

UNCLASSIFIED

AD NUMBER

AD915720

LIMITATION CHANGES

TO:

Approved for public release; distribution is unlimited.

FROM:

Distribution authorized to U.S. Gov't. agencies only; Test and Evaluation; DEC 1973. Other requests shall be referred to Air Force Flight Dynamics Lab., Wright-Patterson AFB, OH 45433.

AUTHORITY

AFFDL ltr 28 Nov 1979

THIS PAGE IS UNCLASSIFIED

AD915720

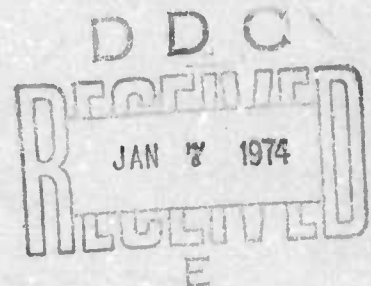
# TECHNOLOGY INTEGRATION FOR CLOSE AIR SUPPORT AIRCRAFT

Larry E. Hove, et al.

GENERAL DYNAMICS  
Convair Aerospace Division  
Fort Worth Operation

Distribution limited to U. S. Government  
agencies only; test and evaluation  
statement applied Jul 73  
Other requests for this document must be  
referred to AF Flight Dynamics Laboratory,  
(PTC), Wright-Patterson AFB, Ohio 45433

JULY 1973



AIR FORCE FLIGHT DYNAMICS LABORATORY  
AIR FORCE SYSTEMS COMMAND  
WRIGHT-PATTERSON AIR FORCE BASE, OHIO



## NOTICE

When Government drawings, specifications, or other data are used for any purpose other than in connection with a definitely related Government procurement operation, the United States Government thereby incurs no responsibility nor any obligation whatsoever; and the fact that the government may have formulated, furnished, or in any way supplied the said drawings, specifications, or other data, is not to be regarded by implication or otherwise as in any manner licensing the holder or any other person or corporation, or conveying any rights or permission to manufacture, use, or sell any patented invention that may in any way be related thereto.

Copies of this report should not be returned unless return is required by security considerations, contractual obligations, or notice on a specific document.


# TECHNOLOGY INTEGRATION FOR CLOSE AIR SUPPORT AIRCRAFT

Larry E. Hove, et al.

GENERAL DYNAMICS  
Convair Aerospace Division  
Fort Worth Operation

Distribution limited to U. S. Government  
agencies only; test and evaluation;  
statement applied Jul 73

Other requests for this document must be  
referred to AF Flight Dynamics Laboratory,  
PTC, Wright-Patterson AFB, Ohio 45433



## FOREWORD

This study program was performed by General Dynamics Corporation, Convair Aerospace Division, Fort Worth, Texas, under Air Force Contract No. F33615-73-C-3082 during the period 1 November 1972 to 1 July 1973. The study was initiated by the Air Force Flight Dynamics Laboratory under Project 1207 and was administered under the technical coordination of Maj. D. R. Seger, PTC.

Included among those who made major contributions to this study are Capt. D. S. Hawkins, USAF 422 FWS; Capt. G. D. Huff, USAF 414 FWS; Capt. S. D. Lawder, USAF 355 TFW; Major J. R. Vineyard, USAF TAC Hdqtrs. (XPDC); and Messrs. L. E. Hove, G. J. Komechak, R. D. Weidler, W. S. Bennett, H. P. Fell, M. Massey, E. L. Gomez, L. R. Kirchdorfer, R. E. Neben, T. E. Peace, R. F. Endres, P. D. Whitter, J. I. Koger, I. G. Kennon, and P. H. Deam, all of Convair.

This document was submitted in June 1973.

The technical report has been reviewed and approved.



---

R. E. Colclough  
Acting Chief, Prototype Division  
Air Force Flight Dynamics Laboratory

## ABSTRACT

The objectives of this technology integration study for close air support aircraft were to perform configuration design and validation using, in part, man-in-the-loop simulation techniques. An advanced technology close air support aircraft configuration known as Lightweight Attack (LWA) Configuration 29 was evolved and justified. The selected configuration embodies powered lift in the form of vectored thrust with supercirculation (VT/SC) and an advanced composite structure. Other advanced technologies which are integrated in LWA Configuration 29 are direct sideforce control (DSFC), variable camber, internal/conformal pallet for stores carriage, close-coupled canard, and modular digital avionics. Results of the study show that such an integrated advanced technology configuration provides significant improvement in total tactical fighter mission capability and in the ability to perform and survive in the ground attack environment.



# T A B L E   O F   C O N T E N T S

<u>Section</u>	<u>Page</u>
1      INTRODUCTION AND SUMMARY	1
1.1    Background	2
1.2    LWA Operational Concept	3
1.3    LWA Design Guidelines	4
1.4    LWA Configuration	5
1.5    LWA Man-in-the-Loop Simulation	7
1.6    Recommendations	8
2      LWA CONFIGURATION 29	9
2.1    General Description	9
2.2    VT/SC and DSFC	11
3      GROUND ATTACK AND LANDING SIMULATION	13
3.1    Simulation Setup	13
3.2    VT/SC Evaluation	15
3.3    DSFC Evaluation	17
3.4    Pilot's Comments	23
3.5    Conclusions	27
4      SURVIVABILITY SIMULATION	29
4.1    Simulation Setup	29
4.2    Aircraft Maneuvers	30
4.2.1    Flight Profiles	30
4.2.2    Weapon Delivery Accuracy	32
4.3    Survivability Evaluations	32
4.3.1    Penetration Simulations	32
4.3.2    Weapon Delivery Simulations	34
4.4    Conclusions	35
 APPENDICES	
A      TECHNOLOGY AND OPERATIONS DEFINITION	37
A.1    Technology Assessment	37
A.2    Operations Analysis	63
B      IN-FLIGHT POWERED LIFT DESIGN TECHNOLOGY DEVELOPMENT	69
B.1    Design Objectives	70
B.2    Vectored Thrust	73
B.3    Jet Flaps	74
B.4    Vectored Thrust with Supercirculation	83
B.5    Externally Blown Flaps	90
C      APPLICATION OF ADVANCED COMPOSITE MATERIALS TO FIGHTER AIRCRAFT STRUCTURE	95
C.1    Design and Fabrication	95
C.2    Cost	98
C.3    Advanced Composite Airplane Development	101

# TABLE OF CONTENTS (Continued)

<u>Section</u>		<u>Page</u>
D	LWA CONFIGURATION 29 EVOLUTION AND JUSTIFICATION	103
	D.1 Non-Parametric Configuration Characteristics	103
	D.2 Reference Configurations	121
	D.3 Mission/Configuration Tradeoffs	143
E	AVIONICS RATIONALE, DESCRIPTION, AND TECHNOLOGY REQUIREMENTS	177
	E.1 Overall Design Approach	177
	E.2 Computer Complex	178
	E.3 Navigation and Guidance	179
	E.4 Electro-Optical Capability	180
	E.5 Radar	181
	E.6 Communications, Command and Control	182
	E.7 Weapons Delivery Equipment	183
	E.8 Defensive System	184
F	VECTORED THRUST/SUPERCIRCULATION AERODYNAMIC DESIGN DISCUSSION	187
	F.1 Design Problem	187
	F.2 Design Approach	188
G	CONFIGURATION SYNTHESIS PROCEDURE	191
	G.1 Force Prediction Methods	191
	G.2 Flight Mechanics/Performance Methods	195
	G.3 Mission Analysis Methods	201
H	PARAMETRIC MISSION/CONFIGURATION DATA	203
I	LWA CONFIGURATION 29 SIMULATION	367
	I.1 Simulation Equations	367
	I.2 Aerodynamics	370
	I.3 Flight Control System	377
J	GROUND ATTACK AND LANDING SIMULATION DATA	385
K	SURVIVABILITY SIMULATION DATA	403
	K.1 AAA Quadratic Predictor	403
	K.2 AAA Probability of Kill Model	404
	K.3 Gun Firing Data	406

# LIST OF FIGURES

<u>Figure</u>		<u>Page</u>
1-1	Low Cost and Flexibility Are LWA Goals	4
1-2	LWA Configuration 29	5
1-3	Baseline Design Requirements for LWA	6
1-4	Man-in-the-Loop Simulation Used TAC Pilots and 23 mm Gun Threat	8
2-1	Configuration 29 General Arrangement	10
2-2	Typical LWA Aerodynamic Performance at M 0.9, 30,000 Feet Altitude	11
2-3	Configuration 29 Direct Lift Capability	11
2-4	LWA Configuration 29 Maximum Side Acceleration	11
3-1	Simulation Facility Block Diagram	13
3-2	Cockpit General Arrangement	14
3-3	Cockpit Modifications for VT/SC and DSFC Controllers	15
3-4	VT/SC Can Decrease Exposure for Given Pullout Speed	16
3-5	VT/SC Allows Increased Pullout Speed	16
3-6	DSFC Did Not Improve Azimuth Pointing Accuracy	19
3-7	DSFC with Yaw Rate Mode and Thumb Switch Gave Consistent Improvement in Elevation Pointing Accuracy	20
3-8	DSFC Improved Weapon Delivery Accuracy up to 30 Percent	21
3-9	DSFC Sideslip Mode with Rudder Pedal Control Provided Smoother Approaches	23
4-1	Weapon Delivery Profile Comparison Shows Typical Evasive Maneuver Using VT/SC and DSFC	31
4-2	Effect of Survivability Maneuvers on Weapon Delivery Accuracy	32
A-1	Vectored Thrust Can Decrease Landing Distance and Increase Turn Rate	38
A-2	NASA Tests of Vectored Thrust with Supercirculation	39
A-3	A Jet-Flap Aircraft - The Hunting H.126	39
A-4	Convair Test Data on Transonic Jet Flaps	39
A-5	Fighter-Type Configurations Have Been Tested with External Blown Flaps	40
A-6	Potential Benefits of Spanwise Blowing	41



# LIST OF FIGURES (Continued)

<u>Figure</u>		<u>Page</u>
A-7	The Supercritical Wing Can Improve Transonic Maneuver Performance	41
A-8	Convair Tests Have Verified Favorable Interference for a Close-Coupled Canard-Delta	42
A-9	Wing-Body Design Integration Can Improve L/D at High Angles of Attack	42
A-10	Cruise Drag Reduction Through CCV	43
A-11	Maneuver Load Control Can Reduce Weight	43
A-12	Direct Sideforce Control Can Potentially Improve Aircraft Effectiveness	44
A-13	Active Flutter Suppression Can Save Weight	45
A-14	Multiplexing Can Reduce Flight Control System Weight	46
A-15	Possible Cycle Arrangements for Powered Lift Concepts	47
A-16	Allowable Turbine Inlet Temperature	47
A-17	Compressor Technology Is Not a Limitation	47
A-18	Supercharged Turbofans (STF) Engine Concept	48
A-19	USAF ARL Cold Thrust Augmentation Transition Corridor	50
A-20	LWA Structural Technology Items	51
A-21	Convair's F-5 Composites Fuselage, an Example of the Structural Complexity Reached with Composites	51
A-22	Advanced Composites Impact Both Performance and Configuration	52
A-23	Benefits of Advanced Composite Airframe on M 0.90 Cruise Advanced Transport	52
A-24	Advantages of Advanced Composites Applied to Hydraulic Systems	53
A-25	Flexible Control Surfaces Incorporating Continuous Actuators	54
A-26	Flexible Structures Applied to Aerodynamic Surfaces	54
A-27	Laminated Titanium Wing Carry-Through Structure Designed for Damage Tolerance	55
A-28	Fail-Safe Design Concept for Advanced Composite Panels	55
A-29	Transparent Structure Potential Uses	55
A-30	Transparent Structure Load Capacity and Weight	56
A-31	Transparent Structure Efficiency	56



## LIST OF FIGURES (Continued)

<u>Figure</u>	<u>Page</u>
A-32 Air Flotation System with Brush Braking and Steering	57
A-33 External Pylon-Mounted Weapons Can Limit Aircraft Performance	58
A-34 Clip On/In Weapon Rack Can Provide Mission Flexibility	58
A-35 Bomb Modification for Internal Loading Efficiency	59
A-36 Typical LWA Weapon Candidates	59
A-37 Modular Weapons Study Matrix	59
A-38 Modular Weapons Guidance Concepts	59
A-39 Weapon Delivery Avionic Equipment Candidates	60
A-40 Weapon Delivery Control and Display Possibilities	61
A-41 General Avionic Equipment Candidates	62
A-42 Approach to Operations Assessment for LWA	63
A-43 Scenarios for LWA Analysis	63
A-44 Runway Availability Can Affect LWA STOL Requirement	64
A-45 Bad Weather Predominates European Winters	64
A-46 Target-Type Distribution	64
A-47 Soviet Aircraft Trends	65
A-48 Projected Tactical Force Structure	65
A-49 Typical Tactics	65
A-50 Target Response Times	66
A-51 Effect of Altitude and Jinking on Probability of Hit	66
A-52 Mission Phases	66
A-53 Mission Radius Considerations	67
A-54 Unrefueled Ferry Range Requirements	67
B-1 Modern-Day Tactical Fighters Have STO Capability	70
B-2 Landing Technique Can Shorten Required Field Length for Conventional Fighter	71
B-3 Steep Approach Angle is Important for Realizing Short Landings	71
B-4 Landing Gear Considerations Can Limit Sink Speed	71

# LIST OF FIGURES (Continued)

<u>Figure</u>		<u>Page</u>
B-5	Limit Sink Speed Can Restrict Approach Angle	71
B-6	Vectored Thrust Quickly Reduces Turn Radius	73
B-7	Convair's STOL Tactical Fighter Study Vectored Thrust Configuration	73
B-8	Digital Simulation Studies Showing Effect of Thrust Vectoring (Fixed) on Air Combat During the Initial 15 Seconds	74
B-9	Jet Flap Lift Augmentation Depends on Momentum Coefficient	75
B-10	An Integrated Duct/Trailing Edge Structure is Desirable	75
B-11	Simple Fixed Jet Angle Nozzle is Likely	76
B-12	Jet Flap Performance is Function of Jet Angle, $\theta_j$	76
B-13	Wing Sweep-Back Decreases Jet Flap Effectiveness	76
B-14	Wing Geometry Affects Jet Flap Duct Losses	77
B-15	Fan Pressure Ratio Can Limit $C_\mu$	77
B-16	Available $C_\mu$ and Wing Geometry Are Strongly Related	77
B-17	Available $C_\mu$ Used for Jet Flap Performance Evaluations	78
B-18	Jet Flap Landing Performance Potential	78
B-19	Jet Flap In-Flight Performance Potential	79
B-20	Conventional Jet Flap Configuration Arrangement	81
B-21	Close-Coupled Canard Jet Flap Configuration Arrangement	82
B-22	NASA/Langley's First Vectored Thrust with Supercirculation Wind Tunnel Model	83
B-23	Vectored Thrust W/Supercirculation Performance is Function of Vector Angle, $\theta_j$	83
B-24	Wing Sweep-Back Decreases Vectored Thrust W/Supercirculation Effectiveness	84
B-25	Available $C_\mu$ Used for VT/SC Performance Evaluations	84
B-26	Vectored Thrust W/Supercirculation In-Flight Performance Potential	85
B-27	Conventional VT/SC Configuration Arrangement	86
B-28	M-Wing VT/SC Arrangement Reduces Thrust Vector - CG Separation	87

# LIST OF FIGURES (Continued)

<u>Figure</u>		<u>Page</u>
B-29	Close-Coupled Canard VT/SC Arrangement Results in Large Positive Static Margin	88
B-30	Removing Weapons Bay Reduces Static Margin for Canard - VT/SC but Still Unsatisfactory	88
B-31	Fan-Air-Only VT/SC Provides Freedom for CG Location	89
B-32	Fan-Air-Only VT/SC Aerodynamic Performance Potential	90
B-33	EBF Performance Is Function of Flap Turning Angle, $\theta$	90
B-34	Wing Sweep-Back Decreases EBF Effectiveness	91
B-35	EBF In-Flight Performance Potential	92
B-36	Conventional EBF Configuration Arrangement	93
B-37	Desired Engine/Wing Location for EBF Compromised by Required Aft Shift of CG	93
C-1	A Thin, Composite Wing Might Be Full Depth Sandwich Construction	96
C-2	Wing/Fuselage Joint Can Use Fail-Safe Lug Fittings	96
C-3	Optimized Composite Laminate Design for a Particular Wing Geometry	97
C-4	Several Structural Concepts Exist for a Composite Fuselage	97
C-5	New Composite Empennage Design Concepts Can Save Weight and Cost	98
C-6	Cost Comparison for an F-111 Part Shows Composites Can Be Lower Cost Than Aluminum	99
C-7	Studies Show Composites To Be Cost Competitive on Simple Material Substitution Basis	100
D-1	Modular Weapons Are Important to LWA Air-to-Ground Flexibility	104
D-2	Smart Bomb Technology Decreases Payload Requirements	104
D-3	LWA Can Be an Effective Booster for Unpowered Stand-Off Weapons	105
D-4	Choice of Gun Caliber for LWA is Tradable	105
D-5	LWA Stores Carriage is Keyed to Flexibility	106
D-6	Convair ATF Studies Show Internal Carriage is Weight Competitive	106

# LIST OF FIGURES (Continued)

<u>Figure</u>		<u>Page</u>
D-7	LWA Internal/Conformal Carriage Concept is Based on Flexible Clip-In Platform	107
D-8	Clip-In Platform Accommodates Universal Weapon Racks for Standard A-G Ordnance Carriage	109
D-9	Clip-In Platform Can Be Missionized for Many Types of Stores	109
D-10	LWA Avionics Approach Is Modular Digital Missionized System	110
D-11	Life-Cycle Costs Are Generally Lower for One Man Crew	112
D-12	Demanding A-G Missions Require Advanced Systems for One Man Crew	112
D-13	Bubble Canopy Costs Some Supersonic Drag	113
D-14	Life-Cycle Costs for Similar Engine Favor One Engine Approach	114
D-15	Combat Experience Does Not Show Differences in Survivability	114
D-16	Engine Weight Tradeoffs Considered in Evolving LWA Reference Configurations	115
D-17	Cruise SFC is One Measure for LWA Engine Cycle Selection	116
D-18	Blowing Momentum is Also Consideration in Cycle Selection	117
D-19	Canard Best Accommodates Both Powered Lift and CCV	119
D-20	LWA Vertical Stabilizers are Consistent with CCV and Direct Sideforce Technologies	120
D-21	Current LWA Approach to the -ilities	120
D-22	LWA Conventional Reference Configuration 26B	122
D-23	High Sink Rate Gear is Stowed in the Wing Box	123
D-24	LWA Internal Bay Integrates Well with Configuration	123
D-25	LWA Vectored Thrust/Supercirculation (VT/SC) Reference Configuration 27	126
D-26	Configuration 27 Utilizes Fan Air Only for VT/SC	126
D-27	Pegasus Plenum Chamber Burning (PCB) is Similar to LWA Wing Duct Burning (WDB)	128
D-28	WDB Thrust Augmentation is a Strong Function of Exhaust Temperature	128
D-29	Simple Vectoring Nozzle Concepts Do Not Satisfy Aerodynamic Requirements	130

# LIST OF FIGURES (Continued)

<u>Figure</u>		<u>Page</u>
D-30	Articulated Pivoting Nozzle is Attractive from All Standpoints	130
D-31	Nozzle Tradeoffs Can Affect Selected WDB Exhaust Temperature	131
D-32	Initial VT/SC Configuration Severely Limited Trimmable Thrust Vector Angle	131
D-33	LWA VT/SC Configuration Evolution is Keyed to Maximizing Trimmable Thrust Vector	132
D-34	Configuration 27 Controllable Thrust Vector at Low Speed	132
D-35	Proper Scheduling of Thrust Vector and Canard Deflection Can Maximize Efficiency	133
D-36	Configuration 27 Aerodynamics for M0.9, 30,000 Feet Altitude Maneuver Evaluations	134
D-37	Configuration 27 Aerodynamics for Ground Attack Maneuver Evaluations	135
D-38	VT/SC Allows Reasonably Short Landings at High Wing Loading	136
D-39	Jet Flap Reference 28	137
D-40	Amount of Jet Flap Air is Variable	138
D-41	Configuration 28 $C_{\mu}$ at Selected Conditions	138
D-42	Jet Flap Wing Duct Concept Uses Main Structural Box as Primary Duct	139
D-43	Low Speed Aileron Can Be Used as Simple Control Device or Blown Flaperon	139
D-44	Jet Flap Wing Duct Concept Integrates Structure and Duct	140
D-45	Wing and Fan Ducts Result in Significant Pressure Losses	141
D-46	Configuration 28 Aerodynamics for M0.9, 30,000 Feet Altitude Maneuver	142
D-47	Configuration 28 Aerodynamics for 150 KTAS, 5000 Feet Altitude Maneuver Evaluations	142
D-48	Mission/Configuration Tradeoff Analysis Steps	143
D-49	Initial Set of Parametric Operational Requirements for LWA is Very Broad	145
D-50	Maneuver and Acceleration Requirements Provide Excellent Ground Attack Capability and Maintain Self-Defense	145

# LIST OF FIGURES (Continued)

<u>Figure</u>		<u>Page</u>
D-51	Quick Reaction Attack Mission Represents Typical Close Air Support Role for LWA	146
D-52	LWA Employment for Interdiction/Strike Role is Basis for Pre-Planned Attack Mission	147
D-53	Escort/Intercept Capability Allows Supplemental Air Superiority Role for LWA	148
D-54	Low Speed Maneuver Dominates Parametric Requirements from Aerodynamic Standpoint	149
D-55	Parametric Analysis Considers More Compatible and Meaningful Instantaneous-g Requirements	150
D-56	Supersonic Acceleration Requirements Provide Adequate Thrust to Generally Meet Other Engine Sizing Requirements	150
D-57	Preliminary Survey Indicates Wing Geometries of Interest	151
D-58	Optimum Cruise is Sufficiently Near Optimum Loiter for Analysis Purposes	155
D-59	TMRs for Minimum Time Subsonic Cruise Are Not Substantially Different Than for Optimum Subsonic Cruise	155
D-60	"Optimum Subsonic" Mission Profile Represents Quick Reaction Attack and Optimum Cruise Pre-Planned Attack Requirements	156
D-61	Sea Level Penetration Speed Can Have a Strong Effect on Parametric Results	156
D-62	"Sea Level Penetration" Mission Profile Represents Pre-Planned Attack Option	156
D-63	Parametric Configuration Variations Do Not Significantly Affect TMRs at Different Supersonic Penetration Speeds	157
D-64	"Supersonic Penetration" Mission Profile Represents Pre-Planned Attack Option	157
D-65	"Supersonic Intercept" Mission Profile Represents Interceptor Role for LWA	158
D-66	Conventional Materials Top-Level Mission/Configuration Tradeoffs Using Representative Wing Geometry	160
D-67	Advanced Composite Materials Top-Level Mission/Configuration Tradeoffs Using Representative Wing Geometry	163
D-68	VT/SC Top-Level Mission/Configuration Tradeoffs	165
D-69	Jet Flaps Top-Level Mission/Configuration Tradeoffs	167

# LIST OF FIGURES (Continued)

<u>Figure</u>		<u>Page</u>
D-70	Mission Profile and Design Requirements for LWA	171
D-71	25,000-Pound Class LWA Baseline Configurations	176
F-1	VT/SC Thrust Recovery Picture is Cloudy	187
F-2	VT/SC Partial Span Loading Results in Induced Drag Increment	188
F-3	Tailoring Planform Can Improve Jet-Induced Loading	189
F-4	Increasing Duct Span is Obviously Helpful	189
F-5	Span Loading Can Be Increased in Outboard Regions with Camber and Twist	189
F-6	Variable Camber in Outboard Region Could Be Answer	190
G-1	Structural Weight Methods - Loading Parameter	194
H-1	Engine Size and Wing Area Used for Parametric Data Can Be Converted to Thrust Loadings and Wing Loadings	204
I-1	Design Flight Conditions	370
I-2	Lift Curve Slope and Intercept	370
I-3	Supercirculation Parameters	371
I-4	Lift Curve Break and Moment Curve Slope	371
I-5	Minimum Drag Coefficient	371
I-6	Minimum Drag Lift Coefficient and Span Efficiency Factors	371
I-7	Jet Flap Drag and Altitude Correction Parameters	372
I-8	Speedbrake and Flap Drag	372
I-9	Canard Lift and Moment Curves	372
I-10	Flap Lift and Moment Curves	373
I-11	Pitch Rate Derivatives	373
I-12	Maximum Lift Coefficient	373
I-13	Sideslip Derivatives	373
I-14	Aileron Derivatives	374
I-15	Sideforce Derivatives	374
I-16	Vertical Tail Derivatives	374

# LIST OF FIGURES (Continued)

<u>Figure</u>		<u>Page</u>
I-7	Yaw Rate Derivatives	375
I-18	Roll Rate Derivatives	375
I-19	Sideslip Derivative Flexibility	375
I-20	Control Derivative Flexibility	376
I-21	Longitudinal Flight Control System	378
I-22	Pitch Acceleration Command	378
I-23	Longitudinal Forward Loop Gain	378
I-24	Acceleration and Angle of Attack Feedback Gains	379
I-25	Jet Flap/Canard Interconnect Gain	379
I-26	Flaperon (Flap)/Canard Interconnect Gain	379
I-27	Lateral-Directional Flight Control System	380
I-28	Roll Rate Command	380
I-29	Rudder Forward Loop Gain and Sideforce Mode Feedback Gain	381
I-30	Sideforce/Rudder Interconnect Gain and Flaperon (Aileron) Forward Loop Gain	381
I-31	Rudder/Flaperon and Sideforce/Flaperon Interconnect Gains	381
J-1	VT/SC Ground Attack Simulation Geometry	386
J-2	DSFC Ground Attack Simulation Evaluation - Pilot A	388
J-3	DSGC Ground Attack Simulation Evaluation - Pilot B	388
J-4	DSFC Ground Attack Simulation Evaluation - Pilot C	389
J-5	Landing Approach With Zero Crosswind-Conventional Configuration	390
J-6	Landing Approach With Zero Crosswind - DSFC Sideslip Mode Engaged, Rudder Pedal Controller	391
J-7	Landing Approach With Zero Crosswind - DSFC Sideslip Mode Engaged, Thumb Controller	392
J-8	Landing Approach With Zero Crosswind - DSFC Yaw Rate Mode Engaged, Rudder Pedal Controller	393
J-9	Landing Approach with Zero Crosswind - DSFC Yaw Rate Mode Engaged, Thumb Controller	394



# LIST OF FIGURES (Continued)

<u>Figure</u>		<u>Page</u>
J-10	Landing Approach With 30 Knot Crosswind - Conventional Configuration	395
J-11	Landing Approach With 30 Knot Crosswind - DSFC Sideslip Mode Engaged, Rudder Pedal Controller	396
J-12	Landing Approach With 30 Knot Crosswind - DSFC Sideslip Mode Engaged, Thumb Controller	397
J-13	Landing Approach With 30 Knot Crosswind - DSFC Yaw Rate Mode Engaged, Rudder Pedal Controller	398
J-14	Landing Approach With 30 Knot Crosswind - DSFC Yaw Rate Mode Engaged, Thumb Controller	399
J-15	Simulator Pilots' Report	400
K-1	Block Diagram of Down-Range Prediction Circuits	403

# L I S T   O F   T A B L E S

<u>Table</u>		<u>Page</u>
1-1	VT/SC Improves the Turning Performance of LWA Configuration 29	7
2-1	Configuration 29 Weight Statement	9
2-2	Configuration 29 Engine Characteristics	9
3-1	DSFC Ground Attack Evaluation Run Matrix for Each Pilot	19
3-2	DSFC Landing Approach Evaluation for Each Pilot	22
4-1	Gun and Projectile Performance Characteristics	29
4-2	Penetration Profile Matrix	32
4-3	Probability of AAA Killing Aircraft	33
D-1	Modular Avionics Approach Allows Minimum Basic System	111
D-2	Internal Bay Impact on Structural Weight for LWA Configuration Approach	123
D-3	Structural Weight Reduction for Configuration 26C	125
D-4	Vectoring Nozzle Design Objectives	129
D-5	VT/SC Implementation Increases Propulsion System Weight	133
D-6	Wing Duct Design Criteria for FPR=4 Fan	138
D-7	Jet Flap Implementation Impacts Propulsion and Wing Weights	141
D-8	Parameters and Ranges of Interest Selected for LWA Parametric Analysis	151
D-9	A Concept of "Mission Configurations" Is Used to Cover Allowance and Payload Variations	152
D-10	A Wing Planform Geometry of $t/c = 0.5$ , $\Lambda_{LE} = 20^\circ$ , and Aspect Ratio = 4 Is a Good Geometry for Top-Level Tradeoff Presentations Relating to Conventional Materials	159
D-11	A $t/c = 0.5$ , $\Lambda_{LE} = 20^\circ$ , and Aspect Ratio = 5 Wing Is Used for Advanced Composite Materials Tradeoff Illustrations	162
D-12	Baseline Payload Requirements for LWA	169
D-13	Acceleration and Maneuver Requirements for LWA	170
D-14	Parametric Configurations Which Meet Acceleration and Maneuver Requirements with Maximum Wing Loading and Minimum Thrust Loading	172
D-15	Selected Characteristics for Advanced Composites Baseline Configuration	172

# LIST OF TABLES (Continued)

<u>Table</u>		<u>Page</u>
D-16	Advanced Composites Baseline Configuration Changes from Reference Configuration 26B	174
D-17	Selected Characteristics for VT/SC Baseline Configuration	174
E-1	Rationale for Avionics Requirements Is Based on LWA Objectives and Operations Studies	177
E-2	Heart of Avionics System Is Computer Complex	178
E-3	Navigation and Guidance Depends Heavily on External Aids	179
E-4	E-O Capability Is Optional but Fully Accommodated by Basic System	181
E-5	A-G Attack Radar Enhances LWA Mission Accomplishment	182
E-6	Optional Digital Data Links Are Provided in Modular C <sup>3</sup> Approach	183
E-7	Advanced Armament Displays and Controls are Included	183
E-8	Defensive Electronics Are Optional	184
H-1	Nine Mission Profile/Mission Configuration Combinations Are Included in the Parametric Data	203
I-1	Lightweight Attack Aircraft (LWA) Simulation and General Equations	368
I-2	LWA Configuration Constants	369
I-3	$C_{l_0}$ and $C_{l_\alpha}$ Versus Blowing Coefficient	376
I-4	Intermediate Power Thrust	376
I-5	Wing Blowing Coefficients	376
I-6	List of Symbols	382
J-1	VT/SC Ground Attack Simulation Evaluation - Pilot A	386
J-2	VT/SC Ground Attack Simulation Evaluation - Pilot B	387
J-3	VT/SC Ground Attack Simulation Evaluation - Pilot C	387
K-1	Gun Firing Data	407

# LIST OF ABBREVIATIONS AND SYMBOLS\*

AAA	- Anti-Aircraft Artillery
A-A	- Air-To-Air
A/B	- Afterburner
A/C	- Aircraft
AC	- Aerodynamic Center
AFAPL	- Air Force Aero Propulsion Laboratory
AF-EWES	- Air Force Electronic Warfare Evaluation/Simulator
AFFDL	- Air Force Flight Dynamics Laboratory
A-G	- Air-To-Ground
AR	- Aspect Ratio
ATF	- Advanced Tactical Fighter
BPR	- Engine By-Pass Ratio
CC&C, C <sup>3</sup>	- Communications, Command, and Control
CCV	- Control Configured Vehicle
CEP	- Circular Error Probability
CG, c.g.	- Center of Gravity
C <sub>D</sub>	- Aerodynamic Drag Coefficient
C <sub>d</sub>	- Section Aerodynamic Drag Coefficient
C <sub>L</sub> , C <sub>LT</sub>	- Aerodynamic Lift Coefficient
C <sub>Lc</sub>	- Aerodynamic Lift Coefficient Due to Circulation
C <sub>l</sub>	- Section Aerodynamic Lift Coefficient
C <sub>M</sub>	- Aerodynamic Moment Coefficient
C <sub>T</sub>	- Engine Thrust Coefficient
C <sub>TJ</sub>	- Thrust Coefficient of Powered Lift Jet
C <sub>TE</sub>	- Thrust Coefficient of Jet Not Used for Powered Lift
C <sub>X</sub>	- Net Axial Force Coefficient, $C_D - C_T \cos \alpha$

---

\* This list includes those symbols and abbreviations which are used throughout the report. Other symbols and abbreviations which are confined to specific sections are defined in those sections.

# LIST OF ABBREVIATIONS AND SYMBOLS (CONT'D.)

DAIS	- Digital Avionics Information System
D.I.M.	- Duct Inlet Mach Number
DSFC	- Direct Sideforce Control
EBF	- Externally Blown Flap
ECM	- Electronic Countermeasures
EO, E-O	- Electro-Optical
FBW	- Fly-by-Wire
FEBA	- Forward Edge of the Battle Area
FLIR	- Forward Looking Infrared
FPR	- Fan Pressure Ratio
F <sub>N</sub>	- Net Thrust
HUD	- Head-Up Display
IIR	- Imaging Infrared
ILS	- Instrument Landing System
INS	- Inertial Navigation System
IR	- Infrared
L/D	- Lift-to-Drag Ratio
L.E.	- Leading Edge
LLTV	- Low Light Level Television
LORAN	- Long Range Aid to Navigation
LTDR	- Laser Target Designator/Ranger
L/W	- Normal Load Factor
LWA	- Lightweight Attack
M	- Mach Number, Moment
MAC	- Mean Aerodynamic Chord
NavSat	- Navigation Satellite
OPR	- Overall Pressure Ratio
P	- Pressure

# LIST OF ABBREVIATIONS AND SYMBOLS (CONT'D.)

PK	- Probability of Kill
PKA	- 5-Minute Probability of Kill
PKK	- 1-Minute Probability of Kill
S, SREF, SW	- Reference Wing Area
S'	- Blown Wing Area
SAM	- Surface-to-Air Missile
S/C	- Supercritical
SFC	- Specific Fuel Consumption
SLS	- Sea Level Static
STO	- Short Takeoff
STOL	- Short Takeoff and Landing
T	- Thrust, Temperature
TAC	- Tactical Air Command
TACAN	- Tactical Aid to Navigation
T.E.	- Trailing Edge
TIT	- Turbine Inlet Temperature
TMR	- Total Mission Radius
T/O	- Takeoff
T/W	- Thrust-to-Weight Ratio
TG	- Gross Thrust
USAF	- United States Air Force
V	- Velocity
V/STOL	- Vertical/Short Takeoff and Landing
VT/SC	- Vectored Thrust/Supercirculation
W	- Air Flow Rate
WDB	- Wing Duct Burning
W/S	- Wing Loading

# LIST OF ABBREVIATIONS AND SYMBOLS (CONT'D.)

$b_F/b$	- Ratio of Blown Span-to-Total Span
$c$	- Wing Chord
$c_\mu$	- Blowing Momentum Coefficient
$r$	- Thrust Recovery
$t/c$	- Thickness Ratio
$\alpha$	- Angle-of-Attack
$\beta$	- Sideslip DSFC Mode
$\delta_{\text{Canard}}$	- Canard Deflection
$\delta_F$	- Flap Deflection
$\delta_H$	- Horizontal Tail Deflection
$\delta_{LE}$	- Leading Edge Flap Deflection
$\theta_j$	- Jet Angle
$\Lambda_{LE}$	- Leading Edge Sweep
$\Lambda_{c/2}$	- 50 Percent Chord Sweep
$\lambda$	- Taper Ratio
$\dot{\psi}$	- Yaw Rate DSFC Mode

## SECTION 1

### INTRODUCTION AND SUMMARY

The Convair Aerospace Division of General Dynamics has completed a study entitled "Technology Integration for Close Air Support Aircraft" for the Air Force Flight Dynamics Laboratory (AFFDL). The work documented in this technical report has resulted in the following conclusions:

- o Through the integrated use of advanced technology, a superior tactical fighter aircraft can be obtained with a lightweight airframe -- thus providing an important step toward reducing the cost of future fighter weapon systems. The advanced technology concepts which have first-order effects on this result are advanced composite structures and powered lift in the form of vectored thrust with supercirculation (VT/SC).
- o Man-in-the-loop simulation evaluations of VT/SC and direct sideforce control (DSFC) indicate significant improvements in air-to-ground weapon delivery accuracy and evasive tactics are attributable to these two advanced technology concepts.

The study consists of two basic tasks: (1) configuration design and parametric analysis and (2) configuration validation and refinement through man-in-the-loop simulation. Section 2 of this report contains a discussion of the first task, and Sections 3 and 4 contain a discussion of the results of the second task. The appendices provide further detail concerning these results.

The two tasks were directed toward the study objectives as stated in the contract statement of work:

"There are a number of advanced and emerging technologies which have a potential impact on the design and operation of future close air support aircraft. The benefits to be gained from the incorporation of one or more of these technologies into a system depends upon the mission to be accomplished. Because the possible close air support roles are numerous and also because there are many advanced and emerging technologies to be considered, a systematic evaluation of potential capabilities against mission requirements is needed. ...The objective of this effort is to obtain design data relative to the integration of advanced and emerging fighter technologies into advanced technology close air support aircraft. Specifically, efforts are to be conducted which will demonstrate how advanced/emerging technologies can best be integrated into fighter aircraft design and the extent to which they provide a superior CAS capability."



## 1.1 BACKGROUND

A Convair-sponsored advanced aircraft development program known as the Lightweight Attack (LWA) program has been closely tied to the subject contractual study. For this reason, the aircraft considered in the AFFDL study are referred to as LWA.

Convair's LWA program began in early 1972. Initial LWA technical efforts resulted in the development of preliminary design techniques for applying powered-lift concepts to maneuvering flight including flight at transonic speeds.<sup>1</sup> An excellent preliminary design data base existed for other technologies of interest such as advanced composite materials.

Operational studies were also conducted during the initial phases of the program.<sup>2</sup> The results of these studies provided guidelines for the LWA concept and parametric operational requirements which could be used to evaluate tradeoffs with configuration variables.

In June 1972, Convair submitted a "Technical Proposal for Technology Integration for Close Air Support Aircraft," Convair Report FZP-1429, to the AFFDL. This proposal which resulted in the subject contract contained technical discussions covering technology assessment, operational considerations, and conceptual configuration designs. Much of this material is contained in Appendices A and B of this report.

In the last half of 1972, Convair completed configuration design and parametric analysis work.<sup>3</sup> These results provided the basis for work on the subject contract which was awarded in November 1972. Much of this information is contained in Appendices C through H.

The major portion of the contractual effort was directed toward man-in-the-loop simulation studies. The impetus for this type of effort in a preliminary

---

<sup>1</sup> "Powered Lift Aerodynamic Studies for the Advanced Technology Close Air Support Fighter," Convair Report MR-A-2099, June 1972 (Confidential).

<sup>2</sup> "Post-1980 Tactical Air Strike Requirements and Capabilities," Convair Report MR-O-351, August 1972 (Confidential).

<sup>3</sup> "Lightweight Attack (LWA) Aircraft Preliminary Configuration Design and Mission/Configuration Tradeoff Studies," Convair Report FZM-6085, January 1973.

design study stems from the apparent fact that certain potential benefits of advanced technology are dependent on man/machine interface considerations. The specific objective of the simulation effort was to evaluate VT/SC and DSFC to determine their contribution to improvements in ground attack performance and survivability.

## 1.2 LWA OPERATIONAL CONCEPT

Studies of future tactical air scenarios and present and future tactical force structures indicate a developing gap in operational capability. This is the inability to accomplish ground attack missions (close air support/interdiction/strike) with relatively large numbers of aircraft which can survive in a hostile environment. The role is now occupied primarily by the F-4--an aircraft designed for air superiority two decades ago.

Survivability is a unique aspect of the LWA concept: first, because it is an attack aircraft which offers both maneuverability and speed as self-defense features and, second, because these features provide the LWA with significant air combat capability.

The need for large numbers influences the LWA concept by dictating a low-cost system. The first step toward low cost is lightweight. Considering future force structures with the sophisticated capabilities of F-111, F-15, and F-14 aircraft that are available or potentially available, it is logical to postulate a new system which does not perform at the extremes of these specialized aircraft (i.e., range, payload, and speed) and which therefore can be lightweight.

The other important factor in the cost equation is the weapon delivery system. Developments in recent years have resulted in quantum jumps in daylight, night, and all-weather delivery accuracies. First and foremost, the LWA concept will optimally accommodate these systems, and this alone will make the LWA a unique aircraft. However, if all such systems were included in the basic LWA, a conflict with the low-cost objective would result.

The emerging concept of modular digital avionics presents the answer to this dichotomy. With this concept, provisions can be made in the LWA airframe to accommodate a full-capability avionics system with minimum impact on the basic avionics

and airframe size. Further, provisions can be made so that the addition of any or all of the full system can be accomplished at essentially only the cost of the added equipment.

In summary, the LWA concept reverses the traditional approach of designing high-performance tactical air forces for air superiority and accepting the ground attack fall-out. In future applications of tactical air power, technology makes it imperative that an optimized ground attack aircraft which can survive through its own capability be available.

### 1.3 LWA DESIGN GUIDELINES

Translation of the LWA operational concept into design guidelines is summarized by two descriptors--low cost and flexibility (Figure 1-1). Low cost is achieved through the establishment of proper requirements and design philosophy. Flexibility, at low cost, is attained by application of new technology.

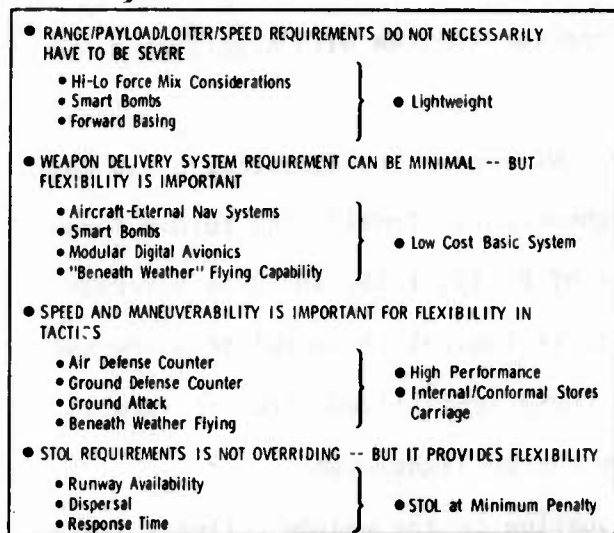


Figure 1-1 Low Cost and Flexibility Are LWA Goals  
takeoff and landing distances and maneuver performance which otherwise require high-lift systems and lower wing loadings.

Internal/conformal carriage provides the capability to carry mission stores throughout the flight envelope. Modular avionics make it possible to design a basic airframe with all provisions for full capability avionics without significant penalty.

A fifth technology which is important to the LWA concept although not a part of the physical airframe design is represented in the concept of modular weapons.

If the full capabilities of the LWA are to be realized, it is clear that new weapon configurations are required. In this regard technology does not pose as much of a problem as the standardization of current and future weapons to a single set of criteria.

#### 1.4 LWA CONFIGURATION

The LWA configuration which was selected for the simulation task is shown in Figure 1-2. The characteristics of LWA Configuration 29 are compatible with the baseline design requirements described in Figure 1-3.

##### FEATURES:

- Powered Lift (Vectored Thrust/Supercirculation)
- Advanced Composite Materials
- Variable Camber
- Internal Bay w/Internal/Conformal Pallet
- Close Coupled Canard
- Direct Sideforce Control
- CCV/ Fly-by-Wire
- Modular Digital Avionics
- Single Wing Duct Burning Turbofan

##### CHARACTERISTICS:

- W/S = 80 lbs/sq. ft. at Transonic Combat Weight
- T/W = 1.3 Sea Level Static, Uninstalled at Supersonic Acceleration Weight
- Wing Geometry
  - $t/c = 0.0625$  (rms)
  - $\Delta LE = 30/47$  Degrees
  - $AR = 4$

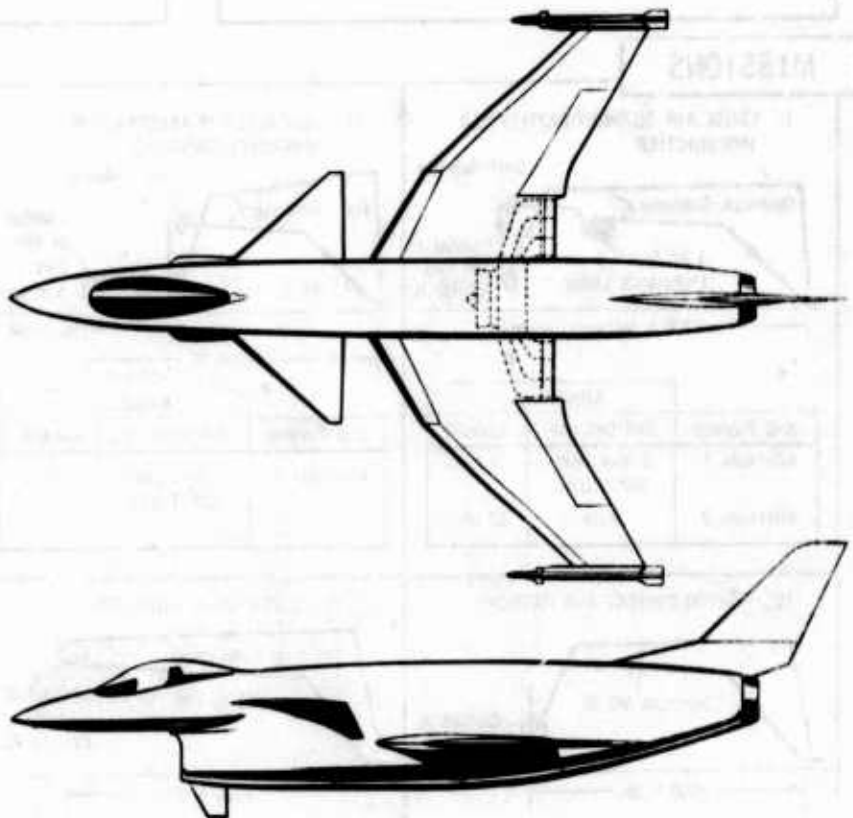


Figure 1-2 LWA Configuration 29

The study results indicate that a 25,000-pound class aircraft of the Configuration 29-type can be optimized to meet or exceed the baseline design requirements. Detail characteristics of the simulated configuration are described in Section 2.

The advanced technology concepts of interest in the simulation task are VT/SC and DSFC. The VT/SC concept is implemented by ducting fan air through two-dimensional, vectorable nozzles located at the inboard wing trailing edge. The nozzle vector angle is essentially zero for cruise and is controllable up to 50 degrees for maneuvering.

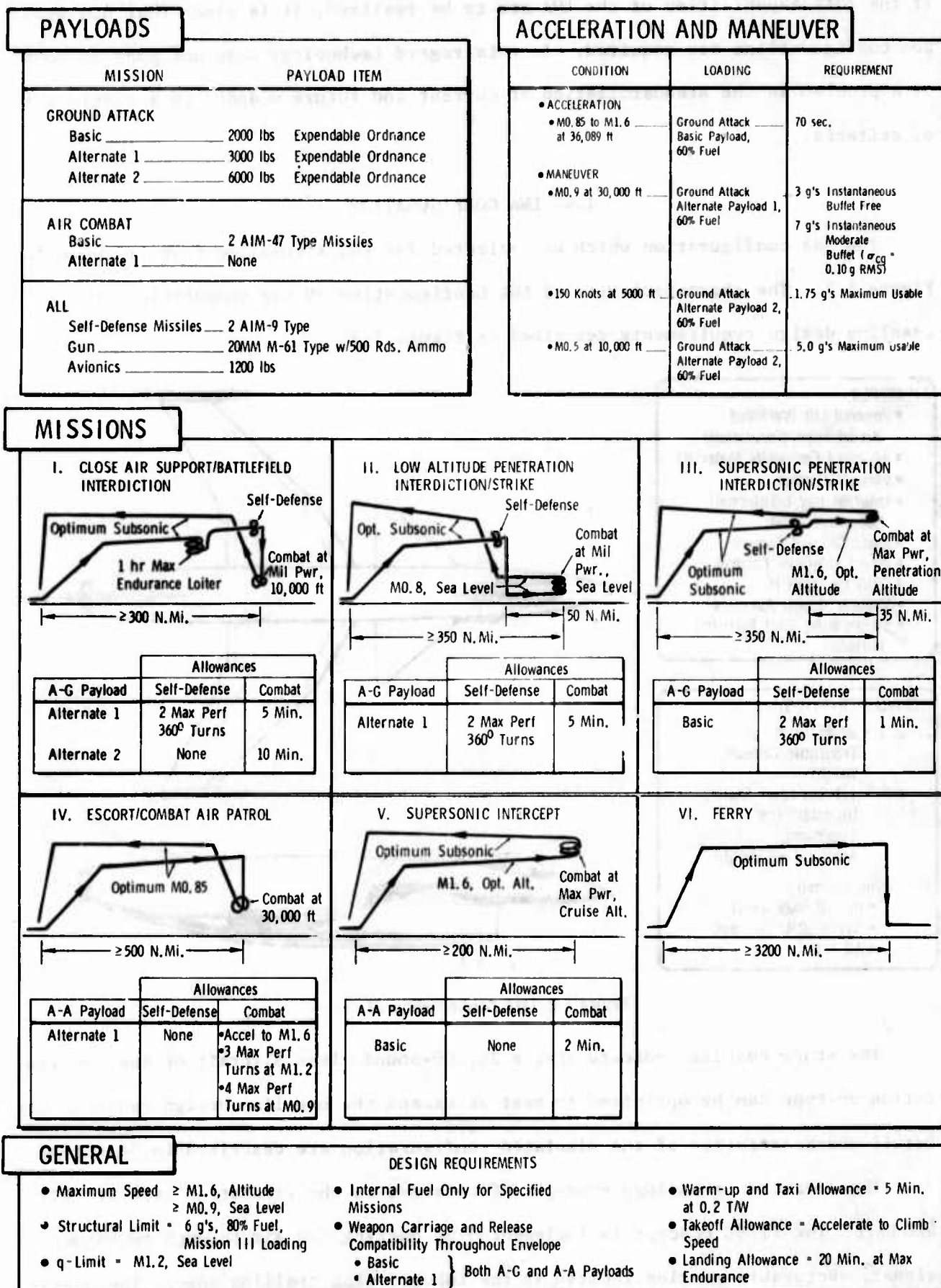


Figure 1-3 Baseline Design Requirements for LWA

The effects of vectoring the nozzles on lift, drag, and thrust can be utilized in several ways. For a given angle of attack, a change in the thrust vector angle produces a lift coefficient increment. Thus, direct lift control is possible. At the same time, induced drag is increased, and horizontal thrust is lost. This results in a speed brake effect if the power setting is not increased.

Table 1-1 VT/SC IMPROVES THE TURNING PERFORMANCE OF LWA CONFIGURATION 29

	BUFFET FREE - g's		SUSTAINED - g's		MAX USEABLE - g's	
	NO VT/SC	VT/SC ( $\theta_1 = 40^\circ$ )	NO VT/SC	VT/SC ( $\theta_1 = 40^\circ$ )	NO VT/SC	VT/SC ( $\theta_1 = 40^\circ$ )
TRANSONIC • MO. 9, 30,000 ft • WDB On • No Flaps	1.8	4.0	3.8	4.8	—	—
LOW SPEED • MO. 5, 10,000 ft • WDB Off • No Flaps	2.2	3.5	3.5	3.8	4.1	5.1

Vector thrust with supercirculation has a large impact on turning performance (Table 1-1). The LWA Configuration 29 approach is to trade the VT/SC turning improvements for increased wing loading. The resulting turning performance is comparable to modern fighters,

but other aspects of mission performance should be better.

Direct sideforce is realized by coordinated deflection of the all-movable vertical tail and twin surfaces (chin fins) located forward of the center of gravity. At low altitude and high subsonic speed, these surfaces are capable of generating greater than 1-g of zero-moment lateral force.

### 1.5 LWA MAN-IN-THE-LOOP SIMULATION

The basic objective of the man-in-the-loop simulation task was to evaluate the effects of VT/SC and DSFC on air-to-ground weapon delivery accuracy and survivability (Figure 1-4). In addition, four other preliminary design areas were addressed:

1. Flight control system design and cockpit control locations and mechanizations
2. Comparison of zero yaw rate sideslip and controlled yaw rate modes of DSFC
3. Effects of crosswind on DSFC utility
4. Impact of DSFC on landing approach.



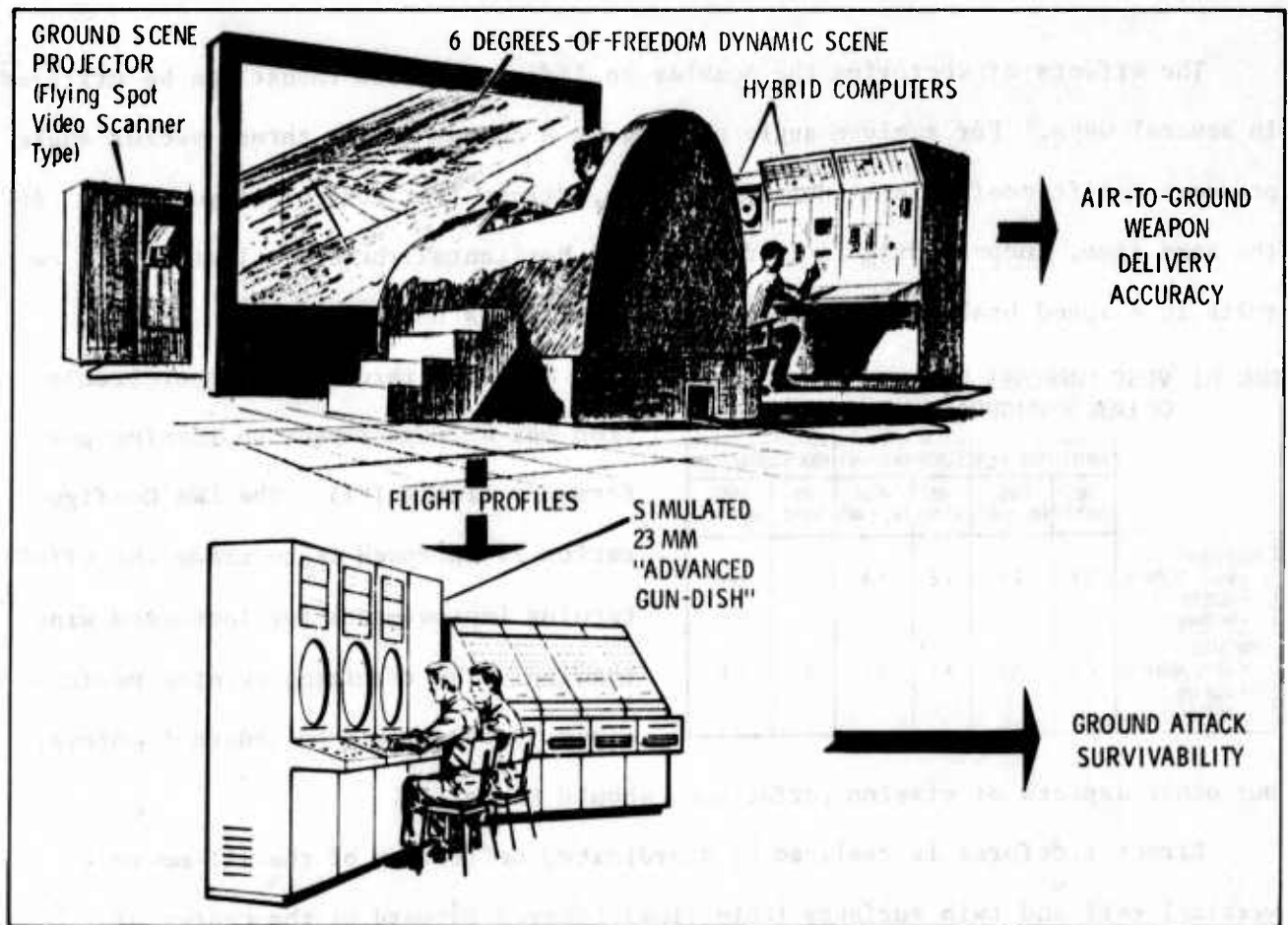


Figure 1-4 Man-in-the-Loop Simulation Used TAC Pilots and 23MM Gun Threat

Another important aspect of the man-in-the-loop simulation work was the opportunity to involve the user, i.e., the pilot, in the early stages of the design process. To maximize this benefit, the USAF Tactical Air Command (TAC) provided three current fighter pilots for the simulation task. The impressions and guidance provided by these pilots are considered equally as important as the quantitative evaluations.

#### 1.6 RECOMMENDATIONS

The results which are documented in this report lead to the following recommendations:

1. A manned flight vehicle program should be undertaken with the objective of demonstrating VT/SC and advanced composites technologies. Other technology concepts which show potential payoff should also be incorporated, e.g., DSFC, CCV/fly-by-wire, and vortex lift enhancement.
2. Utilization of man-in-the-loop simulation as a preliminary design tool should be continued. Simulation provides an excellent medium for communication between the user and the designer.

## SECTION 2

### LWA CONFIGURATION 29

LWA Configuration 29 which was simulated for configuration validation and refinement is described in the following paragraphs. The simulated configuration is very similar to LWA Configuration 27 which is described in Appendix D. Discussions of the basic configuration approach and justification of this approach, presented

in detail in Appendix D, are not repeated here.

Table 2-1 CONFIGURATION 29 WEIGHT STATEMENT

Structure _____	(5,874)
WING _____	1,922
FUSELAGE _____	2,337
CANARD _____	384
VERTICAL TAIL _____	171
CHIN FINS _____	36
LANDING GEAR _____	(620)
MAIN _____	410
NOSE _____	110
LANDING GEAR CONTROLS _____	100
AIR INDUCTION _____	404
Propulsion System _____	(4,137)
ENGINE _____	3,100
FUEL SYSTEM _____	175
ACCESSORIES _____	212
VT/SC DUCT AND NOZZLE _____	650
Systems and Equipment _____	(3,168)
FLIGHT CONTROLS _____	750
INSTRUMENTS _____	93
HYDRAULIC & PNEUMATIC _____	385
ELECTRICAL _____	290
AVIONICS _____	1,200
FURNISHINGS _____	300
AIR CONDITIONING & ANTI-ICING _____	150
Weight Empty _____	13,179
Useful Load _____	(922)
CREW _____	225
GUN INSTALLATION _____	462
WEAPON RACKS _____	180
MISCELLANEOUS _____	55
Basic Operating Weight _____	14,101 lbs

### 2.1 GENERAL DESCRIPTION

The general arrangement and geometrical characteristics of Configuration 29 are shown in Figure 2-1. The primary difference between the Configuration 29 arrangement and that of Configuration 27 is in the location of the internal/conformal bay and the gun.

The configuration incorporates an advanced composites structure. The structural design weight is 22,500 pounds. A weight breakdown is given in Table 2-1. An aircraft gross weight of 21,000 pounds was used in the simulation.

The propulsion system includes an advanced technology turbofan (Table 2-2). The engine thrust is augmented by wing duct burning, but an afterburner is not incorporated. The fan air is ducted to the inboard wing trailing edge and exhausted through a two-dimensional, vectorable nozzle during cruise and VT/SC operation.

Table 2-2 CONFIGURATION 29 ENGINE CHARACTERISTICS

UNINSTALLED SLS THRUST _____	28,000 LB
BY-PASS RATIO _____	1.5
FAN PRESSURE RATIO _____	4.0
OVERALL PRESSURE RATIO _____	30.0
TURBINE INLET TEMPERATURE _____	3200°R
WING DUCT BURNING TEMPERATURE _____	2000°R



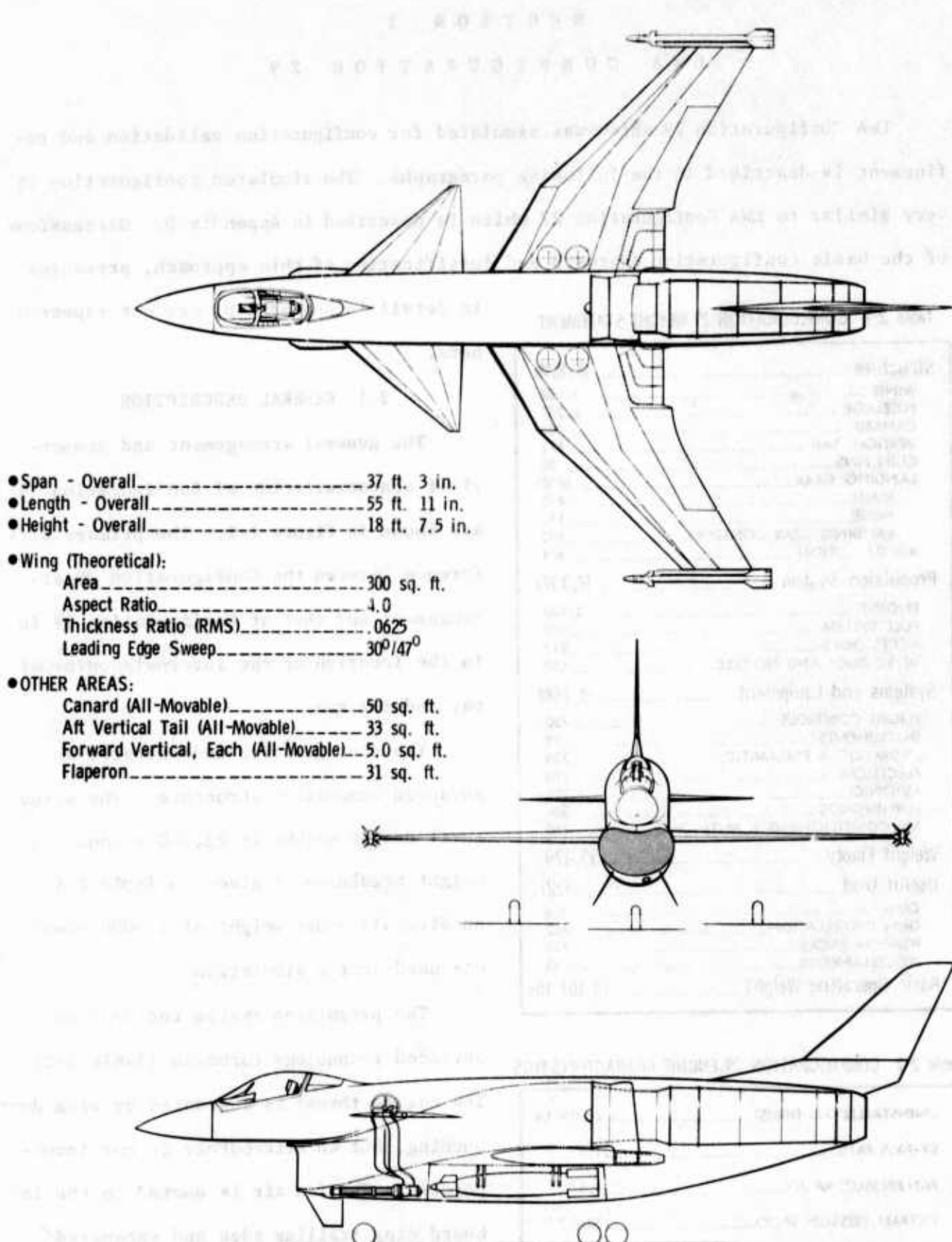


Figure 2-1 Configuration 29 General Arrangement

## 2.2 VT/SC AND DSFC

The objective of implementing VT/SC is to improve maneuver capability. The comparative effect on the aircraft performance is indicated in Figure 2-2. The

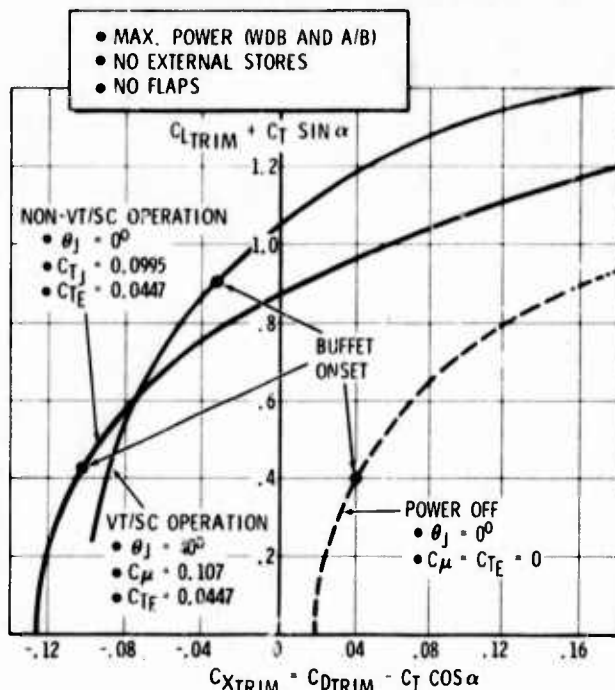


Figure 2-2 Typical LWA Aerodynamic Performance at M0.9, 30,000 Feet Altitude

transonic buffet-free lift coefficient is more than doubled with VT/SC. Above a lift coefficient of 0.6, VT/SC provides higher energy turns. Similar improvements are obtained throughout the speed regime.

The use of VT/SC for direct lift control (i.e., the capability to change lift without an attendant angle-of-attack change) is possible (Figure 2-3). The lift forces which VT/SC is capable of generating are very significant compared to other candidate direct lift approaches.

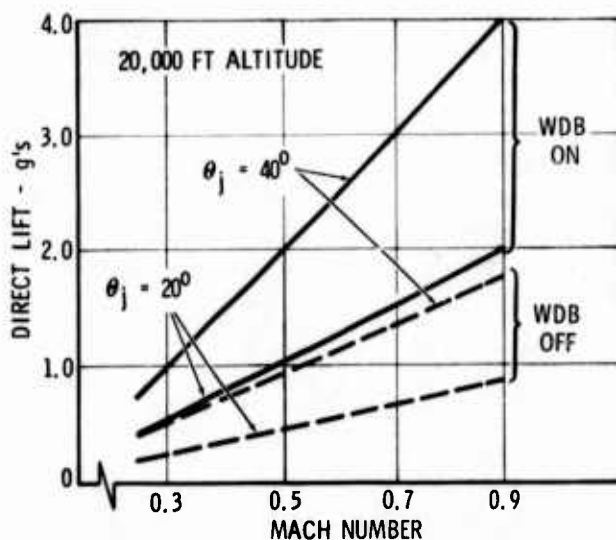


Figure 2-3 Configuration 29 Direct Lift Capability

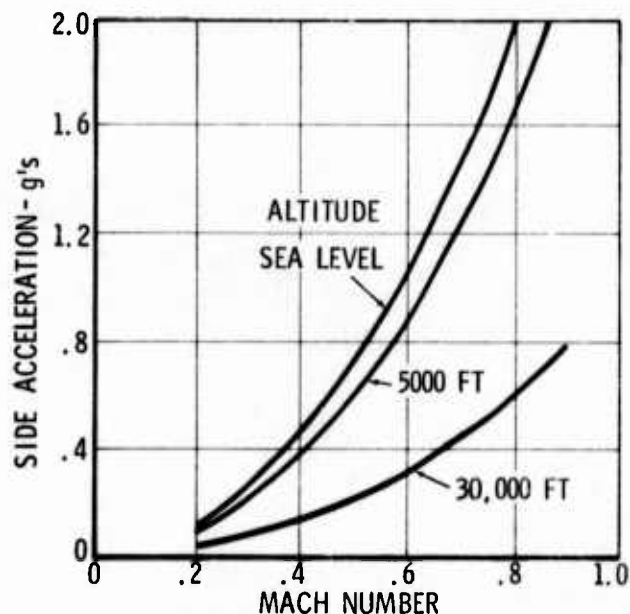


Figure 2-4 LWA Configuration 29 Maximum Side Acceleration

The objective of implementing DSFC is to provide the capability to make lateral flight path changes without rolling the aircraft. Of the several candidate approaches to generating DSFC forces, the chin fins are best, because they result in the largest force and the least coupling with other aircraft axes (Figure 2-4).

## SECTION 3

### GROUND ATTACK AND LANDING SIMULATION

The overall objective of the LWA man-in-the-loop simulation was to determine the effectiveness of the advanced technology concepts of Vectored Thrust/Super-Circulation (VT/SC) and Direct Sideforce Control (DSFC) in realistic manned operational tasks, particularly in those tasks involving severe time constraints or high pilot workload. The simulation task involved (1) developing equations to describe the selected LWA Configuration 29, (2) programming the Convair hybrid computing facility to represent the aircraft, (3) modifying the Convair cockpit facility to fulfill the requirements of the task, and (4) conducting one week of simulation data gathering with three USAF TAC pilots. The simulation setup encompassed the complete airplane flight spectrum; however, the tasks performed by the pilots during the evaluation phase were limited to ground attack weapon delivery, landing, and low altitude survivability maneuvers.

#### 3.1 SIMULATION SETUP

The LWA configuration preliminary design and analysis phase culminated in selection of Configuration 29 as the point design airplane for the simulation

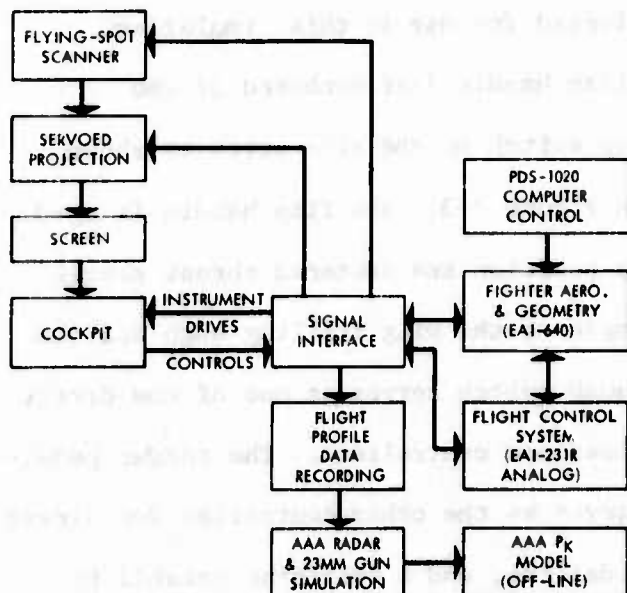


Figure 3-1 Simulation Facility Block Diagram

evaluation. Theoretical and empirical aerodynamic data developed during the design analysis were used as input for the simulation. Weight, inertia, and engine data for the specific configuration were predicted by use of current theoretical and empirical techniques. A full definition of the simulated airplane is presented in Appendix I. The simulation setup is depicted in Figure 3-1.

The equations used to calculate the forces and moments, including those attributed to vectored thrust/supercirculation with variation in power setting and vector angle, and the airplane equations of motion that were developed for the simulation are given in Appendix I. These equations, along with equations to relate the airplane flight path with respect to earth axes, were programmed into a hybrid computer system consisting of an EAI 640 digital computer and two EAI 231-R analog consoles, which provided real time solution.

The hybrid computation was interfaced with the Convair advanced cockpit simulator, visual scene projection system, and peripheral magnetic tape and strip chart recording systems.

The air-to-ground scene projection system consists of a scene transparency, a servoed flying-spot scanner, and servoed projection equipment which produces an earth scene having complete 6 degrees-of-freedom (linear and angular) and perspective cues. The scene was projected onto a screen directly in front of the cockpit. The sight was mounted on the screen to simulate an autocollimated, fixed, depressed reticle bomb sight (Figure 3-2).

The Convair advanced cockpit simulator will accommodate two control stick locations, one center mounted on the floor and one side mounted, plus rudder pedals, throttle with speed brake control, and a complete set of flight and engine instruments. The sidestick location was selected for use in this simulation.

The cockpit was modified to provide a flap handle just outboard of the throttle and to provide a proportional thumb switch on the side stick as shown

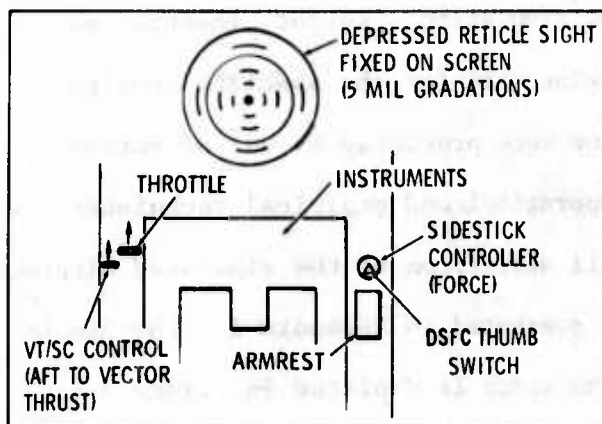
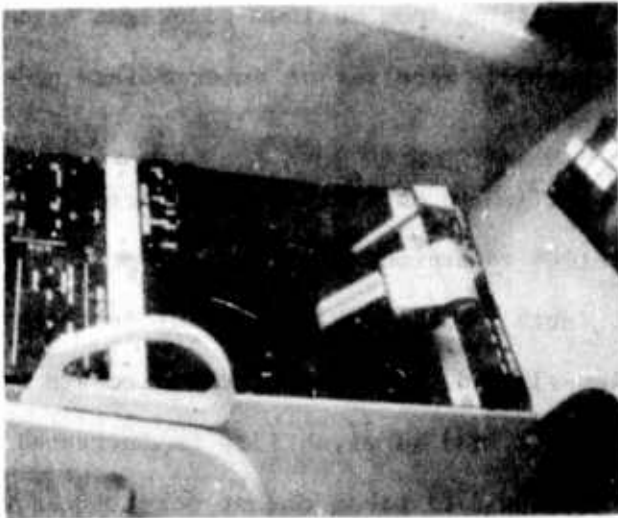


Figure 3-2 Cockpit General Arrangement

in Figure 3-3. The flap handle is used to position the vectored thrust nozzle angle at the wing trailing edge and the thumb switch serves as one of the direct sideforce controllers. The rudder pedals served as the other controller for direct sideforce, and a switching capability was provided to permit the rudder pedals

C Control Handle (Forward Position  
for No Thrust Vectoring)



Direct Sideforce Thumb Switch Control  
(Mounted on Sidestick Controller)

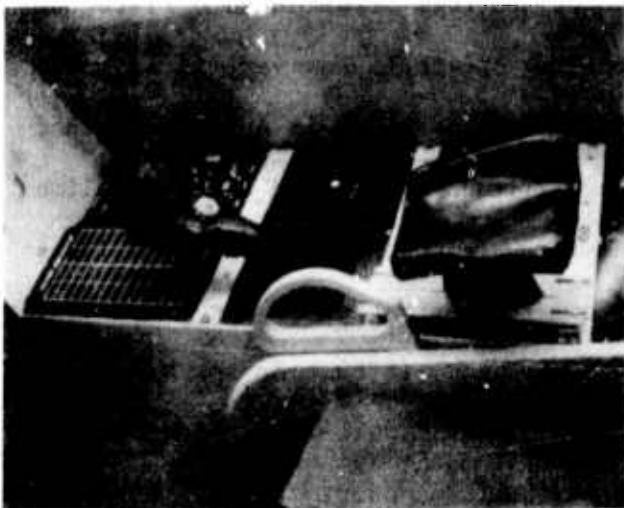


Figure 3-3 Cockpit Modifications for VT/SC  
and DSFC Controllers

to operate in their normal rudder control function or in the sideforce control function. The pitch, roll, and rudder control force gradients were typical for fighter aircraft and are shown in the control system block diagrams of Appendix I.

The command and stability augmentation flight control system developed for Configuration 29 provided two methods of employing the sideforce control as discussed in Section 3.3. The flight control system was checked out prior to the evaluation runs, and the conventional configuration handling qualities were found to be compatible with the requirements of MIL-F-8785B.

### 3.2 VT/SC EVALUATION

The VT/SC evaluation runs consisted of a roll-in from an initial altitude (13,000 feet) and speed (400 and 575 ktas) to a given dive angle (30, 45, and 60 degrees). Three thrust conditions

were evaluated during the dive maneuvers for each type of attack: (1) idle power, no thrust vectoring; (2) 25 percent intermediate power, 50-degree thrust vector; and (3) 50 percent intermediate power, 50-degree thrust vector. Each of the three pilots performed this matrix of 18 runs.

Pullout from each dive was initiated at 4000 feet altitude and the airplane was put into a 60 degree climb back to 10,000 feet. For the non-VT/SC case, the pullout and climb were made with maximum power, that is, with the engine at

intermediate power plus wing duct burning (WDB). However, for the cases with 50 degree thrust vectoring, the available lift resulting from maximum power was beyond the aircraft structural limit, so the VT/SC pullouts were set at intermediate power without WDB.

For a fixed pullout speed, the effect of VT/SC in this attack sequence is to reduce the altitude loss from pullout initiation to minimum altitude and to reduce the time to climb to altitude (Figure 3-4). Both results are beneficial in that

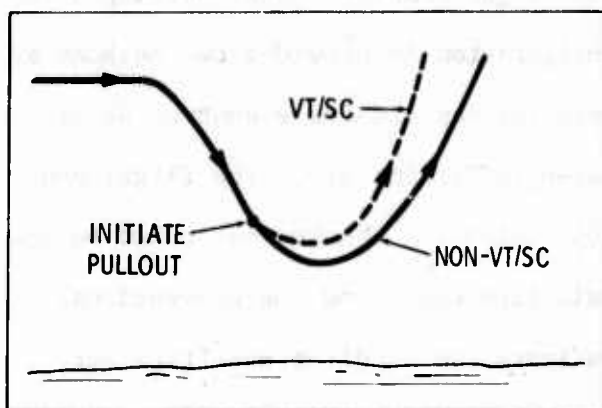


Figure 3-4 VT/SC Can Decrease Exposure for Given Pullout Speed

low-altitude exposure of the aircraft is reduced, and survivability is increased.

The data taken do not permit quantifications of the VT/SC effects in those specific terms. (The different dive power settings resulted in different pullout speeds.) However, it is noted from the data given in Appendix J that the altitude losses and times to climb

for the different power and vector angle settings are roughly the same for fixed initial speed and dive angle. This fact allows quantification of the VT/SC effect by comparing pullout speeds for essentially equivalent altitude losses and times to climb (Figure 3-5). It is noted again that the VT/SC pullout is made at intermediate power and the non-VT/SC operation is at maximum power.

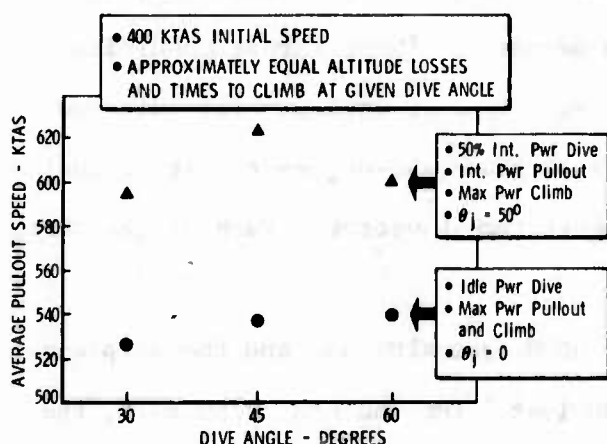


Figure 3-5 VT/SC Allows Increased Pullout Speed

In addition to providing improved turning capability to increase ground attack survivability, the VT/SC can also be employed to improve reattack capability. The ability to perform a reattack maneuver without losing sight of the target or letting the target escape could be very valuable. This feature was not a part of the VT/SC evaluation.



The VT/SC effects were qualitatively noted during the simulated landing approach maneuvers. It was demonstrated that use of the VT/SC considerably reduced the airplane angle of attack during this flight phase as compared to that of the same configuration without use of VT/SC. The decrease in angle of attack greatly improved pilot visibility of the runway, and all of the DSFC landing approach evaluation runs were made with the use of VT/SC.

### 3.3 DSFC EVALUATION

Previous studies on direct sideforce control by Cornell and Boeing provided the background for further investigation of the benefits of sideforce implementation and the control mechanization methods.<sup>1,2</sup> The Cornell study indicated that the pilots preferred an independent sideforce controller, one that was not associated with the primary flight controls; but the thumb wheel mechanization used in the Cornell study was not adequate. The Cornell findings led to the development of the proportional command thumb switch for the LWA simulation evaluation (Figure 3-3).

Results from both studies indicated that rudder pedals would serve as an acceptable method of sideforce control. However, use of the rudder pedals for DSFC precludes normal rudder control. Therefore, one phase of the simulation evaluation was devoted to pilot comparison of these two candidate control methods.

Two types of airplane response can be obtained from application of direct sideforce control input. One mode is to develop a sideslip angle without changing the airplane heading which results in a lateral translation of the airplane flight path. The other mode is to use the sideforce to curve the airplane flight path and, by maintaining zero sideslip, developing a yaw rate and thus a change in airplane heading.

---

<sup>1</sup>Hall, Warren G., A Flight Test Investigation of Direct Side Force Control, Air Force Flight Dynamics Laboratory Technical Report AFFDL-TR-71-106, September 1971.

<sup>2</sup>An Investigation of Direct Sideforce Control for Improving Maneuver Capability of Attack Aircraft, The Boeing Company, Report D 180-14004-1, October 1971.

The first mode was termed the "sideslip" or  $\beta$  mode and the second, the "yaw rate" or  $\dot{\psi}$  mode. In either mode, any aerodynamic coupling between DSFC forces and other axes was removed by the flight control system. The Cornell and Boeing studies were oriented toward use of sideforce control during ground attack and a preference toward the yaw rate mode was indicated for that task. The LWA simulation evaluation was expanded to include landing approach to determine if a change in flight phase would change the preferred sideforce mode. Both modes were incorporated in the LWA simulation, and switching was provided to enable comparative evaluation of the two modes for the ground attack and landing approach runs.

One objective of the simulation was to conduct the runs in a manner to represent a realistic combat situation while maintaining sufficient control on the initial flight conditions to obtain meaningful quantitative data for comparison. To this end, discussions were held with the Air Force TAC pilots prior to the DSFC ground attack evaluation. The pilots desired a roll-in maneuver to the target which would provide them with typical target alignment tasks. Also, in view of the expected future threat, it was felt that high flight speeds would be necessary for survival.

The resultant ground attack evaluation run sequence was as follows: Each run started with a 12,000-foot range and a 12,000-foot lateral offset from the target and included a roll-in from an initial altitude of 13,000 feet at an airspeed of 400 kias. The dive angle was 45 degrees with bomb release at 4000 feet altitude and 558 kias. The depression angle of the fixed sight was set to agree with the above drop condition and thus gave the proper sight pendulum effect.

The run matrix of 30 runs summarized in Table 3-1 was performed by each pilot. The run matrix allowed comparison of the conventional flight control with combinations of the two DSFC controllers and the two DSFC modes with and without crosswind effects. The VT/SC was not used during the DSFC ground attack runs.

The objective of the DSFC ground attack evaluation was to measure and compare pointing errors and bomb miss distances based on the fixed, depressed reticle aiming system. Previous studies have shown that DSFC can effect significant improvements



Table 3-1 DSFC GROUND ATTACK EVALUATION RUN MATRIX FOR EACH PILOT

<p>● INITIAL CONDITIONS: 13,000 FEET ALTITUDE; 400 KIAS; STRAIGHT AND LEVEL</p> <p>● DROP CONDITIONS: 45-DEGREE DIVE ANGLE; 4000 FEET ALTITUDE; 558 KIAS</p>																																					
RUN NO.	1	2	3	4	5	6	7	8	9	10	11	12	13	14	15	16	17	18	19	20	21	22	23	24	25	26	27	28	29	30							
CROSSWIND																																					
● NONE	✓															✓																					
● 30 KTS																✓																✓					
DSFC CONTROLLER																																					
● RUDDER PEDALS					✓						✓											✓						✓									
● THUMB SWITCH											✓						✓											✓						✓			
DSFC MODE																																					
● NONE	✓	✓	✓																																		
● SIDESLIP, $\beta$				✓	✓	✓					✓	✓	✓				✓	✓	✓				✓	✓	✓				✓	✓	✓						
● YAW RATE, $\dot{\psi}$								✓	✓	✓						✓	✓	✓						✓	✓	✓						✓	✓	✓			

in accuracy under these conditions by removing the pendulum effect normally incurred with this type of bomb sight. This study extended these prior investigations to include evaluations of the DSFC controllers and modes.

The computed weapon impact points for each pilot are recorded in Appendix J. The impact points were calculated using vacuum ballistics from the actual release conditions existing when the pilot squeezed the bomb release trigger on the control stick. The averaged azimuth pointing errors at the time of bomb release are shown in Figure 3-6. The azimuth errors were generally small as was expected. Interest-

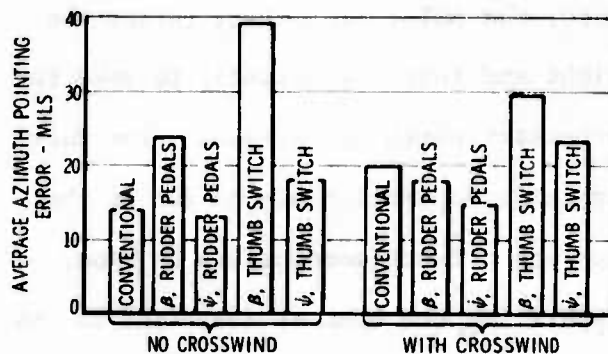


Figure 3-6 DSFC Did Not Improve Azimuth Pointing Accuracy

ingly, the effect of DSFC on azimuth errors was a marginal improvement or even a detrimental effect.

There are three factors which may have some bearing on these results. First, there may have been adequate time during the dive to make the necessary double-roll maneuvers in the conventional configuration to minimize the azimuth

pointing error. From 10 to 15 seconds were available to the pilot for the alignment task. Had this time been reduced, fewer correction maneuvers would have been possible.

Second, the initial roll-in and gross alignment correction was made by conventional control methods; for the DSFC modes, the pilot had to mentally decouple the heading and roll axes for the final tracking tasks. The pilots had a tendency to continue to make heading corrections with roll even while applying the DSFC and thus, in many cases, they did not take full advantage of the DSFC capability.

Third, the pilots did not have enough experience with DSFC to mentally define its region of operation. That is, the pilots did not know for sure how close the initial correction had to be before they could comfortably rely on the DSFC to make the final corrections. It is evident that in order to overcome these last two factors the pilots would need to participate in a more lengthy training program.

Comparisons of average elevation pointing errors are given in Figure 3-7. Use of the DSFC thumb switch controller in the yaw rate mode gave consistent improvement

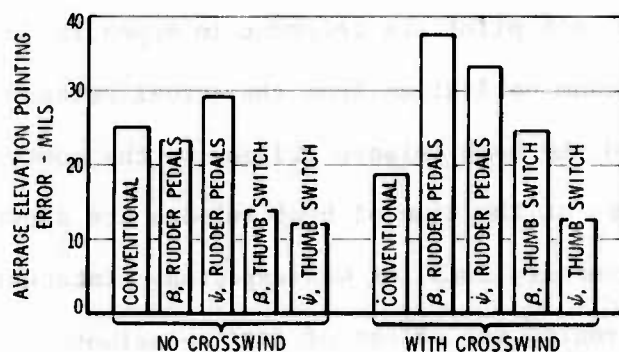


Figure 3-7 DSFC with Yaw Rate Mode and Thumb Switch Gave Consistent Improvement in Elevation Pointing Accuracy

in the elevation pointing accuracy. Apparently the pilot's ability to make the proper elevation corrections is degraded during the double roll maneuver with the sight pendulum effect. By reducing or eliminating the rolling maneuvers with DSFC, the pilot can better relate the sight and target vertically to make the necessary pitch corrections. The fact

that no improvement is shown with the rudder pedal controller may be due to the ease with which the pilots can make elevation and azimuth corrections by hand, a familiar method to them, as compared to separating the control functions to the hand for elevation and to the feet for azimuth correction.

The finding that the elevation pointing error with conventional control with the 30 knot crosswind is less than that for conventional control without crosswind was unexpected. Since the DSFC runs show the expected accuracy degradation with crosswind, it is probable that the average conventional results with crosswind are favorably biased by the relatively small sample size, i.e., nine runs.

The total effect of DSC is measured by the average weapon miss distance (Figure 3-8). This measurement reflects not only the pilot's ability to point the

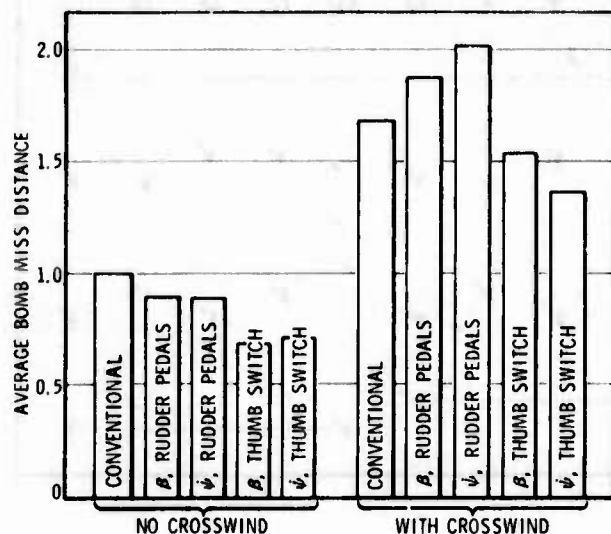


Figure 3-8 DSFC Improved Weapon Delivery Accuracy Up to 30 Percent

aircraft, but also the effect of the different pointing methods on his capability to perform the other necessary functions, i.e., attain the required dive angle, altitude, and speed for weapon release.

Although the effect of DSFC on pointing errors is not consistently good for all DSFC modes and controllers, the bomb miss distances are better for all DSFC cases with no crosswind. It appears,

therefore, that DSFC definitely improves the pilot's ability to achieve the desired angle, altitude, and speed for weapon release.

The rudder pedal controller mode appears inferior to the thumb switch controller with regard to total pilot control coordination for the target tracking task. This may be attributed to the hand/foot coordination difficulty mentioned above. When the thumb switch controller is used, the yaw rate DSFC mode appears somewhat better for both crosswind cases. For this mode, the bomb miss distance improvements with and without crosswind are approximately equal in magnitude, but the percentage improvement is less in the crosswind case.

The use of DSFC during landing was investigated during the simulation by having each pilot complete a matrix of 15 approaches wherein the effects of the DSFC controller, DSFC mode, crosswind and turbulence were evaluated (Table 3-2). The data taken during the runs consisted of time histories of the state variables. Some of the time history data obtained are included in Appendix J. The initial condition of each run was 40,000 feet from the runway with a 5-degree glide slope and a 3000-foot lateral offset to the left of the runway centerline. The pilot task in each case was to make the lateral offset correction and continue the landing

Table 3-2 DSFC LANDING APPROACH EVALUATION RUN MATRIX FOR EACH PILOT

● INITIAL CONDITIONS: 40,000 FEET RANGE; 160 KIAS; 5-DEGREE GLIDE SLOPE															
RUN NO.	1	2	3	4	5	6	7	8	9	10	11	12	13	14	15
CROSSWIND • 0 KTS • 30 KTS	✓	—	—	—	✓	✓	—	—	—	—	—	—	—	—	✓
DSFC CONTROLLER • RUDDER PEDALS • THUMB SWITCH		✓	✓	✓	✓		✓	✓	✓	✓		✓	✓	✓	✓
DSFC MODE • NONE • SIDESLIP, $\beta$ • YAW RATE, $\dot{\psi}$	✓	✓	✓	✓	✓	✓	✓	✓	✓	✓	✓	✓	✓	✓	✓
TURBULENCE • NONE • 11.4 ft/sec rms	✓	—	—	—	—	—	—	—	—	✓	✓	✓	✓	✓	✓

approach until just before touchdown. The crosswind in the problem was from the right and thus the pilot had to overcome both the lateral offset plus the crosswind to align with the runway and then he had to continue the approach while compensating for the crosswind.

Examination of the data indicates that without crosswind a smoother approach can be made with the DSFC sideslip mode engaged than with the conventional configuration (Figure 3-9). Also, it appears that the rudder pedals are preferable with the sideslip mode since the runs made with the rudder pedal are slightly smoother than those with the thumb switch and since the pilot can apparently hold the control with his feet for a longer time with less fatigue than with his thumb.

The yaw rate mode does not appear to offer any improvement since a considerable amount of roll control is still required as well as DSFC. Also, in order to make a lateral displacement correction, the pilot must leave the runway heading and fly a crosstrack until he feels he is nearing the runway centerline. With the sideslip mode, the airplane heading is maintained with that of the runway, and the pilot is given a more positive cue as to when the lateral error has been corrected.

The DSFC sideslip mode can also be used to advantage during crosswind landing to reduce roll and crab angles. The DSFC control power requirements to correct for lateral displacement plus crosswind were found to be quite high; but, if the

Airplane Initial Lateral Offset is 3000 Ft Left of Runway

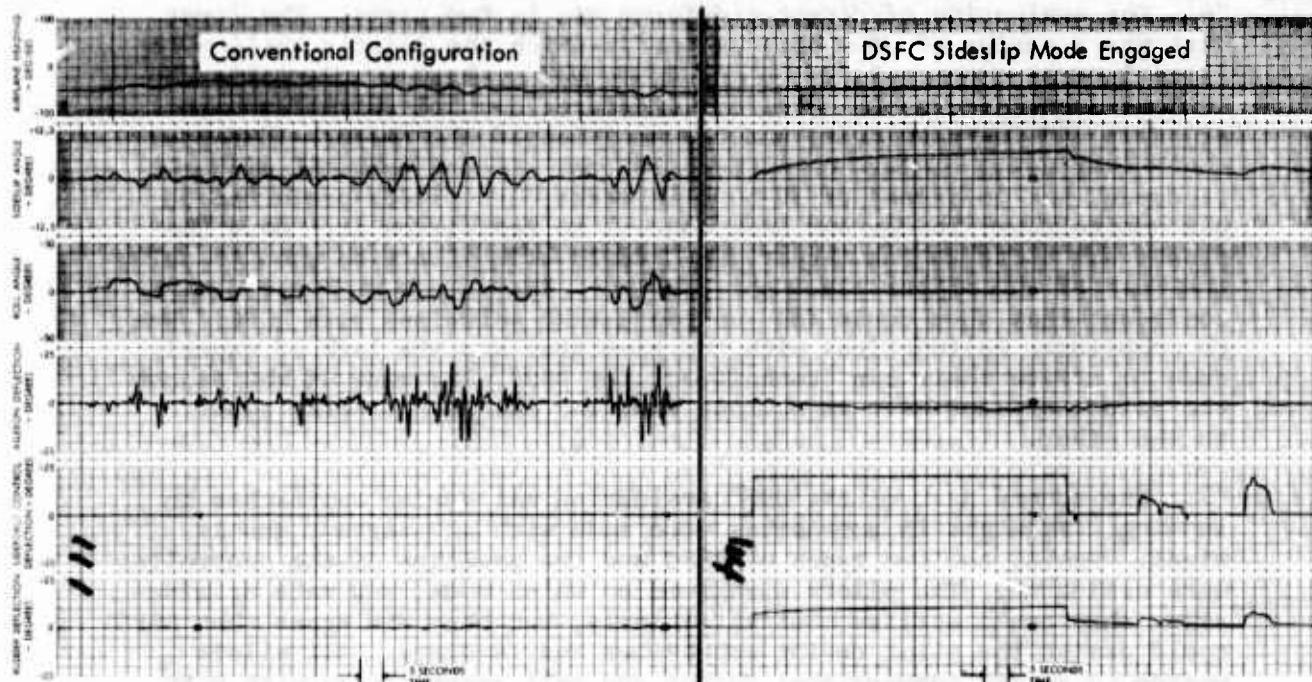


Figure 3-9 DSFC Sideslip Mode with Rudder Pedal Control Provided Smoother Approaches

initial gross lateral displacement is made by conventional techniques, the remainder of the landing problem is considerably simplified with the sideslip mode. It appears that the thumb controller gives a smoother approach than the rudder pedals with crosswind. The yaw rate mode with crosswind, as in the cases without crosswind, does not offer any improvement over the conventional configuration.

### 3.4 PILOT'S COMMENTS

The three USAF TAC pilots who participated in the ground attack simulation task were current in fighter/attack aircraft. All had recent Southeast Asia experience. A "consensus" report was prepared by the pilots, and excerpts related to the evaluations are given below. The complete report is documented in Appendix J.

"5. To evaluate powered lift, each pilot ran through a series of dive bomb passes varying roll-in airspeed, dive angle, power setting and jet flap deflection angle. Data were collected to determine the effect of the jet flap on controlling airspeed in the dive and on decreasing altitude lost during recovery. It was obvious to all pilots that the jet flap would produce somewhat of a speedbrake effect when used in the dive. Maximum utilization of the jet flap during recovery both decreased altitude lost during pullout and decreased time to establish a climb back to above 10,000 feet AGL....



"6. The evaluation of direct sideforce was in two parts. The first part was a series of dive bomb passes in which the pilot's ability to solve lateral pipper placement and drift was evaluated. Variable conditions included crosswind, direct sideforce control (DSFC) in both sideslip and yaw rate modes and the position of the direct sideforce controller using rudders or a thumb switch. If the original pipper placement was in excess of 30-50 mils error, all pilots preferred to use conventional rudder and bank control to reposition it. Once the pipper was close to the target, DSFC could effectively be used to solve the rest of the pipper placement problem. The pilots were not always confident that they could achieve consistent solutions with DSFC. Due to occasional malfunctions with the simulator and the lack of experience to create their own 'techniques' for DSFC placement of the pipper the pilots did not have an obvious feel for one method being superior to the other.

"7. The second part of the DSFC evaluation was during approaches to landing. Straight in approaches were made with and without crosswinds. Again, the two types of DSFC and the position of the controller were evaluated. The pilots disagreed on which mode, yaw rate or sideslip, they could utilize most effectively, but they did agree that DSFC could assist the pilot during approaches and landings. All pilots wanted to retain conventional rudder and roll capabilities with DSFC being an additional instead of a replacement feature. Placement of a DSFC switch on the stick was considered unwise. The control stick is the direct force type and unwanted inputs could be generated while actuating the DSFC switch with the thumb. A throttle location should be considered....

"8. Pilot comments on the mechanization of the simulation: Video field of view was too small. In side slip mode, roll was limited to less than 180 degrees. A fixed armrest for the stick arm was not equally comfortable to each pilot. Rudder force control was not the right magnitude. Using full afterburner and full jet flaps during dive recovery would overflow the computer memory.

"9. Recommendations: Further investigation into the use of powered lift and direct sideforce devices should definitely be continued. However, the advantages in maneuverability that these devices provide should be examined over the entire flight profile. The survivability and defensive ability of a ground attack aircraft should be greatly improved by the proper utilization of these devices. All pilots involved would like to see the next simulation of the LWA address the entire mission profile. The DSFC is available at only a small cost in terms of weight and complexity but provides much in the way of additional maneuverability both offensively and defensively. Incorporating powered lift would not be as cheap, but at combat airspeeds it is cheaper in terms of added weight per unit of lift than conventional aerodynamic lift.

"10. During the week, the pilots spent their free time talking with engineers from many different departments at the plant. These meetings proved to be very informative for both parties involved. All pilots felt it was extremely beneficial to have an opportunity to make operationally oriented inputs at the concept and design phase. Many engineers and their supervisors expressed themselves as hoping there would be future opportunities for dialogue directly with operational pilots. It is recommended that TFWC and TAC favorably consider any future requests from AFFDL, or the aerospace industry, that would allow operational ideas and pilots to be a part of new aircraft design at the concept and design synthesis stage."

In addition to the report quoted above, each pilot commented concerning his own evaluation. Pertinent excerpts from these personal evaluations are presented below.

#### PILOT A

"1. First, and perhaps most important, I feel that bringing the pilots into the development of a future fighter at the conceptual stage is a must. I feel that the limited inputs that were made will be invaluable and save much time and money.

"2. The Vectored-Thrust concept is extremely valuable. The present design problem with negative angle-of-attack developing on the forward canards utilizing maximum wing-burn and maximum aft-stick needs to be worked out; however, any means by which we can obtain more performance, more lift and climb out of the groundfire environment on a quicker basis is a bonus. Care must be taken in development to insure that all of the additional lift capability can be taken advantage of throughout all phases of flight, especially the critical phases such as pull-out of a dive delivery maneuver.

"3. The Direct Side-Force Control is a good concept. The advantages through many phases of flight are obvious. However, your present design does not give enough side-force velocity to be worth the cost. The objective of side-force control should be to avoid ground-fire, not to reduce pendulum-effect errors in the bombing problem. By 1981, I hope we are not working with iron-sight systems for bombing. In modern sighting systems, we do not have pendulum-effect problems, so DSFC should be approached as another addition to the maneuverability of the aircraft, and therefore making the aircraft less vulnerable.

"4. Other areas such as cockpit layout, position of control stick, the fly-by-wire concept, and many other details were discussed at length during the week I was there. These details must be evaluated by pilots before being incorporated into the finished product if we are to optimize the development cycle.

"5. It is absolutely a requirement that as this aircraft is developed further the pilots be brought in again for another evaluation. The benefits from such an evaluation should prove to be immense in terms of time and money saved."

#### PILOT B

"Powered Lift: I could tell that using (the VT/SC) flaps would allow you to roll in at higher airspeeds and power settings and still have the same airspeeds at release, but I didn't really have a feel for how this was so much greater than using regular speed brakes. No doubt on recoveries though. The effect there was loud and clear. After bomb release you can recover with less altitude lost, rotate to a climb attitude quicker, and get back to altitude much faster.

"DSFC-Bombing: I felt like I could make large corrections much easier with conventional controls, but making those last small corrections was aided by either mode. Unless I looked close I wouldn't notice the difference in pipper track using one mode versus the other. Sideslip always seemed slower. I felt like when I was making very small corrections that I'd have the control in and back out before I'd see any response.

"Rudders vs. thumb switch: I know that I'm not sure which I like but that's about all. When using yaw rate I tried to use the thumb switch like a trim button and that seemed pretty natural. Only trouble (was that) it was an off to full-on movement. If I wanted some rate less than full, I felt more sure of my degree of input using rudders. But then this ties up rudders so they aren't conventional. Now sideslip. Again, incremental application would seem best with the thumb. Only thing is I don't know how violent this would be going from off to full-on all the time. Once you're on course and want only a small input I'd rather use rudders. In any case I don't think you want the control on the stick. If you're applying only thumb power for DSFC, you're very likely to cause stick inputs. And as you attempt to change force inputs to the stick, I think it would be difficult to hold a constant position with your thumb.

"DSFC/(Landing) Approach: Sideslip must have enough control authority to compensate for whatever the maximum allowable crosswind for landing is designed to be. I could see very little difference if any at all between conventional and yaw rate. It probably would be less disrupting in actual weather to yaw rather than turn but this wasn't apparent in the simulator. To evaluate the sideslip mode I found it much quicker to yaw or turn to correct to centerline, then align my heading with course and hold that position with sideslip. Sideslip always seemed too slow for the large corrections but could hold you fine once on course. On the approaches I'd attribute any misalignments to poor visual display rather than one mode allowing me to correct to and hold centerline better than another. Holding sideforce inputs with the thumb is going to get tiresome for the 5 minutes or so of the approach. Here I'd much prefer rudders as controls. Somewhat at high speeds, but especially at approach speeds, I felt that DSFC was fighting control of the aircraft when I applied ailerons (or ailerons and rudder when control was on thumb switch) to attempt to maneuver and turn the aircraft. We can't live with this kind of control interference. I think any pilot who "felt" the DSFC trying to fight for control of his aircraft would cut it off and never turn it on again."

#### PILOT C

##### "VECTORED THRUST/POWERED LIFT

"1. Vectored lift, utilized by means of a jet flap system was evaluated with respect to dive bomb runs and landing approaches. Its value as a speed reduction device during the bombing runs was negligible during the pull out, the use of wing burner with full flaps produced excessive delta "G" however, utilizing military power until the nose was level and then selecting wing burner produced very good climb results, and considerably reduced the time required to reach 10,000 MSL.

"2. Use of vectored lift during the landing approach reduced the angle of attack required to maintain the glide path. When using full flaps, however, the aircraft tended to pitch nose down when power was applied.

##### "SIDE FORCE CONTROL STICK

"I would prefer to have the stick in the conventional position so that the aircraft can be flown with either hand.

##### "DIRECT SIDE FORCE CONTROL

"1. Both the sideslip and yaw rate modes of operation have a practical application to dive bombing. The aircraft heading or position can be changed without introducing bank into the tracking problem. Additionally,



a steady ground track can be maintained using the sideslip mode without having to place the aircraft in a crab.

"2. The effectiveness of jinking maneuvers utilizing the yaw rate and sideslip modes is difficult, if not impossible, for the pilot to determine in the simulator.

"3. In utilizing the DSFC modes, I found that using the thumb switch was easiest for me during the initial portion of the tracking problem. In the latter part of the tracking problem, the rudder pedals allowed smoother tracking than the thumb switch.

"4. In using either DSFC mode in conjunction with the rudder pedals, you lose normal rudder operation. Unless there is a compensating rudder-aileron interconnect, it becomes difficult to manually turn the aircraft.

#### "DSFC MODES ON FINAL LANDING APPROACH

"1. Sideslip and yaw rate both have practical uses in the landing approach for course correction. However, in a high crosswind condition sideslip has a limited value due to its reduced effectiveness at low airspeeds. I had trouble trying to manually turn the airplane while the sideslip mode was engaged."

### 3.5 CONCLUSIONS

Considering both the quantitative and qualitative evaluations, the VT/SC and DSFC technology concepts appear to have merit. The VT/SC quantitative evaluations were not particularly amenable to comparative analysis, but the usefulness of the improved turning capability in a ground attack mode was verified by the pilots. Also, it was demonstrated that the VT/SC capability results in considerably improved visibility during the landing approach by decreasing the airplane angle of attack. The use of VT/SC in other flight regimes should be explored through additional simulation activities. Use of a separate lever for VT/SC nozzle vector angle control was not satisfactory. A control location on the throttle is a possibility.

The DSFC offers weapon delivery accuracy improvements for fixed, depressed reticle aiming systems. The DSFC yaw rate mode, wherein the airplane heading is controlled, appears to give better delivery accuracy than the sideslip mode, wherein the airplane lateral translation is controlled. The question of DSFC benefits for a computed-solution-type delivery system could be approached with additional simulation activities.

The DSFC sideslip mode offers a significant improvement to the landing approach problem by providing the pilot with the ability to maintain runway heading while making lateral displacement corrections and/or controlling crosswind. Crosswind control may be a major criterion for sizing the sideforce control surfaces. The DSFC yaw rate mode does not appear to offer any improvement over conventional landing techniques. The preference of different DSFC modes during different airplane flight phases introduces the possibility of multimode DSFC operation available for selection by the pilot.

No clear preference was given by the pilots to either of the two DSFC controllers investigated. They did favor retention of rudder control capability rather than replacement of rudder control for sideforce control, since they do, at times, command rudder during maneuvering. The thumb switch provides good pitch/heading coordination and remains as a candidate controller. However, when used on a fixed, force-sensing control stick, the thumb switch commands can be inadvertently transmitted into the roll channel of the control stick.

## SECTION 4

### SURVIVABILITY SIMULATION

The objective of the survivability simulation was to evaluate the effect of maneuverability on aircraft survivability in the presence of an anti-aircraft artillery (AAA) threat. The evaluation included man-in-the-loop simulation of an advanced radar-controlled, 23-millimeter gun and an aircraft flying both maneuvering and nonmaneuvering flight profiles. The two advanced technologies of interest for the LWA aircraft, Vectored Thrust/Supercirculation (VT/SC) and Direct Sideforce (DSFC), were utilized for maneuver augmentation.

#### 4.1 SIMULATION SETUP

The flight profiles employed in the survivability simulation had been recorded during the man-in-the-loop ground attack simulation of the LWA Configuration 29 (see Figure 3-1) and provided a "man-against-man" situation for the study. The survivability simulation was accomplished by use of the Air Force Electronic Warfare Evaluation Simulator (AF-EWES) located at Convair's Fort Worth facility.

The AF-EWES was configured to simulate a generic AAA fire control radar with associated 23-millimeter gun and projectiles. One 23-millimeter four-barrel gun was simulated. Gun pointing dynamics were assumed identical for all barrels. It

Table 4-1 GUN AND PROJECTILE PERFORMANCE CHARACTERISTICS

PARAMETER	VALUE OR TYPE
● GUN	
NUMBER OF BARRELS	4
RATE OF FIRE, PRACTICAL (RDS/MIN/BARREL)	325
LIMITS (DEG)	
TRAVERSE	360
ELEVATION	0 TO 85
RATES, TRACK (DEG/SEC)	
TRAVERSE, MAXIMUM	80
ELEVATION, MAXIMUM	45
● PROJECTILE	
CALIBER (MM)	23
WEIGHT, API-T (LB)	0.419
FUZE TYPE	POINT DETONATING
RANGE, TACTICAL, MAXIMUM WITH RADAR (FT)	7800
MUZZLE VELOCITY, API-T (FT/SEC)	3052

was also assumed that gravity was the only force acting upon the projectiles. The dispersion of the four-barrel gun was defined as  $\pm 5$  milliradians. Performance characteristics of the gun and projectiles are delineated in Table 4-1.

In order to simulate an advanced technology AAA threat appropriate to the operational time period of the LWA, the linear prediction approach common to present-day fire control directions was

replaced by quadratic prediction. The quadratic prediction circuits and equations are given in Appendix K.

In order for the gun to fire, the following requirements had to be met: (1) the predicted slant range from the radar site to the target aircraft had to be equal to or less than 9800 feet, (2) the elevation angle of the gun barrels had to be equal to or between the limits of 0 and 85 degrees, and (3) the radar operators had to depress a FIRE switch and hold it in the depressed position as long as the radar tracking was satisfactory. Engagements were terminated either (1) after the target aircraft reached an outbound slant range of 12,000 feet from the AAA site or (2) at the end of the particular run.

An aircraft radar cross section of 14dB relative to a 1 square meter cross section (dBsm) was simulated and remained constant throughout an engagement. Scintillation was included on the skin echo return with peak amplitude variations of  $\pm 9$  decibels and a Gaussian frequency distribution after being filtered through a 1-hertz, low-pass filter.

Confidence tests were performed each day on (1) the AAA radar, (2) the AAA digital computer equipment, and (3) the completely integrated AF-EWES AAA system. Control runs were dispersed throughout the test program in order to maintain continuous confidence in the validity of the simulation. In these control runs, the target aircraft was flown along a nonmaneuvering path with an offset of 0.5 nautical mile, an altitude of 5000 feet, and speeds of 400 and 600 knots.

## 4.2 AIRCRAFT MANEUVERS

### 4.2.1 FLIGHT PROFILES

The flight profiles of interest for the survivability evaluation are of two types: penetration and weapon delivery. The penetration profiles investigated ranged from (1) nonmaneuvering, straight and level flight to (2) gentle S-weave turning at constant altitude to (3) hard jinking with altitude changes. Each penetration profile type was flown at two speeds, 400 and 600 kias.

The nonmaneuvering and S-weave profiles were flown using only conventional controls. The jinking penetrations were made with conventional controls and also with VT/SC and DSFC. The penetration profile matrix is given in Table 4-2.

The survivability evaluation for weapon delivery called for each pilot to make three high maneuverability runs in which the AAA site was the target. The initial conditions and drop conditions for these runs were the same as those used for the weapon delivery runs discussed in Section 3; however, the pilots applied DSFC and VT/SC first for evasive maneuver augmentation and then applied DSFC in the terminal tracking phase to help align the target. The nature of these weapon delivery runs is indicated by the time history of a typical profile as shown in Figure 4-1.

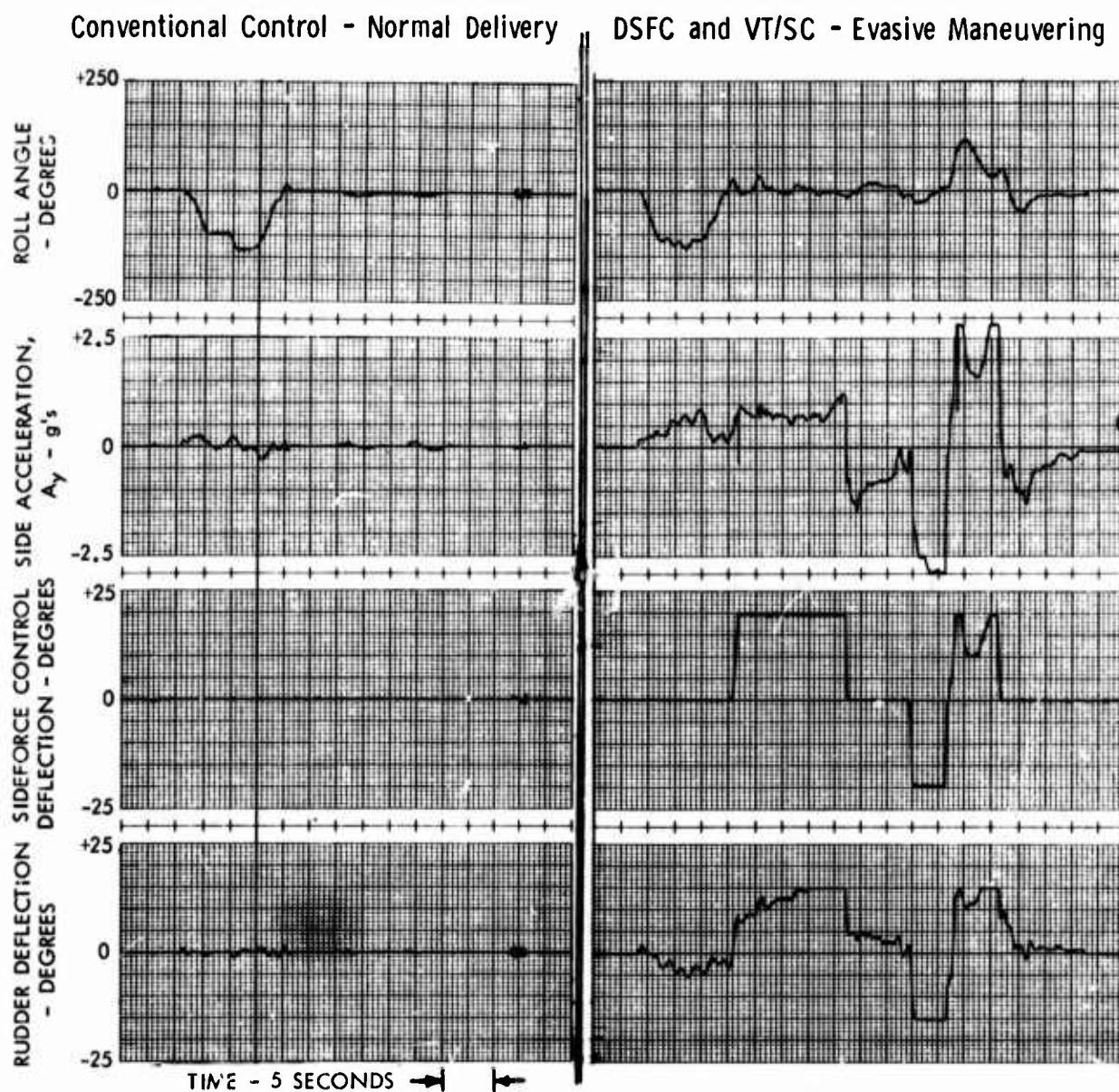


Figure 4-1 Weapon Delivery Profile Comparison Shows Typical Evasive Maneuver Using VT/SC and DSFC

Table 4-2 PENETRATION PROFILE MATRIX

	SPEED	
	400 kias	600 kias
NON-MANEUVERING (Straight and Level Flight)	a	a
S-WEAVE ( $\pm 20^\circ$ Heading Change, $30^\circ$ - $40^\circ$ Bank, Constant Altitude)	a	a
JINKING ( $\pm 60^\circ$ Heading Change, $60^\circ$ - $90^\circ$ Bank, +3000' to -1000' Altitude Changes)	a, b	a, b

<sup>a</sup> LWA CONFIGURATION 29 WITH CONVENTIONAL CONTROLS

<sup>b</sup> LWA CONFIGURATION 29 WITH VT/SC AND DSFC

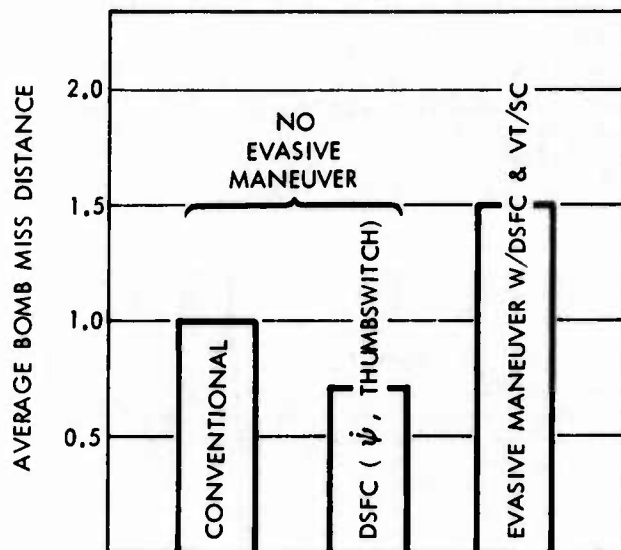


Figure 4-2 Effect of Survivability Maneuvers on Weapon Delivery Accuracy

#### 4.2.2 WEAPON DELIVERY ACCURACY

The effect of the evasive maneuvers on weapon delivery accuracy is of interest, and miss distances were calculated for the nine high maneuverability weapon delivery runs. Average miss distance comparisons are shown in Figure 4-2.

The accuracy degradation compared to the conventional control case is only moderate. This is attributable to the DSFC capability which allows rapid alignment of the aircraft.

#### 4.3 SURVIVABILITY EVALUATIONS

The initial data output of the survivability simulation consists of projectile miss distances and total rounds fired. These data are presented in Appendix K. The evaluation of aircraft survivability was made from these firing data by calculating kill probabilities ( $P_K$ ) by use of

a statistical model, which is described in Appendix K.

Two measures of kill probability were obtained, a 1-minute  $P_K$  and a 5-minute  $P_K$ . The 1-minute data ( $P_{KK}$ ) are based on a crew or engine kill which disables the aircraft within 1 minute. The 5-minute kill ( $P_{KA}$ ) is based on the additional possibility of aircraft disability due to fuel leakage.

##### 4.3.1 PENETRATION SIMULATIONS

The survivability evaluations of the penetration simulations are shown in Table 4-3. The 1-minute kill probabilities  $P_{KK}$  are very low in all cases. Significant points to be made from the 5-minute kill probabilities are as follows:



Table 4-3 PROBABILITY OF AAA KILLING AIRCRAFT

TEST COND NO.	CONTROL MODE	MANEUVER	INITIAL POSITION				NO. OF DATA RUNS	PROBABILITY OF KILL <sup>4</sup>	
			OFFSET <sup>1</sup> (N.MI.)	ALTITUDE (FT)	SLANT RANGE (N.MI.)	SPEED (KT)		P <sub>KK</sub>	P <sub>KA</sub>
4	CONVENTIONAL	NONE	-0.5	1000	4.0	400	3	0.0524	0.9999
5			-1.0				3	0.0209	0.9923
6			-0.5	5000			8	0.0385	0.9993
7			-1.0				3	0.0124	0.9401
AVERAGE								0.0332	0.9877
8	CONVENTIONAL	NONE	-0.5	1000	4.0	600	3	0.0331	0.9984
9			-1.0				3	0.0220	0.9912
10			-0.5	5000			3	0.0093	0.8426
11			-1.0				3	0.0133	0.9041
AVERAGE								0.0194	0.9341
12	CONVENTIONAL	S-WEAVE <sup>2</sup>	-0.5	1000	4.0	400	5	0.0037	0.5504
13			-1.0				5	0.0022	0.4613
14			-0.5	5000			5	0.0000	0.0040
15			-1.0				5	0.0002	0.0545
AVERAGE								0.0015	0.2677
16	CONVENTIONAL	S-WEAVE	-2.0	1000	4.0	600	5	0.0042	0.6275
17			-1.5				5	0.0066	0.6835
18			-1.5	5000			5	0.0001	0.0176
19			-1.0				5	0.0000	0.0000
AVERAGE								0.0027	0.3322
20	CONVENTIONAL	JINK <sup>3</sup>	-0.5	1000	4.0	400	5	0.0000	0.0000
21			-1.0				5	0.0000	0.0000
22			-0.5	5000			5	0.0000	0.0000
23			0				7	0.0000	0.0090
AVERAGE								0.0000	0.0029
24	CONVENTIONAL	JINK	0.5	1500	4.0	600	6	0.0000	0.0000
25			0.25				5	0.0000	0.0000
26			0.5	5000			7	0.0000	0.0000
27								0.0000	0.0000
AVERAGE								0.0000	0.0000
28	VT/SC AND DSFC	JINK	-0.5	1000	4.0	400	5	0.0000	0.0000
29			0				5	0.0000	0.0000
30			-0.5	5000			6	0.0001	0.0258
31			0				5	0.0004	0.0733
AVERAGE								0.0001	0.0248
32	VT/SC AND DSFC	JINK	-1.5	1000	4.0	600	6	0.0000	0.0000
33			-1.0				5	0.0000	0.0000
34			-1.5	5000			5	0.0000	0.0000
35			-1.0				6	0.0000	0.0000
AVERAGE								0.0000	0.0000

## NOTES:

1. Negative offset means the aircraft approaches with the AAA site on the left.
2. Aircraft heading was changed approximately  $\pm 20^\circ$  using  $30^\circ$ - $40^\circ$  bank while maintaining altitude.
3. Aircraft heading was changed approximately  $\pm 60^\circ$  using  $60^\circ$ - $90^\circ$  bank with about +3000, -1000 altitude variation.
4. P<sub>KK</sub> - One minute P<sub>K</sub>  
P<sub>KA</sub> - Five minute P<sub>K</sub> (involves fuel tank vulnerability) See Appendix K.

1. The AAA achieves a 0.9 to 1.0 average  $P_{KA}$  against a nonmaneuvering target. Increasing speed from 400 to 600 kias results in only a small  $P_K$  reduction. The relatively low  $P_K$  for Run Condition 10 is apparently an anomaly due to the limited sample size rather than the specific aircraft flight profile.
2. The  $P_{KA}$ 's for the S-weave profiles are decreased from those of the nonmaneuvering case by an order of 3 to 4. The  $P_K$ 's are lower for the 400 kias profiles than for those at 600 kias. This is attributable to the more pronounced flight path displacements resulting from the lower turn radii at the lower speed. (It is noted that the  $P_K$ 's for this gentle maneuvering profile would be virtually zero if the current-day AAA threats had been simulated using linear predictions rather than a quadratic predictor.)
3. Jinking reduces the AAA kill probability for the quadratic prediction gun considered here to virtually zero. The use of VT/SC and DSFC is not necessary to achieve this result. When jinking flights were flown directly toward the AAA site so that the relative motions between aircraft and gun were reduced, some non-0  $P_K$ 's were obtained.

#### 4.3.2 WEAPON DELIVERY SIMULATIONS

The weapon delivery flight profiles which were evaluated for survivability included (1) conventional controls and normal delivery, (2) DSFC and VT/SC and normal delivery, and (3) DSFC and VT/SC and initial evasive maneuvers. The initial offset distance and altitude were 2 nautical miles and 13,000 feet in all cases. The AAA site was located at the target point.

Nineteen data runs were made and all resulted in 0  $P_K$ 's. This result is a consequence of the roll-in maneuver used to close out the initial offset. The AAA tracking system did not recover from the initial prediction transient in time to achieve kill prior to weapon release and aircraft pull-out.



#### 4.4 CONCLUSIONS

Maneuverability is an effective counter to an advanced quadratic-prediction-type AAA. In a one-on-one situation, hard jinking will probably be necessary to achieve an acceptable level of survivability against future AAA threats. Although VT/SC and DSFC offer additional dimensions of maneuverability, it is not apparent that they will materially affect survivability; however, they can possibly reduce degradation of the pilot's performance of other tasks while he is performing survivability maneuvers.

It should be noted that in this study only one type of threat having an assumed level of advanced technology has been considered. Consideration of other threats such as the various types of surface-to-air missiles or different advanced AAA might result in a survivability distinction between jinking with conventional controls and jinking with DSFC and VT/SC.

A P P E N D I X    A  
T E C H N O L O G Y    A N D    O P E R A T I O N S  
A S S E S S M E N T

The LWA program is directed toward evolution of a weapon system which embodies new approaches to aircraft design and operations. The program does not include synthesis of conventional configurations to meet conventional requirements.

Present and future technologies and operational requirements were assessed early in the program. Knowledge gained from this assessment, supplemented by additional development and analysis as appropriate, has been used to examine the potential performance of integrated, advanced/emerging technology LWA configurations in relation to postulated environments. Important aspects of the technology and operations assessment activities are discussed below.

A.1    TECHNOLOGY ASSESSMENT

A.1.1    AERODYNAMICS

The LWA aerodynamic assessment has centered on achieving the following fighter characteristics:

- o Superior instantaneous and sustained maneuver capability during ground attack and in air-to-air combat
- o High longitudinal acceleration and maximum speed
- o STOL capability.

A number of advanced/emerging aerodynamic concepts offer potential for the improvement of future close air support aircraft. These concepts include

- o Powered Lift
- o Spanwise Blowing

- o Supercritical wing
- o Close-coupled canard
- o Wing-body integrated design.

#### A.1.1.1 Powered Lift

The fighter characteristics listed above lead to high thrust-to-weight airplanes with wings of advanced design. These configuration trends can conceivably result in an advantage for powered lift concepts.

The simplest form of powered lift is the vectored-thrust concept. This arrangement provides STOL performance and increased maneuver capability at low speeds (Figure A-1).

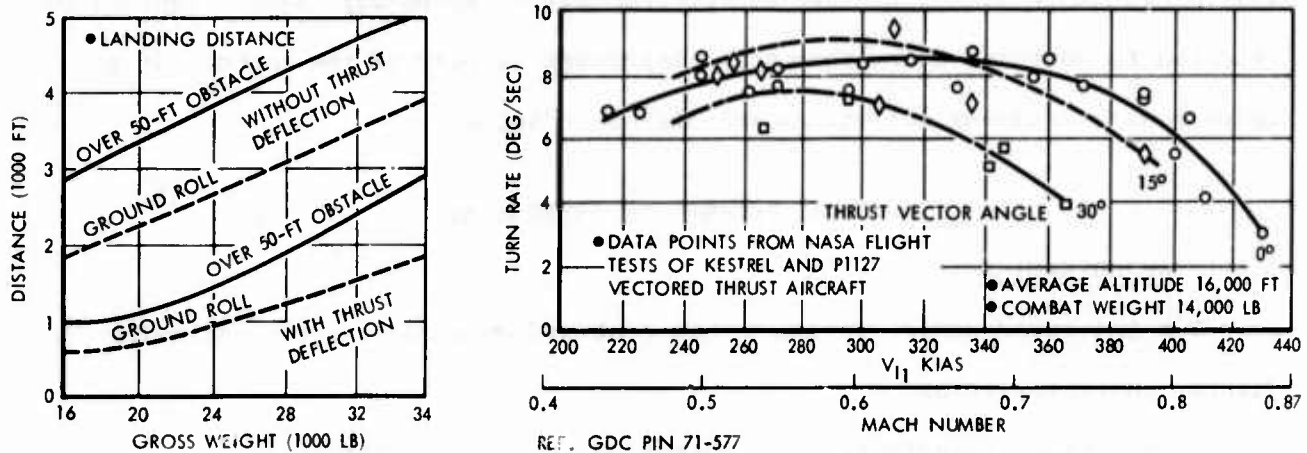


Figure A-1 Vectored Thrust Can Decrease Landing Distance and Increase Turn Rate

The direct aerodynamic problems due to vectoring thrust can be solved, but thrust moment balancing, engine-out performance, and safety requirements can heavily influence a vectored-thrust aircraft configuration.

A new concept for obtaining the benefit of vectored thrust and at the same time augmenting the wing lift is the NASA vectored thrust with supercirculation (VT/SC) concept.<sup>1</sup> In this concept, the engine nozzles are placed at the trailing edge of the wing; when vectoring is applied, the jet induces a large additional circulation on the wing (Figure A-2). NASA is continuing tests of this concept, which holds promise.

<sup>1</sup> Corson, B. W., Jr., Capone, F. J., and Putman, L. E., Lift Induced on a Swept Wing by a Two-Dimensional Partial-Span Deflected Jet at Mach Numbers from .20 to 1.30, NASA TM X-2309, August 1971.

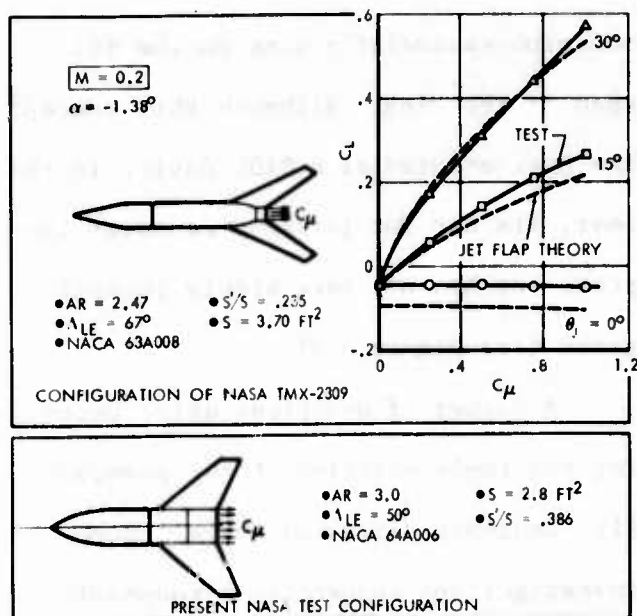


Figure A-2 NASA Tests of Vectored Thrust with Supercirculation

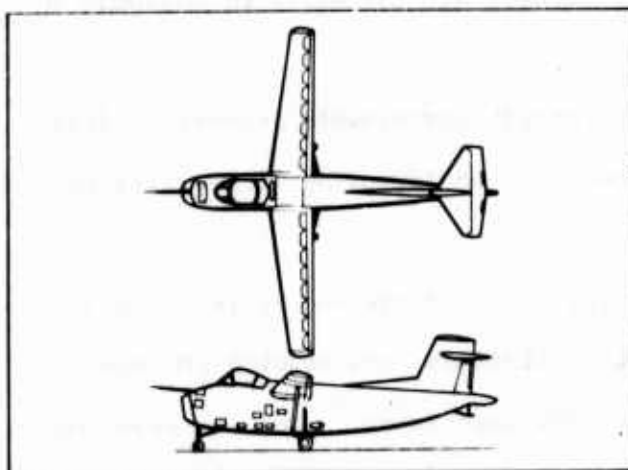


Figure A-3 A Jet-Flap Aircraft - The Hunting H.126

Another powered-lift concept of interest is the external blown flap. As in the case of the vectored thrust with supercirculation, the internal ducting problems of the jet flap are eliminated; in addition, the external blown flap can produce full-span performance. This concept results in a larger lift than the other concepts because the full engine

because of the large lift gain. The VT/SC is achieved by use of a partial-span jet flap of large momentum.

The jet flap has a long test history, and large lift gains have been demonstrated, but these usually impose considerable thrust penalties due to internal ducting losses in the wing and external losses aft of the nozzles. The jet flap airplane shown in Figure A-3 suffered considerable losses of this type because of the use of large amounts of hot, low pressure turbine-exhaust air. Continuing improvements in propulsion technology and recent work on jet flaps at high speeds with small momentum coefficients show promise (Figure A-4).<sup>1,2</sup>

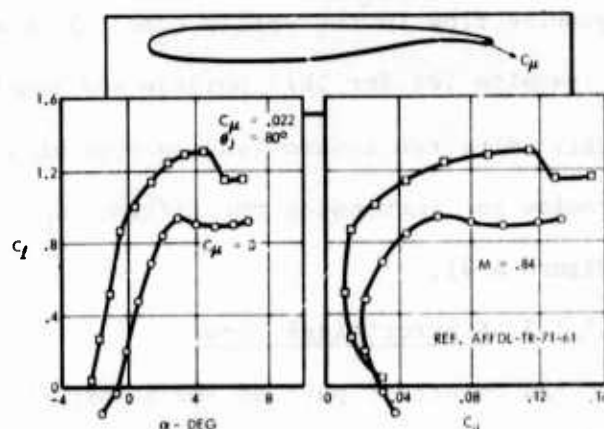


Figure A-4 Convair Test Data on Transonic Jet Flaps

<sup>1</sup> Yoshihara, H., Zonars, D., and Caster, W., High Reynolds Number Transonic Performance of Advanced Planar Airfoils with Jet Flaps, AFFDL-TR-71-61, June 1971.

<sup>2</sup> Grahame, W. E., and Headley, J. W., Jet Flap Investigation at Transonic Speeds, AFFDL-TR-69-117, February 1970.

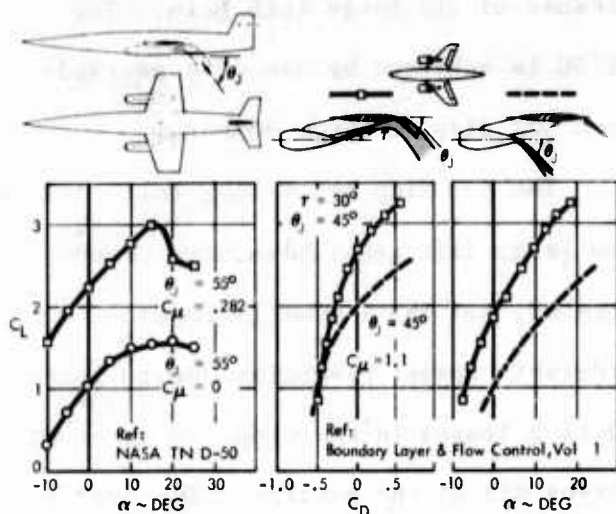


Figure A-5 Fighter-Type Configurations Have Been Tested with External Blown Flaps

momentum essentially acts on the full span of the wing. Although this concept has been studied as a STOL device in the past, its use for inflight maneuver improvement has not been widely investigated (see Figure A-5).

A number of questions arise concerning the implementation of the powered-lift concepts discussed above. Some investigations concerning aerodynamic and other aspects of the problem have

been made to support the LWA program. These studies are discussed in Appendix B.

#### A.1.1.2 Spanwise Blowing

Another concept for enhancing wing lift through aerodynamic/propulsion integration has been considered. This concept is based on improving vortex lift on wings rather than direct lift augmentation.

The stability and strength of a vortex system are increased by inducing a spanwise flow in the vortex core. Several investigators have studied the use of a spanwise jet for this purpose and benefits have been found.<sup>1</sup> Convair Aerospace tests, directed toward leading edge blowing indicate that this concept offers promise for increasing the lifting capability of surfaces in separated flow (Figure A-6).

#### A.1.1.3 Supercritical Wing

An important part of the industry's continuing intensive transonic wing design effort is the supercritical wing as proposed by NASA. The increases in usable subsonic lift available with the supercritical wing through buffet postponement and

<sup>1</sup> Dixon, C. J., Analysis of Experimental Force Data for Lift Augmentation by Spanwise Blowing Over Trailing-Edge Flaps and Aircraft Control Surfaces, Report ERR-11190, Lockheed-Georgia Company, September 30, 1971.

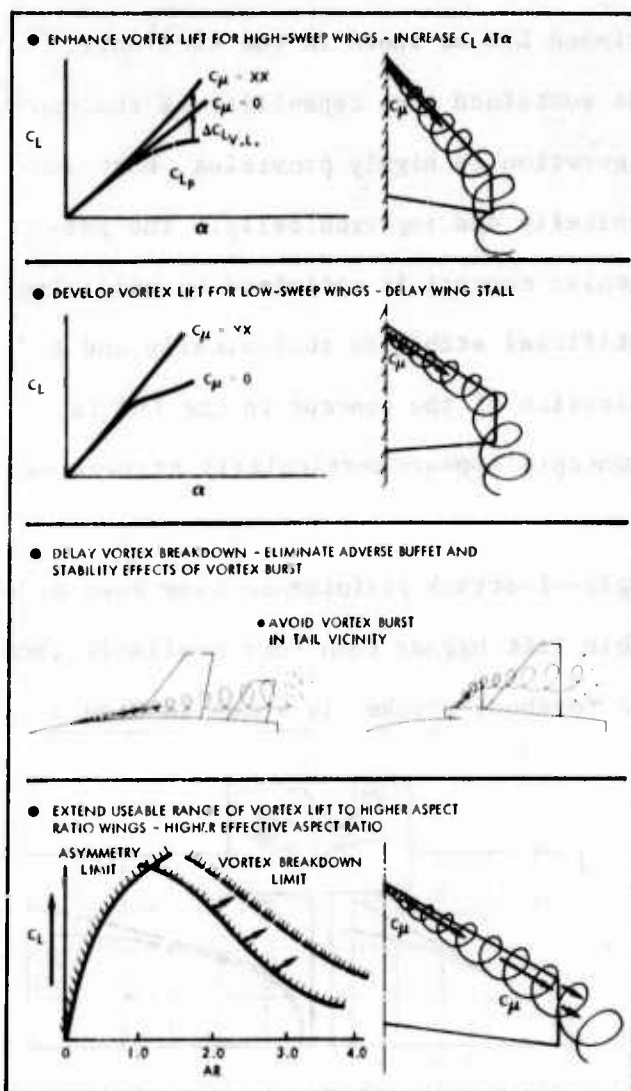


Figure A-6 Potential Benefits of Spanwise Blowing

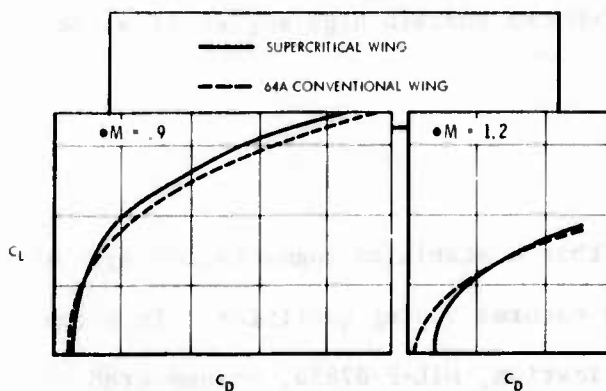


Figure A-7 The Supercritical Wing can Improve Transonic Maneuver Performance

the thicker sections possible through its drag-rise delay can be important to the transonic close air support fighter.

Supersonically, it is not desirable to use thick wing sections, however, and a different approach is required. Recent test data comparing fighter wings with supercritical and 64A sections are shown in Figure A-7. While the supercritical wing is 50 percent thicker, permitting a higher aspect ratio, the drag at transonic maneuver is lower than that of the 64A wing, even though the latter wing is equipped with a variable-deflection leading-edge flap. At supersonic speeds the sustained maneuvering lift coefficients of the two wings are similar. With the supercritical design shown, however, supersonic acceleration is reduced.

#### A.1.1.4 Close-Coupled Canard

Convair studies of fighters have for many years included canard configurations. Recently, however, tests have validated a close-coupled configuration which has negligible-to-favorable interference between canard and wing (Figure A-8).<sup>1</sup> The addition of the canard in the optimum location increased the subsonic and supersonic

<sup>1</sup> Tyler, S. P., Summary Report of Wind Tunnel Tests of a Scale Model of the General Dynamics Convair Delta-Canard Airplane With Bifurcated Inlets, TN-72-SP-02, February 1972.

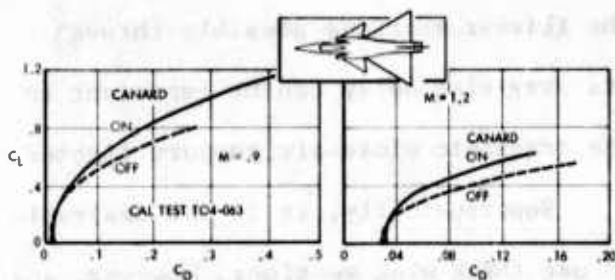


Figure A-8 Canvair Tests Have Verified Favorable Interference for a Close-Coupled Canard-Delta

trimmed L/D as shown in the test data.

The sustained turn capability of the configuration is highly promising, both subsonically and supersonically. The particular concept is optimized by utilizing artificial stability subsonically and a

fixed canard trim supersonically. The application of the concept to the LWA is promising. Integration with powered lift concepts appears particularly attractive.

#### A.1.1.5 Wing-Body Integrated Design

Recent improvements in fighter high-angle-of-attack performance have been made by the design of wing-bodies to develop usable lift higher than that available from the wing alone. One approach of this type, a forebody strake, is shown in Figure A-9. The effect of this design feature is shown as a significant increase in lift and L/D at high angles of attack. A benefit not shown in the lift and drag is a stabilizing influence on the lateral-directional characteristics at high angles. Such devices can extend the load factor capability of high-thrust aircraft which can sustain high angles of attack in turns.

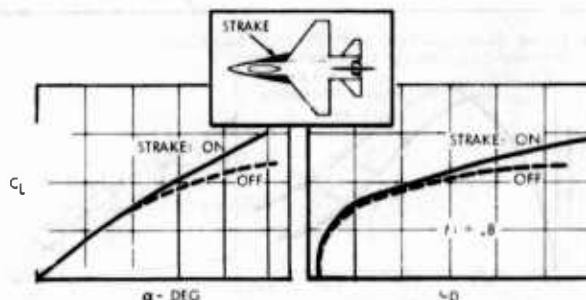


Figure A-9 Wing-Body Design Integration can Improve L/D at High Angles of Attack

#### A.1.2 FLIGHT CONTROL TECHNOLOGY ASSESSMENT

##### A.1.2.1 Control Configured Vehicle

Modern fighter aircraft are designed so that a stability augmentation system (SAS) is usually required to supplement their natural flying qualities. In accordance with military handling qualities specification, MIL-F-8785B, unaugmented aircraft are required to have dynamic and static stability of sufficient magnitude to allow the pilot to fly safely without use of the SAS. With the recent increase in reliability of flight control electronics, wherein the probability of unaugmented flight can be virtually eliminated, the requirement for unaugmented static stability can be relaxed to the point where the unaugmented airframe may be



statically unstable at some flight conditions. This relaxation leads to potential performance improvements through the use of control configured vehicle (CCV) concepts. Increased performance is obtained by allowing lower control surface trim deflections (lower trim drag) and lower tail loads which permits an overall reduction of airplane weight (Figure A-10).

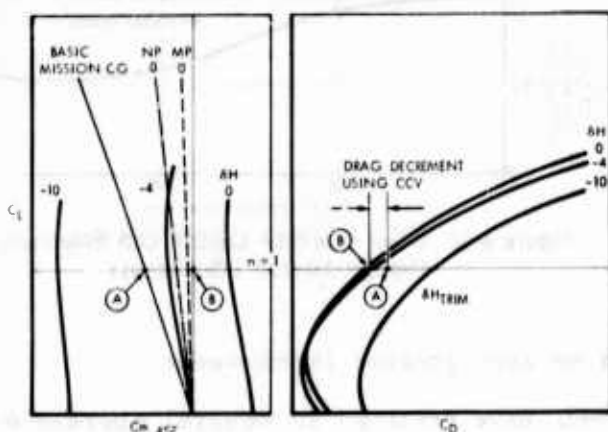


Figure A-10 Cruise Drag Reduction Through CCV

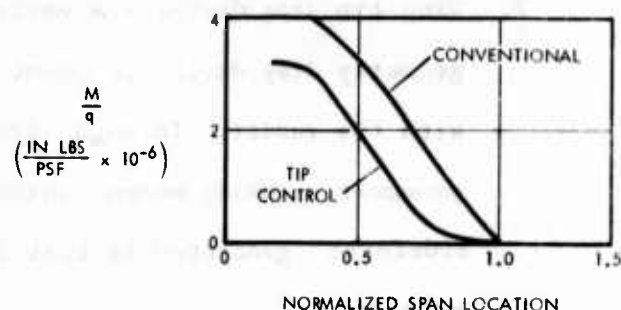
Criteria for the reduced static stability concepts have been developed.<sup>1</sup> Minimum criteria for pitch, roll, and yaw control power, duty cycle, and response time for CCV have been investigated, and these concepts are currently being used by Convair for longitudinal control of the USAF YF-16. The use of CCV in the design of the LWA will

potentially result in performance enhancement.

#### A.1.2.2 Maneuver Load Control

Attention has recently been focused on use of inboard trailing edge or tip controls to change the wing spanwise loading in order to reduce wing bending moment and/or optimize the drag polar. As a typical example, in a study of maneuver load control (MLC) using wing tip control, the spanwise bending moment is shown in Figure A-11 for an aspect ratio 6.7 wing at a design load condition. Use of MLC reduces the spanwise moments, as shown, for the same design condition. These smaller root bending moments can result in lighter structure and higher performance aircraft. Figure A-11 Maneuver Load Control Can Reduce Weight

The use of MLC can permit use of a higher-than normal aspect ratio wing to obtain the associated increased range performance, while at the same time allowing the



<sup>1</sup>"Control Power Criteria and Requirements for Control Configured Vehicles," Convair Report ERR-FW-1265, 31 December 1971.



wing to react structurally during maneuver as a low aspect ratio wing. Thus, the usual high aspect ratio wing structural weight penalty is avoided.

#### A.1.2.3 Direct Sideforce Control

Much attention has been devoted recently to the use of direct sideforce control (DSFC) for improving flight path control. Such control is seen as a significant improvement in the pilot's ability to perform such tasks as air-to-ground weapon delivery, inflight refueling, and short field landing. The type of improvement possible for a particular tracking task is shown in Figure A-12.<sup>1</sup> Use of

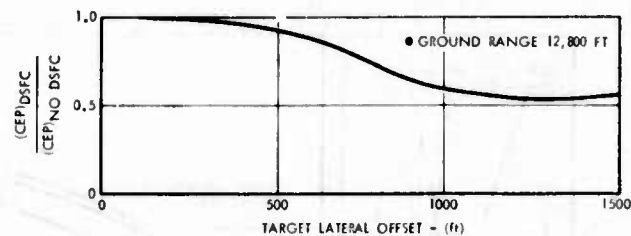


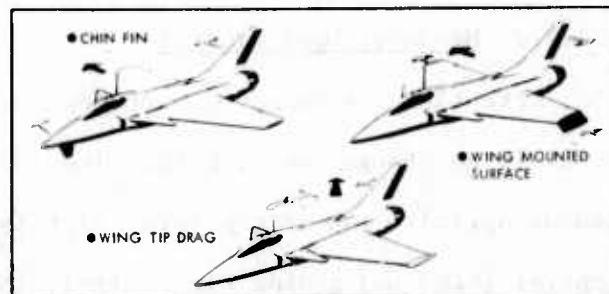
Figure A-12 Direct Sideforce Control Can Potentially Improve Aircraft Effectiveness

DSFC in conjunction with CCV may result in an even greater improvement.

Current programs for development of DSFC have resulted in several approaches.

1. Chin Fin - Sideforce is obtained from a forward located surface which is used in conjunction with the rudder. Both surfaces yield a sideforce.

The roll and yaw moments are minimized by proper location of the surface and by proper ratioing of the surface deflection with the rudder.



Proposed Approaches for DSC

2. Wing tip drag device - A variable geometry drag device is mounted on each wing tip and used in conjunction with the rudder. Through asymmetric actuation, the drag at one wing tip produces a yawing moment which is balanced by a rudder deflection. The sideforce generated is that from the rudder. This method normally has high drag.
3. Wing-mounted sideforce surface - This device, when deflected, yields a sideforce directly. The yaw and roll moments caused by this deflection are minimized by use of ailerons and rudder.

<sup>1</sup> An Investigation of Direct Sideforce Control on Improving Maneuver Capability of Attack Aircraft, The Boeing Company Report D180-4004-1, October 1971.

Cornell Aeronautical Laboratories (CAL) has implemented the second approach in a T-33 and demonstrated validity of the concept. Pilots adapted readily to the new technique. The CAL system was pointed toward weapon delivery. The chin-fin concept was investigated recently by Boeing.<sup>1</sup>

#### A.1.2.4 Gust Alleviation and Active Flutter Suppression

Configurations designed to obtain high aerodynamic efficiency in conjunction with low structural weight can result in surface flutter. Reduction of flutter by redistribution of mass properties, increased stiffness, or modified aerodynamic configuration can result in performance penalties. Flutter suppression by means of automatic flight control systems may be less demanding in terms of weight, power requirements, and drag penalties.

Current development has lead to the flight evaluation of the load alleviation mode stabilization (LAMS) on the B-52. The use of LAMS will result in longer fatigue life (i.e., extended service life for present aircraft) or higher load levels for the same fatigue life and better ride control for crew comfort. The NASA is also pursuing techniques which lead to incorporation of active flutter suppression as an integral part of the configuration design.

In a recent Convair study on advanced transport technology, significant weight reduction was shown through (1) use of controls which condition maneuver loads and (2) provision of the required stiffness through use of composite materials. It

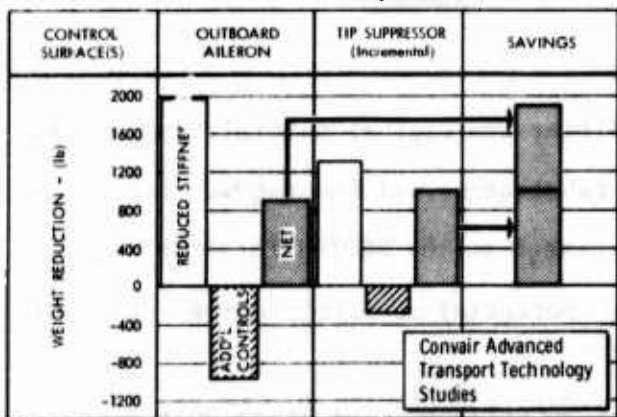


Figure A-13 Active Flutter Suppression Can Save Weight

was found that potential net weight savings from use of active control flutter suppression can be as much as 1800 pounds for this type of aircraft (Figure A-13).

Use of an active ride control system for the LWA can be an asset in that it can reduce pilot fatigue and provide a smoother platform for low-level

<sup>1</sup> Ibid.

attack where turbulence is a significant parameter. Use of control for maneuver and gust load alleviation can also result in a tangible weight saving for the LWA.

#### A.1.2.5 Fly-By-Wire/Multiplexing

The concept of fly-by-wire (FBW) consists of transmitting pilot inputs entirely electrically to the control surfaces rather than with a completely mechanical flight control system. Evolution of FBW to aircraft application has taken many years, and the Convair YF-16 will be the first aircraft with a pure FBW system. The principal advantage in the use of FBW lies in the area of weight saving, increased reliability, maintainability, and survivability. For the LWA, the latter three elements are predominant.

A method of further increasing the efficiency of an FBW flight control system is multiplexing. Multiplexing reduces the total wire count required for FBW by transmitting all flight control signals for each redundant branch on one pair of wires.

Convair recently completed a contract for FDL to prove the applicability of multiplexing to FBW by designing and fabricating an operational breadboard.<sup>1</sup> The investigation also showed benefits from multiplexing in weight decrement, increased reliability, and ease of maintenance (Figure A-14).

Convair and FDL have developed airworthy hardware to demonstrate in actual flight the digital multiplexing concept developed in the initial study. The design, fabrication and testing of this hardware is complete, and the equipment has been tested on the NC131H Total Inflight Simulator (TIFS) aircraft. The weight saving potential of multiplexing applied to

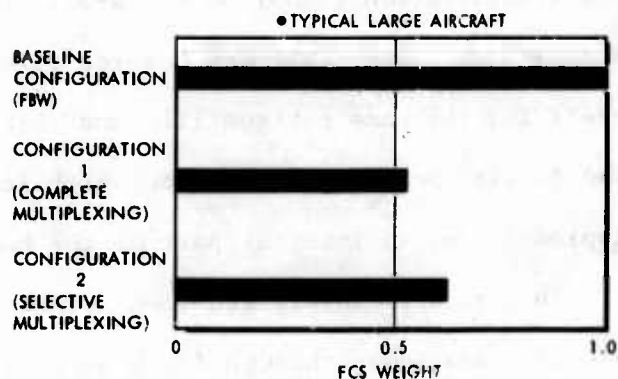


Figure A-14 Multiplexing can Reduce Flight Control System Weight

<sup>1</sup>"Research into Definition and Demonstration of an Optimum Solid State Switching and Multiplexing System For Use On A Fly-By-Wire Flight Control System," AFFDL TR-70-80, June 1970.

the LWA is probably small. However, there are potential advantages in the areas of easier maintenance, increased survivability, and increased reliability.

### A.1.3 PROPULSION TECHNOLOGY ASSESSMENT

#### A.1.3.1 Conventional Gas Generator Cycles

The Airframe/Propulsion System Integration (APSI) and the Advanced Technology Gas Generator (ATEGG) programs sponsored by the Air Force Flight Dynamics Laboratory (AFFDL) and Air Force Aero-Propulsion Laboratory (AFAPL) are continually improving gas generator technology, including the technology to integrate the airframe and propulsion system into a compatible unit.

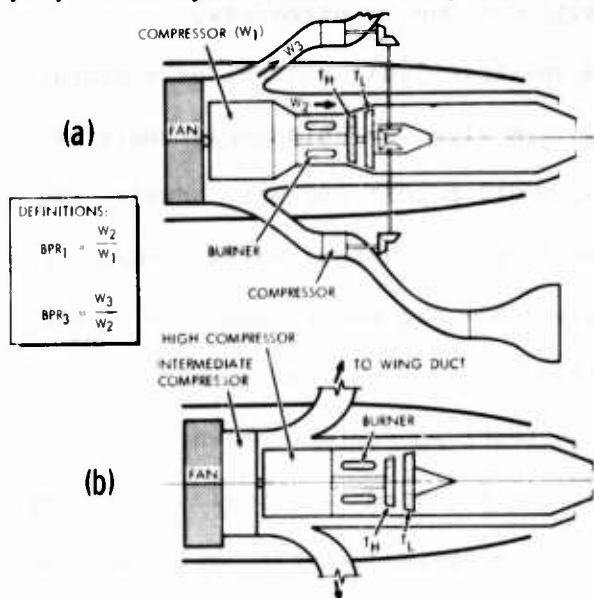


Figure A-15 Possible Cycle Arrangements for Powered Lift Concepts

The possible application to the LWA of jet flaps which require high pressure, relatively cool gas suggests somewhat unconventional cycle arrangements. The two cycle arrangements depicted in Figure A-15 supply air for jet flap applications and also partially decouple the jet flap requirements from the basic mission requirements as far as cycle selection is concerned.

Good cycle performance from such arrangements requires high turbine inlet temperature and high overall compressor pressure ratio. Predicted trends for these parameters are shown in Figures A-16 and A-17. The ATEGG program appears to be providing adequate technology to assure excellent engine performance for the LWA.

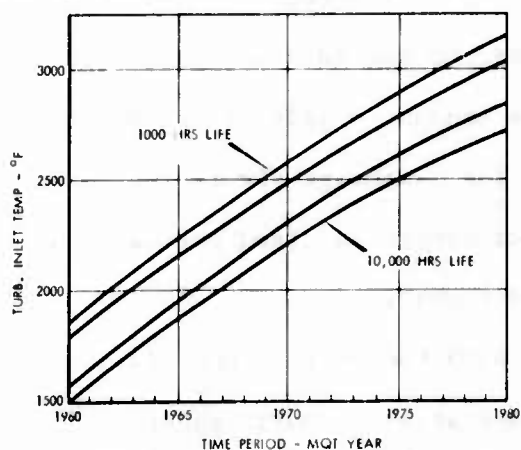


Figure A-16 Allowable Turbine Inlet Temperature Continues to Increase

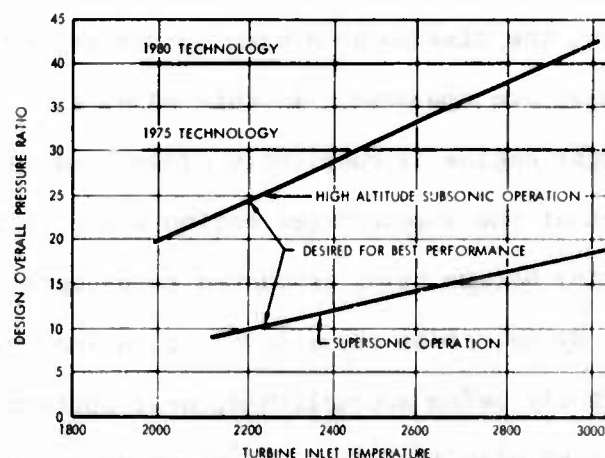


Figure A-17 Compressor Technology is not a Limitation

#### A.1.3.2 Supercharged Gas Generator Cycles

The best currently available engine for subsonic cruise operation is the high-bypass ratio, high-compression ratio, unaugmented turbofan. However, for airplanes that must also perform supersonic cruise, make short takeoffs, and provide high levels of specific excess power at selected flight conditions, the engine cycle must be severely compromised. Bypass ratio and compression ratio must be reduced and augmentation by duct heating or afterburning must be incorporated in order to achieve the best propulsion system consistent with mission requirements.

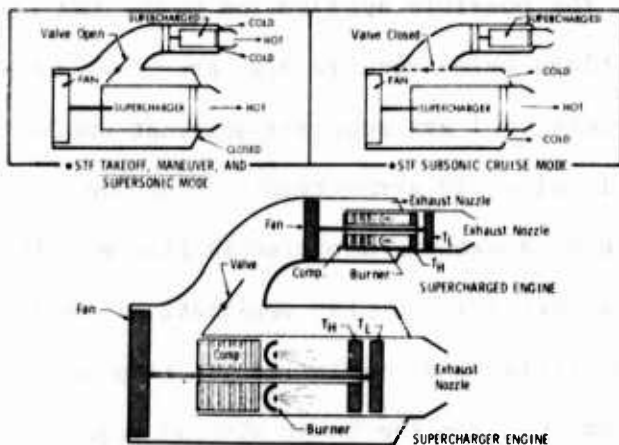


Figure A-18 Supercharged Turbofan (STF) Engine Concept

A variable-cycle engine, or a propulsion system with variable-cycle characteristics, would permit operation during the various flight phases with less compromise to performance and might result in further reduction in airplane size. The supercharged turbofan (STF) powerplant shown in Figure A-18 can be operated to produce performance similar to a variable-cycle engine without

requiring the large variations in internal engine geometry normally associated with variable-cycle engine approaches.

During subsonic cruise, the supercharged engine is turned off and isolated; and the high-bypass ratio, high-compression ratio supercharger engine is operated alone to provide near optimum subsonic cruise engine performance. At other times during the mission when high thrust is needed to perform the task at hand, both engines are operated. In this mode, the fan stream exhaust nozzle of the supercharger engine is completely closed and all of its fan discharge air is fed to the inlet of the supercharged engine where it is further compressed (and partially heated) before being exhausted to produce increased thrust.

By selecting the mode of operation compatible with the part of the mission currently being accomplished, near optimum engine and airplane performance can be achieved with the STF power plant during each part of the mission. Constraints on

physical arrangement and consideration of propulsion system weight may reduce the advantage that appears to result from consideration of the STF.

The discussion of the STF presented above concerns thrust/drag matching for conventional flight. The supercharged air available from the STF may be advantageously used for other purposes. These include blowing flaps for lift control, vectoring for high- and low-speed maneuvers, and pitch and roll control during low speed flight.

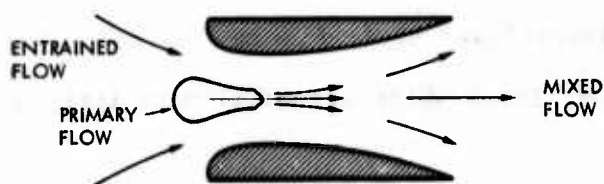
#### A.1.1.3.3 Propulsion Flight Control Force Management System

In order to attain near optimum performance and overall airframe/engine compatibility, an integrated engine/inlet/aircraft flight control system may be desirable. There is a current effort within the AFAPL to develop the design requirements for such a control system.

#### A.1.1.3.4 Cold Thrust Augmentation

The cold thrust augmentation (CTA) concept is of interest as a method to increase propulsive capacity of a given engine under some flight conditions. The CTA technique makes use of engine exhaust and/or bleed air as the primary flow for a series of high-efficiency ejector systems in wings, flaps, canards, etc. The primary flow from the engine source entrains external (cold) flow with the resulting thrust being significantly greater than that of the primary flow alone.

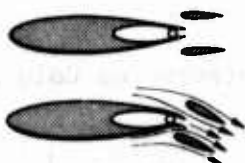
Augmentation ratios of approximately 2.0 are theoretically attainable.



Cold Thrust Augmentation Concept



EJECTOR WING



EJECTOR FLAP

CTA Applications

The CTA concept has been highly developed in recent work of the USAF Aerospace Research Laboratory (ARL). The bulk of the ARL work has been directed toward ejector wings applied to V/STOL aircraft. The type of CTA application which appears best suited for the LWA is an ejector flap.

The ejector flap is desirable, because the ejector wing loses its



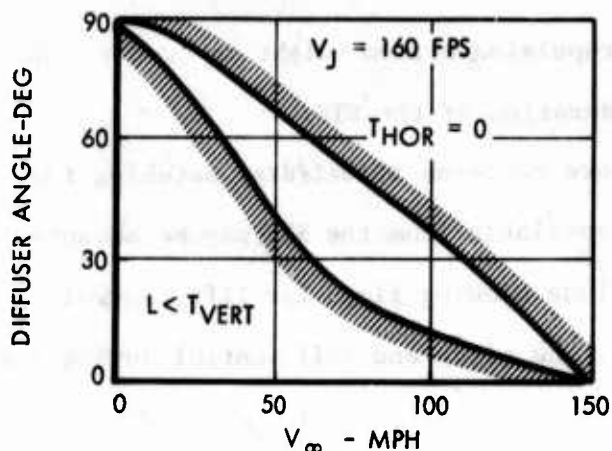
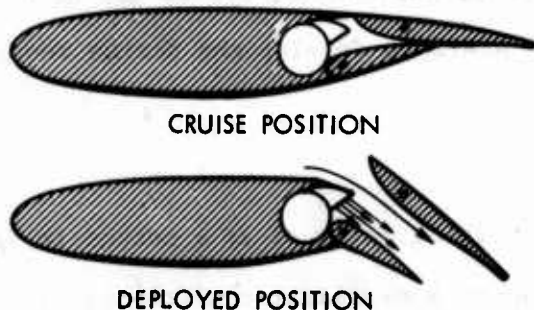


Figure A-19 USAF ARL Cold Thrust Augmentation Transition Corridor



Thick S/C Airfoil could be Advantageous

effectiveness rapidly with an appreciable forward velocity (Figure A-19).<sup>1</sup> Used in conjunction with powered lift concept, CTA can result in benefits to the LWA in the form of (1) increased time on target without aircraft attitude changes, (2) improved low-speed maneuverability for target access, (3) improved evasive capability by virtue of large speed variations, and (4) improved dispersal provided by increased STOL capabilities.

The possibility of obtaining an efficient CTA ejector flap is problematical. The relatively thick supercritical airfoil sections which can provide additional area for ducting and mechanisms while maintain-

ing good cruise characteristics might offer some advantages in this regard.

#### A.1.4 STRUCTURES TECHNOLOGY ASSESSMENT

The revolutionary approaches of current structural design concepts, with advanced composites in particular, amplify the importance of advanced structures to the LWA. It is important to note that the LWA structures investigations are complemented by other advanced technology investigations.<sup>2</sup> Figure A-20 contains a listing of the advanced structures technology items which are of primary interest.

##### A.1.4.1 Advanced Composites Technology

Filamentary materials--primarily graphite and boron fibers impregnated with epoxy, polyimide, or aluminum--have been established as having great potential for

<sup>1</sup>"USAF Aerospace Research Laboratory Presentation on Cold Thrust Augmentation," Unnumbered Charts, 13 April 1972.

<sup>2</sup>"Conceptual Design of Advanced Composite Airframe and Propulsion System," USAFML Contract F33615-72-C-424.



- COMPOSITES TECHNOLOGY
  - Application to Airframes
  - System and Subsystems
  - Producibility
  - Design Criteria
- CONFIGURABLE AERODYNAMIC SURFACES
- VULNERABILITY
  - Metal Structures
  - Composite Structures
- STRUCTURAL TRANSPARENCIES
- AIR CUSHION LANDING GEAR
- STRUCTURAL/FLIGHT CONTROL INTEGRATION
  - Load Alleviation
  - Flutter Suppression
  - Reduced Static Margins
- MAINTAINABILITY

Figure A-20 LWA Structural Technology Items

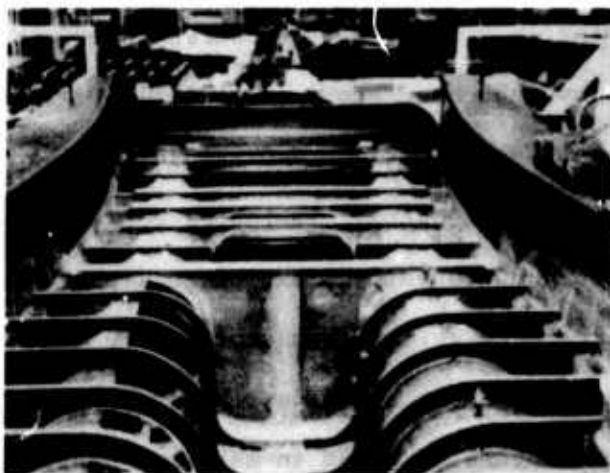


Figure A-21 Convair's F-5 Composites Fuselage, An Example of the Structural Complexity Reached with Composites

increasing the structural performance of aircraft. To date approximately 100 programs have been initiated for aircraft structure, propulsion, missile, and space system components. These programs, conducted on a composite substitution for metal basis, have reflected weight savings from 5 to 54 percent. An example of the structural complexity reached with composites is the F-5 composite fuselage currently being completed at Convair. Extensive information into the detailed designs of major aircraft components has been gained in this program.

Increased payoffs are possible by considering composites at the initiation of the design studies when the higher structural efficiencies could be reinvested in increased performance, range, payload, or operating economy. Examination of certain configuration "shape" parameters

(range, maneuverability, speed, etc.) readily shows that performance is enhanced when the greater composite material structural efficiency is, at least partially, used to enhance the aerodynamic efficiency. For example, composites used to increase the wing aspect ratio instead of only reducing gross weight can produce the effect on range shown in Figure A-22. For a particular aircraft configuration, the direct substitution of composites for aluminum yields a 5 percent increase in range while the optimum composite wing aspect ratio increases the range 20 percent over that of the metal wing.

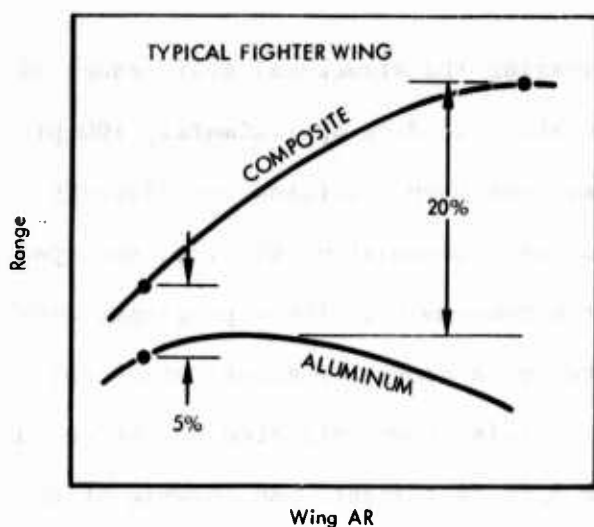


Figure A-22 Advanced Composites Impact Both Performance and Configuration

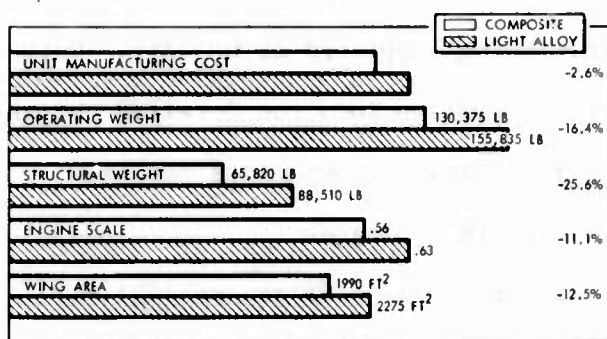


Figure A-23 Benefits of Advanced Composite Airframe on M .90-Cruise Advanced Transport

Ultimately, the extent to which composites are used for the LWA will be based on the overall cost and performance which include a consideration of the synergistic effects discussed above. An example of the total impact (cost, weight, etc.) of composites on an advanced technology transport airplane is shown in Figure A-23.

**A.1.4.1.1 Composites Design Criteria Development.** Advanced composites exhibit significant differences in material performance when compared to metals. Basic laminates without stress concentrates (holes, notches, etc.) show little degradation due to fatigue and retain high residual strengths. Laminates containing stress concentrations exhibit a significant

loss in static strength but retain the excellent fatigue behavior of the basic laminate. In addition, many structural laminates exhibit linear stress-strain behavior to failure as opposed to the nonlinear response observed in metals. Consideration of factors such as these suggests that the traditional design criteria used in metals may not be suitable for efficient and reliable design in composites.

Convair is actively pursuing a criteria approach in which reliability is the design goal. It is believed that structural reliability cannot be guaranteed simply in terms of design allowables for the basic material and conventional design factors for safety. A more desirable approach is to determine design safety factors as a function of design complexity (basic laminates, number of joints, etc.), the intended usage of the structure, and the number of structures to be built.

A.1.4.1.2 Composites Application. The use of composites in aircraft influences design, fabrication, and cost. A detailed discussion of the application of advanced composite materials to fighter aircraft structure is contained in Appendix C.

The use of composites in aircraft systems and subsystems that are not considered part of the airframe structure or propulsion systems is also potentially beneficial. Most approaches to utilizing composites in systems and subsystems are oriented toward weight savings. An example of potential composite usage in hydraulic systems is shown in Figure A-24.

TYPICAL COMPONENTS	% OF COMPONENT WITH COMPOSITE APPLICATION POTENTIAL	NATURE OF COMPOSITES APPLICATION	DESIGN BENEFIT EXPECTED IN ADDITION TO WEIGHT SAVINGS	EST. SAVING IN COMPOSITE COMPONENT WEIGHT %
PUMPS	20	RODS, (CONTINUOUS) CASE (MOLDED + WRAPS)		20
FILTERS	50	HOUSING (MOLDED + WRAPS)		20
ACCUMULATORS	75	MOLDED + WRAPS, METAL REINFORCED		20
RIGID TUBING	75	TAPE WRAPPED GRAPHITE-EPOXY	LOW THERMAL EXPANSION (FEWER BELLOWS) LESS INSULATION	50
REGULATORS	50	MOLDED CASE, SHEET DIAGRAM	BETTER HIGH G TOLERANCE	20
ACTUATORS	75	MOLDED + TAPE WRAPS		30

Figure A-24 Advantages of Advanced Composites Applied to Hydraulic Systems

In some cases, the nature of composites manufacturing can simplify subsystem installation. For example, uncured composite tubing could be routed through the aircraft structure and subsequently cured in place by pumping hot gas through the tubing, thereby eliminating many fittings and

tube bending operations. Another example is that composites can eliminate the necessity for expansion joints in environmental control systems because of their low thermal expansion coefficients.

#### A.1.4.2 Configurable Aerodynamic Surfaces

The effective use of composites in structures usually results in a structure with vastly different stiffnesses in the orthogonal directions, at any particular point in that structure. This effect significantly contributes to the high structural efficiency obtainable with composites but also suggests a means of increasing the aerodynamic performance by controlling the surface contour. Two types of control surfaces are shown in Figure A-25.

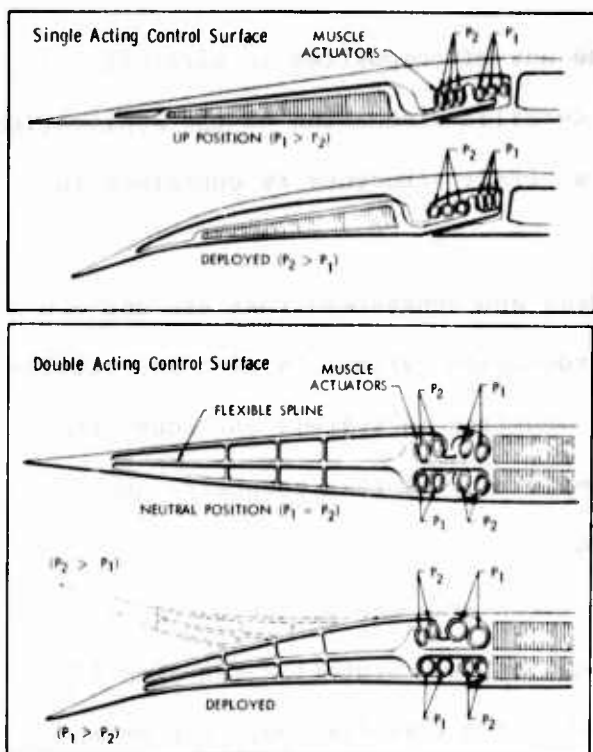


Figure A-25 Flexible Control Surfaces Incorporating Continuous Actuators

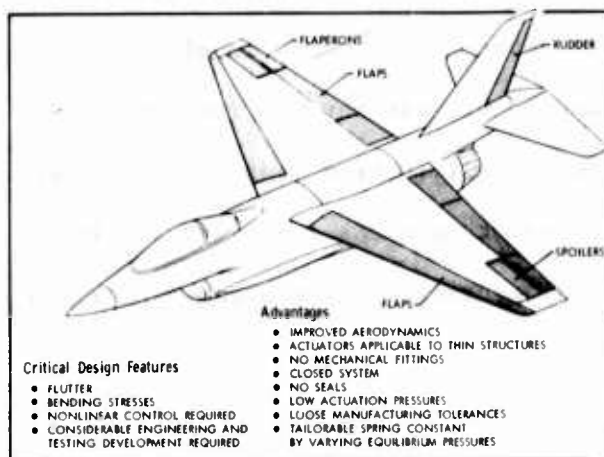


Figure A-26 Flexible Structures Applied to Aerodynamic Surfaces

Studies are continuing to establish the design limits of flexible structures. Depending on the total aerodynamic and system effectiveness, the principle can be extended to large percentages of wing and stabilizer surfaces and to the air-flow control functions of such systems as the environmental control and engine inlet systems. Figure A-26 is an illustration of possible areas for application of flexible structures.

#### A.1.4.3 Vulnerability

Reduction in aircraft vulnerability to combat damage and the increased reliability requirements of advanced aircraft has generated interest in fail-safe structures. Metal and advanced composite damage tolerant structures are currently being studied.

Advances in metal design are principally related to (1) structures designed for fracture control using fracture

mechanics during the design process and

(2) the development of metals with better fracture characteristics. Recent experience and advanced studies have led to the formulation of new design concepts (Figure A-27).

One of the potentially beneficial features of composite materials is the broad range of performance characteristics that can be realized with proper laminate design. A technique of fabricating a laminate with crack-arresting capability is demonstrated by the model shown in Figure A-28. A crack will arrest as it enters

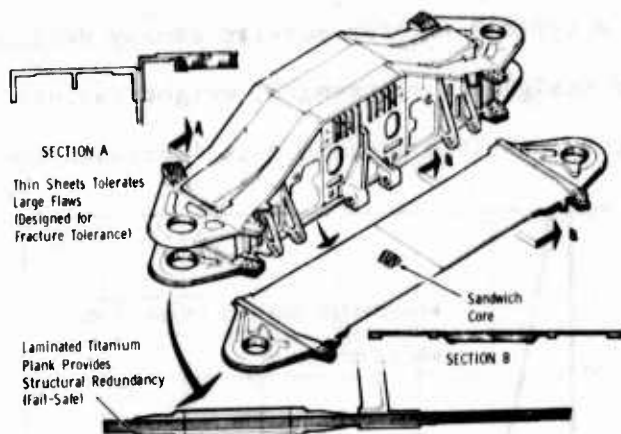


Figure A-27 Laminated Titanium Wing Carry-through Structure Designed for Damage Tolerance

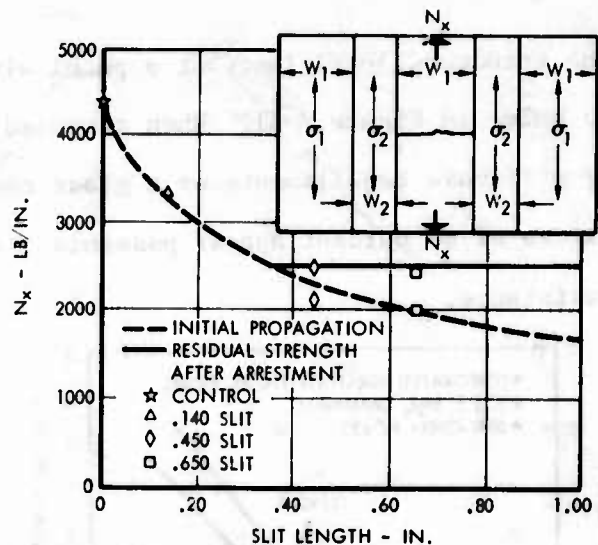


Figure A-28 Fail-Safe Design Concept for Advanced Composite Panels

the low modulus strips providing the stress in the strips is sufficiently below the critical stress required for propagation in the buffer material. The feasibility of the arrestment concept has been demonstrated in static tests of tensile specimens.

#### A.1.4.4 Structural Transparencies

In viewing perforated composite panels fabricated for acoustic treatment studies, it was noticed that there was little image distortion of objects viewed through the panel. This gave rise to an idea of using perforated panels sealed with a transparent film as a structural transparency.

The use of transparencies with high structural efficiency could decrease the weight of typical transparencies such as canopies and improve the maintainability of aircraft systems by permitting visual inspection of avionic components, accessory drive system oil levels, and environmental control equipment (Figure A-29). Access panels would receive less use and in some cases could be eliminated.

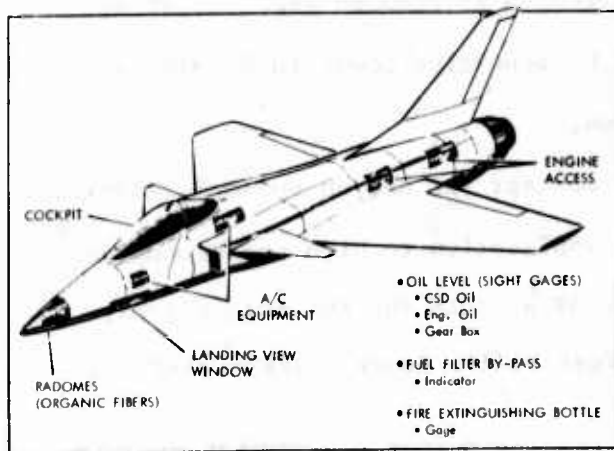


Figure A-29 Transparent Structure Potential Uses

For a particular composite panel where the hole diameter is equal to the panel thickness, the panel weight increase with increasing load is shown in Figure A-30.

The structural efficiency of a panel with holes is compared to that of a panel with no holes in Figure A-31. When compared to a typical fighter acrylic canopy designed by stiffness requirements or a glass canopy designed for strength, weight savings in excess of 60 percent appear possible. Another possible advantage is increased impact resistance.

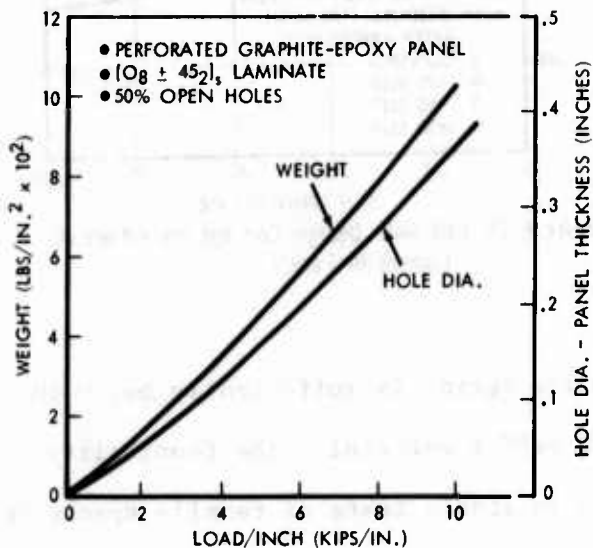


Figure A-30 Transparent Structure Load Capacity and Weight

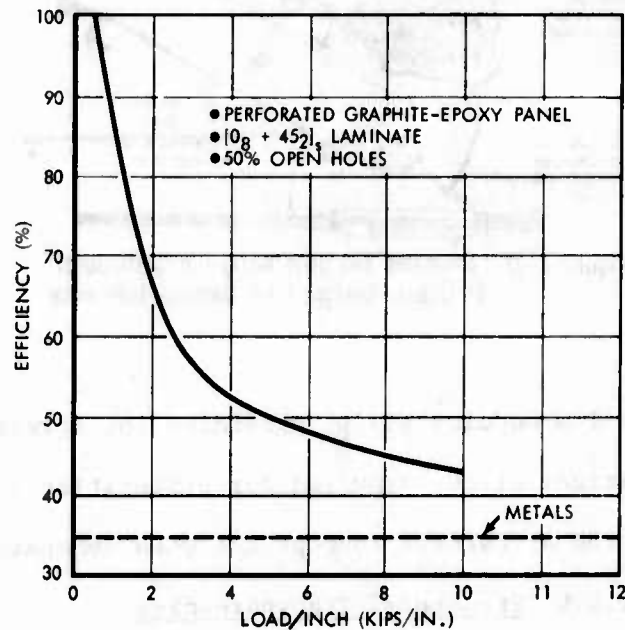


Figure A-31 Transparent Structure Efficiency

#### A.1.4.5 Air Cushion Landing System

An air cushion landing system (ACLS) replaces the aircraft wheel gear with an annular jet air cushion. The objective in considering the ACLS for LWA aircraft is to improve takeoff and landing performance. Potential takeoff and landing advantages are associated with crosswind capability, low footprint pressure, fast retraction, high energy absorption and damping, and improved braking. Any potential weight savings with this system are related directly to reduced gear weight and indirectly to aircraft structure weight. Weight penalties occur in ducting and power plant modification to provide the airflow.

Previous studies have validated the ACLS concept for use on subsonic aircraft, and studies are continuing to investigate its application to high performance aircraft.<sup>1,2</sup> To provide a preliminary assessment of an ACLS for the LWA, a system

<sup>1</sup>Earl, T. Desmond, "Air Cushion Landing Gear Feasibility Study," AFFDL-TR-67-32, May 1967.

<sup>2</sup>Diggs, K. H., and Perez, D. J., "Air Cushion Landing System for STOL Aircraft," V/STOL Technical and Planning Conference, Las Vegas, 25 September 1969.



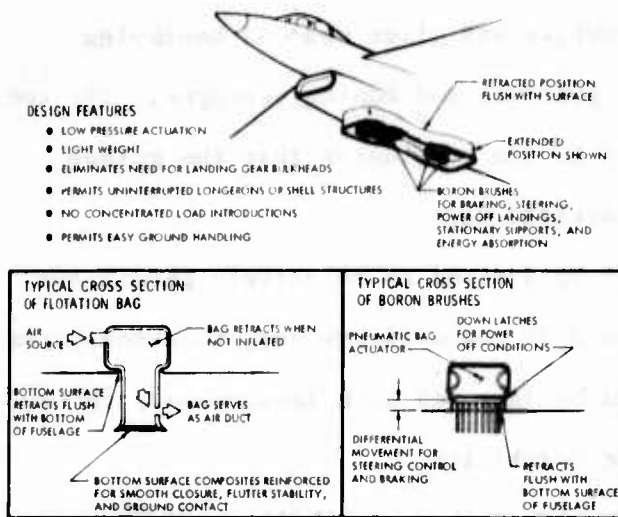


Figure A-32 Air Flotation System with Brush Braking and Steering

similar to the one shown in Figure A-32 has been investigated. In this concept a rigid panel is integrated with the curtain to function as a door during the normal flight and as a skid during the touchdown phase of the landing. Braking and steering control is provided by advanced composite brushes.

The wear characteristics of advanced composites under these conditions remain to be evaluated, but since remarkable wear

characteristics have been found between graphite-epoxy and unlubricated steel, advanced composites may have potential advantages over rubber pads in this area.<sup>1</sup> The preliminary assessment of this ACLS indicates that power requirements are acceptable, a reasonable combination of cushion parameters is available to permit sink rates near 15 ft/sec without imposing unduly high structural loads, and lighter fuselage and gear weights are possible.

#### A.1.5 ARMAMENT/AVIONICS

The accurate delivery of weapons in the presence of the severe threat environment forecasted for future tactical targets imposes demands on aircraft performance and requirements for advanced weapons and avionics that can significantly impact aircraft configurations. The advanced and emerging weapons and avionics concepts which were considered in the LWA configuration development are discussed below.

##### A.1.5.1 Advanced Weapon Technology

Target characteristics together with weapon delivery accuracies set the requirement for ordnance type and size and weapon guidance and control. The advantage of improved accuracy and available technology have led to the accelerated

<sup>1</sup>Berg, C. A., Bartra, S., and Tirosh, J., "Wear and Friction of Two Different Types of Graphite Fiber Reinforced Composite Materials," Dept. of Mech. Engr., Univ. of Mech. Engr., M.I.T., Faculty of Mech. Engr., The Technion (Israel Institute of Technology Haifa, Israel, 1971.



development and/or consideration of guided powered and glide weapons employing radar, electro-optical (EO), and radiometric guidance and homing concepts. The success to date and improvements envisioned lead to the conclusion that the guided weapons will be heavily employed in future tactical wars.

The use of free fall weapons will likely be limited to relatively permissive threat environments and area targets. Accuracy in the delivery and, therefore, the utility of free fall bombs can be expected to be improved with improvements in navigation, target acquisition, and aircraft maneuverability.

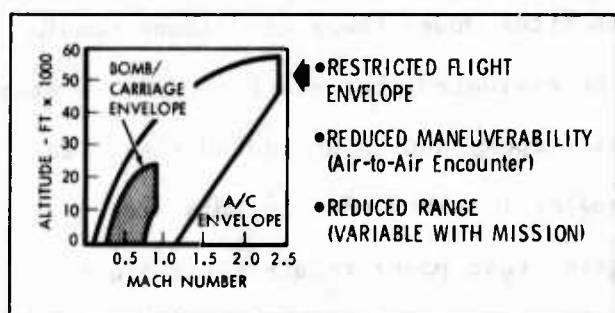


Figure A-33 External Pylon Mounted Weapons can Limit Aircraft Performance

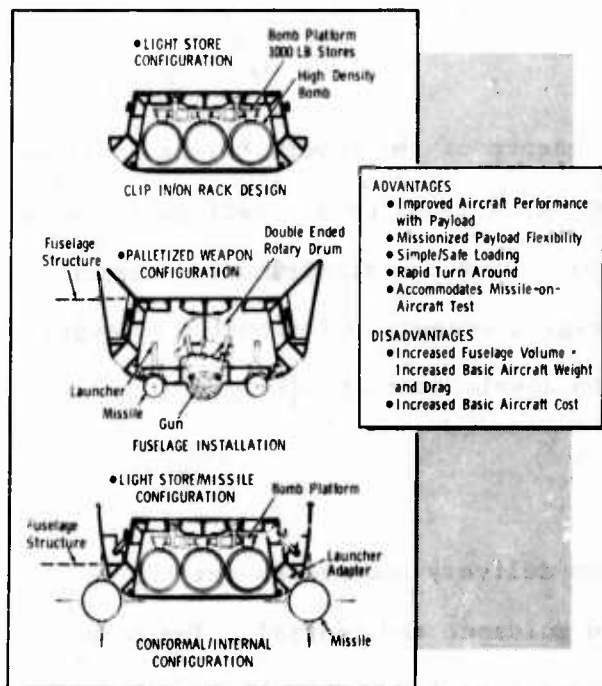


Figure A-34 Clip On/In Weapon Rack can Provide Mission Flexibility

Weapons packaging efficiency becomes critical with internal stores configuration, and the conversion to bluff-shaped weapons (Figure A-35) offers not only good

Aircraft compatibility and operational factors (such as logistics and ordnance selection flexibility to match the mission) will have a significant impact on the design of future weapons. The desire to overcome aircraft performance limitations imposed by pylon-mounting weapons (Figure A-33) has resulted in a search for alternatives. The "clip in/on" weapon rack concept, depicted in Figure A-34 affords not only improved aircraft performance possibilities but is readily adaptable to missionizing payloads and facilitates simple and safe loading operations. Preloading of the racks will provide for rapid aircraft turnaround. All degrees of aircraft submergence are possible from external fuselage mounting through partially submerged/conformal to completely internal arrangements.

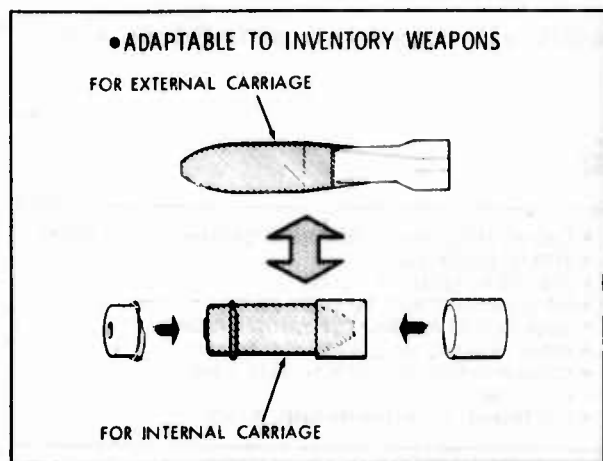


Figure A-35 Bomb Modification for Internal Loading Efficiency

AIR-TO-AIR MISSILES		GUIDED GLIDE WEAPONS		UNGUIDED WEAPONS	
WEAPON	COMMENT	WEAPON	COMMENT	WEAPON	COMMENT
AIM-9J/R Sidewinder	In Development IR Homing - 190 lbs	KMU-353B	Phase II Test EO Guided MK-84 - 2130 lbs	MK-82	Inventory GP 500 lb Bomb
AIM-54 Agile	In Development IR Homing	KMU-388 A/B	Phase II Test Laser Guided MK-82 - 650 lbs	MK-84	Inventory GP 2000 lb Bomb
AIM-7F Sparrow	In Inventory Radar Homing - 500 lbs	KMU-351 A/B	Phase III Prod Laser Guided MK-84 - 2040 lbs	SUU-51	Inventory Dispenser ~ 1000 lbs
AIR-TO-GROUND MISSILES		EGDM/SUU-51	Planned Laser Guided Dispenser ~ 1000 lbs	Rockeye II	Inventory Dispenser 476 lbs
AGM-65A Shrike	In Inventory Radar Homing - 395 lbs	Guided Rockeye	Inventory Laser Guided Anti-Tank Bomb Cluster - 555 lbs	BLU-27/B	Inventory Fire Bomb - 870 lbs
AGM-65 Maverick	Phase III Prod Contrast Image Int. Chng. Sensors Proposed - 475 lbs	Short Range Modular	See Figure A-37 Figure A-38	High Speed FAE	Fuel - Air Explosive to Replace BLU-76/B ~ 2500 lbs
AGM-78D Standard	Phase II Test IR/IR/Inert - 1390 lbs	Long Range Modular	See Figure A-37 Figure A-38	Modular	See Figure A-37 Figure A-38
Site Shooter	Planned Defense Suppression - <190 lbs	GUN		ROCKETS	
Out-Range	Planned Subsonic Cruise - 2020 lbs	WEAPON	COMMENT	WEAPON	COMMENT
		GAU-8 30mm	Air-to-Ground	2.75" FFAR	In Inventory
		GAU-7 25mm	Air-to-Air	Adv. Rocket	Multiple Warheads Ballistic/Guided IOC 1980's

Figure A-36 Typical LWA Weapon Candidates

Warhead Type/WL lbs/#	Unguided Class I	Guided Class I	Guided Class II	Guided Unpowered Class III	Guided Powered Class III
• H. E./800/1	✓	✓	✓		✓
• H. E./1500/2a	✓	✓	✓		✓
• CLUSTER/800/2b	✓	✓	✓		
• HE/2000/3a	✓	✓	✓	✓	
• NAPALM/700/3b	✓	✓	✓		
• H. S. M./1700/3c	✓	✓	✓		
• CLUSTER/2000/4	✓	✓		✓	
• S. O. C./1500/5	✓	✓			✓
• S. O. C./2200/6a	✓	✓		✓	
• FLAME/1375/7	✓	✓			

• CLASS I \_\_\_\_\_ Free Fall  
 • CLASS II \_\_\_\_\_ Powered to Provide 10 n.mi. Standoff at 5 K ft  
 • CLASS III \_\_\_\_\_  
 • Powered - 100 n.mi. to 200 n.mi. (60 K ft) Standoff  
 • Unpowered - 70 n.mi. Standoff at 60 K ft

Figure A-37 Modular Weapons Study Matrix

- LASER SEMI-ACTIVE
- EO CONTRAST SEEKER
- IR IMAGING SEEKER
- AUTO RADIATION SEEKER
- EO AREA CORRELATOR
- MICROWAVE RADIOMETER
- RADIOMETRIC AREA CORRELATOR

Figure A-38 Modular Weapons Guidance Concepts

packaging efficiency but has resulted in improved weapon separation characteristics. Munition thermal limits have been a major factor in limiting aircraft flight envelopes with external stores. Future munitions having thermal limits consistent with aluminum aircraft thermal limitations are planned.

Representative weapons that are expected to be retained in inventory or expected to be developed for use in the 1980-1985 time period are identified in Figure A-36. An advanced tactical rocket particularly suited to the close air support mission is under development with an IOC in the early 1980s possible. The objective of the advanced concept is to provide a low cost weapon with interchangeable ballistic and laser-guided warheads (fragmentation, target marking, penetrating, anti-material flechette).

A summary of the modular weapon concepts currently under consideration is presented in Figure A-37. Basically, the concepts involve the interchangeable weapon sensors, guidance and control, propulsion, warheads and fuses to accommodate mission requirements. The weapon guidance concepts under study are listed in Figure A-38. The potential weapon combinations

and the aircraft avionic accommodations to handle all possible combinations are numerous.

#### A.1.5.2 Advanced Tactical Avionics Technology

##### A.1.5.2.1 Weapon Delivery Equip-

ment. Equipment items in use or proposed

to support adverse weather and night de-

livery of advanced tactical weapons in a

severe threat environment are identified in

Figure A-39. The size, weight, power and

costs of this equipment depend heavily on the functional sophistication demanded by the mission to be performed.

The TFTA radar feature facilitates adverse weather and night low-level threat penetration and weapon delivery. The attack radar provides for adverse weather and night target acquisition and weapon delivery. Radar system improvements currently being implemented or proposed include  $K_a$  and dual frequency operation, shortened radar pulse operation, moving target identification, and a 2.5 nautical mile diameter display.

Current attack radars offer weather penetration capabilities superior to EO sensors but lack the close-in target resolution afforded by EO sensors. Radar employed in conjunction with EO sensors affords both early target recognition and final target resolution.

The EO-aided delivery of weapons involves consideration of LLLTV, IR, Imaging IR (IIR) and LTDR provisions. The simplest concepts, in terms of aircraft requirements, involve the use of laser-guided bombs employed in conjunction with ground designation or other-aircraft laser designation of targets. Aircraft detection and tracking of the laser designated target may involve the use of an onboard laser spot seeker to provide angle and angle rate data employed in the delivery of both guided and unguided weapons. More sophisticated concepts involve the use of aircraft IIR with target acquisition and aiming provisions

- TERRAIN FOLLOWING TERRAIN AVOIDANCE (TFTA) RADAR
- ATTACK RADAR (AR)
- LOW LIGHT LEVEL TV (LLLTV)
- INFRARED/IMAGING INFRARED (IR/IIR)
- LASER TARGET DESIGNATOR/RANGER (LTDR)
- RADAR HOMING AND WARNING (RHAW)
- COMMAND/UPDATE WEAPON DATA LINK
- C<sup>3</sup> SECURITY
- ELECTRONIC COUNTERMEASURES (ECM)

Figure A-39 Weapon Delivery Avionic Equipment Candidates

operated in association with either radar or laser ranging equipment. The addition of an onboard laser target designation and ranging capability adds another level of complexity.

The LLLTV dependence on ambient lighting and limitations in adverse weather make it an unlikely candidate for advanced aircraft employing IIR. TV reception capability to accommodate TV-guided bomb delivery may be desirable. EO sensor pointing and stabilization requirements and, therefore, equipment complexity are intimately related to attack tactics and weapons employed.

Limited adverse weather/night operations, target area navigation nets (e.g., TOA/DME, Loran), FAC beacon/target laser designation support, and self contained weapon guidance capabilities all can relieve LWA radar/EO equipment requirements. Also, the use of weapon-seeker-coordinated EO equipment mounted on weapon "clip in/on" racks can provide greater LWA mission flexibility.

All aspect radar warning with threat identification features and possibly an accurate location/homing capability is desirable to counter the air-to-air and SAM threats. Avionics to provide guided weapon commands and data to update target acquisition information must be considered. The protection of these data links as well as communication links against enemy countermeasures will be required.

A.1.5.2.2 Advanced Controls and Displays. Review of the potential weapon delivery-related controls and displays (Figure A-40) and consideration of addi-

•HEAD UP/HEAD DOWN PILOT DISPLAY Heading/Altitude/Airspeed/Attitude/Terrain/Threat/ DME/TOA/Course Correction/Weapon Release Signal
•AIMING CONTROL/DISPLAY HMS/HMD/Optical Sight/Radar-Cursor/IIR Detected Laser Designated Target Location/IIR-Cross Hair/Laser Target Designation/Ranging
•WEAPONS MANAGEMENT/FIRE CONTROL Weapon Type/Weapon Location/Weapon Thermal Control/Weapon Target Data/Launch/Command-Update/Target Designation
•COUNTERMEASURES RHAW/Jammer

Figure A-40 Weapon Delivery Control and Display Possibilities

tional requirements associated with aircraft management, C<sup>3</sup>, and test and emergency provisions raise serious questions concerning crew size in the performance of advanced tactical missions. Single-pilot operation can be facilitated through (1) helmet-mounted sights and displays; (2) mission constraints in terms of number

of weapon types, target types, and tactics to be employed in a single sortie; and (3) multimode controls and displays which can be preset for compatibility with a missionized payload.

Key considerations in the design of controls and displays are real-world visual correlation; rapid recognition; and minimum space, weight, power and cost. Advanced concepts employing digital readout, safe operating range indicators, go-no go test indicators, emergency indicators, and flight/target/threat situation displays must be considered. The use of common controls and displays for multiple mode operation affords considerable economy in space/weight/cost. Developments in multimode matrix electronic display instruments (MEDIA) employing light emitting diode materials and components should provide highly reliable, survivable and relatively inexpensive flexible format displays for use on advanced aircraft.

A.1.5.2.3 Additional Avionic Equipment. Additional avionic equipment possibilities which are largely self-evident and/or related to previously discussed equipment are summarized in Figure A-41.

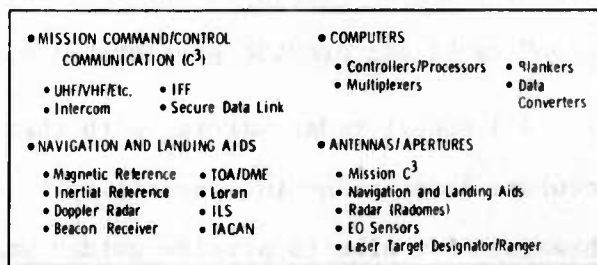


Figure A-41 General Avionic Equipment Candidates

Constraints related to radar antenna mounting/pointing and provisions for EO sensor sighting/aiming and possibly laser firing are expected to be most important in the LWA configuration refinement. Location of the electro-optical platform and whether the installation is a fixed external pod installation or a retractable pod installation will depend upon many factors including sensor numbers and complexity, internal space constraints, and aircraft performance considerations.

## A.2 OPERATIONS ASSESSMENT

### A.2.1 REQUIREMENTS IN THE 1980s

The environment in which tactical aircraft must operate, their mission objectives, and the resulting force compositions must be considered in the design synthesis of new tactical aircraft. Changes in potential conflict environments can be expected to present more stringent demands and add new roles for a new CAS strike system. Convair's approach to establishing system requirements and evaluating configuration concepts (Figure A-42) fully embraces the LWA philosophy of selective incorporation of new technology that is especially adaptable to the post-1980 CAS/strike role.

#### A.2.1.1 Scenarios

Battle scenarios have been developed to characterize the specific missions and objectives assigned to the tactical air strike force. A conventional full-scale conflict is represented by the European NATO/PACT scenario and an intermediate level conflict by the Middle East Arab/Israeli scenario. In Central Europe the enemy will have a high degree of mobility along a 100 n.mi. FEBA. The Middle East scenario is more geographically compact with about one-third the target density of Europe, thus can be defended by aircraft with a shorter combat radius. Available bases vary from 50 to approximately 300 in Europe, dropping to about 5 in Israel or 46 if Cyprus and Crete are allowed (Figure A-44).

The impact of weather on strike aircraft design is exemplified in the European scenario where, during winter, the operational limit is a 3000 foot ceiling/

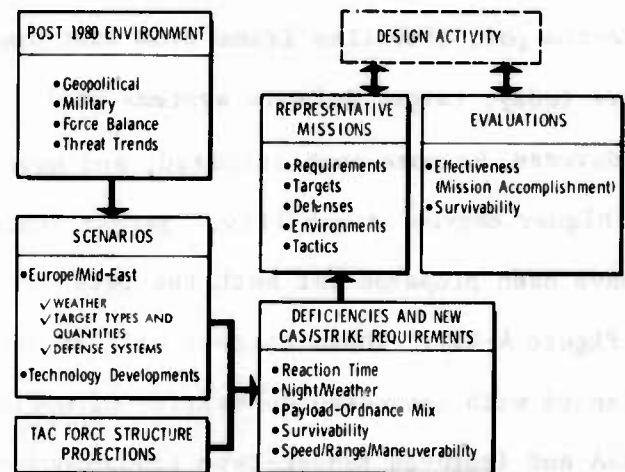


Figure A-42 Approach to Operations Assessment for LWA

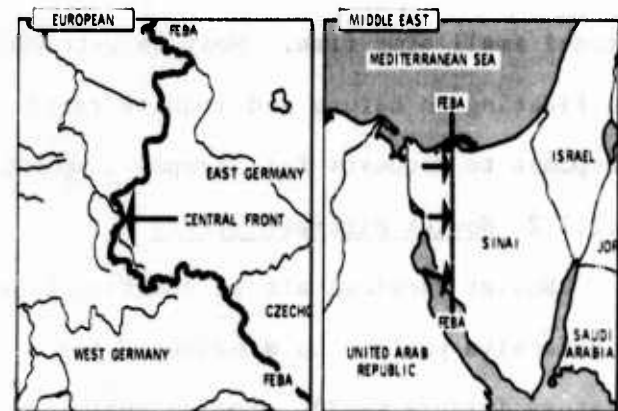


Figure A-43 Scenarios for LWA Analysis



3 mile visibility for 60 percent of the time (Figure A-45). Strike aircraft utilization can be significantly increased if operations can be made below a 3000 foot ceiling or if an all-weather capability is available.

The nature of the ground target complexes will not be significantly different in the post-1980 time frame from what they are today; target defense systems will increase, be more sophisticated, and have a higher degree of mobility. Target lists have been prepared for both theaters (Figure A-46). These targets will be defended with increased quantities of mobile AAA and improved Redeye-type troop-carried surface-to-air weapons as well as conventional small arms fire. Most targets will be fleeting in nature and require rapid response to requests for firepower support.

#### A.2.1.2 Soviet Aircraft Trends

Soviet tactical air is shifting from a defensive posture to a balanced force posture (Figure A-47). The potential impact of this shift on design considerations for the LWA is twofold: (1) a permissive air environment around FEBA cannot be assured, and (2) basing must minimize vulnerability to an air base strike.

#### A.2.1.3 Projected TAC Force Structure

The design of a new tactical fighter must also evolve from a consideration of the other systems it will complement. As noted in Figure A-48, the post-1980

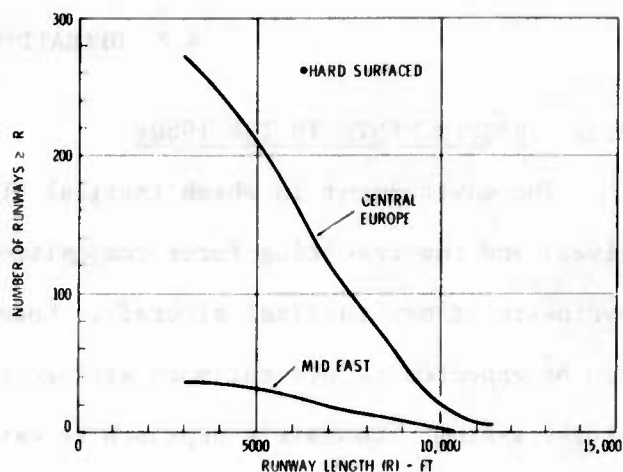


Figure A-44 Runway Availability can Affect LWA STOL Requirement

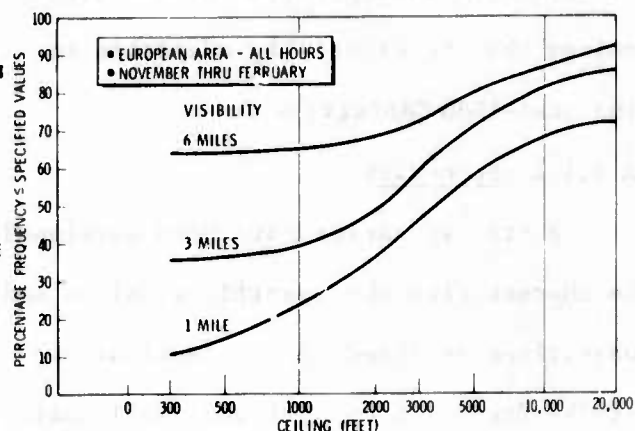


Figure A-45 Bad Weather Predominates European Winters

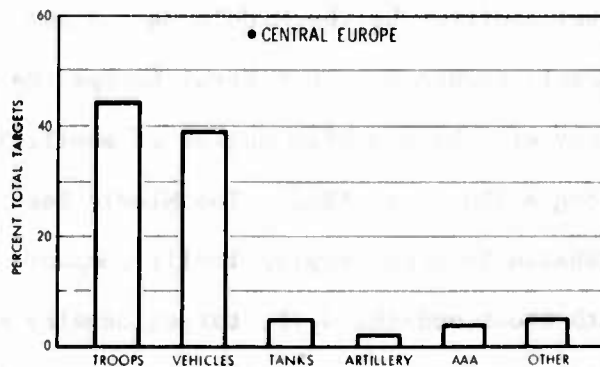


Figure A-46 Target-Type Distribution



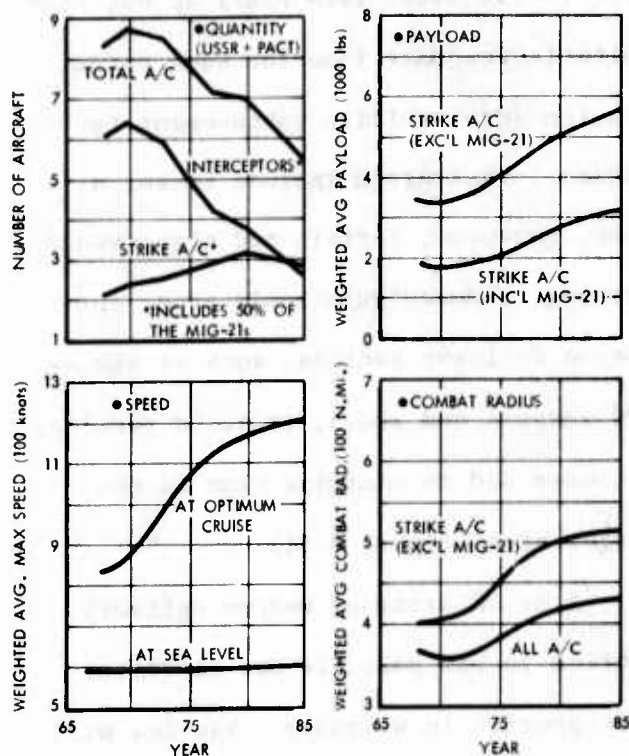


Figure A-47 Soviet Aircraft Trends

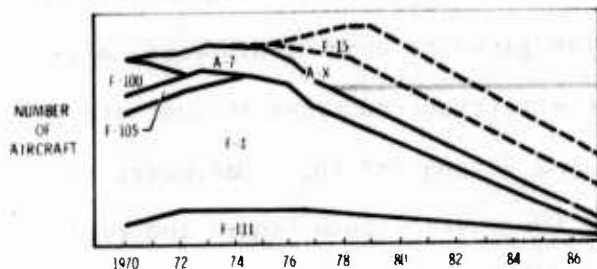


Figure A-48 Projected Tactical Force Structure

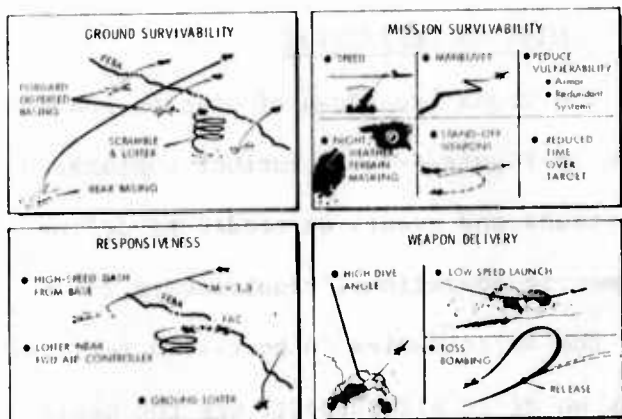


Figure A-49 Typical Tactics

force structure will consist of F-4, A-7, and F-111 aircraft with an average age of 13 years and specialized aircraft (i.e., the F-15 and A-9/10 aircraft used for air superiority and close troop support missions, respectively). The requirements set forth for the LWA design are derived in the context of this total tactical air force, considering specific deficiencies and needs for replacement.

#### A.2.2 TACTICS/EFFECTIVENESS/SURVIVABILITY

The tactics emphasized are those which take maximum advantage of unique or superior performance capabilities afforded by advanced/emerging technologies. The effectiveness standard by which the performance of a given configuration is evaluated is the expected degree of accomplishment (the likelihood that the target is destroyed) for each of the missions in the representative set.

Enhancement of survivability, both on the ground and in-flight, is a dominant consideration in design (Figure A-49). Ground survivability is closely allied with reaction time. As seen in Figure A-50, STOL forward-based aircraft have the highest potential for intercepting immediate targets. Systems based to the

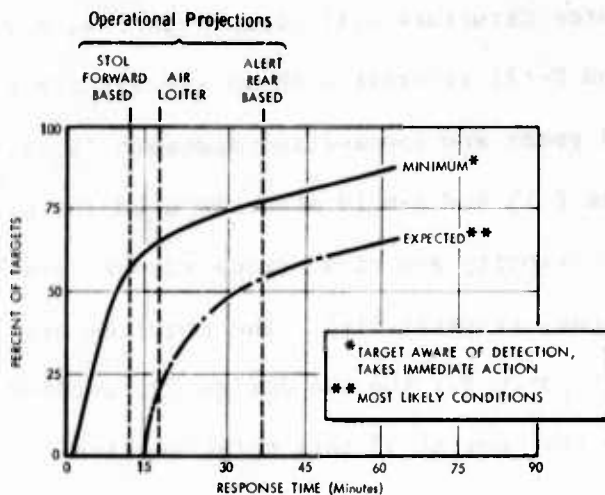


Figure A-50 Target Response Times

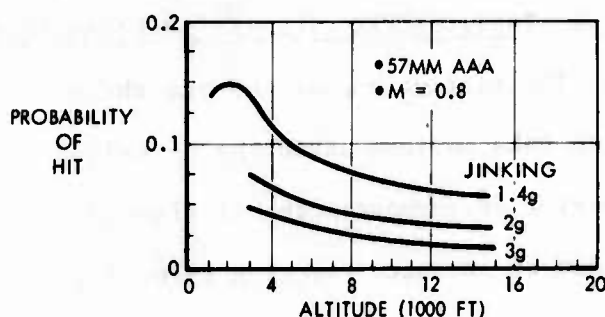


Figure A-51 Effect of Altitude and Jinking on Probability of Hit

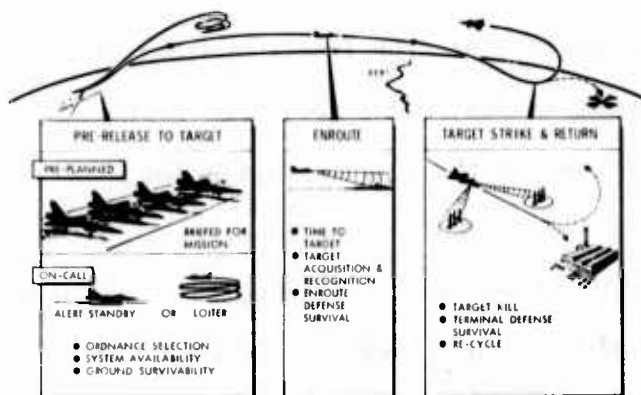


Figure A-52 Mission Phases

rear ( $\approx 150$  miles from FEBA) do not have suitable response time for such targets. Mission survivability enhancement techniques investigated include speed, altitude, maneuver, terrain and night/weather masking, reduced vulnerable area, and weapon delivery tactics, such as stand-off weapons and modes, to avoid terminal defenses and to minimize time in the target area (Figure A-51).

A broad array of weapon delivery tactics is now possible due to recent developments in weaponry. Tactics will include both powered and unpowered weapons and trainable guns. Consideration is also given to cost of ordnance, aircraft attrition reduction through stand-off, and weapon lofting. Maneuvers to allow low-speed weapon launch and rapid acceleration from the target area are potentially required.

### A.2.3 MISSION DEFINITION

The gross breakdown of mission phases shown in Figure A-52 is further subjugated into tasks and events as needed to define parametric operational requirements for

configuration synthesis. As noted previously, the deficiencies in post-1980 tactical air strike capability, with particular emphasis on close air support, are the basis for the representative missions.

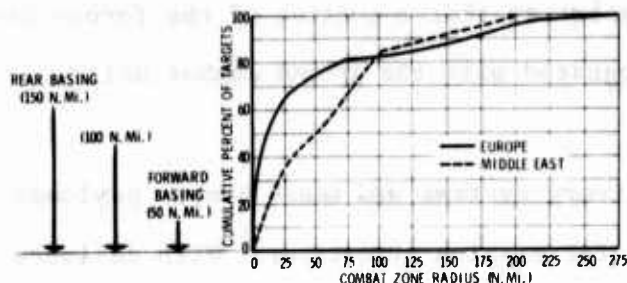


Figure A-53 Mission Radius Considerations

along the front in Europe. An examination of 15 countries of military interest worldwide reveals that 97 percent of the time a 4,000-foot runway is available within 150 n.mi. In Europe the 150 n.mi. pre-penetration distance also provides for adequate lateral mobility along the front to concentrate firepower. This indicates that a 300 n.mi. combat radius is probably satisfactory.

The assumption that CONUS forces will have 30 days to deploy before an attack implies a high level of activity in positioning forces. An unrefueled ferry range of at least 1860 n.mi. is desirable to cover the critical leg to Europe (Figure A-54).

#### A.2.3.2 Availability

In the intense, rapidly changing conditions envisioned, high surge rates will vastly improve system benefits. Surge rates of 4 to 6 sorties per day are desirable. These rates imply a simple, rugged system requiring about 10 maintenance man-hours per flying hour. Some 30,000 pounds of support per day are required per airplane for this type of activity.

The ability to operate down to conditions of a 1,000 foot ceiling and 1 mile of visibility allows operation in Europe 85 percent of the time. The use of systems external to the aircraft for vectoring may be sufficient to attain the needed night/weather capability with nominal costs.

#### A.2.3.3 Responsiveness

Because of the highly fleeting nature of the postulated targets, a response time of approximately 15 minutes is needed. Short field capability ( $\leq 2500$  ft. run-

#### A.2.3.1 Range

As illustrated in Figure A-53, there is a high concentration of targets near the FEBA; 90 percent are within 150 n.mi. A pre-penetration distance of 150 n.mi. provides the choice of numerous fields

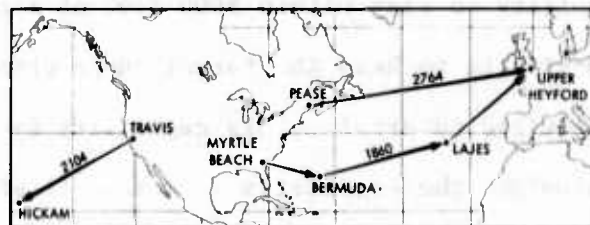


Figure A-54 Unrefueled Ferry Range Requirements

way) or air loiter (1 to 2 hours) is necessary so that a portion of the forces can be rotated near the front and closely integrated with the ground combat units.

#### A.2.3.4 Lethality

With the introduction of improved delivery systems and smart bombs, payloads of 4,000 to 6,000 pounds may be sufficient for mission objectives. With delivery accuracies on the order of 50 foot CEP, there is a high probability (~90%) that a single pass will kill the target. Highly accurate delivery of a single bomb, without random gross errors must be achieved for delivery close to friendly troops. In a low-threat environment, a gun would provide high accuracy at the lowest cost, since a majority of the targets are vulnerable to gun fire.

#### A.2.3.5 Target Acquisition

To counter the enemy's option to move at night and under adverse weather conditions, sensors (FLIR, EO, etc.) are needed to identify moving targets. The ability to stay within 5000 feet of a target for a reattack during daylight is desirable to keep the target under visual surveillance. A low-speed turn radius is required to provide this capability (~2500 feet below 0.6M); such a provision also provides the capability to make a first pass from visual detection of an offset target.

APPENDIX B  
IN - FLIGHT POWERED LIFT DESIGN  
TECHNOLOGY DEVELOPMENT

The in-flight powered lift family of advanced technology concepts is of primary interest to the LWA concept because of its potential to provide STOL capability as well as excellent low- and high-speed maneuver performance in a single configuration. This family includes four concepts of interest to the LWA: (1) vectored thrust, (2) jet flaps, (3) vectored thrust with supercirculation, and (4) externally blown flaps. With the exception of vectored thrust, each of these concepts involves a significant increase in circulation lift due to blowing, i.e., supercirculation.

The potential aerodynamic performance of these concepts is summarized in paragraph A.1.1.1. However, configurations employing these concepts must be designed and evaluated in order to fully determine the real potential of these technologies. An initial assessment of powered lift concepts indicates a great deal of theoretical and experimental lift and drag information related to takeoff and landing. On the other hand, with the exception of simple vectored thrust, there exists only a small amount of data concerning operation of these concepts at flight speeds.

The data that are available on the supercirculation concepts at flight speeds are mostly experimental and represent a wide variety of configurations and conditions. The first step to remedy this situation has led to development of a method for predicting the aerodynamic design parameters related to each concept through correlation of existing theoretical and experimental information.<sup>1</sup>

The resulting method is not necessarily absolute in its results, and its utility lies in (1) providing consistent performance predictions for configuration

---

<sup>1</sup>Mothersole, G. F., et al., "Powered Lift Aerodynamic Studies for the Advanced Technology Close Air Support Fighter," Convair Report MR-A-2099, 1 June 1972 (Confidential).

comparisons and (2) accounting for performance variations as a function of important configuration variables. In perspective, the method is intended for use in determining the directions of further technology development. A discussion of the general evaluations which have been performed and some indication of the relative directions of each of the candidate powered-lift concepts is presented in subsequent paragraphs of this appendix. The configuration performance data presented in this appendix are tail-off. Because of the unique trim problems associated with each of the powered-lift concepts, innovative configuration designs are required to realize the indicated gains.

## B.1 DESIGN OBJECTIVES

### B.1.1 SHORT TAKEOFF AND LANDING

Takeoff and landing requirements for the LWA have not yet been specified. One objective of the LWA operations analysis and configuration design efforts is a parametric evaluation of the effect of different STOL requirements on the configuration and its operational effectiveness. For discussion purposes, a requirement of 1500 feet for takeoff and landing over a 50-foot obstacle is assumed.

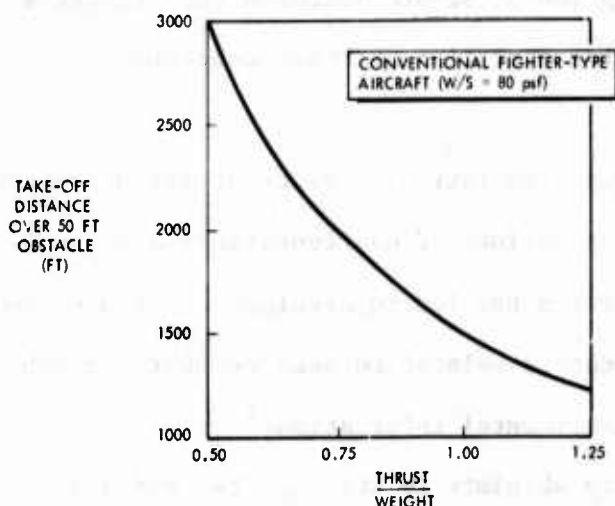


Figure B-1 Modern-Day Tactical Fighters Have STO Capability

For modern day fighters, a 1500-foot takeoff requires only a minimal high-lift system, if any (Figure B-1). A 1500-foot landing is a different matter.

As described in Convair's STOL Tactical Fighter Configuration Study, true short field landings require reduction of the touchdown margin through the use of automatic throttle control and a no-flare landing technique.<sup>1</sup> In addition,

thrust reversal can provide a large reduction in ground roll (Figure B-2).

<sup>1</sup>STOL Tactical Fighter Configuration Study, AFFDL TR-72-127, February 1973.



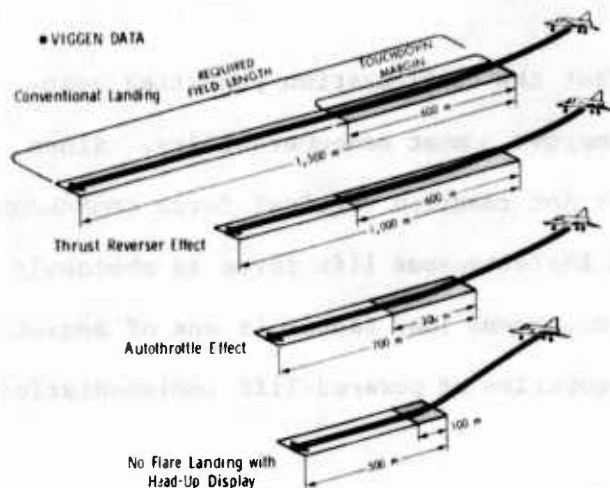


Figure B-2 Landing Technique can Shorten Required Field Length for Conventional Fighter

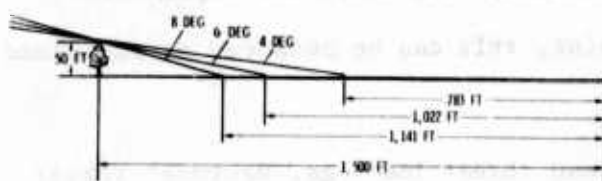


Figure B-3 Steep Approach Angle is Important for Realizing Short Landings

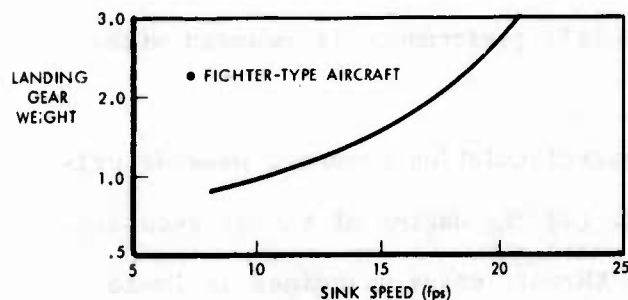


Figure B-4 Landing Gear Considerations can Limit Sink Speed

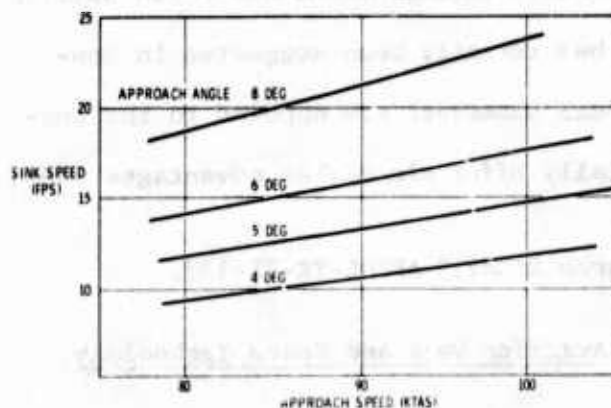


Figure B-5 Limit Sink Speed can Restrict Approach Angle

For a specified landing distance over a 50-foot obstacle, the allowed rollout distance is proportional to the approach angle (Figure B-3). Maximizing the approach angle is important to the achievement of short landings, but the higher sink speeds associated with steep approaches compromise the landing gear design (Figure B-4). Since sink speed is also a function of landing speed, a design objective then becomes to reduce approach speed which is, of course, the purpose of powered lift for STOL use (Figure B-5).

Conceptually, any of the in-flight powered lift approaches will reduce landing speed [ $V_{\text{Approach}} \sim V_{\text{Stall}} \sim f(L_{\text{Max}}, T_{\text{Vert}})$ ]. The effect of vectored thrust is to reduce the required wing lift; use of the other concepts provides increments to the maximum lift available as well as a vectored thrust effect.

The objective then is to integrate the candidate technologies and the total configuration so that undue penalties are not incurred in achieving STOL. Also, there is a tradeoff between the degree of STOL required and the configuration impacts of thrust reverse, sink speed, and powered lift.



### B.1.2 COMBAT MANEUVERS

One tenet of the LWA concept is to offset the configuration penalties associated with STOL by using powered lift to improve combat maneuverability. Since each of the powered-lift concepts involves a jet reaction vertical force component over the basic wing lift, an improvement in instantaneous lift force is obviously realized. The question in the case of instantaneous load factor is one of degree, and the tradeoff is the impact on the configuration of powered-lift implementation versus reduced wing loading.

The lift increments potentially attainable through supercirculation are large, but another aspect of the picture is the efficiency with which the improvements are generated. From a configuration standpoint, this can be measured as sustained lift capability.

For contemporary fighter wing loadings and threat loadings, vectored thrust can improve sustained lift at very low speeds (less than 200 knots), because the wing will reach its maximum lift capability with excess thrust remaining. This is not the case at higher speeds, and sustained lift performance is reduced with simple vectored thrust.

The sustained lift efficiency of the supercirculation concepts depends primarily on (1) the lift augmentation achieved, (2) the degree of thrust recovery, (3) the span loading efficiency, and (4) the thrust losses sustained in implementing the concept.

The possibility of improving combat capability through maneuvers which utilize quick, large decelerations and accelerations has recently been suggested in conjunction with thrust-vectored aircraft.<sup>1,2</sup> Such maneuvers are opposed to the concept of high sustained turn rate, but potentially offer air combat advantages where

---

<sup>1</sup>"V/STOL Tactical Fighter Configuration Research Study," AFFDL-TR-71-157, December 1971.

<sup>2</sup>"Vectored-Thrust Maneuverability Explored," Aviation Week and Space Technology, December 13, 1971.

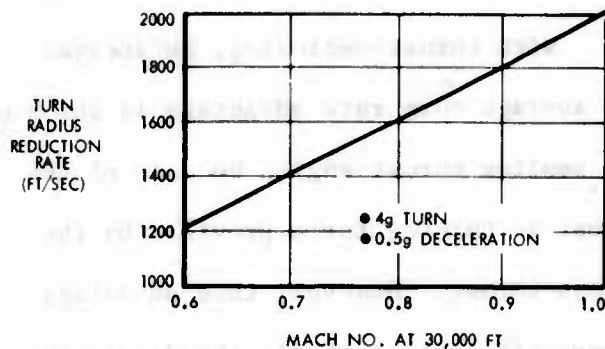


Figure B-6 Vectored Thrust Quick<sup>1</sup>, Reduces Turn Radius

flap concepts can potentially provide the "super speed brake" capability with minor effect on the configuration. The jet flap as presently envisioned does not have the capability to produce deceleration effects as large as the other powered lift concepts. In-flight thrust reverse is an alternative, but less desirable method for achieving a similar deceleration capability.

## B.2 VECTORED THRUST

### B.2.1 STOL TACTICAL FIGHTER CONFIGURATION STUDY

Convair's previous contract study with the Flight Dynamics Laboratory for STOL tactical fighter configurations has provided the basis for LWA vectored thrust

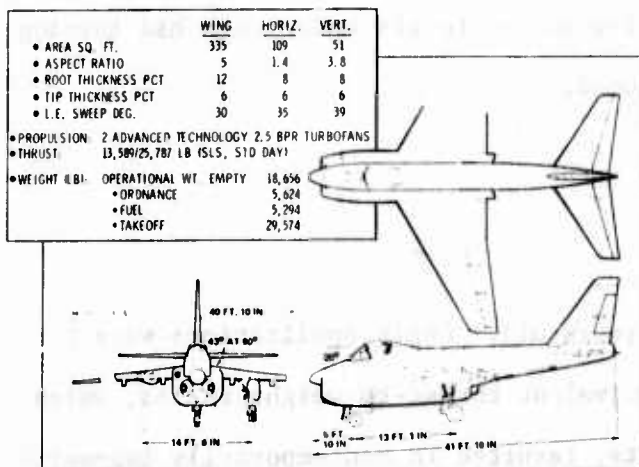


Figure B-7 Convair's STOL Tactical Fighter Study Vectored Thrust Configuration

instantaneous turn radius reductions are appropriate (Figure B-6). The ability to decrease speed in a ground attack dive can also increase aircraft effectiveness.

In addition to the standard vectored-thrust approach, the vectored thrust with supercirculation and externally blown

considerations. The configuration depicted in Figure B-7 was used for comparison purposes with other powered lift configurations.

### B.2.2 VECTORED THRUST FOR AIR COMBAT

Convair has utilized its digital simulation design tool to study the potential of thrust vectoring in air combat.<sup>1</sup>

Some of the results are shown in Figure B-8. Supercirculation effects, which are

attainable with some configurations, are not included in these results.

<sup>1</sup>Wenham, R. J., and Gomez, E. L., A Study Demonstrating the Potential of Thrust Vectoring in Air Combat, Convair Aerospace Division Report MR-A-2098, May 1972.

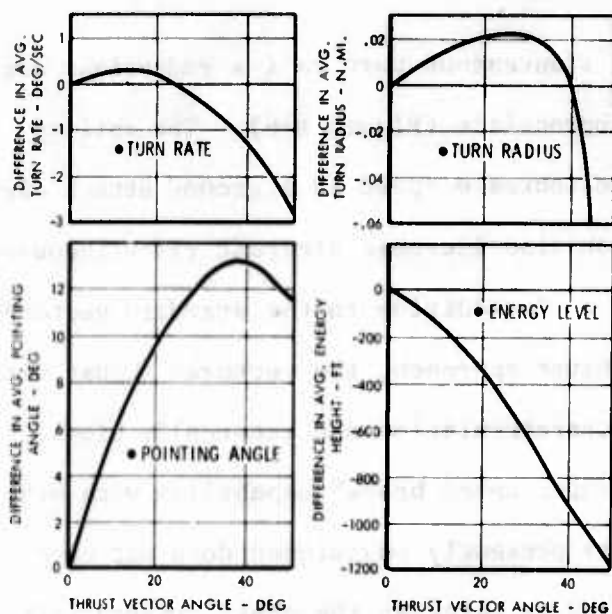


Figure B-8 Digital Simulation Studies Showing Effect of Thrust Vectoring (Fixed) on Air Combat During the Initial 15 Seconds

With thrust-vectoring, an increase in average turn rate advantage is observed at smaller thrust angles because of the boost in turning force provided by the gross thrust. However, this advantage drops off because of (1) the decreasing thrust recovery and (2) the rapidly decaying velocity which drives the aircraft state into the  $C_{L_{max}}$  region, thus reducing the attainable load factor.

The vectoring thrust effect is more pronounced on turn radius advantage. The important measure, however, is the degree to which the thrust-vectoring aircraft has reduced its pointing angle relative to the nonthrust-vectoring aircraft. Beyond a thrust vector angle of 37 degrees, the negative effects on turn radius and turn rate show their influences.

In conclusion, these data emphasize that thrust vectoring must be applied only during brief, tactically wise situations. Extended application would most certainly drive a combatant to relatively low energy levels where both his turning and acceleration potential is severely reduced.

### B.3 JET FLAPS

#### B.3.1 CONCEPTUAL APPROACH

The jet flap concept is more than 15 years old. Early applications were hard to justify partly because the high equivalent thrust-to-weight ratios, which are required to realize aerodynamic benefits, resulted in contemporarily impractical configurations. In the intervening years, engine technology and operational requirements have evolved to a point where operationally useful, high thrust-to-weight aircraft are in existence, and jet flaps could prove practical.

Previous implementation approaches to jet flaps typically employed the total engine exhaust, which resulted in a hot, relatively low pressure gas; e.g., the

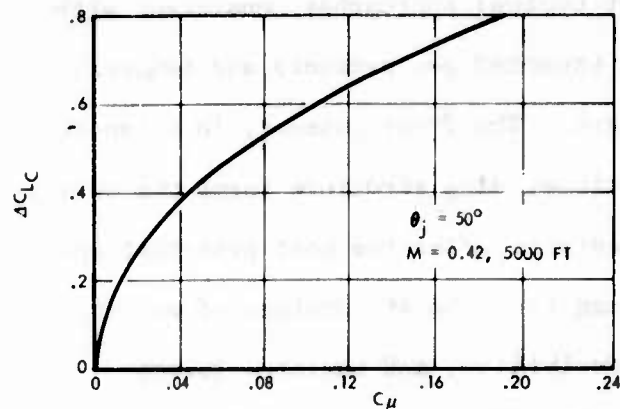


Figure B-9 Jet Flap Lift Augmentation Depends on Momentum Coefficient

exhaust of a current fighter turbofan engine has a nozzle pressure ratio of less than 2.5 and a gas temperature over 700°F. The attendant ducting and exhaust losses can be high; e.g., thrust loss for the Hunting experimental jet flap aircraft from engine to wing exit is estimated to be 28 percent.

The approach to this problem for the LWA is to use air from a high compression ratio fan or a low compression ratio compressor, depending on the preferred terminology. For example, fan air at a static pressure ratio of four has a corresponding temperature of approximately 300°F. For a given amount of air, this greatly reduces

both thrust losses and duct design problems. One disadvantage of using only fan air is the reduced blowing momentum coefficient,  $c_\mu$ , as compared to the total engine momentum (Figure B-9).

For the LWA, the advantages accruing to jet flaps from technology improvements are somewhat offset by application to thin, relatively low aspect ratio wings as compared to the subsonic aircraft for which jet flaps have been considered in the past. Aerodynamic improvements are markedly better for high aspect ratio wings; thin wings result in increased losses for a given  $c_\mu$ .

Several ducting concepts for a thin, fighter-type wing were explored. The three concepts shown in Figure B-10 repre-

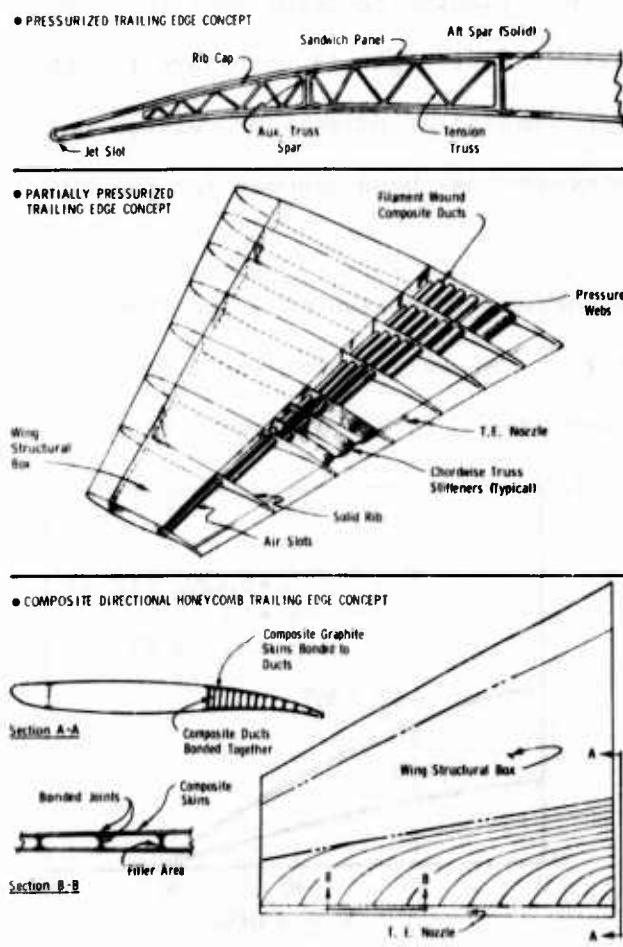


Figure B-10 An Integrated Duct/Trailing Edge Structure is Desirable

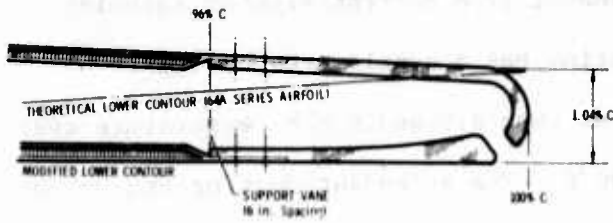


Figure B-11 Simple Fixed Jet Angle Nozzle is Desirable

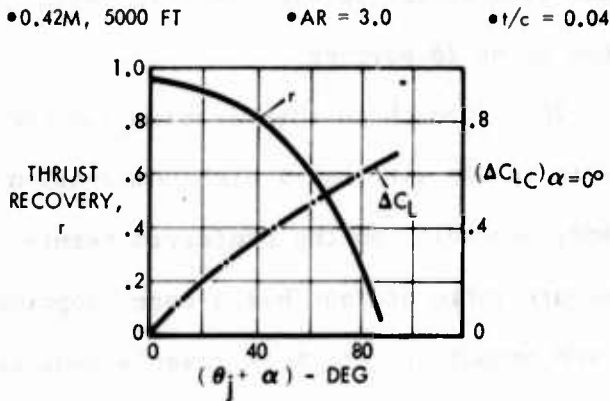


Figure B-12 Jet Flap Performance is Function of Jet Angle,  $\theta_j$

aircraft, because the aircraft uses its jet flap exhaust as primary propulsion for non-high-lift flight. A fixed-jet nozzle arrangement has been assumed for the LWA (Figure B-11).

The selection of the fixed-jet angle is important in design of a jet flap configuration. Both the lift increment and the thrust recovery factor are functions of the jet angle, and selection of this angle can make a large difference in configuration performance (Figure B-12).

The jet flap impacts the overall configuration design process in many ways. For example, it has been shown that the expected lift increment for a jet flap (as well as for the other supercirculation concepts) is a function of wing sweep.

Another area of configuration trade-off is the effect of wing geometry on  $c_{\mu}$ .

sent typical approaches consistent with the expected gas pressure and temperature ranges. The first concept, in which conventional wing structure forms the ducting, appears to offer the most practical approach from the standpoints of weight, producibility, and momentum losses.

The added weight, complexity, and thrust losses associated with a variable-angle jet flap appear to override the aerodynamic advantages. The Hunting jet flap aircraft has a mechanical Coanda flap which turns the jet, but a 5 percent thrust loss is estimated to occur over the flap. A variable jet angle is necessary for this

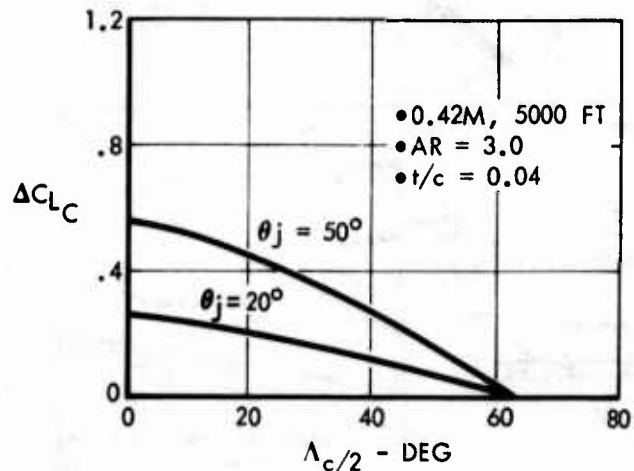


Figure B-13 Wing Sweep-Back Decreases Jet Flap Effectiveness

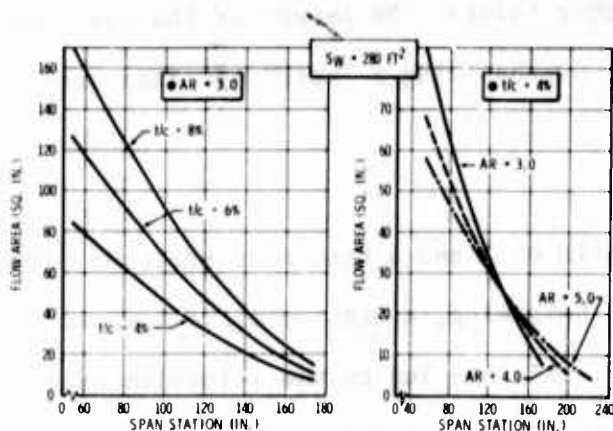


Figure B-14 Wing Geometry Affects Jet Flap Duct Losses

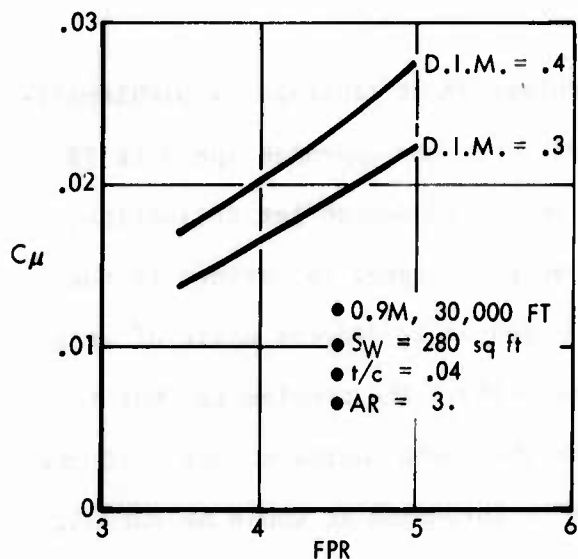


Figure B-15 Fan Pressure Ratio Can Limit  $C_\mu$

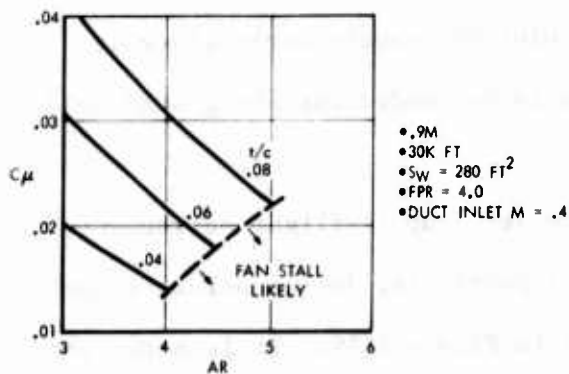


Figure B-16 Available  $C_\mu$  and Wing Geometry are Strongly Related

For a given wing area, the duct flow area is a function of both wing thickness and wing aspect ratio. If duct losses are held constant, maximum  $c_\mu$  becomes a function of these parameters (Figure B-14).

Although turning and temperature losses are important, the primary duct losses are friction losses which are a function of the square of the gas velocity, and the velocity is, in turn, proportional to the duct area. For analysis purposes, holding duct inlet Mach number constant is therefore equivalent to maintaining constant duct losses. The effect of fan pressure ratio and duct inlet Mach number on  $c_\mu$  is shown in Figure B-15 for a given wing planform. Looking at it from the other direction, the variation of  $c_\mu$  as a function of wing geometry for fixed fan pressure ratio and duct inlet Mach number is given in Figure B-16.

Selection of a  $c_\mu$ , a fan pressure ratio, and a net thrust determines the engine bypass ratio which, in turn, ties the engine cycle selection process for the other mission requirements into the jet flap design process. Analysis to

date has shown that sets of the above parameters in the range of interest for jet flaps result in very low bypass ratio engines.



The above discussion indicates, among other things, the impact of the jet flap concept on the configuration design process. Synthesizing a "best" jet flap configuration is not a straightforward task.

### B.3.2 POTENTIAL PERFORMANCE

A 280-square-foot wing with an aspect ratio of 3 and a thickness ratio of 0.04 is used for general comparison purposes. For this wing, a minimum  $c_{\mu}$  of 0.02 at Mach 0.9 and 30,000 feet is thought necessary; this has led to the selection of a turbofan with a fan pressure ratio of 4 corresponding to a wing duct inlet Mach number of 0.4. This design point fan results in the  $c_{\mu}$ 's shown in Figure B-17 at other speeds.

The potential of this jet flap design to achieve short landings is problematical. With a wing loading of 80 pounds per square foot, the approach speed is 98

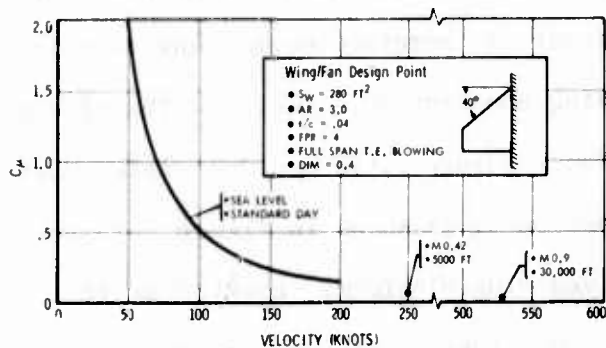


Figure B-17 Available  $C_{\mu}$  Used for Jet Flap Performance Evaluations\*

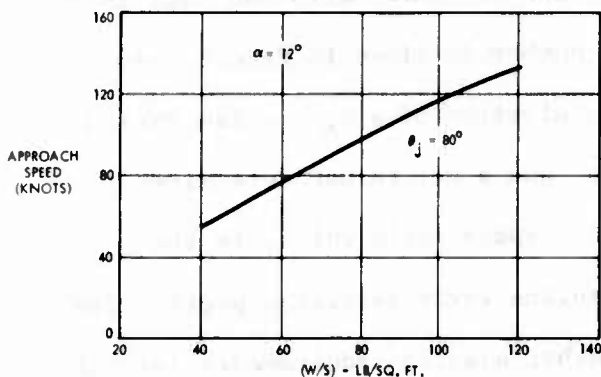


Figure B-18 Jet Flap Landing Performance Potential

knots for an 80 degree jet deflection, where approach speed is defined as the stall speed at 12 degrees angle of attack (Figure B-18). The problem is what to do with the basic engine thrust. If the engine is throttled as would be normal, the available  $c_{\mu}$  is greatly reduced. Thrust reverse during approach is a possible solution, particularly since it appears to be needed for the ground roll phase.

The jet flap in-flight performance for this particular design point is summarized in Figure B-19. It is noted that different total engine thrusts are assumed for the two-maneuver conditions. Review-

ing the salient points, the jet flap advantage in instantaneous lift lies in providing higher lift for a given angle of attack. For practical purposes, wing stall



•  $R = 3.0$

•  $S_{REF} = 280 \text{ SQ FT}$

•  $\Lambda_{LE} = 40^\circ$

•  $l/c = .04$

• VARIABLE L.E. FLAP

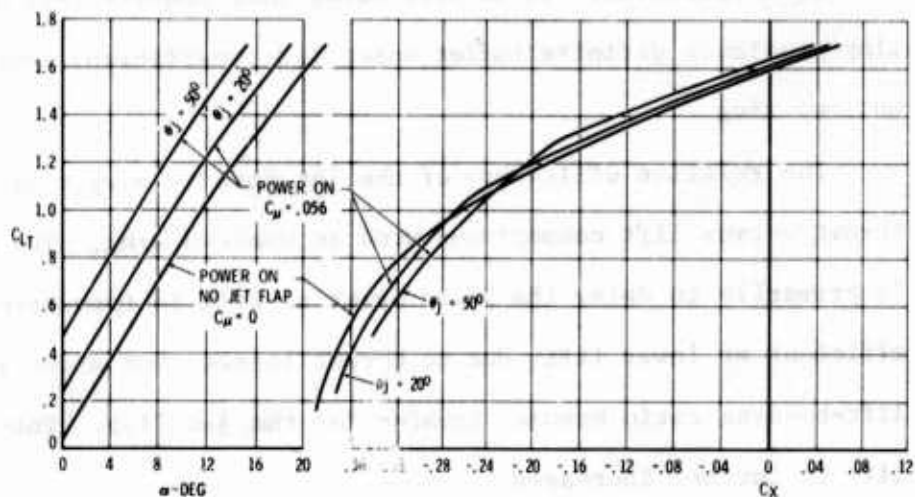
• FULL SPAN T.E. BLOWING

•  $S'/S = .635$

### AERODYNAMIC CHARACTERISTICS

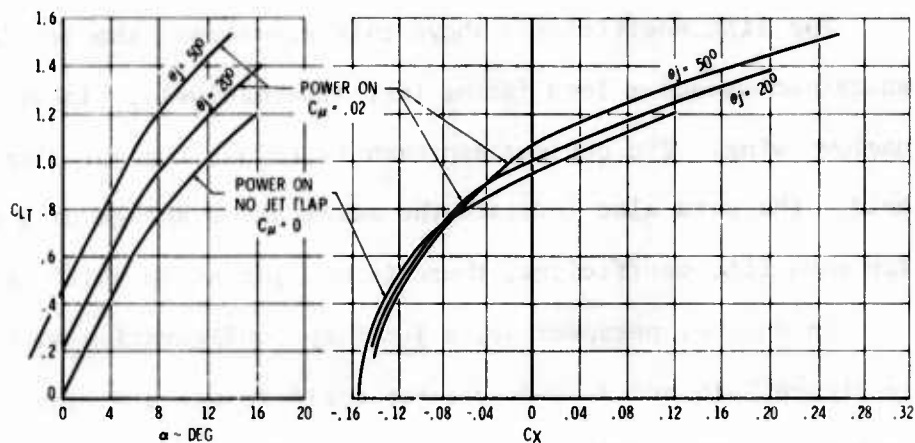
•  $M = 0.42$

• ALTITUDE 5,000 FT



•  $M = 0.9$

• ALTITUDE 30,000 FT



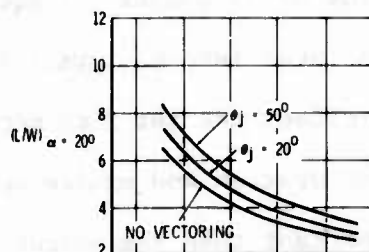
### MANEUVER CAPABILITY

• INSTANTANEOUS

•  $\alpha = 20^\circ$

•  $M = 0.42$

• ALT = 5000 FT

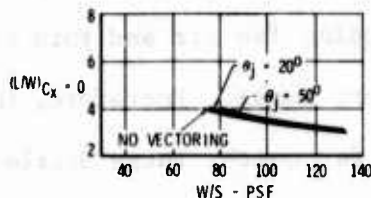


• SUSTAINED

•  $M = 0.42$

• ALT = 5000 FT

•  $T_G/W = 1.015$

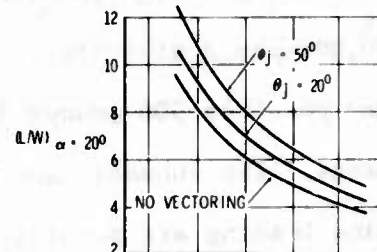


• INSTANTANEOUS

•  $\alpha = 20^\circ$

•  $M = 0.9$

• ALT = 30,000 FT



• SUSTAINED

•  $M = 0.9$

• ALT = 30,000 FT

•  $T_G/W = .752$

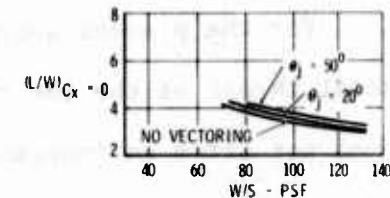


Figure B-19 Jet Flap In-Flight Performance Potential

per se has been eliminated in current fighter designs, so jet flap benefits in total usable instantaneous lift are questionable. However, there are several advantages in configuration design and weapon delivery effectiveness for low angle-of-attack operation. It is also noted that Convair test data on transonic jet flaps indicate definite buffet onset lift coefficient increases over those of an unblown wing.

The relative efficiency of the jet flap is very visible in the drag-minus-thrust versus lift comparisons with an unblown wing. The effect of the jet flap is primarily to delay the polar break as lift is increased. The jet flap is less efficient at lower lifts due to thrust losses, but above some lift coefficient the lift-to-drag ratio becomes greater for the jet flap. This advantage increases as lift is further increased.

For lift coefficients above this crossover, the jet flap results in a better sustained maneuver load factor (or, alternatively, higher specific power) than an unblown wing. The obvious approach is to use the jet flap only above this threshold. The data also indicate the marginal advantage of a variable angle jet; i.e., for each lift coefficient, there is one jet angle which is better than others.

In another perspective, a jet flap configuration with the parameters indicated in Figure B-19 and a 50-degree jet angle requires a wing loading of 88 pounds per square foot to sustain a 4-g maneuver at Mach 0.9 and 30,000 feet. The same unblown wing design requires a wing loading of 74 pounds per square foot. For a 30,000-pound aircraft, this can be translated into 65 square feet less wing area and possibly 500 pounds less weight to offset the jet flap mechanization requirements. The subsonic and supersonic acceleration and cruise advantages of a higher wing loading are possibly even more important than the weight trade.

For the present approach, i.e., using fan air and thin wings, the percent of total thrust of the jet flap air is very small. Therefore, the jet flap concept does not offer an inherent capability for quick, large decelerations and accelerations. Thrust reverse of the primary engine to achieve this capability is a possibility.

### B.3.3 CONFIGURATION CONSIDERATIONS

A conventional configuration approach to a jet flap LWA configuration is shown in Figure B-20. This configuration is balanced to reflect CCV implementation in that the subsonic aerodynamic center (AC) is forward of the center of gravity (CG) by approximately 10 percent of the mean aerodynamic chord (MAC). The basic operating weight is based on a composite structure as are all configuration weights discussed in this appendix.

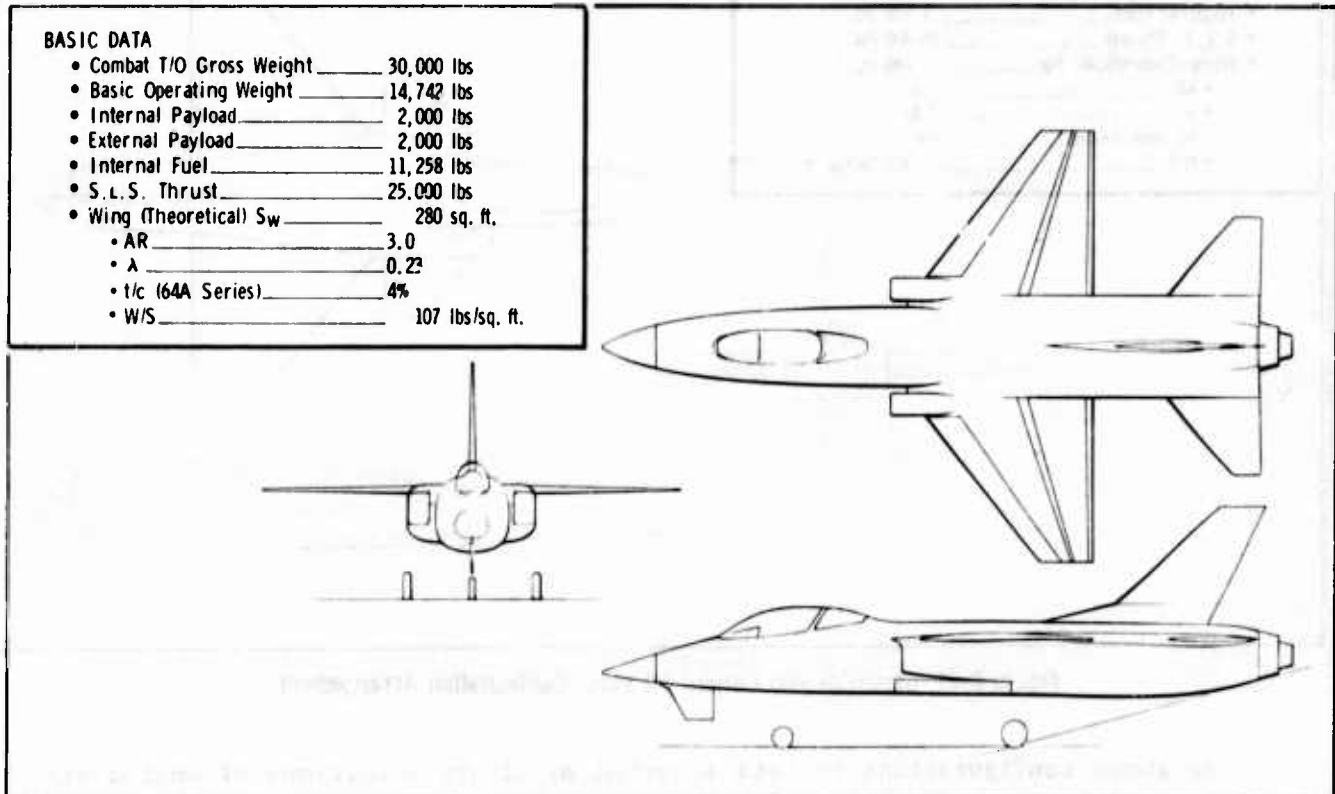


Figure B-20 Conventional Jet Flap Configuration Arrangement

Because of the downwash of the jet flap wing, a T-tail is possibly required. The extent of downwash is dependent on the amount of supercirculation achieved, and, with the relatively low  $c_{\mu}$ 's for jet flaps currently being considered, the need for a T-tail is not necessarily obvious.

Another effect of supercirculation is to cause an aft shift of the center of pressure and a corresponding increase in nosedown moment. The extent of this shift as a function of  $c_{\mu}$  is also being studied.

Both the downwash and moment generation effects are minimized by a canard configuration, i.e., the control surface is removed from the downwash and placed so that the trim forces are lifting. A jet flap LWA configuration utilizing the close-coupled canard approach is depicted in Figure B-21. This configuration is also balanced to reflect CCV.

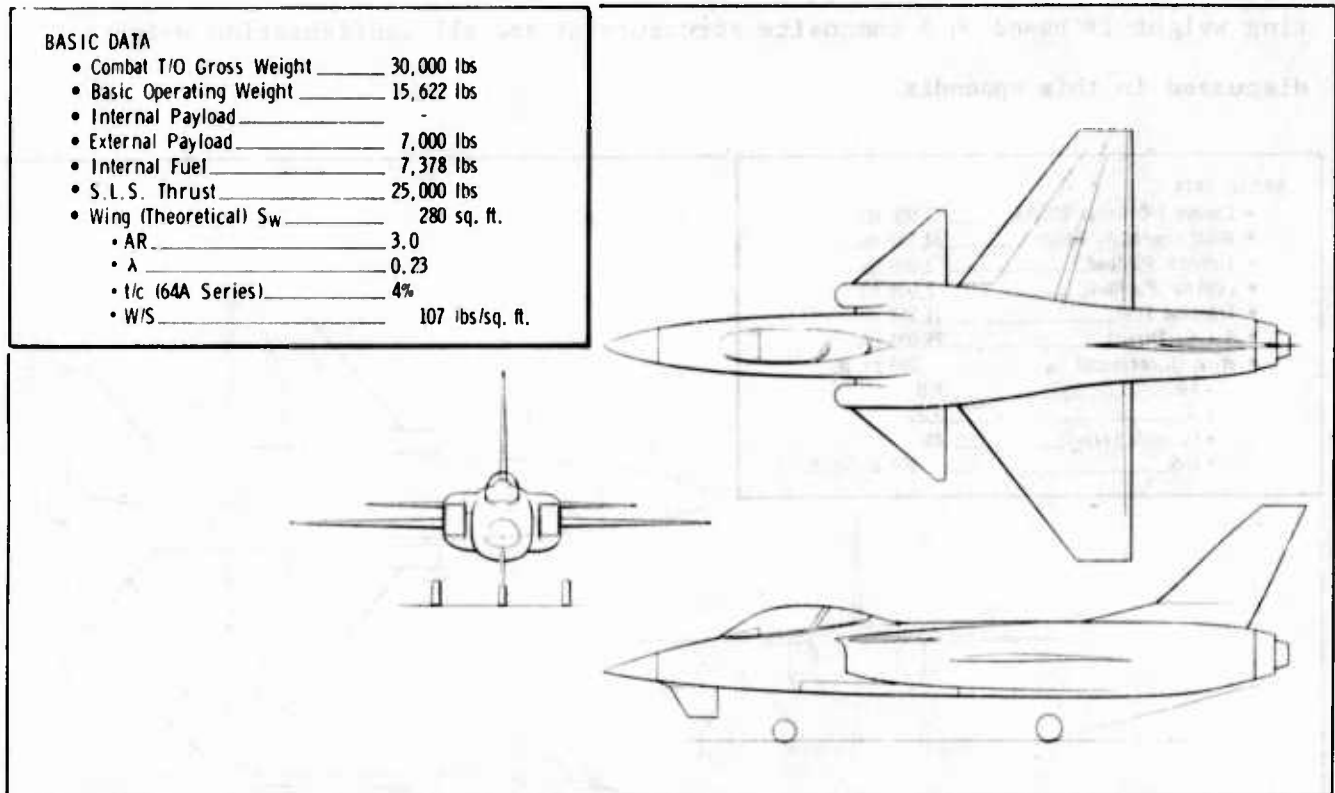


Figure B-21 Close-Coupled Canard Jet Flap Configuration Arrangement

The above configurations reflect somewhat arbitrary selections of engine size, wing loading, aspect ratio, thickness ratio, etc. The purpose of evolving such configurations is to separate workable approaches from unworkable ones before initiating configuration geometry and size studies.

#### B.3.4 GENERAL EVALUATION

The jet flap concept applied to a fighter aircraft does not result in large blowing momentum coefficients compared to those of traditional jet flap approaches. This approach has the effect of minimizing potential gains in lifting capability, which impacts the STOL and instantaneous load factor design objectives.

At moderate lift coefficients and above, the jet flap is a more efficient producer of lift than an unblown wing and potentially can improve sustained maneuver

performance. Another consideration concerning jet flaps for combat maneuvering is the possibility of an expanded buffet envelope. In-flight thrust reverse is one solution to the unanswered problem of excess thrust during landing approach as well as providing for combat decelerations and accelerations.

#### B.4 VECTORED THRUST WITH SUPERCIRCULATION

##### B.4.1 CONCEPTUAL APPROACH

The vectored thrust with supercirculation (VT/SC) concept as generally explained in paragraph A.1.1 is relatively new. The NASA's Langley Research Center

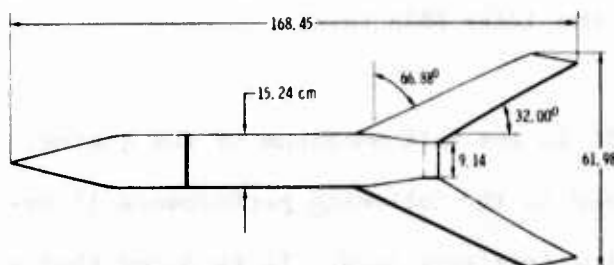


Figure B-22 NASA/Langley's First Vectored Thrust with Supercirculation Wind Tunnel Model

originated the concept and is engaged in an active experimental program. The initial test model consisted of a highly swept, arrow wing planform and a two-dimensional, rectangular nozzle (Figure B-22).

The inherent advantages of VT/SC are the very high  $c_{\mu}$  available, the elimination of internal wing ducting, and the high deceleration and acceleration capability associated with vectored thrust. The only inherent penalty is the weight of the thrust vectoring mechanism; however, the concept poses very special demands on the configuration arrangement, which can, in turn, result in significant penalties.

Convair has found through correlation with the NASA experimental results that the lift augmentation effect of VT/SC corresponds to that of a partial span jet flap. On that basis, the analysis shows similar variations for the parameters  $r$  and  $c_{\mu}$  with jet angle. The low thrust recovery factor for even small jet angles

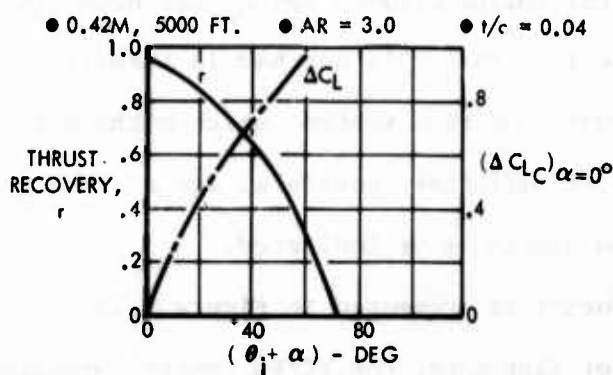


Figure B-23 Vectored Thrust w/Supercirculation Performance is Function of Vector Angle,  $\theta_j$

has been observed in the limited amount of partial span jet flap test data and is attributed to the drag increase from partial span loading. However, the NASA/Langley results indicate significantly higher thrust recovery than that used in these illustrations, and this anomaly is currently being investigated.

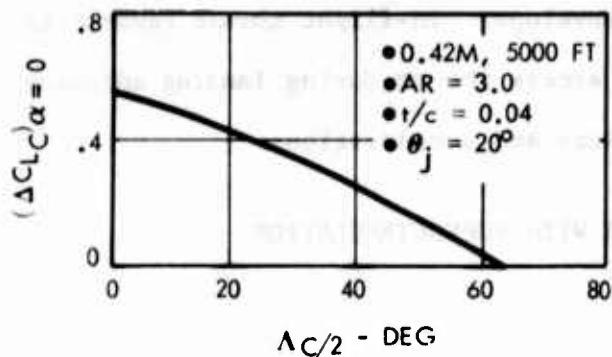


Figure B-24 Wing Sweep-Back Decreases Vectored Thrust w/Supercirculation Effectiveness

#### B.4.2 POTENTIAL PERFORMANCE

The maximum available  $c_{\mu}$  for the VT/SC is the full momentum of the engine. The full engine momentum  $c_{\mu}'$ 's which are used in the following performance illustrations are shown as a function of velocity in Figure B-25. It is noted that a

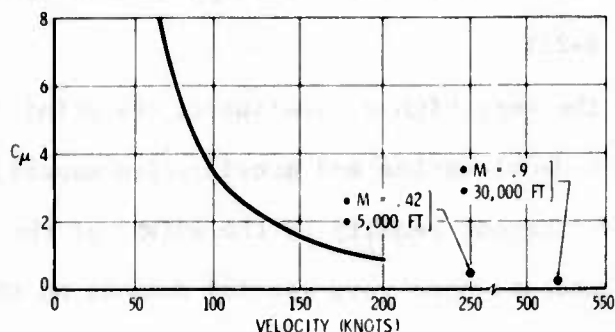


Figure B-25 Available  $C_{\mu}$  Used for VT/SC Performance Evaluation

The latest NASA tests have been conducted with a planform of lower sweep than that used in the initial work, and improved performance was obtained. This is to be expected, since empirical correlations indicate a detrimental effect on supercirculation by sweepback. Circular nozzles were also investigated in the later NASA test.

larger engine is assumed for the low speed maneuver condition than for the landing and high speed maneuver conditions.

With the high  $c_{\mu}$  potentially available for landing, approach speed is expected to be determined by maximum con-

trollable lift rather than actual lift generation capability. However, a landing approach with thrust vectoring at any but very large jet angles or a very low engine power setting poses the same problem as the jet flap, i.e., what to do with the excess horizontal thrust. Throttling the engine reduces the  $c_{\mu}$  and hence the lift increment. Using a large vector angle for landing is not bad in itself; however, it does require a large angle thrust vectoring system, which might not be required otherwise. Short landings appear definitely possible, and a trade between controllability, power setting, and jet angle is indicated.

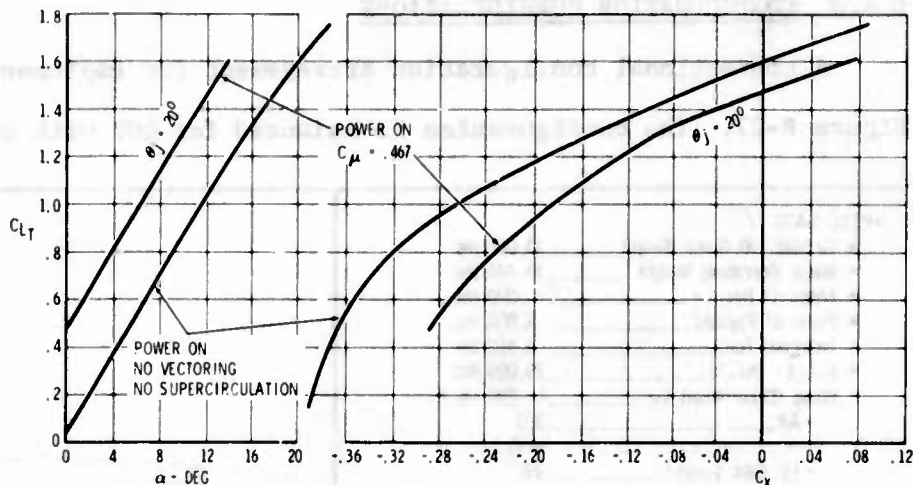
In-flight performance of the VT/SC concept is presented in Figure B-26. Drawing some parallels with the previous jet flap data, the VT/SC concept produces greater lift at a given angle of attack than jet flaps but is less efficient than



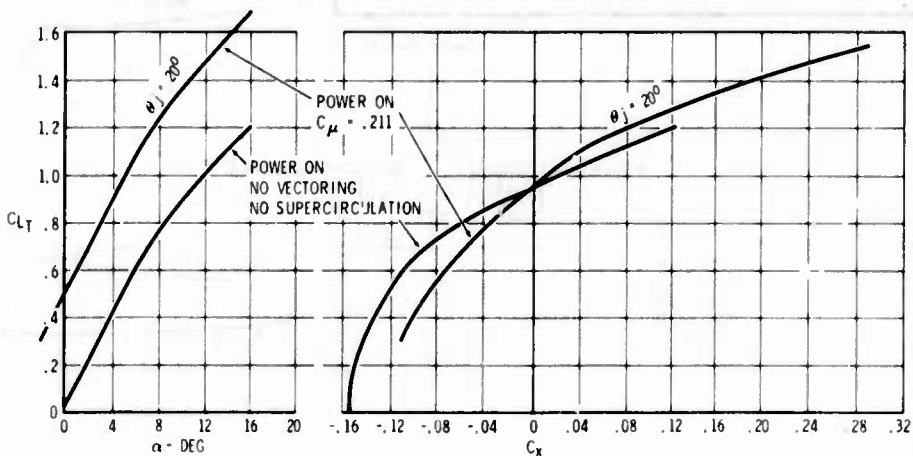
• $R = 3.0$	• $\Delta LE = 40^\circ$	• $S' / S = 0.347$
• $S_{REF} = 280 \text{ SQ FT}$	• $1/c = .04$	
	• VARIABLE I.E. FLAP	

**AERODYNAMIC CHARACTERISTICS**

- $M = 0.42$
- ALTITUDE = 5000 FT

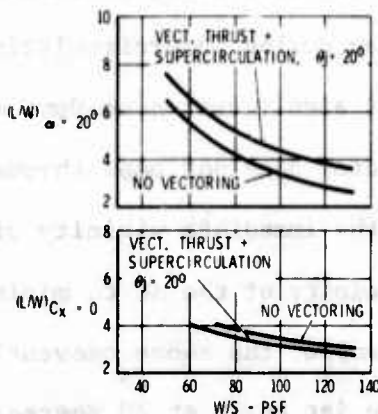


- $M = 0.9$
- ALTITUDE = 30,000 FT

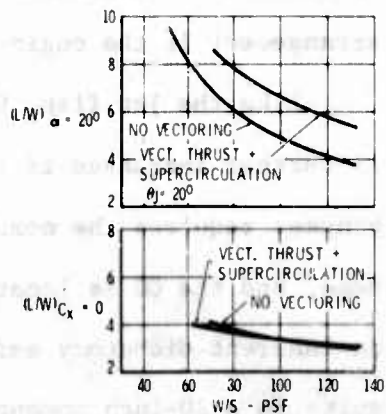


**MANEUVER CAPABILITY**

- INSTANTANEOUS,  $\alpha = 20^\circ$
- $M = 0.42$
- ALT = 5000 FT



- INSTANTANEOUS,  $\alpha = 20^\circ$
- $M = 0.9$
- ALT = 30,000 FT



- SUSTAINED
- $M = 0.42$
- ALT = 5000 FT
- $T_G/W = 1.015$

- SUSTAINED
- $M = 0.9$
- ALT = 30,000 FT
- $T_G/W = .752$

Figure B-26 Vectored Thrust w/Supercirculation In-Flight Performance Potential

an unblown wing except at high speed and high lift coefficients. The prediction obtained indicates the induced drag effect of partial span loading makes VT/SC even less efficient than a standard vectored thrust approach for low speed maneuvers.

#### B.4.3 CONFIGURATION CONSIDERATIONS

A conventional configuration arrangement for implementing VT/SC is shown in Figure B-27. The configuration is balanced for CCV with the CG aft of the AC by

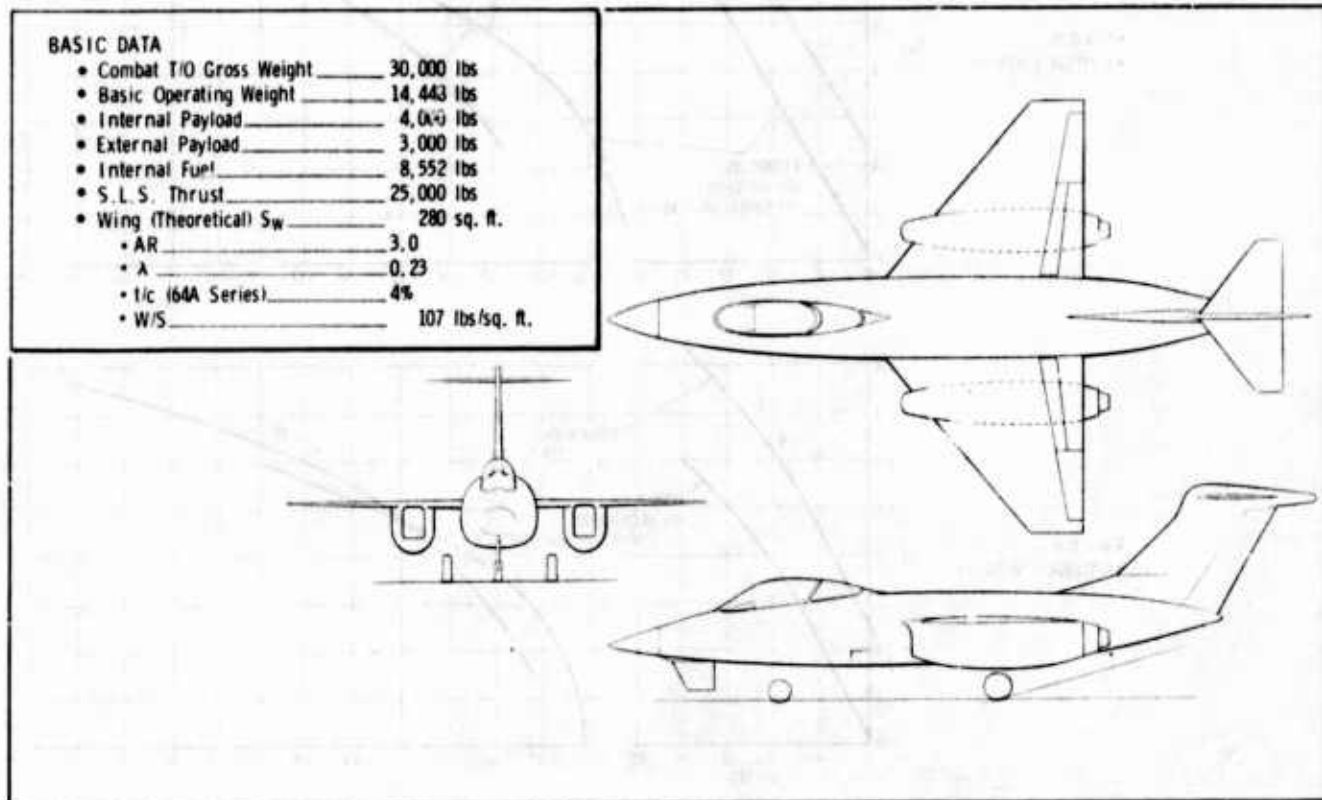


Figure B-27 Conventional VT/SC Configuration Arrangement

approximately 10 percent of the MAC. The overriding concern with this type of arrangement is the engine-out situation during supercirculating operation.

Like the jet flap, VT/SC produces significant nose-down moments. This moment is further increased if the thrust vector does not pass through the CG. The VT/SC concept requires the nozzle to be in the immediate vicinity of the wing trailing edge, and the CG is located in the vicinity of the AC to minimize trim. Therefore, an inherent dichotomy exists. For example, the above conventional arrangement results in a 20-inch moment arm with the jet angle at 20 degrees.

At maneuver speeds and the correspondingly small jet angles which are anticipated, the moment contribution for this degree of offset has a relatively small impact on the trim requirements. However, a combination during landing of low speed and large jet angle does result in significant additional control power requirements.

An M-wing configuration is a possible approach to minimizing the distance between the thrust vector and the AC (and thus, the CG). The arrangement shown in Figure B-28 reduces the moment arm to 12 inches for a 20-degree jet angle. This configuration is also balanced with the CG behind the AC for CCV benefits.

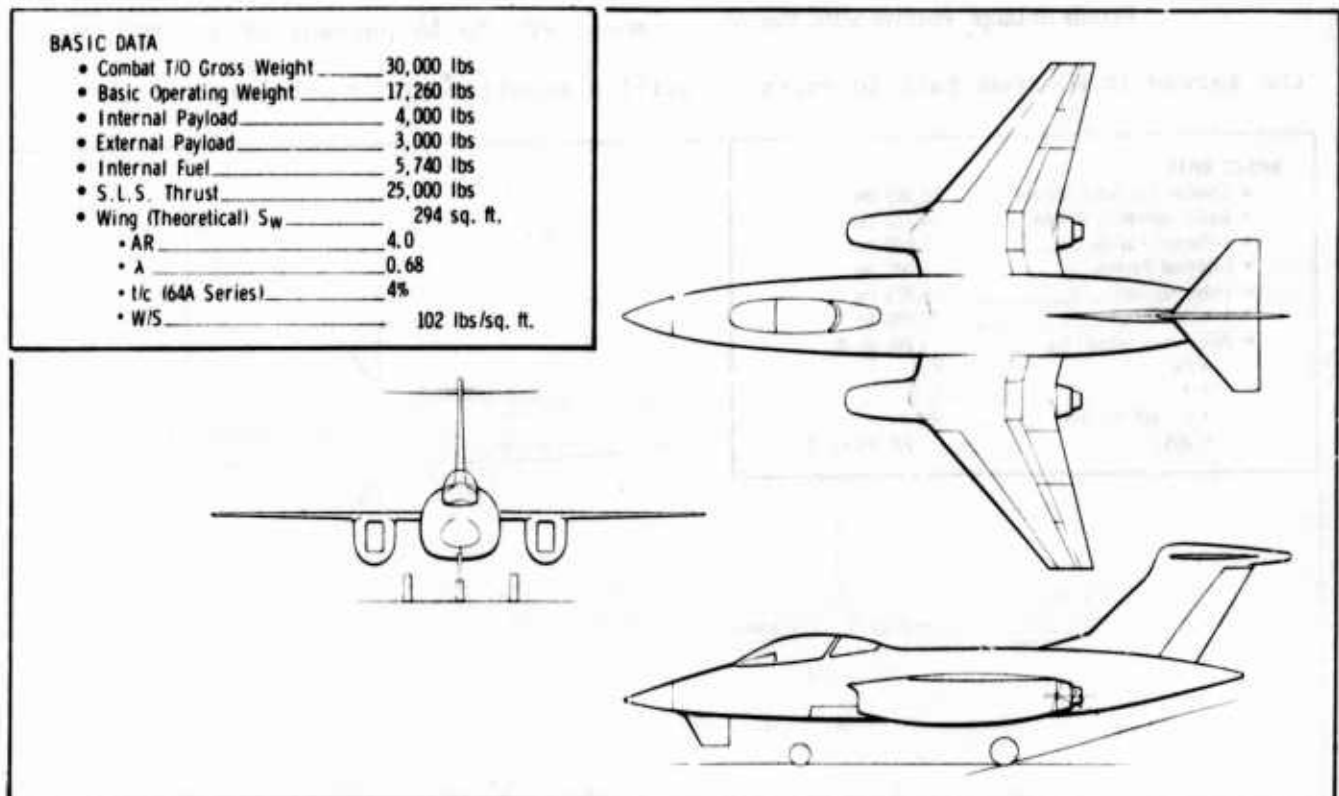


Figure B-28 M-Wing VT/SC Arrangement Reduces Thrust Vector - CG Separation

As for the jet flap, a canard arrangement has some inherent advantages; i.e., the control surface is removed from the downwash, and it becomes a lifting surface. It also allows a centerline propulsion arrangement, thereby alleviating the engine-out roll control problem.

Such an arrangement is shown in Figure B-29. This arrangement also incorporates the features of the jet flap-canard configuration. In analyzing this arrangement, it becomes apparent that the canard approach to VT/SC has an inherent

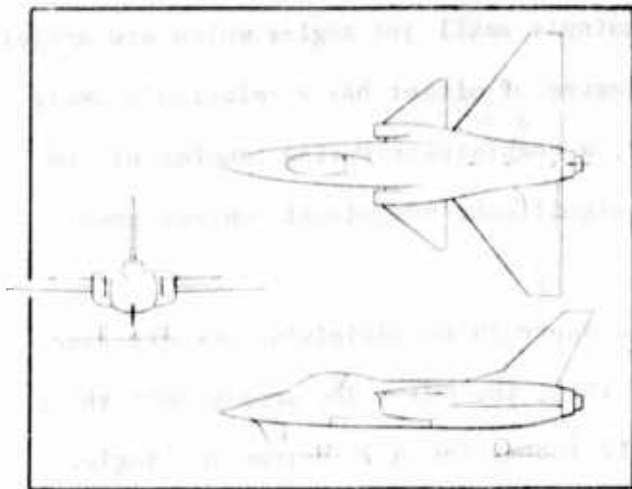


Figure B-29 Close-Coupled Canard VT/SC Arrangement  
Results in Large Positive Static Margin

forward CG location problem. For example, the CG for this configuration when full is at zero percent MAC; when empty, the CG moves forward 17 percent. This is obviously an unacceptable trim situation.

By removing the internal weapons bay and shortening the nose, the above arrangement can be reconfigured as shown in Figure B-30. The full-up CG location is moved aft to 14 percent of the MAC, but

the spread in CG from full to empty is still a significant 13 percent.

#### BASIC DATA

- Combat T/O Gross Weight \_\_\_\_\_ 30,000 lbs
- Basic Operating Weight \_\_\_\_\_ 14,722 lbs
- Internal Payload \_\_\_\_\_ 2,000 lbs
- External Payload \_\_\_\_\_ 5,000 lbs
- Internal Fuel \_\_\_\_\_ 8,278 lbs
- S.L.S. Thrust \_\_\_\_\_ 25,000 lbs
- Wing (Theoretical)  $S_w$  \_\_\_\_\_ 280 sq. ft.
  - AR \_\_\_\_\_ 3.0
  - $\Lambda$  \_\_\_\_\_ 0.23
  - $t/c$  (64A Series) \_\_\_\_\_ 4%
  - $W/S$  \_\_\_\_\_ 107 lbs/sq. ft.

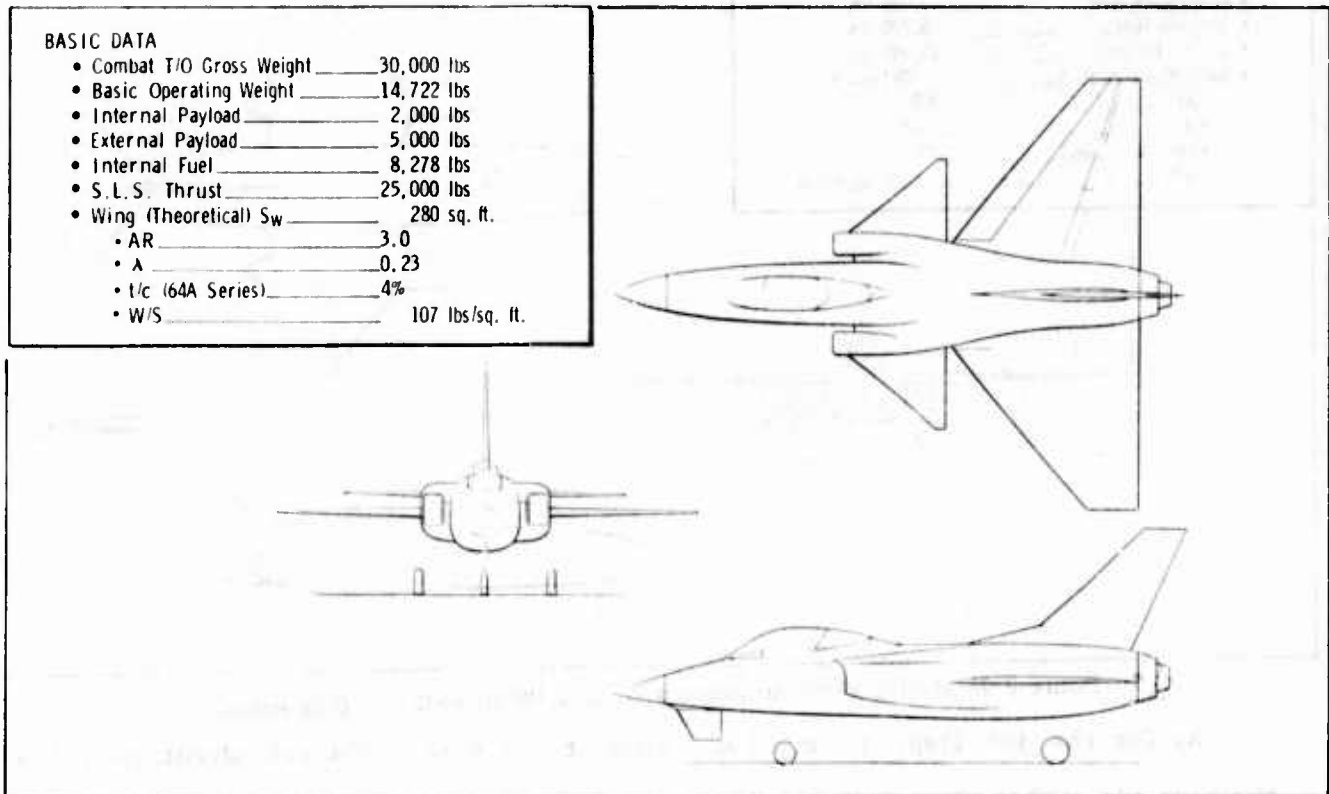


Figure B-30 Removing Weapons Bay Reduces Static Margin for Canard - VT/SC but Still Unsatisfactory

The problem of thrust vector-CG separation is accentuated by the canard approach. For example, the above arrangement has a 38-inch moment arm at the most aft CG location.

An alternative to using the full momentum of the engine is to use only the fan air of a moderate bypass turbofan for blowing (Figure B-31). This approach

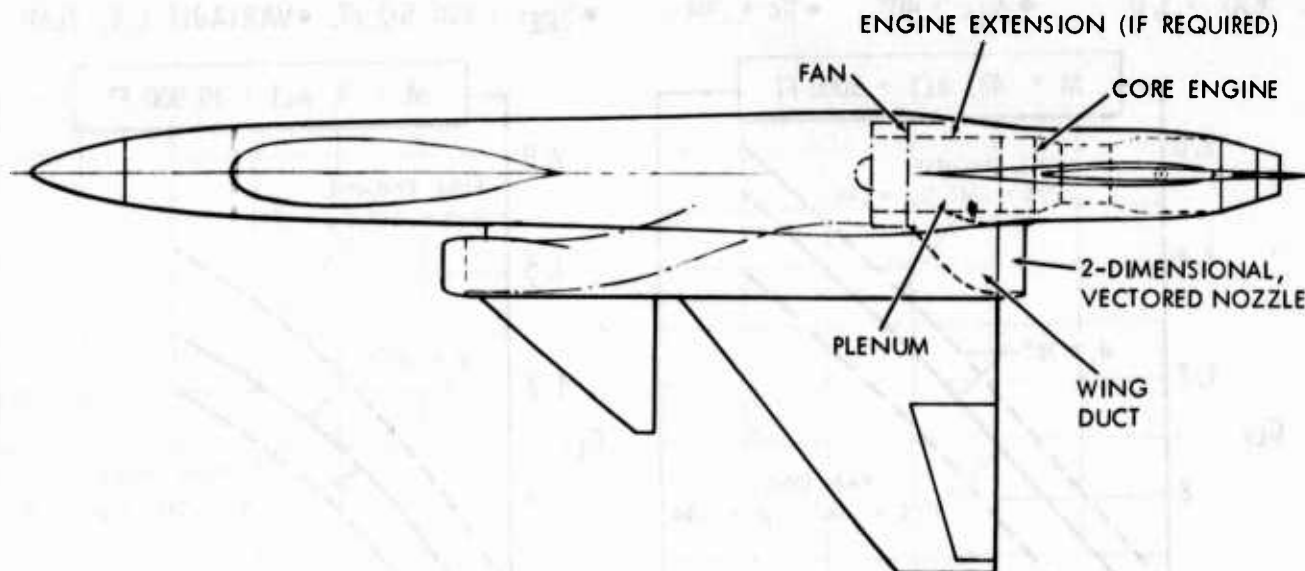


Figure B-31 Fan-Air-Only VT/SC Provides Freedom for CG Location

allows the bulk of the engine weight to be placed aft of the wing trailing edge, which rectifies the nose-heavy situation encountered with the canard configurations described above. Further latitude in CG location is provided by extending the fan drive shaft so that the location of the core engine can be based solely on balance considerations.

The blowing momentum is reduced by about one-half for the bypass ratio 1.5 turbofan engines considered here. Aerodynamic performance comparisons are shown in Figure B-32 for a thrust vector angle of 20 degrees. Although the lift increment is reduced, it is noted that the reduced  $c_{\mu}$  allows a larger trimmable angle for the fan-air-only case if the balance situations are similar. The larger vector angle increases the lift increment, and for the configurations studied here, the trimmable, fan-air-only lift increments are at least as great as the trimmable, full-engine-momentum lift increments.

#### B.4.4 GENERAL EVALUATION

The VT/SC concept is appealing, because it potentially provides large lift increments and deceleration capability with a minimum impact on the propulsion, mechanical, and structural aspects of the configuration. Its potential drawbacks are low thrust recovery and penalizing configuration arrangement requirements. Both problems are subject to alleviation through innovative design approaches.

• AR = 3.0 •  $\Delta LE = 40^\circ$  •  $t/c = .04$

•  $S_{REF} = 280$  SQ. FT. • VARIABLE L.E. FLAP

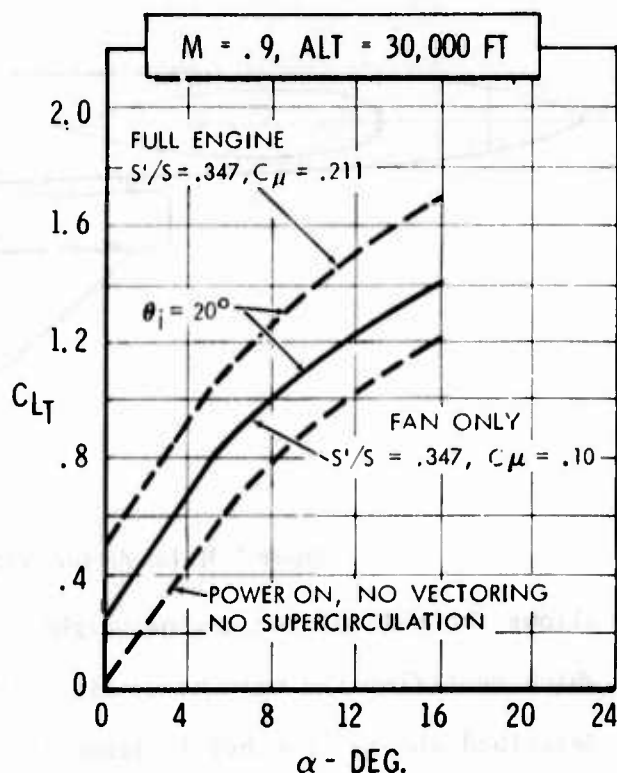
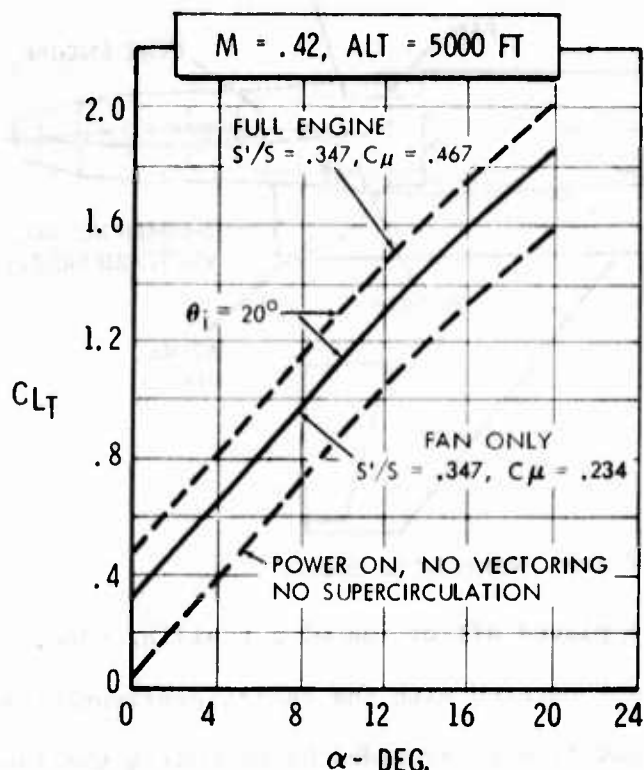


Figure B-32 Fan-Air-Only VT/SC Aerodynamic Performance Potential

## B.5 EXTERNALLY BLOWN FLAPS

### B.5.1 CONCEPTUAL APPROACH

The externally blown flap (EBF) concept is not new and is a favored approach in STOL transport technology. Consideration of EBF for fighters has been restricted, primarily because of concern over (1) blowing flaps with augmented exhaust and (2) engine-out roll control.

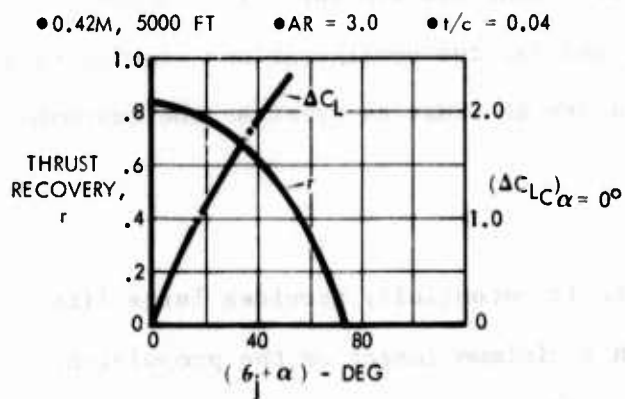


Figure B-33 EBF Performance is Function of Flap Turning Angle,  $\theta$

The effects on EBF performance of jet angle (flap angle, in this case) and sweepback are similar to those of the other supercirculation concepts. For the EBF application to the LWA, a single-slotted flap has been assumed.



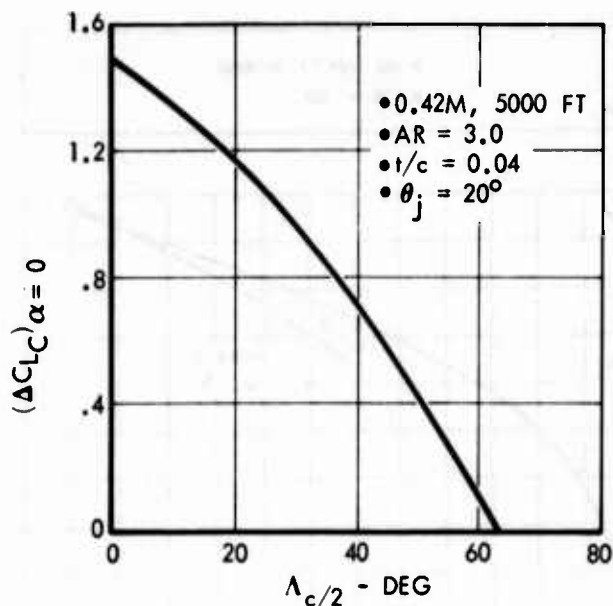


Figure B-34 Wing Sweep-Back Decreases EBF Effectiveness

### B.5.2 POTENTIAL PERFORMANCE

The EBF concept is similar to the VT/SC in that the full engine momentum is the maximum available  $c_{\mu}$ . The values of  $c_{\mu}$  which are used in the EBF performance illustrations are those shown previously in Figure B-25. As noted previously, a larger engine is assumed for the low speed maneuver condition than for the landing and high speed maneuver conditions.

If near full span blowing can be achieved, the performance of EBF is excellent in incremental lift and reasonably efficient. As is the case for VT/SC, short landing performance depends on controllability; and large jet angles and/or low power settings are required in order to minimize excess thrust.

As seen in Figure B-35, the EBF concept is more efficient at very high lift coefficients than an unblown wing. It also has the potential at low lift coefficients of providing rapid, large decelerations. The overriding potential advantage of EBF is, however, a very large instantaneous lift capability.

### B.5.3 CONFIGURATION CONSIDERATIONS

The configuration arrangement constraint of a fixed relationship between the engine nozzle and the wing trailing edge, which is encountered with the VT/SC concept, also exists for EBF. The difference is that, for EBF, the nozzle must be forward of the trailing edge, which tends to worsen the forward CG location problem. The arrangement shown in Figure B-36 has an essentially coincident AC and CG, and the full benefits of CCV cannot be realized.

By placing the CG as far aft as it is in the configuration shown in Figure B-36, the aerodynamic performance is compromised. The inlet ducts are shorter than desired resulting in a low nacelle fineness ratio and marginal inlet performance at super-

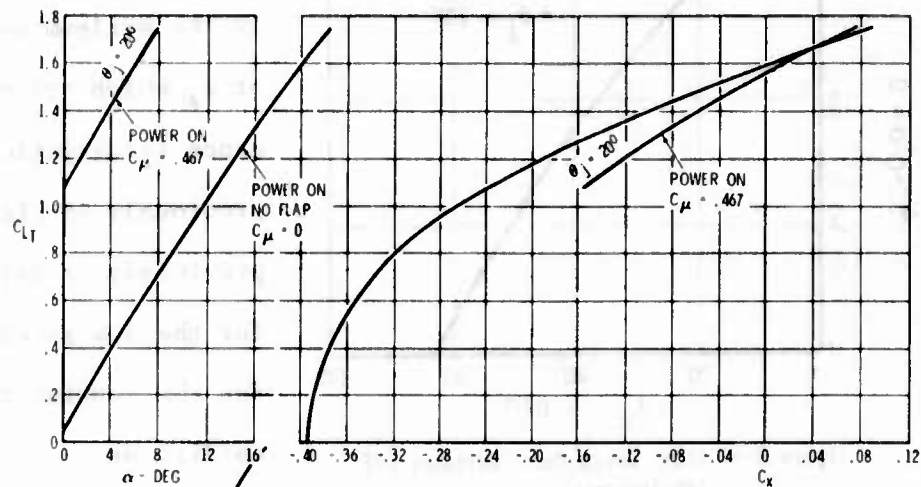
- $M = 3.0$
- $S_{REF} = 280 \text{ SQ FT}$

- $\Delta LE = 40^\circ$
- $t/c = .04$
- VARIABLE I.E. FLAP

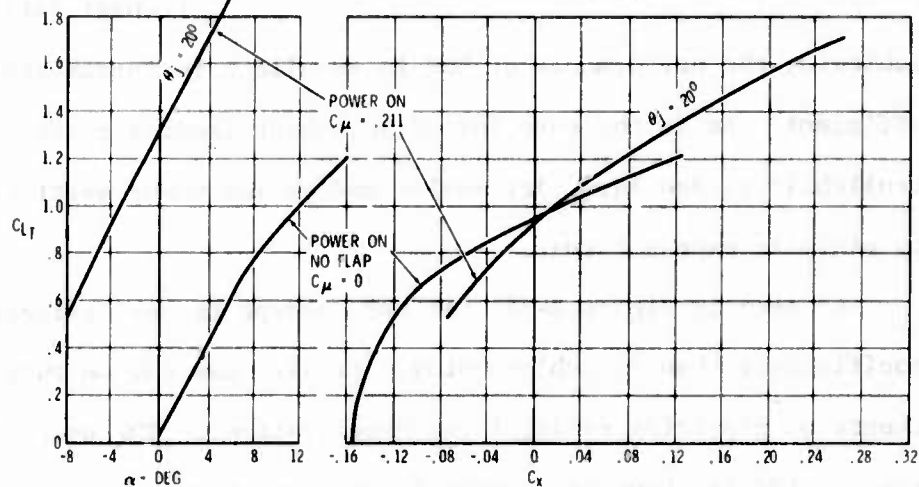
- FULL SPAN T.E. BLOWING
- $S'_{1/5} = .635$

#### AERODYNAMIC CHARACTERISTICS

- $M = 0.42$
- ALT = 5000 FT

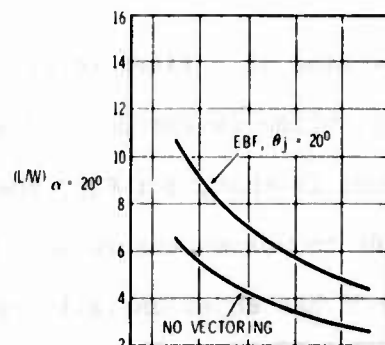


- $M = 0.9$
- ALT = 30,000 FT

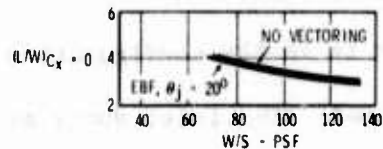


#### MANEUVER CAPABILITY

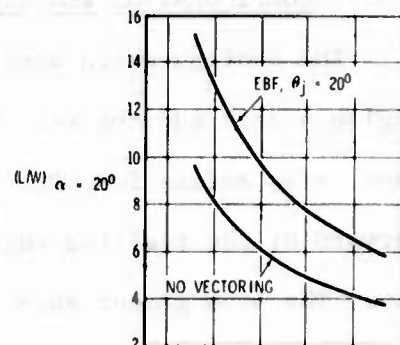
- INSTANTANEOUS,
  - $\alpha = 20^\circ$
  - $M = 0.42$
  - ALT = 5000 FT



- SUSTAINED
  - $M = 0.42$
  - ALT = 5000 FT
  - $T_G/W = 1.015$



- INSTANTANEOUS,
  - $\alpha = 20^\circ$
  - $M = .9$
  - ALT = 30,000 FT



- SUSTAINED
  - $M = 0.9$
  - ALT = 30,000 FT
  - $T_G/W = .752$

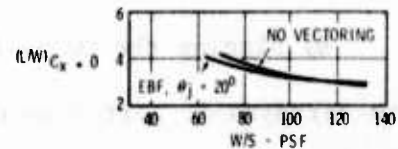


Figure B-35 EBF In-Flight Performance Potential

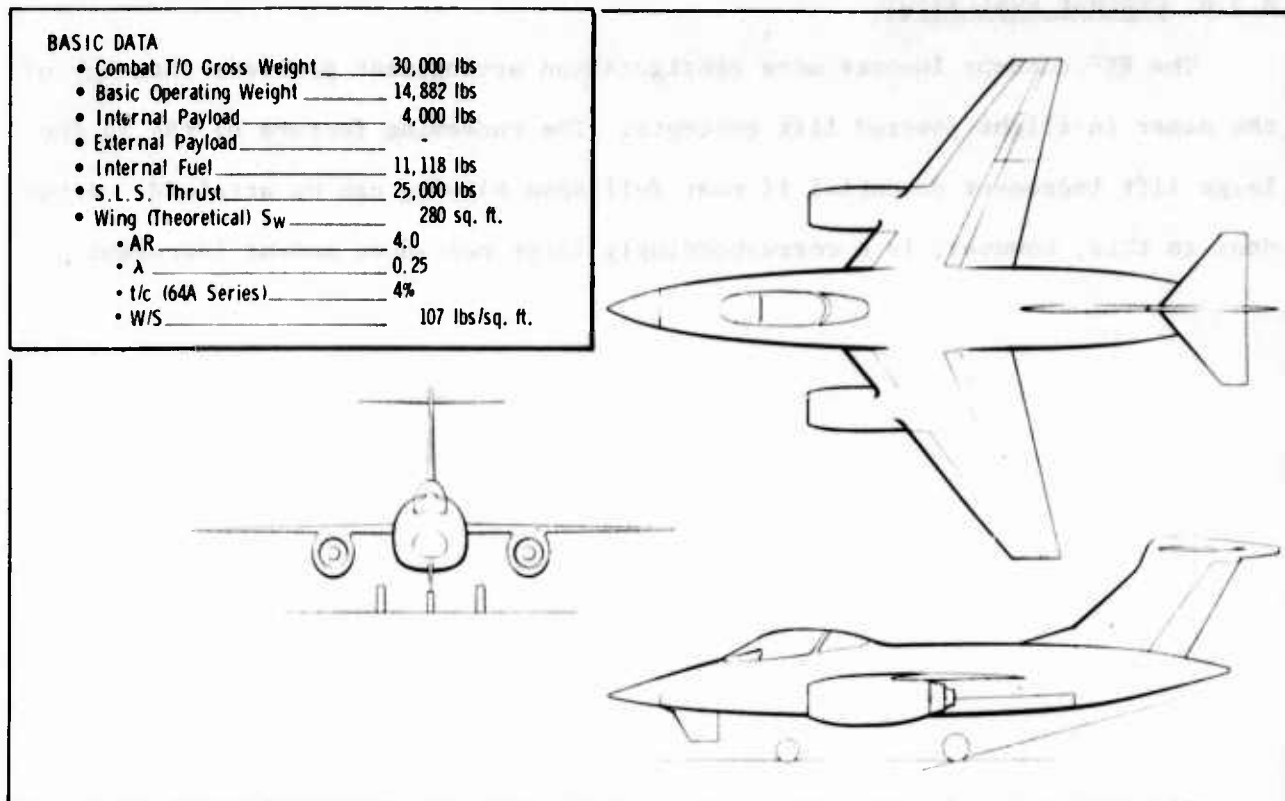


Figure B-36 Conventional EBF Configuration Arrangement

sonic speeds (Figure B-37). The engine is moved further aft than desired resulting in less span blowing than is possible otherwise. Finally, the nacelle is

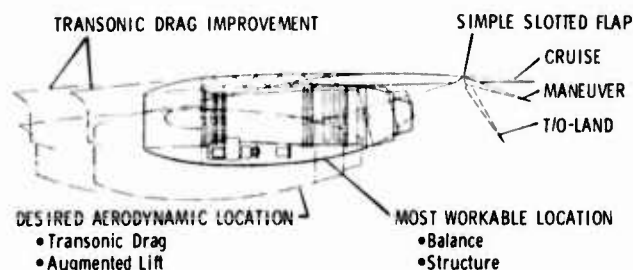


Figure B-37 Desired Engine/Wing Location for EBF Compromised by Required Aft Shift of CG

moved up under the wing both to minimize the required nozzle vectoring angle and to eliminate the need for a pylon. This also reduces the extent of the span being blown.

Several canard approaches to EBF arrangements have been attempted, but all exhibit the same forward CG location problem associated with the VT/SC concept, but to a greater extent. An approach of stacking engine, wing, and fuselage in a P-38, twin-boom-type arrangement promises a workable balance situation but results in unsatisfactory transonic and supersonic characteristics.

#### B.5.4 GENERAL EVALUATION

The EBF concept imposes more configuration arrangement problems than any of the other in-flight powered lift concepts. The redeeming feature of EBF is the large lift increment potential if near full span blowing can be attained. Attendant to this, however, is a correspondingly large nose-down moment increment.

APPLICATION OF ADVANCED  
COMPOSITE MATERIALS TO  
FIGHTER AIRCRAFT STRUCTURE

The high specific strength and stiffness of unidirectional graphite and boron composite materials coupled with their tailorability for specific conditions permit the design of aircraft structural configurations which are not practical with conventional metals. Structural component weight savings of 25 to 35 percent are possible by proper application of advanced composite materials.

The use of advanced composites for aircraft structures has been limited to material substitution or metal reinforcement of selected components. No new aircraft have been designed and built to obtain full advantage of composites technology. The reasons are several. Material costs are very high; the technology is relatively new and confidence is lacking; low cost fabrication and tooling methods must be proven; and a different design methodology is required. However, the potential payoffs in both performance and cost justify continuing emphasis on composites development, and the next logical step is a prototype aircraft.

#### C.1 DESIGN AND FABRICATION

There are several general design and fabrication guidelines for composites. Highly loaded mechanical joints are to be avoided because of the brittle nature of composite materials. Large area, fully inspectable components are desirable. Simultaneous curing and assembling of detail parts reduces processing time and fit problems. Designing for filament dominated load response, rather than mechanical joints, increases the fatigue life of the structure. Through-the-body wing and empennage carry-through structures are preferable to full-chord root splices.

##### C.1.1 WING

The level of structural efficiency achieved in composite wing design as compared to conventional metals is a function of the wing geometry. High aspect

ratio, large area, thin wings are structurally practical with composites and offer obvious aerodynamic advantages on a high performance fighter.

For this type of wing, the most efficient structural arrangement is to put the primary load bearing material in the wing skins. The results are thick wing skins which are tailored to meet the aeroelastic constraints of flutter and divergence. Full-depth sandwich construction is a good choice for this type of wing configuration (Figure C-1).

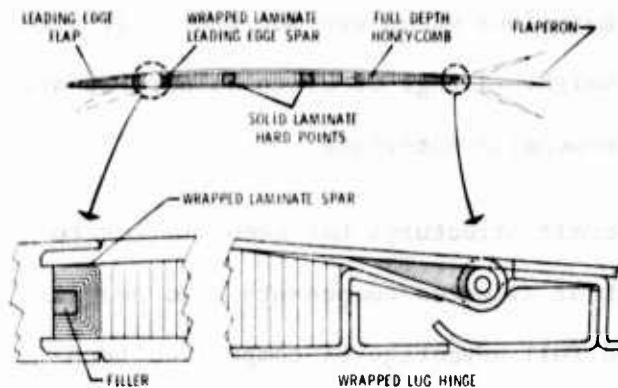


Figure C-1 A Thin, Composite Wing Might be Full Depth Sandwich Construction

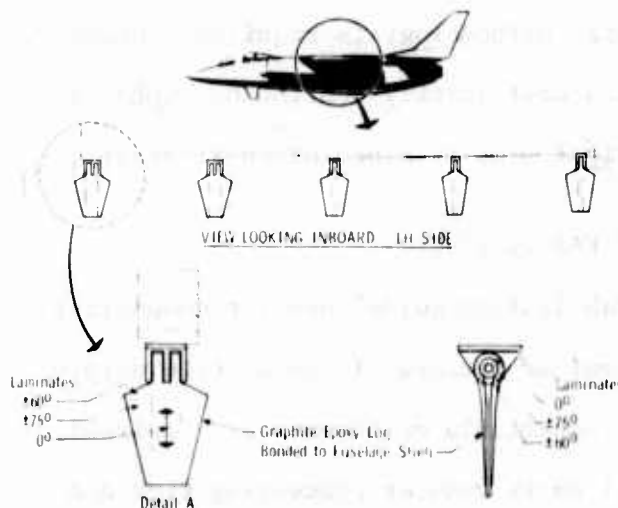


Figure C-2 Wing/Fuselage Joint can Use Fail-Safe Lug Fittings

The wing box is manufactured in one piece from tip-to-tip yielding a simplified, automated lay-up and thereby a low-cost component. Hard points for stores and other attachments are provided by simply replacing the honeycomb core with buildups of laminate material.

A composite wing can be designed for damage tolerance and fail-safety by incorporating crack arresting buffer strips in the skins.<sup>1</sup> With a high wing configuration, multiple-lug, fail-safe fittings appear practical for use in attaching the wing to the fuselage (Figure C-2).

Through the use of an aeroelastic synthesis procedure, the wing skin material distribution that simultaneously satisfies strength, flutter speed, and static aeroelastic constraints is defined. A typical distribution is shown in Figure C-3. A skin efficiency of 2.7 times that of aluminum has been achieved.

<sup>1</sup> See Section A.1.4.3.



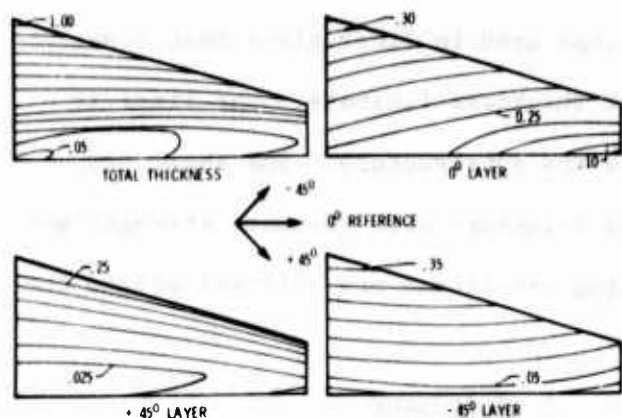


Figure C-3 Optimized Composite Laminate Design for a Particular Wing Geometry

### C.1.2 FUSELAGE

Several viable concepts for composite fuselage structures have been defined. Three of these concepts are (1) sandwich-shell, (2) strong-back, and (3) shell-liner (Figure C-4). The sandwich-shell concept makes use of composite-faced honeycomb sandwich panels to form the outer shell and utilizes both solid laminate and sandwich bulkheads and frames. The sandwich-shell concept has been used in component substitution applications and is considered current technology.

The strong-back fuselage structure concept places the primary load-bearing material in the inlet duct and nacelle structure where a minimum number of penetrations are required for access to systems and equipment. The outer shell of the fuselage is a simple aerodynamic fairing. The major disadvantage of this concept is the low efficiency due to placement of structure near the neutral axis of the beam.

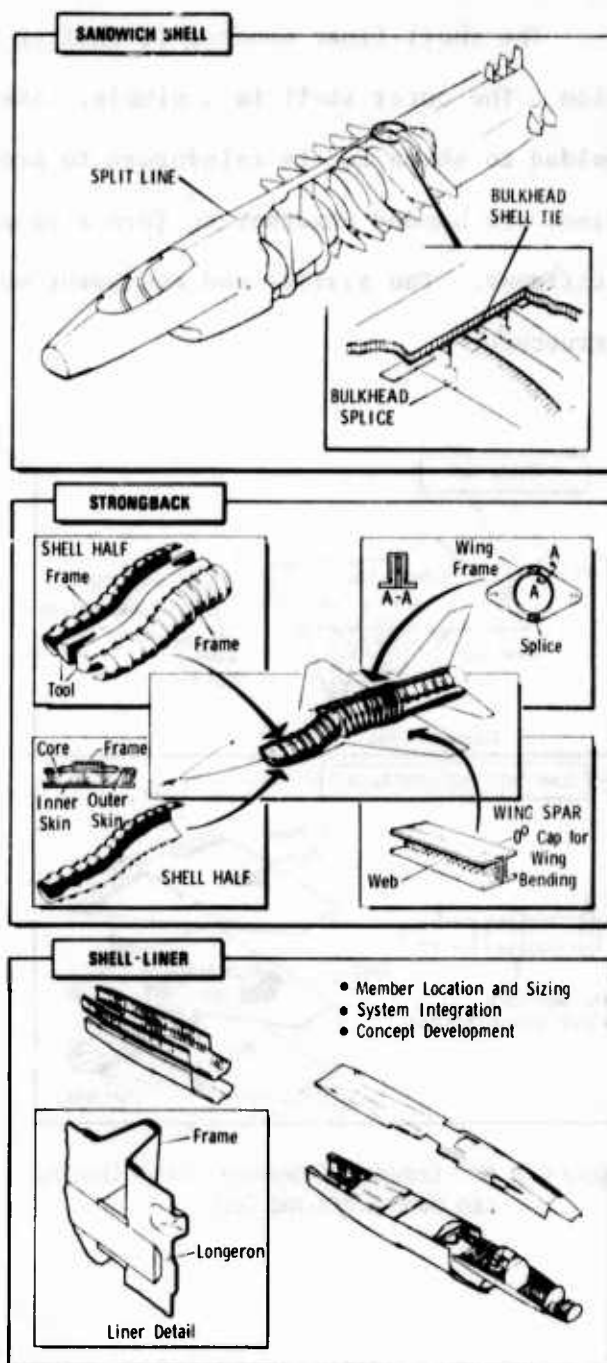


Figure C-4 Several Structural Concepts Exist for a Composite Fuselage

The shell-liner concept is similar to that used in fiber glass boat construction. The outer shell is a simple, constant thickness laminate. The liner is molded to shape and is reinforced to provide the substructure. The shell and liner are bonded together to form a complete structure with adequate strength and stiffness. The systems and equipment mounting provisions are integral within the structure.

### C.1.3 EMPENNAGE

Several fighter aircraft have been designed and flown with advanced composite horizontal and/or vertical tails. These designs have resulted in weight savings and are considered state-of-the-art designs. New concepts that offer increased savings in weight and cost have been defined (Figure C-5).

The objective of these new concepts is to avoid intense load transfer joints at the root chord. In addition, fewer and simpler parts are employed, and additional weight and cost savings are obtained.

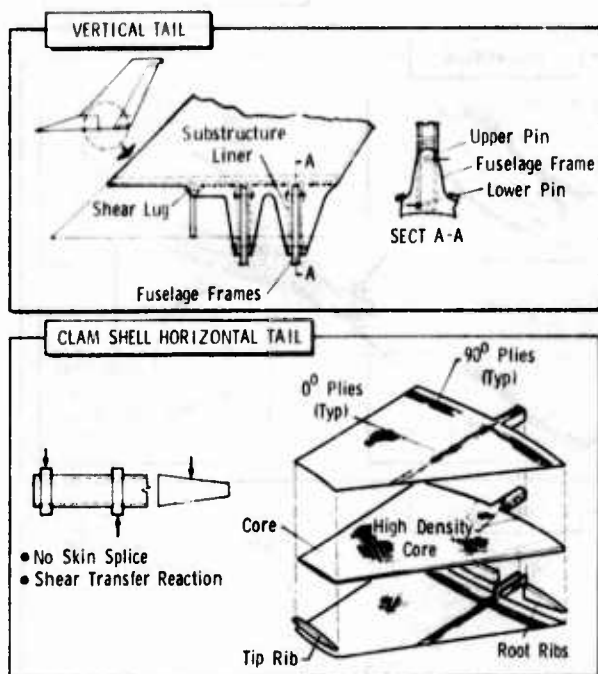


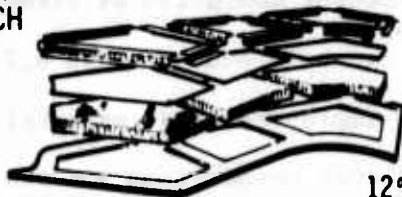
Figure C-5 New Composite Empennage Design Concepts can Save Weight and Cost

### C.2 COST

Advanced composites provide cost-effective airframe components. A recent case in point involving an F-111 part is summarized in Figure C-6.

The use of composites in a total airframe offers potential cost improvements in three areas: (1) lower fabrication cost, (2) reduced operating cost, and (3) reduced quantities of airframes needed to achieve the required function. Lower fabrication costs can be achieved with composites by using simpler parts, fewer parts, less tooling, and lower cost tooling. Assembly cost is also reduced because of the fewer and simpler parts.

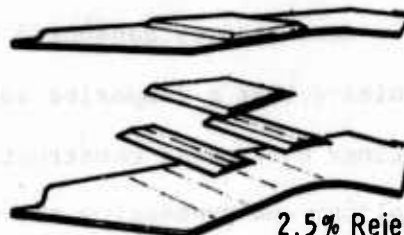
# ALUMINUM SANDWICH



12% Rejection

	OPERATION	QTY	NO. STEPS	MAN HOURS
1	OUTER SKIN	1	13	4.8
2	INNER SKIN	3	4	.5
3	CORE	3	11	2.0
4	EDGE MEMBERS	11	11	1.7
5	PREFIT		13	2.4
6	CLEAN		6	1.5
7	ASSEMBLE		14	3.3
8	BOND		13	2.2
9	POST BOND		6	1.6
10	INSPECTION		5	1.3
11	FINISH		7	2.3
12	TRIM			3.0
13	DRILL			5.0
	SUBTOTAL			31.60
	LABOR COST @ \$13.00			410.80
	MATERIAL COST			12.50
	TOTAL			\$ 423.30

# GRAPHITE SANDWICH



2.5% Rejection

	OPERATION	QTY	NO. STEPS	MAN HOURS
	OUTER SKIN	1	2	.3
	INNER SKIN	1	2	.3
	CORE	1	2	.3
	DOUBLERS	2	3	.2
	ASSEMBLE		7	2.6
	BOND		1	2.0
	POST BOND			.4
	INSPECT		1	1.0
	DRILL		1	.5
	SUBTOTAL			7.6
	LABOR COST @ \$13.00			98.80
	MATERIAL COST			258.00
	TOTAL			\$ 356.80

Figure C-6 Cost Comparison for an F-111 Part Shows Composites can be Lower Cost than Aluminum

Composites effect a reduction in operating cost by improving the service life (composite laminates do not fatigue crack like metal). They are easy to re-pair, corrosion-resistant, and less subject to damage. Operating cost savings have been substantiated by flight experience on the F-111 horizontal tails, wing trailing edge panels, and main landing gear door.<sup>1</sup>

A third area where composites can result in lower cost is in the reduced quantities of airframes needed to do a specific job. That is, an advanced composites aircraft offers increased mission performance and less out-of-commission time for maintenance than a conventional metal aircraft, which means fewer airplanes to do an equivalent job.

<sup>1</sup> "Maintainability Aspects of Composite Structures," Convair Report ERR-FW-1218, December 1971.

Cost studies conducted by Convair during a recent composite airframe study indicate that a composite substitution airframe can be produced at an 8.7 percent savings over metal construction provided certain improvements in material costs, tooling, and processing are achieved.<sup>1</sup> Itemized cost comparisons and sensitivities to the primary cost parameters are shown in Figure C-7.

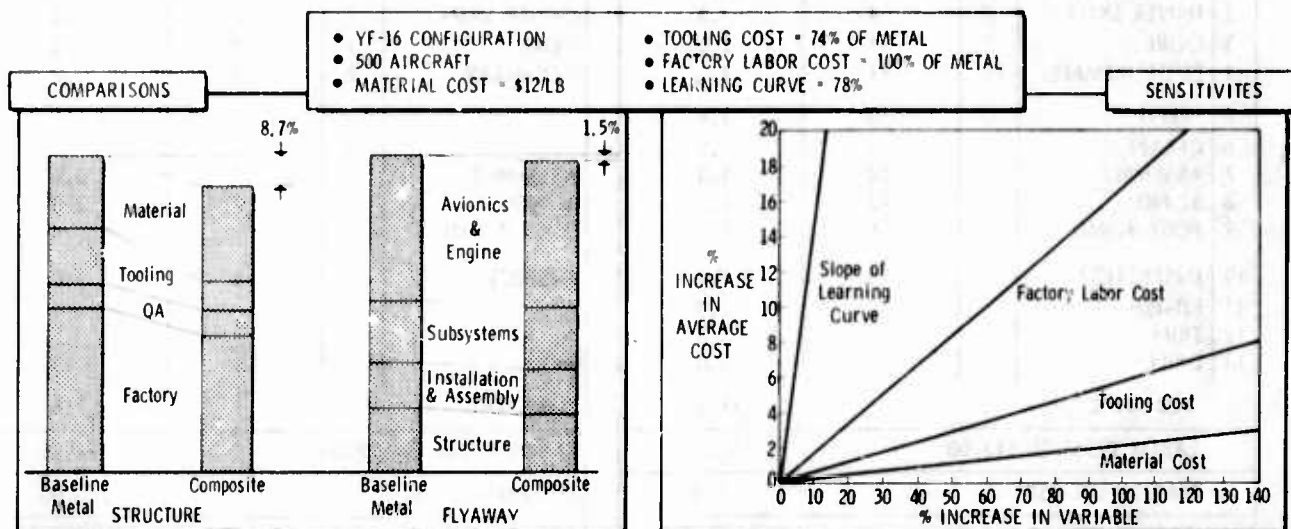


Figure C-7 Studies Show Composites to be Cost Competitive on Simple Material Substitution Basis

Recent developments in the application of composite technology indicate near-term improvements in weight and cost savings, but improvements are dependent upon simplified design concepts and airframe configurations that afford efficient utilization of advanced composites. Research is being done to identify and verify low-cost composite structures for airframes. If one assumes that the planned programs are moderately successful, then composite construction costs should be equivalent to metal construction costs by the 1975-1977 time period.

<sup>1</sup> "Conceptual Design of Advanced Composite Airframes," Report AFML-TR-73-4, February 1973.

### C,3 ADVANCED COMPOSITE AIRPLANE DEVELOPMENT

A near-term prototype is needed to determine the performance, functionability, and cost of an advanced composite airplane. The objective of such a prototype program is to develop the data base for possible production aircraft.

A composite prototype airframe can be fabricated with low cost temporary tooling and will be more easily modified than a metal airframe. These features tend to lower the cost of the prototype and increase its utility for technology development.

## A P P E N D I X D

### L W A C O N F I G U R A T I O N 2 9 E V O L U T I O N

#### A N D J U S T I F I C A T I O N

The selection of LWA Configuration 29 for validation with man-in-the-loop simulation is the result of a four-step technical approach: (1) assessment and, where necessary, development of technology and operational concepts; (2) establishment of basic configuration characteristics which are not subject to tradeoff; (3) development of reference configurations which reflect different technology approaches; and (4) quantification of mission/configuration tradeoffs.

Appendices A through C cover the results of the first step. This appendix is addressed to the last three steps and to the rationale that led to selection of LWA Configuration 29 for man-in-the-loop simulation.

#### D.1 NON-PARAMETRIC CONFIGURATION CHARACTERISTICS

A number of issues which are not, for one reason or another, included in the present mission/configuration tradeoffs are significant factors in developing the basic LWA configuration. From the standpoint of parametric aircraft performance impact, the alternatives in this category are second order, but, in some cases, they are very important to the total weapon system concept.

These issues and the tradeoffs involved are discussed below. In addition, rationale for the LWA configuration approach is provided and supported by tradeoff data when possible. In many cases, results from previous studies and experience are used rather than "reinvent wheels." The configuration areas covered include the following: armament/avionics, crew station, propulsion, control surfaces, and the -ilities.

##### D.1.1 ARMAMENT/AVIONICS

The LWA is first and foremost an air-to-ground weapon delivery system par excellence. It seems evident that future standards will be set by the weapons themselves and the associated delivery systems. Thus, the aircraft's primary objectives are to survive the threat and to accommodate the weapons and systems (in addition, of course, to delivering the weapons at a desired location and time).



The proper integration of modern armament and avionics is central to the success of the LWA concept. Without the ability to carry, protect, and release the desired weapons over a broad Mach/altitude regime, full use of the LWA improved airframe performance and thus the sought-after improvements in survivability and effectiveness cannot be obtained.

The objective of properly accommodating weapons and systems when taken in context with the LWA ground rule of a lightweight, inexpensive aircraft presents a traditional dichotomy. The armament and avionics concepts incorporated in the LWA configuration design are believed to offer new solutions to old problems.

#### D.1.1.1 Armament Concept

The LWA armament concept began with selection of the candidate weapons. The candidates selected are expected to be available in the post-1980 time period.

##### D.1.1.1.1 Air-to-Ground

An important activity with regard to future air-to-ground bombs and missiles is the Modular Weapons Study (Figure D-1). This program has far-reaching implications as to the ultimate success of weapons integration with a high performance aircraft.

The impact on the LWA concept of guided weapons, particularly those developed in recent years, is great. The effect of accuracy on the payload requirements of an aircraft tasked to kill a point target is shown in Figure D-2. It is clear that these "smart" weapons, which have reported CEP capabilities of less than 15 feet, can be traded for aircraft size.

• MODULAR WEAPONS STUDY MATRIX					
Warhead Type/Wt, lbs/ft	Unguided Class I	Guided Class I	Guided Class II	Guided Unpowered Class III	Guided Powered Class III
• H. E. /800/1	✓	✓	✓		✓
• H. E. /1500/2a	✓	✓	✓		✓
• CLUSTER/800/2b	✓	✓	✓		
• HE/2000/3a	✓	✓	✓	✓	
• NAPALM/700/3b	✓	✓	✓		
• H. S. M. /1700/3c			✓		
• CLUSTER/2000/4	✓	✓		✓	
• S. O. C. /1500/5	✓	✓			✓
• S. O. C. /2200/6a	✓	✓		✓	
• FLAME/1375/7	✓	✓			

• CLASS I	Free Fall
• CLASS II	Powered to Provide 10 n. mi. Standoff at 5 K ft
• CLASS III	
	• Powered - 100 n. mi. to 200 n. mi. (60 K ft) Standoff
	• Unpowered - 70 n. mi. Standoff at 60 K ft

• GUIDANCE CONCEPTS	
• Laser Semi-Active	• EO Area Correlator
• EO Contrast Seeker	• Microwave Radiometer
• IR Imaging Seeker	• Radiometric Area Correlator
• Auto Radiation Seeker	

Figure D-1 Modular Weapons are Important to LWA Air-to-Ground Flexibility

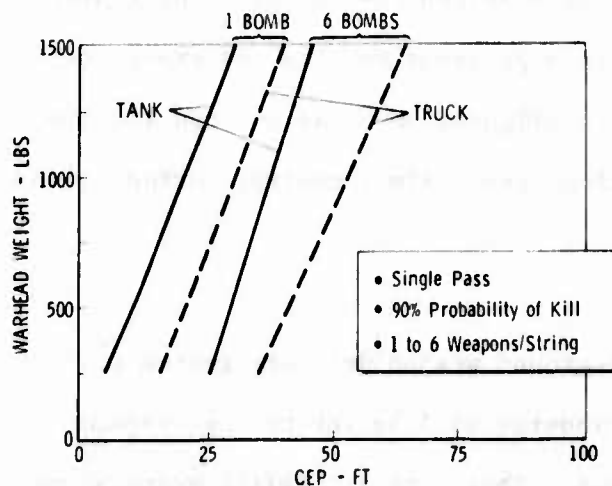


Figure D-2 Smart Bomb Technology Decreases Payload Requirements

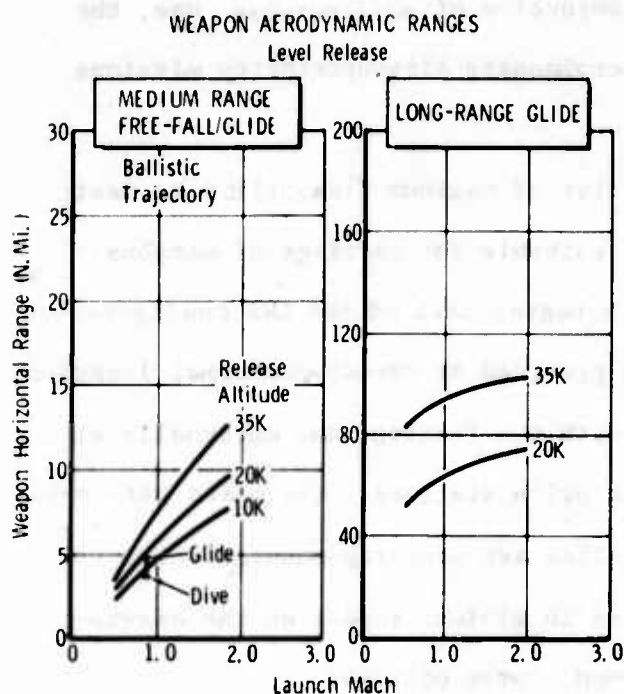


Figure D-3 LWA can be an Effective Booster for Unpowered Stand-off Weapons

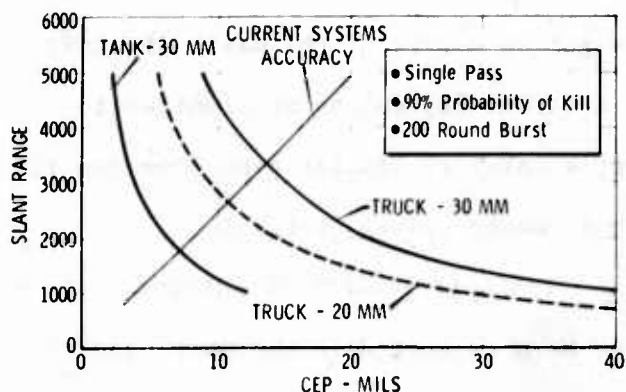


Figure D-4 Choice of Gun Caliber for LWA is Tradable

The need for standoff weapons against certain targets is evident now and is expected to become more imperative in the future. The Convair ATF studies show that an unpowered glide bomb that is boosted by a carrier aircraft can have very significant range (Figure D-3). The supersonic capability of the LWA offers this potential delivery mode, and the weapons carriage approach is consistent with requirements for release and separation at supersonic speeds (although this is a major question requiring development).

For some aspects of the LWA mission concept, a ground attack gun is a likely weapon. The primary question at this point is what caliber of gun is required, because the different calibers available result in greatly different configuration requirements. Data such as shown in Figure

D-4 indicate that the lethality of the smaller caliber guns is not significantly different from that of higher calibers against soft targets. Also, the higher caliber guns require better than state-of-the-art aiming accuracy for realistic attacks against defended hard targets.

#### D.1.1.1.2 Air-to-Air

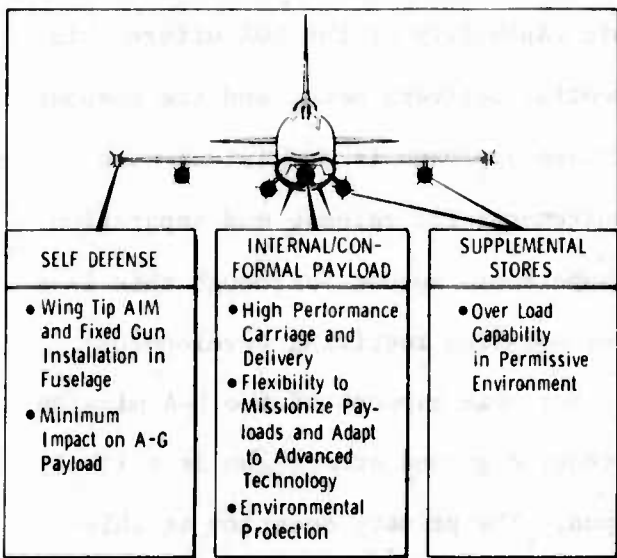
The basic LWA air-to-air armament complement is considered in the context of self-defense. The primary weapon is an IR homing AIM-9 or AIM-84 class missile. The gun discussed above also serves as an air-to-air weapon.

Radar homing air-to-air missiles such as the AIM-7 or AIM-47 are compatible with the LWA carriage concept, but supporting avionics are not included in the

basic system. However, in keeping with the objective of multipurpose use, the LWA attack radar includes a growth mode to accommodate air-superiority missions.

### D.1.1.1.3 Stores Carriage

In consonance with the LWA design objective of maximum flexibility to meet future missions and threats, an internal bay suitable for carriage of weapons, avionics, and/or fuel is incorporated as an integral part of the LWA configuration (Figure -5). Additional weapon carriage is provided at pseudo-conformal locations







beneath the fuselage and externally at wing pylon stations. The basic air-to-air missiles are wing-tip-mounted which results in minimum impact on the air-to-ground stores options.

The LWA configuration approach incorporates a fuselage-mounted M-61 20mm gun as a part of the basic aircraft. The internal bay can be missionized to carry a GAU-8 or similar type 30mm gun if such a weapon proves desirable.

Figure D-5 LWA Stores Carriage is Keyed to Flexibility

D.1.1.1.3.1 Internal Carriage Rationale. Tradeoff studies of internal versus conformal versus external stores carriage have been conducted in the past, and the results have not consistently shown large advantages for any of the three. For example, Convair's ATF studies indicate wide variations depending on the mission and payload assumptions (Figure D-6).

For a high performance ground attack fighter, it seems clear that either internal or conformal carriage is desirable. Since the conformal approach does not result in significantly smaller configurations than internal carriage, the greater flexibility potentially offered by internal carriage argues for its selection.

CONFIGURATION CONCEPT		 Internal Clip-in Pallet (Baseline)	 Conformal Pallet Low-Drag Store (2 KMU 351)	 Pylon- Mounted Low-Drag Store (2 KMU 351) (Pylons Retained)	 Pylon- Mounted High-Drag Store (8 MK 82's) (Pylons Retained)	
RESIZED AIRCRAFT*	DASH RADIUS	TAKEOFF GROSS WEIGHT - MID ALTITUDE AIRCRAFT				
	MANEUVER LEVEL					
	LOW	Moderate	1.00	0.95	1.01	1.23
		High	1.00	0.95	1.01	1.17
	HIGH	Moderate	1.00	1.00	1.12	1.41
		High	1.00	1.00	—	—

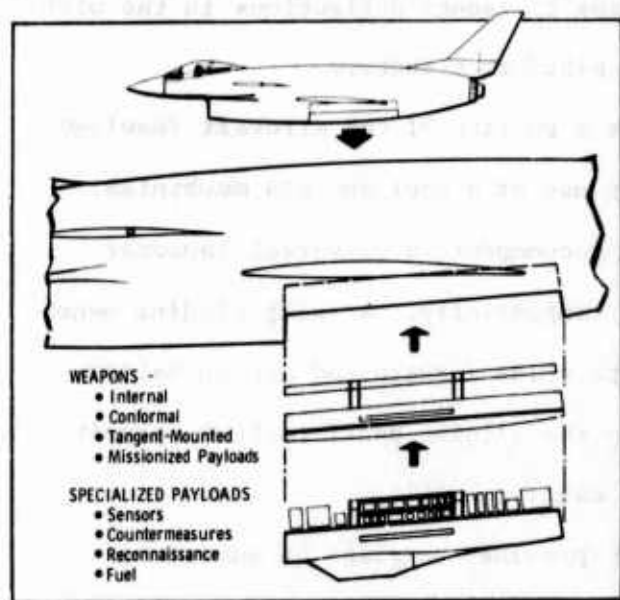
\*Each Aircraft Completely Reoptimized for Same Range, Payload Weight, and Maneuver Level

Figure D-6 Convair ATF Studies Show Internal Carriage is Weight Competitive

The question becomes one of feasibility of concept, i.e., is it possible to provide an internal bay which yields the desired store flexibility? This is certainly a valid question considering experiences with the internal bays of other high performance fighters, specifically those of the F-105 and F-111.

It should be noted that these internal bay designs were not directed toward multistore capability but were intended essentially for one mission, one weapon. In addition, Convair believes that its experience with the F-111, the F-111 internal stores improvement program known as TART, and advanced concept studies such as ATF and LWA have provided a viable multipurpose internal bay concept.<sup>1</sup>

D.1.1.1.3.2 Internal/Conformal Carriage Concept. The basic element of the LWA internal/conformal carriage concept is a clip-in platform that accommodates uni-



versal clip-in weapon racks and is amenable to specialized internal and/or conformal installation of a wide variety of missionized stores. The LWA configurations have not been developed around a specified internal carriage requirement; LWA internal capacity has been determined as a function of overall configuration size and shape. The LWA bay concept can be characterized as providing a 2000-

The clip-in platform is basically a saddle structure with a split sliding

Figure D-7 LWA Internal/Conformal Carriage Concept is Based on Flexible Clip-in Platform

panel on the lower surface. The saddle is designed to function as a plenum for the distribution of ram air above internal stores. Experimental evidence indicates that this ram air reduces turbulence during launch.<sup>2</sup> The air also effects a

<sup>1</sup> "Design Study for Internal Carriage and Release System," Convair Aerospace Division Report ERR-FW-1211, December 1971.

<sup>2</sup> "Supersonic Wind Tunnel Investigation of Flow in Various Bomb Bay Configurations," Cornell Aeronautical Laboratory Report GD-910-C-19, September 1957.

slight positive pressure in the cavity during flight. Ram-air flow is controlled by a pressure sensitive fluidic device.

Although the concept of a sliding panel closure and ram-air plenum appears to offer advantages in loading efficiency and improved local flow for better weapon separation, the concept requires verification. Other provisions which have been suggested for separation improvement are possible without materially altering the basic concept.

The structural legs of the platform are shaped to provide a 10-degree fall angle when the payload is composed of ejection-launched munitions. A longitudinal beam spans the legs of the structure and contains hole patterns for the installation of bomb racks. The racks are attached to place the centers of gravity of the various munitions near the supporting airframe bulkheads to reduce deflections in the platform structure and minimize the weight of the platform structure.

The bottom 12 inches of the platform form a portion of the aircraft fuselage which is attached to the fuselage longerons by use of a pawl and pin mechanism. The shoulders of the platform are designed to accommodate a universal launcher that carries external shoulder-mounted stores tangentially. A split sliding panel for cavity closure during flight is designed to slide forward and aft on balled-block guides. Brush-type seals are used along the sliding panel rails to permit ram-air seepage from a slightly overpressured cavity.

An integral centerline heavy weapons rack provides carriage of munitions heavier than 1000 pounds. The rack accommodates MAU-12 or Super 30-type ejection launchers or elongated single-acting and retractable thrusters. A lightweight, multiposition weapon rack carries stores weighing 1000 pounds and under on Super 14-type ejection launchers (Figure D-8). The lightweight rack may be installed in the platform in a make-up area or preassembled and delivered to the aircraft (with platform installed) for remote installation. The rack concept allows rapid reloading or change-out of payloads, which is important for LWA ground loiter operations.



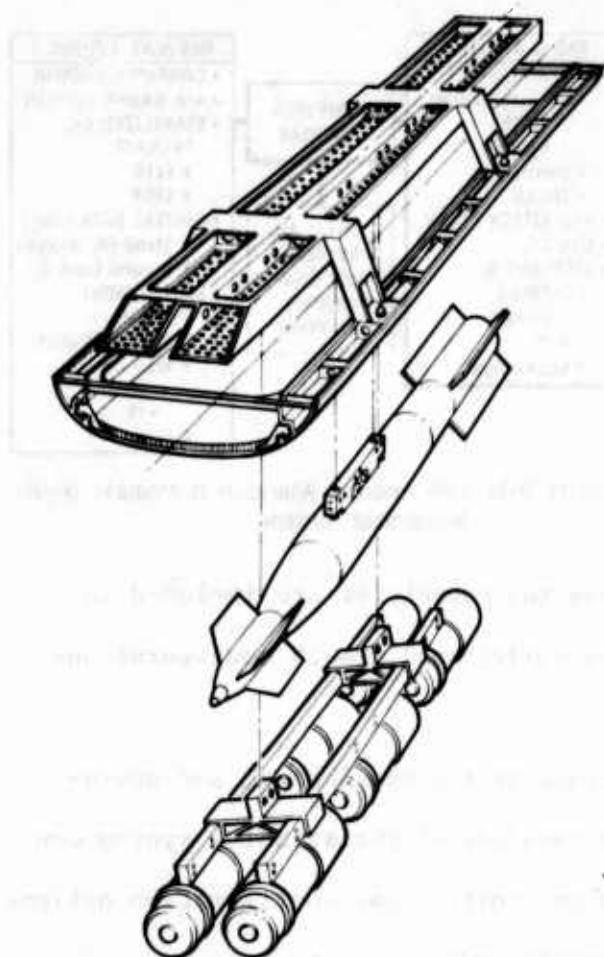


Figure D-8 Clip-in Platform Accommodates Universal Weapon Racks for Standard A-G Ordnance Carriage

The clip-in platform concept also affords considerable flexibility for the installation of missionized stores consisting of weapons and specialized avionic equipment. Alternate palletized payloads include semisubmerged munitions, gun systems, electronic countermeasure transmitters/receivers, FLIR/LLTV/Laser scanning avionics, fuel tanks, and reconnaissance equipment (Figure D-9).

#### D.1.1.2 Avionics Concept

The conceptual approach to the LWA avionics is based on a modular digital system configuration which is initially designed to be easily reconfigured to provide optional or growth capabilities to a basic avionics system (Figure D-10).

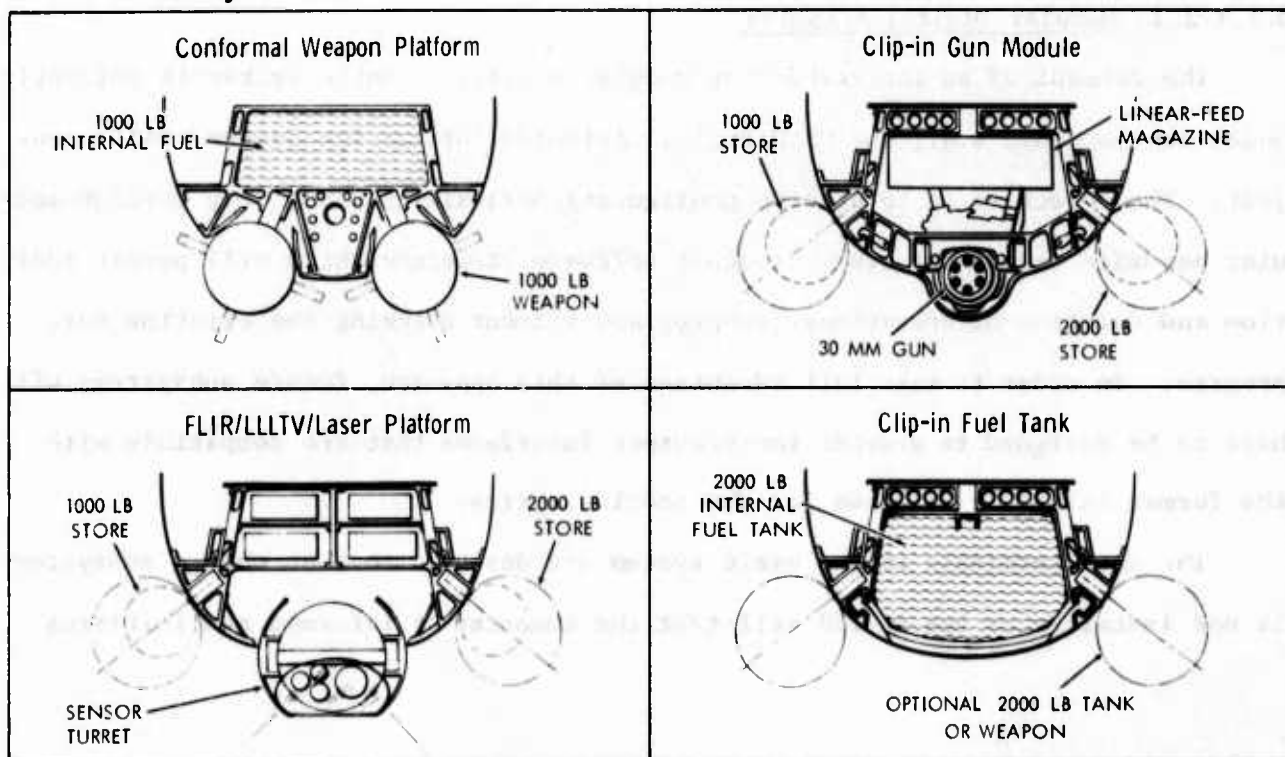


Figure D-9 Clip-in Platform can be Missionized for Many Types of Stores

This modular growth is made possible by two basic features:

1. The avionics system is organized and controlled through a digital computer complex having data bus terminals which provide the software interfaces both for basic subsystems and for planned modular additions.

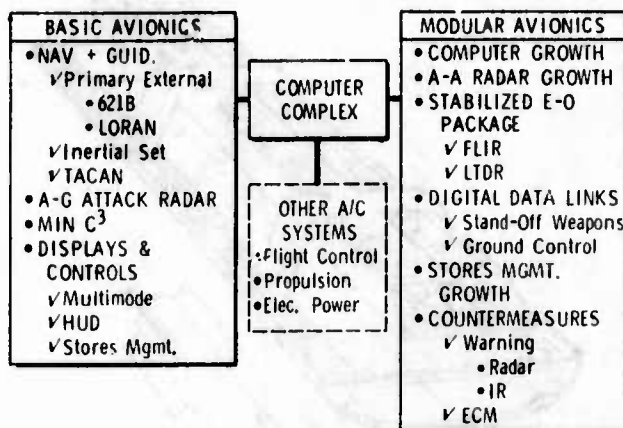


Figure D-10 LWA Avionics Approach is Modular Digital Missionized System

2. Sufficient space, power, and environmental capacities are included in the basic airplane to provide for the anticipated growth configurations as well as for the basic systems.

The implication of the LWA avionics approach in the development and operation of the airplane is that mission-peculiar versions of the avionics system can be obtained with a minimum of turnaround time and cost. Some configuration options might be available to the field commander, whereas others would be depot or manufacturer modification tasks.

#### D.1.1.2.1 Modular Digital Avionics

The concept of an integrated but modular digital avionics system is currently under development, e.g., the USAF Digital Avionics Information System (DAIS) project. The objective is to provide configuration flexibility not only through modular hardware design but also through a software structure which will permit addition and deletion of operational subprograms without changing the existing core program. In order to take full advantage of this approach, future subsystems will have to be designed to provide input/output interfaces that are compatible with the format initially selected for the modular system.

The data terminals in the basic system are designed so that when a subsystem is not installed or has failed self-test the computer is informed and initiates



appropriate action. When the subsystem is installed and operating normally or in an acceptable degraded mode, data are transmitted in the specified standard format.

The computer arrangement may include, in addition to the central processor, dedicated processors in each subsystem, each tailored to the specific computing functions of the subsystem but having a standard interface with the rest of the computer complex. Data conversion is performed within each subsystem. The central computer accomplishes the executive control functions such as mode switching, backup assignments, centralized self-testing, timing, and data bus control, in addition to subsystem computations such as weapon delivery and satellite navigation which are best suited to central computing.

#### D.1.1.2.2 Selected Subsystems

The LWA program groundrules, previous LWA operational studies, and avionics system options have been duly considered for the purpose of defining an avionics system for incorporation in the LWA configuration designs. These considerations are discussed in Appendix E, "Avionics Rationale, Description, and Technology Requirements."

A basic system weighing 482 pounds is defined as well as a modular growth configuration weighing up to 1197 pounds. Current LWA configurations provide for

Table D-1 MODULAR AVIONICS APPROACH ALLOWS  
MINIMUM BASIC SYSTEM

	BASIC SYSTEM		TOTAL GROWTH SYSTEM	
	BAYS	COCKPIT	BAYS	COCKPIT
Computer Complex	30 lbs	- lbs	50 lbs	- lbs
Navigation & Guidance	72	36	72	36
E-O Capability	-	30	170	35
Radars	160	10	250	15
CC&C	26	30	66	33
Weapon Delivery	40	48	50	55
Defensive System	-	-	345	20
	328 lbs	154 lbs	1003 lbs	194 lbs

- Basic System Weight - 482 lbs
- Total Growth System Weight - 1197 lbs

the full growth complement. Table D-1 is a list of the subsystems and associated weights (described in detail in Appendix E).

The internal bay and modular avionics approach also make the LWA concept amenable to configuration for special purpose missions not provided for by the growth system. In particular, electronic warfare or reconnaissance configurations are considered likely candidates.

### D.1.2 CREW STATION

From the standpoint of preliminary configuration design, there are two crew station issues which must be resolved: (1) crew size and (2) pilot visibility. Other questions which are addressed at later stages of configuration development concern instrument arrangement, control and display concepts, stick location, etc. These latter issues are considered at this point only to ensure adequate crew station space to accommodate any of the foreseen alternatives.

#### D.1.2.1 Crew Size

The question of a one- or two-man fighter is an old one, and the answer is largely dependent on the initial assumptions. However, there are two points which are germane. First, many past studies have shown that fighter life cycle costs are lower for one crew member than for two, providing the pilot can accomplish the avionics operating requirements as well as his other functions (Figure D-11).

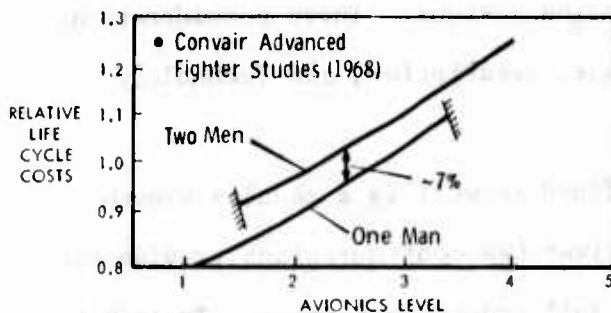


Figure D-11 Life-Cycle Costs are Generally Lower for One Man Crew

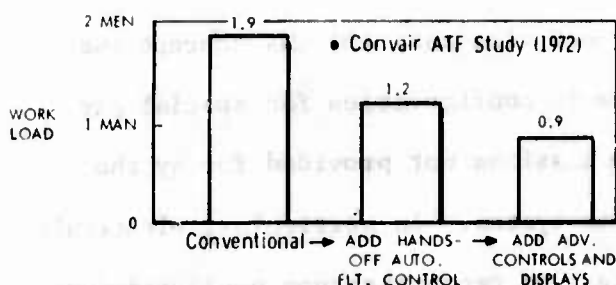


Figure D-12 Demanding A-G Missions Require Advanced Systems for One Man Crew

However, recent Convair ATF studies show that the requirements of a demanding ground attack mission in conjunction with advanced weapon delivery systems definitely indicate the need for two men. This conclusion can be reversed with the application of automatic flight control and advanced controls and displays for weapon delivery which, in turn, add new terms to the cost equation (Figure D-12).

The LWA approach is to assume a one-man crew on the basis of utilizing advanced technology and also the expressed sentiment of many USAF pilots. At a later time, the several technology development programs which are pertinent to this question (e.g., the USAF Multi-Mode-Matrix

Electronic Display Instruments for Aircraft (MEDIA) Program) should be assessed, and cost and work load analyses conducted for specific LWA configurations and missions.

#### D.1.2.2 Pilot Visibility

As indicated by the recent A-X, F-15, and LWF designs, bubble canopies which provide the pilot with 360-degree horizontal vision are accepted fighter design features. The bubble canopy does result in a drag penalty, particularly at supersonic speed (Figure D-13). Because the LWA is not intended to operate supersonically

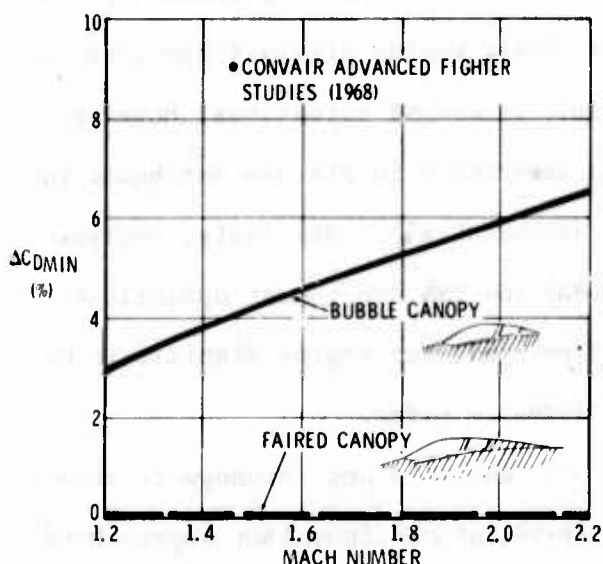


Figure D-13 Bubble Canopy Costs Some Supersonic Drag

over extended periods, the bubble canopy does not overly compromise mission capability, and this configuration feature is incorporated in the LWA designs.

Forty degrees is considered to be excellent over-the-side vision, and the LWA configurations which incorporate the bottom-mounted inlet provide 40-degrees at 50-degrees aft. For alternate configurations incorporating side-mounted inlets, aft over-the-side vision is severely restricted.

Over-the-nose visibility for USAF fighters is usually set by drag considerations which, for high performance aircraft, limit it to around 15 degrees. For a STOL aircraft, the combination of large approach angle and high angle of attack can dictate an increased vision requirement, but probably not over 20 degrees. As the LWA short landing conditions become better defined, the over-the-nose angle can be increased from the present 15 degrees as required.

### D.1.3 PROPULSION

#### D.1.3.1 Number of Engines

The question of one versus two engines for a tactical fighter is also an old one, and the answer is dependent on initial assumptions and specifics of the situation. For example, life cycle cost comparisons of "paper" engines will invariably favor a one engine approach, but comparisons of existing engines, which usually are quite different in concept and development history, can change this conclusion (Figure D-14).

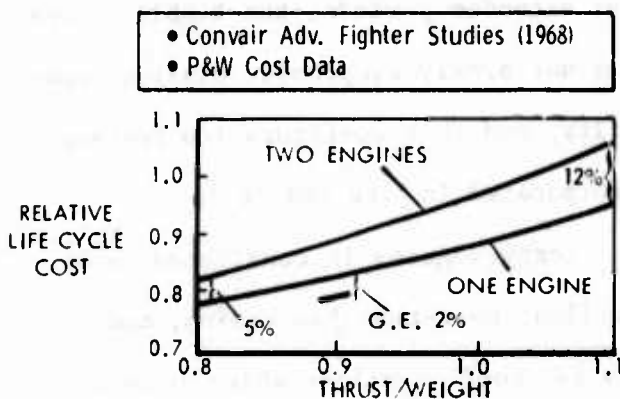


Figure D-14 Life-Cycle Costs for Similar Engine Favor One Engine Approach

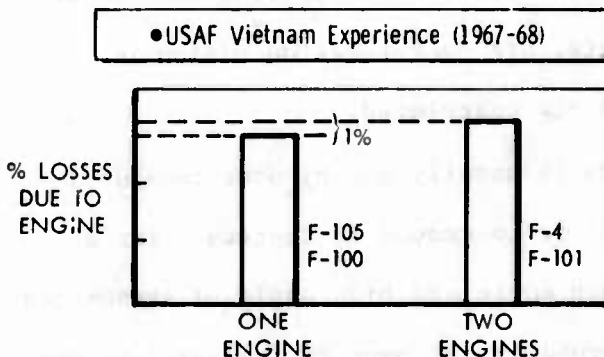


Figure D-15 Combat Experience does not Show Differences in Survivability

#### D.1.3.2 Engine Cycle

Because of the extremely broad nature of the LWA mission/configuration trade-off studies discussed in Section D.3, no engine cycle variables have been included in the overall parametric analysis. Future efforts should logically include an

An intuitive feeling generally exists that single-engine aircraft are more vulnerable in combat situations; however, U.S. experience in SEA has not borne this out (Figure D-15). Similarly, analysis of USAF and USN non-combat operations does not show two-engine fighters to be consistently safer.

The above is not intended to show a single-engine configuration approach is necessarily better, but only to point out that neither is a two-engine approach necessarily better. For powered lift concepts, a single-engine configuration is favored. A single-engine eliminates the propulsion installation complications which are required to prevent asymmetric lift and the consequent large rolling moment due to an engine-out situation.

examination of engine cycle tradeoffs relating to specific mission and configuration variables. The general considerations which resulted in engine cycle selection for the reference configurations described in Section D.2 are discussed here.

The LWA requirements for low specific fuel consumption during cruise and for short supersonic acceleration time point to an augmented engine. Generally speaking, higher thrust-to-weight ratios are obtainable with mixed-flow afterburning turbofans as compared to separate-flow, duct-burning turbofans (Figure D-16). On the other hand, the shorter length of a duct-burning engine can potentially offset this weight advantage by allowing the engine center of gravity to be positioned at a further-aft airplane station, thereby resulting in a shorter configuration.

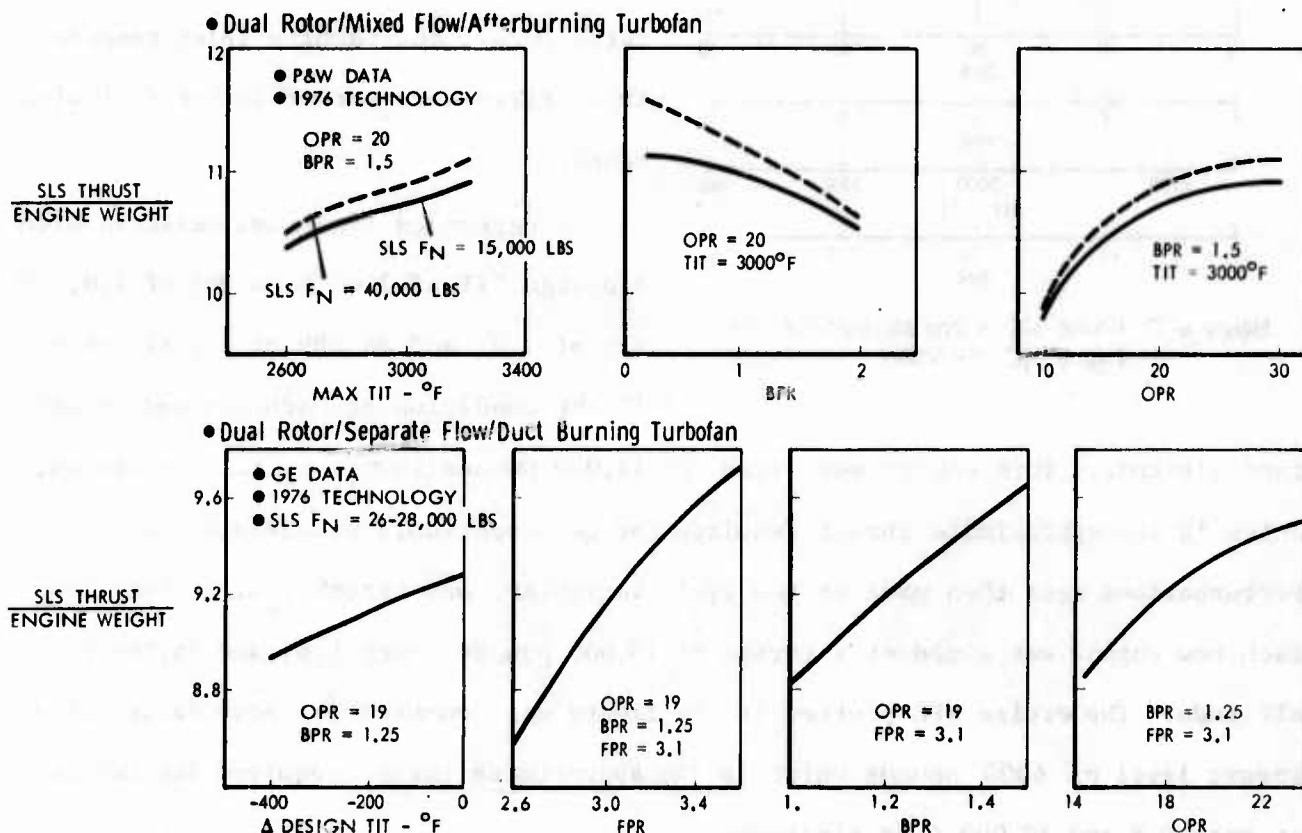


Figure D-16 Engine Weight Tradeoffs Considered in Evolving LWA Reference Configurations

Any configuration differences resulting from choice of augmentation concept are not first-order at this point in the LWA configuration development. Therefore, the duct-burning engine has been selected for the reference configurations, because the engine control problems associated with the powered-lift concepts are far easier to handle with a separate flow cycle.

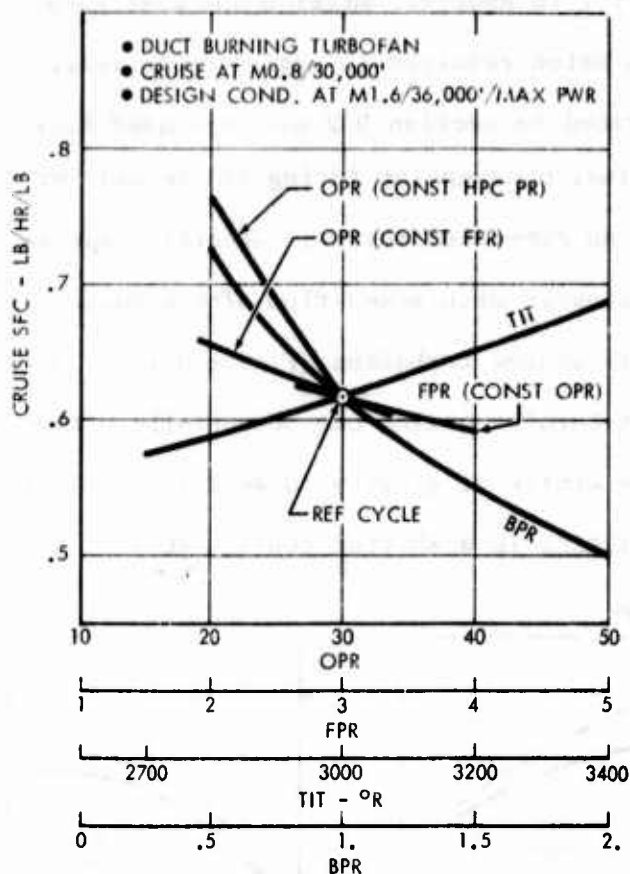


Figure D-17 Cruise SFC is One Measure for LWA Engine Cycle Selection

Specific fuel consumption (SFC) is one measure of engine cycle performance which can be considered parametrically without defining a specific mission and configuration. Figure D-17 illustrates the effect of cycle parameter variations on subsonic cruise SFC for an engine sized for supersonic acceleration. The cycle parameters of interest--bypass ratio (BPR), fan pressure ratio (FPR), overall pressure ratio (OPR), and turbine inlet temperature (TIT)--were varied in the following manner.

A reference cycle was selected with a design TIT of 3000°R, a BPR of 1.0, an FPR of 3.0, and an OPR of 30, all at a flight condition of Mach 1.6 and 36,089

feet altitude. This engine was sized for 15,000 pounds thrust at that condition, which is the approximate thrust required for LWA supersonic acceleration objectives. Perturbations were then made to the cycle variables, one variable at a time, and each new engine was sized at a thrust of 15,000 pounds, Mach 1.6, and 36,089 feet altitude. The cruise SFC plotted in the figure was computed for each design at a thrust level of 6000 pounds which is the approximate thrust required for LWA cruise at Mach 0.8 and 30,000 feet altitude.

With the exception of TIT, cruise SFC is seen to improve as all cycle parameters are increased. Within the time frame of interest, the maximum feasible fan pressure ratio is 4 and the maximum overall pressure ratio for a two-spool engine is 30. At that FPR and OPR, the maximum design BPR is dependent on the design TIT, because sufficient turbine work must be available to drive the fan. This results in a conflict, since a high BPR (favorable) requires a high TIT (unfavorable).



For the powered lift concepts, an important engine performance parameter is the momentum coefficient,  $c_\mu$ , produced by the fan. The effect of engine cycle parameters on  $c_\mu$  is shown in Figure D-18. The important point to note is that the

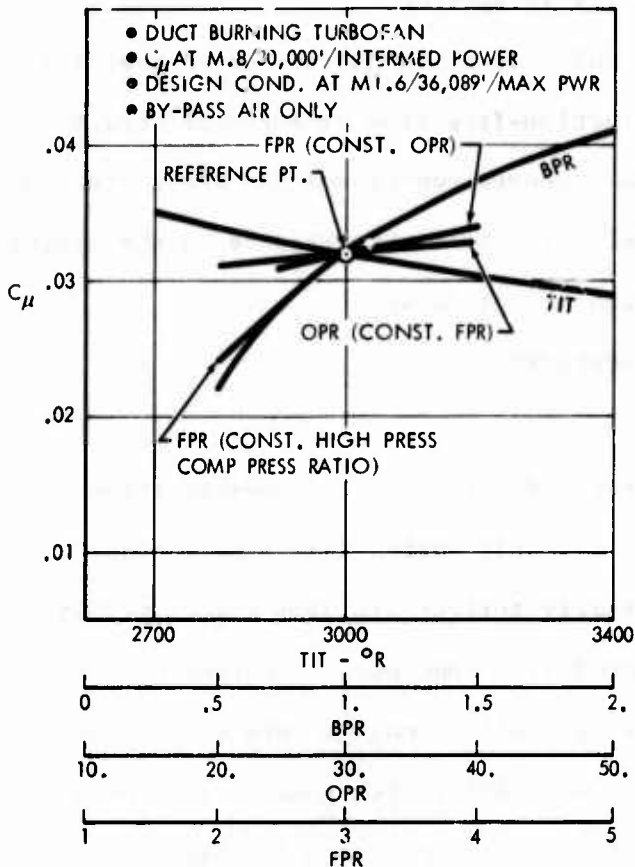


Figure D-18 Blowing Momentum is also Consideration in Cycle Selection

variations which increase  $c_\mu$  also decrease SFC, and no particular conflict between these two parameters is to be expected.

The engine cycles which are chosen for the reference configurations are based on (1) the general considerations above, (2) considerations of unique requirements of the powered lift concepts, and (3) results from similar programs relating to engine cycle, mission, and configuration tradeoffs. More specific analysis will be appropriate in the next phase of LWA configuration development; however, engine availability and cost could ultimately have much to do with engine selection.

#### D.1.3.3 Inlet

The non-configuration-sensitive inlet characteristic which must be determined at this time is inlet type. For the maximum Mach number of 1.6 appearing in the LWA parametric mission requirements, a normal shock inlet is preferred to an inlet with an external-compression surface, either fixed or variable.

A fixed compression surface at Mach 1.6 can provide a 7 percent increase in pressure recovery but at the cost of additional spillage and external drag due to a 13 percent larger inlet capture area. An inlet with the capability of varying compression surface angle and throat area, i.e., a variable geometry inlet, improves pressure recovery and reduces inlet spillage drag, but at considerable cost in complexity and weight.



Inlet performance and weight trade studies for aircraft with mission and flight envelopes similar to those of the LWA show that the normal shock inlet provides the best compromise in terms of performance, weight, development time, cost of fabrication and maintenance, and reliability in service.

For a single-engine aircraft, a bottom inlet location is considered best from the standpoint of pressure recovery and distortion-free flow at angle of attack. Side-mounted inlets are adequate for the LWA maneuver conditions and are preferred for two-engine configurations. Choice of inlet location also depends on the stores carriage concept and the likelihood of foreign object damage.

#### D.1.4 CONTROL SURFACES

##### D.1.4.1 Horizontal Stabilizer

The horizontal stabilizing surface selected for primary LWA consideration is a canard. In addition to utilization of the variable vortex lift from a close coupled canard, the canard avoids the potentially serious problems associated with the very high downwash generated by the powered lift concepts. Previous experience shows that large amounts of blowing at the wing trailing edge create very large downwash angles even for T-tailed configurations. Also, with powered lift creating large nose-down pitching moments, much of the lift advantage is lost with an aft horizontal tail which produces large down-loads to trim.

The canard thus offers the advantages of being ahead of the downwash field plus maximum generation of lift by trimming the blowing moments with an up-load rather than a down-load. A canard used in conjunction with the Control Configured Vehicle (CCV) concept of reduced static stability provides a combination of airplane balance and lift augmentation which gives optimum trim forces throughout the flight spectrum (Figure D-19).

Sizing of the canard has been established from canard/wing vortex lift criteria, and no variations in size for balance and trim have been exercised at this point. Such variations are a possible configuration refinement item. Another factor which needs to be considered is some form of powered lift which can be applied to the canard at low speeds to enhance STOL trim capabilities where thrust capability is high and dynamic pressure for aerodynamic force generation is low.

	Aft Horizontal Tail with Conventional Balance	Aft Horizontal Tail with Reduced Static Stability	Canard with Reduced Static Stability
Subsonic Characteristics - with Thrust Vectoring	<p>TRIM TAIL LOAD (VERY LARGE, DOWN)</p> <p>WING LIFT      VECTORED           THRUST           LIFT</p>	<p>TRIM TAIL LOAD (LARGE, DOWN)</p> <p>WING LIFT      VECTORED           THRUST           LIFT</p>	<p>TRIM CANARD LOAD (LARGE, UP)</p> <p>WING LIFT      VECTORED           THRUST           LIFT</p>
Supersonic Characteristics - No Thrust Vectoring	<p>TRIM TAIL LOAD (LARGE, DOWN)</p> <p>WING LIFT</p>	<p>TRIM TAIL LOAD (SMALL, DOWN)</p> <p>WING LIFT</p>	<p>TRIM CANARD LOAD (SMALL, UP)</p> <p>WING LIFT</p>
Comments	LARGE TRIM TAIL LOADS DECREASE LIFT EFFECTIVE- NESS	TAIL LOADS ARE SMALLER BUT STILL DOWN AT BOTH LOW AND HIGH SPEEDS	TRIM LOADS ARE ALWAYS UP TO MAXIMIZE LIFT EFFECTIVENESS

Figure D-19 Canard Best Accommodates Both Powered Lift and CCV

#### D.1.4.2 Vertical Stabilizer

The application of CCV and fly-by-wire concepts is carried into the selection and preliminary sizing of the vertical stabilizing surfaces. Current handling quality specifications call for minimum levels of Dutch-roll frequency and damping which must be present without use of stability augmentation. That is, the basic airplane, without any control motion, must exhibit inherent directional stability of significant values.

These requirements usually establish the size of the vertical tail. The rudder is then sized to fulfill the control power requirements which are generally smaller than the basic stability requirements and do not require use of the entire vertical stabilizing surface. Incorporation of the CCV concept of reduced static stability into the yaw axis offers the possibility of reducing the vertical tail size by making the tail all-movable and then sizing it based on the combination of augmented stability requirements plus the control requirements (Figure D-20).

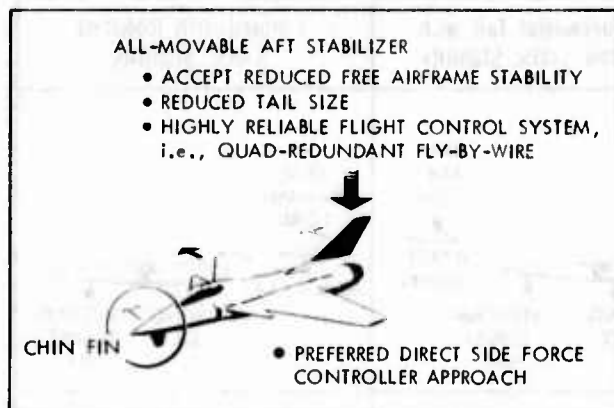


Figure D-20 LWA Vertical Stabilizers are Consistent with CCV and Direct Sideforce Technologies

In addition to an aft vertical stabilizing surface mounted on the top of the fuselage, direct sideforce control studies have lead to the incorporation of "chin fins." These are small vertical surfaces located on the forward, lower part of the fuselage.

In addition to their capability to generate side forces on the airplane to aid in tracking, these surfaces are attractive as directional stabilizing surfaces as well. This is particularly true for high angle-of-attack conditions where the vertical tail generally loses effectiveness because of wing and fuselage flow field effects.

#### D.1.5 THE -ILITIES

At the present point of the LWA configuration development process, the -ilities, i.e., maintainability, reliability, and survivability/vulnerability, are accommodated through conscious preliminary design actions which are based on previous

- FOLLOW GOOD DESIGN PRACTICE AS RELATES TO PRELIMINARY DESIGN
- INCUR NO PENALTIES FOR PARAMETRIC CONFIGURATIONS
  - NO ARMOR
  - STANDARD REDUNDANCY
- PERFORM COST-BENEFIT TRADES AFTER CONFIGURATION IS SELECTED

Figure D-21 Current LWA Approach to the -Iilities

design experience. In the main, the design impacts of the -ilities are not apparent un'il a specific configuration is developed in some detail (Figure D-21).

One area which does have an impact on LWA mission performance is the provision of armor and system redundancy to reduce vulnerability. The issue is,

of course, how far should one go to improve survivability at the cost of performance. A specific configuration and an operational scenario are required to analyze this question. For the present, no penalties are assumed for vulnerability reduction.

## D.2 REFERENCE CONFIGURATIONS

In order to analyze mission/configuration tradeoffs as discussed in the next section, it is necessary to define reference configurations which represent the configuration approaches to be evaluated. The LWA configurations which have been evolved for this purpose represent four technologies: (1) conventional materials, (2) advanced composite materials, (3) vectored thrust/supercirculation, and (4) jet flap.

The conventional configuration embodies the characteristics discussed in Section D.1 in an integrated concept. The advanced technology approaches are derived from the conventional in order to provide a common basis for evaluating potential payoffs.

### D.2.1 CONVENTIONAL MATERIALS - CONFIGURATION 26B

#### D.2.1.1 General Description

The general arrangement of the LWA Conventional Materials Reference Configuration 26B is shown in Figure D-22. The canard/wing arrangement is consistent with the objective of obtaining favorable aerodynamic interference; however, the primary reason for the close-coupled canard approach at this point is its compatibility with the powered-lift concepts to be derived from this configuration.

The wing planform and thickness are similar to those of the Convair YF-16, which facilitates use of that data base. Leading edge flaps are incorporated for maneuver improvement. The leading edge flaps and simple trailing edge flaps provide a high-lift system for takeoff and landing.

The all-movable canard is used for trim. Roll control is provided by inboard flaperons.

A forward, fuselage-mounted vertical surface for direct sideforce control conflicts with the bottom-mounted inlet and associated nose gear location. The double chin fin arrangement provides one solution to this problem. The question of aerodynamic interference (favorable or unfavorable) from these surfaces affecting stores separation requires further investigation.

STRUCTURAL DESIGN WEIGHT	22,500 lbs
SPAN	30 ft.
LENGTH	50 ft. 6 in.
HEIGHT	17 ft.
WING:	
Area	300 sq. ft.
Aspect Ratio	3
Thickness Ratio	4%
Leading Edge Sweep	40°
OTHER AREAS:	
Canard (All-Movable)	47 sq. ft.
Aft Vertical Tail (All-Movable)	33 sq. ft.
Forward Vertical, Each (All-Movable)	5 sq. ft.
Flaperons	33 sq. ft.
Flaps	9 sq. ft.
ENGINE:	
SLS Thrust	23,875 lbs
By-Pass Ratio	1.0
INTERNAL FUEL	7,490 lbs

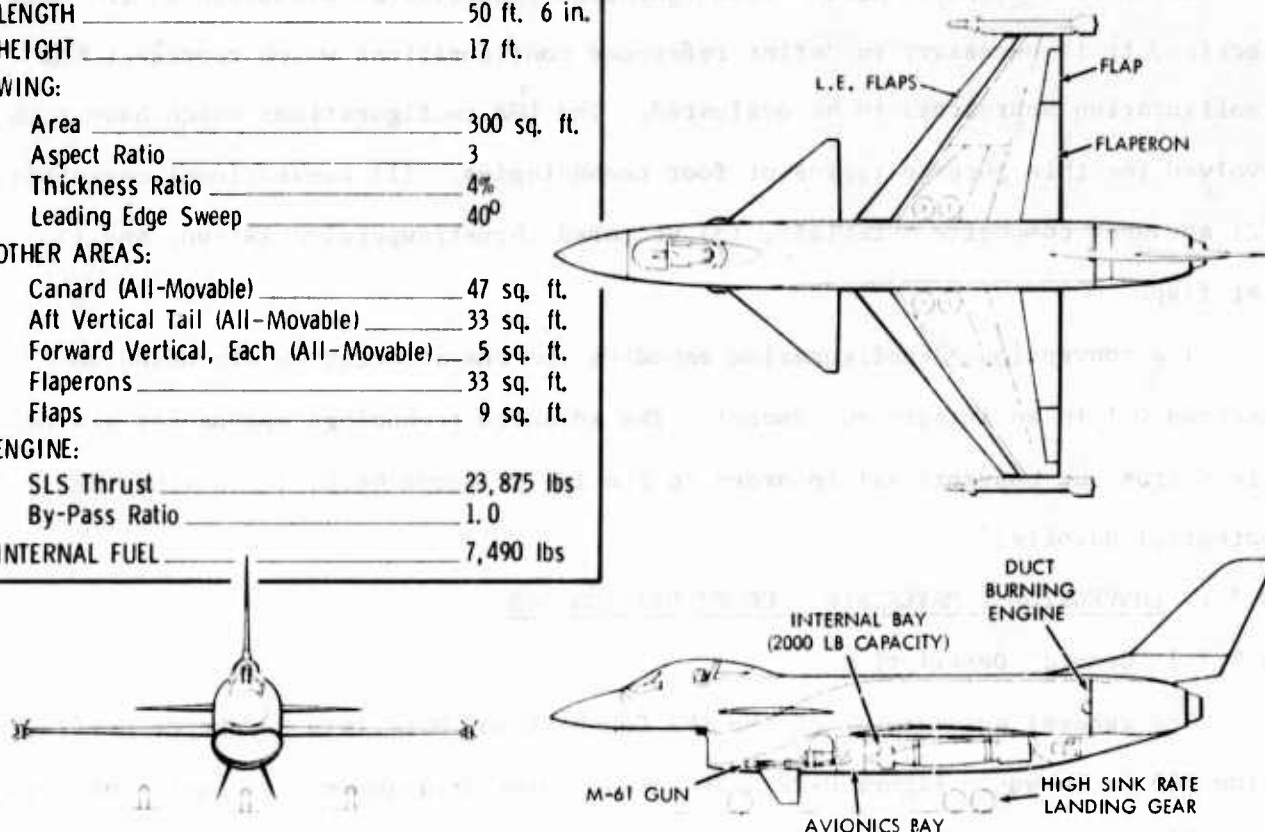


Figure D-22 LWA Conventional Reference Configuration 26B

The duct-burning turbofan has a BPR of 1.0, an OPR of 20, and a TIT of 3100°F. This engine represents a cycle which was shown to have some merit for Convair's ATF designs, and the availability of engine performance data makes its use expedient.

The fixed geometry, normal shock inlet is displaced from the fuselage to avoid ingestion of the fuselage boundary layer. An extension of the upper lip of the inlet in the forward direction forms a splitter plate between the boundary layer and inlet flow which prevents interaction of the inlet normal shock and the airplane boundary layer at reduced engine airflows and supersonic flight speeds. The inlet lip is thickened on the bottom surface and lower sides to prevent separation of the flow at high angles of attack.

A high sink rate landing gear allows no-flare, steep landings (Figure D-23). The gear is structurally designed to USN criteria for carrier landings, i.e., up to 22 feet per second sink rate, and it easily meets any foreseen short landing conditions.

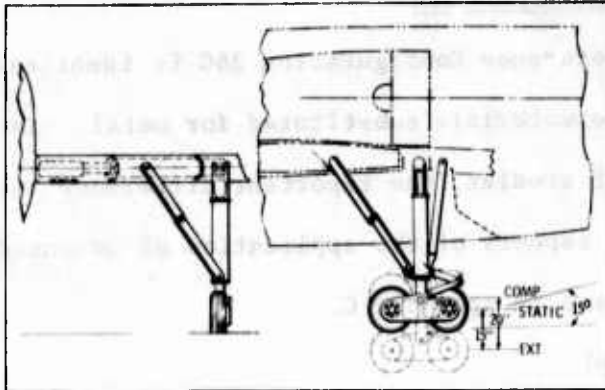


Figure D-23 High Sink Rate Gear is Stowed in the Wing Box

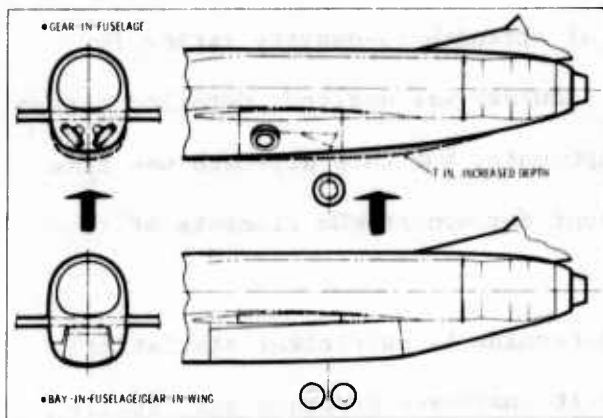


Figure D-24 LWA Internal Bay Integrates well with Configuration

Table D-2 INTERNAL BAY IMPACT ON STRUCTURAL WEIGHT FOR LWA CONFIGURATION APPROACH

COMPONENT	WEIGHT INCREASE
FUSELAGE (Gear Vs. Bay)	+6%
WING (No Gear Vs. Gear)	+27%
TOTAL STRUCTURE	+9%

by other configuration elements (Figure D-24).

The additional fuselage volume obviously results in incremental weight and aerodynamic drag, but comparisons of carriage concepts on an equal performance basis show little difference in aircraft gross weight (paragraph D.1.1.1.3.1). It is of interest from a basic airframe cost standpoint to quantify differences in aircraft structural weights (Table D-2). For the integration approach embodied in Configuration 26B, the internal bay results in less than 10 percent increase in structural weight.

The tandem wheel concept allows the main gear to be retracted into the wing box. A fuselage location for the retracted gear is not practical because of the internal bay.

#### D.2.1.2 Impact of Internal Bay

Integration of an internal bay into a fighter configuration impacts the result in several ways. The LWA approach is to minimize the impact by allowing the bay size to be influenced by the other configuration elements.

Internal bay dimensions are generally determined by some specific store load which is considered compatible with the aircraft concept and mission. In this case, a 2000-pound guided, unpowered bomb of the MWS class fits this description and integrates very well with the single engine and the bottom-mounted inlet; i.e., it is accommodated within the width, depth, and length set



## D.2.2 ADVANCED COMPOSITE MATERIALS - CONFIGURATION 26C

The LWA Advanced Composite Materials Reference Configuration 26C is identical to Configuration 26B with advanced composite materials substituted for metal. In regard to the mission/configuration tradeoff studies, the important difference is in the structural weight variations. Other aspects of the application of advanced composites to LWA configurations are discussed in Appendix C.

### D.2.2.1 Structural Weight Estimation Method

When advanced composite materials were first considered for use in aircraft structures, suitable weight estimation procedures were nonexistent. Gross estimates were made by comparing average values of strength-to-density ratios for aluminum and composite components. If more accuracy was desired, detailed stress analyses were performed on the composite components, but this approach was time consuming. Also, it did not adequately account for nonoptimum elements of the structural weight.

Convair undertook a survey in 1971 to determine if sufficient statistical data were available from both advanced composite hardware programs and detailed analytical studies to allow derivation of statistical-analytical weight prediction methods comparable to those available for metal structures.<sup>1</sup> Although available data are not sufficient to warrant completely new structural weight prediction procedures, advanced composite weight reduction factors have been determined which can be applied to metal weights to give composite structural weights.

It is important to note that these weight reduction factors are not constant for all aircraft, but depend upon configuration concepts and geometry, the structural arrangement, and, most important, the material allowables assumed for the advanced composite material being used. (While the net effect of composite usage varies, the total structural weight saving, as compared to conventional aluminum structure, ranges from 20 to 32 percent.) These factors are continually modified and updated as the results of new studies become available.

---

<sup>1</sup> "Data Summary of Composite Vs. Aluminum Component Weight Comparisons," Convair Report MRS-71-005, 23 August 1971.

Table D-3 STRUCTURAL WEIGHT REDUCTION FOR CONFIGURATION 26C

	WEIGHT REDUCTION FROM CONFIGURATION 26B
WING	35%
CANARD	20
VERTICAL TAIL	24
BODY	36
AIR IND. DUCT	34
TOTAL STRUCTURE	31%

#### D.2.2.2 Configuration 26C Structural Weight

Structural component and system weights for Configuration 26C are determined using the analytical-statistical methods developed by Convair and

discussed in the preceding section. The weight reduction achieved through full composite usage is listed in Table D-3 by component and for the total structure. The weight estimates used in the LWA studies for advanced composite structures represent 1975-1980 technology.

### D.2.3 VECTORED THRUST/SUPERCIRCULATION - CONFIGURATION 27

#### D.2.3.1 General Description

The general arrangement of LWA Vectored Thrust/Supercirculation (VT/SC) Reference Configuration 27 is shown in Figure D-25. Many characteristics are identical to those of Configuration 26B. The structural weights for this configuration are based on advanced composite materials technology as incorporated in Configuration 26C. The aspect ratio is four in anticipation of the effect of advanced composites on planform geometry.

The VT/SC concept, potential performance, and design objectives are generally discussed in Appendix B. Subsequent VT/SC configuration design investigations which led to Configuration 27 have primarily impacted the propulsion system and the wing location and planform.

#### D.2.3.2 Propulsion System

The original NASA concept of vectoring the complete engine thrust at the aft end of the fuselage has been modified in the LWA application. In the LWA approach, fan air only is vectored at an inboard trailing edge location of the wing.

##### D.2.3.2.1 Engine Description

A turbofan with a BPR of 1.5, an FPR of 4, an OPR of 30, and a TIT of 3200°R appears to provide a good engine cycle considering both vectored and non-vectored

STRUCTURAL DESIGN WEIGHT	22,500 lbs
SPAN	34 ft. 8 in.
LENGTH	57 ft. 7 in.
HEIGHT	16 ft. 3 in.
WING (THEORETICAL):	
Area	300 sq. ft.
Aspect Ratio	4
Thickness Ratio	7%
Leading Edge Sweep	30°/47°
OTHER AREAS:	
Canard (All-Movable)	50 sq. ft.
Aft Vertical Tail (All-Movable)	33 sq. ft.
Forward Vertical, Each (All-Movable)	5 sq. ft.
Flaperon	28 sq. ft.
ENGINE:	
SLS Thrust	27,630 lbs
By-Pass Ratio	1.5
Fan Pressure Ratio	4
INTERNAL FUEL	7,266 lbs

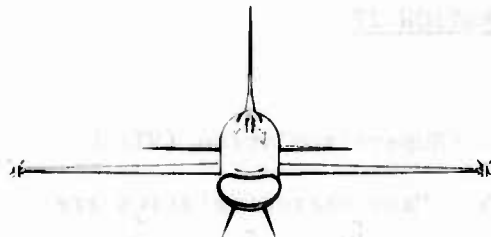
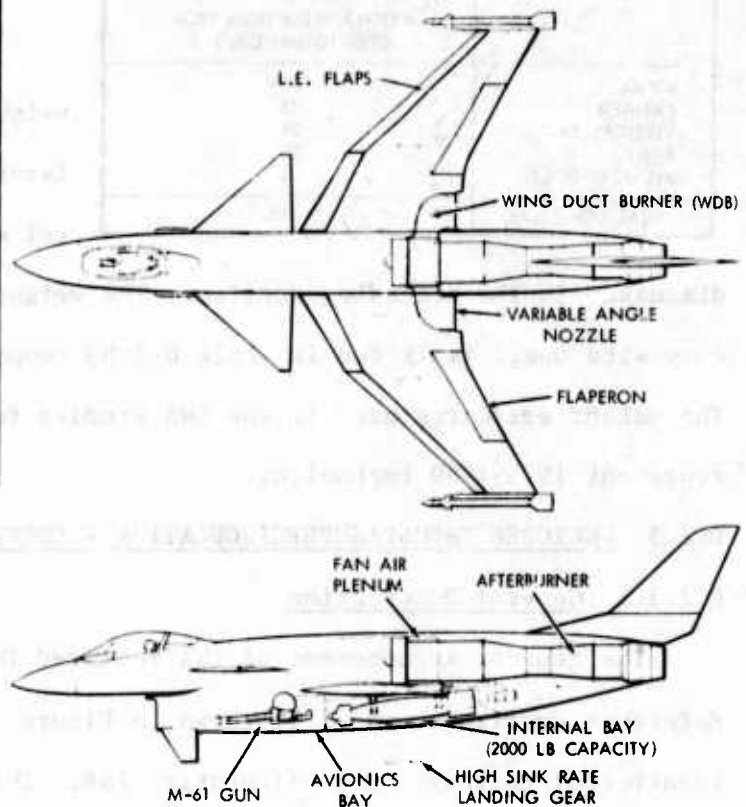


Figure D-25 LWA Vectored Thrust/Supercirculation (VT/SC) Reference Configuration 27

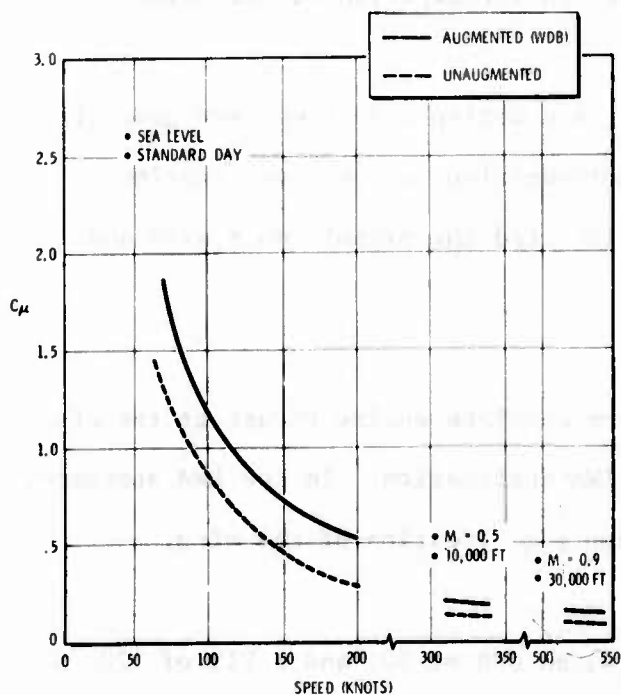


Figure D-26 Configuration 27 Utilizes Fan Air Only for VT/SC

thrust performance (Figure D-26). In order to duct the fan air to the wing trailing edge and keep duct pressure losses within reason, it is necessary to locate the fan air exit sufficiently ahead of the trailing edge so as to require only two, relatively gradual, 90-degree turns of the air. If the complete engine is conventionally located with respect to the fan, the resulting configuration center of gravity (c.g.) is located substantially forward of the desired point.

One solution to this problem, other than ballast weight, is to lengthen the configuration beyond that required by other factors; however, the necessary extension is large because the tailpipe and empennage are not particularly heavy. The approach for Configuration 27 is to physically separate the basic engine from the fan by the length required to properly locate the c.g.

Conceptually, the separation is simply implemented by extending the fan rotor shaft, but the mechanical aspects require further investigation. This approach does not overly extend the configuration length because the c.g. rapidly moves aft as the engine is moved aft.

Configuration 27 incorporates both a wing duct burner and an afterburner. The inclusion of an afterburner in future configurations is questionable because of the low augmentation available, and its desirability requires additional study.

Fan air burning is required to accommodate the conflicting requirements of efficient subsonic cruise and good supersonic acceleration. The approach here is to burn the air in the wing duct. An alternative is to provide valving so that the fan air can be directed into a concentric engine duct and burned conventionally. It is believed that Wing Duct Burning (WDB) is the lighter of the two approaches, and WDB allows VT/SC operation at maneuver conditions requiring augmented thrust (with a correspondingly higher blowing momentum coefficient,  $c_{\mu}$ ).

#### D.2.3.2.2 Wing Duct Burning (WDB)

The concept of diverting burned bypass air out through the fuselage wall and discharging the air from a nozzle location only a short distance aft of the engine fan is not new. Bristol-Siddeley designed and developed such a concept for the Pegasus engine.<sup>1</sup> This concept, known as Plenum Chamber Burning (PCB), burns bypass air at temperatures as high as 2500°R in a plenum chamber a short distance downstream of the fan. The hot exhaust is then routed through a cylindrical duct to a vectorable nozzle (Figure D-27).

---

<sup>1</sup> "Recent Developments in Vectored-Thrust Turbofans," Aircraft Engineering, October, 1965.

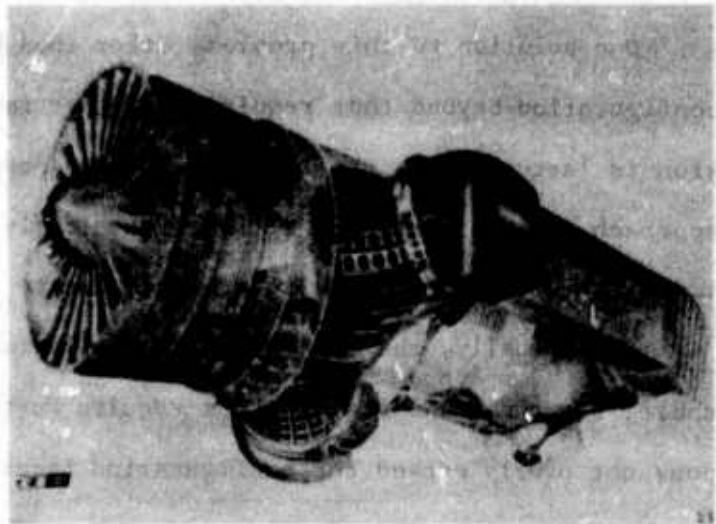
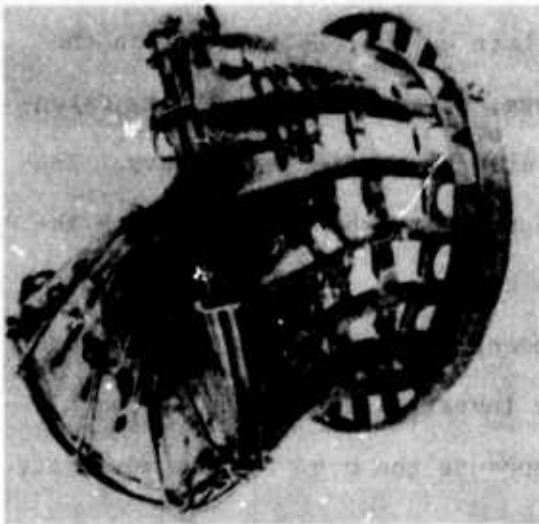


Figure D-27 Pegasus Plenum Chamber Burning (PCB) is Similar to LWA Wing Duct Burning (WDB)

For LWA Configuration 27, a fan plenum collects the bypass air and directs it downward to the bottom of the nacelle. At the bottom of the nacelle, the flow is turned outboard into the wing root and diffused to the burner region.

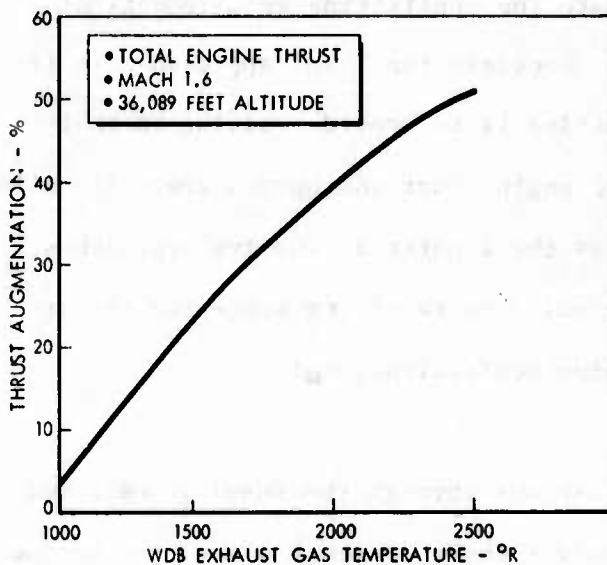


Figure D-28 WDB Thrust Augmentation is a Strong Function of Exhaust Temperature

The WDB exhaust temperature is subject to tradeoff between thrust augmentation and system weight (Figure D-28). For the present, WDB exhaust temperature is 2000°R. Investigations directed toward quantification of temperature tradeoffs are discussed in the next subsection.

Pressure losses of the WDB duct are estimated at about six percent of fan discharge pressure, exclusive of burner pressure losses. An additional pressure

loss of five percent is estimated for flameholder drag and burning.

#### D.2.3.2.3 Vectoring Nozzle

In addition to vectoring thrust, the nozzle for VT/SC concept implementation must perform the functions of a conventional nozzle, i.e., efficiently convert the energy delivered by the engine into propulsive thrust and control the mass flow and pressures in the fan, burner, and duct. Certain aerodynamic requirements must be met in order to maintain high nozzle efficiency throughout the flight envelope.

Both external and internal slopes must be kept to a minimum to avoid adverse boattail drag characteristics or inefficient internal flow expansion. The controlling nozzle throat area must be varied to compensate for temperature variations due to burning or not burning, and the area variation is critically related to the operating pressure ratio defined by the local nozzle total pressure to the free-stream static pressure. Since the operating nozzle pressure ratio varies throughout the flight envelope, a variable internal nozzle area distribution is desired.

Table D-4 VECTORING NOZZLE DESIGN OBJECTIVES

- |  |
|--|
| <ol style="list-style-type: none"> <li>1. MAXIMUM EXTERNAL SLOPE <math>\leq 15</math> DEGREES</li> <li>2. MAXIMUM INTERNAL SLOPES DOWNSTREAM OF THE THROAT <math>\leq 15</math> DEGREES</li> <li>3. MAXIMUM INTERNAL SLOPE UPSTREAM OF THE THROAT <math>\leq 45</math> DEGREES</li> <li>4. OPERATING EXIT AREA TO THROAT AREA RATIO FOR NONBURNING OPERATION 1.5 TO 1.7</li> <li>5. MINIMUM EXIT AREA TO THROAT AREA FOR MAXIMUM DUCT BURNING 1.1</li> <li>6. ACCEPT COOLING AIR</li> <li>7. FUNCTION WITH TWO OR LESS ACTUATORS</li> <li>8. VECTORABLE 45-65 DEGREES</li> <li>9. MINIMUM WEIGHT</li> <li>10. UNIQUE MINIMUM AREA THROAT LOCATION THROUGHOUT THE VARIABLE GEOMETRY ENVELOPE</li> </ol> |
|--|

To accomplish all of the above objectives independently necessitates three separate actuators in the nozzle mechanism. Since this in conjunction with the vectored thrust requirement introduces additional complexity and weight into the system, the capability to independently vary the nozzle internal expansion area ratio is not included in the present studies. The basic design objectives

which have been exercised to identify a viable nozzle concept are listed in Table D-4.

Three nozzle concepts have been investigated for Configuration 27. A pivoting, variable-throat nozzle box is attractive because of its simplicity; however, approach and exit slopes are high (Figure D-29). Also, this concept is probably not acceptable for high temperature operation since air routing for wall cooling appears difficult. A two-flap variable throat nozzle offers simplicity and is amenable to cooling air routing but does not provide proper throat positioning when deflected.

An articulated pivoting nozzle such as depicted in Figure D-30 is attractive from the standpoint of both internal performance and nozzle base drag. This nozzle is limited to about 45 degrees of deflection at the present augmented-to-cold throat area ratio. If a lower WDB temperature is used, a smaller throat area ratio results, and increased nozzle deflections are allowed. However, a smaller augmented throat with the same 45-degree deflection allows a thinner wing section which has obvious advantages.



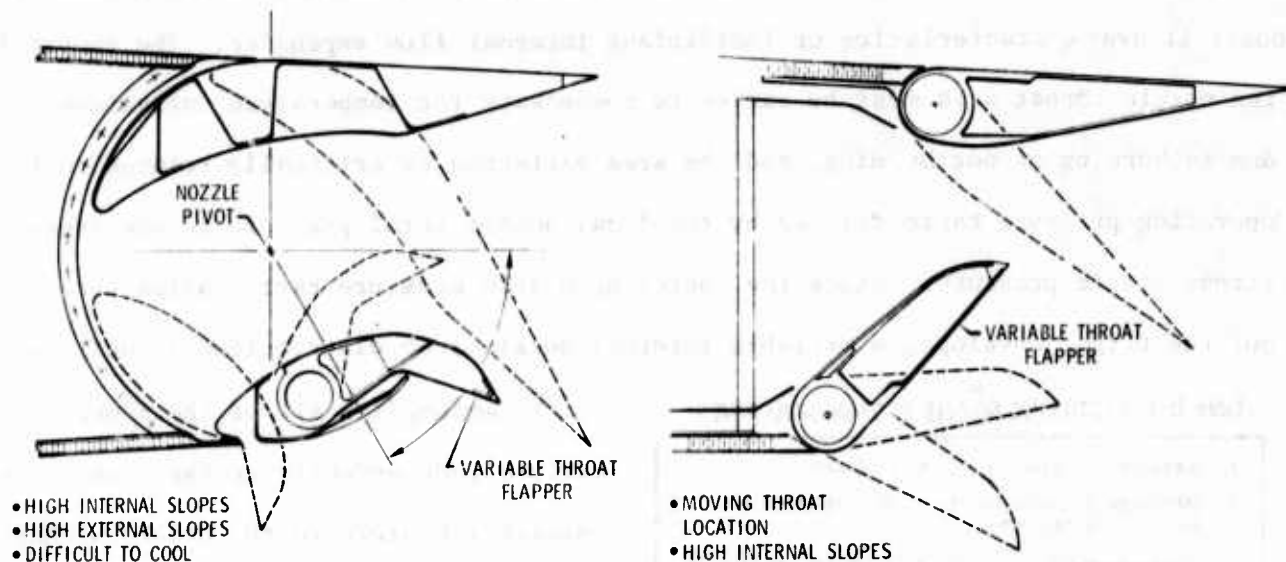


Figure D-29 Simple Vectoring Nozzle Concepts do not Satisfy Aerodynamic Requirements

The above tradeoff relating to selection of a WDB temperature is only one of several which have been identified. The overall trend is to increase WDB temperature to raise the nozzle thrust-to-weight ratio to a maximum and then decrease due to thrust losses and increased nozzle weight (Figure D-31).

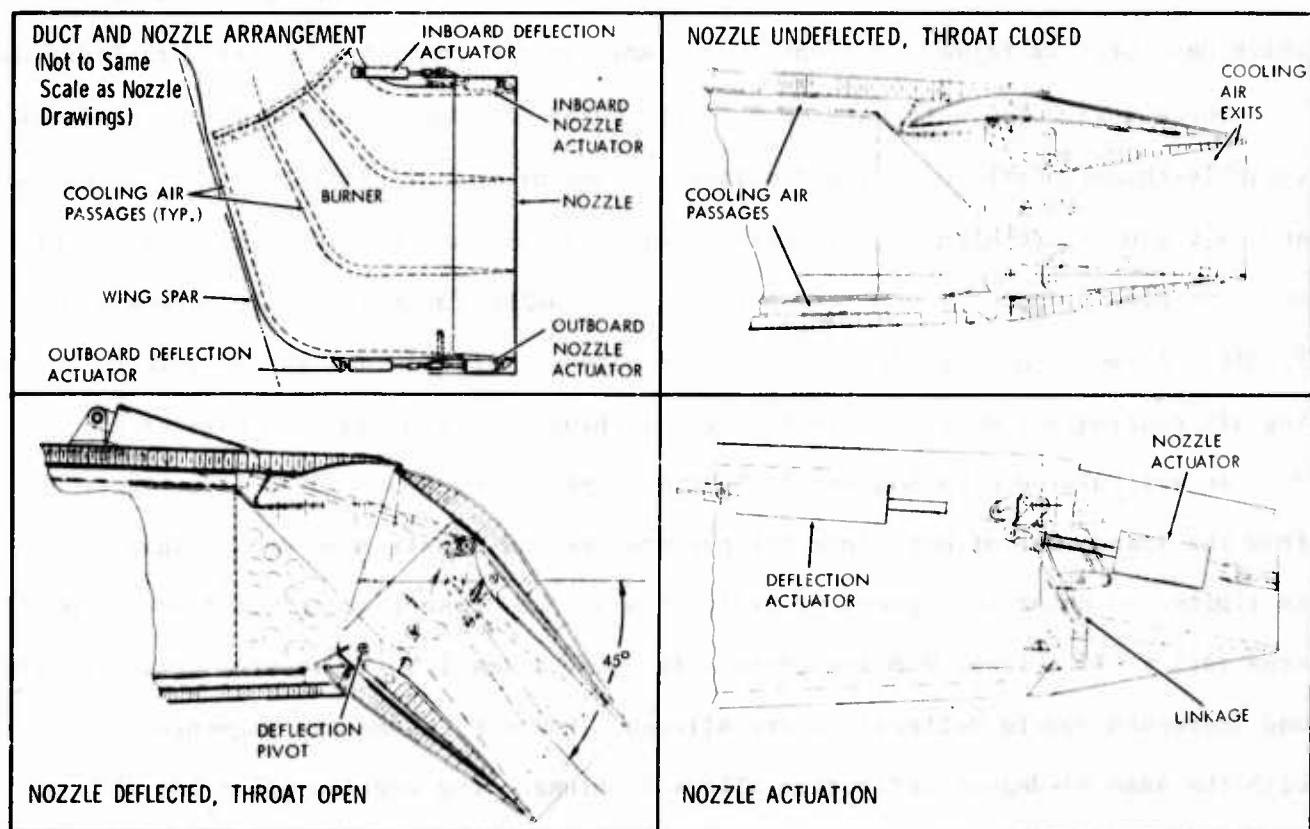


Figure D-30 Articulated Pivoting Nozzle is Attractive from All Standpoints



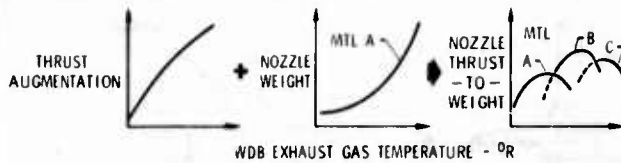


Figure D-31 Nozzle Tradeoffs can Effect Selected WDB Exhaust Temperature

Burning temperature tradeoffs are generally biased toward high temperatures for conventional nozzles; however, the vectored thrust nozzle involves considerations which possibly moderate this trend. Similar tradeoffs exist for the fan pressure ratio, since it sets the operating nozzle pressure ratio.

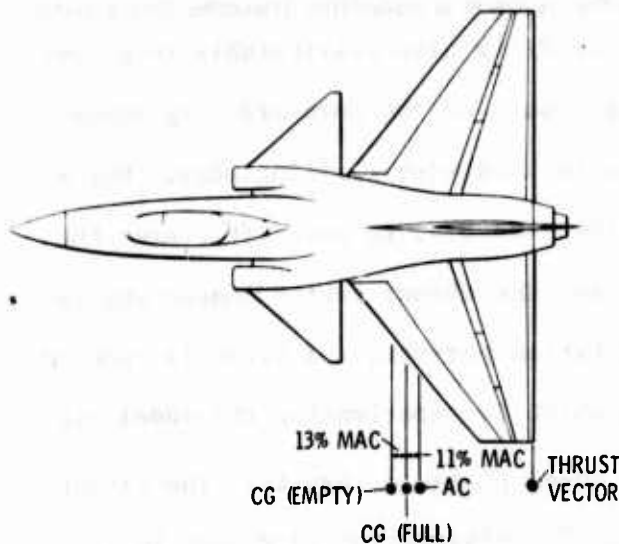


Figure D-32 Initial VT/SC Configuration Severely Limited Trimmable Thrust Vector Angle

#### D.2.3.3 Wing Location and Planform

The conceptually straightforward approach to VT/SC is to vector the full engine thrust at a normal aft location of the nozzle which is also coincident with the trailing edge. Convair efforts to evolve an LWA configuration having this characteristic as well as other desired configuration characteristics result in nose-heavy configurations (Figure D-32). This is not to say that a configuration,

which satisfies the original VT/SC concept and is suitably balanced from a normal trim standpoint, cannot be evolved, because it can--as testified most recently by the SAAB Viggen configuration.

The overriding problem is one of trimming the nose-down moment generated by VT/SC operation at low speed. Although the canard provides a lifting trim force as desired, the canard deflections required for trimming reasonable thrust angles and power settings at low speed are still excessive if the configuration is conventionally balanced.

For this reason, VT/SC configurations with large negative static margins appear necessary. This, in turn, dictates that the engine location be decoupled from the wing trailing edge if such configurations are to be realized. The present approach is to vector only the fan air which is ducted to the inboard portion of the wing trailing edge. The bulk of the engine weight can then be moved aft (Figure 3-12).

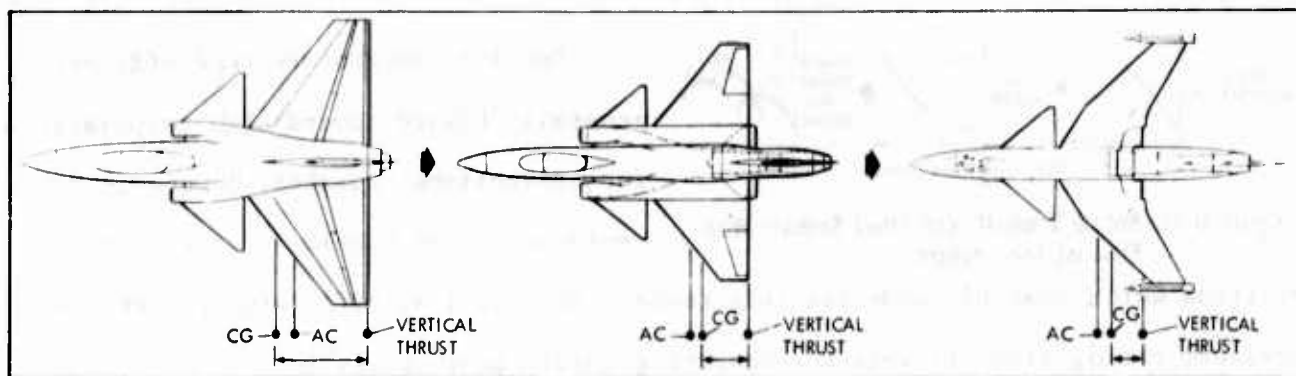


Figure D-33 LWA VT/SC Configuration Evolution is Keyed to Maximizing Trimmable Thrust Vector

The cranked wing planform of Configuration 27 is also attributable to alleviating the trim situation. The relatively high sweep of the outboard wing moves the wing aerodynamic center (a.c.) nearer the inboard wing trailing edge. For a given static margin, moving the a.c. also allows the c.g. to move aft nearer the point of application of the vectored thrust, and the thrust vector moment arm is significantly reduced. Since the lift augmentation potential of VT/SC is reduced by increasing wing sweep, the inboard wing which is experiencing the added circulation is only moderately swept, and the cranked planform results. The larger average sweep and higher wing thickness ratio of Configuration 27 result in a critical Mach number comparable to that of the wing planform of Configuration 26B.

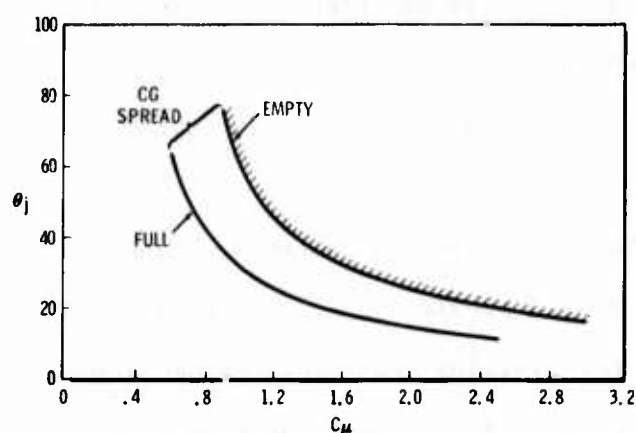


Figure D-34 Configuration 27 Controllable Thrust Vector at Low Speed

The combination of engine/wing decoupling and wing planform tailoring provides the trimmable thrust vectors given in Figure D-34. The configuration is balanced at a static margin between negative 15 and 25 percent of the mean aerodynamic chord. This results in significant trim penalty during cruise and other subsonic

non-VT/SC operations if the canard provides the complete restoring moment.

It is believed that an approach which schedules canard deflection and thrust vector angle to give maximum trimmed lift-to-drag (including lift augmentation and thrust losses due to the vectored thrust) as functions of angles of attack, altitude, and speed will result in flight efficiencies at non-VT/SC operating conditions

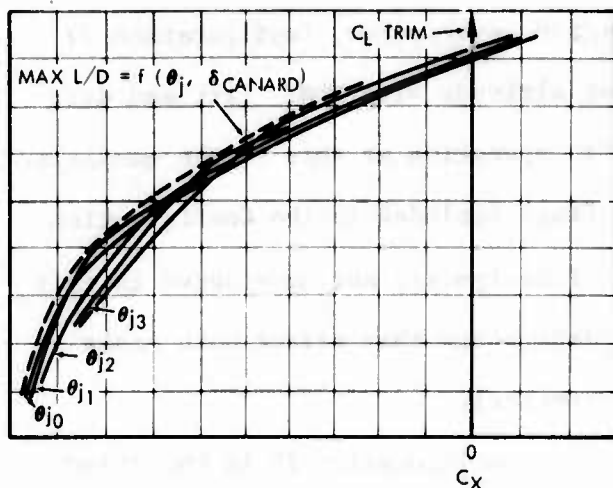


Figure D-35 Proper Scheduling of Thrust Vector and Canard Deflection can Maximize Efficiency

#### D.2.3.4 Performance

The primary adverse performance impact of implementing the Configuration 27 VT/SC concept is the effect on the propulsion system. The concept affects system hardware weight and propulsion efficiency, and the impact can be evaluated as a decrease in thrust-to-weight ratio and an increase in specific fuel consumption (SFC).

Table D-5 VT/SC IMPLEMENTATION INCREASES PROPULSION SYSTEM WEIGHT

	Δ WEIGHT FOR CONFIG. 27 VT/SC
• BASIC ENGINE WITH CONVENTIONAL BURNER	-4%
• PLENUM	+2%
• WDB/NOZZLE	+19%
• ENGINE EXTENSION	+10%
• FUSELAGE PROTECTION	+7%
• TOTAL PROPULSION SYSTEM	+34%

approach is increased 34 percent.

In addition, a 10 percent thrust loss increment at maximum power conditions is attributable to the duct turning, short burner space, and vectoring nozzle. The effect of the Configuration 27 VT/SC approach is then a 33 percent reduction in engine thrust-to-weight ratio and a 10 percent increase in SFC at maximum power conditions.

comparable to, at least, a conventionally balanced aircraft (Figure D-35). A quantitative evaluation of this supposition is greatly dependent on configuration details and therefore would not be particularly meaningful at the present stage of LWA configuration development. The quantified performance of immediate interest is for full VT/SC operation, i.e., for STOL and maneuver augmentation.

The effect of mechanical implementation is seen by comparing the weight of a conventional duct burning turbofan to that of the Configuration 27 arrangement, i.e., a WDB turbofan with turbine exhaust burner (Table D-5). For engines having the same basic size, the weight of the VT/SC

Considering now VT/SC maneuver augmentation performance, Configuration 27 has a  $c_{\mu}$  of 0.107 at Mach 0.9 and 30,000 feet altitude with WDB. Lift and drag-minus-thrust data for both VT/SC and non-VT/SC operation at this flight condition are shown in Figure D-36. The leading edge flaps included in the Configuration

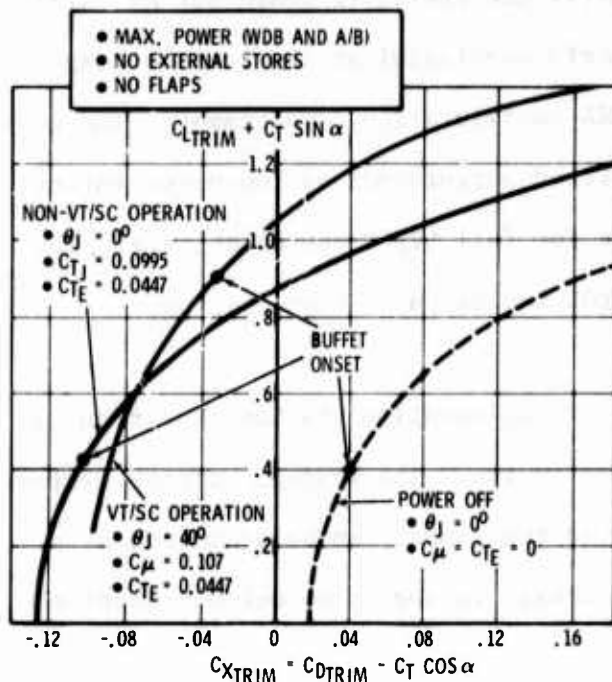


Figure D-36 Configuration 27 Aerodynamics for M0.9, 30,000 Feet Altitude Maneuver Evaluations

27 design are not considered in this data since they affect both modes similarly.

Configuration 27 in the VT/SC mode has a transonic buffet-free instantaneous load factor 2.15 times that for non-VT/SC operation. The effect of VT/SC on buffet onset lift coefficient is to add a lift increment to the corresponding non-VT/SC buffet onset lift coefficient. Since buffet onset occurs at low lift coefficients transonically, the above comparison greatly favors VT/SC.

At non-transonic speeds ( $\leq M0.8$ ), the increase in buffet onset lift coefficient ranges from 50 to 75 percent (Figure D-37). Using 65 percent as nominal, a 65 percent decrease in wing area results. For a Configuration 26C reference, the weight reduction is 1200 pounds, which compares with the approximate 1200 pounds added to the propulsion system by the VT/SC concept.

The non-VT/SC mode requires an additional 59 percent of thrust to equal the maximum sustained lift coefficient for VT/SC operation. This translates to a weight increase of about 1500 pounds which can also be compared to the VT/SC implementation requirements.

Another comparison can be made on the basis of equal  $C_x$  (negative excess power) at buffet onset. This involves both a wing area increase and a thrust

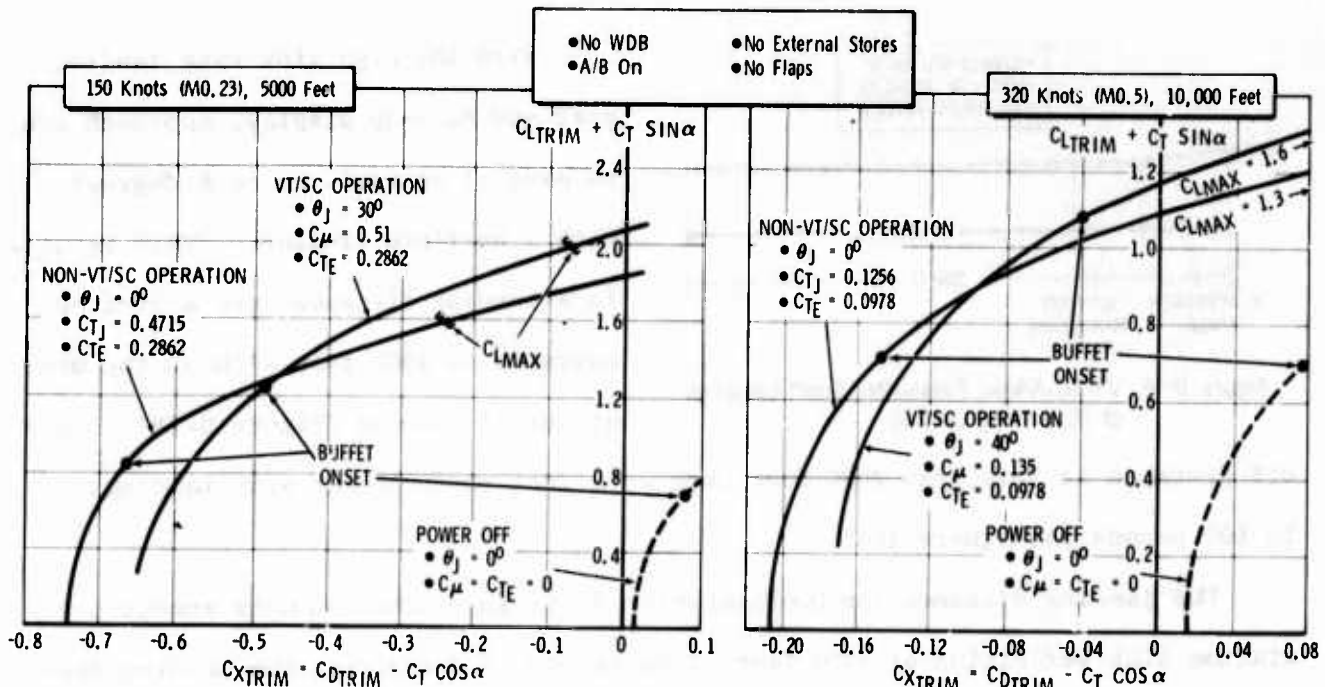


Figure D-37 Configuration 27 Aerodynamics for Ground Attack Maneuver Evaluations

increase for the non-VT/SC case. An approximate estimate of the additional weight required is 2600 pounds compared to the 1200 pounds for VT/SC at non-transonic conditions.

Equal sustained maneuver comparisons are contingent on the thrust recovery assumptions made for the analysis. Thrust recovery is dependent on specific configuration parameters, and the data shown here are empirical and do not reflect improvements which are thought possible. Convair's investigations concerning this subject are discussed in Appendix F.

Although the above single-point comparisons of VT/SC and non-VT/SC operations are of interest, the VT/SC concept must be proved on the basis of all mission requirements and through comparisons with unconstrained, nonpowered lift configurations. For example, the nonpowered lift performance cited above reflects the peculiar wing geometry which is required by VT/SC configuration constraints but which might not be the choice if such constraints were not present.

Considering the landing performance of Configuration 27, previous data from Figure D-34 indicate a trimmable  $c_{\mu}$  of 1.0 at a vector angle of 45 degrees. This translates to an approach speed of about 100 knots at a 12-degree angle of attack and a wing loading of 70 pounds per square foot.

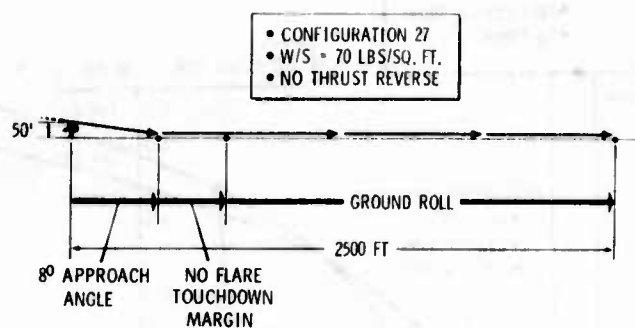


Figure D-38 VT/SC Allows Reasonably Short Landings at High Wing Loading

With the high sink rate landing gear and head-up display, approach can be made at an angle up to 8 degrees with a no-flare landing. This results in a landing distance over a 50-foot obstacle of 2500 feet without the use of thrust reverse (Figure D-38). Take-

off distance is less than 2000 feet over a 50-foot obstacle for wing loadings up to 100 pounds per square foot.

The landing distance for Configuration 27 is above the commonly accepted minimum STOL definition of 1500 feet. One method of decreasing the landing distance is to increase the canard effectiveness through either blowing or some other lift augmentation scheme to provide trim for larger thrust vector angles and/or higher  $c_{\mu}$ . The disadvantages of this approach are not only the implementation requirements of the canard augmentation, but also the considerations associated with providing nozzle vectoring angles greater than 45 degrees. The landing distance can be reduced by about one-third if thrust reverse is incorporated, but this decision also must be made in light of its effect on the total LWA concept.

#### D.2.4 JET FLAP - CONFIGURATION 28

##### D.2.4.1 General Description

The general arrangement of LWA Jet Flap Reference Configuration 28 is shown in Figure D-39. Many of its characteristics are derived from Configuration 26B, and the use of advanced composites is assumed. The wing thickness ratio is five percent in order to better accommodate the jet flap air ducting requirements.

The jet flap precludes incorporation of a flaperon, and spoilers are included for primary roll control. Outboard blown ailerons supplement the spoilers for low speed operations. This results in something less than a full span jet flap, but the ailerons appear necessary for landing control.



STRUCTURAL DESIGN WEIGHT	22,500 lbs
SPAN	34 ft. 8 in.
LENGTH	52 ft. 9 in.
HEIGHT	16 ft. 5 in.
WING (Theoretical):	
Area	300 sq. ft.
Aspect Ratio	4
Thickness Ratio	5%
Leading Edge Sweep	30°
OTHER AREAS:	
Canard (All-Movable)	49 sq. ft.
Aft Vertical Tail (All-Movable)	33 sq. ft.
Forward Vertical, Each (All-Movable)	5 sq. ft.
Flaperon	10 sq. ft.
Spoilers	19 sq. ft.
ENGINE:	
SLS Thrust	30,500 lbs
By-Pass Ratio	1.5
Fan Pressure Ratio	4
INTERNAL FUEL	7,087 lbs

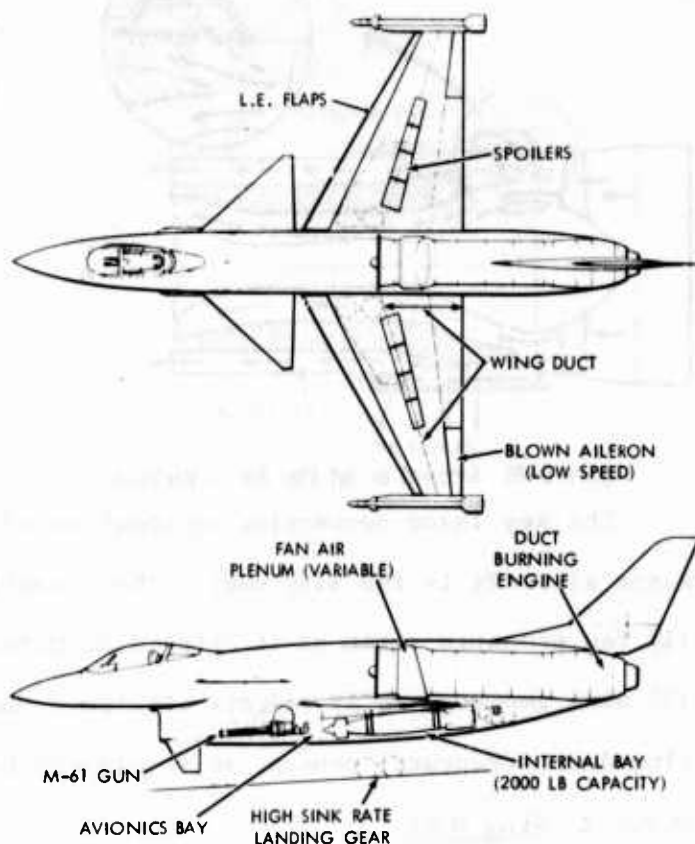
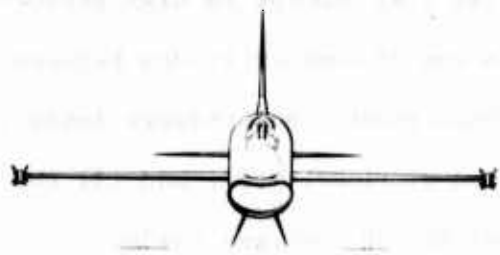


Figure D-39 Jet Flap Reference Configuration 28

As in the case of Configuration 27, the engine fan exit must be located forward of the wing duct entrance in order to keep turning losses reasonable. Separating the fan from the rest of the engine results in the shortest, properly balanced configuration. Since the engine weight that is moved aft includes the duct burner, the separation length is not as great as that required for Configuration 27.

The basic engine cycle is identical to that of Configuration 27 with a higher duct burning temperature. Air for jet flap operation is diverted from the fan duct, or plenum, into the wing duct.

The engine BPR of 1.5 provides more air than can be blown efficiently due to the flow restrictions of a fighter wing duct. So as not to unduly compromise BPR, a valve arrangement is envisioned for diverting variable amounts of jet flap air (Figure D-40). At sustained maneuver conditions where duct losses are critical, less than one-third of the available fan air is diverted (Figure D-41). The remainder can be burned for thrust augmentation if desired.

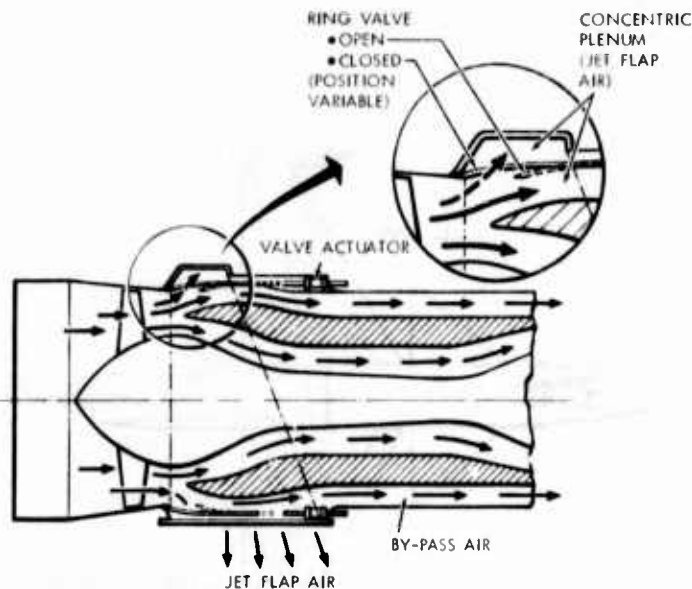


Figure D-40 Amount of Jet Flap Air is Variable

The key issue concerning application of the jet flap concept to high performance aircraft is the wing duct. The situation is one of complex trades between (1) fan pressure ratio as it affects structural requirements and pressure losses, (2) wing geometry as it affects available duct cross-sectional area, and (3) the wing duct structural concept as it affects both weight and pressure losses.

#### D.2.4.2 Wing Duct

##### D.2.4.2.1 Design Requirements

The selected FPR is four and represents a favorable trade of significantly lower pressure losses for small structural weight increases. Design criteria for pressure and temperature at various maneuver conditions are given in Table D-6.

Table D-6 WING DUCT DESIGN CRITERIA FOR FPR = 4  
FAN

MACH NO.	0.4	0.6	0.8	1.0
ALTITUDE (FT)	S.L.	S.L.	20,000	20,000
PRESSURE (PSIA)	67	74	46	53
TEMPERATURE (°R)	878	895	852	879

is, of course, determined by the mass flow and the duct cross-sectional area. The duct area is constrained by wing geometry, so, for a given configuration, mass flow rate is the primary variable for adjusting duct Mach number. From a lift augmen-

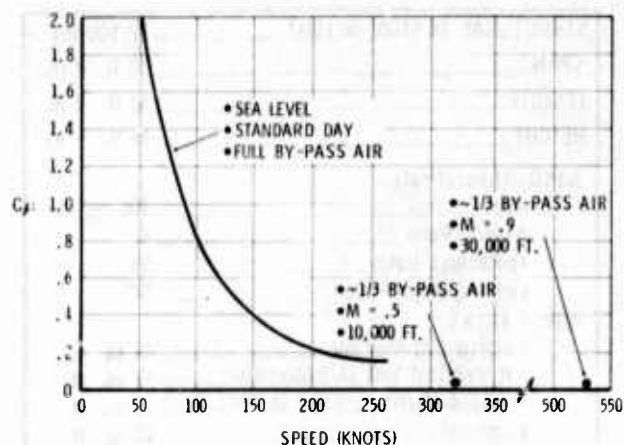


Figure D-41 Configuration 28  $C_L$  at Selected Conditions

A first step to minimize pressure losses is to keep the air velocity low in the duct. A good rule of thumb is a duct Mach number of 0.2 to 0.3.

The duct Mach number for a fixed FPR

mentation standpoint, selecting a required mass flow rate is difficult, because the situation is one of the higher the  $c_{\mu}$  the better.

Early in the LWA powered lift studies, it was determined that a minimum  $c_{\mu}$  of around 0.02 is required to provide meaningful lift augmentation at Mach 0.9, 30,000 feet altitude. Preliminary analyses at that time also indicated that this mass flow resulted in typical duct losses small enough to allow improvements in sustained load factor for the jet flap over an unaugmented wing. For these reasons, this blowing momentum coefficient is used as a gauge for guiding the duct conceptual design.

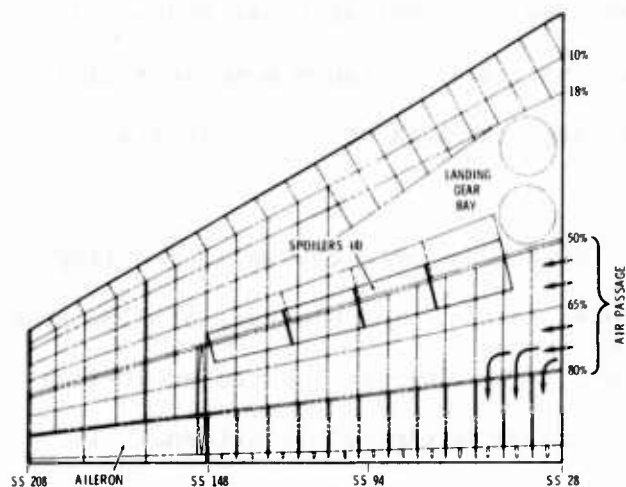


Figure D-42 Jet Flap Wing Duct Concept Uses Main Structural Box as Primary Duct

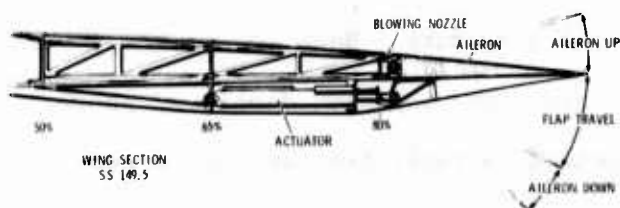


Figure D-43 Low Speed Aileron can be Used as Simple Control Device or Blown Flaperon

and main wing boxes.

The outboard 60 inches of the wing trailing edge are utilized for a low speed aileron. The main wing box/duct provides air so that the aileron can be blown whenever the jet flap is operating (Figure D-43).

#### D.2.4.2.2 Duct Concept

A flow area of 75 square inches at each wing duct inlet is required to maintain a Mach 0.2 flow velocity for a  $c_{\mu} = 0.02$  at Mach 0.9, 30,000 feet altitude. In order to achieve this value for the Configuration 28 wing geometry, the main structural box is designed as the duct. This box extends from the 50 to 80 percent wing chord line as shown in Figure D-42.

An auxiliary forward torque box assists in beaming landing loads on the main box. The main landing gear attach fitting spans the gear bay and distributes loads between the forward

The spoilers are mounted at mid-chord so as not to block air flow to the jet flap. Access to the spoiler actuators is through the landing gear bay for the two inboard segments and through removable cover plates for the two outboard segments.

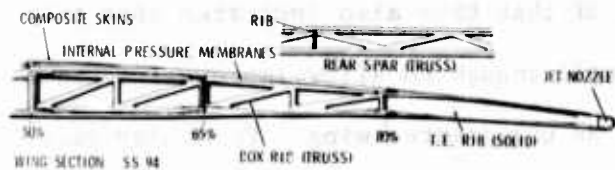


Figure D-44 Jet Flap Wing Duct Concept Integrates Structure and Duct

To eliminate pressure loads on the wing skins and reduce the magnitude of differential thermal expansion loads, the wing box duct is formed of a series of stainless steel pressure

membranes, or pillows, which concentrate the pressure loads at truss spars and ribs (Figure D-44). The wing trailing edge consists of pressure membranes tied to solid ribs. The ribs, spars, and pillows are stainless steel to withstand the high temperatures.

The flow is down the main box and turns 90 degrees into the solid trailing edge rib passages and through the fixed, choked nozzle. The blockage of flow area by each rib and spar truss is about 50 percent. The ribs are located at 10-inch intervals on the basis of skin gage requirements as determined by external air loads. Sandwich skins allow wider rib spacing, but the skin depth eliminates valuable flow area.

The resulting wing is structurally inefficient, and the duct is not particularly efficient due to the blockage by internal structure. However, of the several wing duct concepts considered, the integral structure approach described above appears to be the only concept which is structurally realistic, and it is considered marginal.

#### D.2.4.2.3 Pressure Loss Estimation

Duct pressure loss is a key performance parameter in determining the lift augmentation efficiency of the jet flap concept, but calculation of pressure losses in duct configurations such as described above is difficult. The estimation approach taken here is to divide the duct into two spanwise passages representing the two flow areas between the three main spars.

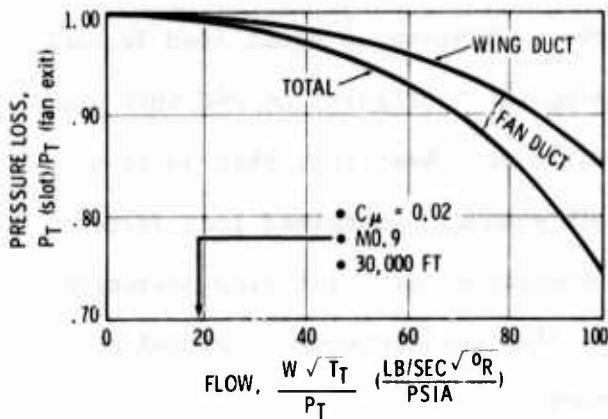


Figure D-45 Wing and Fan Ducts Result in Significant Pressure Losses

each of the truss members. Rounded truss edges are assumed. The pressure loss versus flow rate for the total duct is then obtained by summing the flows through the passages for a given pressure loss (Figure D-45).

Because the blowing slot is choked, similar corrected weight flows occur at all flight conditions for a fixed percentage of bypass air. For the reference condition of  $c_\mu = 0.02$  at  $M0.9$ , 30,000 feet altitude, the estimated wing duct loss is 1.5 percent. An additional 0.5 percent pressure loss at this condition is incurred in the duct between the fan and the wing.

#### D.2.4.3 Performance

The impact of the jet flap on aircraft weight is a primary concern. The weight increments associated with the engine and the wing are discussed in the preceding sections. In Table D-7, the increments are presented as percentages of a comparable conventional component. The actual weight increase for Configuration 28 is 1150 pounds.

Table D-7 JET FLAP IMPLEMENTATION IMPACTS PROPULSION AND WING WEIGHTS

		$\Delta$ WEIGHT FOR CONFIG. 28 JET FLAP
● PROPULSION		
● BASIC ENGINE		0
● PLENUM VALVING		+ 4%
● ENGINE EXTENSION		+ 10%
● TOTAL PROPULSION		+ 14%
● WING STRUCTURE		
● BASIC WING W/FLAPERONS (CONV.)		
OR SPOILERS (JET FLAP)		-12%
● WING BOX DUCT		+ 50%
● TRAILING EDGE SKINS		+ 4%
● TOTAL WING STRUCTURE		+ 42%

The maneuver performance at Mach 0.9, 30,000 feet altitude is shown in Figure D-46. At buffet onset, the nonpowered lift case requires 75 percent additional wing

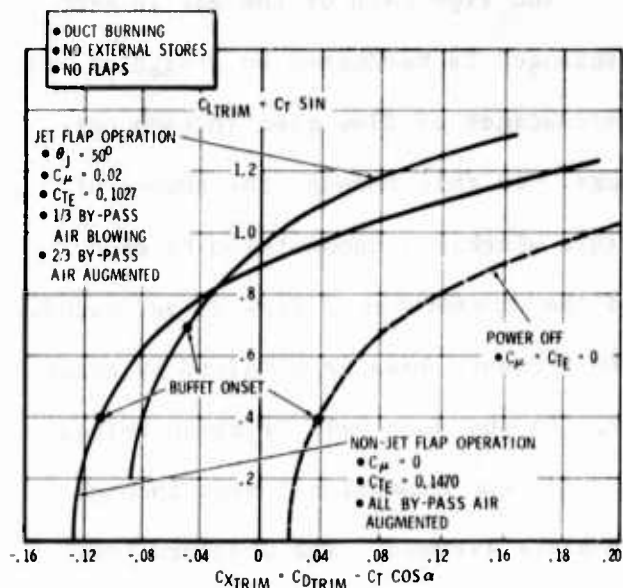


Figure D-46 Configuration 28 Aerodynamics for M0.9, 30,000 Feet Altitude Maneuver Evaluations

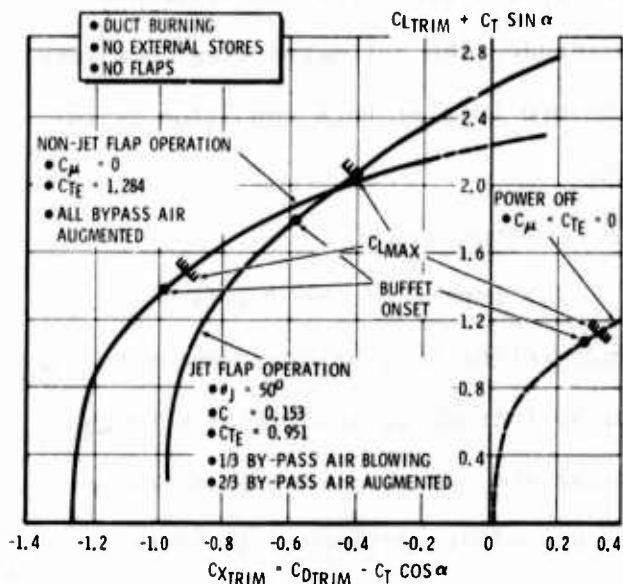


Figure D-47 Configuration 28 Aerodynamics for 150 KTAS, 5000 Feet Altitude Maneuver Evaluations

area to achieve an equal load factor.

Using the Configuration 26C unit wing weight as a baseline, this is about 1400 pounds. Sustained load factor comparisons favor jet flap operation for lift coefficients above buffet onset.

As speed decreases, instantaneous load factor comparisons for equal buffet levels are not as favorable for the jet flap (Figure D-47). Because of the particular Configuration 28 wing geometry, the buffet-onset and maximum lift coefficients are essentially equal at subsonic conditions.

As for Configuration 27, the maneuver comparisons cited above do not reflect the total configuration and performance impact of powered lift concepts. Overall mission performance must be considered in comparison to unconstrained, nonpowered lift configurations.

The amount of fan air diverted for landing is not constrained by pressure loss considerations as it is for maneuver performance. However, a maximum

trimmable lift coefficient exists, and this limits the landing  $c_{\mu}$  to less than that available using the total bypass air. Landing distance performance of Configuration 28 is estimated to be 2500 feet over a 50-foot obstacle.



### D.3 MISSION/CONFIGURATION TRADEOFFS

One of the primary objectives of Convair's LWA studies to date has been to define design requirements which are operationally germane to and compatible with the concept of a light attack system. The first step toward this goal consists of analyses in which the post-1980 time period is viewed from the standpoint of operational requirements with only very general consideration given to systems and technology.<sup>1</sup> The major points from these operational studies are summarized in Appendix A.

The second step in the requirements definition process involves evaluation of the interaction between mission requirements and aircraft configuration parameters and is the subject of this section. The purpose of this step is to reduce the many requirements to a compatible set and to examine these requirements within the framework of new technologies and configuration geometry and size variations. The hope is that, with proper application of technology and selection of configuration geometry and size, operational goals need be only minimally compromised.

#### D.3.1 ANALYSIS APPROACH

An understanding of the approach used in the mission/configuration tradeoff analysis facilitates an understanding of the significance of the results presented in following subsections. The sequential steps of the analysis are depicted in Figure D-48.



Figure D-48 Mission/Configuration Tradeoff Analysis Steps

The parametric operational requirements reflect only slightly the configuration implications. Hence, many are redundant, and certain combinations are unattainable with a lightweight system.

<sup>1</sup> "Post-1980 Tactical Air Strike Requirements and Capabilities," Convair Report MR-O-351, August 1972. (Confidential)

These redundancies are eliminated in a first-pass mission/configuration survey, and a range of pertinent requirements which is consistent with the gross weight objectives is established. This survey also provides guidance for selecting the numerical range of interest for configuration variables such as wing area, engine size, aspect ratio, wing sweep, and thickness ratio.

The mission and configuration variables established through the survey are quantified by parametric analysis. The primary effects being measured are the impact of configuration geometry and size on mission performance. The only advanced technology of interest which has a completely parametric effect on these factors is advanced composite materials. Parametric analyses are accomplished for configurations incorporating both conventional and advanced composite structures. The resulting data provide a meaningful measure of the potential payoff of advanced composites in addition to serving as mission/configuration tradeoff data.

The magnitude of the parametric analysis task should not be understated. In fact, it is only practical through the use of specialized, automated procedures. For the analyses discussed here, the primary concern is to obtain results which are sufficiently accurate to show proper trends of the mission/configuration tradeoffs. The absolute value of any computed performance measure is of second-order importance at this time, and this fact is reflected in the computational approach and, subsequently, in the results. The procedure which Convair used to perform the parametric analyses is described in Appendix G.

The powered lift technologies do not affect the mission/configuration tradeoff picture as viewed in this section in a completely parametric way as do advanced composites. The impact of powered lift can be inferred from the unpowered lift parametric data and the unique characteristics of powered lift configurations -- represented in this case by Configurations 27 and 28. Other advanced technology concepts such as variable camber, CCV, and advanced transonic airfoils can be similarly evaluated by use of the parametric data base.

The result of the mission/configuration tradeoff analyses, described on subsequent pages, is to reduce a very large number of alternatives to a much smaller

number. One is cautioned against any feeling that the questions concerning requirement setting and configuration selection have closed-form solutions. In the end, judgment and compromise will always be required. The purpose of this analysis and subsequent iterations of a similar, but finer, nature is to provide meaningful and logical guidance for the decision process.

### D.3.2 PARAMETRIC OPERATIONAL REQUIREMENTS

The parametric operational requirements as originally derived and documented in the Convair report on "Post-1980 Tactical Air Strike Requirements and Capabilities" include maneuver, acceleration, and mission definitions (Figure D-49).

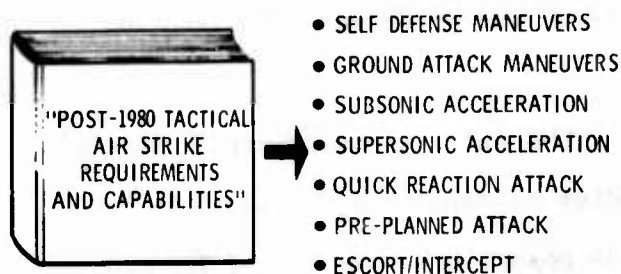


Figure D-49 Initial Set of Parametric Operational Requirements for LWA is Very Broad

#### • MANEUVERABILITY

	SPEED	ALTITUDE	PARAMETRIC RANGE OF SUSTAINED LOAD FACTOR*
• SELF DEFENSE			
A.	M = 0.8	5,000'	6.2 to 7.4 g's
B.	M = 0.9	15,000'	5.25 to 6.4 g's
C.	M = 1.2	25,000'	4.3 to 5.3 g's
• GROUND ATTACK			
A.	150 KNOTS	10,000'	1.5 to 2.5 g's

#### • ACCELERATION

	SPEED	ALTITUDE	PARAMETRIC RANGE OF ACCELERATION TIME*
• SUBSONIC	250 to 550 KTS.	10,000'	20 to 30 SECONDS
• SUPERSONIC	M 0.85 to M-1.6	CRUISE	50 to 80 SECONDS

\*Full Payload, 60% Fuel

Figure D-50 Maneuver and Acceleration Requirements Provide Excellent Ground Attack Capability and Maintain Self Defense

The high-speed sustained-maneuver requirements correspond to specific energy ( $P_s$ ) points that are equal to or greater than those of the most numerous or best threat aircraft currently in existence. In keeping with the guideline objective of self-defense rather than complete air-superiority capability for the LWA, future aircraft threats are not projected in the operations analysis. The Mach-altitude points specified here are obtained by using available data for the threats (Figure D-50).

The ground-attack maneuver requirement is predicated on a similar A-X design point, i.e., 2.2-g sustained maneuver at 150 knots, 5000 feet altitude, tropical day atmosphere. Justification of the demanding A-X design requirement generally takes three routes.

This capability permits (1) operation in very severe weather conditions (nominally 1000-foot ceiling, 1 mile visibility), (2) helicopter escort, and (3) effective

use of inexpensive weapons and associated systems (basically a 30mm gun and unguided, free-fall bombs). None of the above arguments has escaped challenge during the often-controversial A-X history; the primary concern is usually expressed over the survivability of an aircraft flying at such low speeds in any but the most permissive environments.

The subsonic acceleration time range of interest is consistent with a high thrust-to-weight ratio aircraft and guarantees the propulsive capability for performing post-attack survivability maneuvers. The range of supersonic acceleration times covers the F-15 and LWF capabilities and is somewhat better than the F-4 at the upper end. It is shown in the operations analysis that a supersonic acceleration time between 60 and 80 seconds is adequate to outrun threat AIMs assuming current rear-hemisphere detection ranges.

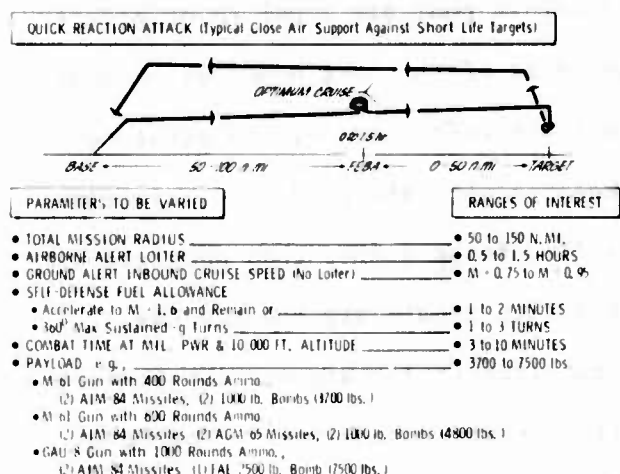


Figure D-51 Quick Reaction Attack Mission Represents Typical Close Air Support Role for LWA

The quick reaction attack mission radius as described in Figure D-51 is made possible by the use of forward basing to reduce range requirements. Forward basing is made technically possible by STOL capability; however, the geopolitical considerations associated with some potential operational situations envisioned for the LWA could present forward basing difficulties. This

situation is accommodated by combinations of radius and loiter time at the upper ends of both parametric ranges, since loiter time is directly translatable into increased mission radius.

The rationale for varying cruise speed to the target from a ground alert standpoint is predicated on the desire for minimum response time. Self-defense fuel allowance considerations are based on typical tactics, e.g., (1) supersonic acceleration and dash to evade a ground-vectored aircraft threat or (2) turning maneuvers to avoid surface-to-air missiles. The self-defense fuel allowance ranges of interest correspond to one or more such maneuvers.

Combat time allowance is based on the assumption that a single pass in a ground attack mode nominally requires three minutes. The range of interest then is one to three passes.

Payload weight is relatively light. The primary rationale for this is the effectiveness of smart bombs and missiles which result in "more bang per pound." The specific payload items listed are given simply to illustrate the weight range of interest.

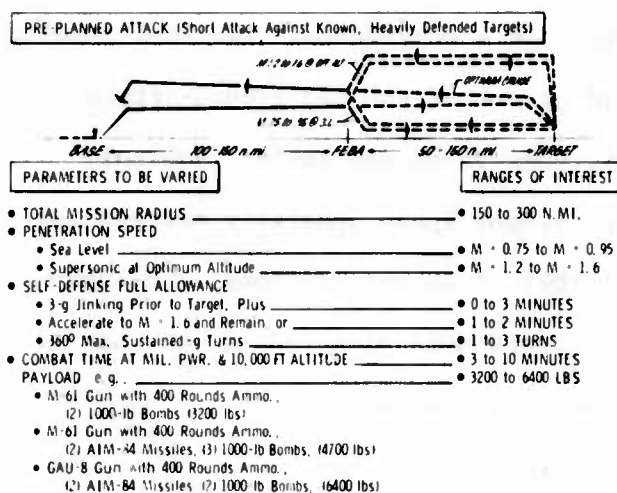


Figure D-52 LWA Employment for Interdiction/Strike Role is Basis for Pre-Planned Attack Mission

The pre-planned attack mission profile shown in Figure D-52 consists of subsonic cruise at altitude with the possibility of dash maneuvers in the vicinity of the target either at subsonic speed and sea level, or at supersonic and altitude. The mission radius range of interest is based on a conventional tactical situation such as might occur in the European theater. Other projected employments of the LWA --

such as "brushfire" conflicts with geopolitical constraints on basing -- could require greater mission radii. These missions generally require less self-defense allowance and/or no dash maneuver which adds substantially to the basic mission radius.

Variations of subsonic and supersonic penetration speeds are of interest, because the effectiveness of the dash maneuver for increasing aircraft survivability is a function of speed. The self-defense fuel allowance includes the capability for the tactics specified for the quick-reaction attack mission plus the capability for a 3-g jinking flight profile prior to weapon delivery to improve survivability.

Combat time and payload weight rationale for the pre-planned attack mission is similar to that for the quick reaction attack mission. Because of the more specific nature of the pre-planned attack targets, somewhat lighter payloads are envisioned for this mission type.

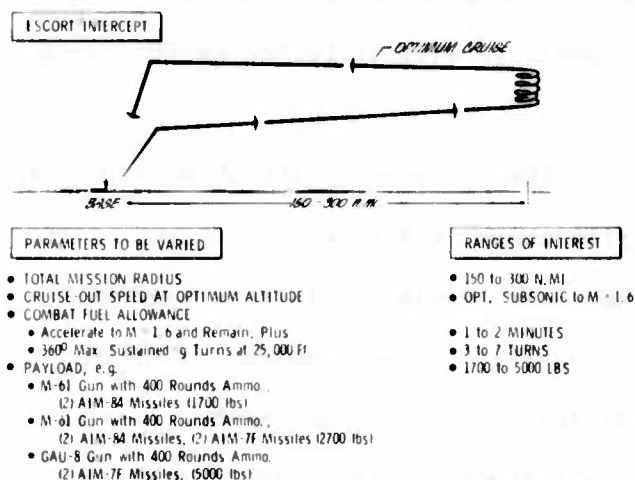


Figure D-53 Escort/Intercept Capability Allows Supplemental Air Superiority Role for LWA

Escort/intercept missions are defined parametrically in Figure D-53. The mission radius range of interest is consistent with both point intercepts in a conventional tactical theater and escort of the LWA ground-attack missions discussed above. Subsonic cruise-out speed generally corresponds to that of escort missions, and supersonic speed is directed toward that of intercept missions.

Combat fuel allowance for the escort/intercept missions is set to allow varying degrees of persistence in an air-to-air engagement. The payload weights of primary interest are small, because the LWA is primarily a visual day fighter when employed in the escort/intercept role.

### D.3.3 MISSION/CONFIGURATION SURVEY

The mission/configuration survey is a process of selectively quantifying the different operational requirements for various parametric configurations. Conventional Configuration 26 is the reference configuration for the survey.

#### D.3.3.1 Maneuverability and Acceleration

Maneuverability and acceleration requirements are the primary determinants of wing loading and thrust loading, respectively. Figure D-54 is indicative of the wing loading associated with each of the parametric maneuver requirements. It is clear that the 150 knot condition is predominant.



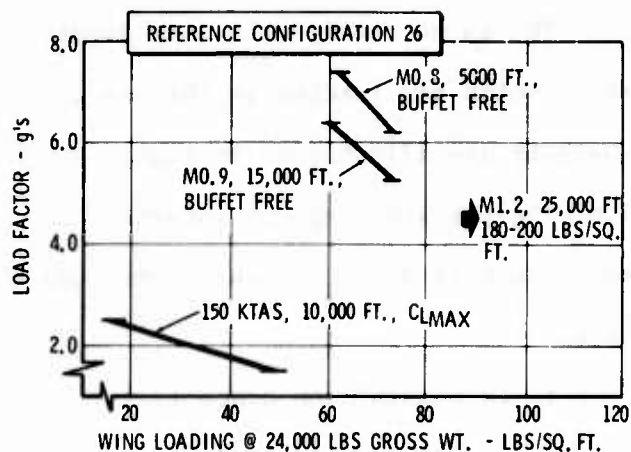


Figure D-54 Low Speed Maneuver Dominates Parametric Requirements from Aerodynamic Standpoint

The specification of self-defense maneuver requirements based only on sustained-maneuver capability of the threat presents a problem. The threat aircraft are only thrust-limited at the conditions considered, and the sustained-g's are not indicative of the threats' instantaneous-g capability.

Because of this situation, a transonic maneuver parametric requirement

range of 2 to 4 g's at Mach 0.9 and 30,000 feet altitude, instantaneous and buffet-free, is added. The increase in lift for the mild-to-moderate buffet region ranges from 50 to 150 percent at transonic conditions, so the buffet-free range of interest corresponds to an in-buffet range which generally brackets the structural limits of the LWA. From an operational requirement standpoint, it is more realistic to specify an in-buffet maneuver requirement; however, buffet onset is easier to predict as a function of wing geometry and therefore is used in the parametric analysis for convenience.

The uncertain justification of the 150-knot requirement indicates that the condition should not be allowed to drive all of the parametric configurations; however, such is the case, even with the 1.5-g lower limit. In order to effect a suitable overlap with the transonic requirement, the range of interest at 150 knots is changed to 1 to 2 g's maximum usable load factor, and the altitude is lowered to 5000 feet, standard atmosphere.

Another ground attack condition which is operationally justifiable is included in the parametric considerations as a backup in the event the 150-knot requirement is discarded completely. The instantaneous load factor range of interest is 4 to 6 g's at 320 knots (Mach 0.5), 5000 feet altitude, and maximum lift coefficient.

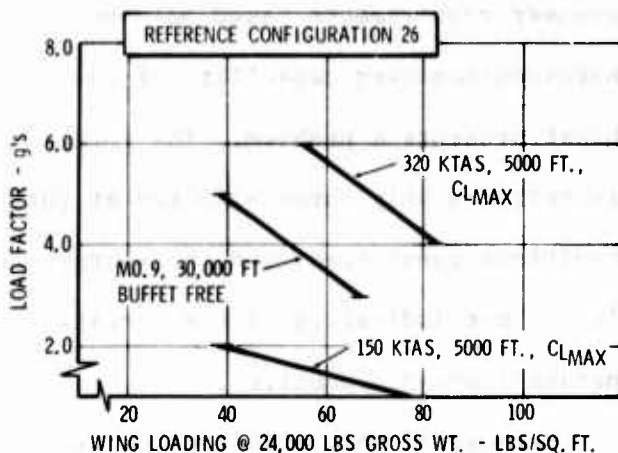


Figure D-55 Parametric Analysis Considers More Compatible and Meaningful Instantaneous g Requirements

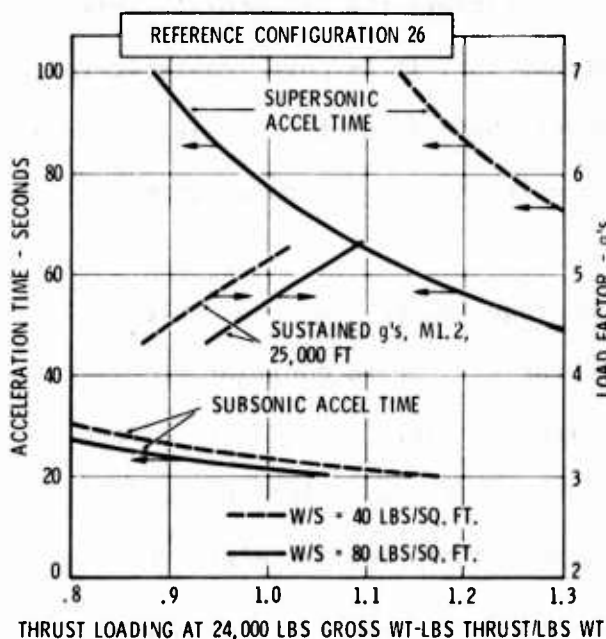


Figure D-56 Supersonic Acceleration Requirements Provide Adequate Thrust to Generally Meet Other Engine Sizing Requirements

The three aerodynamic lift requirements which are tracked in the parametric analysis are illustrated in Figure D-55. The wing loading range of interest is approximately 40 to 80 pounds per square foot.

It is possible to concentrate maneuverability considerations on instantaneous capability, because the minimum supersonic acceleration requirement of 80 seconds generally results in adequate thrust loading to meet or exceed the sustained maneuver requirements. This is illustrated in Figure D-56 for the Mach 1.2, 25,000 feet altitude sustained-maneuver condition which requires the highest thrust loading of the specified sustained maneuvers.

It can also be seen in Figure D-56 that a thrust loading sufficient to perform an acceleration from Mach 0.85 to Mach 1.6 in 80 seconds or less is adequate to meet the subsonic acceleration requirement. The thrust-to-weight range of interest for the parametric studies is from 1.0 to 1.5.

### D.3.3.2 Configuration Geometry Variables

In addition to thrust and wing area variations, the other configuration variables exercised in the complete parametric analysis relate to wing planform geometry, i.e., aspect ratio, thickness, and sweep. The effects of these parameters on wing structural weight and aerodynamics result in the first-order mission/configuration tradeoffs of interest.

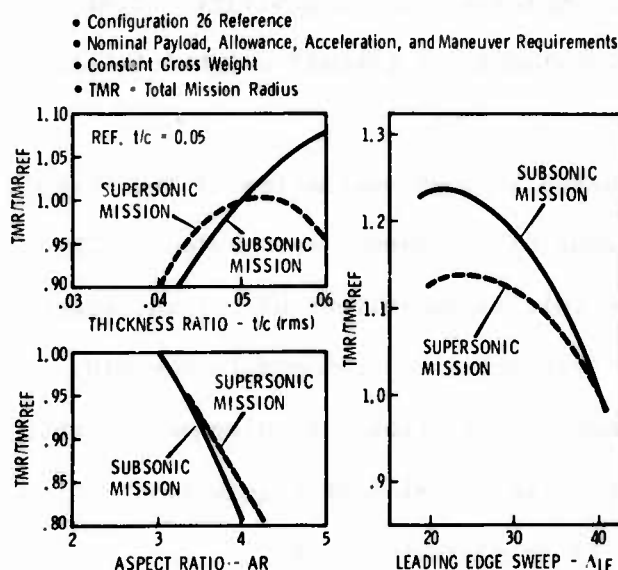


Figure D-57 Preliminary Survey Indicates Wing Geometries of Interest

The conflicting trends of subsonic mission performance versus supersonic mission performance provide a means of bracketing the ranges of interest for the three geometry parameters. In Figure D-57, the effects of varying each parameter from the Configuration 26 reference are shown for nominal missions representing the two speed regimes.

It is noted at this point that all five configuration variables -- wing loading, thrust-to-weight, aspect ratio, thickness, and sweep -- are very inter-related in their effects on mission performance. (This is evidenced by the need for the complete parametric analysis.) The data cited above and in the preceding section only provide guidance for selecting the numerical ranges of interest to be considered in the complete analysis (Table D-8).

Table D-8 PARAMETERS AND RANGES OF INTEREST SELECTED FOR LWA PARAMETRIC ANALYSIS

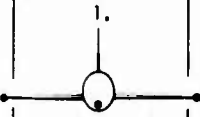
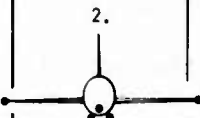
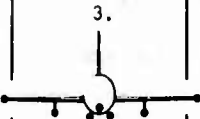
PARAMETER	RANGE OF INTEREST
Wing Loading (W/S)	40-80
Thrust Loading (T/W)	1.0-1.5
Aspect Ratio (AR)	3-5
Wing Thickness Ratio (t/c)	0.04-0.06
Leading Edge Sweep ( $\Lambda_{LE}$ )	20-40 Degrees

### D.3.3.3 Allowances and Payloads

The effects of the self-defense and combat allowance variations on the parametric analysis results are manifest in two forms: (1) partially determining the takeoff weight/mission radius relationships and (2) providing emphasis on performance at the conditions where the allowance is taken; e.g., the self-defense fuel allowance which corresponds to a specified number of maximum sustained-g turns tends to favor the configuration with maximum sustained turn capability. Similarly, the payload variations are primary determinants of takeoff weight/mission radius relationships.

The mission/configuration survey encompasses a rough evaluation of the takeoff weight/mission radius relationships as functions of allowances and payload. The results are then viewed in the context of the initial guidelines of a lightweight system. As shown in Table D-9, the approach selected to accommodate the many allowance and payload variations of the parametric operational requirements within a practical computational task is based on specific "mission configurations" which cover the parametric ranges of interest with three discrete points.

Table D-9 A CONCEPT OF "MISSION CONFIGURATIONS" IS USED TO COVER ALLOWANCE AND PAYLOAD VARIATIONS

Mission Configuration	Typical Scenario	Fuel	Payload	Allowances (Self-Defense/Combat)	Sizing Criteria Exercised	Parametric Study TOGW
1. 	POINT TARGET, HIGH THREAT	● INTERNAL	● INTERNAL 2000 LBS ● WING-TIP A-A MISS. ● M-61 GUN	● ACCEL TO M1.6/3 MIN. MIL PWR	● STRUCTURAL WT. 80% FUEL, 6g's ● SUPERSONIC ACCEL TIME	● 24,000 LBS
2. 	MULTIPLE TARGETS, MODERATE THREAT	● INTERNAL	● INTERNAL 2000 LBS ● SHOULDER 1000 LBS ● WING-TIP A-A MISS. ● M-61 GUN	● ONE 360° MAX PERF TURN/ 6.5 MIN MIL PWR	● HIGH SPEED MANEUVERS ● SUBSONIC ACCEL TIME	● 25,000 LBS
3. 	AREA TARGET, PERMISSIVE ENVIRONMENT	● INTERNAL ● INTERNAL BAY 2000 LBS	● SHOULDER 2000 LBS ● WING PYLON 4000 LBS ● WING-TIP A-A MISS. ● M-61 GUN	● NONE/10 MIN MIL PWR	● LOW SPEED MANEUVERS	● 30,000 LBS

The first tenet of the mission/configuration approach is that the LWA takeoff weight is determined by the fuel and payload loading desired. Structural g-load limits are simply varied with aircraft weight. (Convair is investigating the possibility of sensing loadings with strain gauges or other devices located at critical points. Pilot cues are provided as any load reaches a critical value. The result is a reduced pilot work load as well as a possibly more efficient structure.)

Mission Configuration 1 is a clean configuration with internal payload and wing-tip mounted AIMS. This loading, which corresponds to the lower end of the payload variations of interest, results in the highest performance capability of the LWA and therefore is consistent with employment in a high threat environment. The resulting self-defense allowance is an acceleration to Mach 1.6, which is the largest of the three mission configuration self-defense allowances. It also follows that a single-pass combat allowance is consistent with a heavily defended target as well as the limited payload of Mission Configuration 1.

The structural weight as calculated for the parametric analysis is based on Mission Configuration 1, and the supersonic acceleration times also relate to this configuration. The takeoff weight for Mission Configuration 1 is 24,000 pounds which, with the payload and allowances assumed, provides mission radii for the different mission types within the ranges of interest indicated by the parametric operational requirements.

Mission Configuration 2 provides an additional 1000 pounds of external, shoulder-mounted stores, effecting a medium payload relative to the range of interest. The self-defense allowance is one subsonic turn, and the combat time provided is consistent with the increased payload. The parametric analysis uses Mission Configuration 2 for calculating self-defense maneuverability and subsonic acceleration capabilities.

An important aspect of the Mission Configuration 2 definition is the all-subsonic, high performance allowance and sizing conditions. When this mission configuration is used to perform an all-subsonic mission profile, the result is parametric data which have no explicit supersonic characteristics.

Mission Configuration 3 provides a 2000-pound fuel cell installation in the internal bay and 6000 pounds of external stores. This mission configuration provides the upper end of the payload range of interest. No self-defense allowance is defined, and combat time is increased because of the increased payload. Ground attack maneuverability is measured for this loading.

When examined for all-subsonic missions, Mission Configuration 3 parametric data provide additional contrasts between supersonic, high-subsonic, and moderate-subsonic aircraft design objectives. It is noted that Mission Configuration 3 is consistent with A-X type performance objectives.

The mission configuration definitions do not include some variations in self-defense fuel allowance which are indicated to be of interest by the parametric operational requirements. These are the number of sustained-g turns, the number of minutes of jinking, and the number of minutes at Mach 1.6.

The primary effect of a specific number of sustained-g turns is to trade mission radius for number of turns. Since this trade is similar for all configurations within the range of interest, variation of the number of turns within the complete parametric analysis will have a negligible effect on the results. Mission radius/number of turns tradeoffs will be quantified after the mission/configuration matrix is reduced by parametric analysis.

A similar rationale exists for omitting the jinking maneuver in the complete parametric analysis. The length of time that a Mach 1.6 evasive maneuver is maintained has minimal impact on the parametric analysis for the small range of interest (0-to-2 minutes). As it turns out, the effect of this maneuver in an otherwise all-subsonic mission is approximated in the pre-planned attack mission profile which includes a Mach 1.6 penetration dash that can be easily converted to minutes (one minute at Mach 1.6 = 15 nautical miles).

A final justification of the particular mission configuration definitions is the fact that, for the quick reaction attack mission profile, each mission configuration has basically the same mission radius. This provides a normalizing frame of reference for the parametric analysis results.



#### D.3.3.4 Mission Profiles

##### D.3.3.4.1 Quick Reaction Attack

For a fixed configuration, the difference between optimum subsonic cruise conditions and optimum loiter conditions is a function of engine performance (i.e., the different fuel flow rates), and these differences become small as thrust-to-

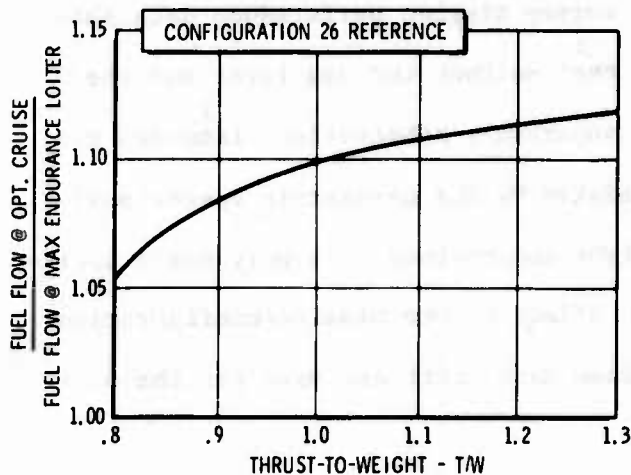


Figure D-58 Optimum Cruise is Sufficiently Near Optimum Loiter for Analysis Purposes

weight reaches the relatively large values of interest for the LWA (Figure D-58). For this reason, the loiter segment of the quick reaction attack mission profile is not explicitly considered. The assumption is that mission radius is convertible to loiter time in about the same proportions for all configurations of interest.

In the above rationale, a fixed engine cycle is assumed. Loiter/mission radius tradeoffs will have a greater impact on future parametric analyses in which engine cycle variations, particularly variations in bypass ratio, are considered.

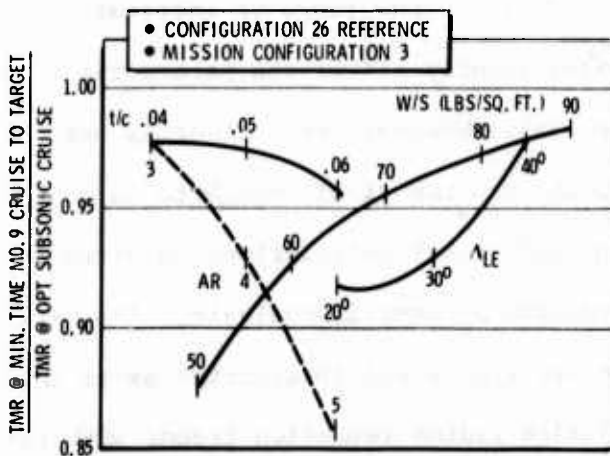


Figure D-59 TMR's for Minimum Time Subsonic Cruise are not Substantially Different than for Optimum Subsonic Cruise

The parametric operational requirement consideration of a cruise-to-target condition which provides faster response time to the target from a ground alert situation does not sufficiently impact the parametric analysis to warrant in-

corporation (Figure D-59). The resulting mission profile which is employed in the parametric analysis for the quick reaction attack mission is shown in Figure D-60.

#### D.3.3.4.2 Pre-Planned Attack

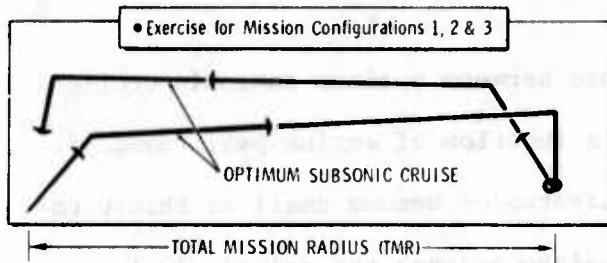


Figure D-60 "Optimum Subsonic" Mission Profile Represents Quick Reaction Attack and Optimum Cruise Pre-Planned Attack Requirements

be varied up to 150 nautical miles, as indicated by the parametric operational requirements, and remain within the LWA weight constraints. If only small variations of penetration radius are allowed, no effect on the mission/configuration tradeoffs are to be expected; therefore, fixed dash radii are used for the parametric analysis.

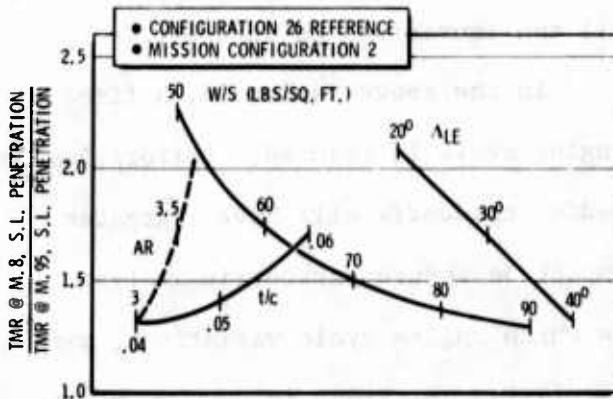


Figure D-61 Sea Level Penetration Speed can have a Strong Effect on Parametric Results

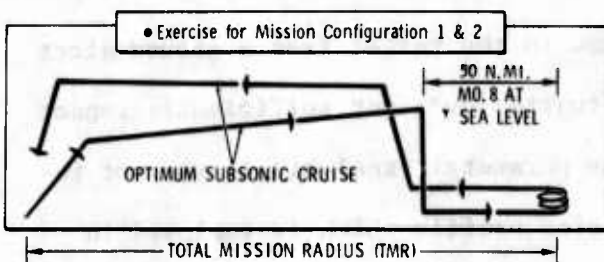


Figure D-62 "Sea Level Penetration" Mission Profile Represents Pre-Planned Attack Option

The optimum cruise option for the pre-planned attack mission is also satisfied by the "optimum subsonic" mission profile shown in Figure D-60. The survey mission performance data show that neither the sea level nor the supersonic penetration distances can

The sea level penetration radius is held constant at 50 nautical miles. The data in Figure D-61 show that variations in subsonic sea level dash speed within the range of interest significantly affect the parametric analysis; however, this trade is not considered important enough to warrant the additional calculations required for complete parametric analysis. The data in the figure are instructive as to the mission radius reduction trends with increased penetration speed as a function of the configuration variables. The "sea level penetration" mission profile used in the parametric analysis is depicted in Figure D-62.

The selected supersonic penetration radius is 35 nautical miles. The penetration altitude is held constant at 40,000 feet for the parametric analysis to eliminate the requirement to solve for an optimum altitude for each configuration. This calculation convenience has no effect on the parametric trends and very little effect on the actual numerical results.

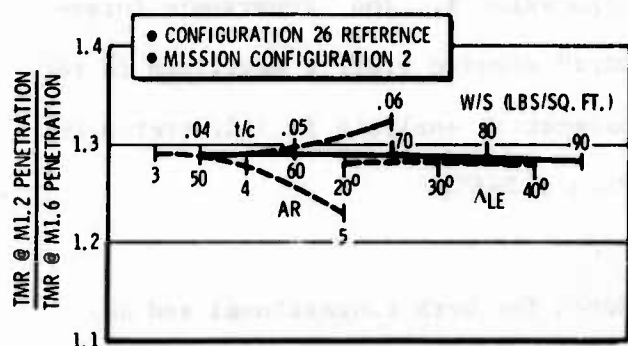


Figure D-63 Parametric Configuration Variations do not Significantly Affect TMR's at Different Supersonic Penetration Speeds

Because the LWA is sized for a maximum speed of Mach 1.6, there is very little parametric configuration variation between penetration speeds from Mach 1.2 to Mach 1.6 (Figure D-63). The parametric analysis exercises one "supersonic penetration" mission profile with a dash speed of Mach 1.6 (Figure D-64).

#### D.3.3.4.3 Escort/Intercept

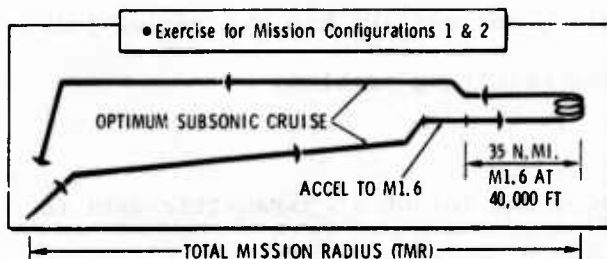


Figure D-64 "Supersonic Penetration" Mission Profile Represents Pre-Planned Attack Option

The lower end of the cruise-out speed range as specified by the parametric operational requirements for the escort/intercept mission is optimum subsonic. This speed corresponds to that used for escort-type missions, and the mission profile is the optimum subsonic

mission profile described previously. The parametric data for this profile and Mission Configurations 1 and 2 correspond directly to those of the escort mission where the combat allowances of 3 and 6.5 minutes at military power is roughly equivalent to 2+ and 5 maximum sustained-g turns at Mach 0.9, 15,000 feet altitude, respectively.

As in the case of the supersonic penetration pre-planned attack mission, there is little parametric configuration tradeoff between supersonic cruise-out speeds less than and equal to Mach 1.6, so only the Mach 1.6 case is considered

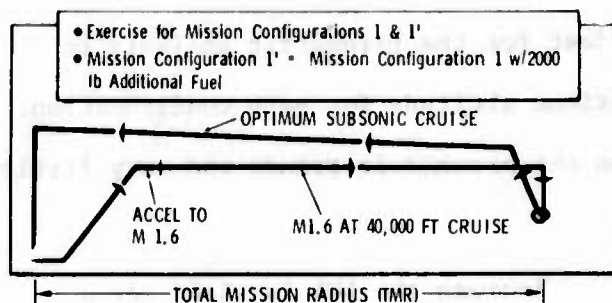


Figure D-65 "Supersonic Intercept" Mission Profile Represents Interceptor Role for LWA

in the parametric analysis. A combat fuel allowance for three maximum sustained-g turns at Mach 0.9, 15,000 feet altitude is used in lieu of the combat allowance specified for Mission Configuration 1. The "supersonic intercept" mission profile exercised in the parametric analysis is illustrated in Figure D-65).

#### D.3.4 PARAMETRIC ANALYSIS

A complete parametric analysis is presented for both conventional and advanced composite materials in Appendix H. The application of the data obtained and the impact of powered lift technology on the LWA mission/configuration trade-offs are described below.

Although the discussion presented here is somewhat driven by specific guidelines for the LWA concept, the basic data in Appendix H are quite general and can be utilized in a number of ways. In other words, one can set his own set of initial goals and apply the parametric data to the resulting problem.

##### D.3.4.1 Conventional Materials

The initial question is how to reduce the large amount of parametric data to something that can be visualized in the absence of specified requirements and without completely arbitrary judgements. The approach described here is based on the two objectives of this study: (1) quantification of mission/configuration trade-offs rather than selection of "optimum" configurations and (2) consideration of "compromise" requirements and configurations which yield a versatile LWA concept. In the exercise described here, the second objective is assumed and the first is partially accomplished.

The three wing planform geometries which result in the largest mission radii for each of the four mission profiles, the one common mission configuration, the four wing loadings, and the five thrust loadings are extracted from the data.

A single constraint is applied to all configurations, i.e., a supersonic acceleration time equal to or less than 80 seconds.

The same geometries appear throughout the tabulation and some appear for almost all mission profiles, wing loadings, and thrust loadings. It is concluded that such a geometry can be used to illustrate wing loading and thrust loading tradeoffs versus mission requirements.

Table D-10 reveals two cuts through the tabulation for a nominal thrust loading and a nominal wing loading. A wing leading edge sweep of 20 degrees appears almost exclusively. The thickness and aspect ratio combinations vary according to generally predictable trends, but a combination of 0.05 thickness ratio and aspect ratio of 4 appears for almost all mission profiles, wing loadings, and thrust loadings.

Table D-10 A WING PLANFORM GEOMETRY OF  $t/c = 0.05$ ,  $\Lambda_{LE} = 20^\circ$ , AND ASPECT RATIO = 4 IS A GOOD GEOMETRY FOR TOP-LEVEL TRADEOFF PRESENTATIONS RELATING TO CONVENTIONAL MATERIALS

● MISSION CONFIGURATION 1						● SUPERSONIC ACCELERATION TIME ≤ 80 SEC.					
ENGINE SIZE = 0.9 (T/W = 1.29 UNINSTALLED AT TAKEOFF)						WING AREA = 350 FT <sup>2</sup> (W/S = 68.6 AT TAKEOFF)					
OPTIMUM SUBSONIC MISSION PROFILE						SUPERSONIC PENETRATION MISS. PROF.					
TMR RATING	t/c	$\Lambda_{LE}$ (DEG.)	AR	$S_w$ (FT <sup>2</sup> )	TMR (N.M.I.)	TMR RATING	t/c	$\Lambda_{LE}$ (DEG.)	AR	$S_w$ (FT <sup>2</sup> )	TMR (N.M.I.)
1	.06	20	5	280	741	1	.05	20	4	280	372
2	.06	↓	4	↓	673	2	.06	↓	4	↓	363
3	.05	↓	4	↓	645	3	.05	↓	3	↓	344
1	.06	20	5	350	722	1	.05	20	4	350	316
2	.06	↓	4	↓	672	2	.05	↓	3	↓	306
3	.05	↓	4	↓	637	3	.06	↓	4	↓	305
1	.06	20	4	420	603	1	.05	20	3	420	245
2	.05	↓	4	↓	569	2	.04	↓	3	↓	243
3	.06	↓	3	↓	555	3	.06	↓	3	↓	228
1	.05	20	3	490	474	1	.04	20	3	490	171
2	.05	↓	4	↓	473	2	.05	↓	3	↓	162
3	.04	↓	3	↓	446	3	.05	↓	4	↓	117
SEA LEVEL PENETRATION MISS. PROFILE						SUPERSONIC INTERCEPT MISS. PROFILE					
TMR RATING	t/c	$\Lambda_{LE}$ (DEG.)	AR	$S_w$ (FT <sup>2</sup> )	TMR (N.M.I.)	TMR RATING	t/c	$\Lambda_{LE}$ (DEG.)	AR	$S_w$ (FT <sup>2</sup> )	TMR (N.M.I.)
1	.06	20	5	280	467	1	.04	20	3	280	228
2	.06	↓	4	↓	463	2	.05	↓	4	↓	221
3	.05	↓	4	↓	441	3	.05	↓	4	↓	217
1	.06	20	4	350	400	1	.04	20	3	350	191
2	.06	↓	3	↓	386	2	.05	↓	3	↓	183
3	.05	↓	4	↓	378	3	.05	↓	4	↓	176
1	.06	20	3	420	311	1	.04	20	3	420	156
2	.05	↓	3	↓	305	2	.05	↓	3	↓	150
3	.06	↓	4	↓	282	3	.05	↓	4	↓	140
1	.05	20	3	490	193	1	.04	20	3	490	127
2	.04	↓	3	↓	179	2	.05	↓	3	↓	121
3	.05	↓	4	↓	126	3	.05	↓	4	↓	111
OPTIMUM SUBSONIC MISSION PROFILE						SUPERSONIC PENETRATION MISS. PROF.					
TMR RATING	t/c	$\Lambda_{LE}$ (DEG.)	AR	ENG. SIZE (IN. MI.)	TMR (N.M.I.)	TMR RATING	t/c	$\Lambda_{LE}$ (DEG.)	AR	ENG. SIZE (IN. MI.)	TMR (N.M.I.)
1	.06	20	4	.8	800	1	.04	20	3	.8	389
2	.05	↓	4	↓	742	2	.05	↓	4	↓	374
3	.05	↓	5	↓	705	3	.06	↓	4	↓	364
1	.06	20	5	.9	722	1	.05	20	4	.9	316
2	.06	↓	4	↓	672	2	.05	↓	3	↓	306
3	.05	↓	4	↓	637	3	.06	↓	4	↓	305
1	.06	20	5	1.0	612	1	.05	20	4	1.0	258
2	.06	↓	4	↓	569	2	.05	↓	3	↓	255
3	.05	↓	4	↓	535	3	.06	↓	4	↓	251
SEA LEVEL PENETRATION MISS. PROFILE						SUPERSONIC INTERCEPT MISS. PROFILE					
TMR RATING	t/c	$\Lambda_{LE}$ (DEG.)	AR	ENG. SIZE (IN. MI.)	TMR (N.M.I.)	TMR RATING	t/c	$\Lambda_{LE}$ (DEG.)	AR	ENG. SIZE (IN. MI.)	TMR (N.M.I.)
1	.06	20	4	.8	505	1	.04	20	3	.8	249
2	.04	↓	3	↓	491	2	.05	20	3	↓	198
3	.05	↓	4	↓	475	3	.04	30	3	↓	197
1	.06	20	4	.9	400	1	.04	20	3	.9	191
2	.06	↓	3	↓	386	2	.05	↓	3	↓	183
3	.05	↓	4	↓	378	3	.05	↓	4	↓	176
1	.06	20	4	1.0	305	1	.04	20	3	1.0	175
2	.06	↓	3	↓	304	2	.05	↓	3	↓	167
3	.05	↓	3	↓	296	3	.05	↓	4	↓	160



Maneuver performance is not explicitly considered in this exercise. The selected wing geometry has a relatively low buffet onset lift coefficient transonically due primarily to the low wing sweep. The analysis described below should be viewed with this fact in mind.

Top-level mission/configuration tradeoffs of the selected wing planform geometry are illustrated in Figure D-66. Mission Configuration 2 performance is shown for the ground attack mission profiles because the Total Mission Radii (TMRs) for this configuration are generally less by a small amount than those for Mission

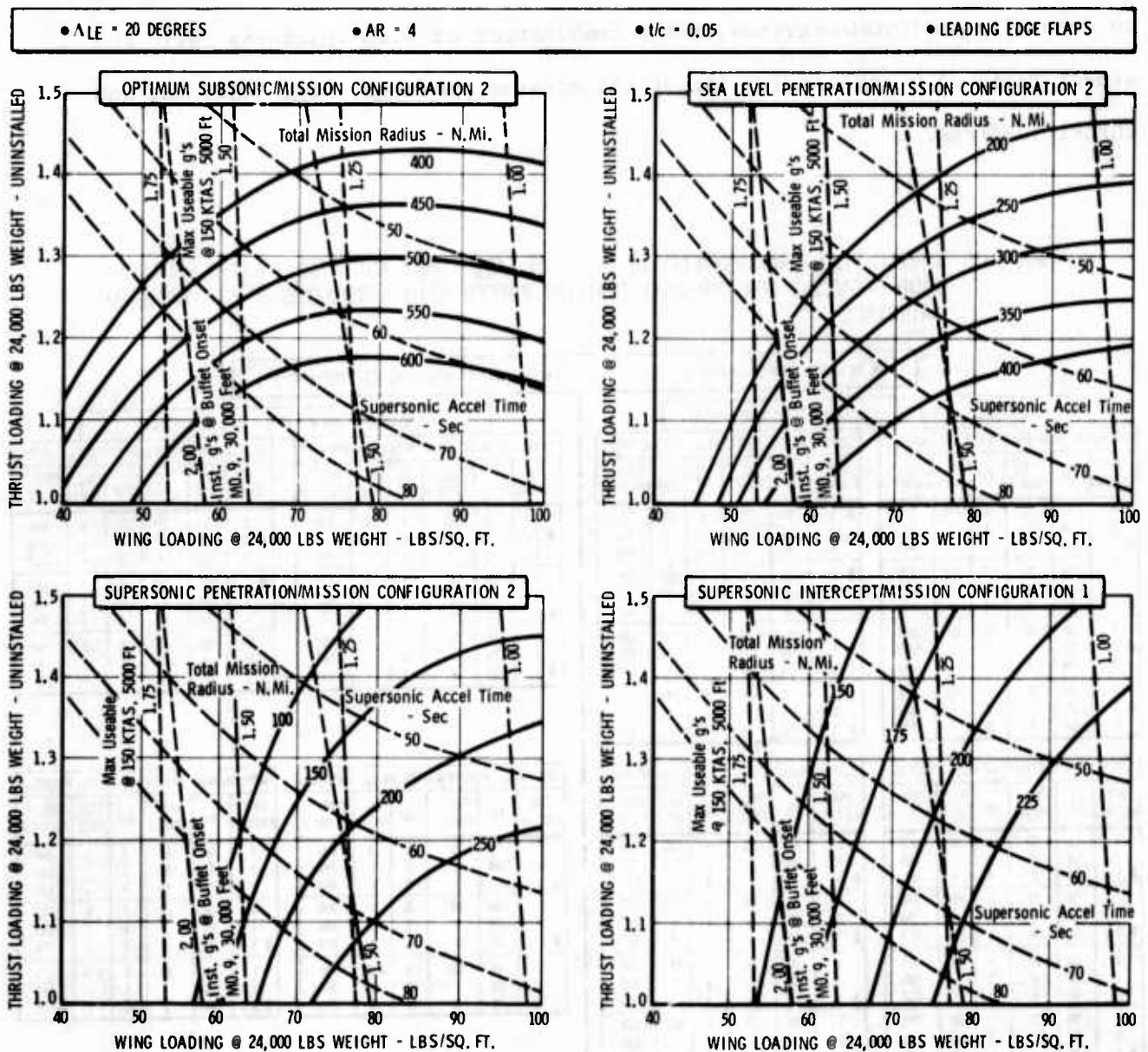


Figure D-66 Conventional Materials Top-Level Mission/ Configuration Tradeoffs Using Representative Wing Geometry



Configurations 1 and 3. The supersonic intercept mission profile is shown for Mission Configuration 1 rather than 1' for the same reason.

By relating the parametric TMR and loiter requirements for the different operational mission types to the four mission profiles, ranges of interest for the four TMRs shown can be implied:

- |                          |                         |
|--------------------------|-------------------------|
| • Optimum Subsonic       | 400-650 nautical miles  |
| • Sea Level Penetration  | 200-350 nautical miles  |
| • Supersonic Penetration | 200-350 nautical miles  |
| • Supersonic Intercept   | 150-300 nautical miles. |

Although these ranges of interest are broad, three points can be made concerning the mission/conventional material configuration tradeoffs:

1. It is possible to select a nominal set of requirements and a configuration which nominally satisfy the subsonic mission types.
2. The supersonic mission types severely constrain maneuver capability (wing loading).
3. A conventional material configuration selection which satisfies the most easily met maneuver and acceleration requirements provides marginal TMRs except for the supersonic penetration mission profile.

#### D.3.4.2 Composite Materials

Table D-11 contains the same two cuts through the parametric data for composite materials as given in the preceding section for conventional materials. A leading edge sweep of 20 degrees is again predominate. An aspect ratio of 5 in conjunction with a thickness ratio of 0.05 is most evident for all but the supersonic intercept mission profile. Inspection of the complete data shows that the supersonic intercept TMR for this geometry is within 10 percent of the third highest TMR in all cases except for combinations of very low wing loading and very high thrust loading.

Table D-11 A  $t/c = 0.05$ ,  $\Lambda_{LE} = 20^\circ$ , AND ASPECT RATIO = 5 WING IS USED FOR ADVANCED COMPOSITE MATERIALS TRADEOFF ILLUSTRATIONS

MISSION CONFIGURATION 1						SUPERSONIC ACCELERATION TIME $\leq 80$ SEC.					
ENGINE SIZE = 0.9 (T/W = 1.29 UNINSTALLED AT TAKEOFF)						WING AREA = 350 FT <sup>2</sup> (W/S = 68.0 AT TAKEOFF)					
OPTIMUM SUBSONIC MISSION PROFILE						SUPERSONIC PENETRATION MISS. PROF.					
TMR RATING	$t/c$	$\Lambda_{LE}$ (DEG.)	AR	$S_w$ (FT <sup>2</sup> )	TMR (N.M.I.)	TMR RATING	$t/c$	$\Lambda_{LE}$ (DEG.)	AR	$S_w$ (FT <sup>2</sup> )	TMR (N.M.I.)
1	.06	20	5	280	1294	1	.05	20	5	280	677
2	.05	20	5	↓	1213	2	.06	20	5	↓	675
3	.06	30	5	↓	1166	3	.06	30	5	↓	661
1	.06	20	5	350	1303	1	.05	20	5	350	630
2	.05	20	5	↓	1204	2	.06	20	5	↓	629
3	.06	30	5	↓	1162	3	.05	↓	4	↓	606
1	.06	20	5	420	1276	1	.05	20	5	420	548
2	.05	↓	5	↓	1179	2	.05	↓	4	↓	542
3	.06	↓	4	↓	1112	3	.04	↓	4	↓	524
1	.05	20	5	490	1058	1	.05	20	4	490	455
2	.05	↓	4	↓	1026	2	.04	↓	4	↓	452
3	.04	↓	4	↓	948	3	.05	↓	5	↓	438
SEA LEVEL PENETRATION MISS. PROFILE						SUPERSONIC INTERCEPT MISS. PROFILE					
TMR RATING	$t/c$	$\Lambda_{LE}$ (DEG.)	AR	$S_w$ (FT <sup>2</sup> )	TMR (N.M.I.)	TMR RATING	$t/c$	$\Lambda_{LE}$ (DEG.)	AR	$S_w$ (FT <sup>2</sup> )	TMR (N.M.I.)
1	.06	20	5	280	947	1	.04	20	3	280	339
2	.05	20	5	↓	888	2	↓	20	4	↓	338
3	.06	30	5	↓	860	3	↓	30	3	↓	331
1	.06	20	5	350	888	1	.04	20	3	350	292
2	.05	↓	5	↓	823	2	↓	20	4	↓	284
3	.06	↓	4	↓	827	3	↓	30	3	↓	283
1	.06	20	5	420	786	1	.04	20	3	420	248
2	.06	↓	4	↓	748	2	↓	30	3	↓	240
3	.05	↓	5	↓	740	3	↓	20	4	↓	237
1	.05	20	4	490	646	1	.04	20	3	490	211
2	↓	↓	5	↓	608	2	↓	30	3	↓	204
3	↓	↓	3	↓	597	3	↓	20	4	↓	199
OPTIMUM SUBSONIC MISSION PROFILE						SUPERSONIC PENETRATION MISS. PROF.					
TMR RATING	$t/c$	$\Lambda_{LE}$ (DEG.)	AR	ENG. SIZE (N.M.I.)	TMR (N.M.I.)	TMR RATING	$t/c$	$\Lambda_{LE}$ (DEG.)	AR	ENG. SIZE (N.M.I.)	TMR (N.M.I.)
1	.06	20	5	.8	1453	1	.05	20	5	.8	714
2	.05	↓	5	↓	1353	2	.06	↓	5	↓	710
3	.06	↓	4	↓	1270	3	.05	↓	4	↓	683
1	.06	20	5	.9	1303	1	.05	20	5	.9	630
2	.05	20	5	↓	1204	2	.06	↓	5	↓	629
3	.06	30	5	↓	1162	3	.05	↓	4	↓	606
1	.06	20	5	1.0	1153	1	.05	20	5	1.0	550
2	.05	20	5	↓	1060	2	.06	20	5	↓	549
3	.06	30	5	↓	1029	3	.06	30	5	↓	525
SEA LEVEL PENETRATION MISS. PROFILE						SUPERSONIC INTERCEPT MISS. PROFILE					
TMR RATING	$t/c$	$\Lambda_{LE}$ (DEG.)	AR	ENG. SIZE (N.M.I.)	TMR (N.M.I.)	TMR RATING	$t/c$	$\Lambda_{LE}$ (DEG.)	AR	ENG. SIZE (N.M.I.)	TMR (N.M.I.)
1	.06	20	5	.8	1028	1	.04	20	3	.8	307
2	.05	↓	5	↓	962	2	↓	20	4	↓	298
3	.06	↓	4	↓	948	3	↓	30	3	↓	298
1	.06	20	5	.9	828	1	.04	20	3	.9	292
2	.05	↓	5	↓	828	2	↓	20	4	↓	284
3	.06	↓	4	↓	827	3	↓	30	3	↓	283
1	.06	20	5	1.0	755	1	.04	20	3	1.0	273
2	.06	↓	4	↓	709	2	↓	20	4	↓	266
3	.05	↓	5	↓	699	3	↓	30	3	↓	264

The wing geometry of 0.05 thickness, 20-degree sweep, and aspect ratio of 5 is selected as adequately representative to show the top-level tradeoffs for the wing and thrust loadings of interest (Figure D-67). Again, the relatively low Mach 0.9 buffet onset lift coefficient resulting from a 20-degree wing sweep is noted.

There are six points to be made concerning the effects of advanced composite materials:

1. At any given wing and thrust loading, the TMRs for the two subsonic profiles are roughly double those of the conventional material configurations.
2. The effect of composites on the supersonic penetration TMR depends on the maneuver and acceleration levels. At lower wing loadings, the TMR of the composite configuration is three or four times larger than that of the conventional material configuration with the same wing and thrust loading.
3. The supersonic intercept TMR is increased by about 50 percent for the advanced composite material configurations.

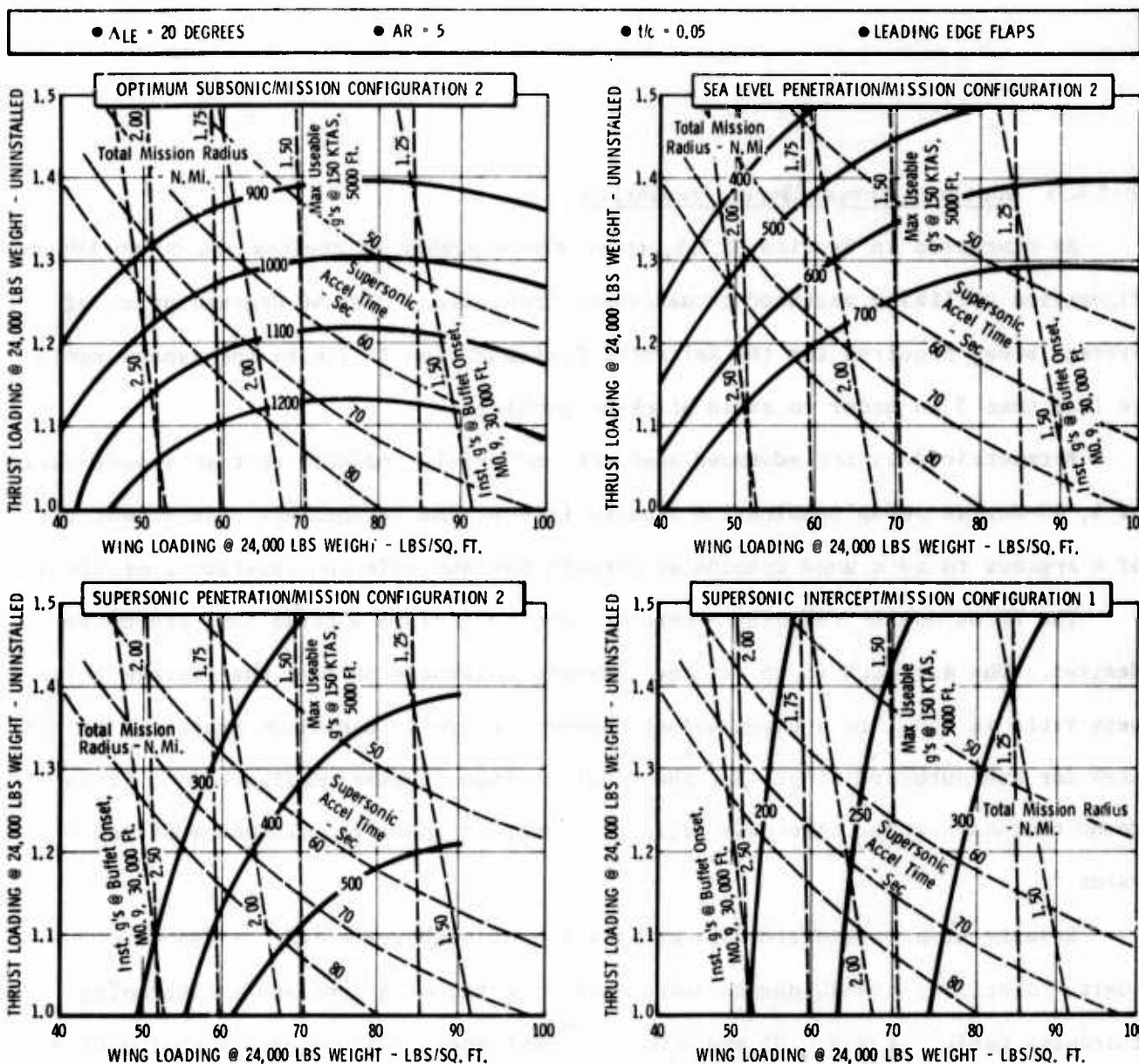


Figure D-67 Advanced Composite Materials Top-Level Mission/Configuration Tradeoffs Using Representative Wing Geometry

4. For a given wing sweep, the higher aspect ratio resulting from application of composites provides higher maximum lift coefficients. This allows maneuver requirements to be satisfied with less wing area, which further improves TMR performance. (If wing taper ratio is held constant, as done for the parametric analysis, effective wing sweep increases with aspect ratio. This increases transonic buffet onset lift coefficient; however, attributing this apparent benefit to advanced composites is somewhat artificial.)
5. Unlike the conventional materials situation, the application of advanced composite materials allows consideration of nominal acceleration and maneuver levels while maintaining adequate TMRs for all the subject mission profiles.
6. The TMRs of both subsonic mission profiles are significantly greater than those thought likely to be operationally required. In other words, additional payload or self-defense and combat allowance is available for these mission types. This suggests the possibility of selecting wing geometry to provide better maneuver and/or supersonic mission performance at the expense of subsonic performance.

#### D.3.4.3 Vectored Thrust/Supercirculation

As discussed in Section D.2.3, there are a number of constraints on an LWA configuration utilizing vectored thrust/supercirculation. The 40 degrees or so of average sweep required for the Reference Configuration 27 limits the aspect ratio to less than 5 in order to avoid pitch-up problems.

Parametric data for advanced composite materials indicate that an aspect ratio of 5, 40-degree sweep combination results in poor  $TMR$  performance. An aspect ratio of 4 appears to be a good compromise between the subsonic and supersonic missions.

The VT/SC nozzle requires a thicker inboard airfoil section than otherwise desired. The approach is to set the outboard thickness so that the average thickness ratio is equal to a given value; however, there is a minimum practical thickness for the outboard wing. For the Configuration 27-type configuration, it is found that an average thickness ratio of 0.0625 is about the minimum achievable value.

Results of a parametric data examination of nonpowered lift, advanced composite materials, the 40-degree sweep, aspect ratio of 4 indicate a compromise thickness ratio between 0.05 and 0.06. The thickness ratio constraint of 0.0625 represents a penalty, particularly in supersonic performance.

A wing geometry of 0.0625 thickness ratio, 40-degree leading edge sweep, and aspect ratio of 4 is selected for illustrating the top-level tradeoffs for VT/SC configurations. The data in Figure D-68 include the propulsion weight and fuel consumption penalties discussed previously for Reference Configuration 27.

The VT/SC data are based on the bypass ratio 1.0 engine cycle used in the preceding analyses and do not reflect the 1.5 bypass ratio of the Reference Configuration 27 engine. Compared to the reference VT/SC configuration, the parametric configurations then have (1) lower drag and dry weight, (2) different engine performance at different flight conditions, and (3) less  $c_{\mu}$ .

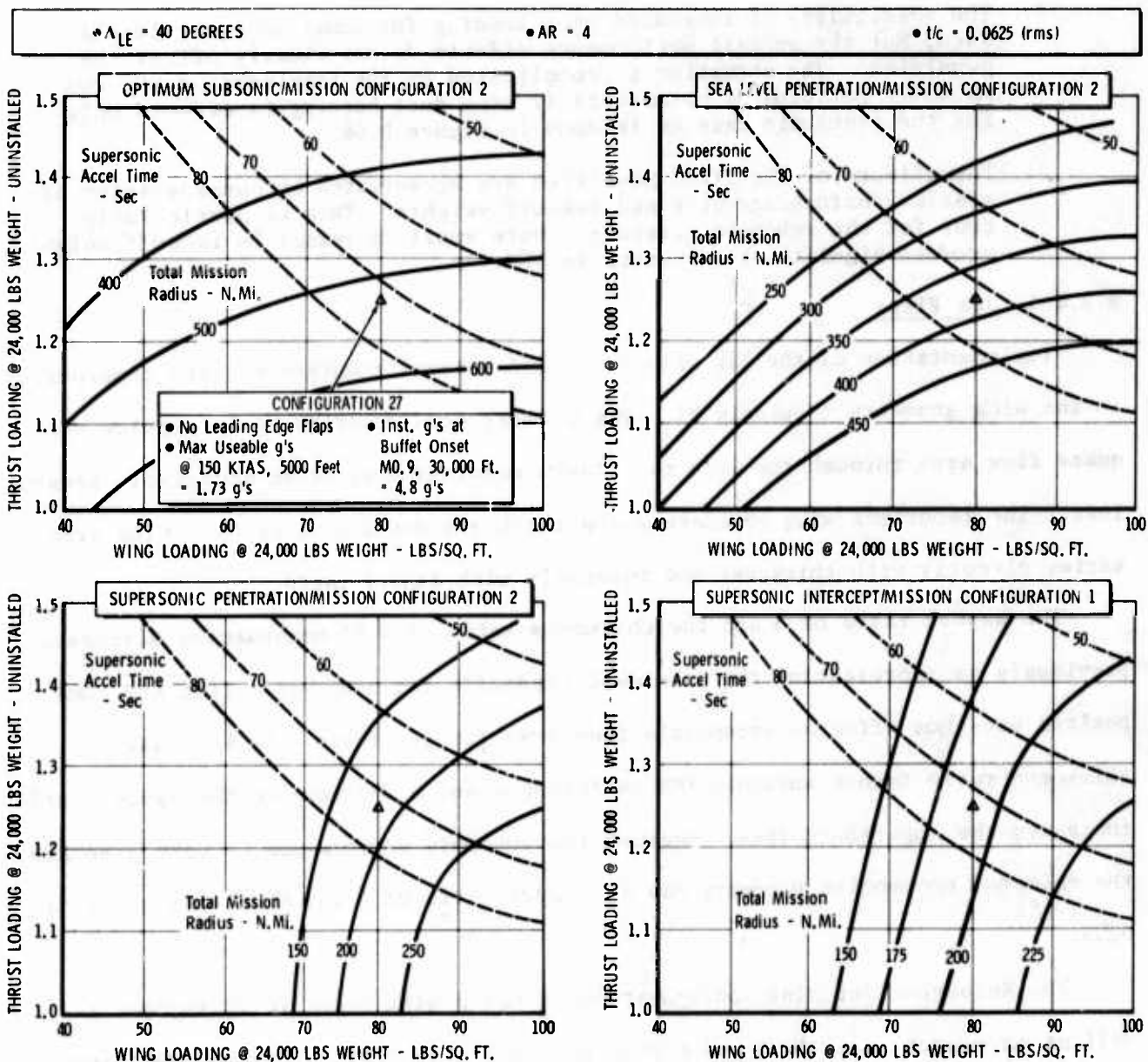


Figure D-68 VT/SC Top-Level Mission/Configuration Tradeoffs

The effects of the first two items are similar to the accuracy expectations of the parametric synthesis procedure. Maneuver potential is indicated using the higher  $c_{\mu}$  of a 1.5 bypass ratio engine. A study to select engine bypass ratio on the basis of tradeoffs between the various flight conditions is a possible step in the future development of the VT/SC concept.

Three points can be made concerning VT/SC potential:

1. The weight increase, thrust loss, and configuration constraints associated with VT/SC are very evident in TMR reductions for all mission profiles.



2. The possibility of increased wing loading for equal maneuver levels is seen, but the overall performance effects do not clearly offset the penalties. The situation is complicated by the imbalance of the two maneuver performance parameters if wing duct burning is assumed only for the transonic case as is done in Figure D-68.
3. The effects of the VT/SC penalties are accentuated by consideration of mission performance at fixed takeoff weights. This is particularly true for the subsonic missions, where small increases in takeoff weight produce significant increases in TMR.

#### D.3.4.4 Jet Flaps

Implementation of the jet flap in an LWA concept requires certain compromises in the wing geometry (Appendix B). The primary consideration is to provide adequate flow area through the wing to allow a meaningful  $c_{\mu}$  at an acceptable pressure loss. The important wing parameters are thickness and aspect ratio. Flow area varies directly with thickness and inversely with aspect ratio.

The aspect ratio of 5 and the thickness ratio of 0.05 combination discussed previously as representing the top-level tradeoffs for nonpowered lift and composites does not offer an acceptable flow area for jet flaps. An increase in thickness ratio favors subsonic TMR performance and a decrease in the aspect ratio increases the supersonic TMRs. Because the subsonic performance is very adequate, the selected compromise geometry has an aspect ratio of 4 and thickness ratio of 0.05.

The Reference Jet Flap Configuration 28 has a wing sweep of 30 degrees as well as an aspect ratio of 4 and a thickness ratio of 0.05. Although the parametric data show better TMR performance with a 20-degree sweep, the reference configuration geometry is reasonably representative and is used to illustrate mission/configuration tradeoffs in Figure D-69.

The data include the engine and wing weight increments previously discussed for jet flap implementation. A bypass ratio of 1.0 is used rather than the 1.5 of Configuration 28 for the reasons discussed previously. Since only one-third of the fan air is diverted to the jet flap for the Configuration 28 aerodynamic performance illustrations presented in paragraph D.2.4.3, the data are extrapolated to the parametric configuration.



•  $\Lambda_{LE} = 30$  DEGREES

• AR = 4

•  $t/c = 0.05$

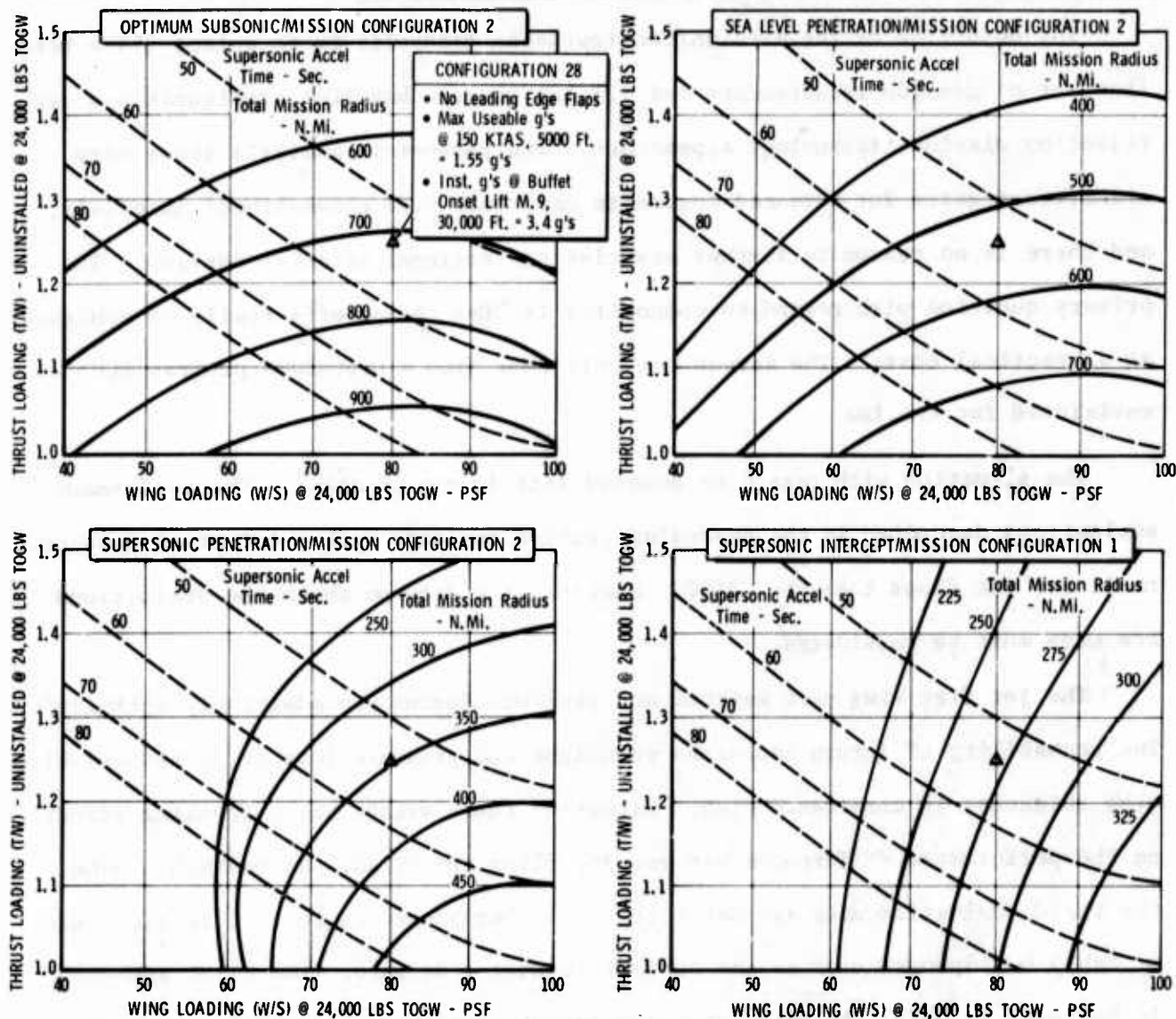


Figure D-69 Jet Flap Top-Level Mission/Configuration Tradeoffs.

Three points can be made concerning jet flap potential:

1. For a given wing loading and thrust loading within the ranges of interest, TMR performance for the jet flap is better than that for VT/SC. Much of this difference is attributable to the different wing geometries of the two concepts, particularly the lower sweep and thickness of the jet flap.
2. Maneuver capability of Configuration 28 indicates a required lower wing loading to achieve equal maneuver performance with Configuration 27. Because the primary weight penalty for the jet flap is a direct function of wing area, the TMR advantages of the jet flap are reduced with decreased wing loading.
3. Jet flap low speed maneuver improvements do not result in TMR performance that is competitive with the advanced composite, unpowered lift configuration potential. The buffet onset improvements at Mach 0.9 do result in competitive TMR comparisons.

#### D.3.5 BASELINE MISSION/CONFIGURATION SELECTION RATIONALE

The objective of the mission/configuration tradeoffs is to select (1) a baseline set of mission requirements and (2) one or more baseline configurations representing distinct technology approaches. The parametric analysis shows very significant gains for advanced composite materials over conventional materials, and there is no reason to further exercise conventional material designs. The primary question with regard to composites is "Can the payoffs really be achieved at a practical cost?" The answer can only come from a prototype program such as envisioned for the LWA.

The situation with regard to powered lift is not as clear. The performance evaluations described in the preceding section indicate better potential mission radii for jet flaps than for VT/SC. However, the data on which the evaluations are made must be considered.

The jet flap wing duct weights and pressure losses are admittedly optimistic. The probability of future increases in weight and pressure loss or, alternatively, wing thickness is considered high. Either of these events has a leveling effect on the performance differences between jet flaps and VT/SC. On the other hand, the VT/SC evaluation data are not felt to be overly optimistic and, in fact, can probably be improved upon as the concept is better defined. The VT/SC approach is believed to offer the least risk and lowest cost LWA program with the same potential performance payoff as the full-span jet flap concept.

The two baseline configurations to be defined embody (1) advanced composite materials and (2) vectored thrust/supercirculation. Other technology approaches such as variable camber, CCV (unconstrained by powered lift considerations), and advanced transonic airfoils can be evaluated as extensions of the advanced composite materials baseline configuration.

The baseline mission requirements for the LWA and the associated selection rationale are described below. In general, the basic selection rationale is (1) the requirement is within the originally specified parametric operational

requirements range of interest and (2) the requirement is achievable within the LWA guidelines and other specified requirements as indicated by the parametric analysis results.

#### D.3.5.1 Payload, Acceleration, and Maneuverability

Payload is specified to provide three options for ground attack missions and two options for air combat missions. Each option includes two AIM-9 type missiles

Table D-12 BASELINE PAYLOAD REQUIREMENTS FOR LWA

MISSION	PAYLOAD ITEM
<b>GROUND ATTACK</b>	
Basic _____	2000 lbs Expendable Ordnance
Alternate 1 _____	3000 lbs Expendable Ordnance
Alternate 2 _____	6000 lbs Expendable Ordnance
<b>AIR COMBAT</b>	
Basic _____	2 AIM-47 Type Missiles
Alternate 1 _____	None
<b>ALL</b>	
Self-Defense Missiles _____	2 AIM-9 Type
Gun _____	20MM M-61 Type w/500 Rds. Ammo
Avionics _____	1200 lbs

and an M-61 type gun. Specified payload options are listed in Table D-12. The avionics complement for calculating performance is the full capability system as defined in Appendix E.

Supersonic acceleration time is specified as 70 seconds with the basic ground attack payload. Lower acceleration times appear to have little utility

for defensive purposes, and the TMR performance penalties are great. For the LWA configurations exercised to date, this specification generally results in an acceleration time for Alternate Ground Attack Payload 1 which is less than 80 seconds, i.e., the upper limit of the parametric operational requirement. A subsonic acceleration requirement is not necessary with the above supersonic requirement.

The self-defense maneuver level specification is expressed as instantaneous load factor capability rather than sustained g's for reasons discussed in Section D.3.3.1. Both a buffet-free condition and a moderate-buffet condition are specified for the transonic requirement in order to circumvent the pitfalls of considering only one or the other. The moderate-buffet condition offers the better operational basis of the two.

The ground-attack maneuver requirements are generally compatible with the self-defense levels as well as each other. Acceleration and maneuver requirements are summarized in Table D-13.

### D.3.5.2 Mission Profiles

Table D-13 ACCELERATION AND MANEUVER REQUIREMENTS FOR LWA

CONDITION	LOADING	REQUIREMENT
• ACCELERATION • M0.85 to M1.6 at 36,089 ft	Ground Attack Basic Payload, 60% Fuel	70 sec.
• MANEUVER • M0.9 at 30,000 ft	Ground Attack Alternate Payload 1, 60% Fuel	3 g's Instantaneous Buffet Free 7 g's Instantaneous Moderate Buffet ( $\sigma_{Cq} = 0.10$ g RMS)
• 150 Knots at 5000 ft	Ground Attack Alternate Payload 2, 60% Fuel	1.75 g's Maximum Usable
• M0.5 at 10,000 ft	Ground Attack Alternate Payload 2, 60% Fuel	5.0 g's Maximum Usable

Earlier presentations of the wing and thrust loading parametric data for fixed wing geometry form the basis for the acceleration and maneuver requirement selections above. Now that these levels are set, it is possible to examine the parametric data in a way which provides better identification of the effects of wing geometry variations on the mission/configuration tradeoffs. Inspection of the complete parametric data for advanced

composite materials indicates only a limited number of configurations will meet the acceleration and maneuver requirements. (The moderate buffet transonic maneuver condition can not be included, because it is not a part of the parametric analysis data.)

A significant point is the effect of wing geometry, particularly sweep, on the buffet-onset lift coefficient and on the maximum lift coefficient. The indication is that a sweep higher than the 20 degrees utilized previously provides better TMR performance when the specified acceleration and maneuver levels are applied.

The sum of the various cuts through the parametric data is the basis for the general design requirements and mission profiles specified in Figure D-70. The performance required to meet these requirements within the LWA guidelines is felt to be marginally compatible with a nonpowered lift, advanced composite materials configuration. More importantly, the total capability represented by these requirements represents a superior aircraft which will fill an important place in the tactical force picture.

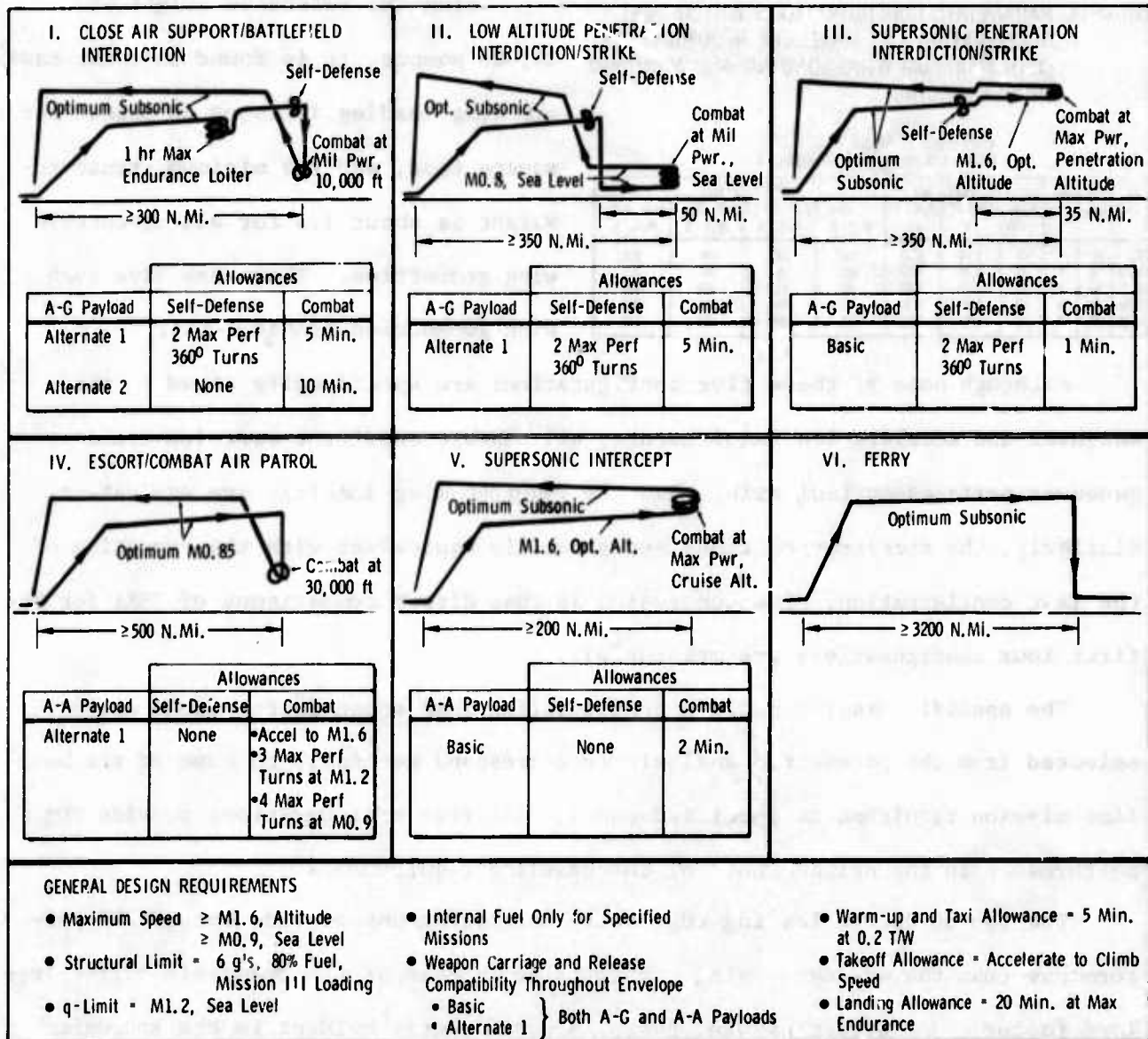


Figure D-70 Mission Profile and Design Requirements for LWA

### D.3.5.3 Advanced Composites

#### D.3.5.3.1 Parametric Configuration Considerations

Selection of the baseline configuration representing a nonpowered lift, advanced composite materials approach begins with inspection of the parametric data. The first point to note is that, of the 20 configurations which meet or exceed the maneuver and acceleration requirements, those with maximum wing loading and minimum thrust loading provide the best TMR performance for all missions.



Table D-14 PARAMETRIC CONFIGURATIONS WHICH MEET ACCELERATION AND MANEUVER REQUIREMENTS WITH MAXIMUM WING LOADING AND MINIMUM THRUST LOADING

• W/S = 57 @ 24,000 LBS  
• T/W = 1.29 UNINSTALLED @ 24,000 LBS

U/C (%)	A/E (DEG)	AR	ACCEL TIME (SEC)	150 KTAS, 5000 FT g's	MO. 9, 30,000 FT g's	TMR'S (N.M.I.)			
						OPT. SUB./ M.C. 2	S.L. PEN./ M.C. 2	SUP. PEN./ M.C. 1	SUP. INT./ M.C. 1
0.05	30	4	61	1.74	3.02	836	526	506	218
0.05	30	5	64	1.78	3.10	861	495	487	202
0.05	40	4	61	1.72	3.82	656	412	419	199
0.06	40	3	64	1.75	3.42	675	456	416	201
0.06	40	4	69	1.79	3.56	731	469	421	189

Using the reference weight of 24,000 pounds, it is found that the maximum wing loading is about 60 pounds per square foot, and the minimum thrust-to-weight is about 1.3 for all acceptable wing geometries. There are five such wing geometries (Table D-14).

Although none of these five configurations are specifically sized to the maneuver and acceleration requirements, all exhibit about the same low-speed maneuver performance indicating that the required wing loadings are equivalent. Similarly, the acceleration times are generally equivalent with the exception of the last configuration. The conclusion is that direct comparisons of TMRs for the first four configurations are meaningful.

The specific mission profile configuration TMRs shown in the table are selected from the parametric analysis to correspond generally to some of the baseline mission requirements specified above. All five configurations provide TMR performance in the neighborhood of the baseline requirements.

The two 30-degree leading edge sweep configurations provide better TMR performance than the 40-degree wings, but at the expense of the transonic buffet-free load factor. The effect of wing sweep is particularly evident in the subsonic

TMRs. The selected characteristics for the advanced composite materials baseline configuration are identified in Table D-15.

Table D-15 SELECTED CHARACTERISTICS FOR ADVANCED COMPOSITES BASELINE CONFIGURATION

- WING LOADING = 50 POUNDS PER SQUARE FOOT AT TRANSONIC COMBAT WEIGHT
- THRUST LOADING = 1.4 SEA LEVEL STATIC, UNINSTALLED AT SUPERSONIC ACCELERATION WEIGHT
- WING THICKNESS RATIO = 0.05
- WING LEADING EDGE SWEEP = 30 DEGREES
- WING ASPECT RATIO = 4

It is noted that the present objective is not to select an "optimum" configuration but to define a baseline LWA configuration which can be a starting point for more detailed design efforts.

The present objective is therefore to select a "near-optimum" configuration.



#### D.3.5.3.2 Other Configuration Considerations

It is now germane to reconsider the nonpowered lift reference configuration approach, Configuration 26B, described in Section A.21. In particular, the inlet/internal bay/main landing gear interrelation is of interest.

The bottom-mounted inlet and internal bay are found to be quite compatible from a fuselage lines standpoint (see Figure D-24); however, this combination precludes locating the main landing gear in the fuselage. The gear must then be located in the wing at some weight penalty.

Consideration of the selected nonpowered lift planform indicates that a wing-located gear is a marginal fit within the approximately 10 inches of thickness available. In view of the weight and possible aerodynamic penalties, an alternate configuration approach of side-mounted inlets and fuselage-located gear is possibly best.

Incorporation of the close-coupled canard in the earlier reference configurations is justified on the basis of its advantages for the powered-lift concepts. The canard does pose certain configuration constraints, and its contribution to a nonpowered lift configuration are not firmly established.

If a conventional horizontal tail is used, the wing can be placed at either a high-, low-, or mid-fuselage location. The internal bay and landing gear preclude a low wing. A mid-wing is not considered the best structural concept for advanced composite materials, but a mid-wing is considered the preferable aerodynamic approach.

The number of engines is also an open question, because the unique requirements of powered lift are not a consideration. Availability of engine candidates will probably determine whether one or two engine configuration approaches will be pursued in future studies. The advanced composites baseline configuration is compared to Reference Configuration 26B in Table D-16.

Table D-16 ADVANCED COMPOSITES BASELINE CONFIGURATION CHANGES FROM REFERENCE CONFIGURATIONS 26B

CONFIGURATION CHANGES	REMARKS
WING LOADING, THRUST LOADING, WING GEOMETRY	♦ Tailored for Specified Requirements
INLET LOCATION • Bottom to Side	♦ Allow Fuselage Location for Main Landing Gear
MAIN LANDING GEAR LOCATION • Wing to Fuselage	♦ Less Weight, Eliminate Possible Adverse Impact on Wing Thickness
HORIZONTAL STABILIZER • Canard to Conventional Tail	♦ Reduce Configuration Arrangement Constraints
WING LOCATION • Mid to High	♦ Improve Structural Efficiency of Advanced Composites
NUMBER OF ENGINES • One to Either One or Two	♦ No Powered Lift Complications of One-Engine-Out Situation

tial changes are in the category of baseline perturbations for future design iterations.

The wing planform geometry of Reference Configuration 27 is selected for the baseline. The combat wing loading is 80 pounds per square foot and combat thrust loading is 1.3, both of which are somewhat higher than those of Configuration 27. The parametric aspects of the selected VT/SC baseline configuration are summarized in Table D-17.

Table D-17 SELECTED CHARACTERISTICS FOR VT/SC BASELINE CONFIGURATION

• WING LOADING - 80 POUNDS PER SQUARE FOOT AT TRANSONIC COMBAT WEIGHT
• THRUST LOADING - 1.3 SEA LEVEL STATIC, UNINSTALLED AT SUPERSONIC ACCELERATION WEIGHT
• WING THICKNESS RATIO - 0.0625 (rms)
• WING LEADING EDGE SWEEP - 30/47 DEGREES
• WING ASPECT RATIO - 4

Future work with this configuration should include consideration of an existing or near-term engine; and bypass ratio will be determined, or at least constrained, by this consideration. The 1.5 bypass ratio of Configuration 27 is assumed for the baseline VT/SC configuration.

Preliminary layouts of the baseline configuration indicate that the engine extension incorporated in Configuration 27 will not be required. Elimination of

#### D.3.5.4 Vectored Thrust/Supercirculation

The baseline VT/SC configuration is almost uniquely determined by the constraints associated with the concept. From a mission standpoint, the parametric analysis results indicate the desirability of both decreasing the wing sweep and reducing the thickness. Some improvement in this direction is possible, but poten-

The other configuration characteristics of the baseline are similar to those of Configuration 27. The engine afterburner is eliminated which increases the basic engine size and, in turn, the amount of fan air. This requires a proportionately larger vectoring nozzle if the bypass ratio remains the same.

the engine extension reduces the VT/SC weight penalty as well as an element of uncertainty associated with the VT/SC concept.

#### D.3.6 SIMULATION CONFIGURATION SELECTION

The two advanced technology configuration approaches which offer most promise of satisfying the majority of the baseline mission requirements with a 25,000 pound class aircraft are depicted in Figure D-71. The first-order difference in the two configurations is that the powered lift concept known as vectored thrust/supercirculation is incorporated in Configuration 29. Other differences point up second-order configuration issues. Further development of these configurations will allow comparisons of powered lift and also other configuration alternatives. .

Indications are that the powered-lift configuration approach possibly can meet or exceed the baseline mission requirements at a lower weight than the Configuration 32 approach. There are a number of questions concerning both configurations which must be addressed with more in-depth design before final conclusions are drawn.

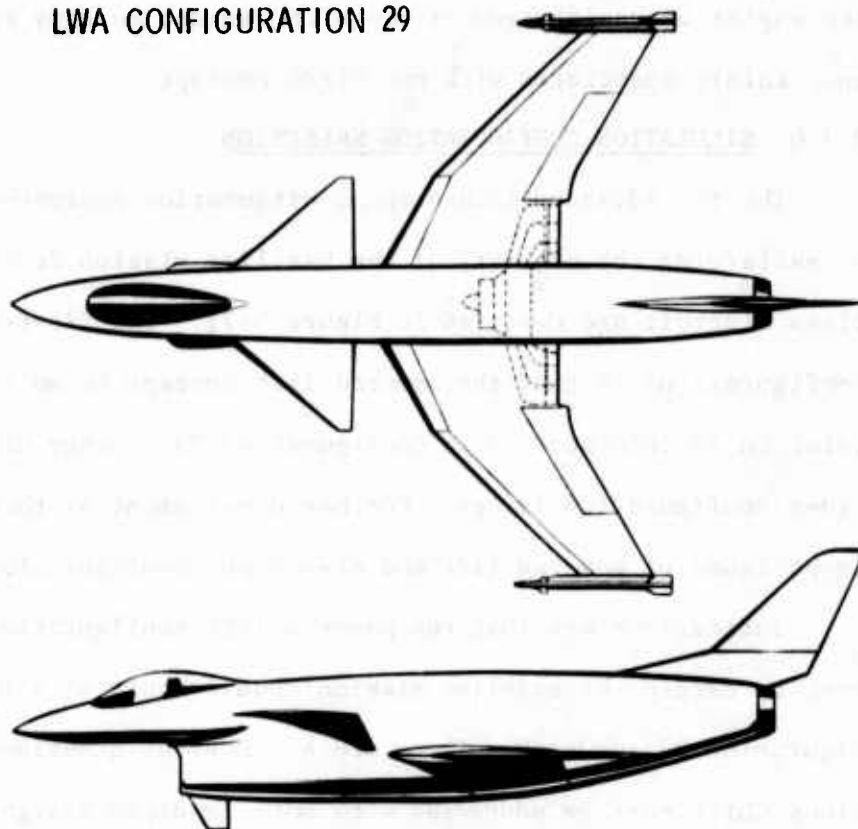
Some of these questions relate to potential benefits of powered lift in modes which may not be as easily quantified as "lifting capability," e.g., the use of powered lift in dive bombing. Man-in-the-loop simulation is an appropriate means for evaluating some potential benefits of powered lift over unpowered lift, and it follows that the powered-lift configuration is the logical choice for the simulation task.

**FEATURES:**

- Powered Lift (Vectored Thrust/Supercirculation)
- Advanced Composite Materials
- Variable Camber
- Internal Bay w/Internal/Conformal Pallet
- Close Coupled Canard
- Direct Sideforce Control
- CCV/Fly-by-Wire
- Modular Digital Avionics
- Single Wing Duct Burning Turbofan

**CHARACTERISTICS:**

- W/S = 80 lbs/sq. ft. at  
Transonic Combat  
Weight
- T/W = 1.3 Sea Level Static,  
Uninstalled at  
Supersonic  
Acceleration Weight
- Wing Geometry
- $t/c = 0.0625$  (rms)
  - $\Lambda_{LE} = 30/47$  Degrees
  - AR = 4

**LWA CONFIGURATION 29****FEATURES:**

- Advanced Composite Materials
- Variable Camber
- Internal Bay w/Internal/Conformal Pallet
- Direct Sideforce Control
- CCV/Fly-by-Wire
- Modular Digital Avionics
- One or Two Augmented Turbofans (Single Engine Shown)

**CHARACTERISTICS:**

- W/S = 50 lbs/sq. ft. at  
Transonic Combat  
Weight
- T/W = 1.4 Sea Level Static,  
Uninstalled at  
Supersonic Acceleration  
Weight
- Wing Geometry
- $t/c = 0.05$
  - $\Lambda_{LE} = 30$  Degrees
  - AR = 4

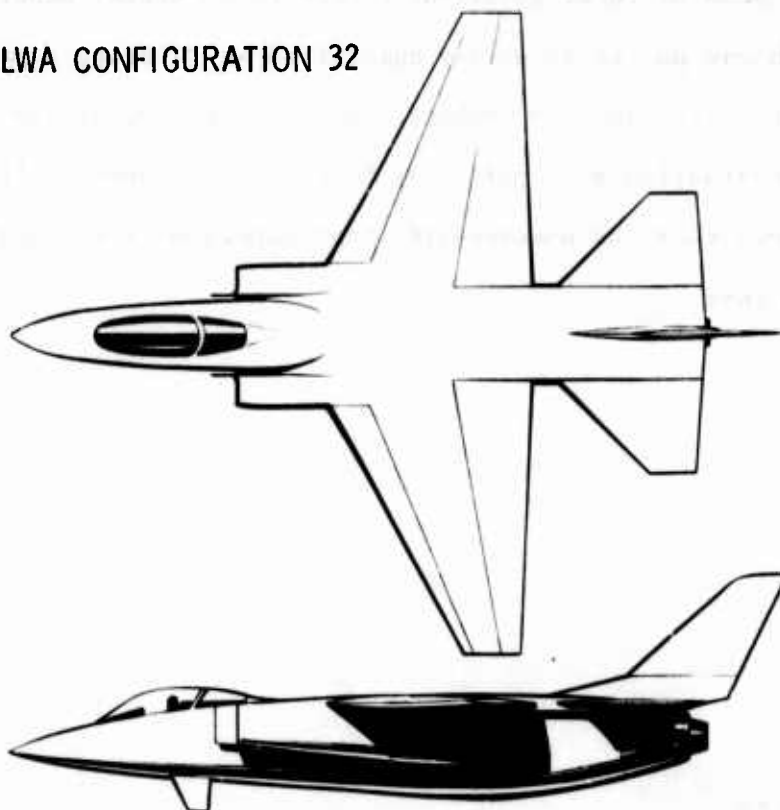
**LWA CONFIGURATION 32**

Figure D-71 25,000-Pound Class LWA Baseline Configurations

# APPENDIX E AVIONICS RATIONALE, DESCRIPTION, AND TECHNOLOGY REQUIREMENTS

Avionics requirements for the LWA are based on the projected missions, threat structure, and other operational considerations previously defined. A summary of these operational requirements and their translation into avionics requirements is shown in Table E-1. In the following discussion, these requirements will be

Table E-1 RATIONALE FOR AVIONICS REQUIREMENTS IS BASED ON LWA OBJECTIVES AND OPERATIONS STUDIES

OPERATIONAL REQUIREMENT	→	RESULTANT AVIONICS REQUIREMENT
• AVAILABILITY (HIGH RELIABILITY/MAINTAINABILITY, FAST TURN-AROUND)	→	• AUSTERE AIRBORNE SYSTEM • EXTENSIVE RELIANCE ON EXTERNAL SYSTEMS FOR NAVIGATION AND WEAPON DELIVERY
• LETHALITY	→	• SMART BOMB CAPABILITIES • FREE-FALL ACCURACY
• MISSION FLEXIBILITY AT LOW COST	→	• MODULAR DESIGN • GROWTH PROVISIONS
• TARGETS WITHIN 200 N.MI. OF FEBA	→	• LINE-OF-SIGHT COMMUNICATIONS • SHORT-RANGE NAVIGATION
• SURVIVABILITY IN HEAVILY DEFENDED ENVIRONMENT	→	• LONG-RANGE SENSOR (RADAR) • AIR-TO-AIR CAPABILITY • PROVISIONS FOR DEFENSIVE SYSTEMS (INTERNAL) • PROVISIONS FOR STAND-OFF WEAPON DATA LINK

translated in terms of their impact on the avionics system design approach and on the selection of specific types of equipment.

## E.1 OVERALL DESIGN APPROACH

The operational effectiveness of future weapon systems will be increasingly measured in terms of high reliability and low cost of ownership without sacrifice of mission capabilities. These criteria combined with the requirement for fast turnaround

from forward bases make it essential that the avionics system be as austere as possible to maximize mean time between failures and ease of maintenance. The basic design approach, then, is to provide a minimum of basic avionics equipment, with extensive reliance on external aids such as ground-based radio networks for navigation and weapon delivery.

At the same time, the airplane must be flexible for use under varying operational conditions and mission requirements. This requirement is incompatible with an austere system if conventional approaches to system design are employed. To circumvent this, the avionics system must be of a modular design which permits rapid changes in capability as a function of varying mission needs and

provides flexibility to add new capabilities without redesigning the complete system.

The design approach to the LWA avionics is based on using a modular system configuration which is designed initially to afford easy reconfiguration to provide optional or growth capabilities. The concept of a modular digital avionics system is discussed in Appendix A, Section A.1.1.2.

Descriptions of the various system elements and the rationale for their selection are presented below.

## E.2 COMPUTER COMPLEX

The initial system contains one central processor and the necessary memory and input/output units. This computer is designed to take full advantage of the lightweight and high reliability benefits of microminiaturized integrated circuit components and to be capable of modular growth. Potential growth consists primarily of adding memory modules; however, the software would be designed to permit interfacing of dedicated processors, if necessary, for growth capabilities.

The weights in Table E-2 are only rough estimates. A great deal of study and analysis remains to be performed before the computer for this system can be accurately sized. The computation requirements, input/output signal and data conversion requirements, operational

Table E-2 HEART OF AVIONICS SYSTEM IS  
COMPUTER COMPLEX

SYSTEM ELEMENT	LOCATION		INSTALLED IN BASIC AIRPLANE	PROVISIONS ONLY
	BAYS	COCKPIT		
DIGITAL COMPUTER	30 LB		30 LB	MEMORY AND PROCESSOR GROWTH TO 50 LB TOTAL

modes, redundancy requirements, control and display interfaces, memory storage requirements, and the operational and support software structure will have to be analyzed. Computer configuration will also be impacted by the state-of-the-art of the subsystems with which it interfaces. Use of existing subsystems will in general require greater complexity in interfacing and data conversion, whereas subsystems yet to be developed can (as pointed out earlier) be designed to provide specified hardware and software interfaces.



### E.3 NAVIGATION AND GUIDANCE

Navigation system requirements are determined primarily by three aspects of the LWA mission:

1. Capability for rapid response, which necessitates a simple airborne system that can navigate accurately to a target area on short notice. Such a capability can be provided by radio navigation.
2. Accurate weapon delivery, which requires positioning in the launch "basket" for smart weapons and accurate velocity data for free-fall delivery
3. Short range to targets, which permits line-of-sight radio navigation. In the event radio navigation facilities are not available, backup autonomous navigation can be provided by an inertial reference unit having reasonable accuracy.

Primary navigation is accomplished by means of an externally aided radio navigation system, which is assumed to be a satellite system of the 621-B type ( $\pm 20$  feet one-sigma accuracy design goal). A simple receiver unit, working in conjunction with a central computer, provides this capability. This system can provide extremely accurate position data for navigation and weapon delivery in the same coordinate system being used by other operational elements in the battle area. The receiver is readily adaptable to a LORAN C/D configuration (60-600 feet accuracy) in the event that the NavSat capability is not operational when this airplane is produced. (Table E-3)

Table E-3 NAVIGATION AND GUIDANCE DEPENDS HEAVILY ON EXTERNAL AIDS

SYSTEM ELEMENT	LOCATION		INSTALLED IN BASIC AIRPLANE	PROVISIONS ONLY
	BAYS	COCKPIT		
1. INERTIAL NAVIGATION SYSTEM	30 LB		30 LB	
2. NAV SAT/LORAN RECEIVER	10 LB		10 LB	
3. TACAN	25 LB	2 LB	27 LB	
4. ILS		7 LB	7 LB	
5. BEACON TRANSPONDER	5 LB	2 LB	7 LB	
6. COMPASS TRANSMITTER	2 LB		2 LB	
7. MISSION CONTROL PANELS		25 LB	25 LB	

A lightweight inertial navigation set (INS) having about 1 n.mi./hr. unaided accuracy will provide the instantaneous velocity component and attitude data required for accurate free-fall weapon delivery, at a low cost. It provides autonomous position

measurement during missions in which radio navigation is degraded or unavailable and can be position-updated by the radio navigation system when that system is operative. The INS also serves as the primary source of attitude data for various subsystems including the flight instruments. Magnetic heading data are obtained from a remote compass transmitter.

Except for the velocity data requirement, all of these functions could be furnished with lower accuracy by a less sophisticated attitude-heading reference system. However, the need for accurate velocity in free-fall weapon delivery is of overriding importance on the LWA mission.

TACAN and ILS capabilities are provided on the assumption that they will still be required as the primary means of en route navigation, position reporting, and instrument landing in the civil air traffic control system. If the NavSat system capability evolves to its full maturity as a worldwide general purpose navigation system and is accepted by all using agencies, then the TACAN and ILS systems may not be required.

Additional operational flexibility for navigation, weapon delivery, and battlefield command and control is provided by means of a beacon transponder, which operates in conjunction with a ground based or airborne radar tracking system. The system also provides an air refueling rendezvous capability.

The mission control panels provide the input/output interfaces between the crew and the INS, central computer, and operational mode switching functions. These panels contain data readouts, mode switches, and data entry keyboard.

All navigation and guidance capabilities are provided initially in the basic airplane; no additional space is allotted for added navigation and guidance functions. Growth is accomplished by substitution of advanced capability systems within the same space envelopes.

#### E.4 ELECTRO-OPTICAL CAPABILITY

In order to provide a smart bomb capability in the basic airplane, a multi-mode display is employed for delivery of E-O weapons having imaging seeker heads. The display also presents superimposed vertical situation data and time-shared

radar data. Such a display enables the airplane to deliver smart bombs of the Walleye/Hobo type with very little weight and cost penalty. Delivery of laser guided bombs from the basic airplane requires external laser designation.

Full E-O weapon delivery capabilities are available in a growth package. This package provides the functions of self-contained day or night E-O target acquisition, cursor designation and target tracking, and laser target designation and ranging for delivery of laser-guided bombs. The laser ranger may be used to provide very accurate target range data for free-fall as well as smart bomb delivery in clear weather. (Table E-4)

Table E-4 E-O CAPABILITY IS OPTIONAL BUT FULLY ACCOMMODATED BY BASIC SYSTEM

SYSTEM ELEMENT	LOCATION		INSTALLED IN BASIC AIRPLANE	PROVISIONS ONLY
	BAYS	COCKPIT		
1. E-O PACKAGE	(170 LB)	(5 LB)		175 LB
• FLIR				
• SENSOR	40 LB			
• ELECTRONICS	30 LB			
• LTDR				
• TRANSMITTER & RECEIVER	10 LB			
• ELECTRONICS	10 LB			
• STABILIZATION				
• SYSTEM				
• GIMBALS/DRIVES	50 LB			
• ELECTRONICS	30 LB	5 LB		
2. MULTIMODE VERTICAL DISPLAY		30 LB	30 LB	

Interfaces are provided in the basic airplane for growth to the E-O configuration with a minimum of modification. These interfaces include space and access provisions for installing the E-O package and its fairing, electrical power, cooling, and signal data bus terminal(s) for access to the central computer and to other subsystem interfaces.

The E-O package is designed so that the FLIR can be replaced by a low-light-level TV for optimization of the E-O capability as a function of daylight and weather conditions. This interchangeability also requires two different fairing windows.

## E.5 RADAR

The operational survivability of this weapon system in a heavily defended environment will be greatly enhanced by the use of an air-to-ground attack radar. Increased survivability is achieved in two ways: (1) provision of a terrain following mode permits low-altitude penetration, and (2) the long-range target detection capability facilitates the use of standoff weapons which can be delivered outside of SAM/AAA zones. (Table E-5)

Table E-5 A-G ATTACK RADAR ENHANCES LWA MISSION ACCOMPLISHMENT

SYSTEM ELEMENT	LOCATION		INSTALL IN BASIC AIRPLANE	PROVISIONS ONLY
	BAYS	COCKPIT		
1. AIR-TO-GROUND ATTACK RADAR	150 LB	10 LB	160 LB	GROWTH TO 250 LB SYSTEM WITH AIR-TO-AIR MODES
2. RADAR ALTIMETER	10 LB		10 LB	

The radar is also essential to provide a cueing display for all-weather target detection. For many LWA missions the targets are either imprecisely located or mobile, making them impossible to locate in bad weather without a sensor of this

type. Even in good weather, a radar may be required to provide the topographical and cultural clues necessary to initially locate the target area. In addition to its basic ground mapping modes, the radar has terrain following and avoidance modes for low altitude penetration, a beacon interrogator for use with ground transponders in locating targets, moving target indication for locating moving vehicles, and air-to-ground ranging for bad-weather weapon delivery.

The radar is of modular design to facilitate growth to incorporate air-to-air modes. Addition of all-weather air-to-air detection and weapon delivery capabilities can be accomplished by adding the necessary processing and computing units, using space allotted for that purpose in the initial installation.

A radar altimeter is also provided for purposes of altitude calibration and as an accurate source of altitude data for use in terrain following and blind letdown modes.

#### E.6 COMMUNICATIONS, CCMAND AND CONTROL

For most LWA roles and missions, low-power line-of-sight transmission and receiving equipment will be sufficient to provide the necessary communication and identification capabilities.

Voice communication for Air Force tactical operations utilizes the UHF band (225-400 MHz). Two identical UHF sets are provided for purposes of redundancy and for simultaneous operation of both traffic control and strike control functions. A VHF-FM set is also included to provide a capability for direct communication with Army units for strike control. The direction-finding unit provides bearing information for homing on a UHF transmitter and is included primarily to facilitate rendezvous with a tanker for refueling. A voice scrambler

is used to enhance communications security. An intercom set is included to provide functions of mixing, channel selection, volume control, and signal conditioning and to permit communication between crew and ground personnel during ground operations. (Table E-6)

Table E-6 OPTIONAL DIGITAL DATA LINKS ARE PROVIDED IN MODULAR C<sup>3</sup> APPROACH

SYSTEM ELEMENT	LOCATION		INSTALLED IN BASIC AIRPLANE	PROVISIONS ONLY
	BAY	COCK- PIT		
1. COMMUNICATIONS	(16 LB)	(27 LB)	43 LB	
• UHF (2)		18 LB		
• VHF-FM		5 LB		
• ADF	6 LB			
• SECURE VOICE	10 LB			
• INTERCOM		4 LB		
2. AIR-TO-GROUND IFF	10 LB	3 LB	13 LB	
3. DATA LINK	(40 LB)	(3 LB)		40 LB
• STAND-OFF WEAPON LINK	20 LB			
• GROUND CONTROL LINK	20 LB	3 LB		

A lightweight air-to-ground IFF set is employed to meet the requirements for military and civil air traffic identification, command, and control.

Space and interface provisions are included for future installation of data link equipment for remote display and control of stand-off weapon guidance and a separate data

link for use in conjunction with a ground digital command and control network.

#### E.7 WEAPON DELIVERY EQUIPMENT

A head-up display with electronic symbol generation will provide visual flight reference, warning cues, target sighting designation, and navigation and attack steering for weapon delivery, all superimposed on the real world visual scene. The symbology, display format, mode control, stabilization, and command steering functions are compatible and integrated with those of the vertical multi-mode display to facilitate the head-up/head-down transition. Both displays are controlled from the digital computer complex through interfaces which offer a maximum of flexibility for reprogramming and modular growth. (Table E-7)

Table E-7 ADVANCED ARMAMENT DISPLAYS AND CONTROLS ARE INCLUDED

SYSTEM ELEMENT	LOCATION		INSTALLED IN BASIC AIRPLANE	PROVISIONS ONLY
	BAY	COCKPIT		
1. HEAD-UP DISPLAY	20 LB	30 LB	50 LB	
2. ARMAMENT CONTROLS	10 LB	10 LB	20 LB	
3. MISSILE ANCILLARIES	10 LB	8 LB	18 LB	GROWTH TO 30 LB TO INCLUDE AGILE TYPE WEAPON

An armament control panel in the cockpit and associated armament programming units are provided to accomplish the visual functions of armament selection, status readout, arming, release, and control of gun firing.

Missile ancillaries include interface electronics for an air-to-air IR missile and a tracking handle unit in the cockpit for lock-on and release of E-O guided weapons and for guidance update of stand-off weapons. Growth provisions are included for additional interface electronics for advanced air-to-air weapons of the Agile type.

#### E.8 DEFENSIVE SYSTEM

Defensive avionics equipment is not installed in the basic airplane. The rationale for this approach is as follows:

1. In general, the basic airplane will rely on its inherent maneuverability or on selection of the optimum speed, altitude, and time of day for penetration in order to avoid attrition due to the threats expected on a particular mission.
2. In dense threat environments, the defensive tasks of warning and counter-measures are assigned to special EW systems such as an EF-111 type aircraft or high-powered ground-based jammers.

However, provisions are made for future internal installation of various defensive subsystems in order to permit autonomous operation of the LWA in heavily defended environments. Space, power, and cooling are provided for the electronics, antennas, cable routing, displays and controls associated with these subsystems. Antenna installations are replaced by access plates or fillets.

(Table E-8)

Table E-8 DEFENSIVE ELECTRONICS ARE OPTIONAL

SYSTEM ELEMENT	LOCATION		INSTALLED IN BASIC AIRPLANE	PROVISIONS ONLY
	BAY	COCKPIT		
1. MULTIBAND RADAR WARNING	40 LB	10 LB		50 LB
2. IR TAIL WARNING & FLARE DISPENSER	50 LB	5 LB		55 LB
3. IR WARNING (LOWER HEMISPHERE)	50 LB			50 LB
4. MULTIBAND ECM	200 LB	5 LB		205 LB
5. INTERFERENCE BLANKER	5 LB			5 LB

Omnidirectional multiband radar warning provides crew warning when defensive radars (SAM or AAA) or airborne threat radars have locked on or launched missiles. ECM equipment (internally mounted) provides the necessary techniques such as jamming or trackbreaking in the ap-

propriate frequency bands to counter the transmitting threats. IR warning sets



on the tail and underside of the aircraft, together with an IR flare dispensing capability, furnishes warning and countermeasures for nontransmitting threats including aircraft or missiles approaching from the rear as well as ground-based missile threats (SAM and Redeye types).

# APPENDIX F VECTORED THRUST / SUPERCIRCULATION AERODYNAMIC DESIGN DISCUSSION

## F.1 DESIGN PROBLEM

Recent NASA test results and Convair analyses of other pertinent experimental data indicate that lift augmentation comparable to a pure jet flap can be achieved with the vectored thrust/supercirculation (VT/SC) concept throughout the subsonic-transonic flight regime.<sup>1-3</sup> However, the NASA results also show thrust recoveries to be lower than those expected for a full span jet flap (Figure F-1).

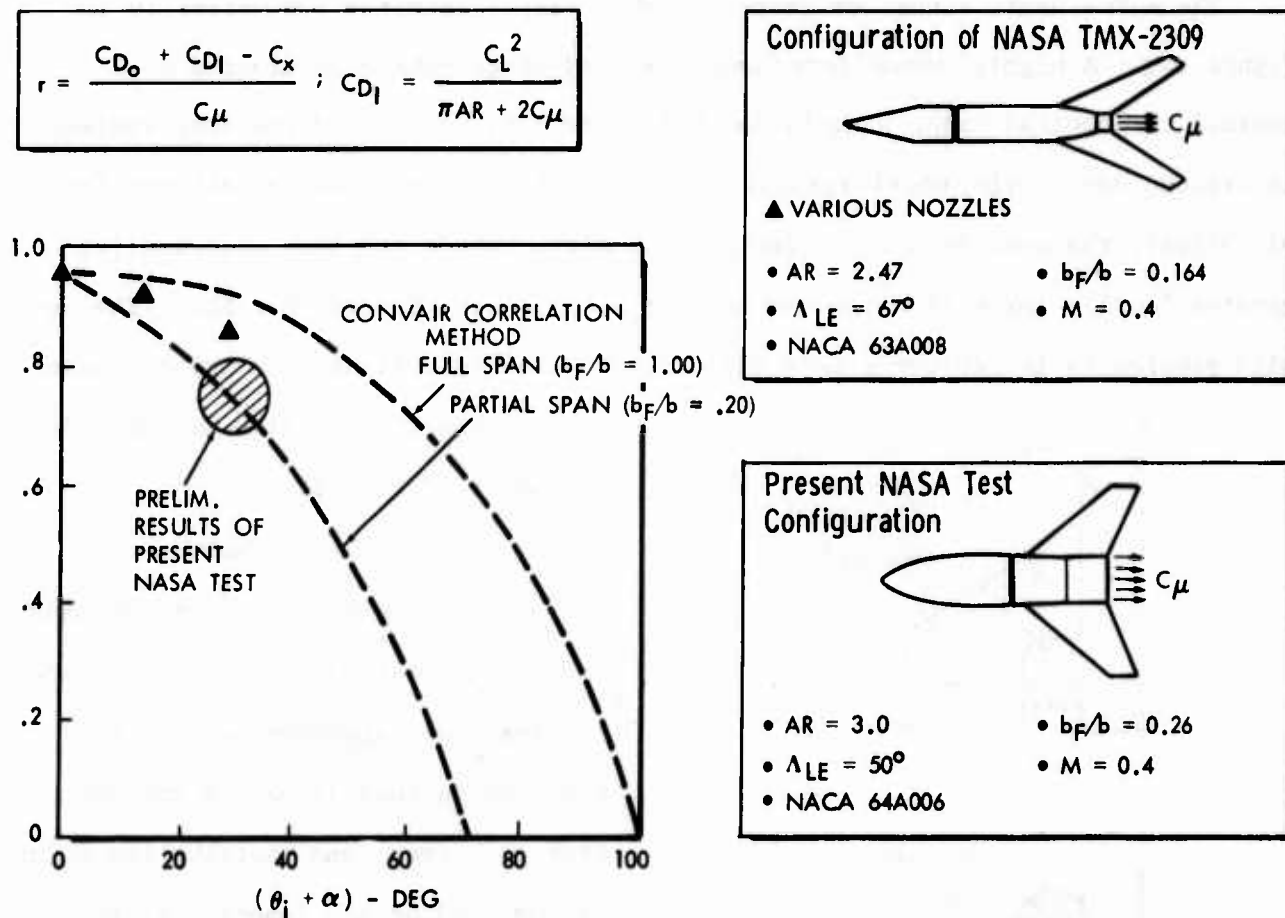


Figure F-1 VT/SC Thrust Recovery Picture is Cloudy

- <sup>1</sup> Corson, B. W., Capone, J., Putman, L. E., Lift Induced on a Swept Wing by a Two Dimensional Partial-Span Deflected Jet at Mach Numbers from 0.20 to 1.30, NASA TM X-2309, August 1971.
- <sup>2</sup> NASA unpublished data.
- <sup>3</sup> Mothersole, G. F., Whitten, P. D., and Smith, C. W., Powered Lift Aerodynamic Studies for the Advanced-Technology Close-Air-Support Fighter, Convair Report MR-A-2099, June 1972.

Convair studies of the NASA data indicate that the drag penalties associated with the partial span loadings generated by the short-span jet are significant. For example, approximately two-thirds of the calculated incremental drag can be attributed to the "peaky" span load distribution.

It seems apparent that the efficiency of the VT/SC concept is strongly dependent on the overall configuration. Since these partial-span-induced drag penalties significantly affect the sustained maneuver performance of VT/SC configurations, successful application of the VT/SC concept depends on innovative design which efficiently integrates the VT/SC concept with the complete configuration.

The aerodynamic situation described above is illustrated schematically in Figure F-2. A highly nonuniform spanwise load distribution is created on a typical trapezoidal swept wing by the deflected jet, and an induced drag increment is created due to the nonelliptical loading. The more the loading differs from elliptical, the greater the induced drag penalty. Since the high momentum jet creates locally large lift increments, the drag penalty is considerable. The design problem is to achieve a more uniform span loading distribution while retain-

ing the short span, high momentum jet of the VT/SC concept.

## F.2 DESIGN APPROACH

Several possible design approaches exist for creating a more uniform span loading. One approach is to tailor the wing so that it has an unblown (jet off) span load distribution which is improved by the inboard loading produced by the jet. This amounts to a wing with some degree of outboard loading. Two powerful planform variables for wings of this type are sweep and taper (Figure F-3).

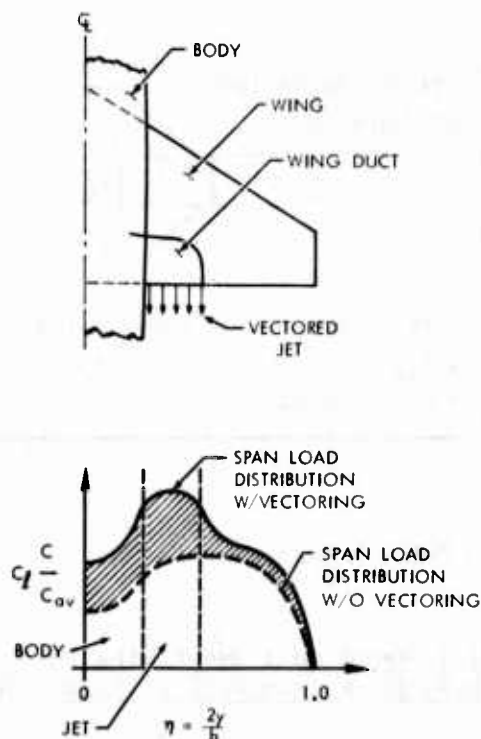


Figure F-2 VT/SC Partial Span Loading Results in Induced Drag Increment

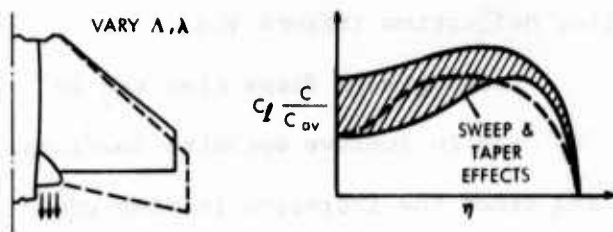


Figure F-3 Tailoring Planform can Improve Jet-Induced Loading

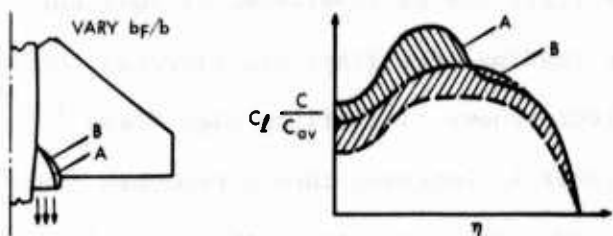


Figure F-4 Increasing Duct Span is Obviously Helpful

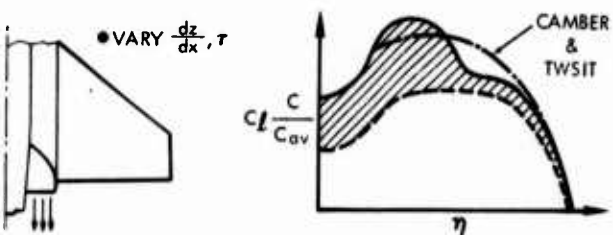


Figure F-5 Span Loading can be Increased in Outboard Regions with Camber and Twist

In general, outboard loaded designs are contrary to accepted design practice, in that they tend to exhibit tip stall and other undesirable characteristics. The amount of outboard loading is thus limited to some reasonable level by the configuration requirements for non-vector thrust operation.

Another important possible configuration design variable is the spanwise extent of the nozzle. If the momentum of the jet is spread across a larger percent of the span, the peak in the load distribution is reduced and a more uniform load distribution achieved (Figure F-4). Of course, this effect must be traded against the increased nozzle length.

A third design approach is to tailor the spanwise twist and camber distribution to produce a loading

favorable for application of the localized lift loading from the jet. This approach complements that of varying planform sweep and taper (Figure F-5).

Another approach entails the addition of camber to the wing to provide increased loading in a particular spanwise region to smooth out the overall distribution. This approach can be implemented by a simple trailing-edge flap outboard of the jet nozzle. Entrainment of the flow over the flap due to the carry-over circulation effects from the jet may also increase the effectiveness of the flap through boundary layer control action. Additional control over the

circulation may be obtained by varying the flap deflection (Figure F-6).

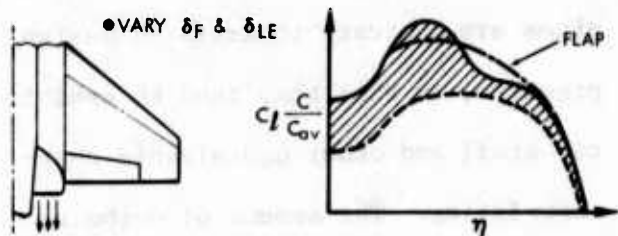


Figure F-6 Variable Camber in Outboard Region could be Answer

Leading edge flaps also can be employed to improve spanwise loadings; and, since the increased leading-edge pressures generated by the supercirculation can possibly create the need for some type of device to prevent

separation at the leading edge, leading-edge flaps can be considered as dual purpose devices. Convair studies indicate that leading-edge flaps can suppress leading edge separation and thus enhance the effectiveness of trailing-edge flaps<sup>1</sup> and proper combination of these flaps may result in improved thrust recovery over a wider range of angle of attack than for fixed solutions such as those previously discussed.

<sup>1</sup> McAllister, J. D., Benepe, D. B., Whitten, P. D., and Kaftan, G., Wing Roll Control Devices for Transonic High Lift Conditions, AFFDL-TR-69-124, Part I, January 1970, and Part II, February 1971.

## APPENDIX G

### CONFIGURATION SYNTHESIS PROCEDURE

The LWA parametric data of Appendices D and H are the products of a Convair configuration synthesis procedure known as CDC 6600 Procedure R1F. The procedure is a preliminary configuration design guide and is not applicable to detailed analysis. The procedure is used to identify trends, define the interaction between major design variables, and provide estimates of aircraft performance potential and gross sizing. The elements of the synthesis procedure are described in subsequent paragraphs.

#### G.1 FORCE PREDICTION METHODS

##### G.1.1 AERODYNAMICS

Aerodynamics methodology enables the prediction of the minimum drag and drag-at-lift characteristics of a complete configuration as a function of Mach number and lift condition. At a specified Mach number and lift condition, total drag is defined as the sum of the minimum drag and drag-due-to-lift.

Subsonically, the minimum drag is defined by the sum of the friction and form drags. Drag rise is added to this sum at Mach numbers above the drag divergence Mach number. Drag divergence Mach is calculated internally and is a function of the airfoil characteristics. Supersonically ( $M \geq 1.0$ ), the wave drag is added to the friction drag to define minimum drag. The wave drag is defined as the sum of the wave drags of the following components: (1) canopy, (2) fuselage, (3) nacelle, (4) wing, (5), vertical tail, and (6) horizontal tail (or canard).

Drag-due-to-lift is defined for a two-segment displaced "envelope" polar. The polar-break lift coefficient ( $CL_{BRK}$ ) separates the polar into two regions (1) the region below polar break is defined in terms of polar displacement ( $\Delta C_L$ ) and span efficiency factor ( $e_0$ ) and (2) the region above polar break is defined in terms of a lower span efficiency ( $e_1$ ) which is due to separation effects and reflects the reduced efficiency of the wing at higher lift coefficients. The



$C_{LBRK}$ ,  $\Delta C_L$ , and  $e_0$  are scaled from the reference by configuration-dependent (leading edge sweep, aspect ratio, thickness ratio) scaling functions.

#### G.1.2 STABILITY AND CONTROL

Initial tail sizes for the procedure are those established from the pre-design analysis of the baseline configuration, utilizing the current balance and control techniques. This tail/wing area relation is then maintained for the wing variation analysis.

#### G.1.3 PROPULSION

The synthesis procedure does not provide for the prediction of propulsion data (thrust and fuel flow) internally. Coefficients for a series of fourth-order polynomial curve fit equations provide the required data at any given Mach number-altitude condition for the engine design being considered.

Maximum power thrust and fuel flow are curve fit against Mach number at five user specified altitude levels by an equation of the form:

$$F_i = \sum_{k=0}^{k=4} A_{ik} M^k \quad (G-1)$$

where A represents the coefficients and M is the Mach number. If the altitude at which maximum power engine performance is to be computed does not coincide with one of the user specified altitudes, the referenced thrust and specific fuel consumption are determined at the closest altitude above and below the altitude of interest. Thrust and specific fuel consumption at the desired altitude are then determined by linear interpolation.

Intermediate power (maximum dry power) thrust and fuel flow are similarly curve fit with (1) Mach number at sea level and (2) altitude at Mach 0.9.

The ratio of partial-afterburning fuel flow to maximum power fuel flow is established as a function of the ratio of partial-afterburning thrust to maximum power thrust. A similar technique is employed for the reduced dry-power data.

#### G.1.4 WEIGHTS

Weights are computed by a variety of techniques. Fixed items such as system weights, armament, and avionics are input when available from design data. When

these data are not available from design layouts and detailed analyses, statistical estimates which encompass a large number of variables and equations are used to derive the input data.

Composite weight increments are estimated based on previous analysis and component experience and on stress/stiffness derived analytical values in specific areas, such as the basic fuselage structure. In the parametric variations, emphasis is placed on obtaining correct trends for major lifting surface weights (wing, tail), since that is where the major aerodynamic/structural interactions occur.

The basic wing weight equation is of the form,

$$W_w = \alpha F + \beta S_E \quad (G-2)$$

where  $S_E$  is the exposed wing area and  $\beta$  is a constant which can be altered to reflect different methods of construction, different levels of high-lift system complexity, etc. The function

$$F = \frac{N W_d b_s^2 \left[ \frac{0.556 + \lambda}{1 + \lambda} + 0.0632 (1 - \cos 4\Lambda) \right] K_R}{t_R (2.28 + \lambda t)} \quad (G-3)$$

is a load-dependent parameter derived as shown in Figure G-1. In this equation,  $N$  = ultimate design load factor,  $W_d$  = design weight,  $b_s$  = structural span,  $\Lambda$  = quarter chord sweep,  $\lambda$  = planform taper ratio,  $\lambda_t$  = thickness taper ratio,  $t_R$  = root thickness, and  $K_R$  = expanded root factor (usually  $\approx 1.0$ ).

In Equation G-2, the function  $\alpha$  is a material characteristic parameter, i.e.,

$$\alpha = 0.90 \times 10^{-5} \left[ C_\alpha + \frac{\alpha_t}{1.61} \left( \frac{(\gamma/\rho) a l}{(\gamma/\rho) c} - C_\alpha \right) \right] \quad (G-4)$$

In this equation,  $\alpha_t$  is a constant which accounts for the fact that the load-carrying material is not concentrated along the maximum wing thickness line;  $\alpha_t$  is primarily a function of airfoil characteristics, except for extremely thin wings where the skin thickness is comparable to the wing thickness. Usually,  $\alpha_t \approx 1.35$ . The constant  $C_\alpha$  accounts for the amount of load-carrying "nonoptimum" material in the wing. For a "statistically average" aluminum wing,  $C_\alpha$  is 1.0; it is greater

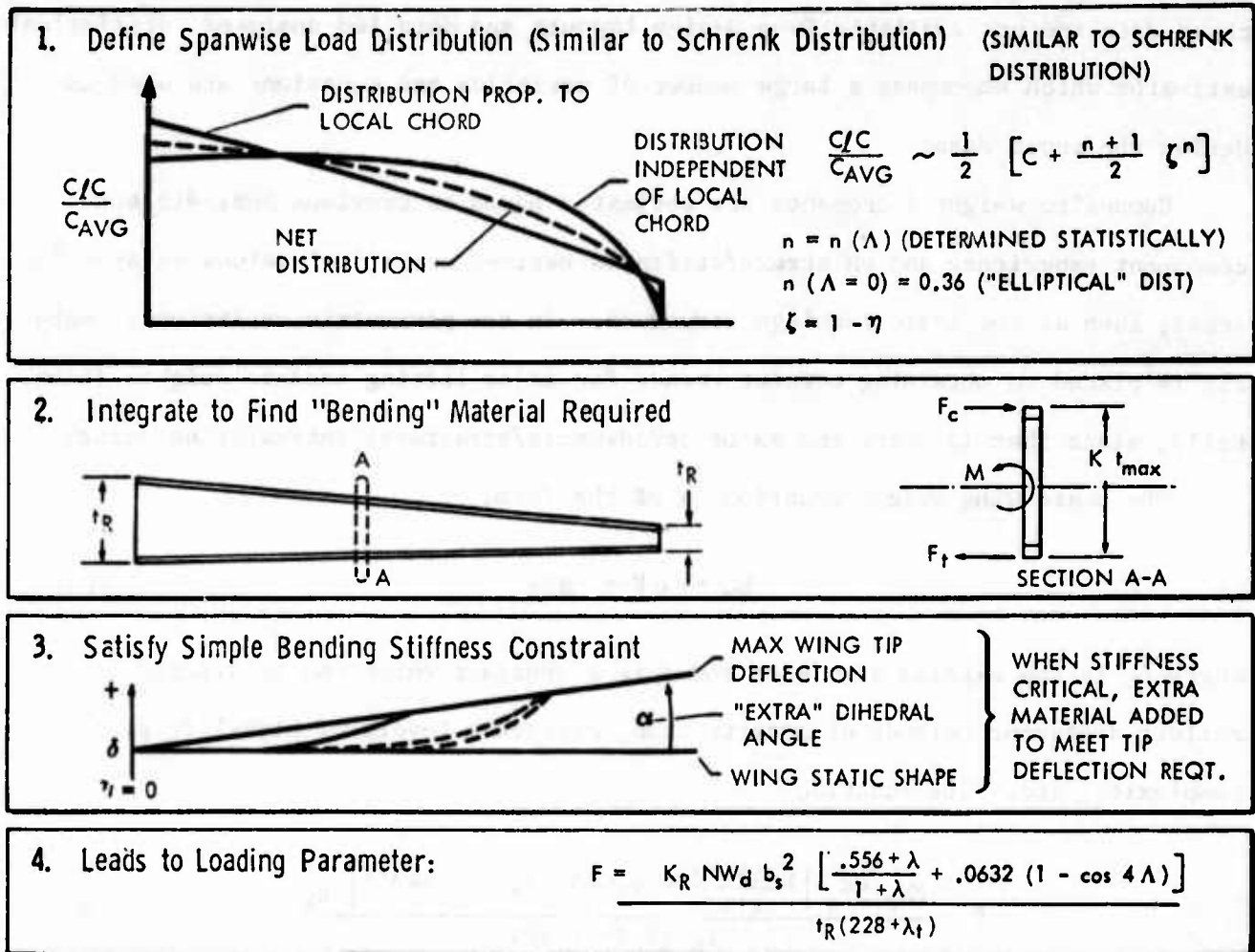


Figure G-1 Structural Weight Methods - Loading Parameter

than 1 when more nonoptimum material is required; and it is less than 1 when the structural design is more efficient. For composite wings, the nonoptimum efficiency is strongly dependent on the design concept.

The  $(\gamma/\rho)_a$  term in Equation G-4 represents the maximum allowable stress-over-density of aluminum and  $(\gamma/\rho)_c$  is an equivalent term for different material properties. The term, which can be modified as necessary for elastic characteristics, is defined as

$$(\gamma/\rho)_c = \begin{cases} \frac{\gamma_M}{\rho} & \text{for } 0 < \frac{b_s}{t_R} \leq \left( \frac{b_s}{t_R} \right)_o \\ \frac{\gamma_M \left( \frac{b_s}{t_R} \right)_o}{\rho \left( \frac{b_s}{t_R} \right)} & \text{for } \left( \frac{b_s}{t_R} \right)_o < \frac{b_s}{t_R} < \infty \end{cases} \quad (G-5)$$

$$\left(\frac{b_s}{t_R}\right)_0 = \frac{(\Delta y/b_s)_{\text{design}}}{\alpha t \left(\frac{\gamma_M}{E}\right) \left\{ \frac{(1-\lambda t)}{(1-\lambda_t)^2} - \lambda t \ln \frac{1}{\lambda t} \right\}} \quad (G-6)$$

where  $\gamma_M$  is the average effective ultimate strength,  $\rho$  is the density,  $E$  is the average effective modulus, and  $(\Delta y/b_s)$  is a maximum allowable deflection at the tip. For metals, the  $E$  and  $\gamma_M$  values are fixed characteristics of the material; however, for composites, they are functions of the basic material properties and the average fiber orientations of the wing load-carrying structure.

## G.2 FLIGHT MECHANICS/PERFORMANCE METHODS

Flight mechanics/performance methodology is available for defining the various types of performance data necessary for each mission phase (warm-up and take-off allowance, acceleration and climb, cruise, loiter, combat, etc.). Assumptions are made to permit the basic equations of motion to be integrated for each mission phase to provide simplified analytical approximations.

### G.2.1 WARM-UP AND TAKEOFF ALLOWANCE

Warm-up and takeoff allowance is defined as the sum of the fuel required to taxi at sea level for a specified time at a thrust-to-weight ratio of 0.2 plus the fuel required to accelerate at sea level, maximum power from brake release to a specified initial climb speed.

### G.2.2 CLIMB AND ACCELERATION

Climb and acceleration performance is defined for (1) subsonic climb at dry power and (2) acceleration at a constant altitude. The methodology involved for each of these segment types is discussed below.

#### G.2.2.1 Subsonic Climb at Dry Power

Fuel and distance to climb are defined assuming that (1) thrust is in the direction of motion, (2) Mach number is constant, (3) climb angle is constant, and

(4) thrust (T) may be represented by  $T = C_T p$  over a limited altitude range.

Because climb is performed at constant Mach number, it may be further assumed that the velocity is constant since the speed of sound is approximately 1000 feet per second, i.e., isothermal atmosphere. With these assumptions, the equations of motion for climb in a vertical plane may be written as

$$\begin{aligned} m\dot{V} &= 0 = T - D - W\sin\gamma \\ mV\dot{\gamma} &= 0 = L - W\cos\gamma \\ \dot{h} &= V\sin\gamma \\ \dot{R} &= V\cos\gamma \\ \dot{W} &= -(\text{SFC})T = -FF \end{aligned} \quad (\text{G-7})$$

Integration of these equations yields simplified analytical expressions for fuel and distance to climb.

#### G.2.2.2 Acceleration at a Constant Altitude

Time and fuel to accelerate at maximum power and constant altitude from an initial Mach number  $M_i$  to a final Mach number  $M_f$  are defined by integrating the equations of motion in a vertical plane using a trapezoidal integration scheme. The acceleration is range free and is performed at constant weight.

The equations of motion in a vertical plane for constant altitude may be written as

$$\begin{aligned} m\dot{V} &= T - D - W\sin\gamma^0 \\ mV\dot{\gamma} &= L - W\cos\gamma = 0 \\ \dot{W} &= -(\text{SFC})(T) \end{aligned} \quad (\text{G-8})$$

These equations may be numerically integrated for small Mach increments to define incremental time and fuel to accelerate. These increments are summed over the entire acceleration Mach schedule to define the total time and fuel to accelerate.

### G.2.3 CRUISE

Four types of subsonic cruise segments are optionally available. Subsonic cruise segments may be defined as

1. "Optimum" Mach number/"optimum" altitude cruise
2. "Optimum" Mach number/constant altitude cruise
3. Constant Mach number/"optimum" altitude cruise
4. Constant Mach number/constant altitude cruise (i.e., dash).

"Optimum" cruise Mach number is limited to Mach numbers less than or equal to the drag divergence Mach number. Dash segments are defined as constant Mach number/constant altitude cruise. The dash Mach number may be specified as any speed since it is not constrained by drag divergence Mach number.

Cruise performance is computed from the classical Brequet range equation

$$R = \left(\frac{L}{D}\right) \left(\frac{V}{SFC}\right) \ln w_0/w_f \quad (\text{N.MI.}) \quad (\text{G-9})$$

where

$L/D$  is lift-to-drag ratio

$V$  is velocity (knots)

$SFC$  is specific fuel consumption (lb/hr/lb)

$w_0$  is initial cruise weight (lb)

$w_f$  is final cruise weight (lb).

If the cruise range ( $R$ ) is specified, the cruise fuel is

$$\Delta W_{\text{Cruise}} = w_0 - w_f = w_f \left( \frac{w_0}{w_f} - 1 \right), \quad (\text{G-10})$$

or

$$\Delta W_{\text{Cruise}} = w_f \left( e^{R/C_R} - 1 \right) \quad (\text{G-11})$$

where

$C_R$  = range constant (N.MI.)

=  $(L/D) (V/SFC)$ .



Dash performance (constant Mach and altitude cruise) is computed from

$$\Delta R = (SR) (\Delta W_{\text{Cruise}}) \quad (G-12)$$

where

SR = specific range constant (n.mi/lb)

$\Delta W$  = velocity divided by fuel flow (V/FF)

FF = fuel flow (lb/hr = (SFC) (T)).

The specific range constant is insensitive to weight for low lift conditions.

#### G.2.4 COMBAT

##### G.2.4.1 Sustained Turn Maneuvers

Sustained turn maneuvers are performed at specified Mach number, altitude, and power setting conditions. The fuel required to perform a specified number of sustained turns is defined for each condition.

A sustained turn implies that the velocity is constant. Therefore, in the direction of motion,

$$m\dot{V} = 0 = T - D - W \sin \gamma. \quad (G-13)$$

The flight path angle is zero since the turn is performed at constant altitude. Equation G-13 may therefore be written as

$$T - D = 0. \quad (G-14)$$

Equation G-14 may be used to solve for the lift condition necessary to sustain the turn in the following manner:

$$T - D = T - (C_{D_{\text{Min}}} + K C_L^2) qS = 0 \quad (G-15)$$

Solving for  $C_L$  yields

$$C_L = C_{L_{\text{Sust}}} = \sqrt{\frac{T/qS - C_{D_{\text{Min}}}}{K}} \quad (G-16)$$

In banked flight, the expression for the rate of change of flight path angle with respect to time ( $\dot{\gamma}$ ) is

$$mV\dot{\gamma} = L\cos\phi - w\cos\gamma \quad (G-17)$$

where

$\phi$  = roll angle.

Equation G-17 may be arranged to define the load factor (lift-to-weight ratio):

$$\frac{L}{W} = n = \frac{1}{\cos\phi} \quad (G-18)$$

where  $n$  = load factor.

In the turning plane, the centrifugal force must be balanced by the lift component, i.e.,

$$\frac{mV^2}{R} = L\sin\phi \quad (G-19)$$

where  $R$  = turn radius. Equations G-18 and G-19 may be manipulated to define the turn radius as

$$R = \frac{V^2}{g_c \sqrt{n^2 - 1}} \quad (G-20)$$

The turn rate is defined as the ratio of the velocity to turn radius, i.e.,

$$\phi_{\text{Sust}} = \frac{g_c}{V} \sqrt{n^2 - 1} \quad (G-21)$$

Equations G-16 and G-18 may be used to define the sustained load factor.

The fuel required to perform  $N$  sustained turns is defined as

$$\Delta W_N \text{ Turns} = \left[ \frac{\text{SFC}_A \times T_A}{3600} \right] \left[ \frac{360 N}{\phi_{\text{Sust}}} \right] \quad (G-22)$$

where

$N$  = number of  $360^\circ$  turns desired

$\phi$  = sustained turn rate (Deg/Sec)

$SFC_a$  = maximum power specific fuel consumption at the turn condition Mach and altitude (lb/hr/lb)

$T_a$  = maximum power thrust at the turn condition (lb).

#### G.2.4.2 Energy Gains

Combat allowance may be requested as the fuel required to gain a specified amount of energy ( $E_s$ ) based on the energy rate ( $\dot{E}_s$ ) at a specified maneuver Mach, altitude, load factor, power setting, and weight condition. The energy rate is defined as

$$\dot{E}_s = P_s = \left( \frac{T-D}{W} \right) V \quad (G-23)$$

where

$T$  = thrust (lb)

$D$  = drag (lb) =  $C_D qS$

$W$  = weight (lb)

$V$  = velocity (ft/sec).

The drag ( $D$ ) is evaluated at the Mach, altitude, and load factor condition. The fuel required to gain a specified energy is defined from

$$\Delta W_{\text{Combat}} = \left( \frac{E_s}{P_s} \right) \dot{w} \quad (G-24)$$

where

$E_s$  = specified energy gain (ft)

$P_s$  = energy rate from Equation G-23 at the specified maneuver condition (ft/sec)

$\dot{w}$  = fuel flow at the specified maneuver condition (lb/sec).

### G.3 MISSION ANALYSIS METHODS

The mission as currently defined in the synthesis procedure is composed of 12 mission segments. Each mission segment may be retained or deleted on an option basis. This option capability permits a number of missions to be defined from the basic 12 mission segments. The order in which these segments may be utilized is fixed by present program logic. This order is as follows:

1. Landing reserve
2. Inbound cruise
3. Inbound climb to cruise path
4. Inbound dash
5. Ordnance drop
6. Combat
7. Outbound dash
8. Outbound acceleration to dash speed or combat acceleration
9. Outbound loiter
10. Outbound cruise
11. Outbound climb
12. Warm-up, takeoff, and acceleration to climb speed allowance.

Notice that the mission segments are listed in reverse order and that the mission with the full complement of twelve segments is a radius mission about the ordnance drop/combat points.

The listing is presented in reverse order because the purpose of the mission analysis base is to define (1) a vehicle sized to meet the specified mission requirements or (2) the performance potential for a specific vehicle size.

For the purposes of discussion, the first case is considered. Based on an initial assumed fuel required to perform the specified mission, the weight methodology (Section G.1.4) is utilized to define an associated empty weight (since design weight is a function of the fuel). The mission is integrated by computing the fuel required to perform each mission segment in the order described

above (i.e., reverse order) to define the fuel required to perform the total mission and hence the takeoff gross weight. This new fuel weight is used to perform successive iterations through the mission until convergence is established between the assumed fuel and the required fuel.

Range is accounted for in cruise, climb, acceleration to dash speed, and dash. Decelerations, descents, loiter, and combat are range free. Cruise and dash range requirements are specified. The specified cruise range is decreased for (1) the inbound leg by the inbound climb range and (2) the outbound leg by the sum of the range to accelerate to dash speed and the outbound climb range.

# APPENDIX H PARAMETRIC MISSION / CONFIGURATION DATA

Parametric data are defined, using the synthesis procedure discussed in Appendix G, for LWA Reference Configurations 26B and 26C utilizing conventional materials and composite materials, respectively. The aerodynamic and weight characteristics of the reference configurations are used to calibrate the synthesis procedure.

Twelve performance parameters are monitored in the parametric analyses. Nine of these parameters are mission profile/mission configuration dependent; three are maneuver dependent.

Mission profiles and mission configurations are defined in Section D.3.3. The nine mission profile/mission configuration combinations are shown in Table H-1.

The three maneuver parameters moni-

Table H-1 NINE MISSION PROFILE/MISSION CONFIGURATION COMBINATIONS ARE INCLUDED IN THE PARAMETRIC DATA

MISSION PROFILE	MISSION CONFIGURATION
OPTIMUM SUBSONIC.....	.....1, 2, & 3
SEA LEVEL PENETRATION.....	.....1 & 2
SUPERSONIC PENETRATION.....	.....1 & 2
SUPERSONIC INTERCEPT.....	.....1 & 1'

tored are

1. Supersonic acceleration time from M0.85 to M1.6, 36,089 feet, maximum power
2. Low speed maneuverability at 150 KTAS, 5000 feet, maximum usable lift ( $Cl_{max}$ )
3. Transonic maneuverability at M0.9, 30,000 feet, buffet free.

The parametric data are presented for each material category as a function of the engine size, wing area, and wing geometry (aspect ratio, leading edge sweep, and thickness ratio). Engine size and wing area variations define carpet plots for each performance parameter and geometry combination.

Lines of constant acceleration time or g-capability at one or both of the maneuver conditions may be plotted on the mission radius plots to define the intersection of an acceleration time line and g-capability line. This intersection point defines the engine/wing size required to meet the specified acceleration time and maneuver load factor.



Engine size may be converted to thrust loading for each mission configuration. Similarly, wing area may be converted to wing loading (Figure H-1).

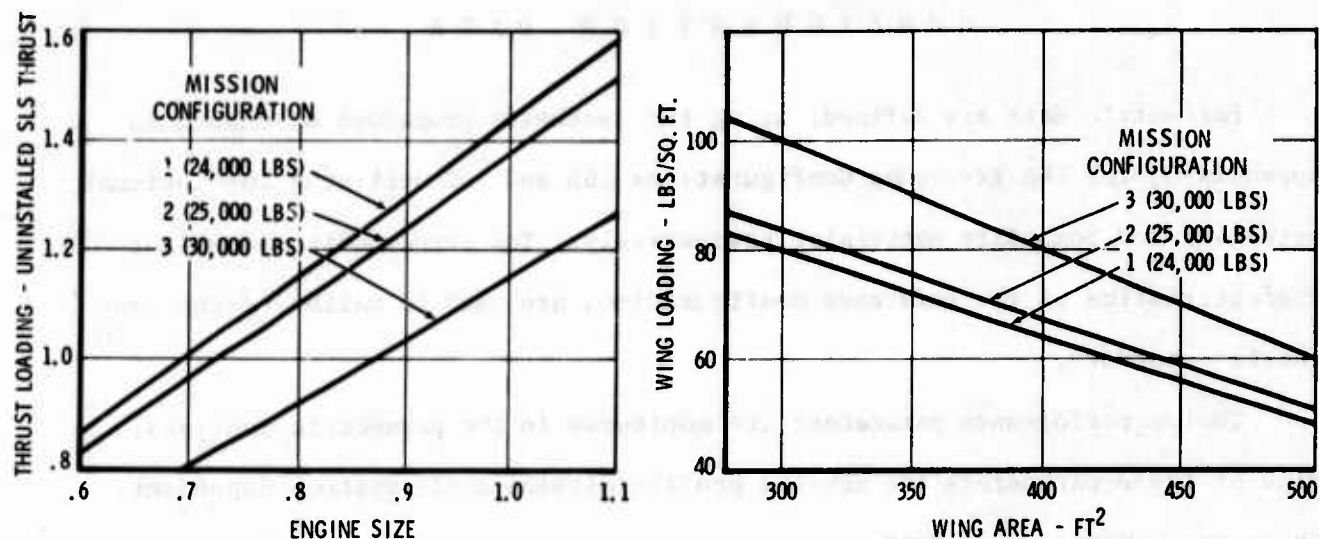
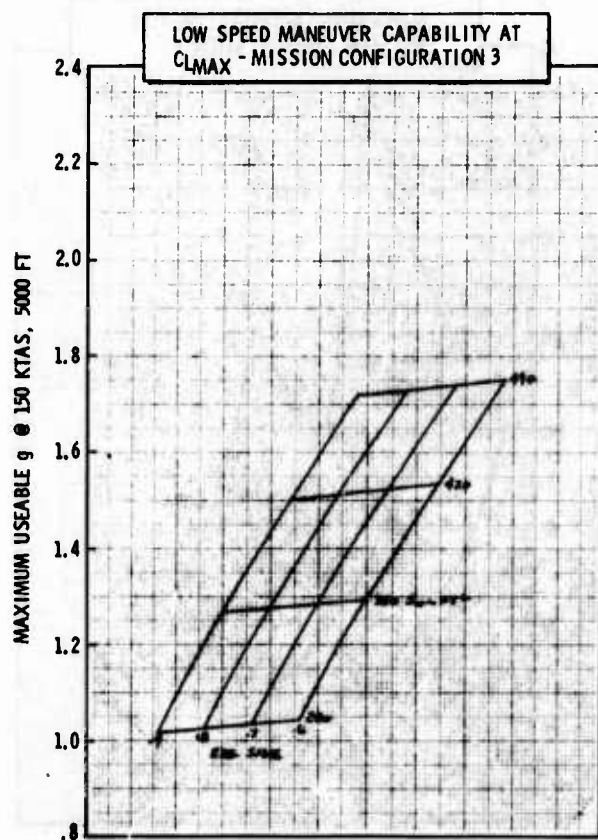
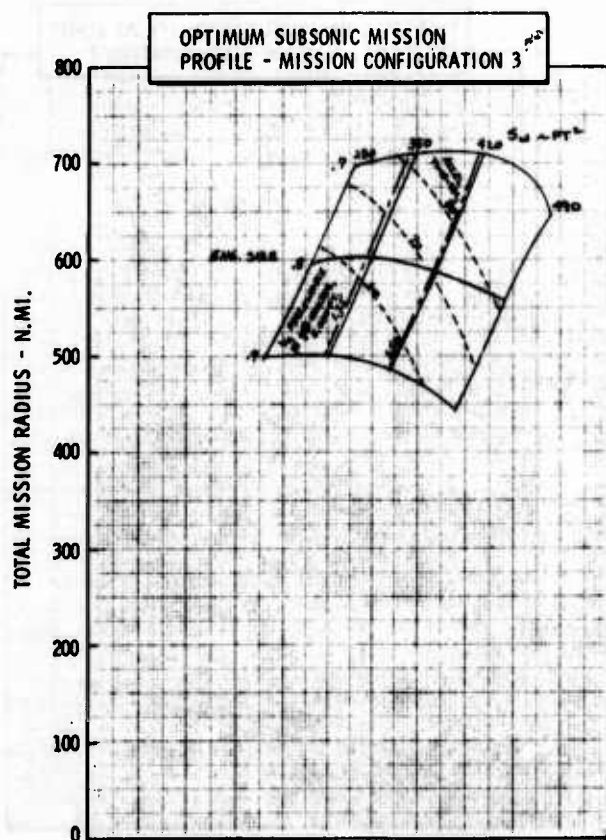
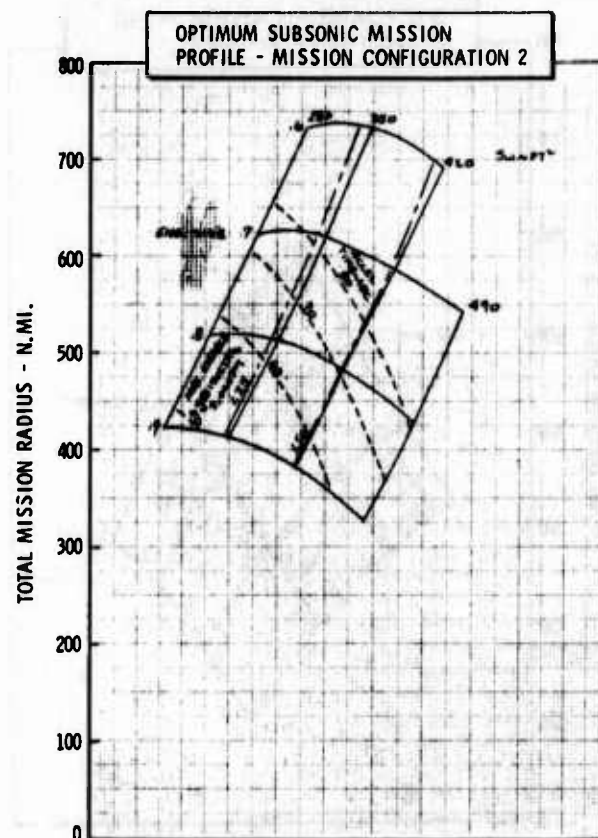
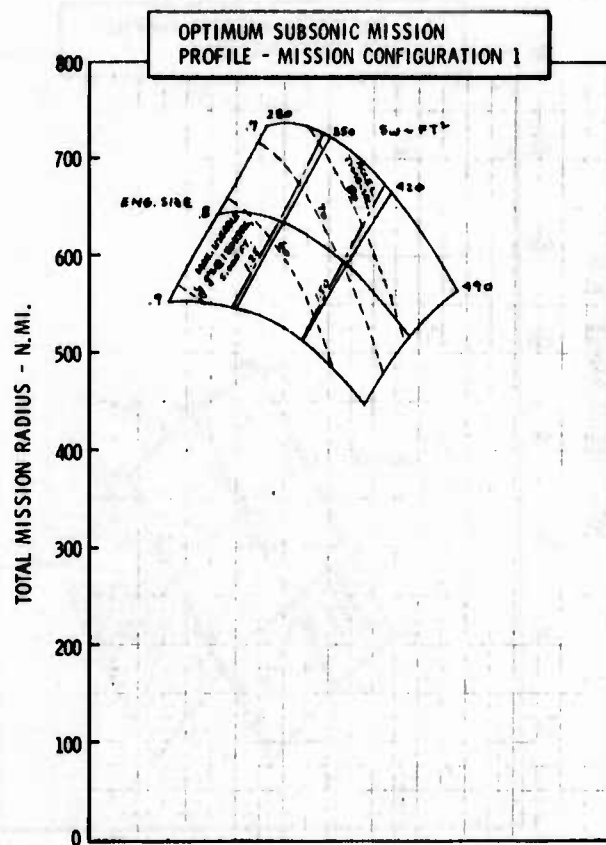


Figure H-1 Engine Size and Wing Area Used for Parametric Data can be Converted to Thrust Loadings and Wing Loadings

•  $\Delta_{LE} = 20^\circ$

• AR - 3.0

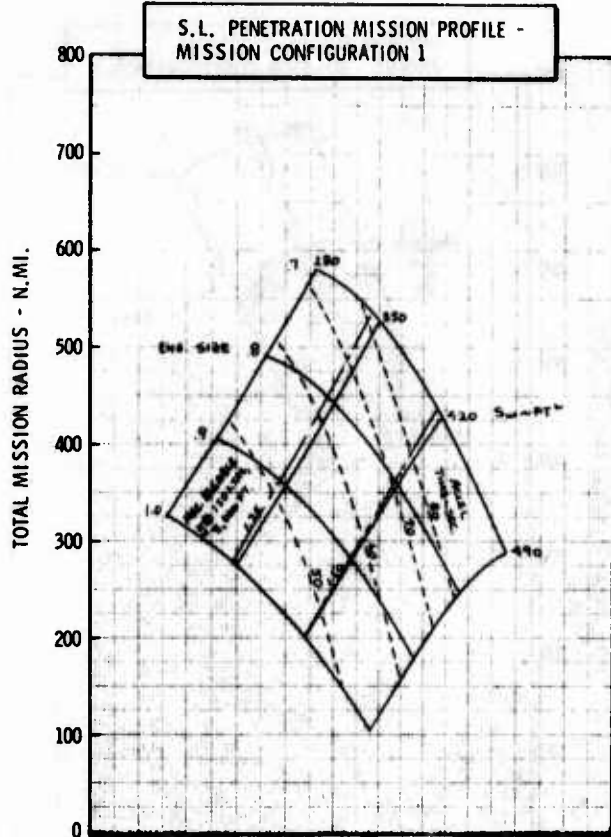
•  $t/c = .04$



**Figure H-2a LWA Mission/Configuration Tradeoff Parametric Data**

• CONVENTIONAL MATERIALS

•  $\Delta LE = 20^\circ$



• AR = 3.0

•  $t/c = .04$

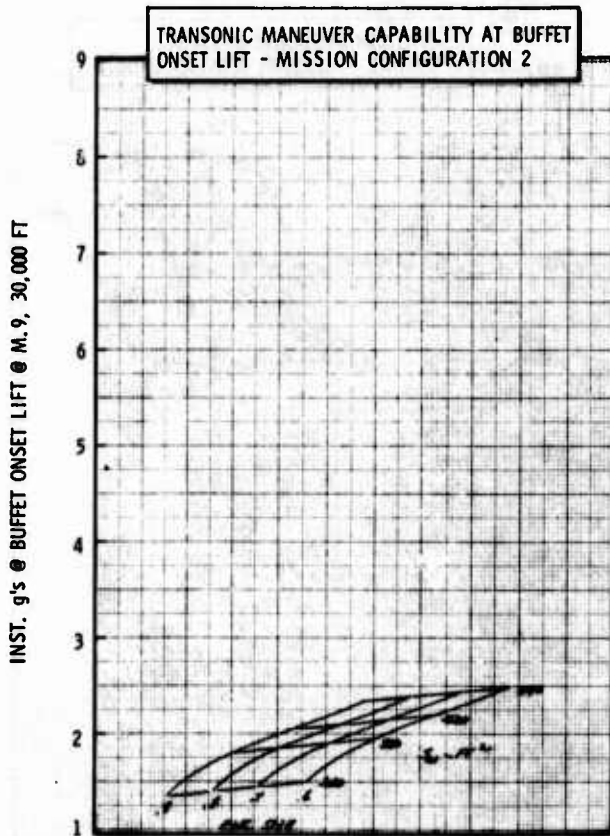
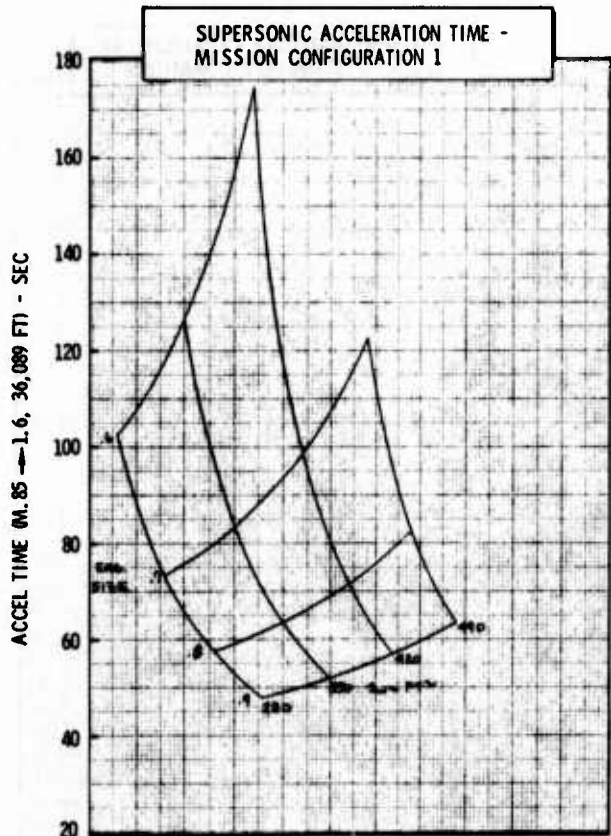
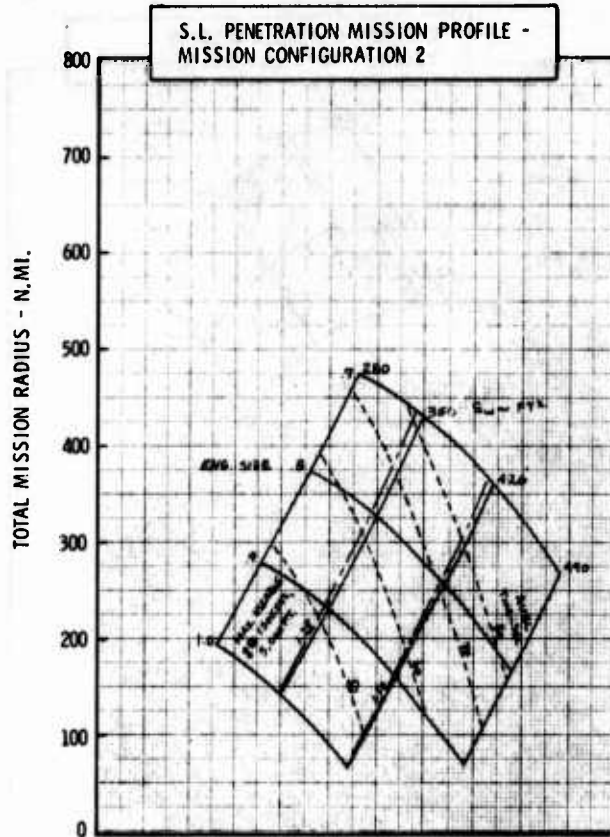


Figure H-2b LWA Mission/Configuration Tradeoff Parametric Data

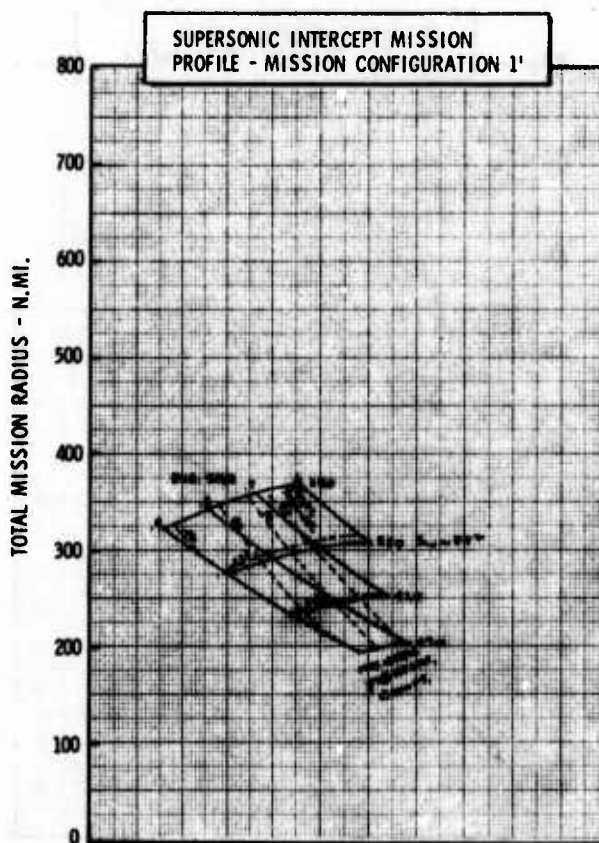
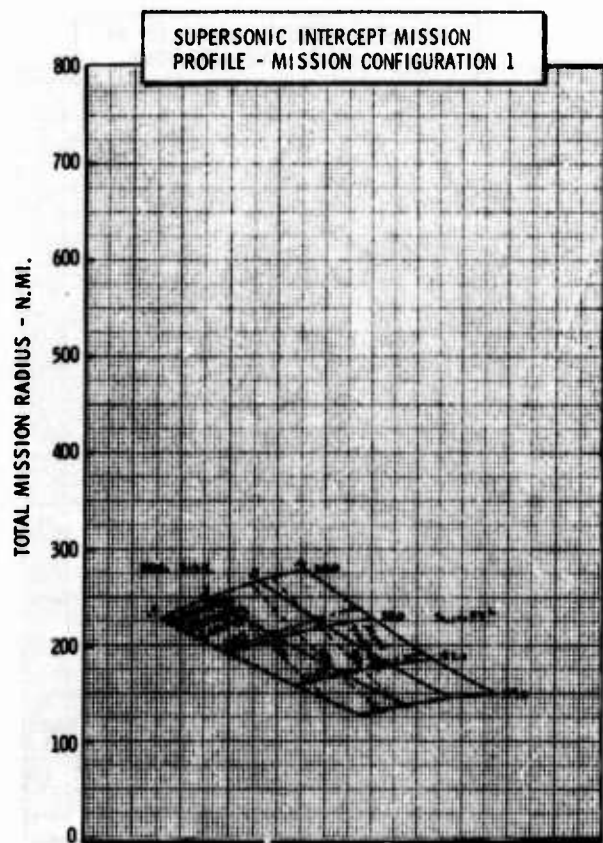
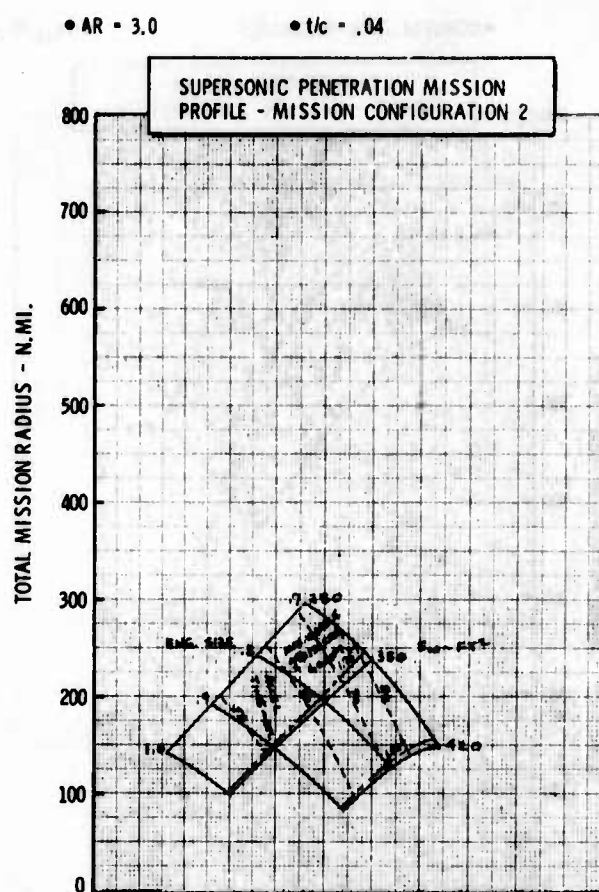
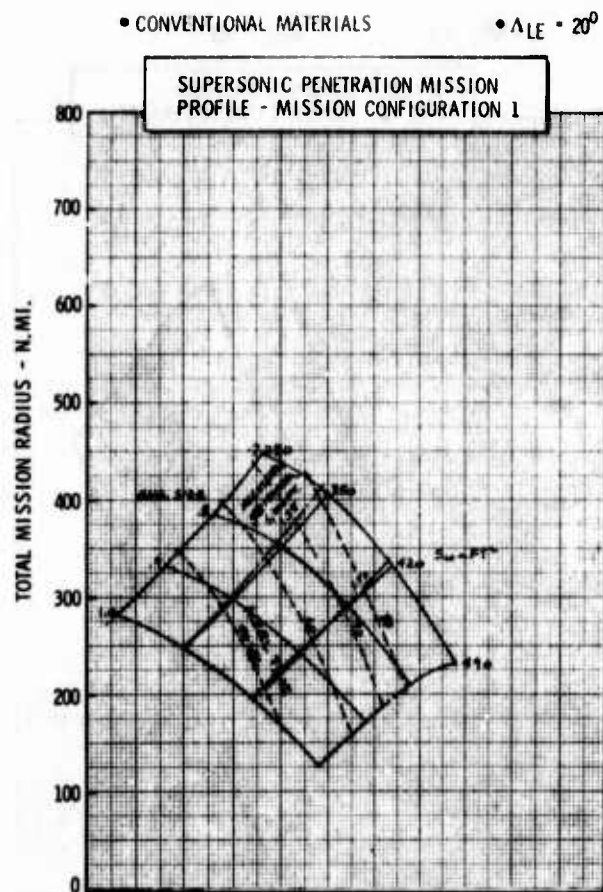


Figure H-2c LWA Mission/Configuration Tradeoff Parametric Data



• CONVENTIONAL MATERIALS

•  $\Delta LE = 20^\circ$

•  $AR = 4.0$

•  $t/c = .04$

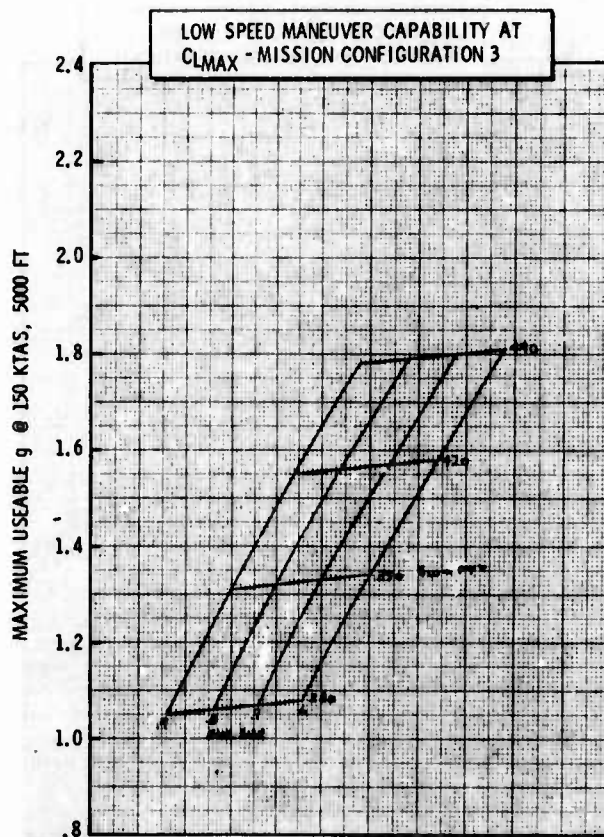
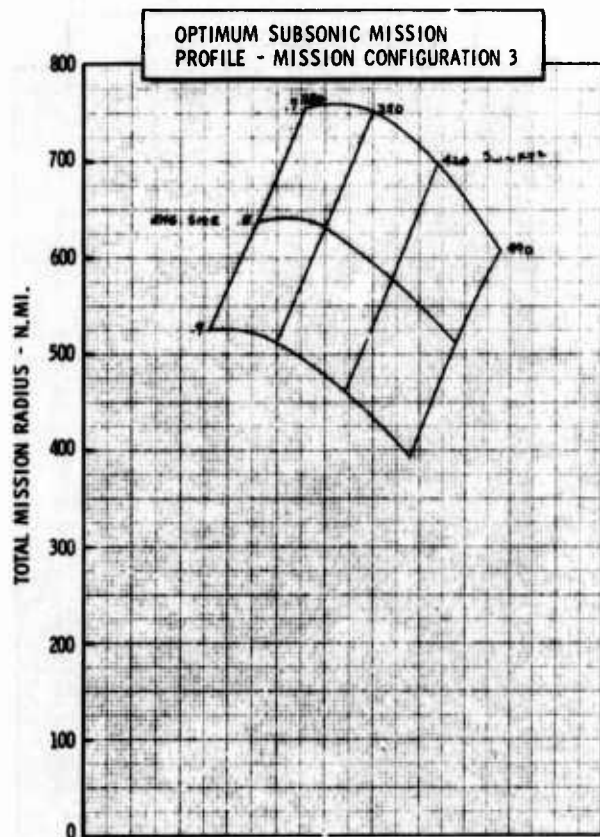
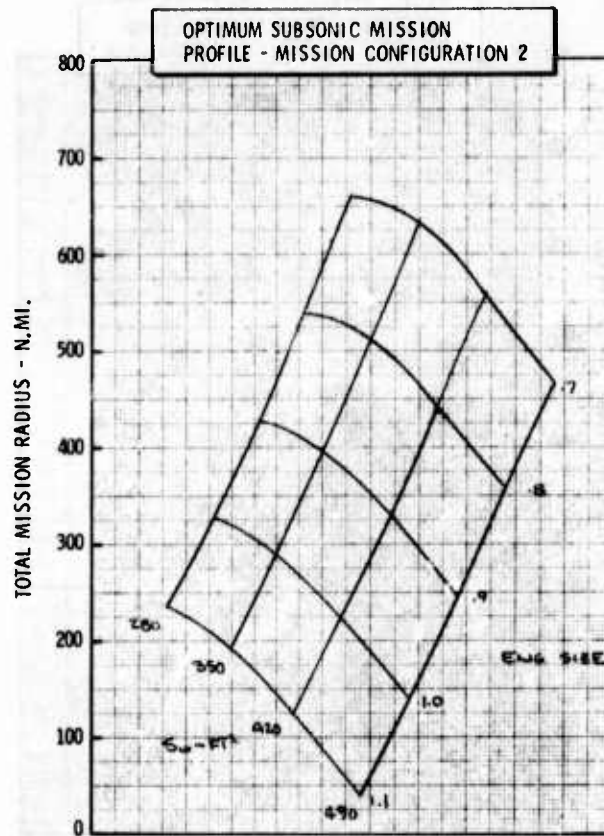
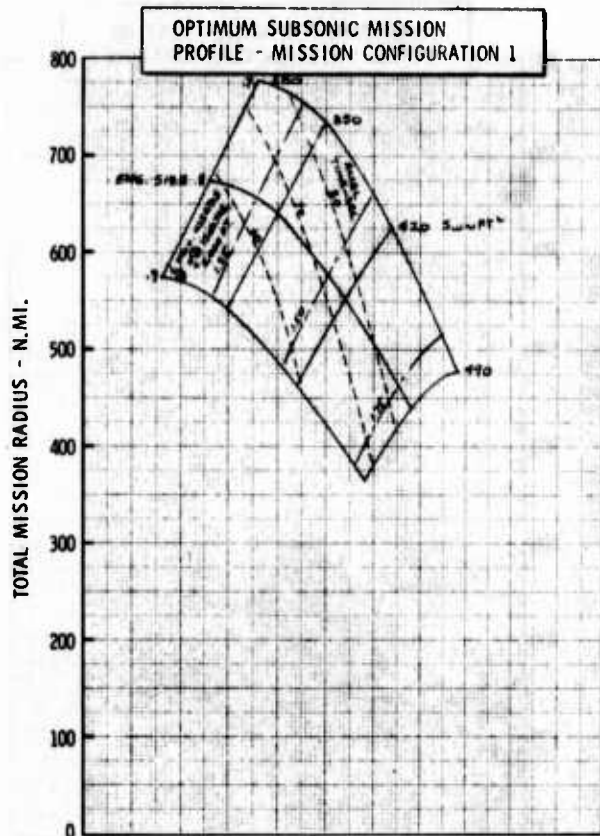


Figure H-3a LWA Mission/Configuration Tradeoff Parametric Data

• CONVENTIONAL MATERIALS

•  $\Delta LE = 20^\circ$

• AR = 4.0

•  $t/c = .04$

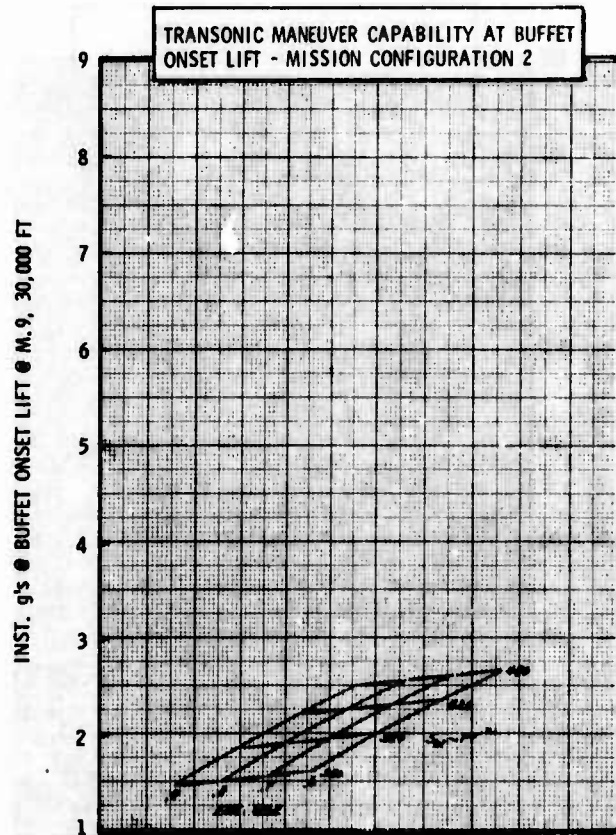
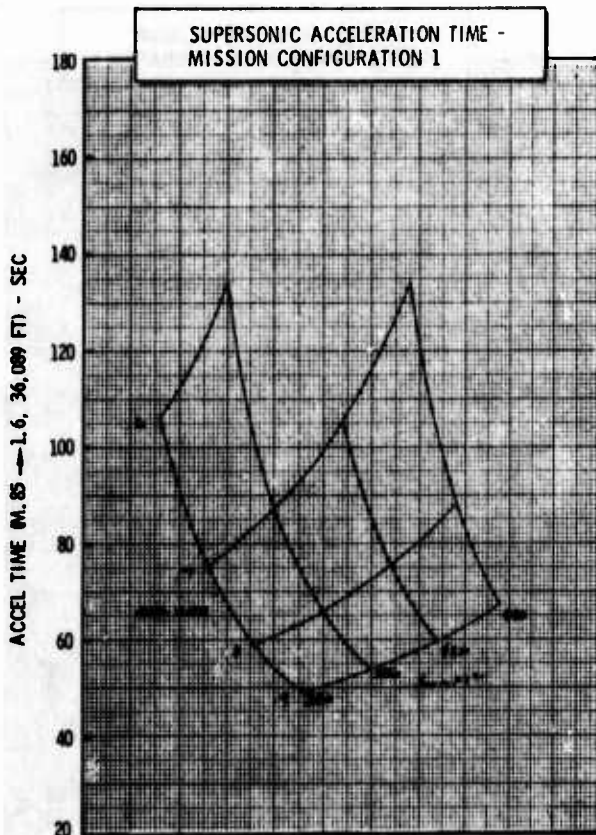
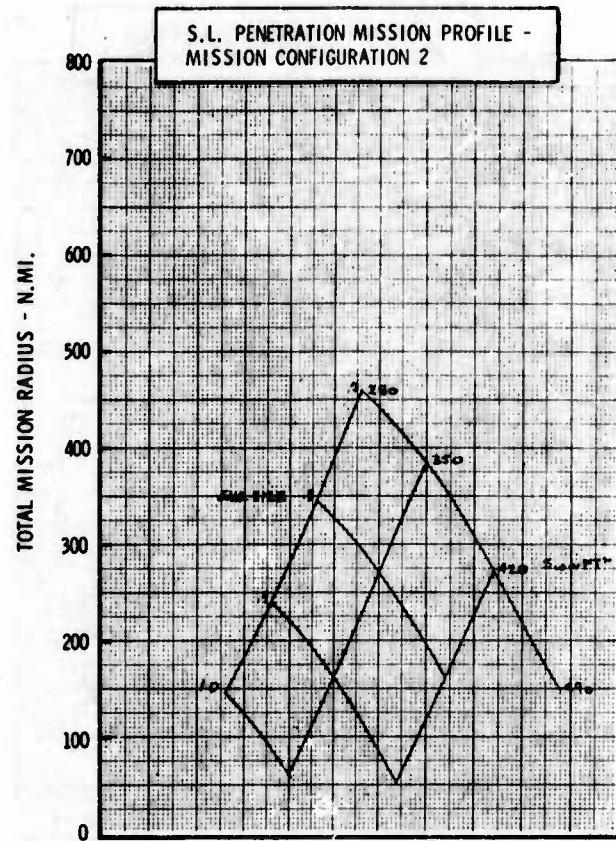
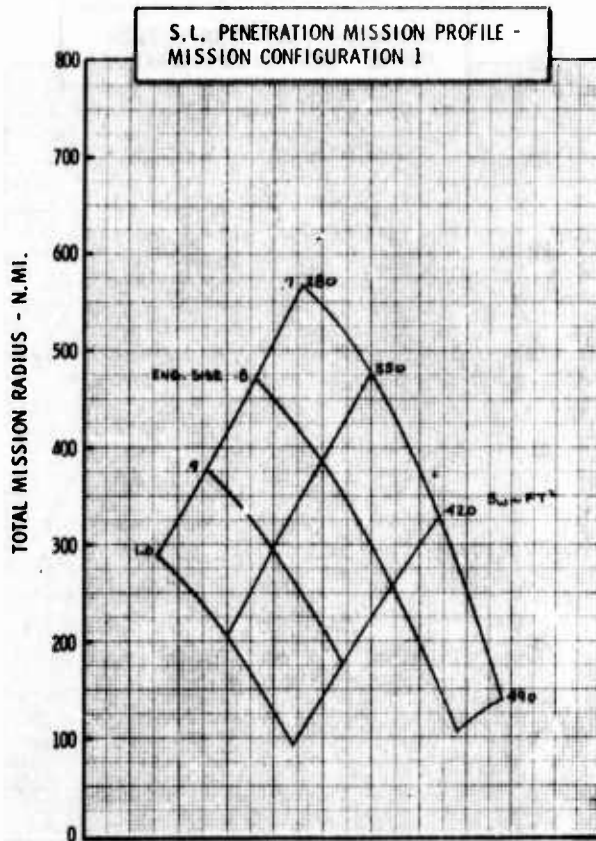


Figure H-3b LWA Mission/Configuration Tradeoff Parametric Data



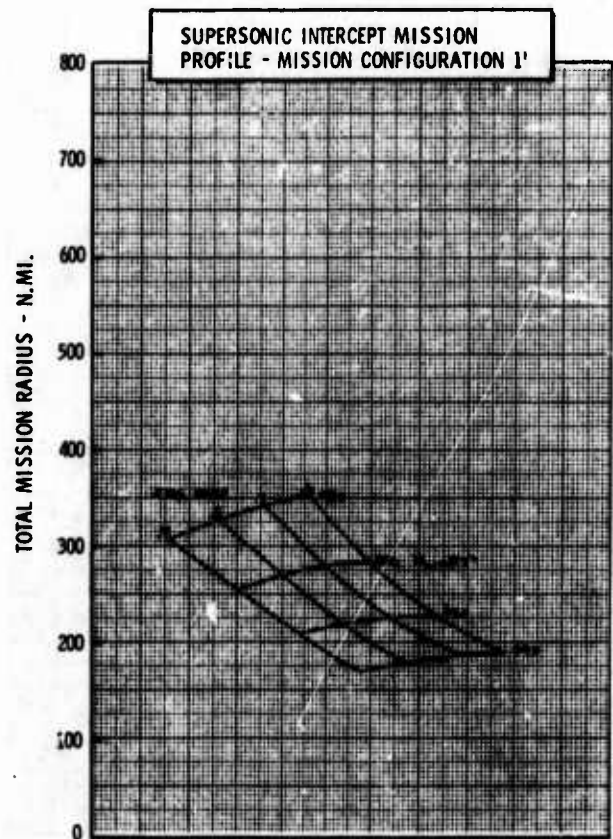
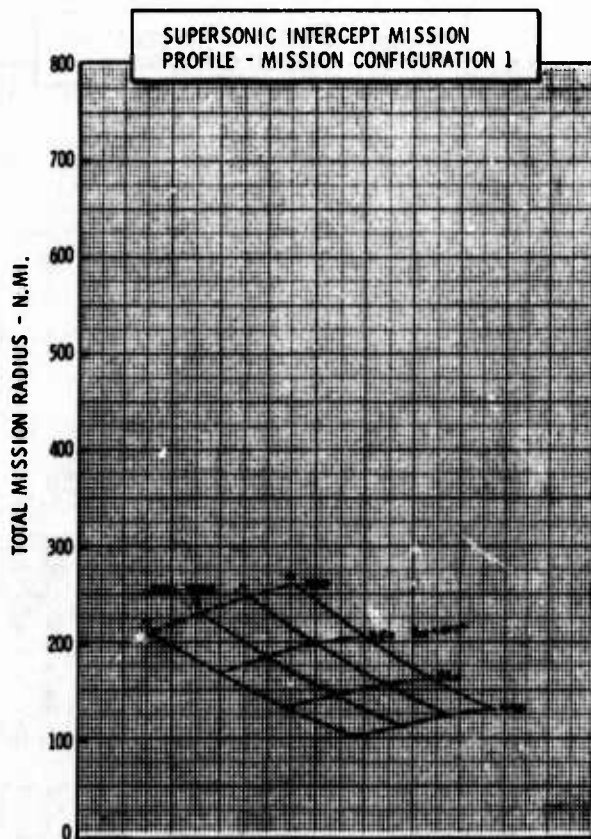
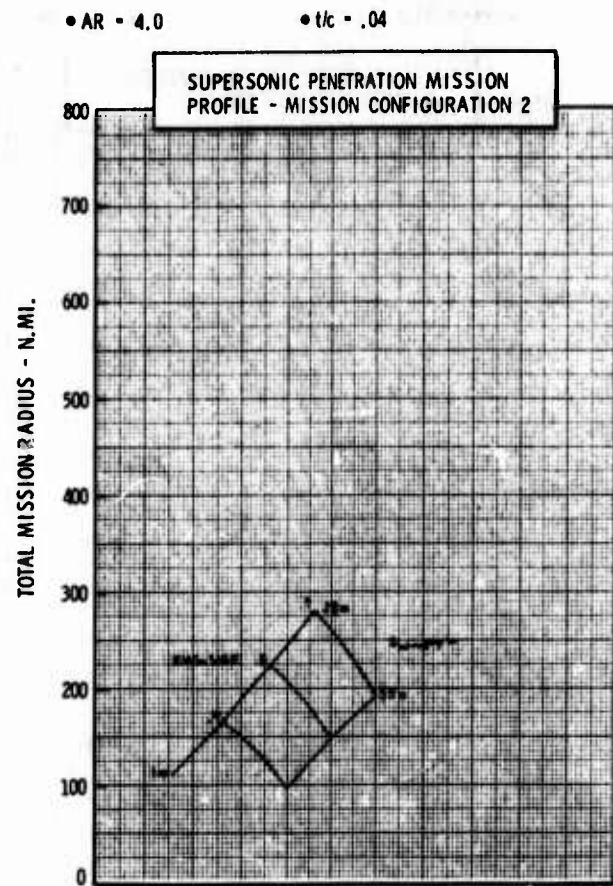
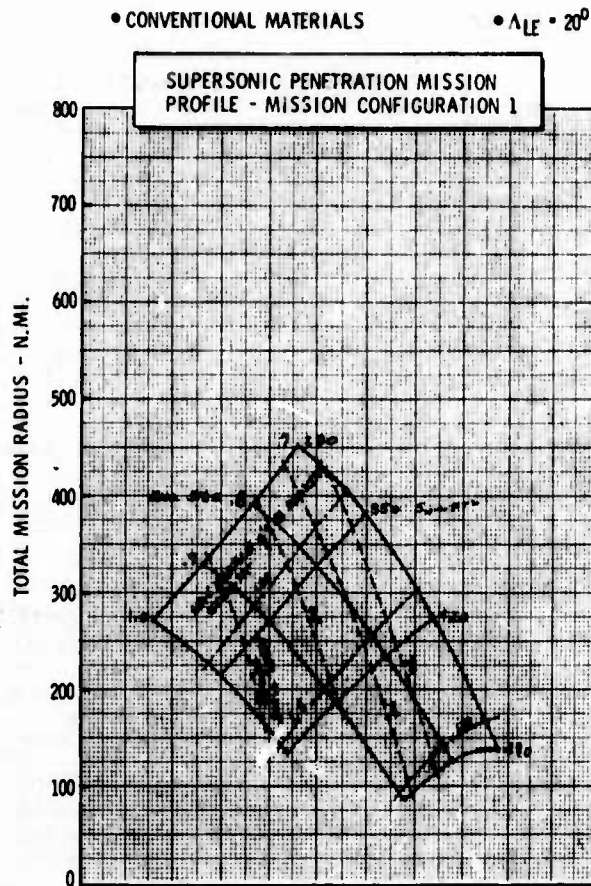
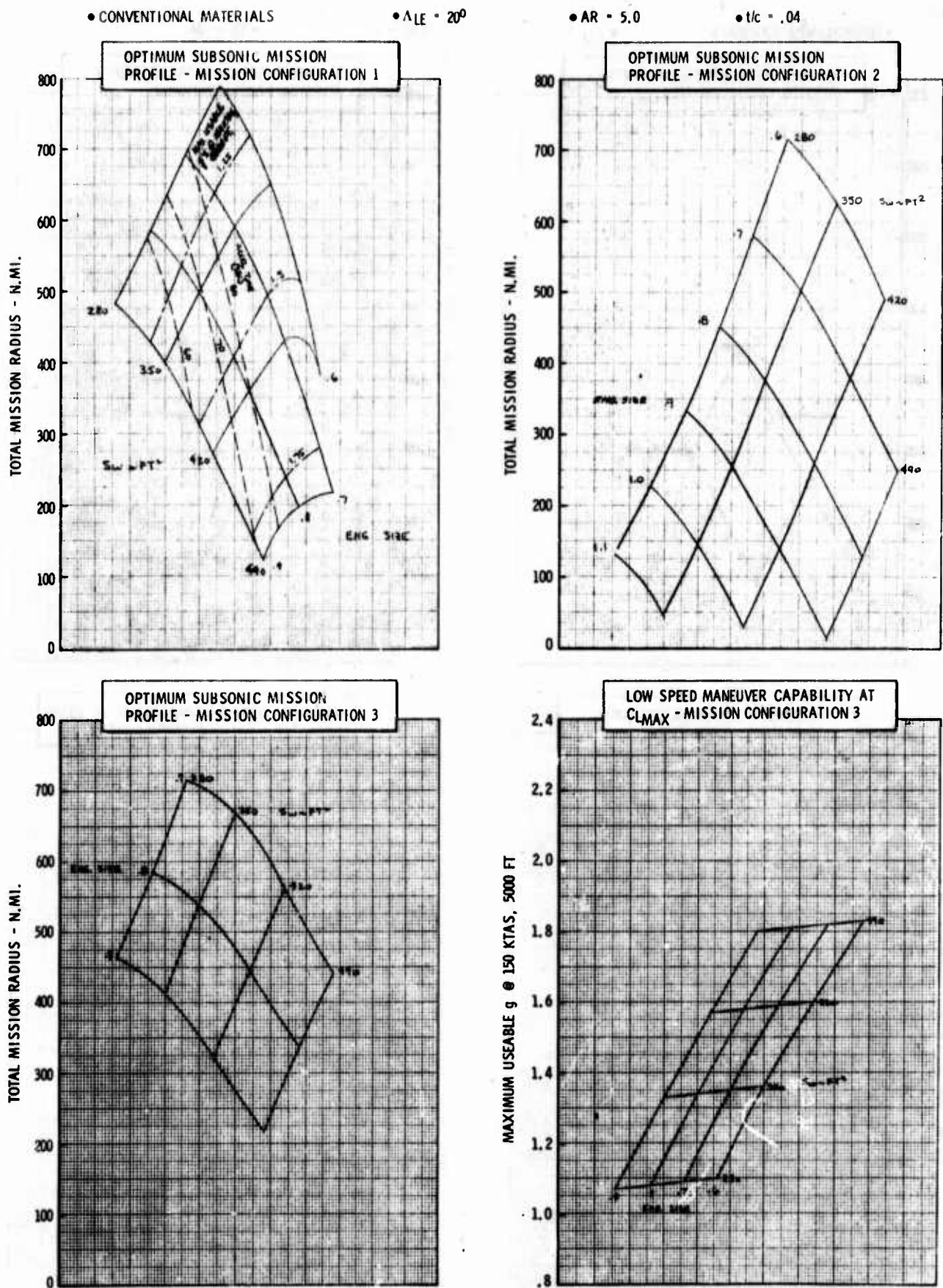
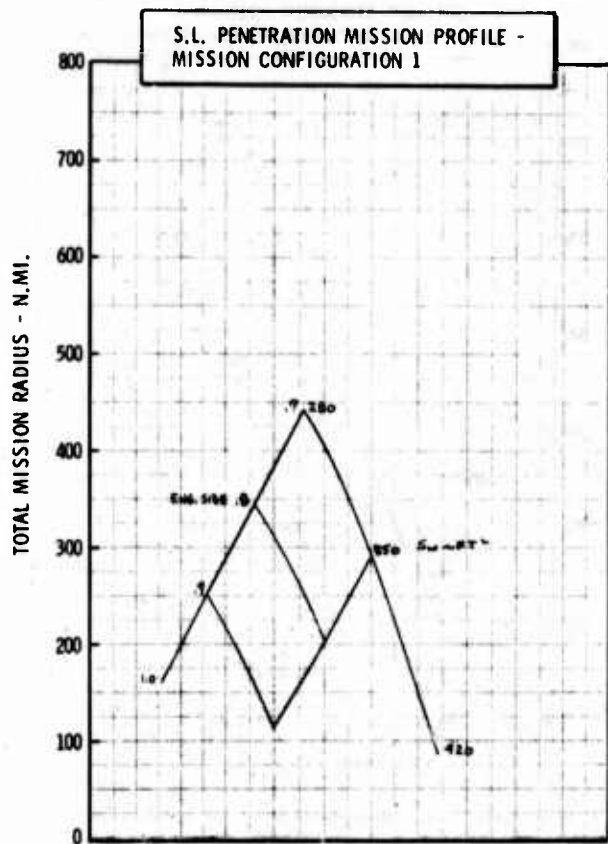


Figure H-3c LWA Mission/Configuration Tradeoff Parametric Data



• CONVENTIONAL MATERIALS

•  $\Delta LE = 20^\circ$



• AR = 5.0

•  $t/c = .04$

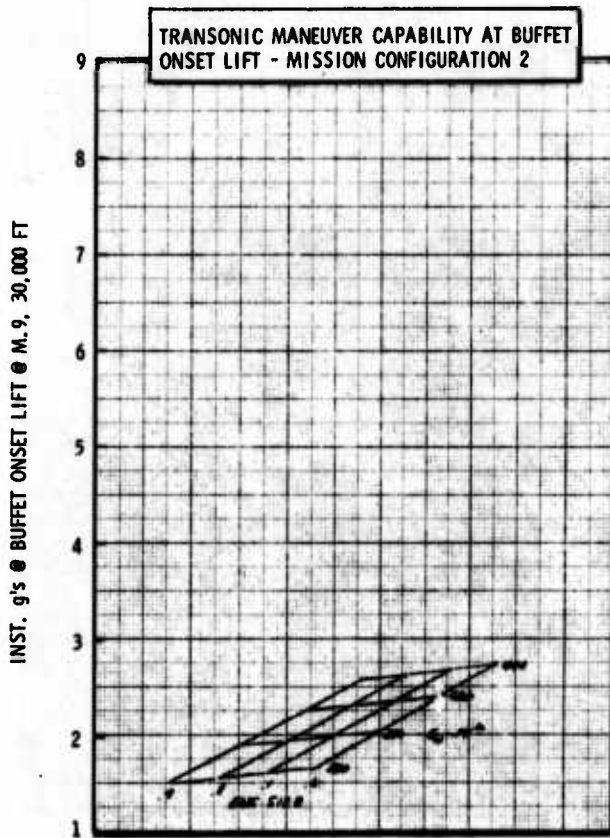
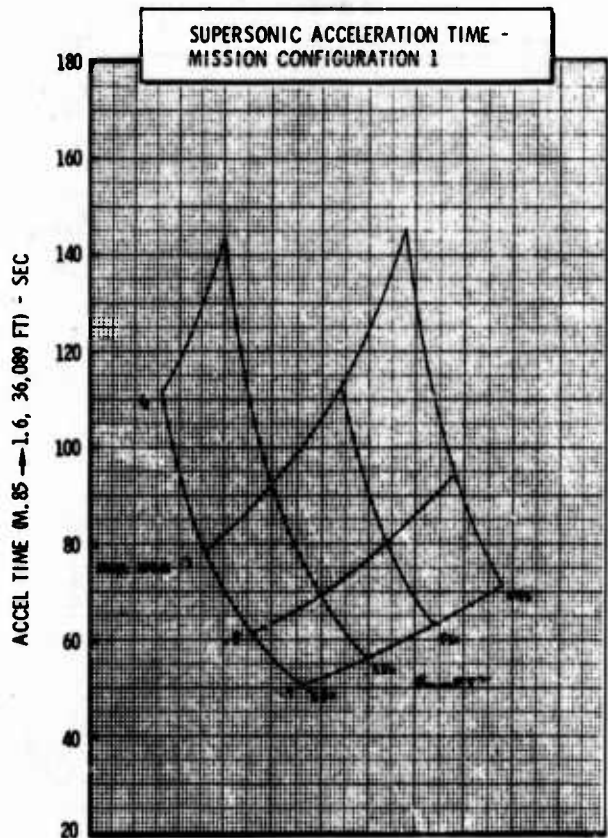
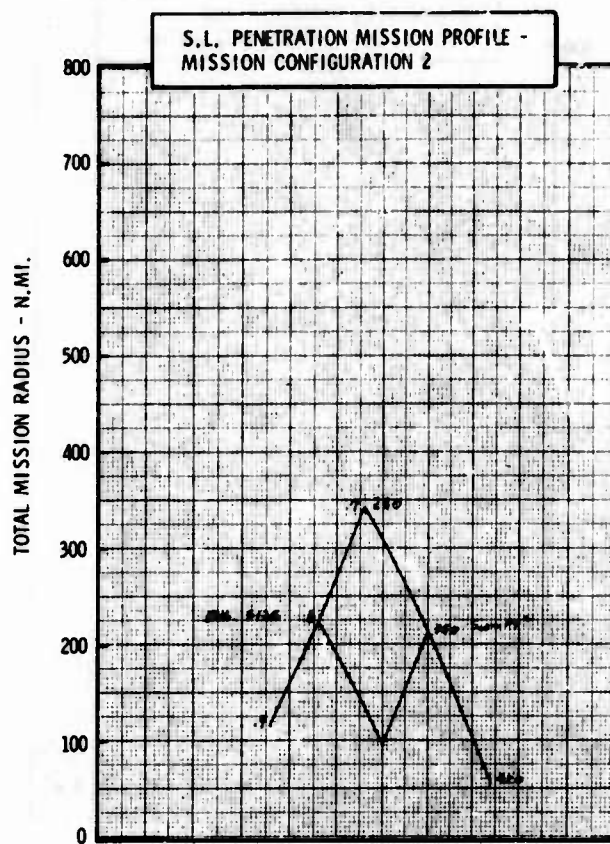


Figure H-4b LWA Mission/Configuration Tradeoff Parametric Data



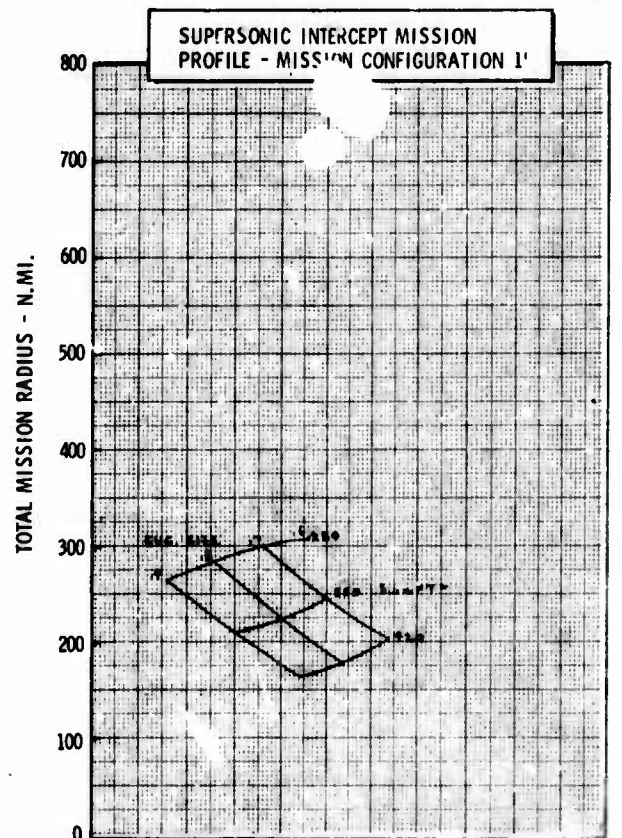
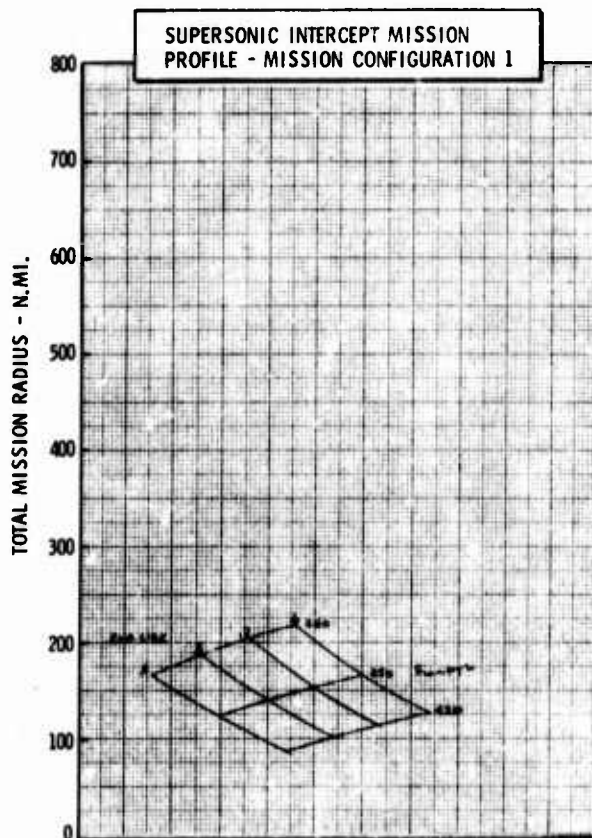
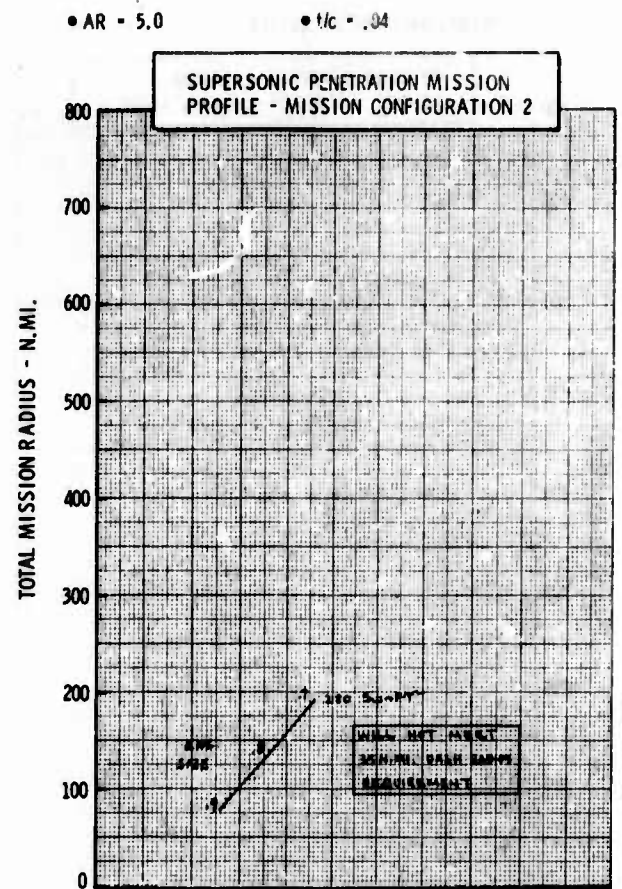
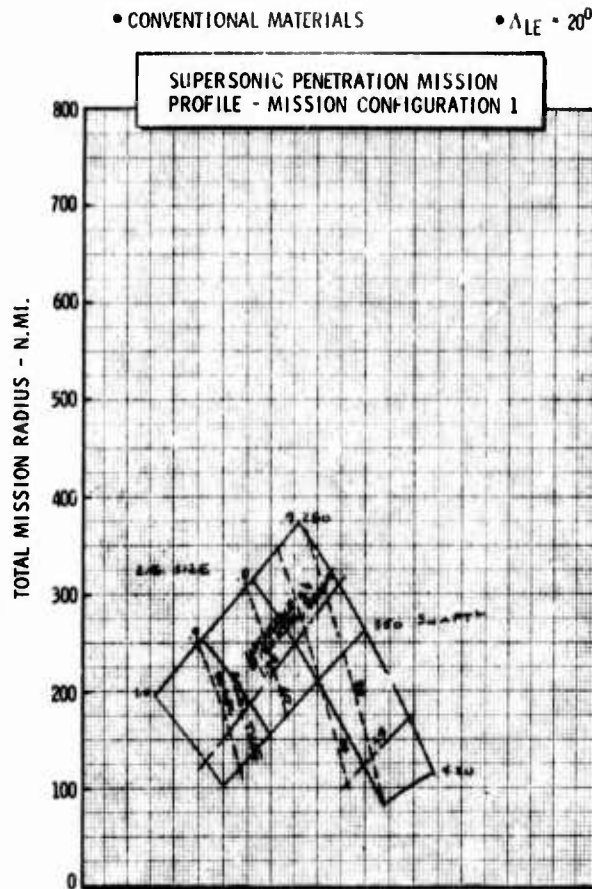


Figure H-4c LWA Mission/Configuration Tradeoff Parametric Data

• CONVENTIONAL MATERIALS

•  $\Delta LE = 30^\circ$

•  $AR = 3.0$

•  $t/c = .04$

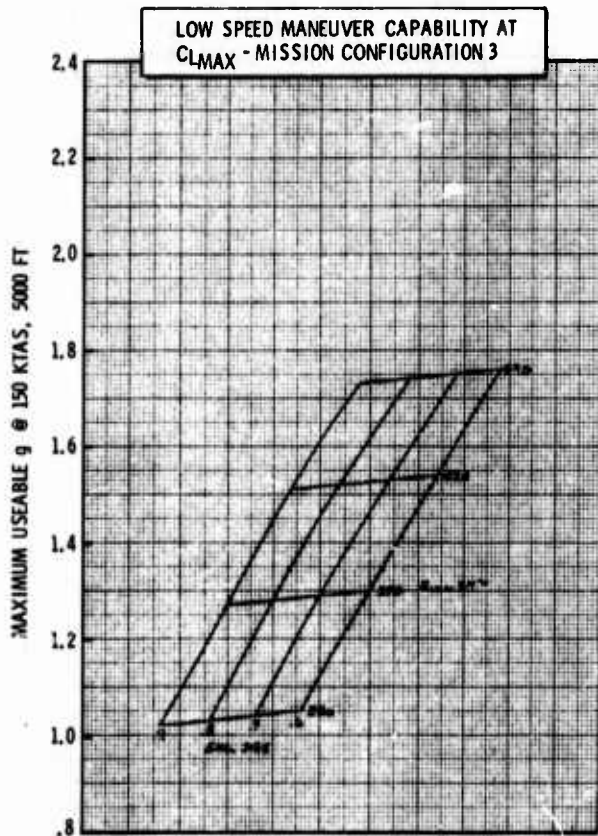
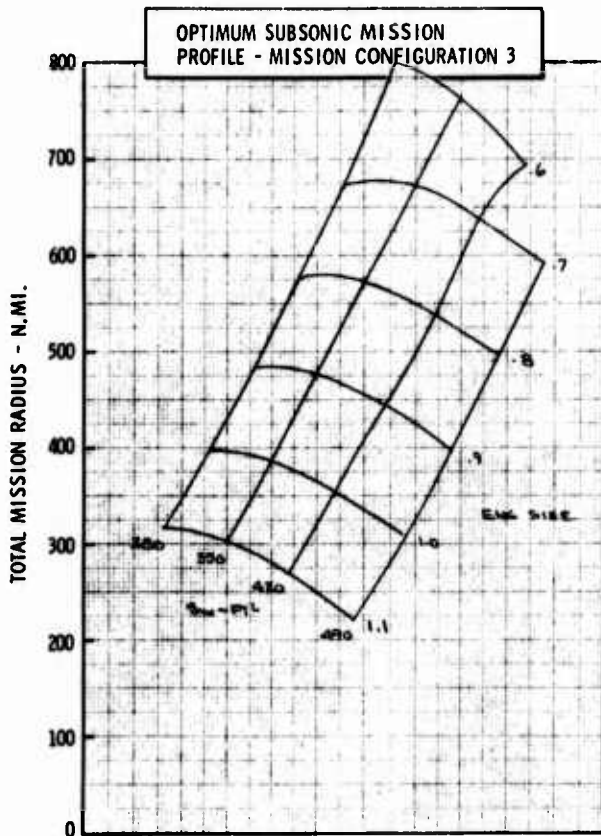
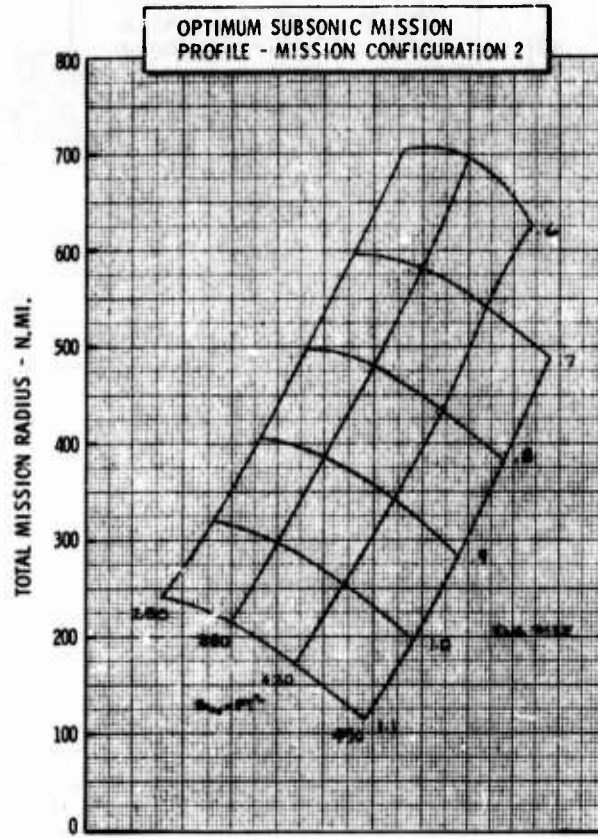
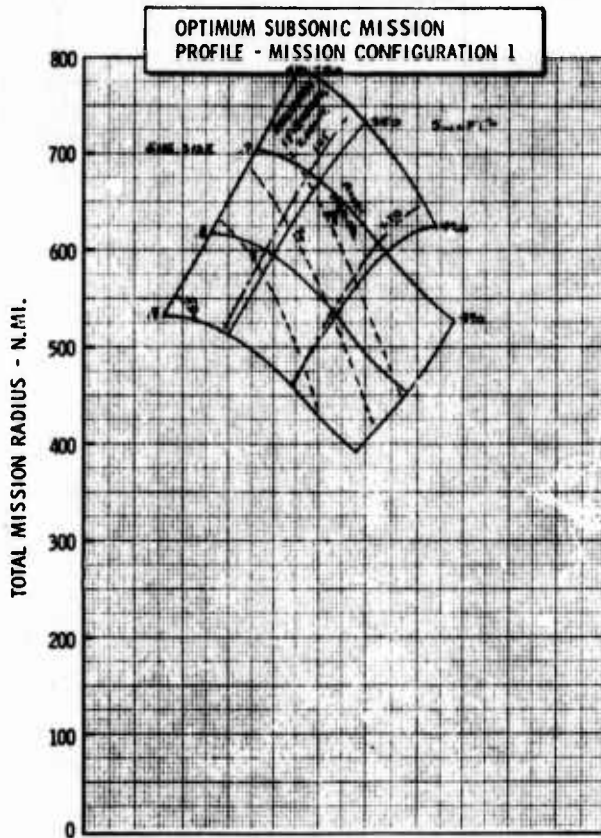


Figure H-5a LWA Mission/Configuration Tradeoff Parametric Data

• CONVENTIONAL MATERIALS

•  $\Delta LE = 30^\circ$

•  $AR = 3.0$

•  $t/c = .04$

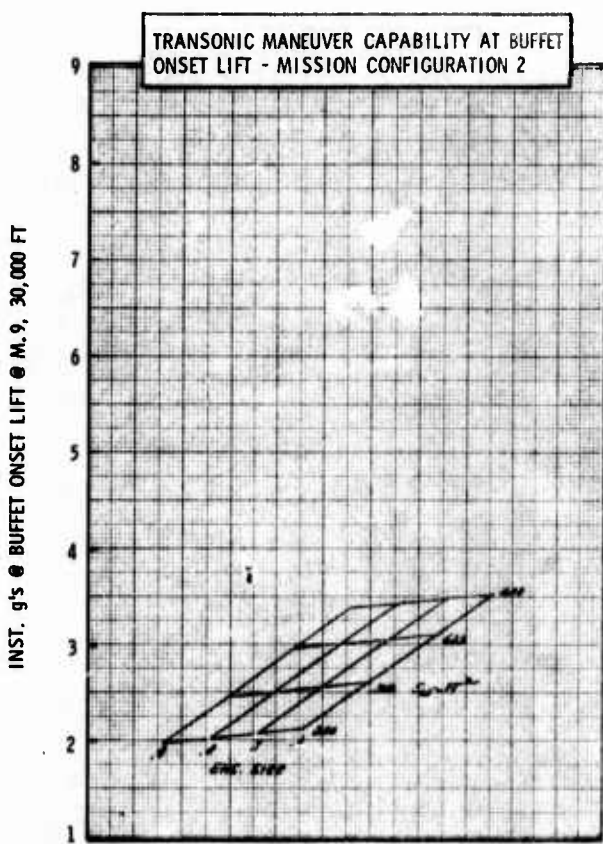
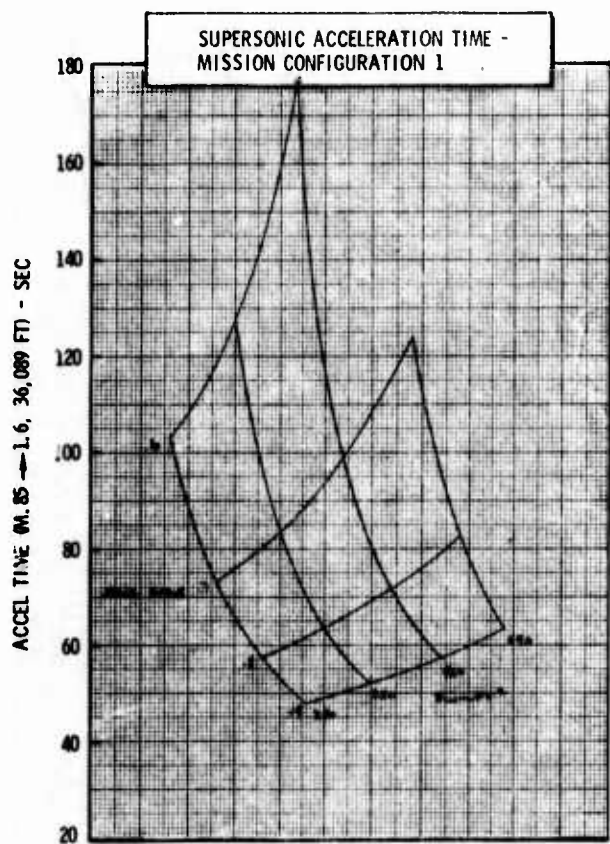
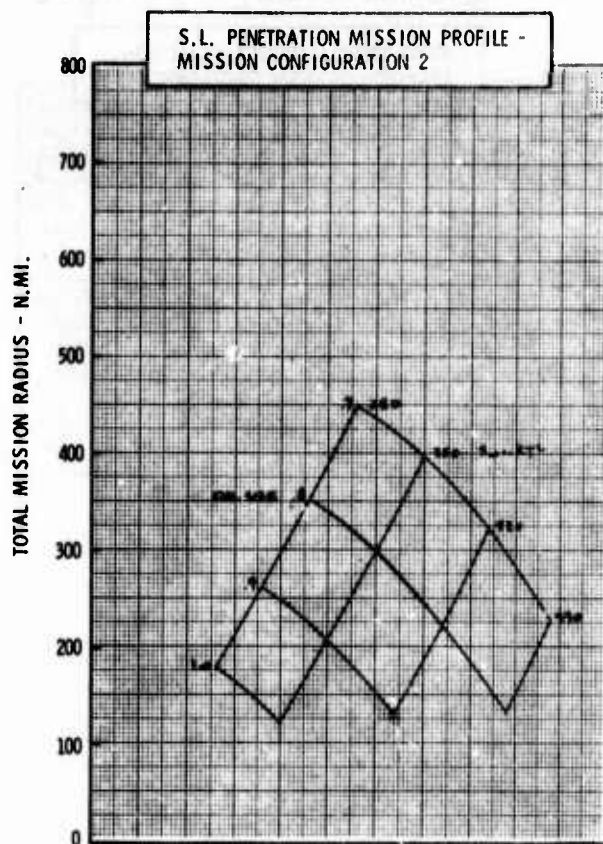
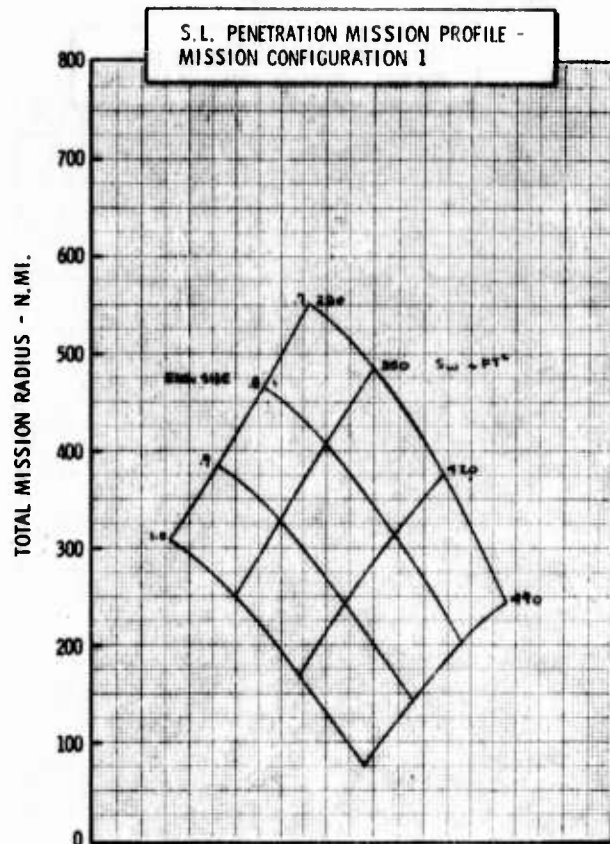


Figure H-5b LWA Mission/Configuration Tradeoff Parametric Data



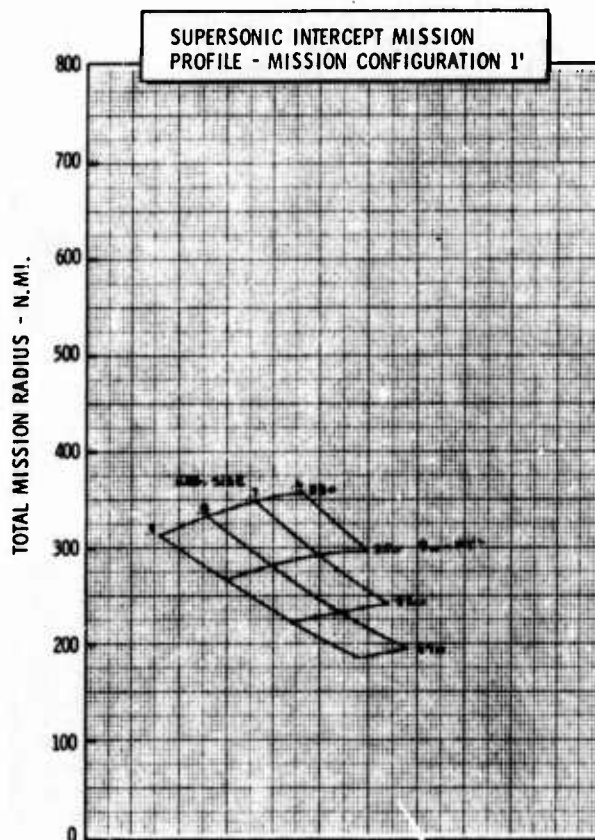
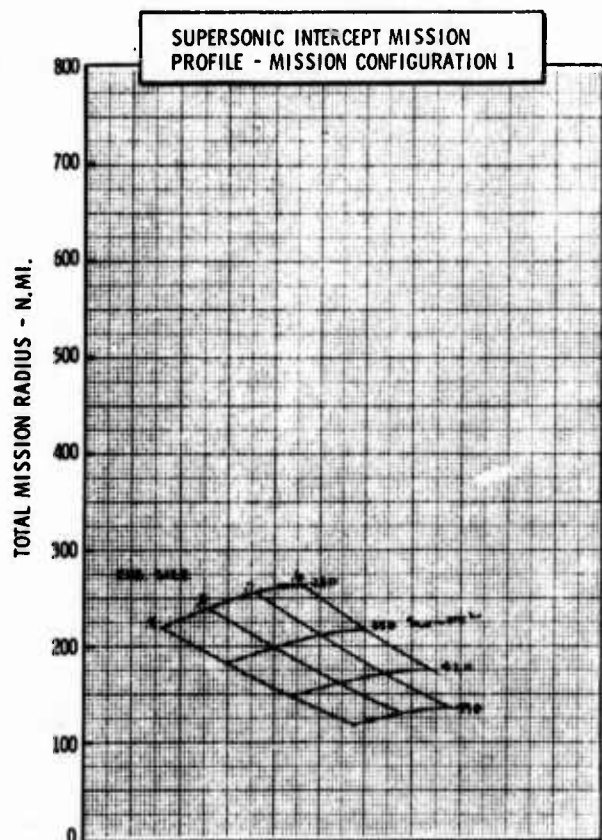
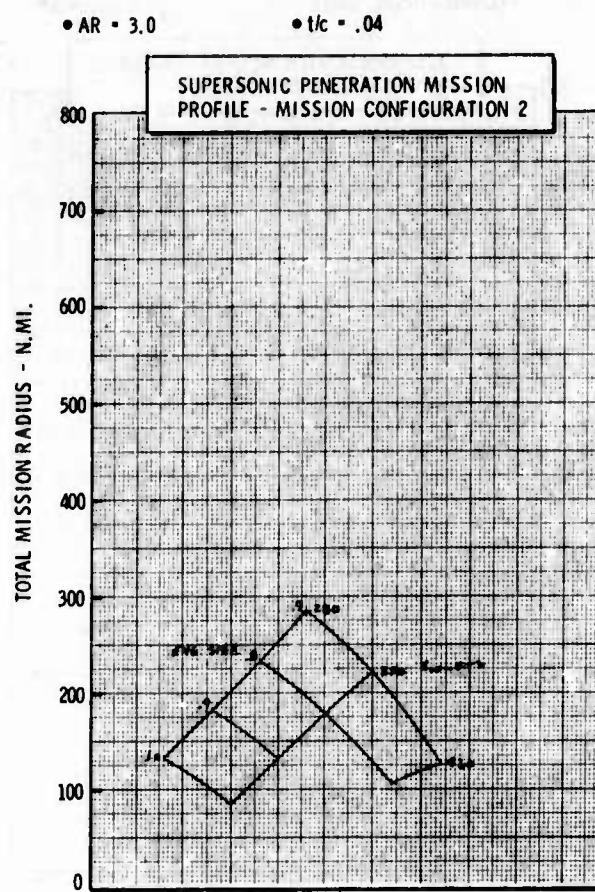
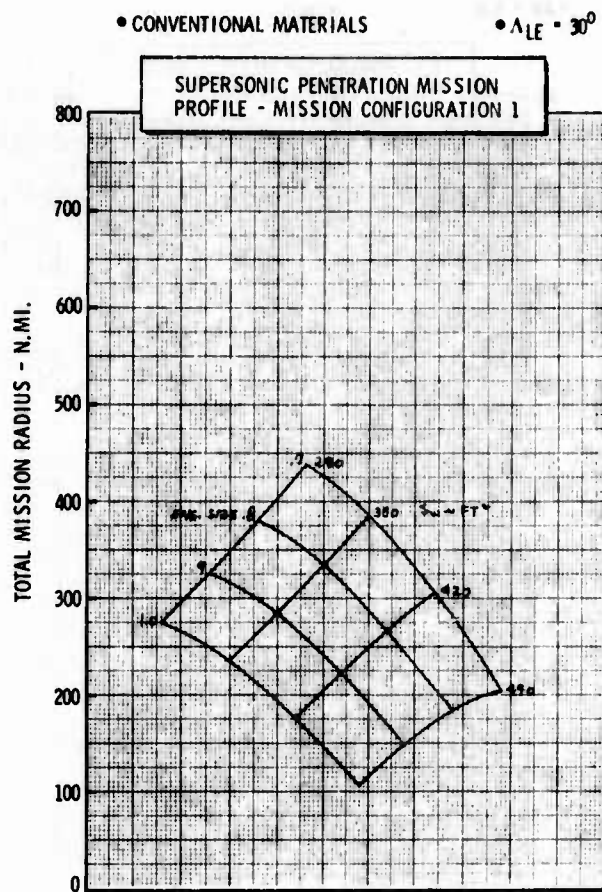


Figure H-5c LWA Mission/Configuration Tradeoff Parametric Data

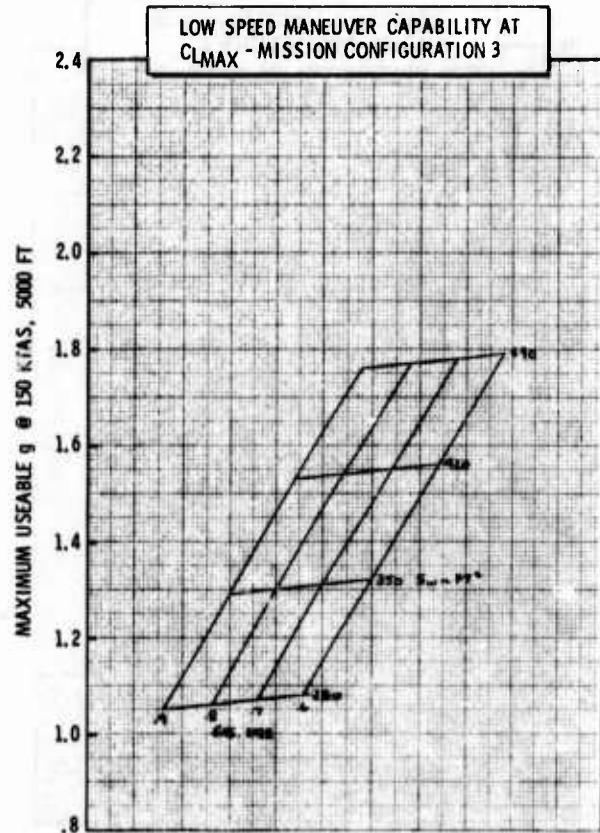
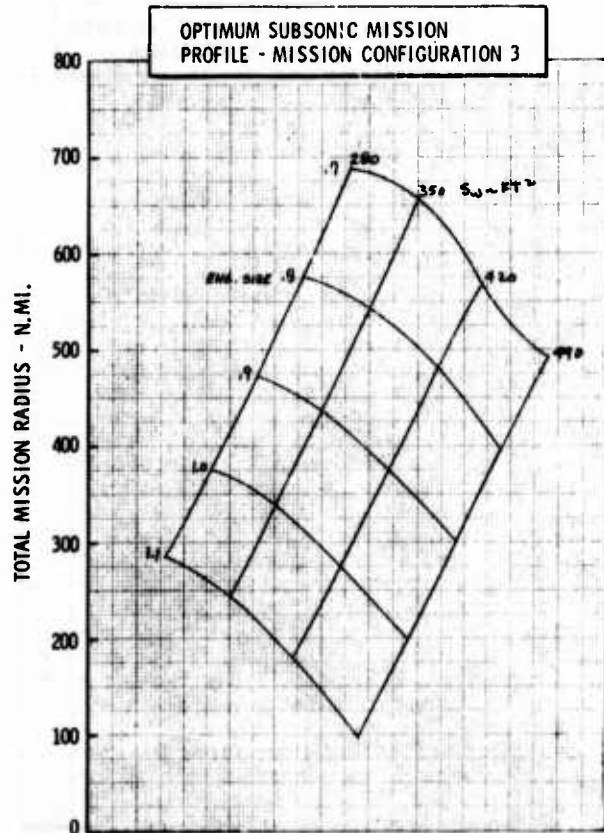
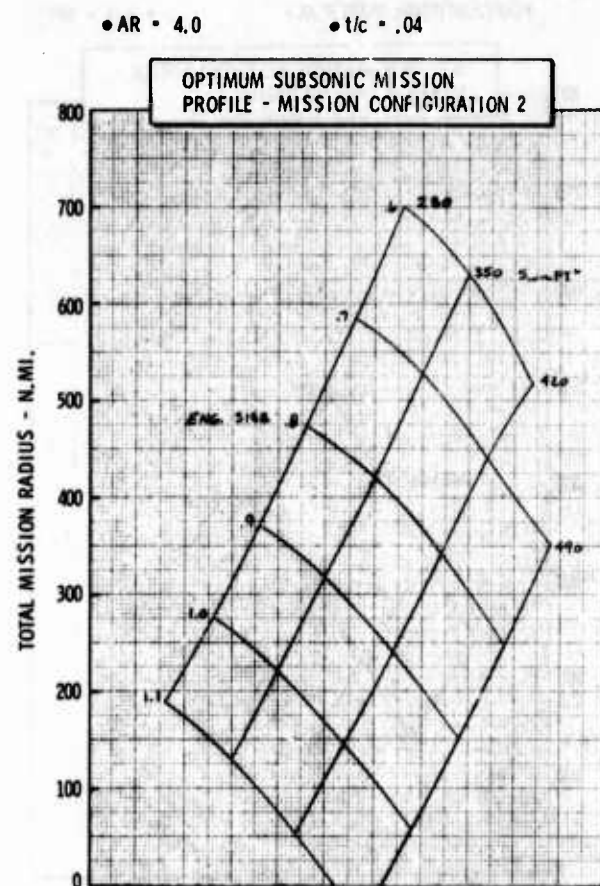
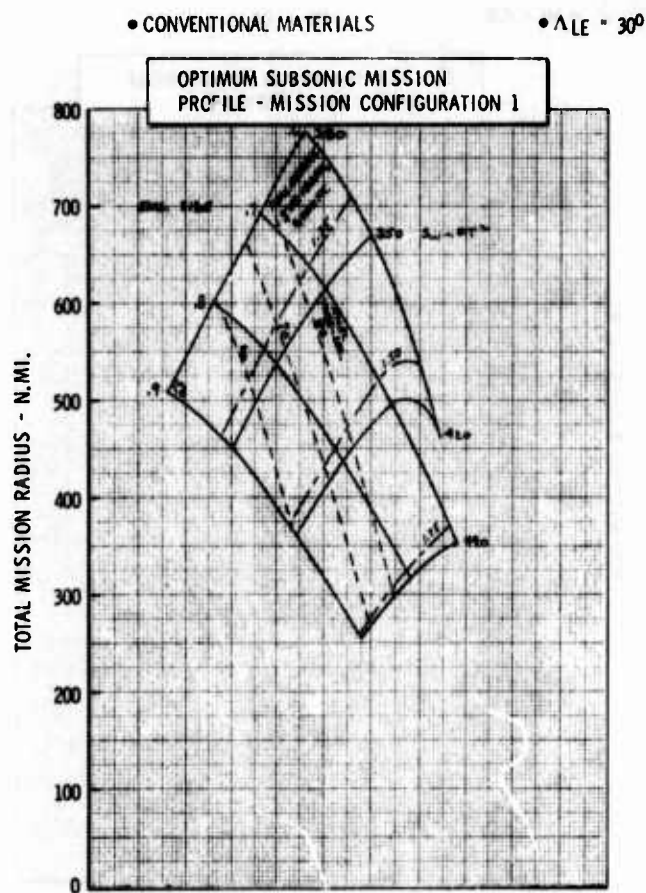


Figure H-6a LWA Mission/Configuration Tradeoff Parametric Data





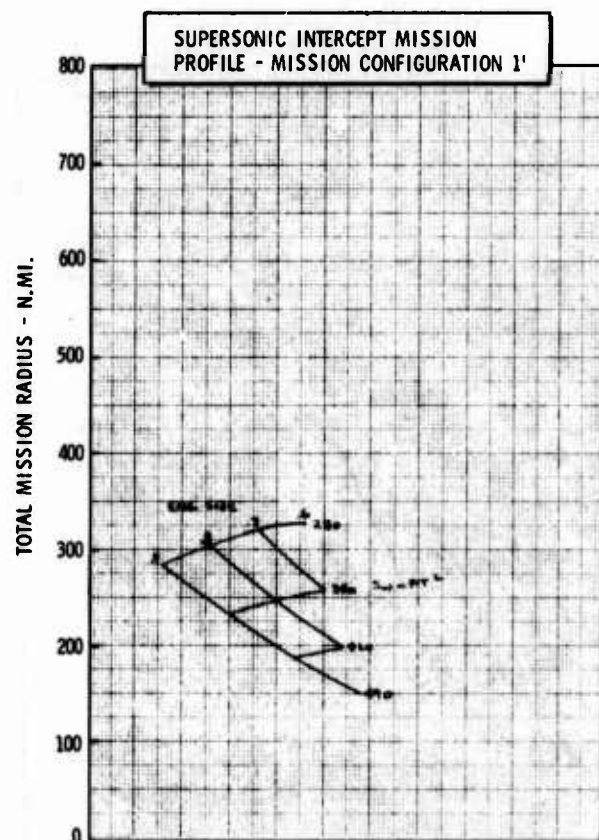
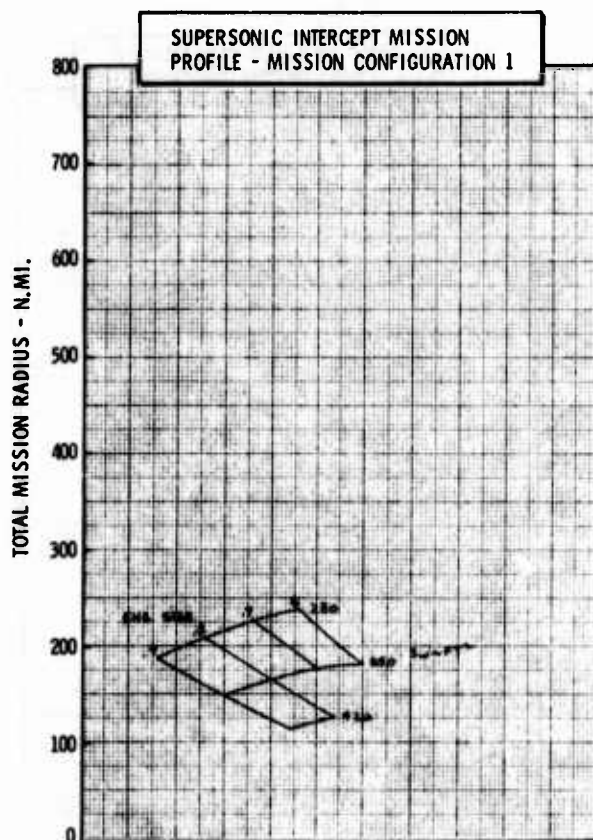
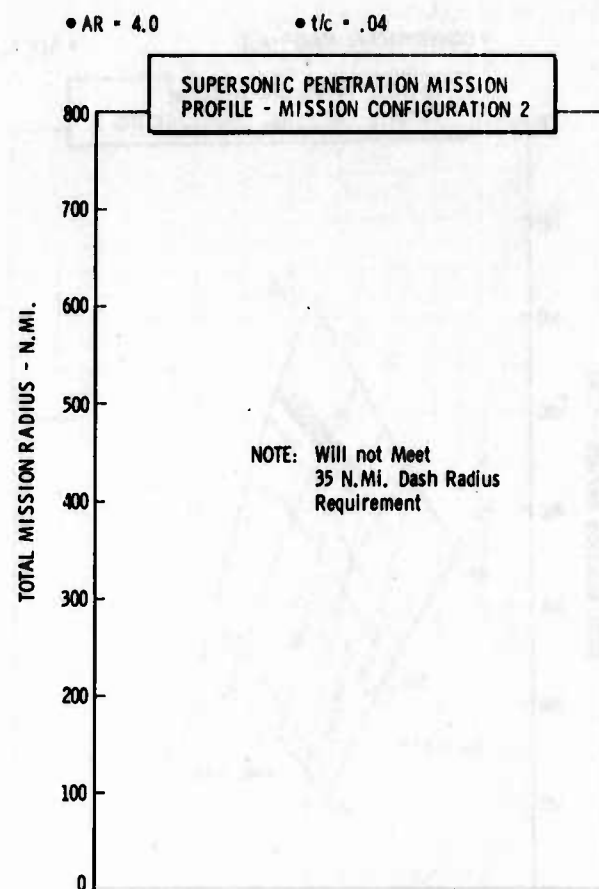
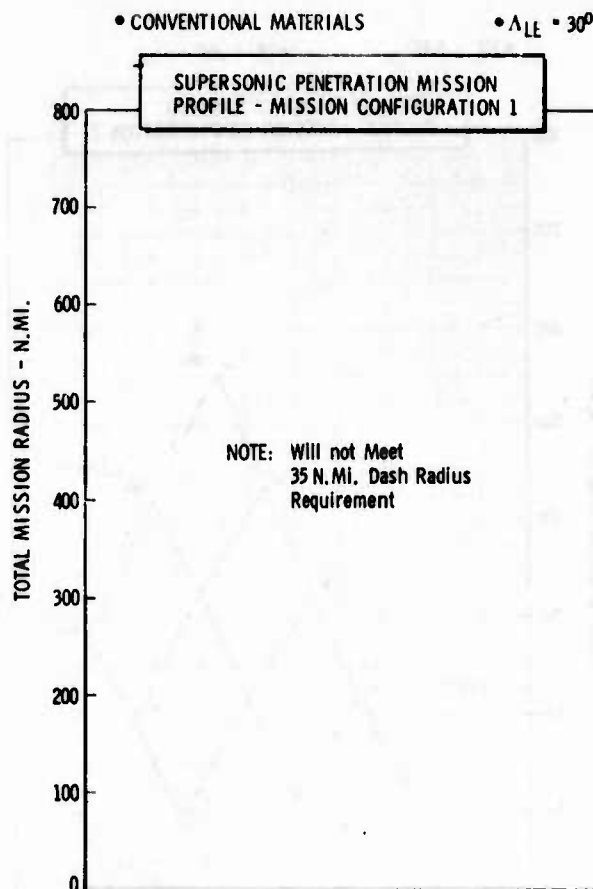


Figure H-6c LWA Mission/Configuration Tradeoff Parametric Data

• CONVENTIONAL MATERIALS

•  $\Delta L_F = 30^\circ$

•  $AR = 5.0$

•  $t/c = .04$

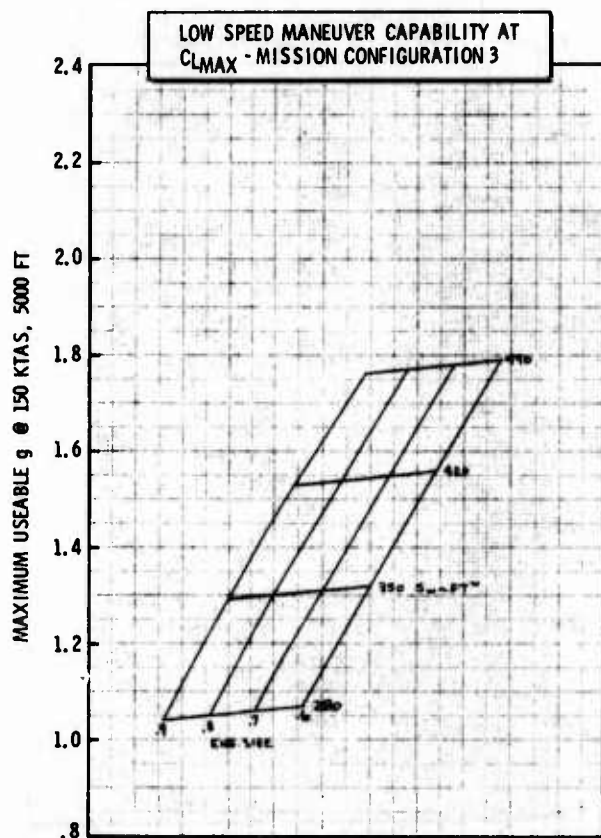
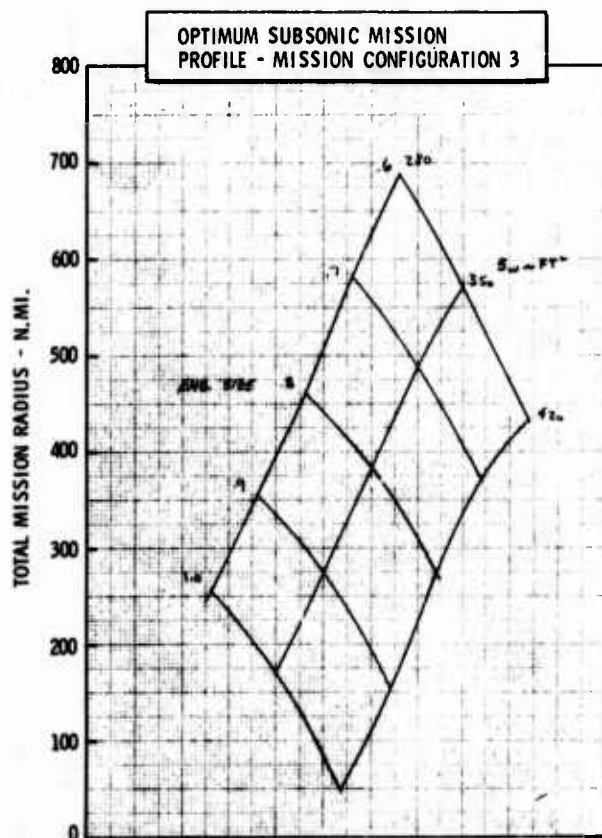
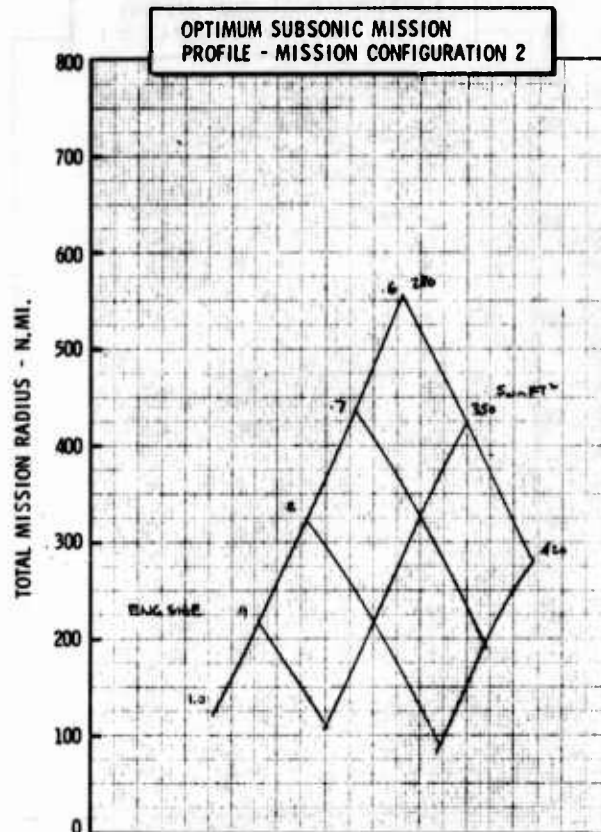
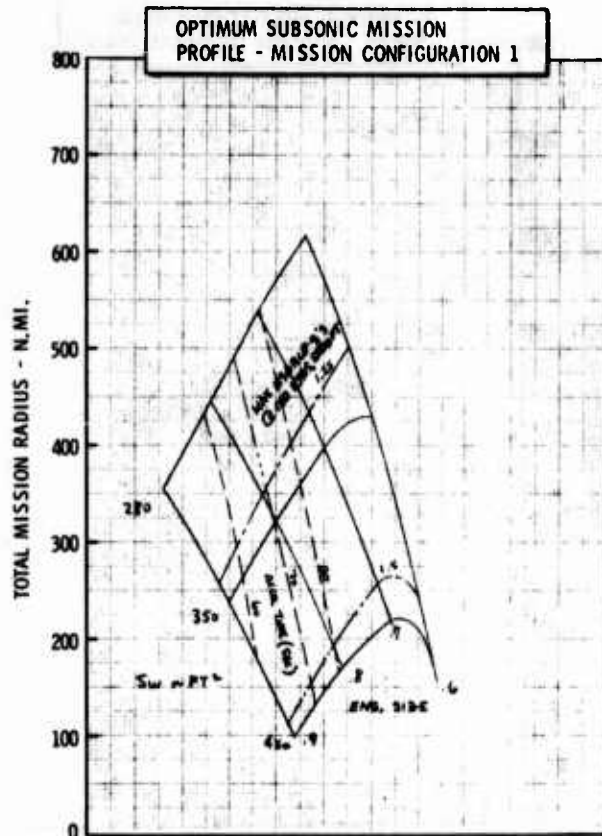


Figure H-7a LWA Mission/Configuration Tradeoff Parametric Data

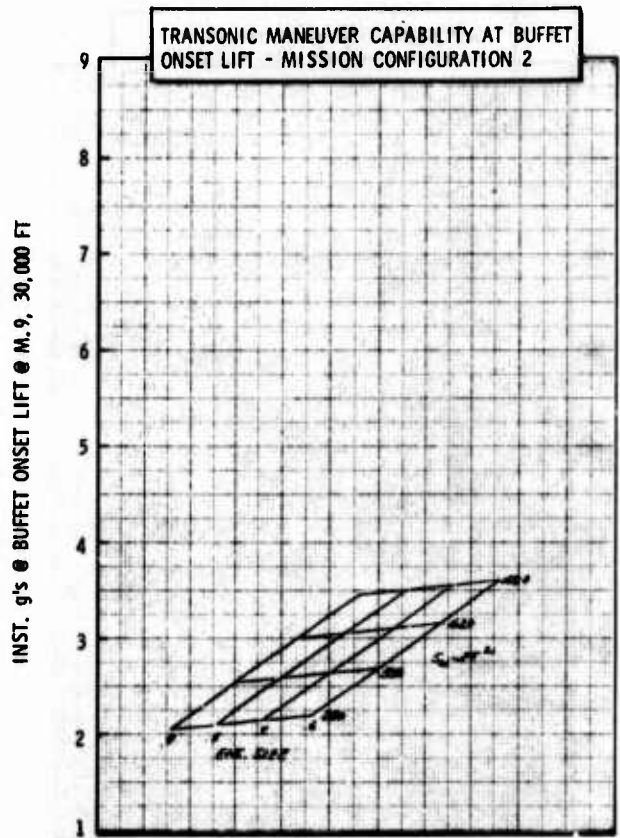
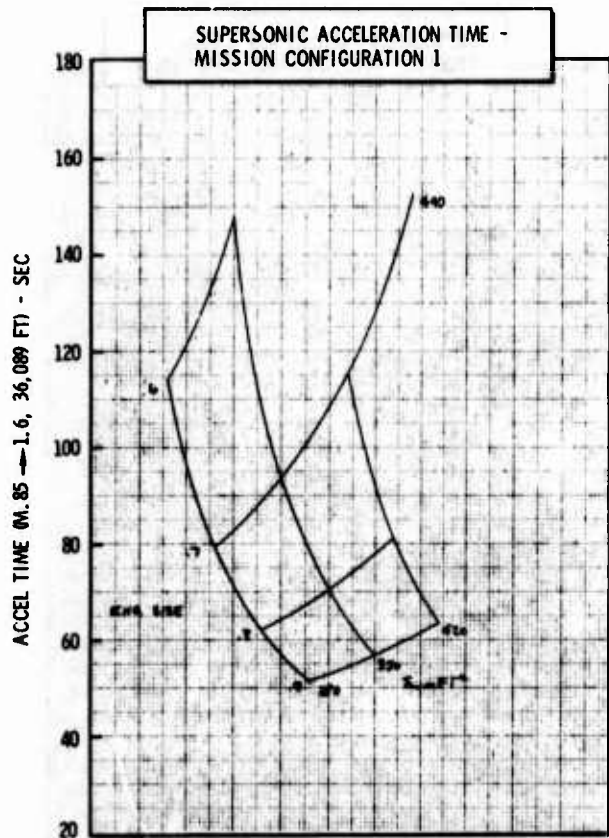
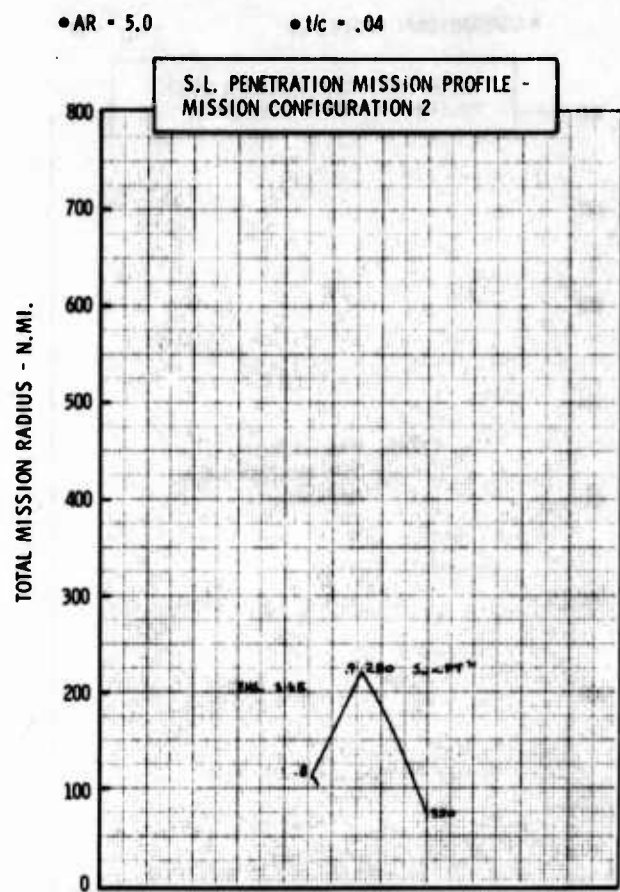
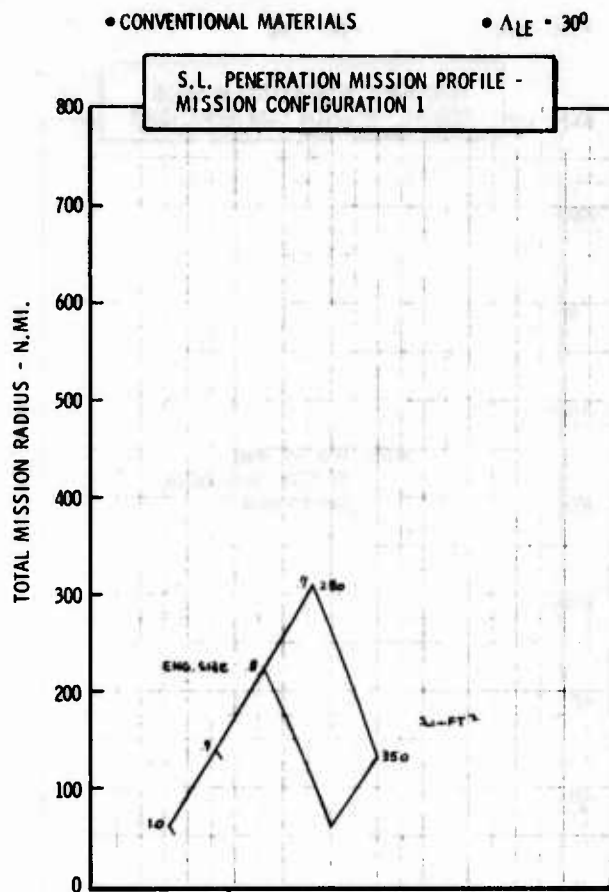


Figure H-7b LWA Mission/Configuration Tradeoff Parametric Data



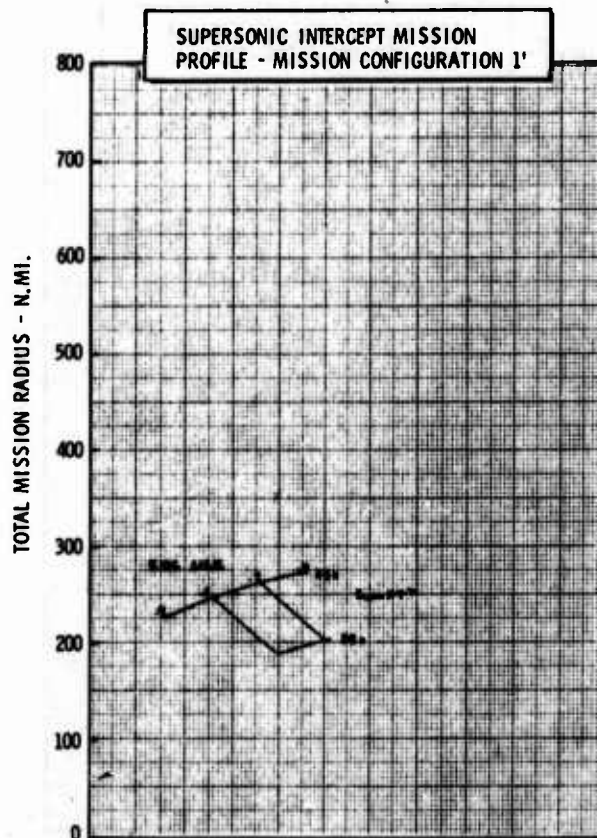
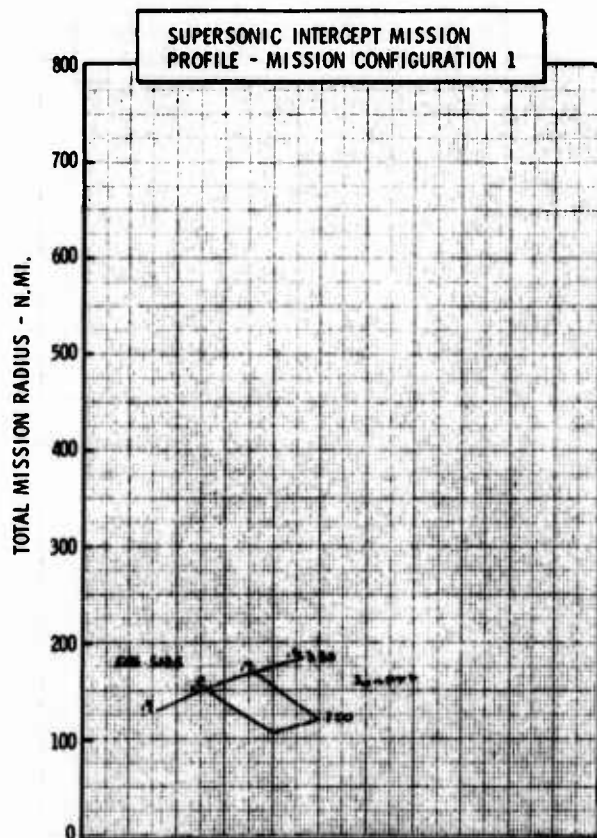
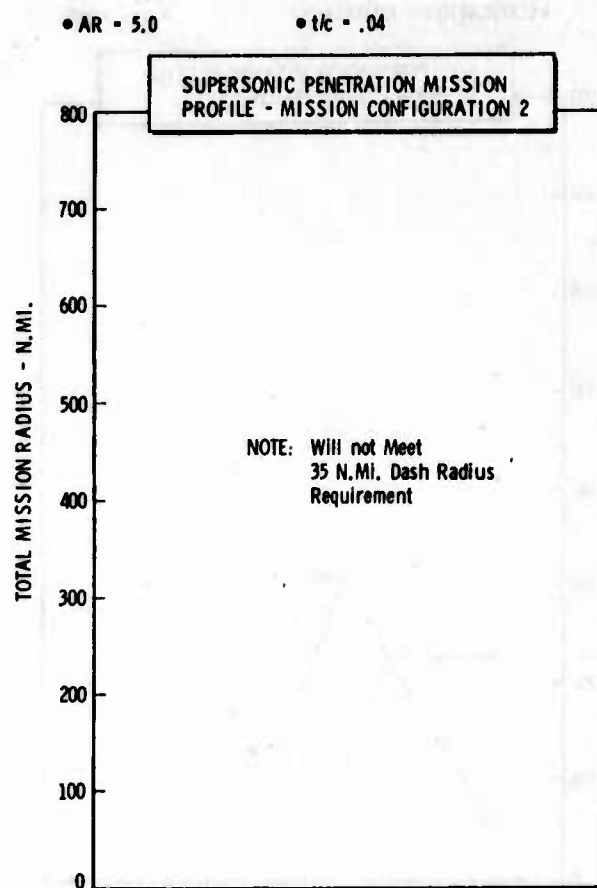
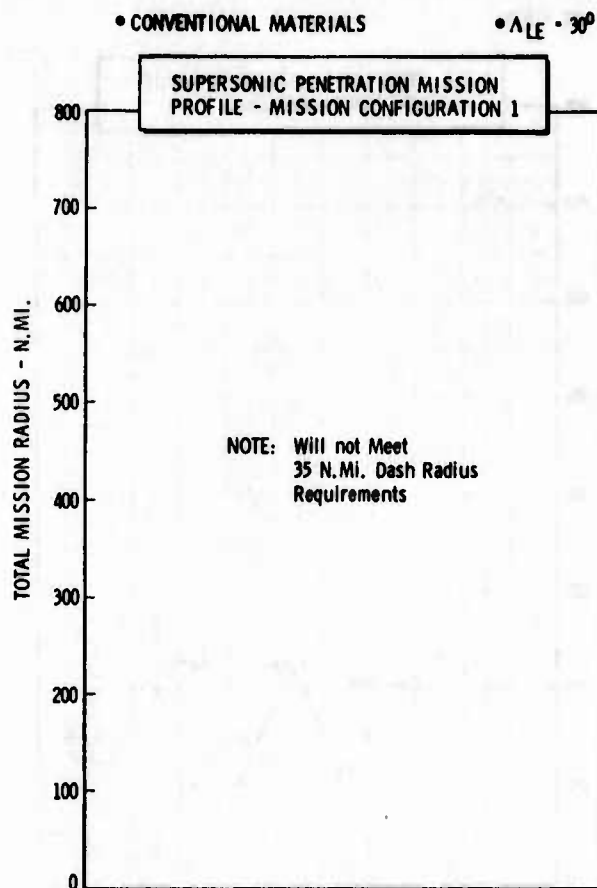


Figure H-7c LWA Mission/Configuration Tradeoff Parametric Data

• CONVENTIONAL MATERIALS

•  $\Delta LE = 40^\circ$

•  $AR = 3.0$

•  $t/c = .04$

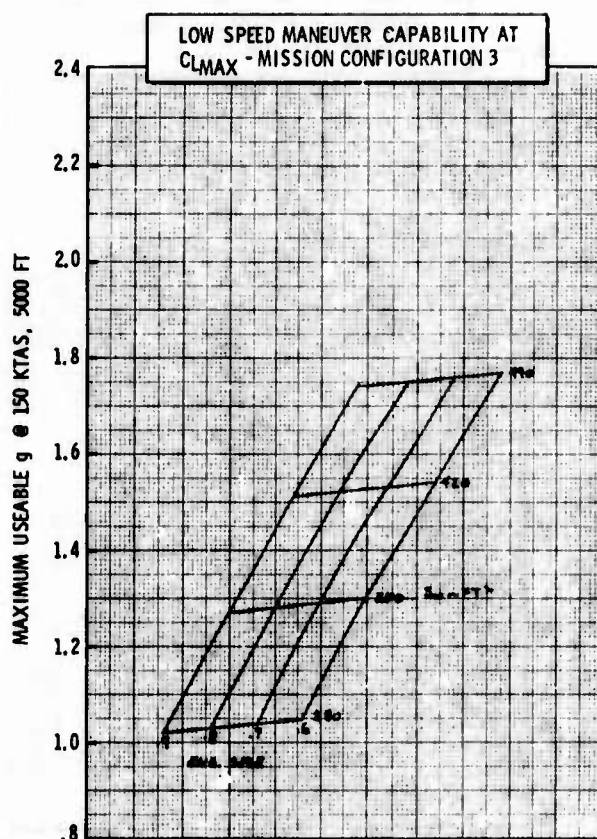
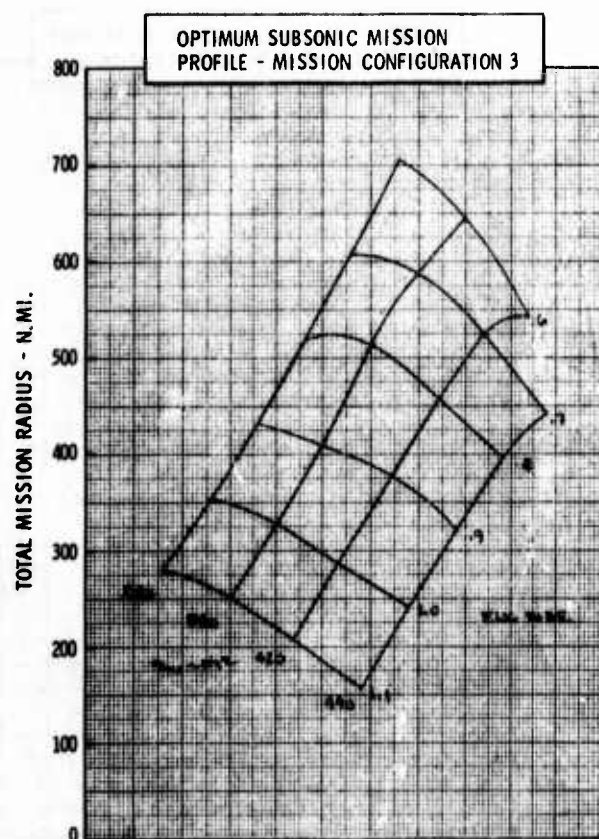
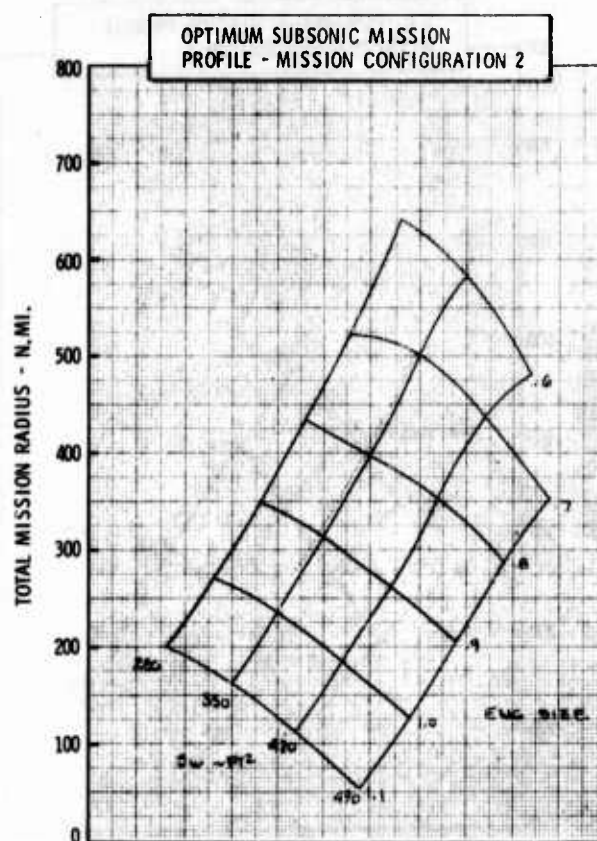
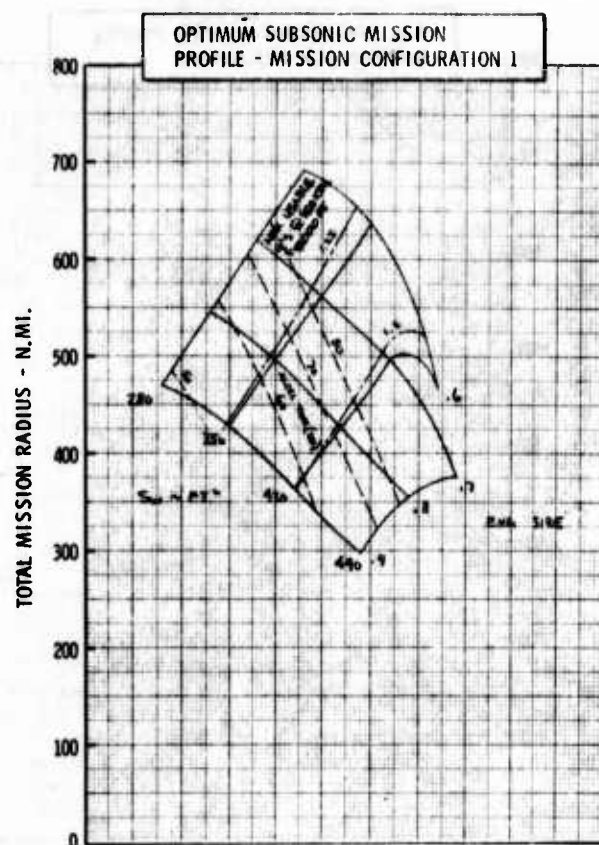


Figure H-8a LWA Mission/Configuration Tradeoff Parametric Data

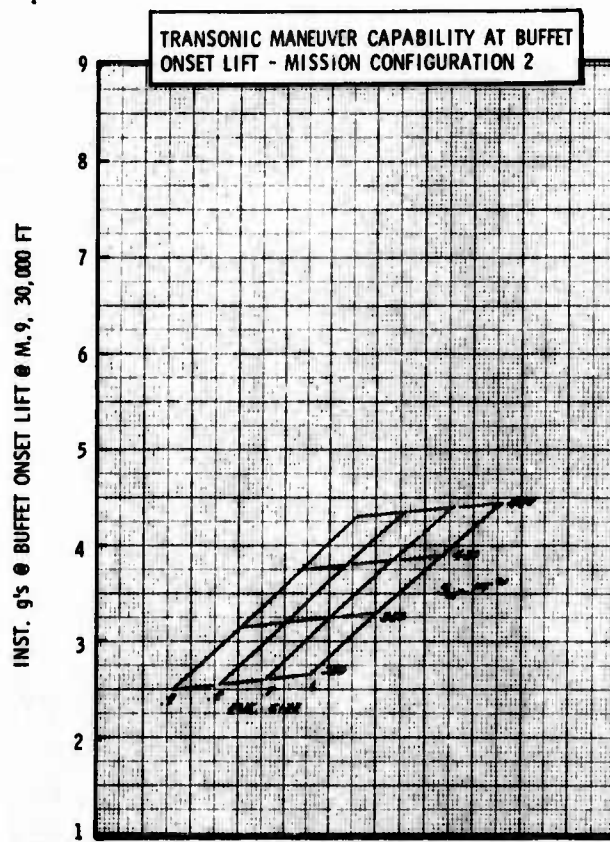
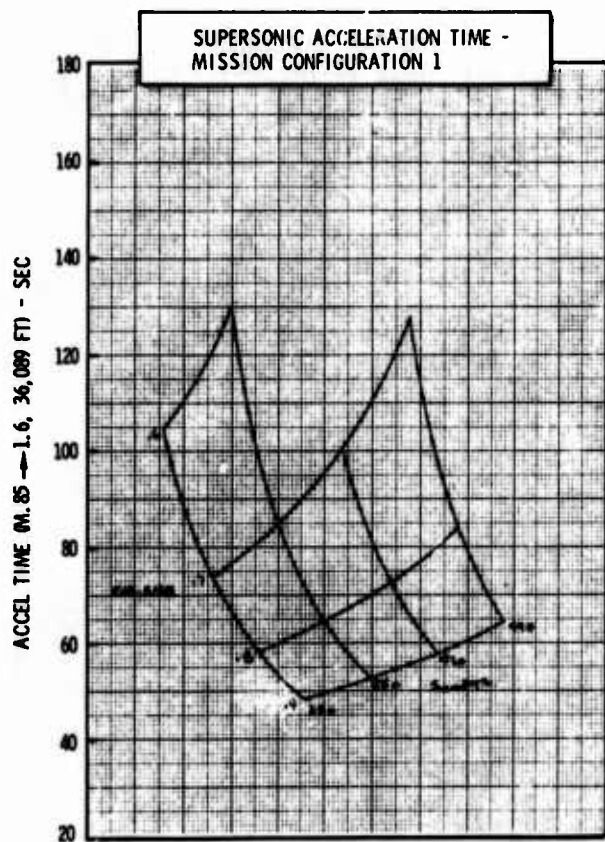
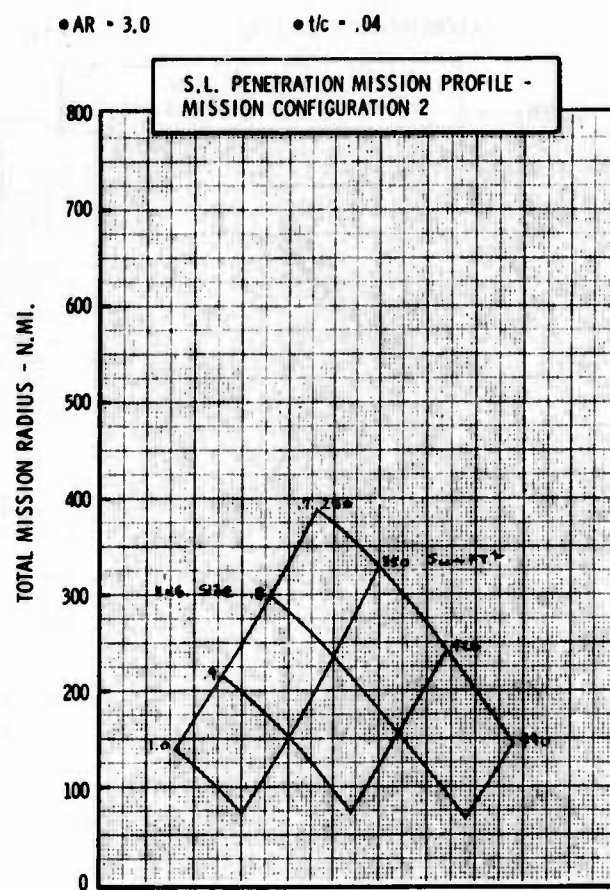
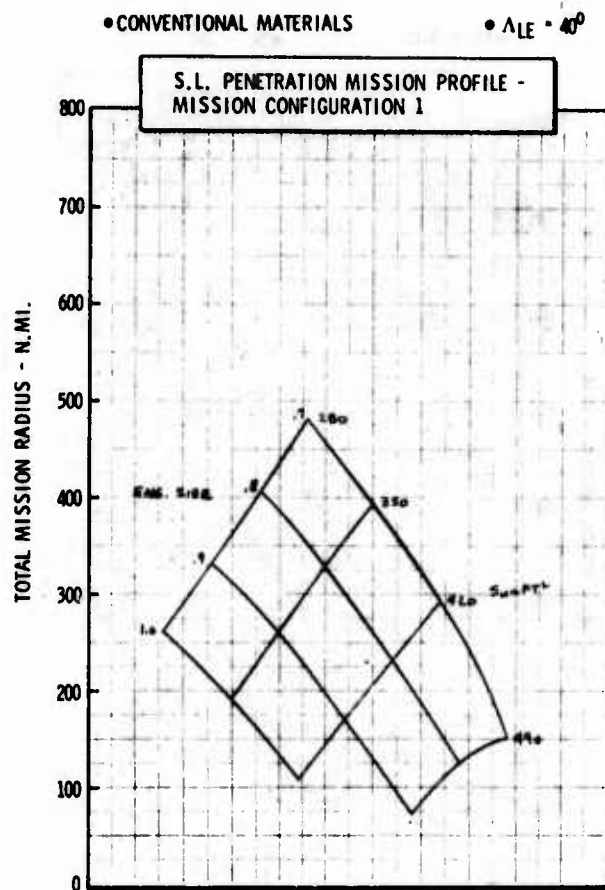


Figure H-8b LWA Mission/Configuration Tradeoff Parametric Data

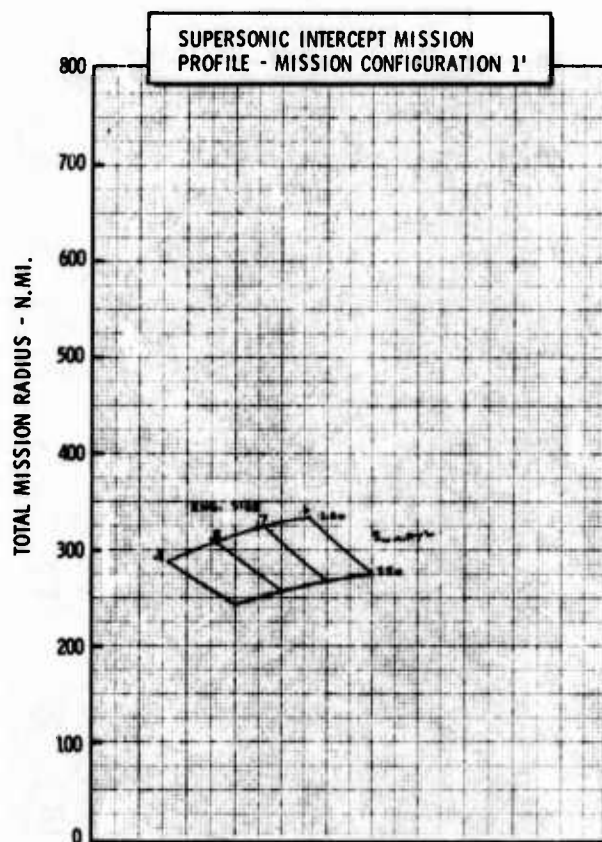
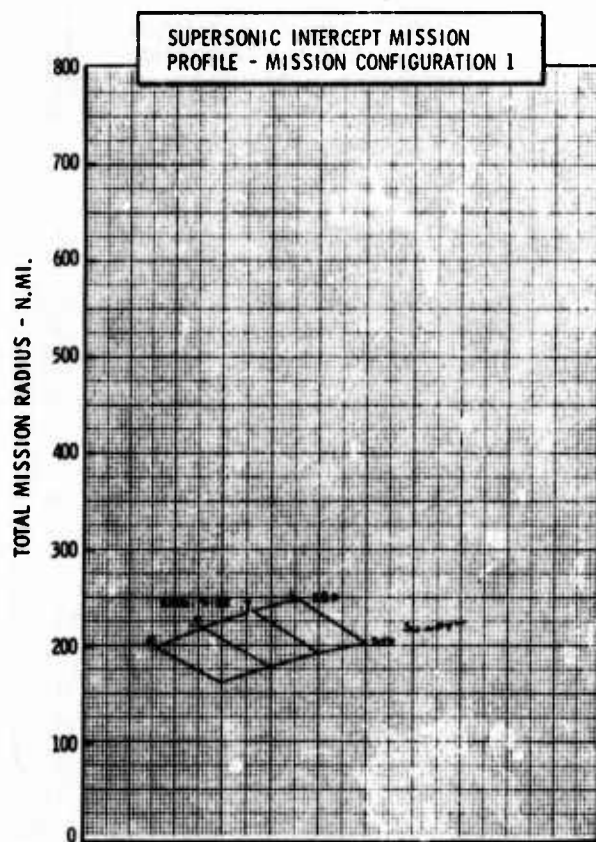
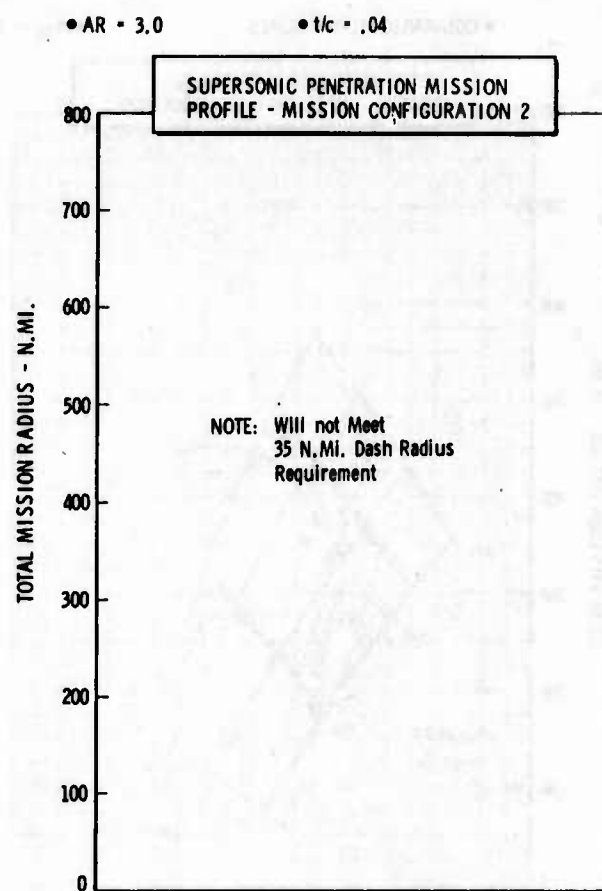
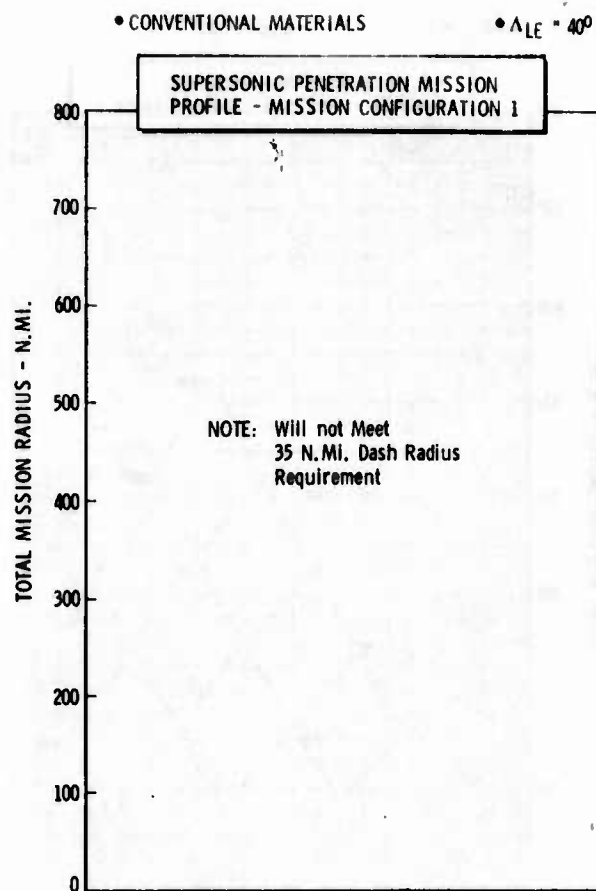


Figure H-8c LWA Mission/Configuration Tradeoff Parametric Data



• CONVENTIONAL MATERIALS

•  $\Lambda_{LE} = 40^\circ$

•  $AR = 4.0$

•  $t/c = .04$

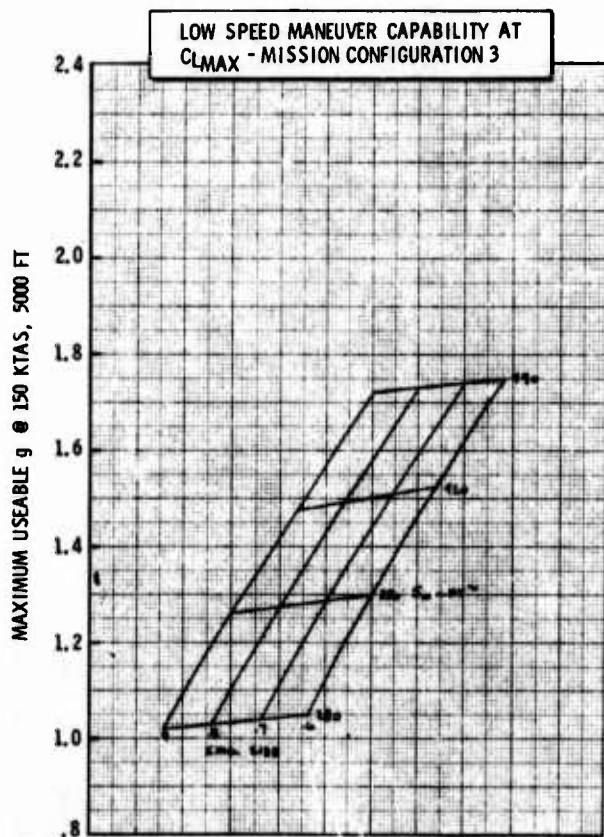
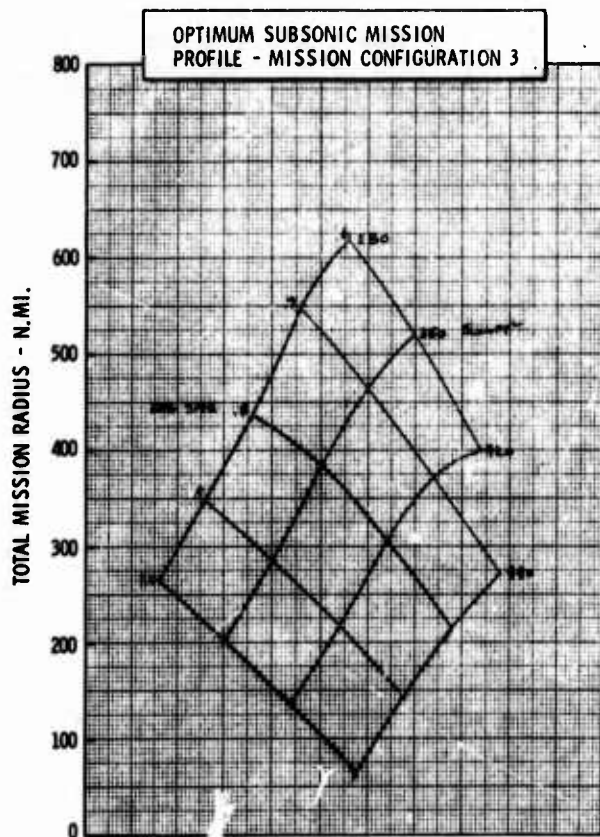
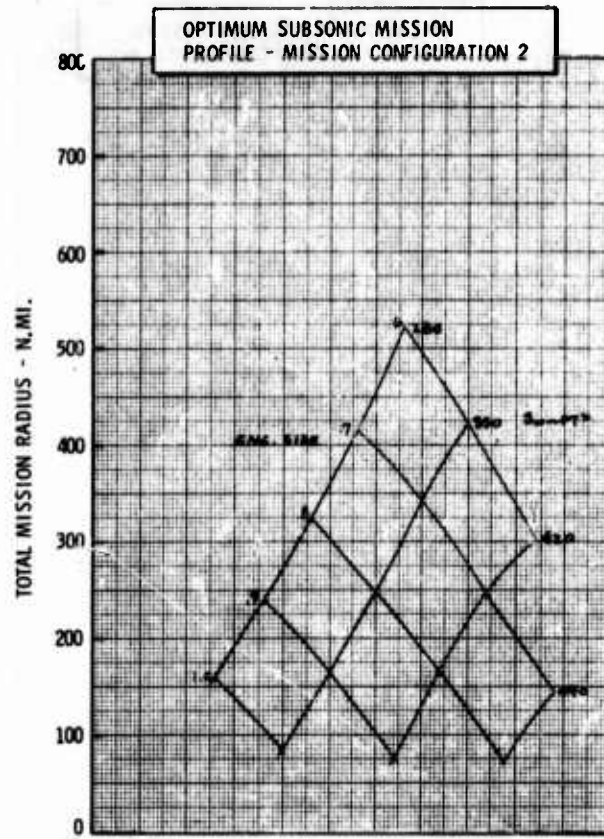
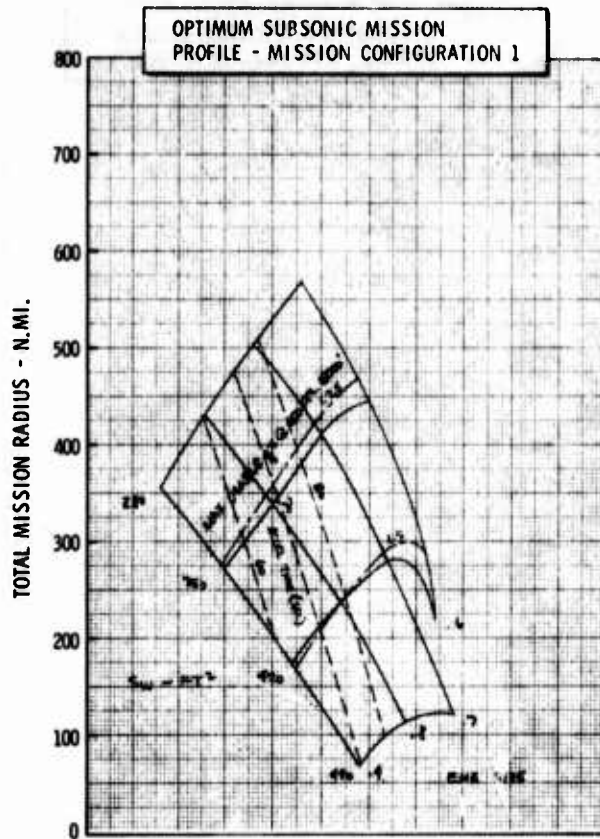


Figure H-9a LWA Mission/Configuration Tradeoff Parametric Data

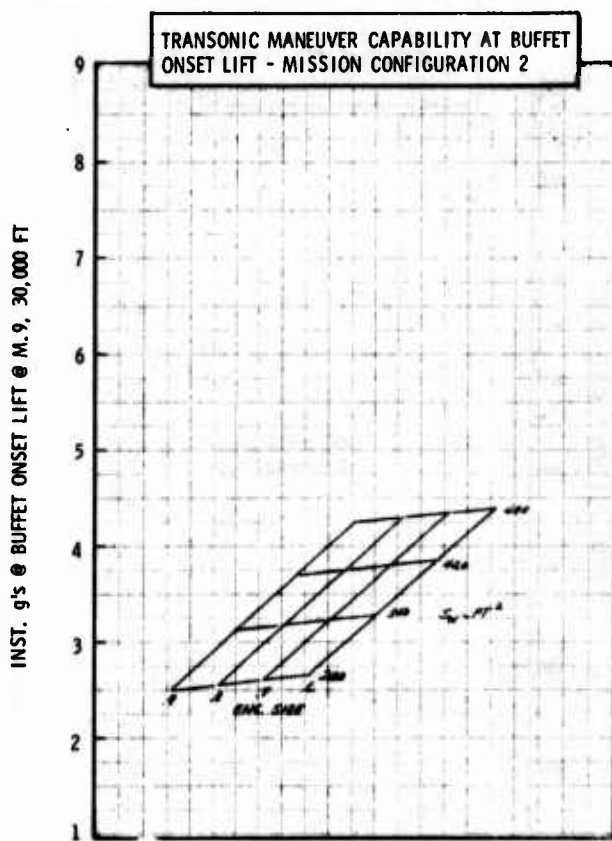
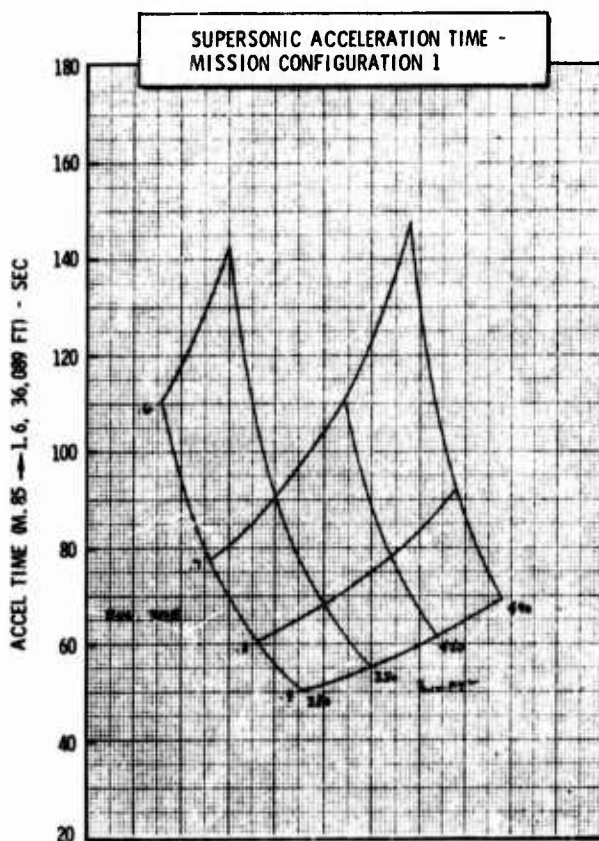
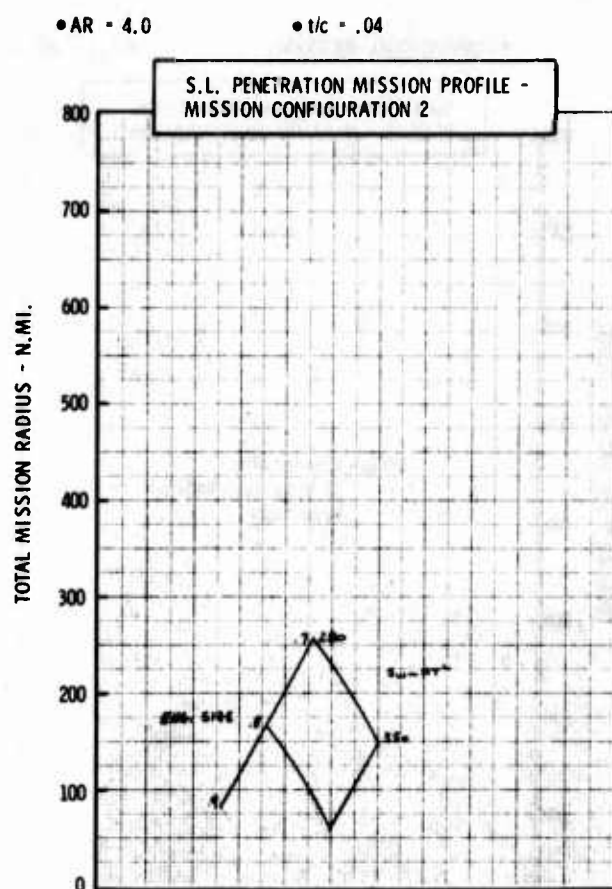
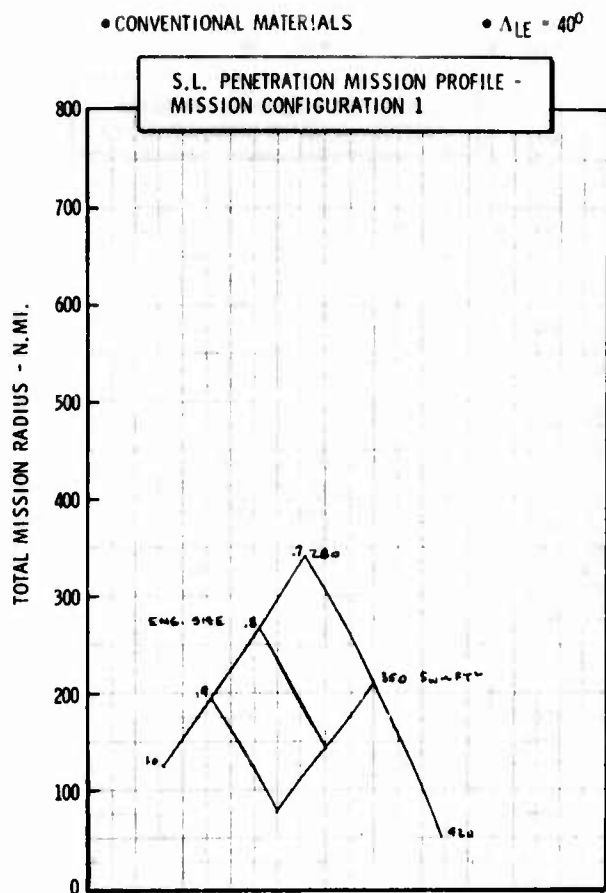


Figure H-9b LWA Mission/Configuration Tradeoff Parametric Data



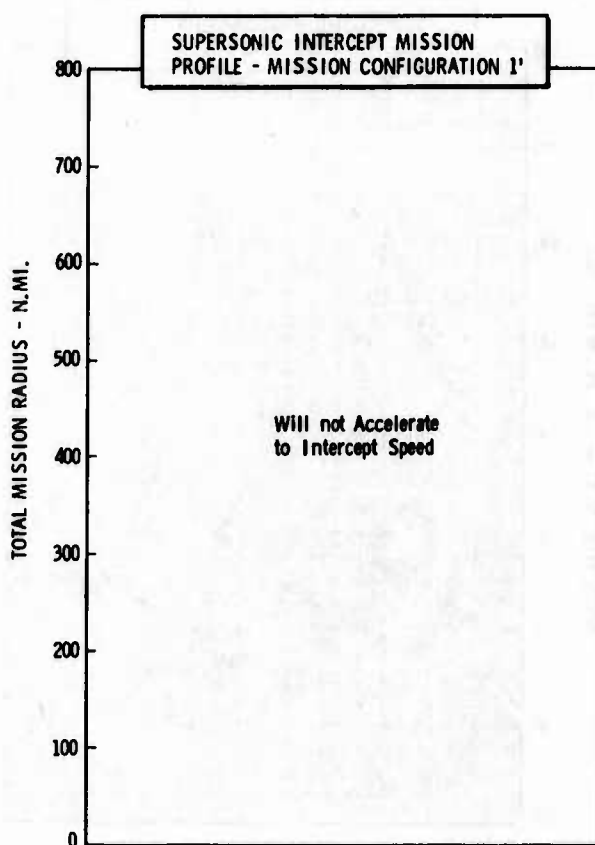
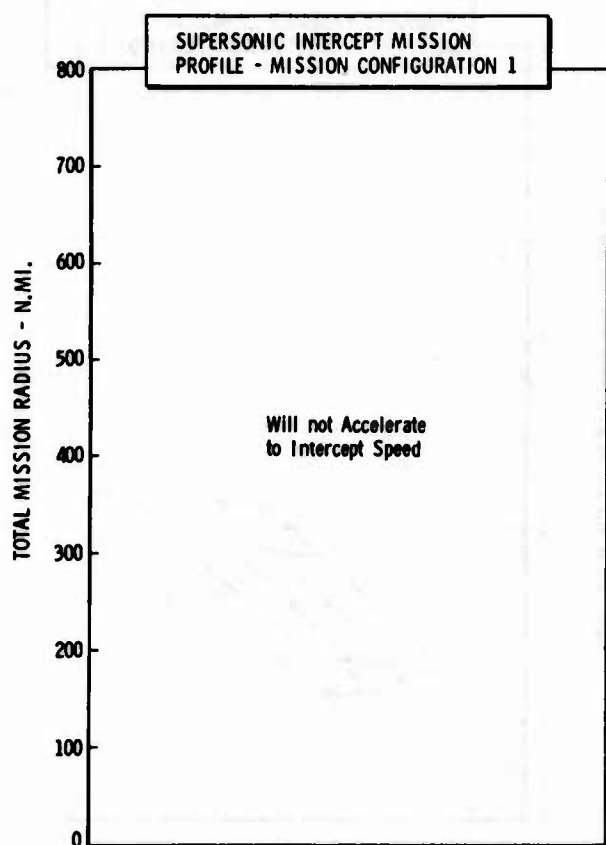
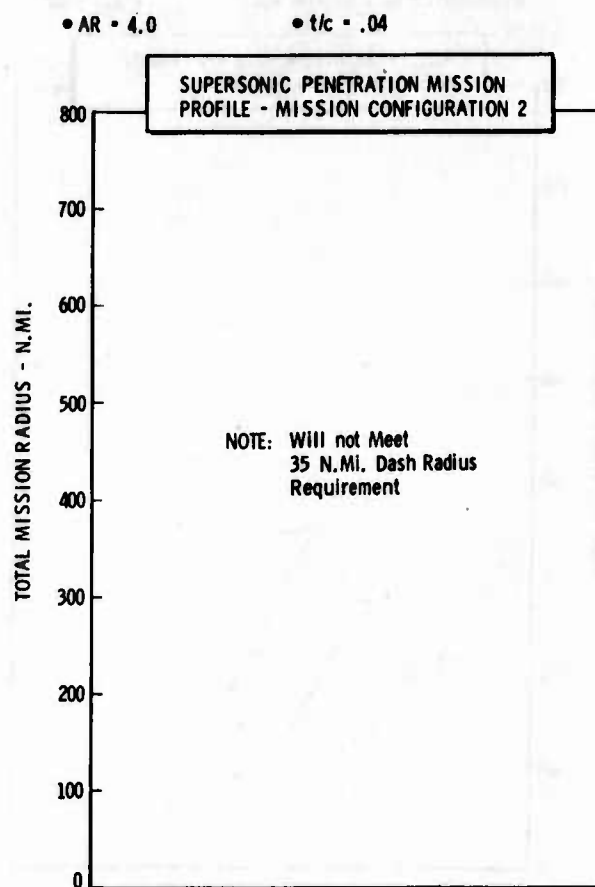
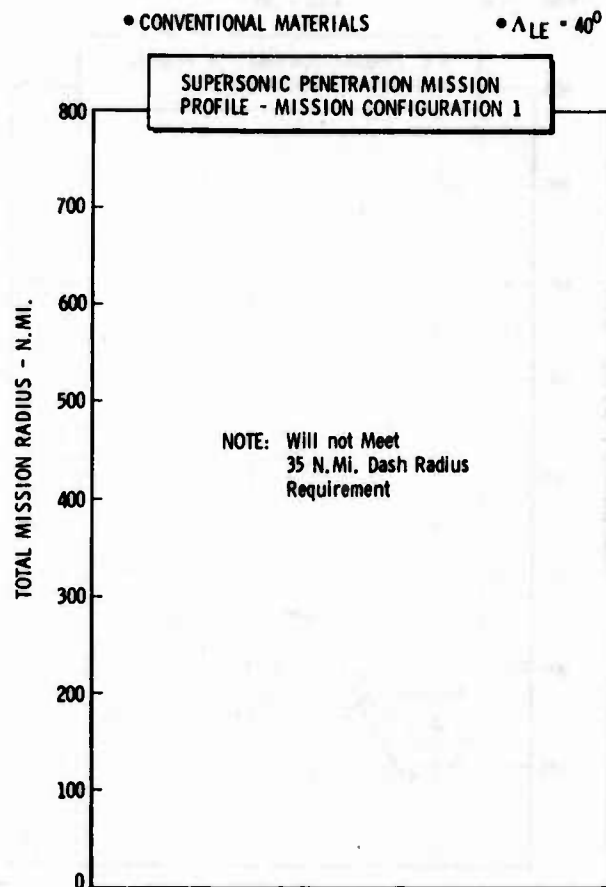


Figure H-9c LWA Mission/Configuration Tradeoff Parametric Data

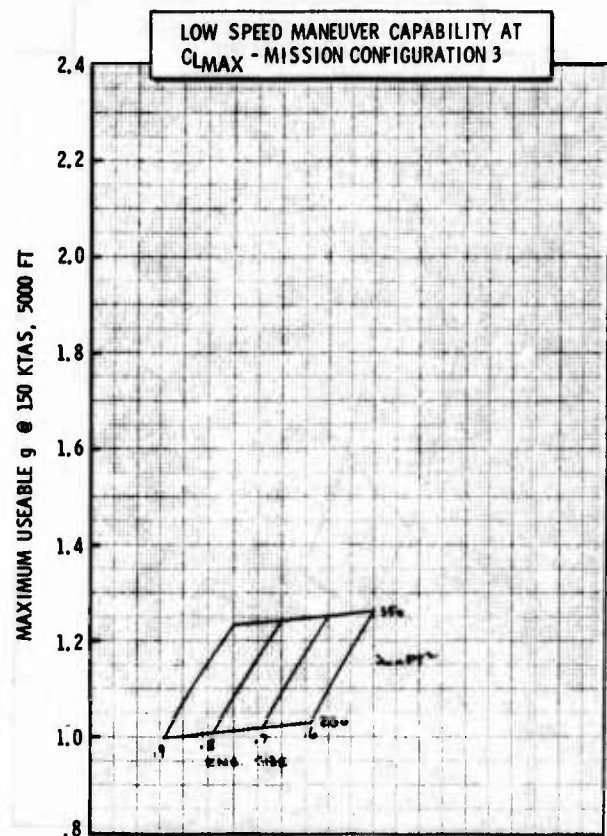
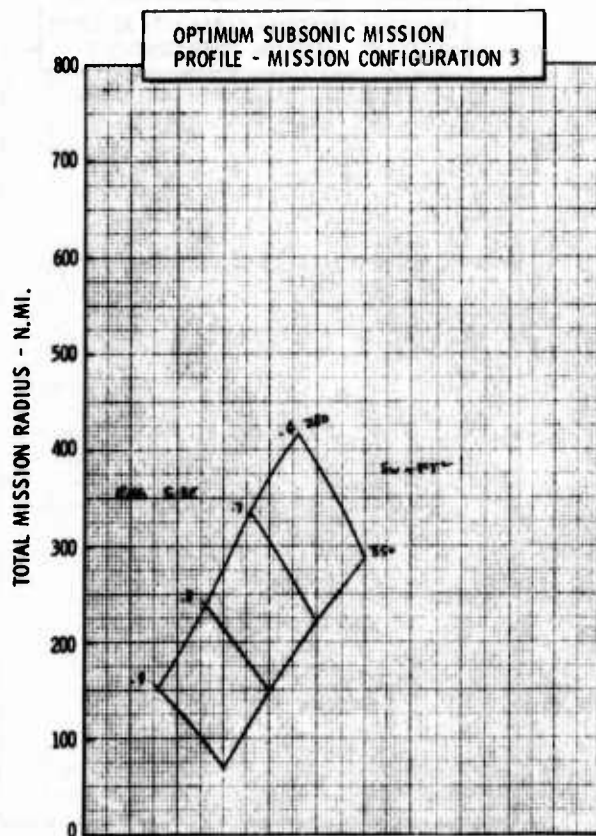
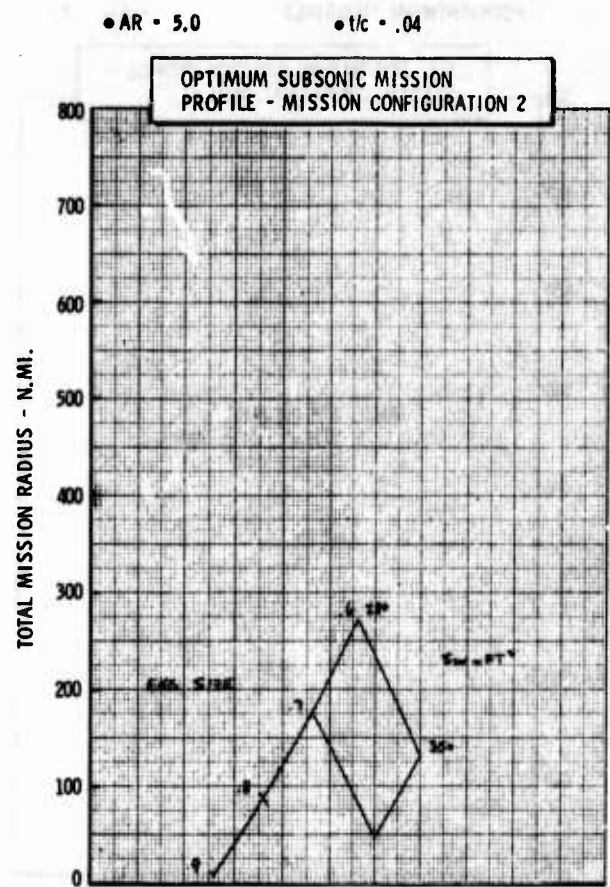
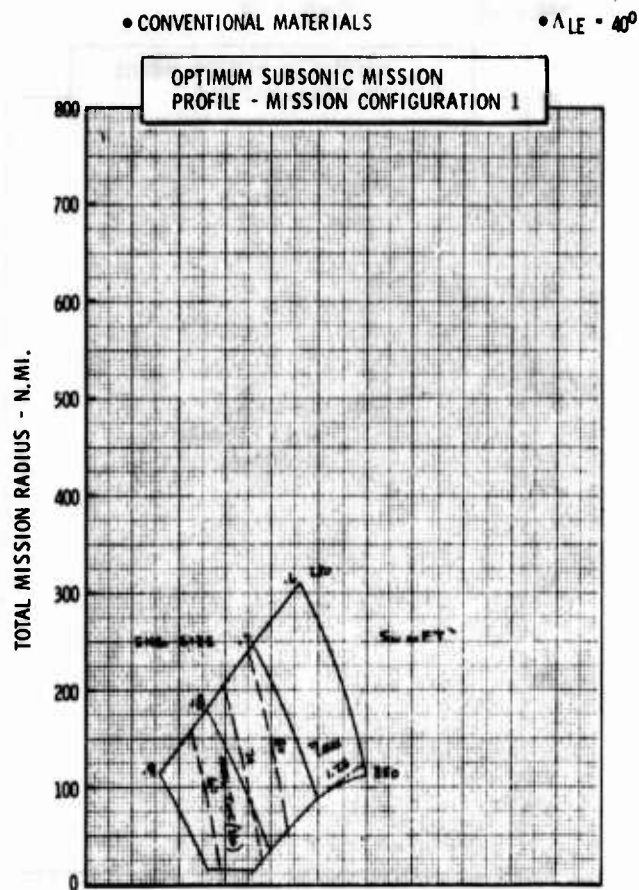


Figure H-10a LWA Mission/Configuration Tradeoff Parametric Data

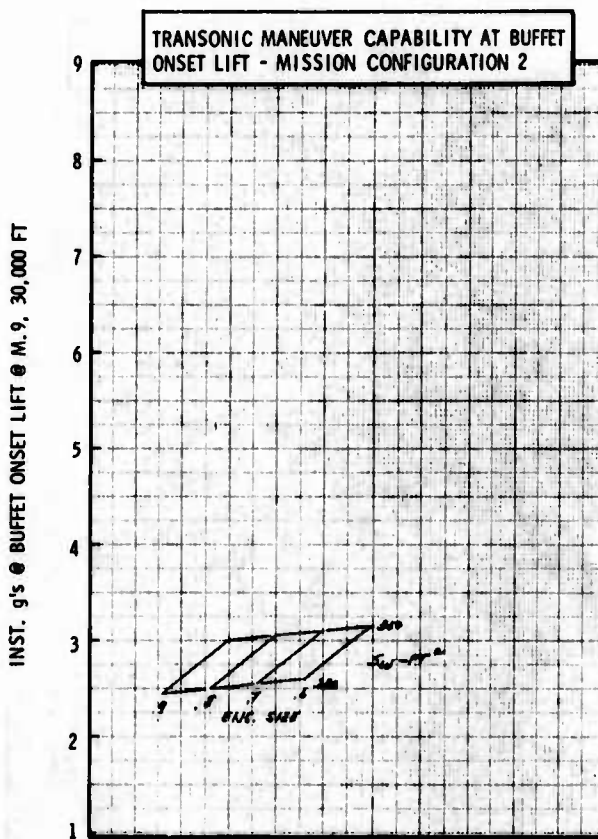
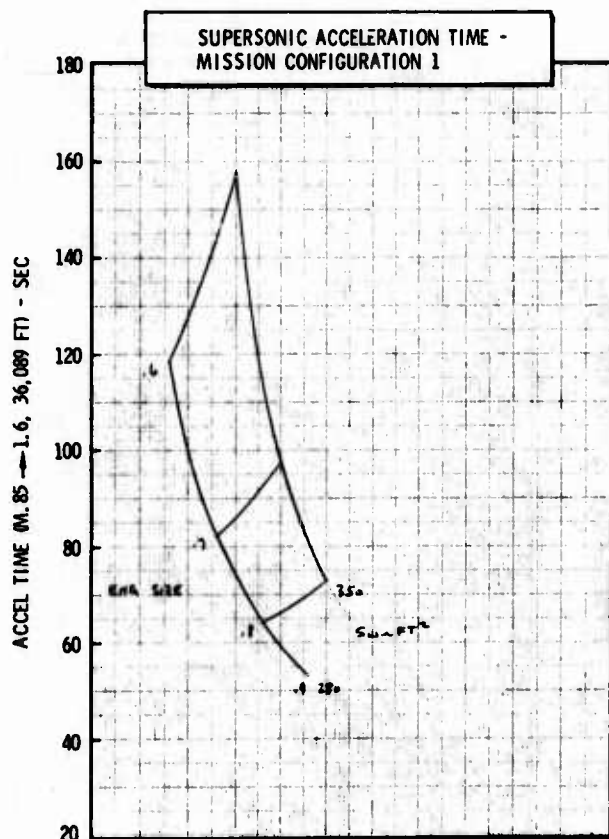
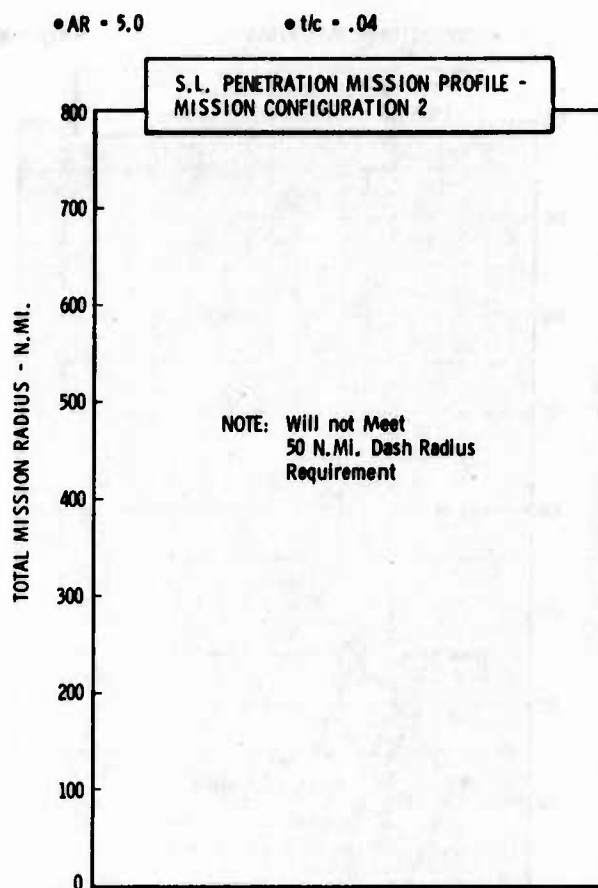
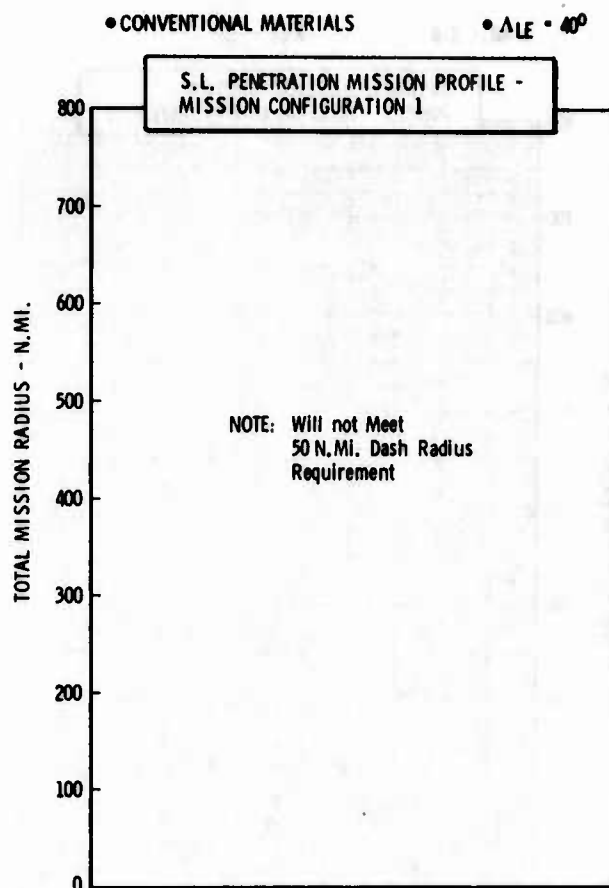


Figure H-10b LWA Mission/Configuration Tradeoff Parametric Data

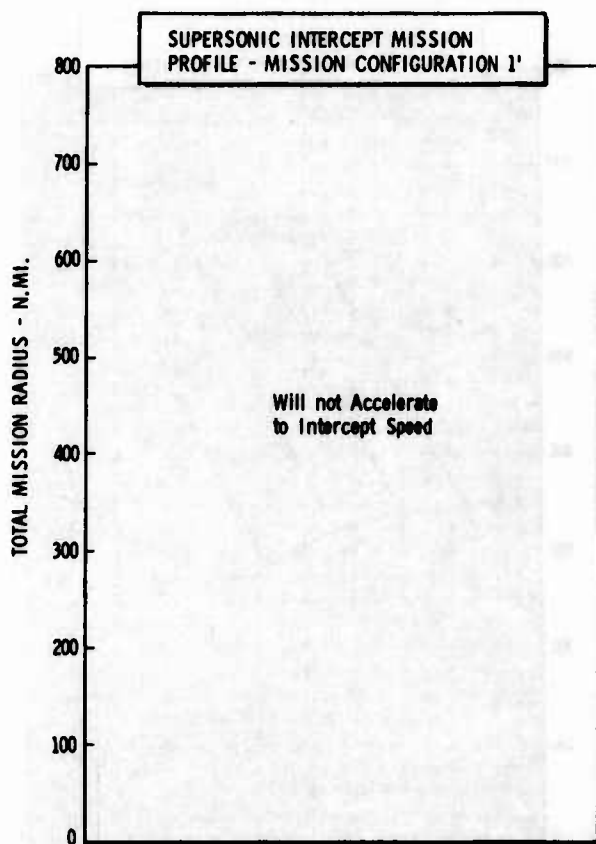
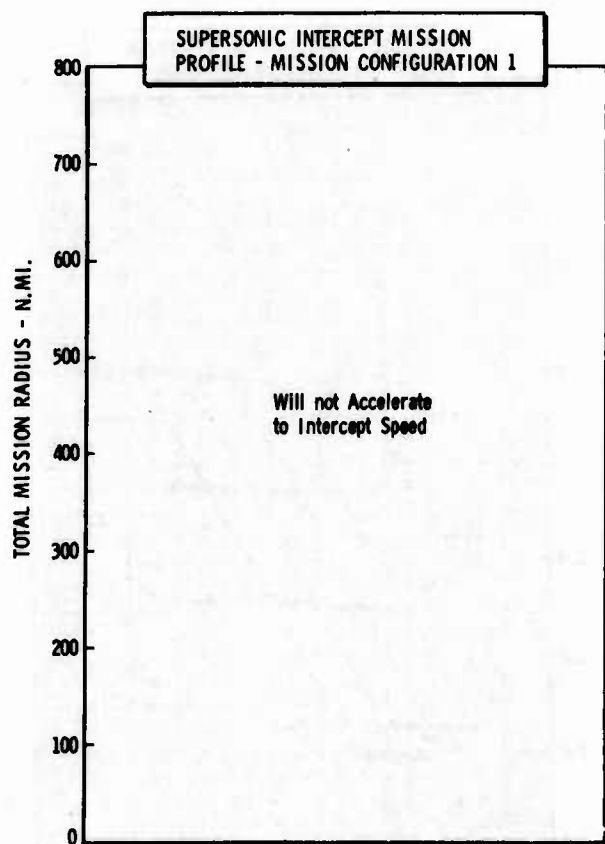
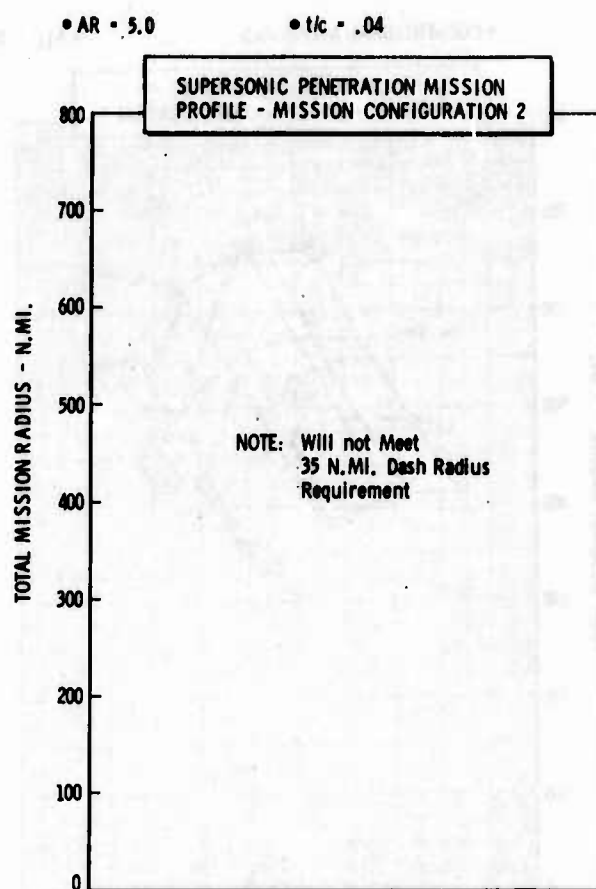
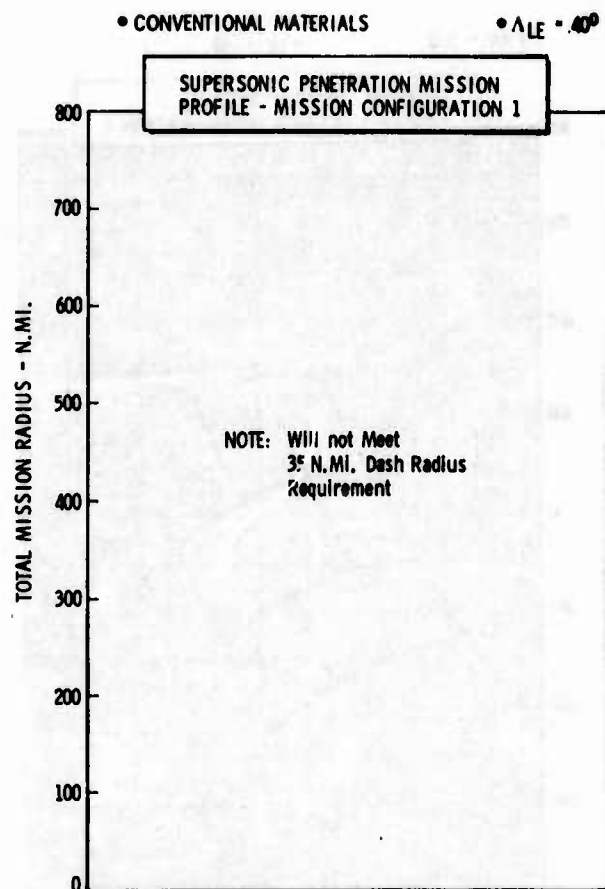


Figure H-10c LWA Mission/Configuration Tradeoff Parametric Data

• CONVENTIONAL MATERIALS

•  $\Delta LE = 20^\circ$

•  $AR = 3.0$

•  $t/c = .05$

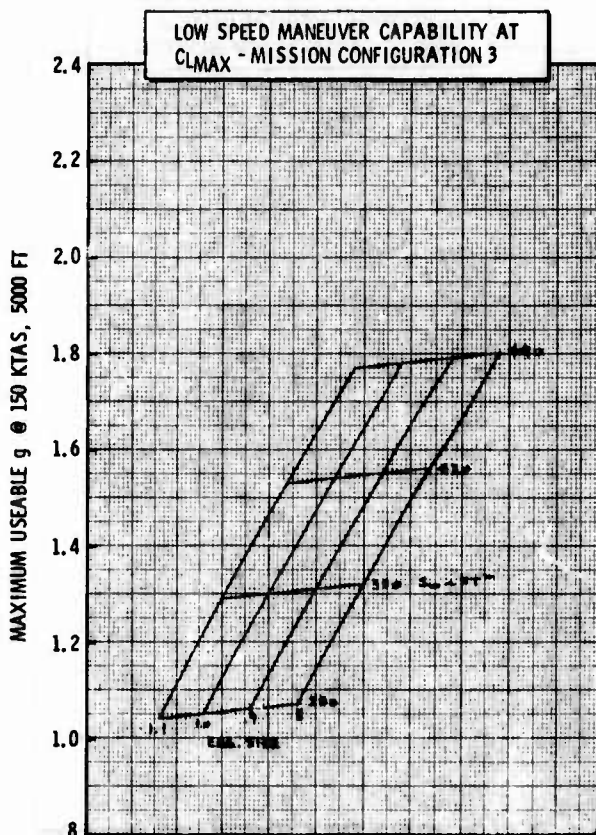
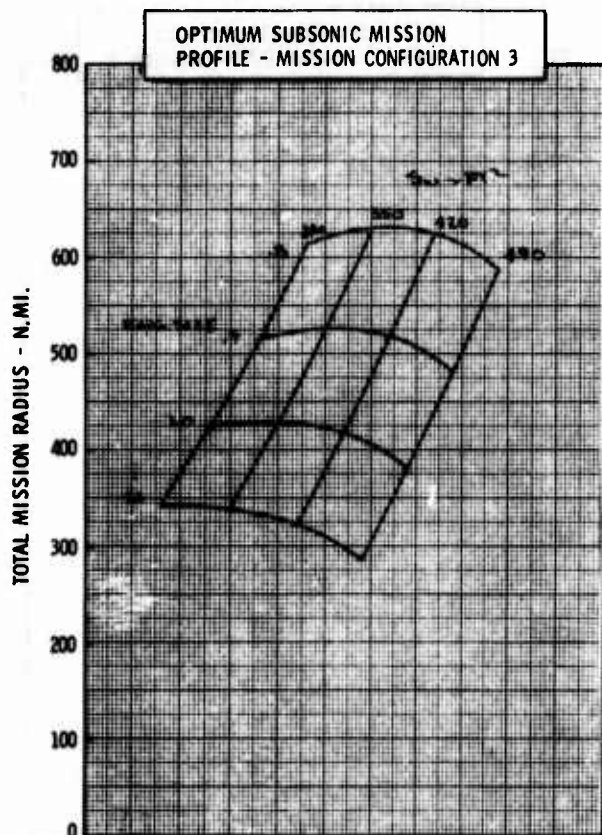
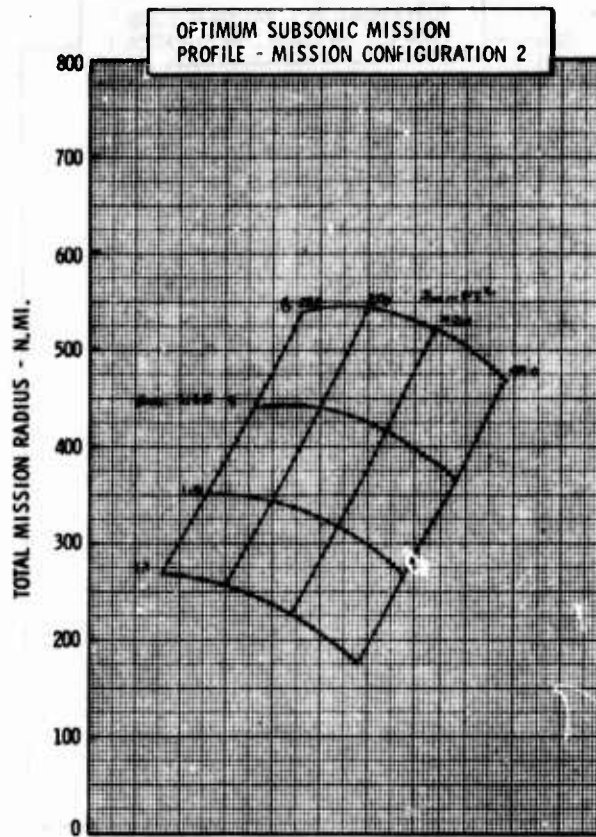
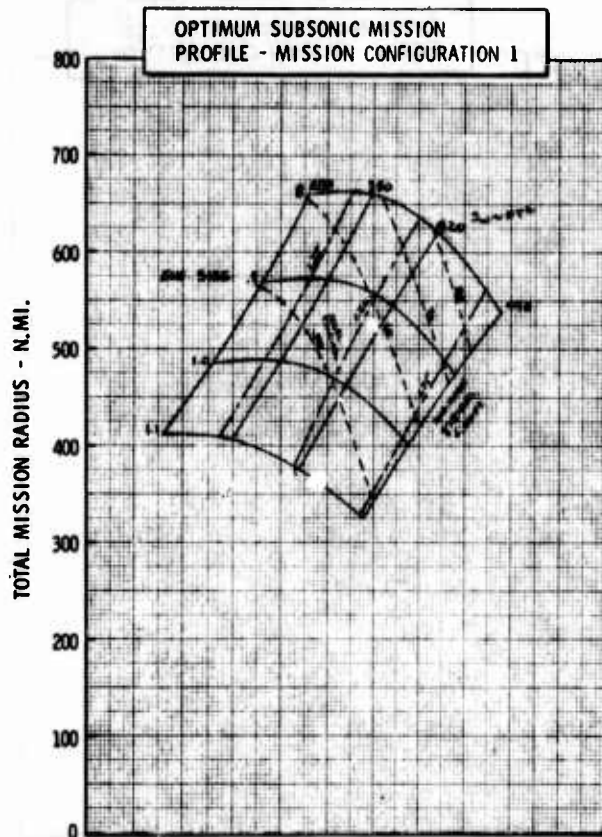


Figure H-11a LWA Mission/Configuration Tradeoff Parametric Data



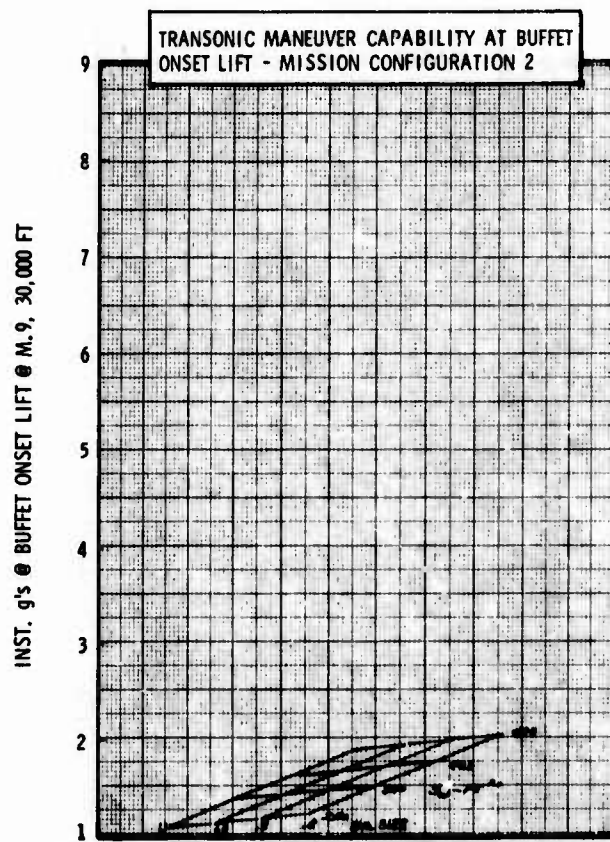
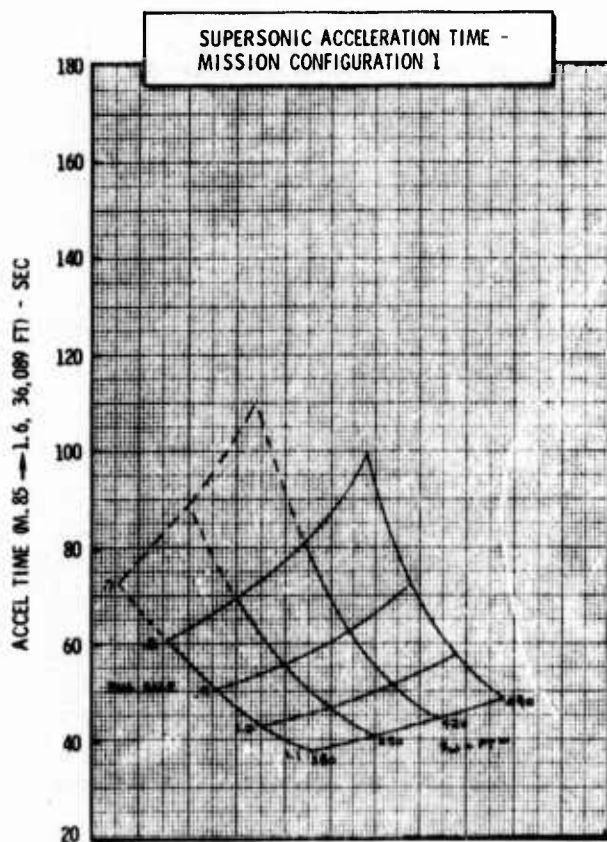
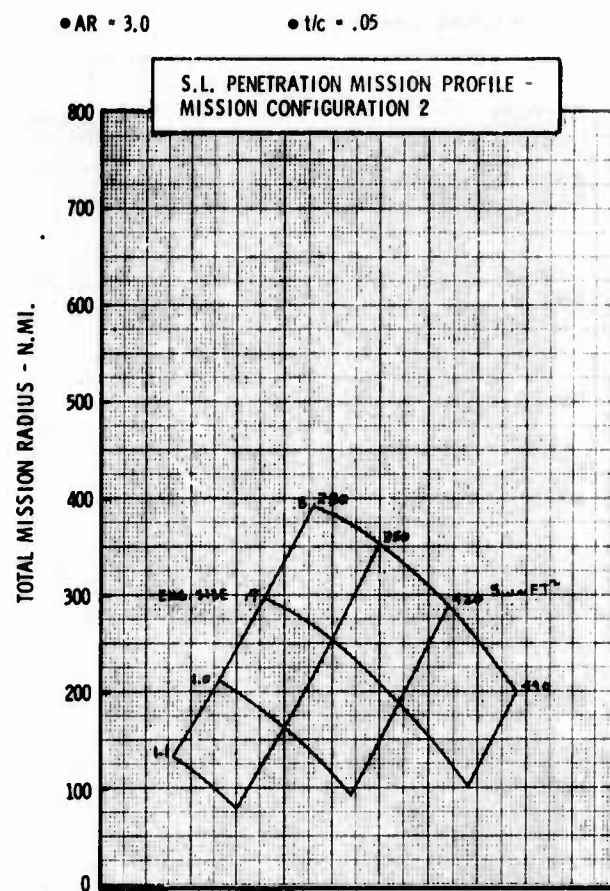
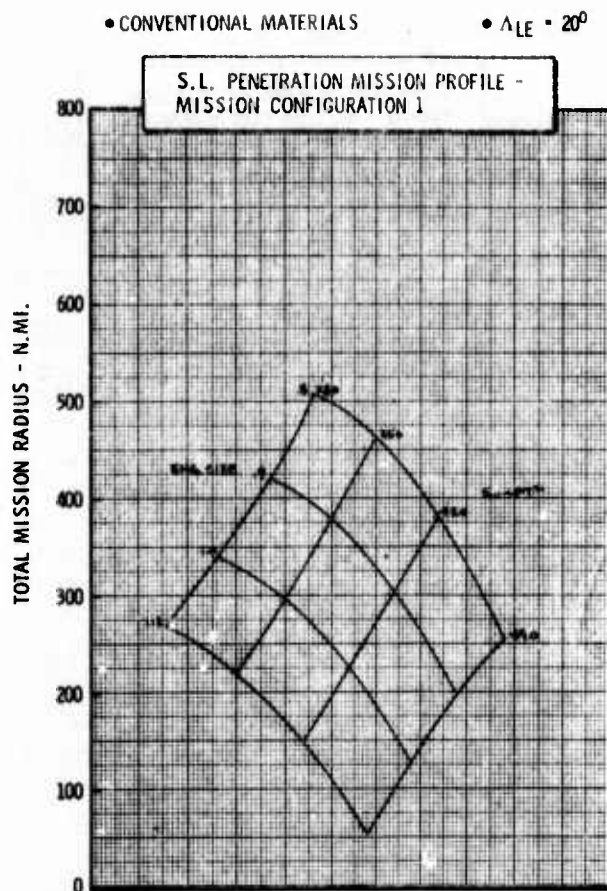


Figure H-11b LWA Mission/Configuration Tradeoff Parametric Data



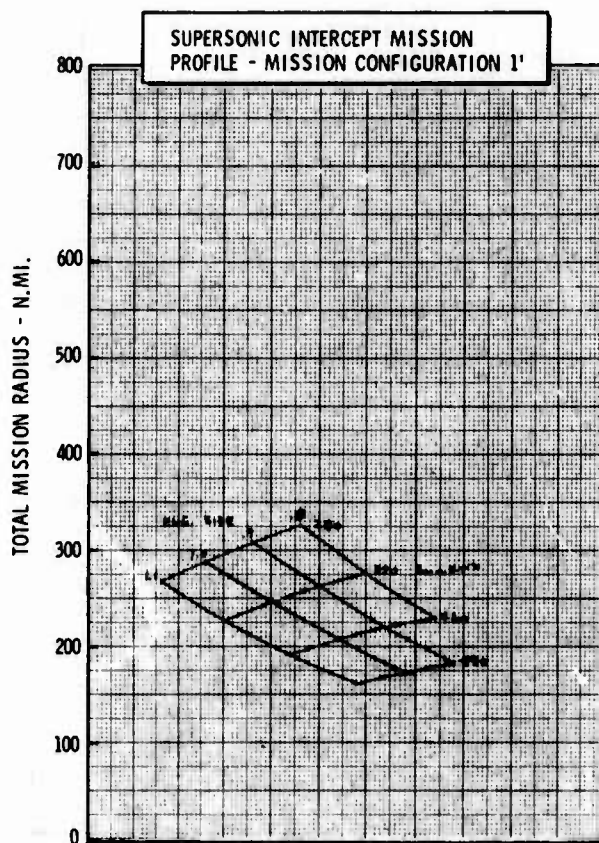
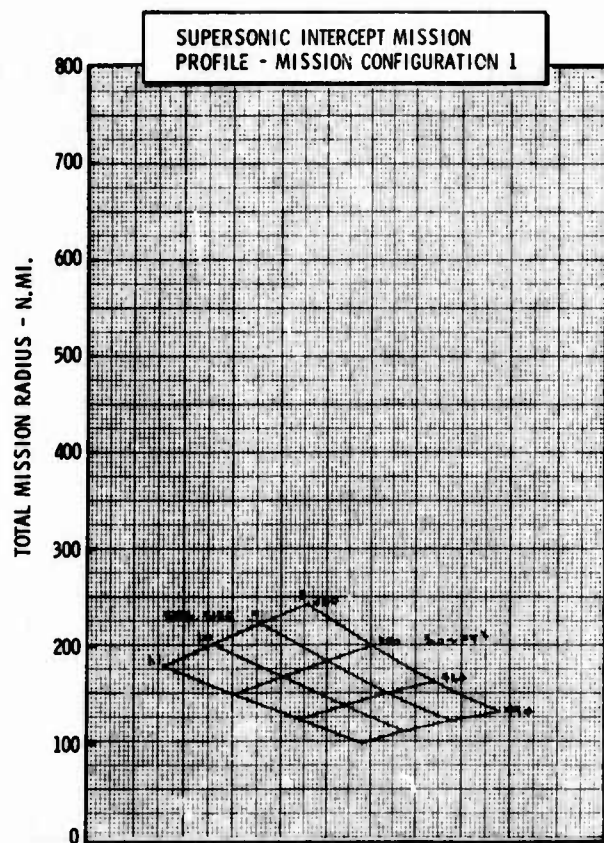
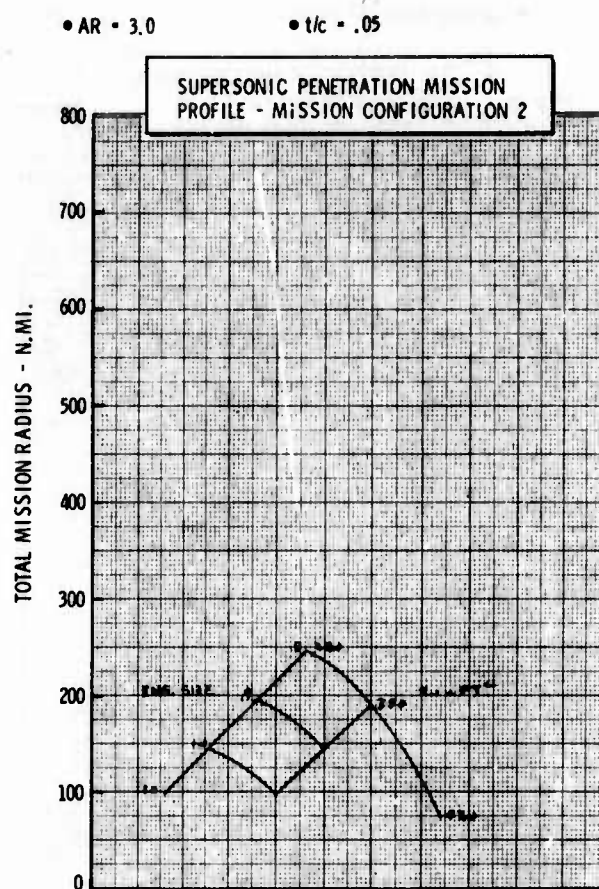
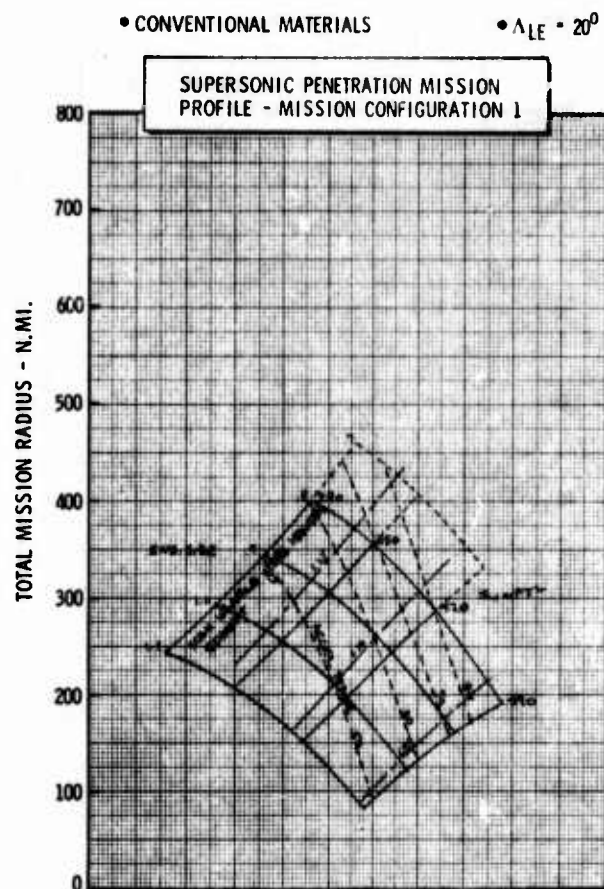


Figure H-11c LWA Mission/Configuration Tradeoff Parametric Data

• CONVENTIONAL MATERIALS

•  $\Delta LE = 20^\circ$

•  $AR = 4.0$

•  $t/c = .05$

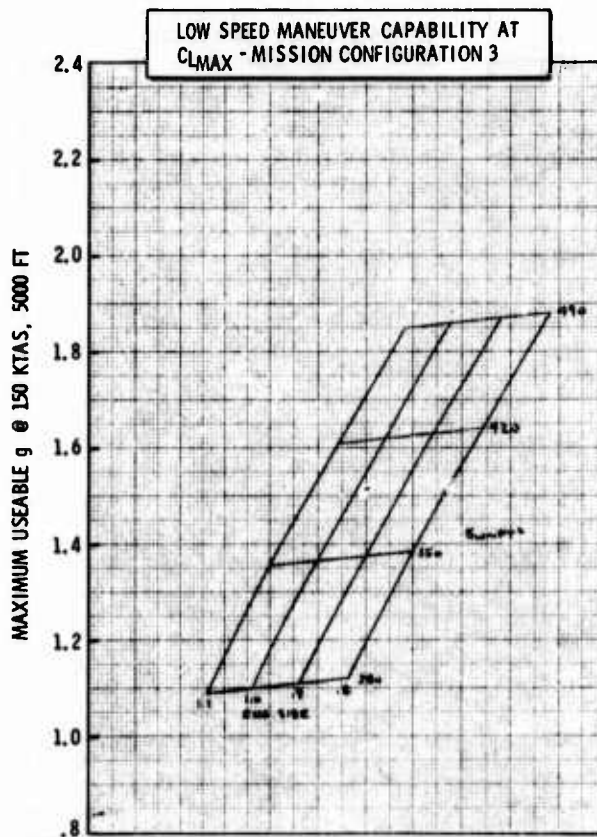
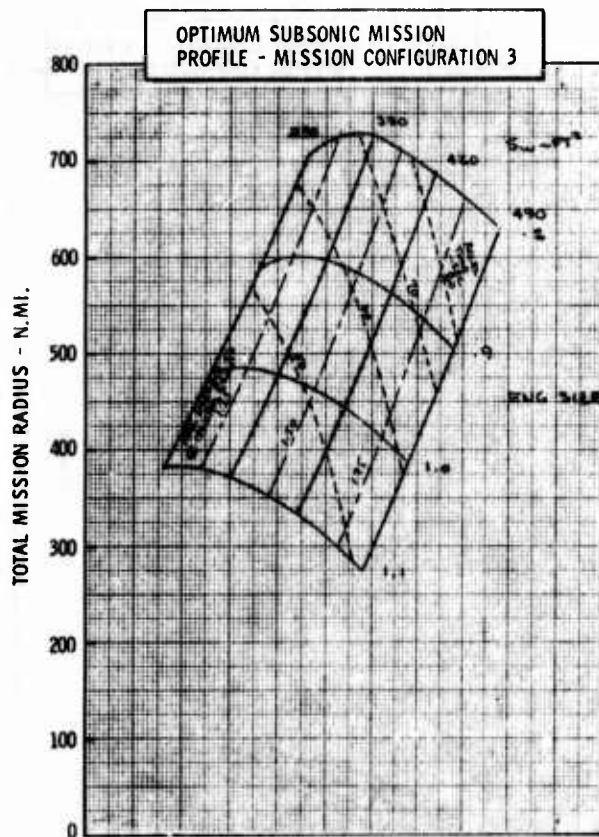
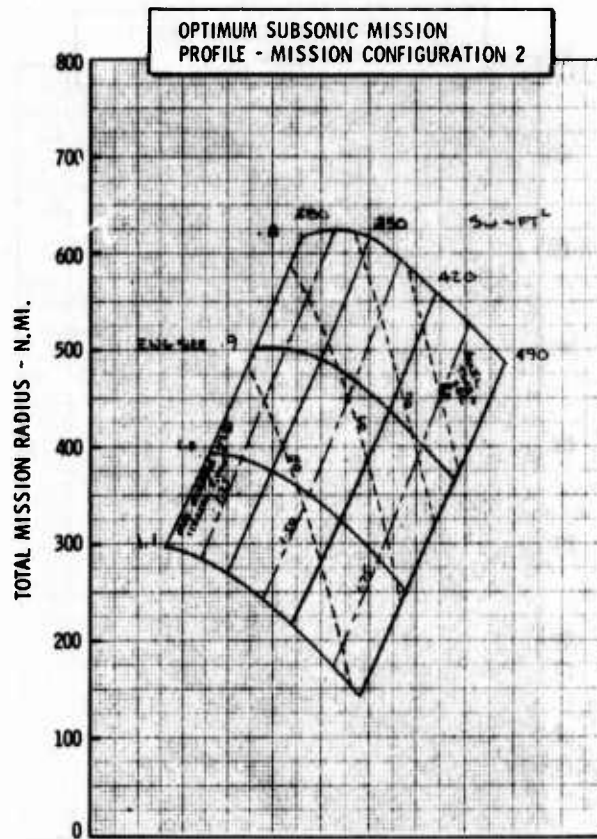
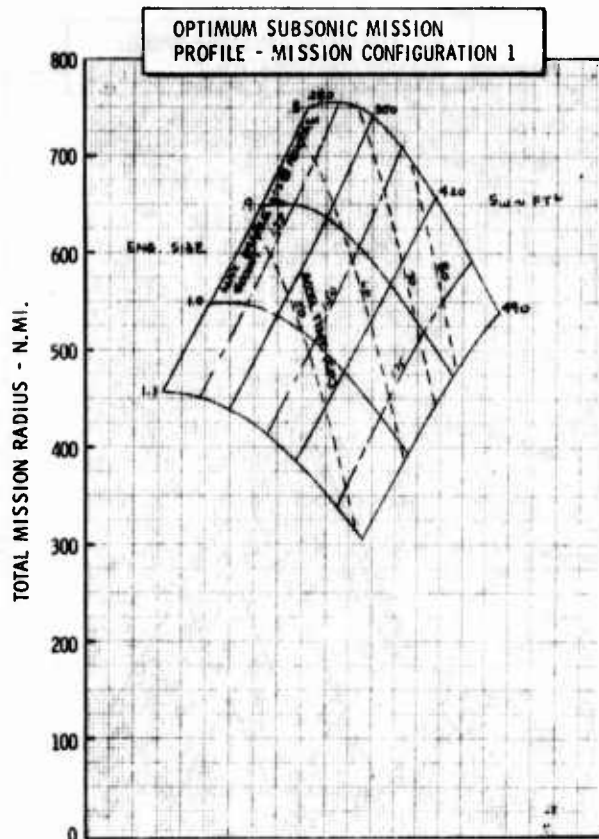
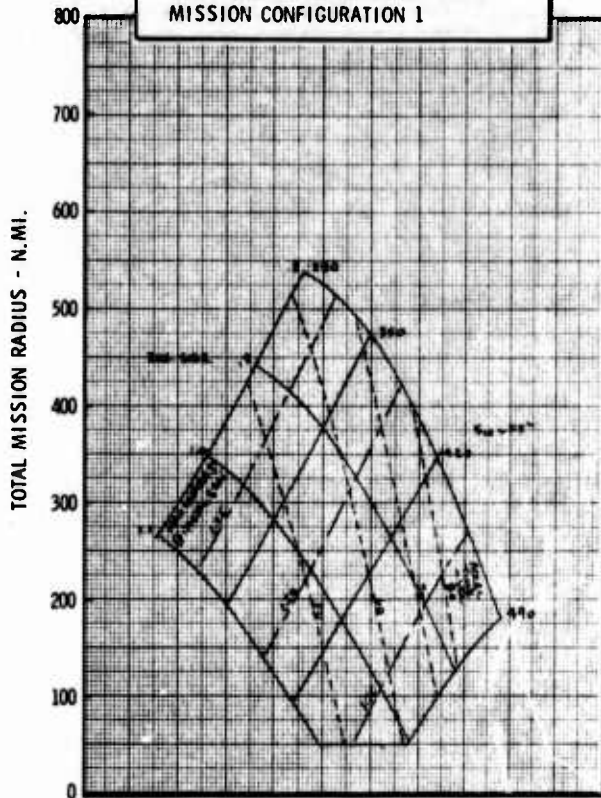


Figure H-12a LWA Mission/Configuration Tradeoff Parametric Data

• CONVENTIONAL MATERIALS

•  $\Delta LE = 20^\circ$

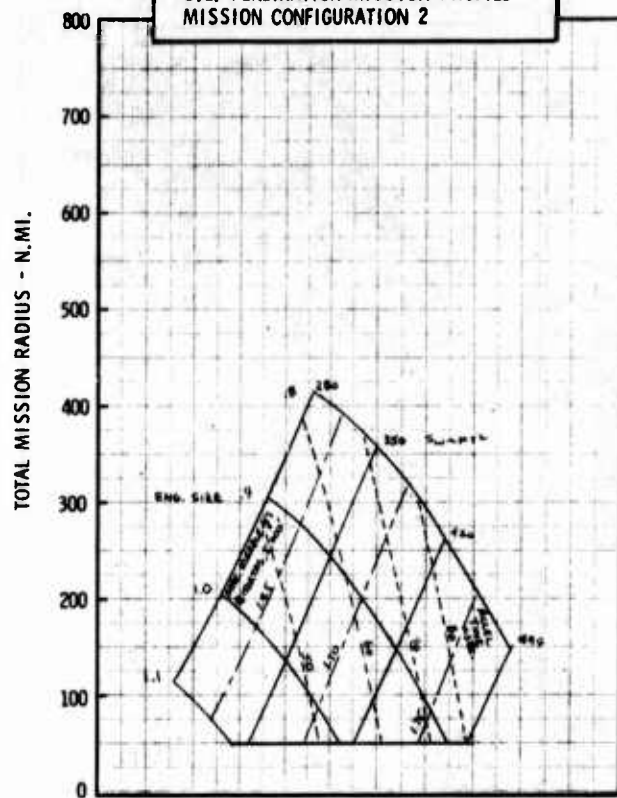
S.L. PENETRATION MISSION PROFILE -  
MISSION CONFIGURATION 1



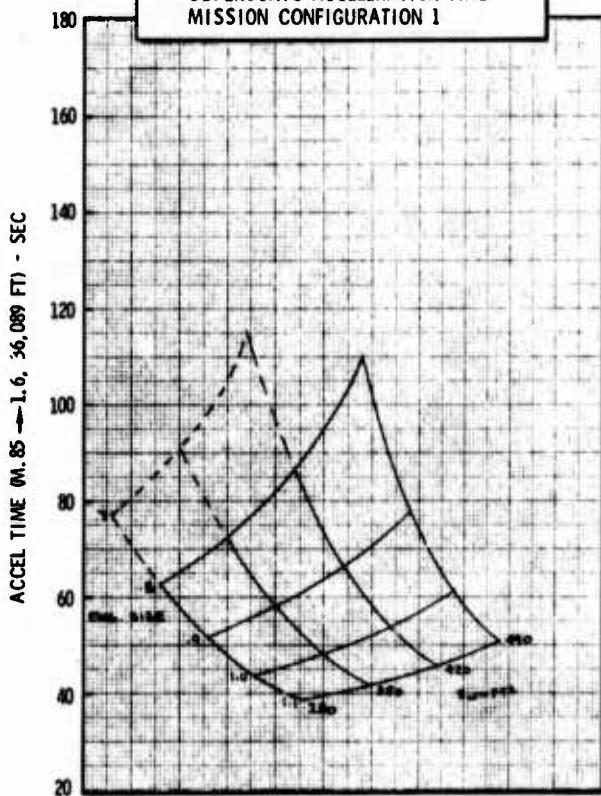
•  $AR = 4.0$

•  $t/c = .05$

S.L. PENETRATION MISSION PROFILE -  
MISSION CONFIGURATION 2



SUPERSONIC ACCELERATION TIME -  
MISSION CONFIGURATION 1



TRANSONIC MANEUVER CAPABILITY AT BUFFET  
ONSET LIFT - MISSION CONFIGURATION 2

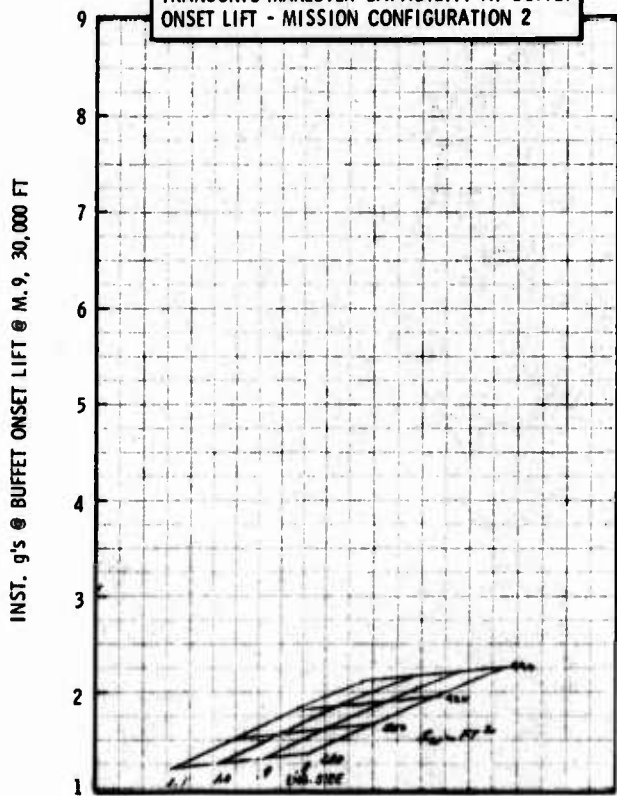


Figure H-12b LWA Mission/Configuration Tradeoff Parametric Data



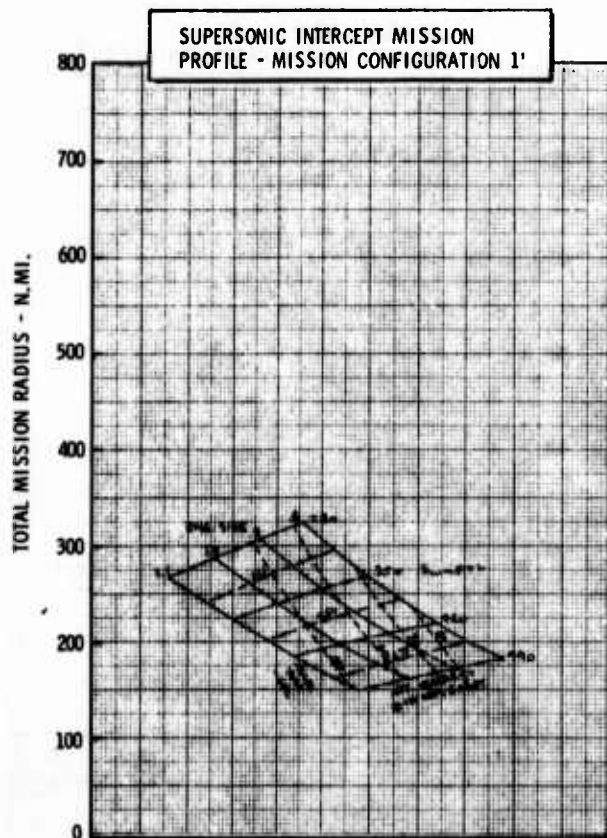
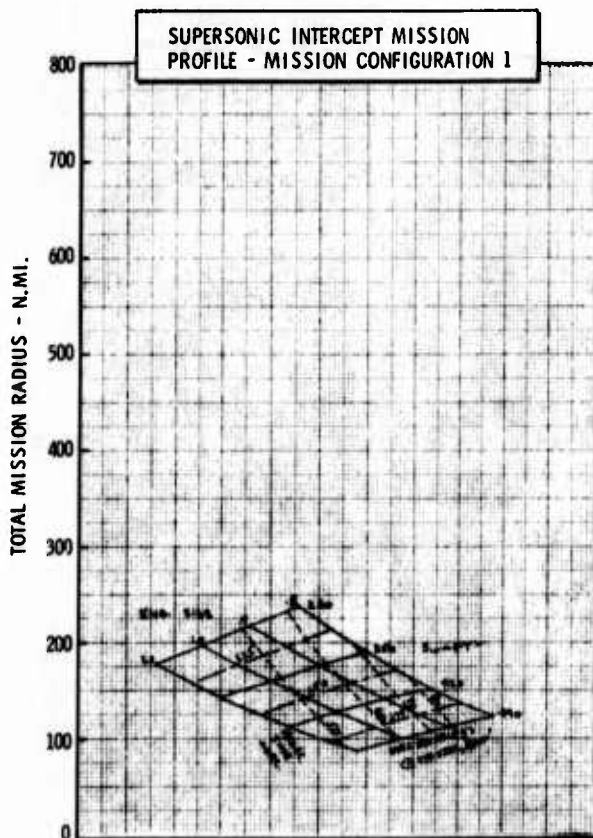
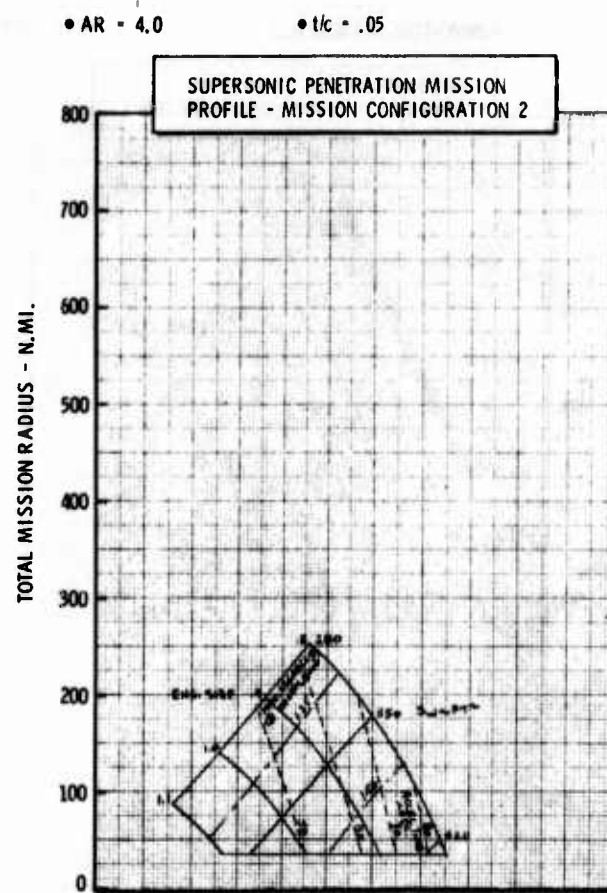
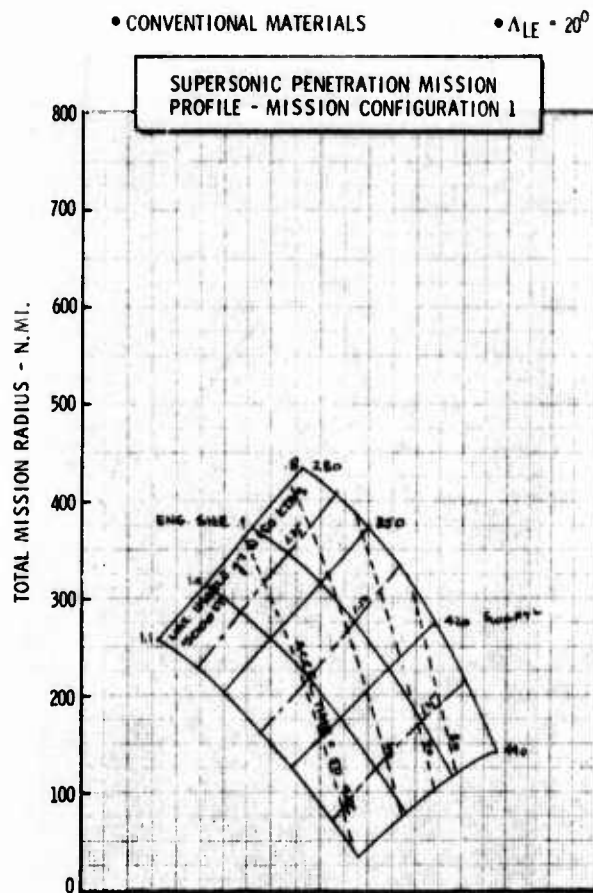


Figure H-12c LWA Mission/Configuration Tradeoff Parametric Data

• CONVENTIONAL MATERIALS

•  $\Delta LE = 20^\circ$

•  $AR = 5.0$

•  $t/c = .05$

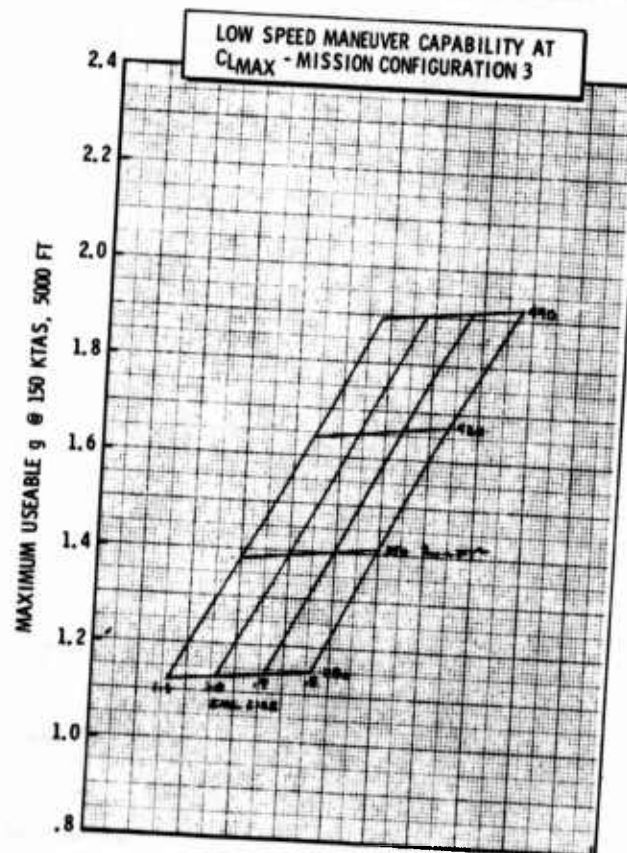
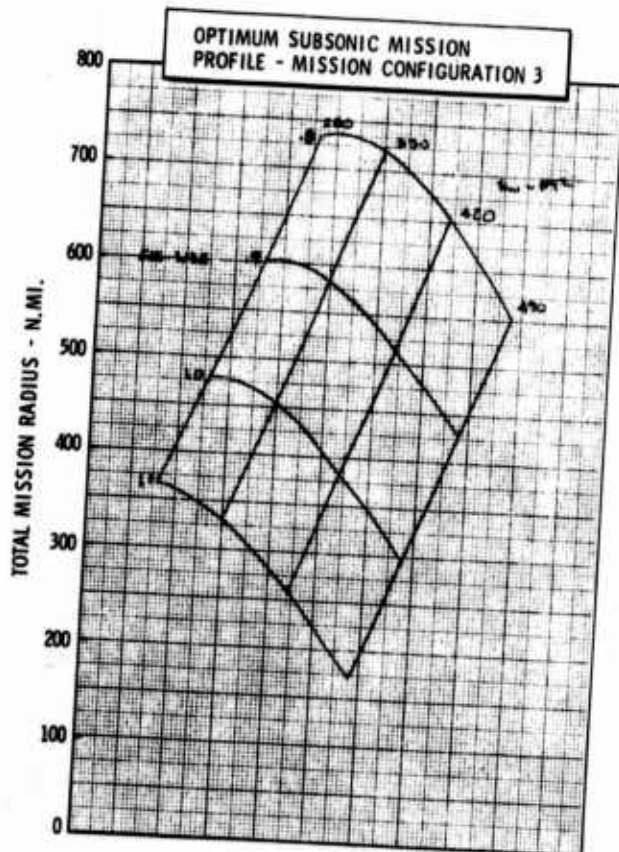
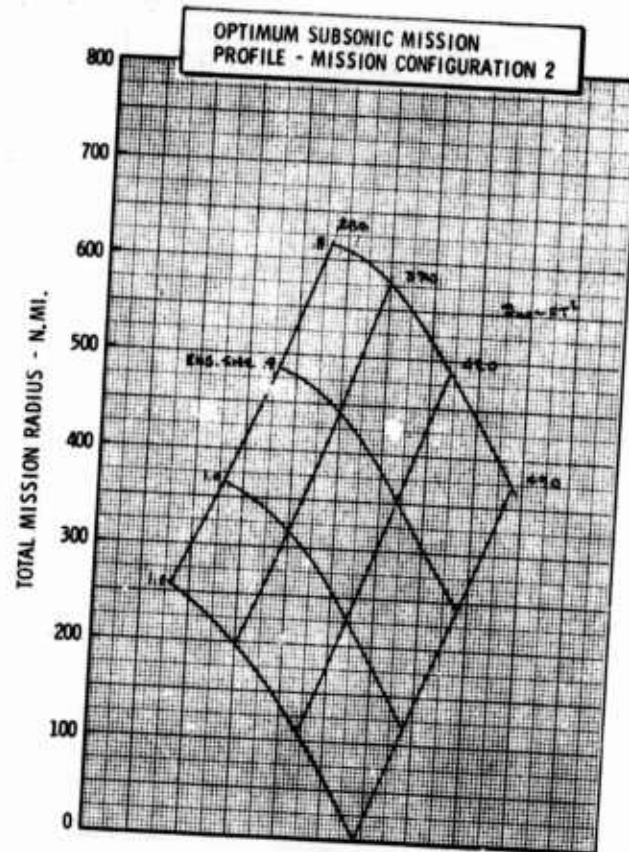
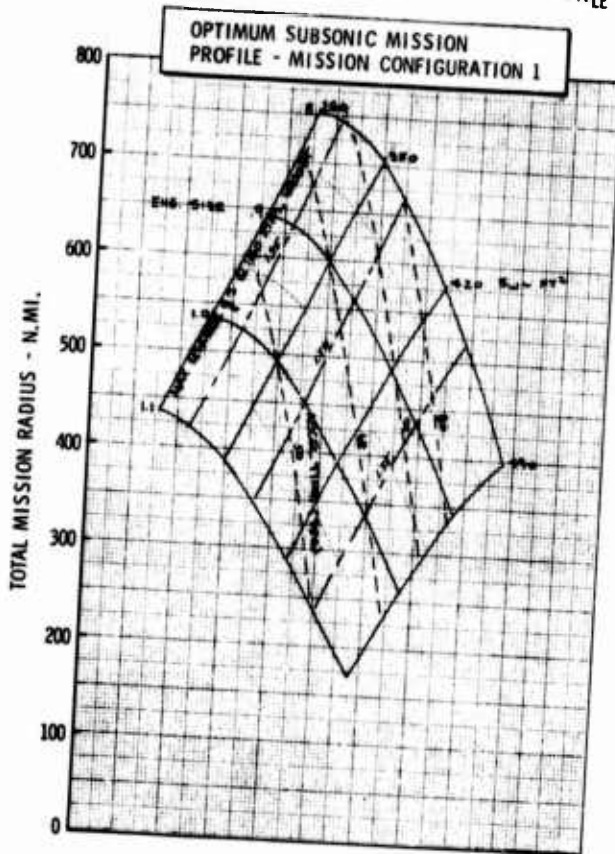


Figure H-13a LWA Mission/Configuration Tradeoff Parametric Data

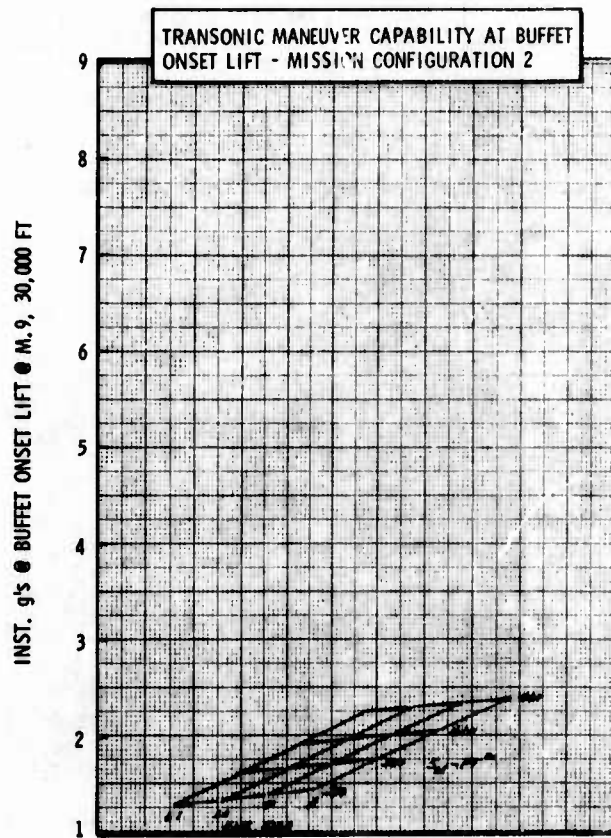
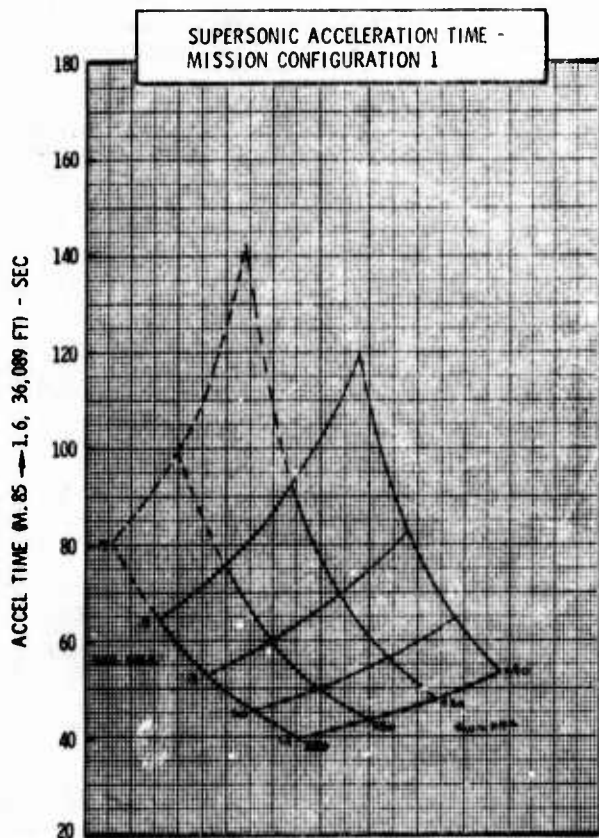
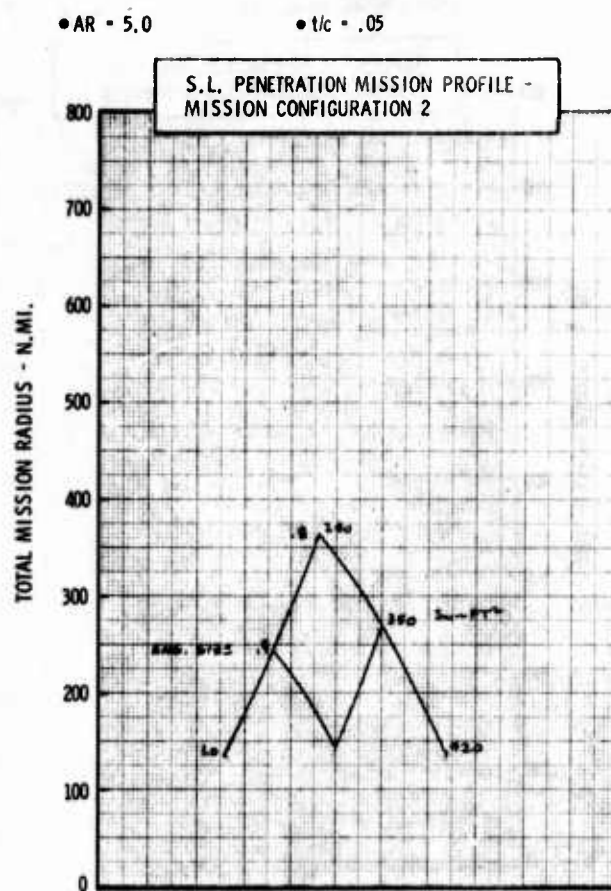
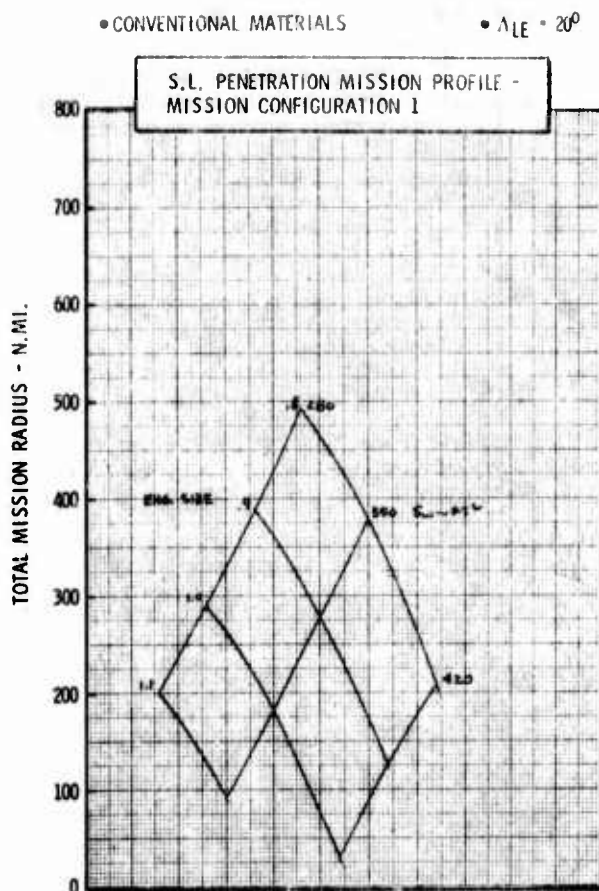


Figure H-13b LWA Mission/Configuration Tradeoff Parametric Data



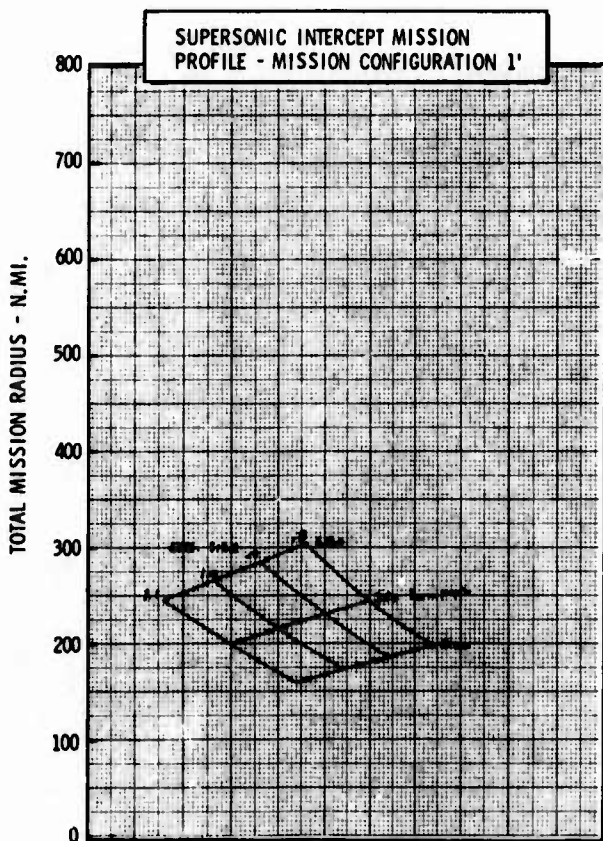
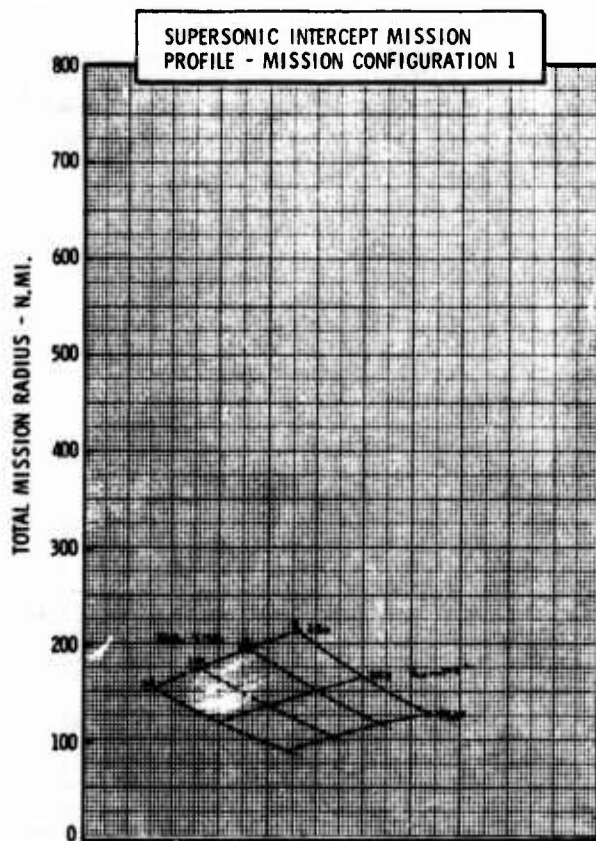
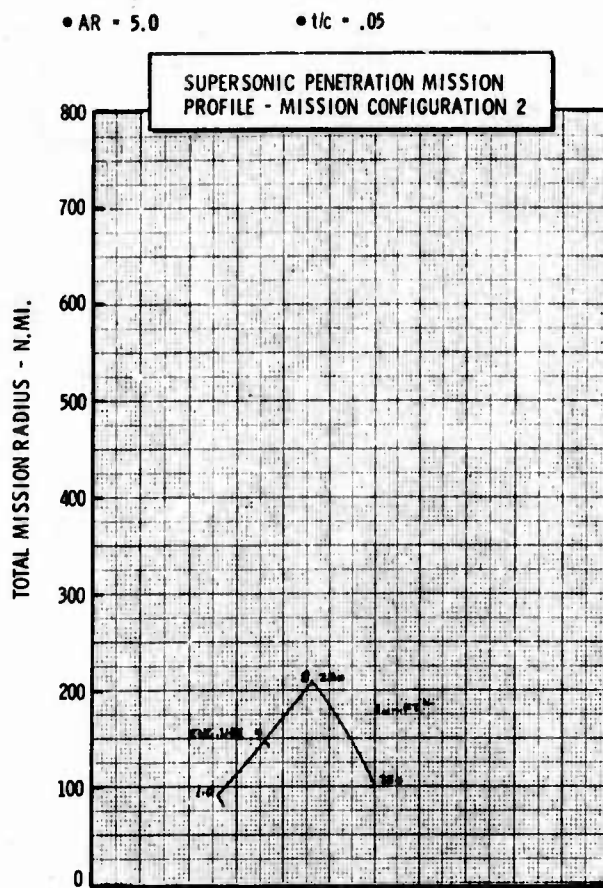
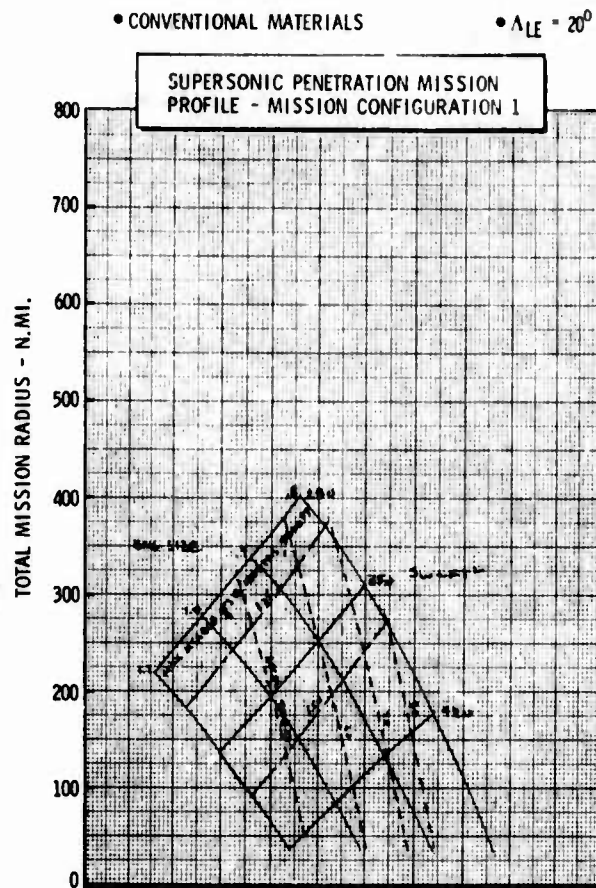


Figure H-13c LWA Mission/Configuration Tradeoff Parametric Data

• CONVENTIONAL MATERIALS

•  $\Delta LE = 30^\circ$

•  $AR = 3.0$

•  $t/c = .05$

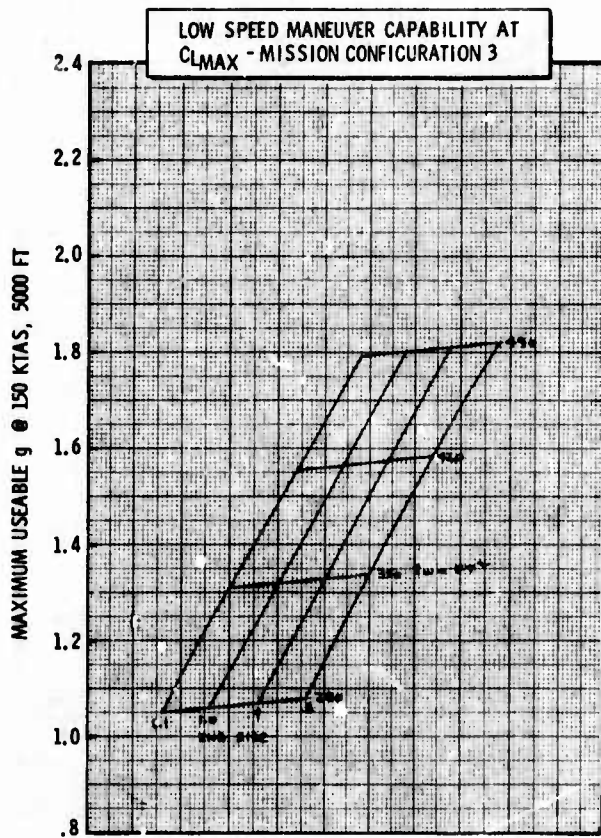
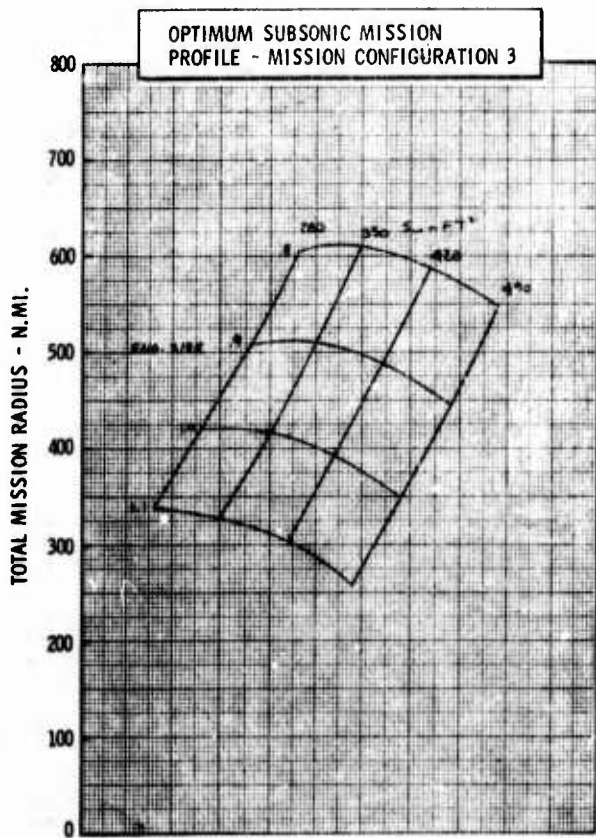
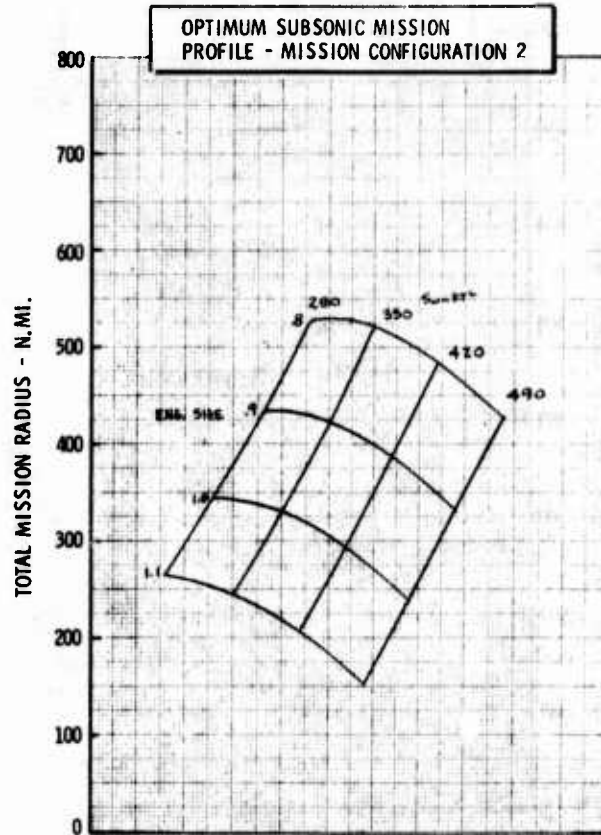
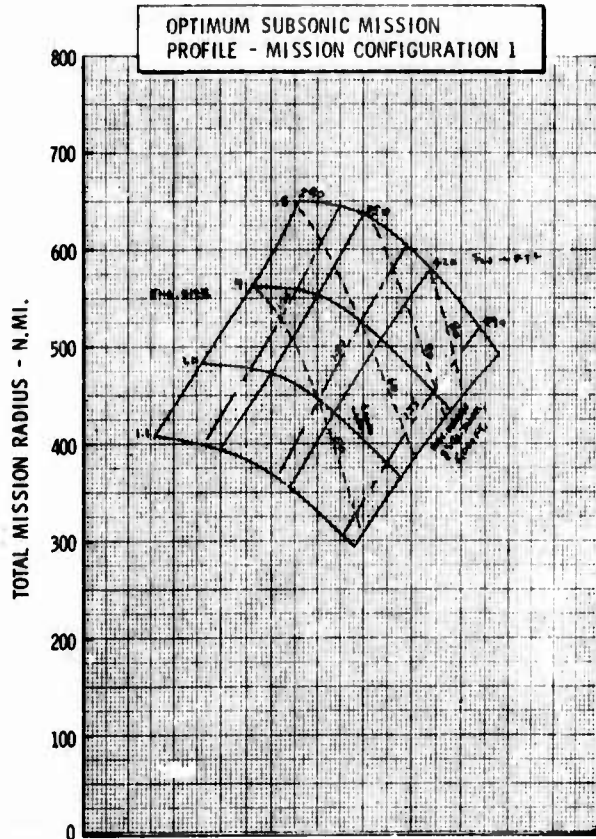


Figure H-14a LWA Mission/Configuration Tradeoff Parametric Data

• CONVENTIONAL MATERIALS

•  $\Delta LE = 30^\circ$

•  $AR = 3.0$

•  $t/c = .05$

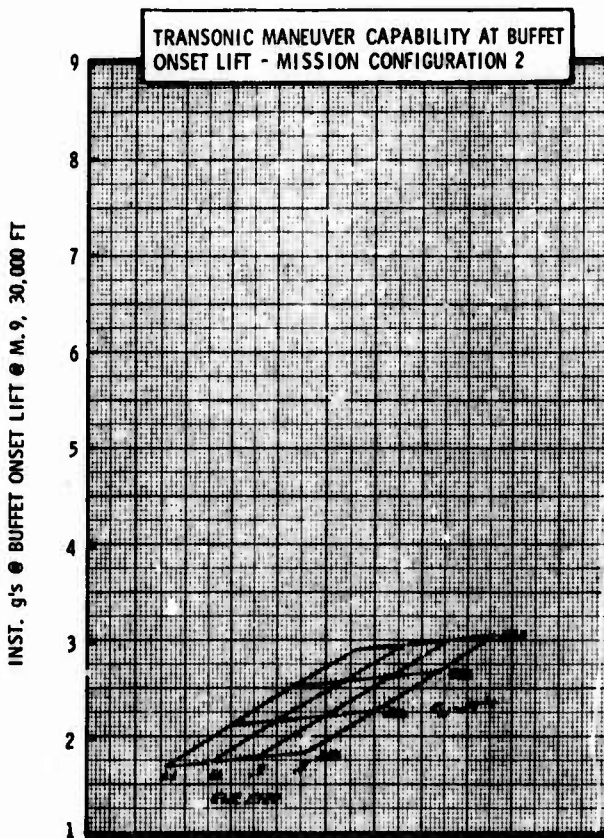
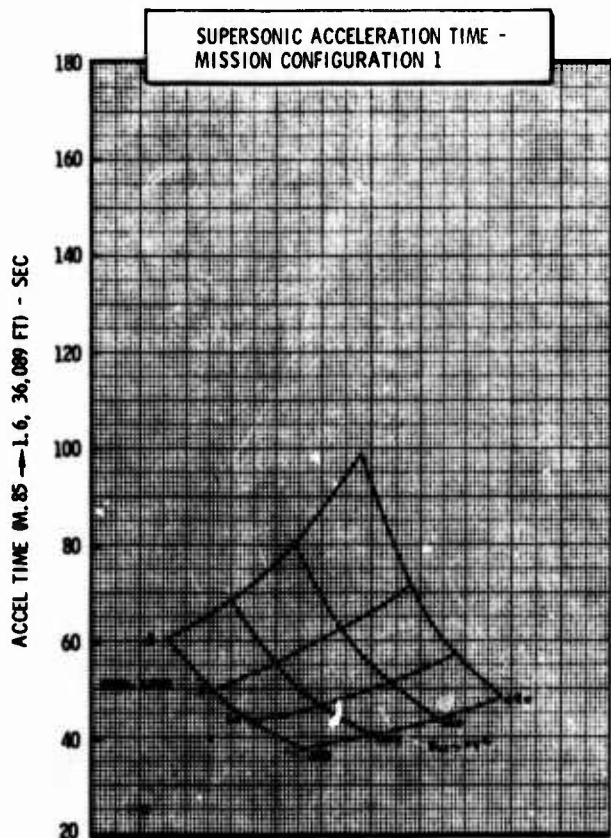
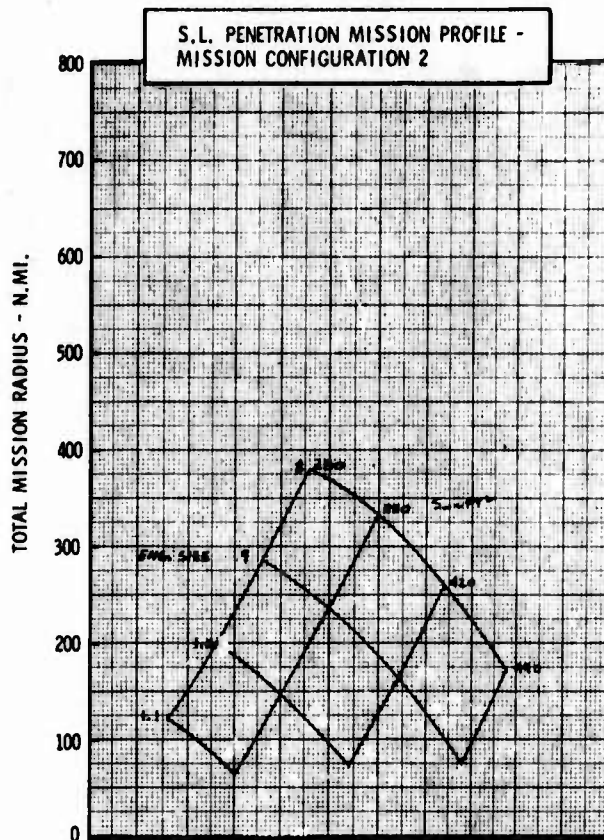
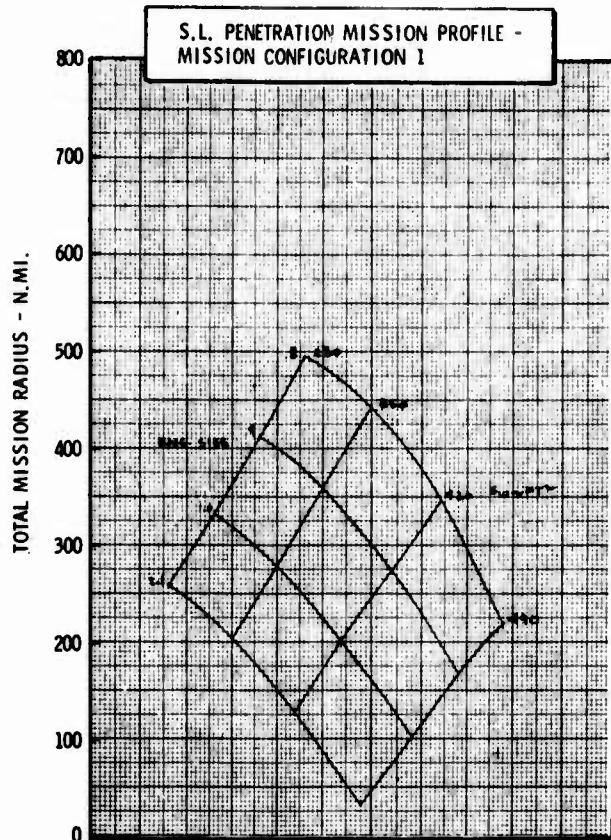


Figure H-14b LWA Mission/Configuration Tradeoff Parametric Data



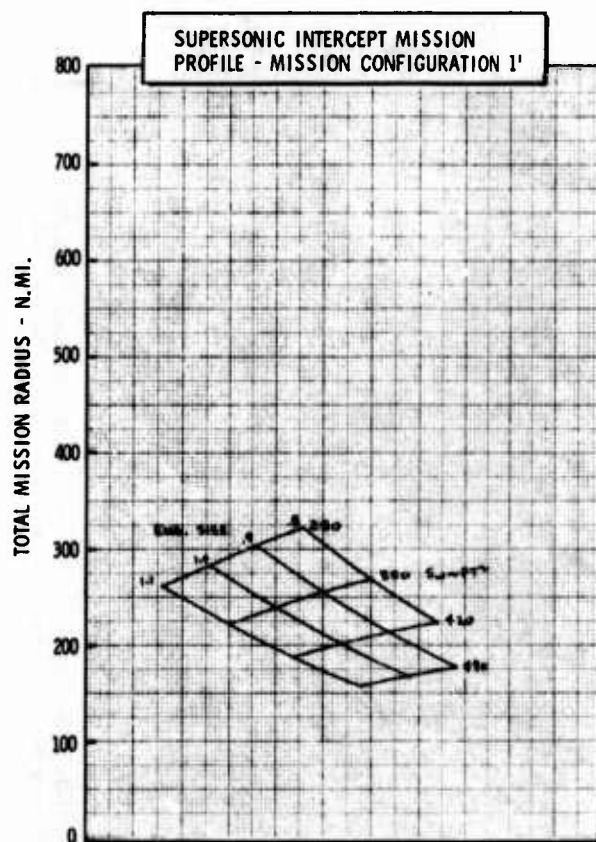
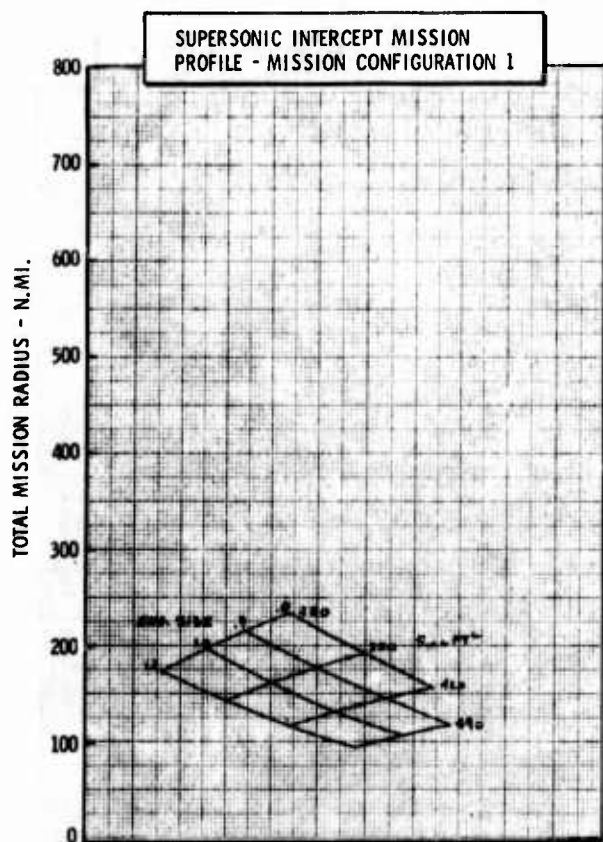
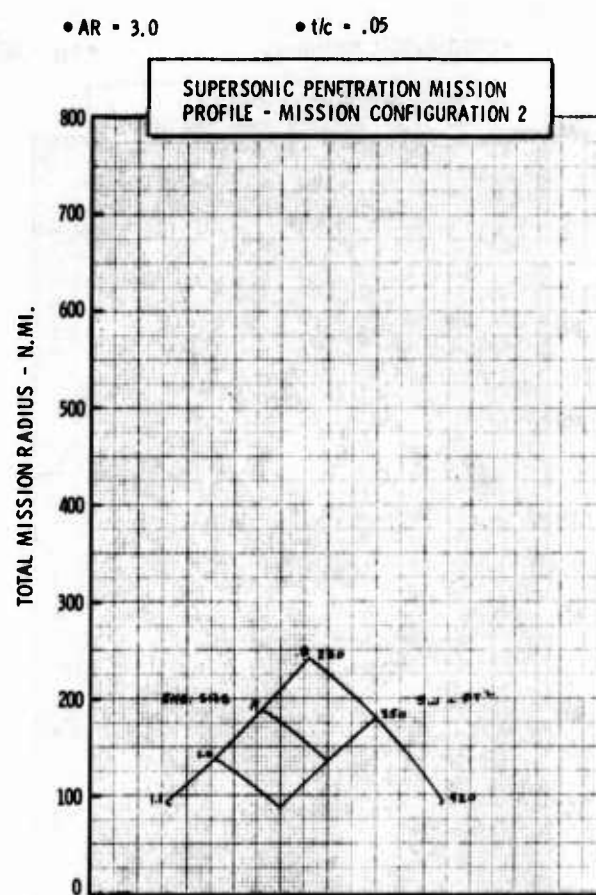
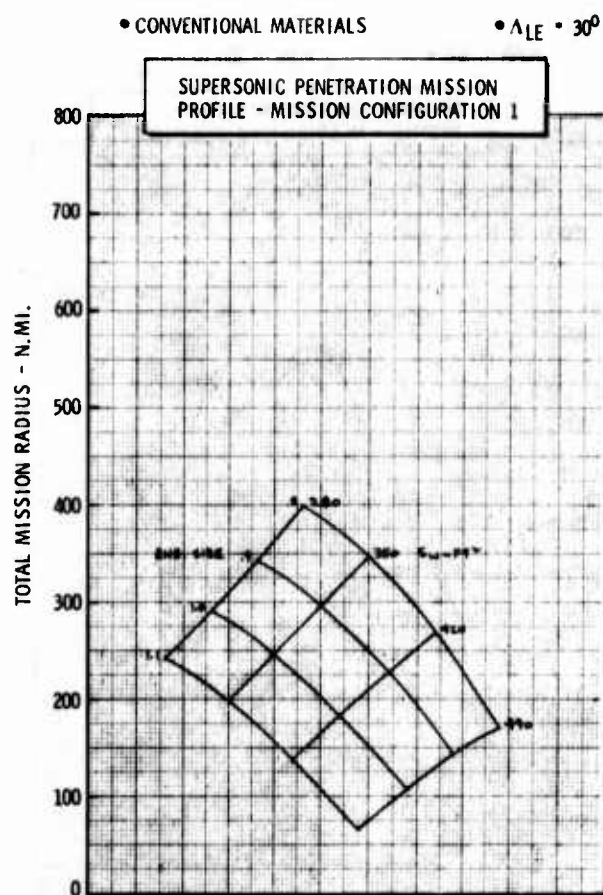


Figure H-14c LWA Mission/Configuration Tradeoff Parametric Data

• CONVENTIONAL MATERIALS

•  $\Lambda_{LE} = 30^\circ$

•  $AR = 4.0$

•  $t/c = .05$

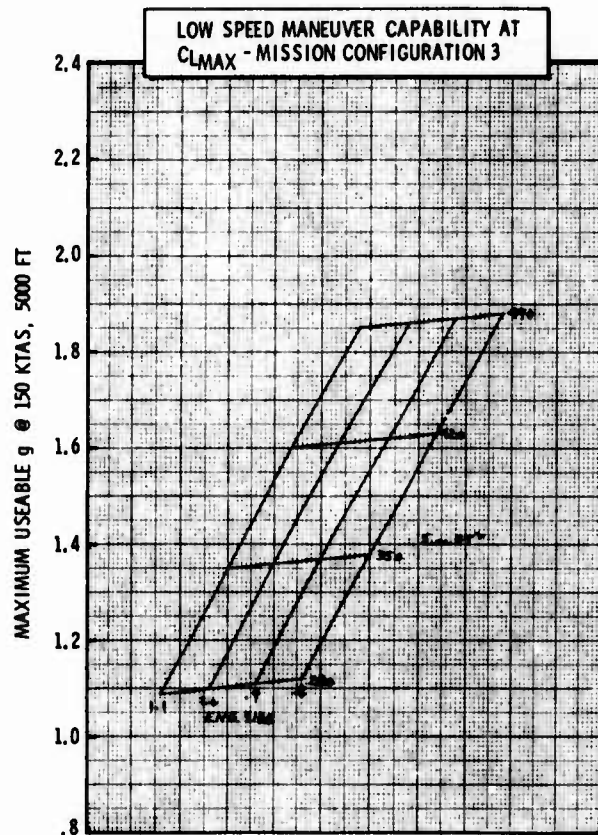
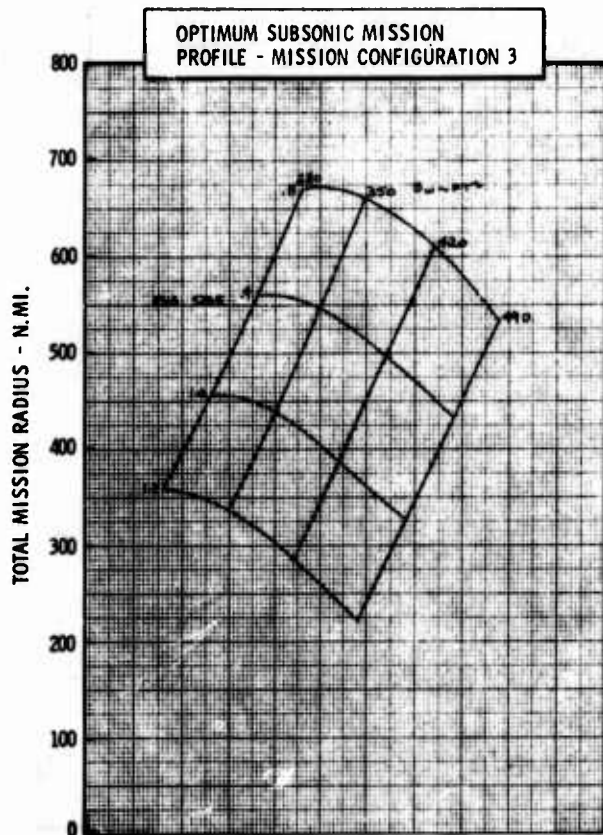
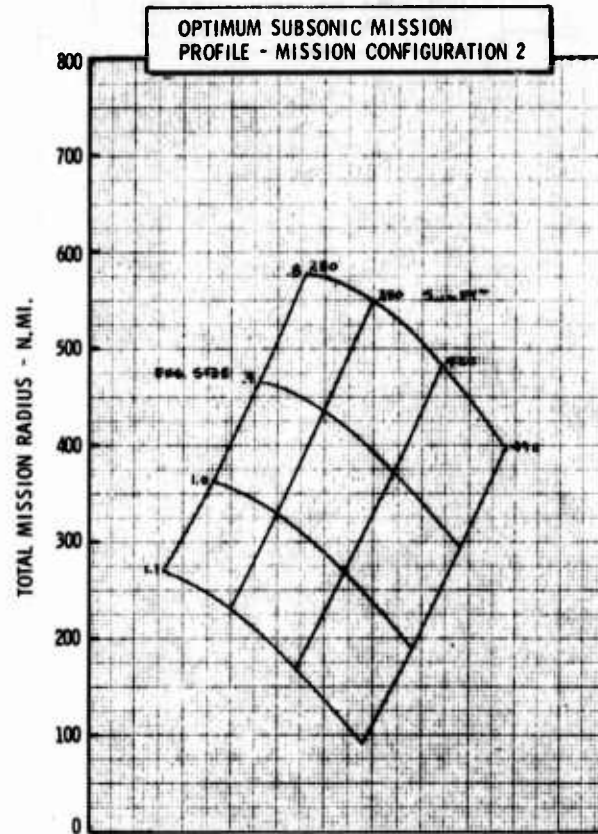
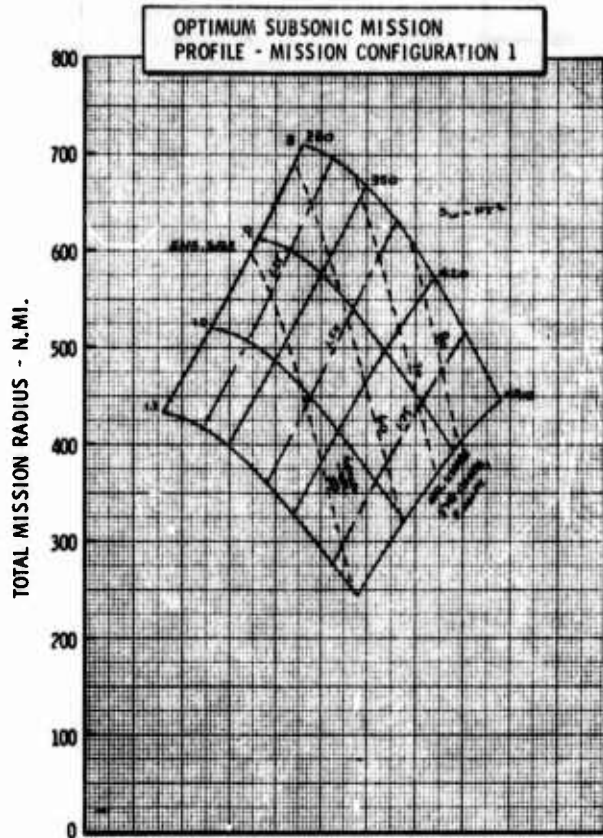


Figure H-15a LWA Mission/Configuration Tradeoff Parametric Data

• CONVENTIONAL MATERIALS

•  $\Delta LE = 30^\circ$

•  $AR = 4.0$

•  $t/c = .05$

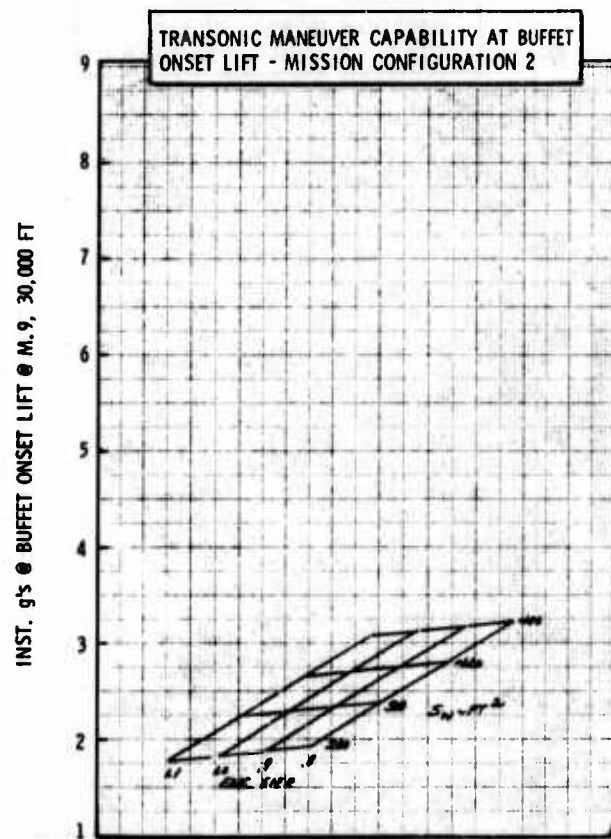
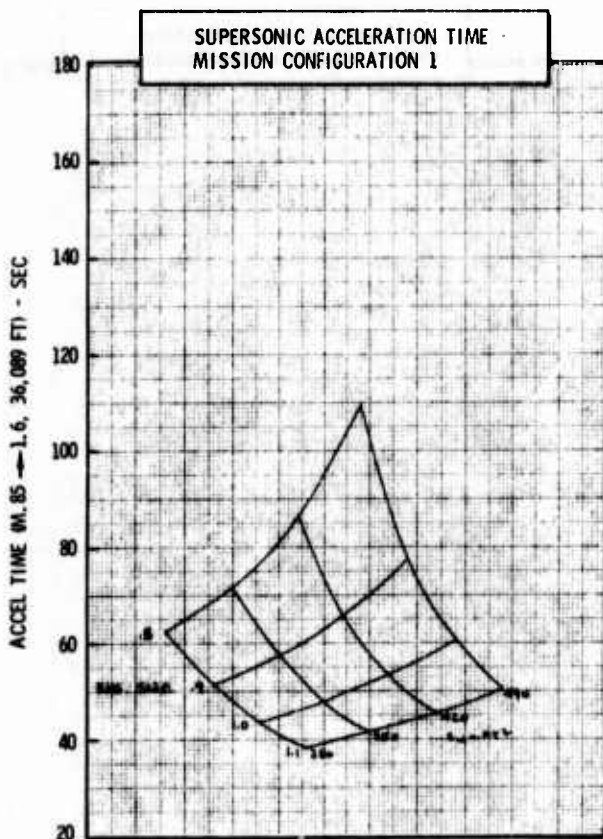
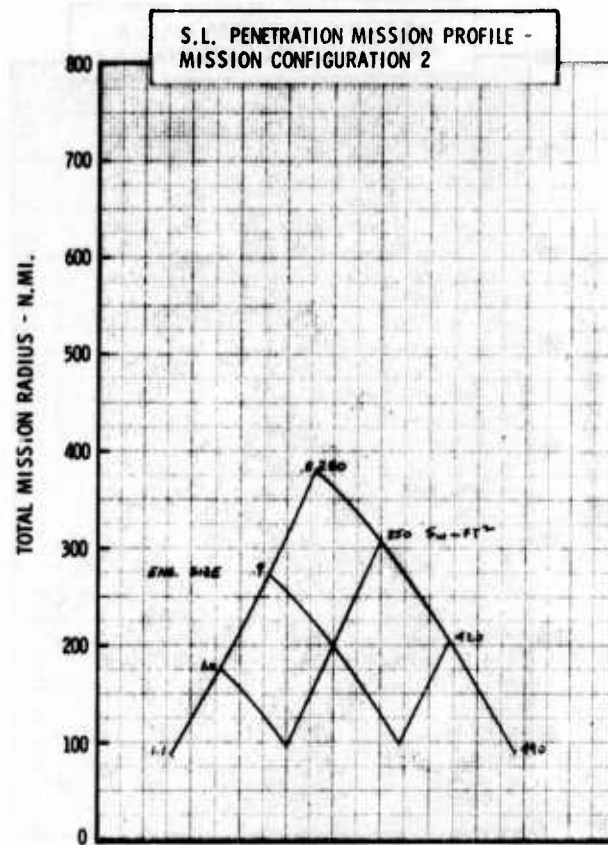
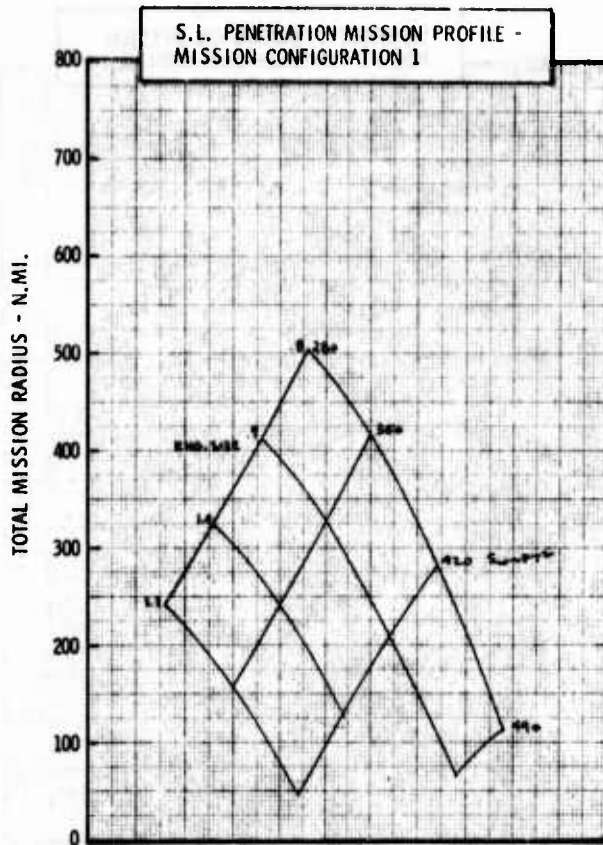
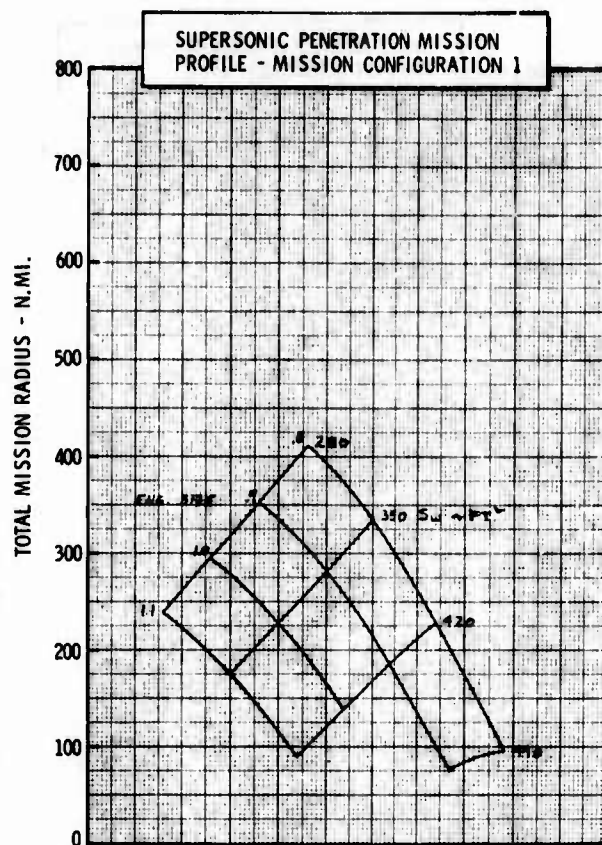


Figure H-15b LWA Mission/Configuration Tradeoff Parametric Data



• CONVENTIONAL MATERIALS

•  $\Delta LE = 30^\circ$



• AR = 4.0

•  $t/c = .05$

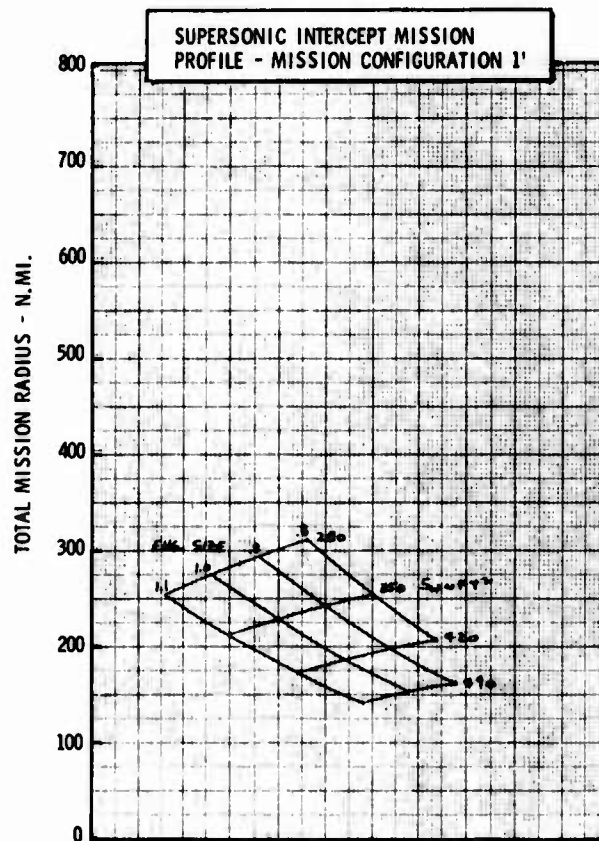
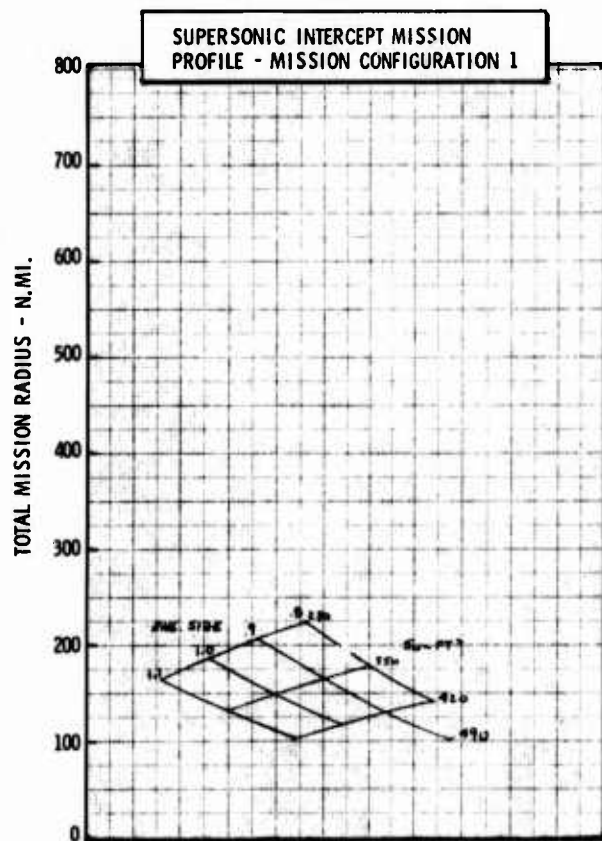
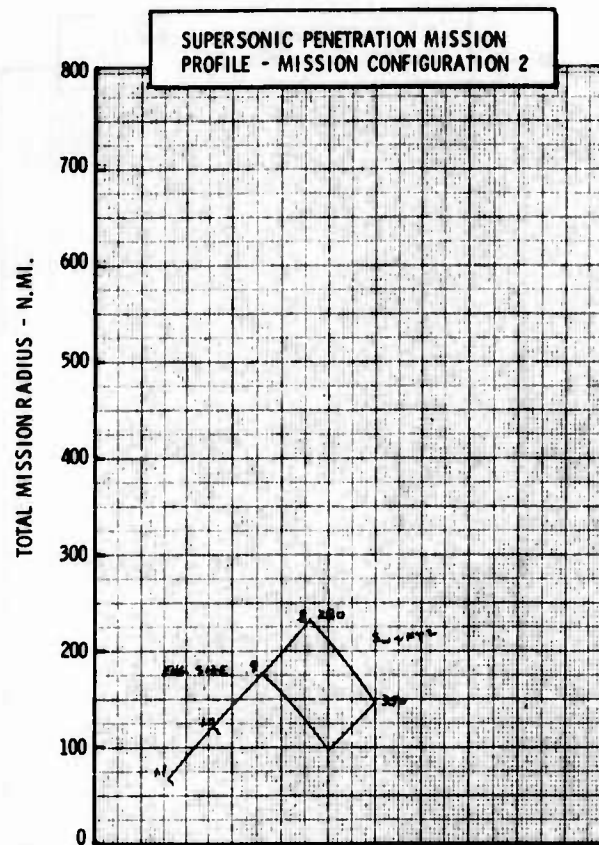


Figure H-15c LWA Mission/Configuration Tradeoff Parametric Data

• CONVENTIONAL MATERIALS

•  $\Delta LE = 30^\circ$

•  $AR = 5.0$

•  $t/c = .05$

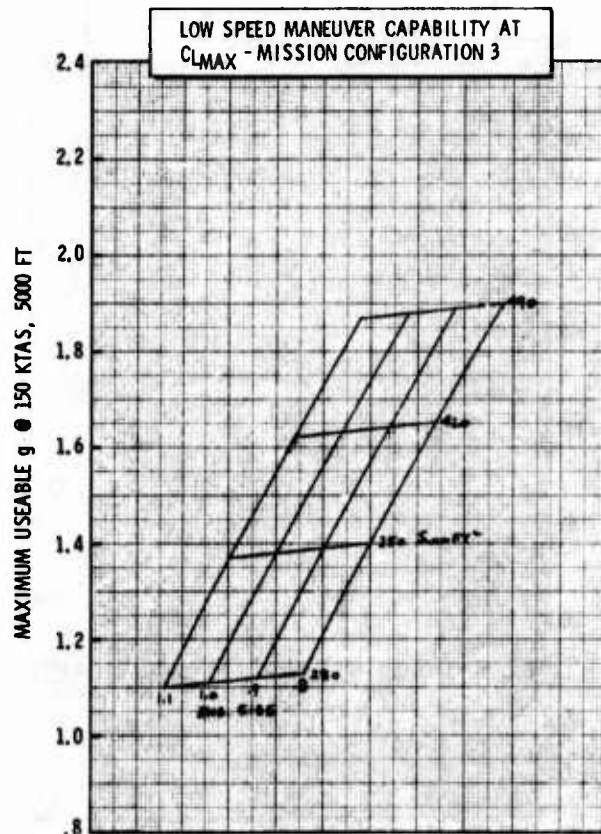
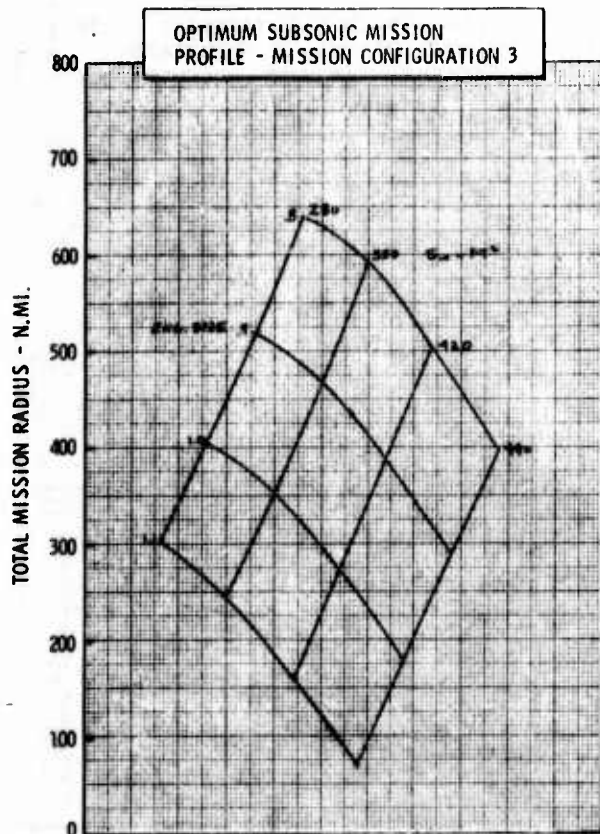
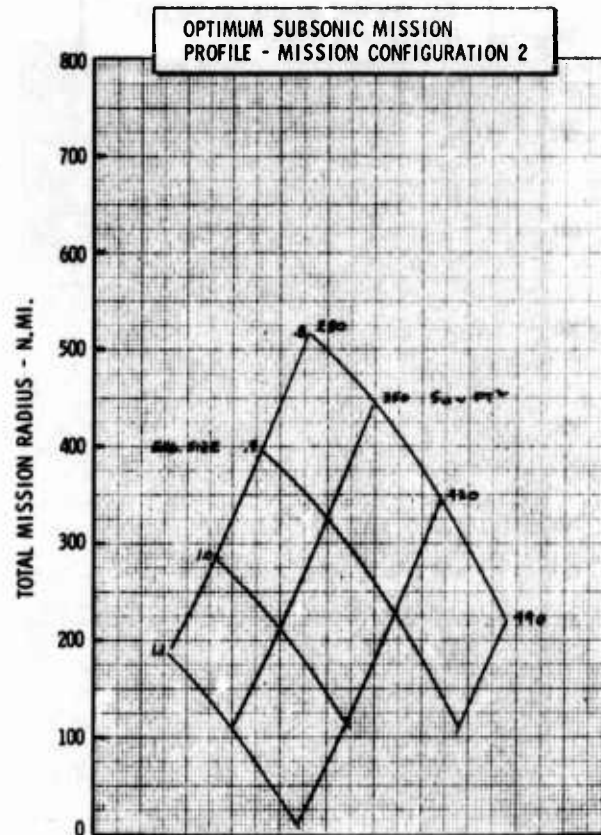
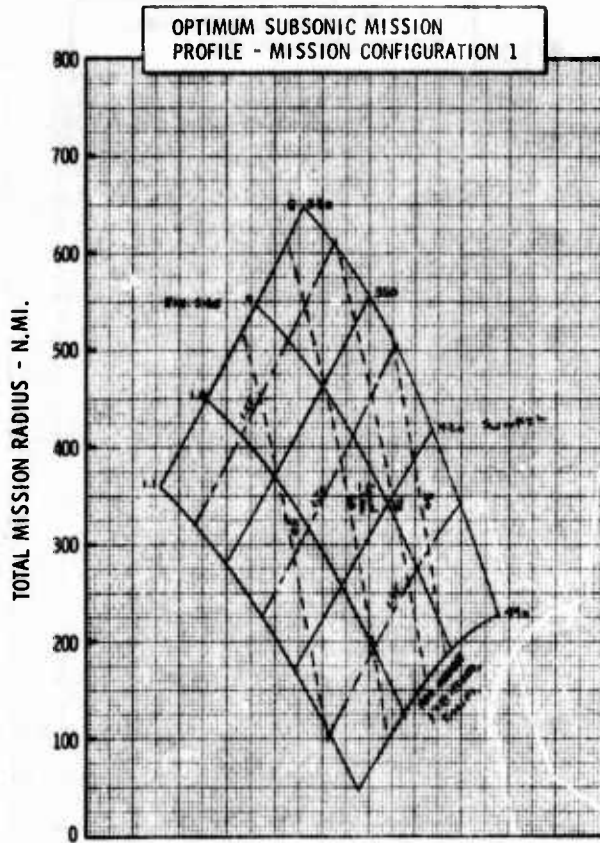


Figure H-16a LWA Mission/Configuration Tradeoff Parametric Data

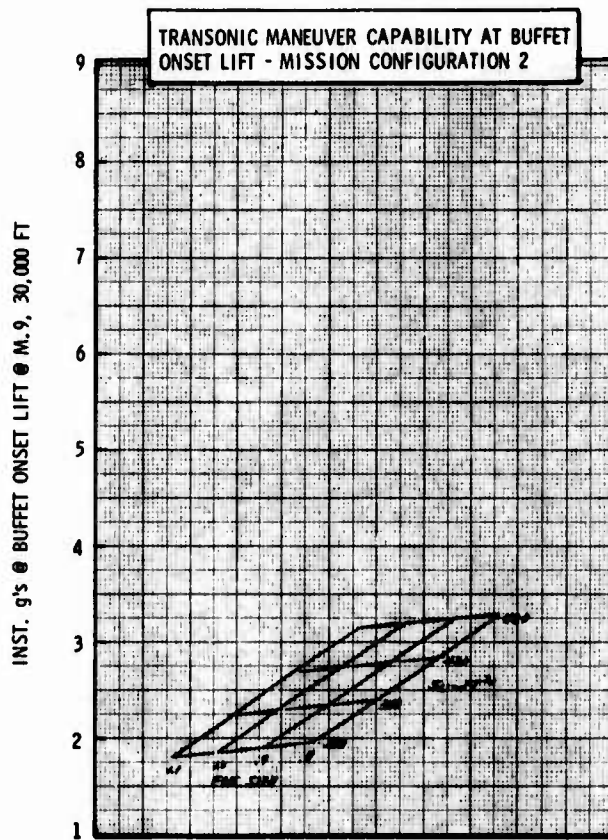
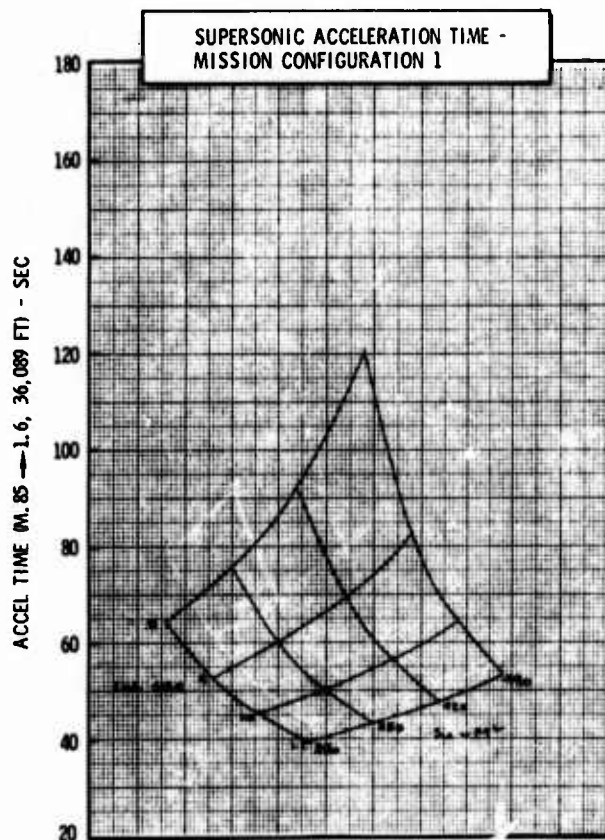
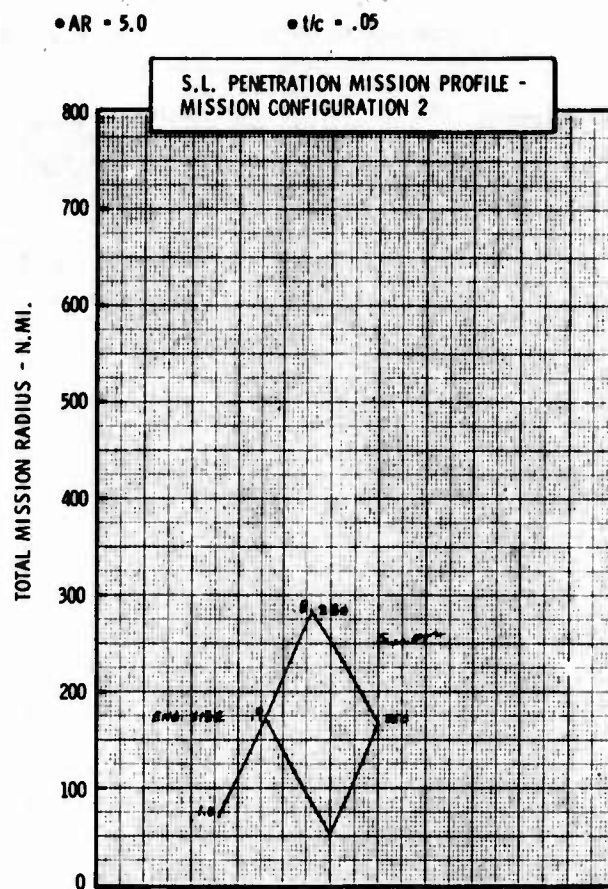
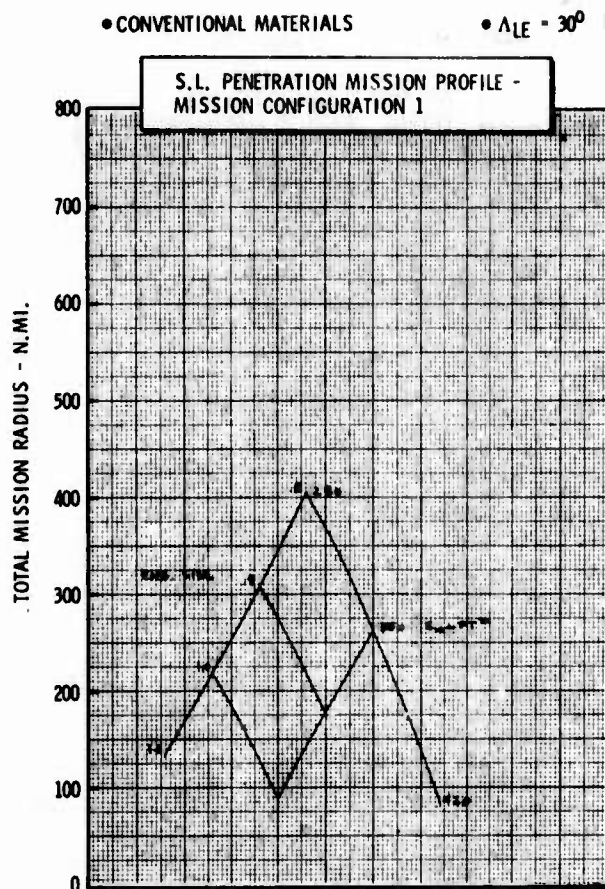


Figure H-16b LWA Mission/Configuration Tradeoff Parametric Data



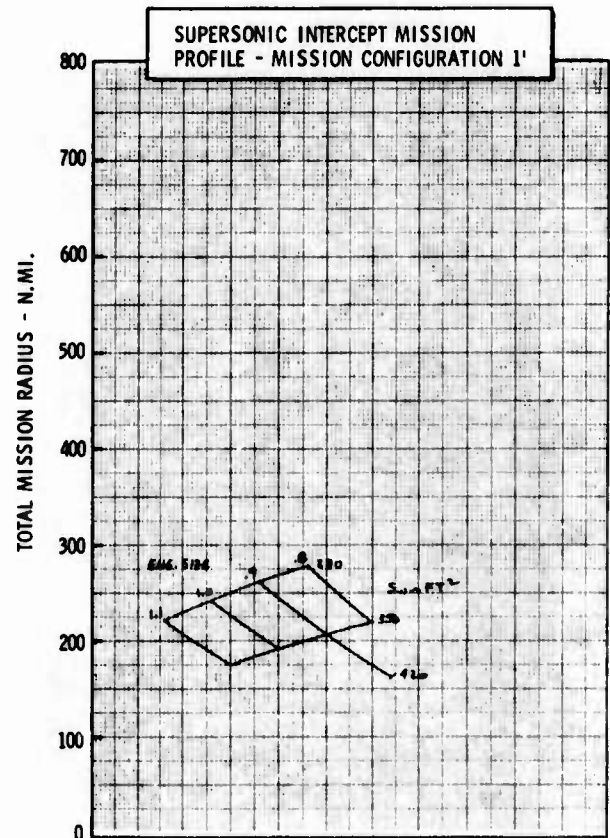
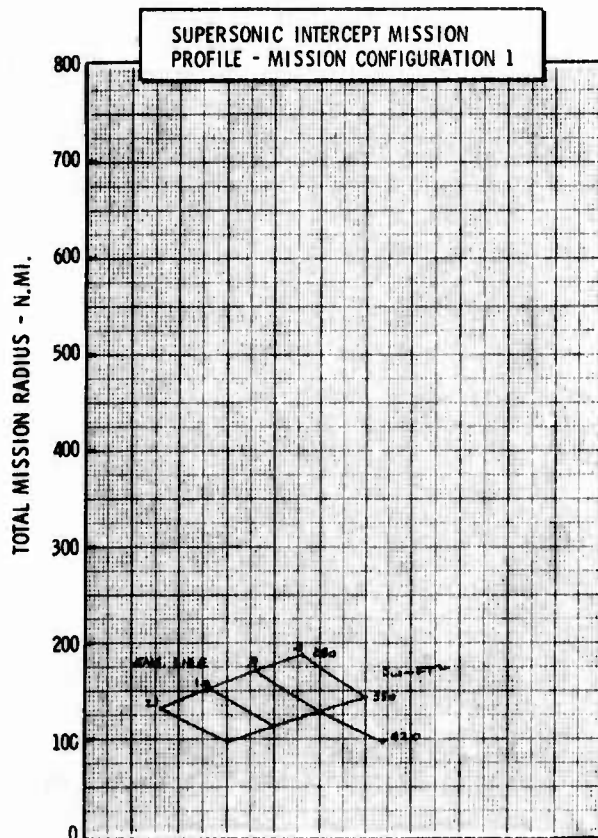
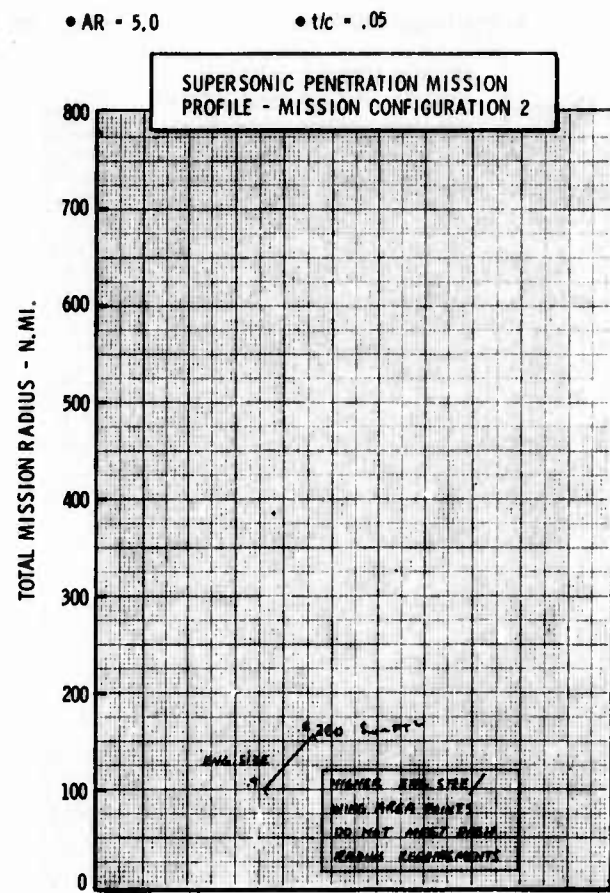
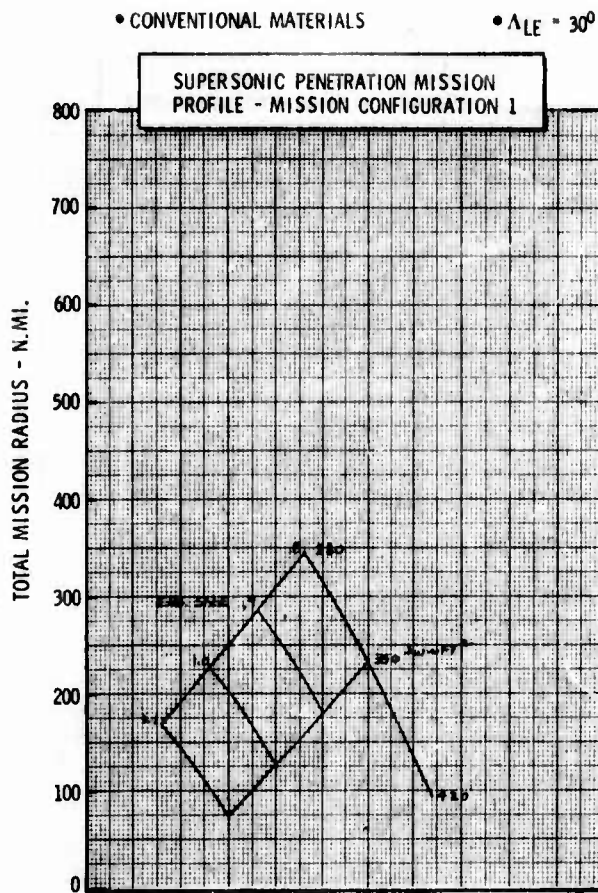


Figure H-16c LWA Mission/Configuration Tradeoff Parametric Data

• CONVENTIONAL MATERIALS

•  $\Delta LE = 40^\circ$

•  $AR = 3.0$

•  $t/c = .05$

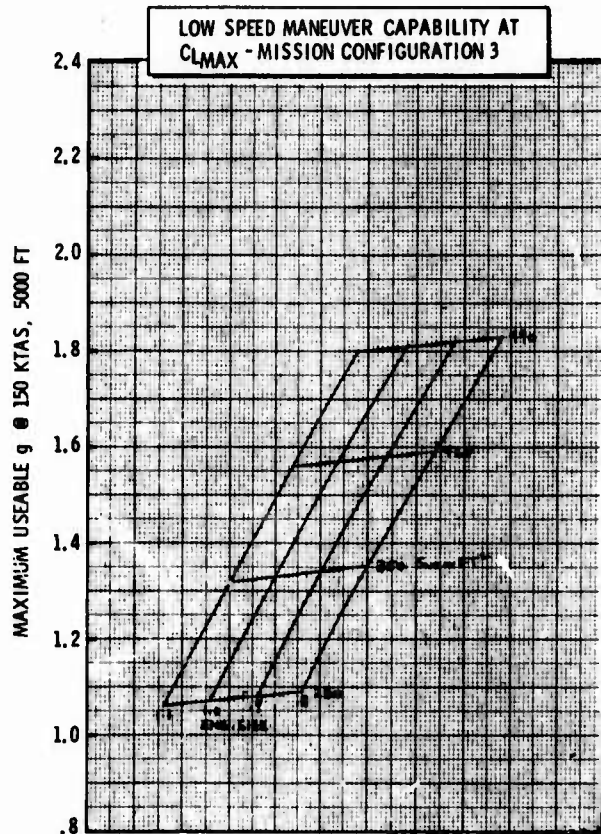
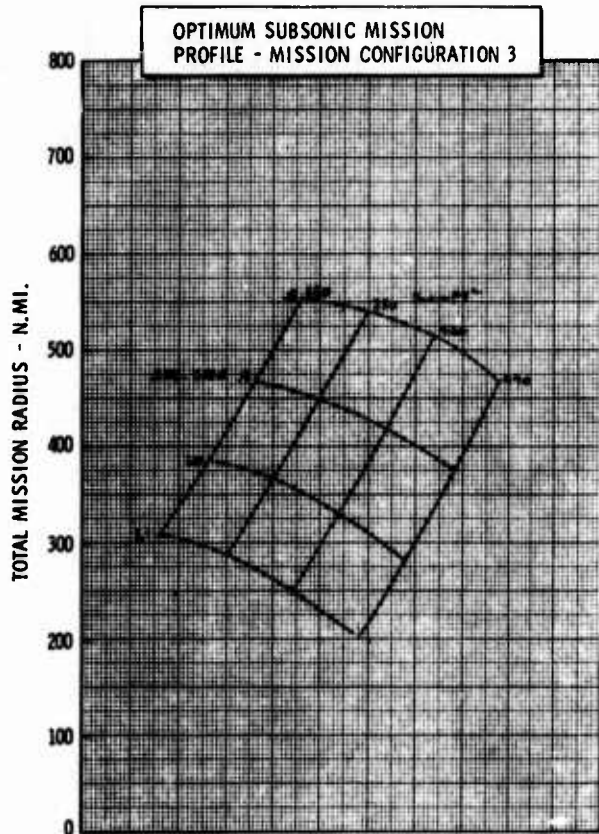
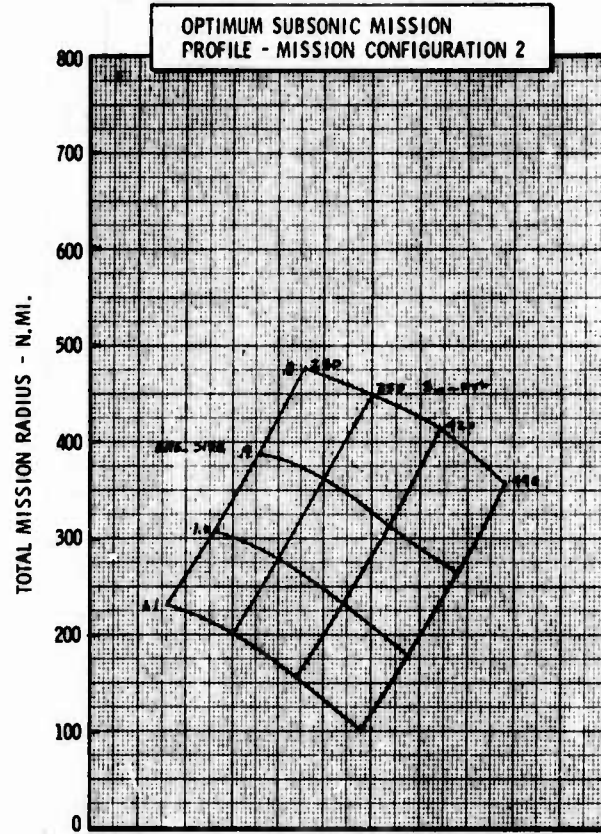
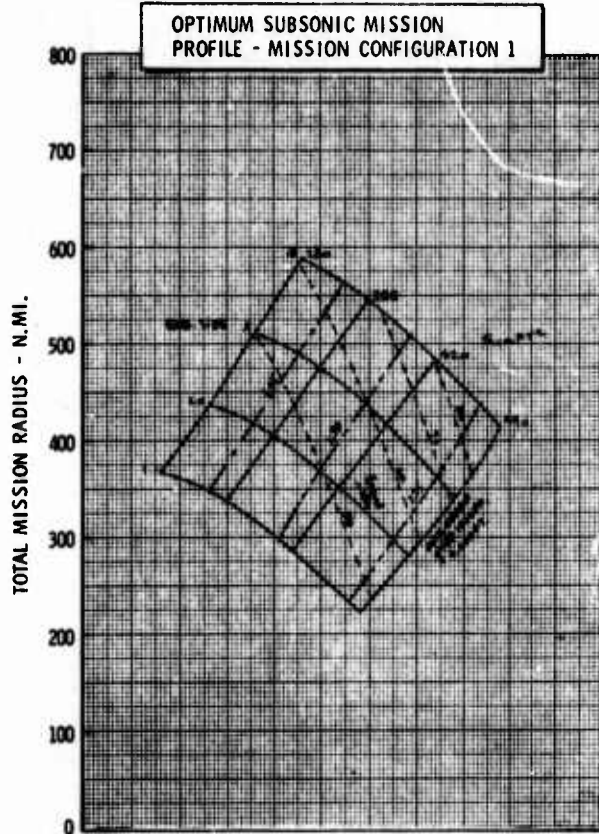


Figure H-17a LWA Mission/Configuration Tradeoff Parametric Data

• CONVENTIONAL MATERIALS

•  $\Delta_{LE} = 40^\circ$

• AR = 3.0

•  $t/c = .05$

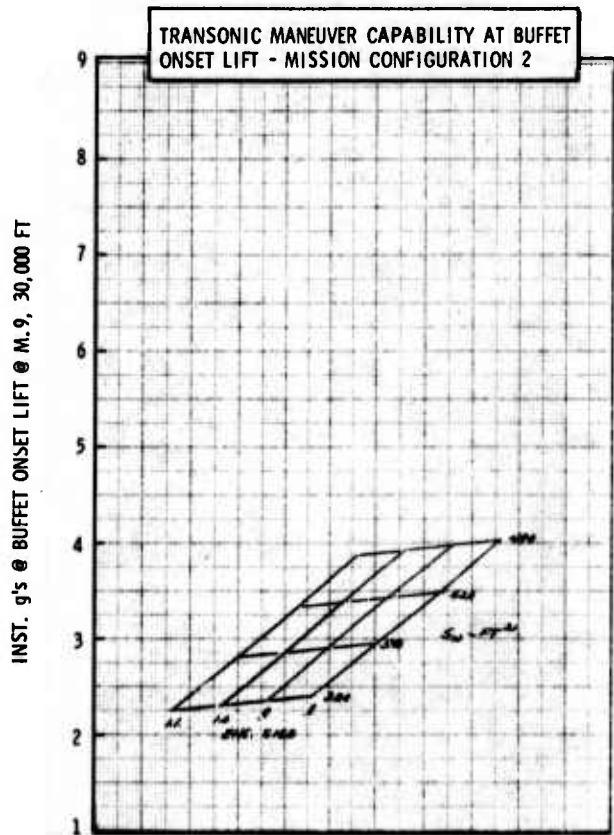
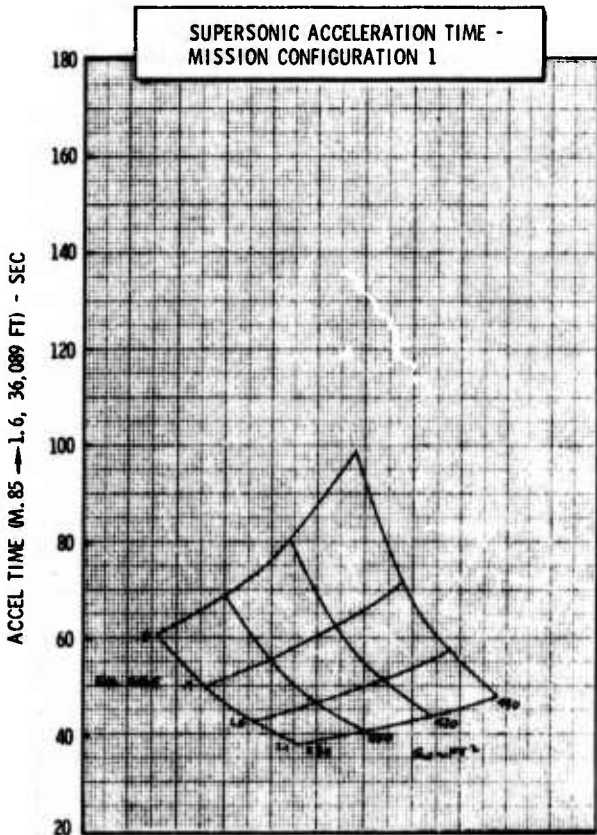
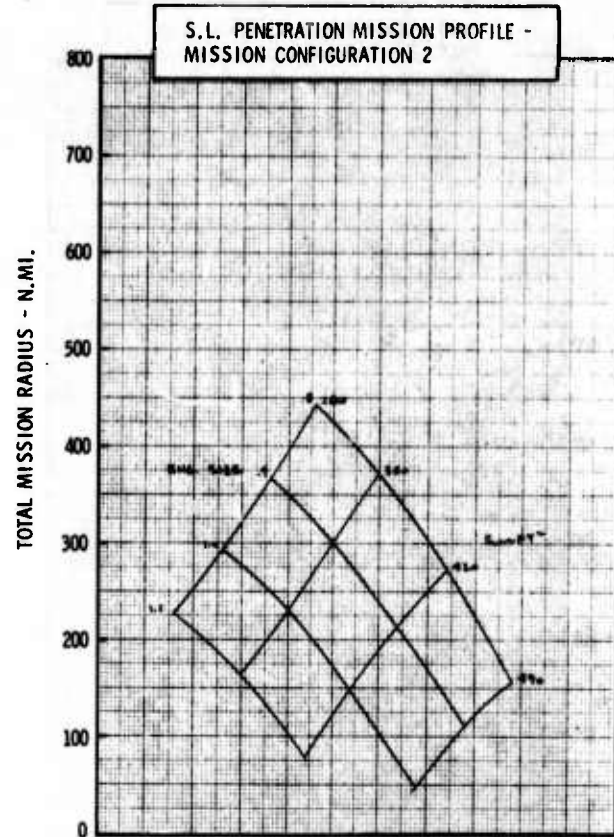
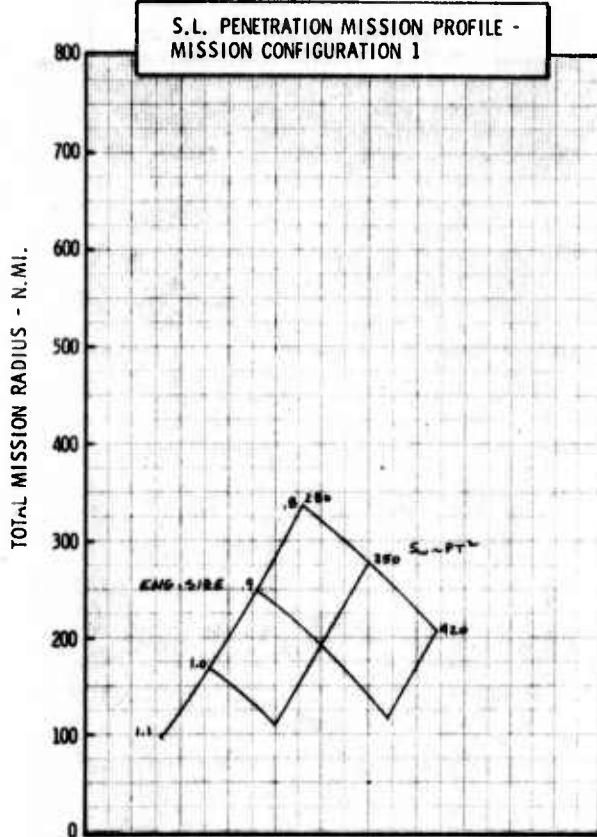


Figure H-17b LWA Mission/Configuration Tradeoff Parametric Data



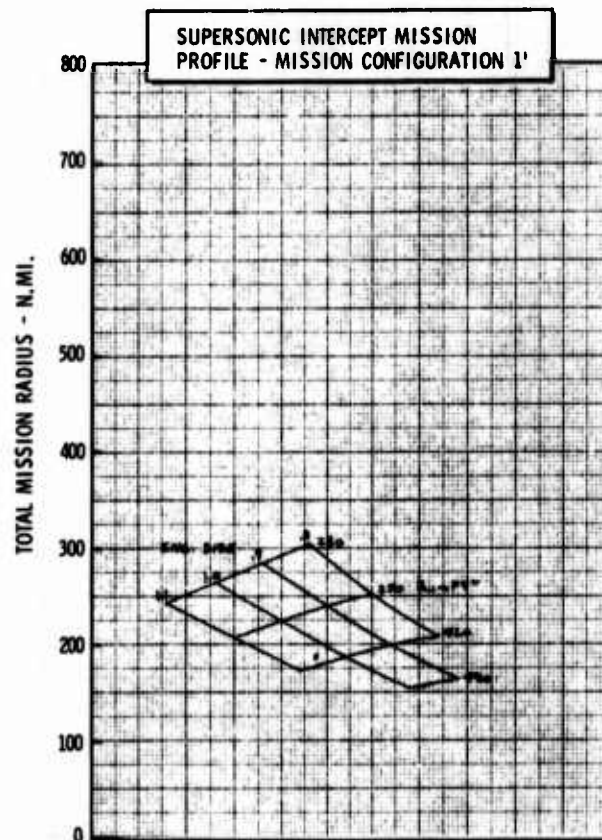
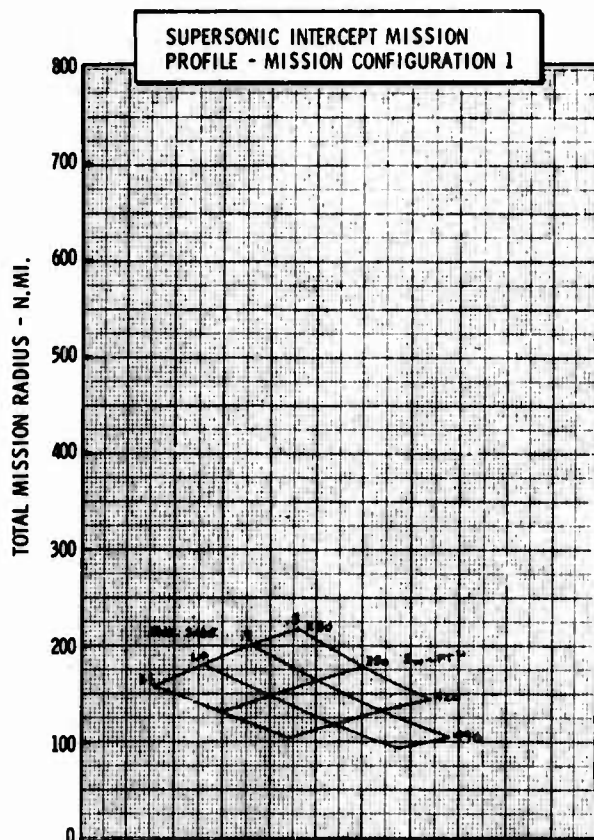
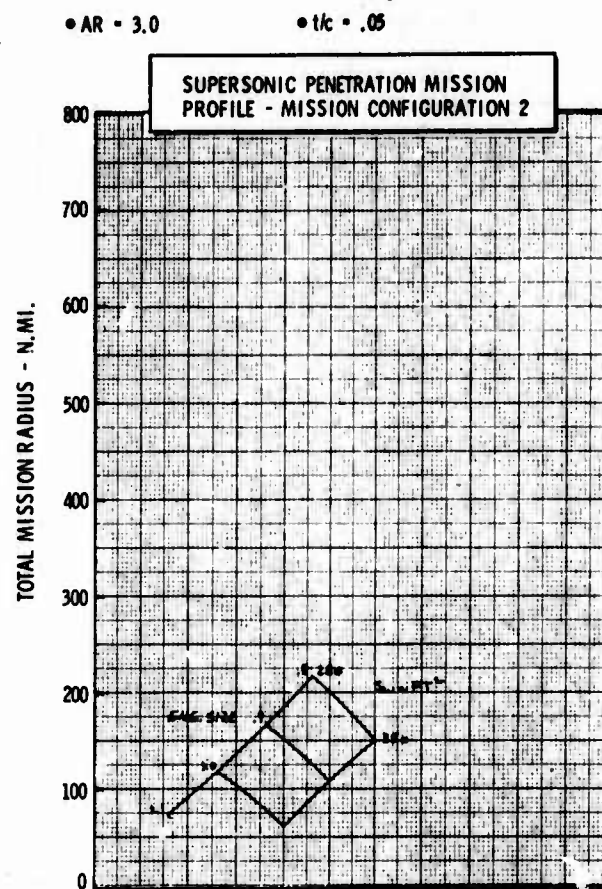
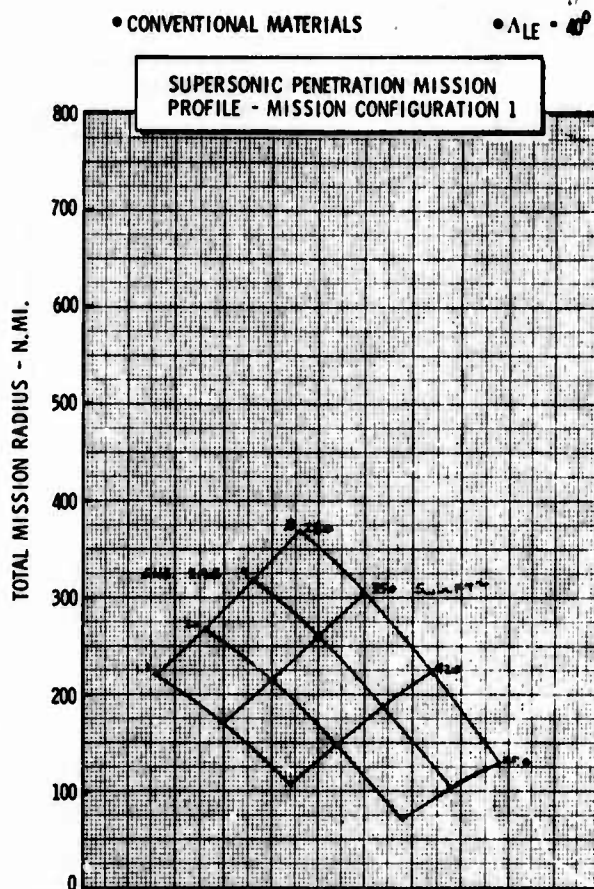


Figure H-17c LWA Mission/Configuration Tradeoff Parametric Data

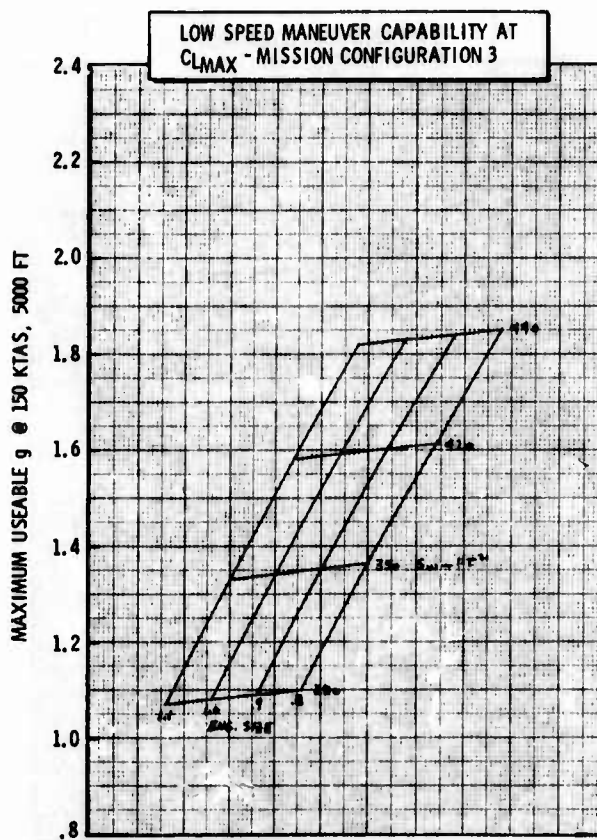
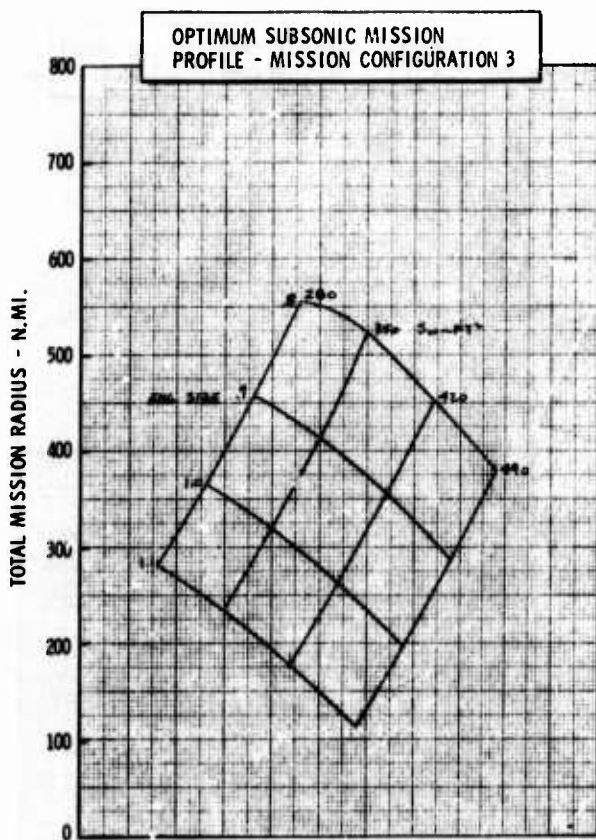
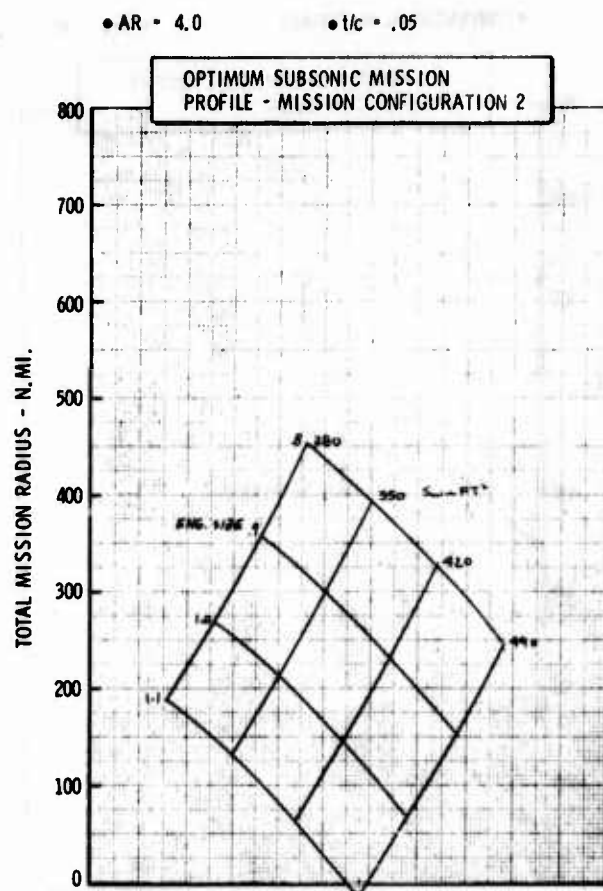
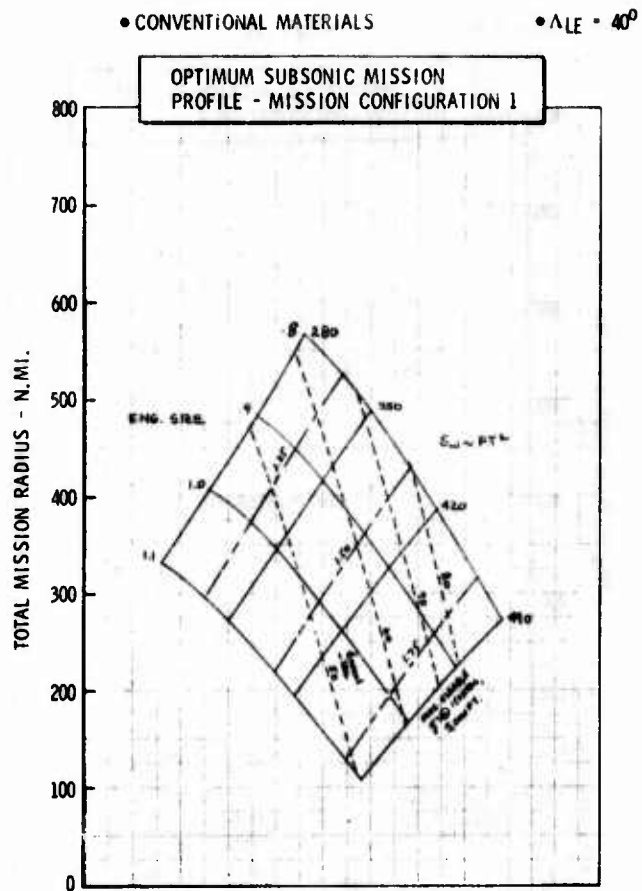


Figure H-18a LWA Mission/Configuration Tradeoff Parametric Data

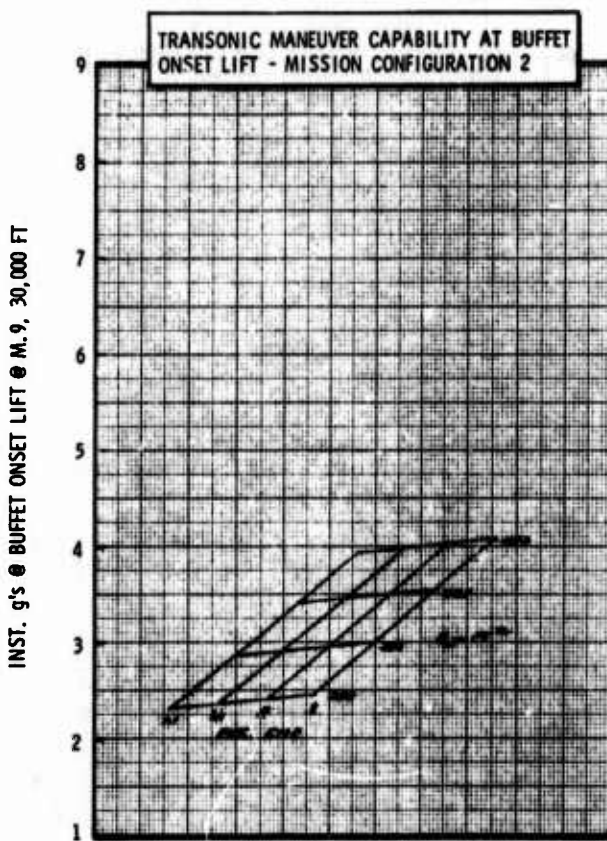
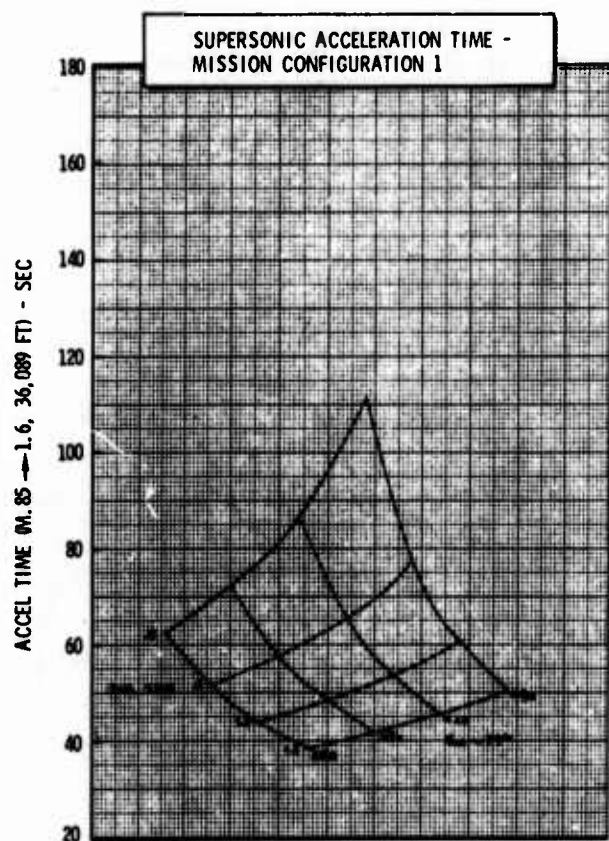
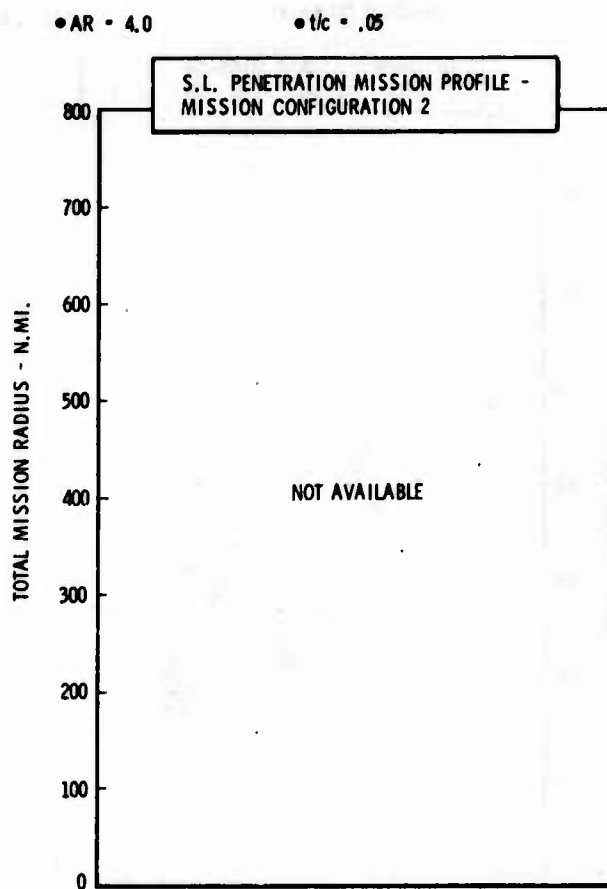
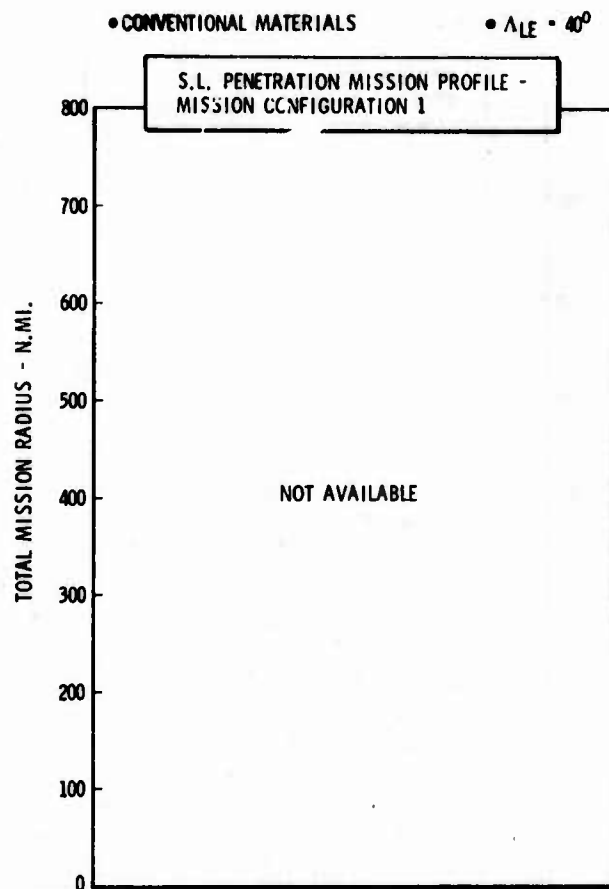


Figure H-18b LWA Mission/Configuration Tradeoff Parametric Data



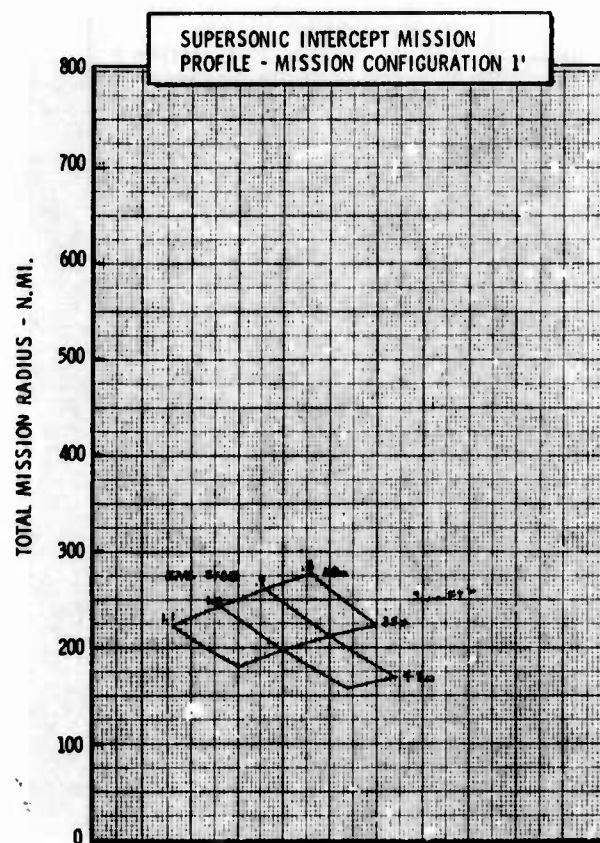
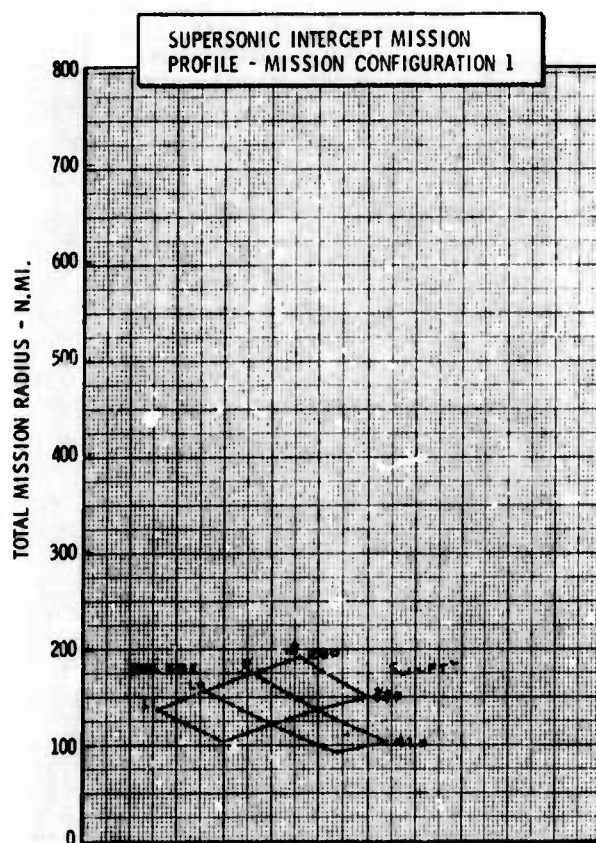
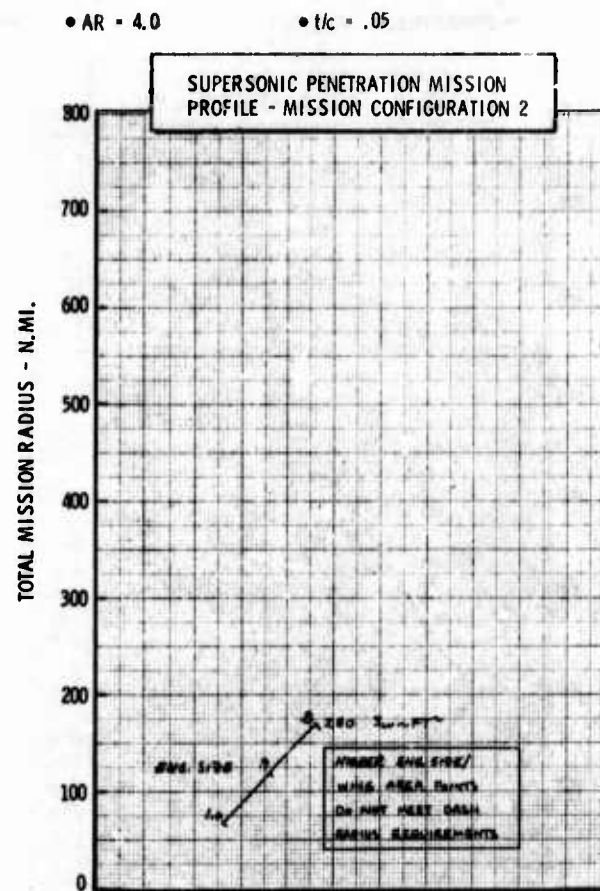
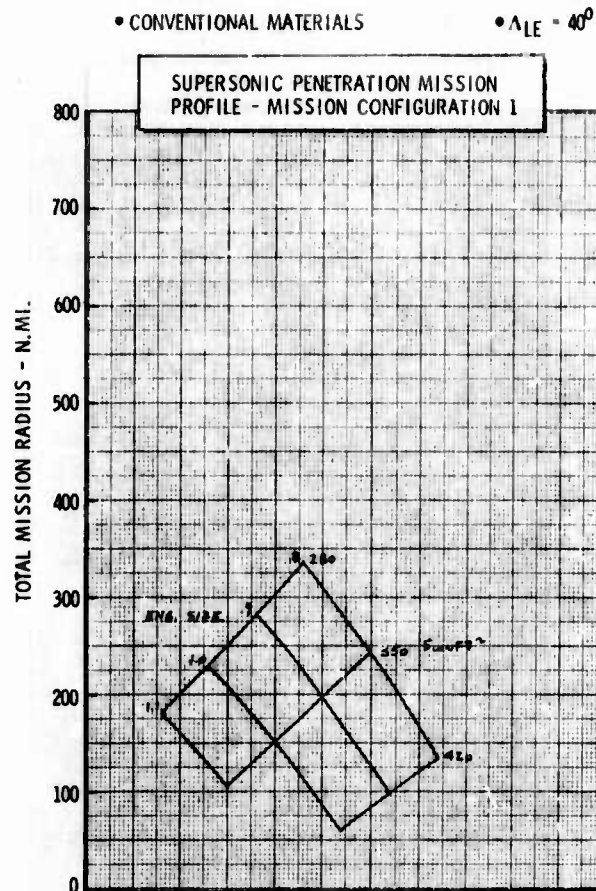


Figure H-18c LWA Mission/Configuration Tradeoff Parametric Data

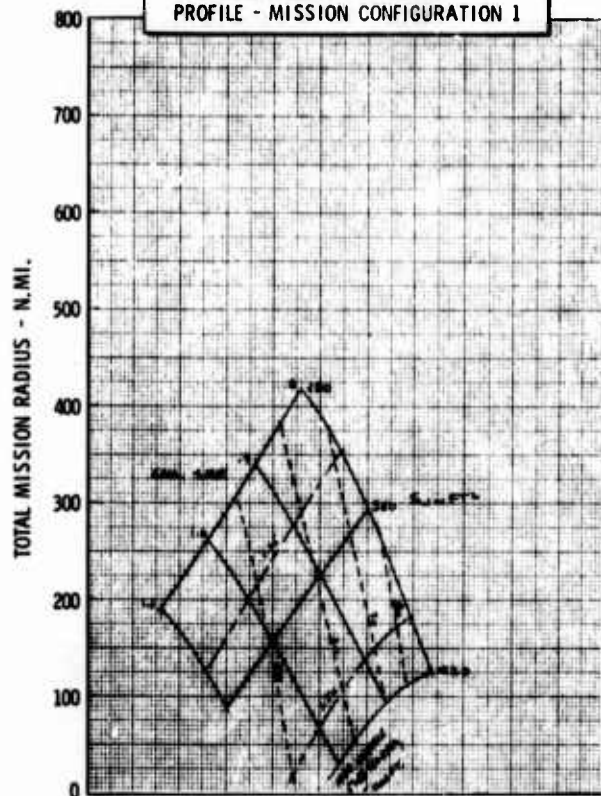
• CONVENTIONAL MATERIALS

•  $\Lambda_{LE} = 40^\circ$

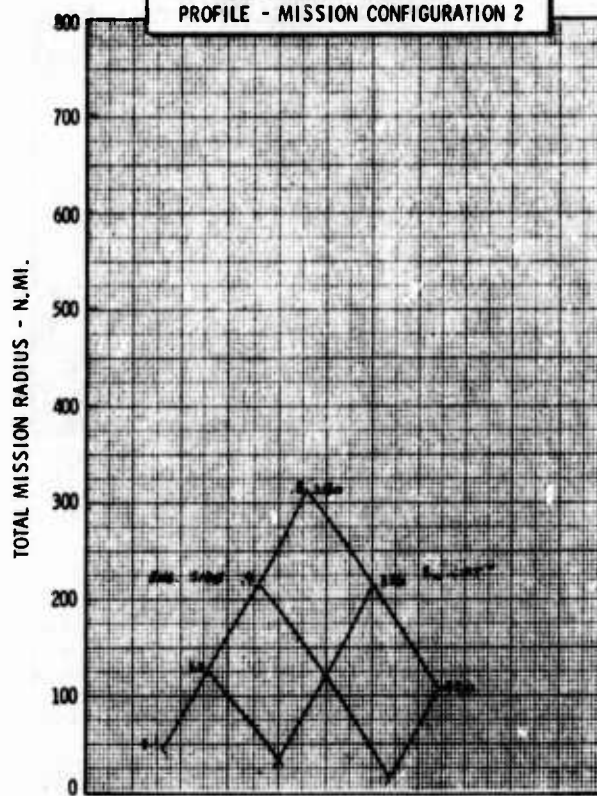
•  $AR = 5.0$

•  $t/c = .05$

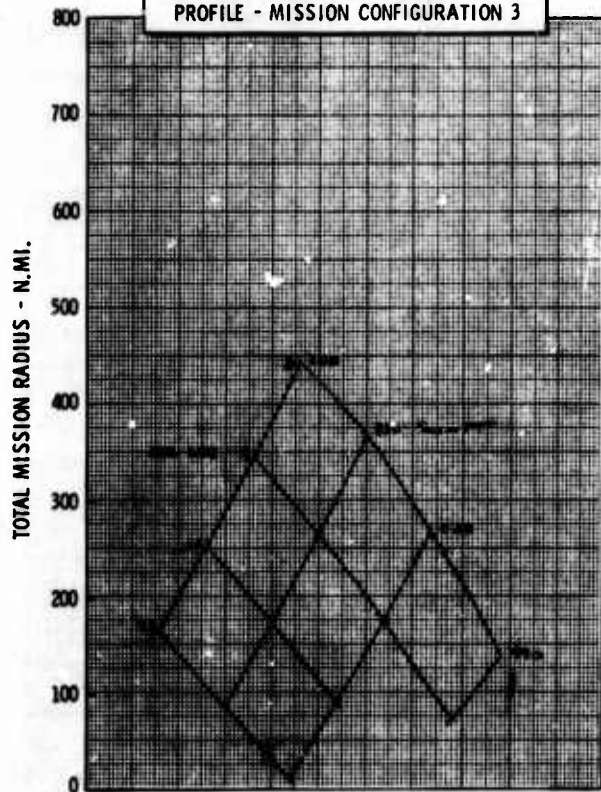
OPTIMUM SUBSONIC MISSION  
PROFILE - MISSION CONFIGURATION 1



OPTIMUM SUBSONIC MISSION  
PROFILE - MISSION CONFIGURATION 2



OPTIMUM SUBSONIC MISSION  
PROFILE - MISSION CONFIGURATION 3



LOW SPEED MANEUVER CAPABILITY AT  
 $CL_{MAX}$  - MISSION CONFIGURATION 3

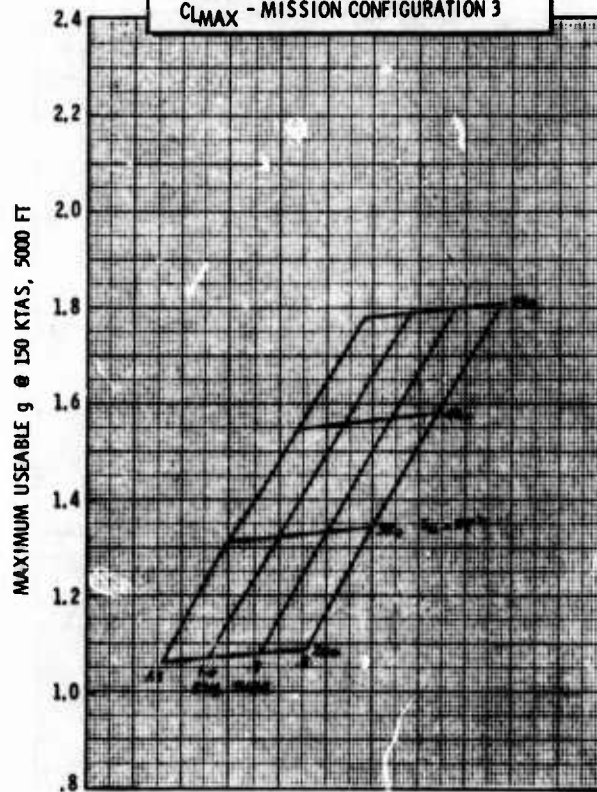


Figure H-19a LWA Mission/Configuration Tradeoff Parametric Data

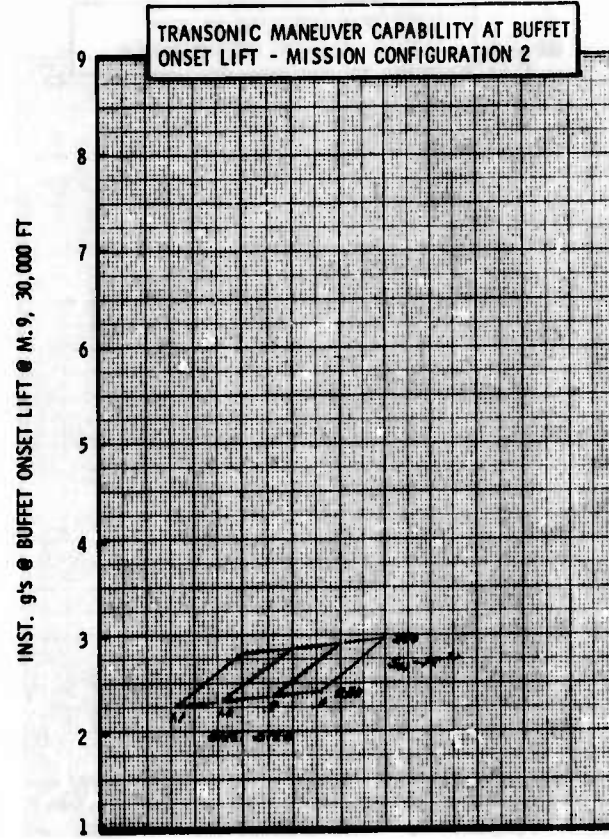
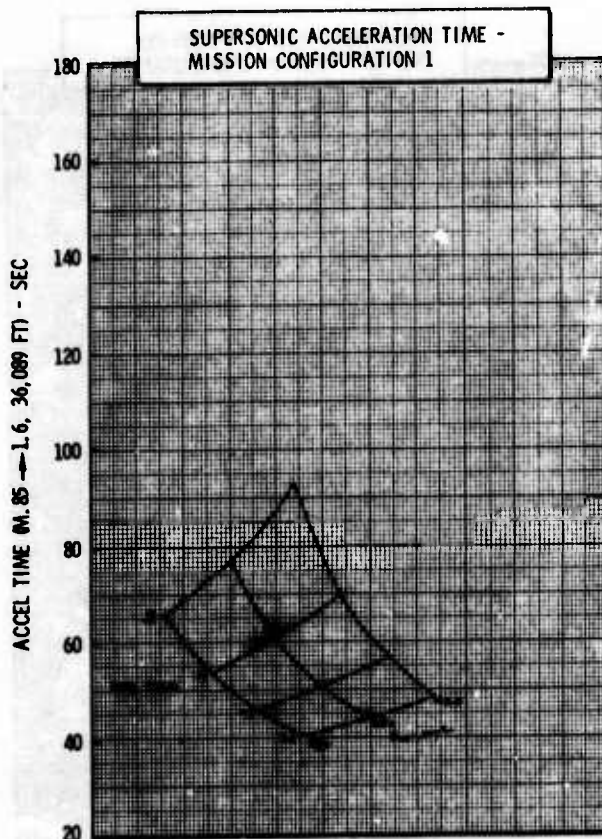
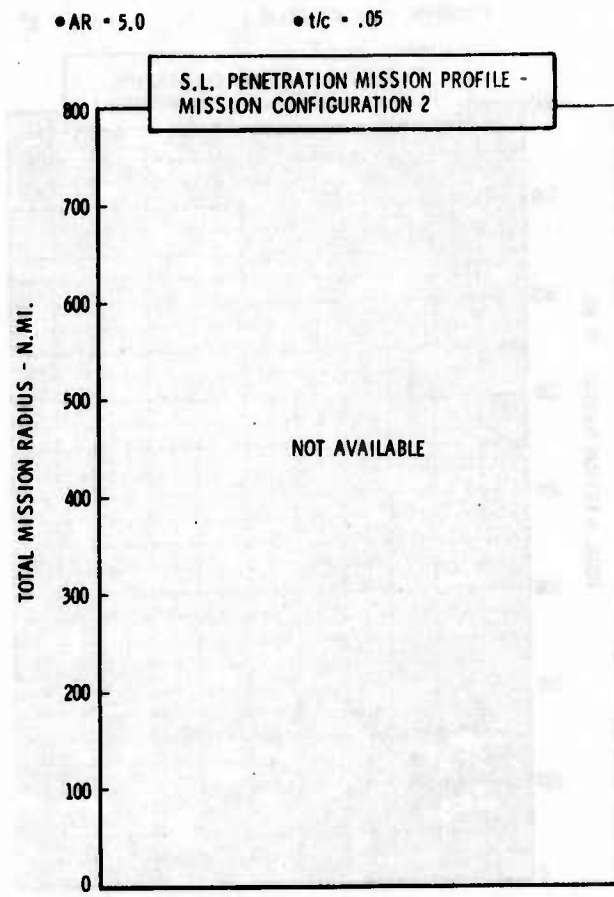
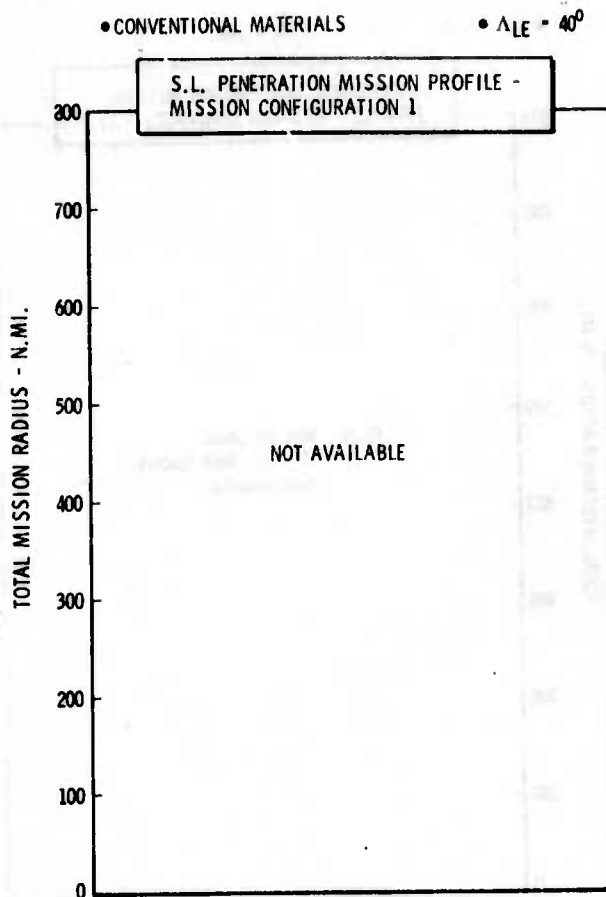


Figure H-19b LWA Mission/Configuration Tradeoff Parametric Data



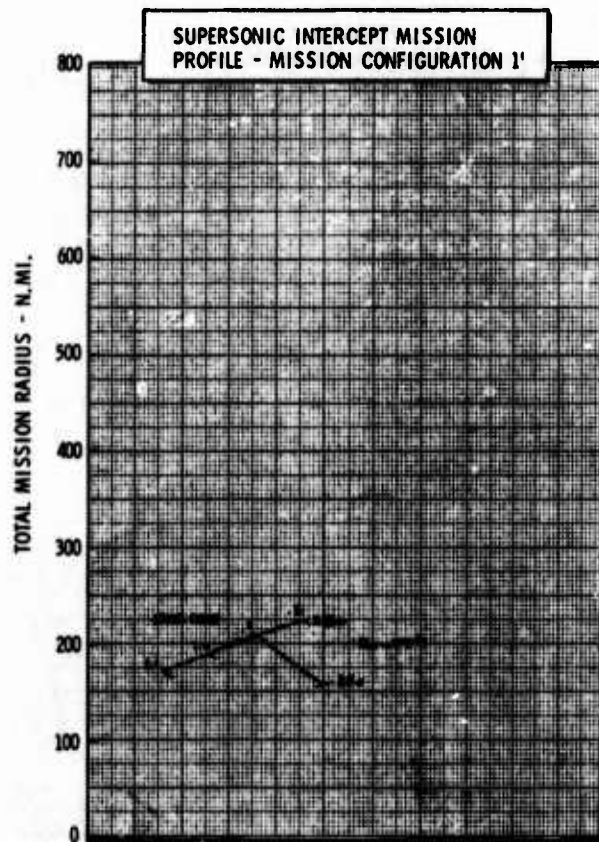
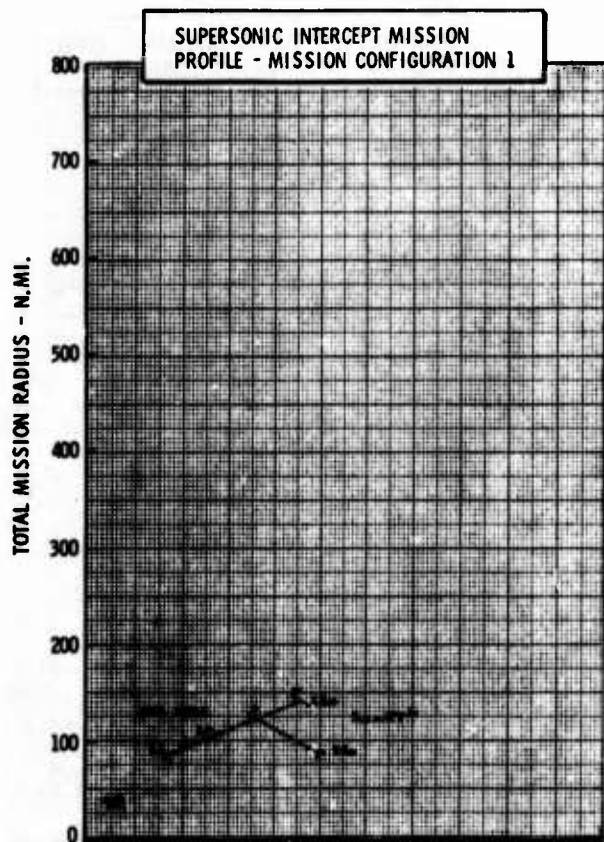
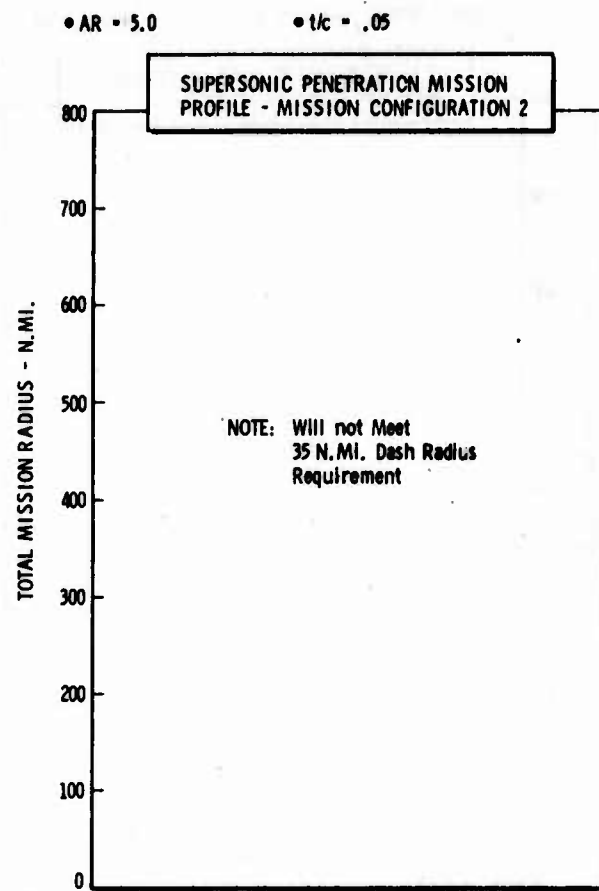
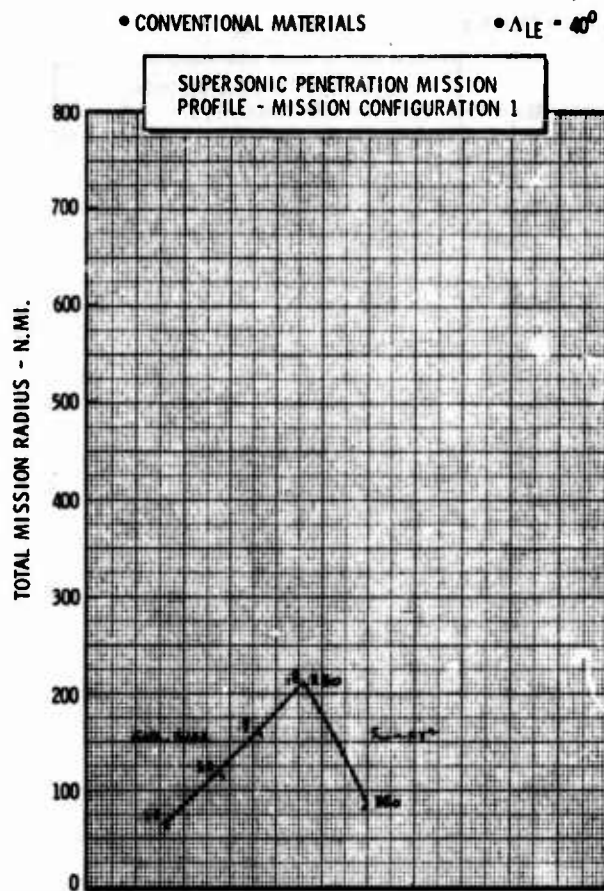


Figure H-19c LWA Mission/Configuration Tradeoff Parametric Data

• CONVENTIONAL MATERIALS

•  $\Lambda_{LE} = 20^\circ$

•  $AR = 3.0$

•  $t/c = .06$

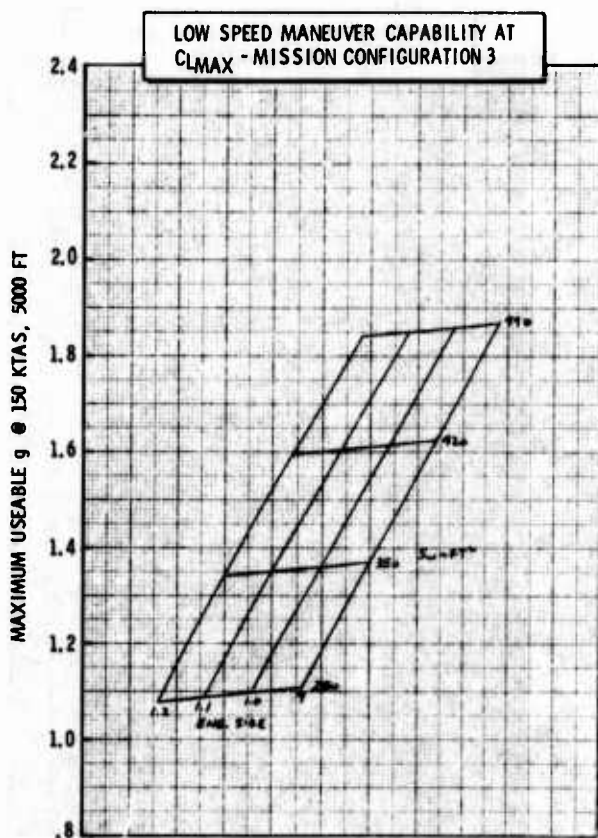
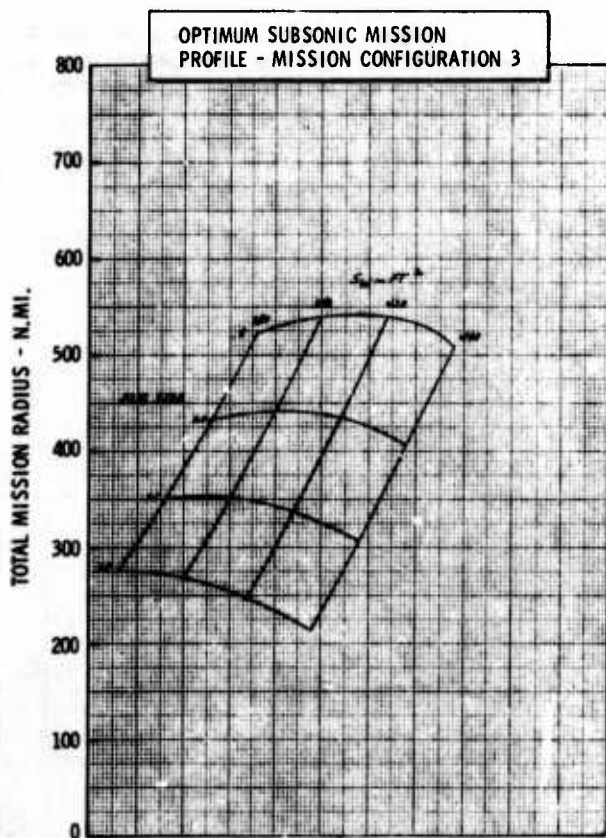
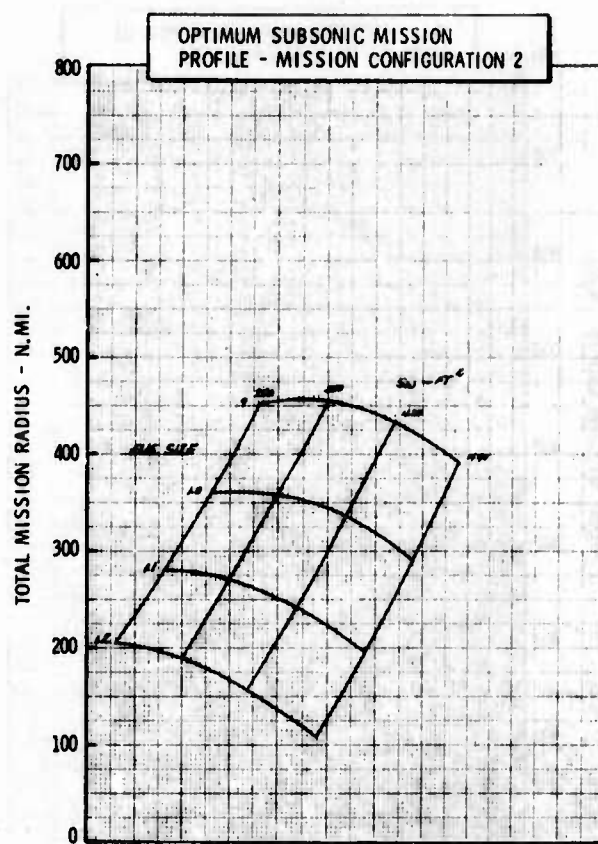
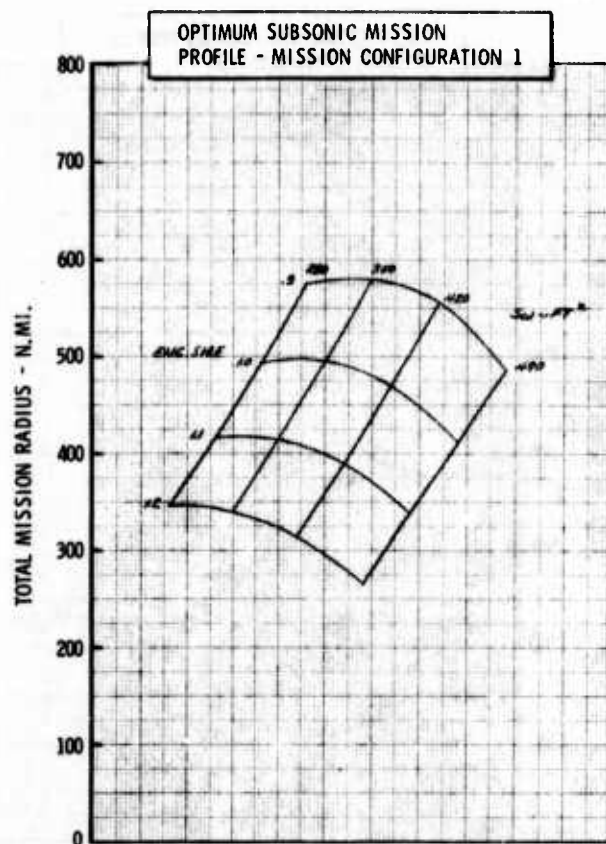


Figure H-20a LWA Mission/Configuration Tradeoff Parametric Data

• CONVENTIONAL MATERIALS

•  $\Delta LE = 2^\circ$

•  $AR = 3.0$

•  $t/c = .06$

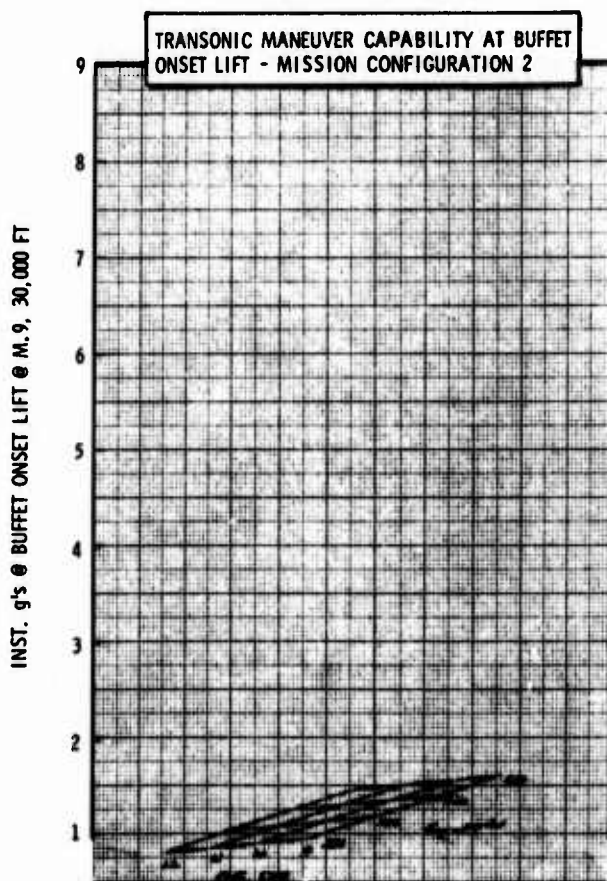
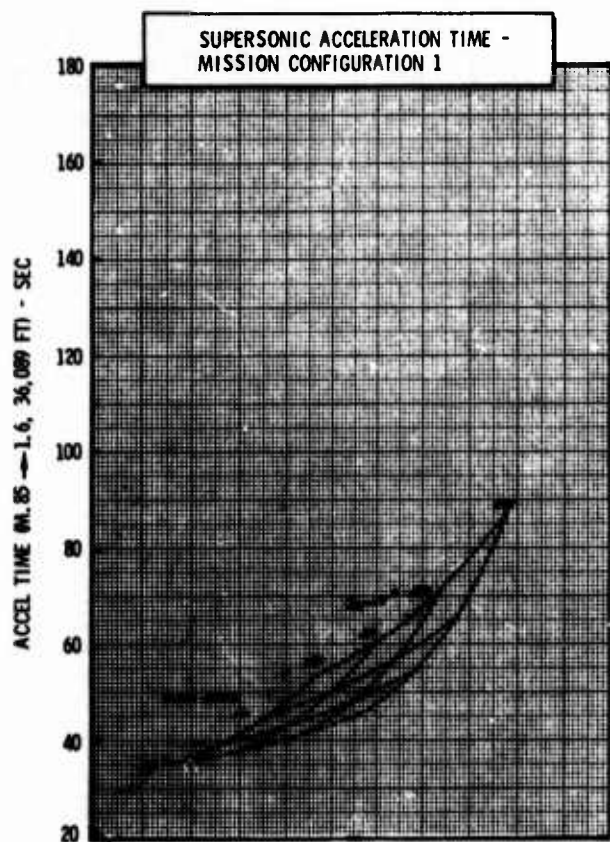
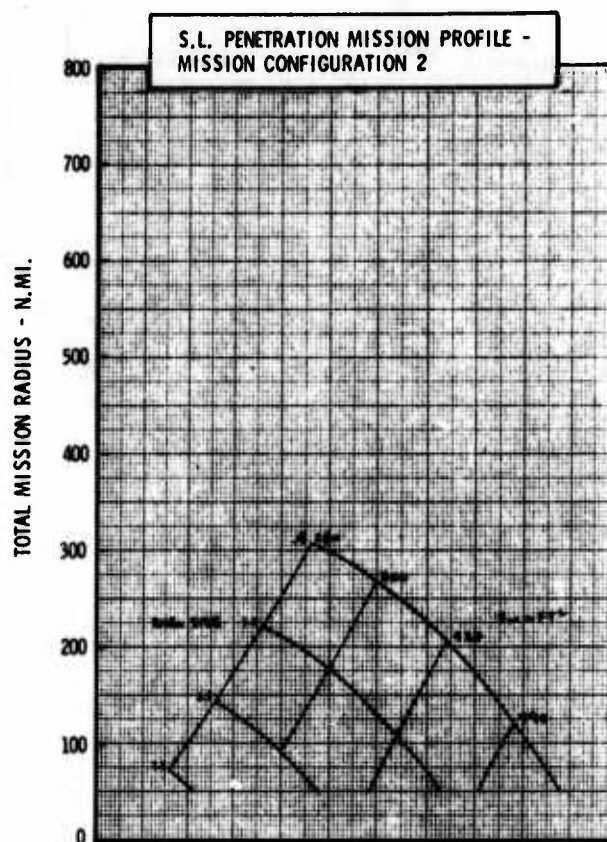
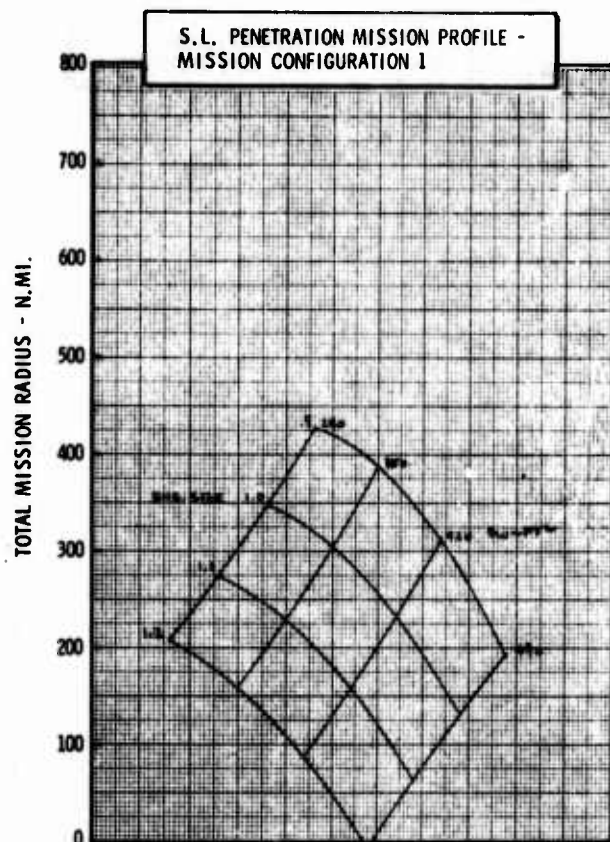


Figure H-20b LWA Mission/Configuration Tradeoff Parametric Data



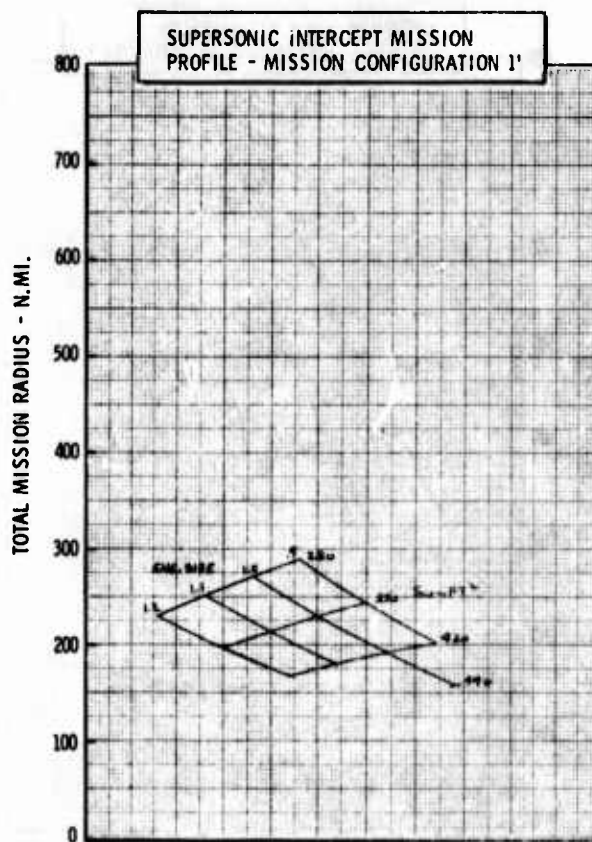
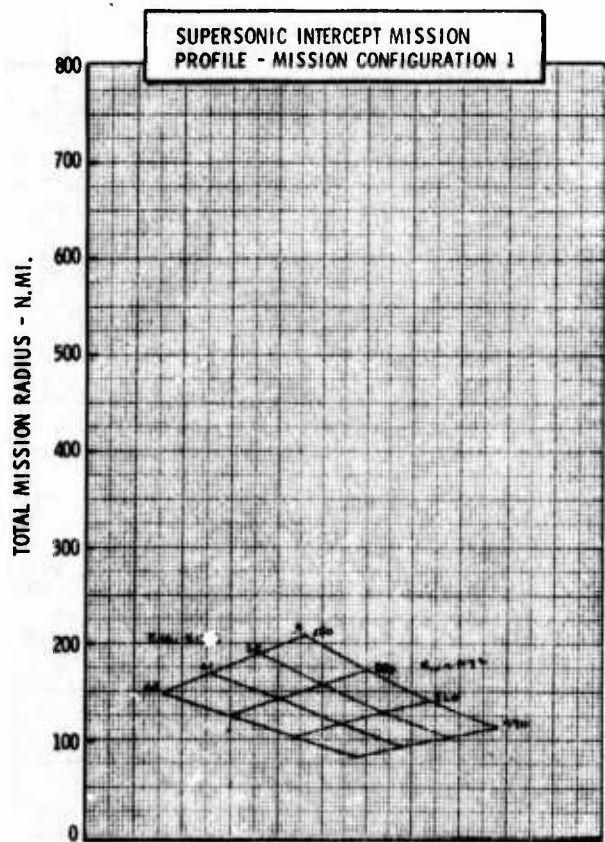
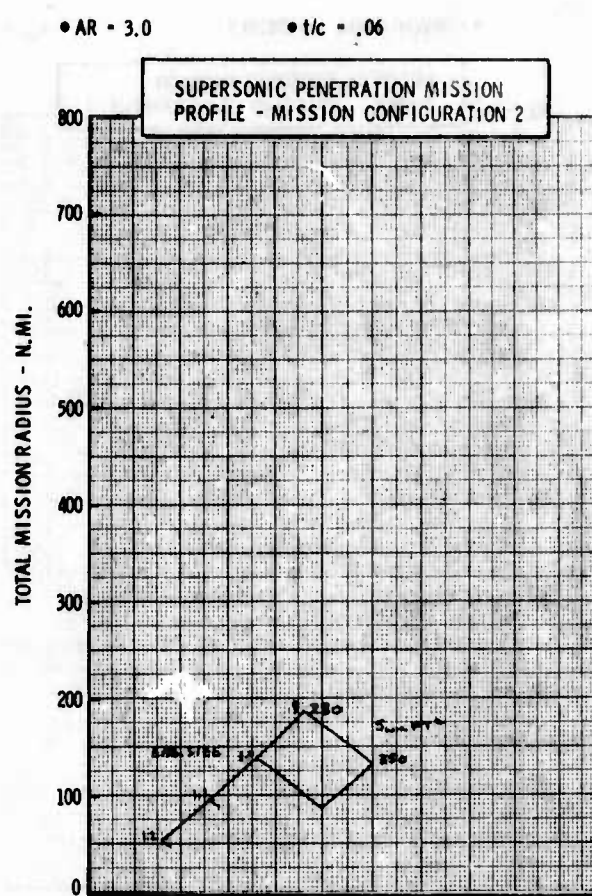
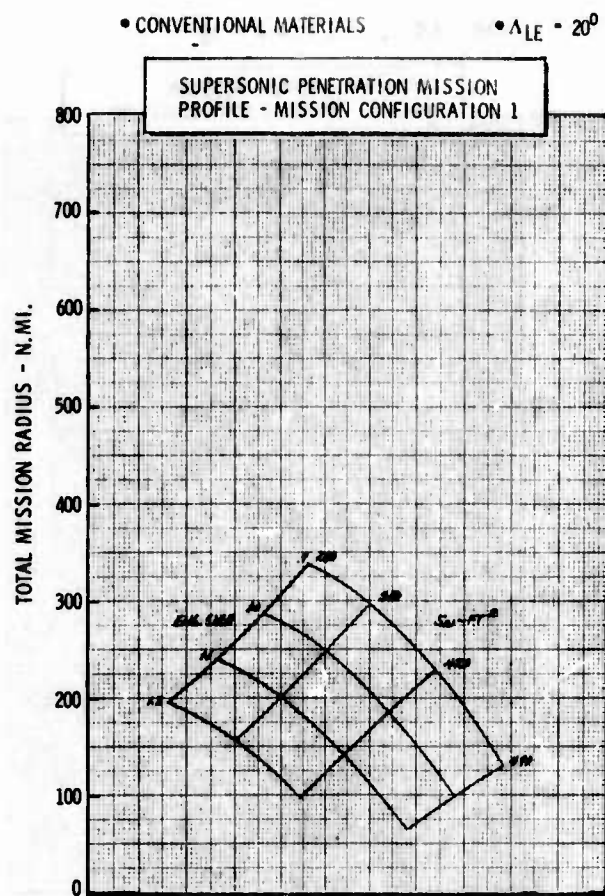


Figure H-20c LWA Mission/Configuration Tradeoff Parametric Data

• CONVENTIONAL MATERIALS

•  $\Delta LE = 20^\circ$

•  $AR = 4.0$

•  $t/c = .06$

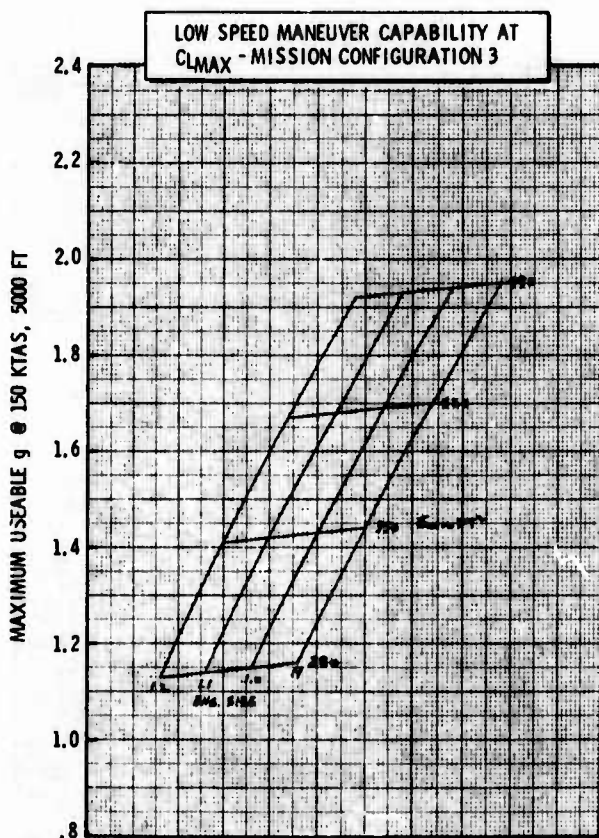
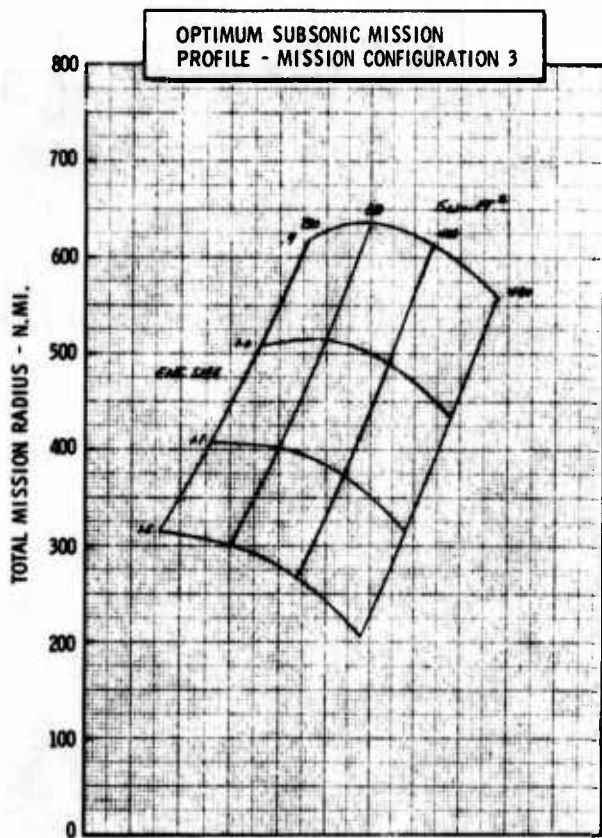
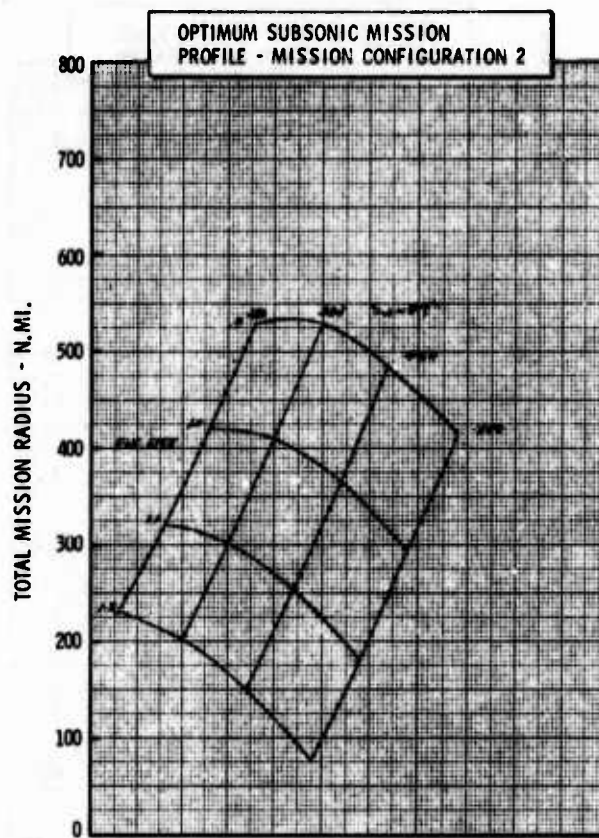
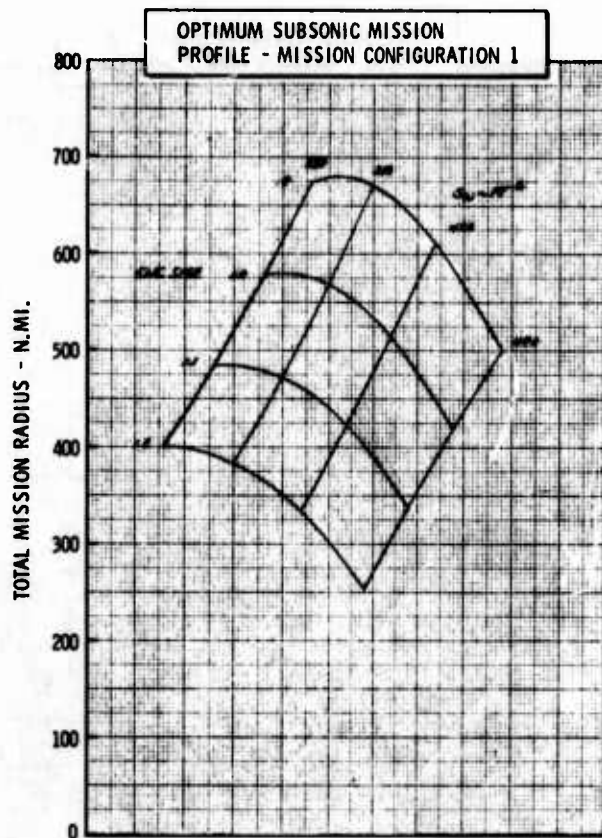


Figure H-21a LWA Mission/Configuration Tradeoff Parametric Data

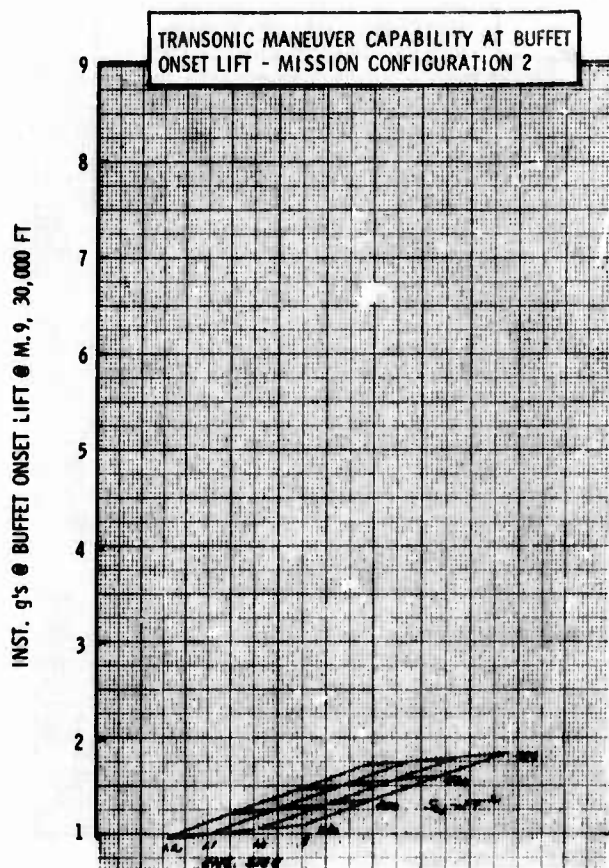
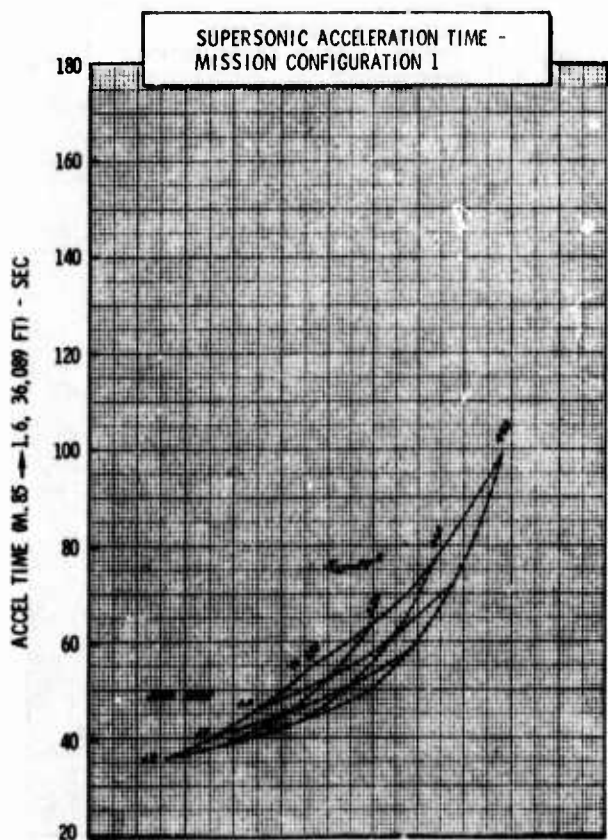
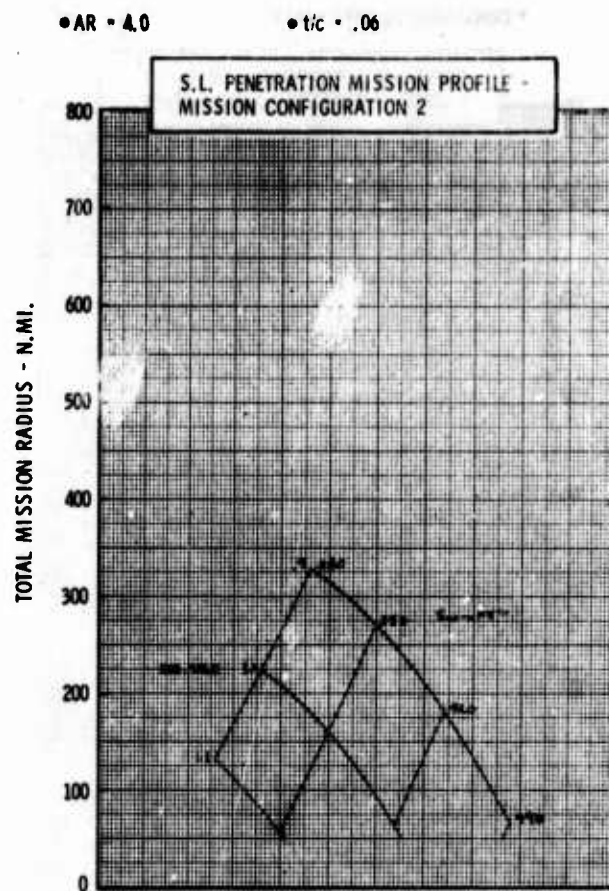
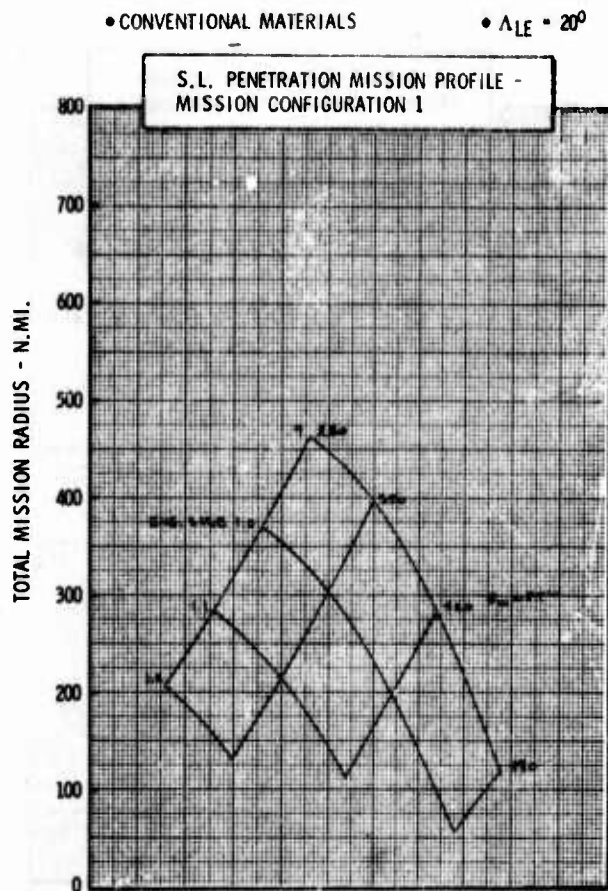


Figure H-21.b LWA Mission/Configuration Tradeoff Parametric Data



• CONVENTIONAL MATERIALS

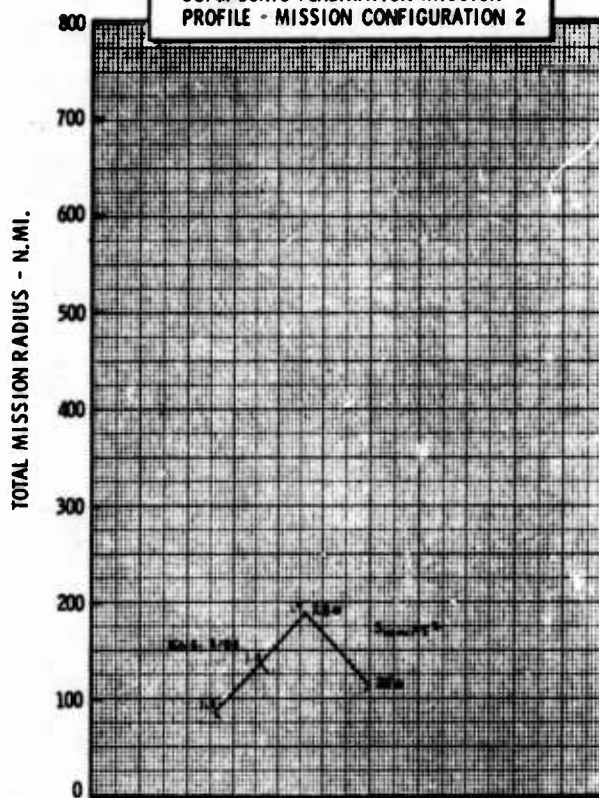
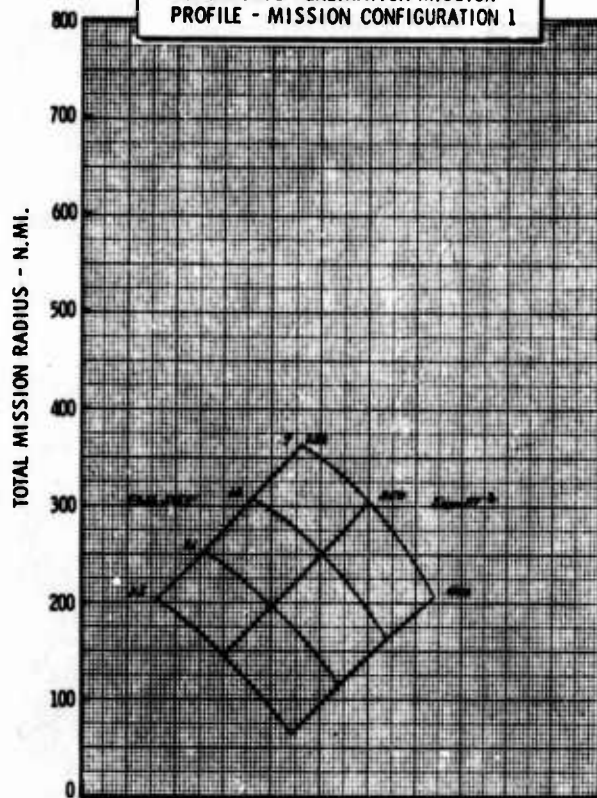
•  $\Lambda_{LE} = 20^\circ$

•  $AR = 4.0$

•  $t/c = .06$

SUPERSONIC PENETRATION MISSION  
PROFILE - MISSION CONFIGURATION 1

SUPERSONIC PENETRATION MISSION  
PROFILE - MISSION CONFIGURATION 2



SUPERSONIC INTERCEPT MISSION  
PROFILE - MISSION CONFIGURATION 1

SUPERSONIC INTERCEPT MISSION  
PROFILE - MISSION CONFIGURATION 1'

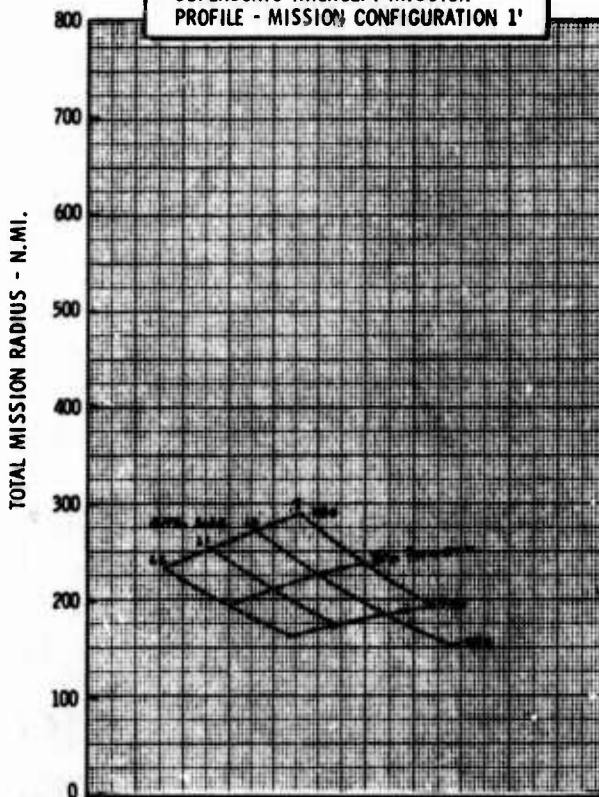
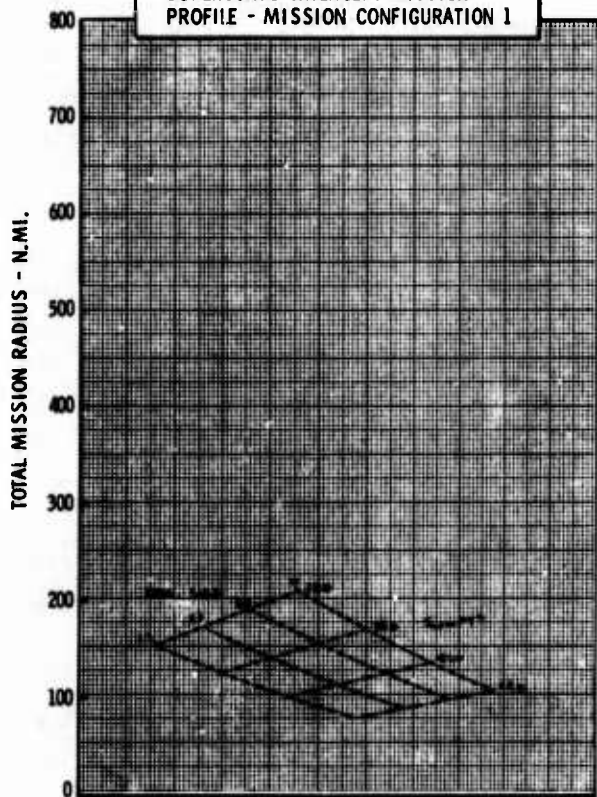


Figure H-21c LWA Mission/Configuration Tradeoff Parametric Data

• CONVENTIONAL MATERIALS

•  $\Delta LE = 20^\circ$

•  $AR = 5.0$

•  $t/c = .06$

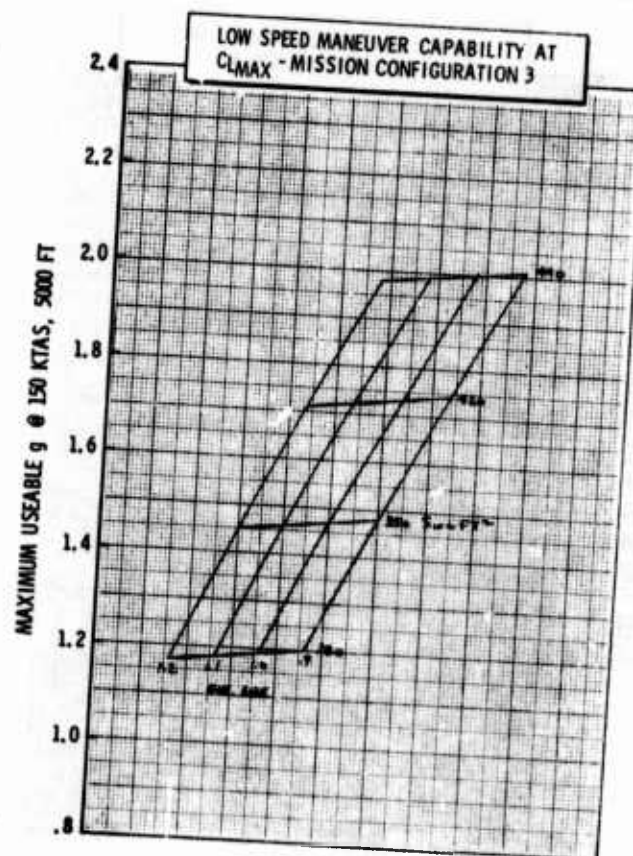
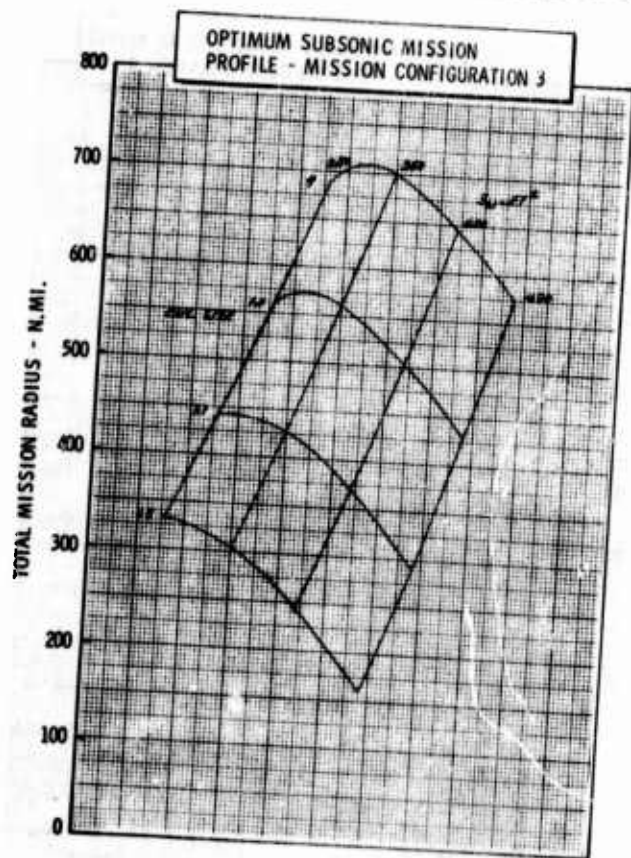
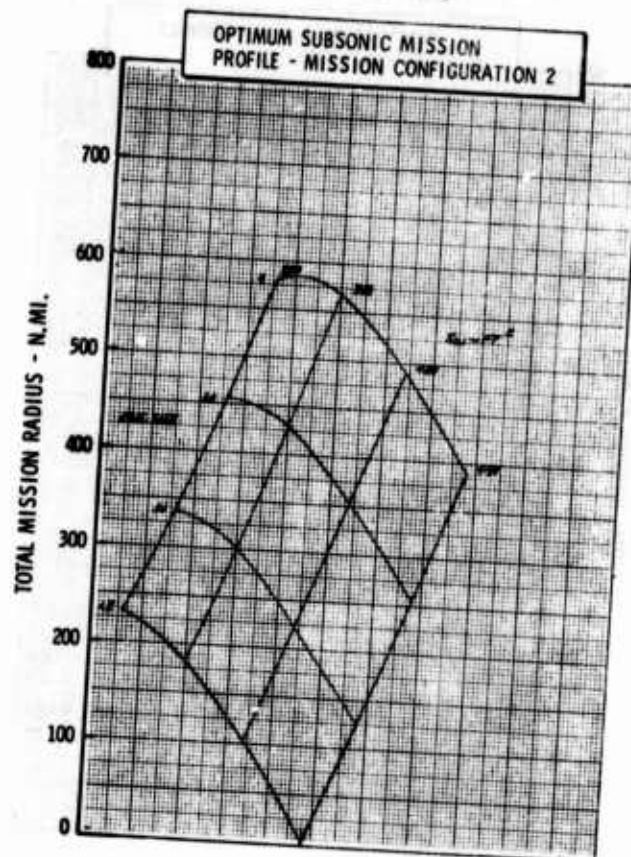
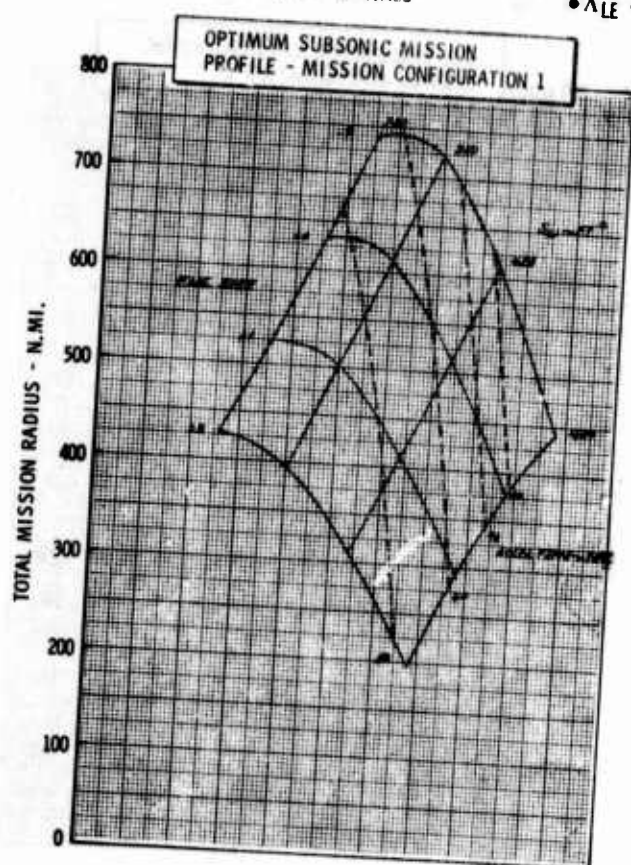


Figure H-22a LWA Mission/Configuration Tradeoff Parametric Data

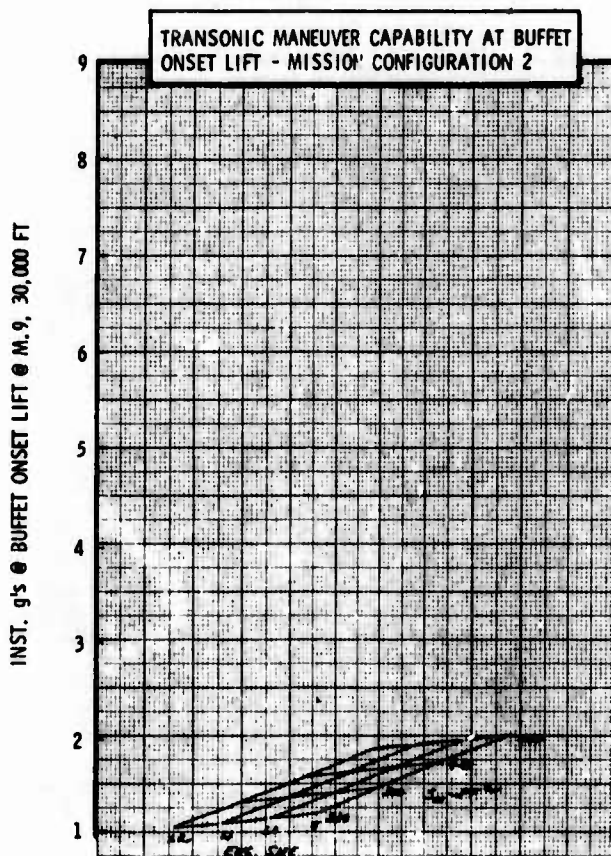
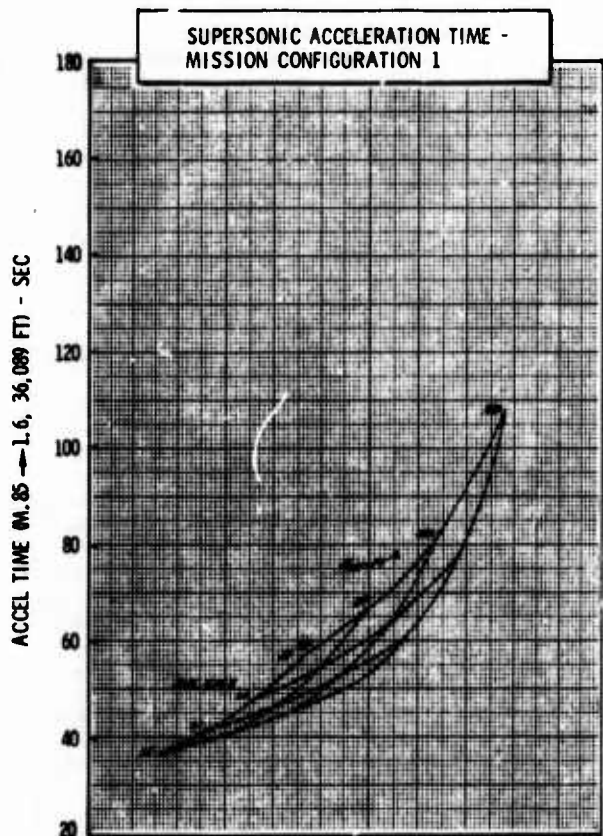
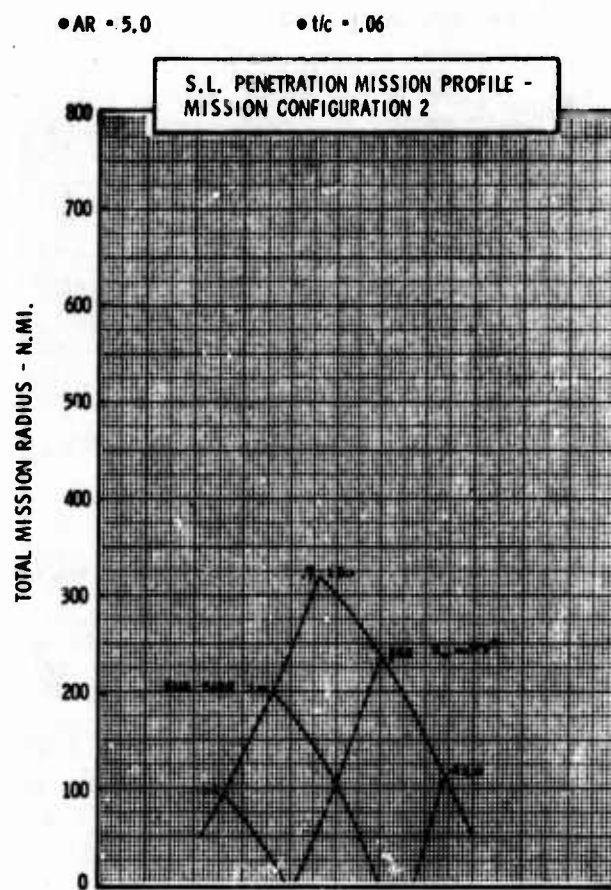
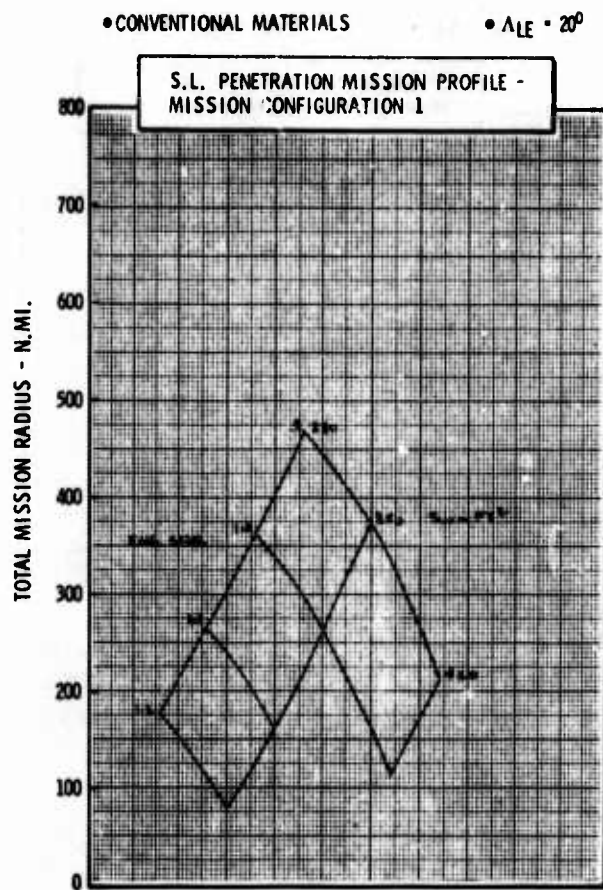


Figure H-22b LWA Mission/Configuration Tradeoff Parametric Data



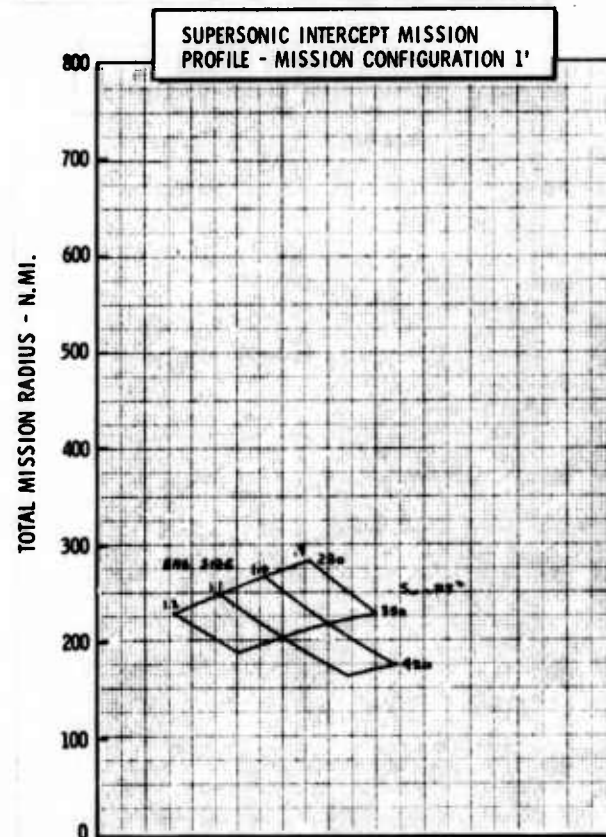
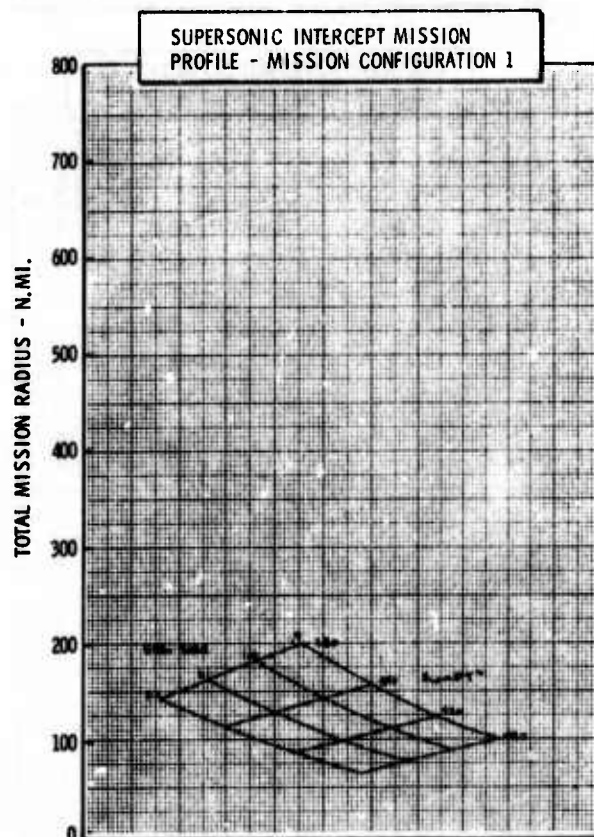
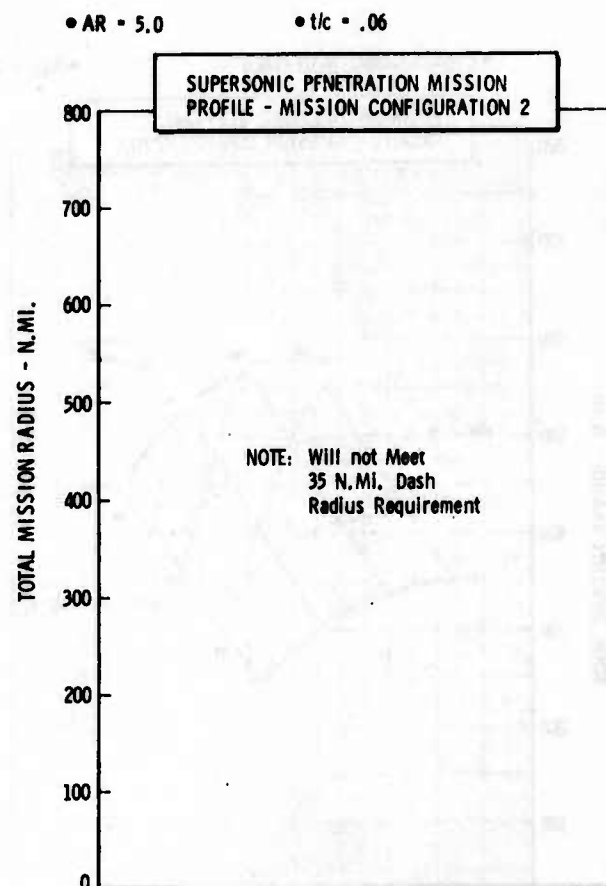
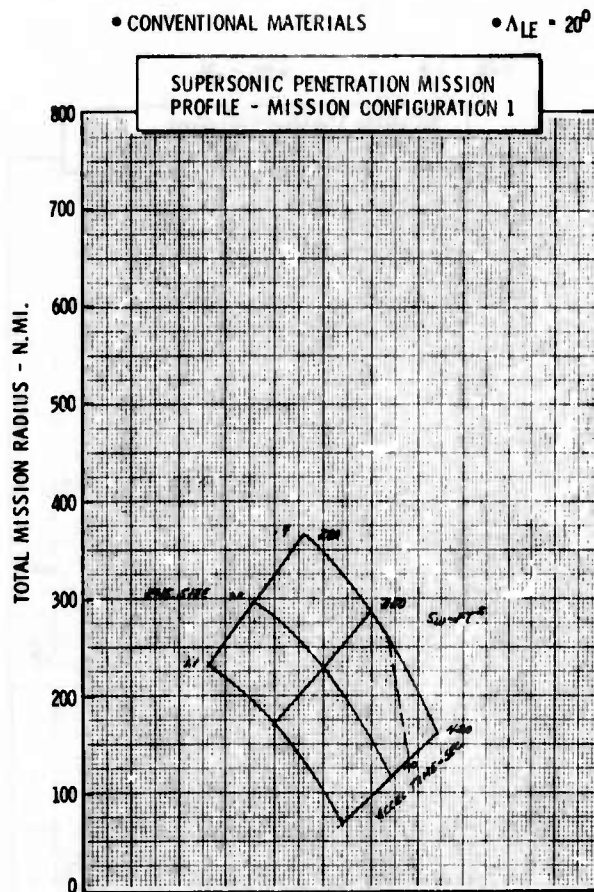


Figure H-22c LWA Mission/Configuration Tradeoff Parametric Data

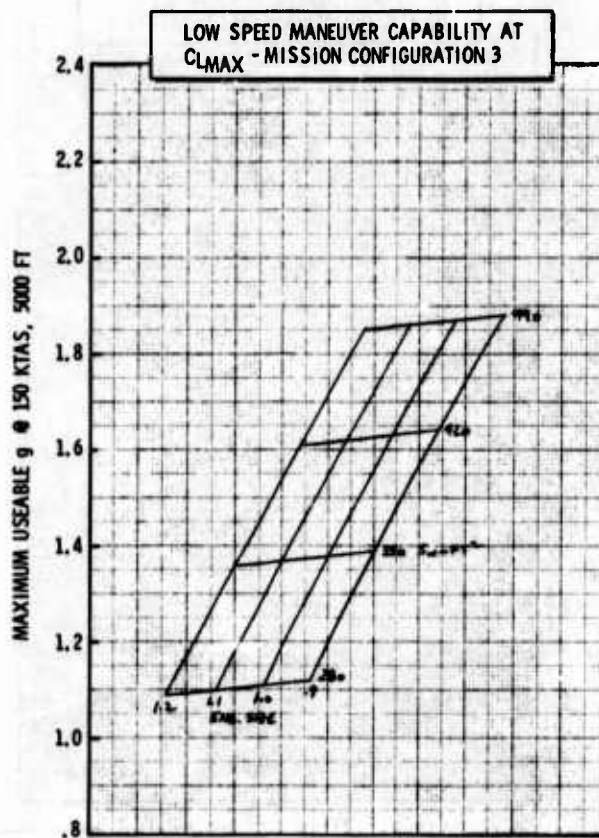
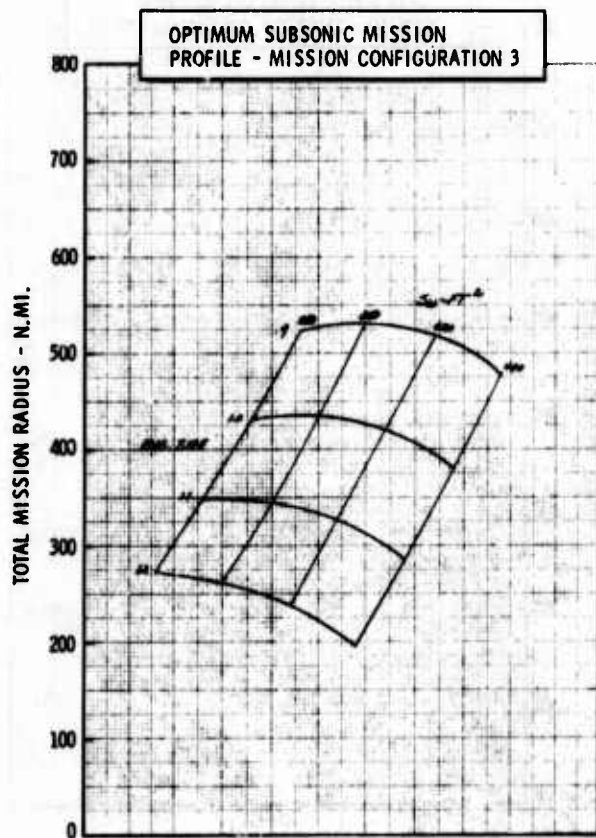
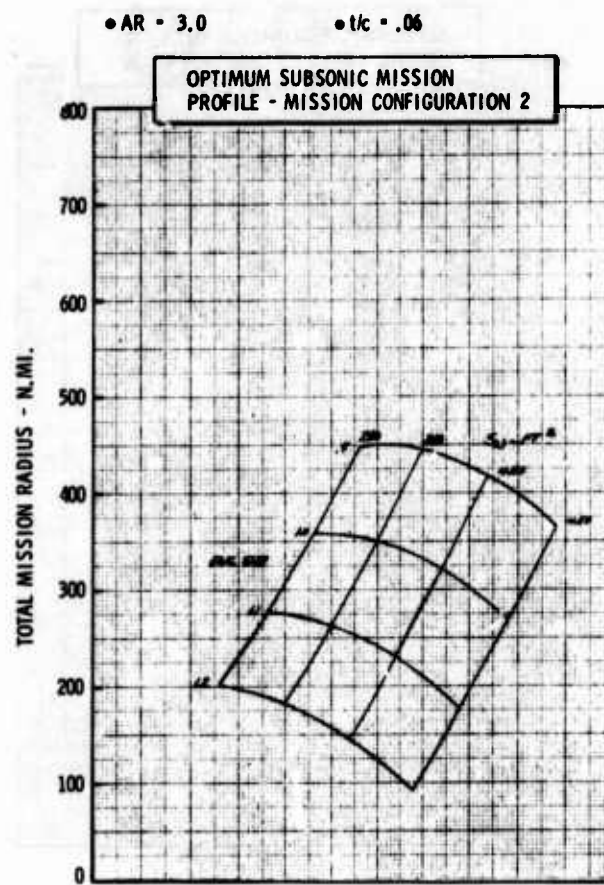
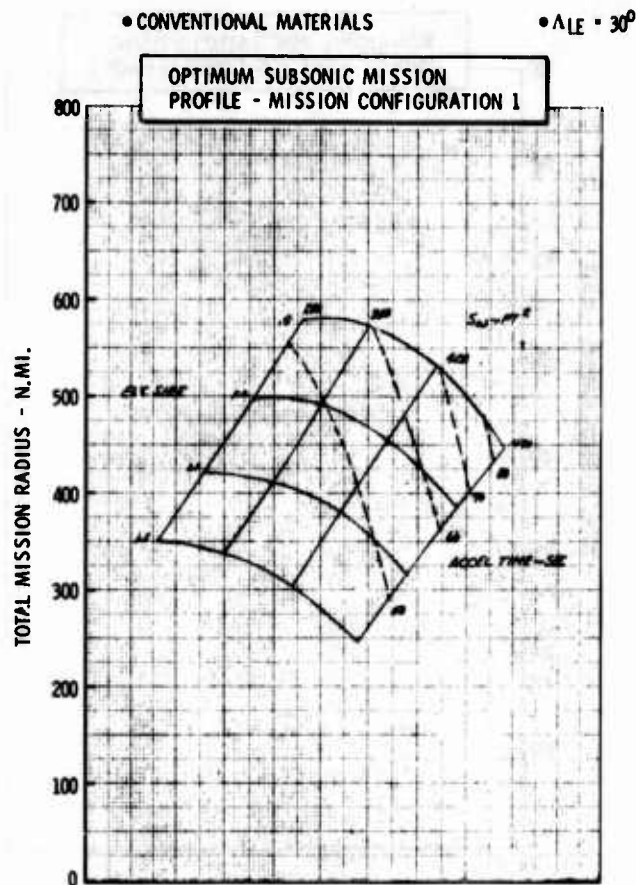


Figure H-23a LWA Mission/Configuration Tradeoff Parametric Data



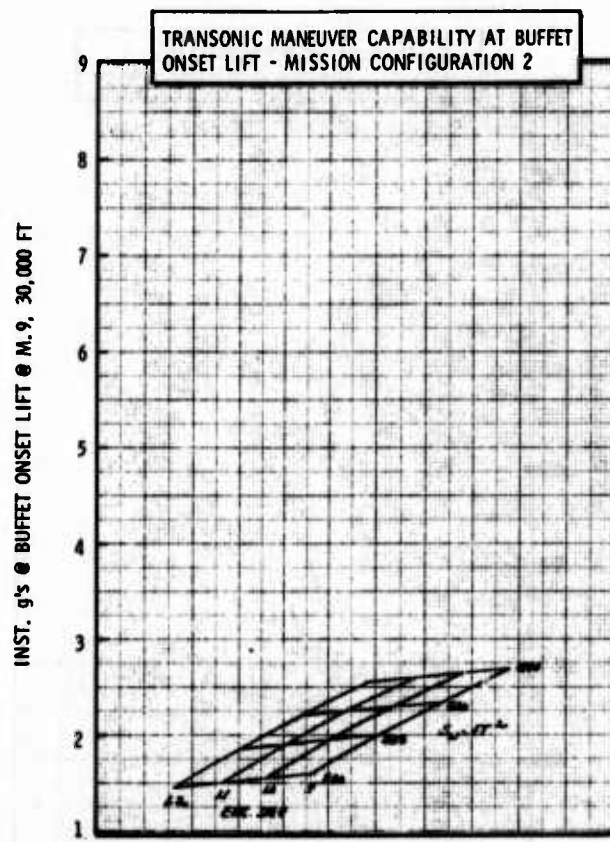
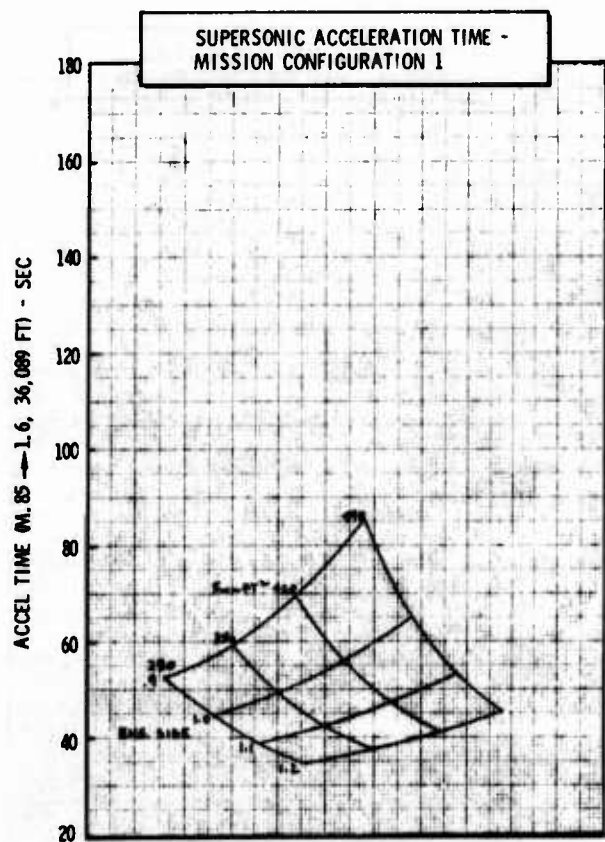
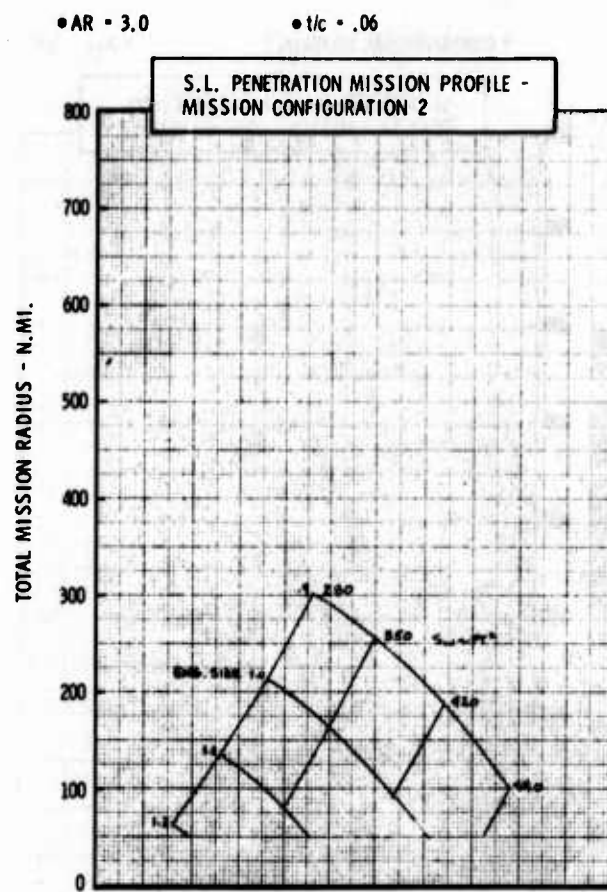
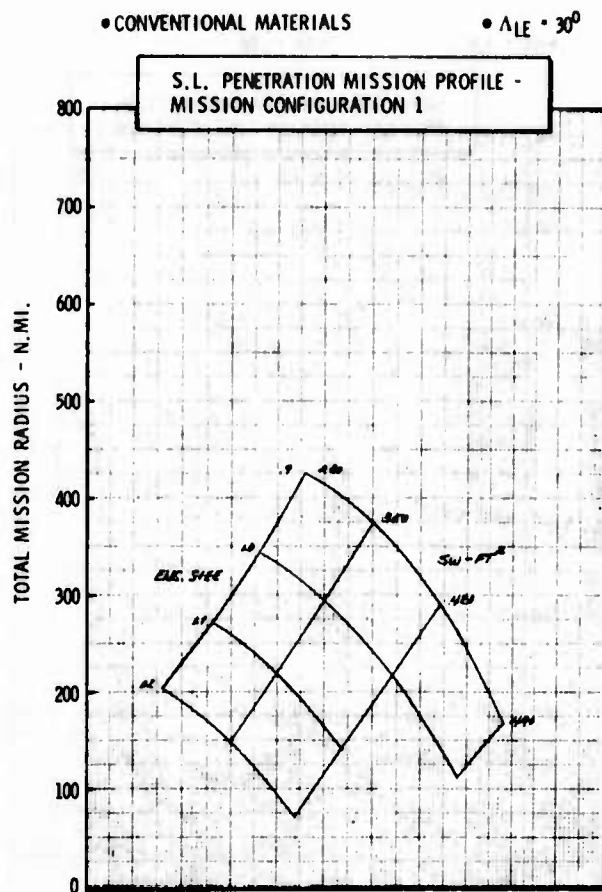


Figure H-23b LWA Mission/Configuration Tradeoff Parametric Data

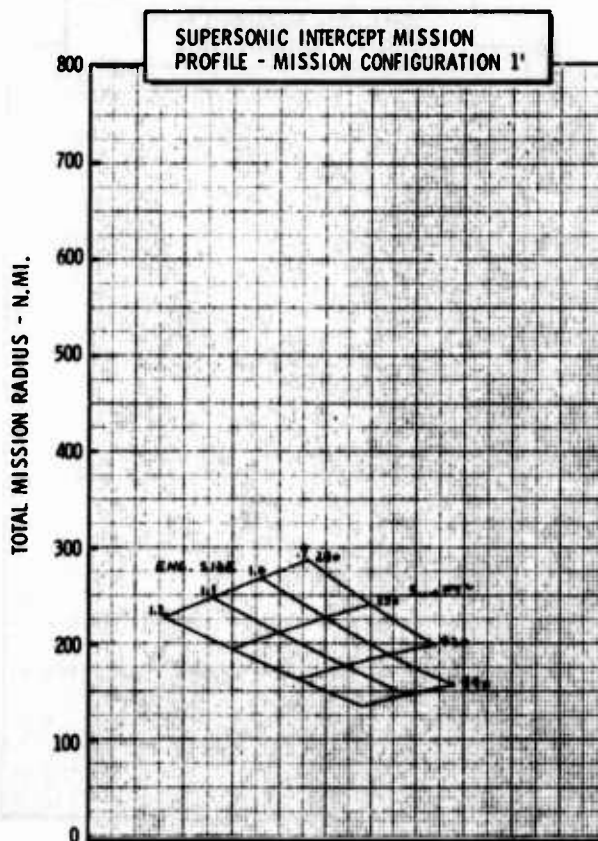
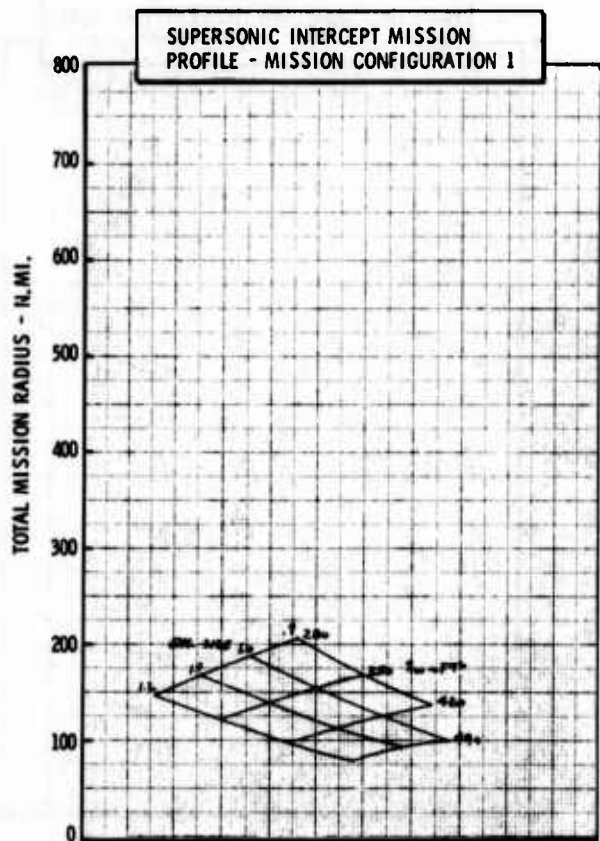
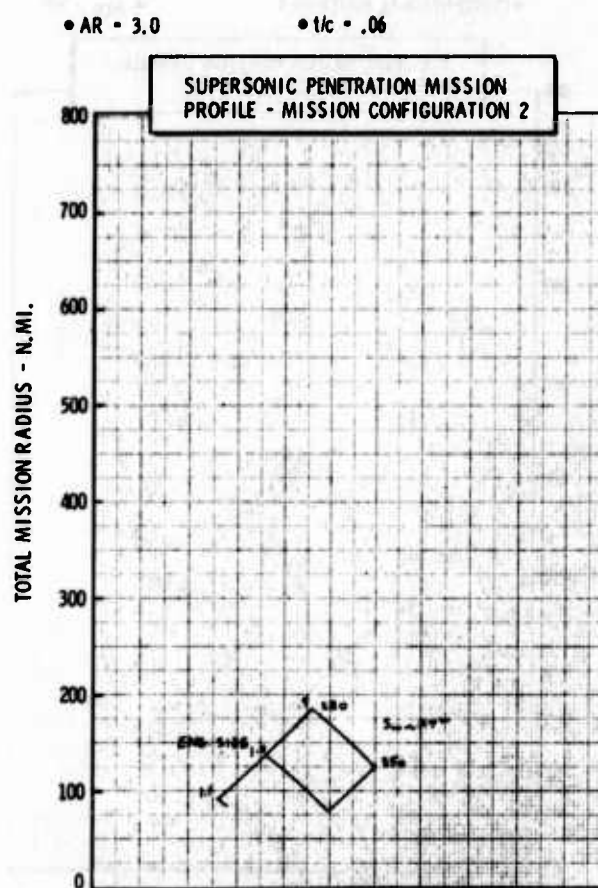
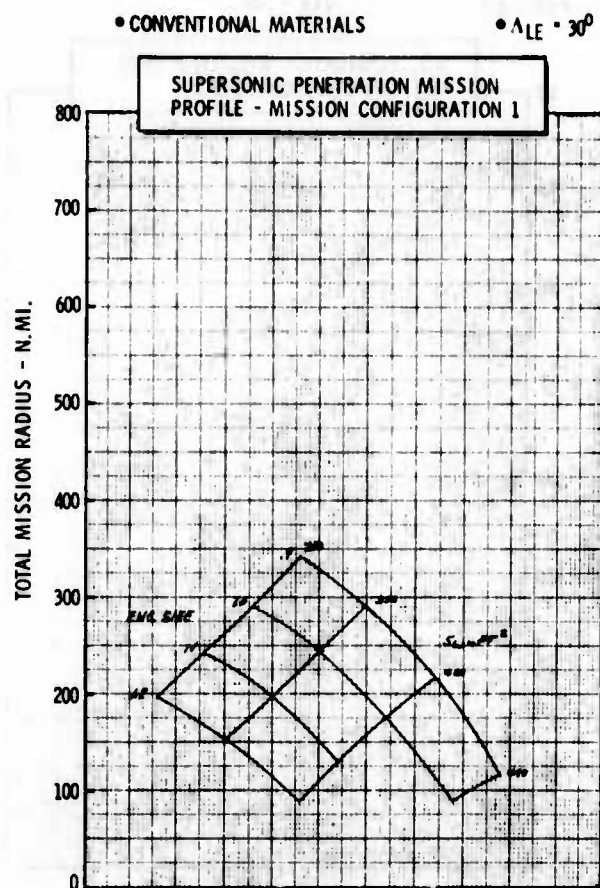


Figure H-23c LWA Mission/Configuration Tradeoff Parametric Data

• CONVENTIONAL MATERIALS

•  $\Delta LE = 30^\circ$

•  $AR = 4.0$

•  $t/c = .06$

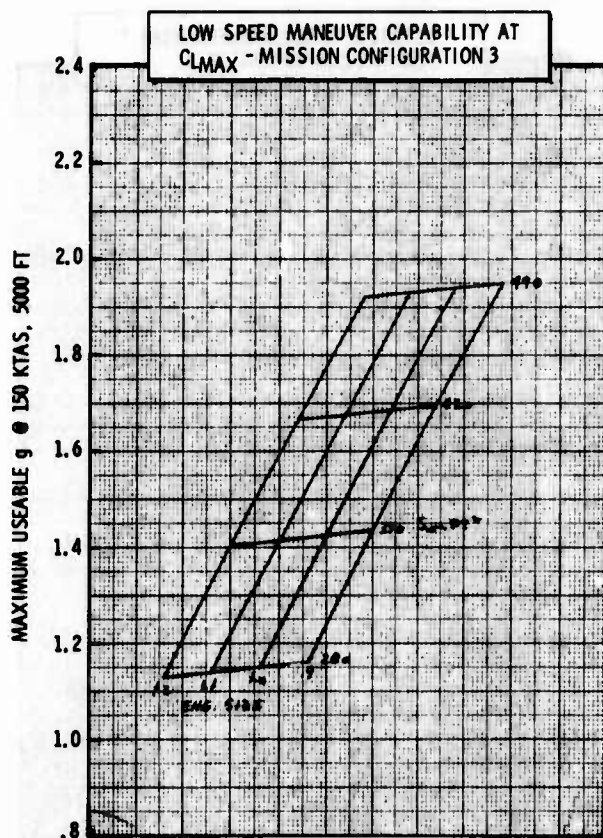
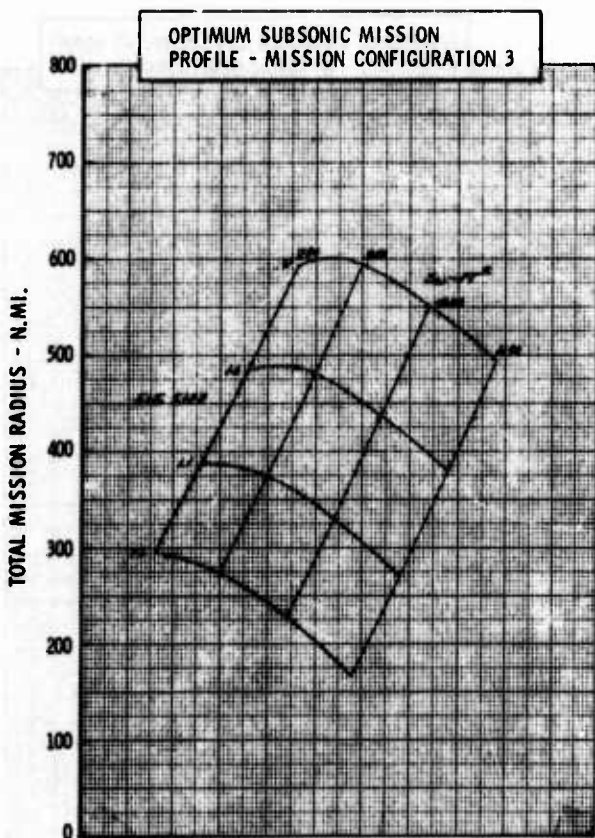
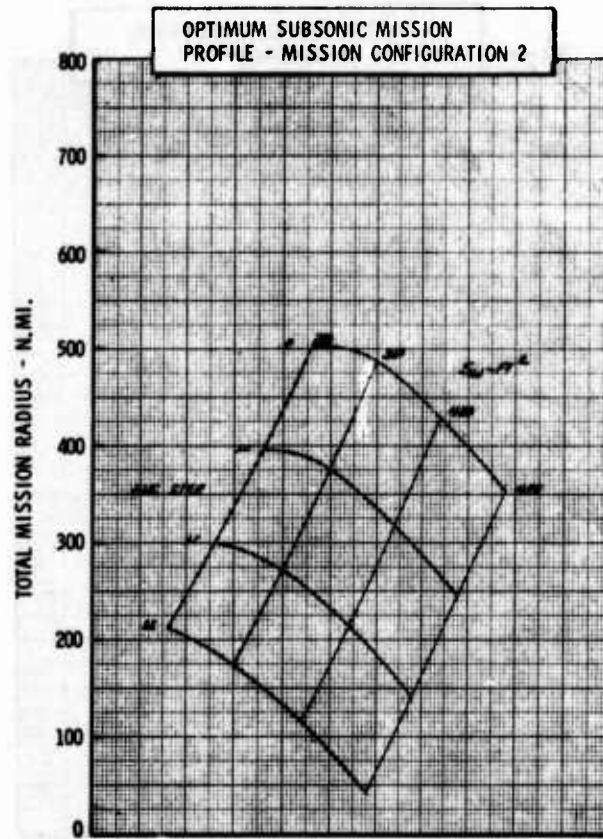
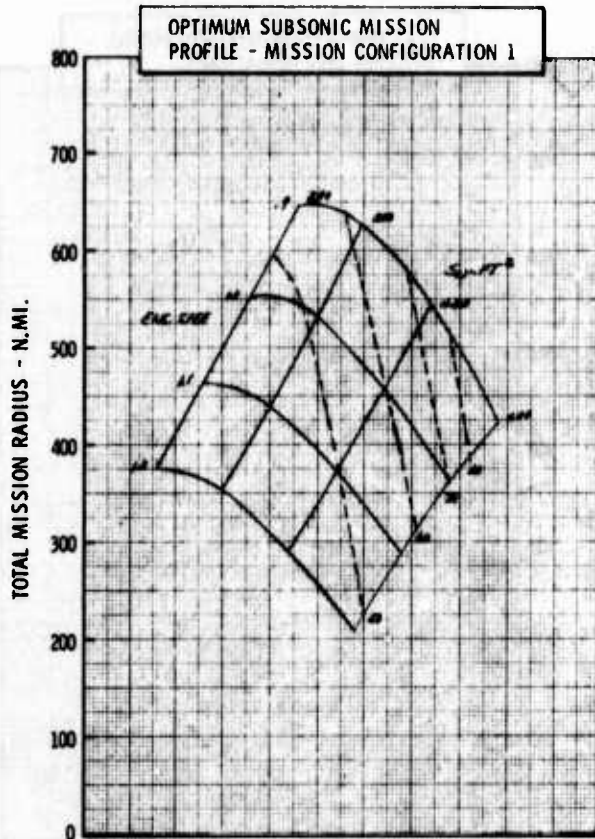


Figure H-24a LWA Mission/Configuration Tradeoff Parametric Data



• CONVENTIONAL MATERIALS

•  $\Delta LE = 30^\circ$

• AR = 4.0

•  $t/c = .06$

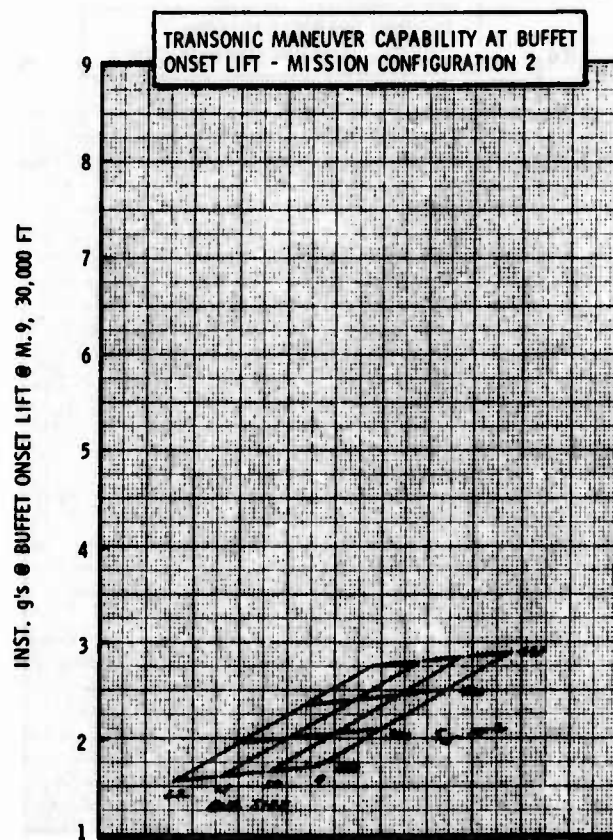
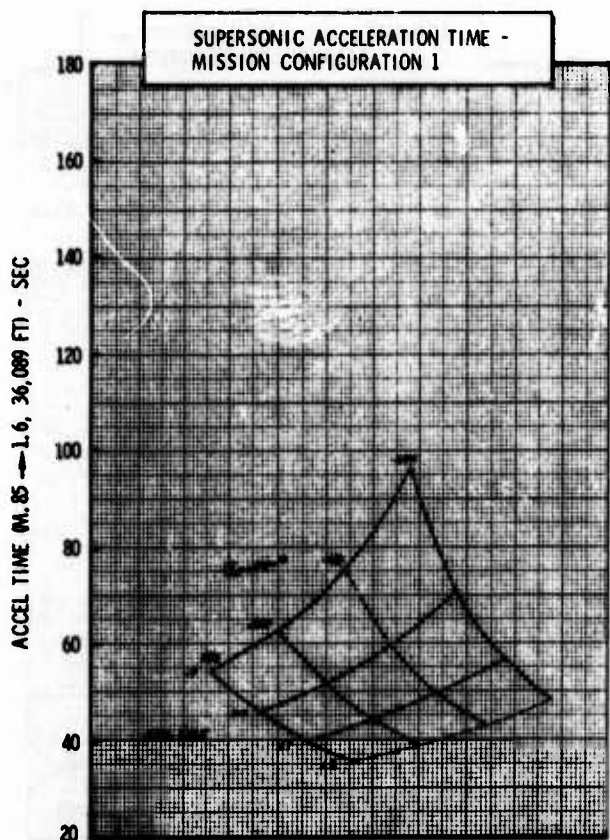
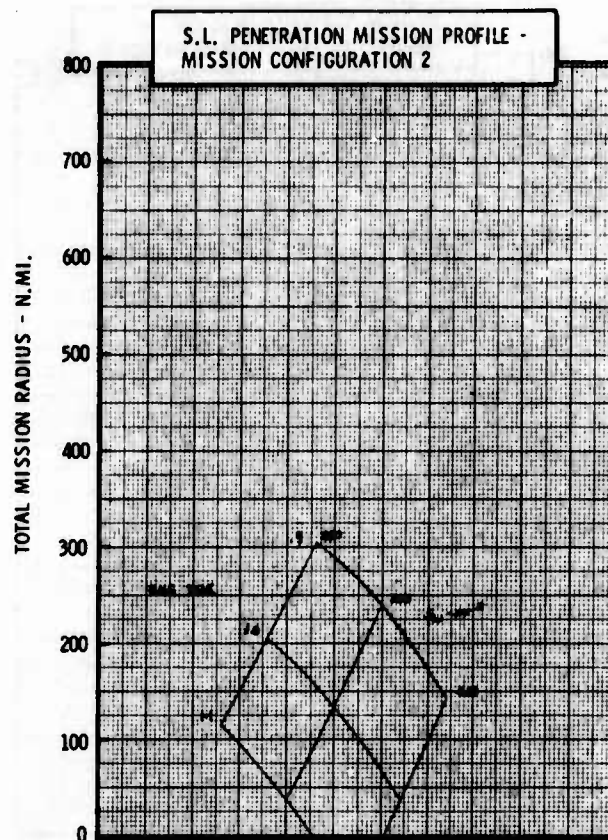
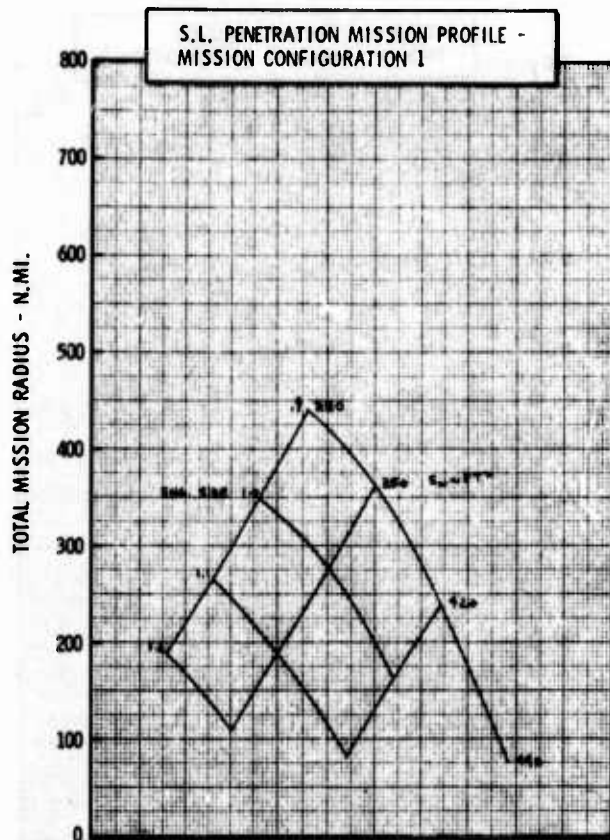


Figure H-24b LWA Mission/Configuration Tradeoff Parametric Data

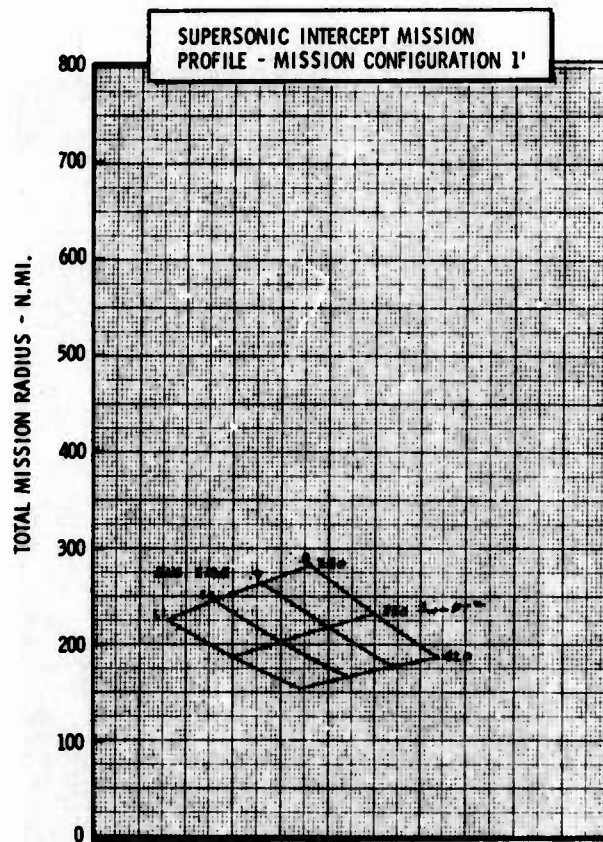
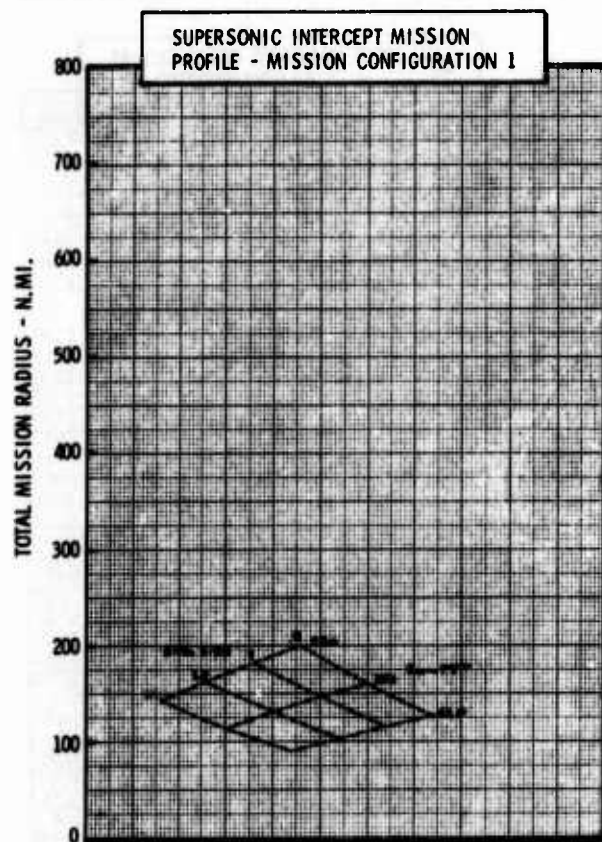
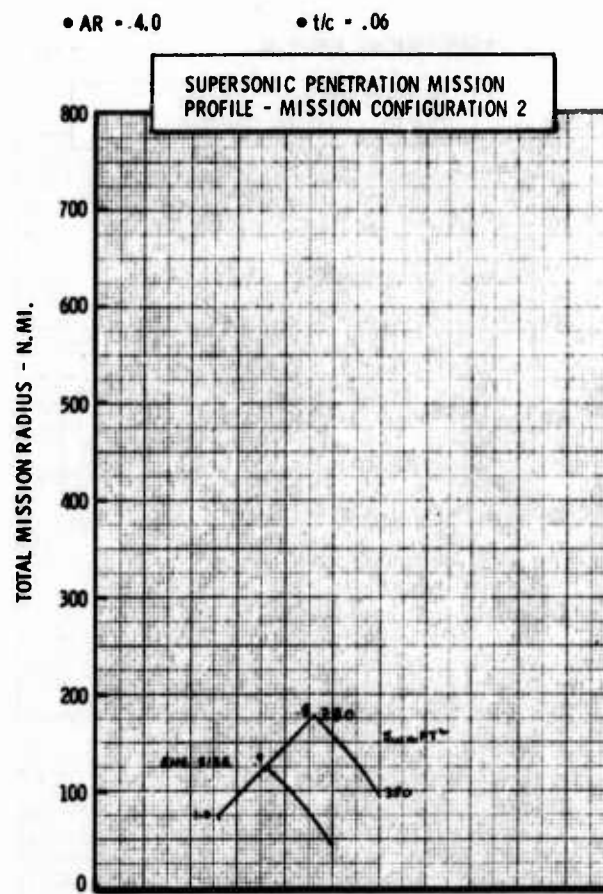
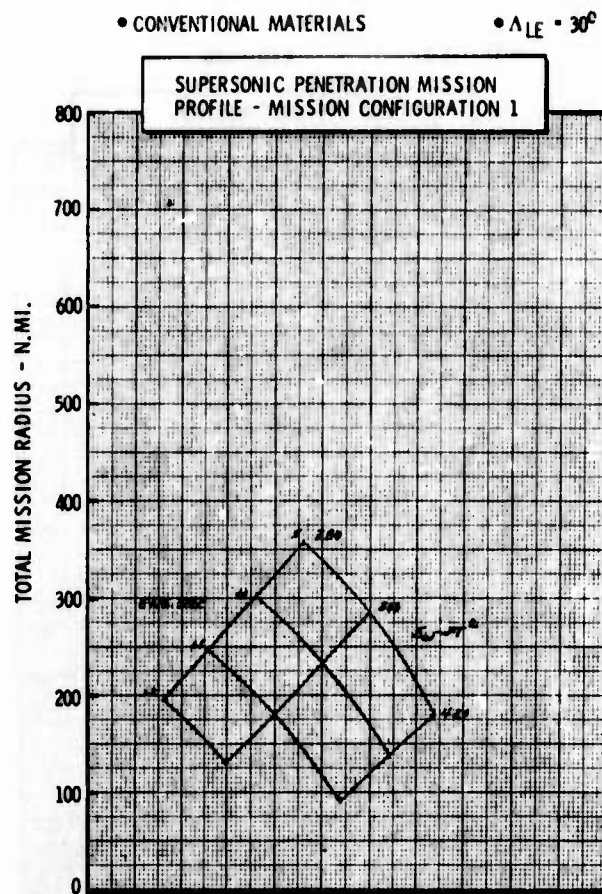


Figure H-24c LWA Mission/Configuration Tradeoff Parametric Data



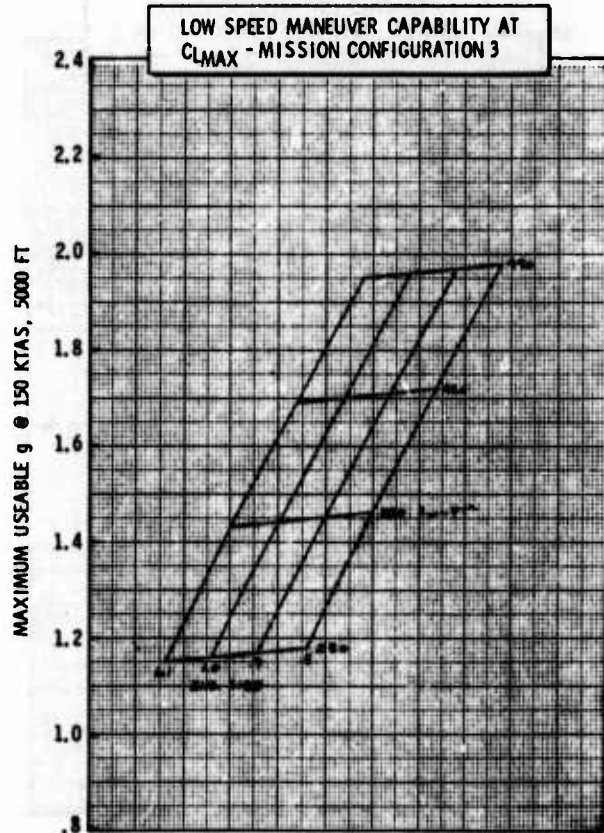
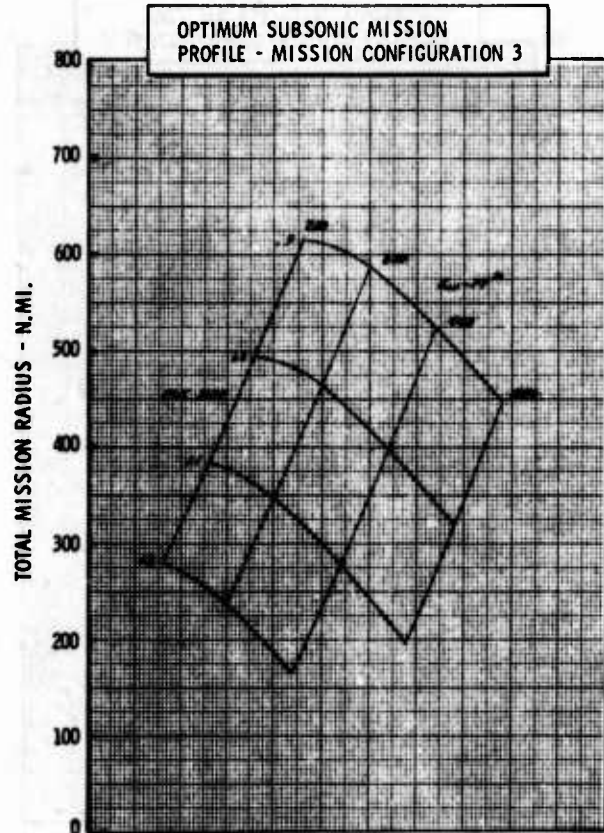
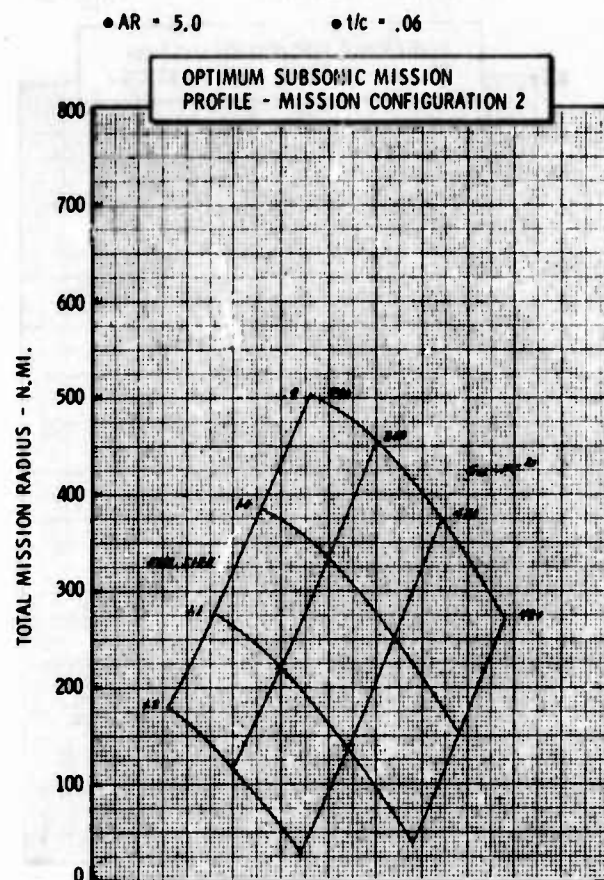
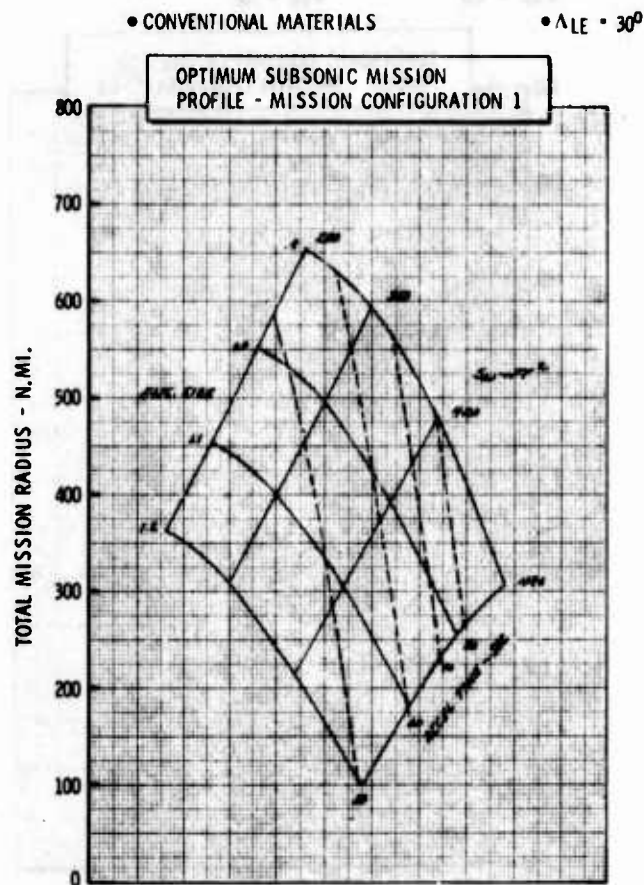


Figure H-25a LWA Mission/Configuration Tradeoff Parametric Data

• CONVENTIONAL MATERIALS

•  $\Delta LE = 30^\circ$

• AR = 5.0

•  $t/c = .06$

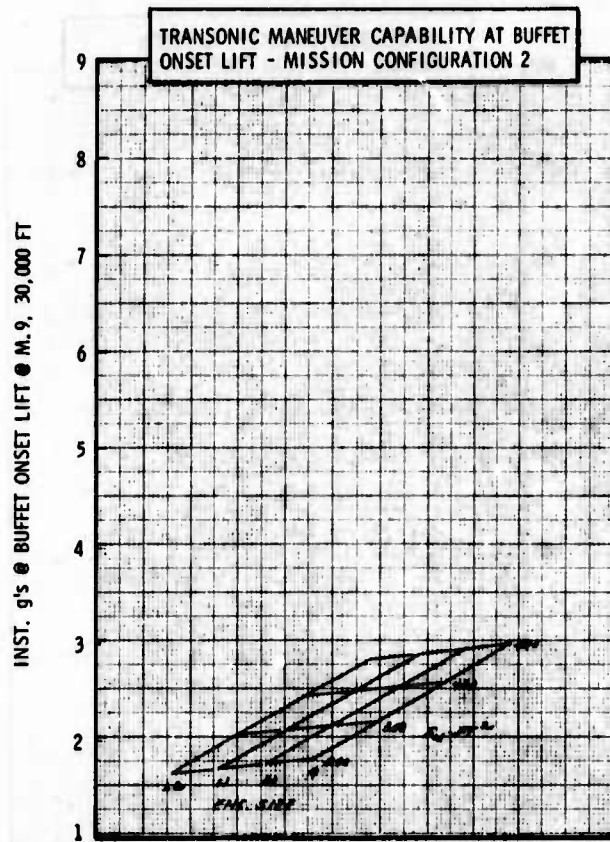
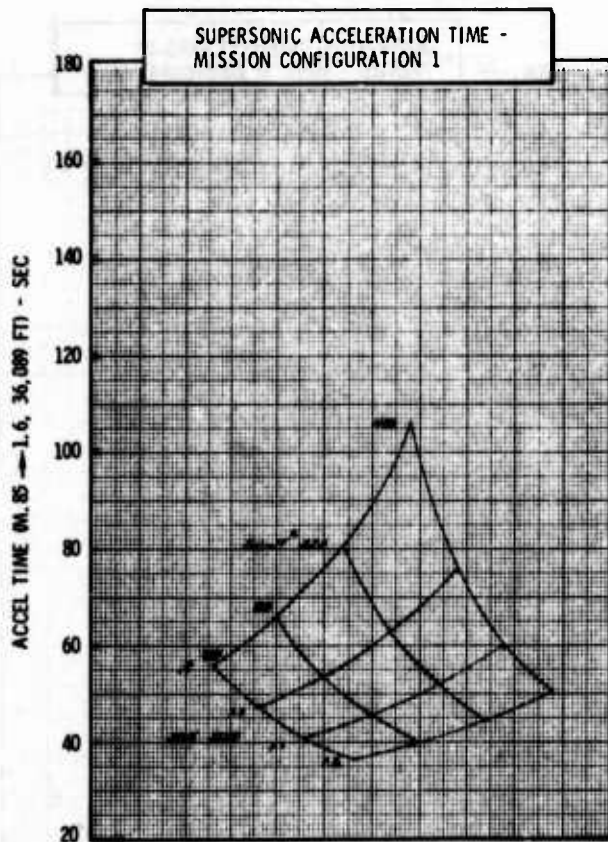
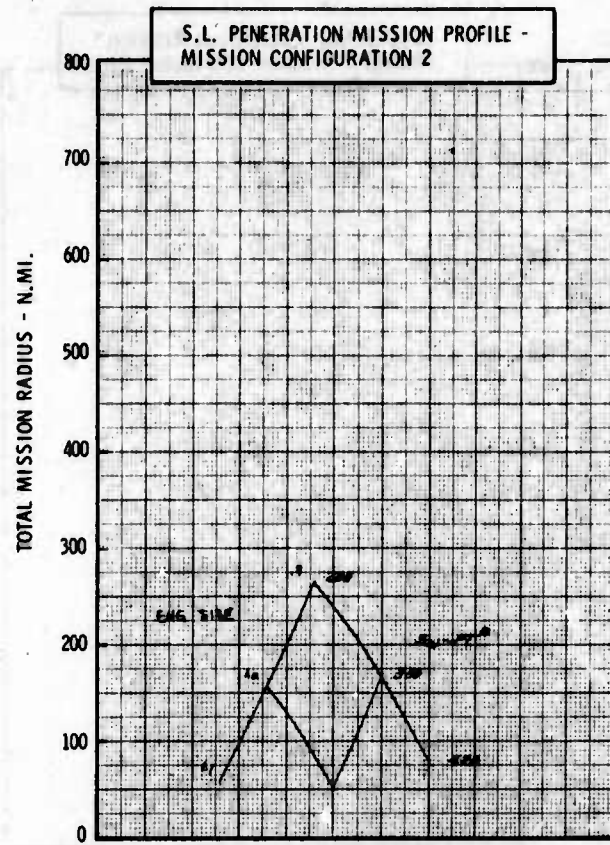
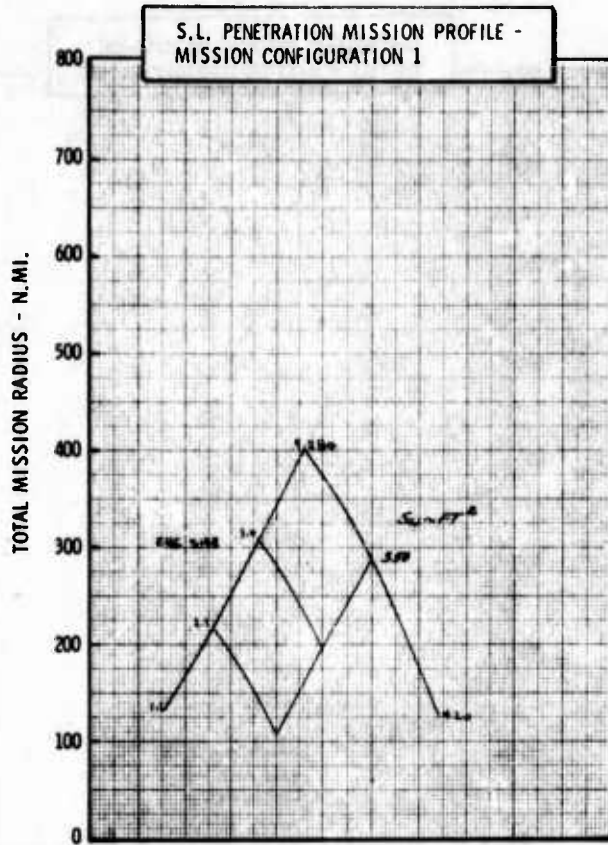


Figure H-25b LWA Mission/Configuration Tradeoff Parametric Data

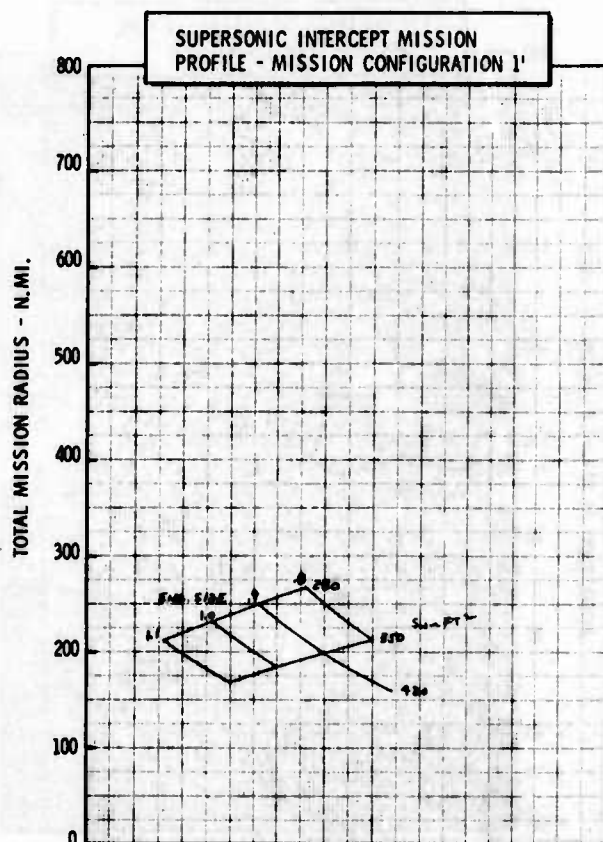
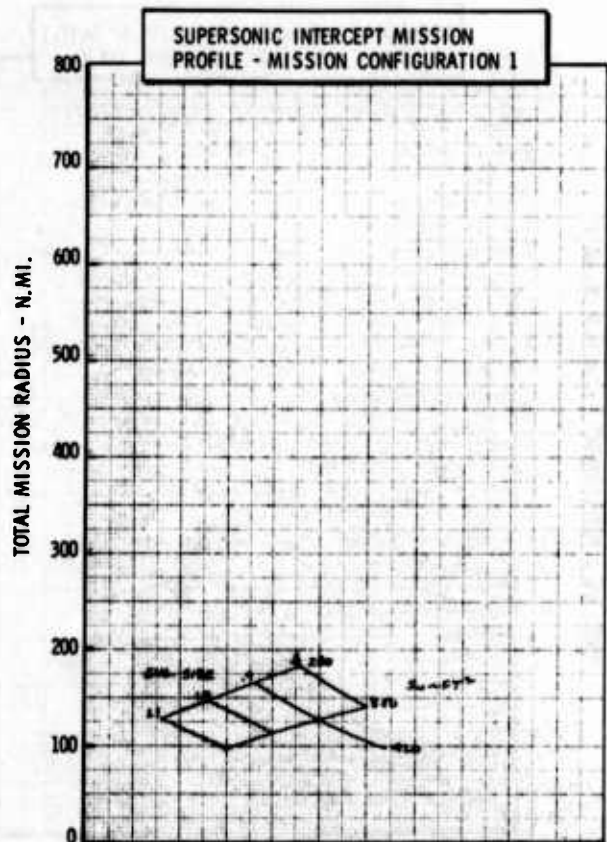
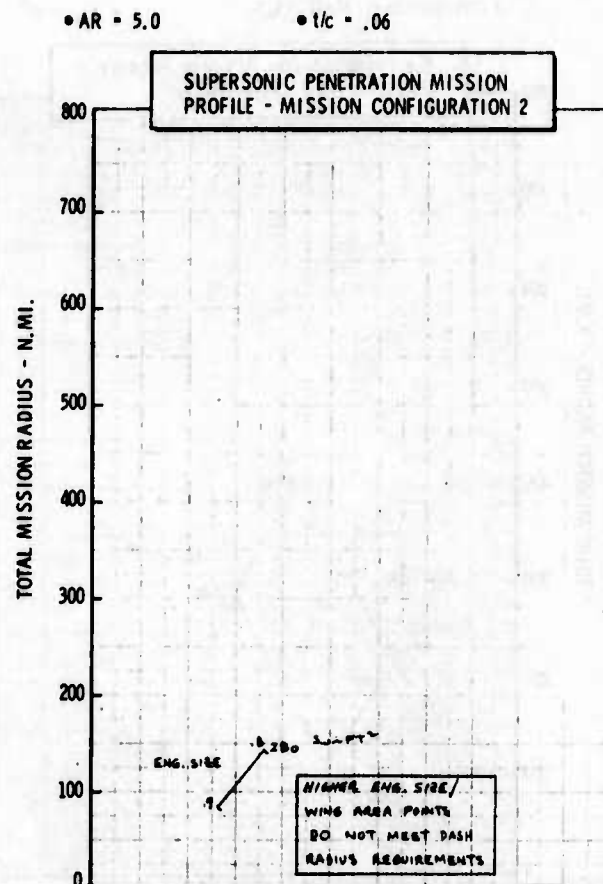
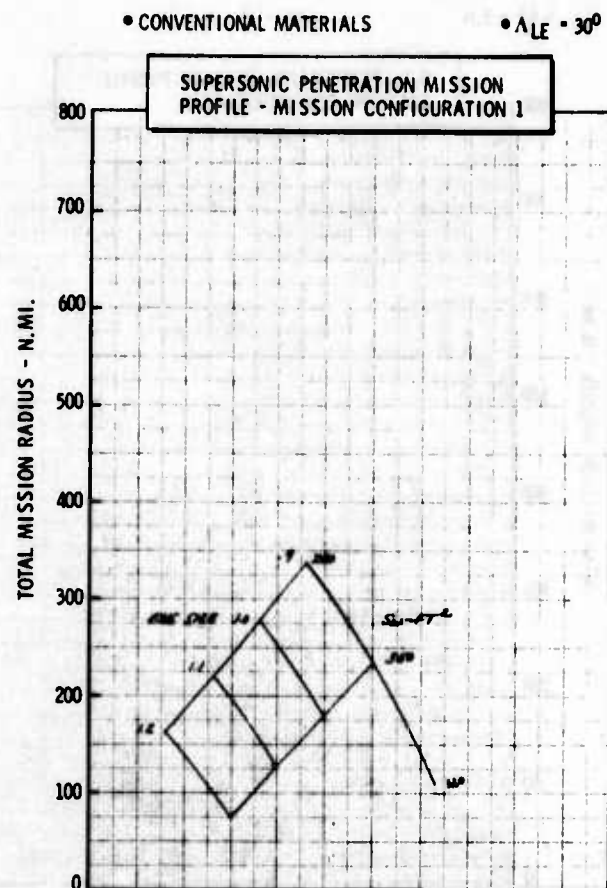


Figure H-25c LWA Mission/Configuration Tradeoff Parametric Data



• CONVENTIONAL MATERIALS

•  $\Lambda_{LE} = 40^\circ$

•  $AR = 3.0$

•  $t/c = .06$

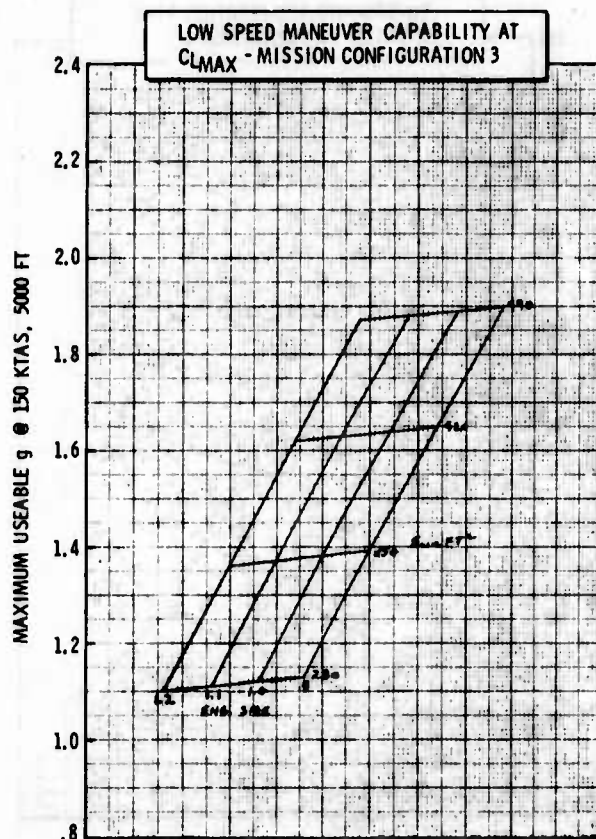
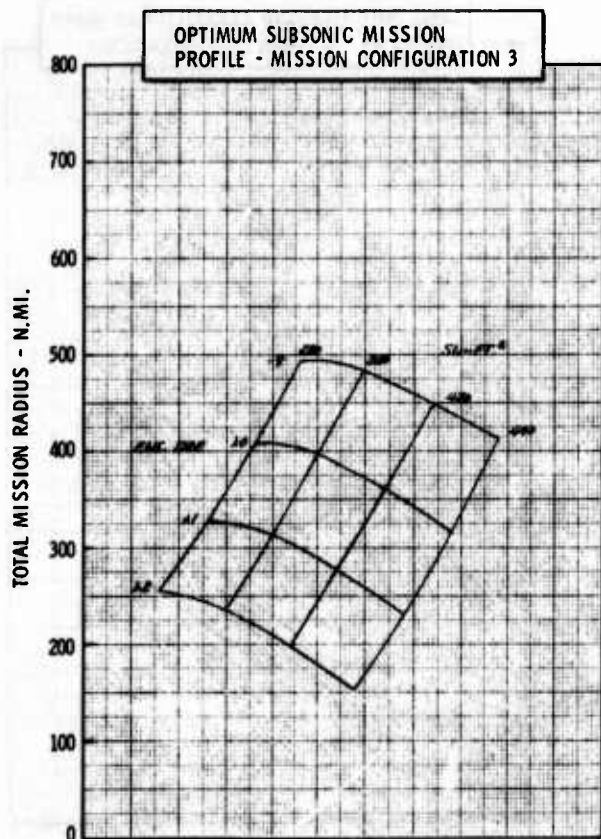
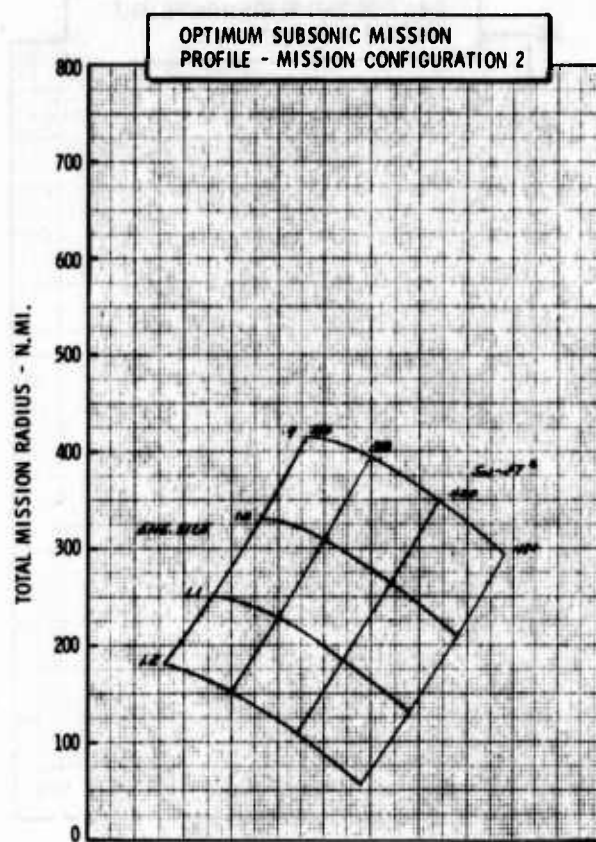
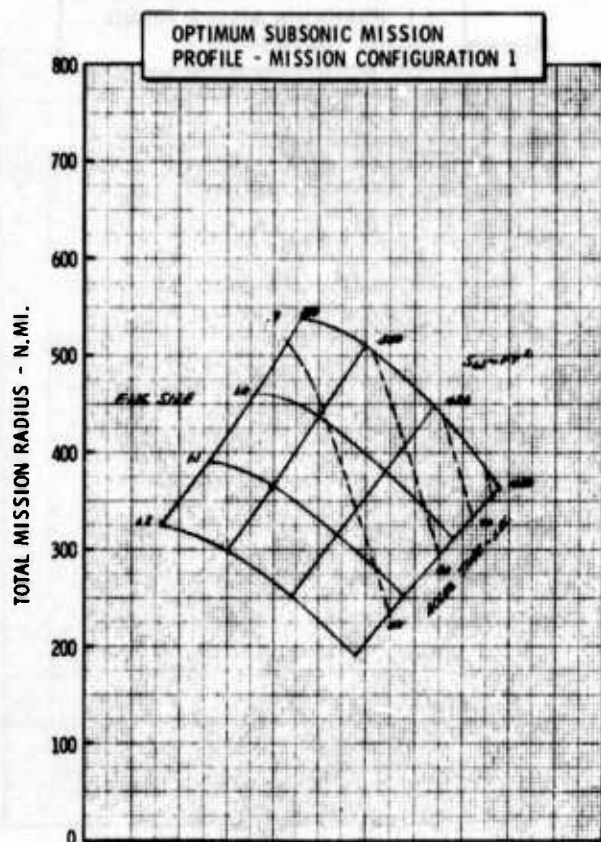


Figure H-26a LWA Mission/Configuration Tradeoff Parametric Data

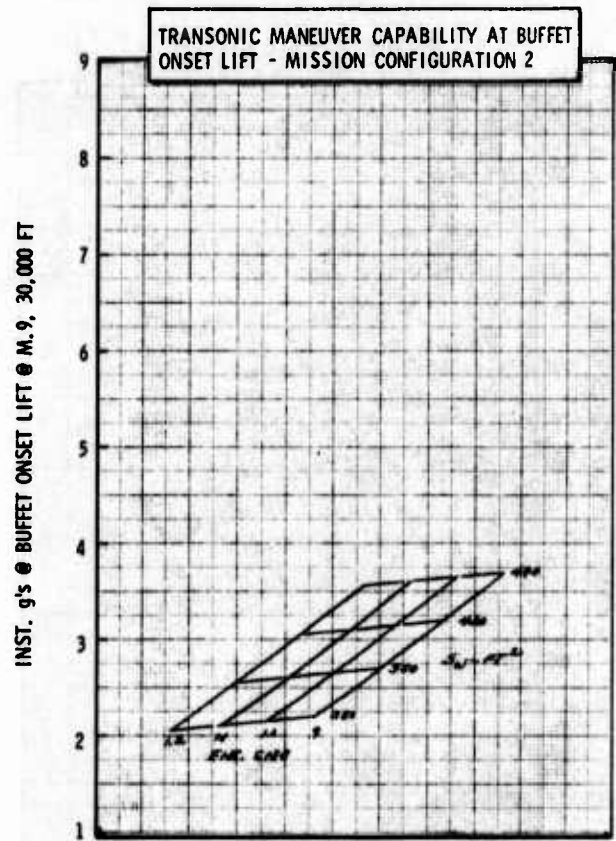
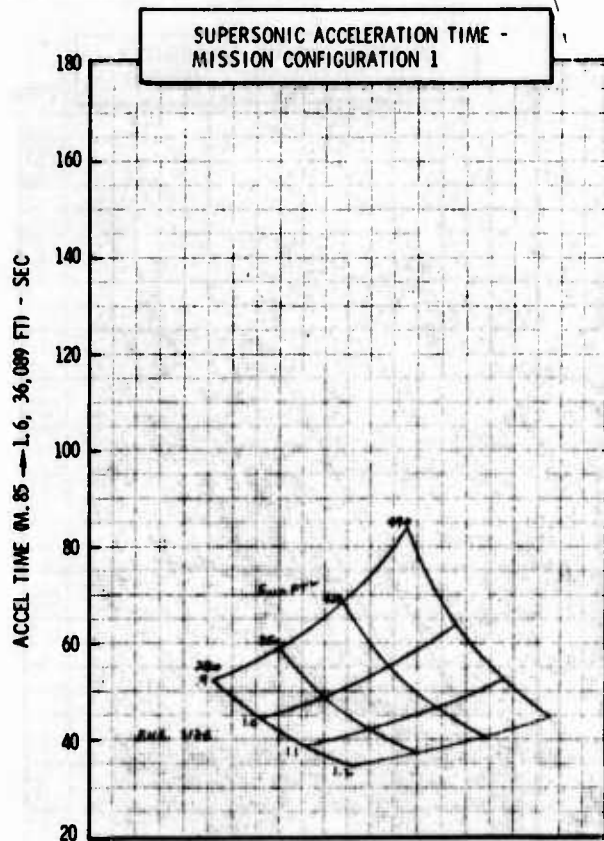
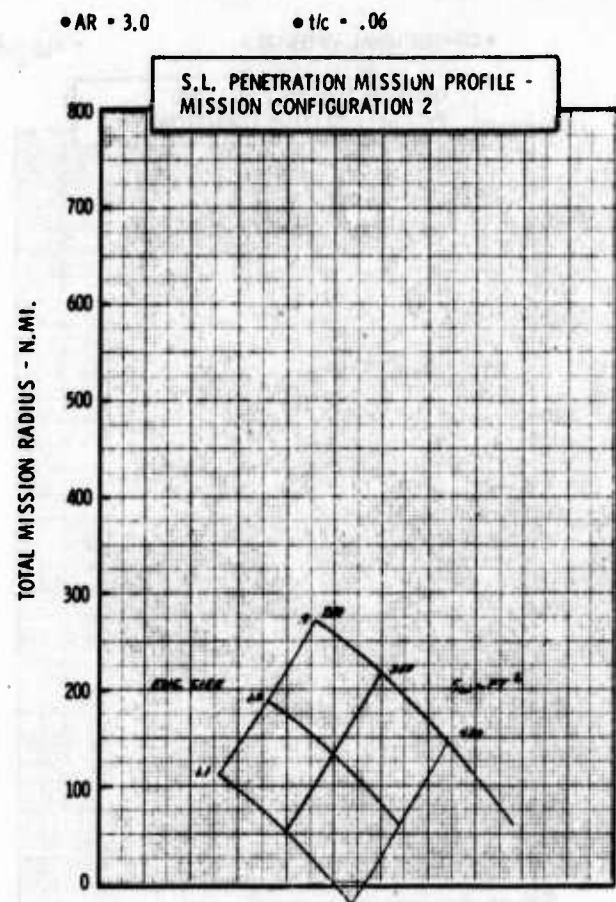
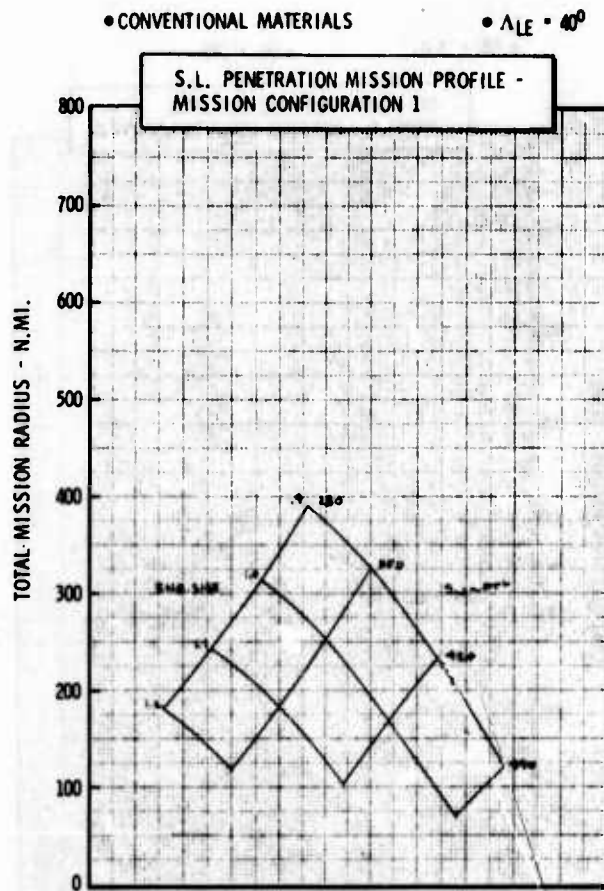


Figure H-26b LWA Mission/Configuration Tradeoff Parametric Data



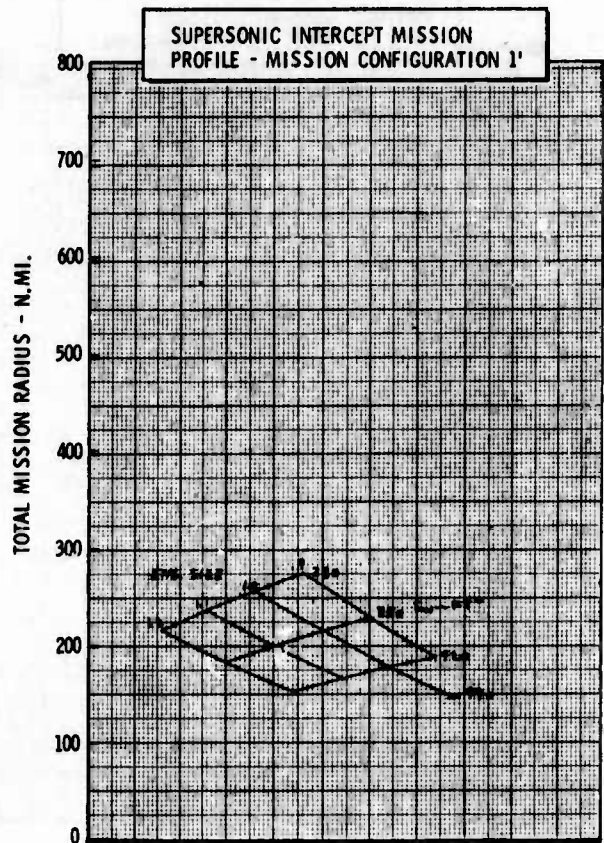
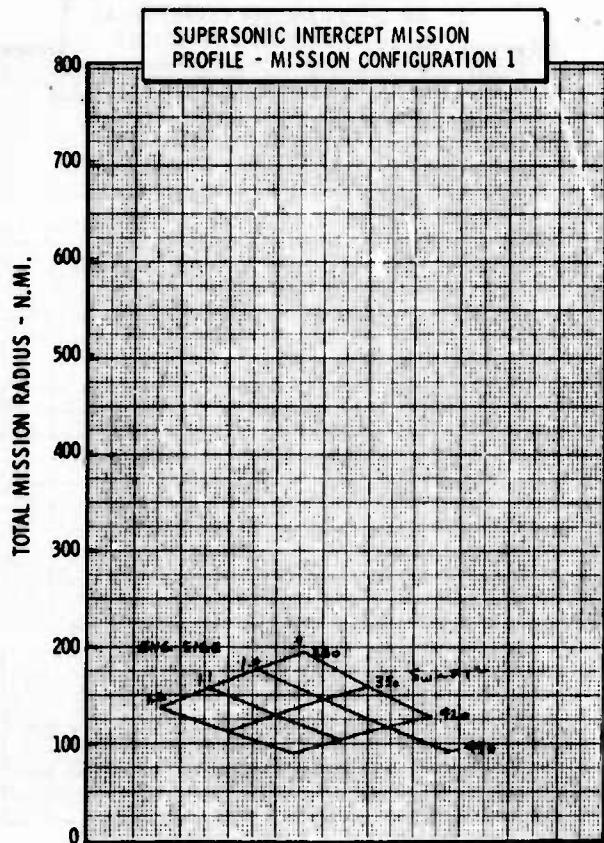
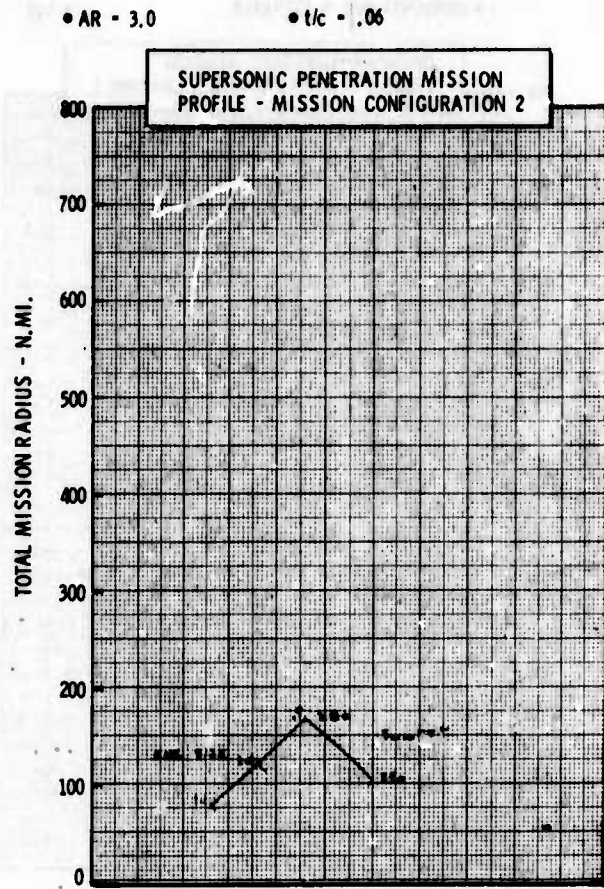
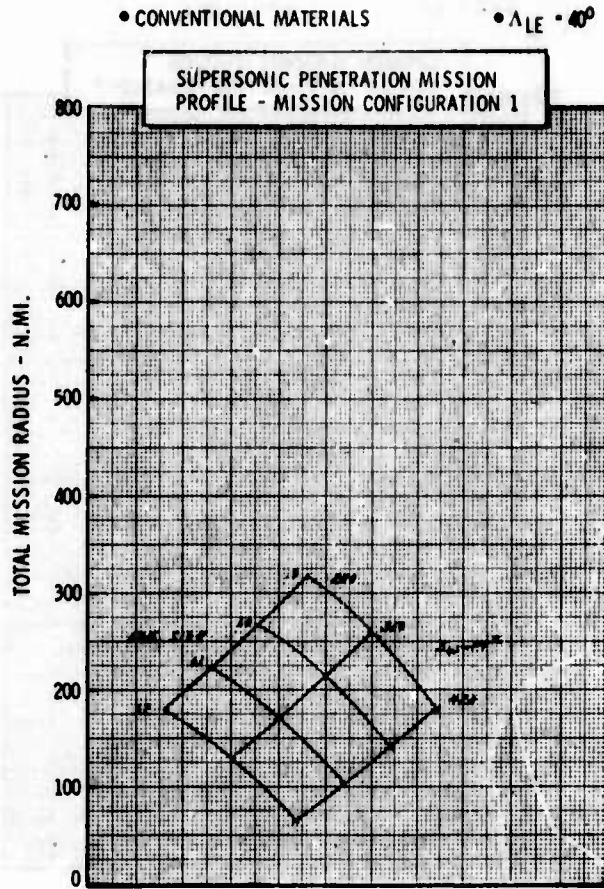


Figure H-26c LWA Mission/Configuration Tradeoff Parametric Data

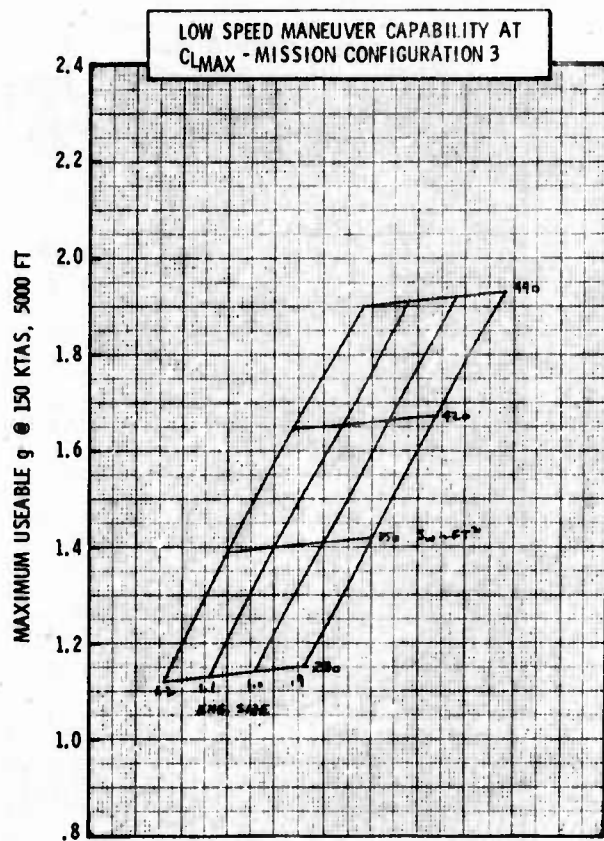
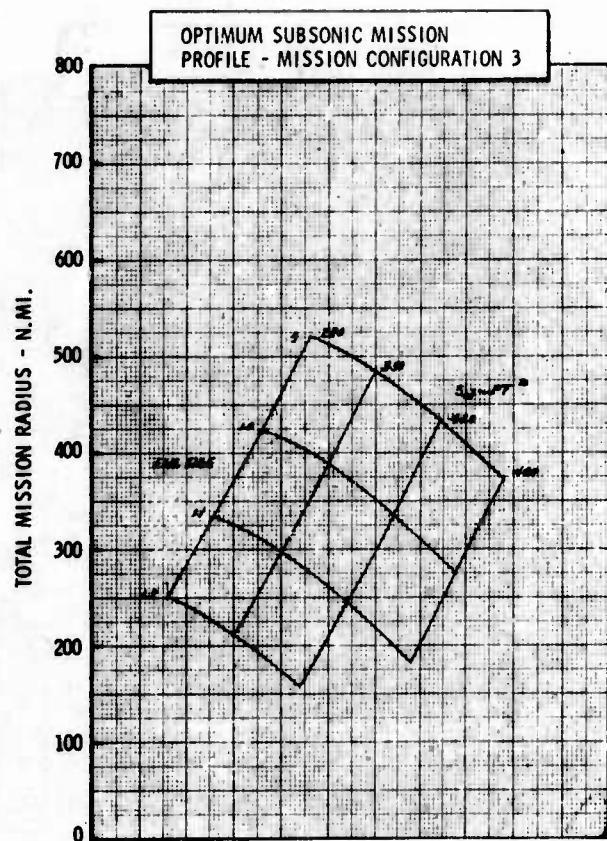
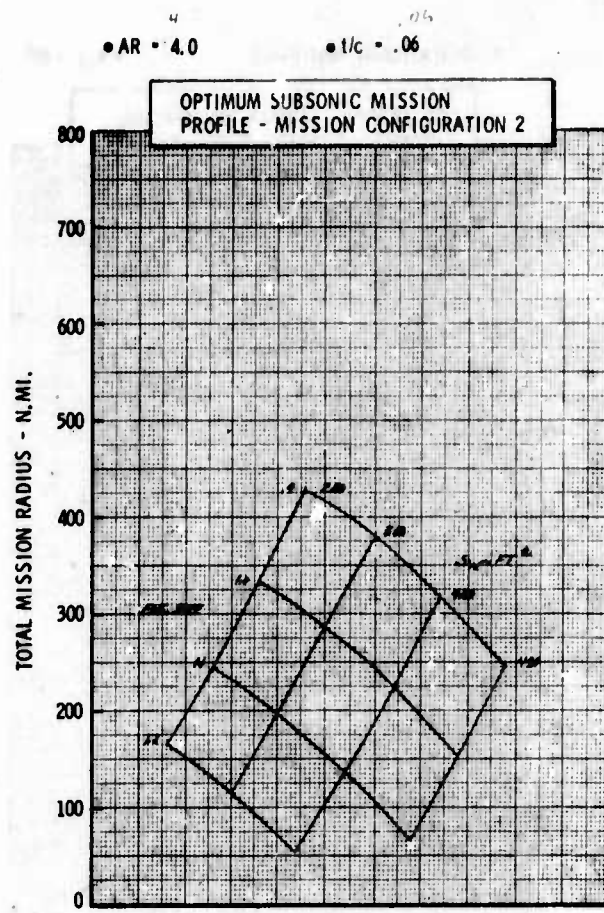
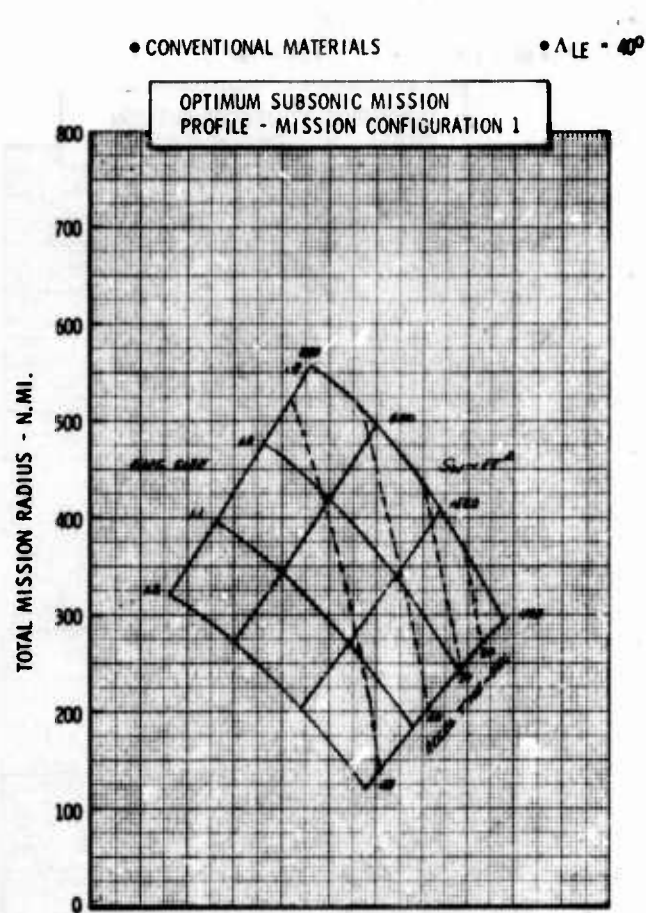


Figure H-27a LWA Mission/Configuration Tradeoff Parametric Data

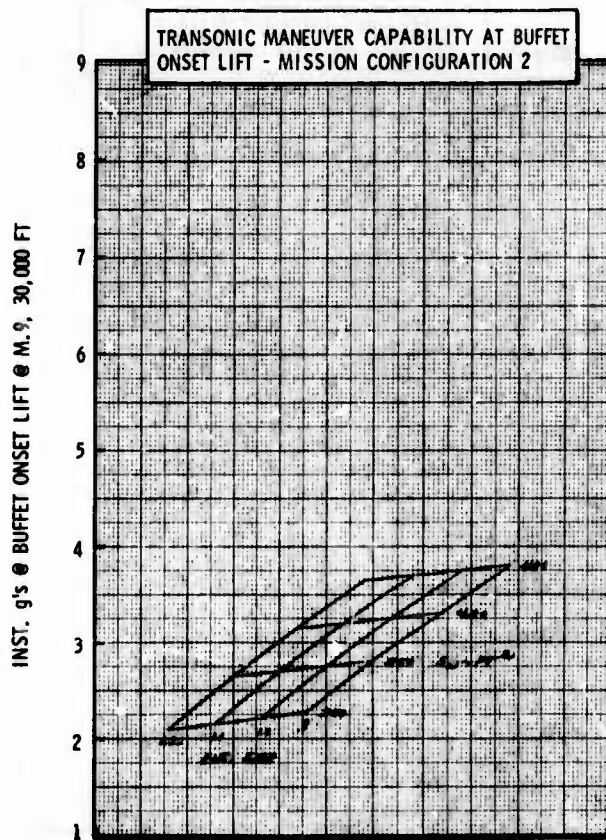
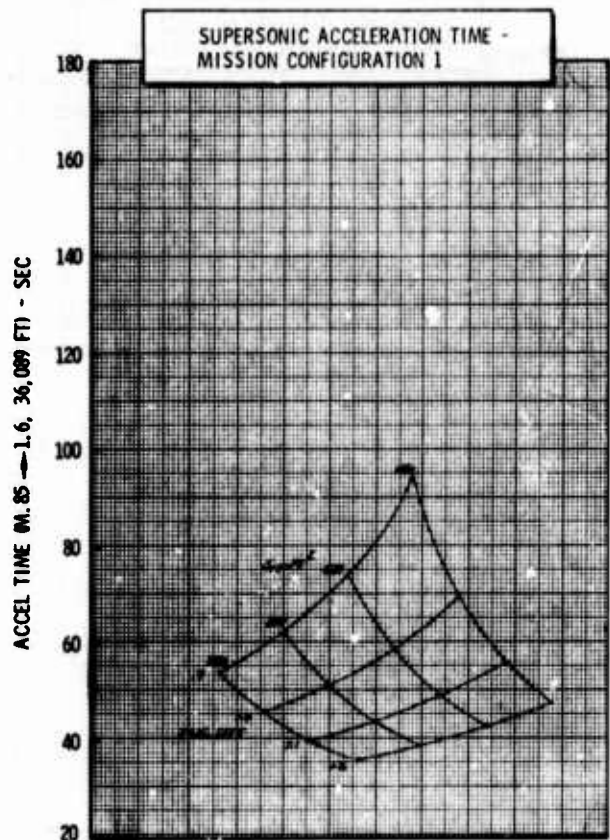
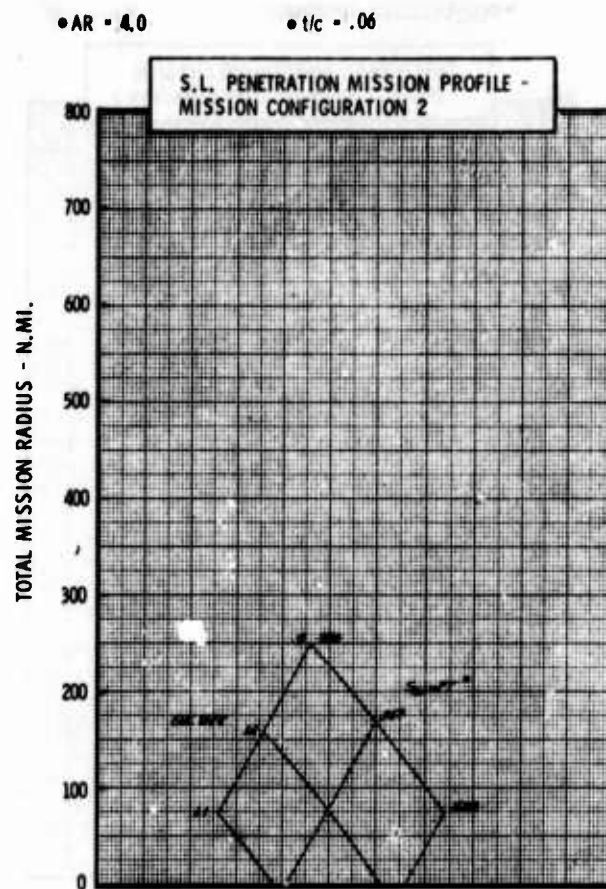
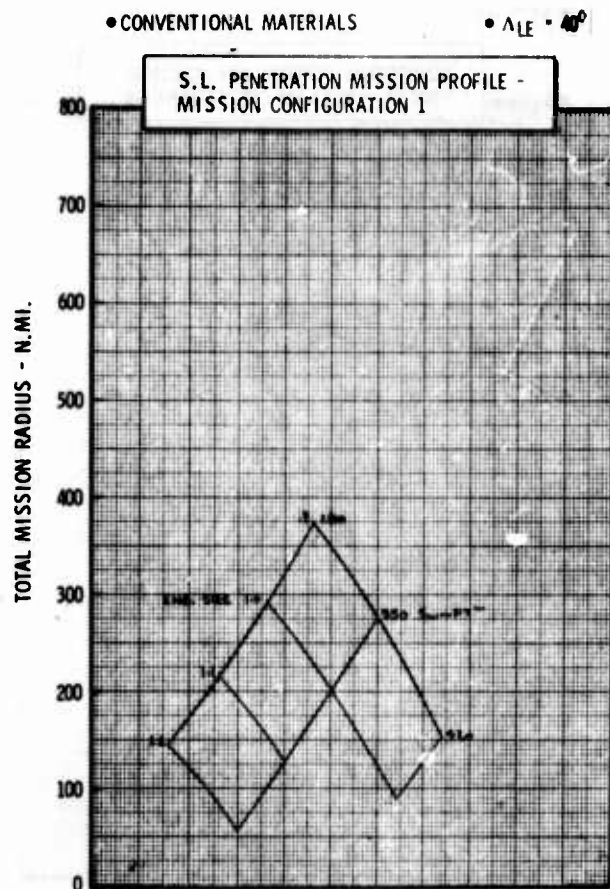


Figure H-27b LWA Mission/Configuration Tradeoff Parametric Data





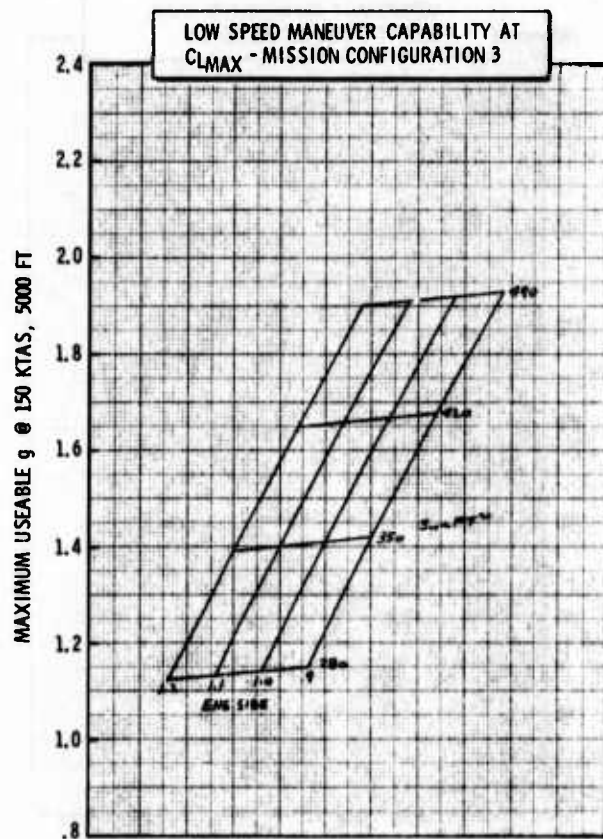
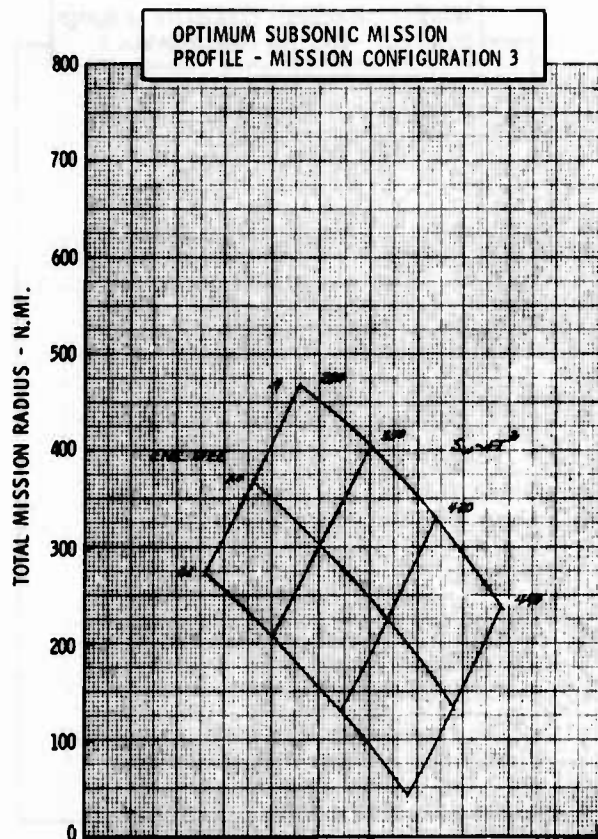
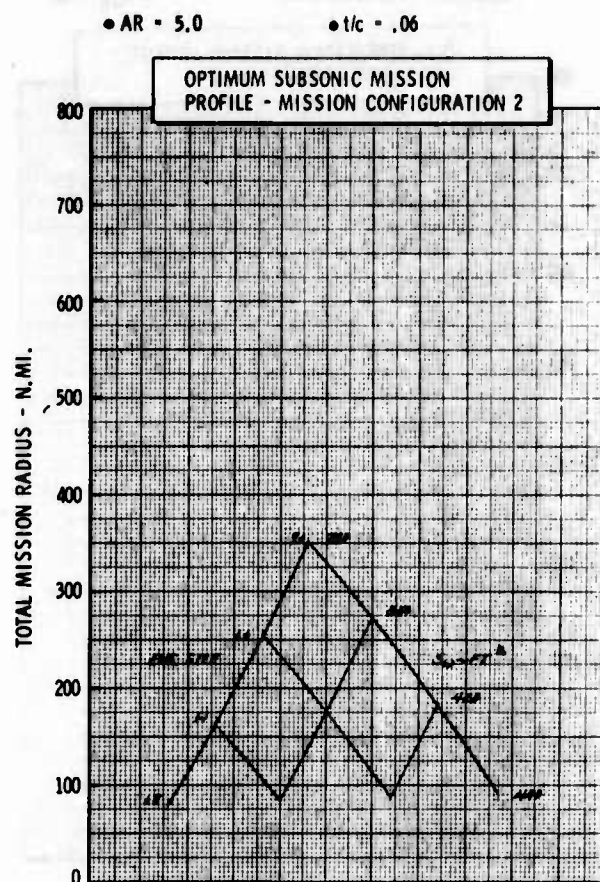
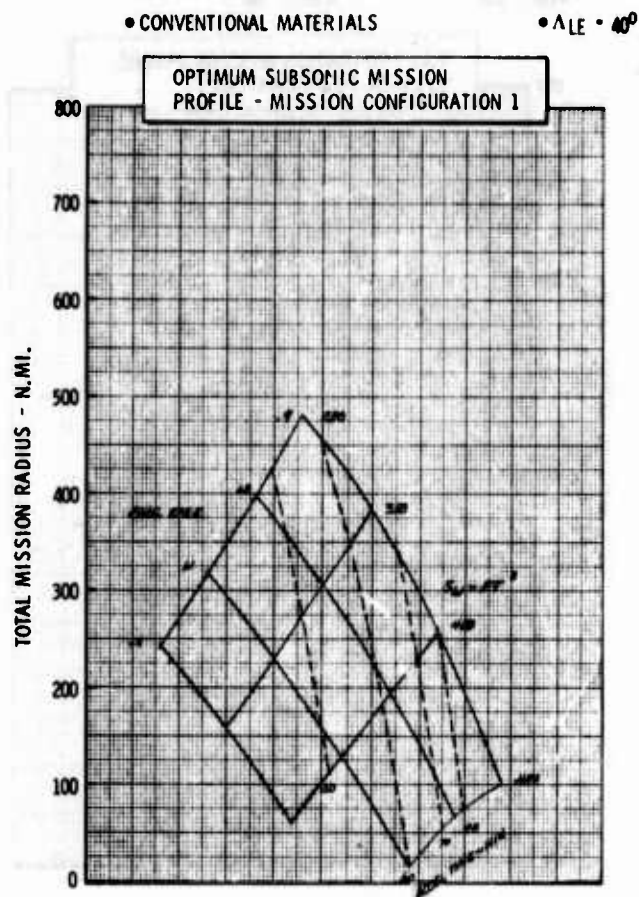


Figure H-28a LWA Mission/Configuration Tradeoff Parametric Data



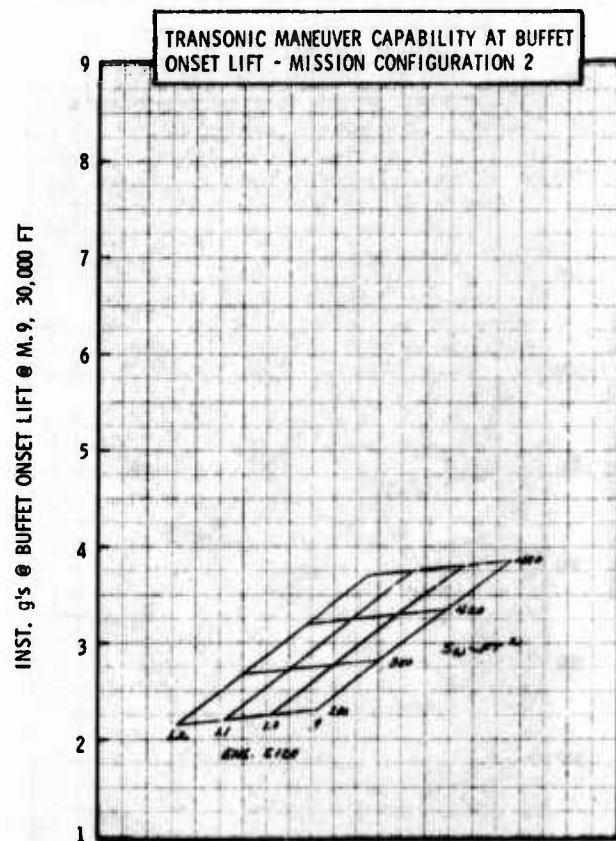
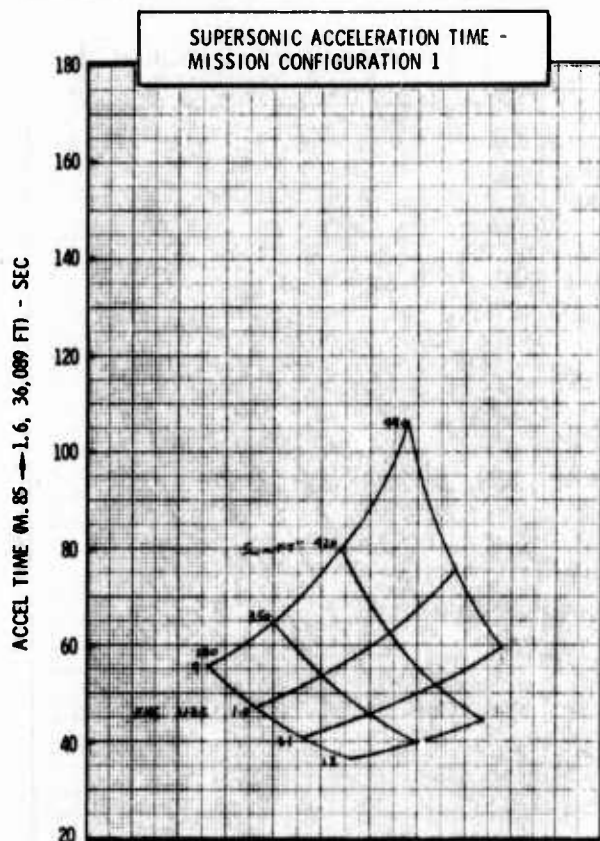
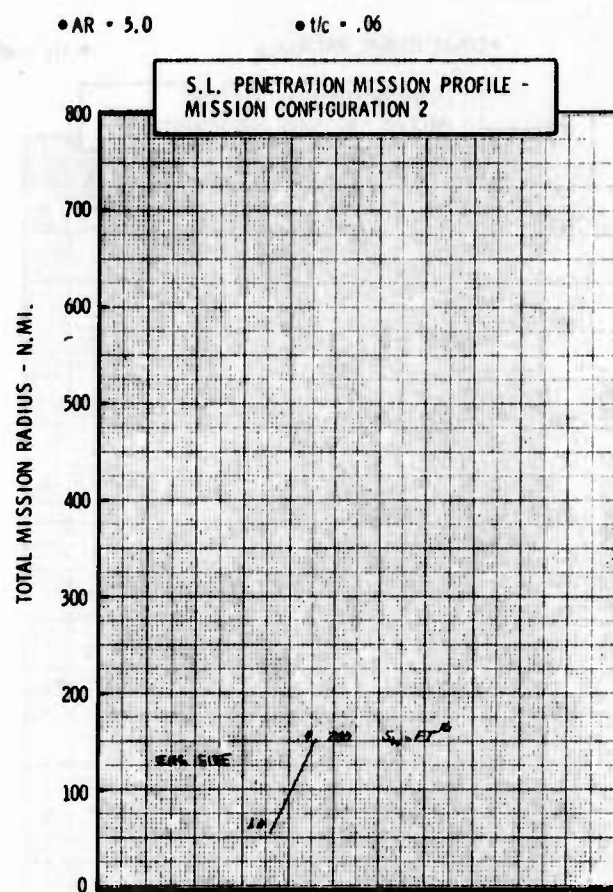
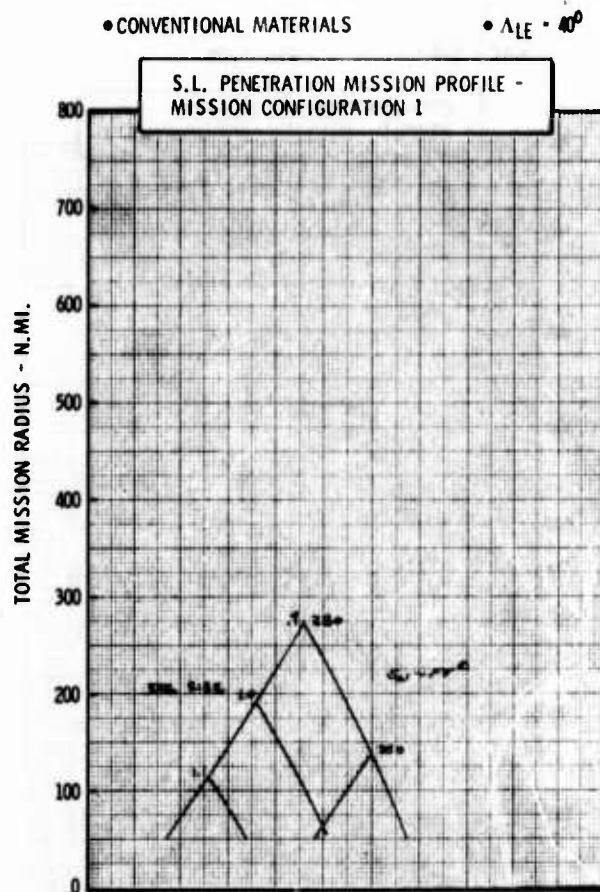
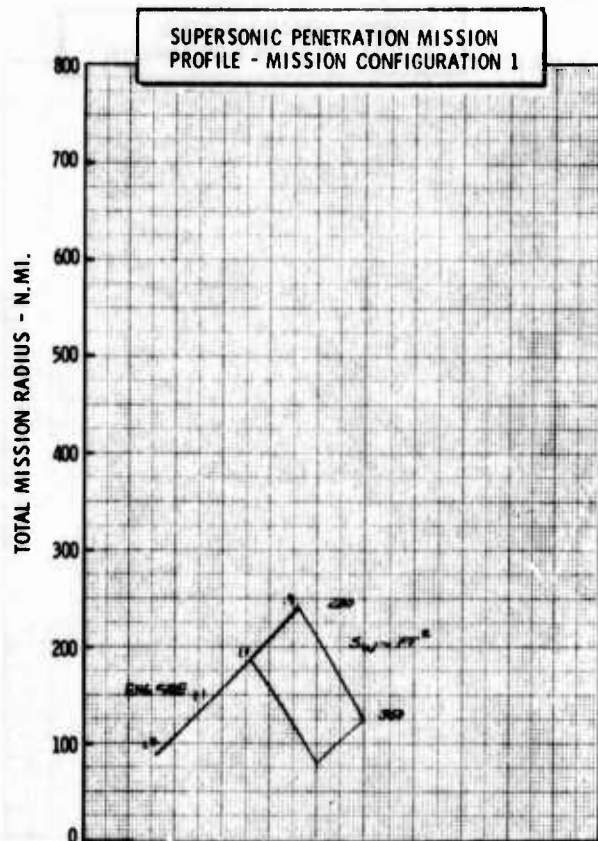


Figure H-28b LWA Mission/Configuration Tradeoff Parametric Data

• CONVENTIONAL MATERIALS

•  $\Delta_{LE} = 40^\circ$



• AR = 5.0

•  $t/c = .06$

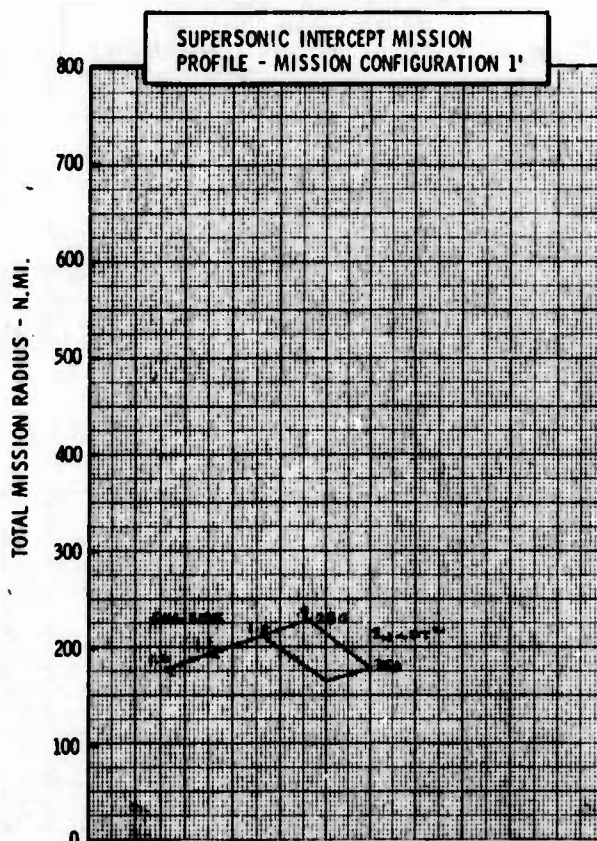
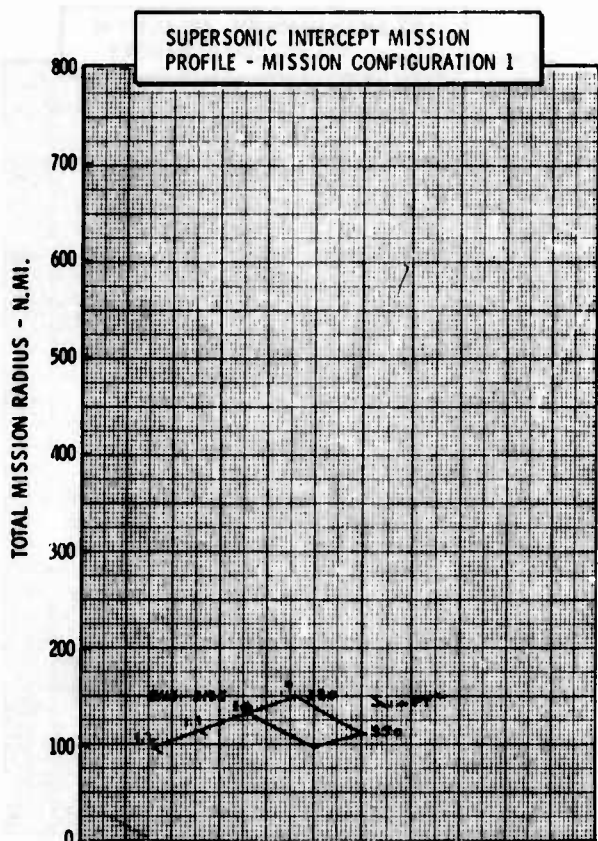
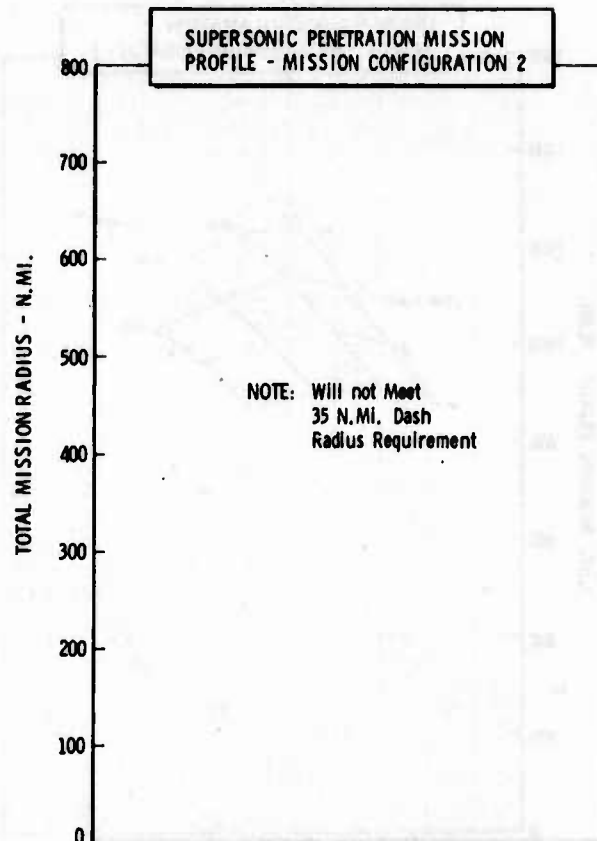


Figure H-28c LWA Mission/Configuration Tradeoff Parametric Data

• COMPOSITE MATERIALS

•  $\Delta LE = 20^\circ$

•  $AR = 3.0$

•  $t/c = .04$

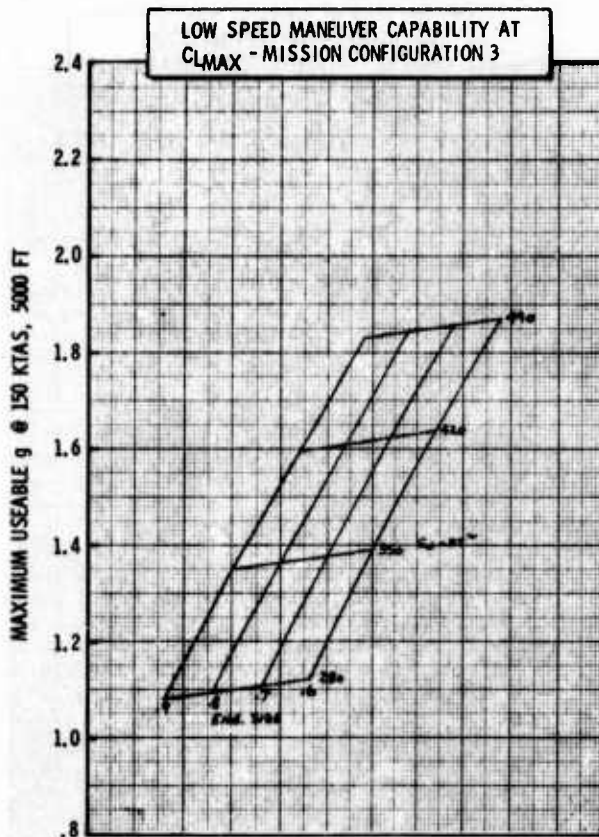
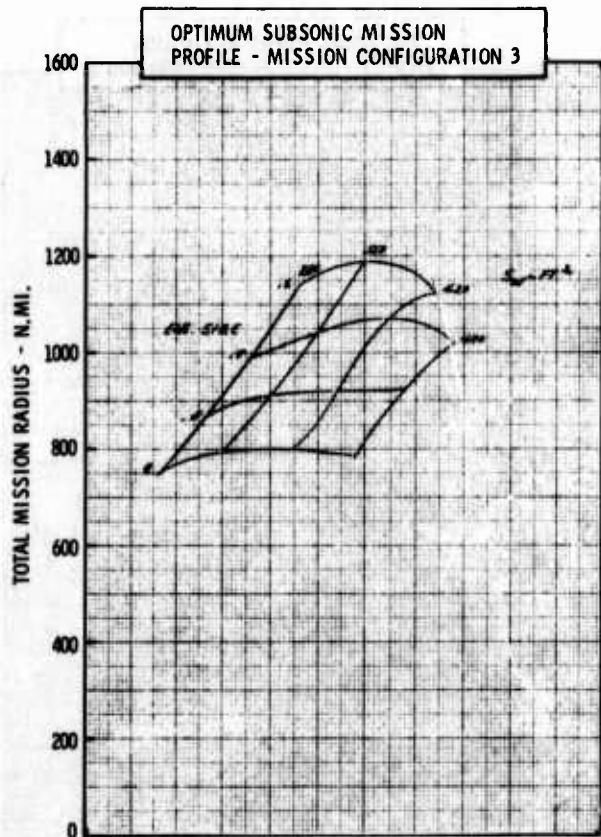
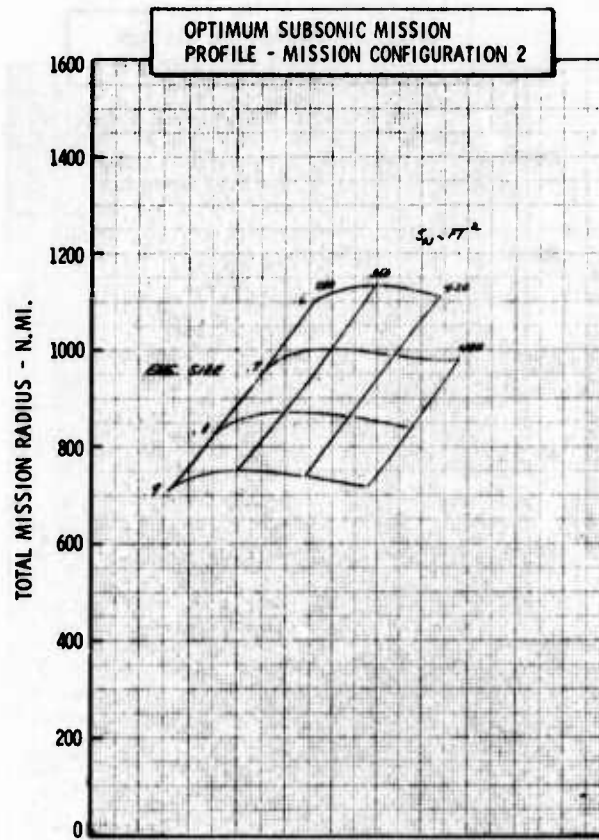
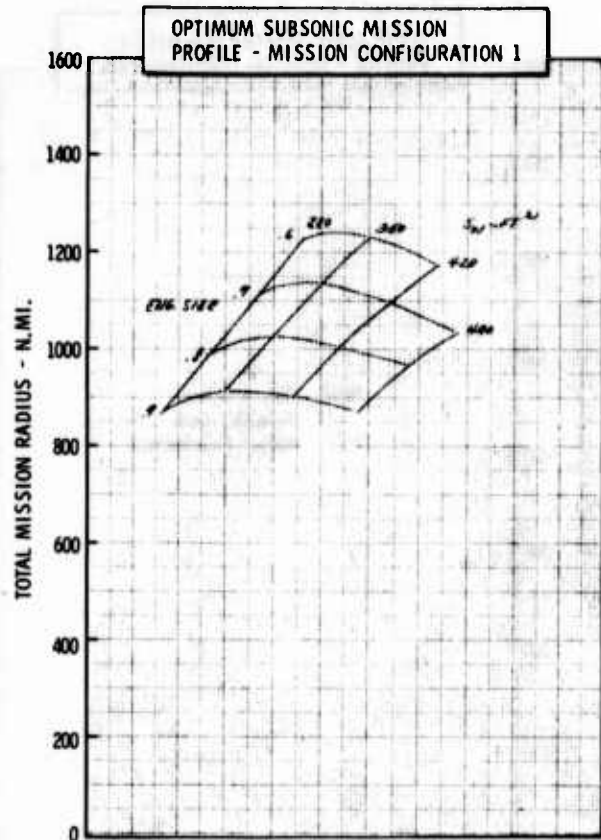


Figure H-29a LWA Mission/Configuration Tradeoff Parametric Data



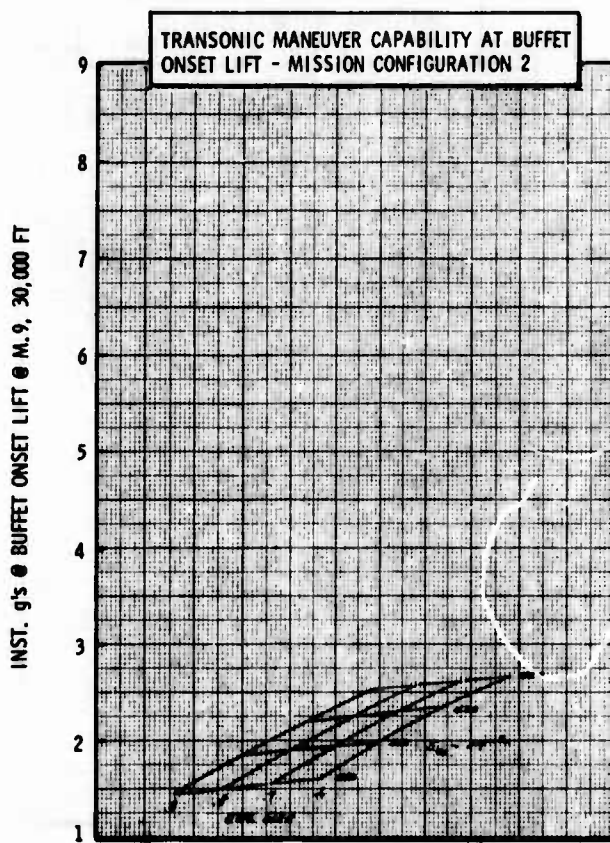
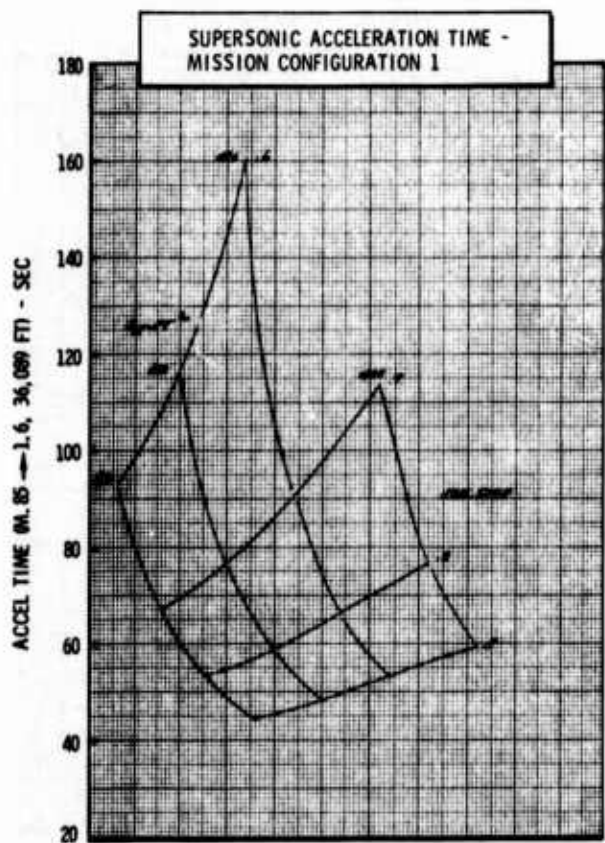
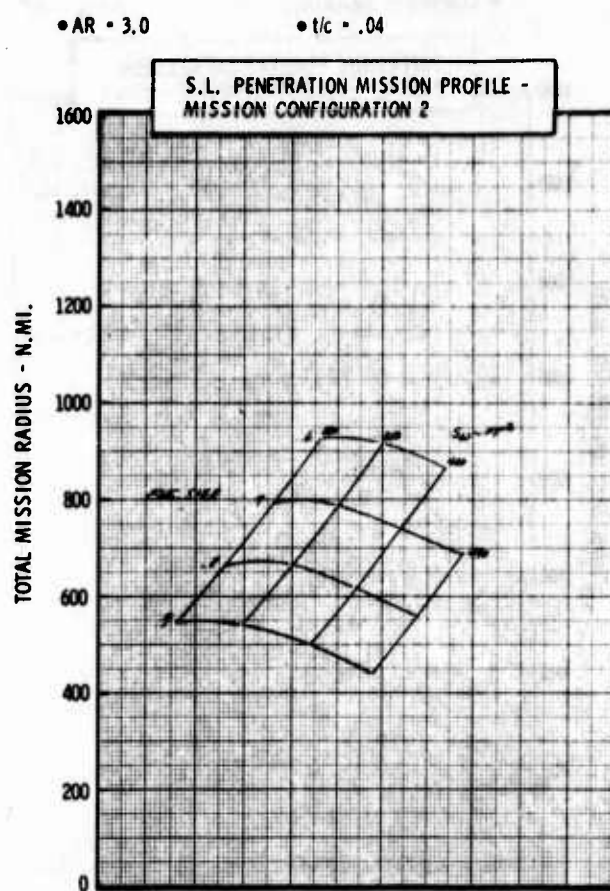
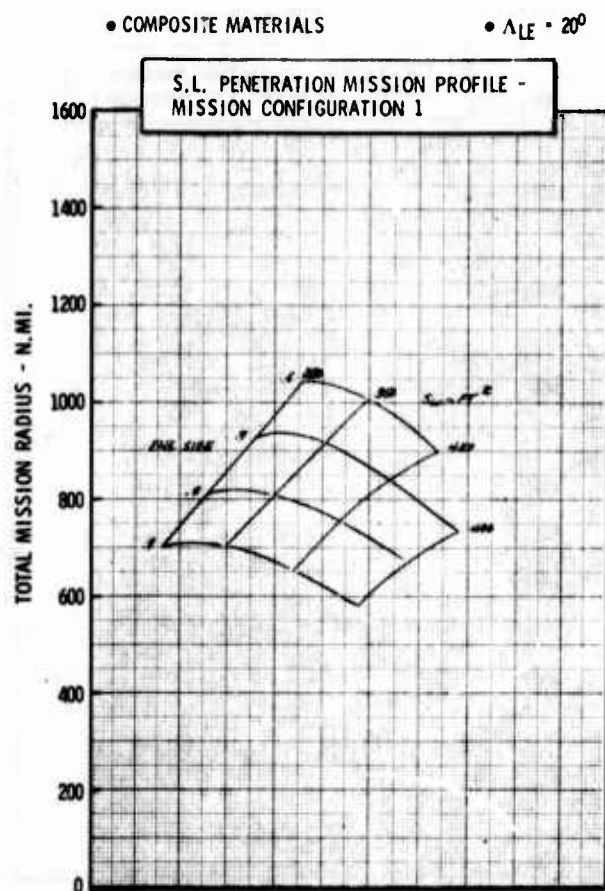
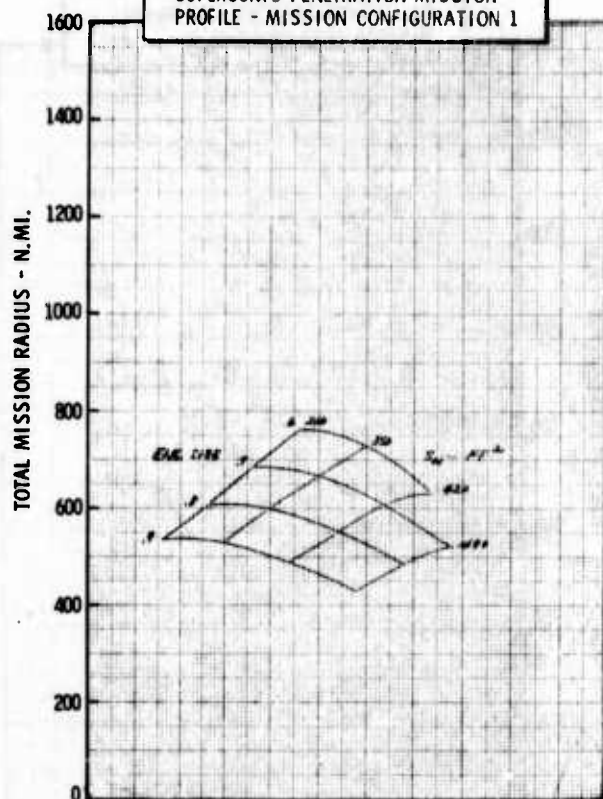


Figure H-29b LWA Mission/Configuration Tradeoff Parametric Data

• COMPOSITE MATERIALS

•  $\Lambda_{LE} = 20^\circ$

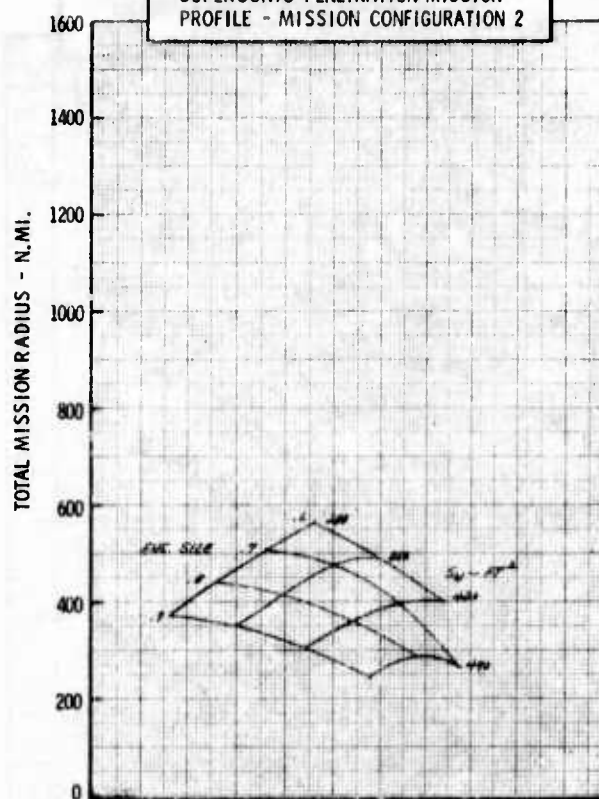
SUPERSONIC PENETRATION MISSION  
PROFILE - MISSION CONFIGURATION 1



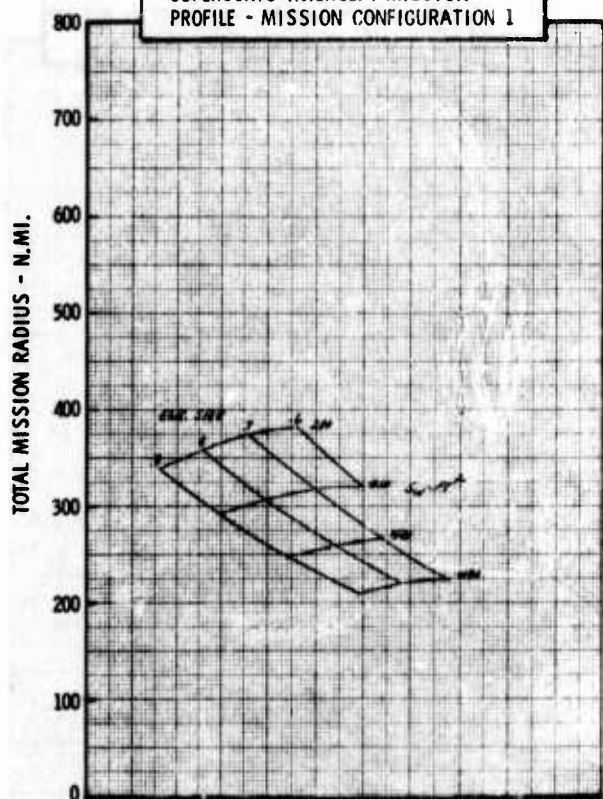
• AR = 3.0

•  $t/c = .04$

SUPERSONIC PENETRATION MISSION  
PROFILE - MISSION CONFIGURATION 2



SUPERSONIC INTERCEPT MISSION  
PROFILE - MISSION CONFIGURATION 1



SUPERSONIC INTERCEPT MISSION  
PROFILE - MISSION CONFIGURATION 1'

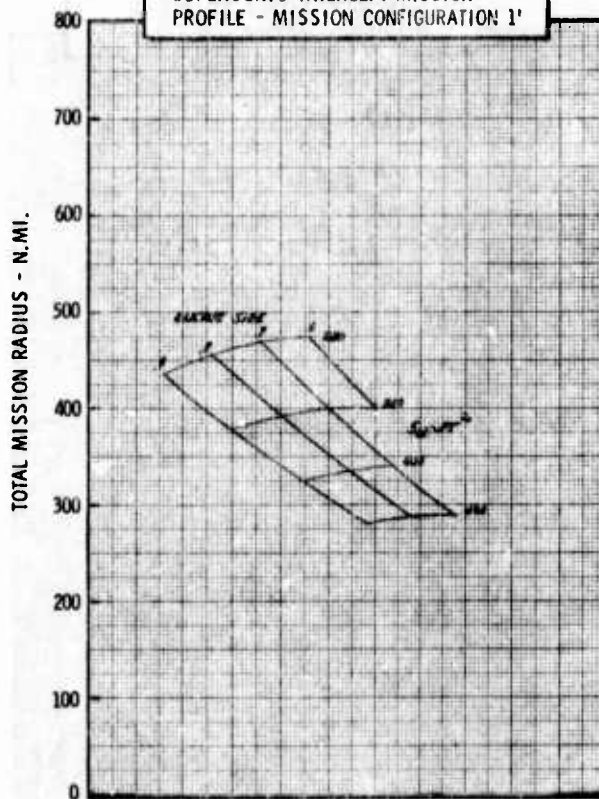


Figure H-29c LWA Mission/Configuration Tradeoff Parametric Data



• COMPOSITE MATERIALS

•  $\Delta LE = 20^\circ$

•  $AR = 4.0$

•  $t/c = .04$

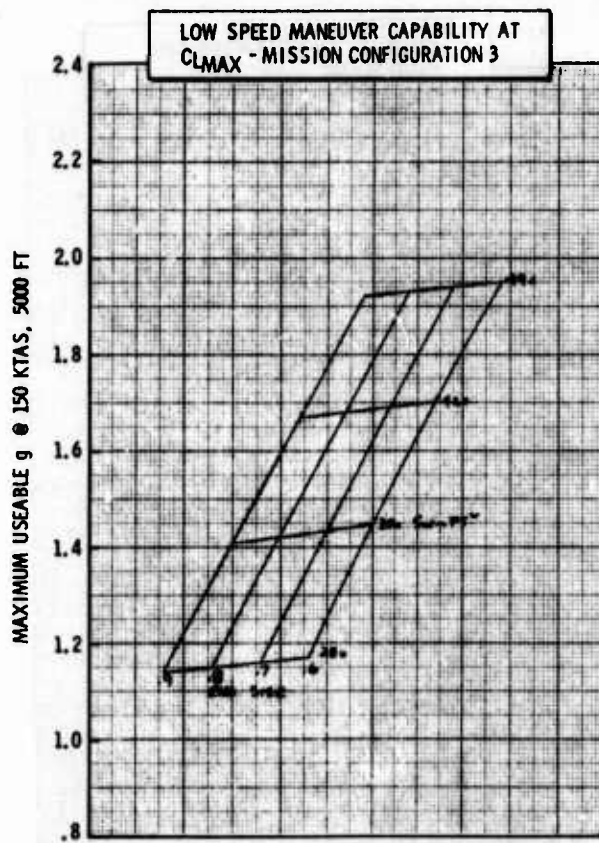
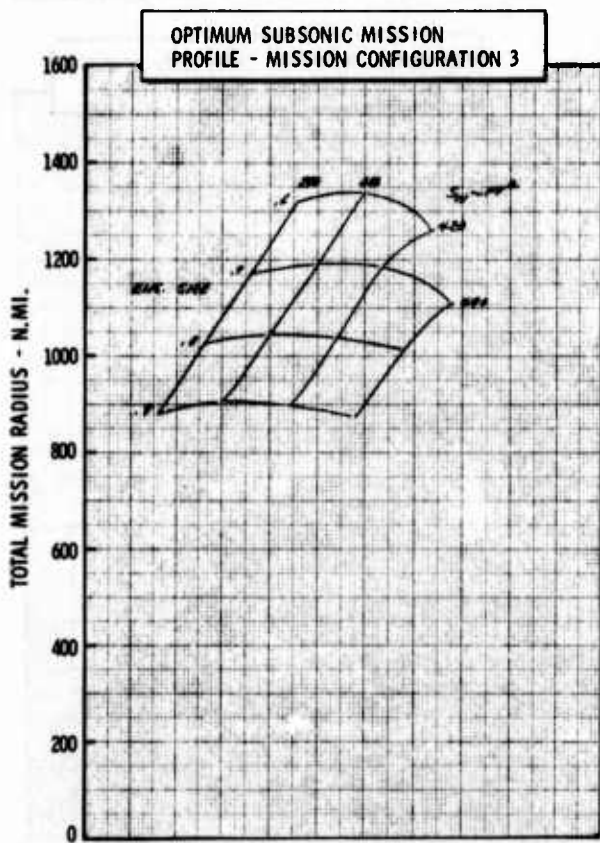
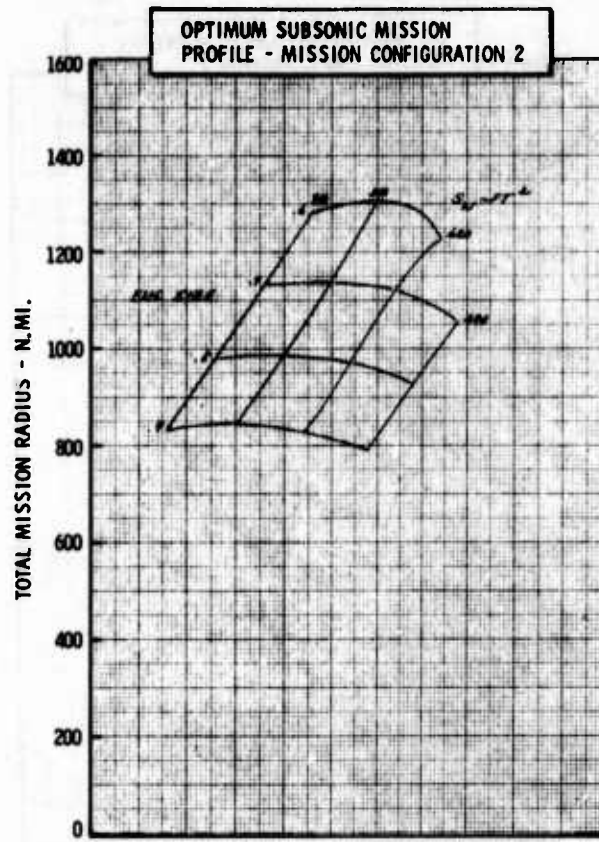
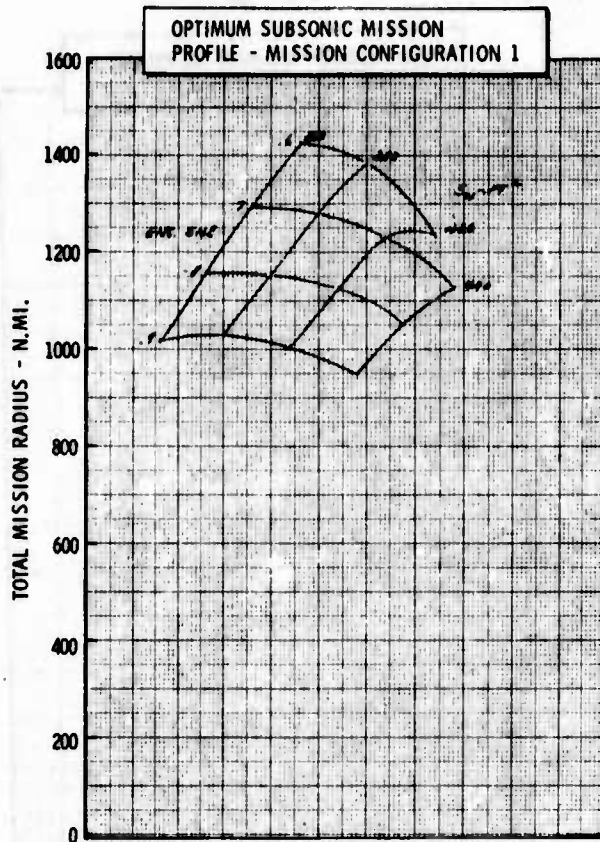


Figure H-30a LWA Mission/Configuration Tradeoff Parametric Data

• COMPOSITE MATERIALS

•  $\Lambda_{LE} = 20^\circ$

• AR = 4.0

•  $t/c = .04$

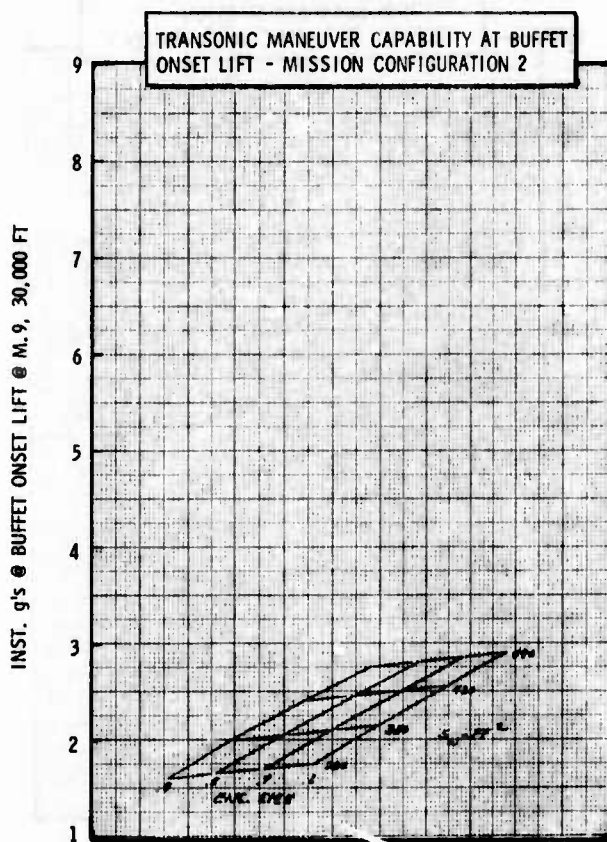
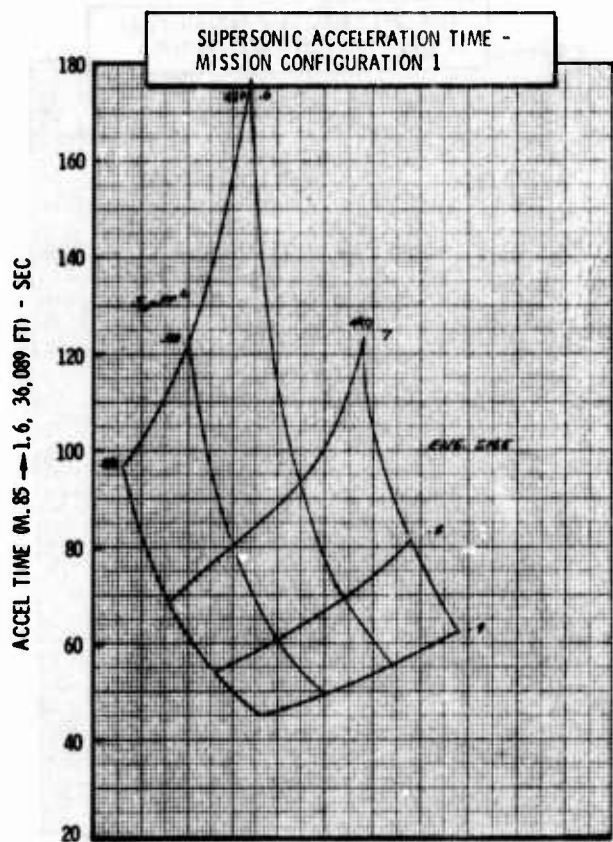
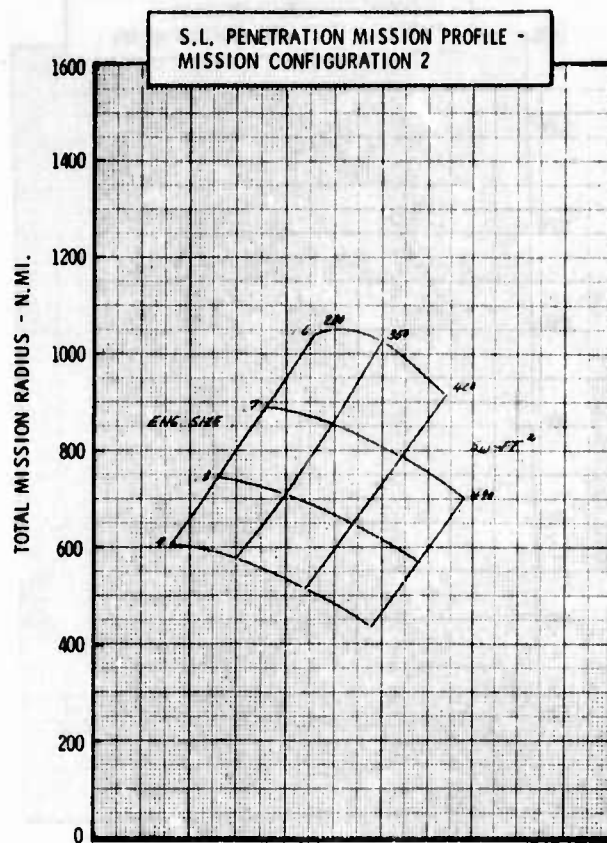
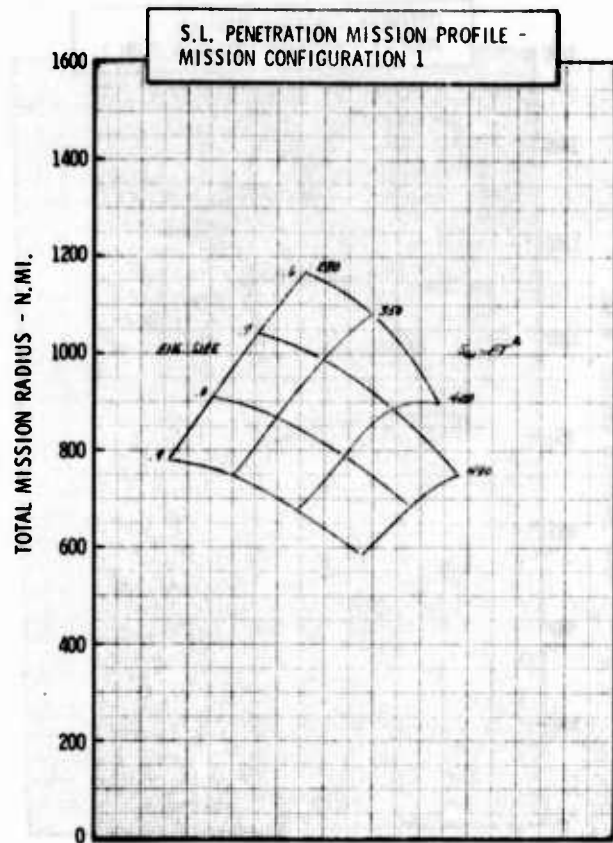


Figure H-30b LWA Mission/Configuration Tradeoff Parametric Data

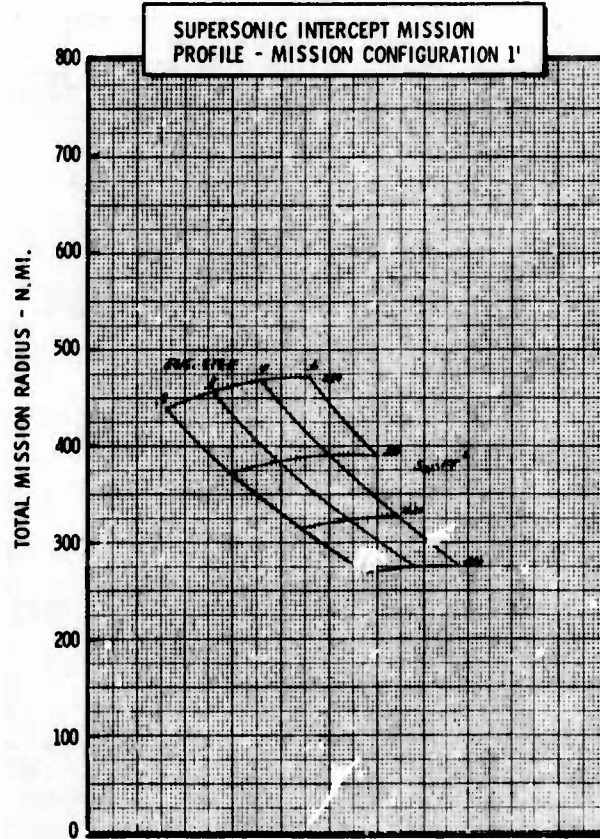
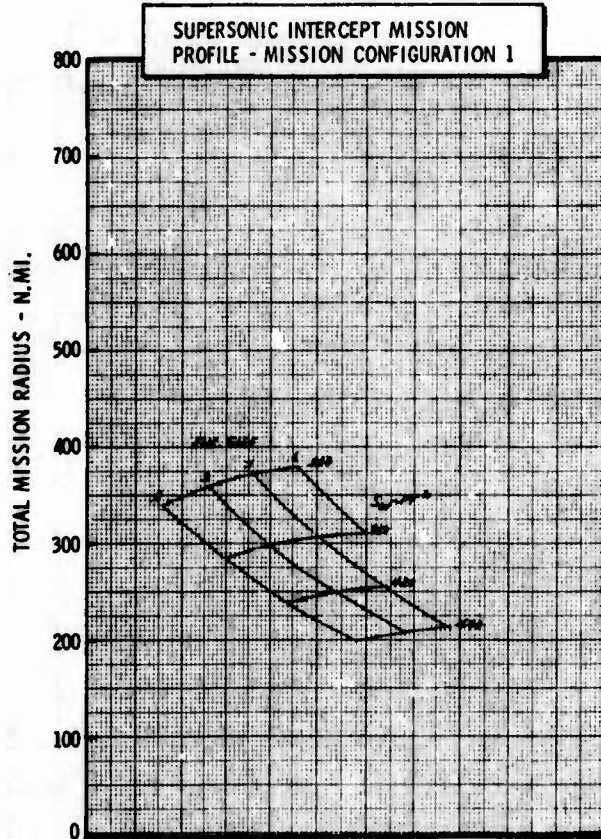
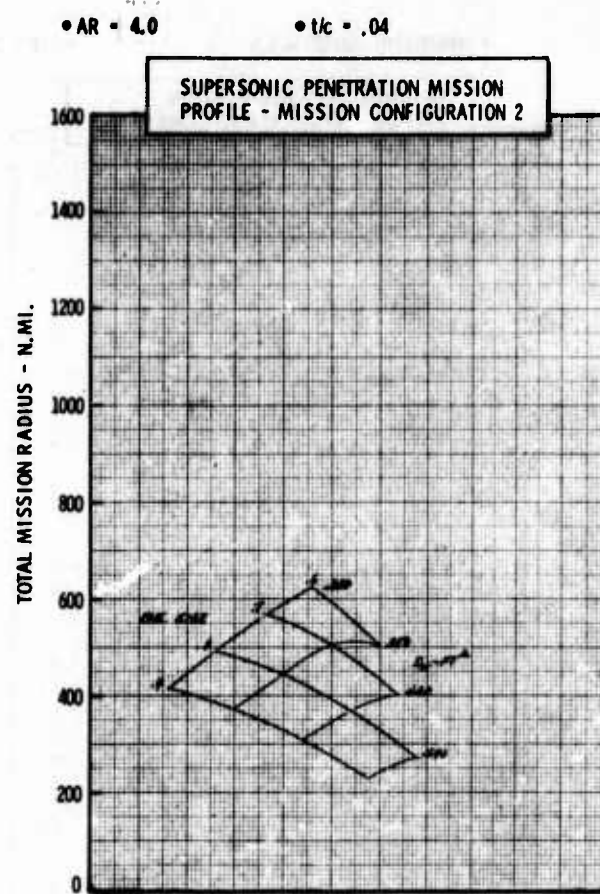
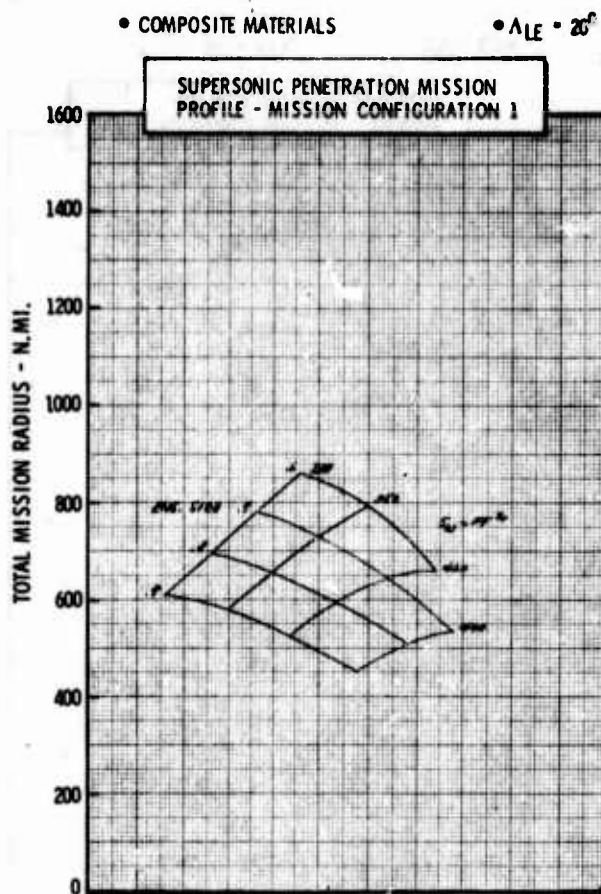


Figure H-30c LWA Mission/Configuration Tradeoff Parametric Data



• COMPOSITE MATERIALS

•  $\Lambda_{LE} = 20^\circ$

•  $AR = 5.0$

•  $t/c = .04$

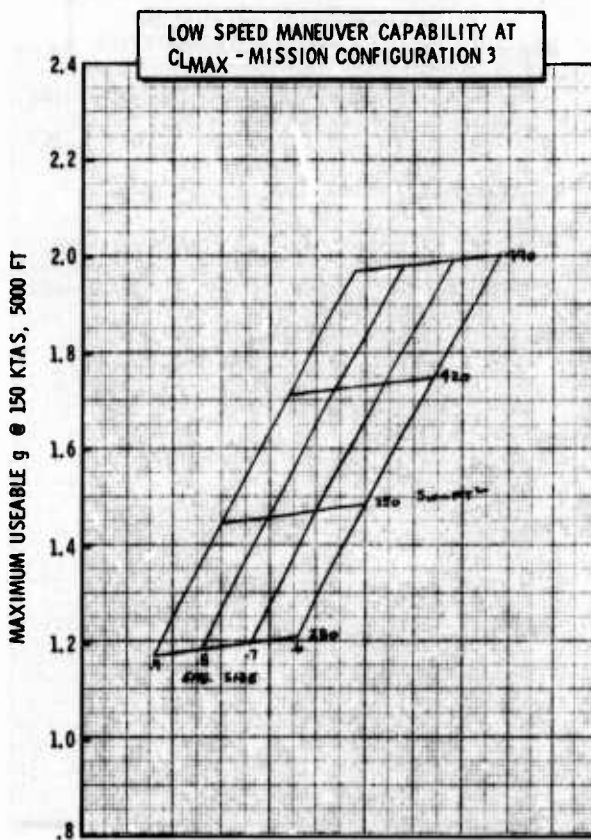
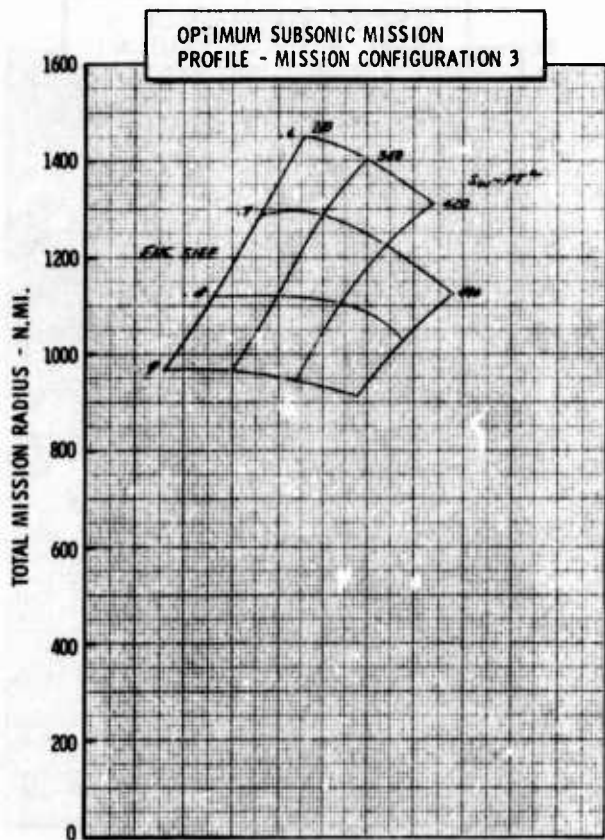
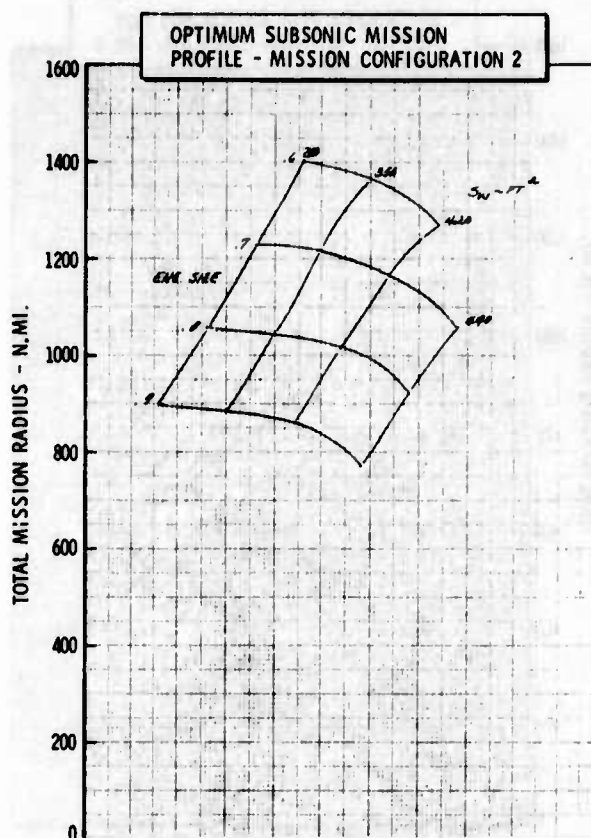
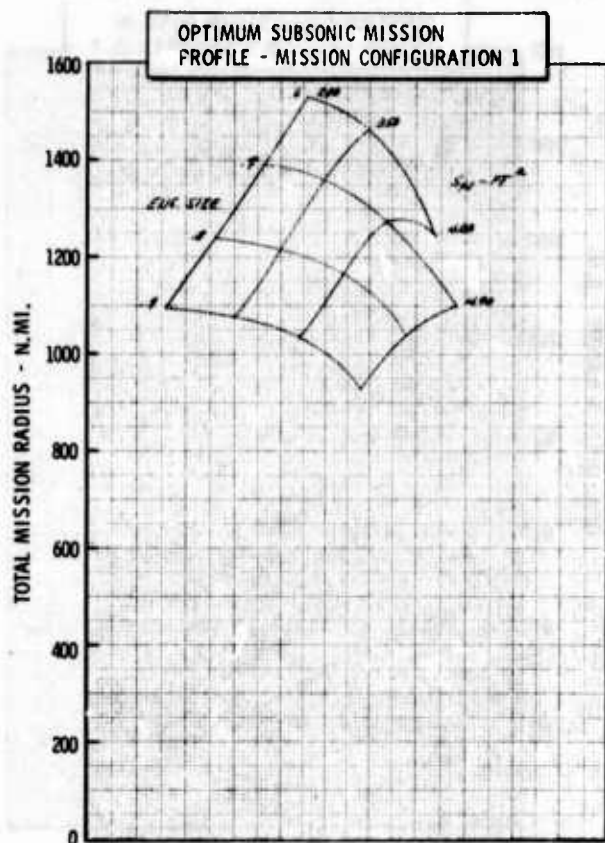
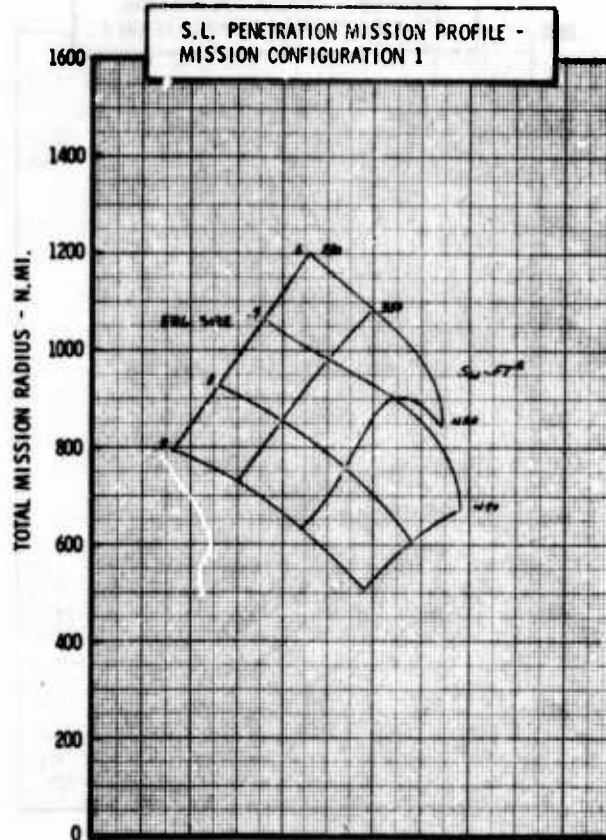


Figure H-31a LWA Mission/Configuration Tradeoff Parametric Data

• COMPOSITE MATERIALS

•  $\Delta LE = 20^\circ$



• AR = 5.0

•  $t/c = .04$

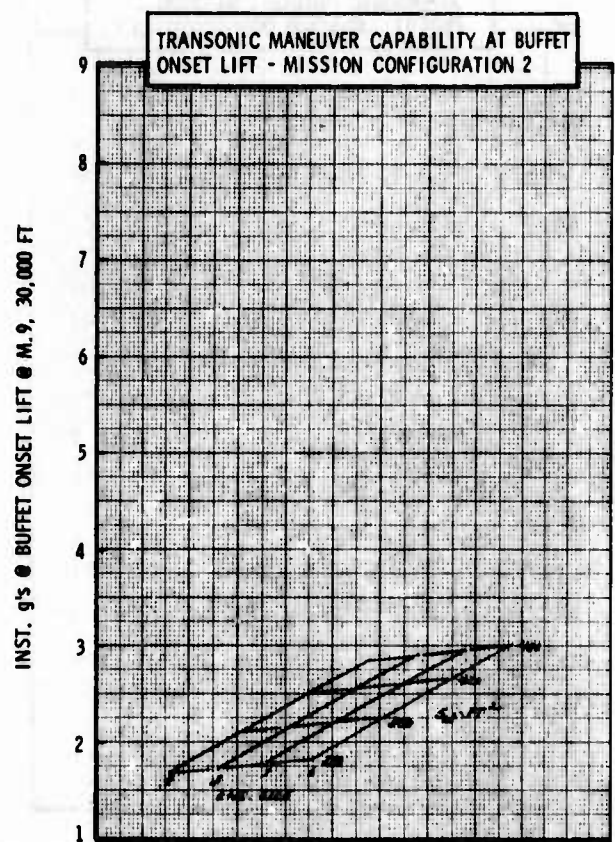
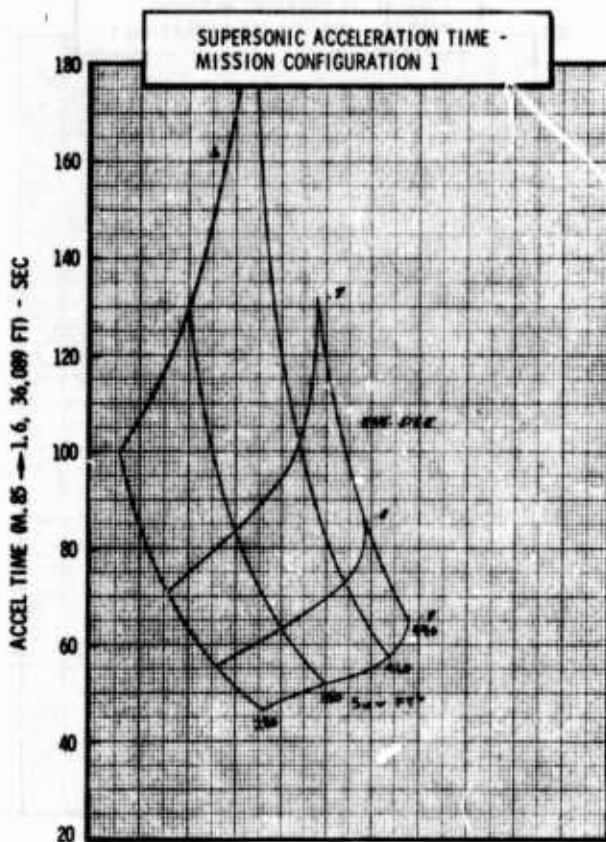
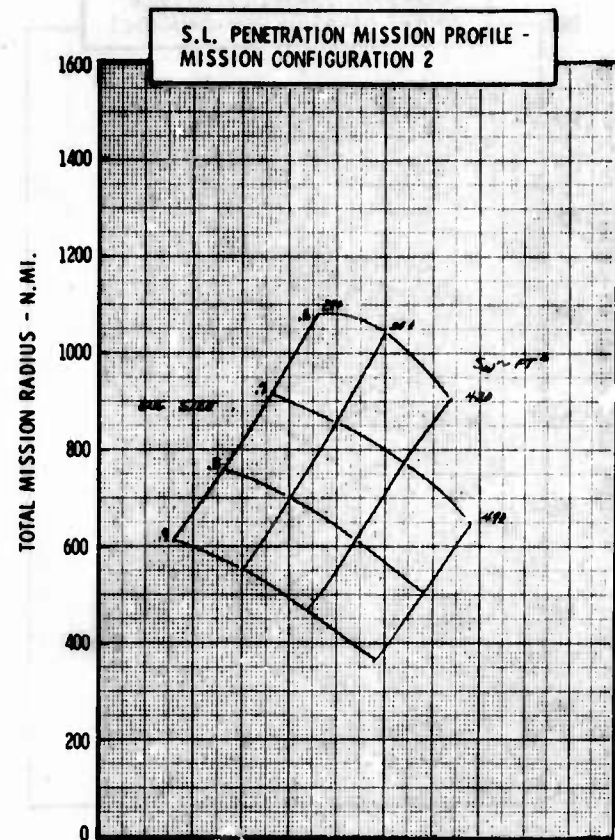


Figure H-31b LWA Mission/Configuration Tradeoff Parametric Data



• COMPOSITE MATERIALS

•  $\Lambda_{LE} = 20^\circ$

•  $AR = 5.0$

•  $t/c = .04$

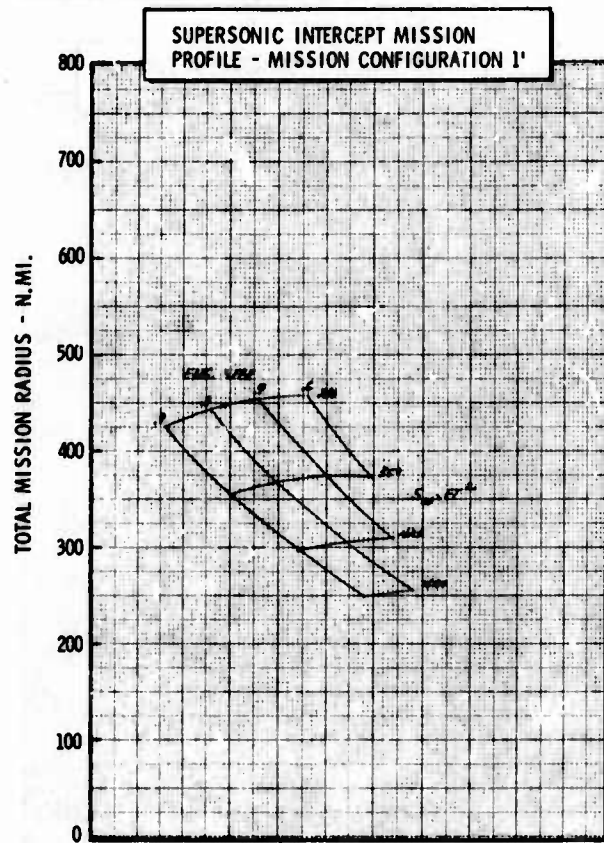
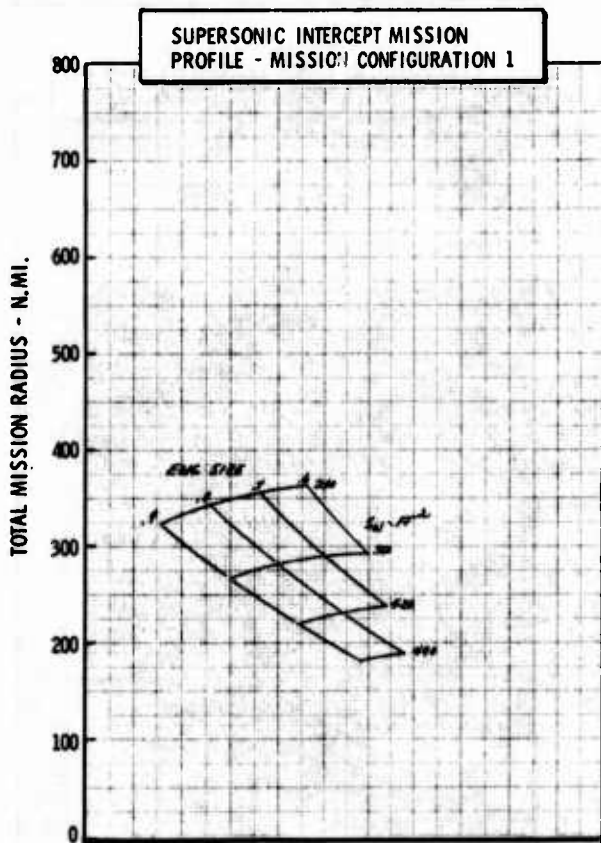
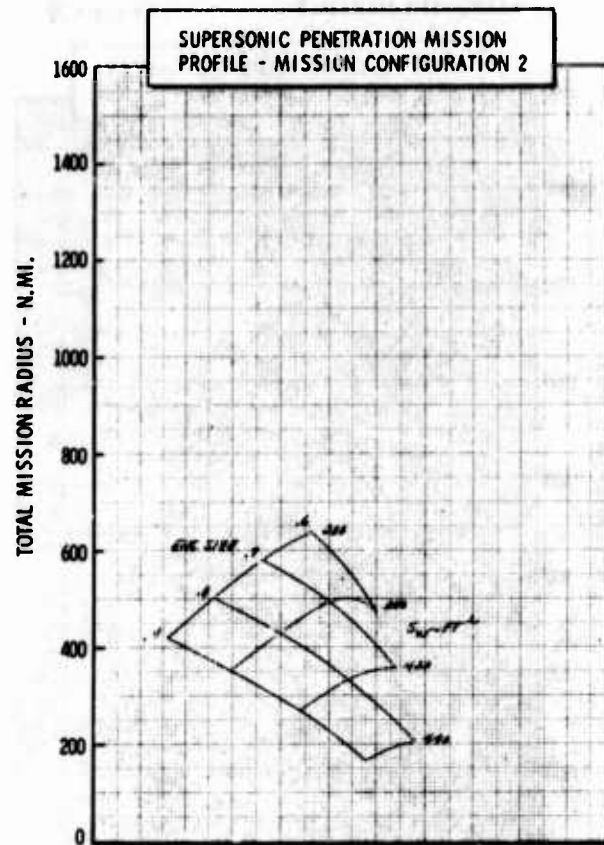
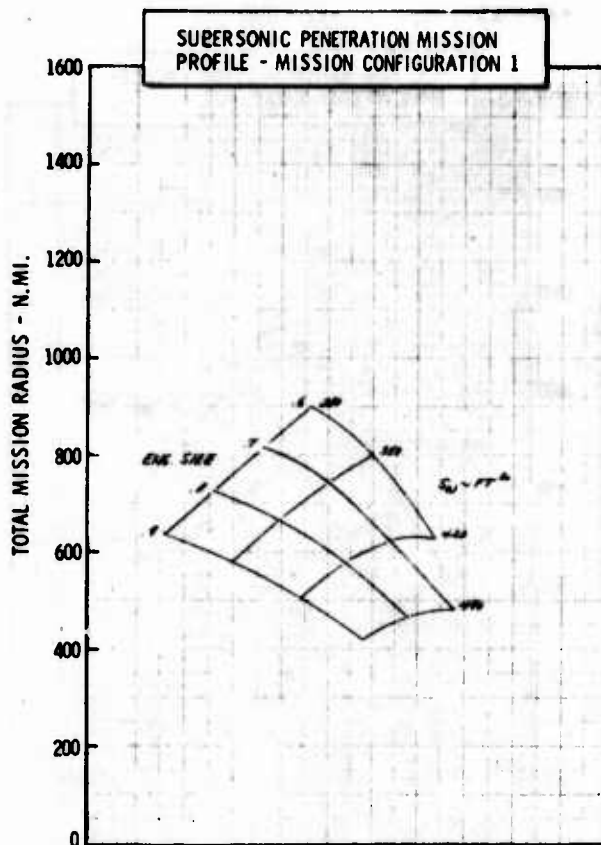


Figure H-31c LWA Mission/Configuration Tradeoff Parametric Data

• COMPOSITE MATERIALS

•  $\Delta LE = 30^\circ$

•  $AR = 3.0$

•  $t/c = .04$

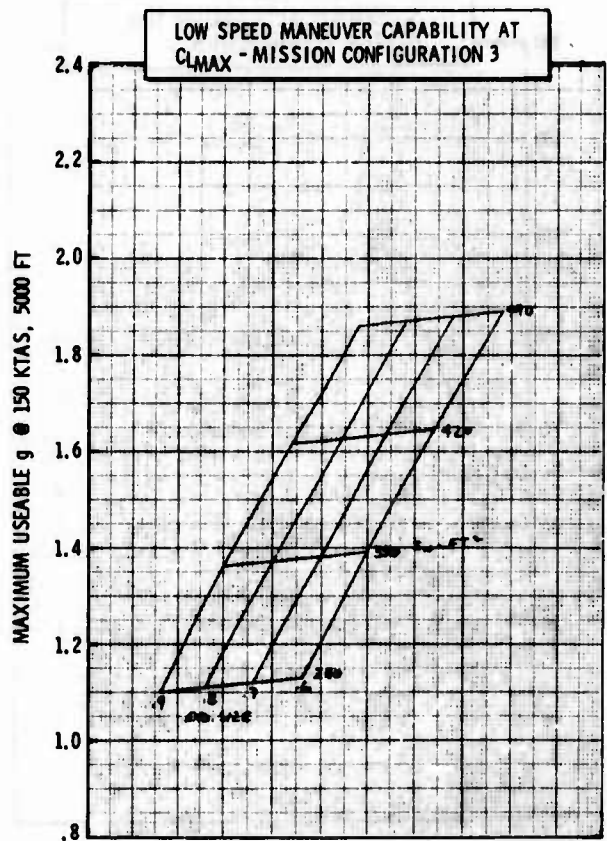
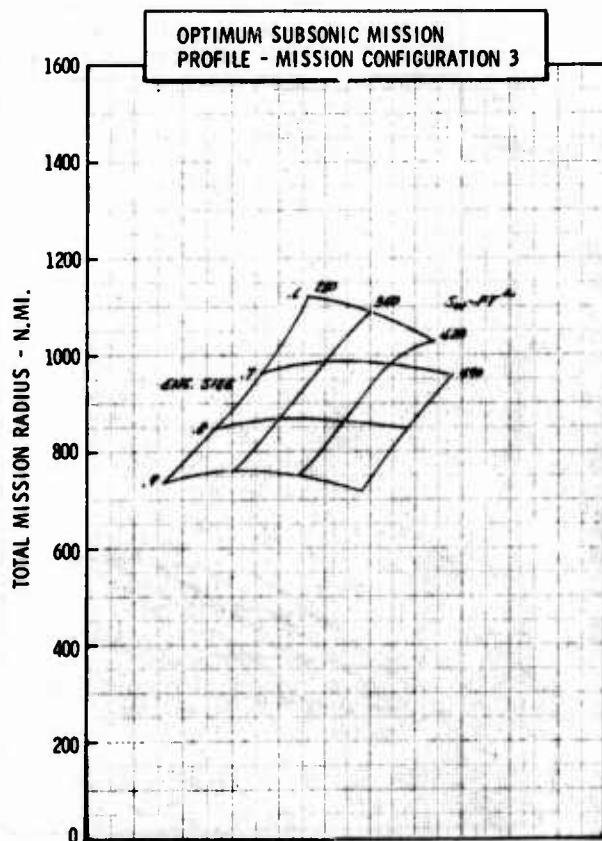
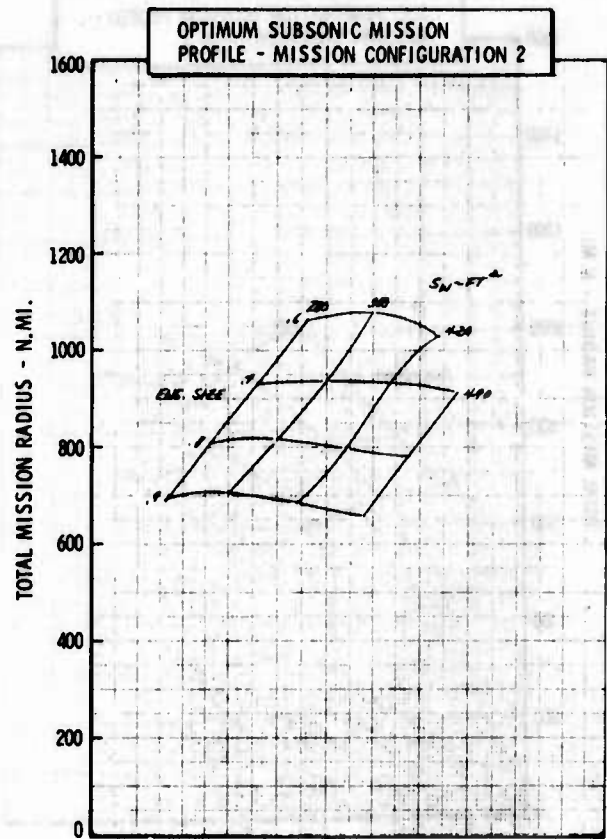
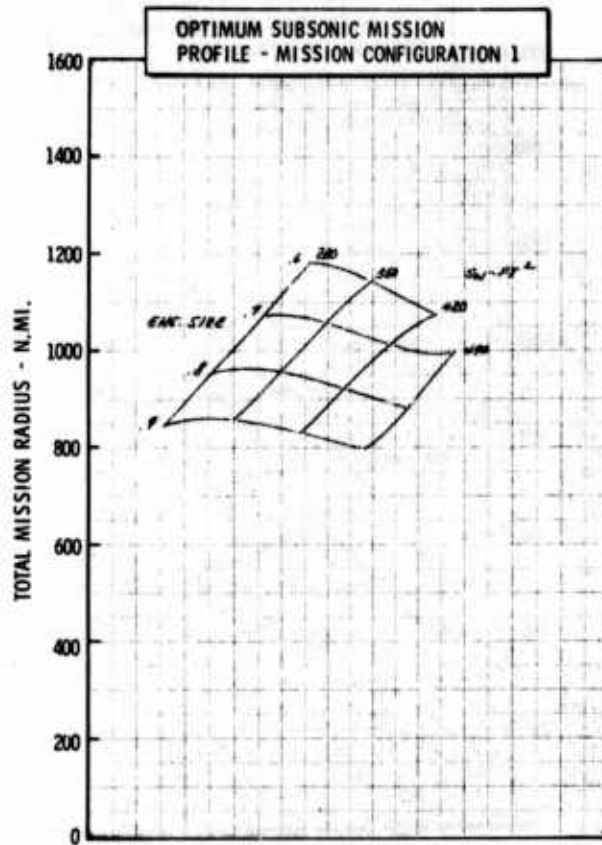


Figure H-32a LWA Mission/Configuration Tradeoff Parametric Data

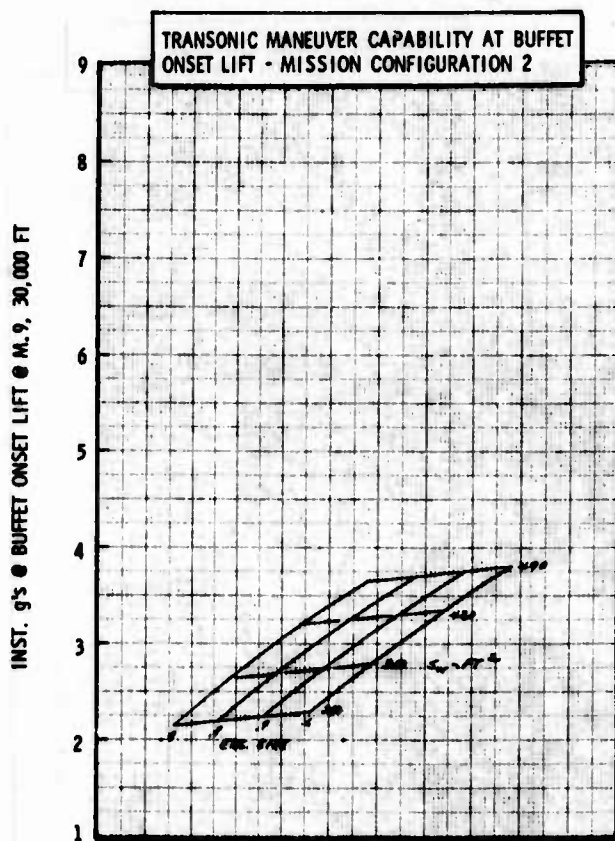
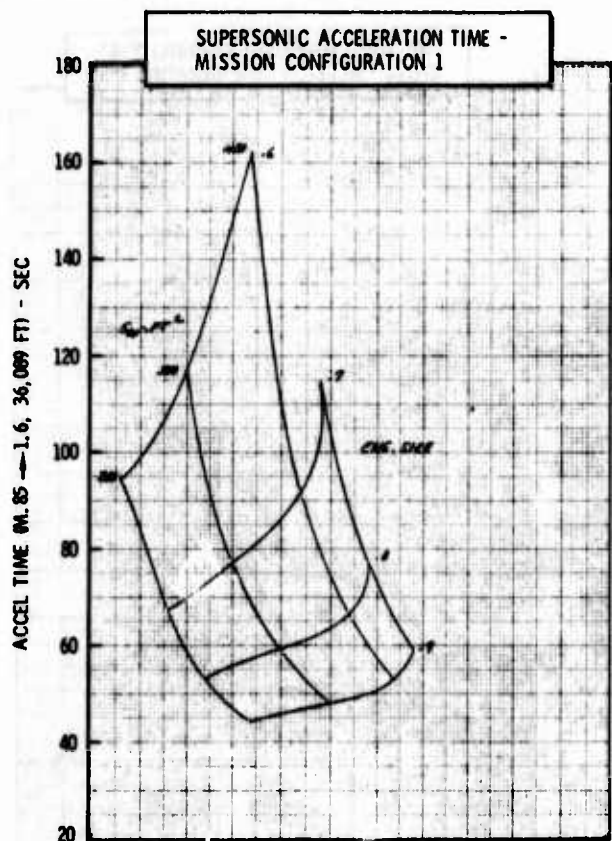
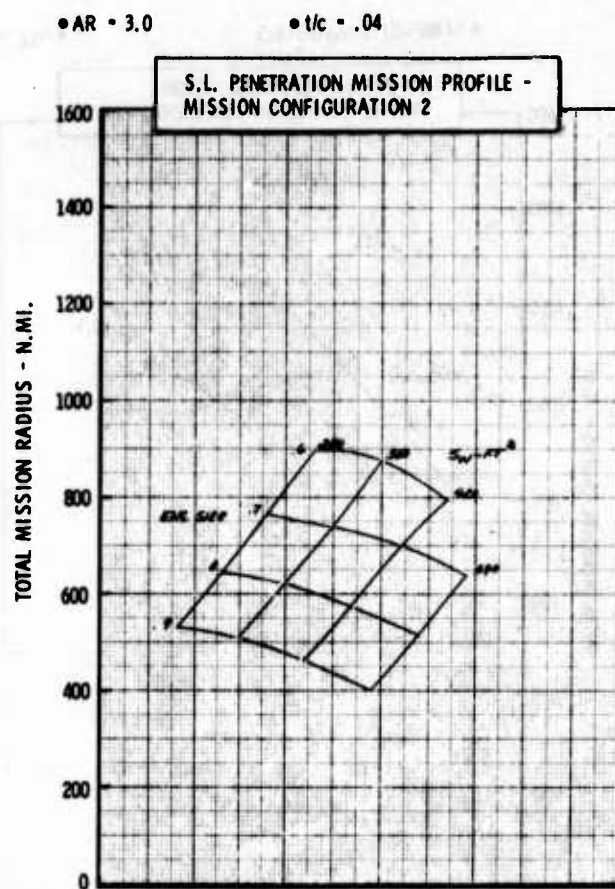
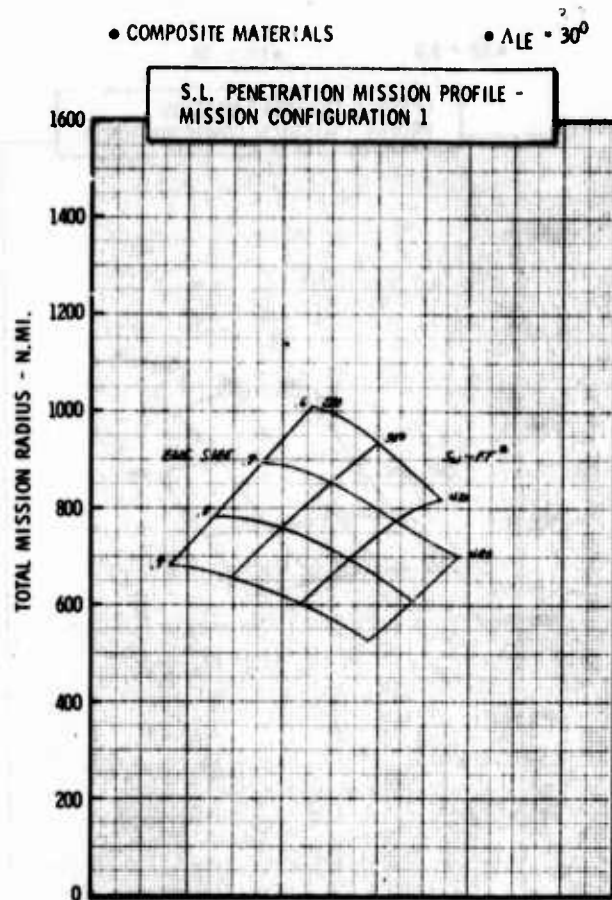


Figure H-32b LWA Mission/Configuration Tradeoff Parametric Data



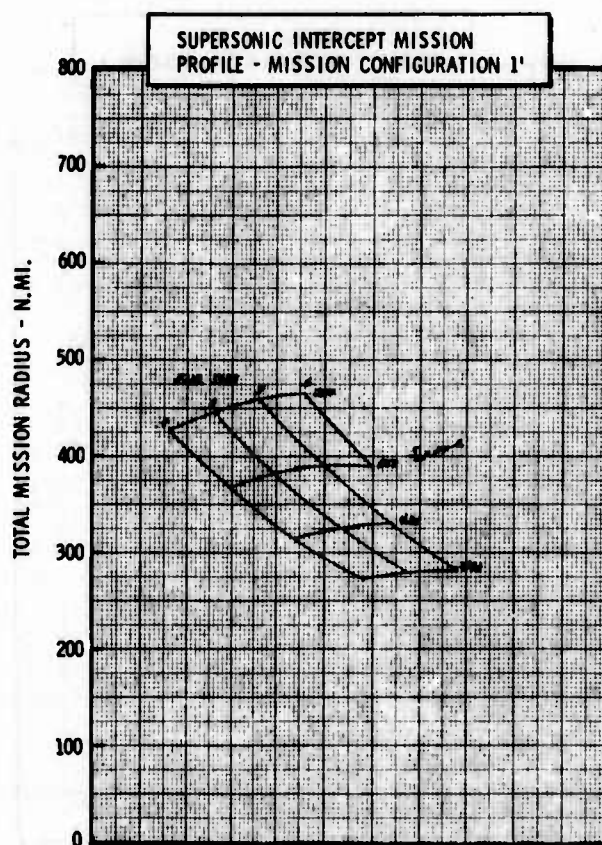
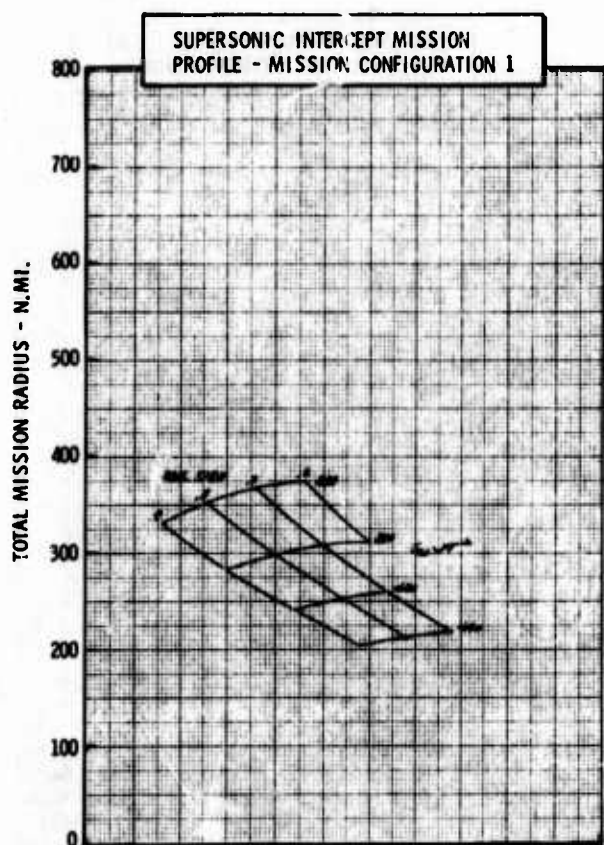
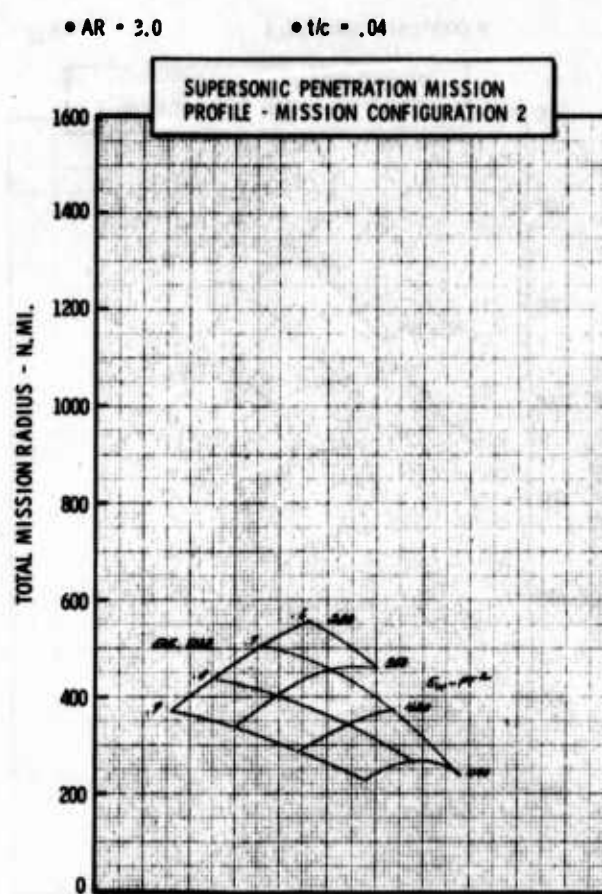
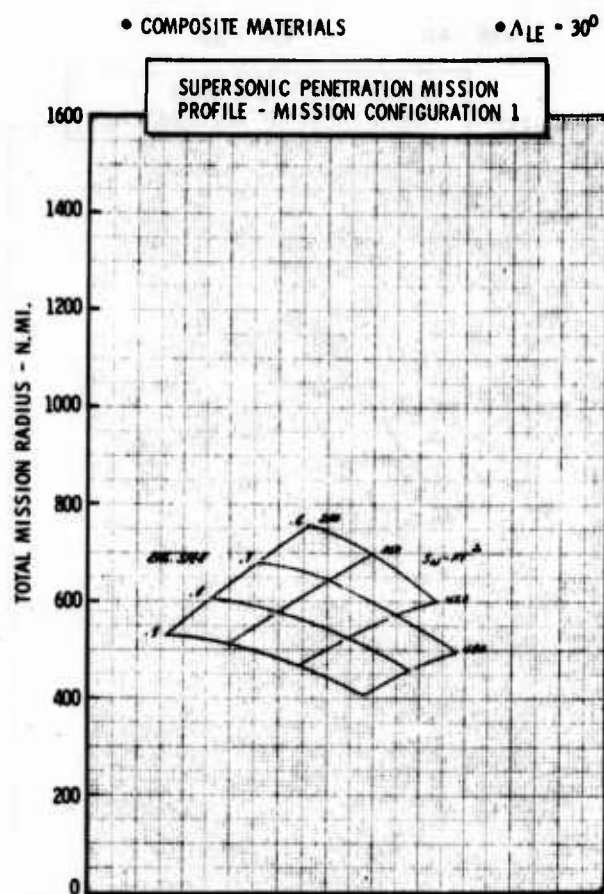


Figure H-32c LWA Mission/Configuration Tradeoff Parametric Data

• COMPOSITE MATERIALS

•  $\Lambda_{LE} = 30^\circ$

•  $AR = 4.0$

•  $t/c = .04$

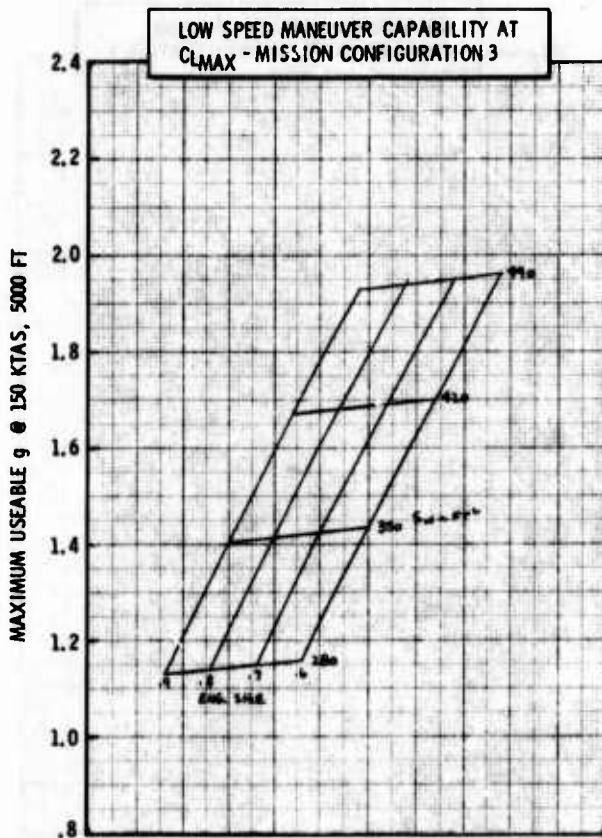
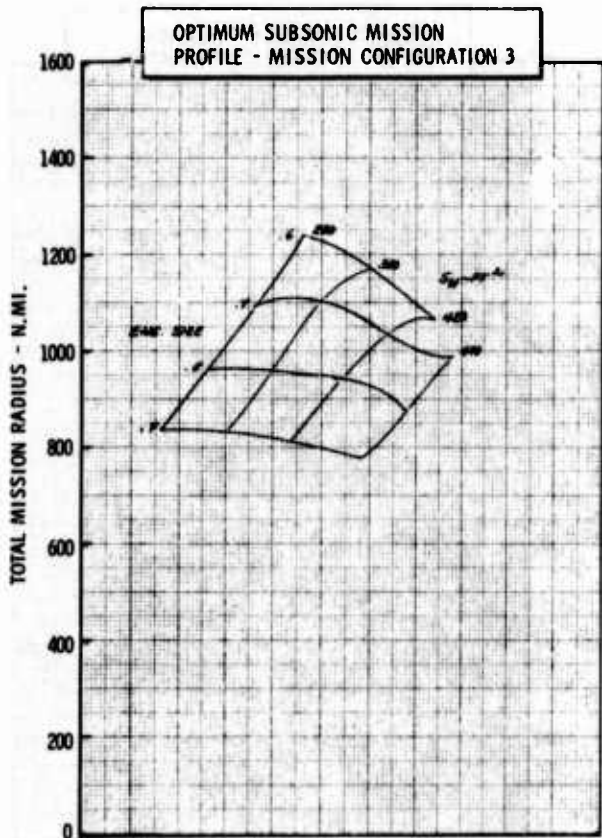
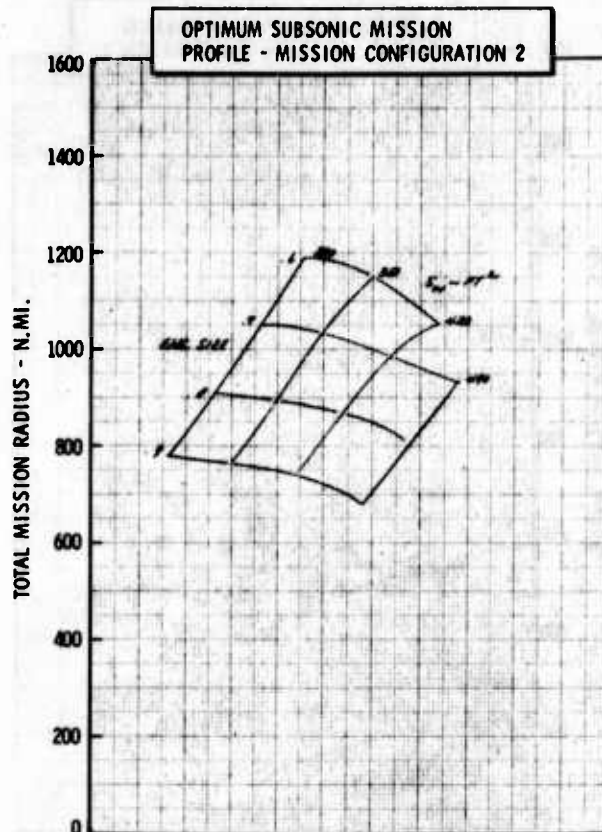
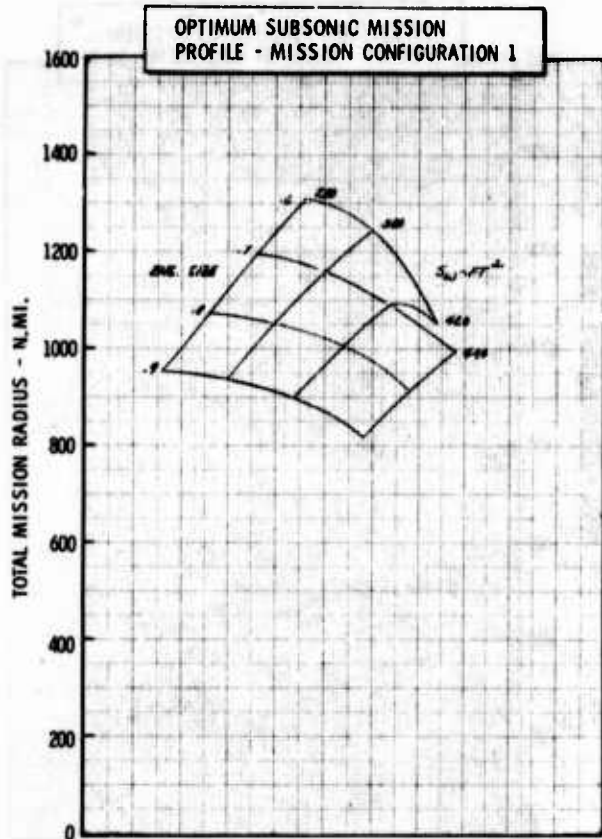


Figure H-33a LWA Mission/Configuration Tradeoff Parametric Data



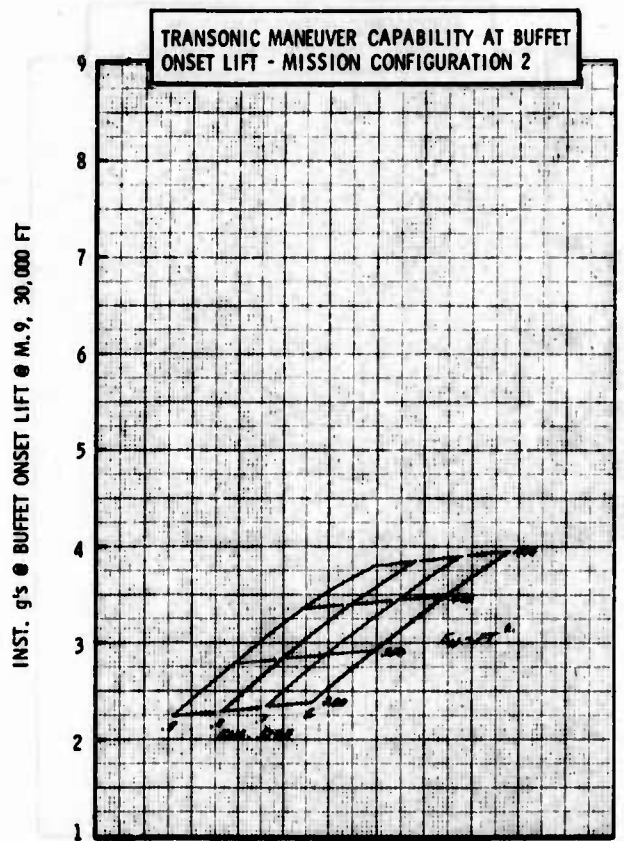
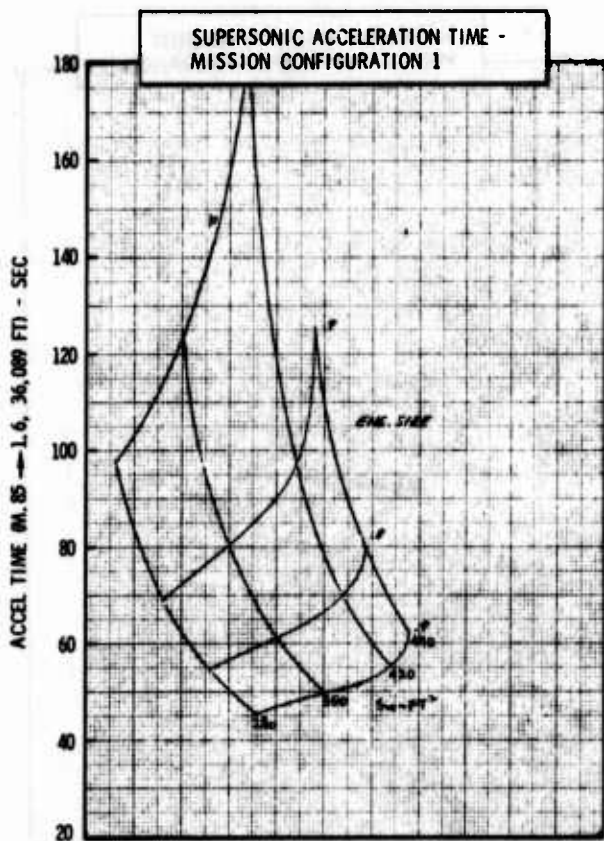
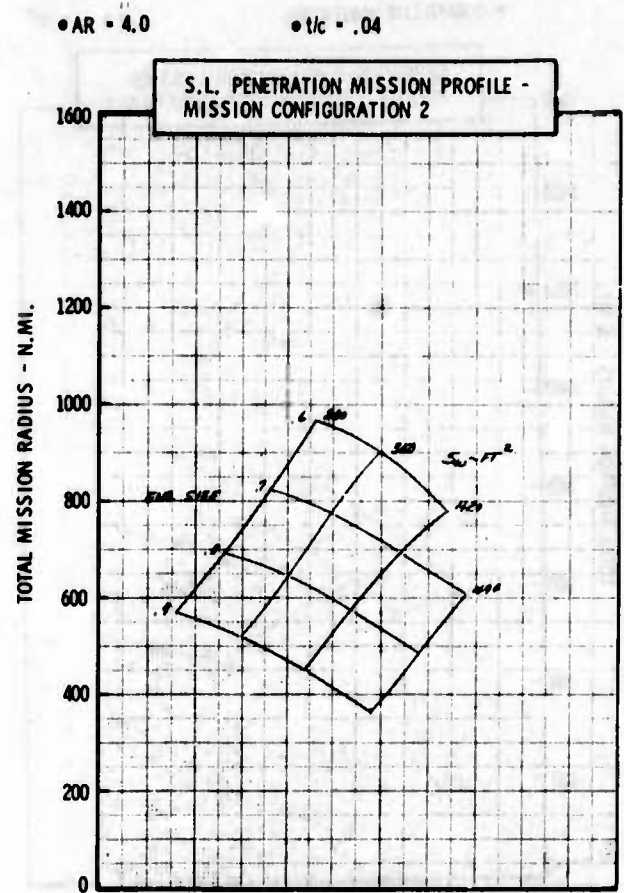
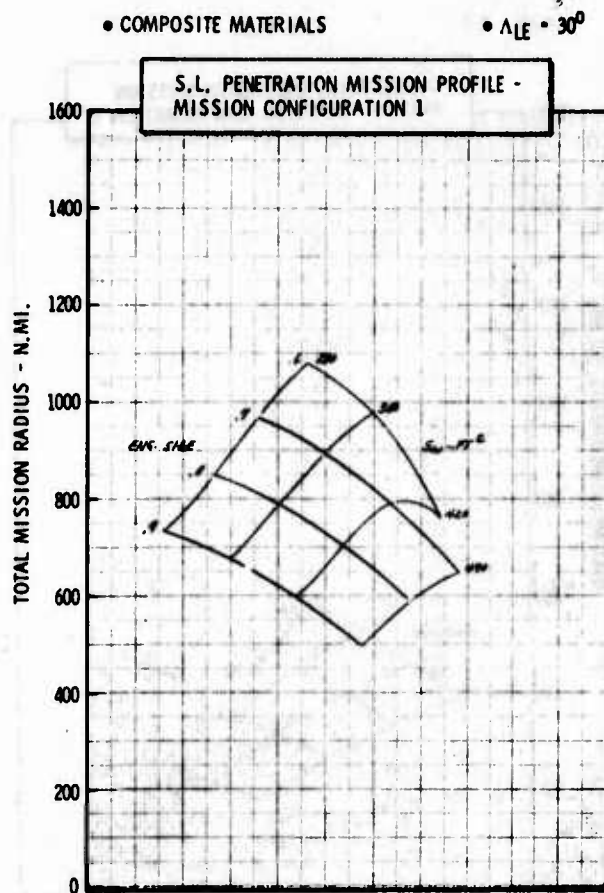
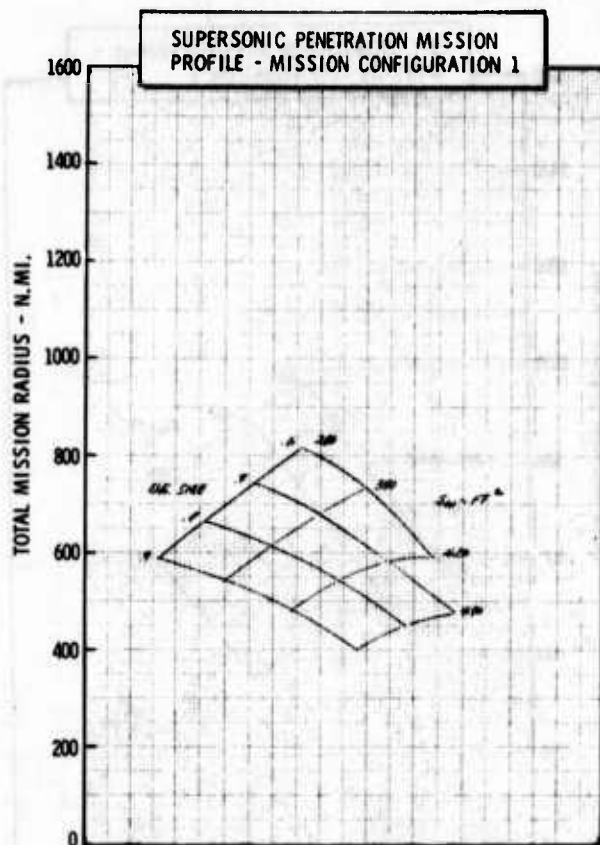


Figure H-33b LWA Mission/Configuration Tradeoff Parametric Data

• COMPOSITE MATERIALS

•  $\Lambda_{LE} = 30^\circ$



• AR = 4.0

•  $t/c = .04$

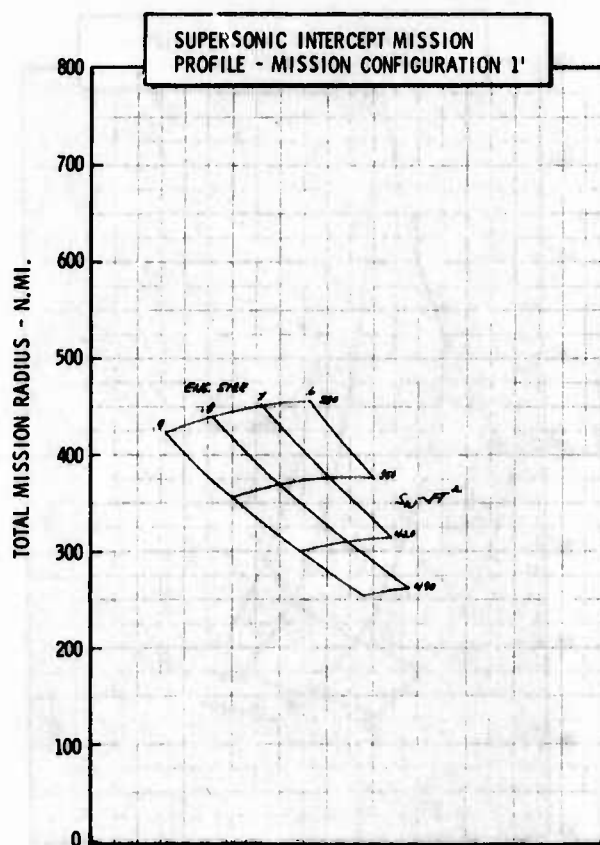
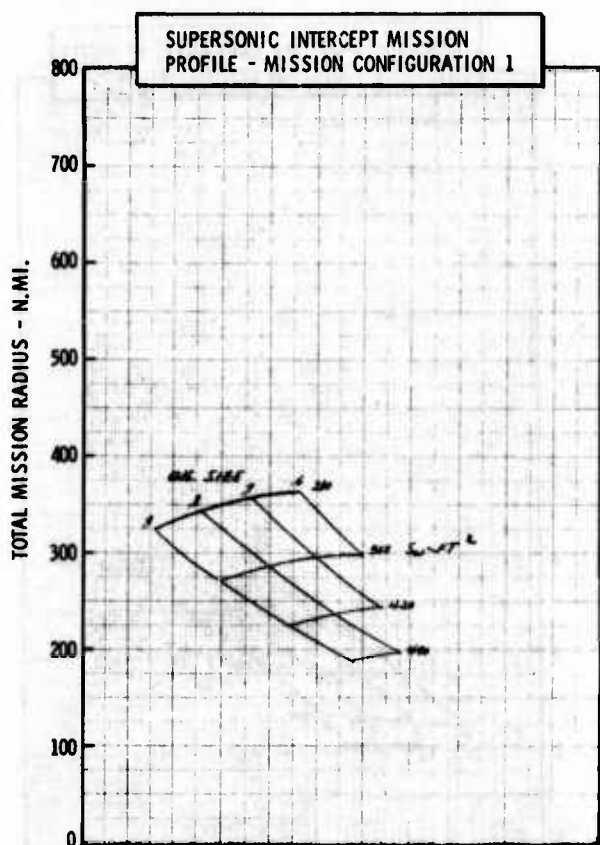
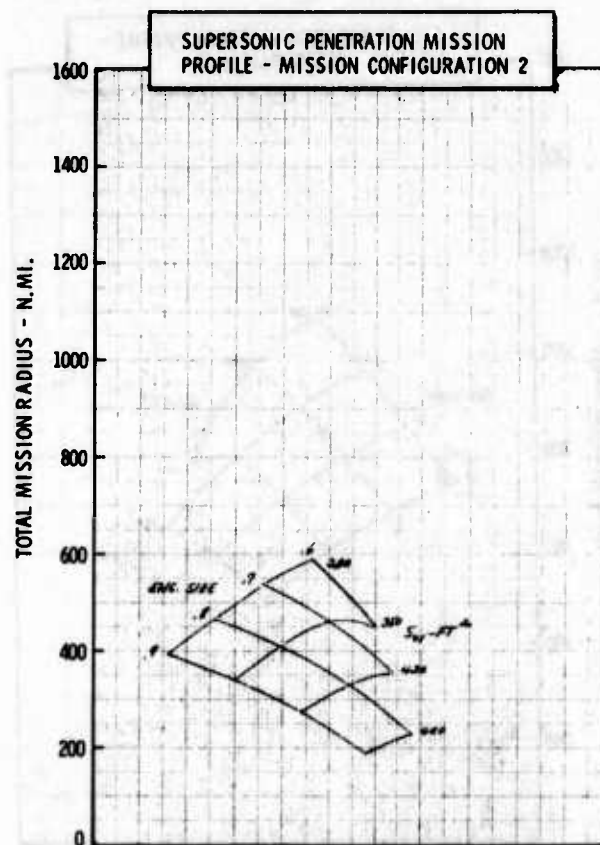


Figure H-33c LWA Mission/Configuration Tradeoff Parametric Data

• COMPOSITE MATERIALS

•  $\Delta LE = 30^\circ$

•  $AR = 5.0$

•  $t/c = .04$

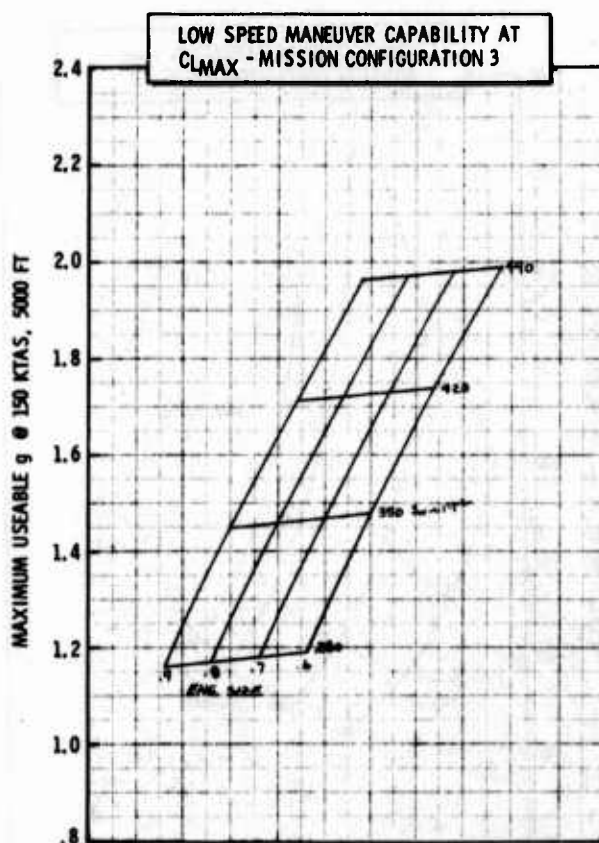
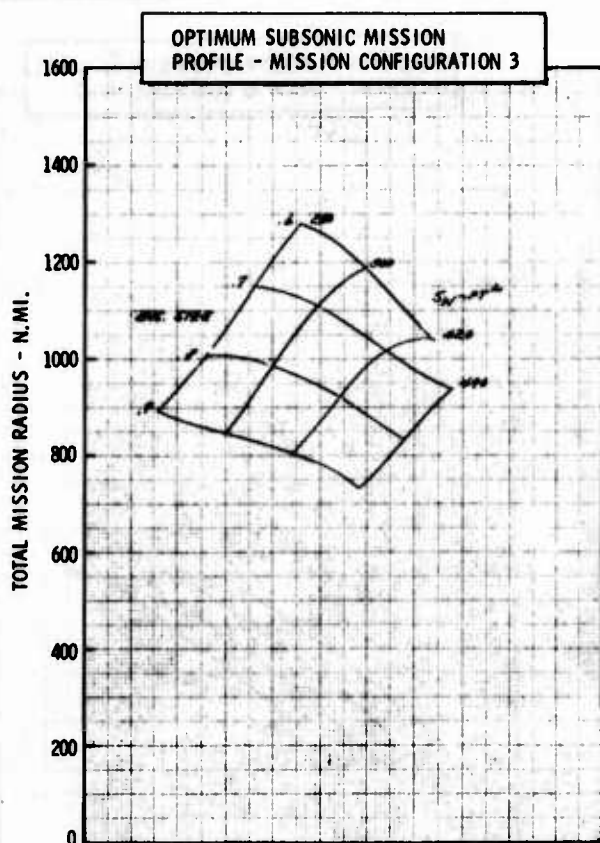
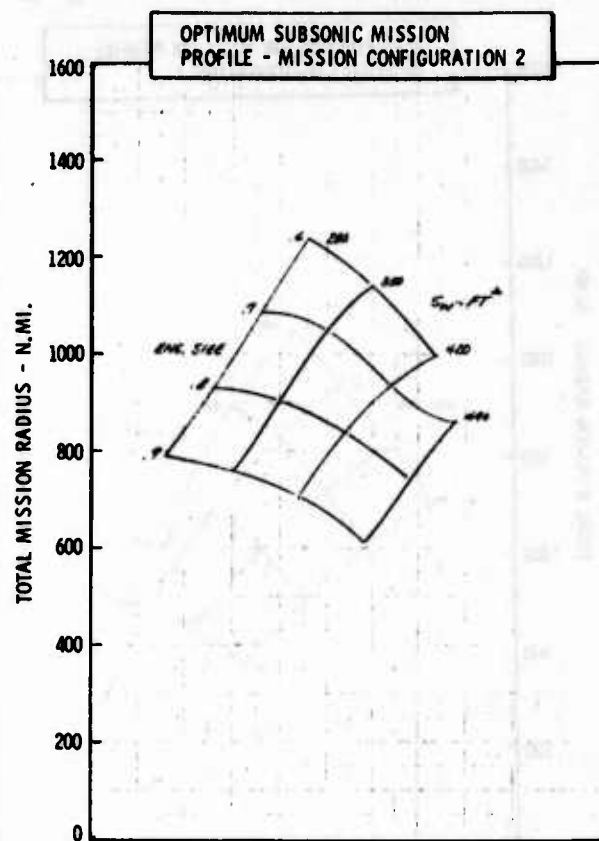
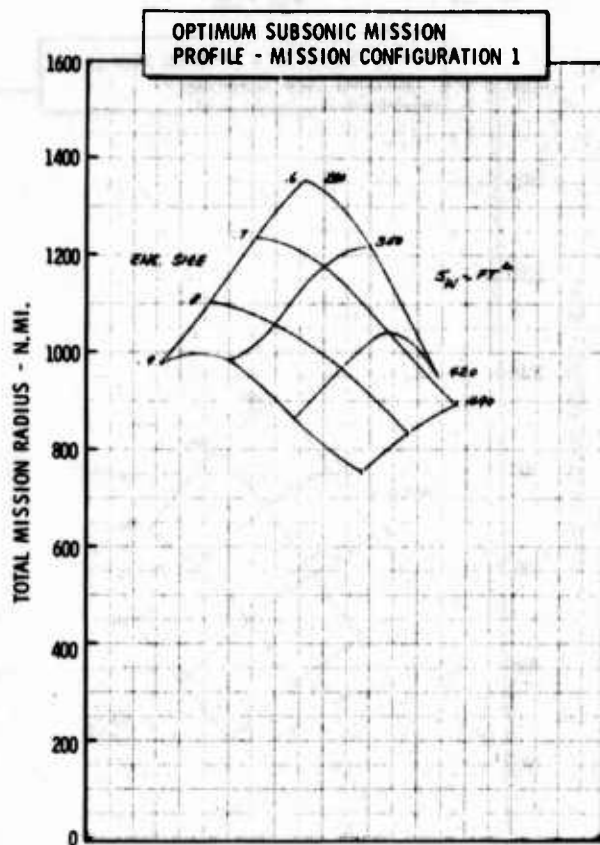


Figure H-34a LWA Mission/Configuration Tradeoff Parametric Data

• COMPOSITE MATERIALS

•  $\Delta LE = 30^\circ$

• AR = 5.0

•  $t/c = .04$

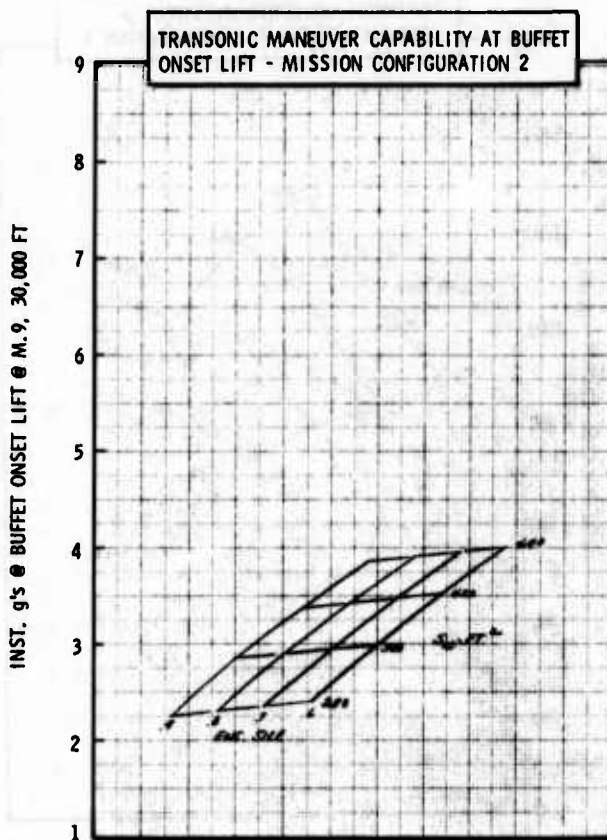
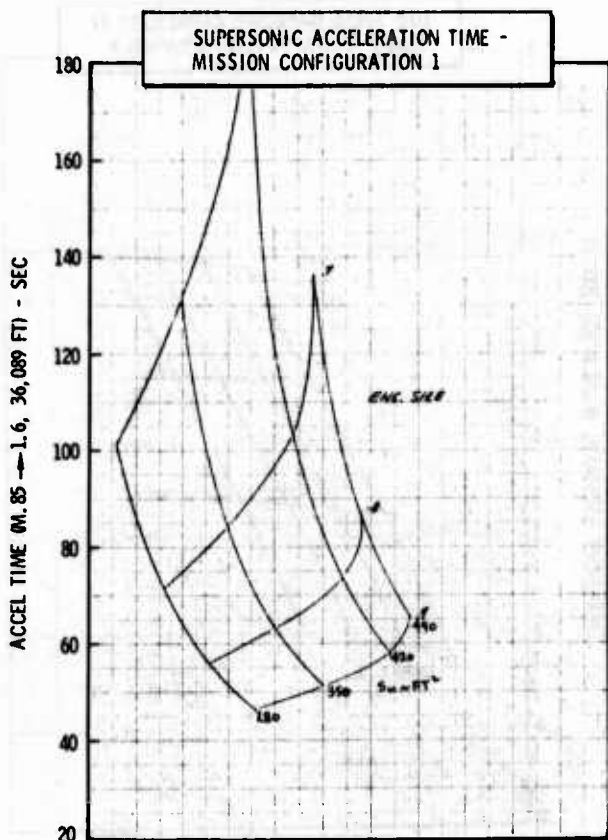
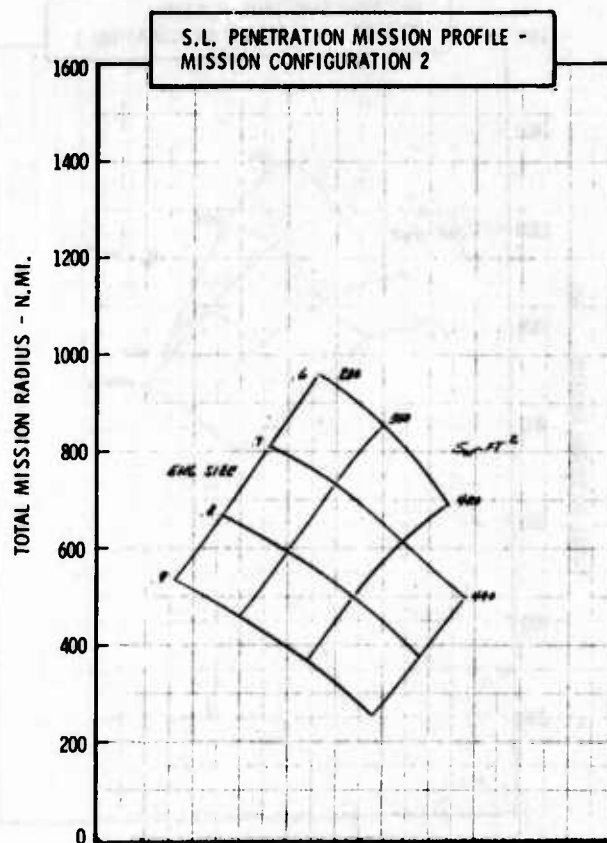
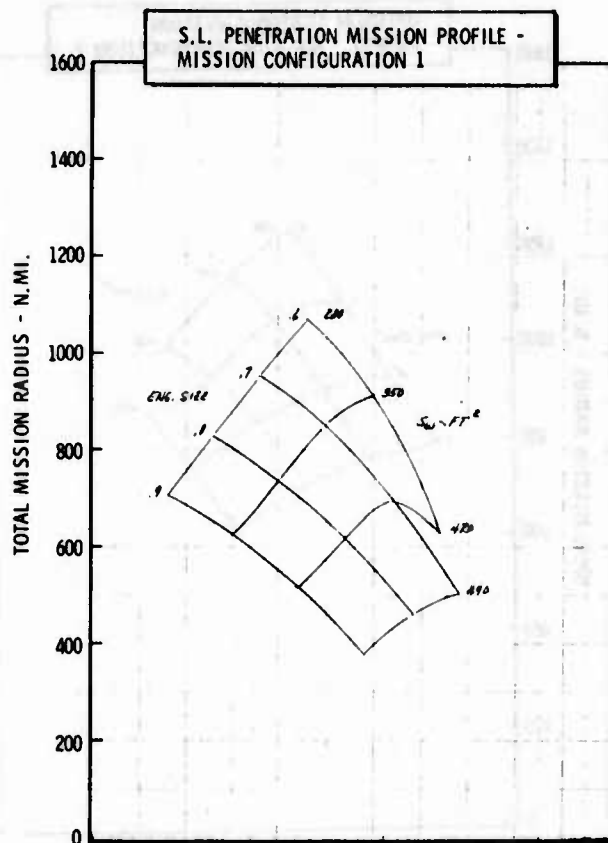


Figure H-34b LWA Mission/Configuration Tradeoff Parametric Data



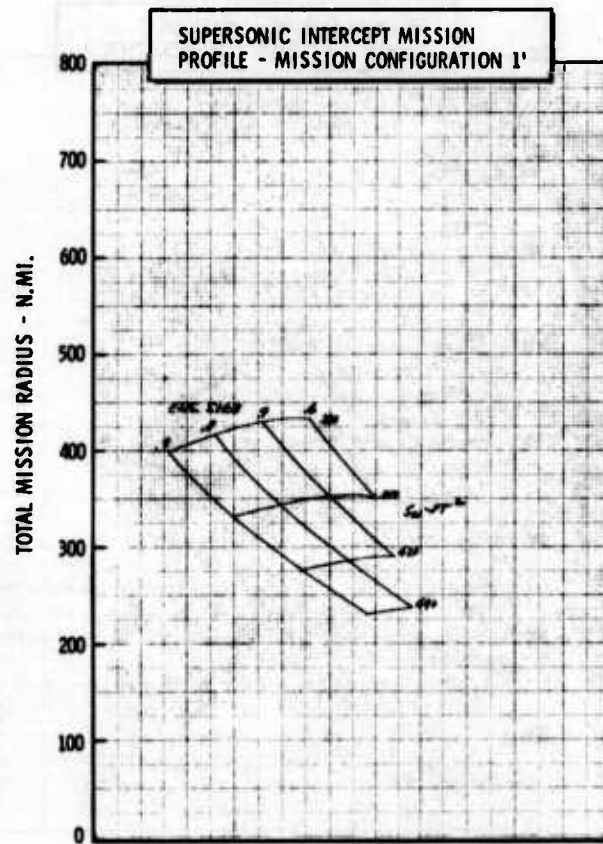
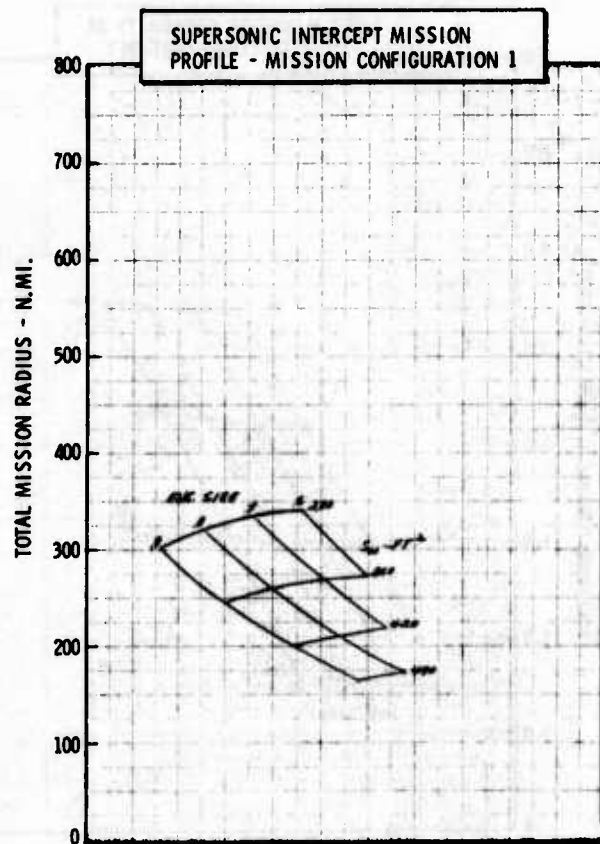
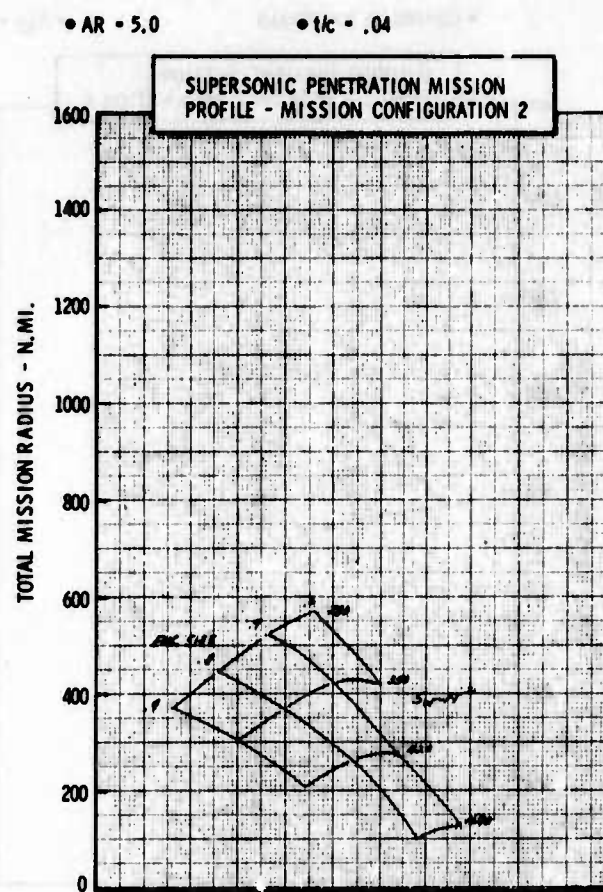
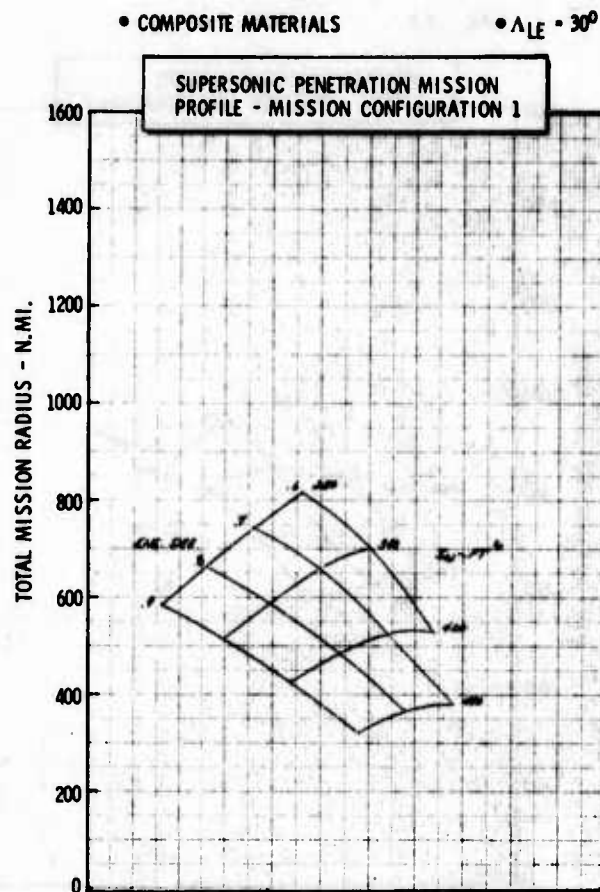


Figure H-34c LWA Mission/Configuration Tradeoff Parametric Data



• COMPOSITE MATERIALS

•  $\Lambda_{LE} = 40^\circ$

•  $AR = 3.0$

•  $t/c = .04$

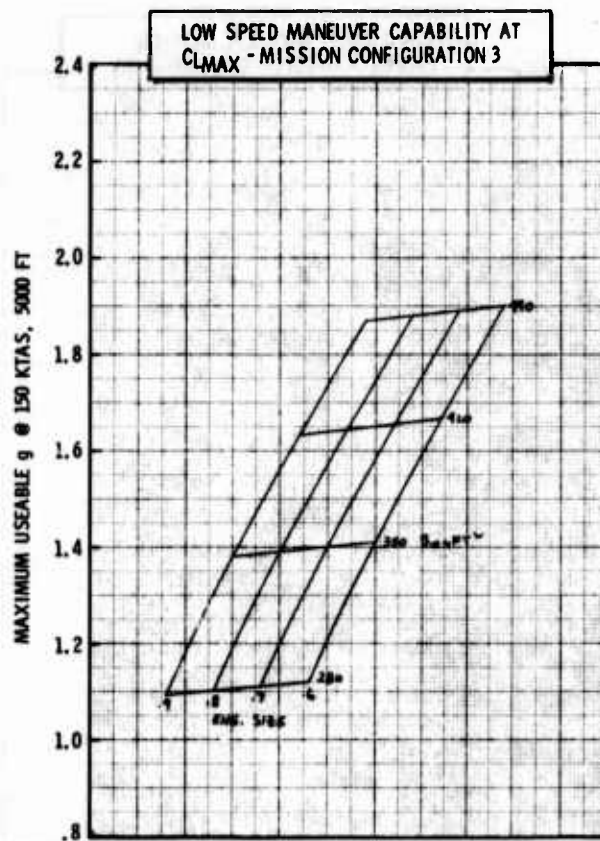
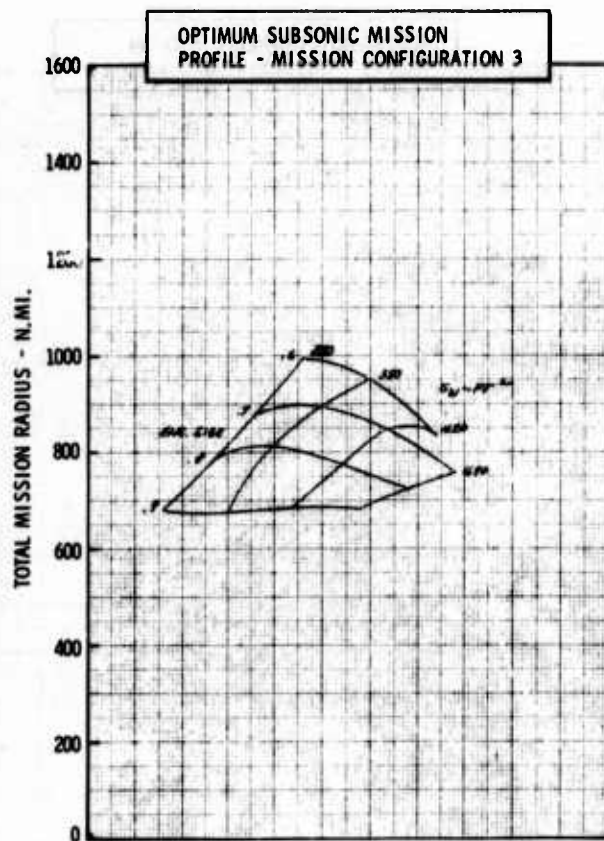
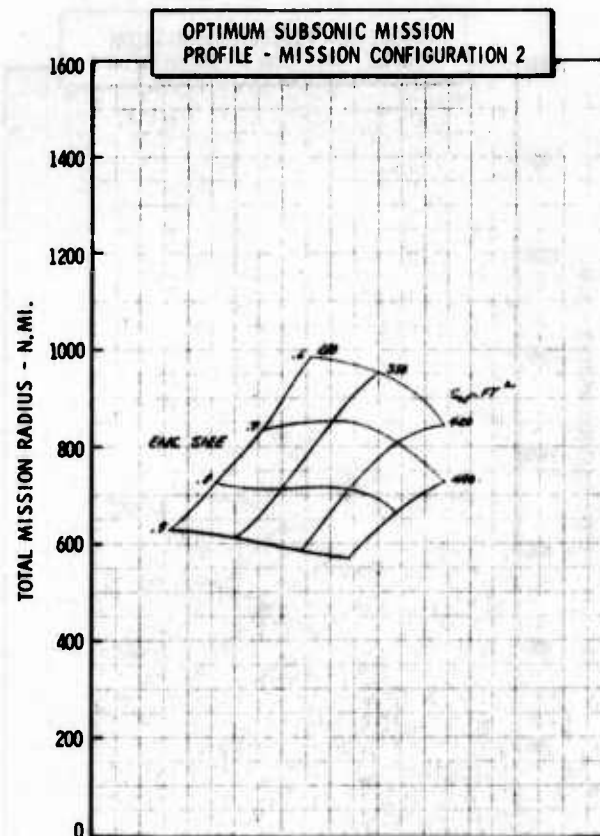
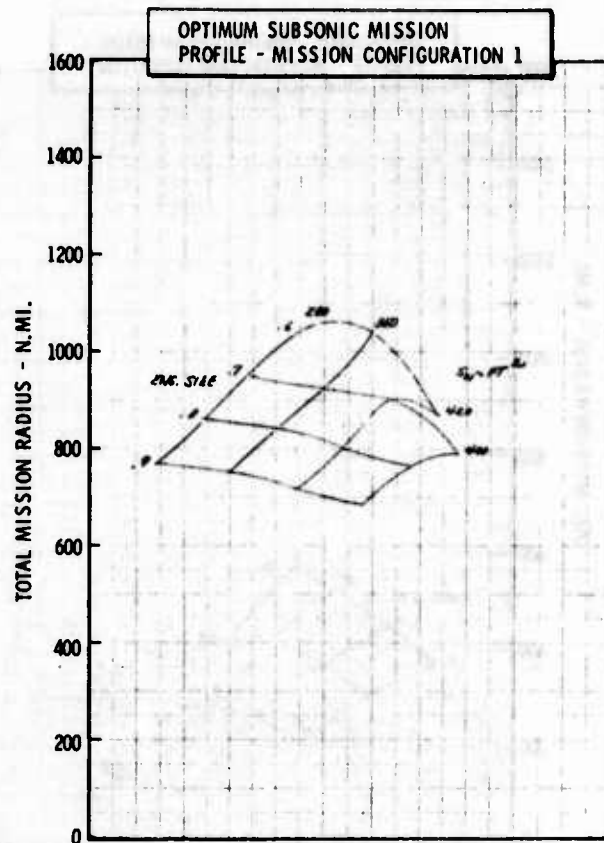


Figure H-35a LWA Mission/Configuration Tradeoff Parametric Data

• COMPOSITE MATERIALS

•  $\Delta LE = 40^\circ$

•  $AR = 3.0$

•  $tlc = .04$

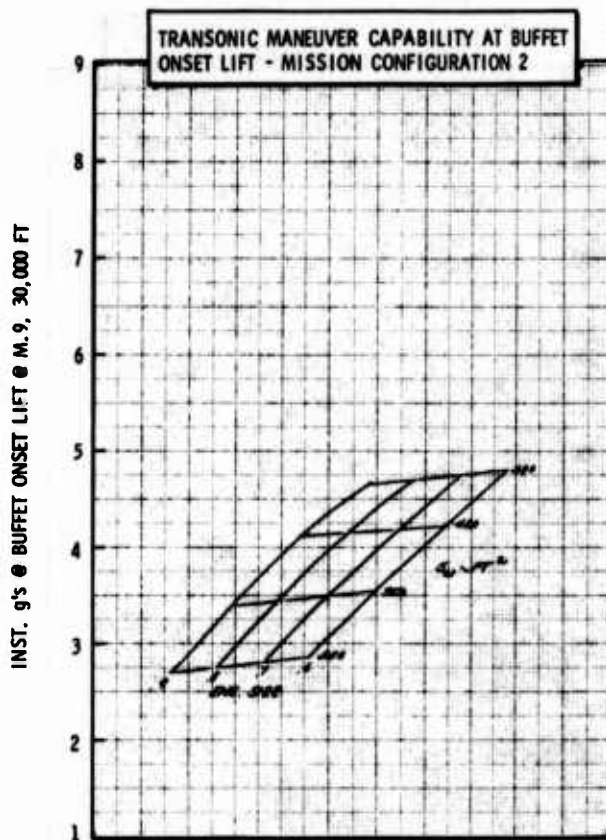
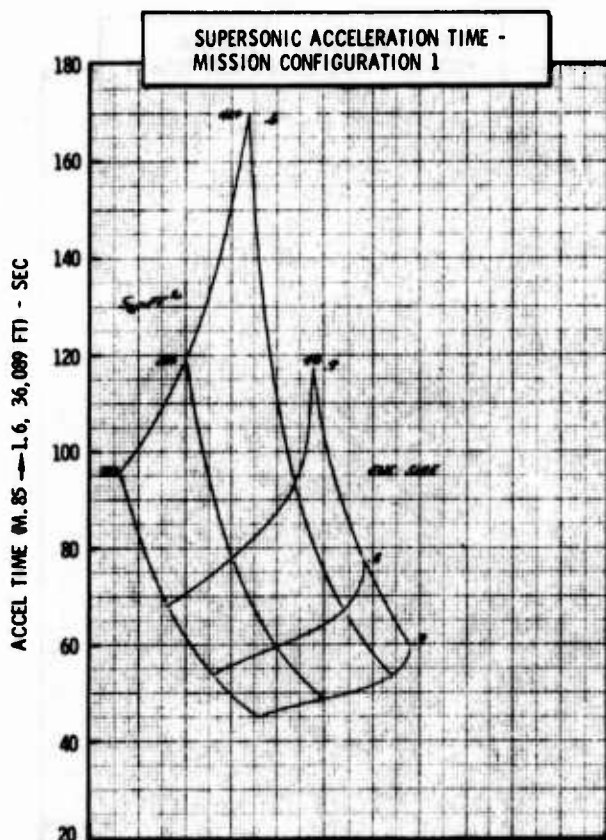
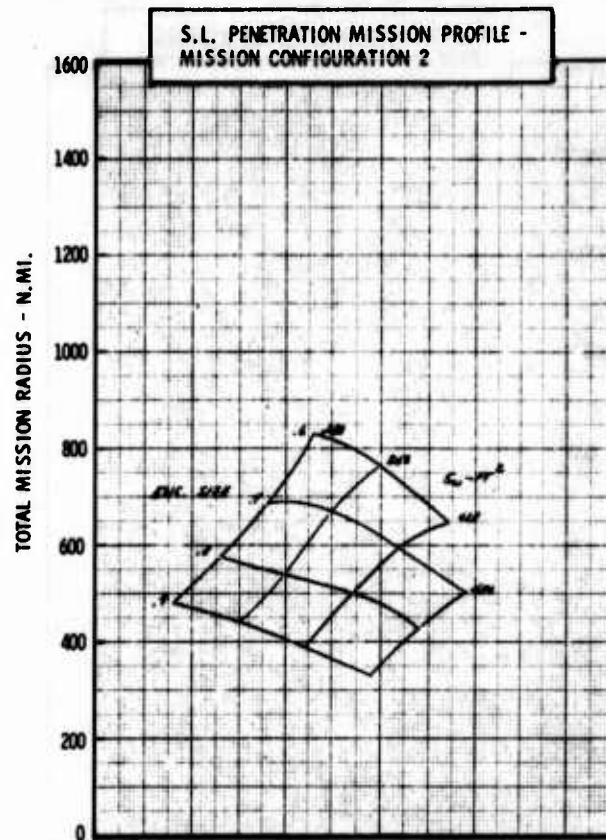
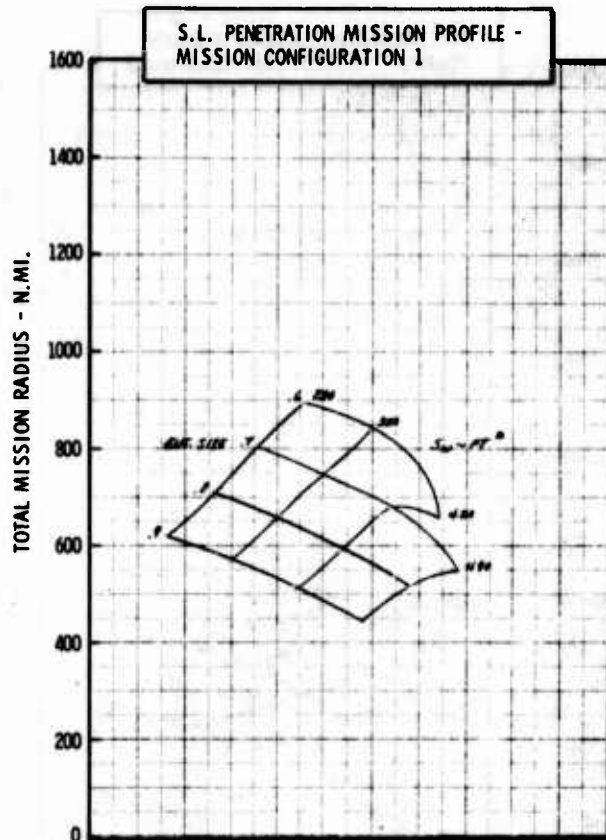


Figure H-35b LWA Mission/Configuration Tradeoff Parametric Data

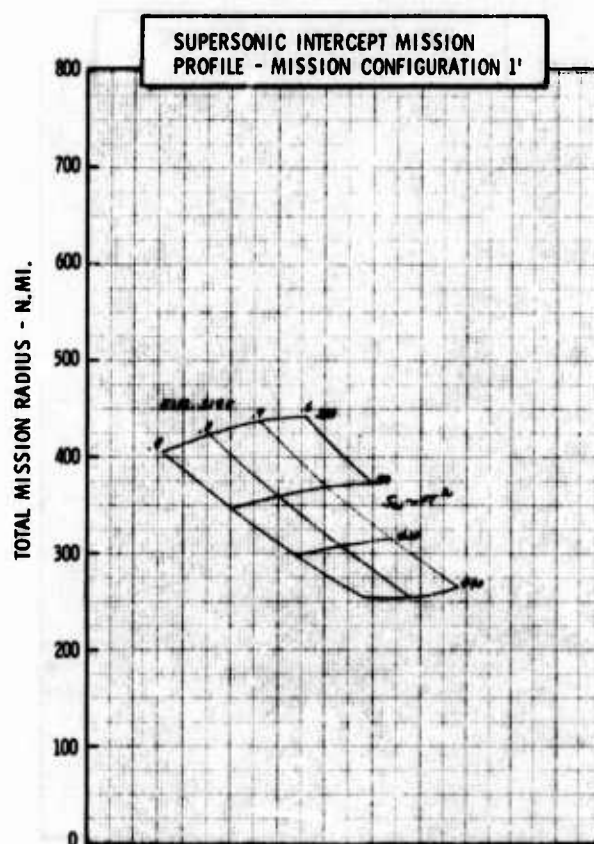
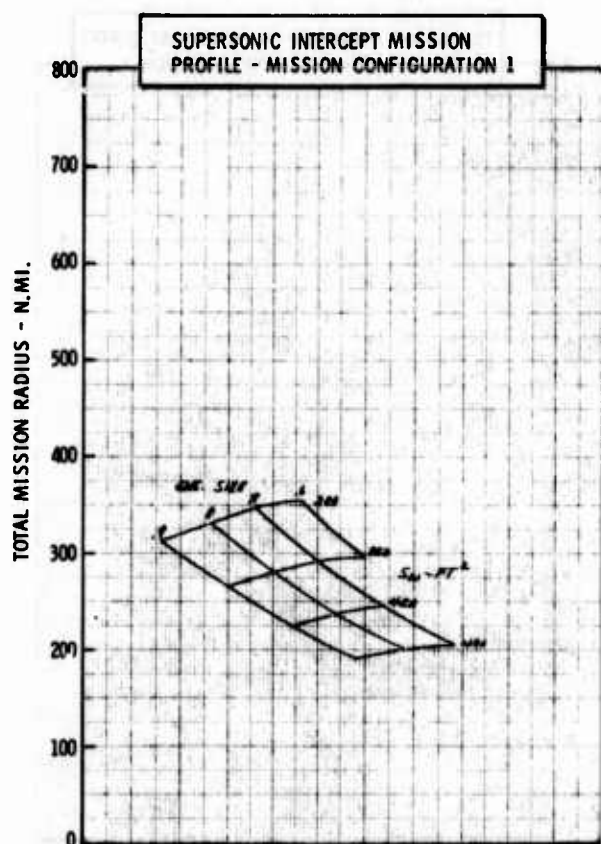
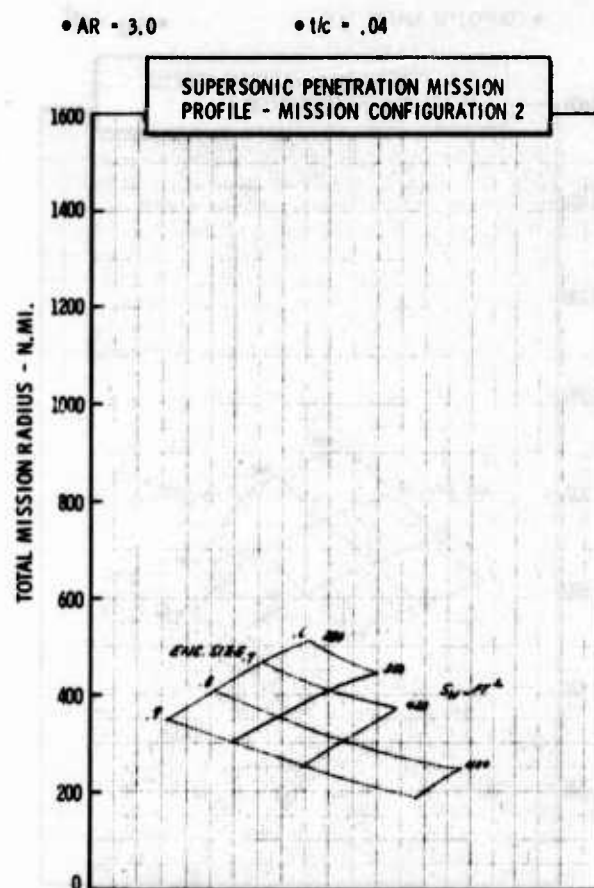
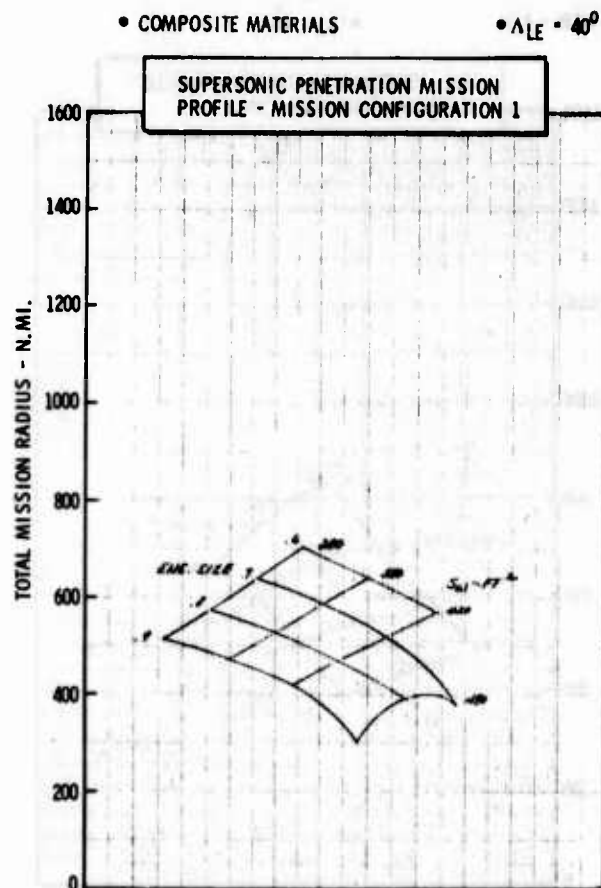


Figure H-35c LWA Mission/Configuration Tradeoff Parametric Data

• COMPOSITE MATERIALS

•  $\Delta LE = 40^\circ$

•  $AR = 4.0$

•  $t/c = .04$

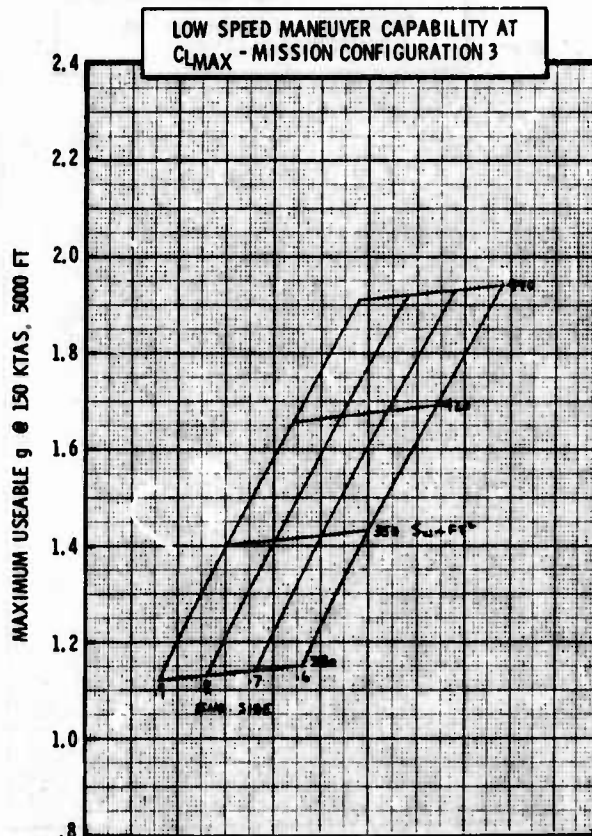
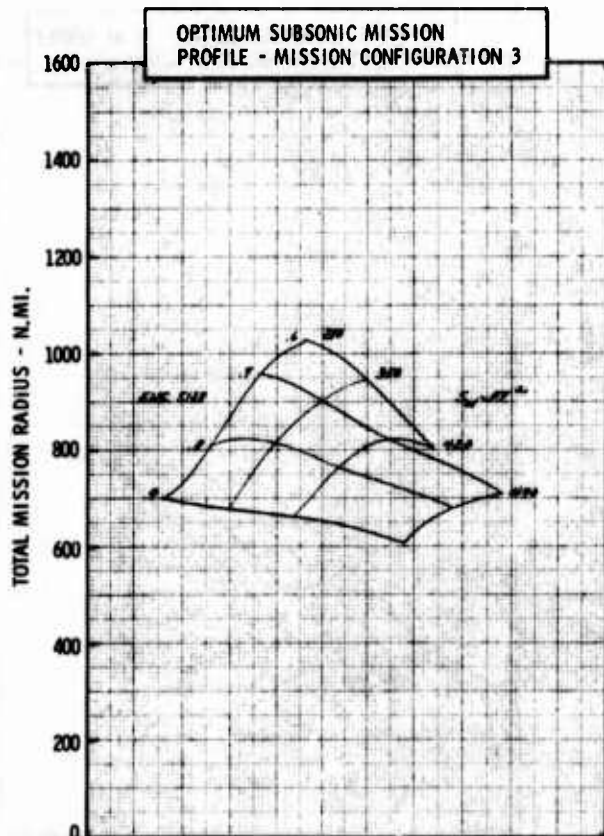
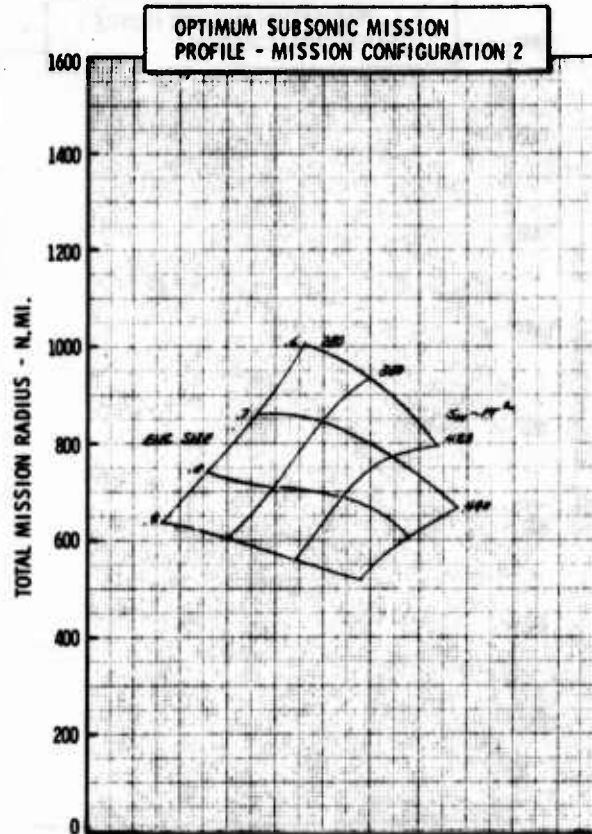
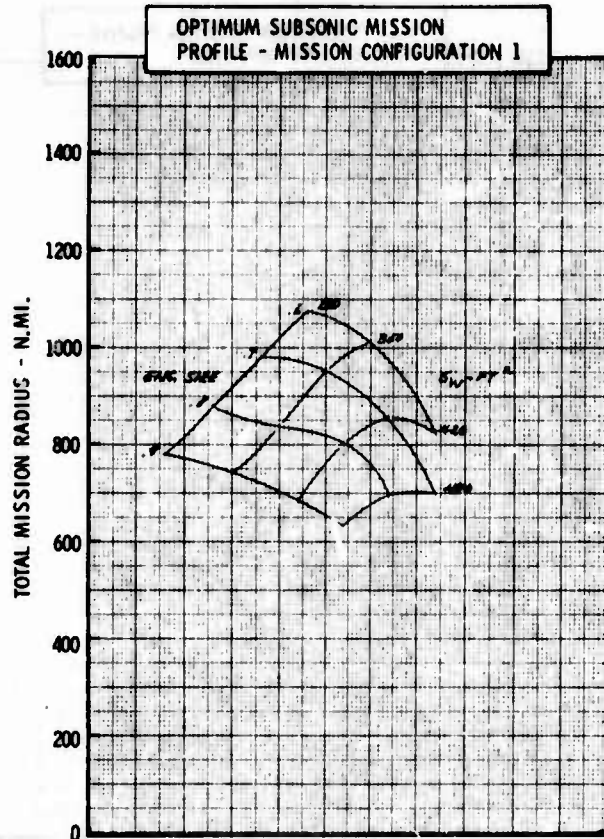


Figure H-36a LWA Mission/Configuration Tradeoff Parametric Data



• COMPOSITE MATERIALS

•  $\Delta LE = 40^\circ$

•  $AR = 4.0$

•  $t/c = .04$

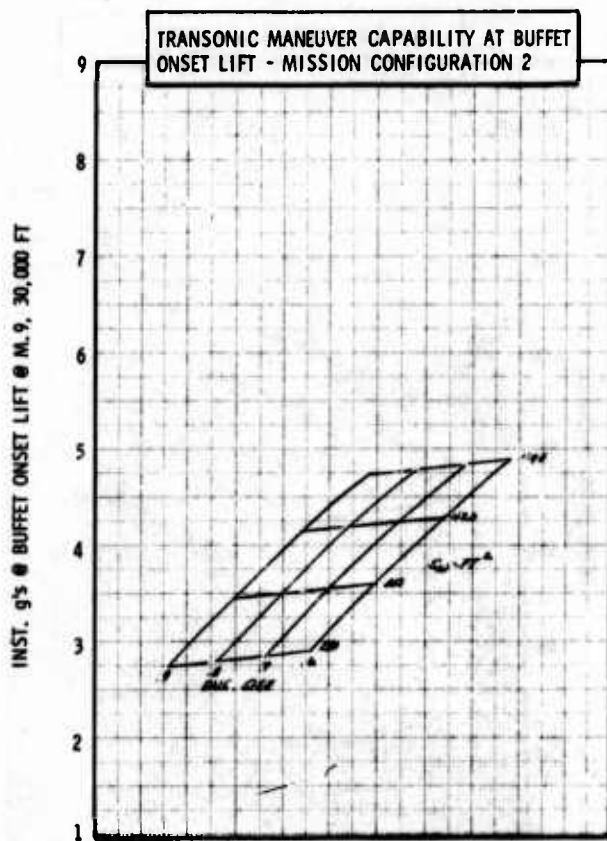
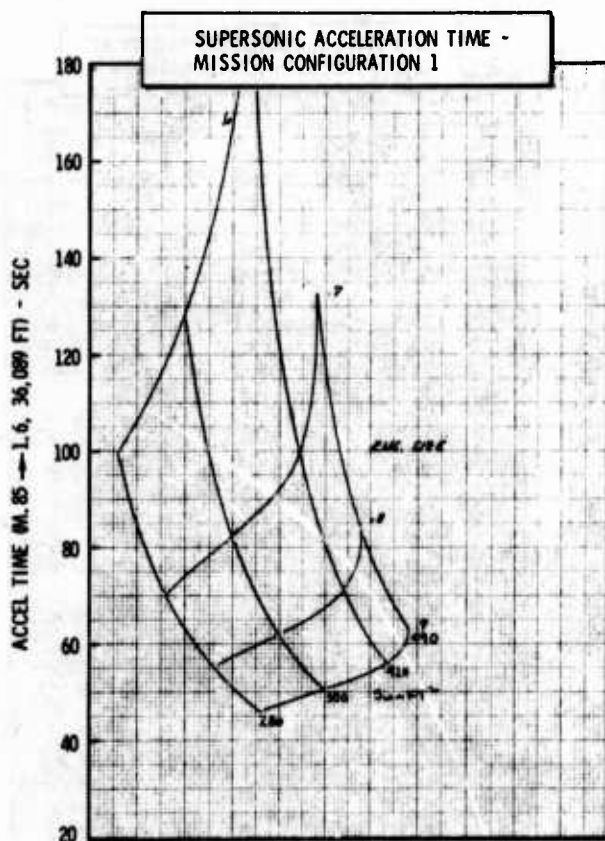
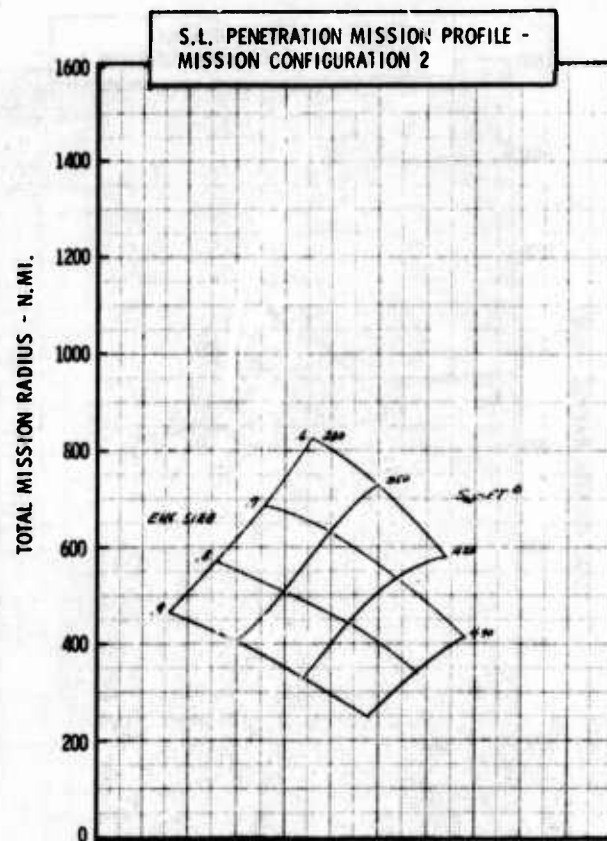
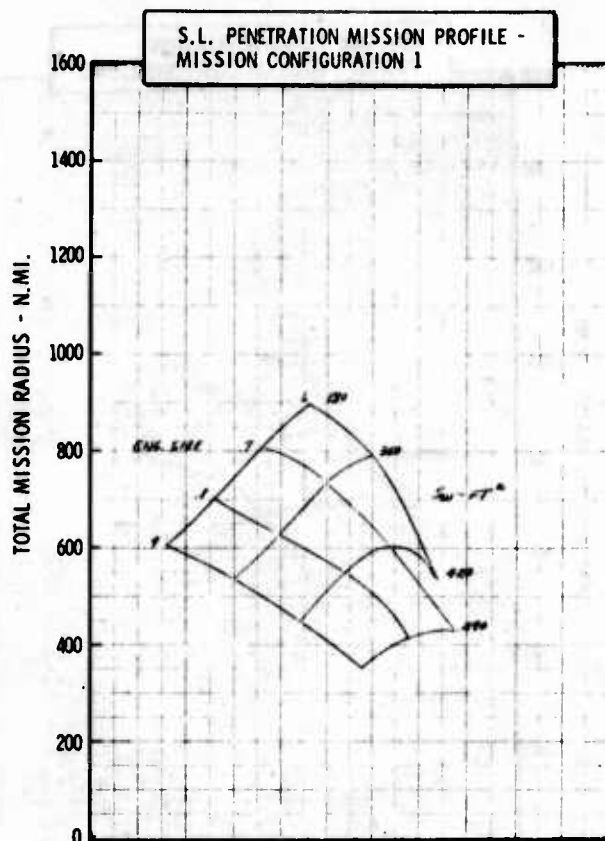


Figure H-36b LWA Mission/Configuration Tradeoff Parametric Data



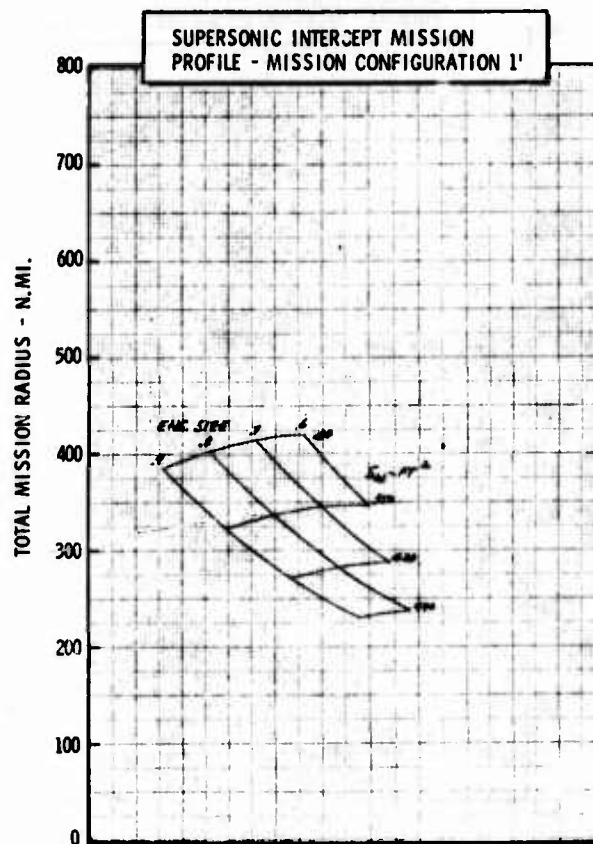
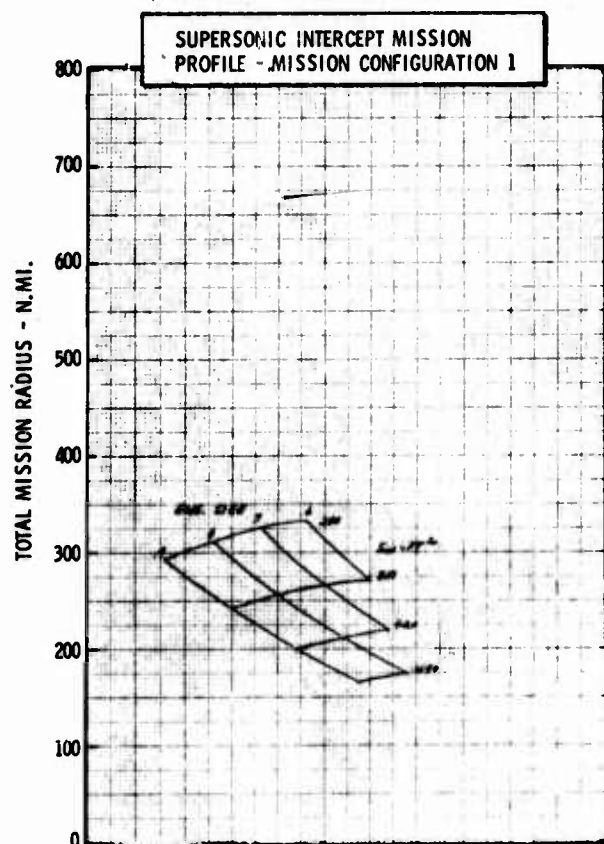
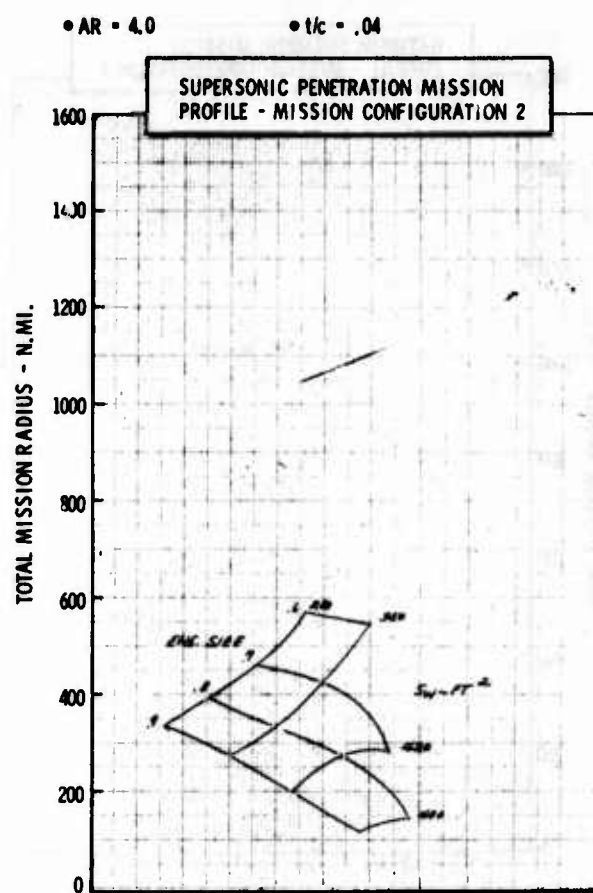
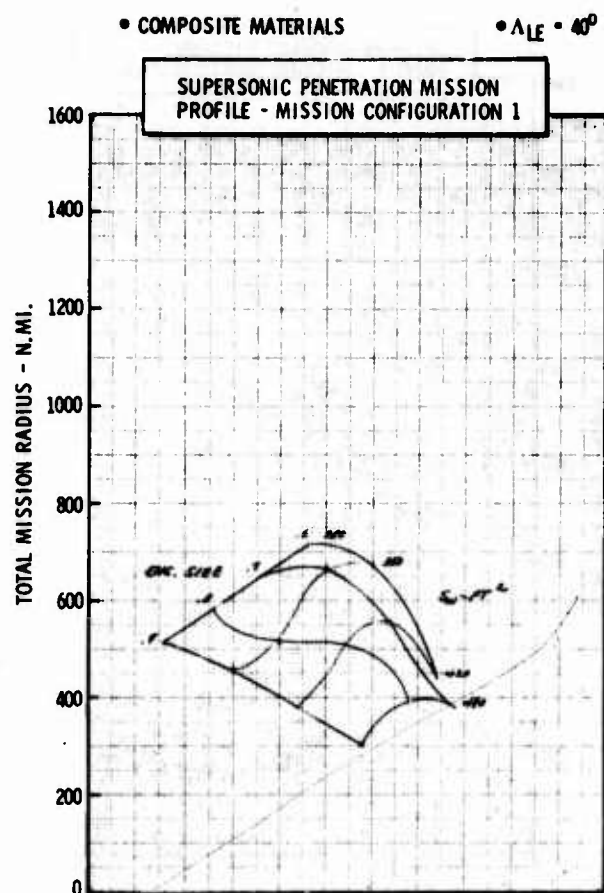


Figure H-36c LWA Mission/Configuration Tradeoff Parametric Data

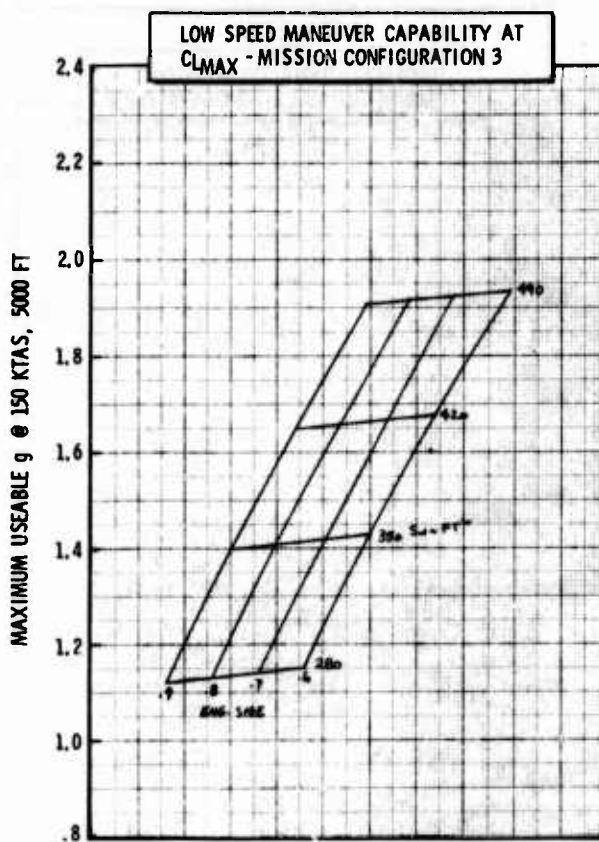
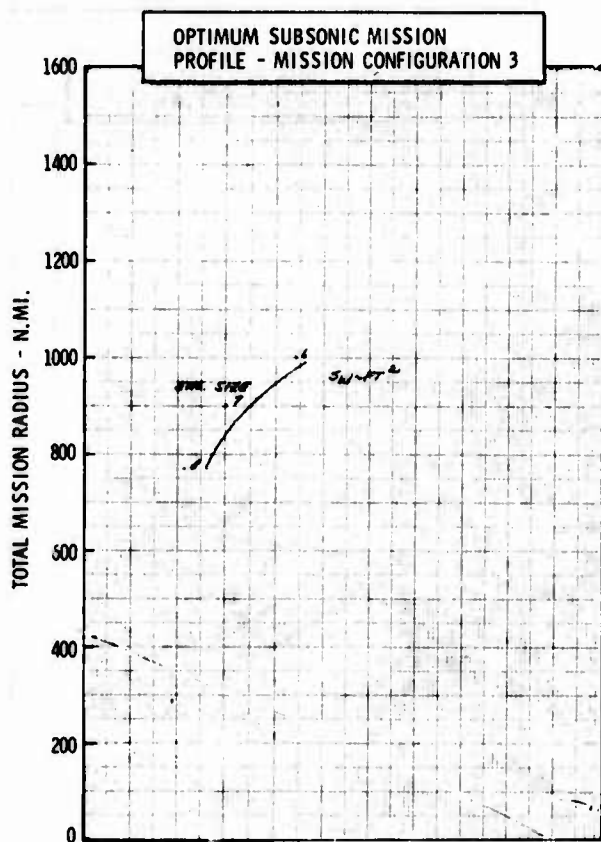
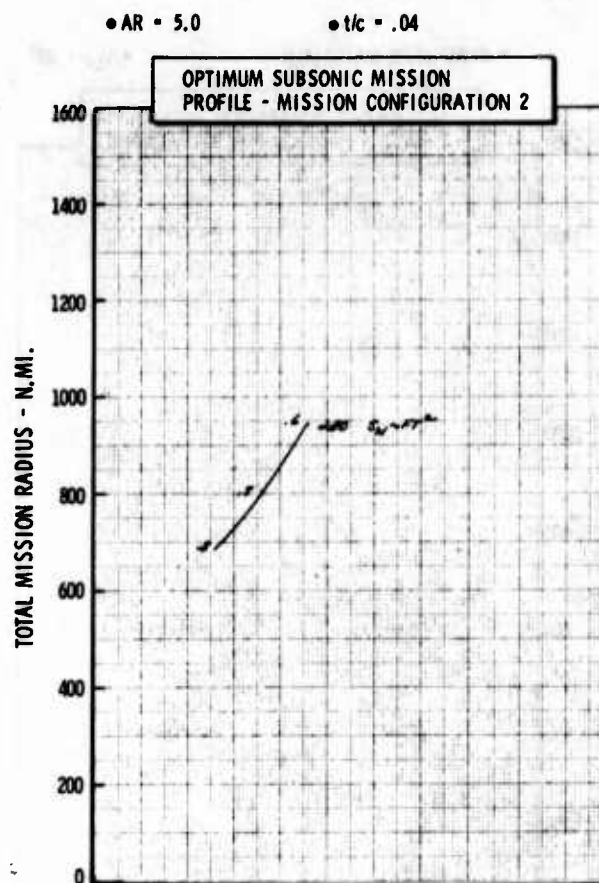
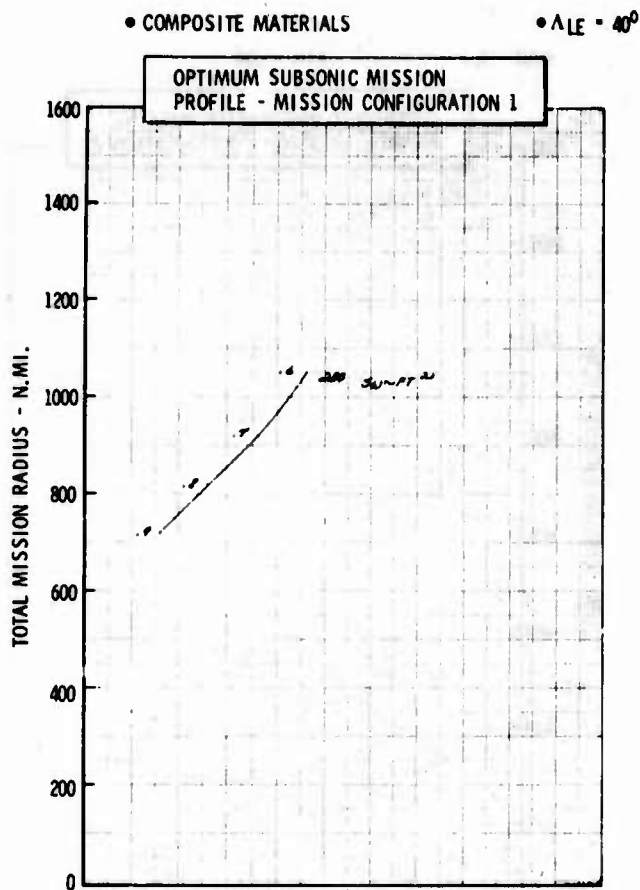


Figure H-37a LWA Mission/Configuration Tradeoff Parametric Data

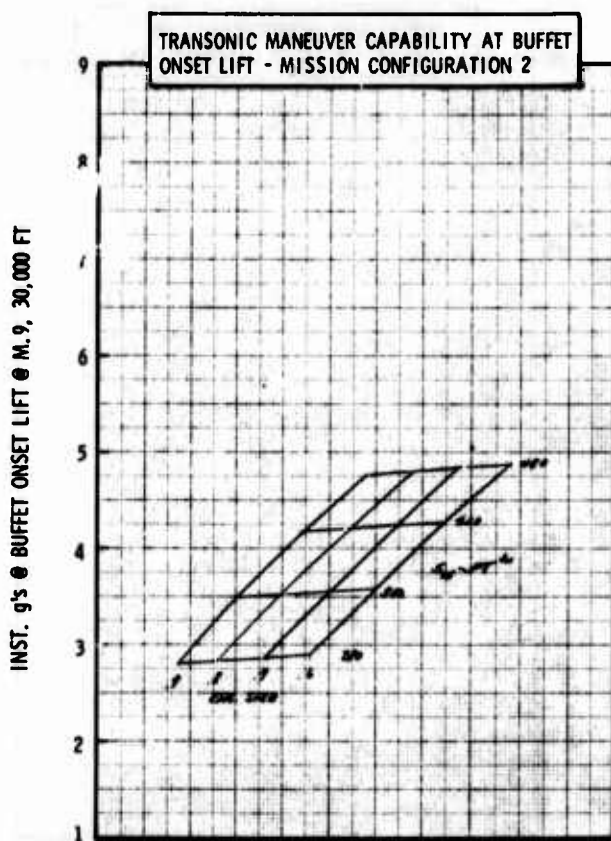
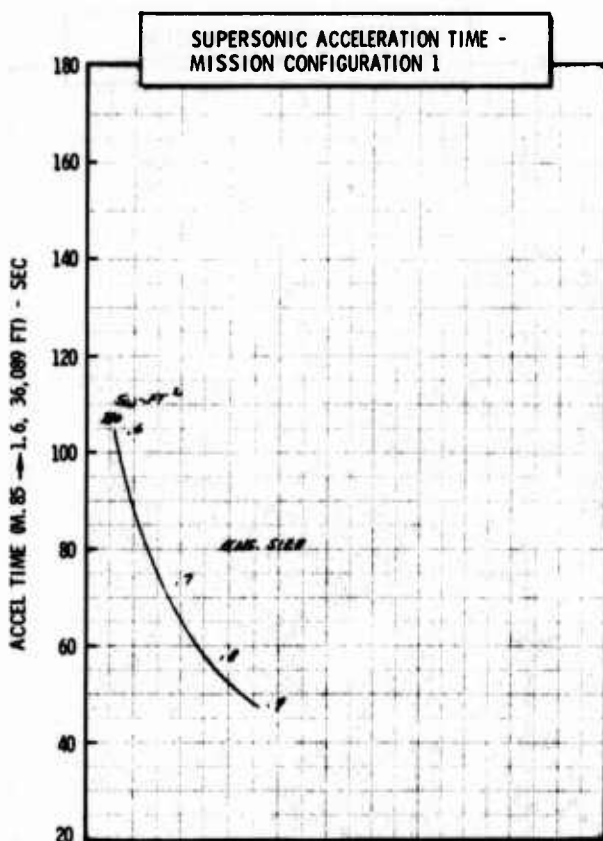
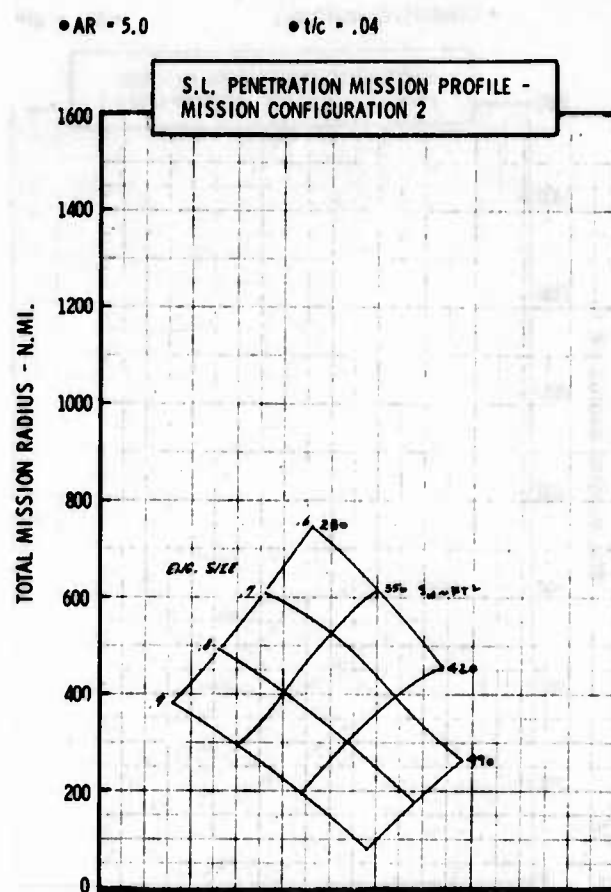
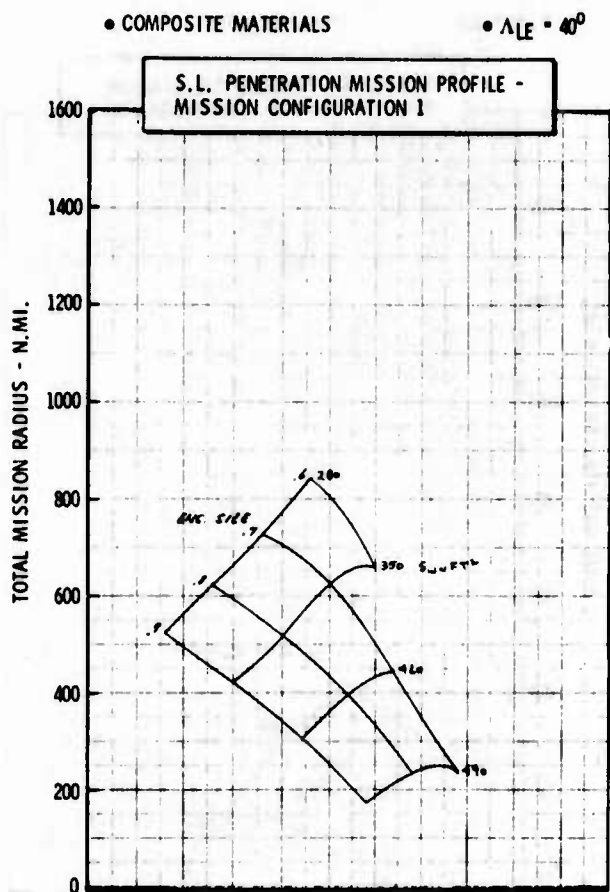
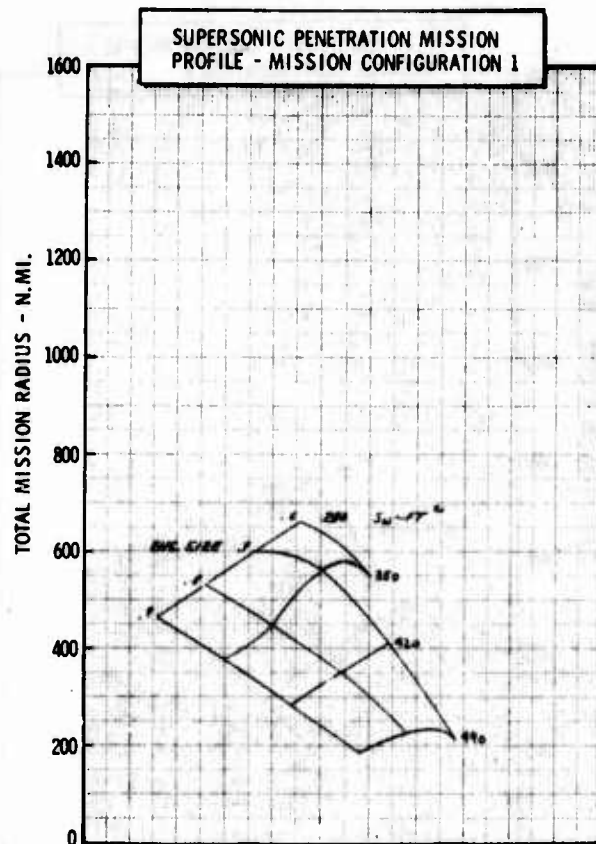


Figure H-37b LWA Mission/Configuration Tradeoff Parametric Data

• COMPOSITE MATERIALS

•  $\Lambda_{LE} = 40^\circ$



• AR = 5.0

•  $t/c = .04$

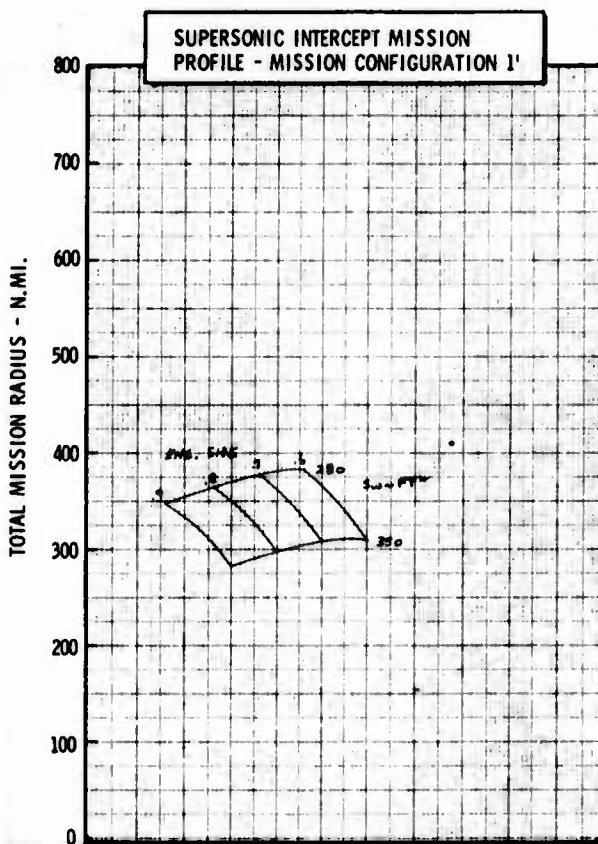
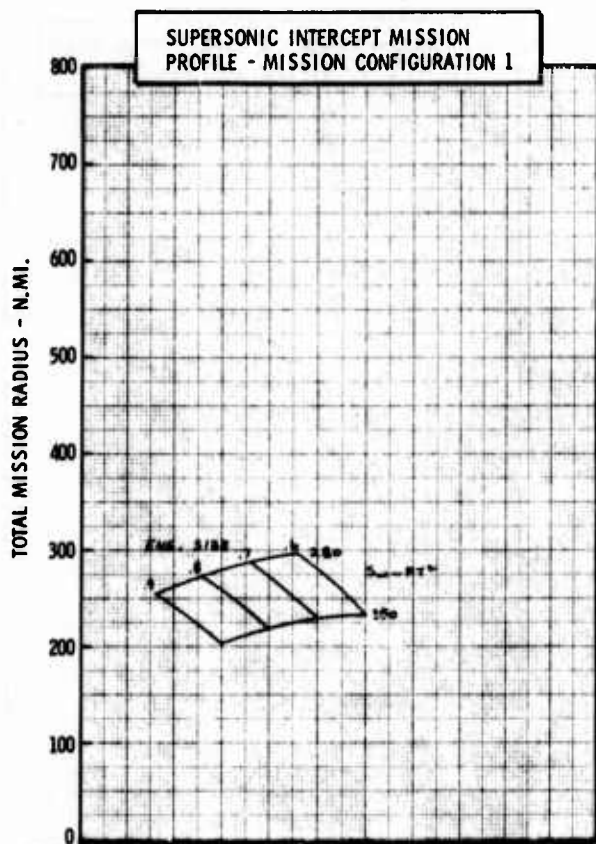
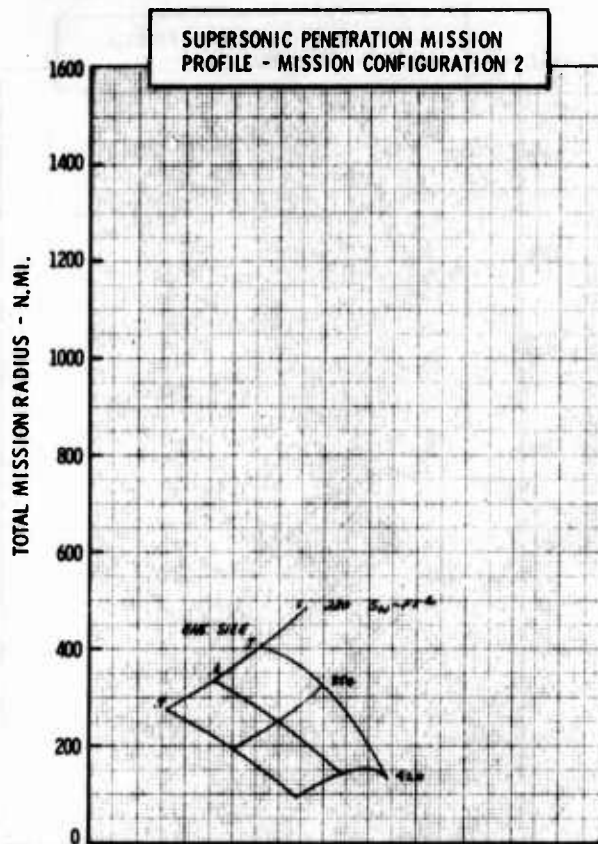


Figure H-37c LWA Mission/Configuration Tradeoff Parametric Data



• COMPOSITE MATERIALS

•  $\Lambda_{LE} = 20^\circ$

•  $AR = 3.0$

•  $t/c = .05$

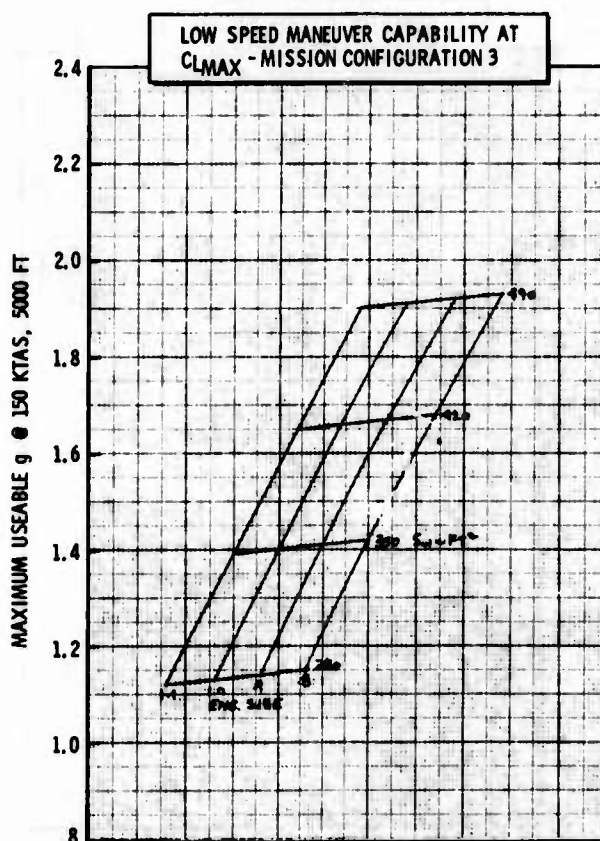
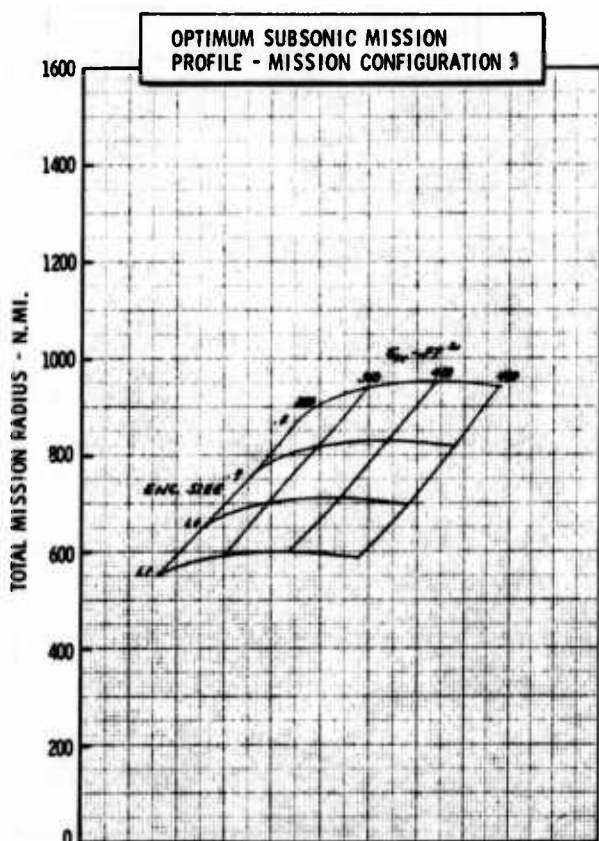
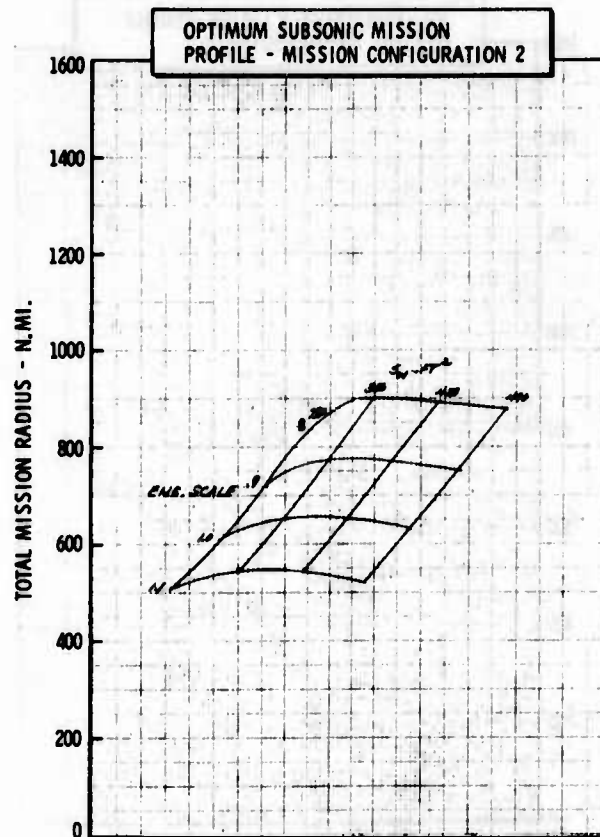
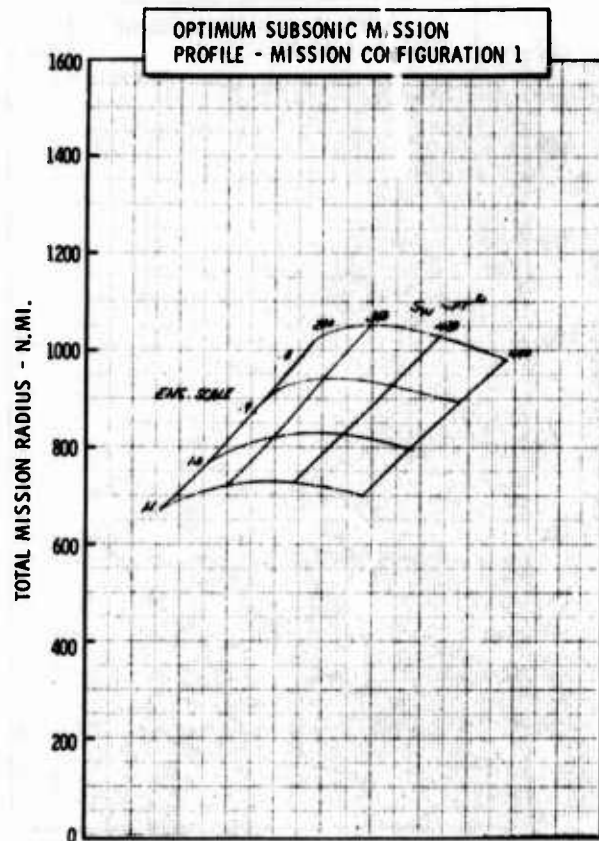


Figure H-38a LWA Mission/Configuration Tradeoff Parametric Data



• COMPOSITE MATERIALS

•  $\Delta LE = 20^\circ$

•  $AR = 3.0$

•  $t/c = .05$

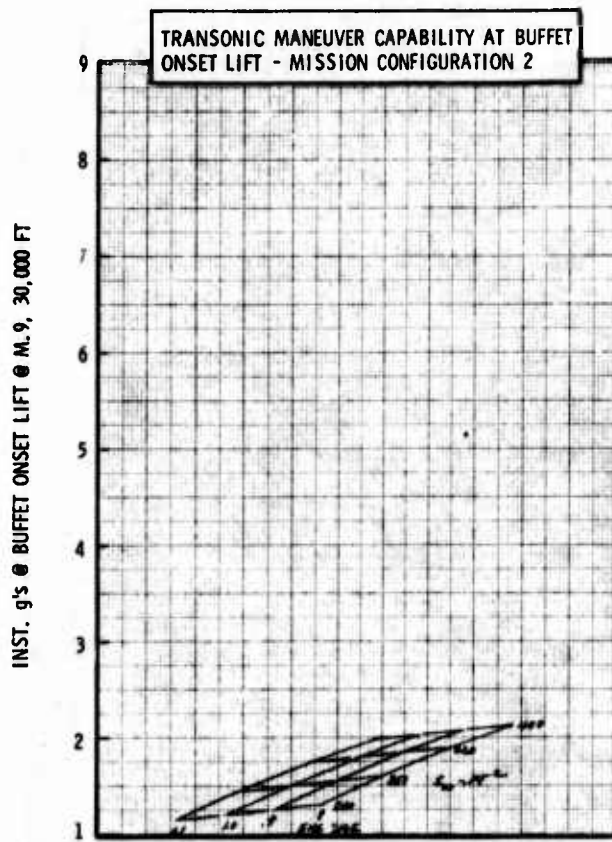
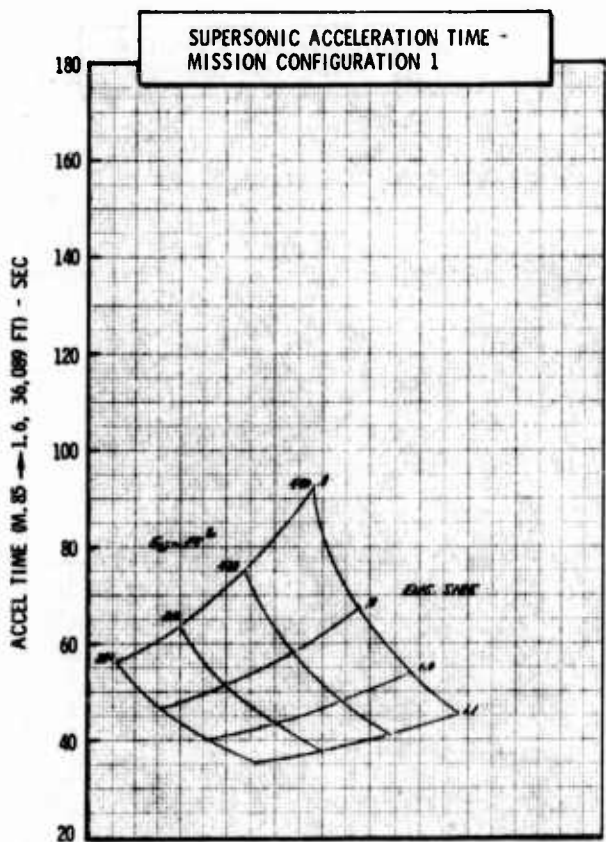
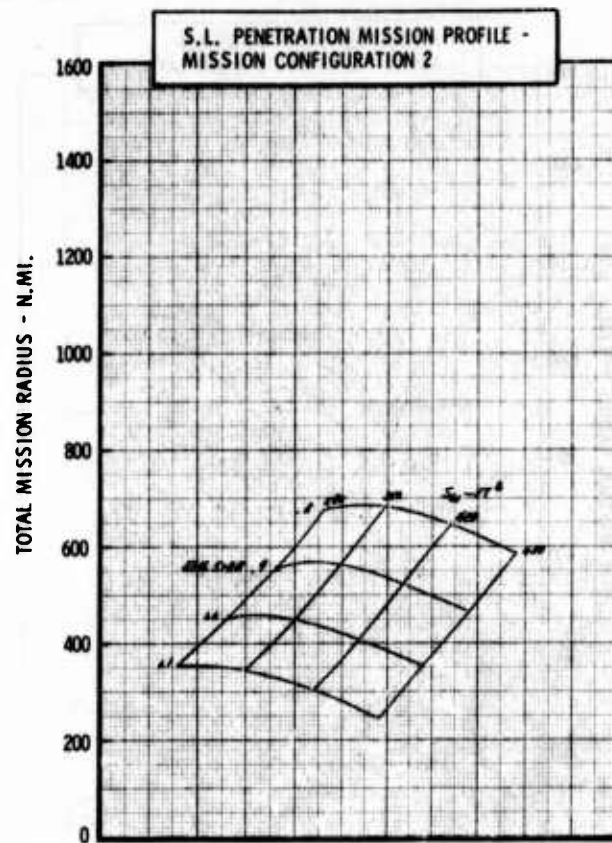
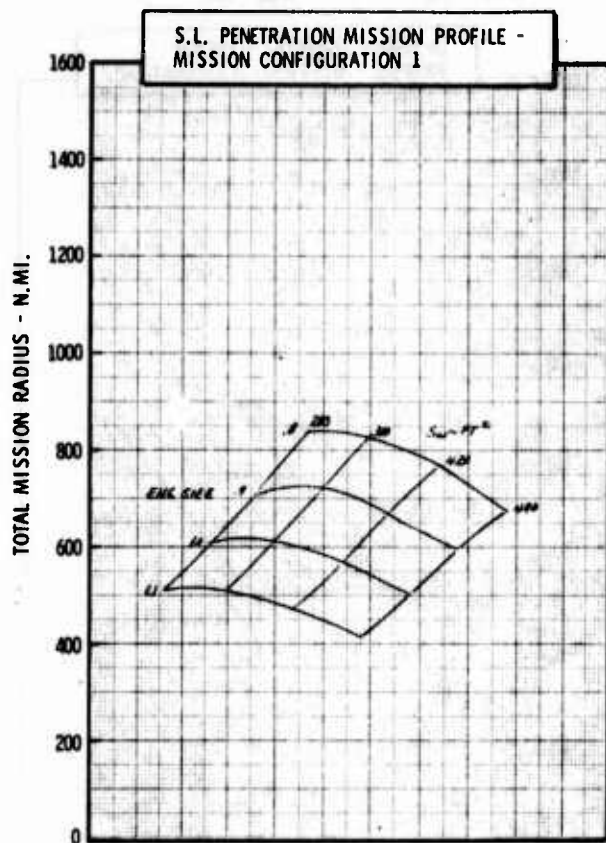


Figure H-38b LWA Mission/Configuration Tradeoff Parametric Data

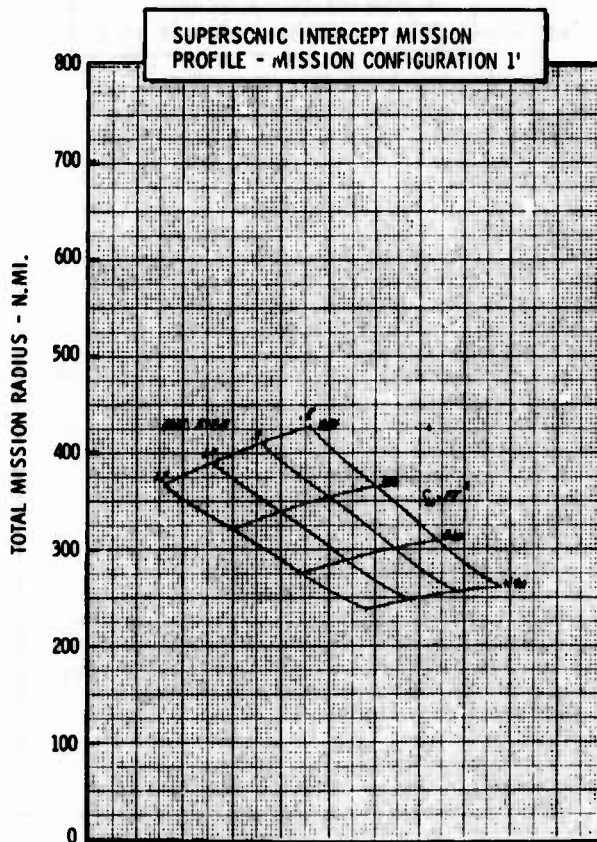
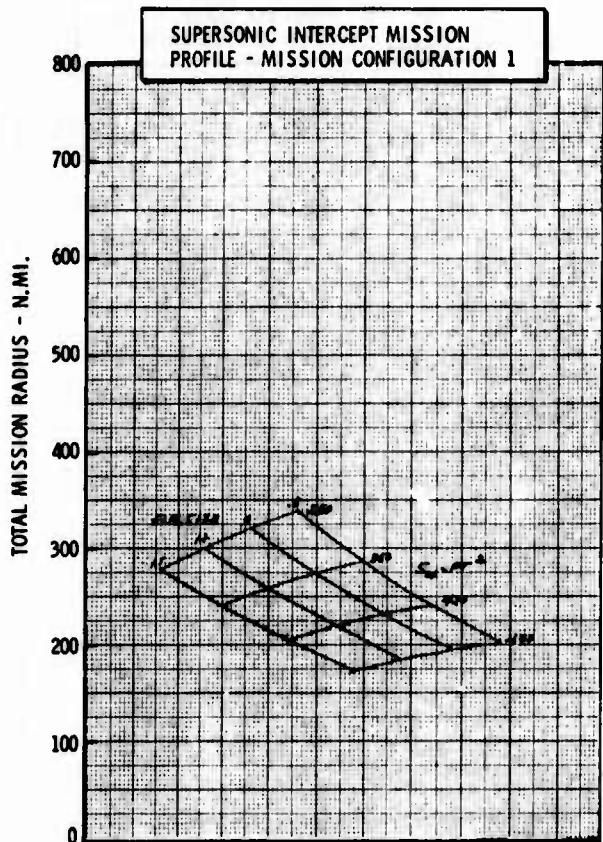
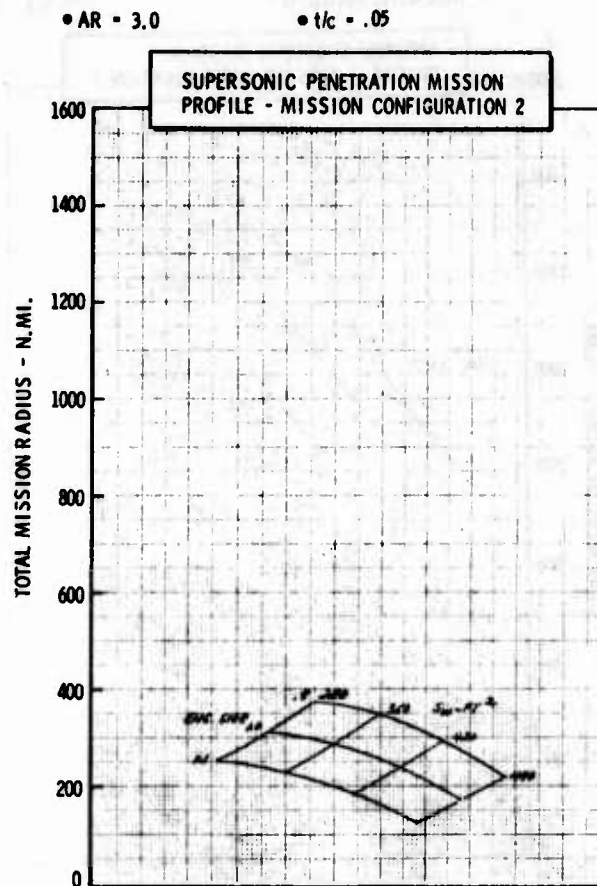
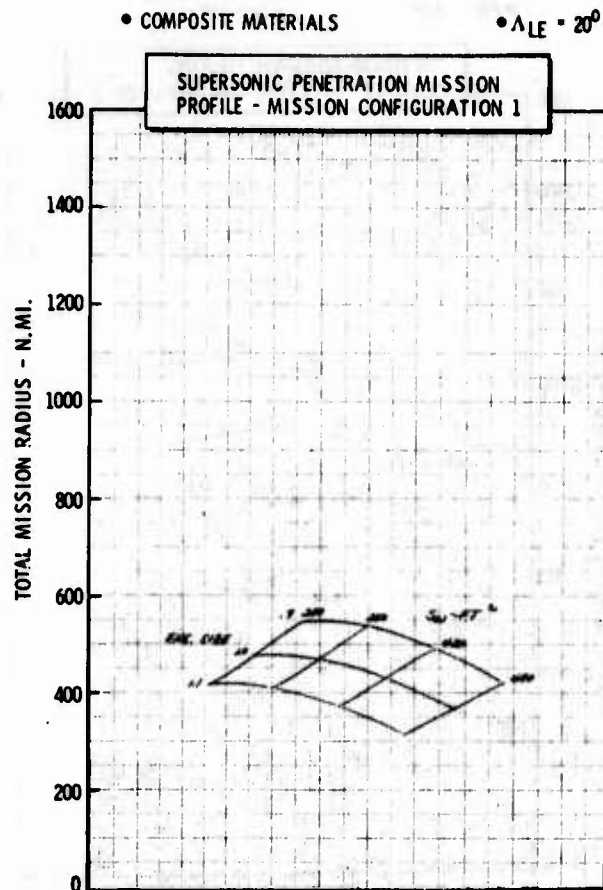


Figure H-38c LWA Mission/Configuration Tradeoff Parametric Data

• COMPOSITE MATERIALS

•  $\Delta LE = 20^\circ$

•  $AR = 4.0$

•  $t/c = .05$

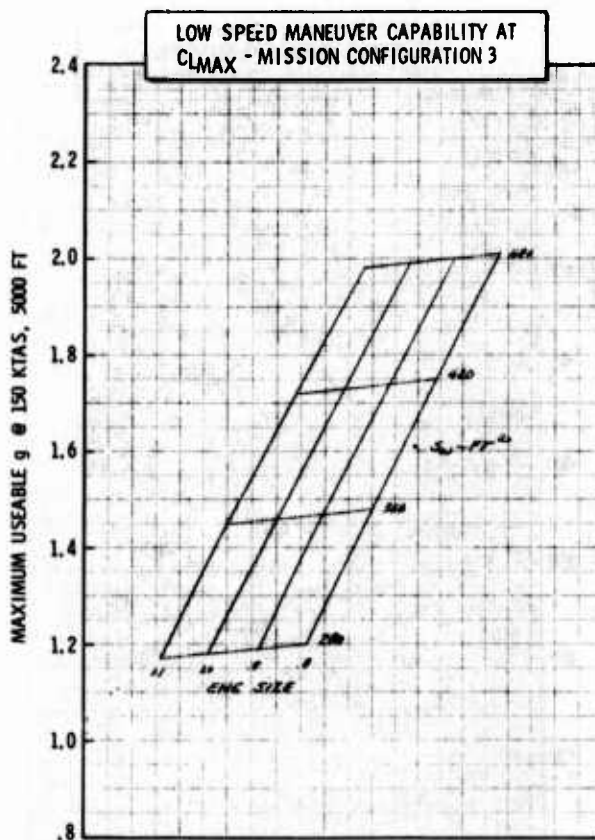
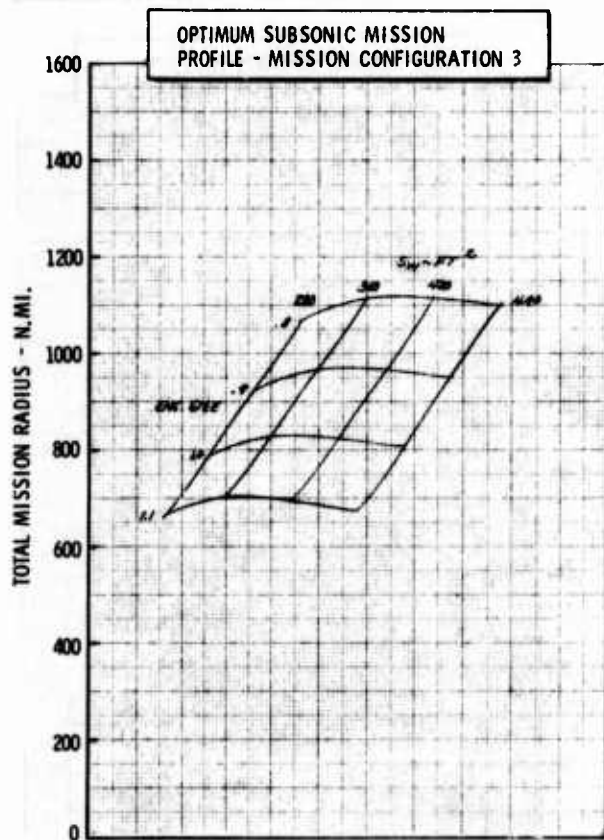
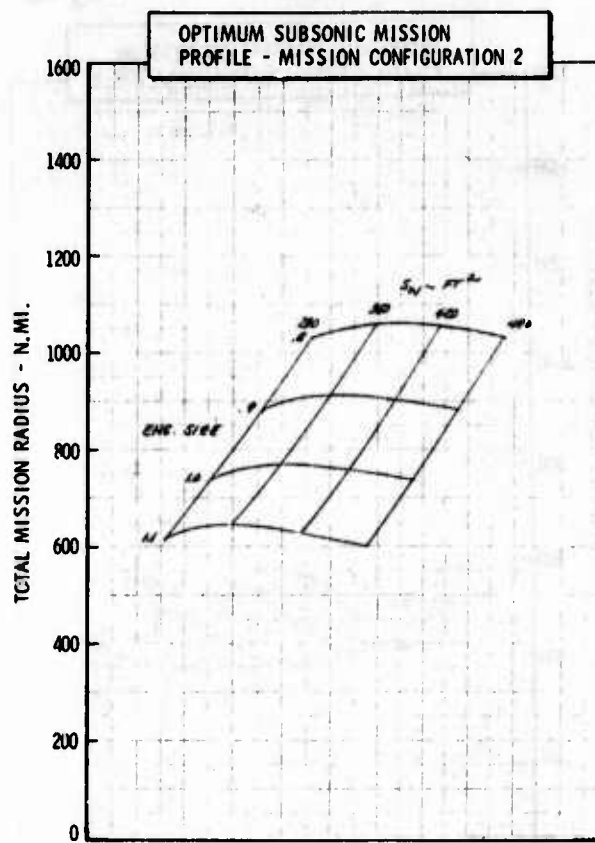
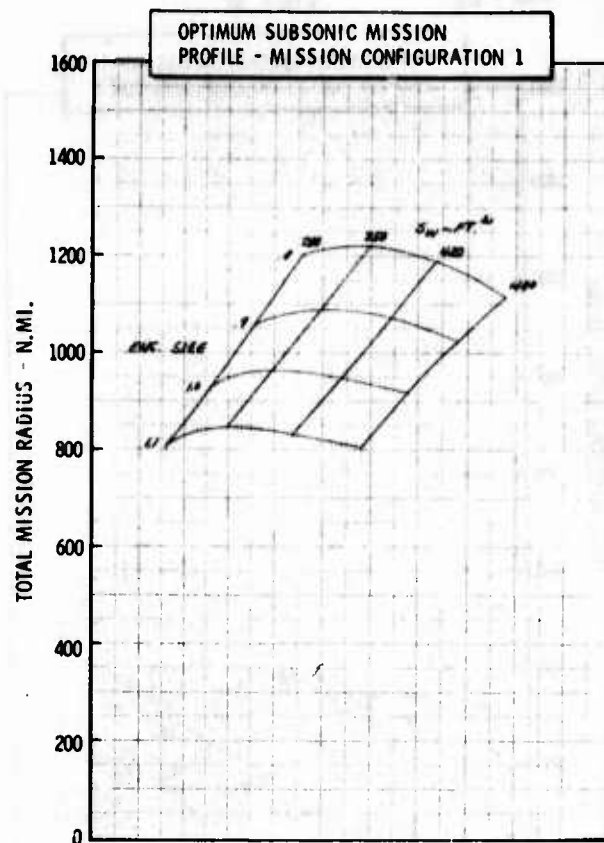


Figure H-39a LWA Mission/Configuration Tradeoff Parametric Data

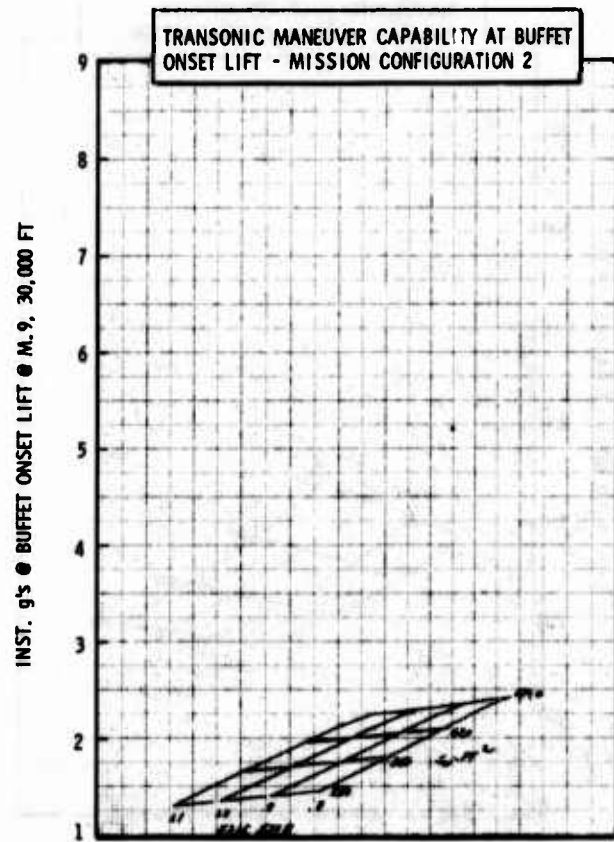
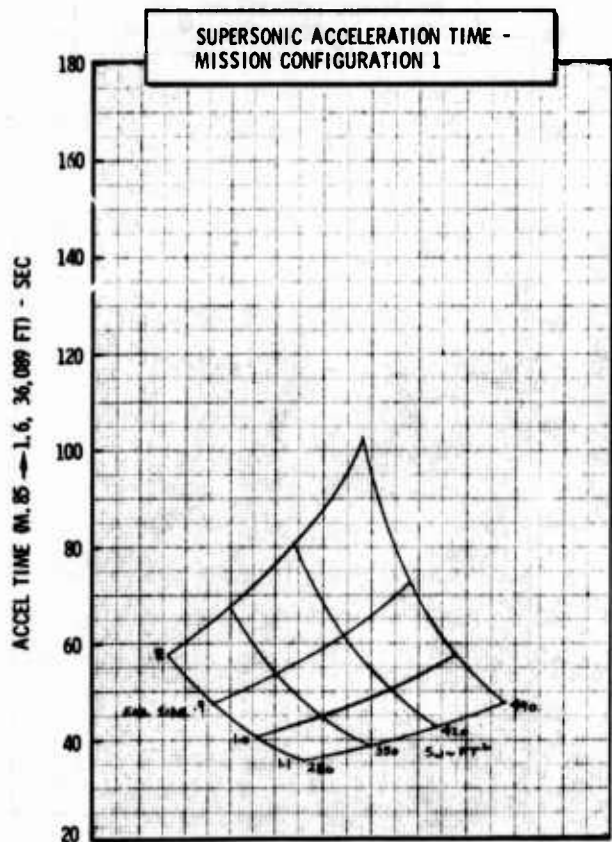
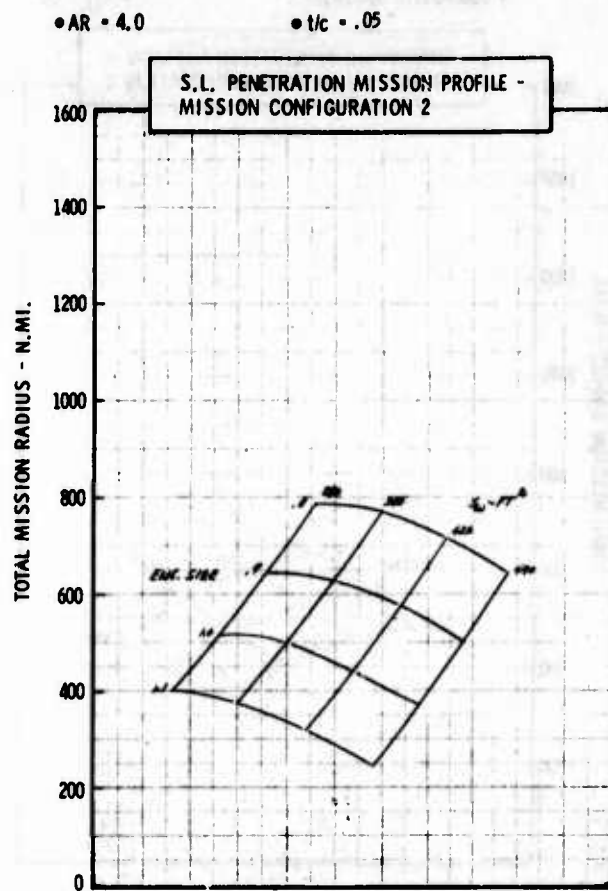
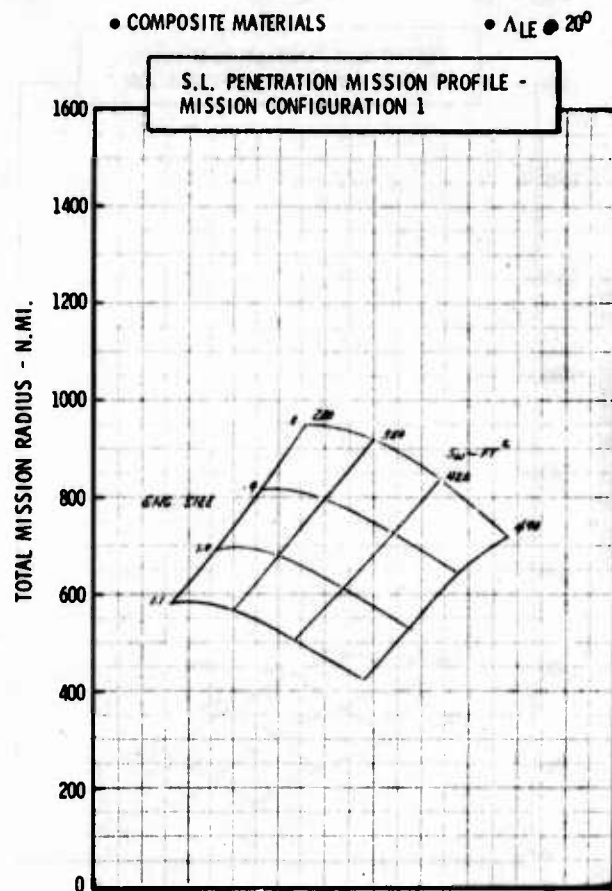


Figure H-39b LWA Mission/Configuration Tradeoff Parametric Data



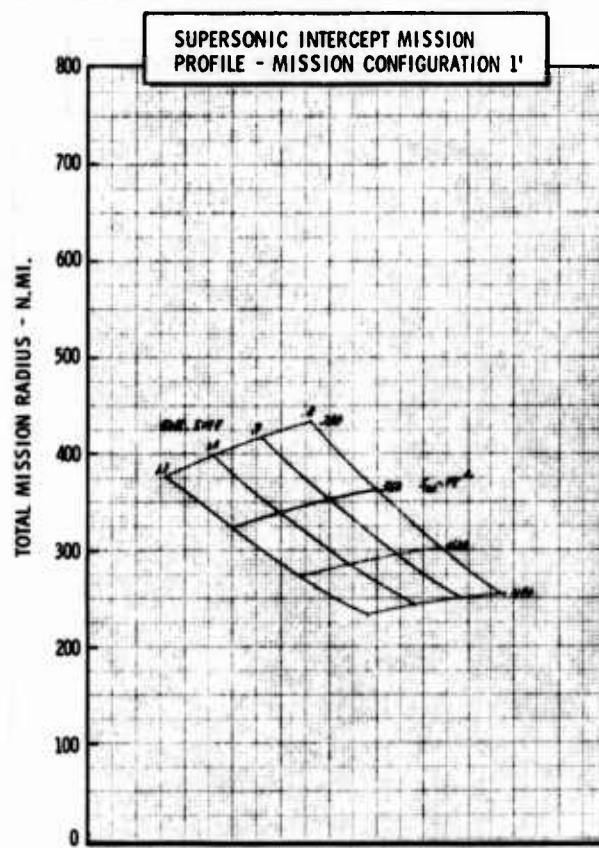
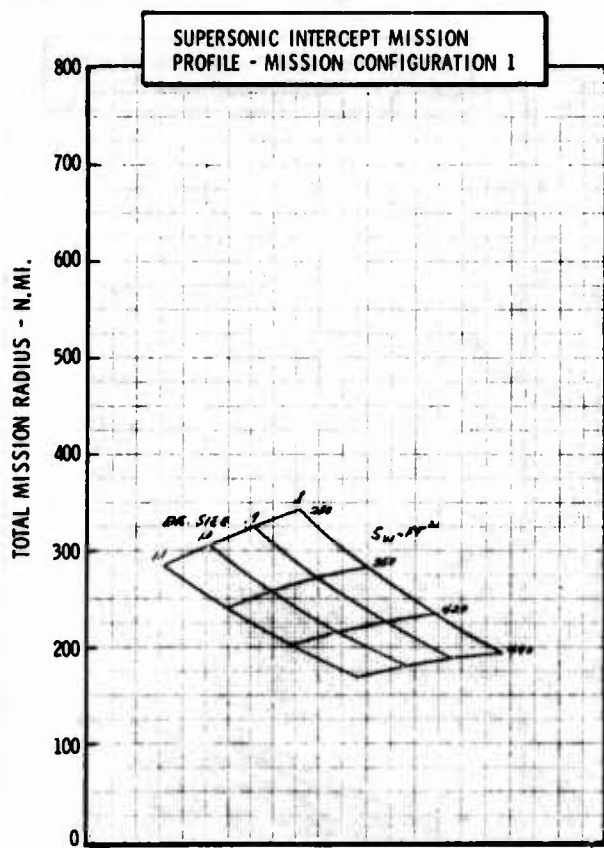
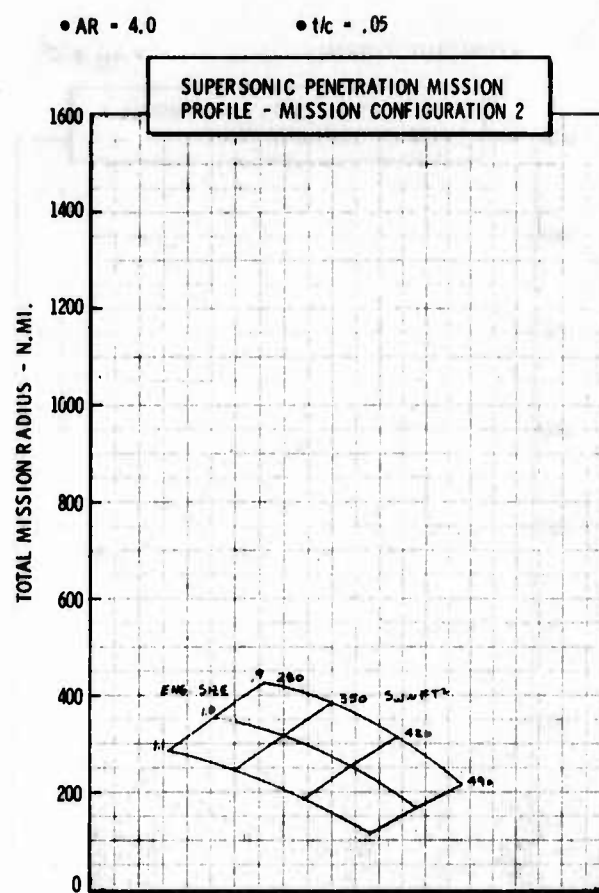
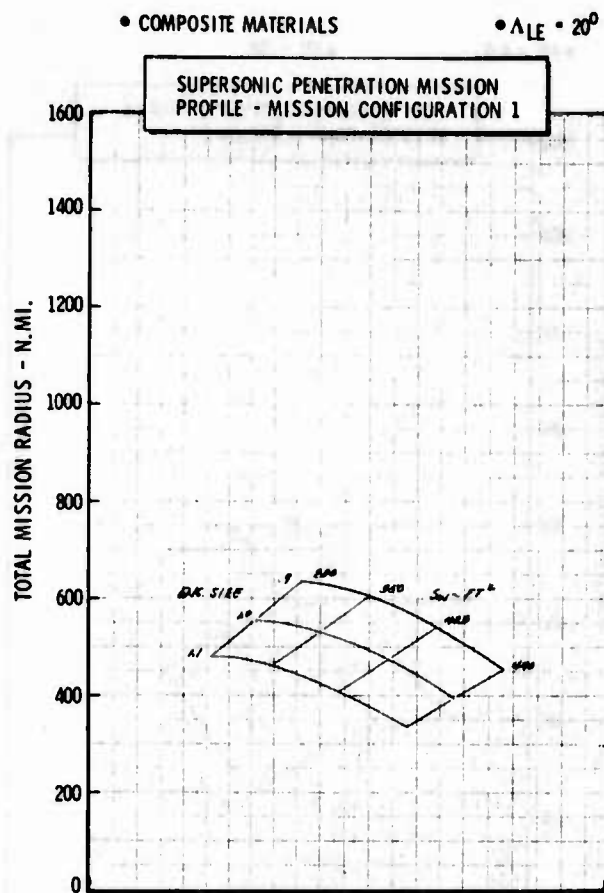


Figure H-39c LWA Mission/Configuration Tradeoff Parametric Data



• COMPOSITE MATERIALS

•  $\Lambda_{LE} = 20^\circ$

•  $AR = 5.0$

•  $t/c = .05$

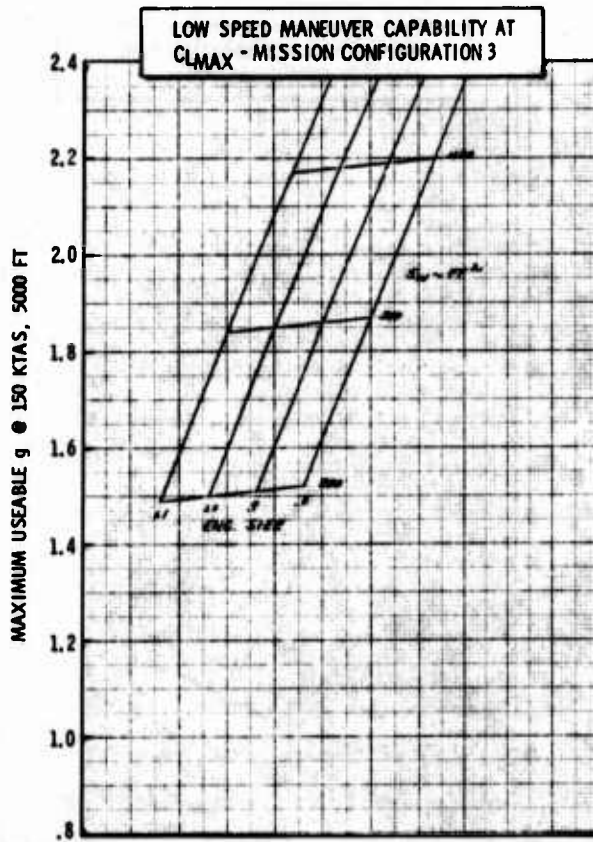
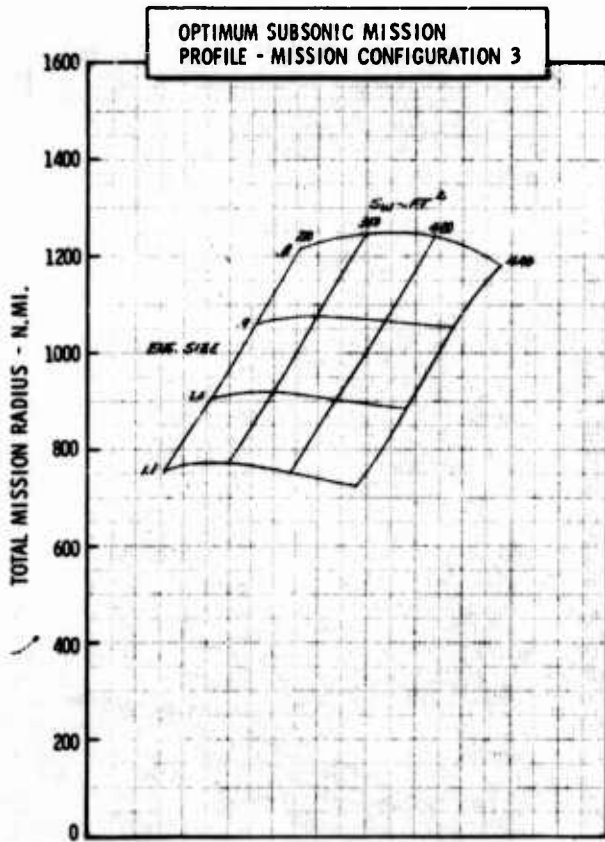
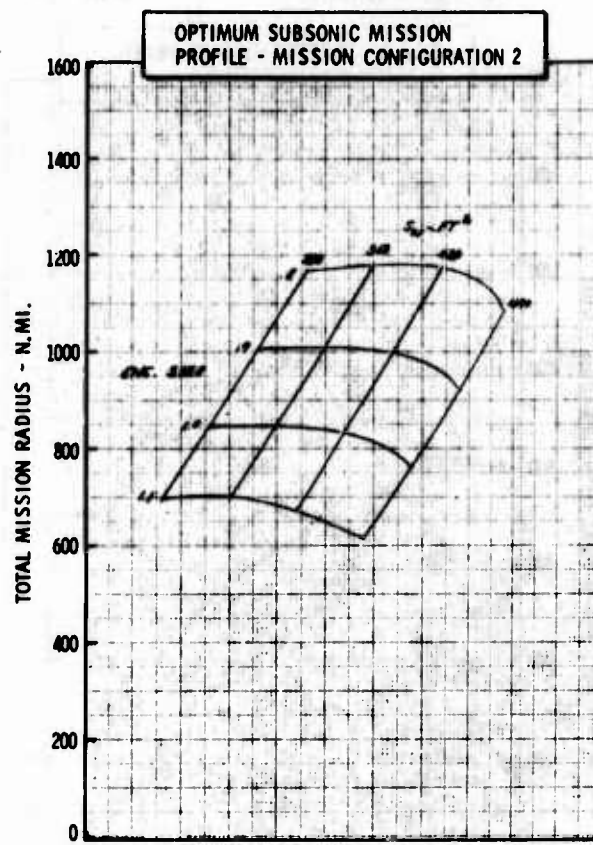
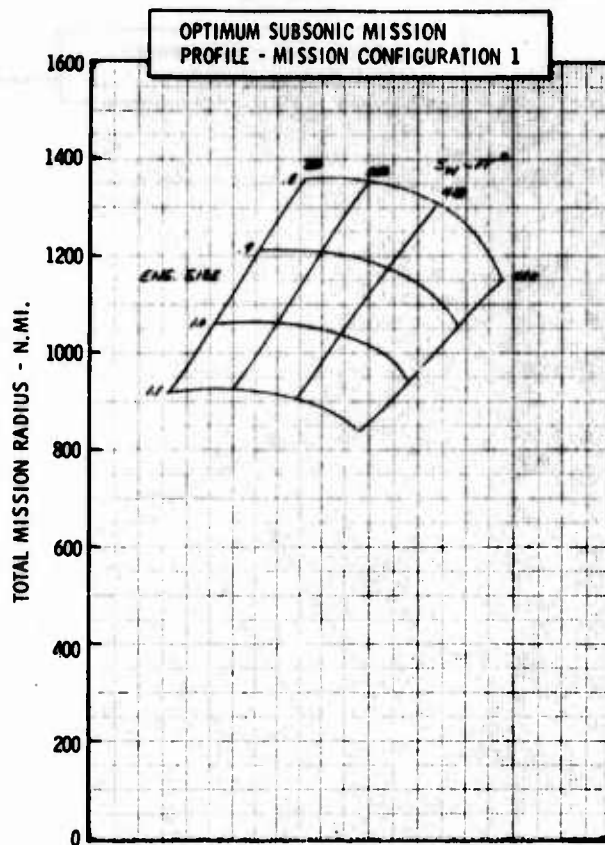


Figure H-40a LWA Mission/Configuration Tradeoff Parametric Data

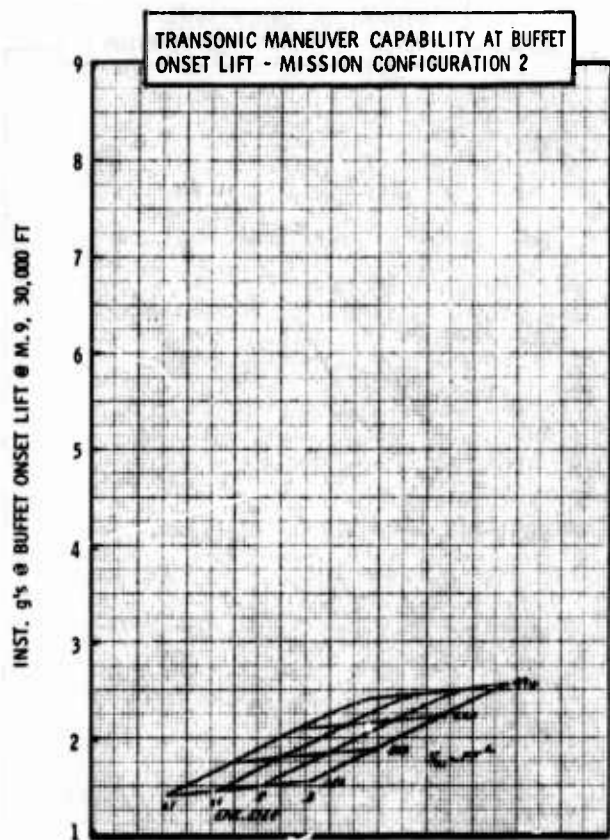
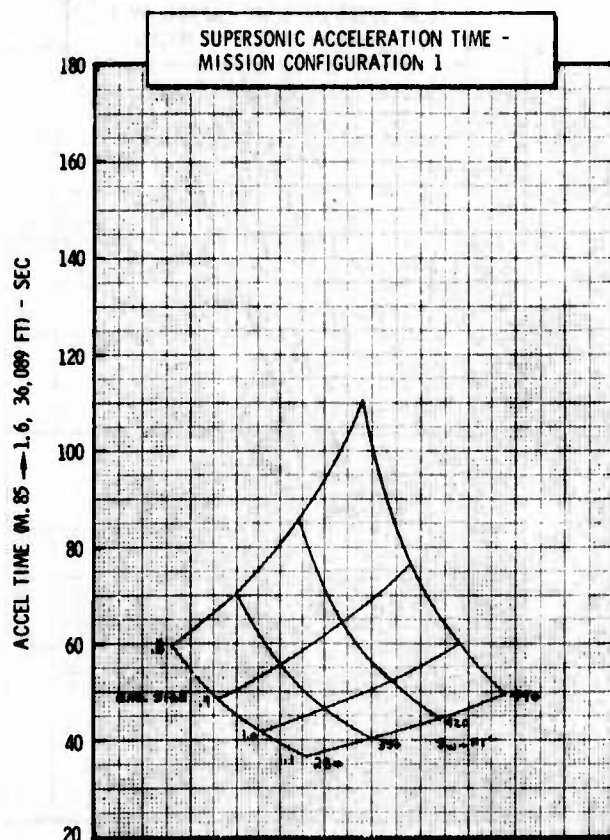
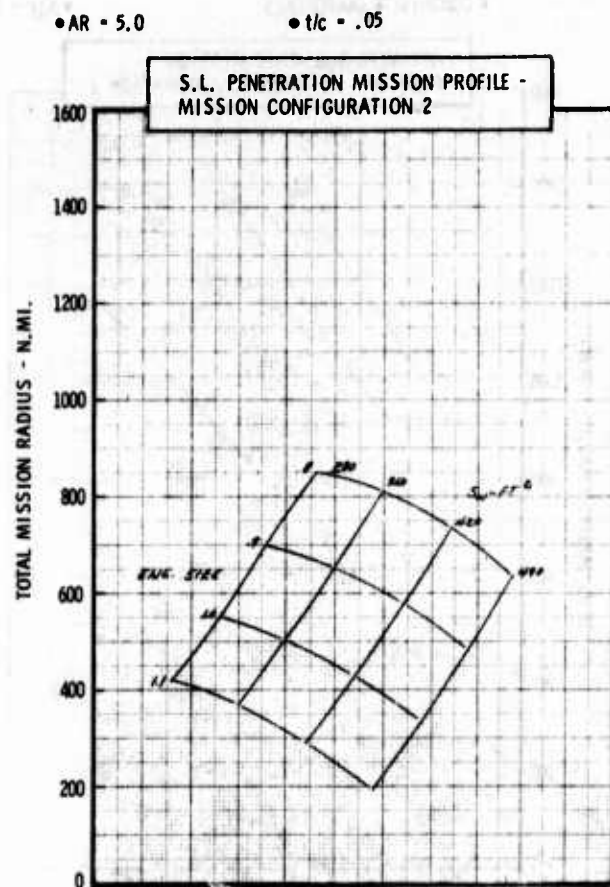
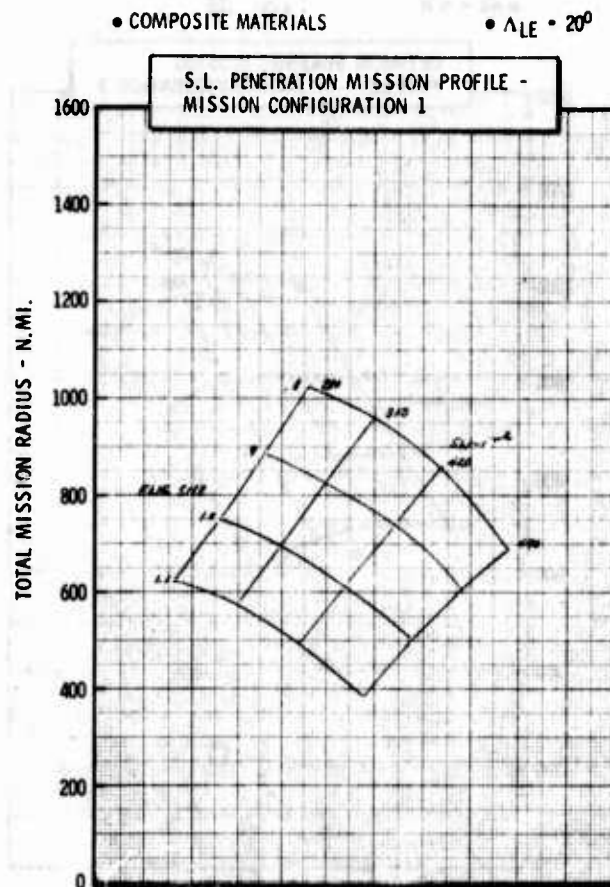


Figure H-40b LWA Mission/Configuration Tradeoff Parametric Data

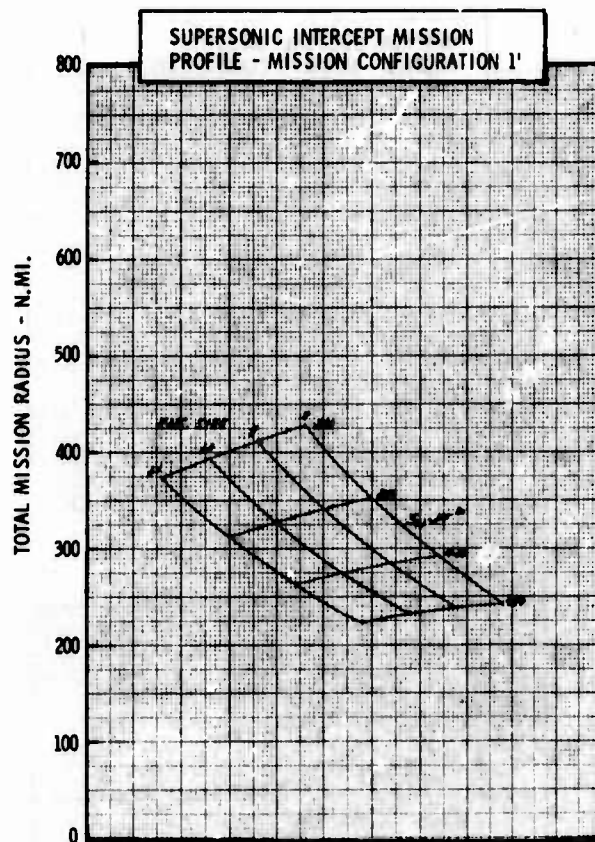
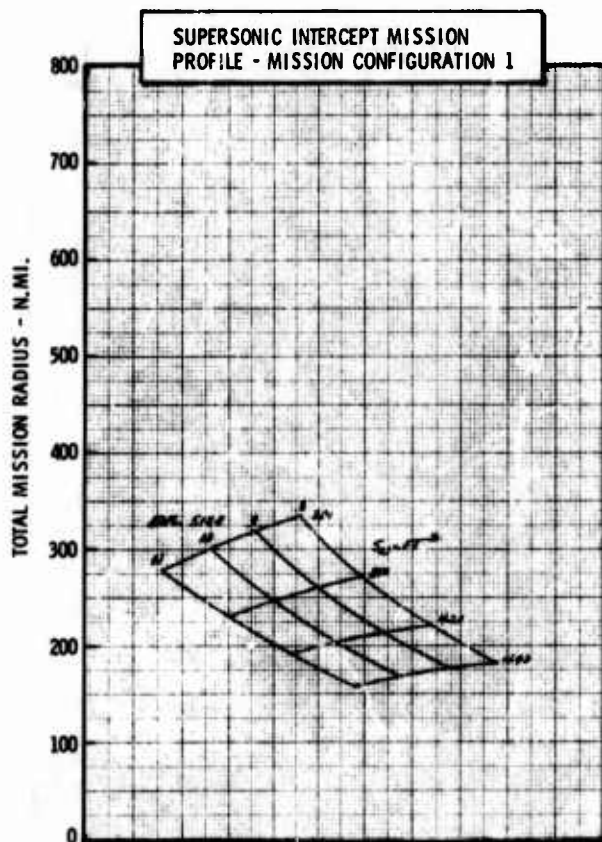
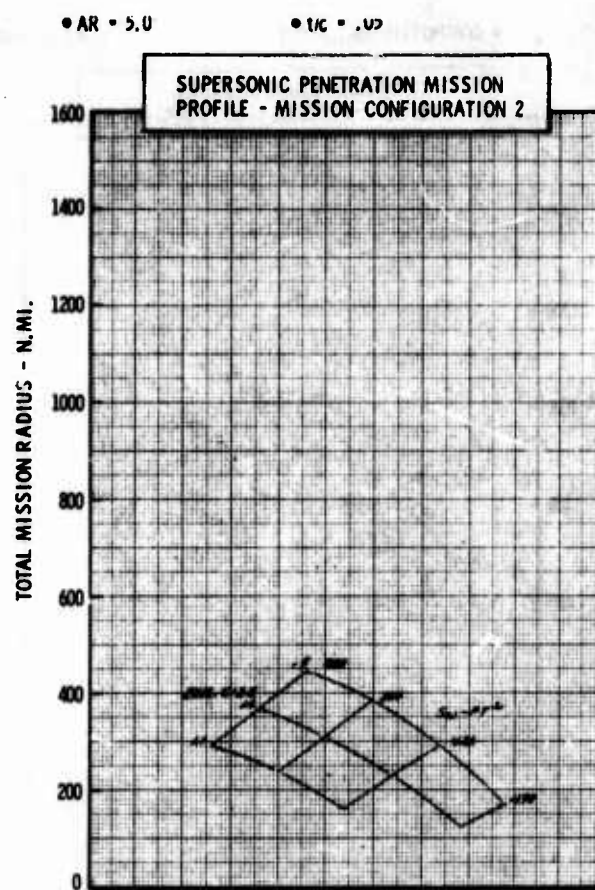
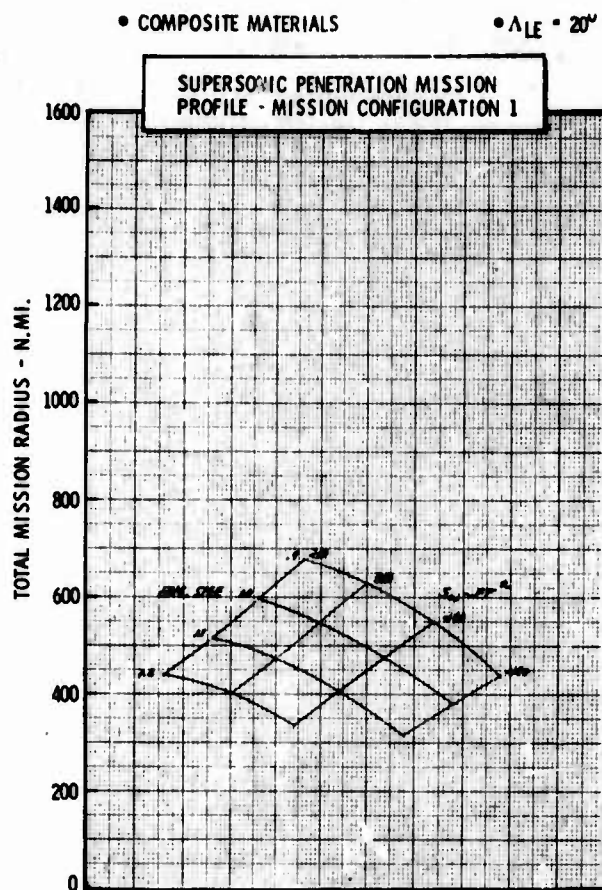


Figure H-40c LWA Mission/Configuration Tradeoff Parametric Data



• COMPOSITE MATERIALS

•  $\Lambda_{LE} = 30^\circ$

•  $AR = 3.0$

•  $t/c = .05$

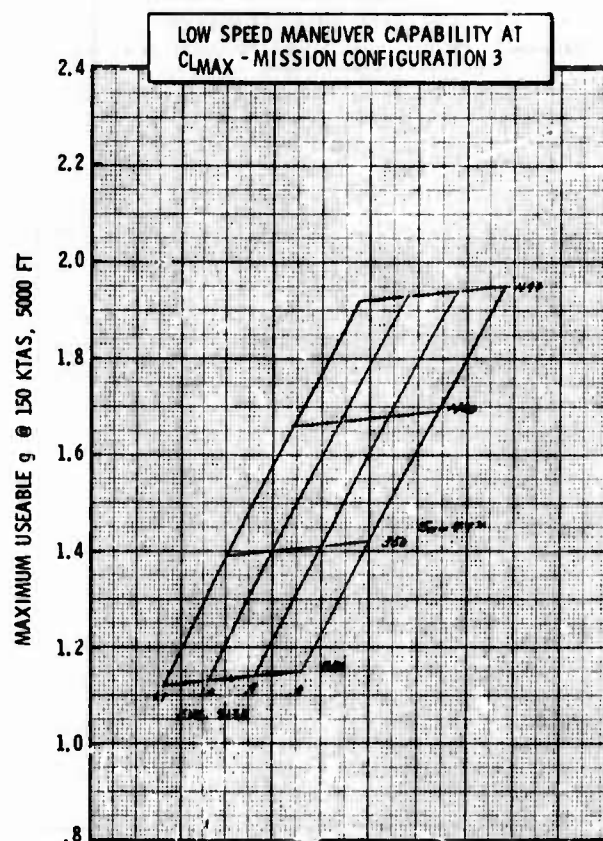
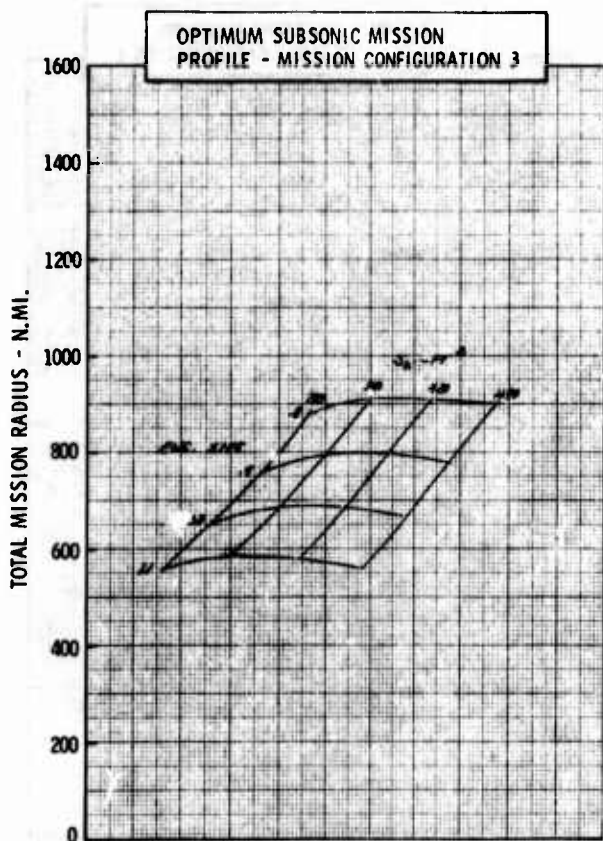
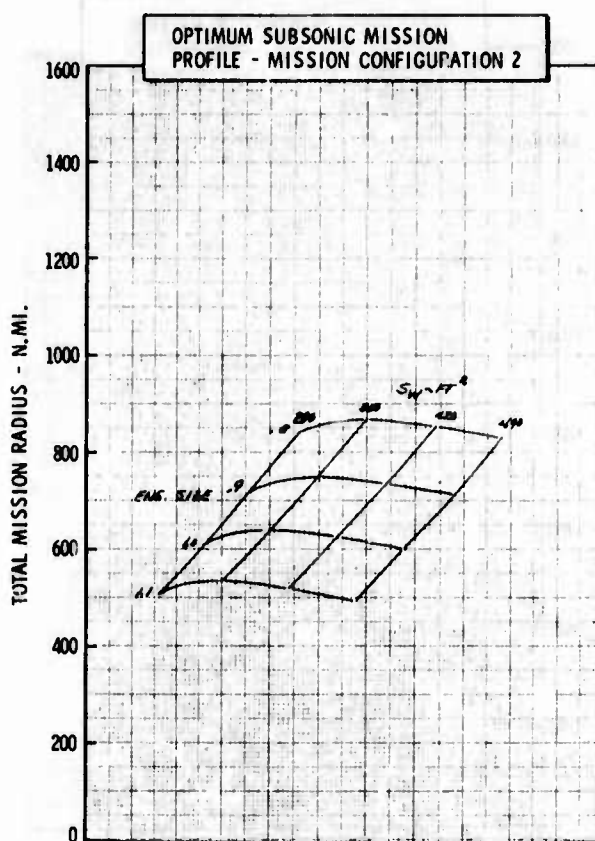
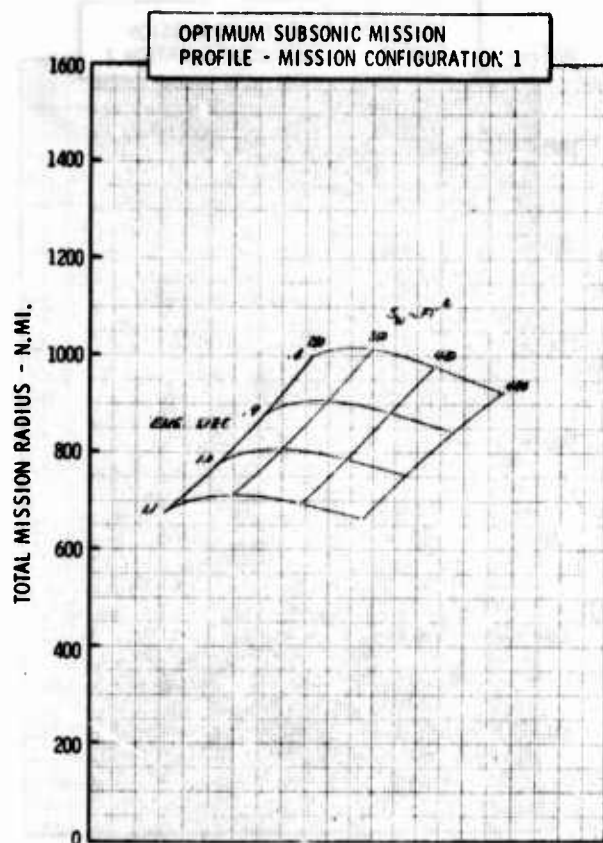


Figure H-41a LWA Mission/Configuration Tradeoff Parametric Data

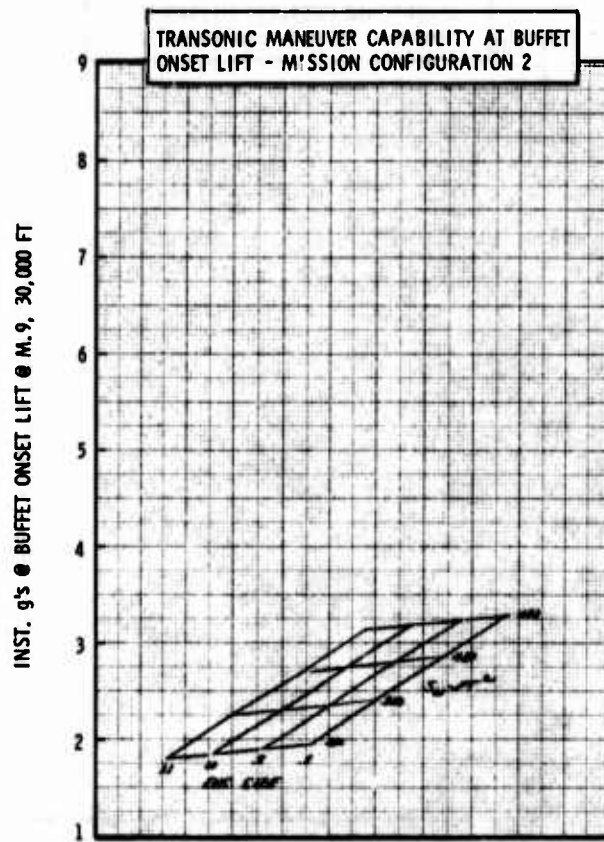
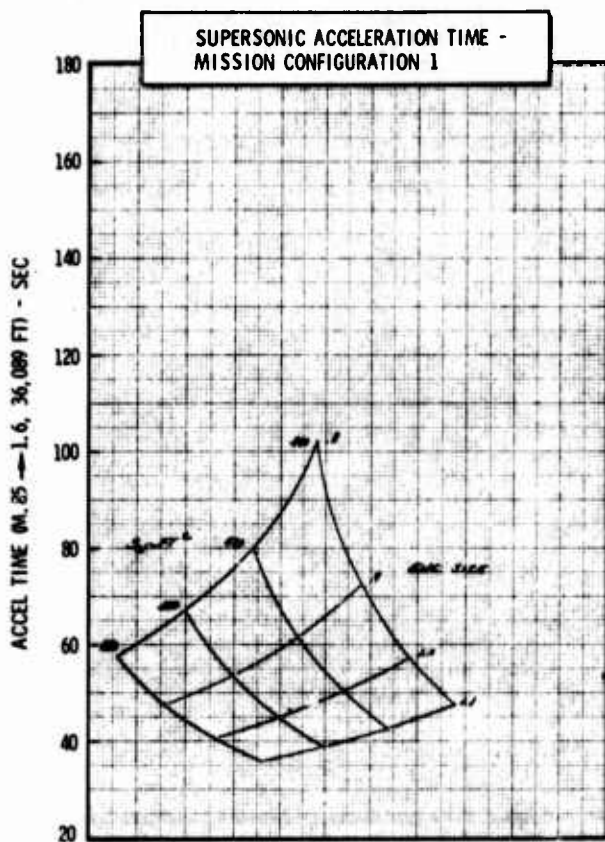
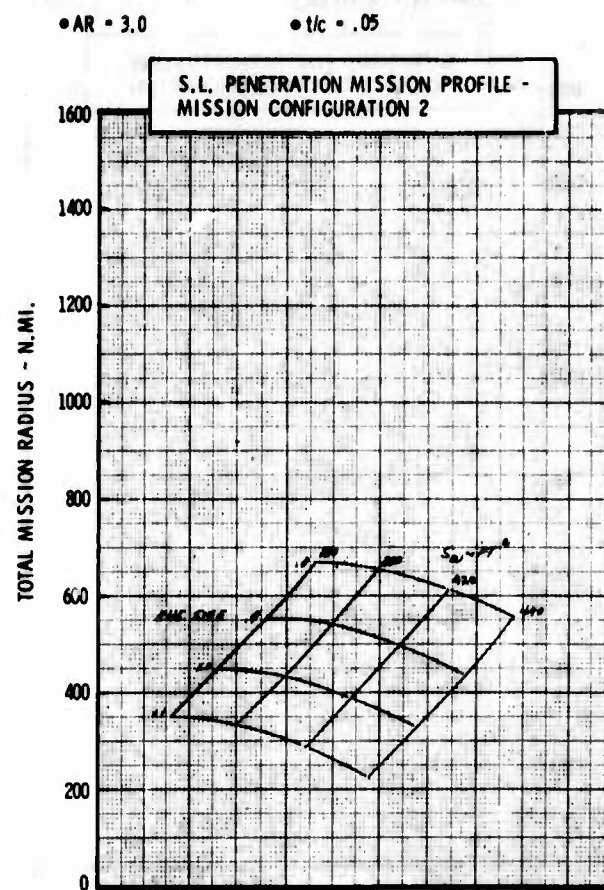
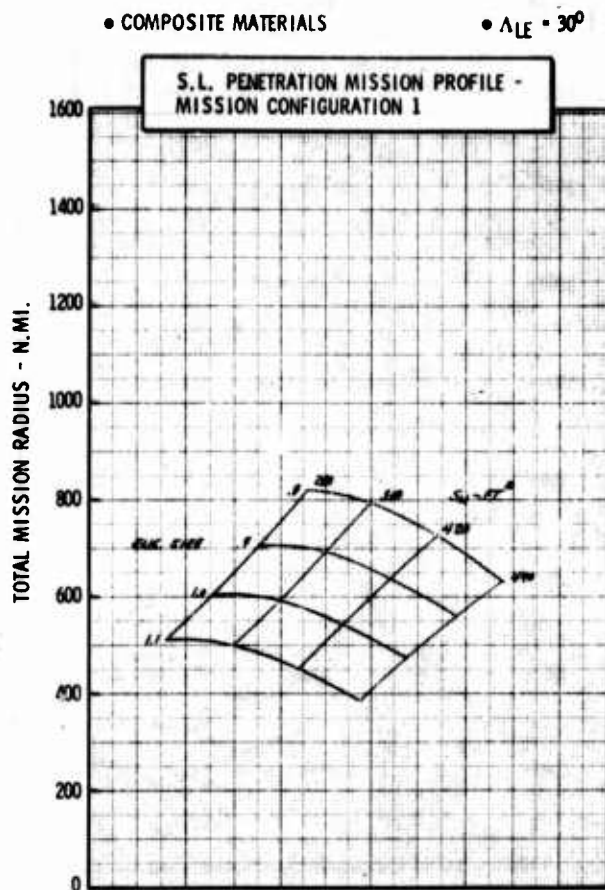
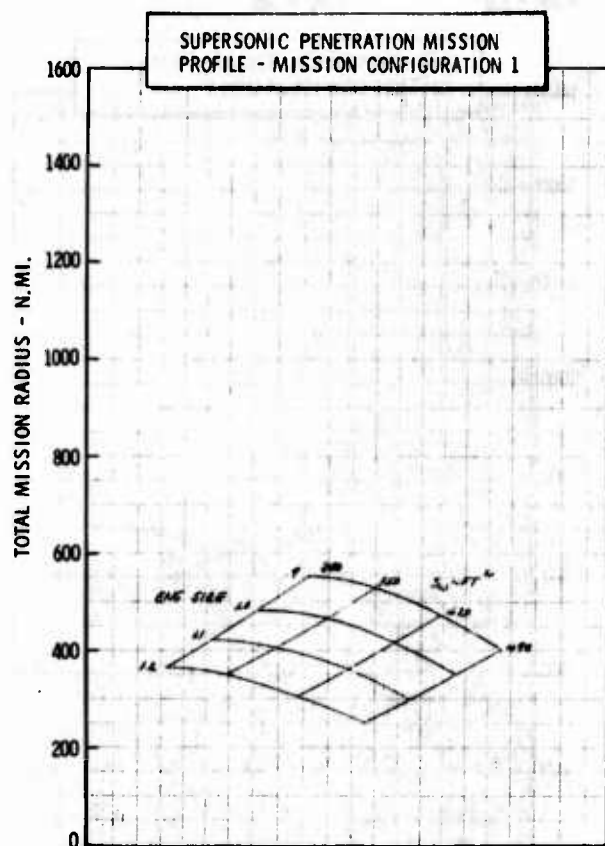


Figure H-41b LWA Mission/Configuration Tradeoff Parametric Data



• COMPOSITE MATERIALS

•  $\Delta LE = 30^\circ$



• AR = 3.0

•  $t/c = .05$

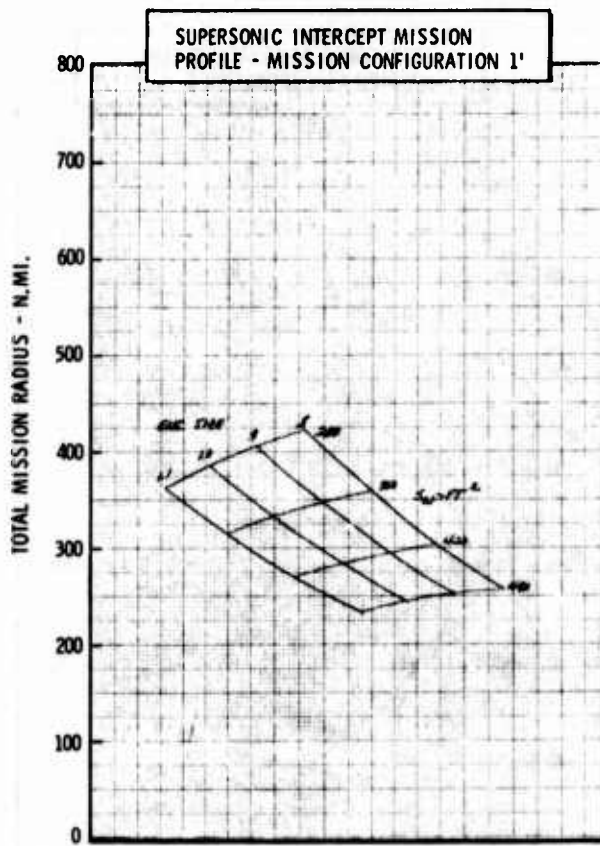
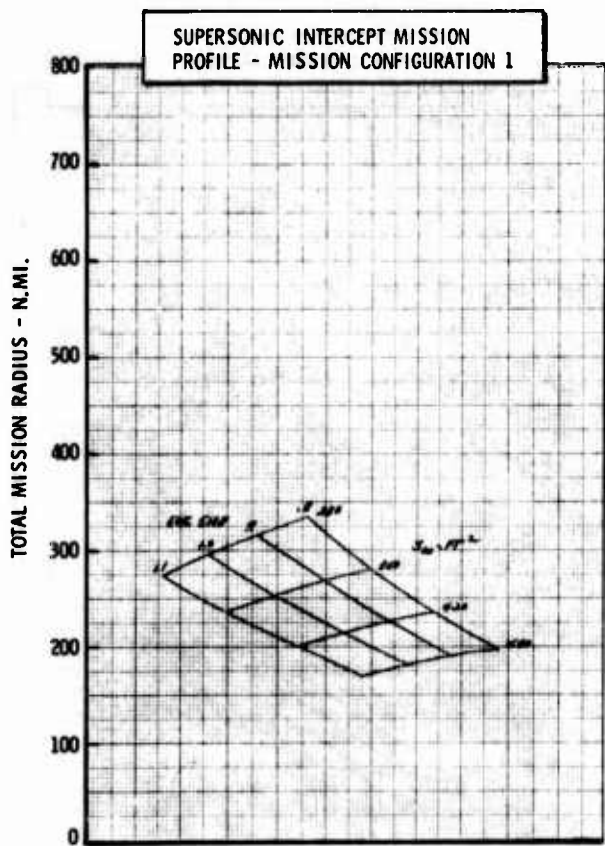
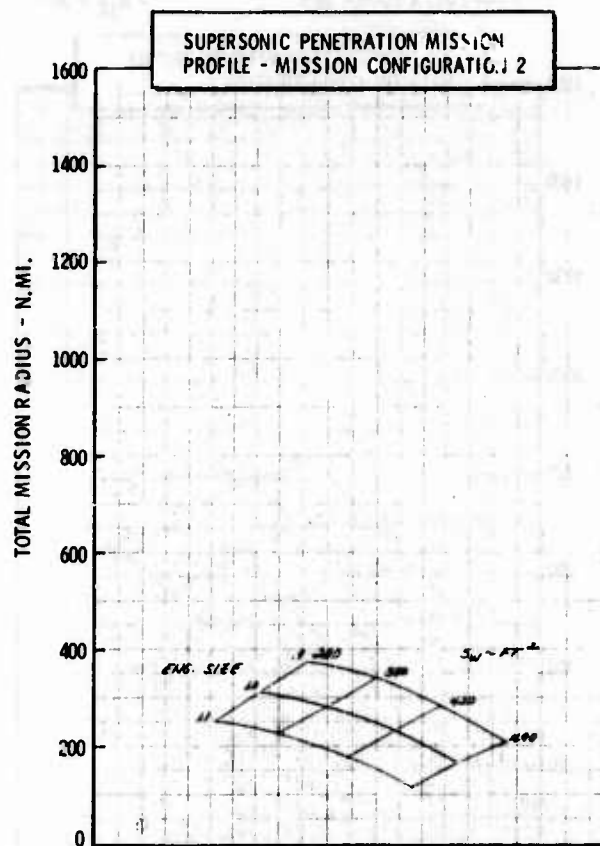


Figure H-41c LWA Mission/Configuration Tradeoff Parametric Data

• COMPOSITE MATERIALS

•  $\Delta LE = 30^\circ$

•  $AR = 4.0$

•  $t/c = .05$

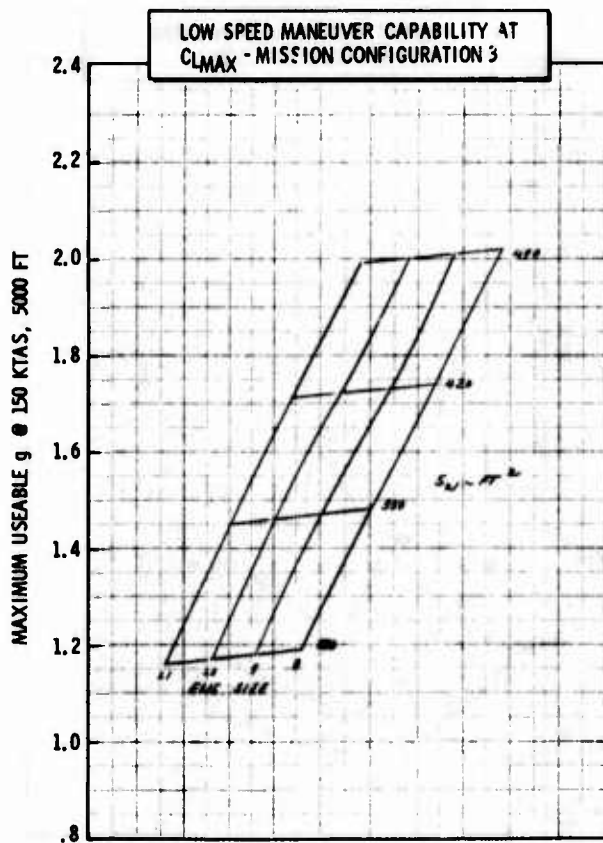
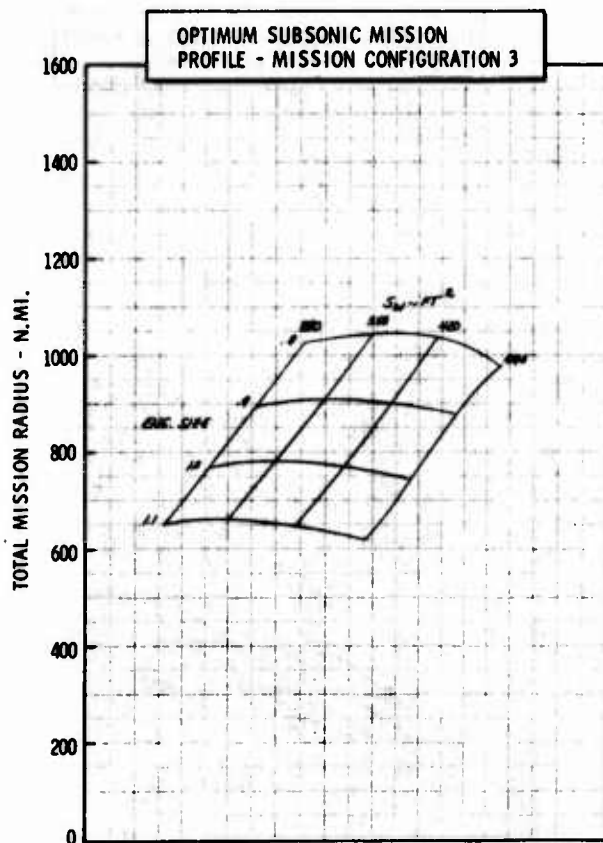
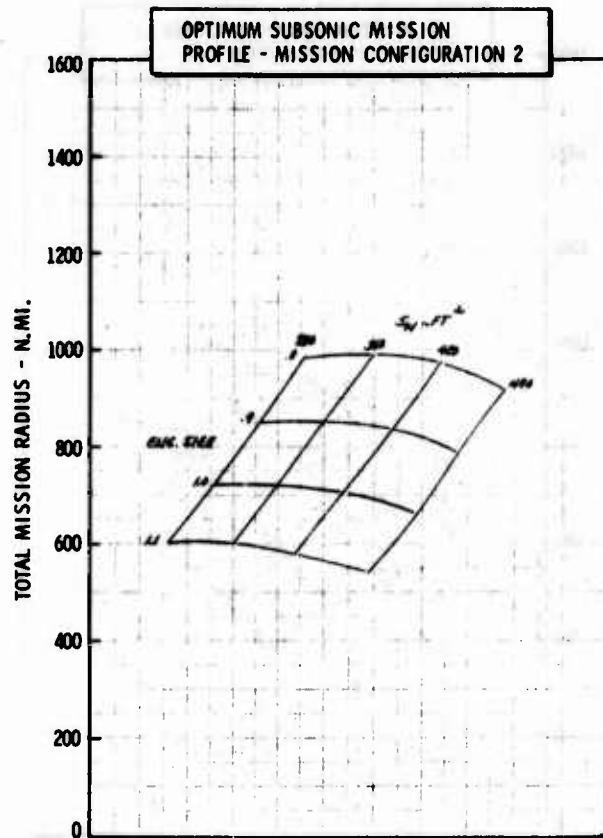
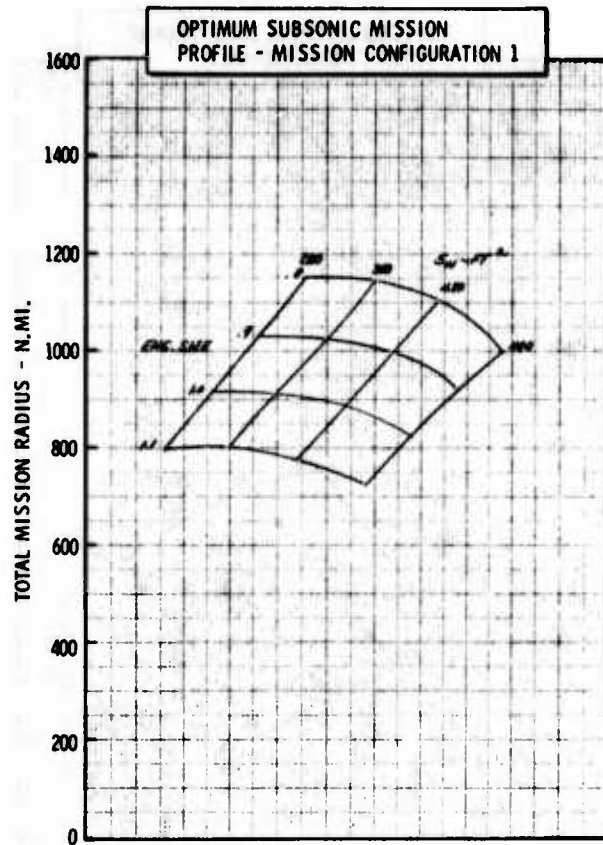


Figure H-42a LWA Mission/Configuration Tradeoff Parametric Data

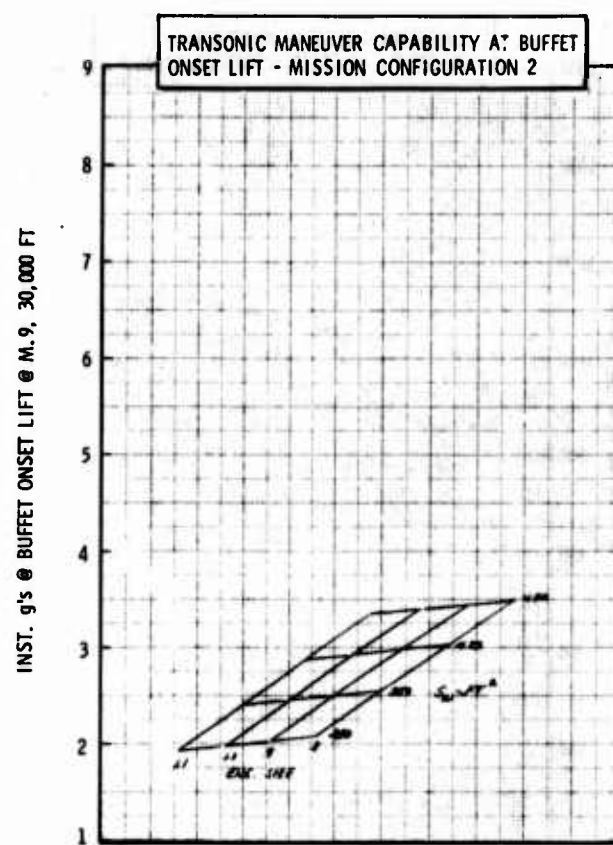
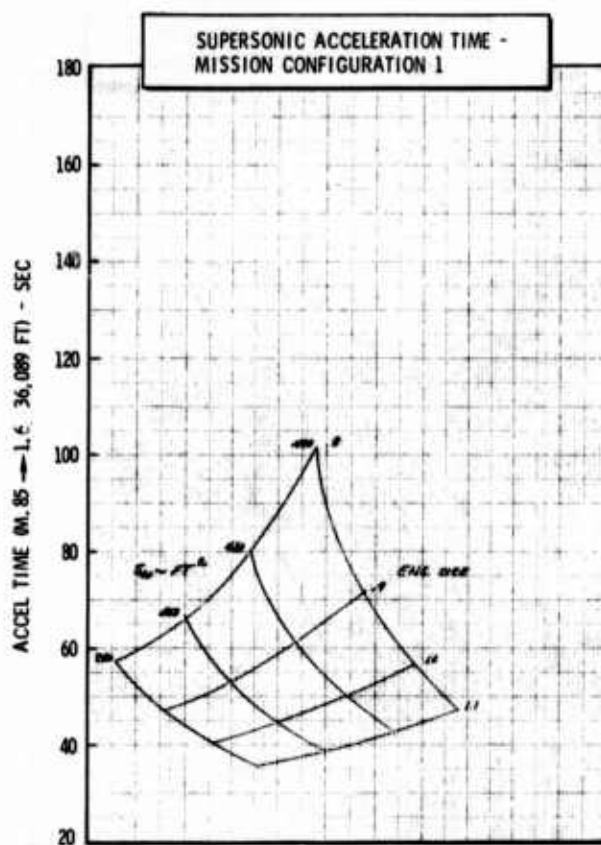
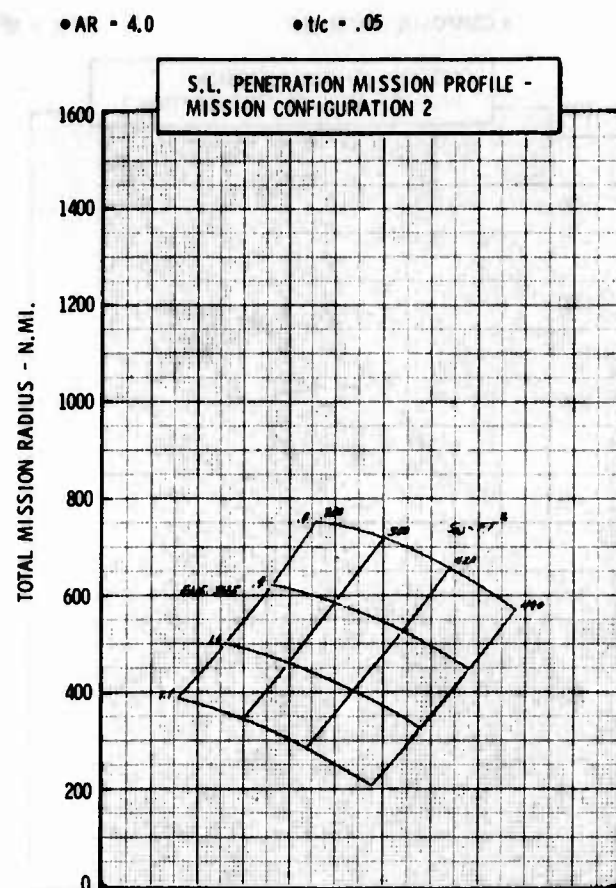
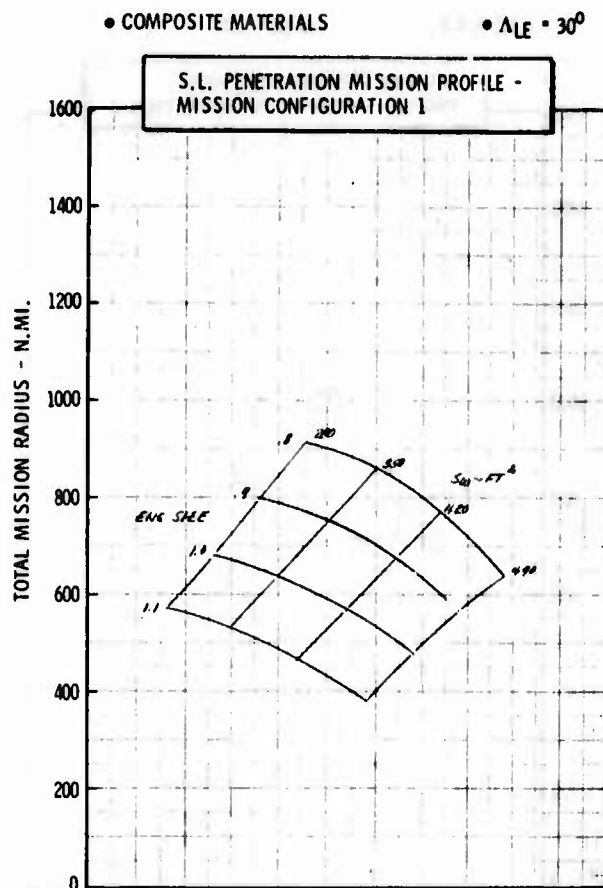


Figure H-42b LWA Mission/Configuration Tradeoff Parametric Data

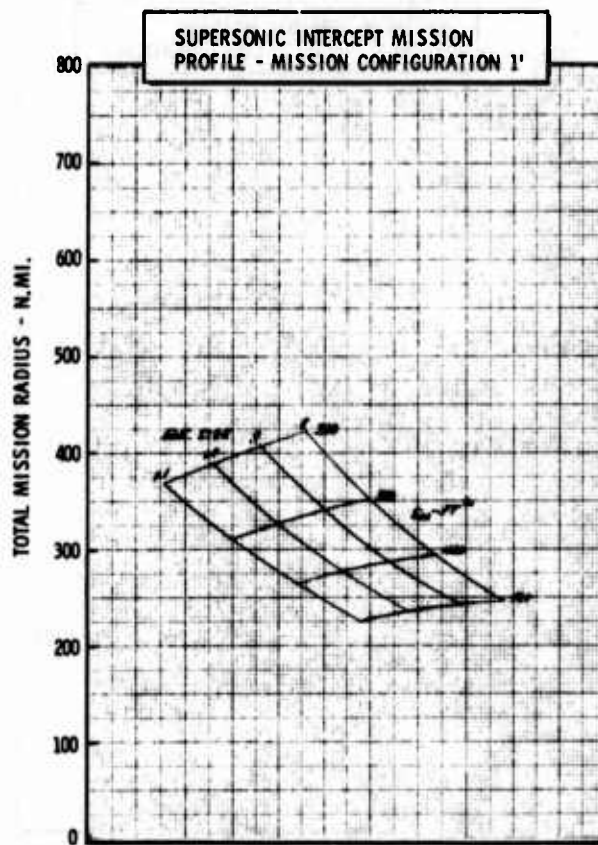
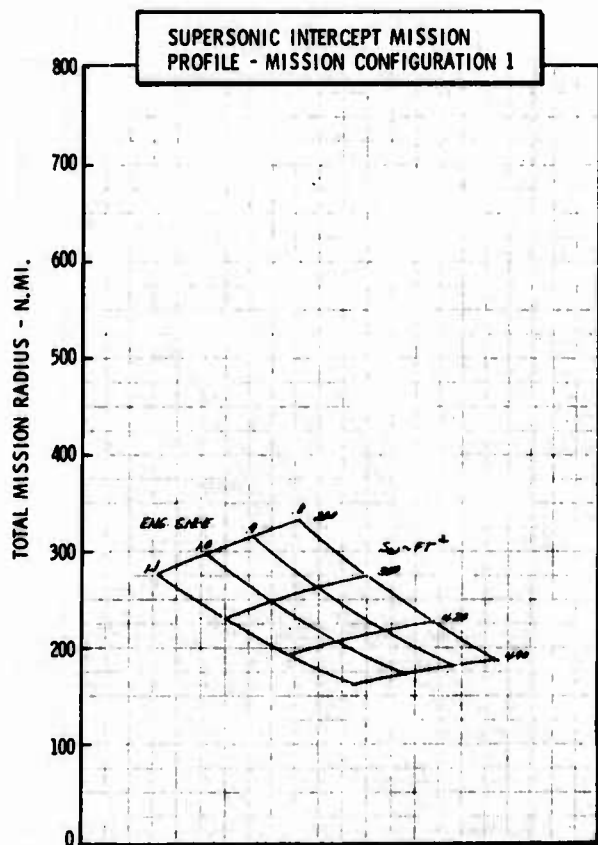
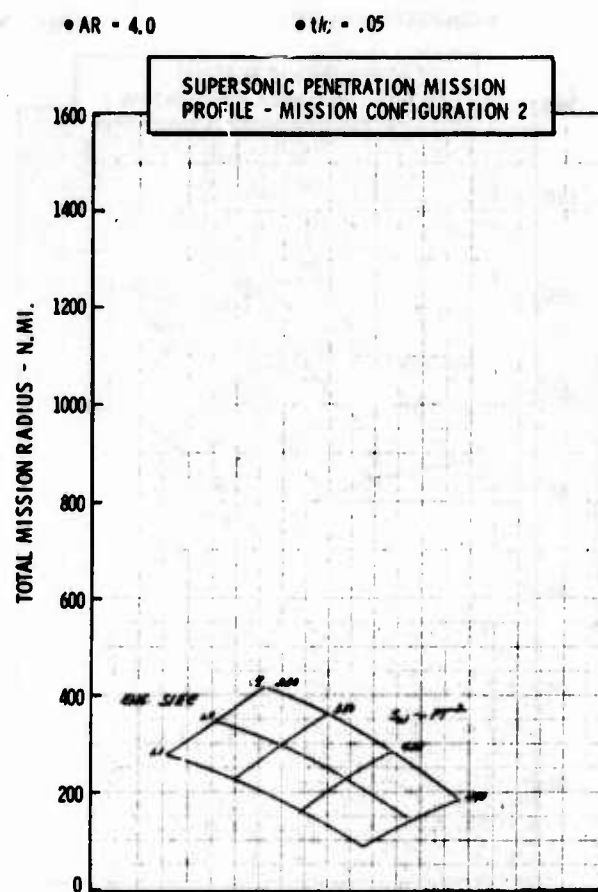
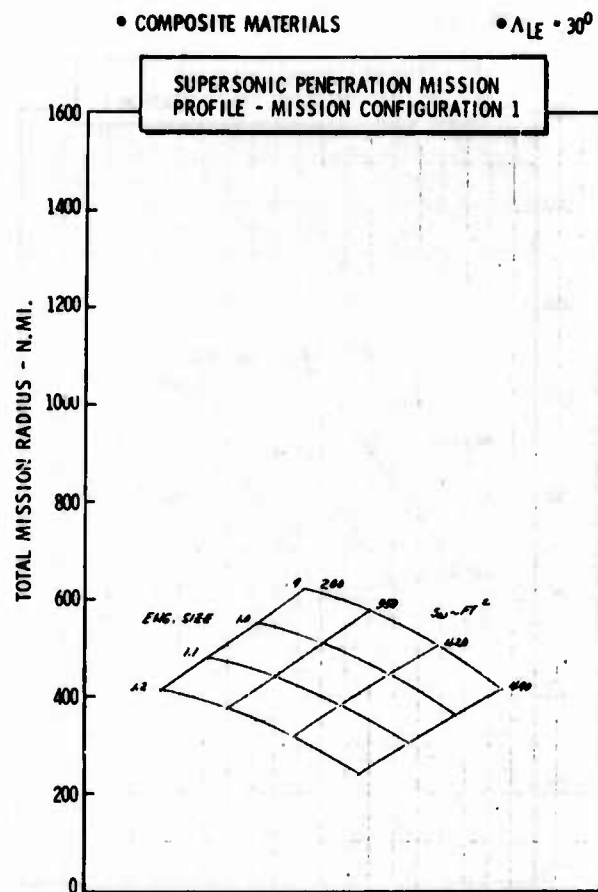


Figure H-42c LWA Mission/Configuration Tradeoff Parametric Data



• COMPOSITE MATERIALS

•  $\Lambda_{LE} = 30^\circ$

•  $AR = 5.0$

•  $t/c = .05$

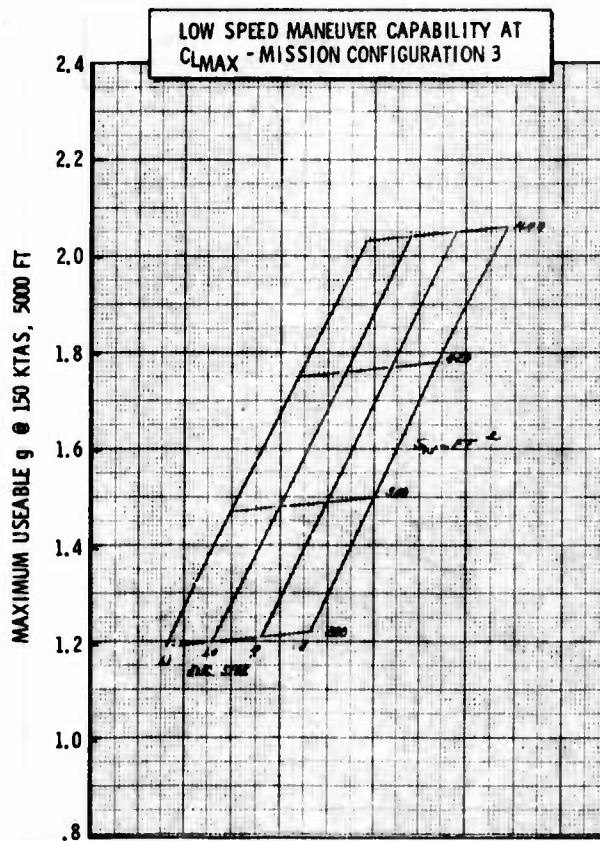
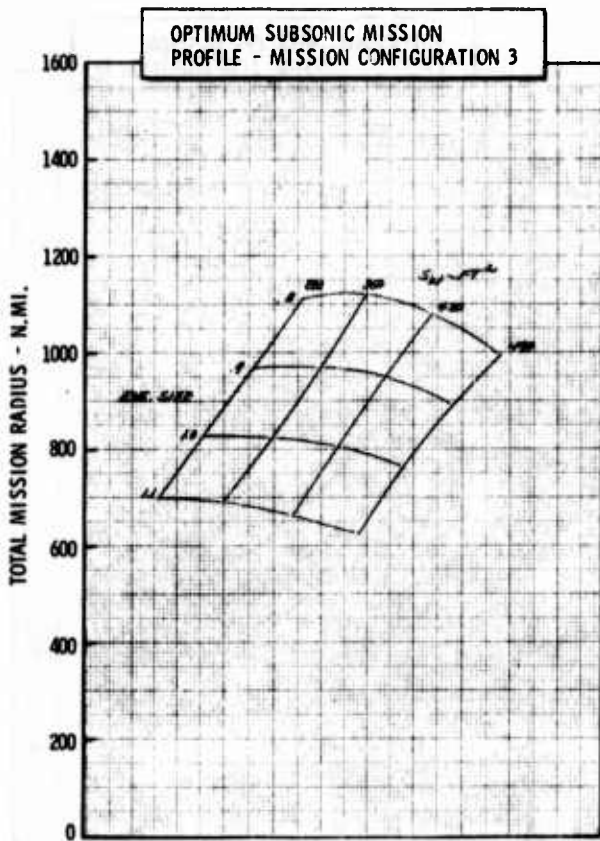
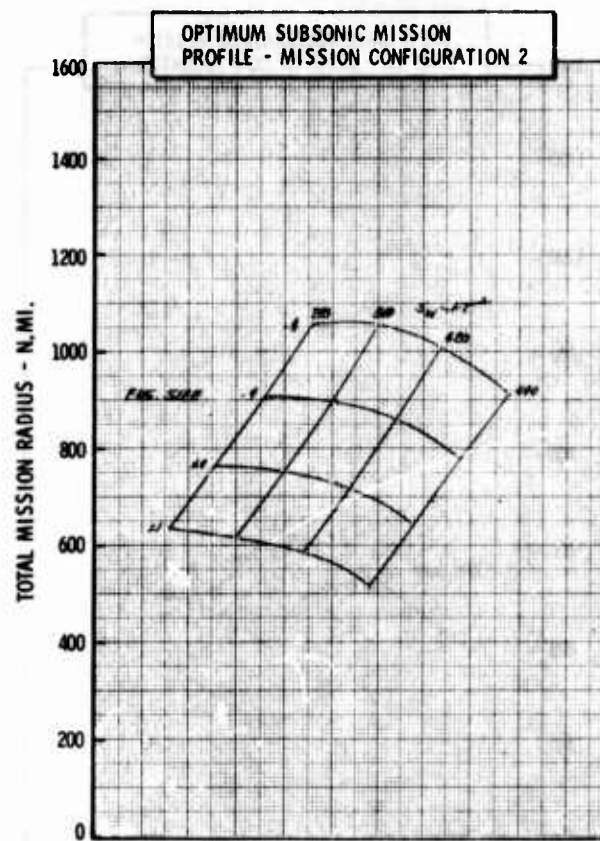
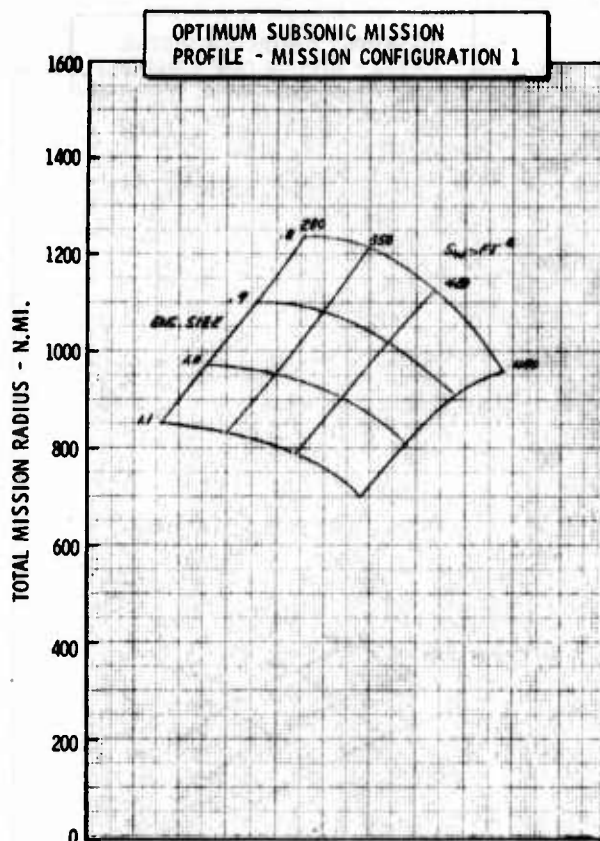


Figure H-43a LWA Mission/Configuration Tradeoff Parametric Data



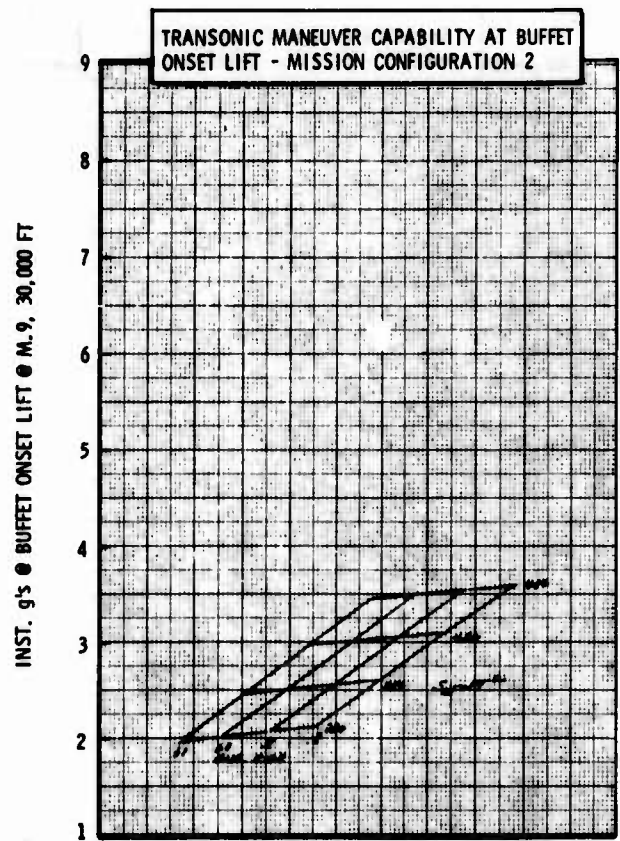
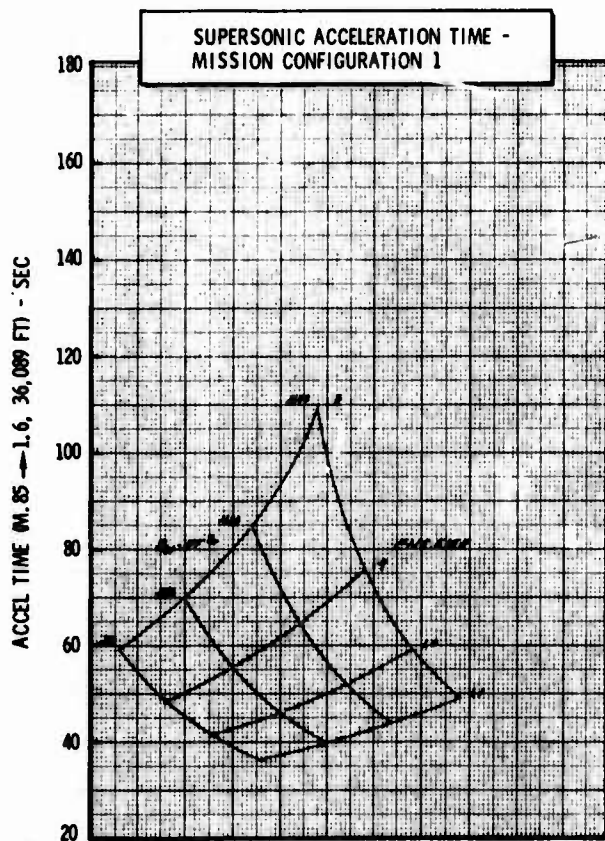
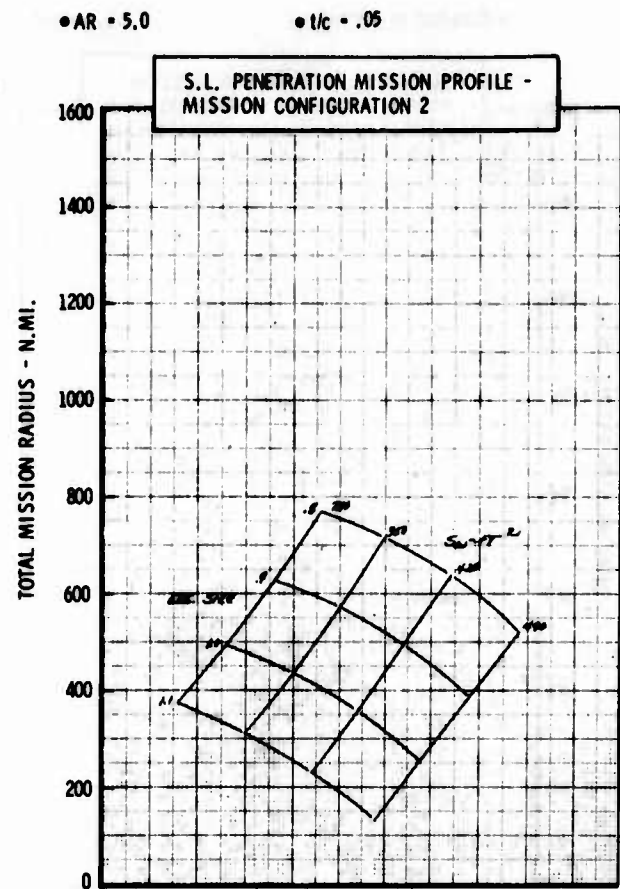
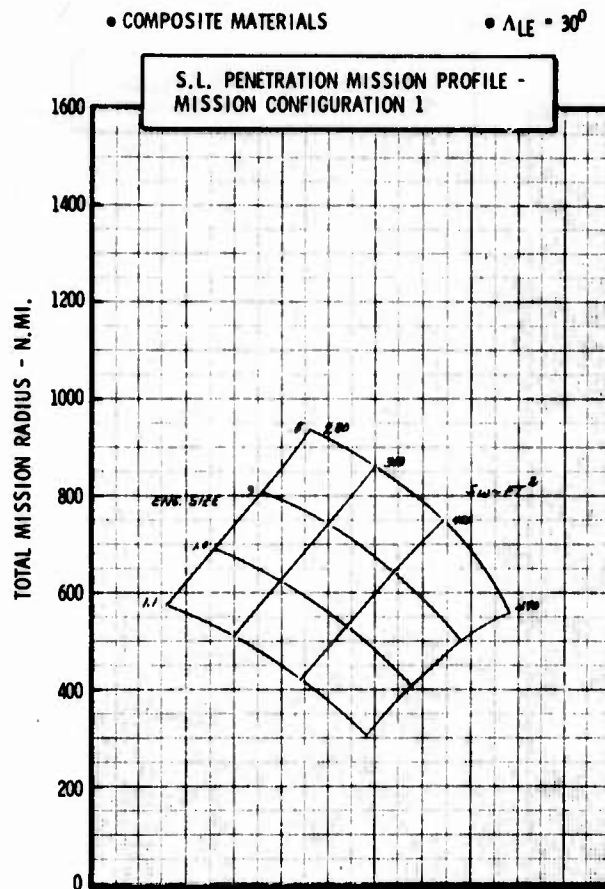


Figure H-43b LWA Mission/Configuration Tradeoff Parametric Data

• COMPOSITE MATERIALS

•  $\Lambda_{LE} = 30^\circ$

•  $AR = 5.0$

•  $1/c = .05$

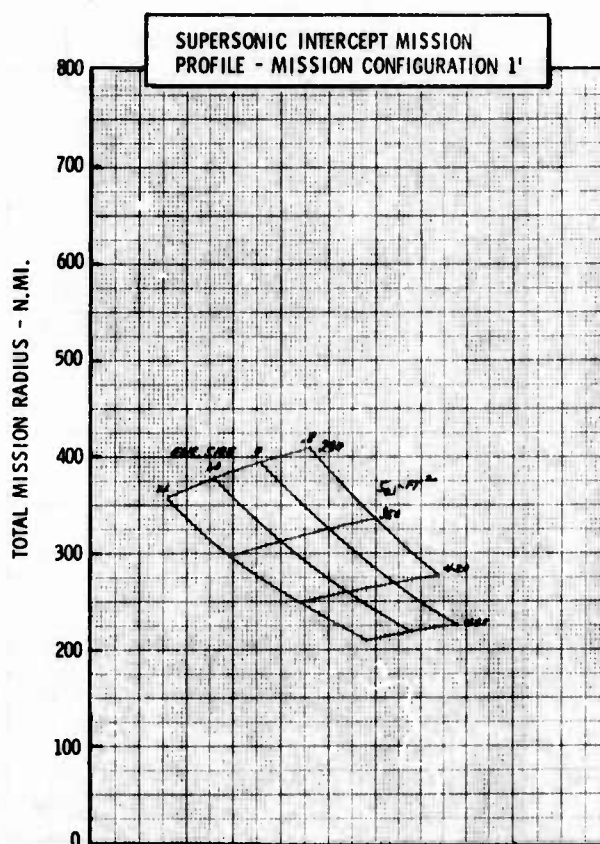
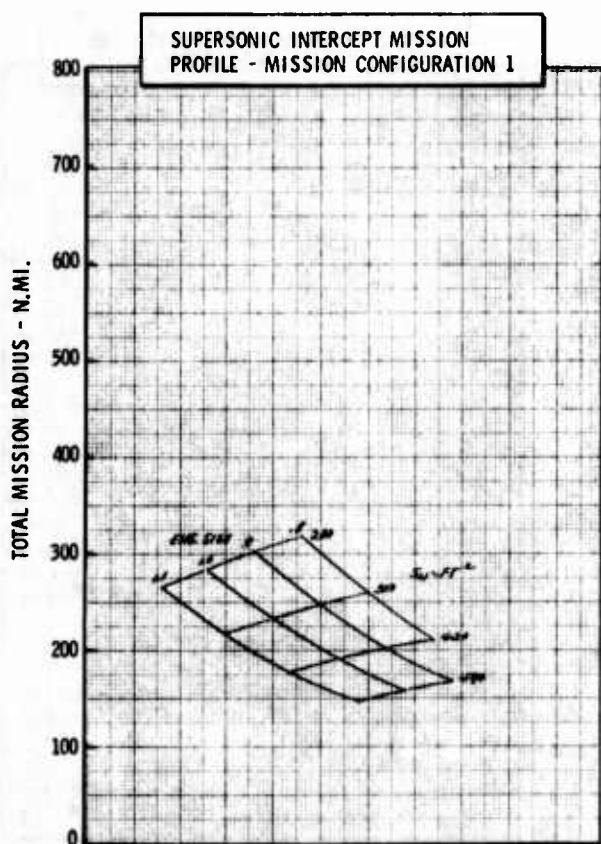
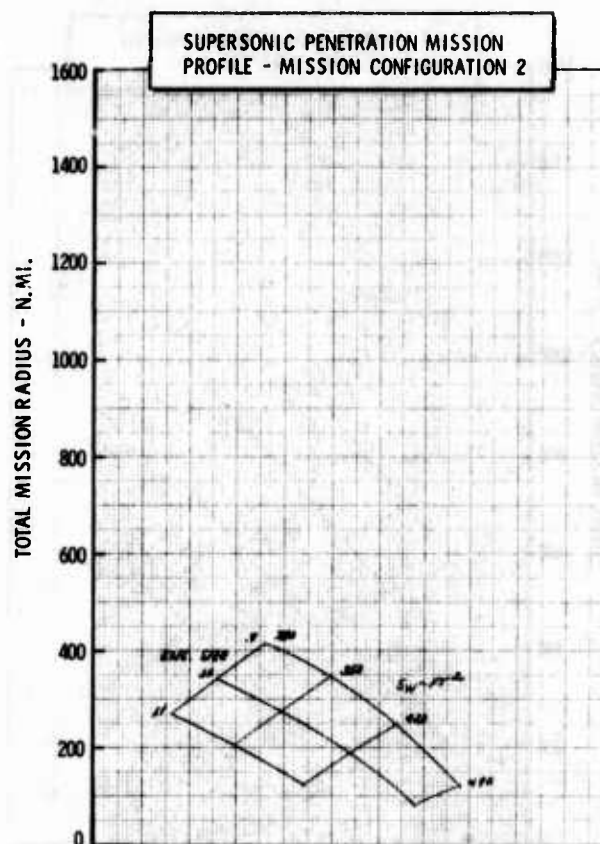
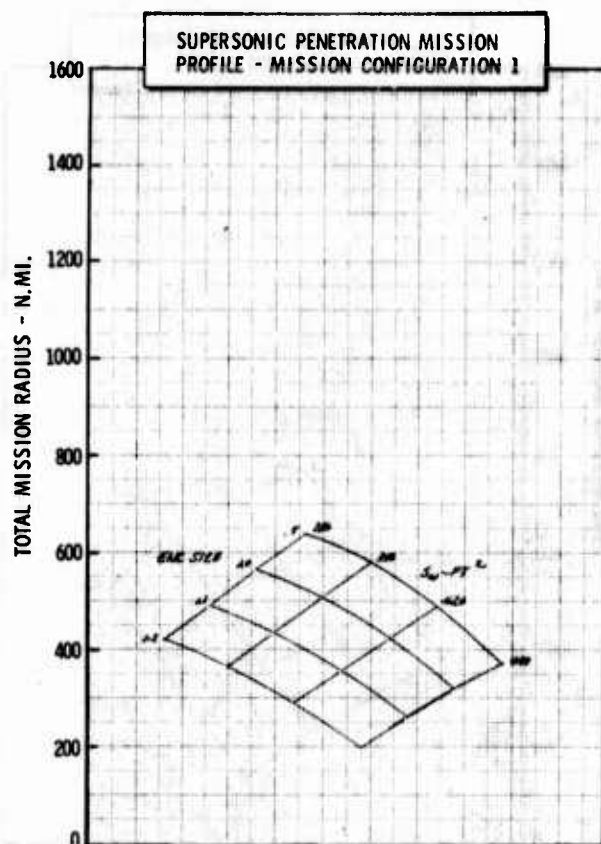


Figure H-43c LWA Mission/Configuration Tradeoff Parametric Data

• COMPOSITE MATERIALS

•  $\Lambda_{LE} = 40^\circ$

•  $AR = 3.0$

•  $t/c = .05$

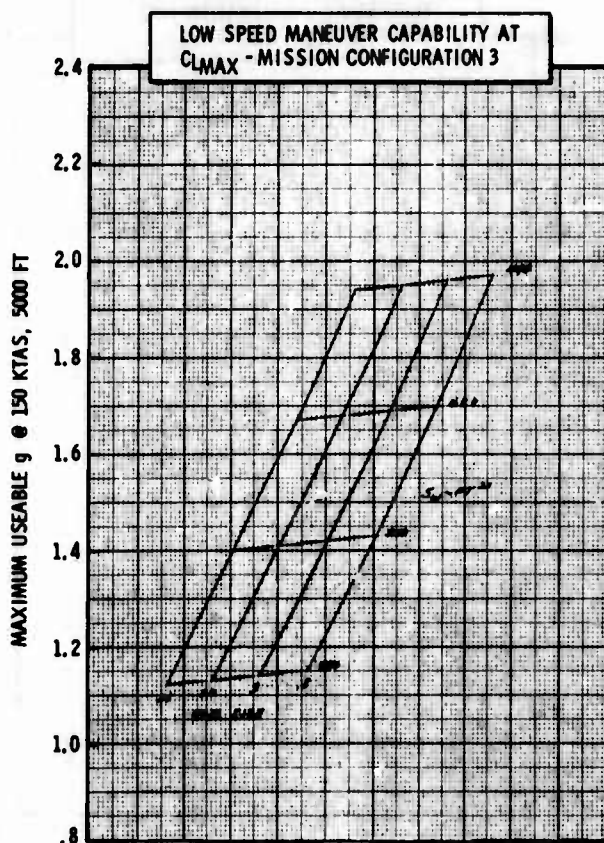
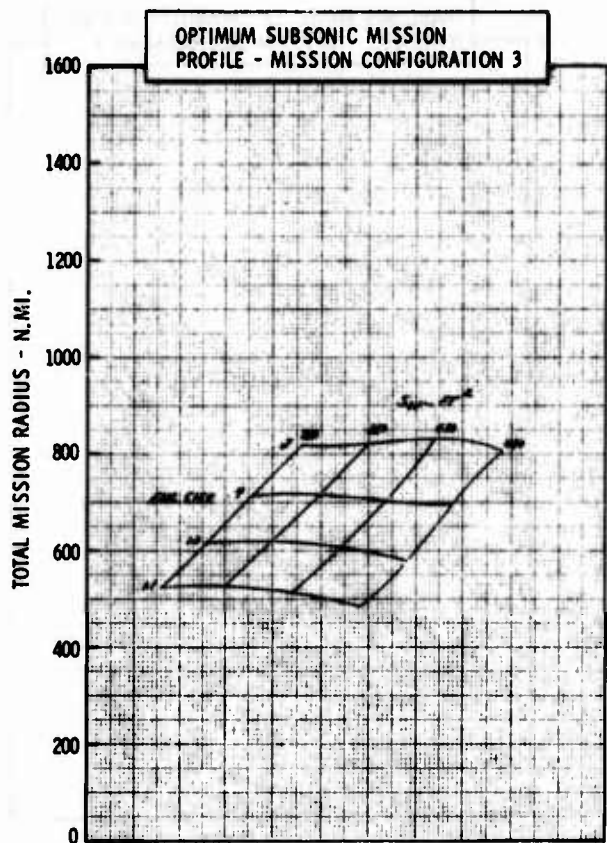
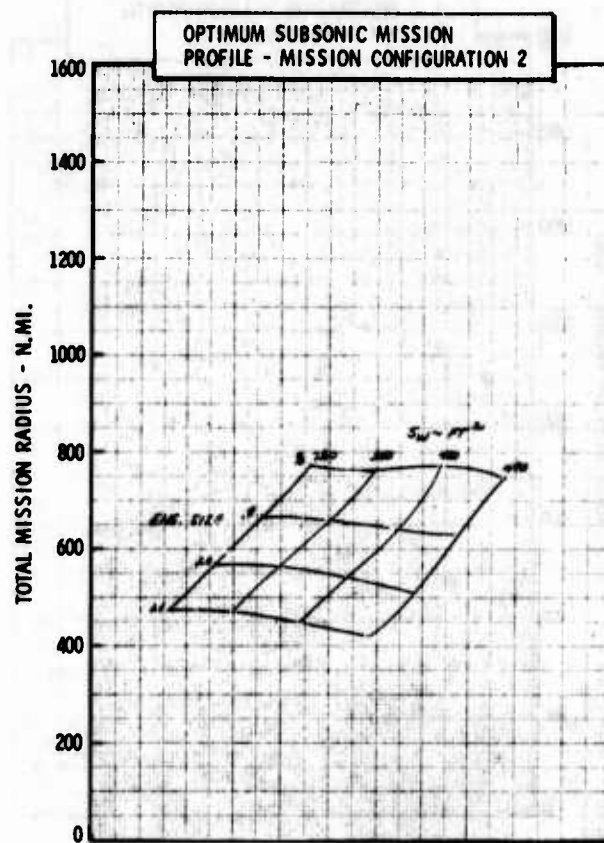
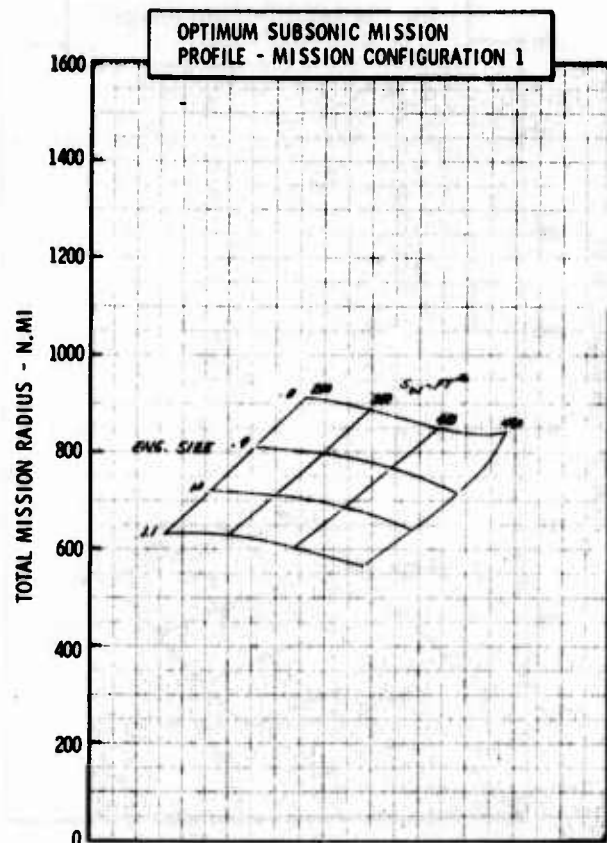


Figure H-44a LWA Mission/Configuration Tradeoff Parametric Data

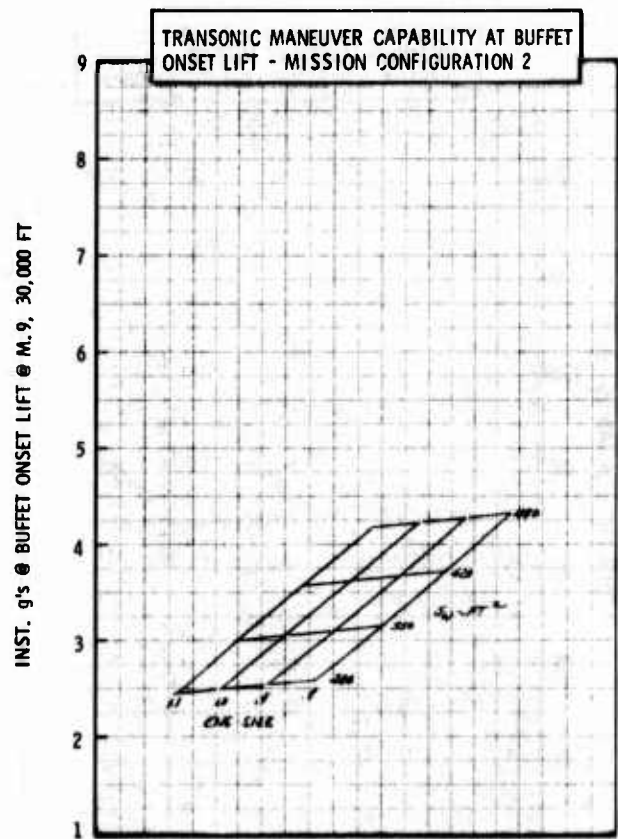
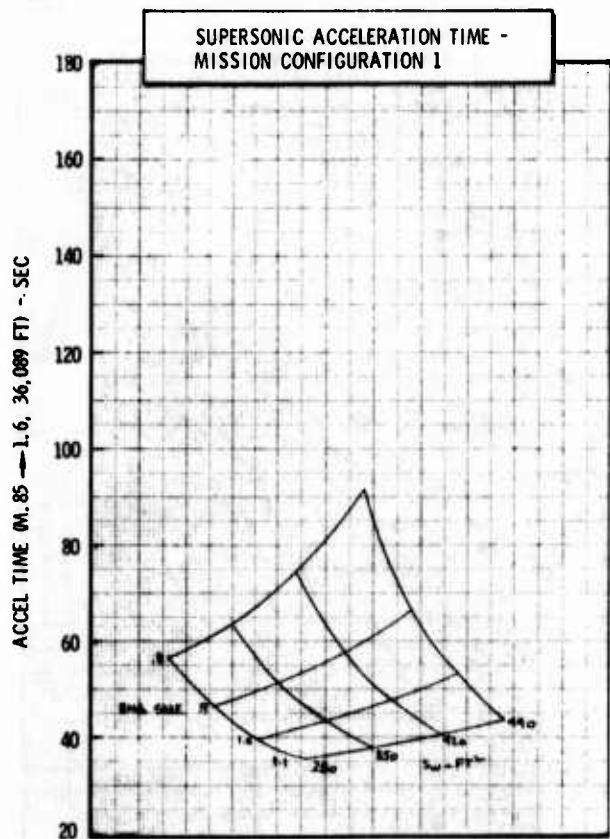
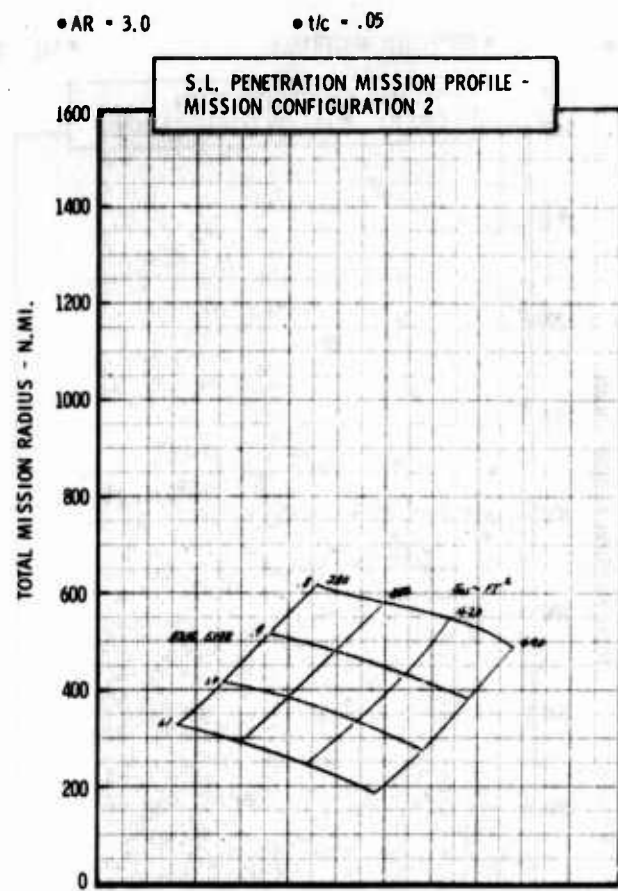
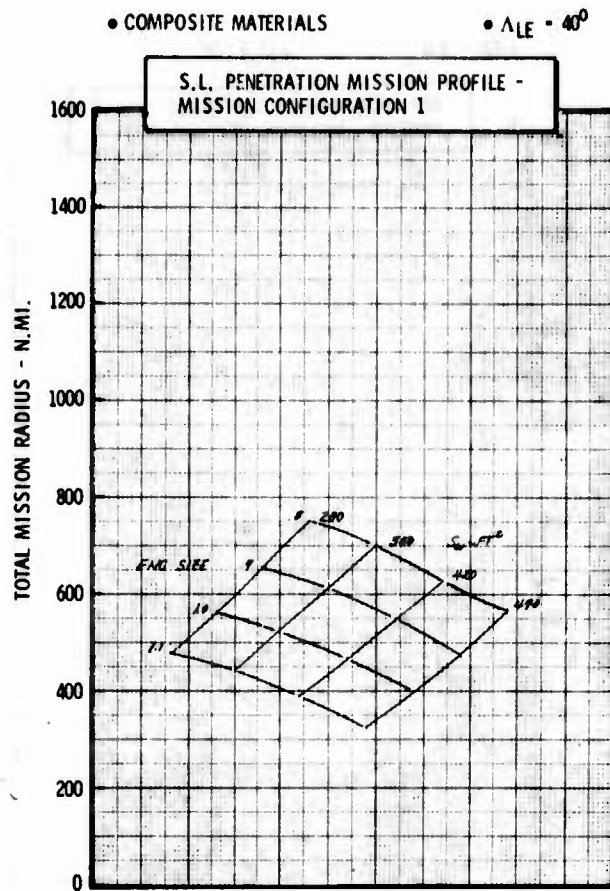


Figure H-44b LWA Mission/Configuration Tradeoff Parametric Data



• COMPOSITE MATERIALS

•  $\Lambda_{LE} = 40^\circ$

•  $AR = 3.0$

•  $t/c = .05$

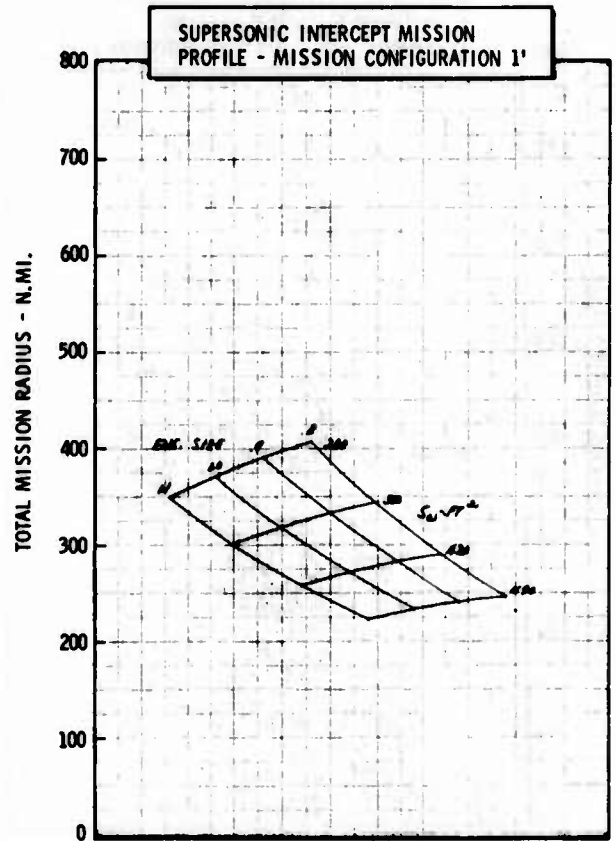
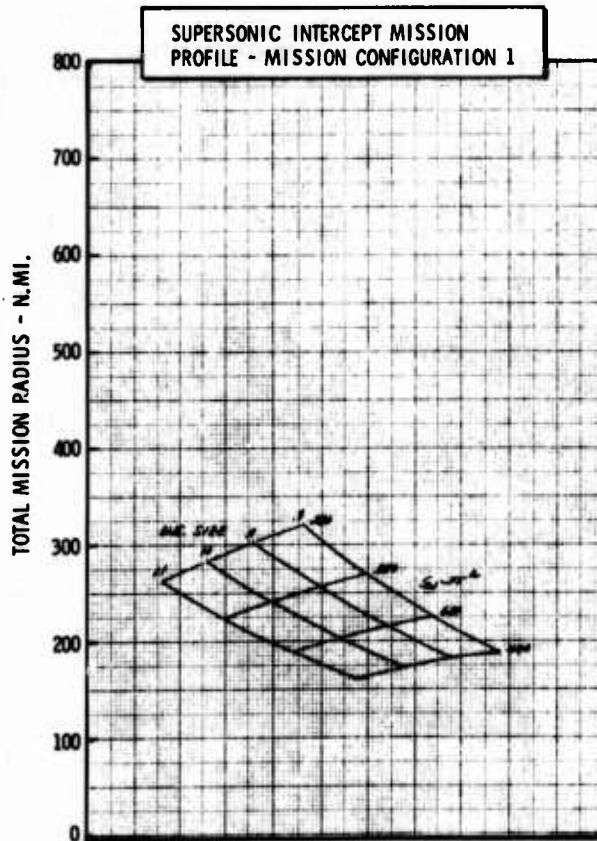
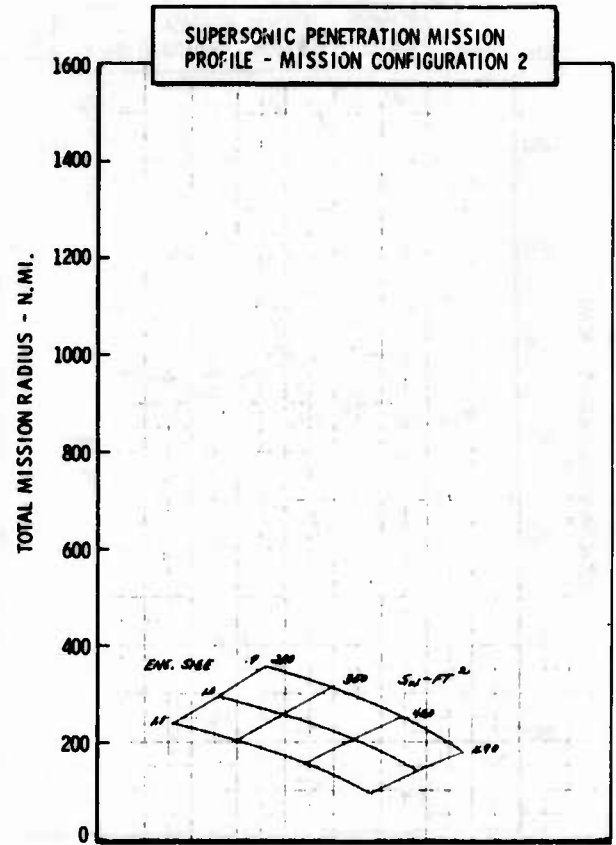
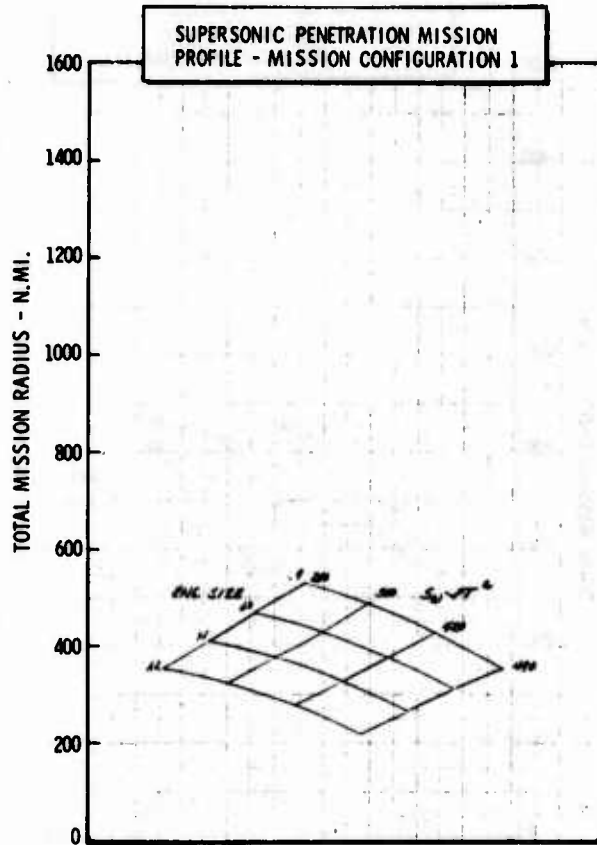


Figure H-44c LWA Mission/Configuration Tradeoff Parametric Data



• COMPOSITE MATERIALS

•  $\Delta LE = 40^\circ$

•  $AR = 4.0$

•  $t/c = .05$

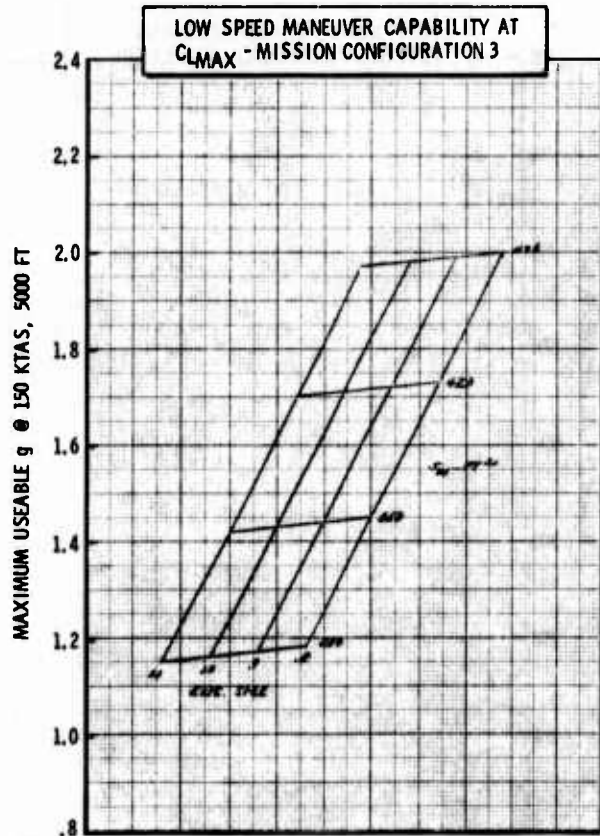
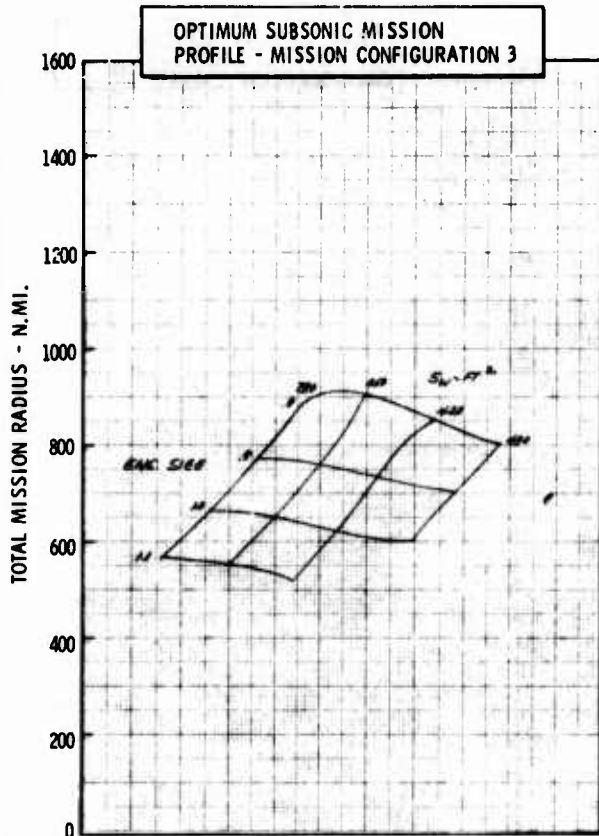
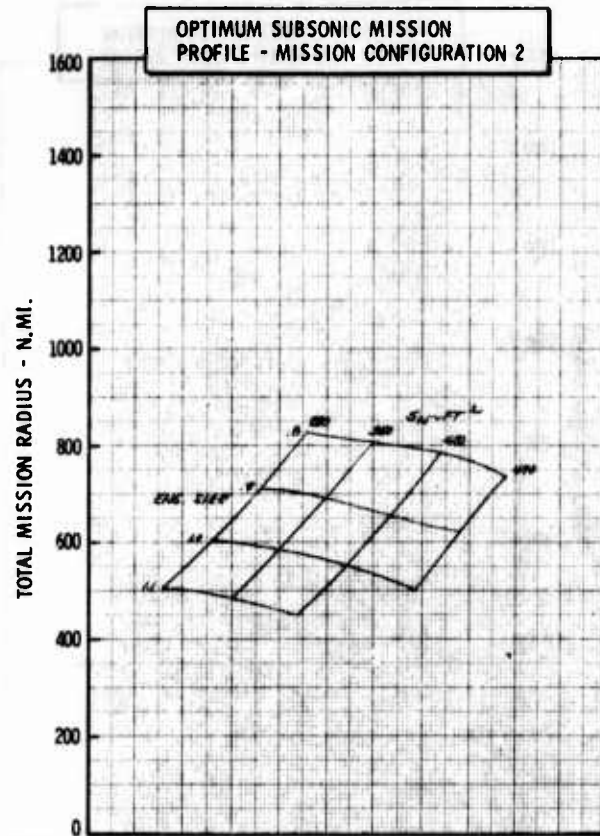
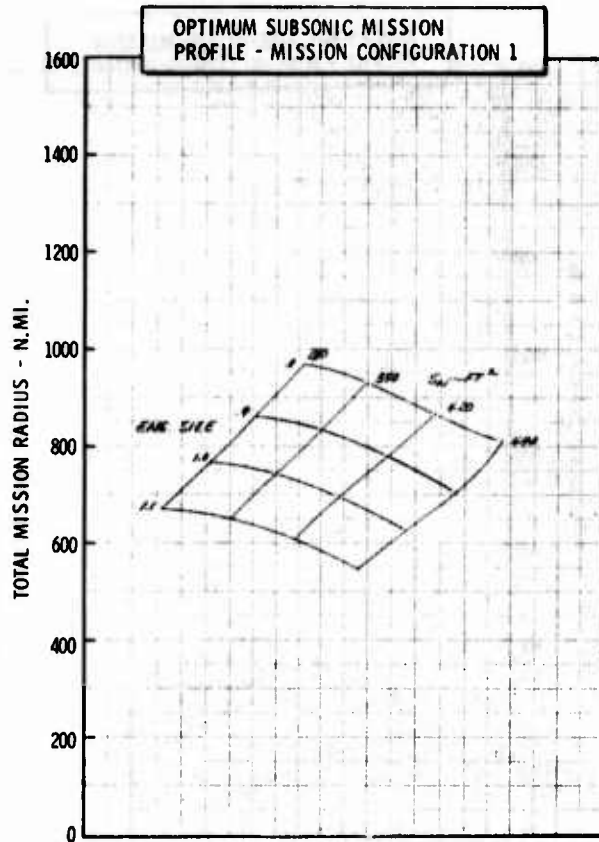
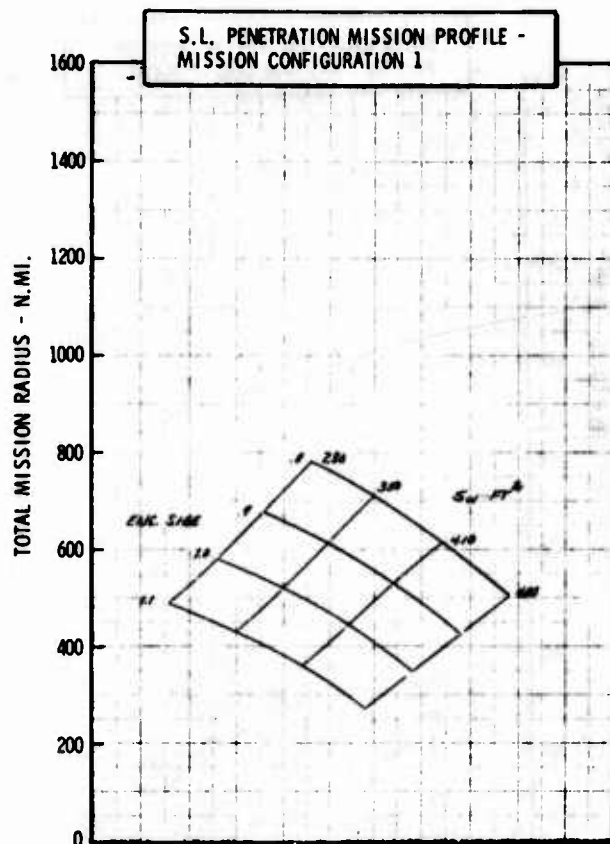


Figure H-45a LWA Mission/Configuration Tradeoff Parametric Data

• COMPOSITE MATERIALS

•  $\Delta LE = 40^\circ$



•  $AR = 4.0$

•  $t/c = .05$

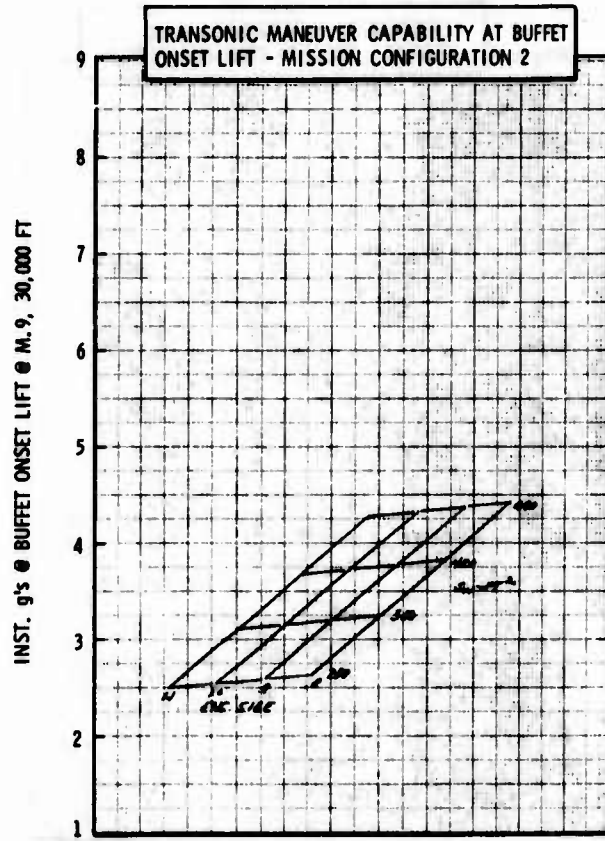
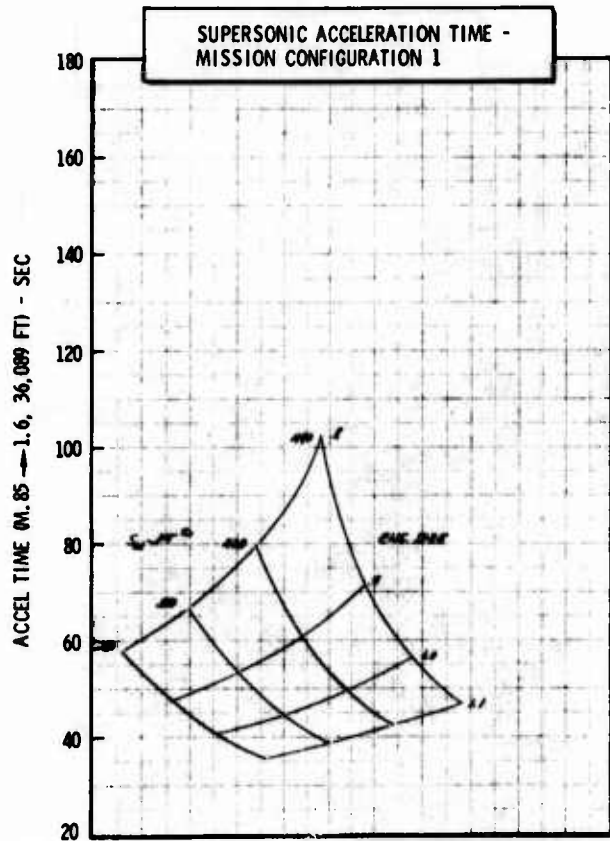
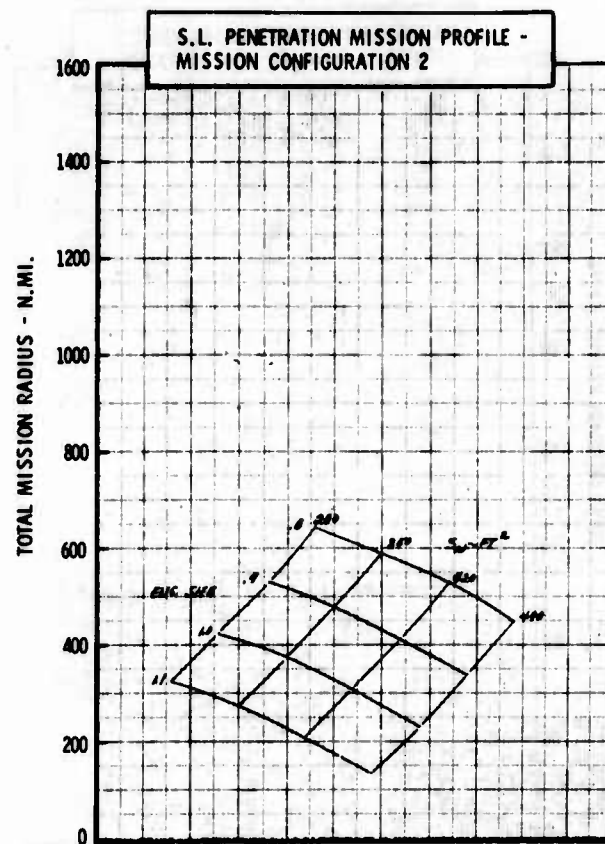
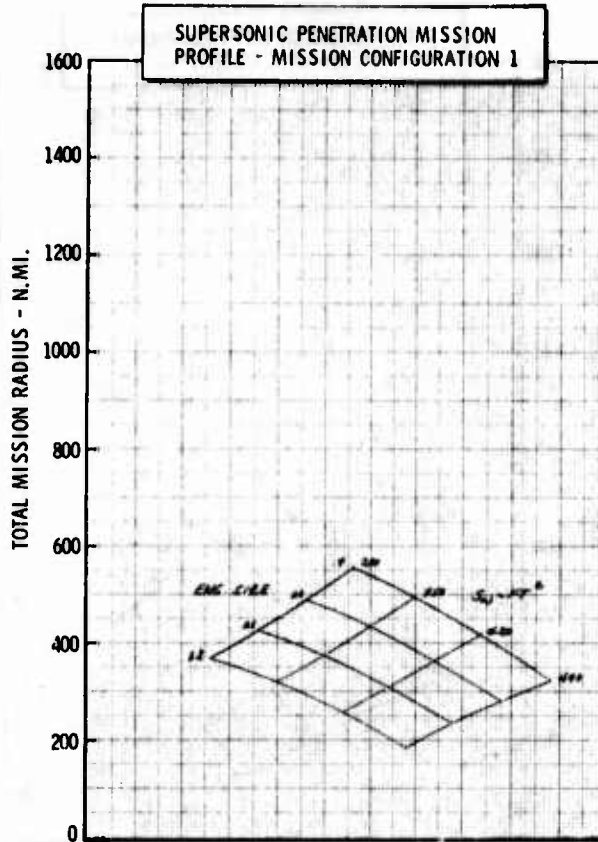


Figure H-45b LWA Mission/Configuration Tradeoff Parametric Data

• COMPOSITE MATERIALS

•  $\Delta LE = 40^\circ$



•  $AR = 4.0$

•  $t/c = .05$

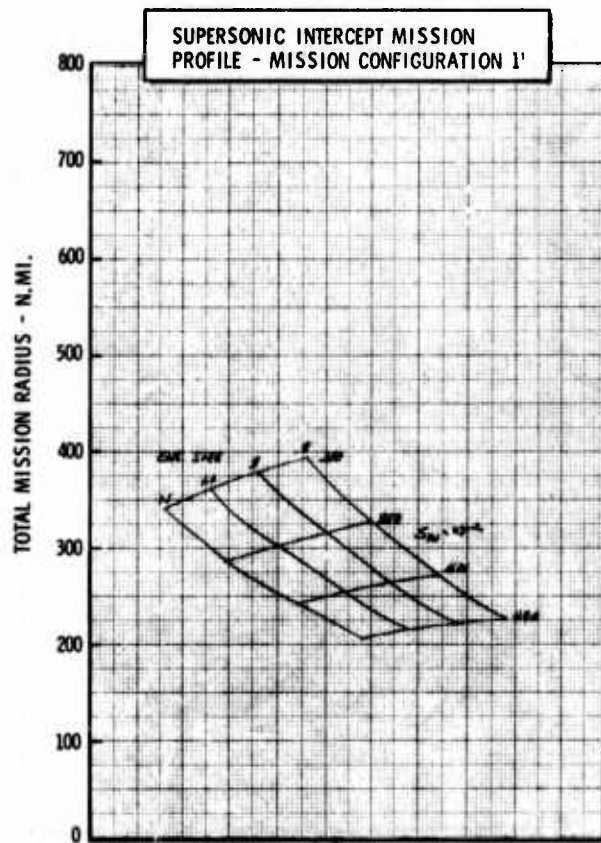
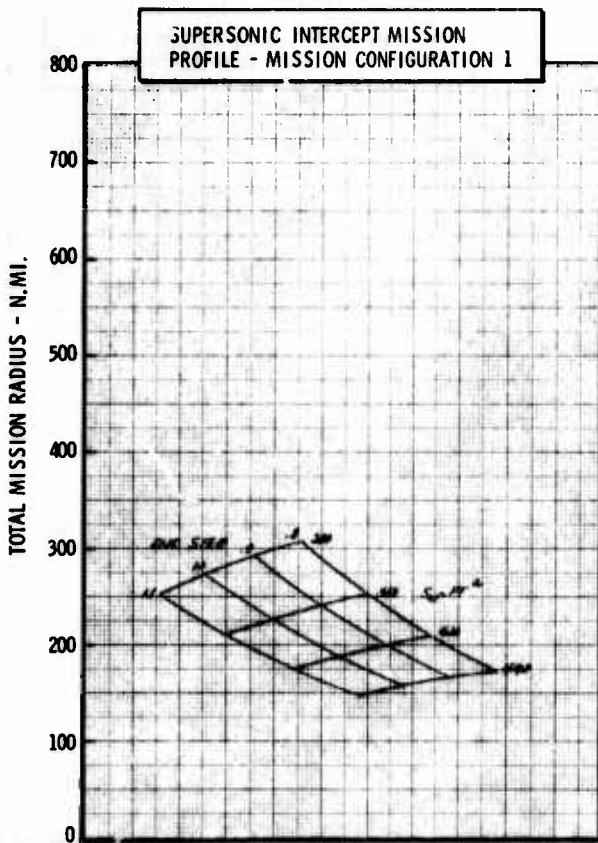
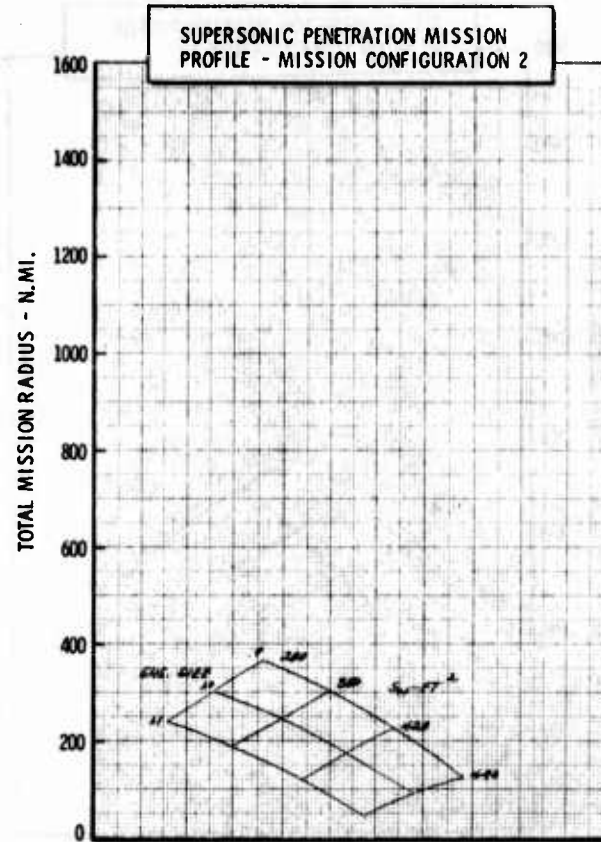


Figure it-45c LWA Mission/Configuration Tradeoff Parametric Data

• COMPOSITE MATERIALS

•  $\Delta LE = 40^\circ$

•  $AR = 5.0$

•  $t/c = .05$

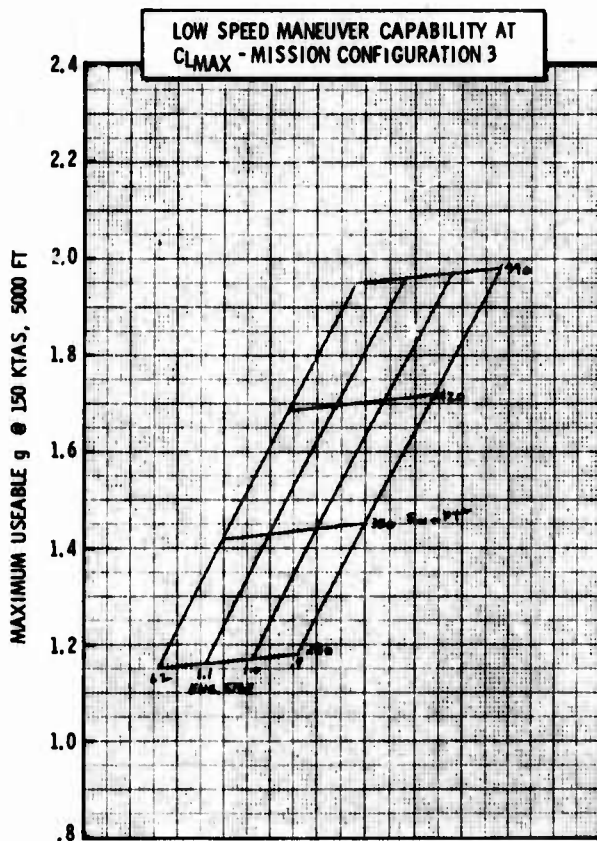
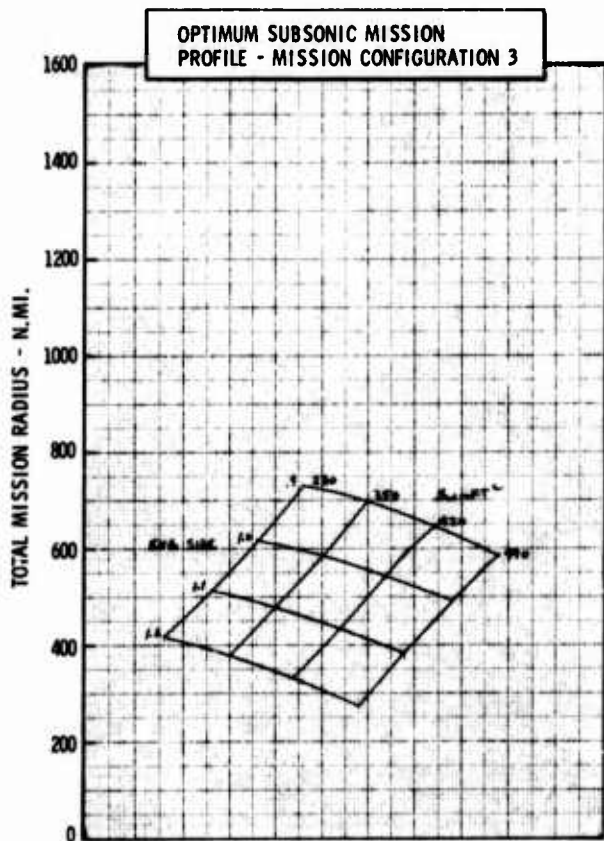
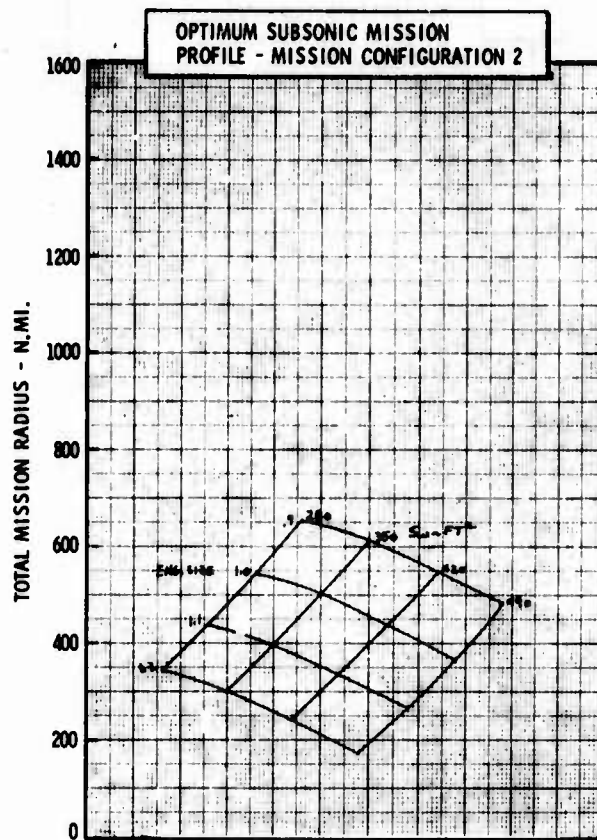
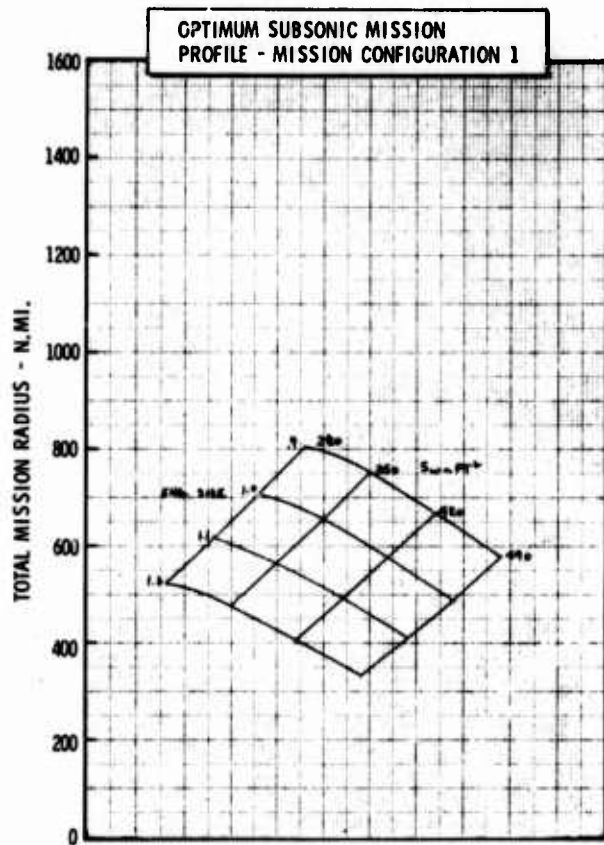


Figure H-46a LWA Mission/Configuration Tradeoff Parametric Data



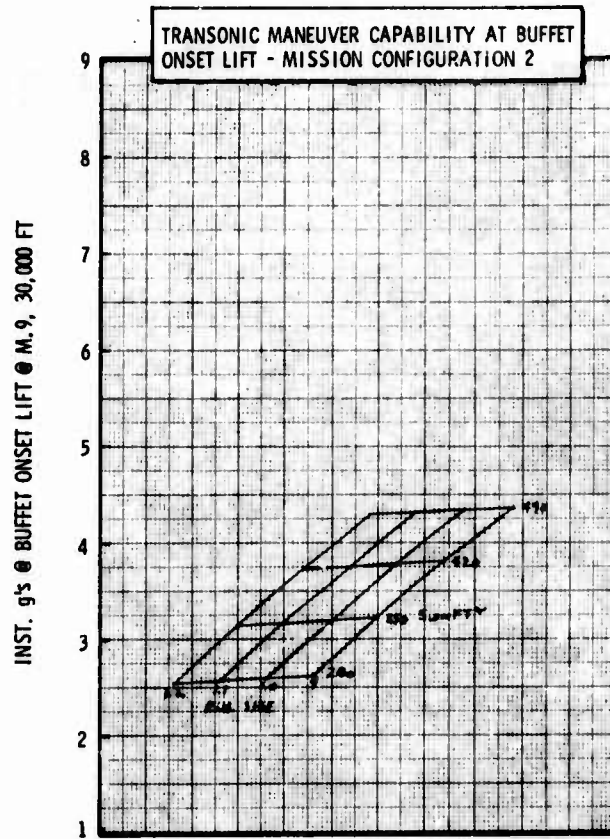
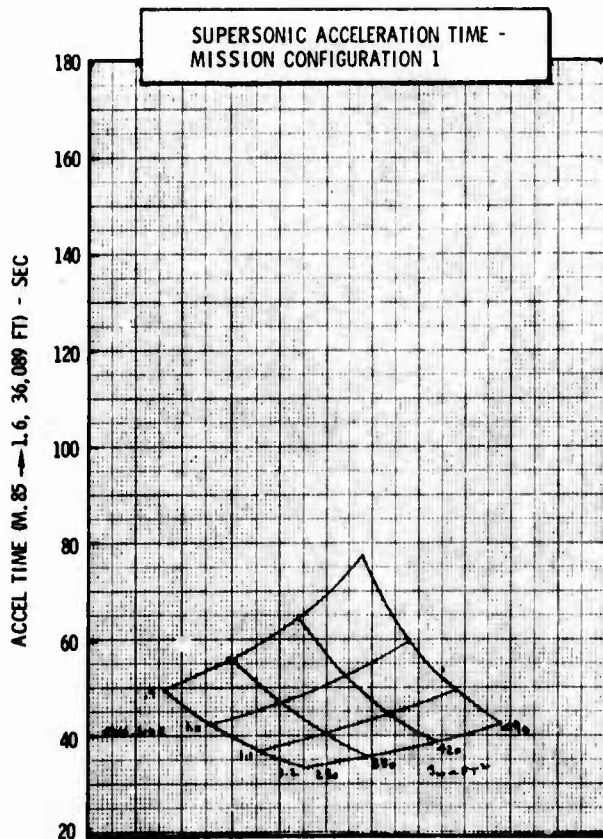
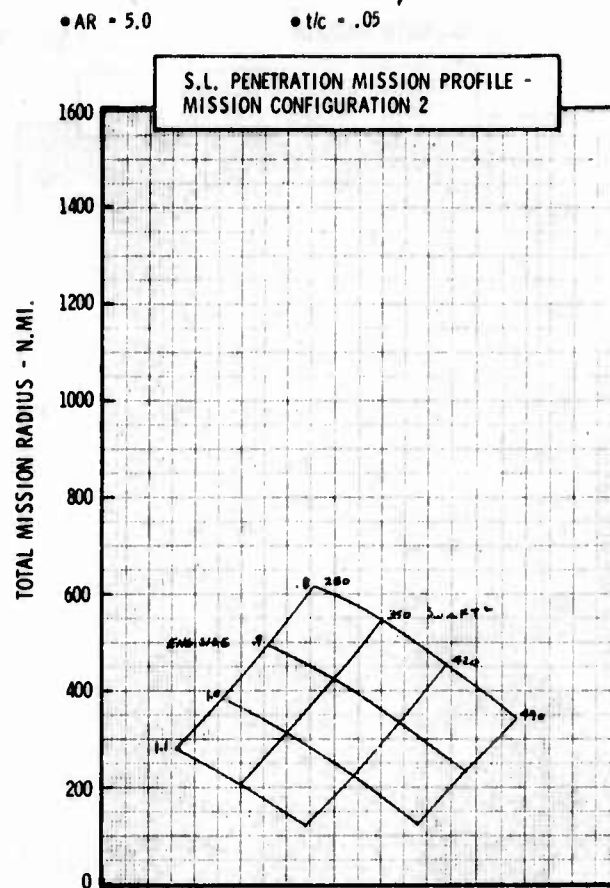
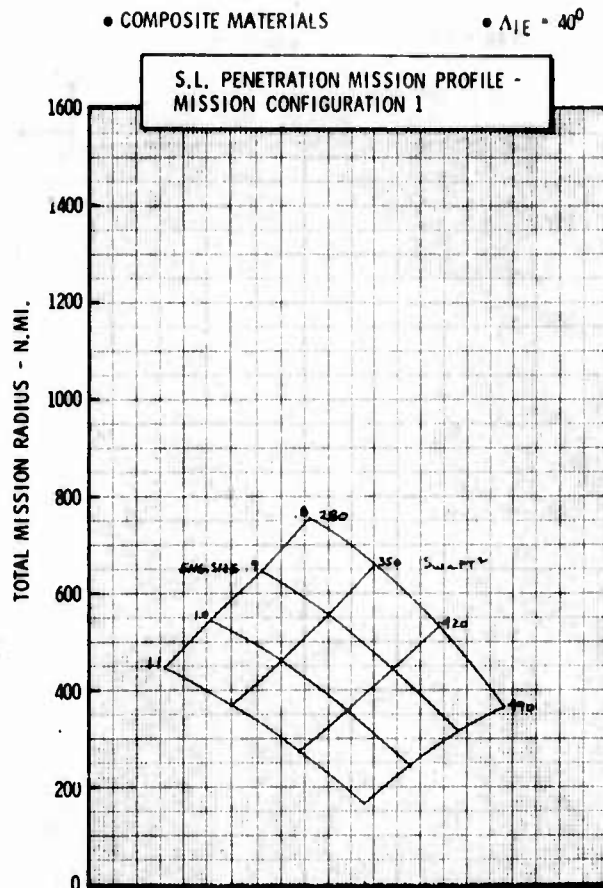


Figure H-46b LWA Mission/Configuration Tradeoff Parametric Data



•  $\Lambda_{LE} = 40^\circ$

• t/c = .05

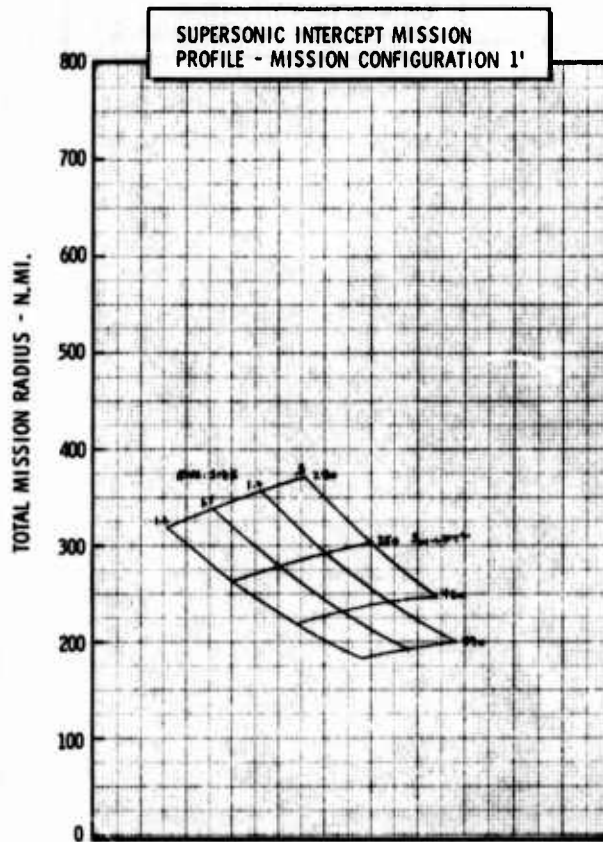
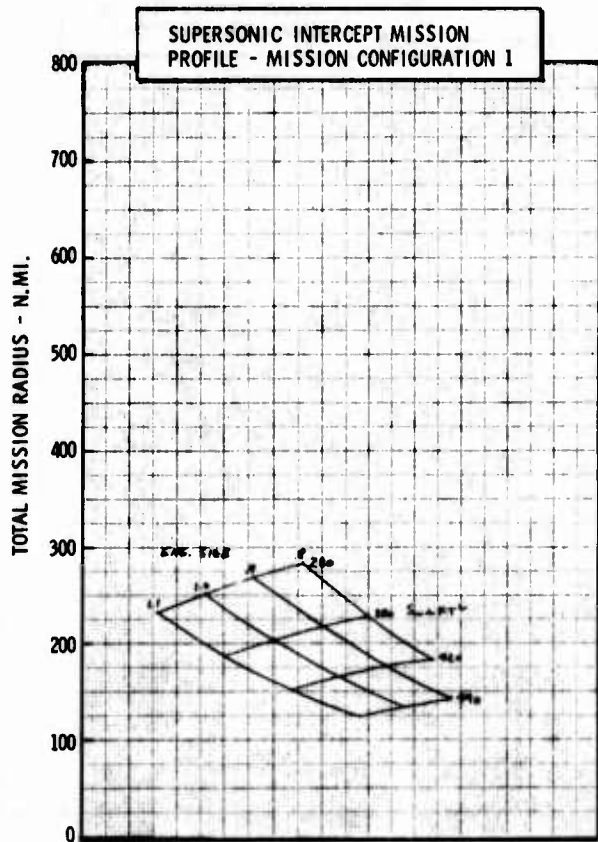
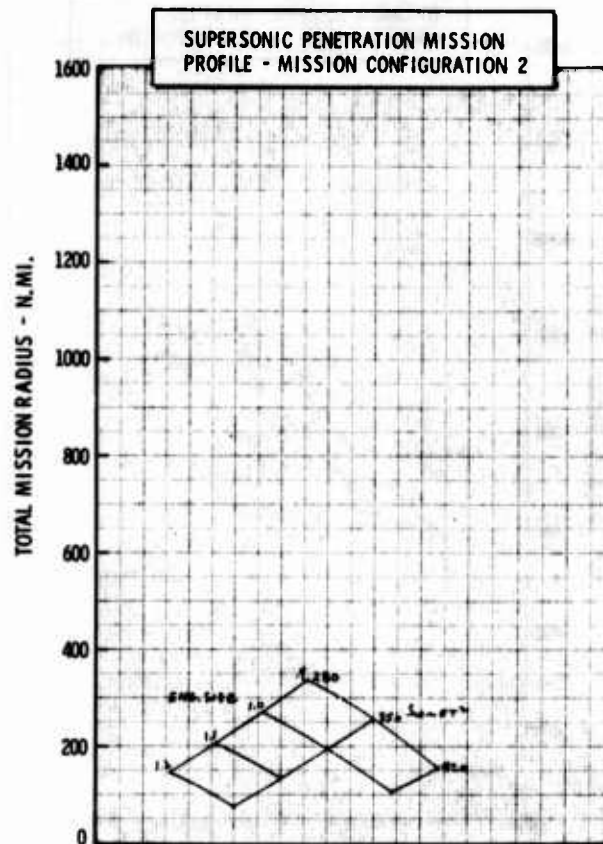
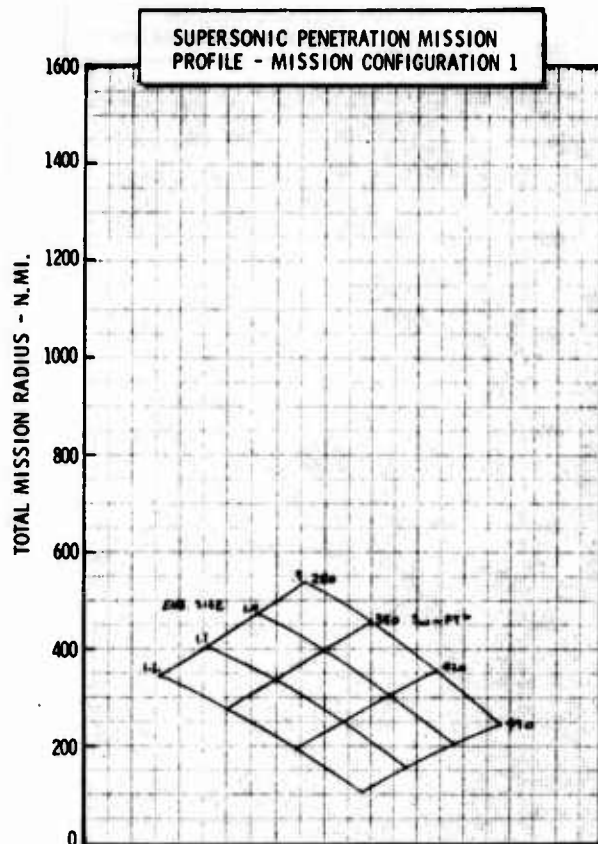


Figure H-46c LWA Mission/Configuration Tradeoff Parametric Data

• COMPOSITE MATERIALS

•  $\Delta LE = 20^\circ$

•  $AR = 3.0$

•  $t/c = .06$

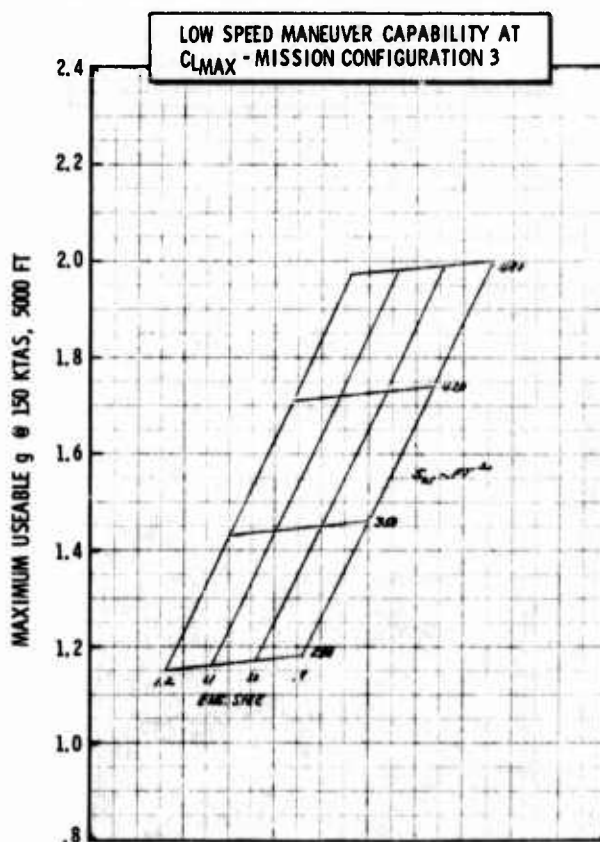
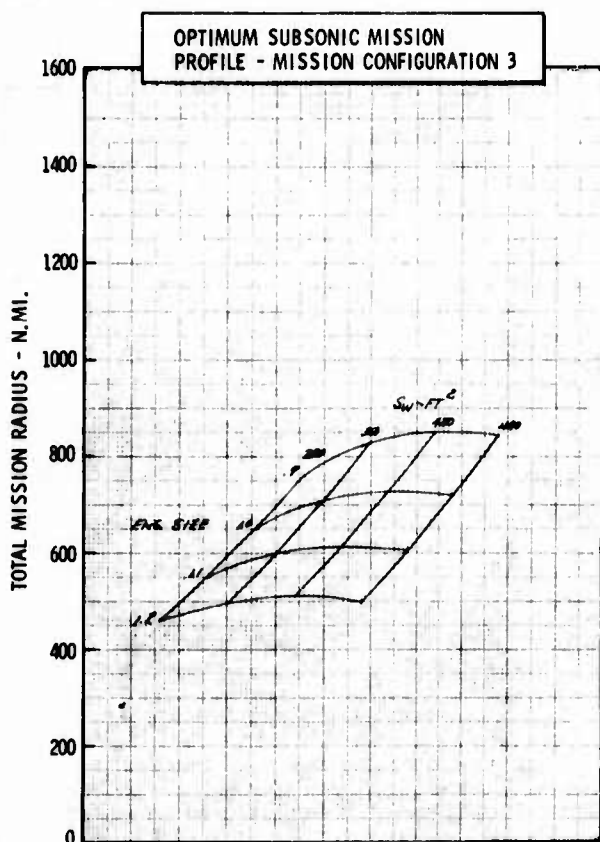
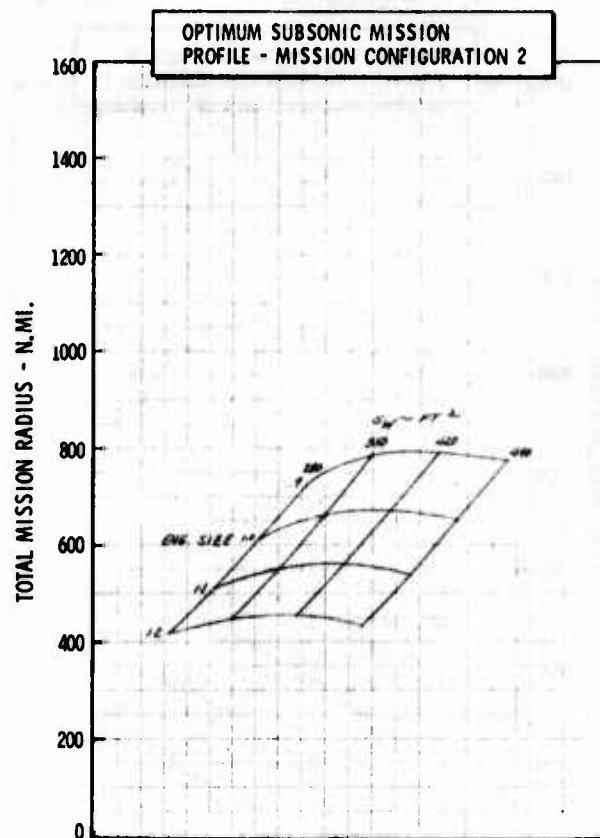
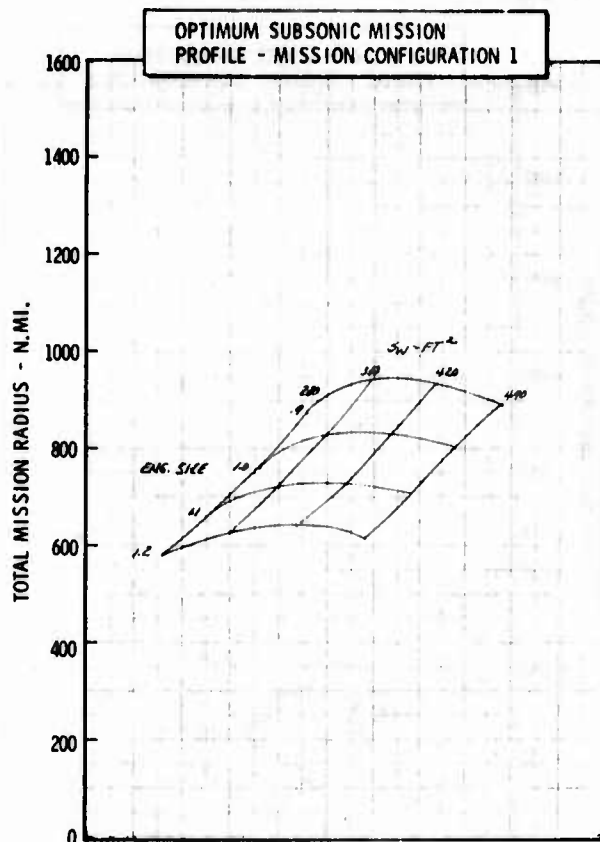


Figure H-47a LWA Mission/Configuration Tradeoff Parametric Data

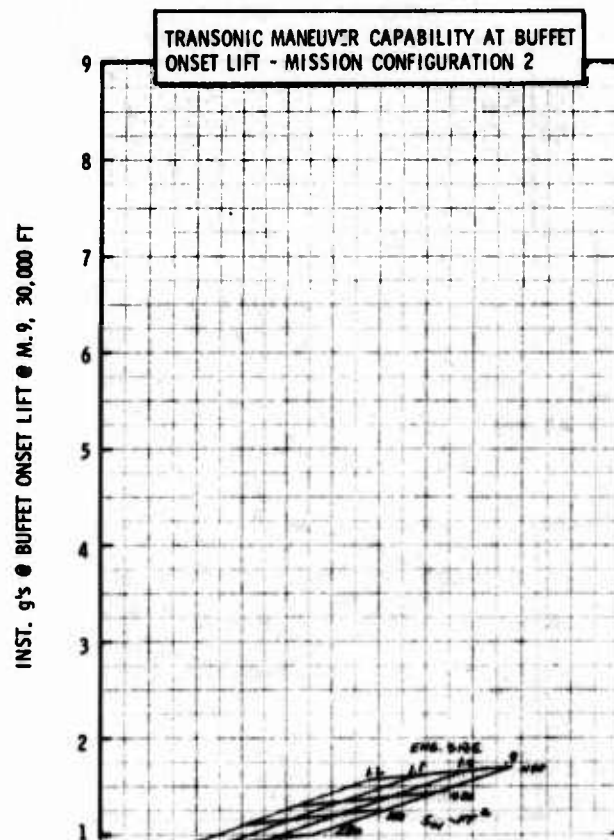
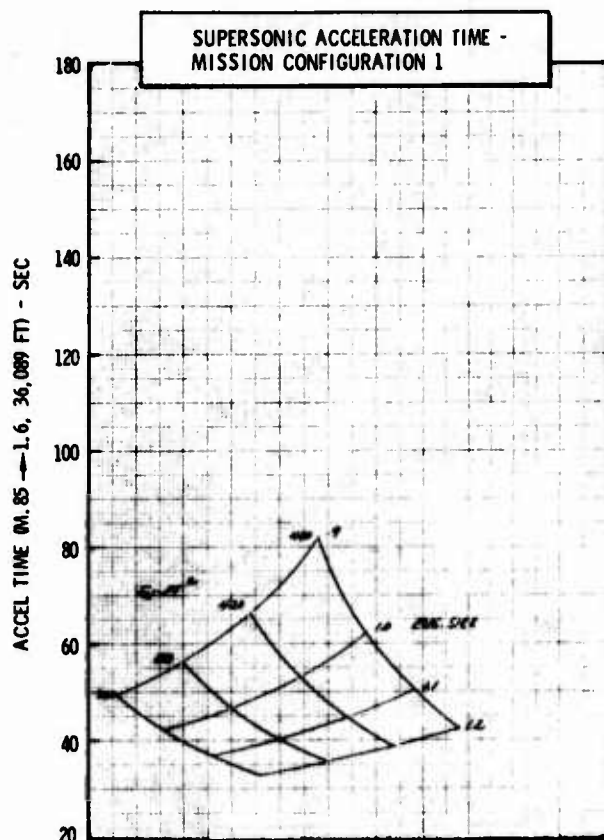
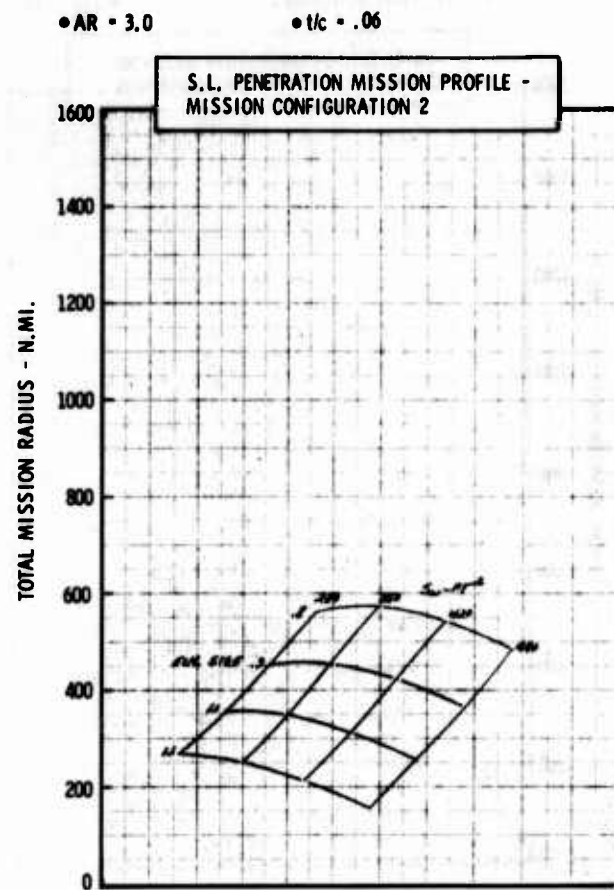
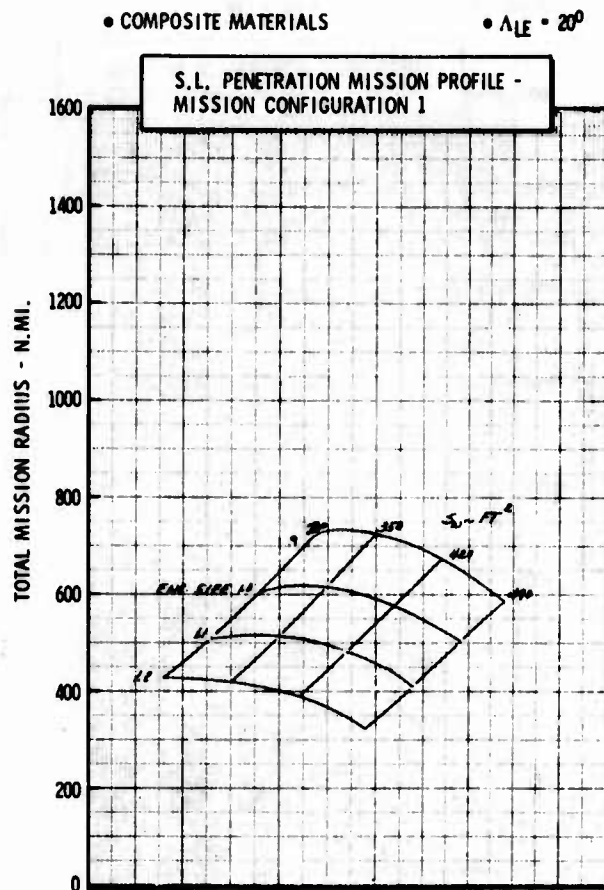


Figure H-47b LWA Mission/Configuration Tradeoff Parametric Data

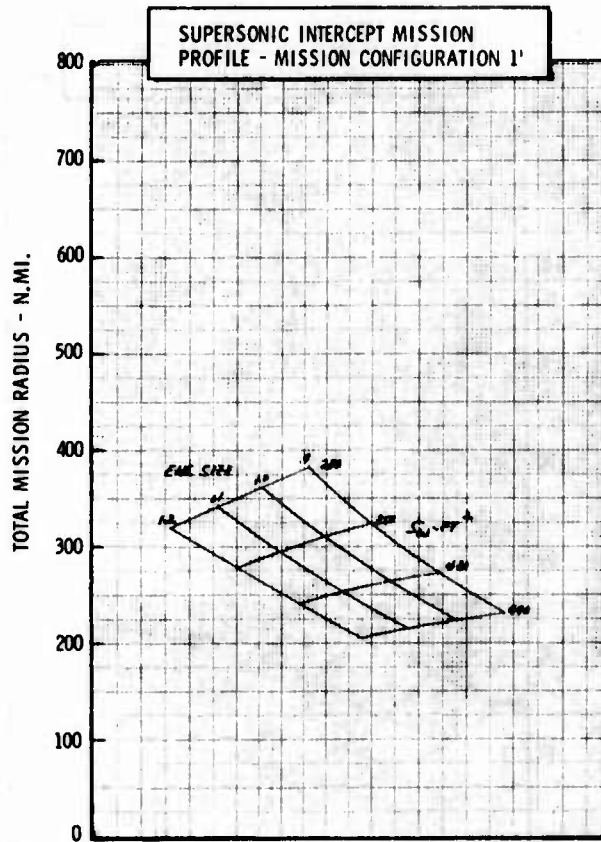
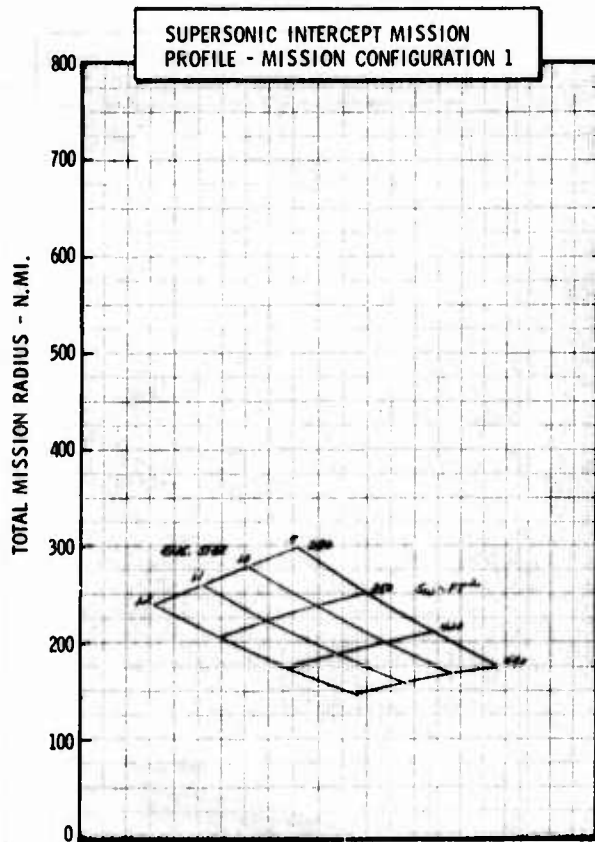
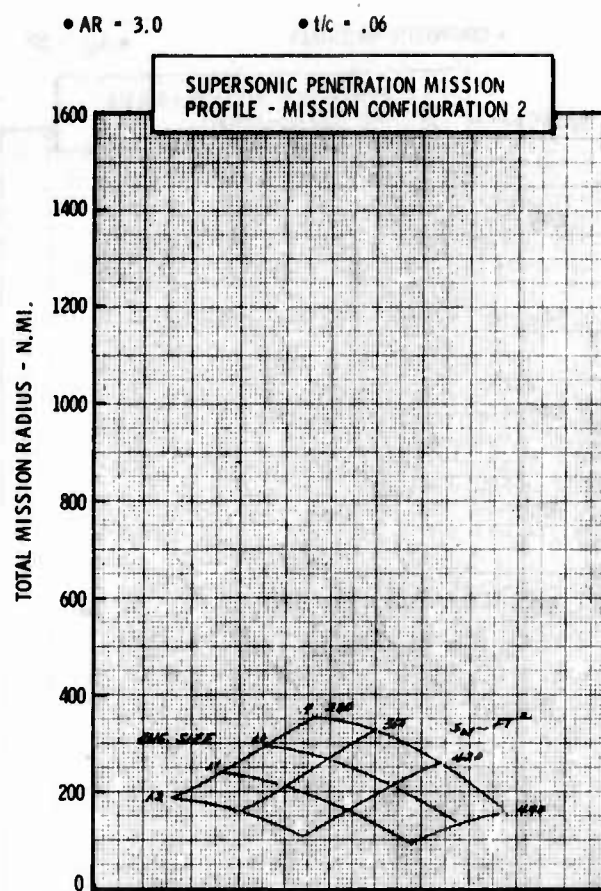
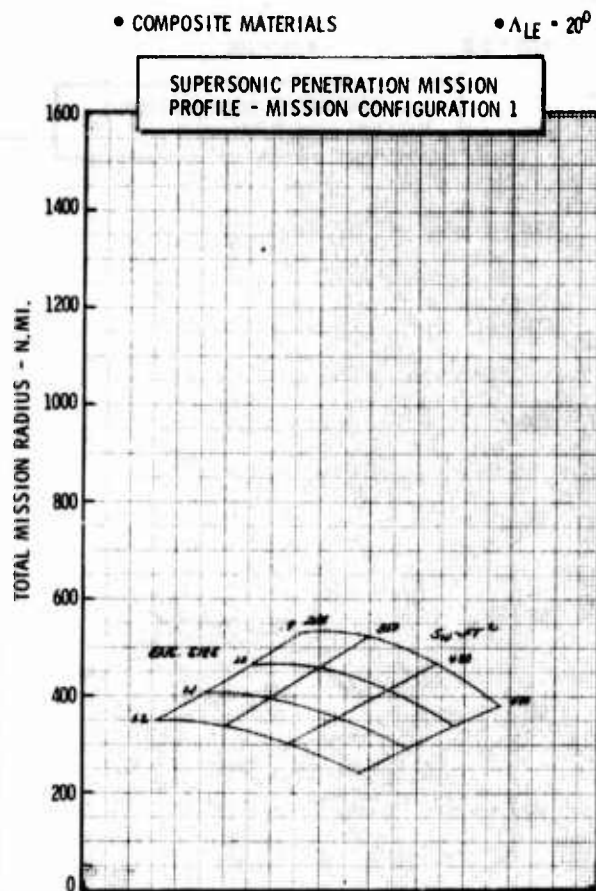


Figure H-47c LWA Mission/Configuration Tradeoff Parametric Data



• COMPOSITE MATERIALS

•  $\Delta LE = 20^\circ$

•  $AR = 4.0$

•  $t/c = .06$

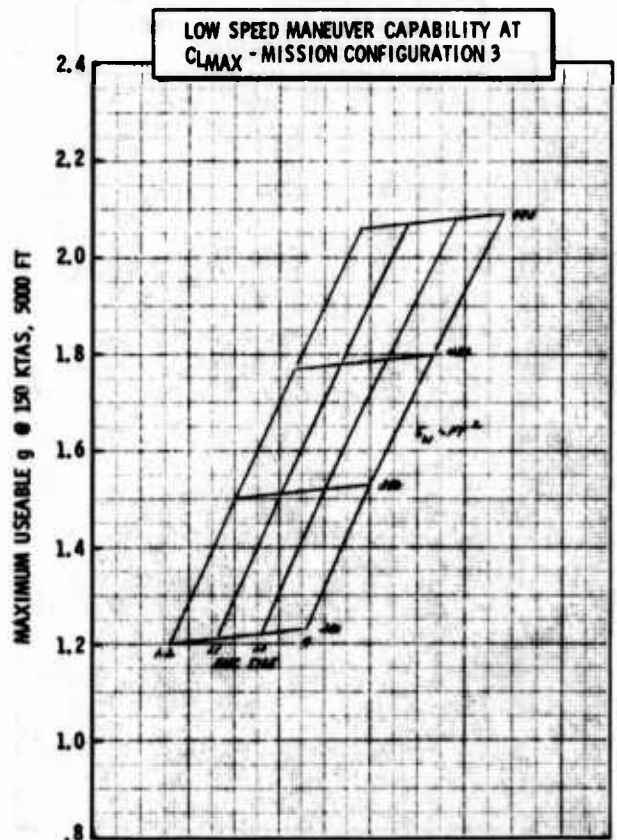
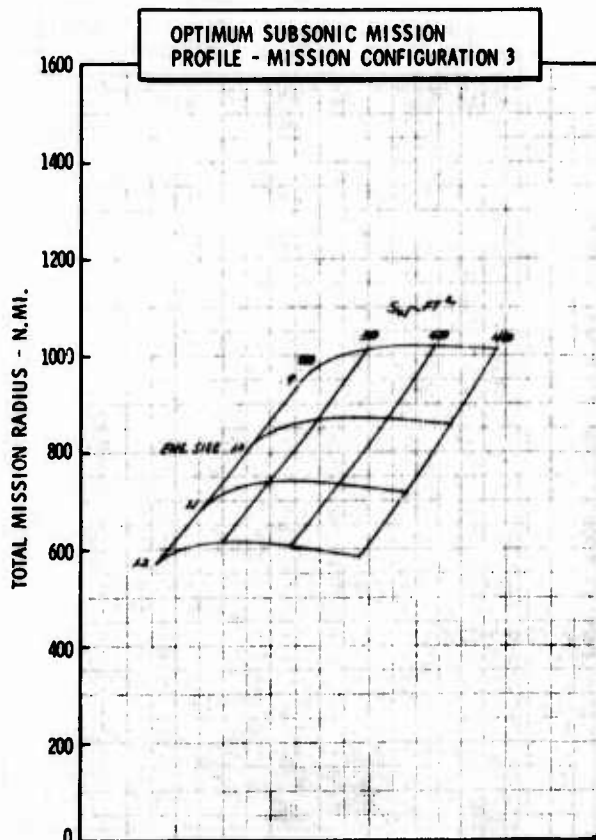
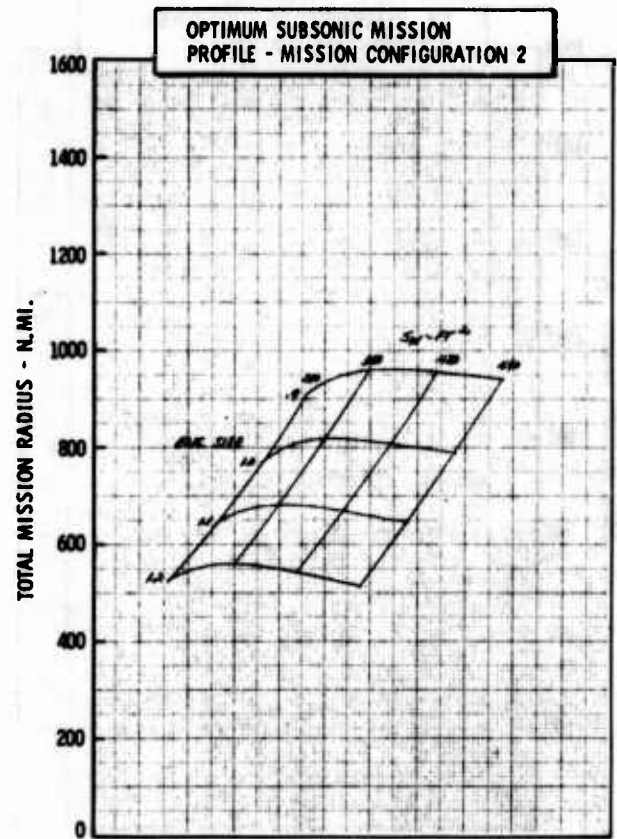
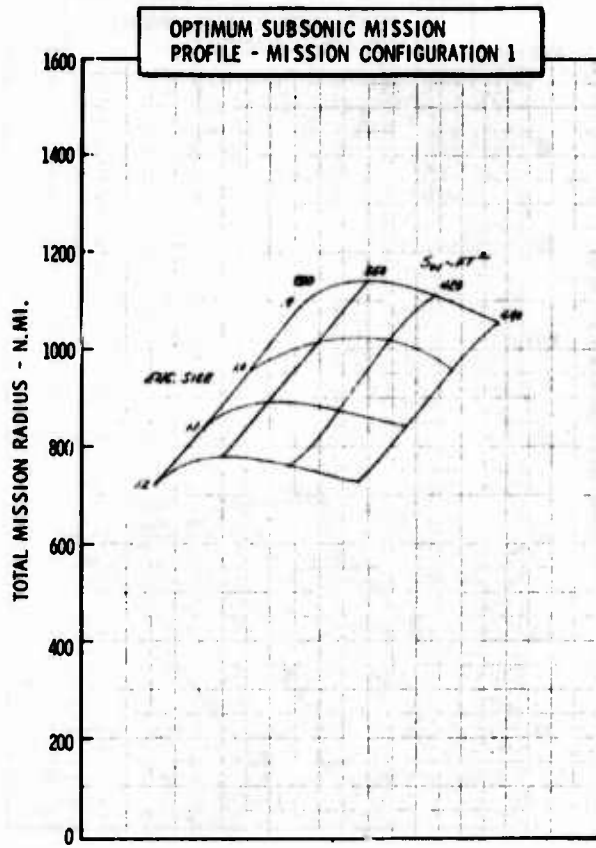


Figure H-48a LWA Mission/Configuration Tradeoff Parametric Data



• COMPOSITE MATERIALS

•  $\Delta LE = 20^\circ$

•  $AR = 4.0$

•  $t/c = .06$

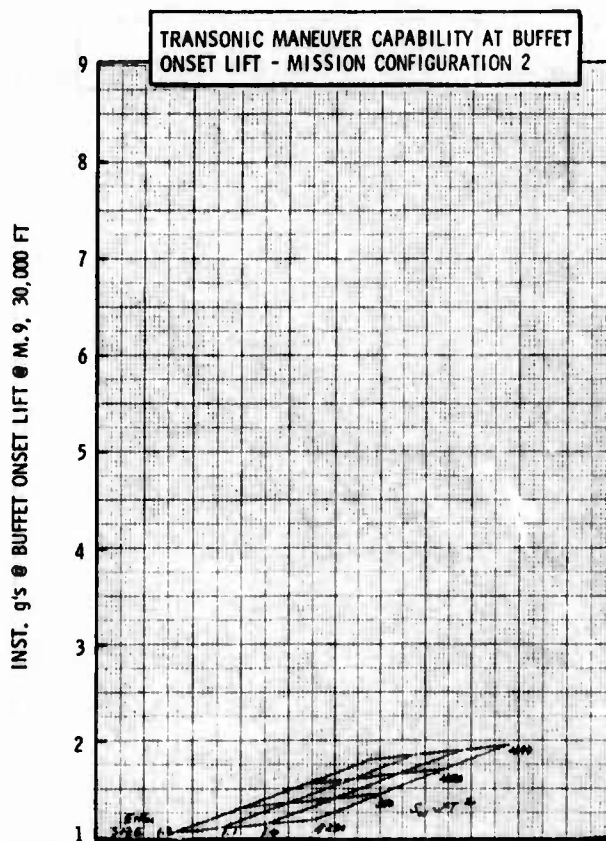
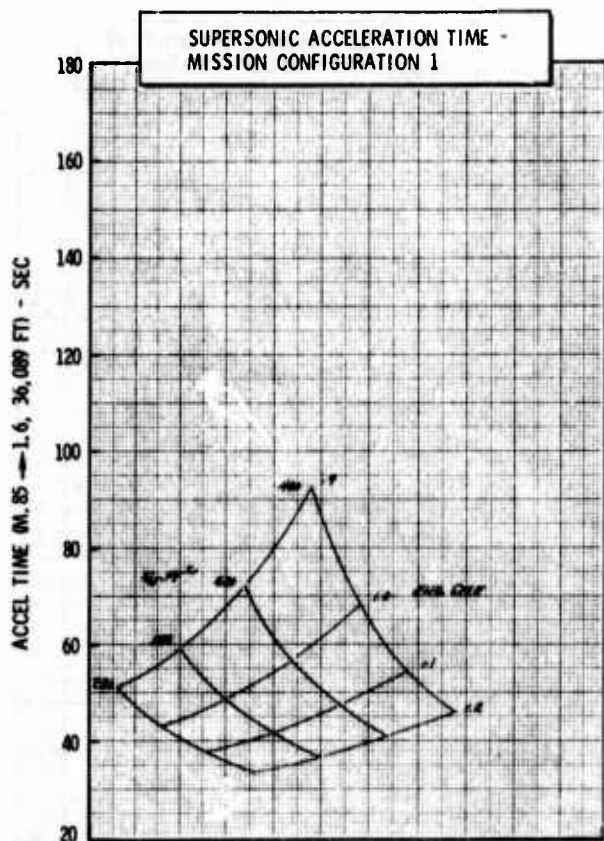
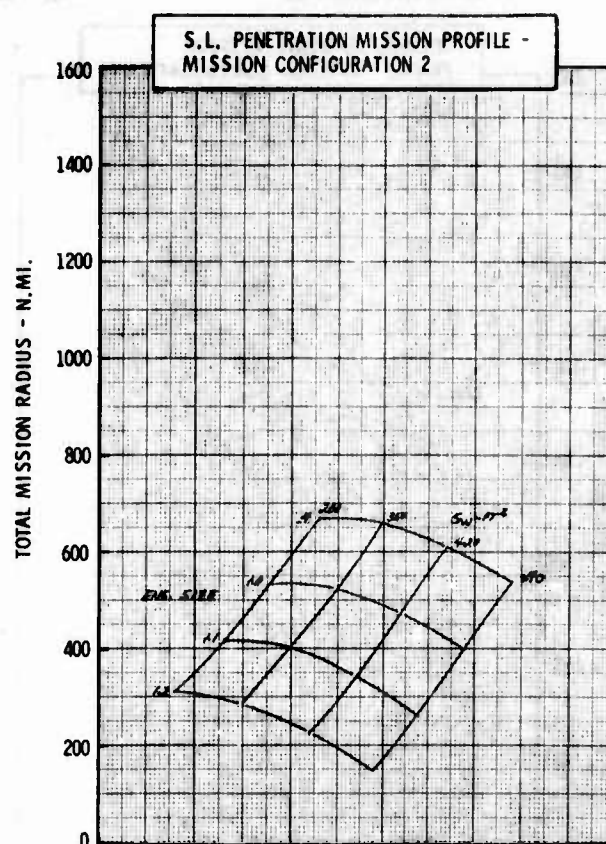
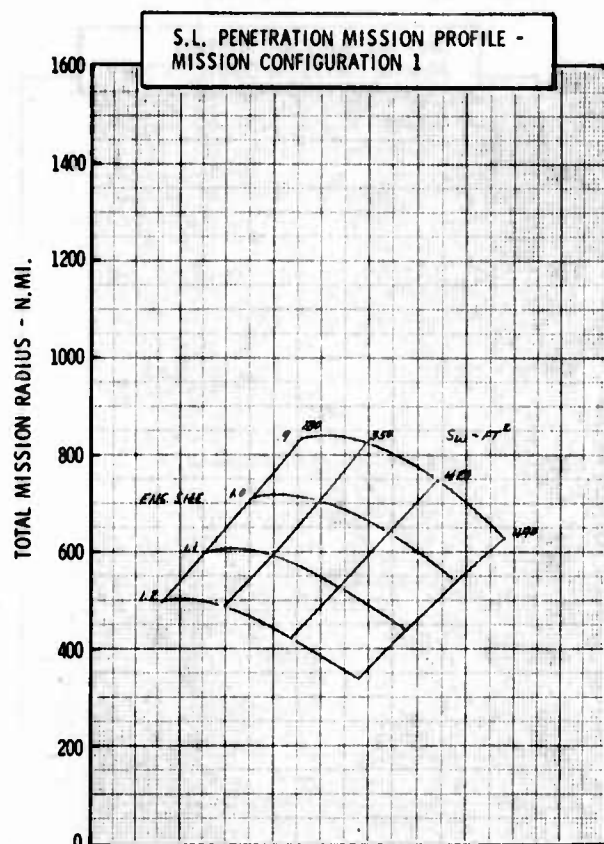


Figure H-48b LWA Mission/Configuration Tradeoff Parametric Data

• COMPOSITE MATERIALS

•  $\Delta LE = 20^\circ$

•  $AR = 4.0$

•  $t/c = .06$

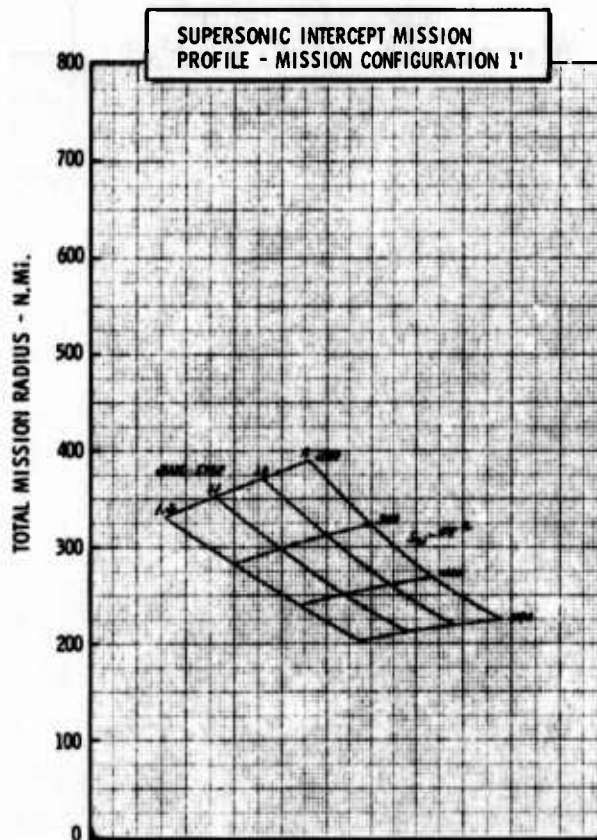
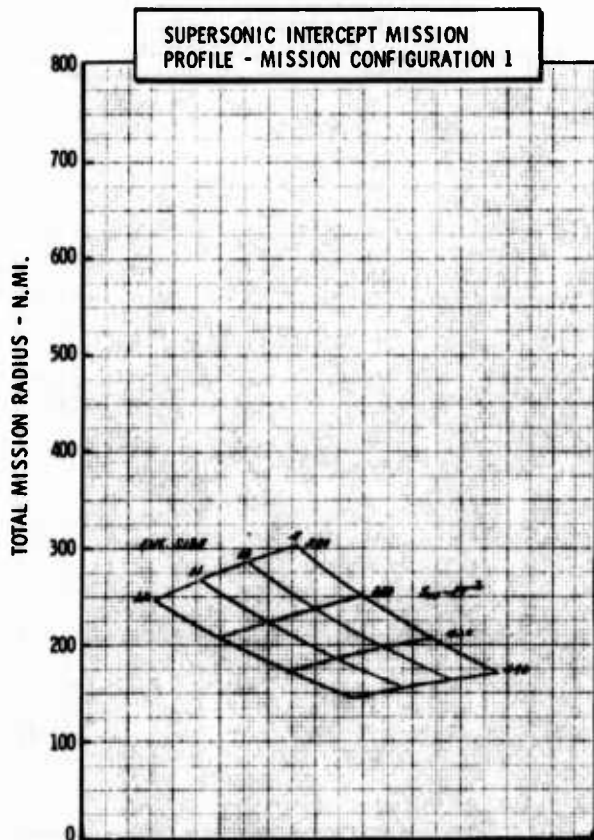
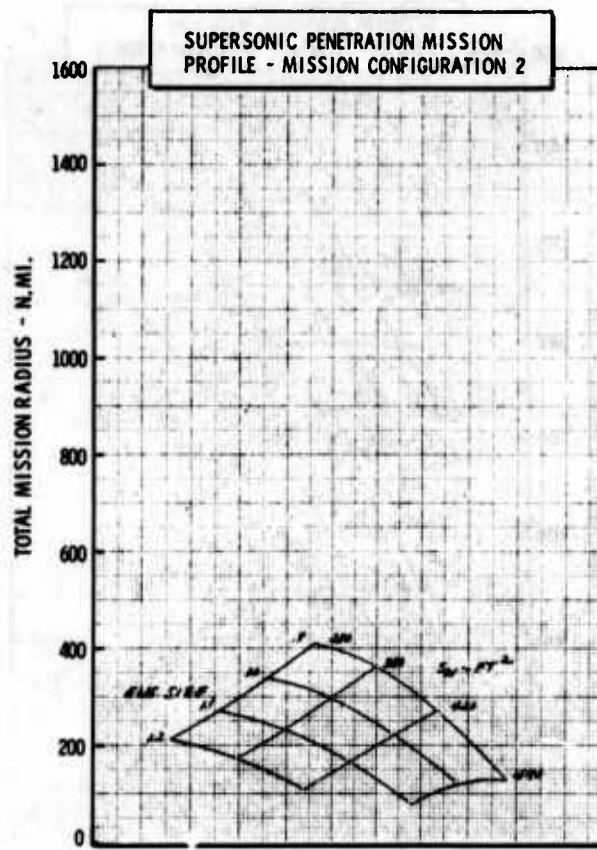
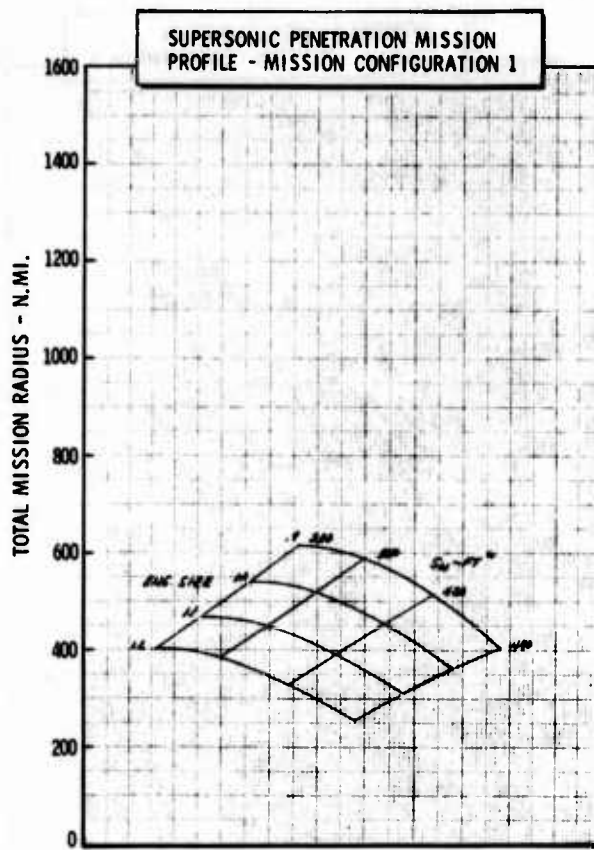


Figure H-48c LWA Mission/Configuration Tradeoff Parametric Data

• COMPOSITE MATERIALS

•  $\Lambda_{LE} = 20^\circ$

•  $AR = 5.0$

•  $t/c = .06$

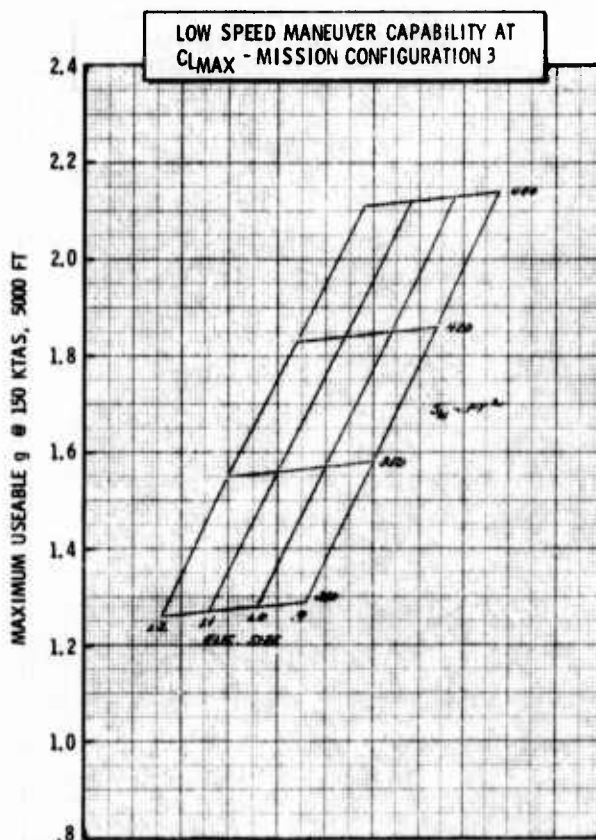
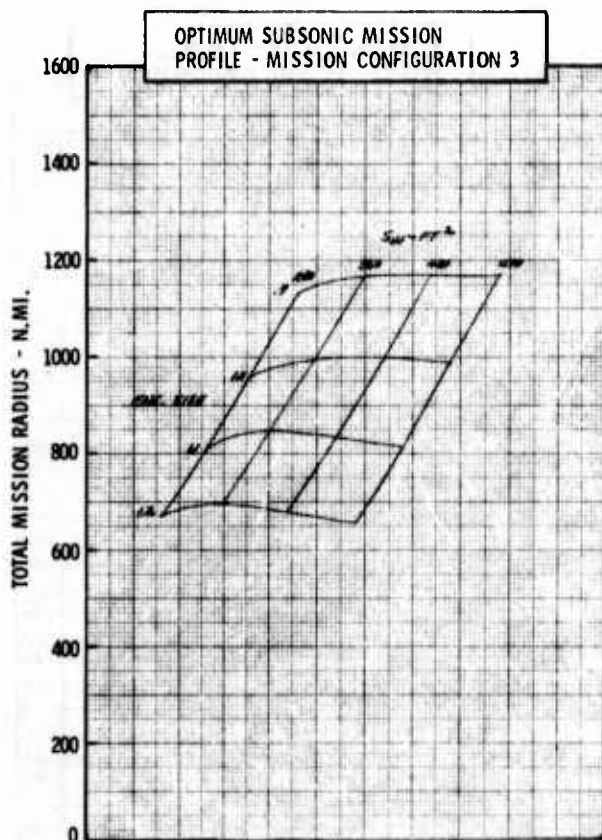
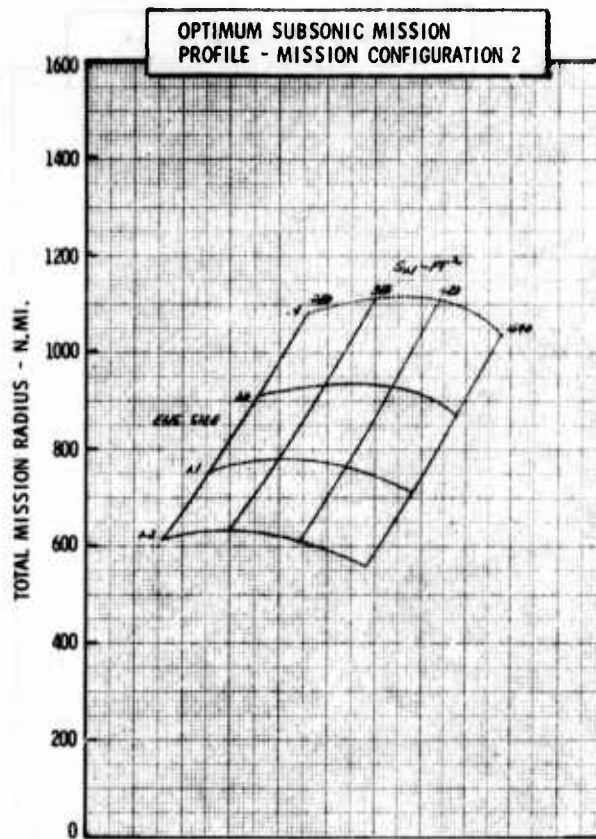
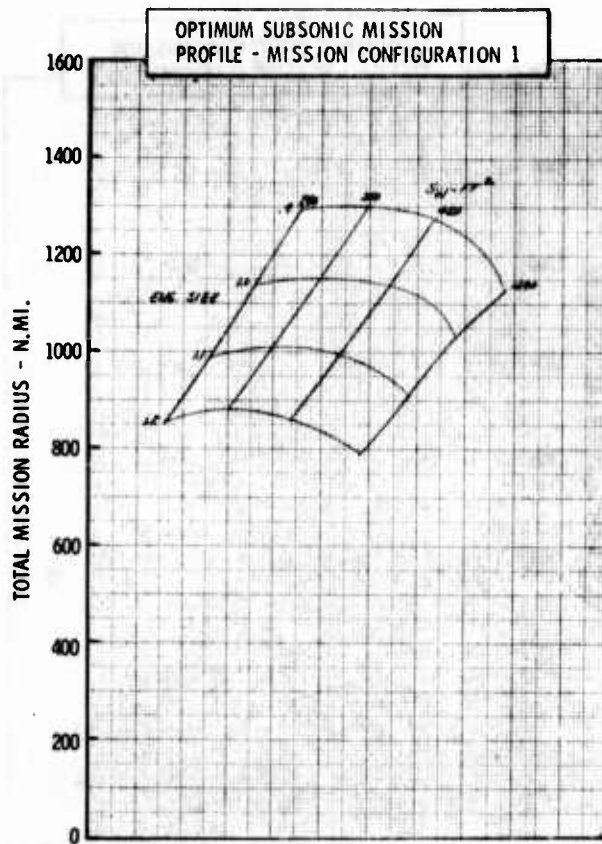


Figure H-49a LWA Mission/Configuration Tradeoff Parametric Data



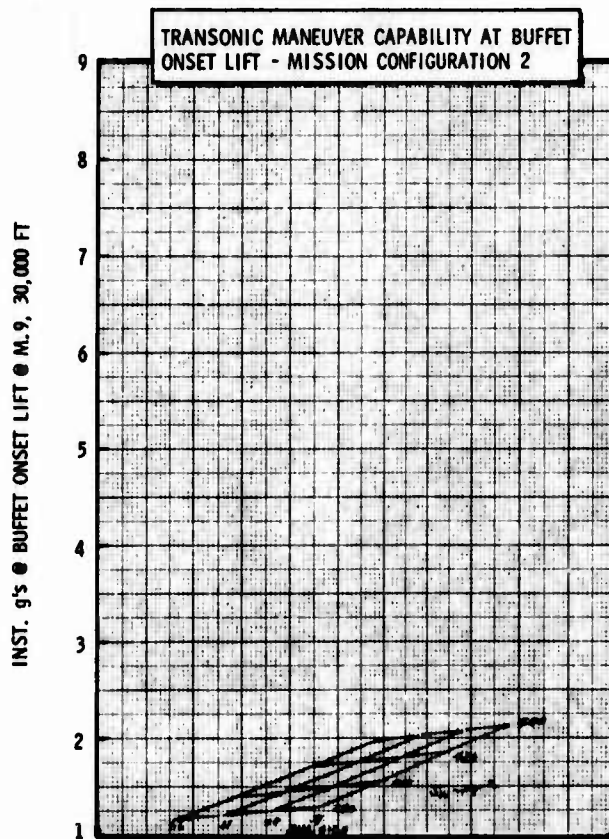
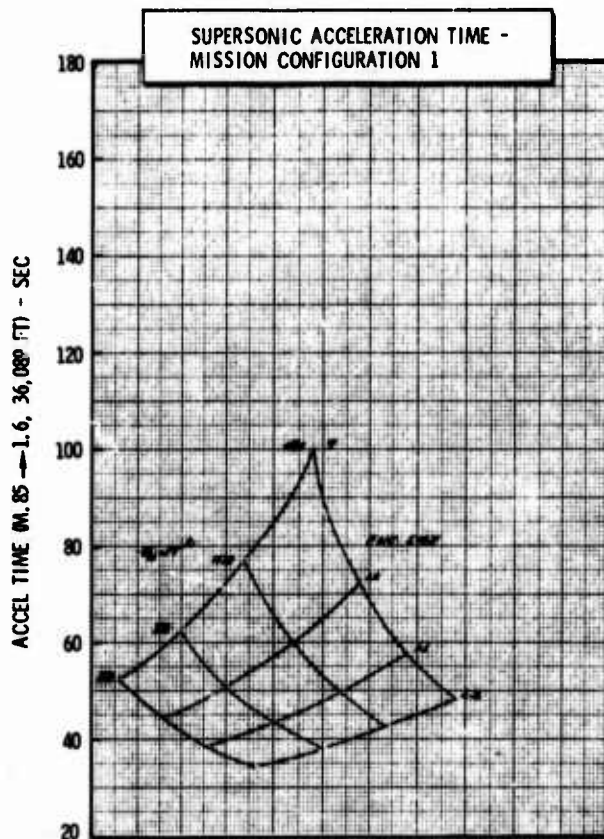
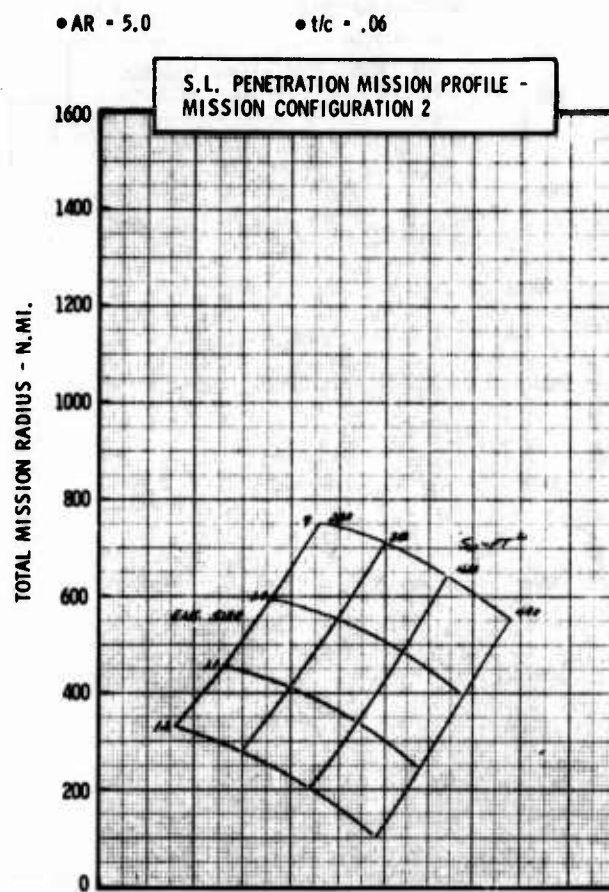
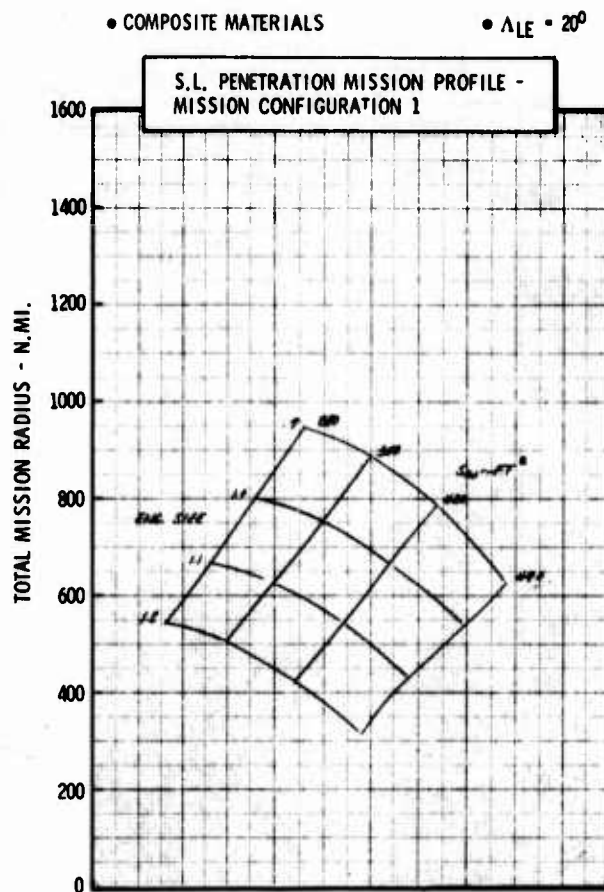
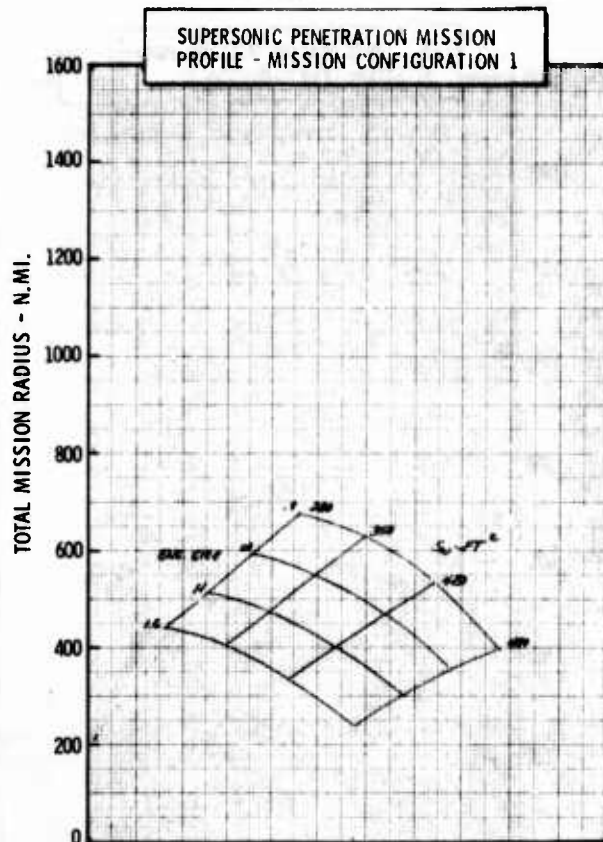


Figure H-49b LWA Mission/Configuration Tradeoff Parametric Data

• COMPOSITE MATERIALS

•  $\Lambda_{LE} = 20^\circ$



• AR = 5.0

•  $t/c = .06$

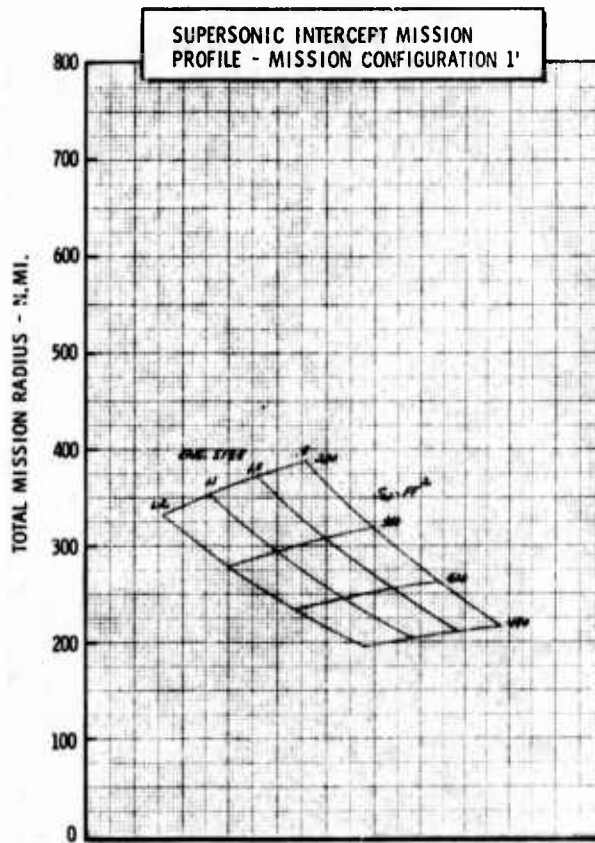
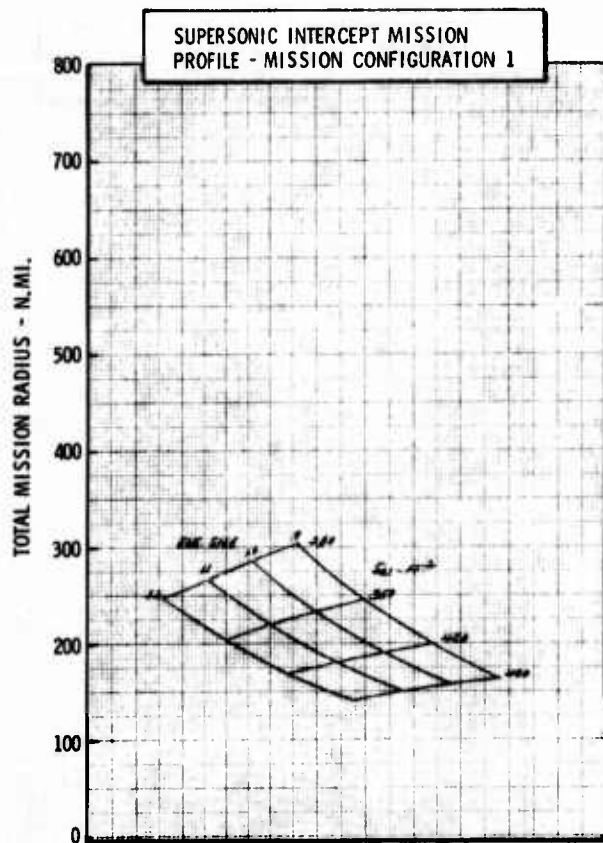
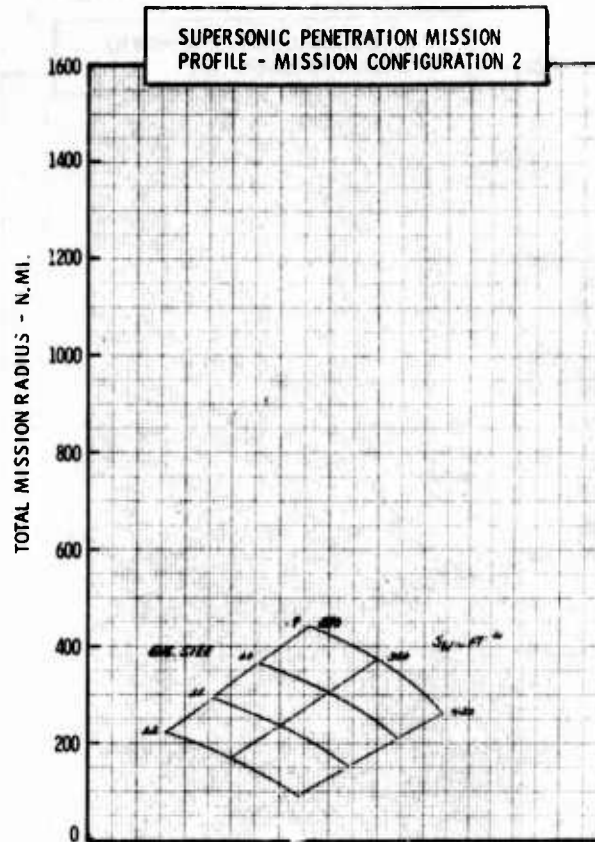


Figure H-49c LWA Mission/Configuration Tradeoff Parametric Data



• COMPOSITE MATERIALS

•  $\Lambda_{LE} = 30^\circ$

•  $AR = 3.0$

•  $t/c = .06$

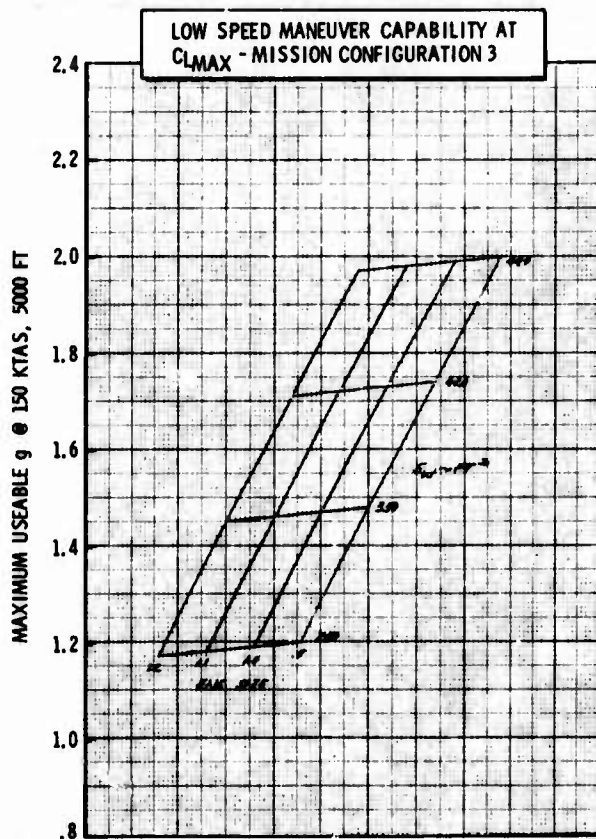
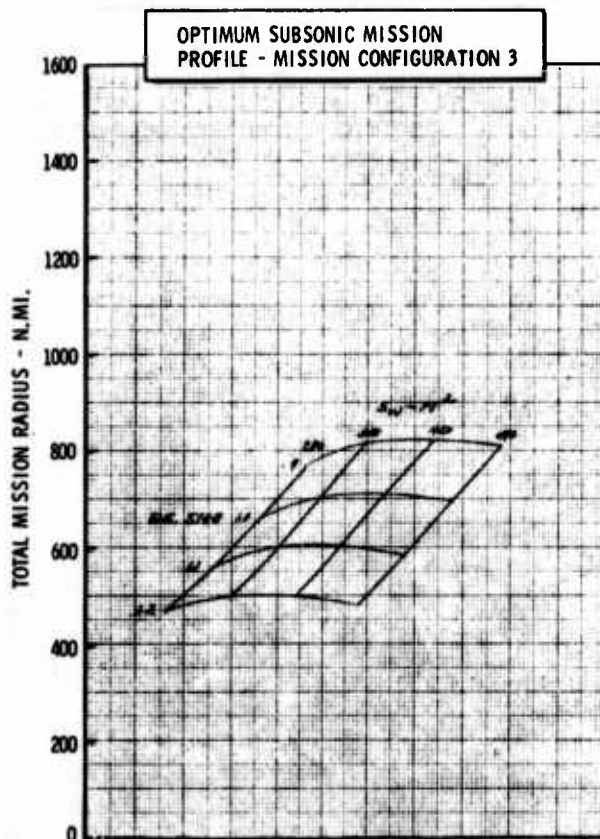
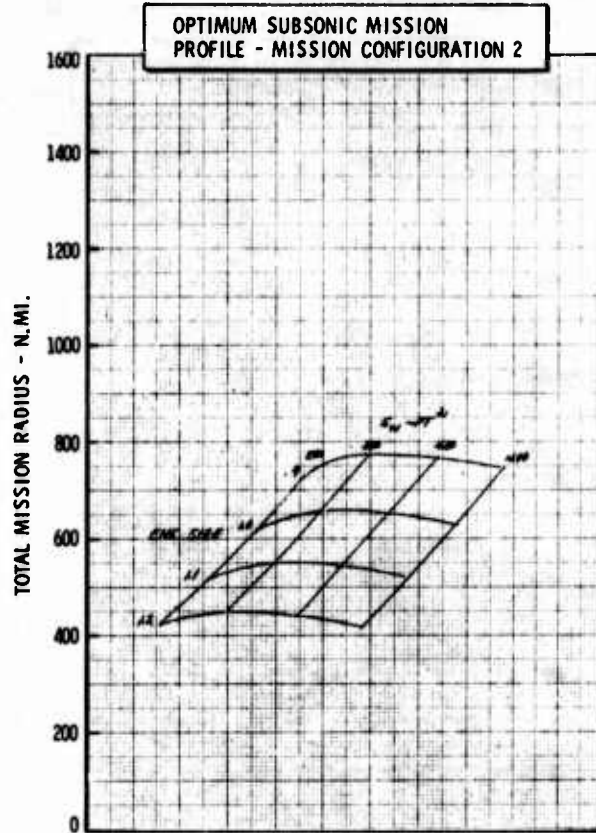
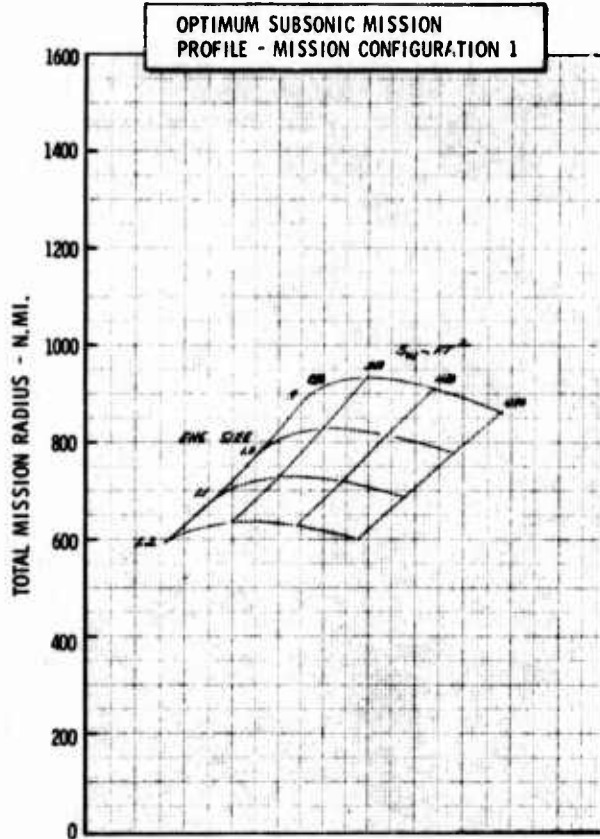


Figure H-50a LWA Mission/Configuration Tradeoff Parametric Data

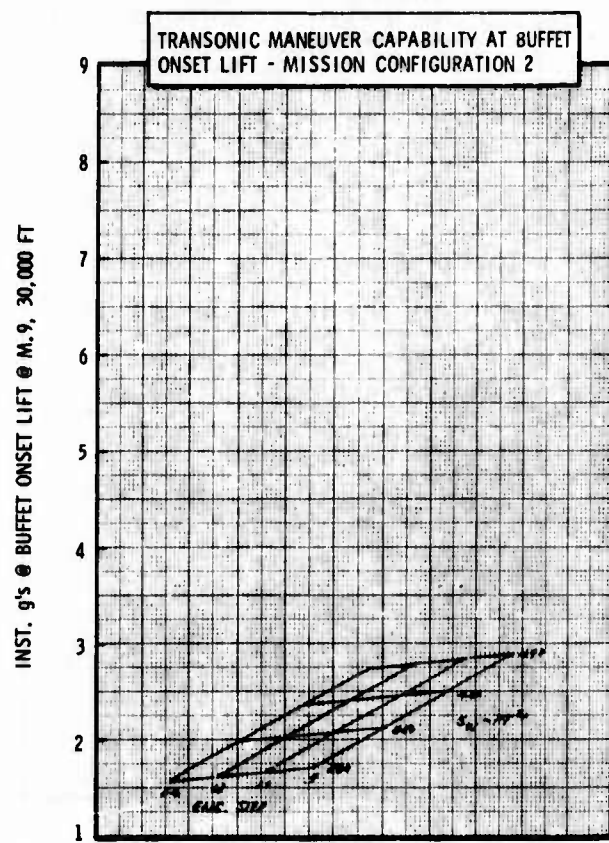
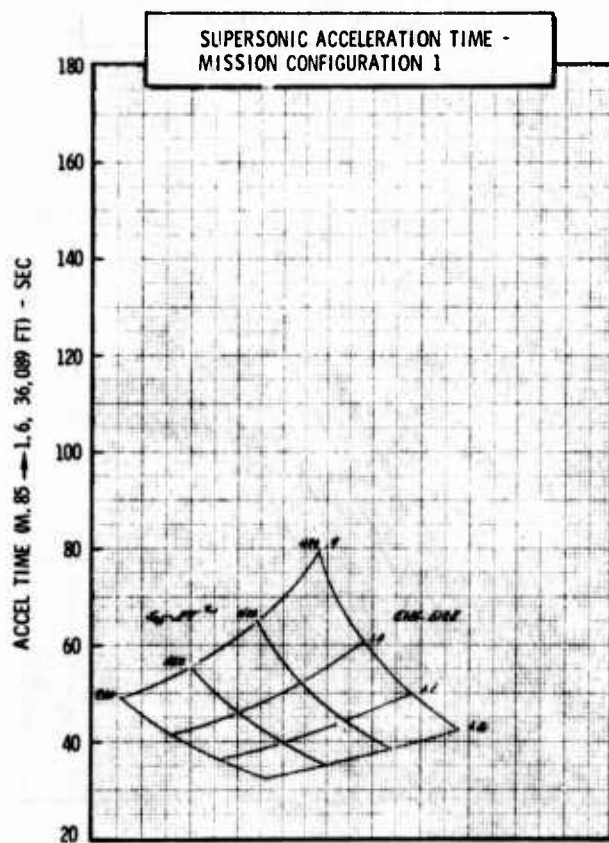
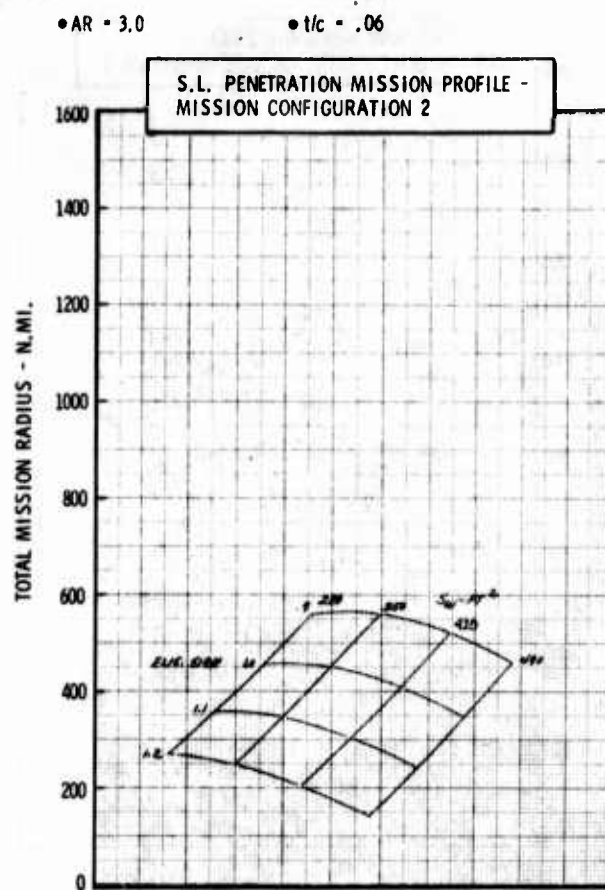
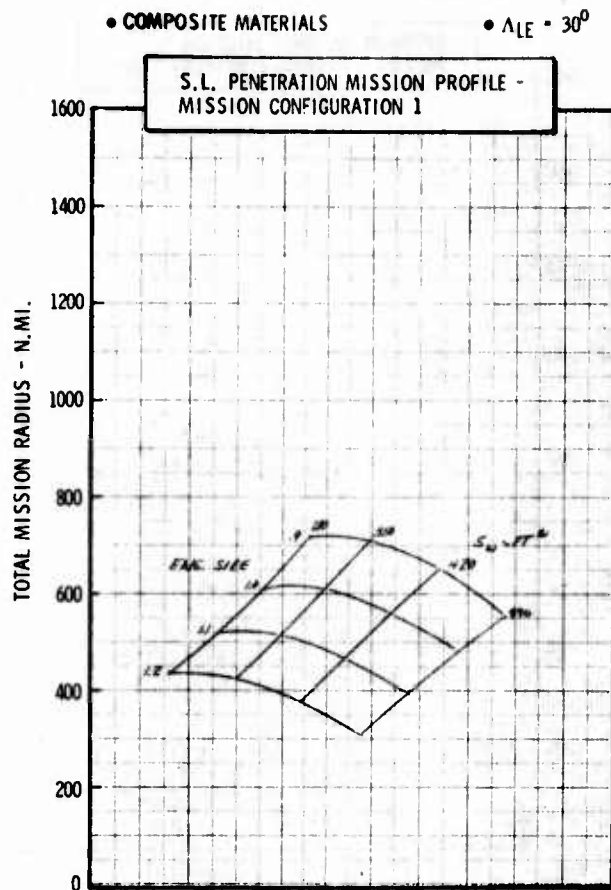
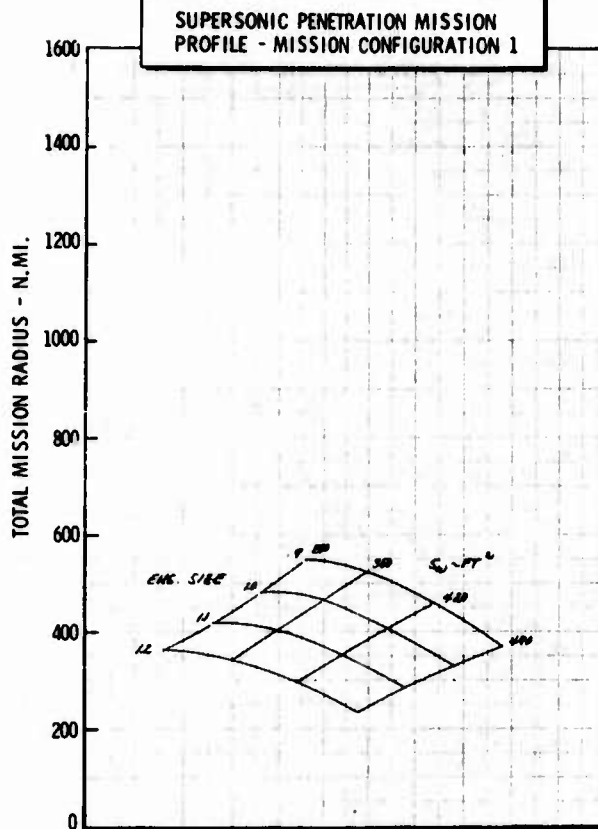


Figure H-50b LWA Mission/Configuration Tradeoff Parametric Data

• COMPOSITE MATERIALS

•  $\Delta_{LE} = 30^\circ$



• AR = 3.0

•  $t/c = .06$

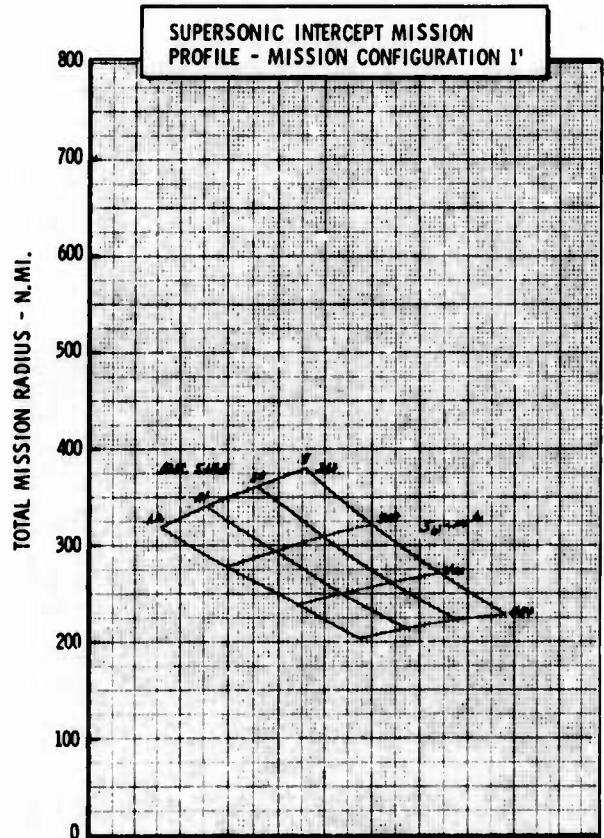
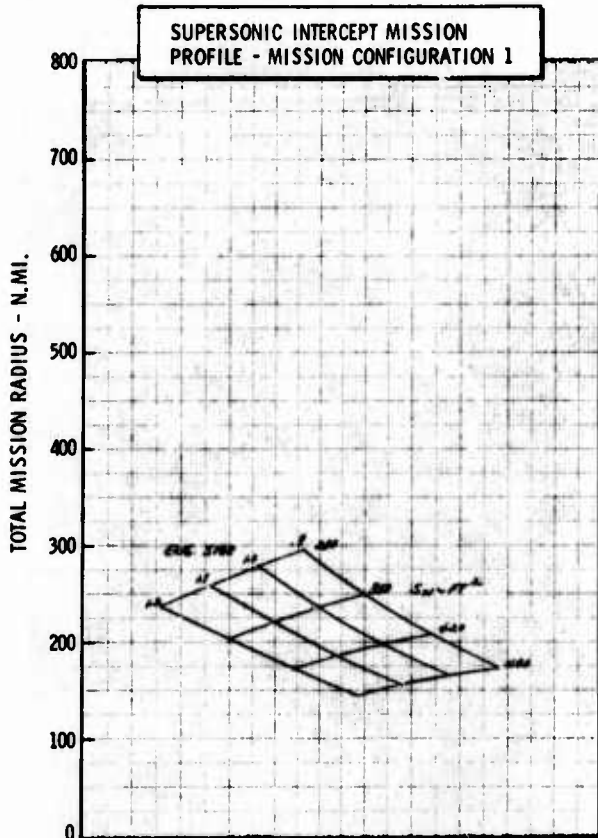
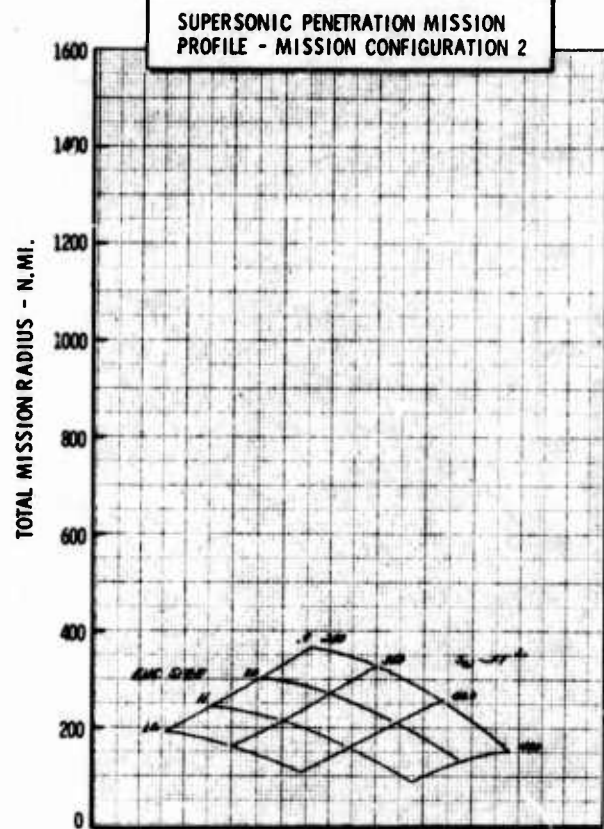


Figure H-50c LWA Mission/Configuration Tradeoff Parametric Data



• COMPOSITE MATERIALS

•  $\Delta LE = 30^\circ$

•  $AR = 4.0$

•  $t/c = .06$

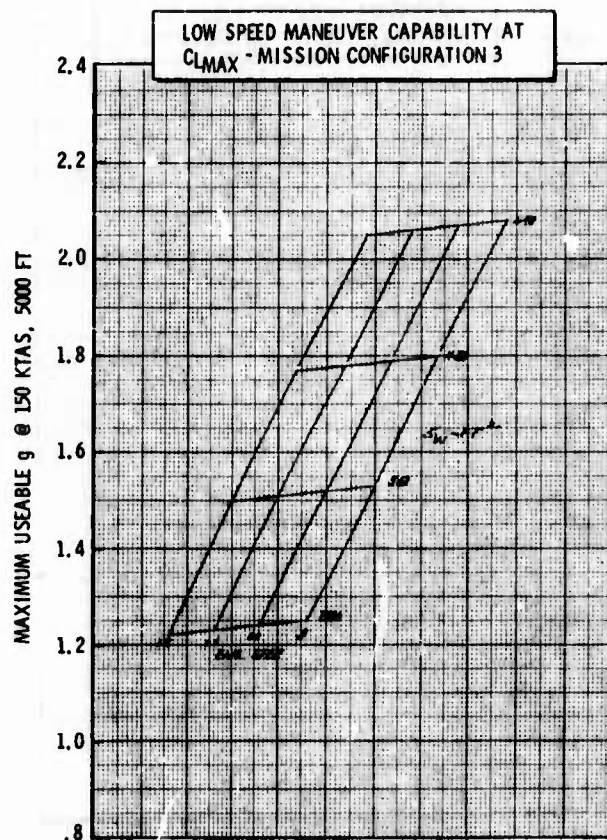
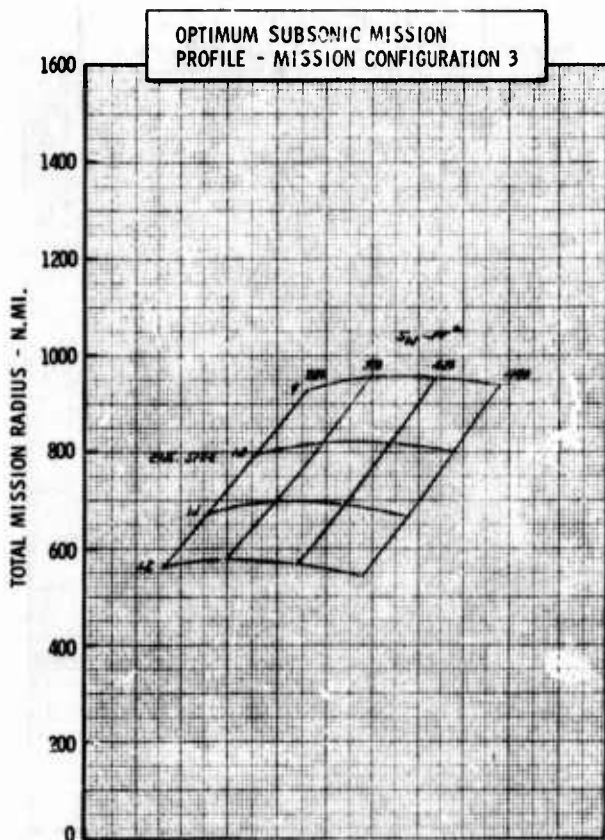
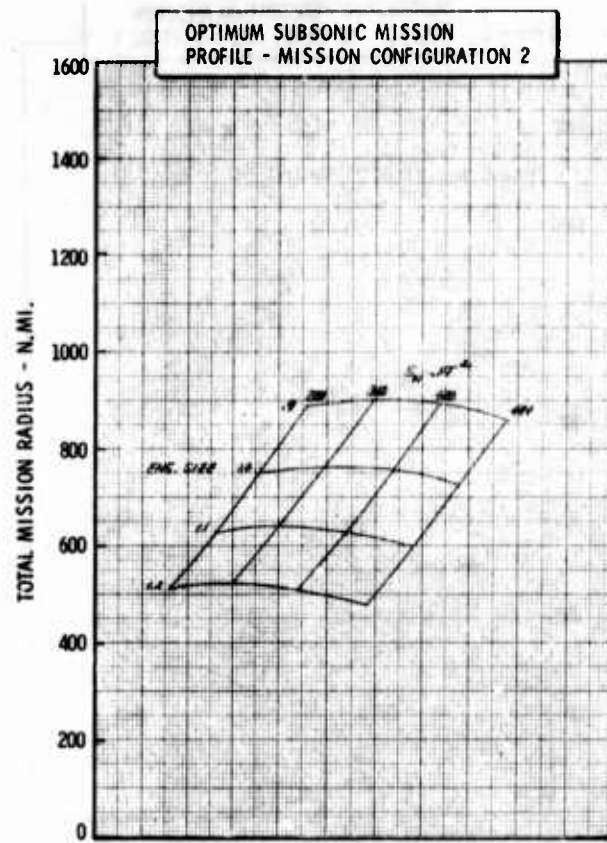
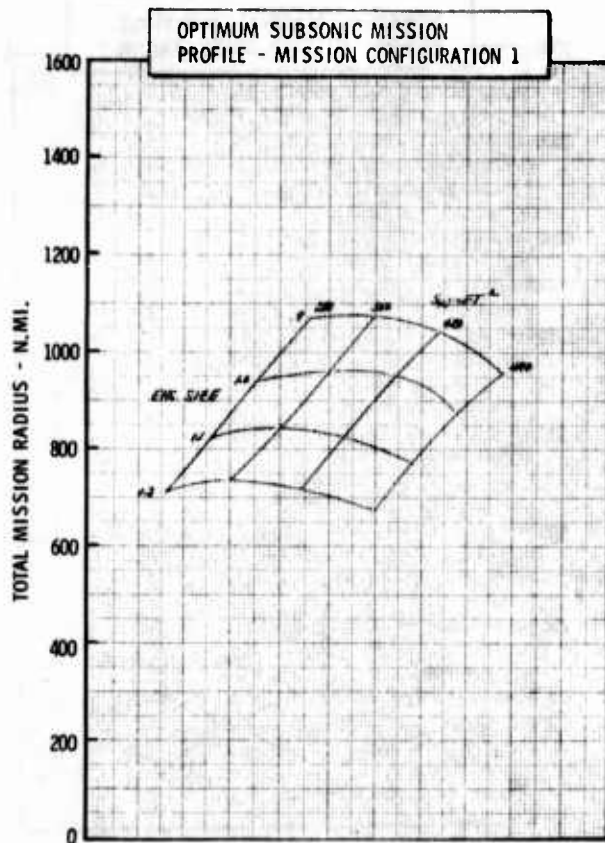


Figure H-51a LWA Mission/Configuration Tradeoff Parametric Data

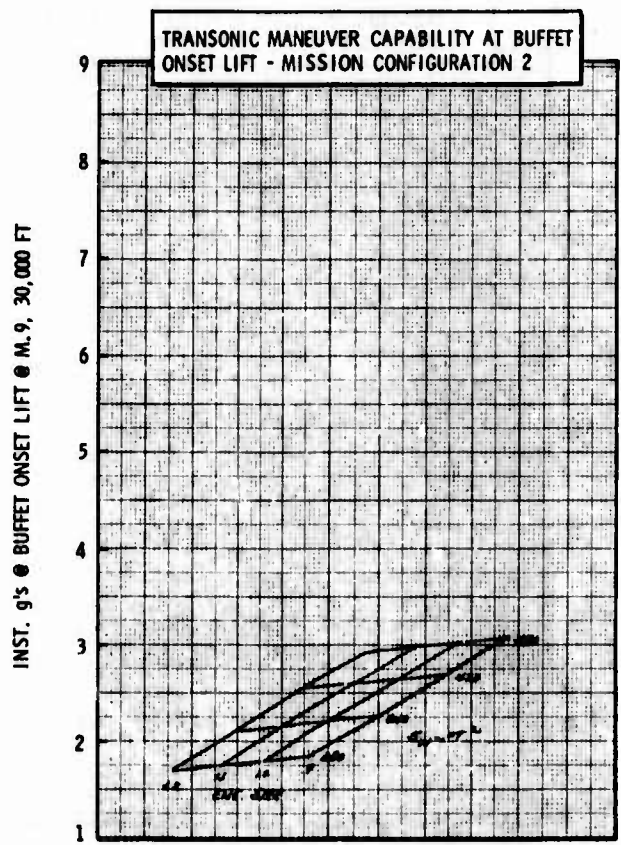
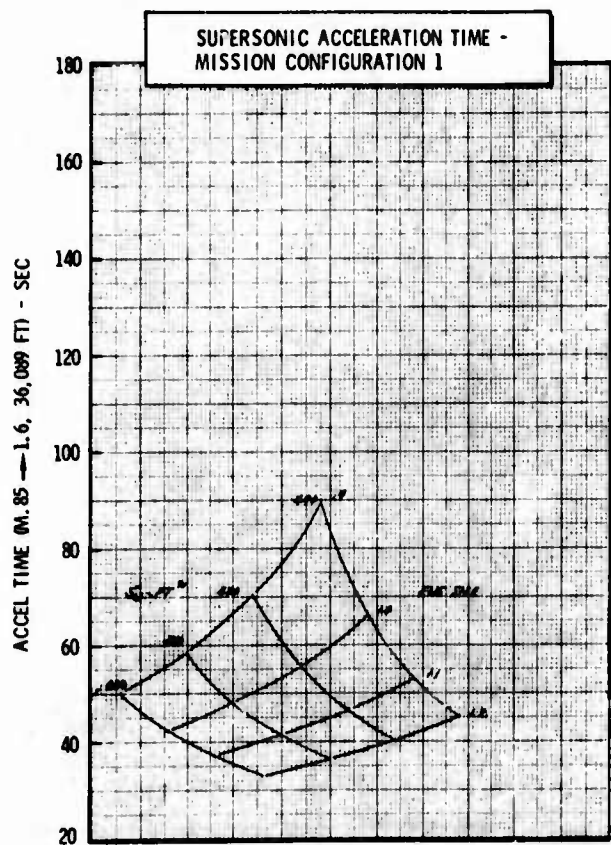
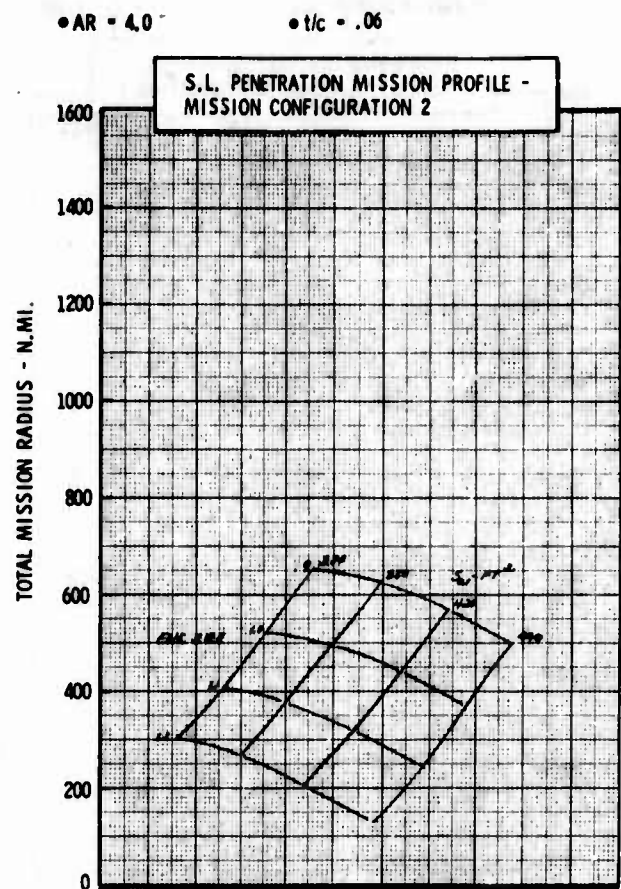
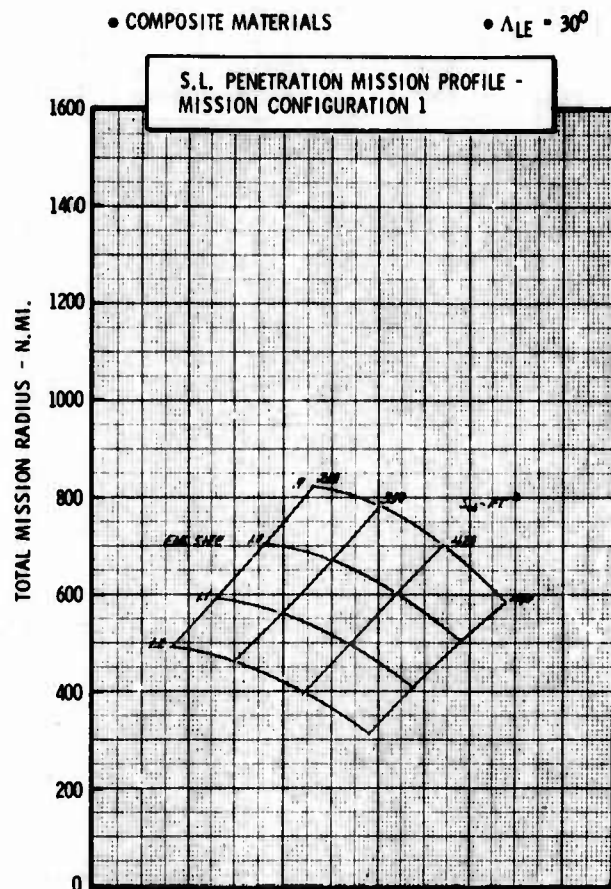
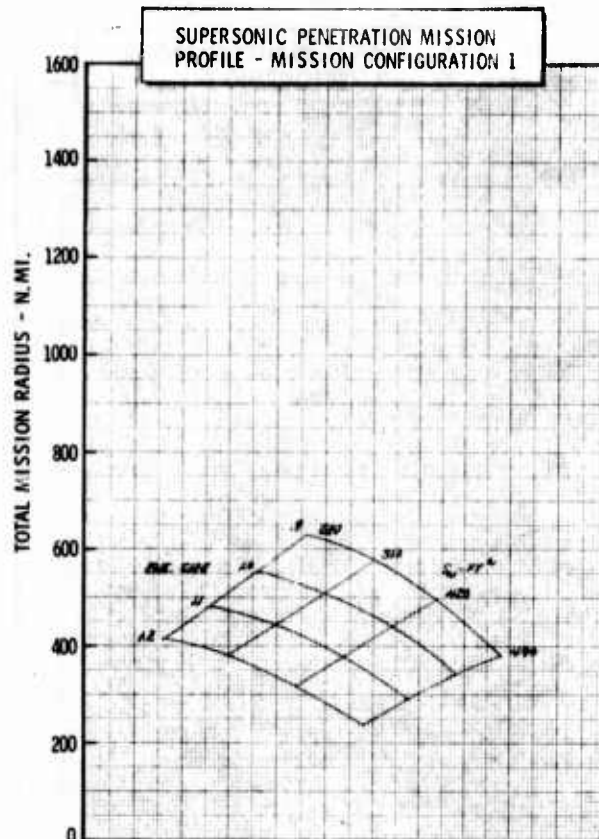


Figure H-51b LWA Mission/Configuration Tradeoff Parametric Data



• COMPOSITE MATERIALS

•  $\Delta LE = 30^\circ$



• AR = 4.0

•  $t/c = .06$

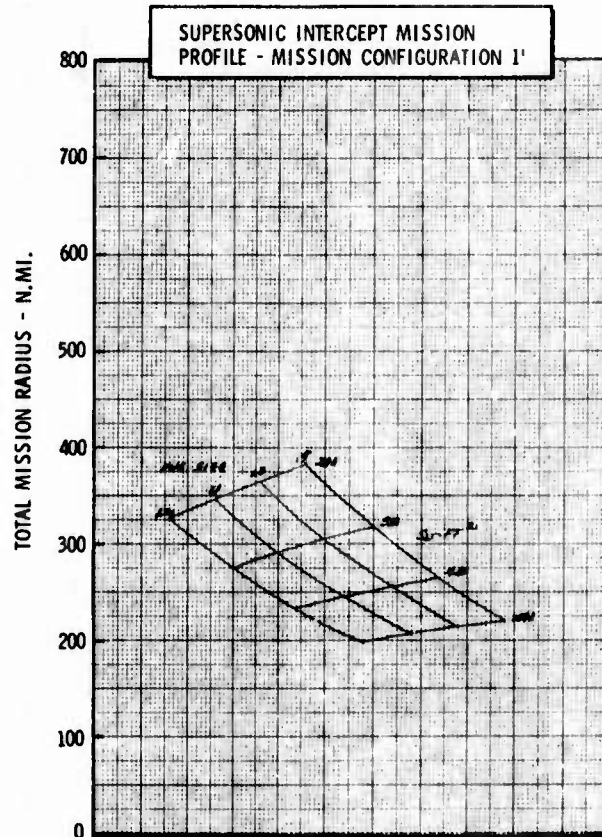
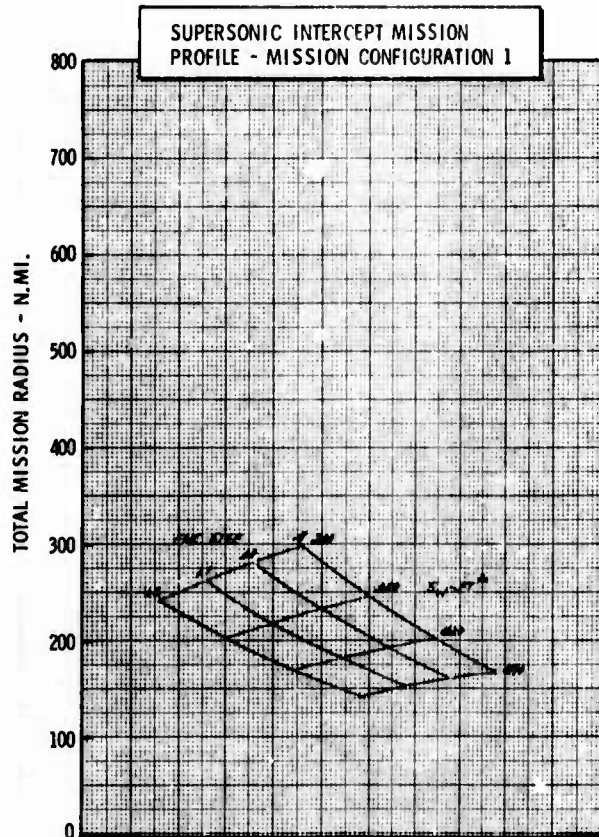
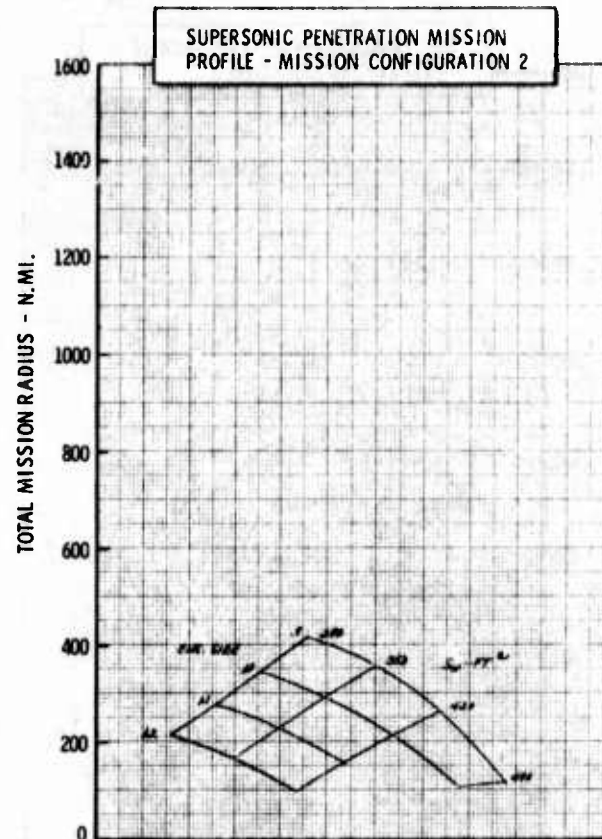


Figure H-51c LWA Mission/Configuration Tradeoff Parametric Data

• COMPOSITE MATERIALS

•  $\Delta LE = 30^\circ$

•  $AR = 5.0$

•  $t/c = .06$

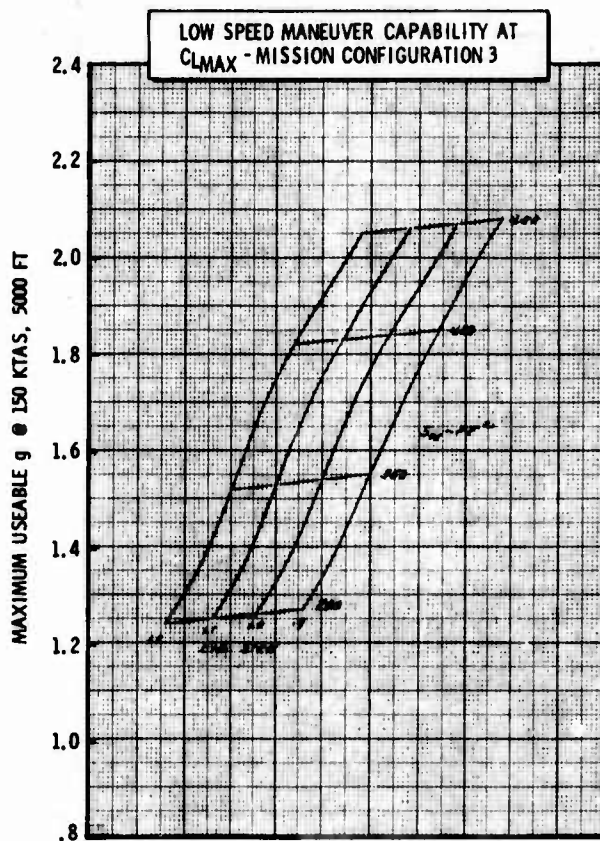
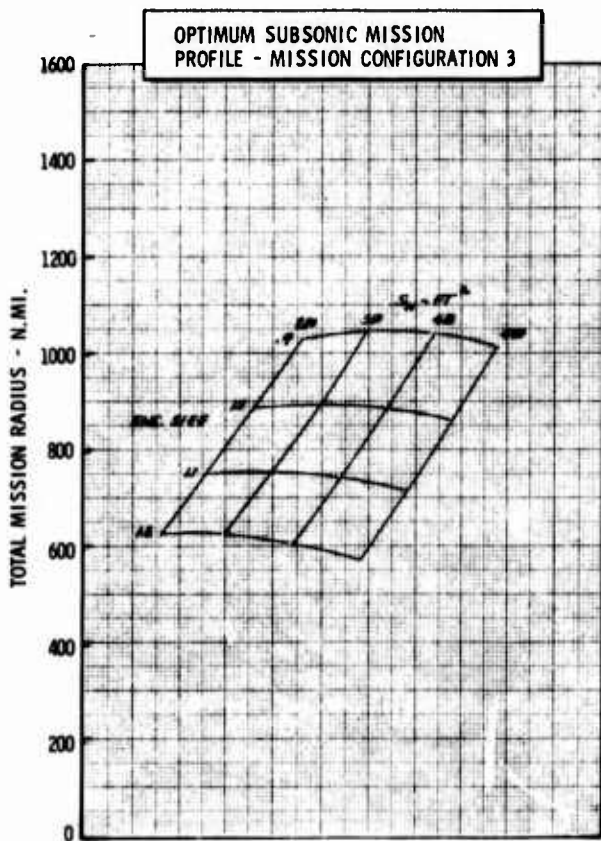
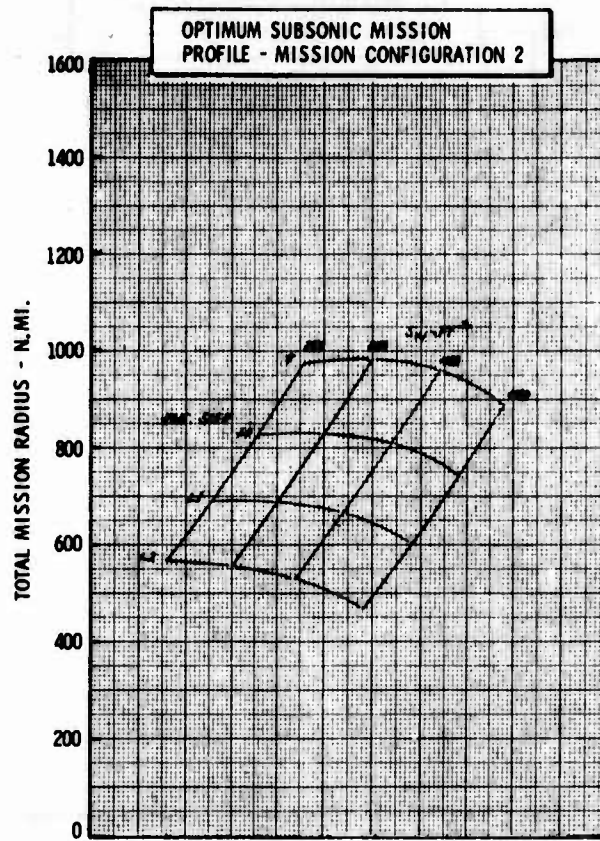
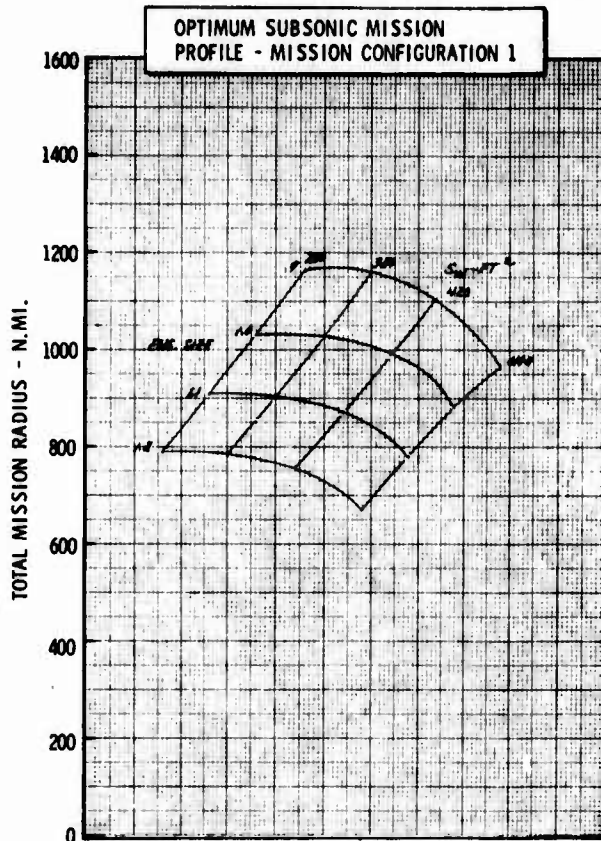


Figure H-52a LWA Mission/Configuration Tradeoff Parametric Data

• COMPOSITE MATERIALS

•  $\Delta LE = 30^\circ$

•  $AR = 5.0$

•  $t/c = .06$

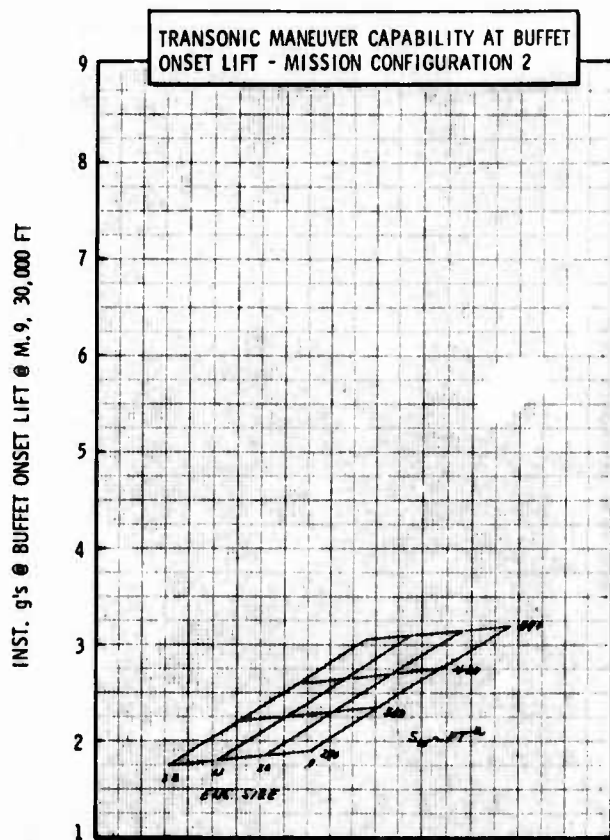
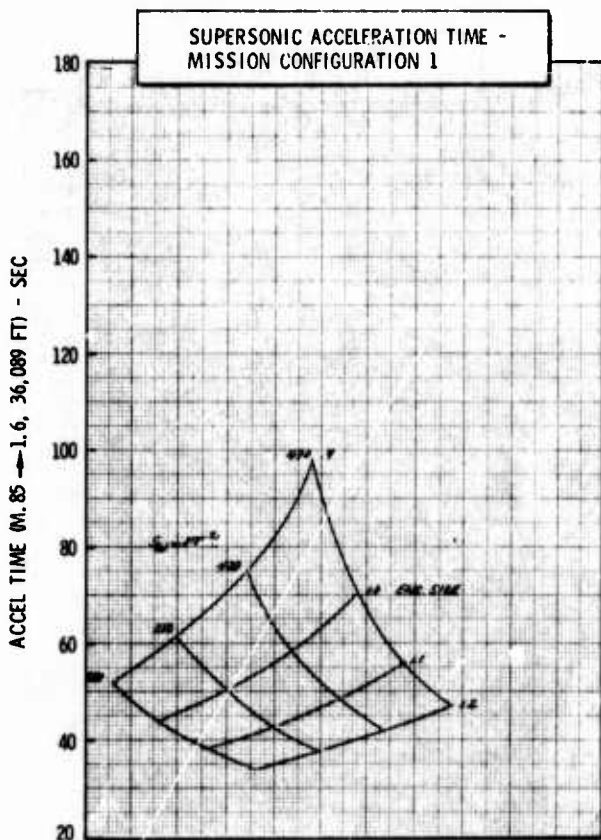
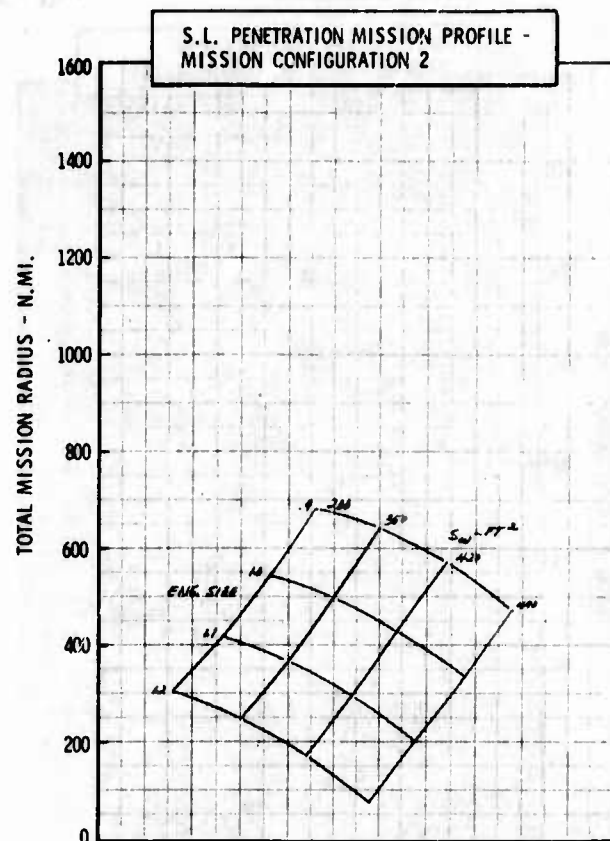
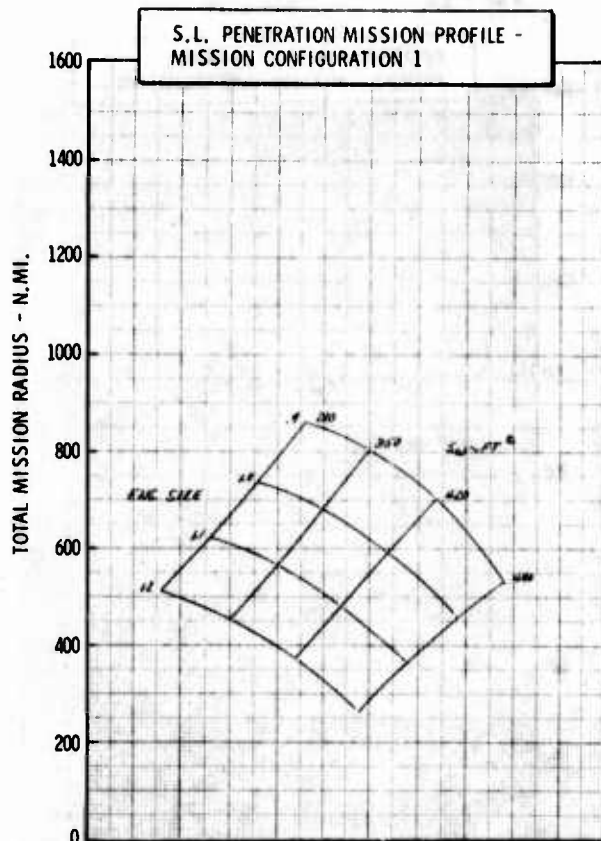
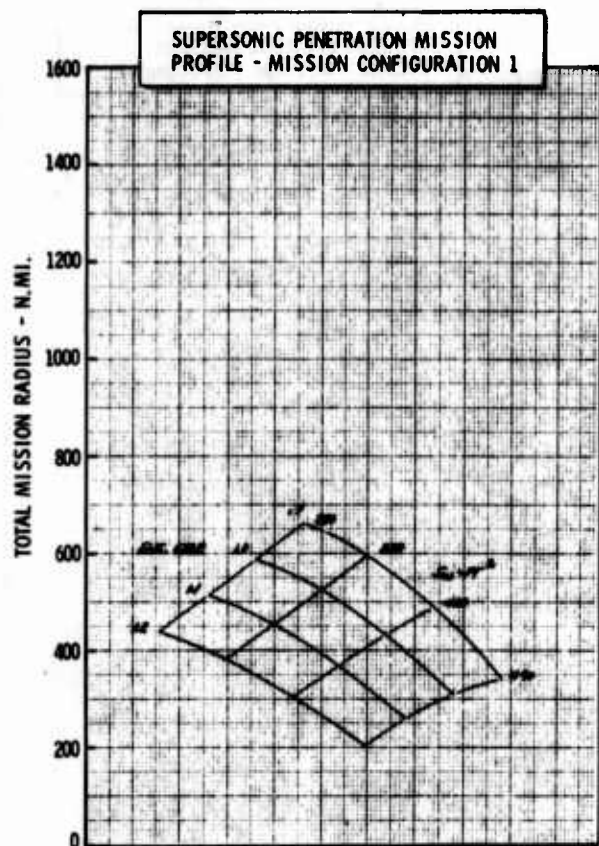


Figure H-52b LWA Mission/Configuration Tradeoff Parametric Data



•  $\Delta_{LE} = 30^\circ$



• t/c = .06

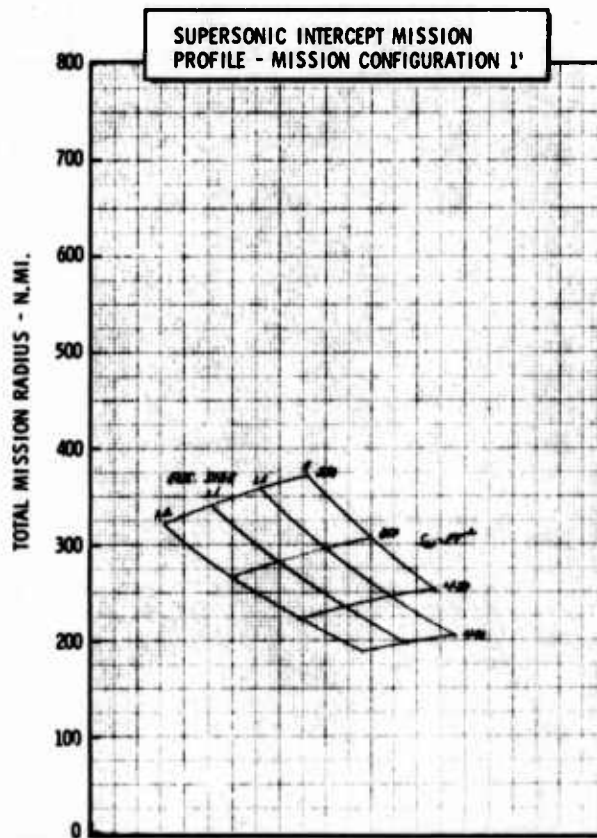
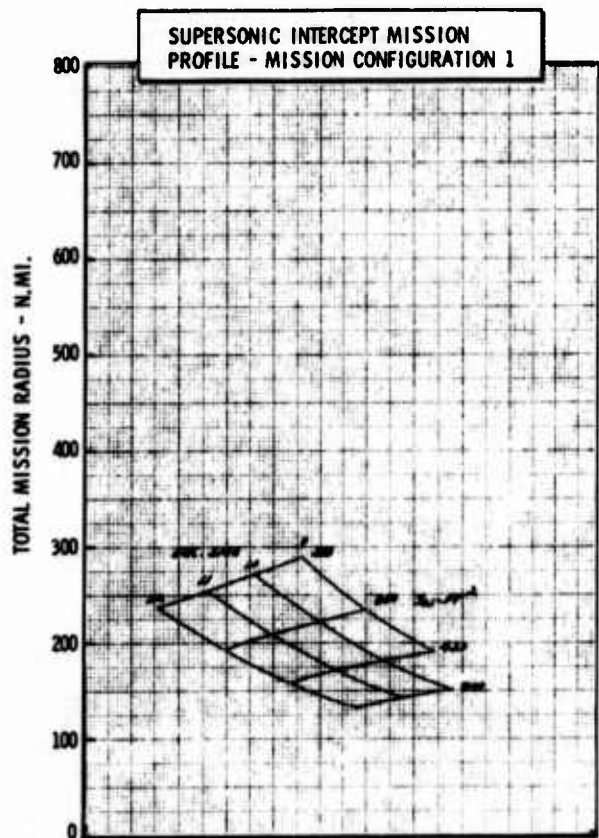
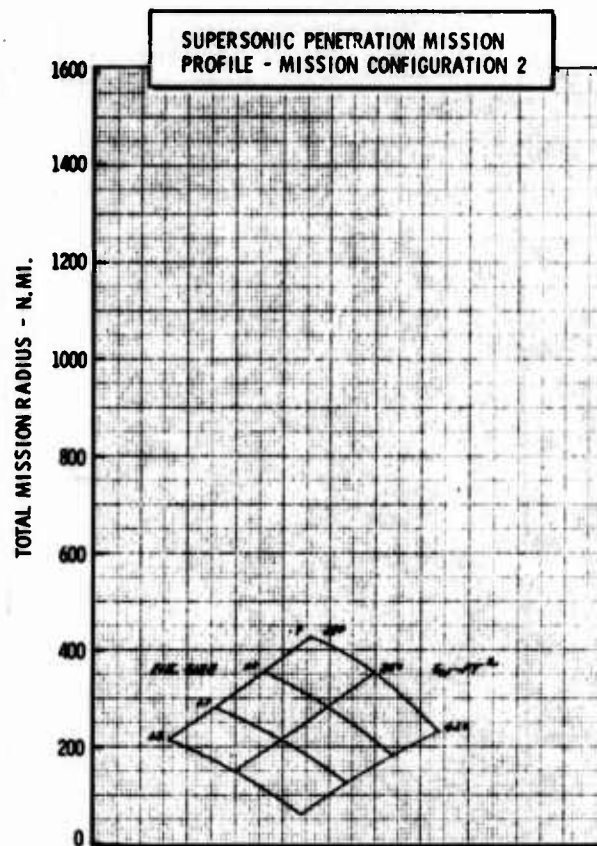


**Figure H-52c LWA Mission/Configuration Tradeoff Parametric Data**

• COMPOSITE MATERIALS

•  $\Delta LE = 40^\circ$

•  $AR = 3.0$

•  $t/c = .06$

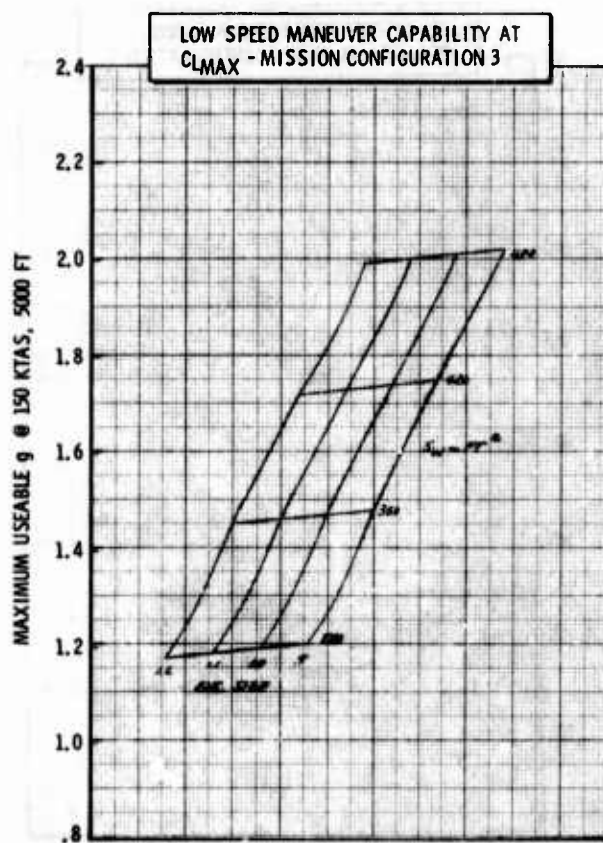
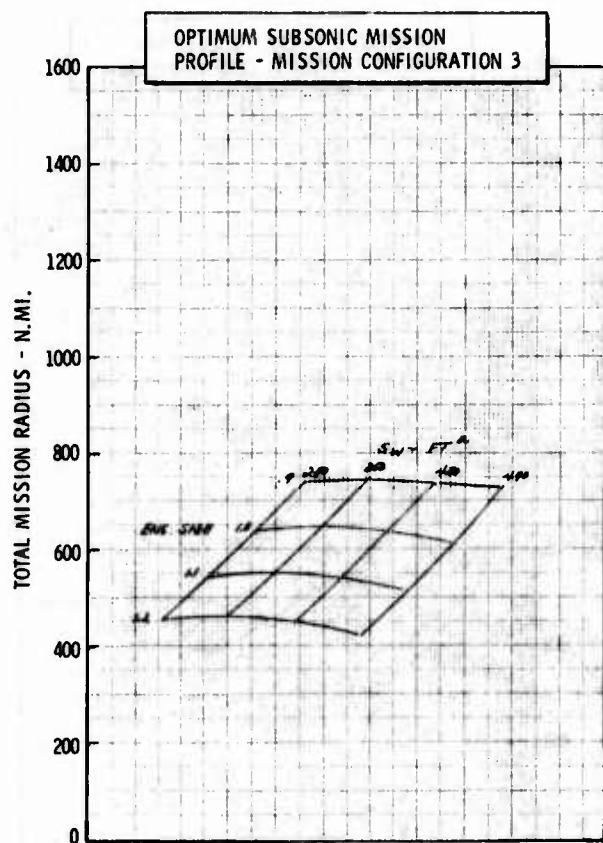
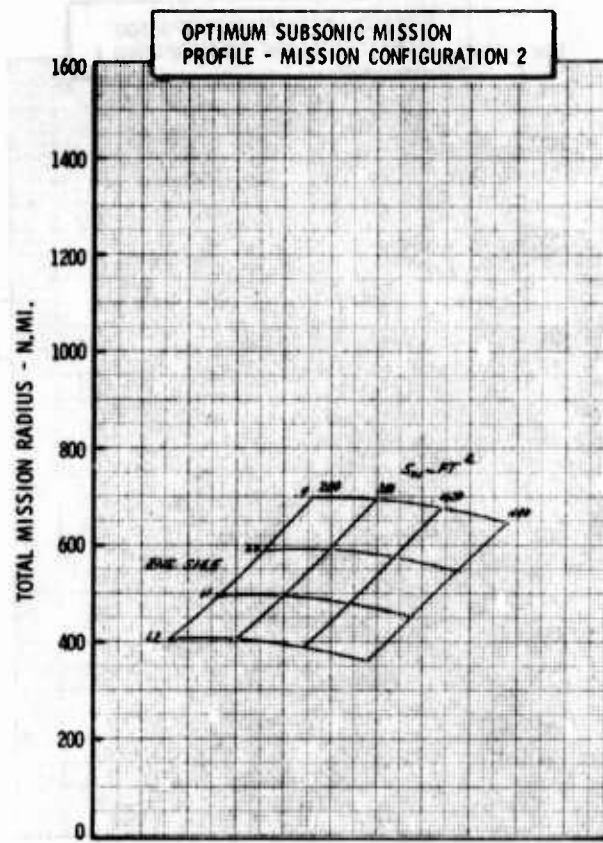
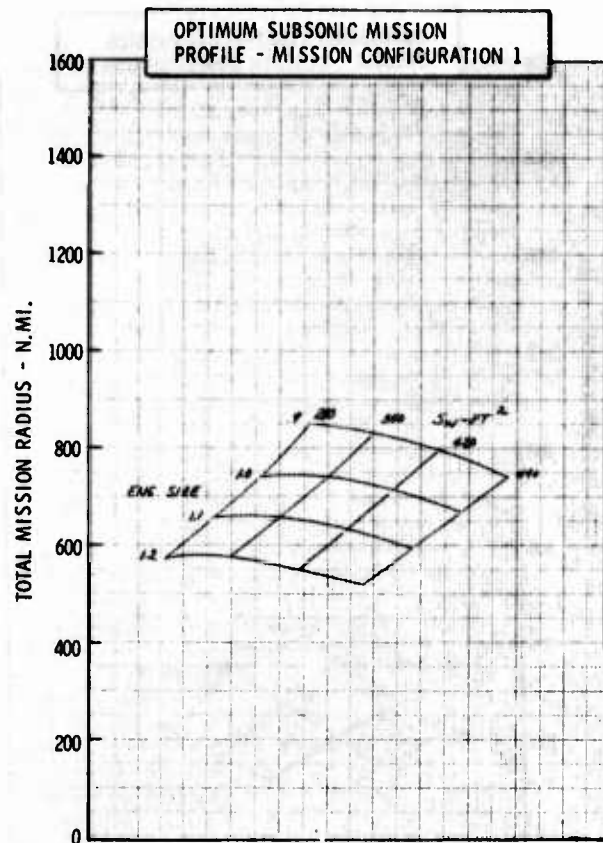


Figure H-53a LWA Mission/Configuration Tradeoff Parametric Data



• COMPOSITE MATERIALS

•  $\Delta LE = 40^\circ$

•  $AR = 3.0$

•  $t/c = .06$

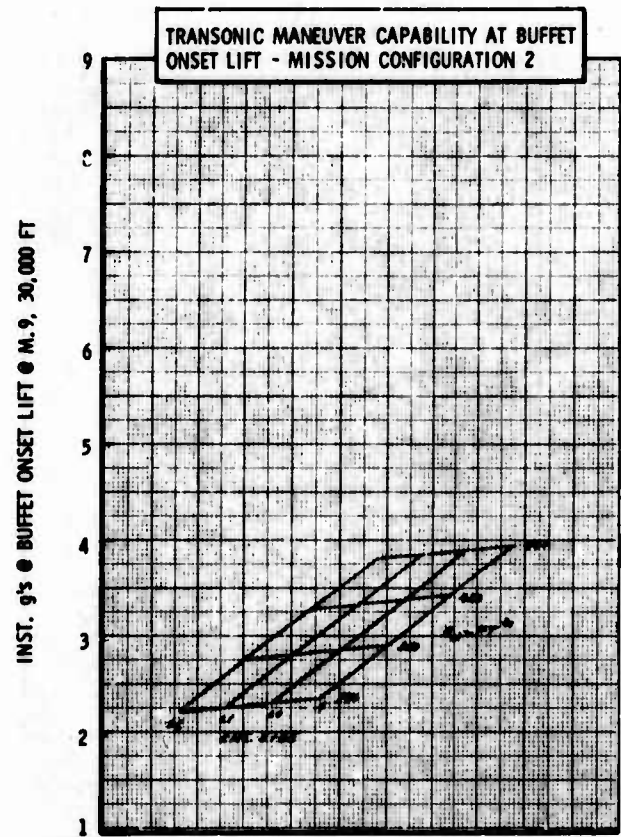
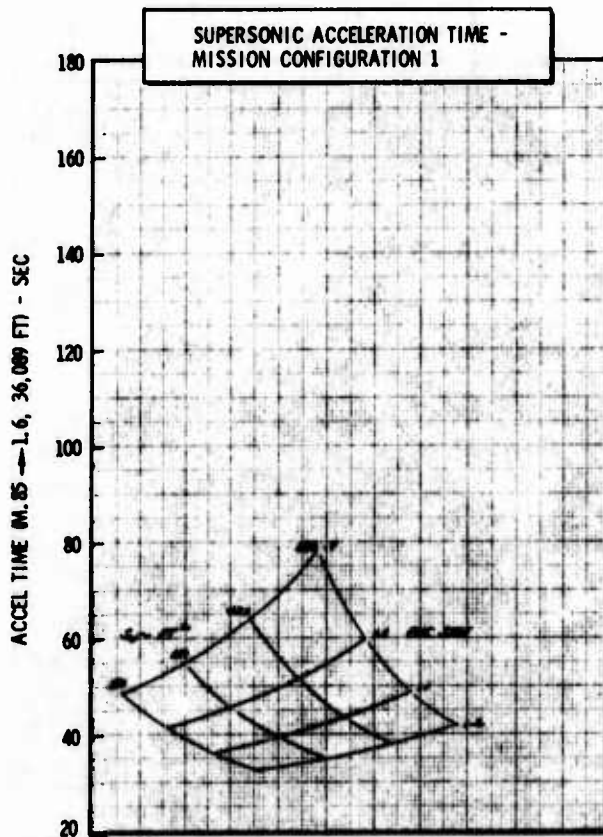
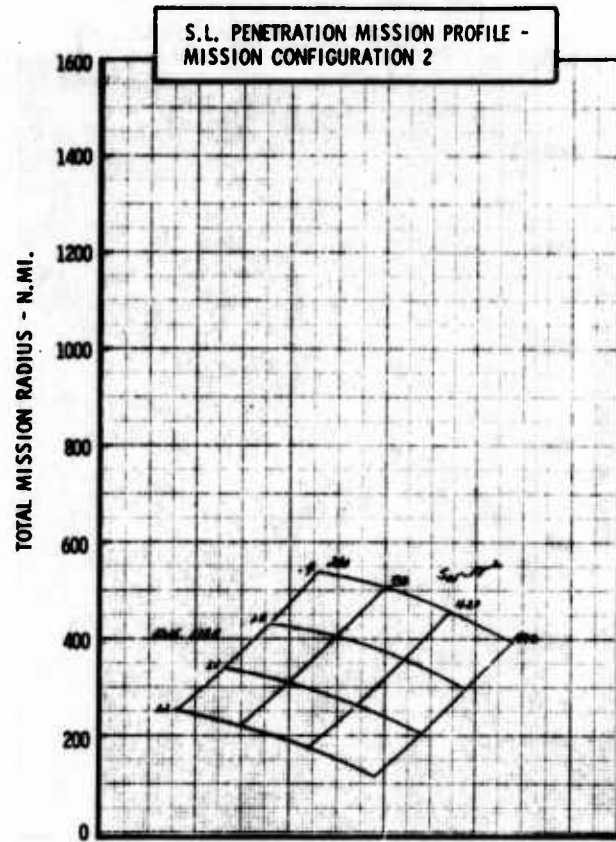
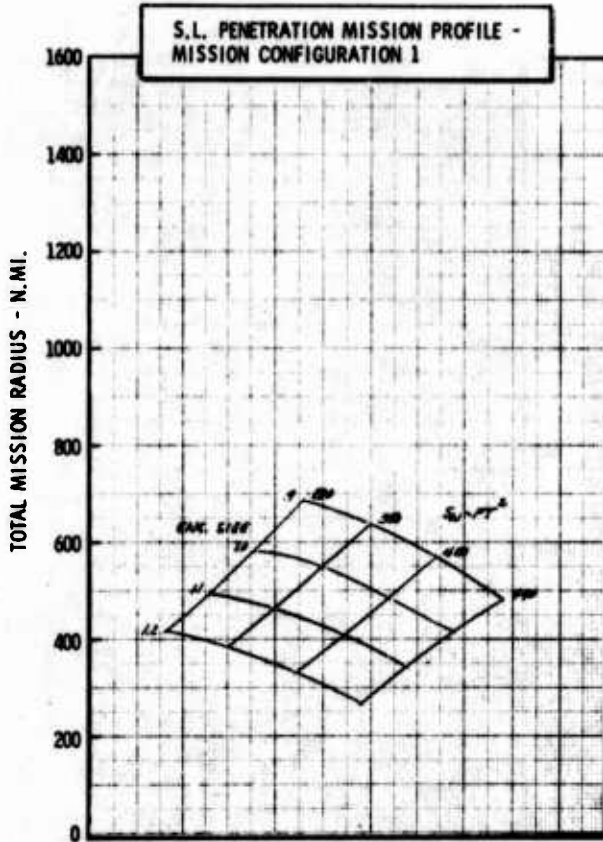


Figure H-53b LWA Mission/Configuration Tradeoff Parametric Data

•  $\angle E = 40^\circ$

• t/c = .06

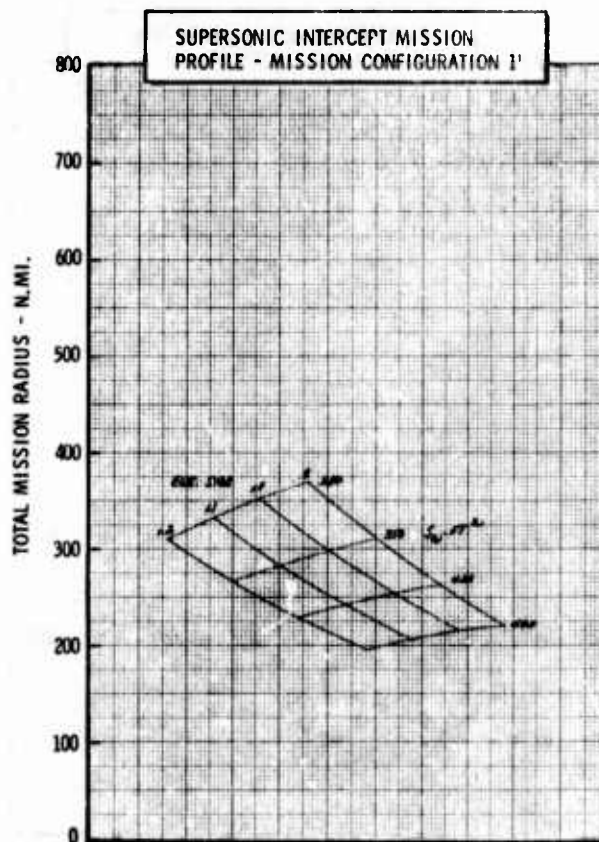
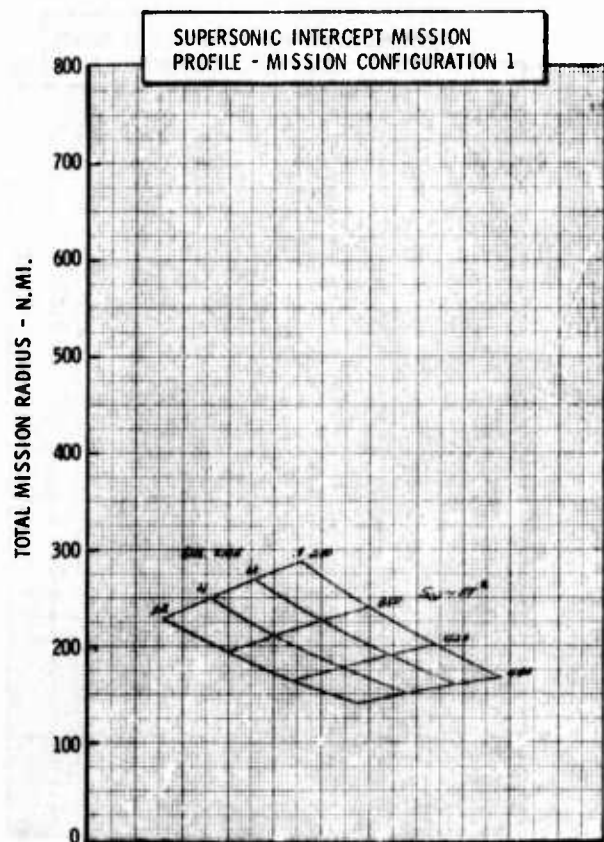
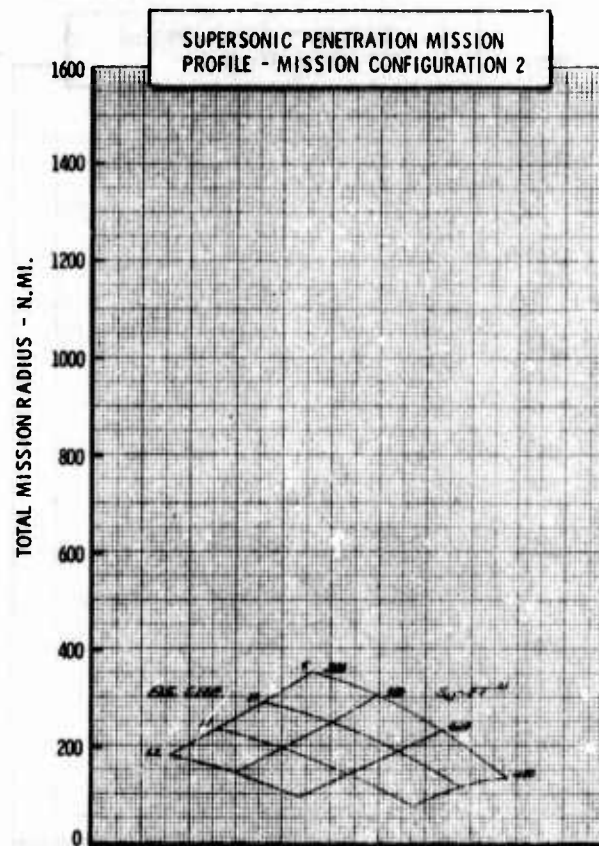
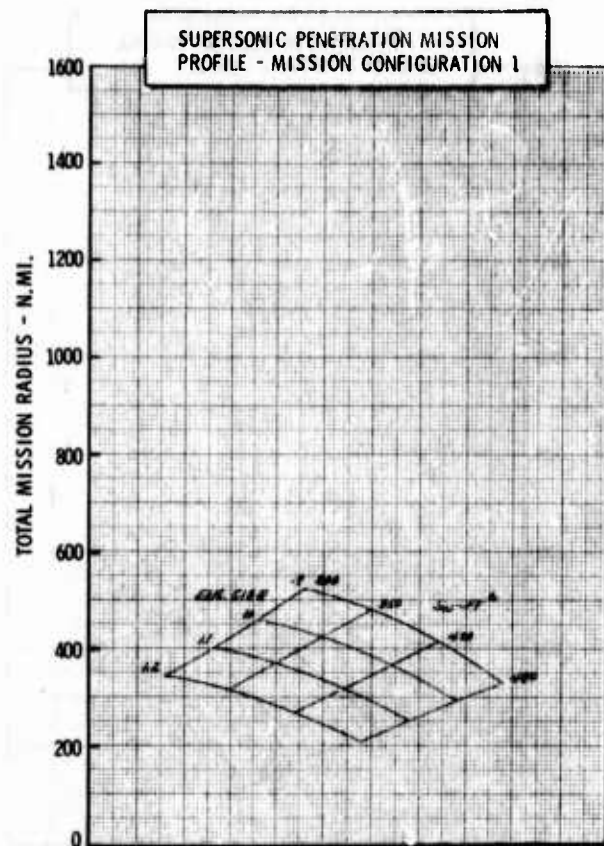


Figure H-53c LWA Mission/Configuration Tradeoff Parametric Data

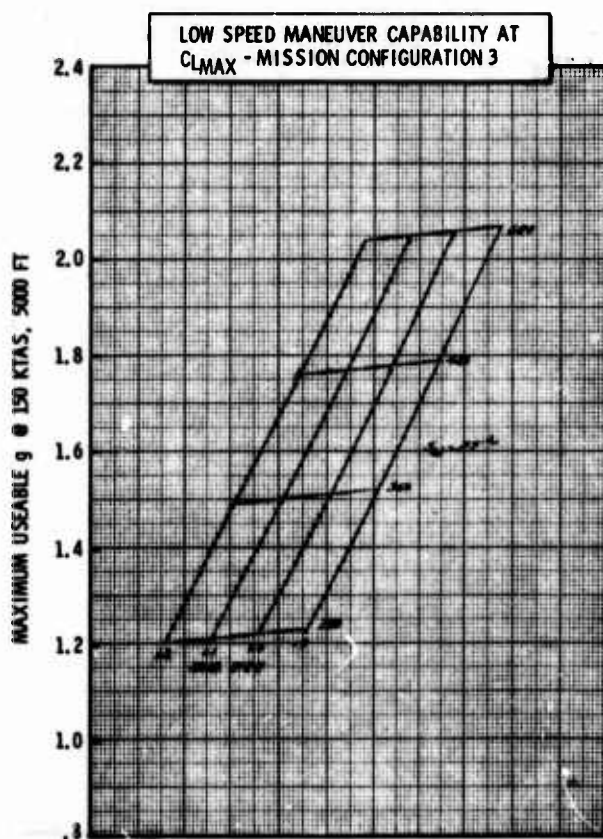
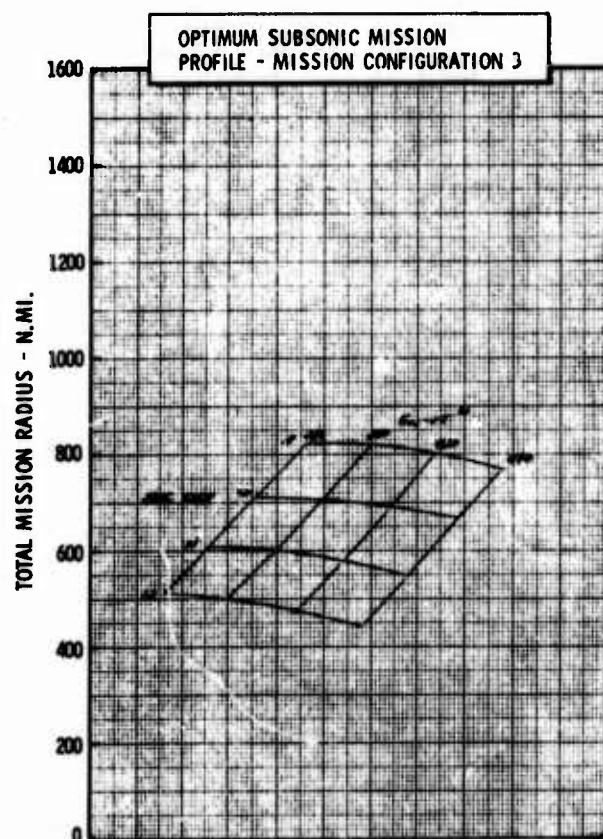
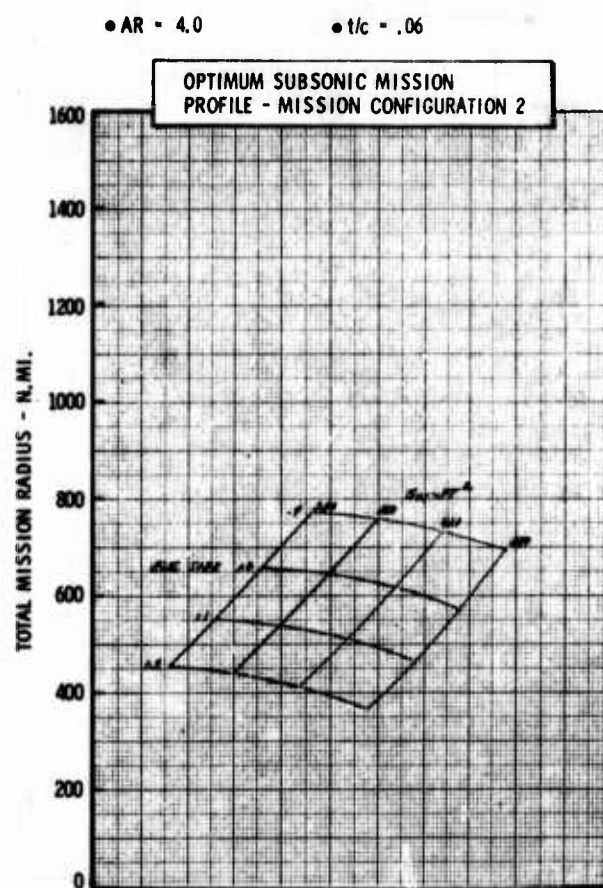
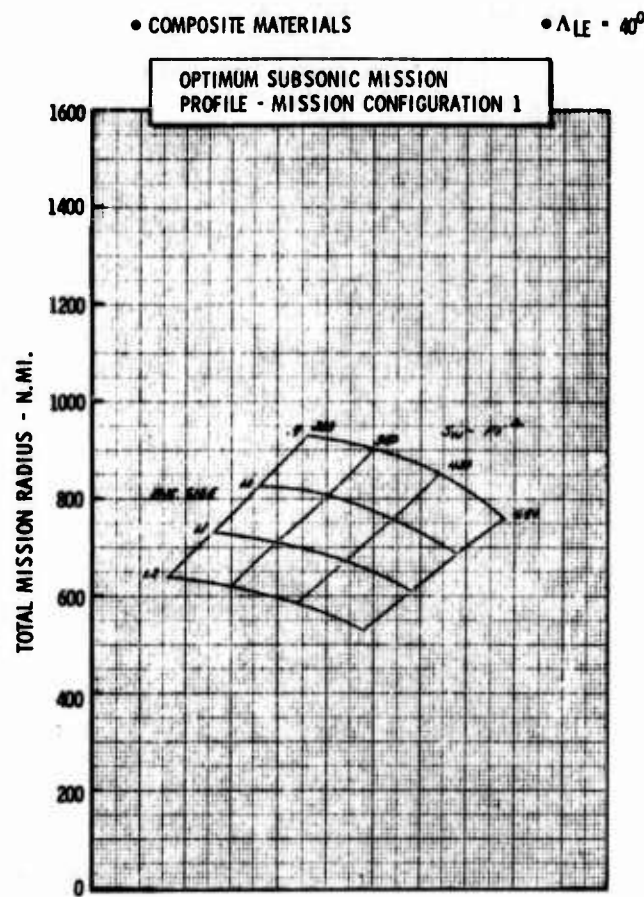
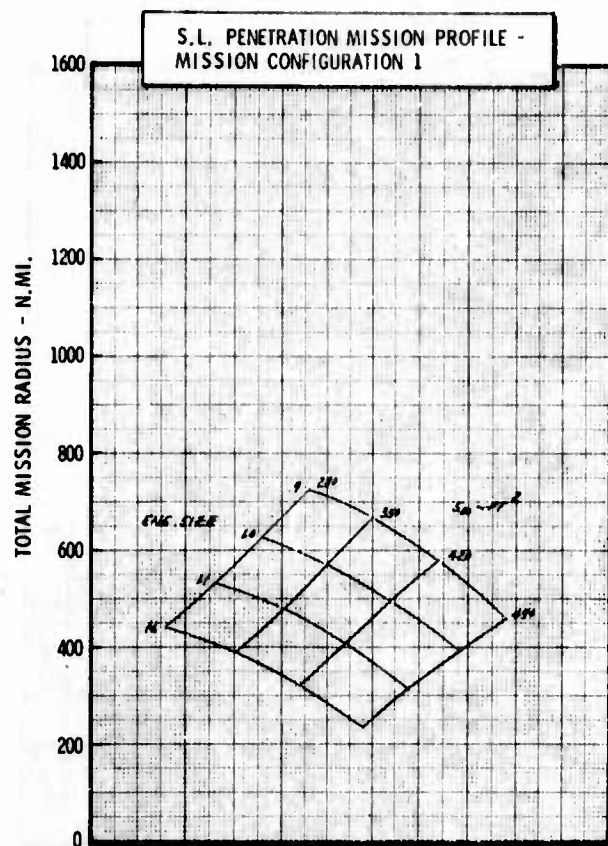


Figure H-54a LWA Mission/Configuration Tradeoff Parametric Data



•  $\Delta LE = 40^\circ$



• t/c = .06

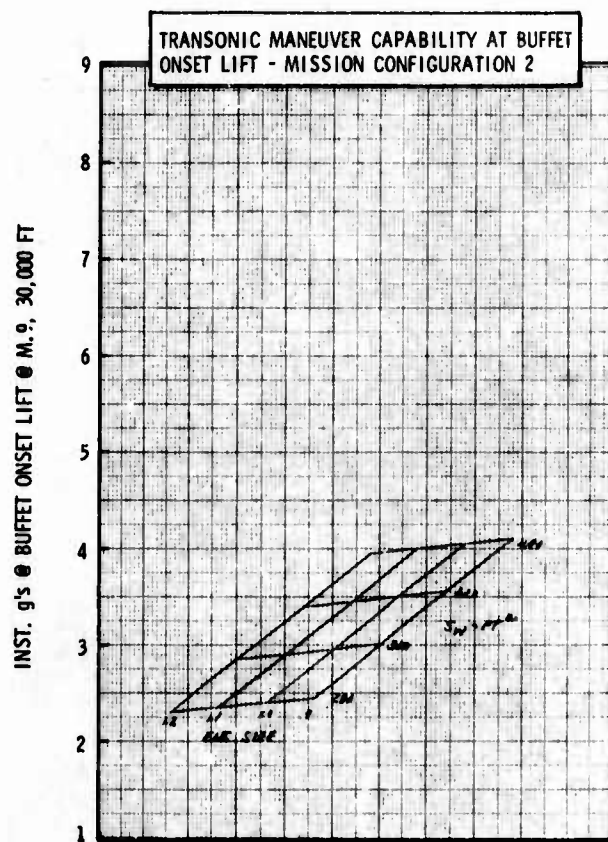
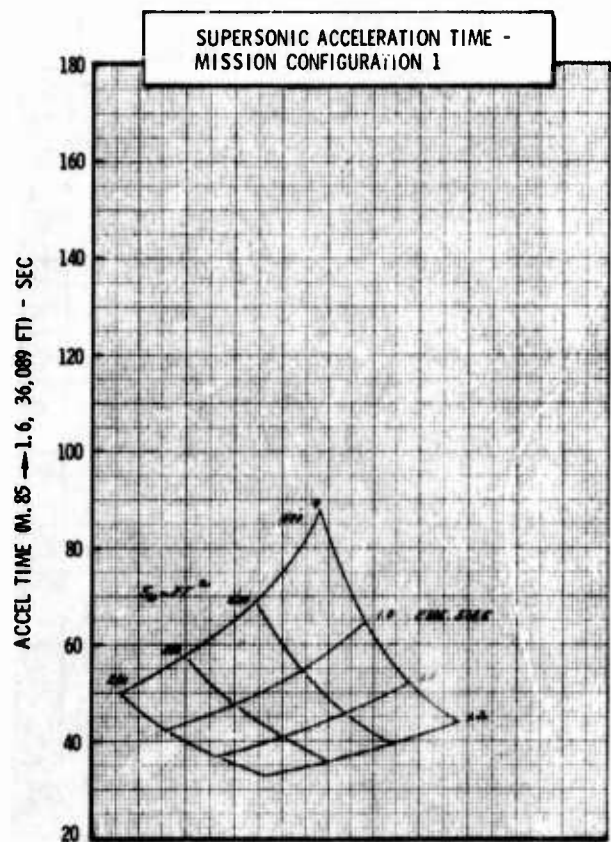
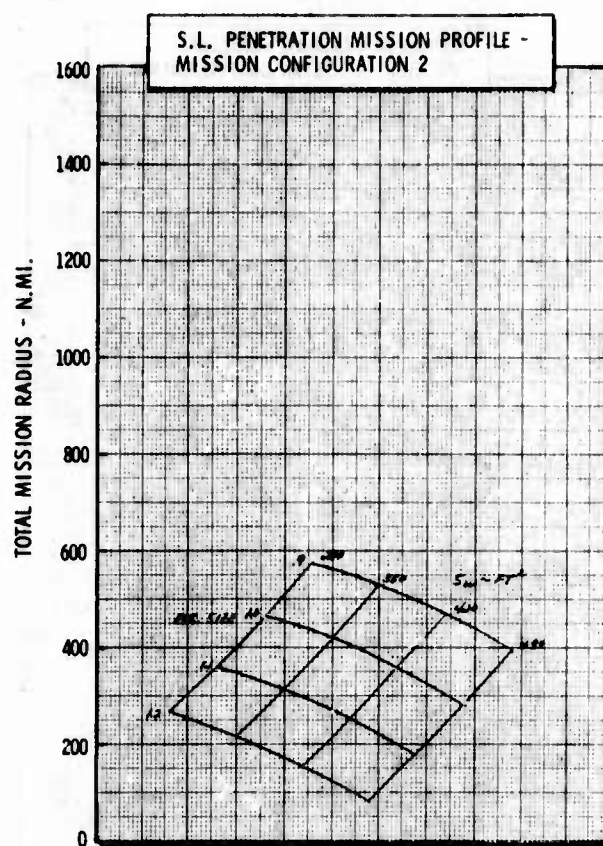


**Figure H-54b LWA Mission/Configuration Tradeoff Parametric Data**

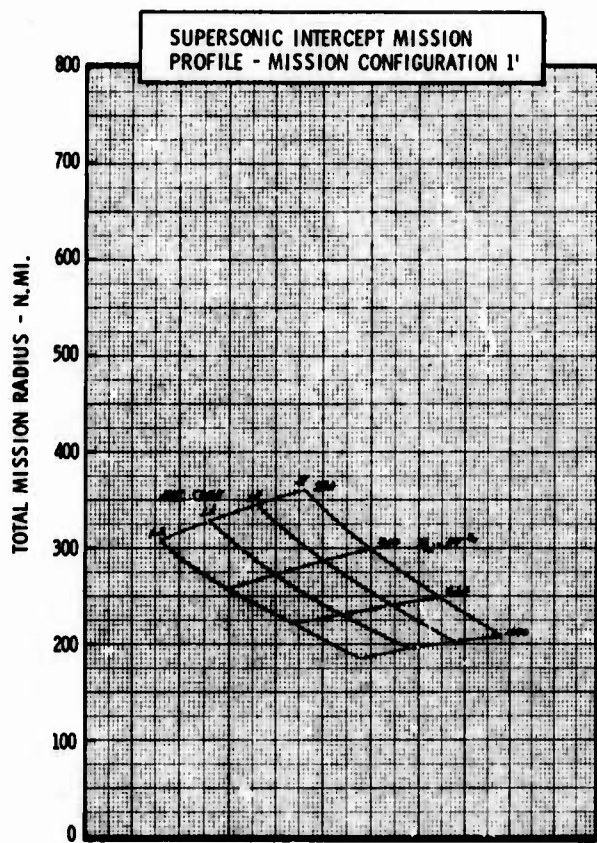
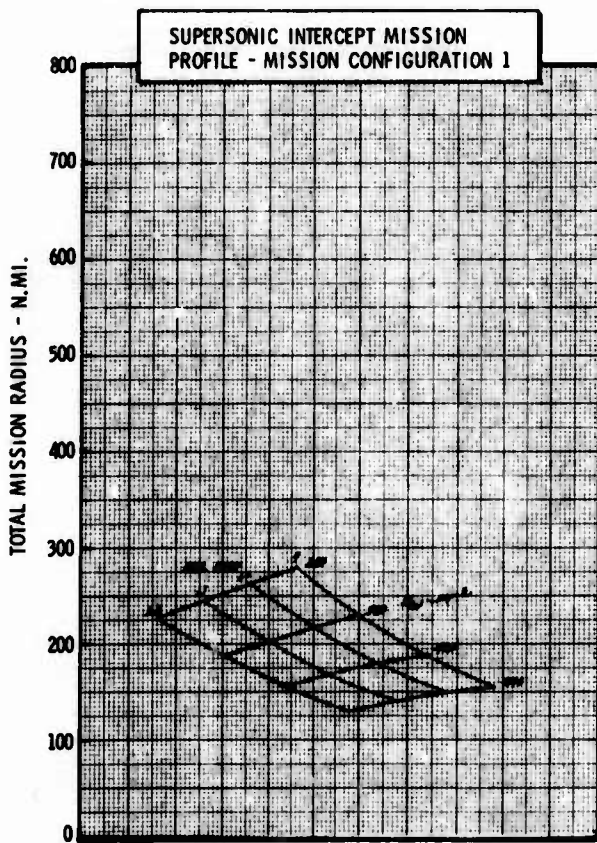
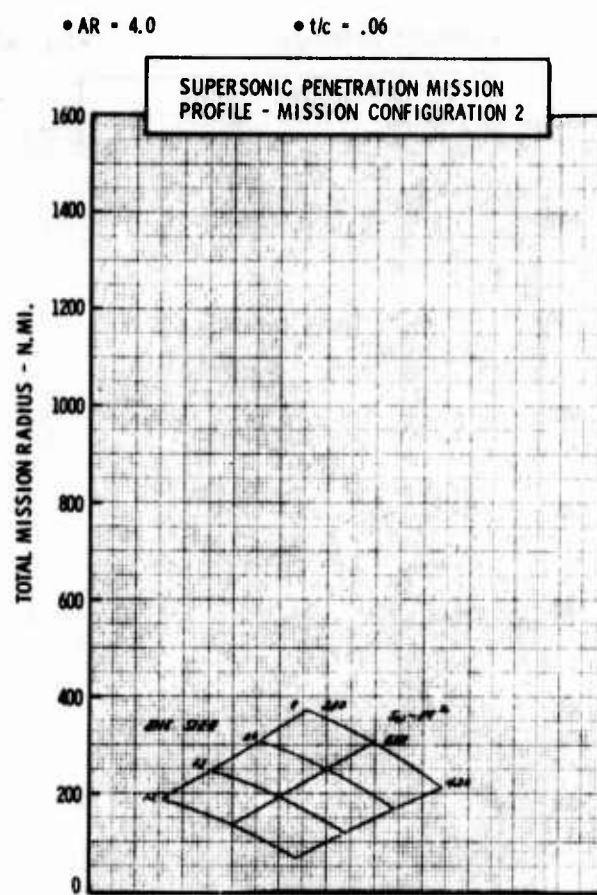
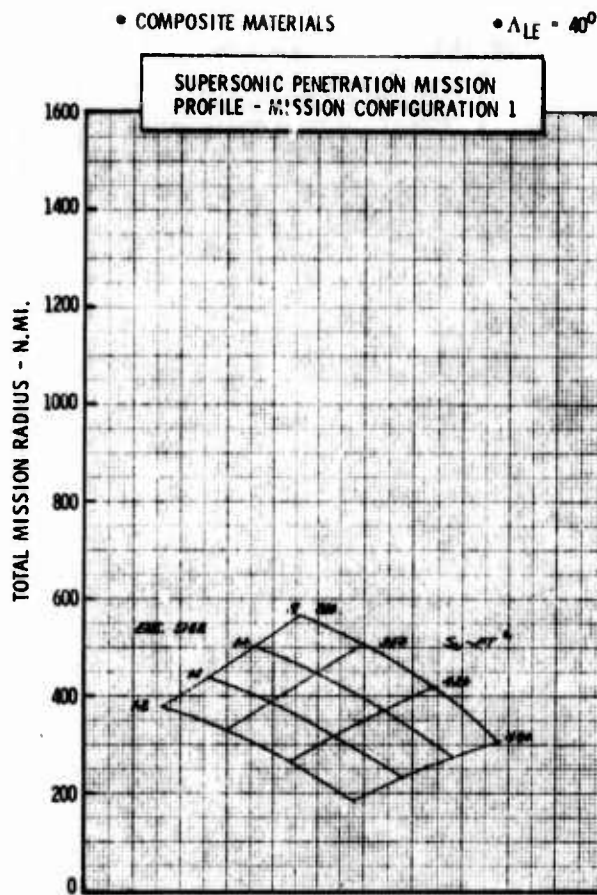


Figure H-54c LWA Mission/Configuration Tradeoff Parametric Data



• COMPOSITE MATERIALS

•  $\Delta LE = 40^\circ$

•  $AR = 5.0$

•  $t/c = .06$

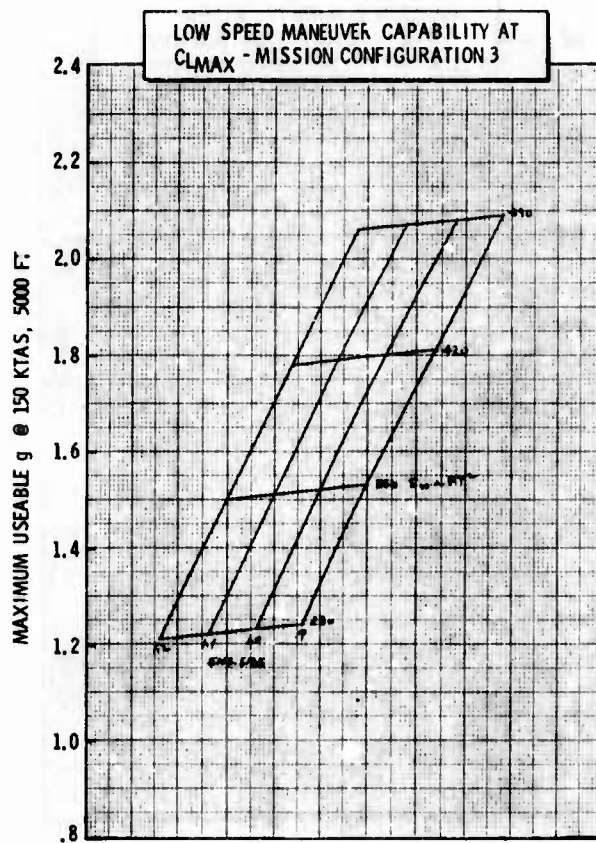
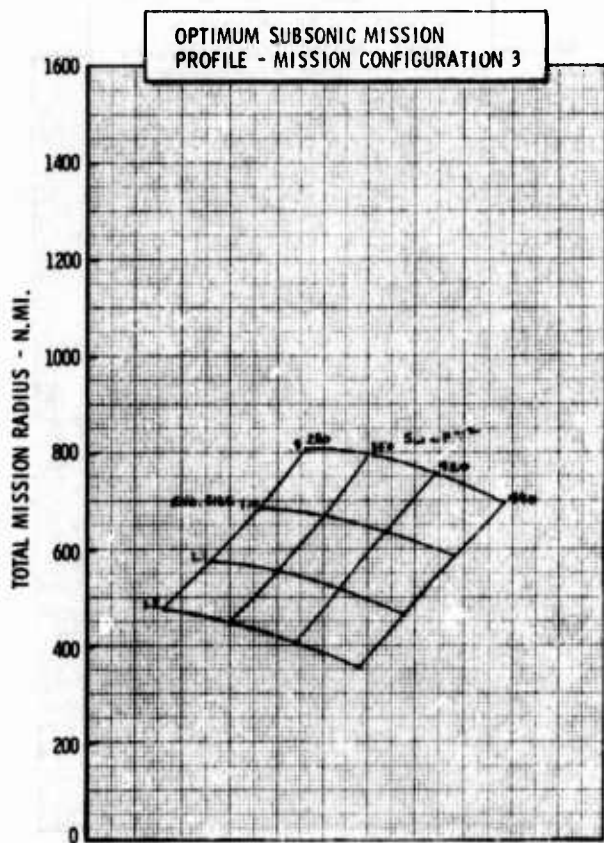
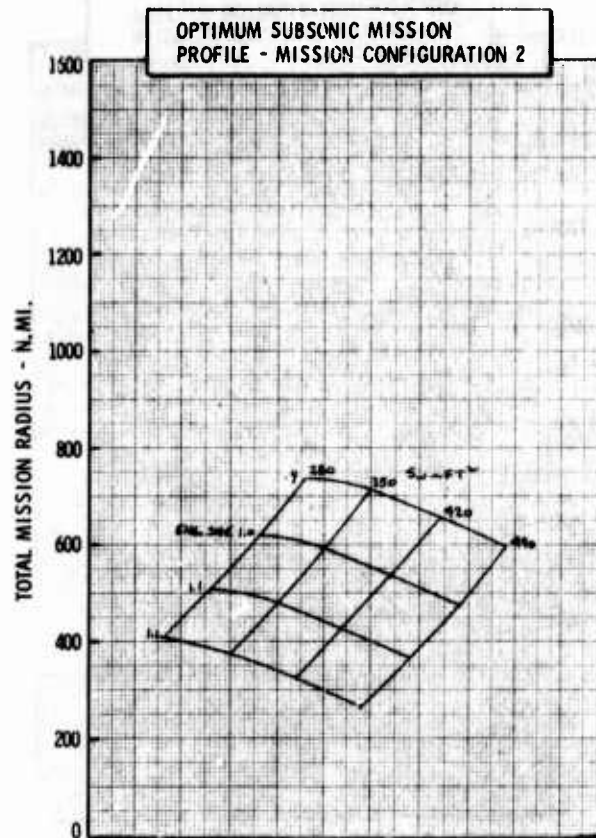
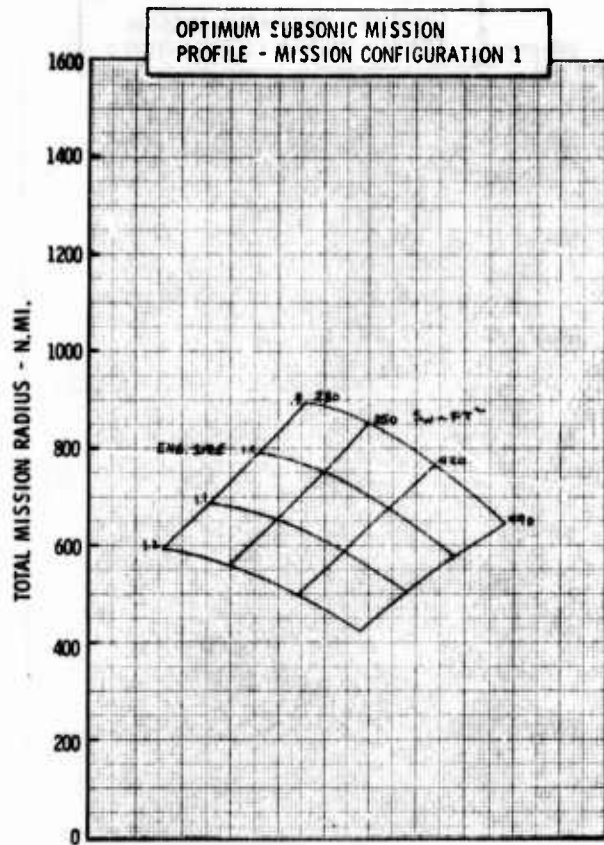


Figure H-55a LWA Mission/Configuration Tradeoff Parametric Data

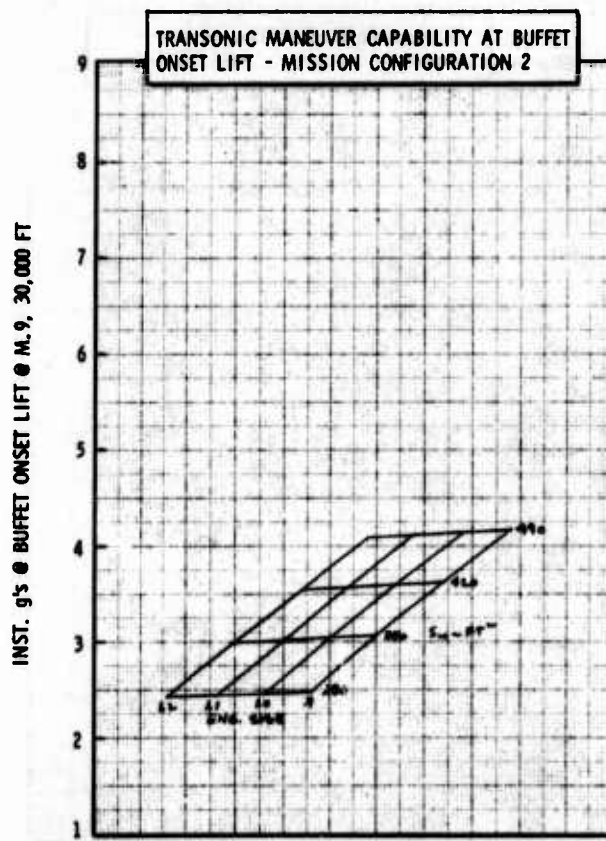
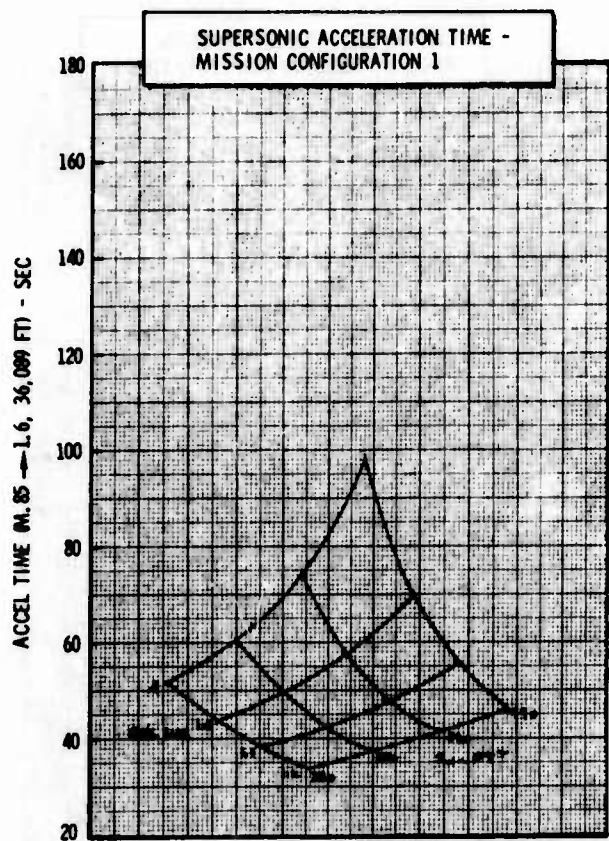
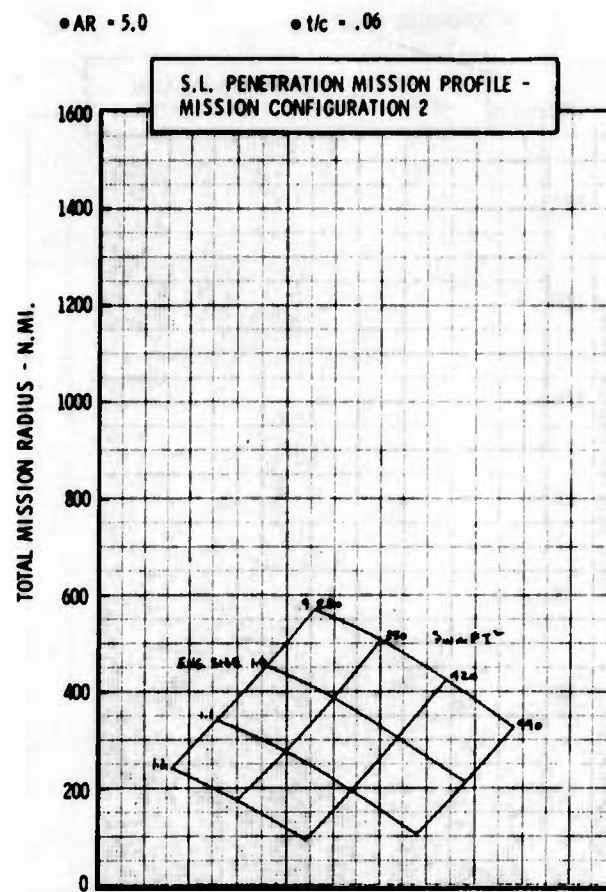
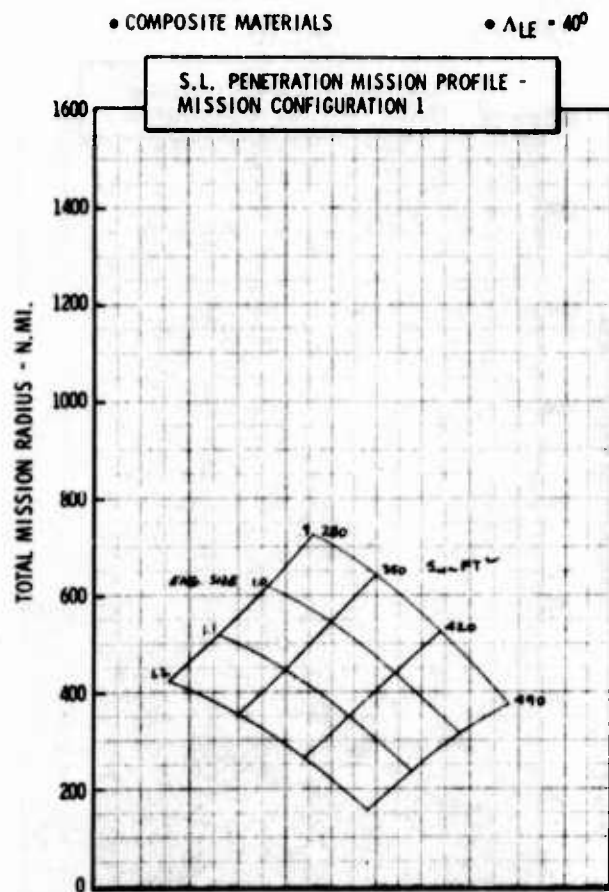
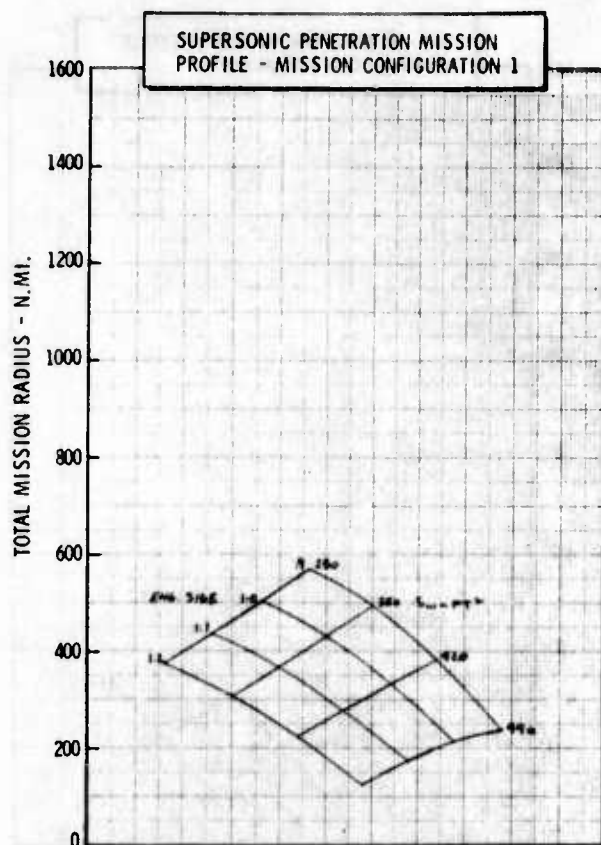


Figure H-55b LWA Mission/Configuration Tradeoff Parametric Data

• COMPOSITE MATERIALS

•  $\Lambda_{LE} = 40^\circ$



• AR = 5.0

•  $t/c = .06$

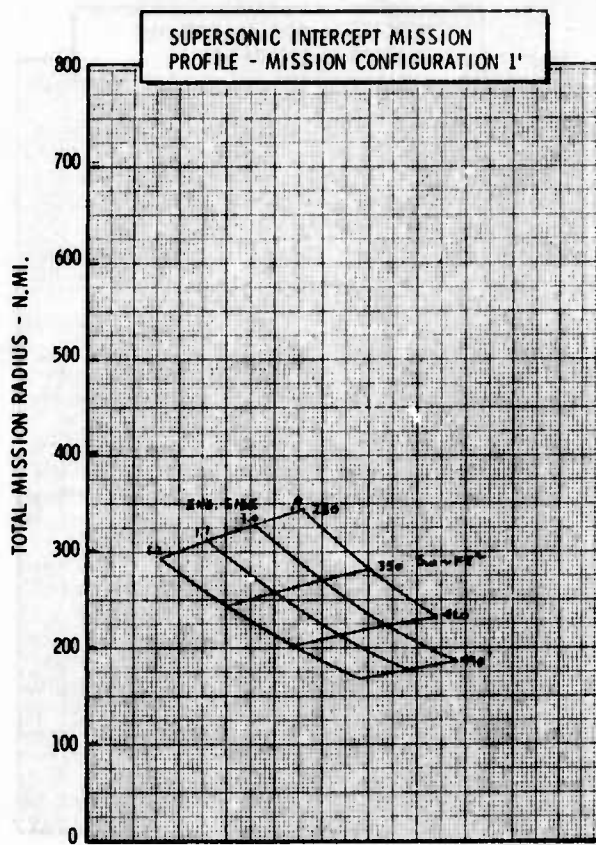
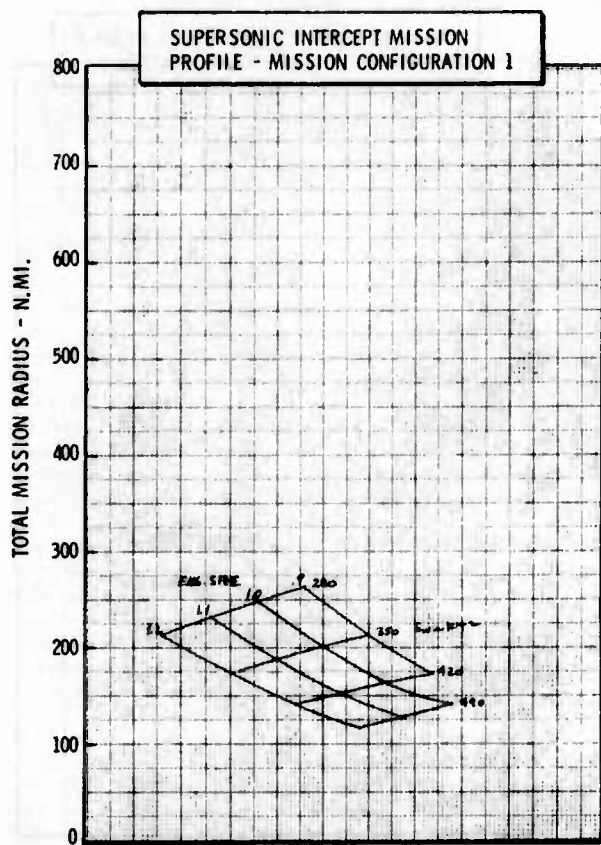
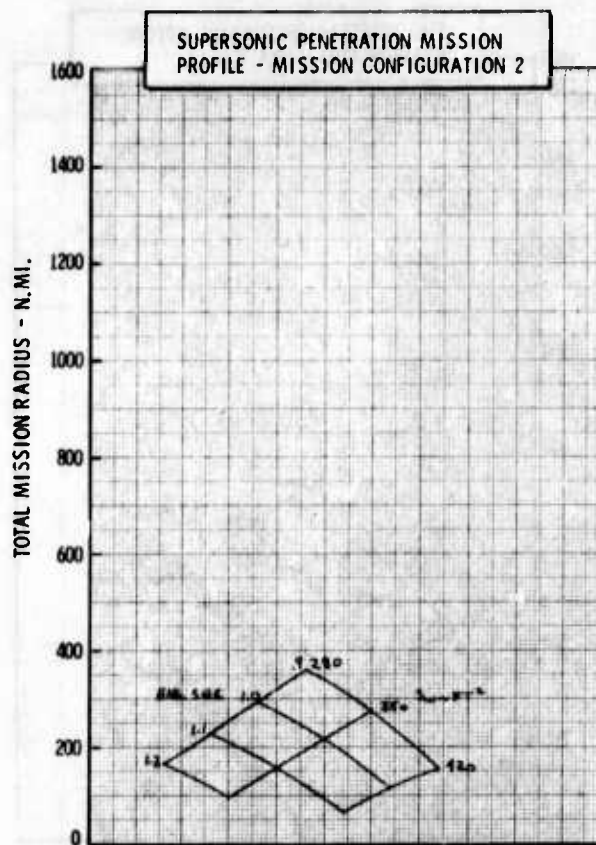


Figure H-55c LWA Mission/Configuration Tradeoff Parametric Data

## APPENDIX I

### LWA CONFIGURATION 29 SIMULATION

Simulation of the flight characteristics of the Lightweight Attack (LWA) aircraft has been accomplished on the EAI 640/231R hybrid computer in six degrees of freedom with limited nonlinear and flexibility effects. This computer simulation was utilized in conjunction with the advanced cockpit simulator and the optical display system to evaluate target tracking, weapon delivery, handling qualities, and precision landing approaches with wing jet flaps and various sideforce control modes. The simulation is flyable over the power approach and cruise envelope although the validity decreases with large excursions from the Mach-altitude flexibility schedule. The hybrid computer consists of two consoles of EAI 231-R analog equipment tied to an EAI 640 digital computer. The equations of motion, aerodynamic data, and flight control system data used in the LWA simulation are defined in this appendix. A list of symbols is included at the end of the appendix.

#### I.1 SIMULATION EQUATIONS

The LWA simulation equations are presented in Table I-1. Significant features of these equations include (1) 6-degrees-of-freedom, (2) jet flap and supercirculation effects, (3) sideforce control surface effects, and (4) nonlinear lateral-directional derivatives as a function of angle of attack and Mach number.

The sign convention for control surface, with the exception of the sideforce control surface, is such that a negative control surface deflection causes positive moments. Positive moments are defined to give climbing turn to the right.

Reference constants and physical data used in the simulation are presented in Table I-2.



Table 1-1 LIGHTWEIGHT ATTACK AIRCRAFT (LWA) SIMULATION GENERAL EQUATIONS

Equations of Motion

$$\begin{aligned}\dot{u} &= vr - wq + (1/m)(X_{AERO} + X_{THRUST}) - g \sin \theta \\ \dot{v} &= wp - ur + (1/m)(Y_{AERO}) + g \cos \theta \sin \phi \\ \dot{w} &= uq - vp + (1/m)(Z_{AERO}) + g \cos \theta \cos \phi \\ \dot{p} &= [(I_{yy} - I_{zz})qr + I_{xz}(\dot{r} + pq) + L_{AERO}] / I_{xx} \\ \dot{q} &= [(I_{zz} - I_{xx})pr + I_{xz}(r^2 - p^2) + M_{AERO} + M_{THRUST}] / I_{yy} \\ \dot{r} &= [(I_{xx} - I_{yy})pq + I_{xz}(\dot{p} - qr) + N_{AERO}] / I_{zz}\end{aligned}$$

Velocities and Rates

$$\begin{aligned}u &= u_0 + \int_0^t \dot{u} dt & p &= p_0 + \int_0^t \dot{p} dt \\ v &= v_0 + \int_0^t \dot{v} dt & q &= q_0 + \int_0^t \dot{q} dt \\ w &= w_0 + \int_0^t \dot{w} dt & r &= r_0 + \int_0^t \dot{r} dt \\ V &= (u^2 + v^2 + w^2)^{1/2} \\ M &= V/a\end{aligned}$$

where

$$\begin{aligned}a &= f(h) \\ u_0 &= V_0 \cos \alpha_0 \cos \beta_0 \\ v_0 &= V_0 \sin \beta_0 \\ w_0 &= V_0 \sin \alpha_0 \cos \beta_0\end{aligned}$$

Load Factor

$$A_N = - (Z_{AERO} / W)$$

Thrust

$$\begin{aligned}X_{THRUST} &= T_{ENG} \\ M_{THRUST} &= -1.765(T_{ENG})\end{aligned}$$

Attitude Angles and Rates

$$\begin{aligned}(\psi, \theta, \phi \text{ Sequence}) \\ \theta &= \theta_0 + \int_0^t \dot{\theta} dt & \dot{\theta} &= 57.3(q \cos \phi - r \sin \phi) \\ \phi &= \phi_0 + \int_0^t \dot{\phi} dt & \dot{\phi} &= 57.3(p) + \dot{\psi} \sin \theta \\ \psi &= \psi_0 + \int_0^t \dot{\psi} dt & \dot{\psi} &= 57.3(q \sin \phi + r \cos \phi) / \cos \theta\end{aligned}$$

Wind Angles

$$\begin{aligned}\alpha &= \tan^{-1} w/u + \alpha_G \\ \beta &= \sin^{-1} v/V + \beta_G\end{aligned}$$

Forces and Moments

$$\begin{aligned}X_{AERO} &= C_x \dot{q} S & L_{AERO} &= C_l \dot{q} S b \\ Y_{AERO} &= C_y \dot{q} S & M_{AERO} &= C_m \dot{q} S \bar{c} \\ Z_{AERO} &= C_z \dot{q} S & N_{AERO} &= C_n \dot{q} S b\end{aligned}$$

where

$$\begin{aligned}\dot{q} &= 1481(p/p_0)M^2 \\ p/p_0 &= f(h)\end{aligned}$$

Accelerometer Equations

$$\begin{aligned}A_{N_{ACC}} &= - \left( \frac{Z_{AERO}}{W} \right) - 1 + \frac{\Delta I_{AN} \dot{q}}{1845} \\ A_{Y_{ACC}} &= \left( \frac{Y_{AERO}}{W} \right) + \frac{\Delta I_{AY} \dot{r}}{1845}\end{aligned}$$

Lift Coefficient

$$\begin{aligned}C_L &= C_L' + \Delta C_{Lc} \\ C_L' &= C_{L_{C_{\mu}=0}} + \Delta C_{L\delta c} + \Delta C_{L\delta f} \\ C_{L_{C_{\mu}=0}} &= C_{L_{\alpha_0}} (\alpha - \alpha_{L0}) & C_L &\leq C_{LBR} \\ &= C_{L_{\alpha_0}} (\alpha_{BR} - \alpha_{L0}) + C_{La1} (\alpha - \alpha_{BR}) & & \\ & & C_L &> C_{LBR} \\ \alpha_{BR} &= \left( \frac{C_{LBR}}{C_{L_{\alpha_0}}} \right)_{C_{\mu}=0} + \alpha_{L0}\end{aligned}$$

$$\Delta C_{L\delta c} = C_{L\delta c} \delta_c \quad C_{L\delta c} = f(M)$$

$$\Delta C_{L\delta f} = C_{L\delta f} \delta_f \quad C_{L\delta f} = f(M)$$

$$\Delta C_{Lc} = \Delta C_{L1} + 1.05 \left[ \left( \frac{\partial \Delta C_L}{\partial M} \right)_{M_{LD}} \right] M^2$$

$$\Delta C_{L1} = [C_{L1}(\alpha) C_{\mu, \theta_1} - 4.42a] F_s$$

$$F_s = f(\theta)$$

$$\begin{aligned}C_{L1}(\alpha) C_{\mu, \theta_1} &= 1.06F [0.26\theta C_{1\theta_1} + \nu \alpha C_{1\alpha}] \\ &\quad - .06C_{\mu}' (\theta_1 + \alpha)\end{aligned}$$

where  $\theta_1$  and  $\alpha$  are in radians

$$\nu = \left[ \frac{.26C_{1\alpha} + 4.64}{C_{1\alpha}} \right] C_{\mu}'$$

$$C_{\mu}' = C_{\mu} / .26$$

$$C_{1\alpha}, C_{1\theta_1} = f(C_{\mu}')$$

$$\begin{aligned}F &= (4 + .64 C_{\mu}) / (6 + .6\sqrt{C_{\mu}} \\ &\quad + .88 C_{\mu})\end{aligned}$$

$$\frac{\partial \Delta C_L}{\partial M} = f(\Delta C_{L1})$$

$$C_{LMAX} = (C_{LMAX})_{C_{\mu}=0} + (\Delta C_{Lc})_{\alpha_{BR}}$$

Drag Coefficient

$$C_D = C_{DMIN} + C_{DL} - r' C_{\mu} + \Delta C_{DSB} + \Delta C_{D\delta c} + \Delta C_{D\delta f}$$

$$C_{DMIN} = C_{DMINALT} + \Delta C_{DALT}$$

$$C_{DMINALT} = f(M)$$

$$\Delta C_{DALT} = f(M)$$



Table 1-1 (Cont'd)

$$C_{DL} = K_0(C_L - \Delta C_{L0})^2 \quad C_L < C_{LBR}$$

$$= \left[ \sqrt{K_0}(C_{LBR} - \Delta C_{L0}) + \sqrt{K_1}(C_L - C_{LBR}) \right]^2$$

$$C_L > C_{LBR}$$

$$K_0 = \frac{1}{\pi AR e_0 + 2C_{\mu}}$$

$$K_1 = \frac{1}{\pi AR e_1 + 2C_{\mu}}$$

$$e_0 = f(M) \quad ; \quad e_1 = f(M)$$

$$C_{LBR} = (C_{LBR})_{C_{\mu}=0} + (\Delta C_{Lc})_{a_0}$$

$$\Delta C_{L0} = (C_{L0})_{C_{\mu}=0} + [(\Delta C_{Lc})_{a_0}] / .38$$

$$(\Delta C_{L0})_{C_{\mu}=0} = f(M)$$

$$a_0 = \left( \frac{\Delta C_{L0}}{C_{L00}} \right)_{C_{\mu}=0} + a_{L0}$$

$$r' = f(\theta_1 + \alpha)$$

$$\Delta C_{D_{SB}} = C_{D_{SB}} \delta_{SB}$$

$$\Delta C_{D_{\delta c}} = C_{D_{\delta c}} \delta_c^2$$

$$C_{D_{\delta c}}^2 = [.000047 + .000178(C_L')^2] 1.272$$

$$M < .6$$

$$= [.000025 + .000039(C_L')^2] 1.272$$

$$M > .9$$

$$= \text{linear interpolation} \quad .6 < M < .9$$

$$\Delta C_{D_{\delta f}} = C_{D_{\delta f}} \delta_f^2$$

Axial Force Coefficient

$$C_x = C_L \sin \alpha - C_D \cos \alpha$$

Normal Force Coefficient

$$C_z = -C_L \cos \alpha - C_D \sin \alpha - C_{Nq} \left( \frac{q\bar{c}}{2V} \right)$$

$$C_{Nq} = f(M)$$

Sideforce Coefficient

$$C_y = (R_{y\beta} C_{y\beta} + C_{y\delta a} \delta_a + C_{y\delta s} \delta_s + C_{y\delta r} \delta_r)_{\text{AERO}} + (C_{yp} + C_{yr}) (b/2V)_{\text{STATIC}}$$

$$R_{y\beta}, C_{y\beta}, C_{y\delta a}, C_{y\delta s}, C_{y\delta r} = f(M)$$

$$C_{yp}, C_{yr} = f(M, \alpha)$$

Pitching Moment Coefficient

$$C_m = C_{m0} + C_{ma}(\alpha - \alpha_{L0}) + C_{m\delta c} \delta_c + C_{m\delta f} \delta_f$$

$$+ \Delta C_{m_{JET}} + C_{mq} \left( \frac{q\bar{c}}{2V} \right) + C_L' \left( \frac{CG - CG_{REF}}{100} \right)_{@C_{\mu}}$$

$$C_{m0}, C_{ma}, C_{m\delta c}, C_{m\delta f}, C_{mq} = f(M)$$

$$\Delta C_{m_{JET}} = -C_{\mu} \sin \theta_j (CP_{JET} - CG) + C_{\mu} \cos \theta_j (Z_{CG} - Z_{JET})_{@C_{\mu}}$$

where  $(CP_{JET} - CG), (Z_{CG} - Z_{JET})$  are fractional  $\bar{c}$

Rolling and Yawing Moment Coefficient

$$C_l = C_{lB} + (C_{lp} + C_{lr}) \frac{b}{2V}$$

$$C_n = C_{nB} + (C_{np} + C_{nr}) \frac{b}{2V} + C_{y_{AERO}} \left( \frac{CG - CG_{REF}}{100} \right) \frac{\bar{c}}{b}_{\text{STATIC}}$$

$$C_{lB} = C_{lS} \cos \alpha - C_{nS} \sin \alpha$$

$$C_{nB} = C_{lS} \sin \alpha + C_{nS} \cos \alpha$$

$$C_{lS} = R_{l\beta} C_{l\beta} + R_{l\delta a} C_{l\delta a} + C_{l\delta r} \delta_r + C_{l\delta s} \delta_s$$

$$C_{nS} = R_{n\beta} C_{n\beta} + C_{n\delta a} \delta_a + C_{n\delta r} \delta_r + C_{n\delta s} \delta_s$$

$$R_{l\beta}, C_{l\beta}, R_{l\delta a}, C_{l\delta a}, C_{l\delta s}, C_{l\delta r}, C_{l\delta r} = f(M)$$

$$R_{n\beta}, C_{n\beta}, C_{n\delta a}, R_{n\delta r}, C_{n\delta r} = f(M)$$

$$C_{lr}, C_{np}, C_{nr} = f(M, \alpha)$$

Mass

$$m = W/32.2$$

Altitude

$$h = u \sin \theta - v \cos \theta \sin \phi - w \cos \theta \cos \phi$$

$$h = h_0 + \int_0^t h dt$$

Thrust

$$\text{Engine: } T_{ENG} = R_T T_{MIL}$$

$$T_{MIL} = f(M, h)$$

$$R_T = 1.0$$

Full Throttle

$$R_T = 0.$$

Idle Throttle

where  $R_T$  is linearly interpolated between throttle settings

$$\text{Jet: } C_{\mu} = R_T C_{\mu \text{ NO BURNING}} \quad \text{Variable Throttle Position}$$

$$C_{\mu} = C_{\mu \text{ BURNING}} \quad \text{Throttle in Afterburner}$$

Table 1-2 LWA CONFIGURATION CONSTANTS

S	300.	ft <sup>2</sup>
$\bar{c}$	9.388	ft
b	34.75	ft
CG	15.0	% $\bar{c}$
CG <sub>REF</sub>	25.0	% $\bar{c}$
W	21053.	lbs
I <sub>xx</sub>	16508.	slug - ft <sup>2</sup>
I <sub>yy</sub>	55182.	slug - ft <sup>2</sup>
I <sub>zz</sub>	64025.	slug - ft <sup>2</sup>
I <sub>xz</sub>	136.	slug - ft <sup>2</sup>
CP <sub>JET</sub> - CG	3.304	ft
Z <sub>CG</sub> - Z <sub>JET</sub>	0.984	ft

## I.2 AERODYNAMICS

Aerodynamic derivatives and coefficients were established for the design flight conditions shown in Figure I-1. The data are given in Figures I-2 through I-20 and Table I-3. The aerodynamic data have been flexibilized on the Mach-altitude schedule shown in Figure I-1. Large deviations from this schedule will cause the flexibilizing factor to be in error, however, the area of interest for this program is well covered by this schedule.

The maximum lift coefficient utilized in the simulator was limited to the value shown in Figure I-12.

The thrust variation with Mach number and altitude for Intermediate Power and jet flap operation is presented in Tables I-4 and I-5, respectively. Engine thrust and wing blowing adjustments were made with the throttle. Wing burning was initiated by advancing the throttle to the afterburner position.

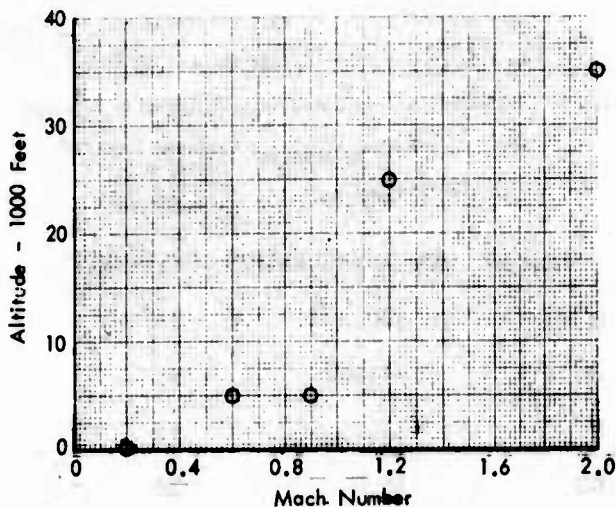


Figure I-1 Design Flight Conditions

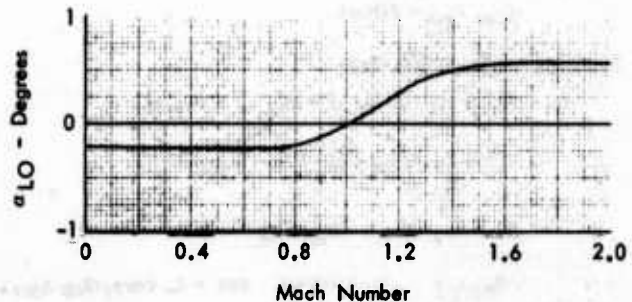
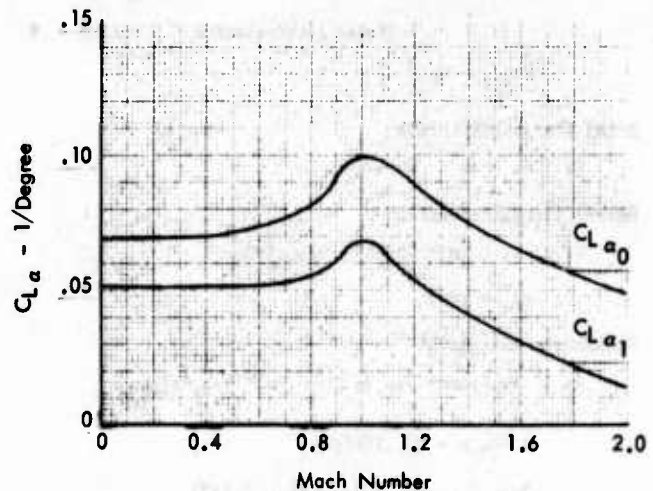


Figure I-2 Lift Curve Slope and Intercept

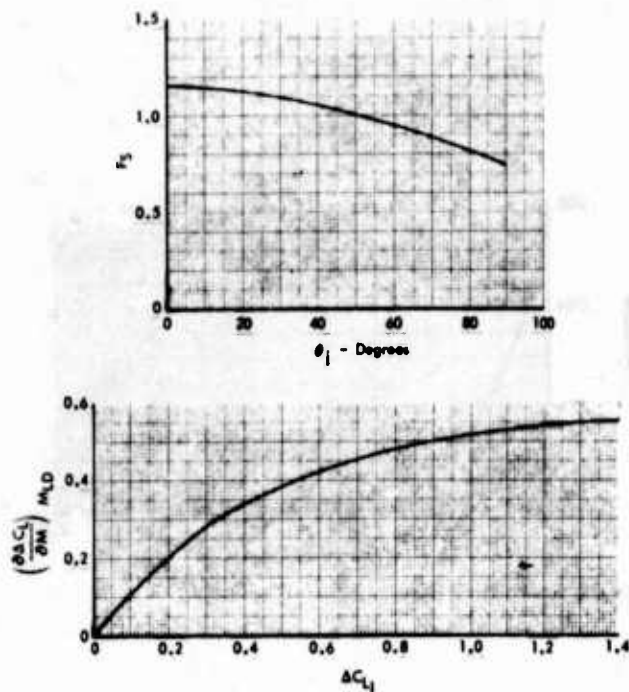


Figure 1-3 Supercirculation Parameters

$$C_{DMin} = C_{DMin} + K_B \left( \frac{.001}{M} \right) \left( 1 - \frac{\theta_i}{30} \frac{1}{LM} \right)$$

$K_B = 1.0$  Wing Burning

$K_B = 0.3$  No Wing Burning

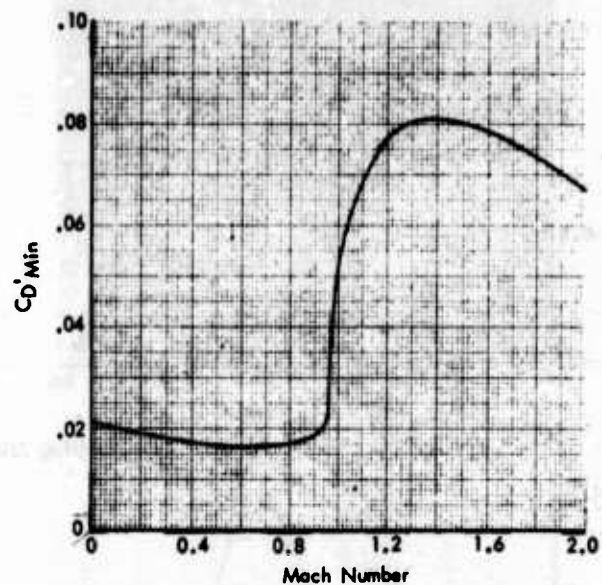


Figure 1-5 Minimum Drag Coefficient

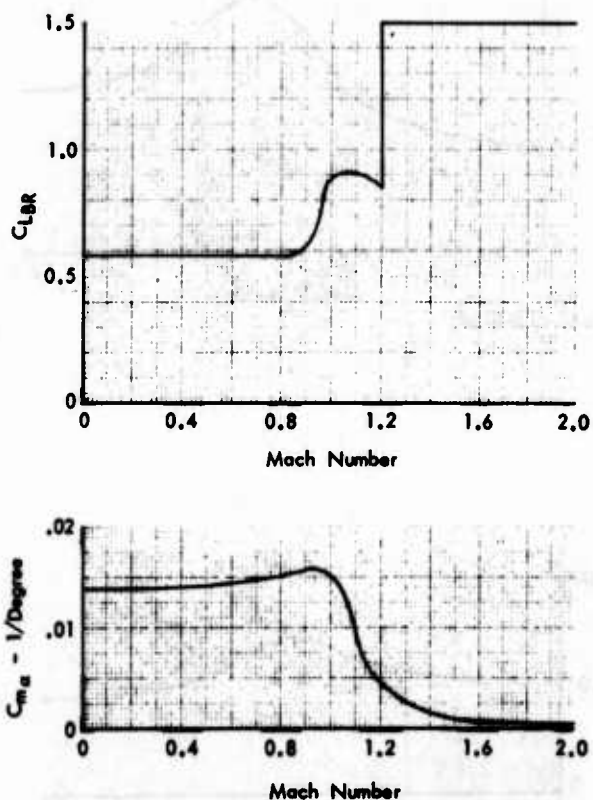


Figure 1-4 Lift Curve Break and Moment Curve Slope

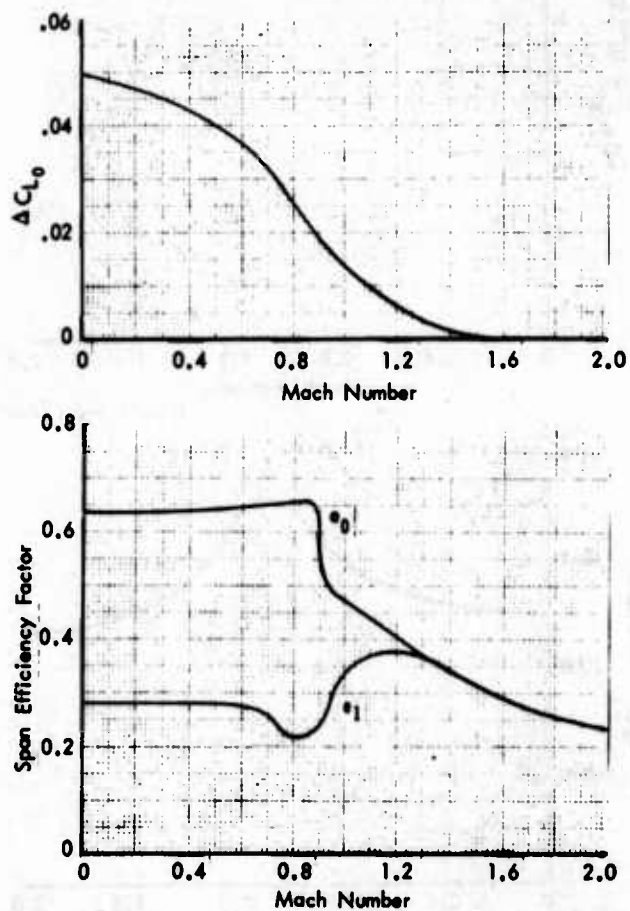


Figure 1-6 Minimum Drag Lift Coefficient and Span Efficiency Factors

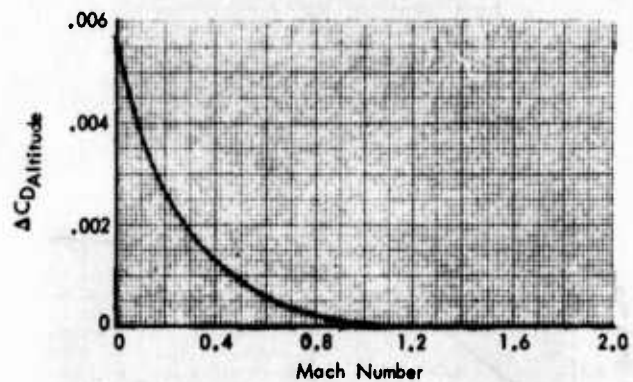
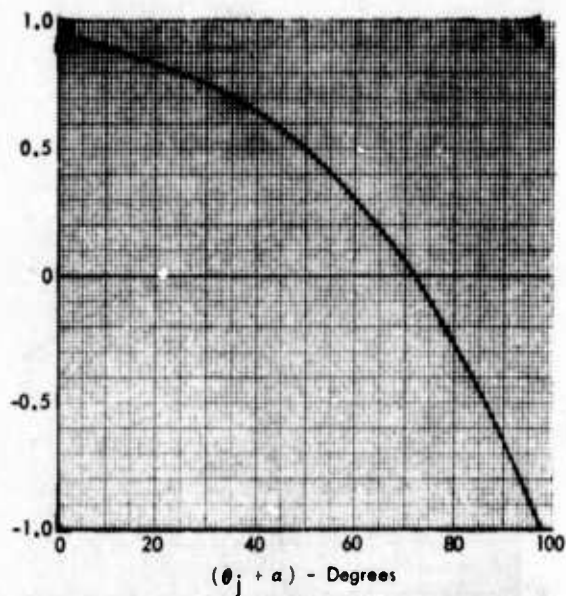


Figure 1-7 Jet Flap Drag and Altitude Correction Parameters

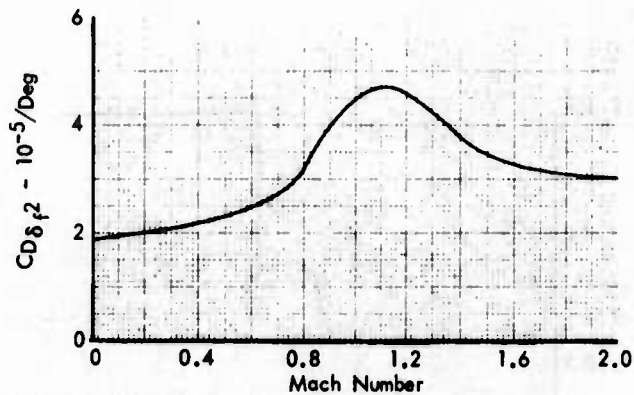
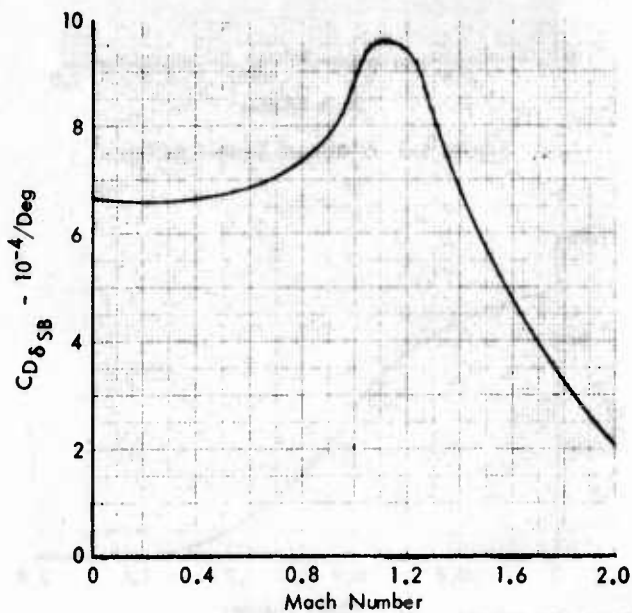


Figure 1-8 Speedbrake and Flap Drag

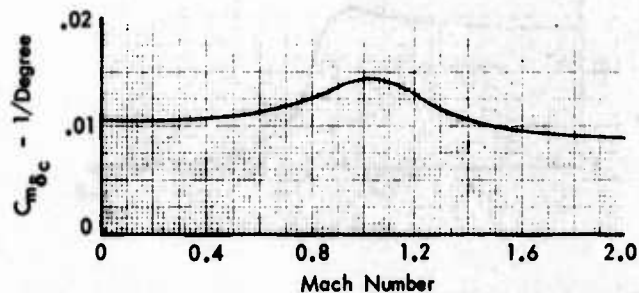
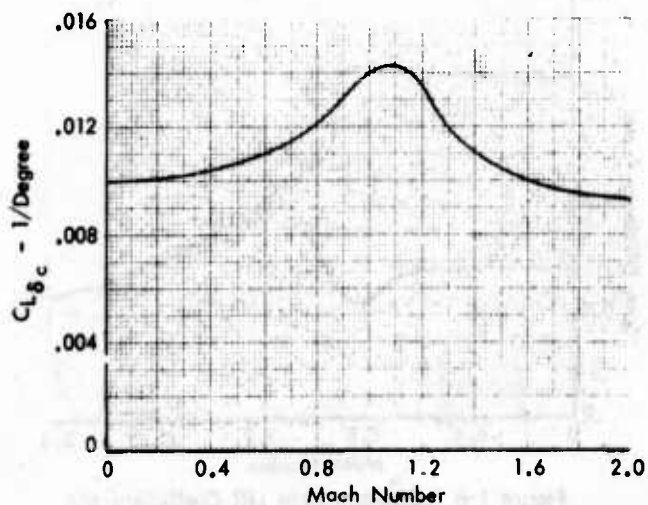


Figure 1-9 Canard Lift and Moment Curves



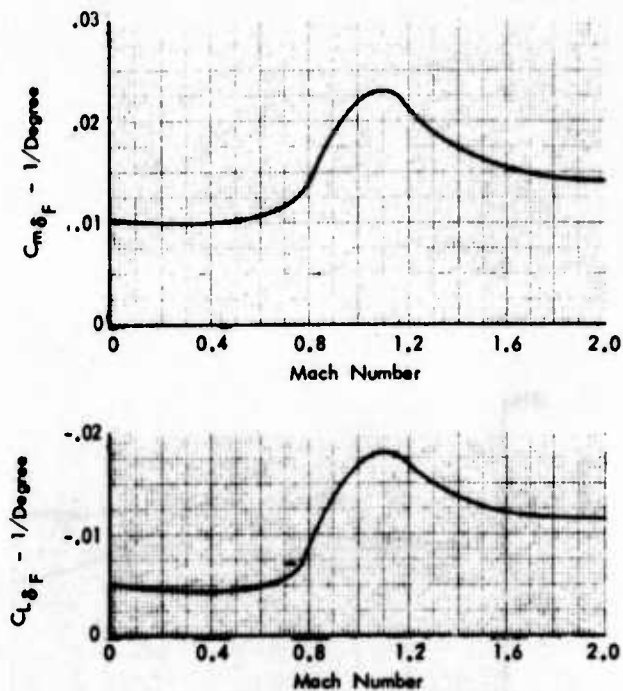


Figure 1-10 Flap Lift and Moment Curves

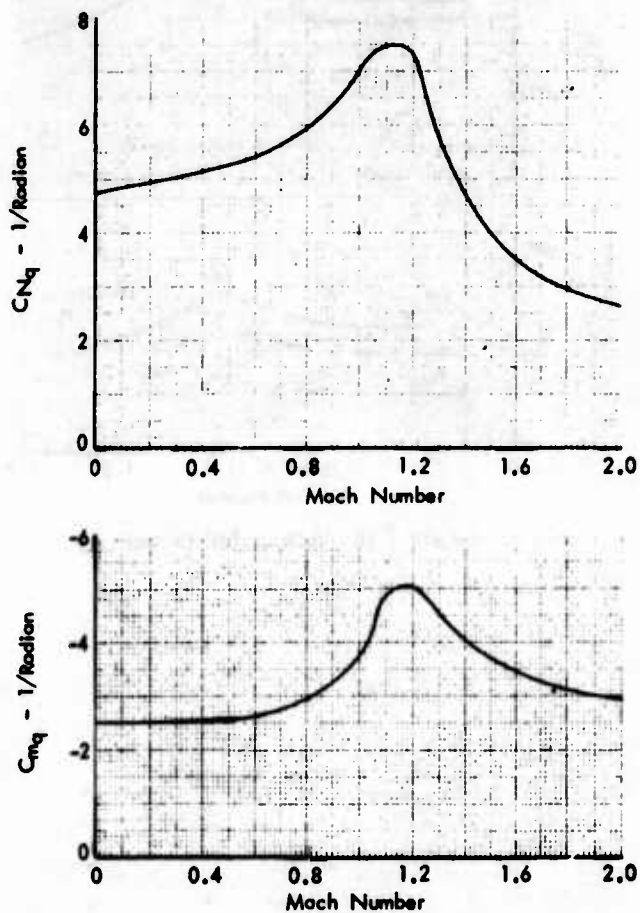


Figure 1-11 Pitch Rate Derivatives

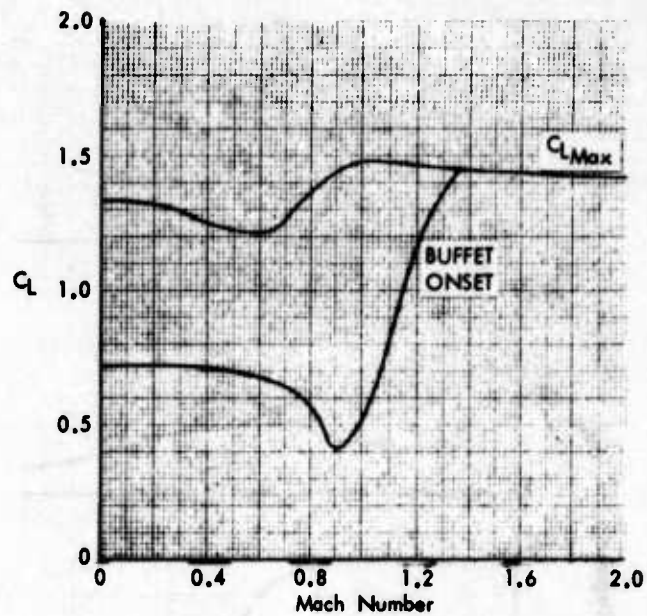


Figure 1-12 Maximum Lift Coefficient

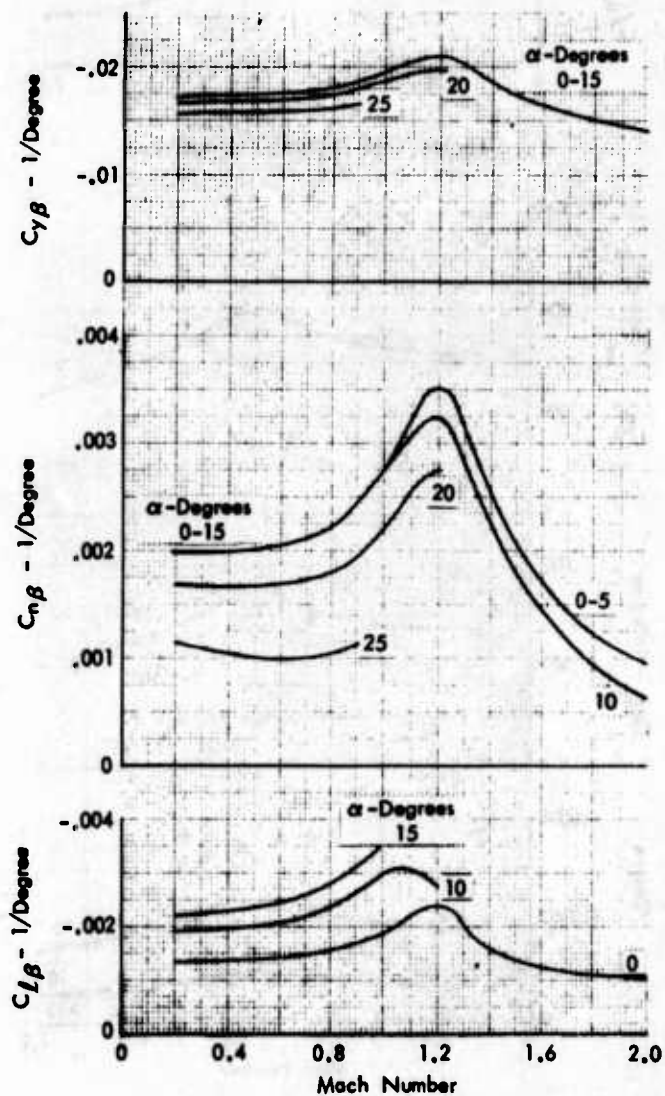


Figure 1-13 Sideslip Derivatives



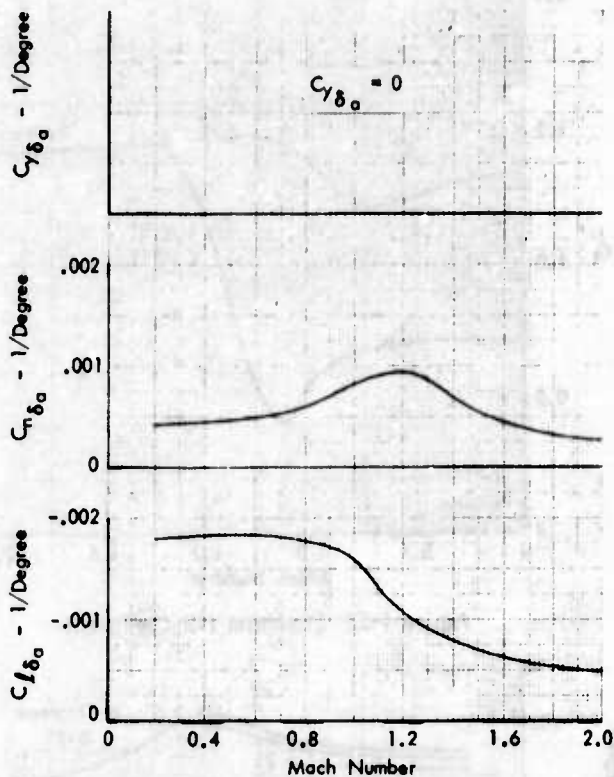


Figure I-14 Aileron Derivatives

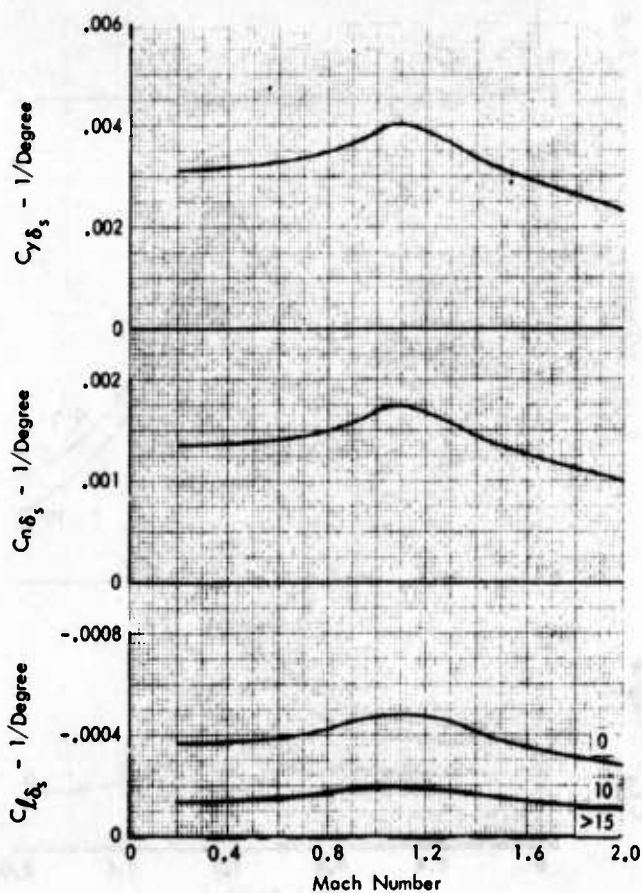


Figure I-15 Sideforce Derivatives

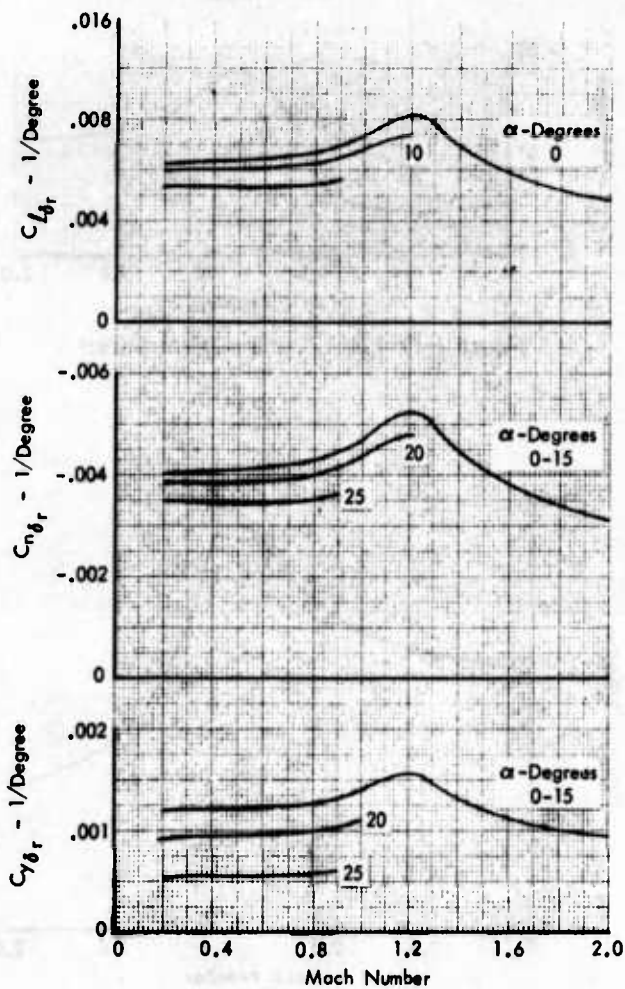


Figure I-16 Vertical Tail Derivatives

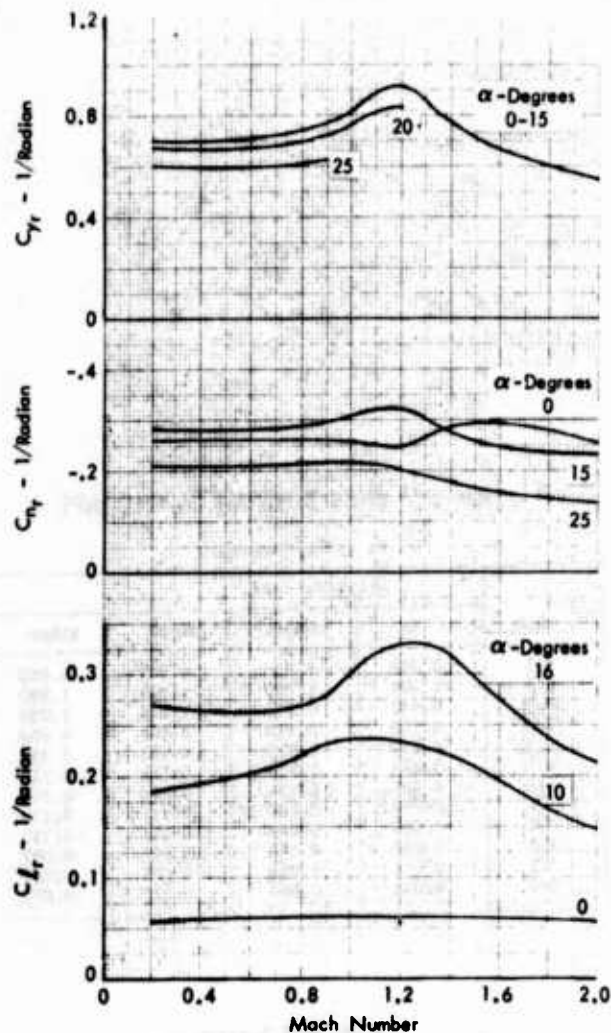


Figure 1-17 Yaw Rate Derivatives

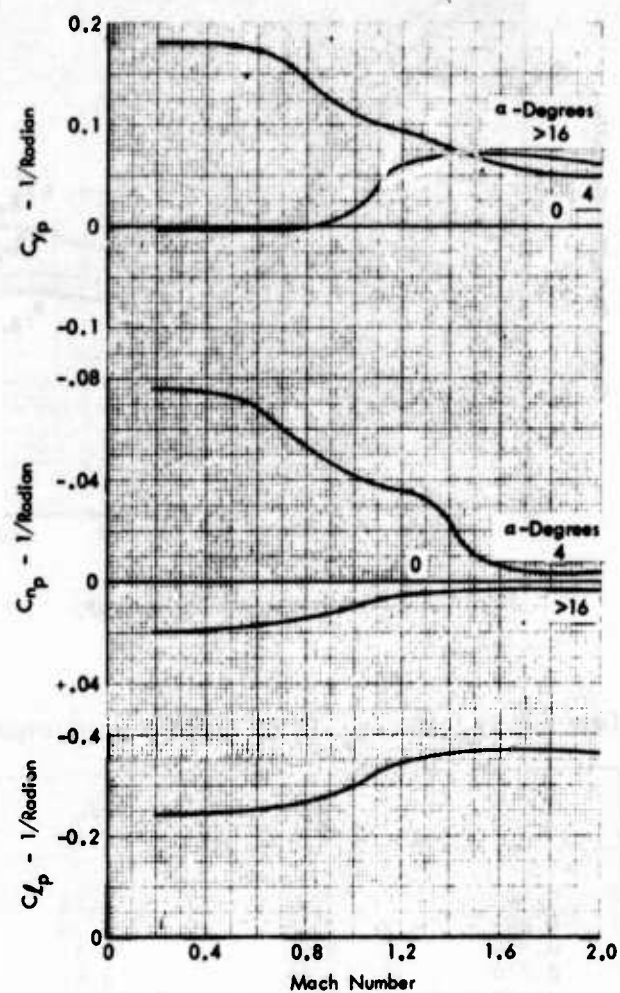


Figure 1-18 Roll Rate Derivatives

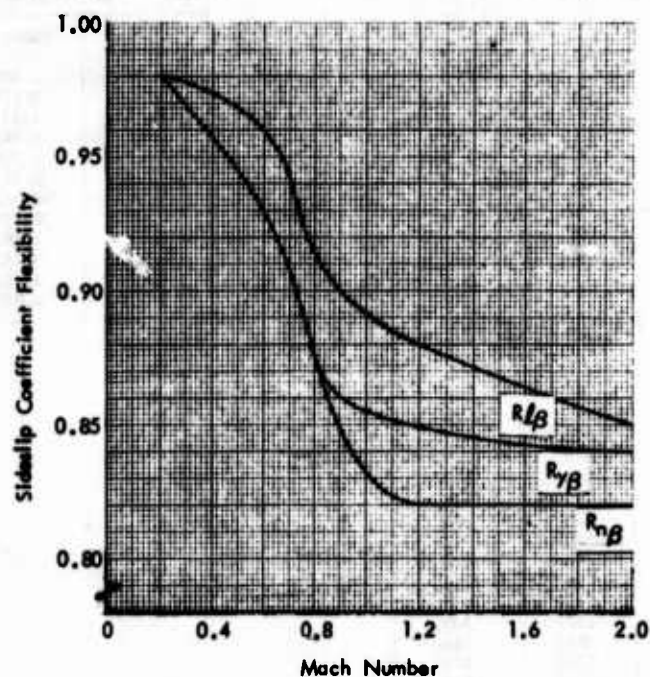


Figure 1-19 Sideslip Derivative Flexibility

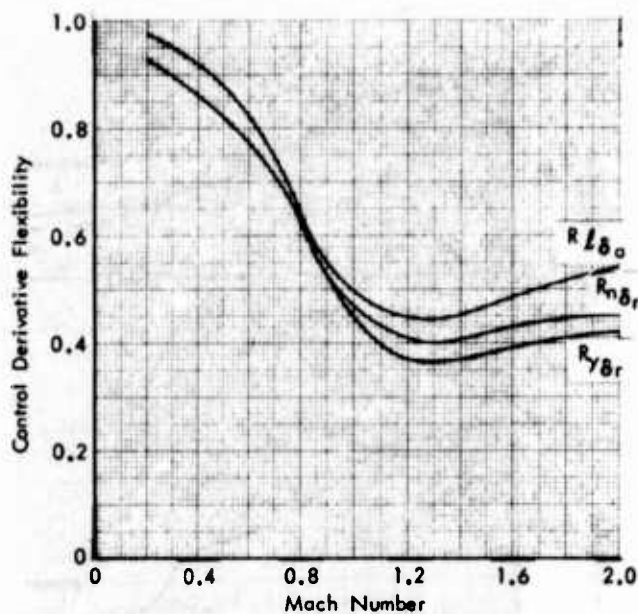


Figure 1-20 Control Derivative Flexibility

Table 1-3  $C_{l_\theta}$  AND  $C_{l_\alpha}$  VERSUS BLOWING COEFFICIENT

$C_{\mu'}$	$C_{l_\theta}$	$C_{l_\alpha}$
0.00	0.00	6.28
0.005	0.25	6.30
0.020	0.52	6.35
0.060	0.90	6.48
0.150	1.42	6.75
0.300	2.06	7.13
0.800	3.55	8.20
1.200	4.50	8.79
1.800	5.73	10.08
2.800	7.60	11.78
4.000	9.64	13.63
5.000	11.24	15.11
50.000	83.24	87.11

Table 1-4 INTERMEDIATE POWER THRUST

Mach	Altitude ~ Ft			
	0	20000.	36089.	65600.
0.1	11110.	2000.	3800.	600.
0.2	9600.	2800.	3700.	700.
0.3	8150.	3540.	3650.	800.
0.4	6700.	4500.	3550.	810.
0.5	5206.	4950.	3423.	826.
0.7	1548.	3600.	2967.	711.
0.9	-3664.	1747.	2333.	562.
1.1	-11308.	-1100.	1325.	309.
1.3	-16630.	-5382.	-224.	-84.
1.5	-19821.	-10476.	-2414.	-628.
1.7	-21700.	-15300.	-5005.	-1243.
2.0	-23500.	-19100.	-8000.	-2600.

Table 1-5 WING BLOWING COEFFICIENTS

Mach	$C_\mu$ (Wing Burning)			
	Altitude ~ Ft			
	0.	20000.	36089.	65600.
0.1	5.500	5.750	6.000	6.000
0.2	1.400	1.780	1.990	1.990
0.3	0.642	0.697	1.030	1.030
0.4	0.370	0.510	0.600	0.600
0.5	0.253	0.323	0.360	0.359
0.7	0.145	0.189	0.218	0.218
0.9	0.101	0.134	0.162	0.163
1.1	0.079	0.106	0.131	0.132
1.3	0.065	0.088	0.113	0.113
1.5	0.056	0.076	0.097	0.097
1.7	0.051	0.068	0.088	0.088
2.0	0.048	0.061	0.077	0.077

Mach	$C_\mu$ (No Wing Burning)			
	Altitude ~ Ft			
	0.	20000.	36089.	65600.
0.1	3.630	3.800	3.850	3.850
0.2	0.928	1.170	1.300	1.300
0.3	0.425	0.573	0.640	0.640
0.4	0.240	0.345	0.375	0.375
0.5	0.168	0.208	0.226	0.225
0.7	0.097	0.123	0.138	0.138
0.9	0.069	0.088	0.104	0.104
1.1	0.055	0.071	0.085	0.085
1.3	0.046	0.060	0.074	0.074
1.5	0.040	0.052	0.065	0.065
1.7	0.038	0.048	0.060	0.060
2.0	0.036	0.045	0.054	0.054

### I.3 FLIGHT CONTROL SYSTEM

A block diagram of the longitudinal flight control system of the LWA simulation is presented in Figure I-21. The longitudinal flight control system is basically a command and stability augmentation system with pitch rate and normal acceleration feedback and normal acceleration and angle of attack limiting. The system predominately utilizes normal acceleration and pitch rate feedback for cruise speeds and angle of attack and pitch rate feedback at reduced speeds.

The pitch command is presented in g's as a function of longitudinal stick force in Figure I-22. The command gradient and the breakout force shown are for the advanced cockpit side stick controller.

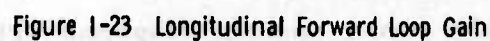
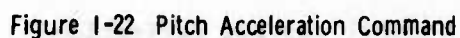
The forward loop gain and the angle-of-attack and normal acceleration feedback gains are scheduled as a function of impact pressure as shown in Figure I-23 and I-24. The canard deflection commanded to cancel pitching moments from the jet flap deflection and the flap action of the flaperon is presented in Figures I-25 and I-26, respectively.

In the lateral-directional control system (Figure I-27), stability augmentation is provided by roll rate feedback to the flaperons and lateral acceleration and yaw rate feedback to the rudder. The roll stick force is fed into the roll command augmentation loop and commands roll rate as shown in Figure I-28. The rudder and aileron feedback loop gains are presented in Figures I-29 and I-30.

Two modes of sideforce operation are available, the  $\beta$  mode and the  $\dot{\psi}$  mode. The  $\beta$  mode yields a vehicle sideslip with no heading change; while the  $\dot{\psi}$  mode provides yaw rate while holding sideslip to near zero.

The  $\dot{\psi}$  mode feedback gain,  $K_{\dot{\psi}}$ , is shown in Figure I-29. The sideforce control was operated from a thumb switch on the side stick controller and from the rudder pedals. When the rudder pedals were used for sideforce control, the rudder was disconnected from the pedals. Interconnects from the sideforce surface command to the rudder and the flaperons (Figures I-30 and I-31) were used to cancel yawing and rolling moments resulting from the sideforce control surface deflection.

A roll attitude hold circuit with control stick steering was included to maximize the effectiveness of the sideforce control modes.





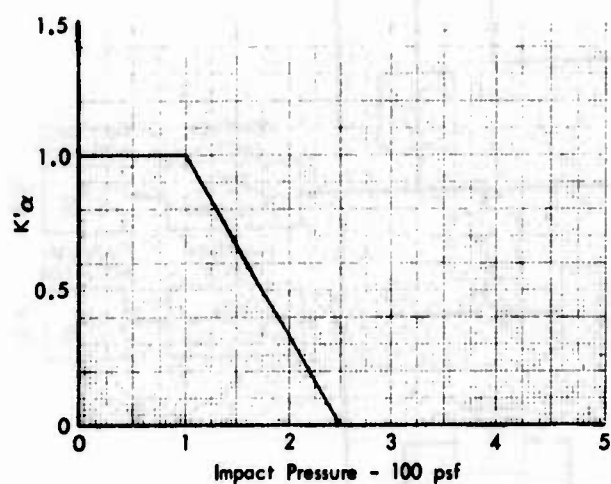
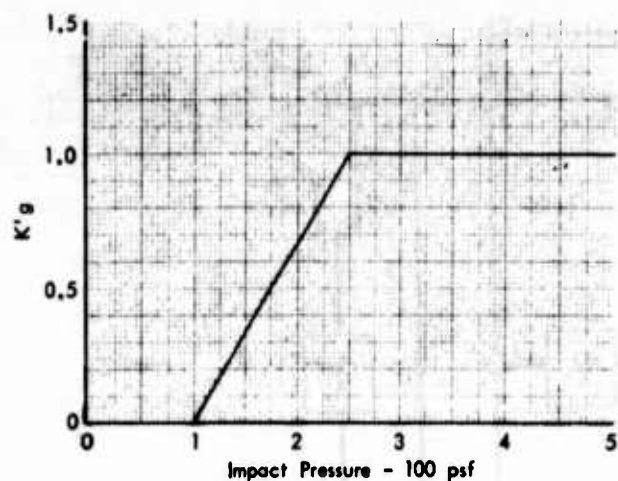


Figure 1-24 Acceleration and Angle of Attack Feedback Gains

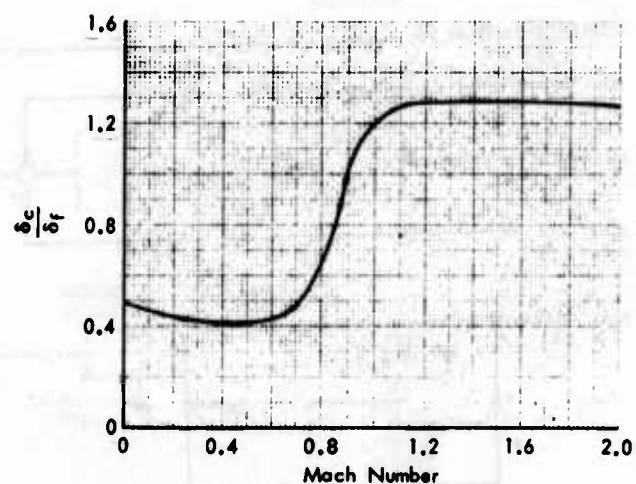


Figure 1-26 Flaperon (Flap)/Canard Interconnect Gain

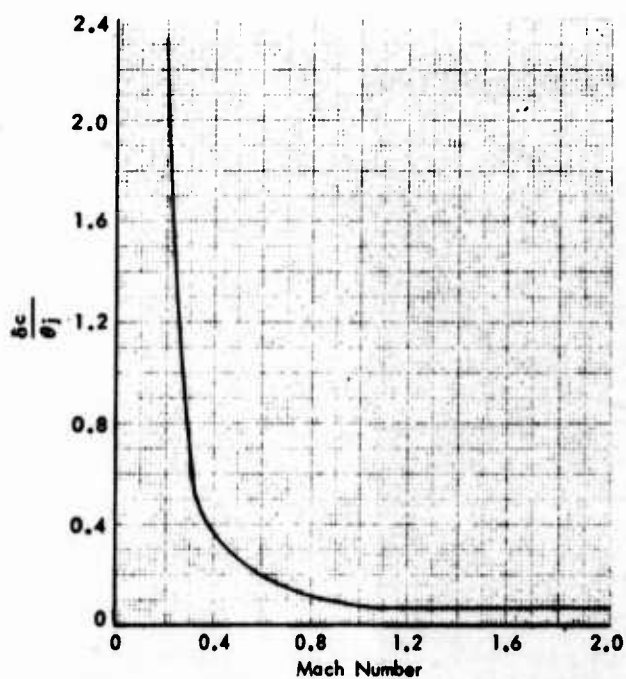


Figure 1-25 Jet Flap/Canard Interconnect Gain

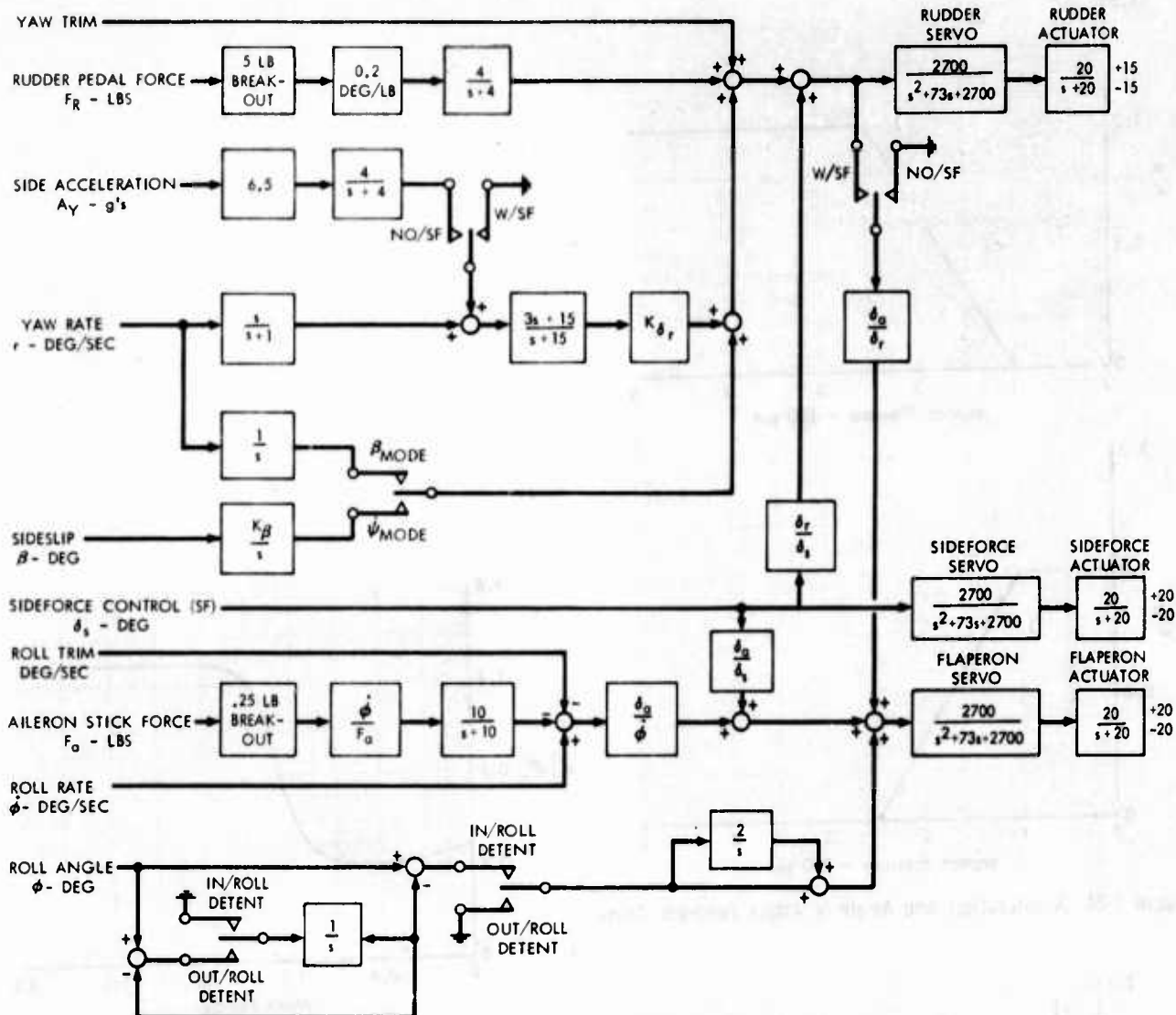


Figure 1-27 Lateral-Directional Flight Control System

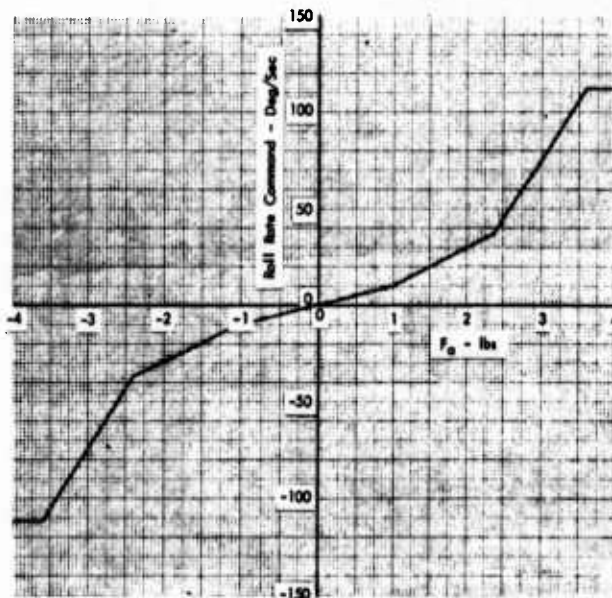


Figure 1-28 Roll Rate Command

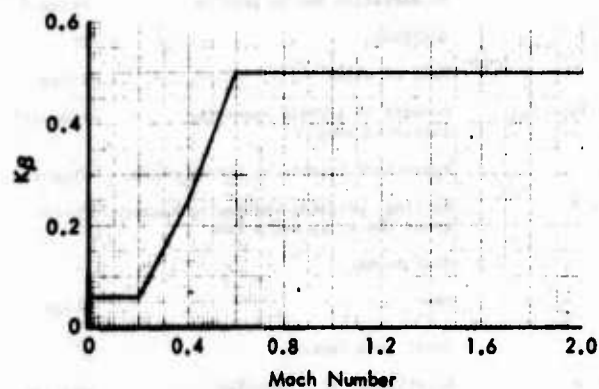
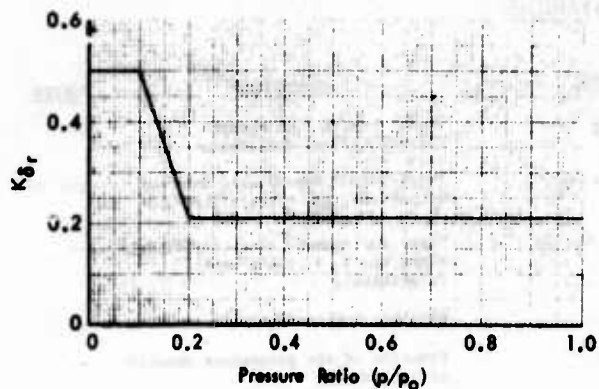


Figure 1-29 Rudder Forward Loop Gain and Sideforce Mode Feedback Gain

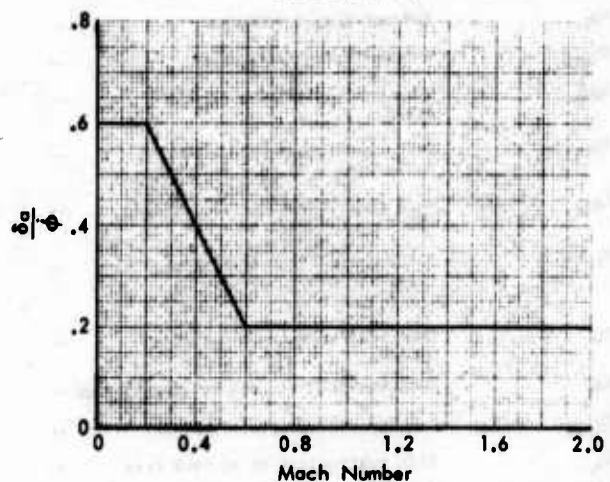
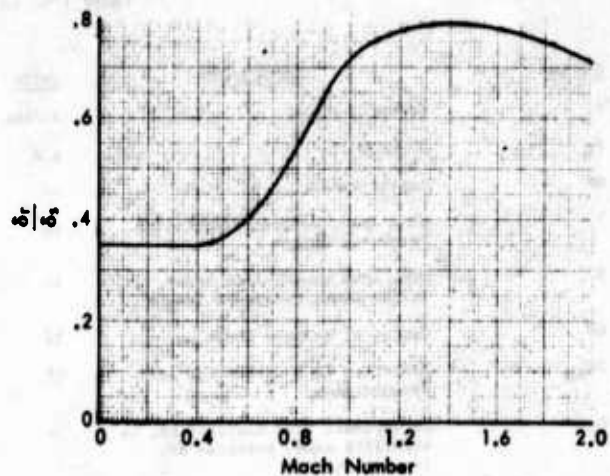


Figure 1-30 Sideforce/Rudder Interconnect Gain and Flaperon (Aileron) Forward Loop Gain

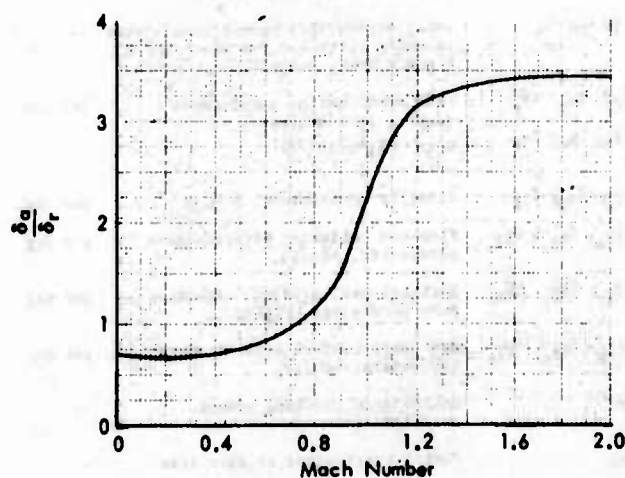
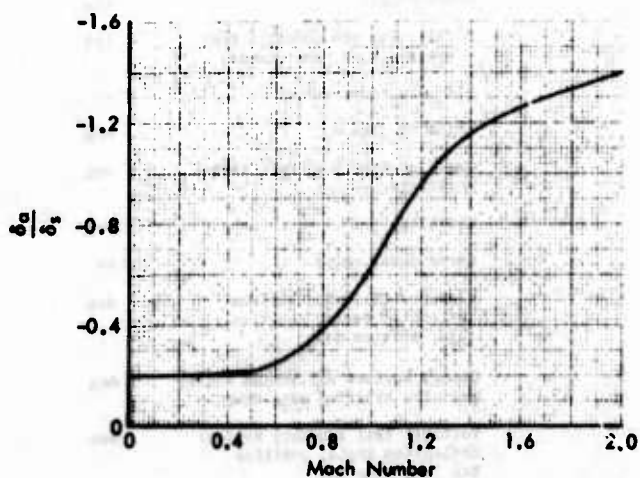


Figure 1-31 Rudder/Flaperon and Sideforce/Flaperon Interconnect Gains

Table I-6 LIST OF SYMBOLS

SYMBOL	DEFINITION	UNITS	SYMBOL	DEFINITION	UNITS
$a$	Speed of sound	ft/sec	$C_{m\delta f}$	Moment coefficient due to flap (flap) deflection	--
$A_N$	Load factor	$g$ 's	$C_{mq}, C_{Nq}$	Longitudinal aerodynamic damping derivatives, $C_{ij} = \partial C_i / \partial (j\dot{\epsilon} / 2V)$	per rad
AR	Aspect ratio	--	$C_X, C_Y, C_Z$	Total aerodynamic force coefficients along the x, y, and z axes, respectively	--
b	Wing span, lateral-directional reference length	ft	$C_\mu$	Wing blowing coefficient	--
$\bar{c}$	Wing mean aerodynamic chord, longitudinal reference length	ft	$f( )$	Function of the parameters denoted in parenthesis	--
CG	Center of gravity location	% $\bar{c}$	g	Acceleration due to gravity	ft/sec <sup>2</sup>
CG <sub>REF</sub>	Reference CG location for aerodynamic data	% $\bar{c}$	h	Altitude	ft
$C_D$	Aerodynamic drag coefficient, in stability axes, positive aft (-x direction)	--	$\dot{h}$	Rate of climb	ft/sec
$C_{D_L}$	Induced drag coefficient	--	$I_{xx}, I_{yy}, I_{zz}$	Moments of inertia about the indicated axes	slug-ft <sup>2</sup>
$C_{D_{MIN}}$	Minimum drag coefficient	--	$I_{xz}$	Product of inertia on the xz plane	slug-ft <sup>2</sup>
$C_{D_{SB}}$	Drag coefficient due to speed break	--	L, M, N	Rolling, pitching and yawing moments about the x, y, and z axes	ft-lbs
$C_{D_{\delta c}}$	Drag coefficient due to canard deflection	--	M	Mach number	--
$C_{D_{\delta f}}$	Drag coefficient due to flap (flap) deflection	--	m	Mass	slugs
$C_L$	Aerodynamic lift coefficient, in stability axes, positive up (-z direction)	--	n	Total load factor	$g$ 's
$C_L'$	Lift coefficient without wing blowing	--	p, q, r	Rotational rates (angular velocities) in roll, pitch and yaw axes	rad/sec
$C_{L_c}$	Lift coefficient due to wing blowing	--	$(p/p_0)$	Atmospheric ambient pressure ratio, $f(h)$	--
$C_{L_{MAX}}$	Lift coefficient limit imposed	--	$\bar{q}$	Dynamic pressure	lbs/ft <sup>2</sup>
$C_{L_0}$	Lift coefficient at minimum drag	--	$r'$	Jet flap drag parameter	--
$C_{L_\alpha}$	Lift curve slope, $\partial C_L / \partial \alpha$	per deg	t	Time	sec
$C_{L_{\delta c}}, C_{m_{\delta c}}$	Canard effectiveness parameters, $\partial C_i / \partial \delta_c$	per deg	TMIL	Intermediate power thrust	lbs
$C_{L_{\delta f}}, C_{m_{\delta f}}$	Flap (flap) effectiveness parameters, $\partial C_i / \partial \delta_f$	per deg	u, v, w	Linear velocity components along the x, y, and z axes	ft/sec
$C_{L_{C_\mu=0}}$	Lift coefficient due to angle of attack with no wing blowing	--	V	Total airplane velocity, coincident with the relative wind	ft/sec
$C_l, C_m, C_n$	Total aerodynamic moment coefficients in roll, pitch and yaw about the x, y and z axes, respectively	--	W	Gross weight	lbs
$C_{l_p}, C_{n_p}, C_{y_p}$	Lateral-direction aerodynamic damping derivatives, $C_{ij} = \partial C_i / \partial (j\dot{\epsilon} / 2V)$	per rad	X, Y, Z	Axial, side and normal forces along the x, y, and z axes	lbs
$C_{l_r}, C_{n_r}, C_{y_r}$			x, y, z	Airplane body axes	--
$C_{l_\beta}, C_{n_\beta}, C_{y_\beta}$	Sideslip derivatives, $\partial C_i / \partial \beta$	per deg	$\alpha$	Angle of attack	deg
$C_{l_{\delta_a}}, C_{n_{\delta_a}}, C_{y_{\delta_a}}$	Flap (aileron) effectiveness parameters, $\partial C_i / \partial \delta_a$	per deg	$\alpha_{L_0}$	Angle of attack at zero lift coefficient	deg
$C_{l_{\delta_r}}, C_{n_{\delta_r}}, C_{y_{\delta_r}}$	Vertical tail (rudder) effectiveness parameters, $\partial C_i / \partial \delta_r$	per deg	$\beta$	Sideslip	deg
$C_{l_{\delta_s}}, C_{n_{\delta_s}}, C_{y_{\delta_s}}$	Sideslip surface effectiveness parameters, $\partial C_i / \partial \delta_s$	per deg	$\Delta$	Incremental value	--
$C_m$	Aerodynamic pitching moment coefficient	--	$\delta_a$	Flap (aileron) surface deflection angle, positive right aileron down	deg
$C_{m_0}$	Moment coefficient at zero lift	--	$\delta_c$	Canard surface deflection angle, positive trailing edge down	deg
$C_{m_{JET}}$	Moment coefficient due to the wing jet flap	--	$\delta_r$	Vertical tail (rudder) surface deflection angle, positive trailing edge lift	deg
$C_{m_\alpha}$	Moment curve slope, $\partial C_m / \partial \alpha$	per deg	$\delta_s$	Sideslip surface deflection angle, positive trailing edge lift	deg
$C_{m_{\delta c}}$	Moment coefficient due to canard deflection	--	$\theta, \phi, \psi$	Euler angles in pitch, roll and yaw	deg

Table 1-6 (Cont'd)

<u>SYMBOL</u>	<u>DEFINITION</u>	<u>UNITS</u>
$\theta_j$	Wing jet flap deflection	deg
( $\dot{\phantom{x}}$ )	Denotes differentiation with respect to time	--
( )AERO	Aerodynamic contribution	--
( )AERO STATIC	Contribution due to static aerodynamic parameters inclosed in the parenthesis	--
( )B	Body axes reference	--
( )BR	Referenced to break in lift curve	--
( )o	Initial condition	--
( )REF	Reference condition or value	--
( )s	Reference to stability axes	--
( )THRUST	Thrust contribution	--



## S I M U L A T I O N   D A T A

contain typical landing approach data for DSFC evaluation.

simulator pilots' report is reproduced as Figure J-15.

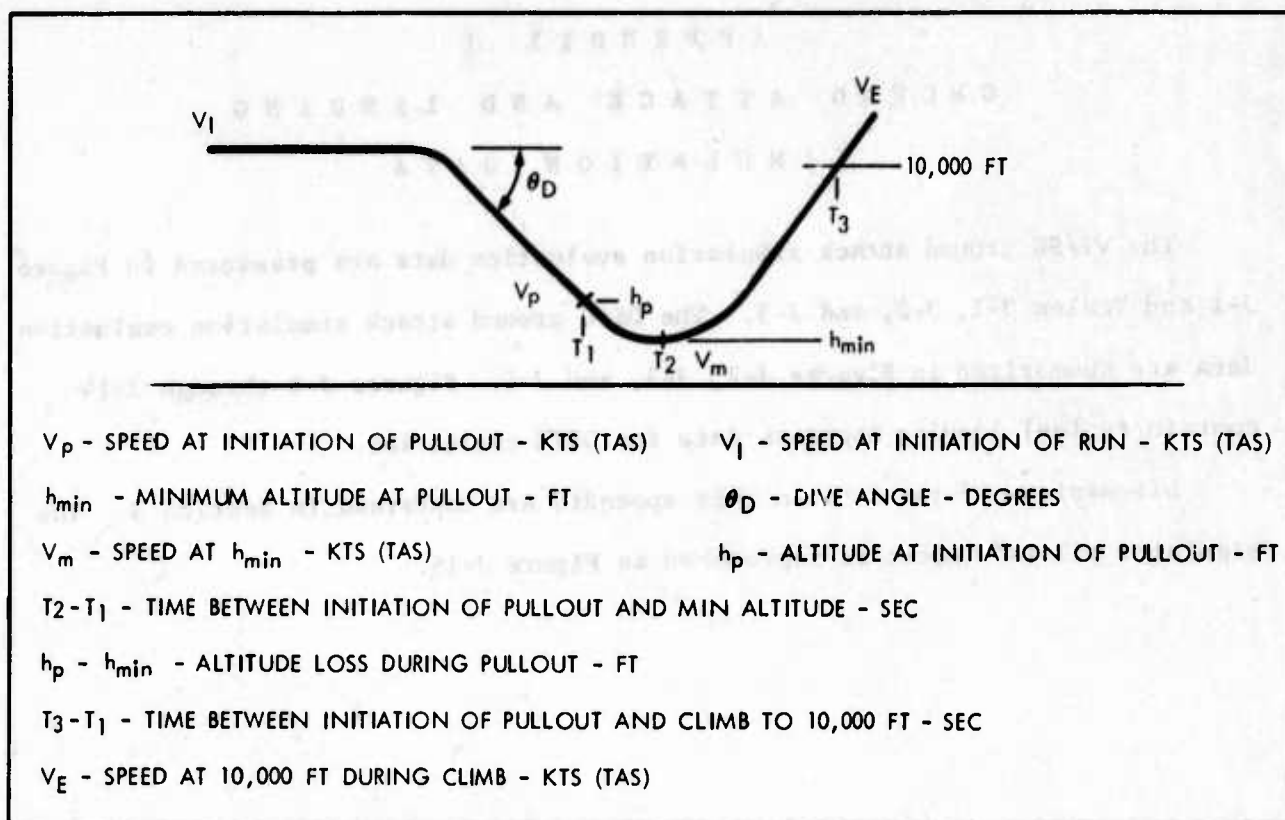


Figure J-1 VT/SC Ground Attack Simulation Geometry

Table J-1 VT/SC GROUND ATTACK SIMULATION EVALUATION - PILOT A

RUN	THROTTLE SETTING	$\theta_j$ (DEG)	$V_I$ (KTAS)	$\theta_D$ DIVE ANGLE (DEG)	$h_p$ (FT)	$V_p$ (KTAS)	$h_{min}$ (FT)	$V_m$ (KTAS)	$h_p - h_{min}$ (FT)	$T_2 - T_1$ (SEC)	$V_E$ (KTAS)	$T_3 - T_1$ (SEC)
1	IDLE	0	400	60	3600	390.5	900	550.3	2700	6.25	488.2	20.75
2	25%	50		60	3900	562.1	600	562.1	3300	6.75	562.1	20.35
3	50%	50		60	3700	597.6	500	603.6	3200	7.00	621.3	20.30
4	IDLE	0		45	3600	508.9	2000	491.1	1600	5.00	568.0	19.00
5	25%	50		45	3600	568.0	2000	612.4	1600	6.00	579.9	17.25
6	50%	50		45	3600	665.7	2000	686.4	1600	4.50	636.1	17.00
7	IDLE	0		30	3800	517.8	3000	556.2	800	6.50	579.9	14.20
8	25%	50		30	3700	579.9	2900	562.1	800	4.00	562.1	14.50
9	50%	50	400	30	3750	597.6	3000	621.3	750	6.75	576.9	14.50
10	IDLE	0	575	60	3750	609.5	100	612.4	3650	7.50	597.6	21.50
11	25%	50		60	3800	636.1	400	615.4	3400	7.00	621.2	21.50
12	50%	50		60	3800	639.1	900	627.0	2900	6.50	568.0	20.50
13	IDLE	0		45	3700	609.5	1400	579.9	2300	6.00	603.6	18.50
14	25%	50		45	3900	621.3	2000	609.5	1900	5.50	562.1	17.00
15	50%	50		45	3700	636.1	1600	621.3	2100	5.50	573.9	20.00
16	IDLE	0		30	3600	606.5	2600	576.9	1000	3.50	621.3	15.00
17	25%	50		30	3700	615.4	2800	597.6	900	3.50	556.2	15.25
18	50%	50	575	30	3800	621.3	3000	609.5	800	3.50	562.1	15.00

Table J-2 VT/SC GROUND ATTACK SIMULATION EVALUATION - PILOT B

RUN	THROTTLE SETTING	$\theta_j$ (DEG)	$V_I$ (KTAS)	$\theta_D$ DIVE ANGLE (DEG)	$h_p$ (FT)	$V_p$ (KTAS)	$h_{min}$ (FT)	$V_m$ (KTAS)	$h_p - h_{min}$ (FT)	$T_2 - T_1$ (SEC)	$V_E$ (KTAS)	$T_3 - T_1$ (SEC)
1	IDLE	0	400	60	3600	553.3	400	650.9	3200	7.00	597.6	21.00
2	25%	50	↓	60	3400	576.9	400	629.0	3000	6.75	582.8	20.75
3	50%	50		60	3600	592.5	500	615.4	3100	6.25	576.9	20.75
4	IDLE	0		45	3600	538.5	1600	615.4	2000	5.25	600.6	16.00
5	25%	50		45	3700	562.1	2000	562.1	2700	5.25	582.8	17.25
6	50%	50		45	3500	597.6	1750	629.0	1750	5.00	576.9	17.25
7	IDLE	0		30	3600	532.5	3000	562.1	600	3.25	562.1	14.00
8	25%	50		30	3700	550.3	3100	562.1	600	3.75	576.9	14.00
9	50%	50		30	3700	597.6	3100	629.0	600	3.00	562.1	14.00
10	IDLE	0		60	3500	615.4	-300	639.1	3800	7.25	585.8	22.00
11	25%	50		60	3800	621.3	150	621.3	3650	7.00	585.8	21.50
12	50%	50		60	3700	636.1	150	629.0	3550	7.25	562.1	21.50
13	IDLE	0		45	3800	606.5	1500	579.9	2300	5.75	615.4	18.25
14	25%	50		45	3700	629.0	1800	629.0	1900	4.25	579.9	17.75
15	50%	50		45	3700	633.1	1700	621.3	2000	5.00	568.0	17.72
16	IDLE	0		30	3800	597.6	2900	630.2	900	3.50	606.5	14.75
17	25%	50		30	3900	606.5	2800	605.9	1100	3.75	579.9	15.25
18	50%	50		30	3900	615.4	2900	609.5	1000	3.50	579.9	15.25

Table J-3 VT/SC GROUND ATTACK SIMULATION EVALUATION - PILOT C

RUN	THROTTLE SETTING	$\theta_j$ (DEG)	$V_I$ (KTAS)	$\theta_D$ DIVE ANGLE (DEG)	$h_p$ (FT)	$V_p$ (KTAS)	$h_{min}$ (FT)	$V_m$ (KTAS)	$h_p - h_{min}$ (FT)	$T_2 - T_1$ (SEC)	$V_E$ (KTAS)	$T_3 - T_1$ (SEC)
1	IDLE	0	400	60	3600	526.6	700	636.1	2900	6.75	597.6	20.25
2	25%	50	↓	60	3700	585.8	600	612.4	3100	6.50	579.9	20.75
3	50%	50		60	3800	592.6	600	612.4	3200	6.50	579.9	20.75
4	IDLE	0		45	3750	562.1	1600	629.0	2150	5.25	600.6	18.00
5	25%	50		45	3800	573.9	2000	562.1	1800	5.00	573.9	17.50
6	50%	50		45	3900	603.6	1900	612.4	2000	5.00	579.9	17.50
7	IDLE	0		30	3900	532.5	2800	576.9	1100	3.75	562.1	14.50
8	25%	50		30	3700	579.9	2900	562.1	800	3.75	573.9	15.00
9	50%	50		30	3800	606.5	3000	609.5	800	3.25	576.9	14.50
10	IDLE	0		60	3700	592.5	200	659.8	3500	7.25	603.6	21.25
11	25%	50		60	3900	629.0	400	629.0	3500	7.25	585.8	21.00
12	50%	50		60	3600	633.1	200	615.4	3400	7.00	579.9	21.50
13	IDLE	0		45	3900	597.6	1500	609.5	2400	5.25	597.6	18.00
14	25%	50		45	3600	615.4	1800	606.5	1800	4.75	576.9	17.75
15	50%	50		45	4000	629.0	2000	621.3	2000	4.75	579.9	17.50
16	IDLE	0		30	3800	592.5	2800	600.6	1000	4.00	562.1	15.00
17	25%	50		30	3900	609.5	2900	603.6	1000	3.25	579.9	15.00
18	50%	50		30	3800	615.4	2900	606.5	900	3.75	579.9	15.00

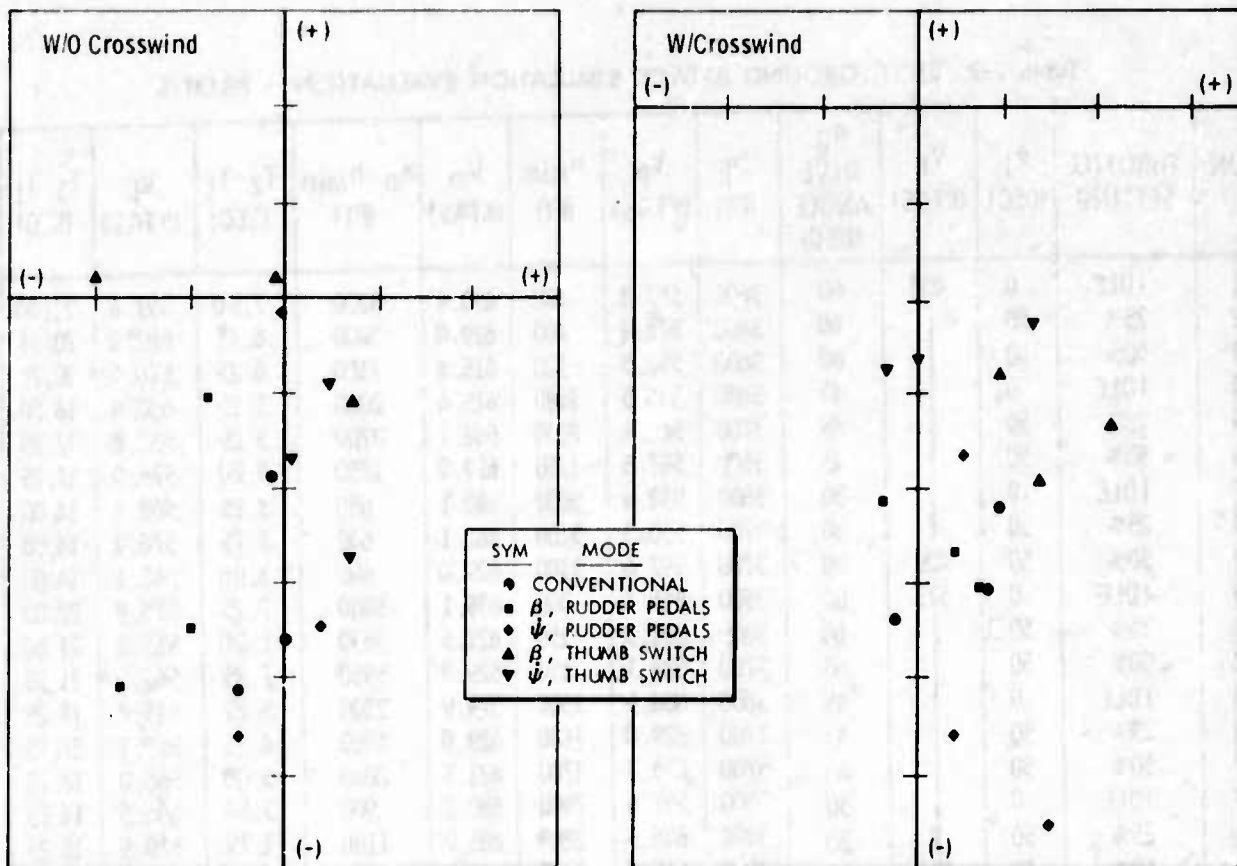


Figure J-2 DSC Ground Attack Simulation Evaluation - Pilot A

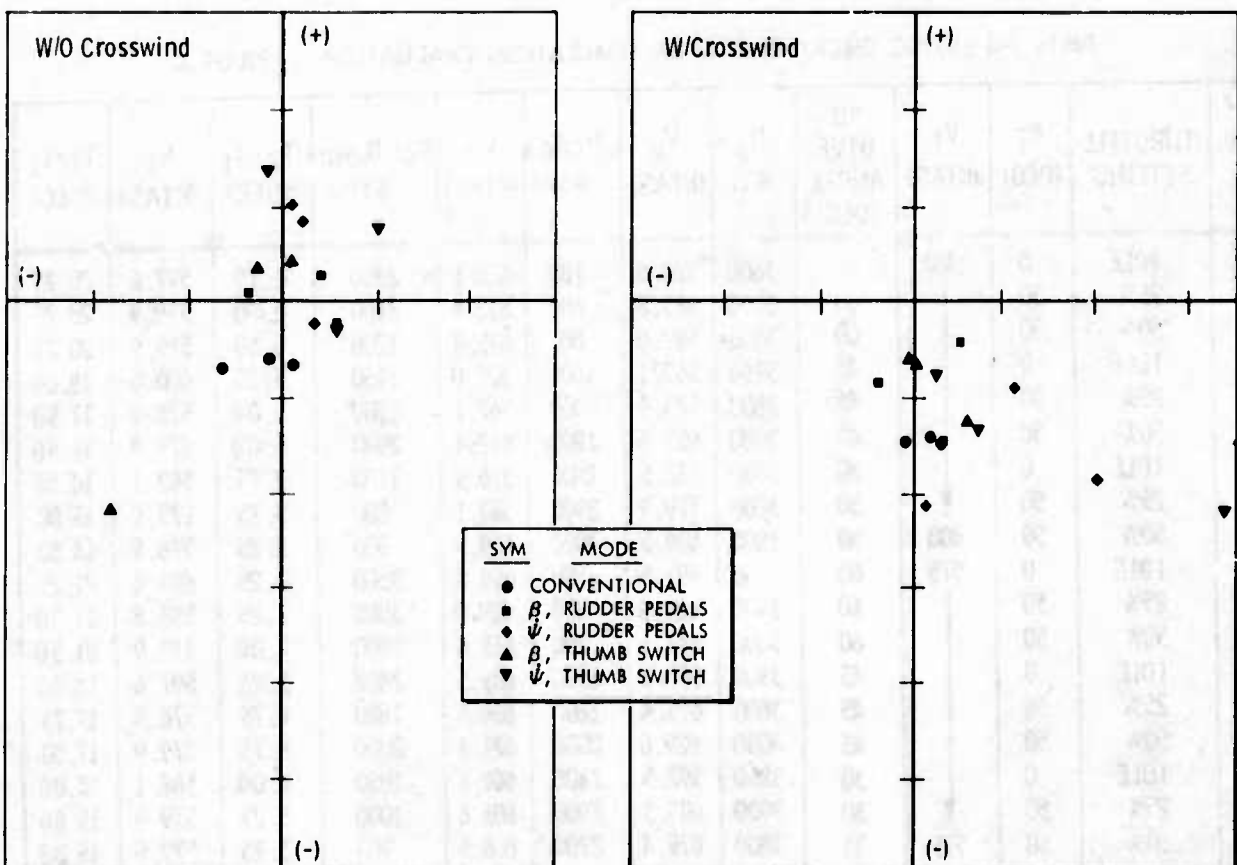


Figure J-3 DSC Ground Attack Simulation Evaluation - Pilot B

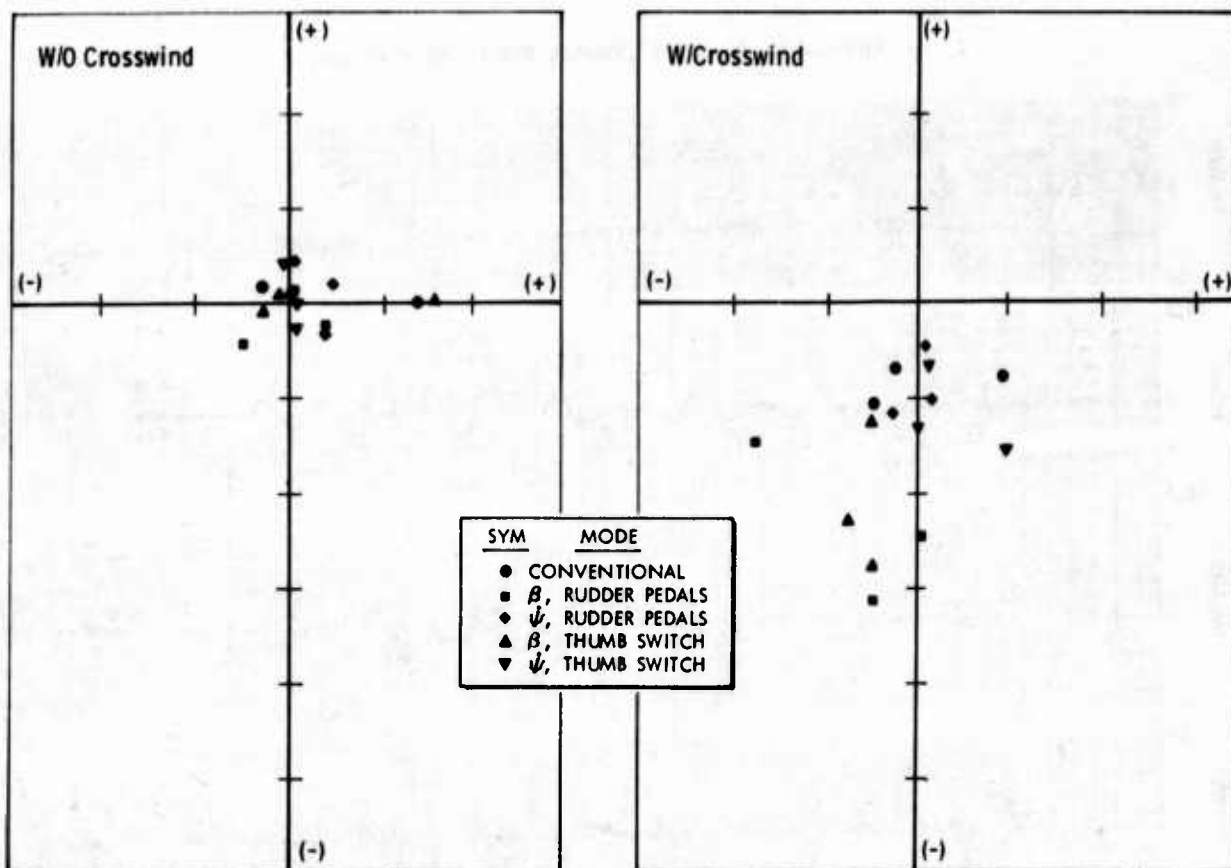


Figure J-4 DSC Ground Attack Simulation Evaluation - Pilot C



Airplane Initial Lateral Offset is 3000 Ft Left of Runway

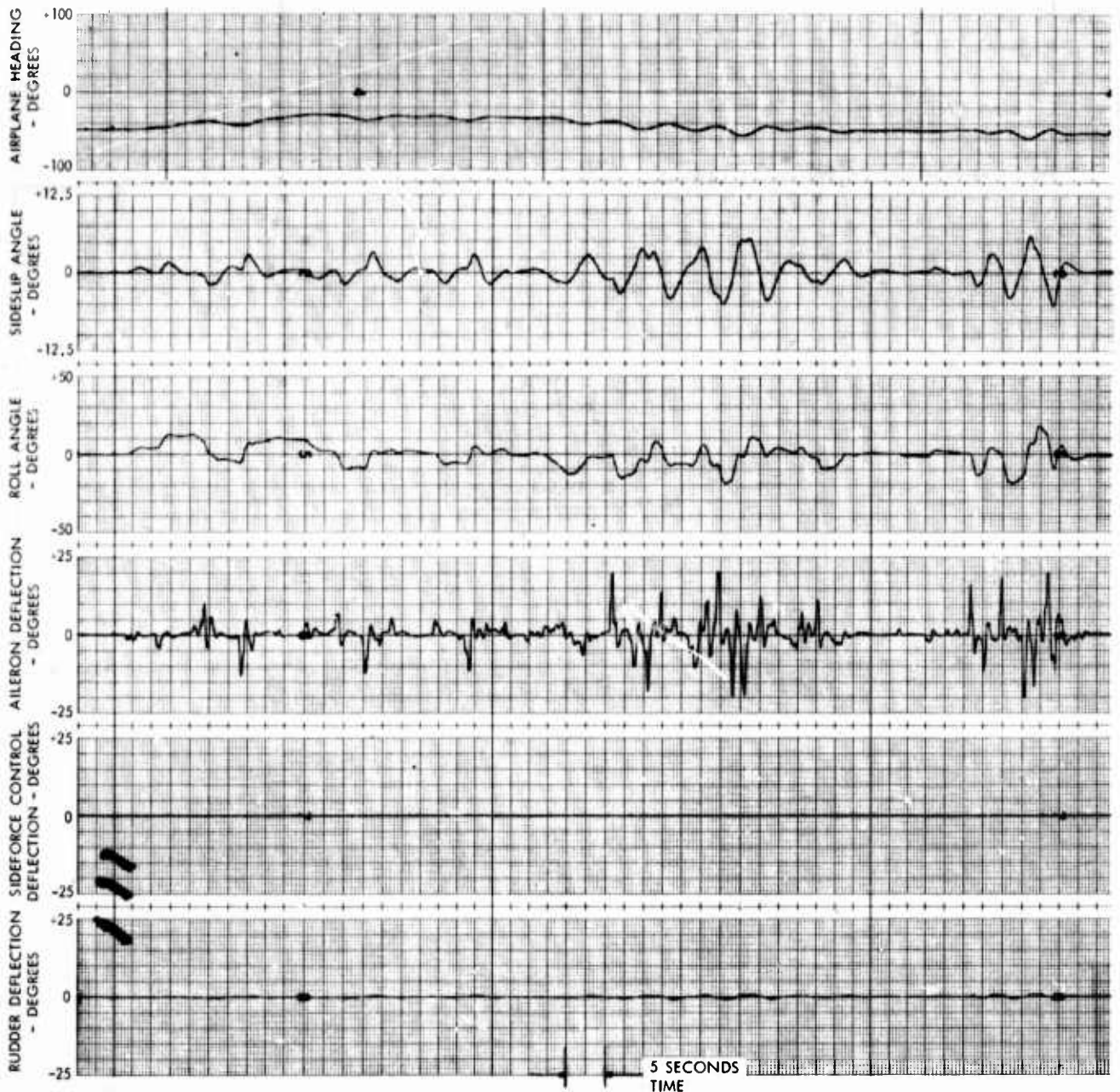


Figure J-5 Landing Approach with Zero Crosswind - Conventional Configuration

Airplane Initial Lateral Offset is 3000 Ft Left of Runway

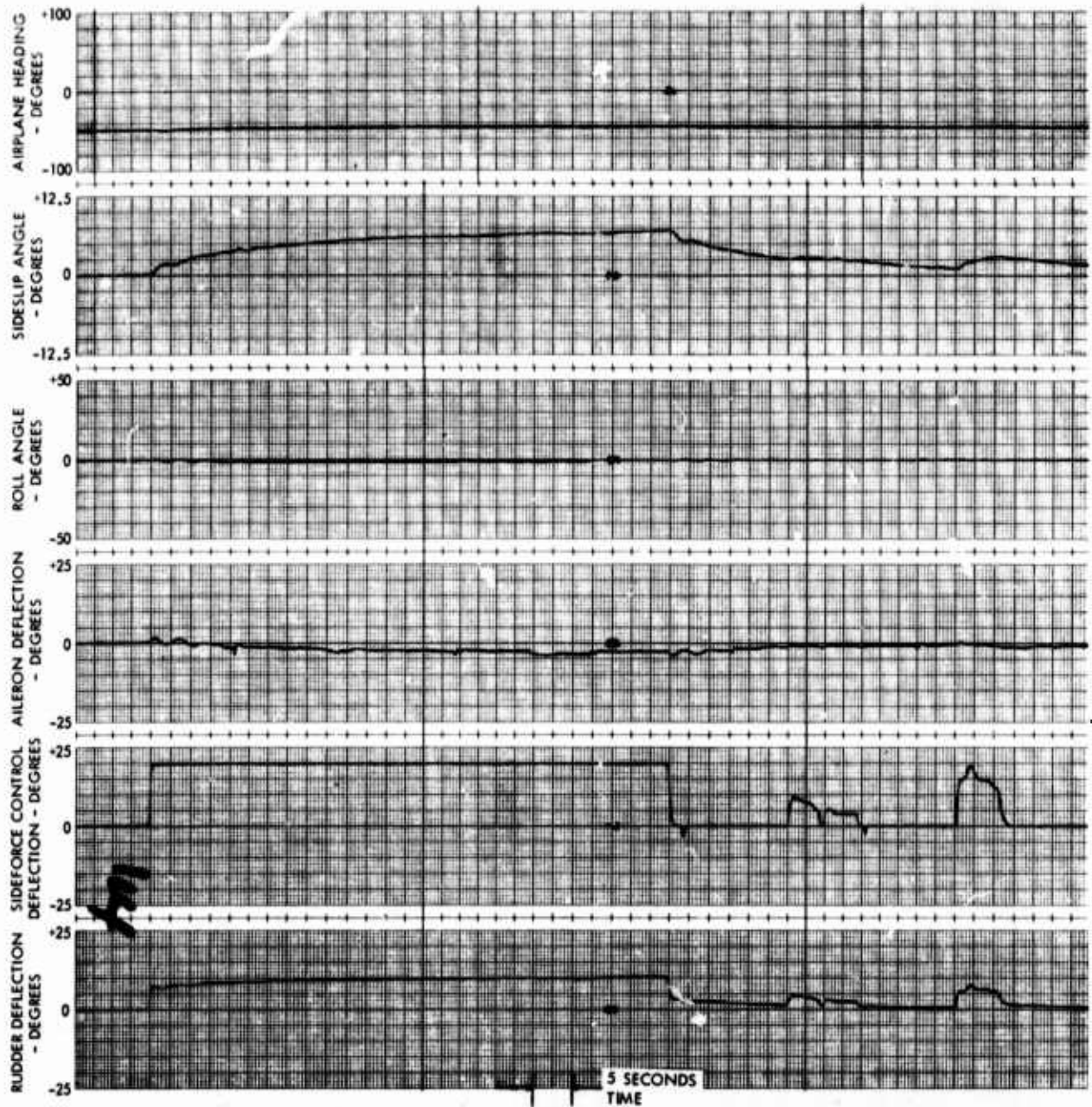


Figure J-6 Landing Approach with Zero Crosswind, DSFC Sideslip Mode Engaged, Rudder Pedal Controller

Airplane Initial Lateral Offset is 3000 Ft Left of Runway

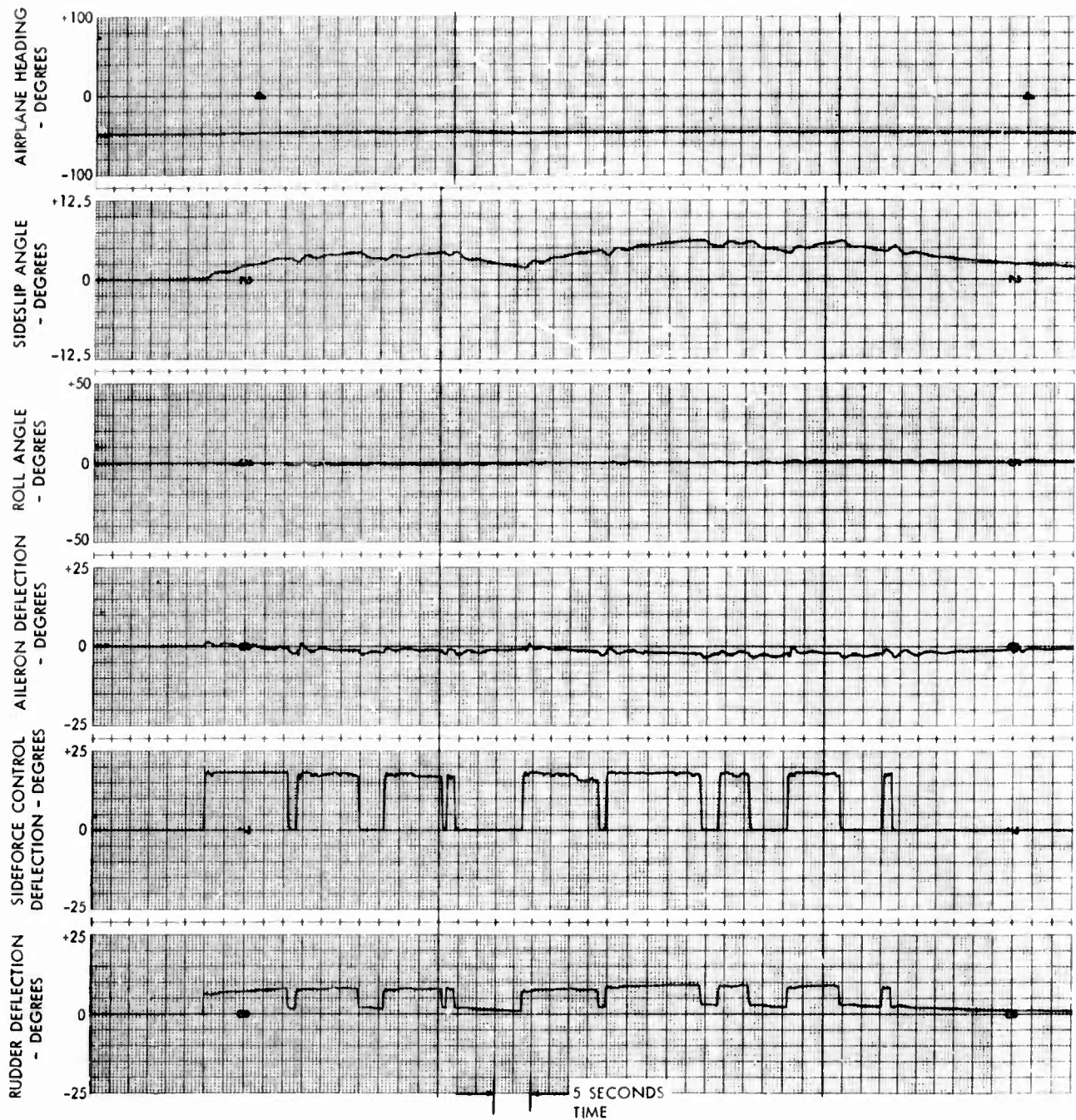


Figure J-7 Landing Approach with Zero Crosswind - DSFC Sideslip Mode Engaged, Thumb Controller



Airplane Initial Lateral Offset is 3000 Ft Left of Runway

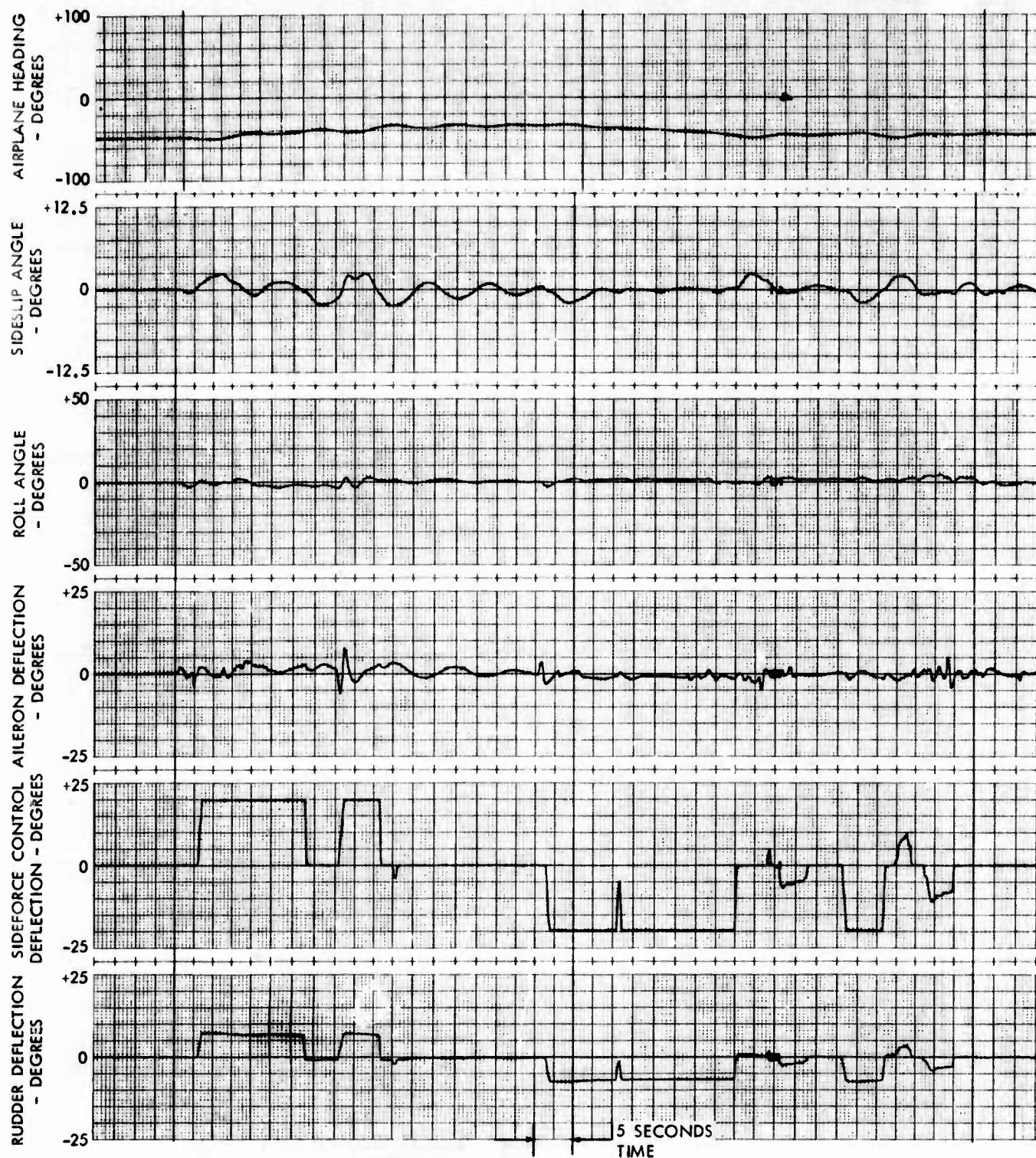


Figure J-8 Landing Approach with Zero Crosswind - DSFC Yaw Rate Mode Engaged, Rudder Pedal Controller

# Airplane Initial Lateral Offset is 3000 Ft Left of Runway

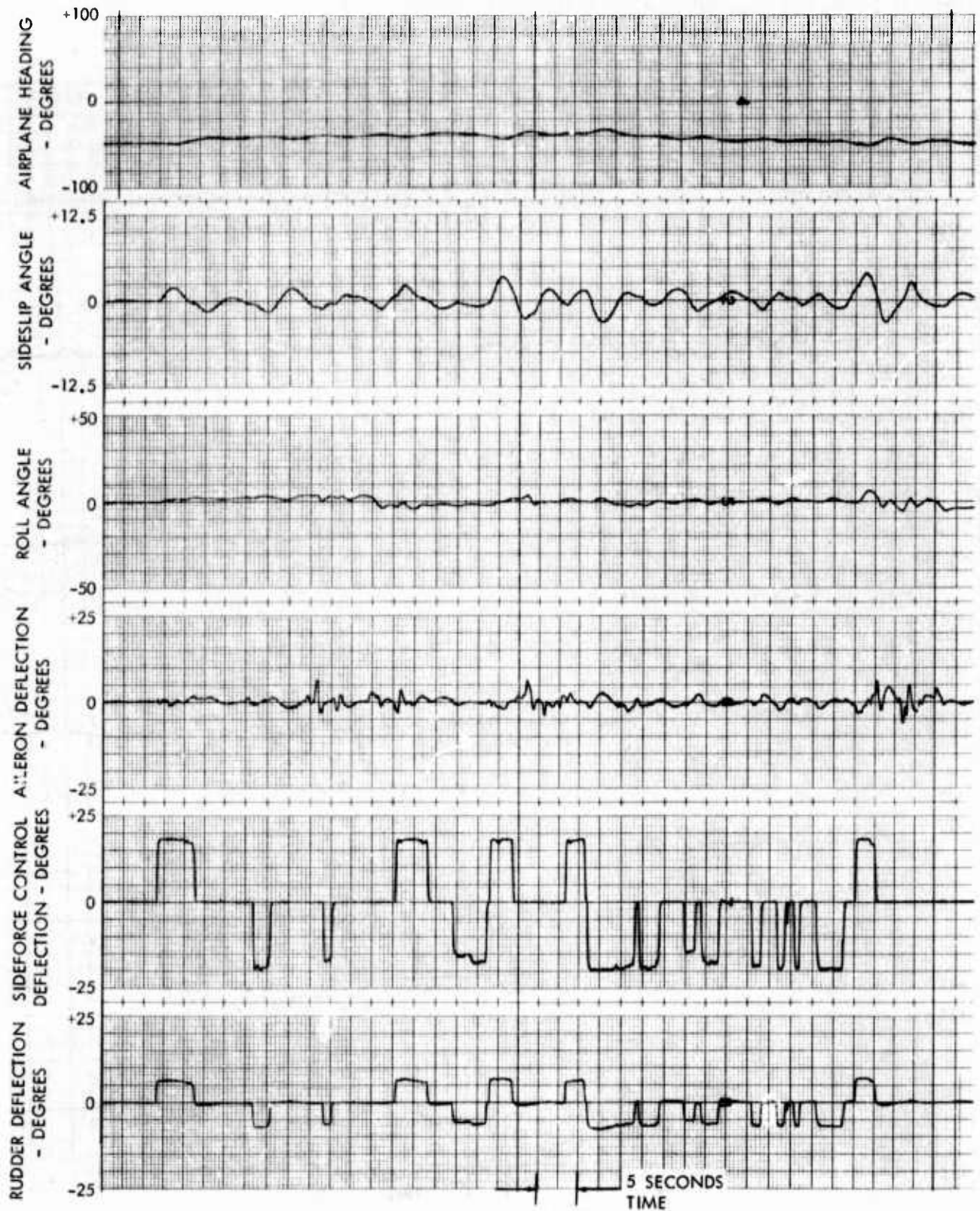


Figure J-9 Landing Approach with Zero Crosswind - DSFC Yaw Rate Mode Engaged, Thumb Controller



● Airplane Initial Lateral Offset is 3000 Ft Left of Runway

● Crosswind is from the Right

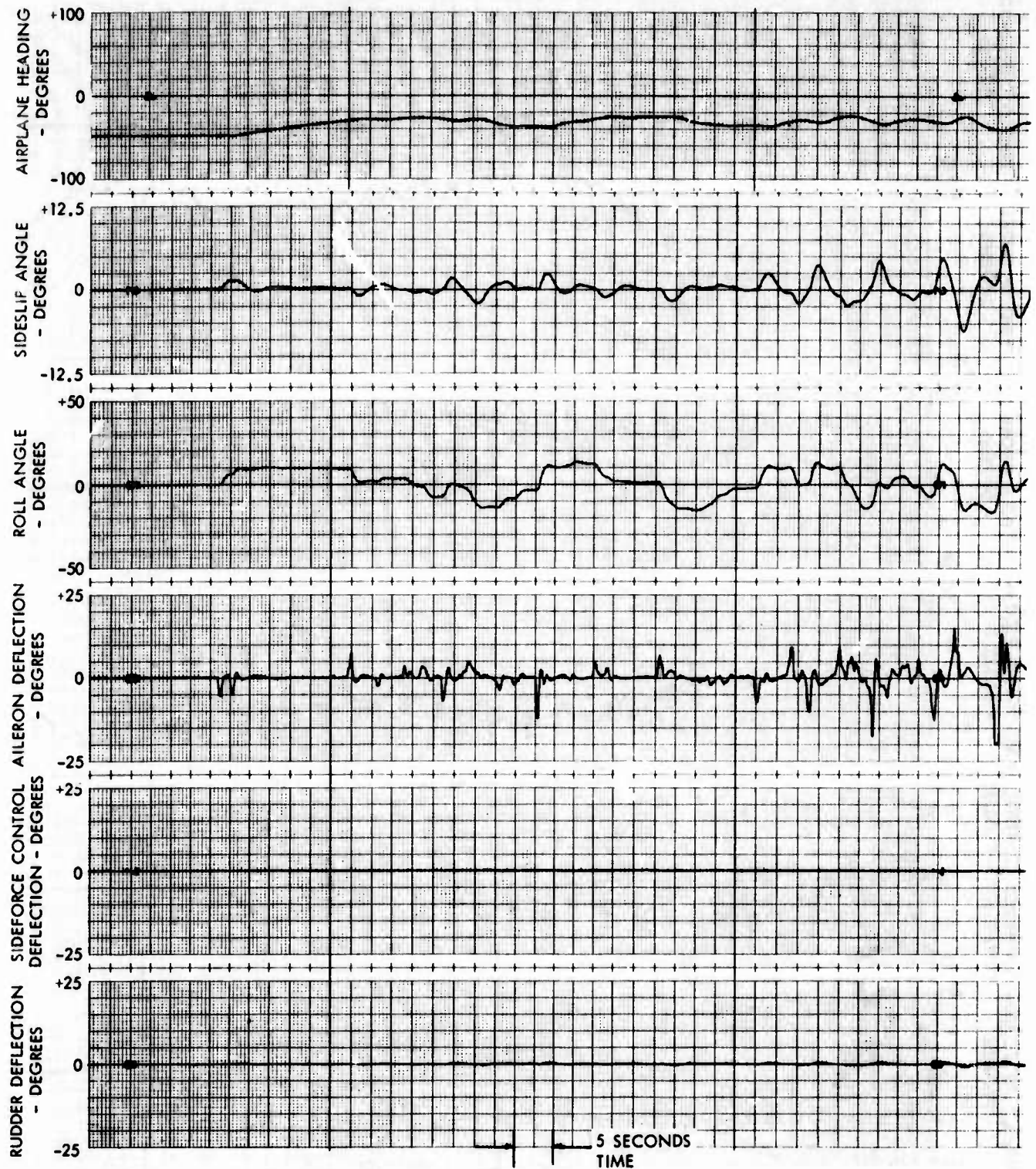


Figure J-10 Landing Approach with 30 Knot Crosswind - Conventional Configuration

- Airplane Initial Lateral Offset is 3000 Ft Left of Runway
- Crosswind is from the Right

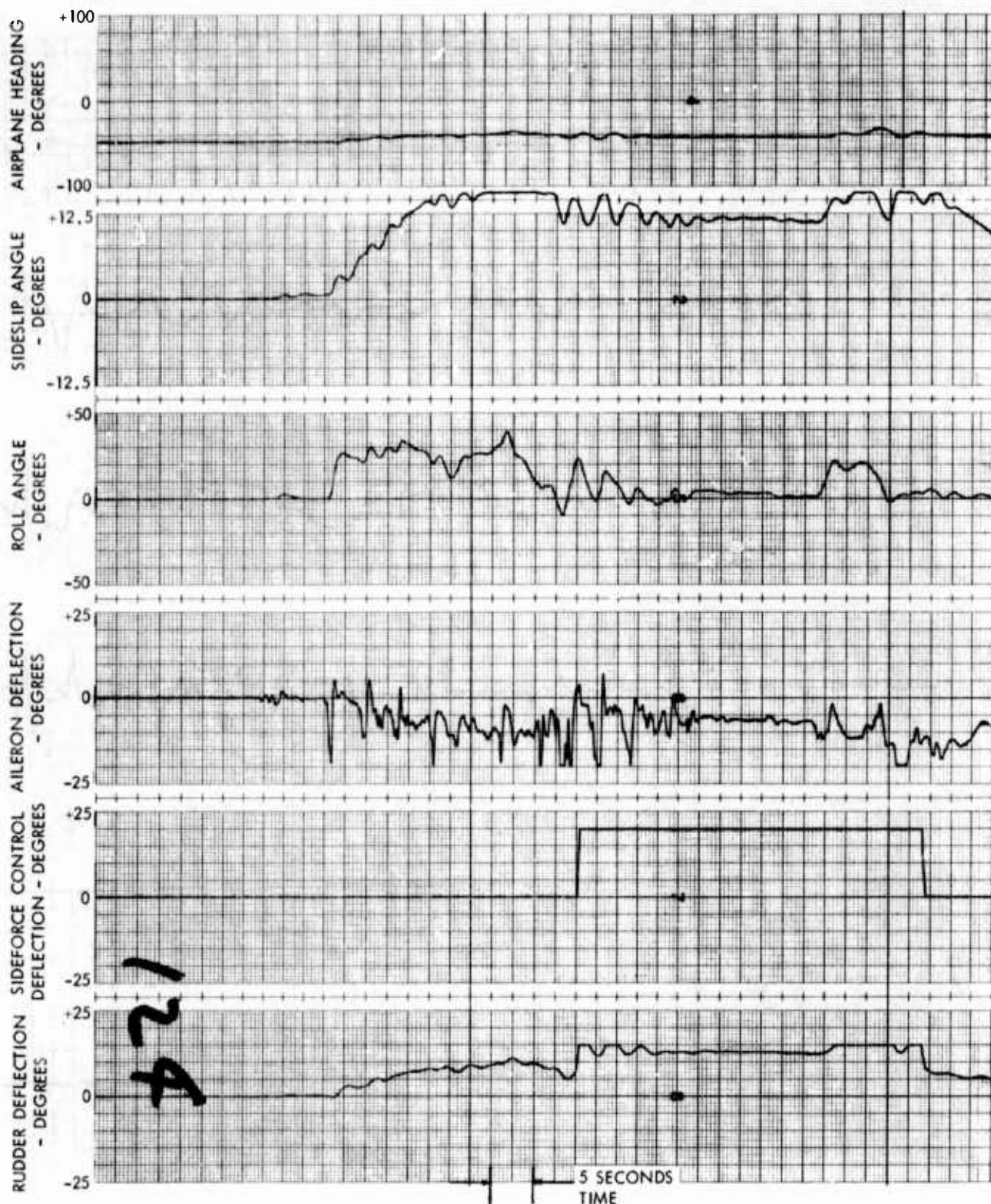


Figure J-11 Landing Approach with 30 Knot Crosswind - DSFC Sideslip Mode Engaged, Rudder Pedal Controller

- Airplane Initial Lateral Offset is 3000 Ft Left of Runway
- Crosswind is from the Right

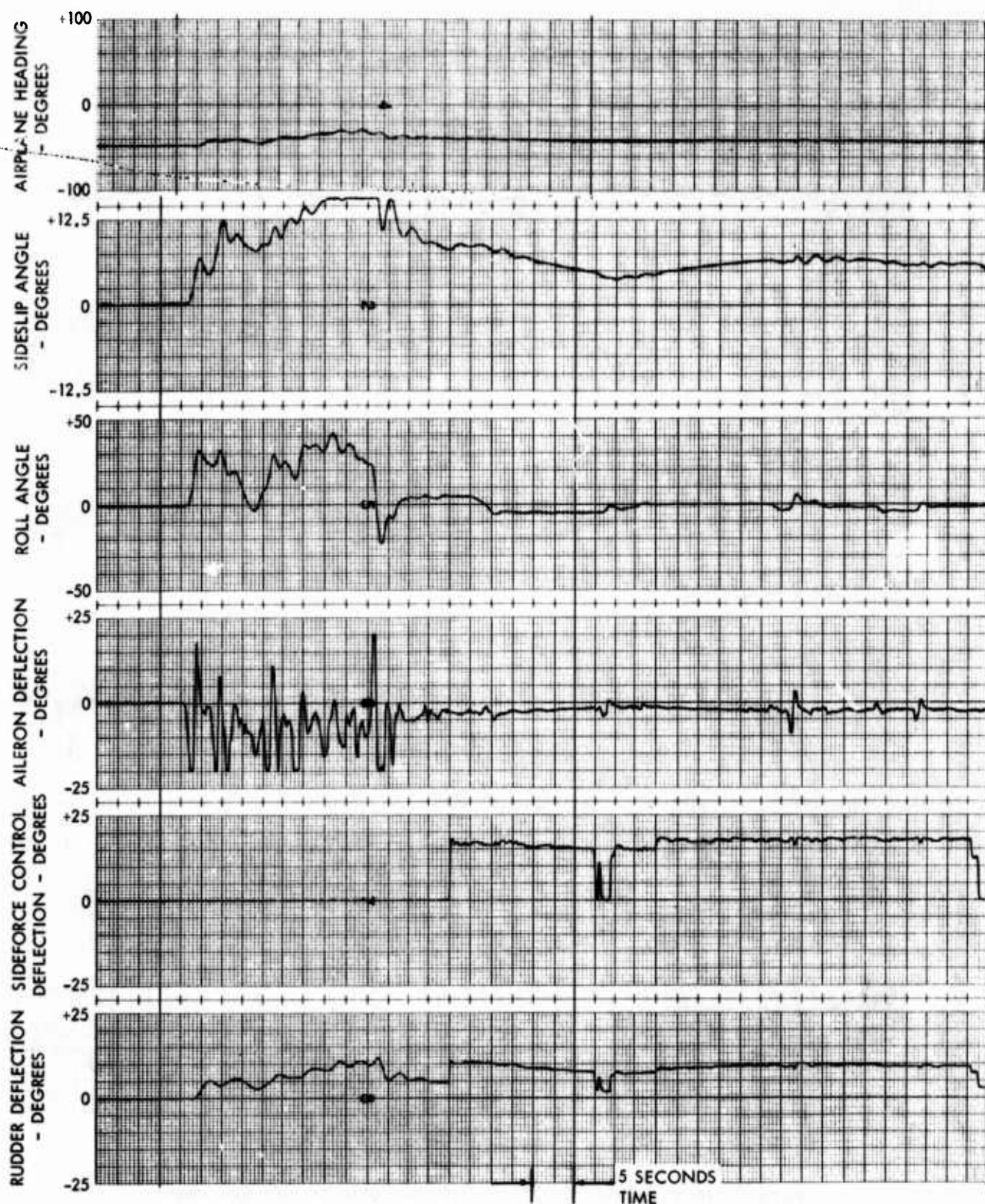


Figure J-12 Landing Approach with 30 Knot Crosswind - DSFC Sideslip Mode Engaged, Thumb Controller



● Airplane Initial Lateral Offset is 3000 Ft Left of Runway ● Crosswind is from the Right

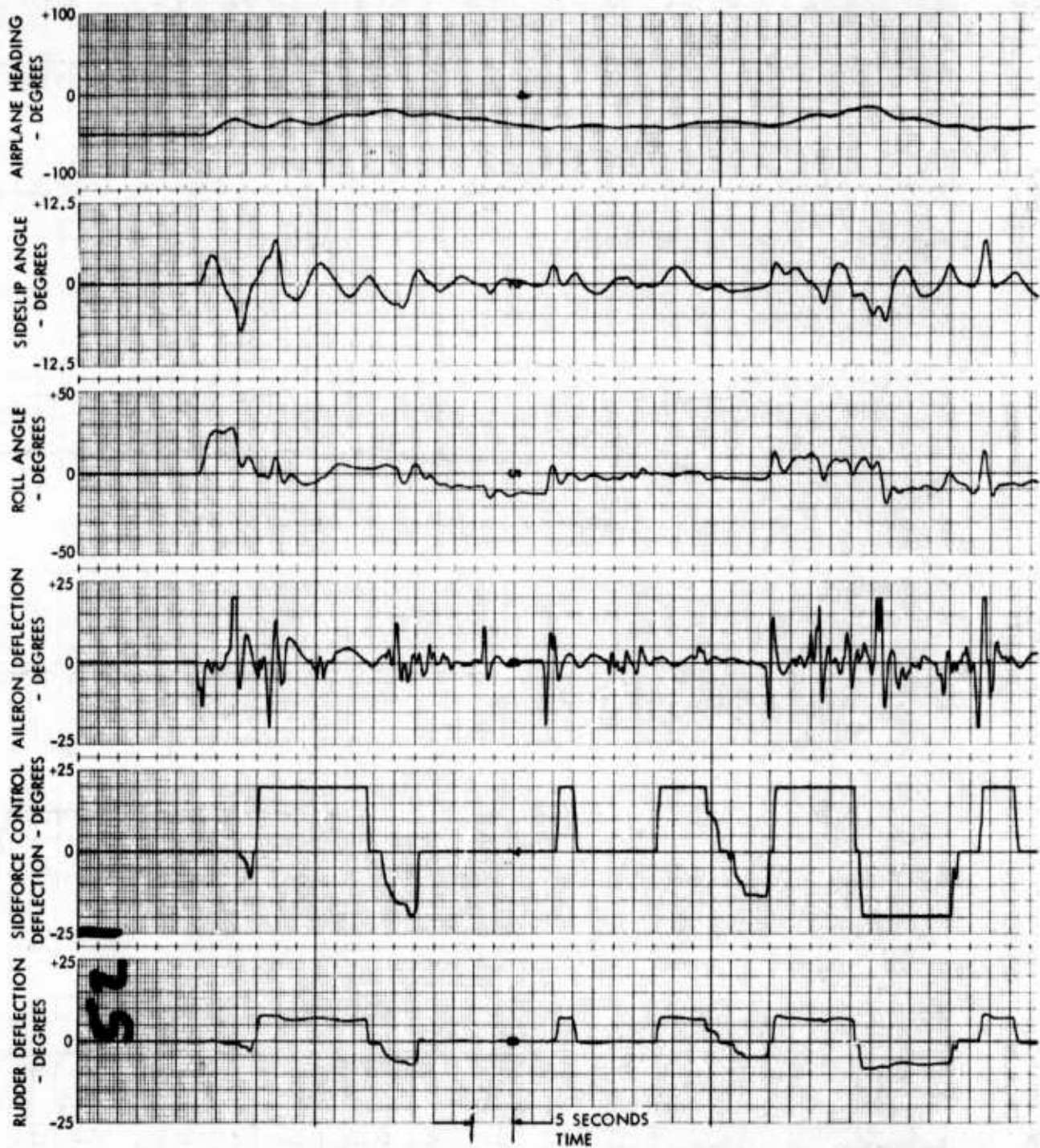


Figure J-13 Landing Approach with 30 Knot Crosswind - DSFC Yaw Rate Mode Engaged, Rudder Pedal Controller

● Airplane Initial Lateral Offset is 3000 Ft Left of Runway

● Crosswind is from the Right

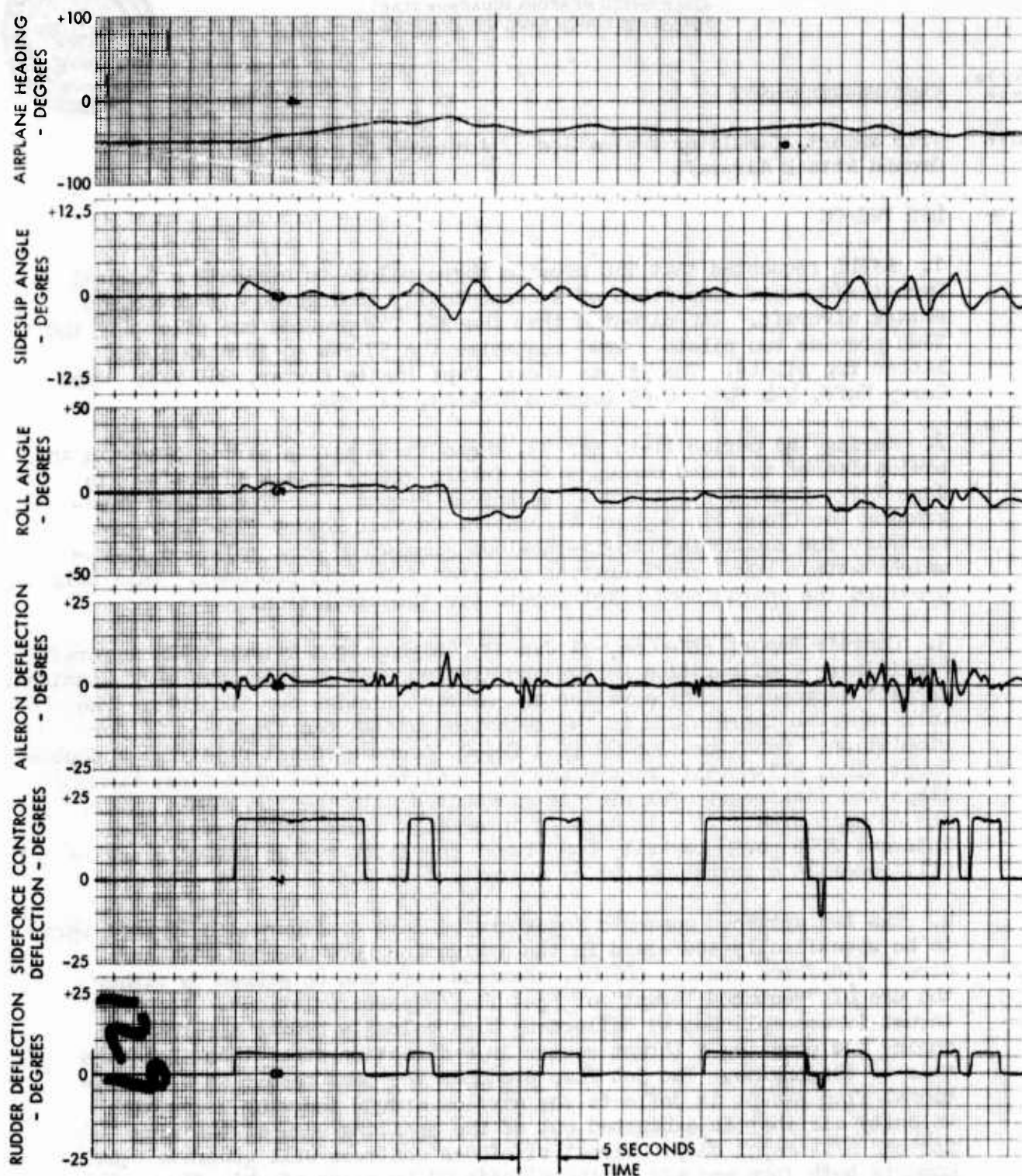


Figure J-14 Landing Approach with 30 Knot Crosswind - DSFC Yaw Rate Mode Engaged, Thumb Controller



DEPARTMENT OF THE AIR FORCE  
422d FIGHTER WEAPONS SQUADRON (TAC)  
NELLIS AIR FORCE BASE, NEVADA 89110



REPLY TO  
ATTN OF:

Capt Hawkins/4997

29 Mar 73

SUBJECT:

Trip Report, Simulator Evaluation of Advanced Concepts for Future  
Ground Attack Aircraft

TO:

422 FWS/CC

1. AFFDL requested that TAC provide three pilots to evaluate a General Dynamics/Convair simulation of a conceptually configured air-to-ground attack aircraft. TAC directed that the 355 TFW provide one pilot and the TFWC provide two pilots. TFWC requested the 57 FWW to furnish these latter two pilots. The pilots were; Capt Shelby Lawder, 355 TFW; Capt Gerry Huff, 414 FWS; Capt Douglas Hawkins, 422 FWS.
2. During the period 11-16 Mar 73, these three pilots participated in an evaluation of advanced concepts for future ground attack aircraft. In June 1972, Convair submitted a "Technical Proposal for Technology Integration for Close Air Support Aircraft", Convair Report FZP-1429. A contract for conducting man-in-the-loop simulation of a selected lightweight attack (LWA) configuration resulted from this proposal. This trip provided the operational pilot inputs for the simulation.
3. Convair Report FZM-6085, 31 Jan 73, "Lightweight Attack (LWA) Aircraft Preliminary Configuration Design and Mission/Configuration Tradeoff Studies", details a proposed configuration and characteristics for two LWAs. The work reported therein led to the selection of LWA Configuration 29 for simulation. Configuration 29 is a 22,500 pound aircraft utilizing a double swept wing, all-movable canard and vertical tail, dual chin fins, L.E. flaps and flaperons. The wing is midmounted with the air intake under the cockpit area. It will have an internally mounted M-61 gun and an internal 2000 pound capacity bomb bay. The large bypass turbofan engine will generate a thrust/weight of approximately 1.5:1.
4. The two advanced concepts incorporated into Configuration 29 that were to be specifically addressed in the evaluation were powered lift and direct sideforce control (DSFC). Powered lift can be gained by either the use of "vectored thrust" or "jet flap/supercirculation". Vectored thrust is accomplished by deflecting high velocity bypass air from the engine and creating a thrust vector in a direction other than along the axis of the engine. The jet flap produces the same result as a conventional flap except it deflects the airflow around the wing using high velocity air that is exhausted out of the trailing edge of the wing instead of a metal flap. Direct sideforce controls will generate equal moments both fore and aft of the plane's CG by means of chin fins. This will allow the aircraft to generate a lateral vector without any associated roll. Creating a slight delta moment, coupled with an antiroll mode in the fly-by-wire flight controls, will permit a controlled yaw rate.

Figure J-15 Simulator Pilots' Report

5. To evaluate powered lift, each pilot ran through a series of dive bomb passes varying roll-in airspeed, dive angle, power setting and jet flap deflection angle. Data were collected to determine the effect of the jet flap on controlling airspeed in the dive and on decreasing altitude lost during recovery. It was obvious to all pilots that the jet flap would produce somewhat of a speedbrake effect when used in the dive. Maximum utilization of the jet flap during recovery both decreased altitude lost during pullout and decreased time to establish a climb back to above 10,000 feet AGL. Formal data reduction has not been completed at this time.

6. The evaluation of direct sideforce was in two parts. The first part was a series of dive bomb passes in which the pilot's ability to solve lateral pipper placement and drift was evaluated. Variable conditions included crosswind, direct sideforce control (DSFC) in both sideslip and yaw rate modes and the position of the direct sideforce controller using rudders or a thumb switch. If the original pipper placement was in excess of 30-50 mils error, all pilots preferred to use conventional rudder and bank control to reposition it. Once the pipper was close to the target, DSFC could effectively be used to solve the rest of the pipper placement problem. The pilots were not always confident that they could achieve consistent solutions with DSFC. Due to occasional malfunctions with the simulator and the lack of experience to create their own 'techniques' for DSFC placement of the pipper, the pilots did not have an obvious feel for one method being superior to the other.

7. The second part of the DSFC evaluation was during approaches to landing. Straight in approaches were made with and without crosswinds. Again, the two types of DSFC and the position of the controller were evaluated. The pilots disagreed on which mode, yaw rate or sideslip, they could utilize most effectively, but they did agree that DSFC could assist the pilot during approaches and landings. All pilots wanted to retain conventional rudder and roll capabilities with DSFC being an additional instead of a replacement feature. Placement of a DSFC switch on the stick was considered unwise. The control stick is the direct force type and unwanted inputs could be generated while actuating the DSFC switch with the thumb. A throttle location should be considered. Formal data reduction of this phase has not been completed either.

8. Pilot comments on the mechanization of the simulation: Video field of view was too small. In sideslip mode, roll was limited to less than 180 degrees. A fixed armrest for the stick arm was not equally comfortable to each pilot. Rudder force control was not the right magnitude. Using full afterburner and full jet flaps during dive recovery would overflow the computer memory.

## Figure J-15 Simulator Pilots' Report (Cont'd)

9. Recommendations: Further investigation into the use of powered lift and direct sideforce devices should definitely be continued. However, the advantages in maneuverability that these devices provide should be examined over the entire flight profile. The survivability and defensive ability of a ground attack aircraft should be greatly improved by the proper utilization of these devices. All pilots involved would like to see the next simulation of the LWA address the entire mission profile. The DSFC is available at only a small cost in terms of weight and complexity but provides much in the way of additional maneuverability both offensively and defensively. Incorporating powered lift would not be as cheap, but at combat airspeeds it is cheaper in terms of added weight per unit of lift than conventional aerodynamic lift.

10. During the week, the pilots spent their free time talking with engineers from many different departments at the plant. These meetings proved to be very informative for both parties involved. All pilots felt it was extremely beneficial to have an opportunity to make operationally oriented inputs at the concept and design phase. Many engineers and their supervisors expressed themselves as hoping there would be future opportunities for dialogue directly with operational pilots. It is recommended that TFWC and TAC favorably consider any future requests from AFFDL, or the aerospace industry, that would allow operational ideas and pilots to be a part of new aircraft design at the concept and design synthesis stage.

*Douglas S. Hawkins*

DOUGLAS S. HAWKINS, CAPT, USAF

Figure J-15 Simulator Pilots' Report (Cont'd)

### K.1 AAA QUADRATIC PREDICTOR

is shown in Figure K-1. Prediction circuits for offset range and altitude are similar to those for down range. The predicted target position basic equations are

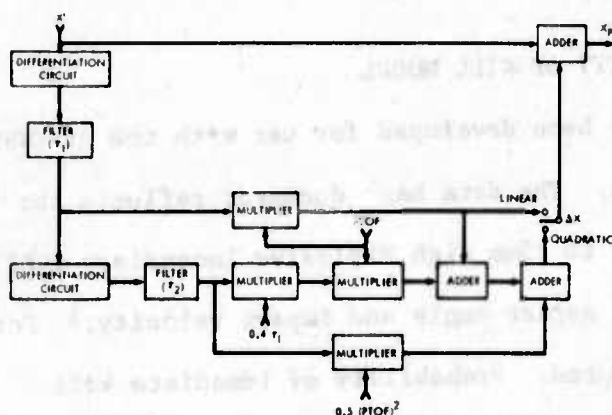


**Figure K-1 Block Diagram of Down-Range Prediction Circuits'**

$$X_p = X' + \Delta X \quad (K-1)$$

$$Y_p = Y' + \Delta Y \quad (K-2)$$

$$Z_p = Z' + \Delta Z \quad (K-3)$$

$\Delta X$  = Predicted target down-range movement during the predicted Projectile Time-of-Flight (PTOF)

$\Delta Y$  = Predicted target offset-range movement during the PTOF

$\Delta Z$  = Predicted target altitude movement during the PTOF.

$$\Delta X = 0.5 \ddot{X} \tau_1 \tau_2 (\text{PTOF})^2 + (\dot{X} \tau_1 + 0.4 \tau_1 \ddot{X} \tau_1 \tau_2) \text{PTOF} \quad (\text{K-4})$$

$$\Delta Y = 0.5 \ddot{\tau}_1 \tau_2 (\text{PTOF})^2 + (\dot{\tau}_1 + 0.4 \tau_1 \ddot{\tau}_1 \tau_2) \text{PTOF} \quad (\text{K-5})$$

$$\Delta Z = 0.5 \ddot{\tau}_1 \tau_2 (\text{PTOF})^2 + (\dot{\tau}_1 + 0.4 \tau_1 \ddot{\tau}_1 \tau_2) \text{PTOF} \quad (\text{K-6})$$

 $\ddot{x}_{T_1 T_2}$  = Smoothed tracked target down-range acceleration $\dot{x}_{T_1}$  = Smoothed tracked target down-range rate

$\tau_1$  = Time constant of data-smoothing filter No. 1

PTOF = Predicted projectile time-of-flight

$\ddot{Y}_{T_1 T_2}$  = Smoothed tracked target offset-range acceleration

$\dot{Y}_{T_1}$  = Smoothed tracked target offset-range rate

$\ddot{Z}_{T_1 T_2}$  = Smoothed tracked target altitude acceleration

$\dot{Z}_{T_1}$  = Smoothed tracked target altitude rate.

## K.2 AAA PROBABILITY OF KILL MODEL

A probability of kill ( $P_k$ ) model has been developed for use with the AF-EWES anti-aircraft artillery (23mm) simulation. The data base document reflects the vulnerability of the areas of an aircraft to 23mm High Explosive Incendiary (HEI) ground fired projectiles as a function of aspect angle and impact velocity.<sup>1</sup> For this test, two categories of  $P_k$  were computed. Probability of immediate kill ( $P_{KK}$ ) is the probability that the aircraft immediately enters uncontrolled flight when struck by the projectiles. Probability of 5-minute kill ( $P_{KA}$ ) is the probability that the aircraft will enter uncontrolled flight within 5 minutes after being struck by the projectiles.

### K.2.1 TARGET VULNERABILITY

As an initial ground rule, data from an inventory fighter aircraft were used to establish vulnerability data although it was realized that the  $P_k$  for this aircraft would not apply directly to the LWA aircraft but would give a comparative basis to examine the effectiveness of several types of maneuvers. The target aircraft for which the data were taken has 10 vulnerable components which were considered: (1) pilot, (2) observer, (3) engine 1, (4) engine 2, and (5) six fuselage fuel tanks. The aircraft wing tanks are assumed to be empty, and the fuselage fuel tanks are assumed to be full.

In order to achieve an immediate kill, either both pilots or both engines must be hit, i.e., pilots and engines are considered multiply vulnerable. In addition to the immediate kill considerations, the 5-minute kill includes vulner-

<sup>1</sup> "The Vulnerability of Several Aircraft and Missiles to Impacting Fragments and Ground Fired Projectiles" (U), BRL 1786, August 1966 (SECRET RESTRICTED DATA).



ability of the fuel tanks. Fuel tanks are singly vulnerable, i.e., one HEI projectile striking one fuel tank can cause a 5-minute kill. All vulnerable areas of the aircraft were located at specified points within the aircraft with respect to the aircraft center of gravity (with the assumed fuel status).

#### K.2.2 P<sub>K</sub> COMPUTATIONS

The available vulnerability data reflected the assumption that a 23mm projectile could contribute to an immediate or a 5-minute kill by inflicting structural damage to the airframe. In order to kill the aircraft, a 23mm projectile would have to physically strike a vulnerable area (contact fusing). Probability of kill, then, included the probability (on a single-shot basis) that a vulnerable area would be hit with each projectile miss distance as measured from the aircraft center of gravity.

The output data from the AF-EWES simulation provide the number of shots within miss distance bins for every data run. Bins of two feet were utilized for this test; therefore, the number of shots were segregated into miss distances (1) less than 2 feet, (2) between 2 and 4 feet, (3) between 4 and 6 feet, (4) etc., out to the maximum miss distance of 200 feet. In the probability of kill model, the vulnerable components were located at the correct positions with respect to the aircraft center of gravity; therefore, for a given aspect angle, the vulnerable areas of the components within each miss distance bin could be measured and divided by the total area of the appropriate miss distance bin. Thus, the probability of a particular component being hit is derived for a given miss distance and aspect angle. Since a highly maneuverable target was involved in the test, the above procedure was accomplished for all four aspect angles represented in the data base document; and an average probability was derived for each vulnerable component, each projectile miss distance bin, and seven projectile impact velocities.

The following equations were used to compute the  $P_{KK}$  and  $P_{KA}$  of each shot fired.

$$P_{KK} = 1 - [1 - P_K(\text{Pilot}) P_K(\text{Observer})] [1 - P_K(\text{Engine 1}) P_K(\text{Engine 2})].$$

$$P_{KA} = 1 - [1 - P_K(\text{Pilot}) P_K(\text{Observer})] [1 - P_K(\text{Engine 1}) P_K(\text{Engine 2})] \times \\ [1 - P_K(\text{Fuel Tank 1})] [1 - P_K(\text{Fuel Tank 2})] \times \\ [1 - P_K(\text{Fuel Tank 3})] [1 - P_K(\text{Fuel Tank 4})] \times \\ [1 - P_K(\text{Fuel Tank 5})] [1 - P_K(\text{Fuel Tank 6})].$$

After derivation of the single-shot probabilities, cumulative probabilities were computed for each data run.

$$P_K = 1 - [1 - P_K(\text{single shot, miss distance bin No. 1})] S1 \times \\ [1 - P_K(\text{single shot, miss distance bin No. 2})] S2 \times \\ \dots$$

where S1 = The number of shots in miss distance bin No. 1

S2 = The number of shots in miss distance bin No. 2, etc.

The cumulative  $P_K$ 's (both categories) for each data run within a test condition were then averaged to provide a mean probability of kill for each test condition.

### K.3 GUN FIRING DATA

The gun firing data which was input to the  $P_K$  model is given in Table K-1.

Table K-1 GUN FIRING DATA

TEST COND NO.	CONTROL MODE	MANEUVER	INITIAL POSITION				NO. OF DATA RUNS	PROJECTILE		MISS DISTANCE		
			OFFSET <sup>1</sup> (N.M.I.)	ALTITUDE (FT)	SLANT RANGE (N.M.I.)	SPEED (KT)		TOTAL FIRED	PERCENT < 20 FT (%)	MEAN (FT)	STANDARD DEVIATION (FT)	90% CONF. INTERVAL (%)
4	CONVENTIONAL	NONE	-0.5	1000	4.0	400	3	1,776	46.3	26	21	3.1
5			-1.0				3	1,740	27.4	33	21	2.7
6			-0.5	5000			8	2,968	39.1	26	16	1.7
7			-1.0				3	1,104	25.5	33	19	2.9
AVERAGE								8,288	36.8	28	19	1.2
8	CONVENTIONAL	NONE	-0.5	1000	4.0	600	3	1,200	43.2	27	20	3.6
9			-1.0				3	1,008	35.1	29	20	3.6
10			-0.5	5000			3	1,008	22.4	37	22	3.7
11			-1.0				3	768	27.6	36	23	2.7
AVERAGE								3,984	32.9	32	22	1.8
12	CONVENTIONAL	S-WEAVE <sup>2</sup>	-0.5	1000	4.0	400	5	2,720	5.2	80	64	2.5
13			-1.0				5	1,760	6.7	90	51	2.2
14			-0.5	5000			5	2,240	0.2	173	60	1.2
15			-1.0				5	680	1.3	112	48	2.4
AVERAGE								7,600	3.6	121	64	1.0
16	CONVENTIONAL	S-WEAVE	-2.0	1000	4.0	600	5	1,600	9.3	109	73	2.7
17			-1.5				5	1,143	13.6	93	68	3.5
18			-1.5	5000			5	939	0.4	153	68	2.4
19			-1.0				5	409	0.2	156	49	2.6
AVERAGE								4,091	7.6	121	73	1.5
20	CONVENTIONAL	JINK <sup>3</sup>	-0.5	1000	4.0	400	5	3,120	0	509	160	0.9
21			-1.0				5	1,520	0	515	112	0.9
22			-0.5	5000			5	1,920	0	778	124	0.6
23			0				7	4,928	0.1	738	131	0.4
AVERAGE								11,488	0.06	653	180	0.4
24	CONVENTIONAL	JINK	0.5	1500	4.0	600	6	1,152	0	383	138	1.8
25			0.25				5	560	0	273	99	2.5
26			0.5	5000			7	112	0	196	28	2.2
27								1,824	0	337	138	1.6
AVERAGE												
28	VT/SC AND DSFC	JINK	-0.5	1000	4.0	400	5	1,408	0	432	125	1.3
29			0				5	2,240	0	381	156	1.4
30			-0.5	5000			6	864	0.6	375	117	1.7
31			0				5	1,600	0.6	478	147	1.3
AVERAGE								6,112	0.2	417	147	0.7
32	VT/SC AND DSFC	JINK	-1.5	1000	4.0	600	6	1,728	0	554	103	0.7
33			-1.0				5	2,125	0	419	116	1.0
34			-1.5	5000			5	880	0	767	93	0.7
35			-1.0				6	2,323	0	696	132	0.7
AVERAGE								7,056	0	587	174	0.6

## NOTES:

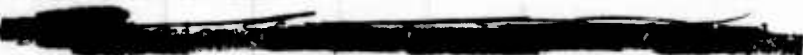
1. Negative offset means the aircraft approaches with the AAA site on the left.
2. Aircraft heading was changed approximately  $\pm 20^\circ$  using  $30^\circ$ - $40^\circ$  bank while maintaining altitude.
3. Aircraft heading was changed approximately  $\pm 60^\circ$  using  $60^\circ$ - $90^\circ$  bank with about  $\pm 3000$ ,  $\pm 1000$  altitude variation.

Unclassified

Security Classification

DOCUMENT CONTROL DATA - R & D

(Security classification of title, body of abstract and indexing annotation must be entered when the overall report is classified)

1. ORIGINATING ACTIVITY (Corporate author) General Dynamics Corporation, Convair Aerospace Division, P.O. Box 748, Fort Worth, Texas 76101		2a. REPORT SECURITY CLASSIFICATION (Unclassified)	
		2b. GROUP	
3. REPORT TITLE TECHNOLOGY INTEGRATION FOR CLOSE AIR SUPPORT AIRCRAFT			
4. DESCRIPTIVE NOTES (Type of report and inclusive dates) Final Technical Report			
5. AUTHOR(S) (First name, middle initial, last name) Larry E. Hove, et al.			
6. REPORT DATE July 1973		7a. TOTAL NO. OF PAGES 407	7b. NO. OF REFS 20
8a. CONTRACT OR GRANT NO. F33615-73-C-3082		9a. ORIGINATOR'S REPORT NUMBER(S) Convair Report FZM-6139	
b. PROJECT NO. 1207		9b. OTHER REPORT NO(S) (Any other numbers that may be assigned this report) AFFDL-TR-73-57	
c.			
d.			
10. DISTRIBUTION STATEMENT 			
11. SUPPLEMENTARY NOTES		12. SPONSORING MILITARY ACTIVITY AFFDL Wright-Patterson AFB, Ohio 45433	
13. ABSTRACT The objectives of this technology integration study for close air support aircraft were to perform configuration design and validation using, in part, man-in-the-loop simulation techniques. Advanced technology close air support aircraft configuration known as Lightweight Attack (LWA) Configuration 29 was evolved and justified. The selected configuration embodies powered lift in the form of vectored thrust with supercirculation (VT/SC) and an advanced composites structure. Other advanced technologies which are integrated in LWA Configuration 29 are direct sideforce control (DSFC), variable camber, internal/conformal pallet for stores carriage, close-coupled canard, and modular digital avionics. Results of the study show that such an integrated advanced technology configuration provides significant improvement in total tactical fighter mission capability and in the ability to perform and survive in the ground attack environment.			

DD FORM 1 NOV 65 1473

Unclassified

Security Classification

Unclassified

Security Classification

14.	KEY WORDS	LINK A		LINK B		LINK C	
		ROLE	WT	ROLE	WT	ROLE	WT
	Close Air Support Aircraft Ground Attack Simulation Survivability Analysis Advanced Composites Structure Powered Lift Jet Flaps Vectored Thrust Direct Sideforce Control Modular Digital Avionics STOL Fighter Aircraft Advanced Technology Fighter Trade Studies						

Unclassified

Security Classification